FEB - FRESENIUS ENVIRONMENTAL BULLETIN
Founded jointly by F. Korte and F. Coulston
Production by PSP - Vimy Str. 1e, 85354 Freising, Germany in
cooperation with PRT-Parlar Research & Technology
Vimy Str 1e, 85354 Freising
Copyright© by PSP and PRT, Vimy Str. 1e, 85354 Freising, Germany
All rights are reserved, especially the right to translate into foreign language or other processes - or convert to a machine language, especially for data processing equipment - without written permission of the publisher. The rights of reproduction by lecture, radio and television transmission, magnetic sound recording or similar means are also reserved.
Printed in Germany-ISSN 1018-4619

FEB-EDITORIAL BOARD

CHIEF EDITOR:
Prof. Dr. Dr. H. Parlar
Parlar Research & Technology-PRT
Vimy Str.1e
85354 Freising, Germany

MANAGING EDITOR:
Dr. P. Parlar
Parlar Research & Technology
PRT, Vimy Str.1e
85354 Freising, Germany

CO-EDITORS:

Environmental Spectroscopy
Prof. Dr. A. Piccolo
Universita di Napoli "Frederico II"
Dipto. Di Scienze Chemica Agrarie
Via Universita 100, 80055 Portici, Italy

Environmental Biology
Prof. Dr. G. Schuurmann
UFZ-Umweltzentrum
Sektion Chemische Ökotoxikologie
Leipzig-Halle GmbH,
Permoserstr.15, 04318
04318 Leipzig, Germany
Prof. Dr. I. Holoubek
Recetox-Tocoen
Kamenice126/3, 62500 Brno, Czech Republic
Prof. Dr. M. Hakki Alma
Igdir Universitesi
76000, Igdir, Turkey

Environmental Analytical Chemistry
Prof. Dr. M. Bahadir
Lehrstuhl für Ökologische Chemie
und Umweltanalytik
TU Braunschweig
Lehrstuhl für Ökologische Chemie
Hagenring 30, 38106 Braunschweig, Germany
Dr. D. Kotzias
Via Germania29
21027 Barza(Va), Italy

Environmental Management
Dr. K. I. Nikolaou
Env.Protection of Thessaloniki
OMPEPT-54636 Thessaloniki
Greece

Environmental Toxicology
Prof. Dr. H. Greim
Senatkommision – DFG / TUM
85350 Freising, Germany

Environmental Proteomic
Dr. A. Fanous
Halal Control GmbH
Kobaltstr. 2-4
D-65428 Rüsselsheim, Germany

Environmental Education
Prof. Dr. C. Bayat
Esenyurt Üniversitesi
34510 Esenyurt, Istanbul, Turkey

Environmental Medicine
Prof. Dr. I. Tumen
Bartin Üniversitesi
74100, Bartin, Turkey

Advisory Board
K. Bester, K. Fischer, R. Kallenborn
DCG. Muir, R. Niessner,W.Vetter,
A. Reichlmayr-Lais, D. Steinberg,
J. P. Lay, J. Burhenne, L. O. Ruzo

Marketing Manager
Cansu Ekici, B. of B.A.
PRT-Research and Technology
Vimy Str 1e
85354 Freising, Germany
E-Mail: parlar@wzw.tum.de
parlar@prt-parlar.de
Phone: +49/8161887988

Fresenius Environmental Bulletin is abstracted/indexed in:
Biology & Environmental Sciences, BIOSIS, CAB International, Cambridge Scientific abstracts, Chemical Abstracts, Current Awareness, Current Contents/Agriculture, CSA Civil Engineering Abstracts, CSA Mechanical & Transportation Engineering, IBIDS database, Information Ventures, NISC, Research Alert, Science Citation Index (SCI), Scisearch, Selected Water Resources Abstracts

CONTENTS

ORIGINAL PAPERS

NATIONAL AMBIENT AIR QUALITY STANDARDS AND GUIDELINES: A GLOBAL REVIEW 2612
Sabah A Abdul-Wahab, Amani Alnahdi, Ali Elkamel, Emmanuel Ikhile

EVALUATION OF THE RECREATIONAL POTENTIAL OF KUTAHYA URBAN FOREST 2629
Mehmet Cetin, Hakan Sevik, Ugur Canturk, Cansel Cakir

SPECTROPHOTOMETRIC MEASUREMENTS OF RHODAMINE B AS A DYE TRACER FOR BRINE OUTFALL LABORATORY EXPERIMENTS 2635
Naim Sezgin, Emin Ahmet Yesil, Mehmet Altun, Ugur Emre Temelli, Semih Nemlioglu

COCONUT OIL-LOADED CHITOSAN NANOPARTICLES FOR THE TREATMENT OF ACNE VULGARIS: CYTOTOXICITY, ANTIBACTERIAL ACTIVITY, AND ANTIBIOFILM PROPERTIES 2642
Rabia Cakir-Koc, Yasemin Budama-Kilinc, Zeynep Kaya, Buse Berber Orcen, Ezgi Ucarkus

THE EFFECTS OF OLIVE MILL WASTEWATER IN FOUR ADSORBENTS ON GERMINATION CHARACTERISTICS OF WHEAT (*TRITICUM AESTIVUM* L.) 2649
Ilkay Yavas

GLOBAL TRENDS AND PERFORMANCES OF CELLULOSE MATERIALS DEGRADATION RESEARCH 2654
Zhanying Liu, Yaping Yan, Qiuping Zhang, Shuli Zhang, Qunhui Wang, Jianguo Liu

INTEGRATING GIS TO DETERMINE THE SPATIAL DISTRIBUTION OF PRINCIPAL COMPONENTS AND THE SOURCES OF HEAVY METALS IN FARMLAND SOILS NEAR MINING AREA IN TONGLING, CHINA 2662
Hong Jiang, Jingru Nie, Shanshan Fan, Guoqing Yin, Youhua Ma, Tiezheng Ma, Qiang Wang, Rungui Shi

NUMERICAL SIMULATION OF THE HYDRODYNAMICEFFECTS OF AN ARTIFICIAL ISLAND 2671
Xiaofeng Guo, Chuhan Chen, Junjian Tang

OPTIMIZATION OF PHOTODEGRADATION OF o-TOLUIDINE IN WATER WITH NANO SPHERICAL CoFe2O4 / COPPER SLAG AS A CATALYST 2682
Rezvan Zeynolabedin, Kazem Mahanpoor

TRACE METALS IN VEGETABLE PLANTS (*ALLIUM CEPA L., CAPSICUM ANNUM* L. *LYCOPERSICON ESCULENTUM* MILL. AND *BETA VULGARIS* L.) FROM THE ZETA VALLEY OF MONTENEGRO 2690
Sladjana Krivokapic, Dragana Petrovic

DETERMINATION OF CYTOTOXIC EFFECTS OF PROCHLORAZ AND TRALKOXYDIM IN BARLEY (*HORDEUM VULGARE* L.) ROOTS 2697
Selda Metin-Kir, Filiz Vardar, Meral Unal

REMEDIATION OF A URANIUM-CONTAMINATED GROUNDWATER USING THE PERMEABLE REACTIVE BARRIER TECHNIQUE COUPLED WITH HYDROXYAPATITE-COATED QUARTZ SANDS 2703
Weimin Zhang, Yadan Guo*, Zhiping Pan, Yiran Li, Hua Zeng

DETERMINATION OF NATURAL RADIOACTIVITY LEVELS OF CONCRETE CORE AND CEMENTS IN ESKISEHIR AREA 2717
Ugur Emre Temelli

TRANSPOSON MUTAGENESIS AND CLONING ANALYSIS OF *MamZ* GENE IN *MAGNETOSPIRILLUM GRYPHISWALDENSE* MSR-1 2724
Lei Zhou, Ruixue Guo, Sha Wu, Junjie Xu, Minghua Xiong, Ying Li, Feng Li, Guangli Wang

PROGRESS IN THE BIODEGRADATION OF CHLORONICOTINYL INSECTICIDE ACETAMIPRID 2735
Qianqian Yang, Yiran Wang, Guangli Wang, Feng Li

STATUS AND PREDICTION OF NO_2 AS AN AIR POLLUTANT IN ISFAHAN, IRAN 2743
Masoud Masoudi, Soraya Gerami

FUNGI COLONIZING CHRYSANTHEMUMS PLANTS CULTIVATED IN THE FIELD IN DIFFERENT PROTECTION SYSTEMS 2751
Marek Kopacki, Stanislaw Parafiniuk, Barbara Skwarylo-Bednarz

COMPARISON OF ANTIBIOTIC SENSITIVITY RATIO OF *ESHERICHIA COLI* AND *KLEBSIELLA PNEUMONIAE* STRAINS ISOLATED FROM VARIOUS CLINICAL SPECIMENS IN INTENSIVE CARE UNIT 2761
Nur Ceyhan-Guvensen, Dilek Keskin, Funda Sankur

SPATIAL ECONOMETRIC ANALYSIS OF ENVIRONMENTAL REGULATION IN CHINA 2768
Yuanhua Yang, Guohua Niu, Dengli Tang, Mengjue Zhu

USE OF WATER QUALITY INDICES AS A TOOL IN WATER RESOURCES MANAGEMENT 2777
Ireneusz Cymes

CHEMICAL DIVERSITY OF ESSENTIAL OIL FROM LEAVES OF *ZIZIPHORA CLINOPODIOIDES* GROWING IN VAN, TURKEY 2785
Nese Okut, Nilufer Selcuk, Mehmet Yagmur, Bunyamin Yildirim

USE OF THE WATER QUALITY INDEX (CCME-WQI) IN AN EVALUATION OF THE IMPACT OF DAM RESERVOIRS ON QAULITY OF GROUNDWATER 2791
Ireneusz Cymes

DINOFLAGELLATE CYST STUDIES IN THE SEDIMENTS OF TURKISH COASTAL WATERS AND FUTURE ASPECTS 2800
Serdar Uzar, Hilal Aydın, Emine Erdem Yurur

EFFECTS OF DEFICIT IRRIGATION ON PEPPER YIELD UNDER VARIOUS GREENHOUSE CONDITIONS 2809
Waheed Ahmed Siddiqui, Zhu Mei, LiXue Ling

STUDY OF THE RELATIONSHIP BETWEEN ECONOMIC GROWTH AND ENVIRONMENTAL QUALITY WITH THE KUZNETS CURVE IN GUANGXI, CHINA 2818
Yuping Xu, Miao Wang, Man Qin, Huaxian Shi, Bowen Sui, Xinzhong Jia, Dongliang Lu

"NEW FINDINGS" ON *BOSTRICHUS CAPUCINUS* LINNAEUS, 1758 (COLEOPTERA: BOSTRICHIDAE) IN TURKEY 2829
Inanc Ozgen

A MODIFIED RAINFALL SIMULATOR: DESIGN PRINCIPLES, RAINFALL CHARACTERISTICS AND SIMULATION ABILITY TO NATURAL RAINS 2834
Tugrul Yakupoglu, Nutullah Ozdemir, Imanverdi Ekberli, Elif Ozturk

GEOGRAPHICAL DISTRIBUTION, CHEMICAL SPECIATION AND RISK ASSESSMENT OF HEAVY METALS IN TING RIVER: THE INFLUENCE OF HEAP BIOLEACHING PLANT ON THE NEARBY RIVER 2844
Jiankang Wen, Mingjiang Zhang, Xingyu Liu, Xinglan Cui, Xiao Yan, Biao Wu, Bowei Chen

SPECIES DIVERSITY IN LENTIC, LOTIC, MARINE AND TERRESTRIAL BIOTOPES OF GOKCEADA SALT LAKE WETLAND (CANAKKALE, TURKEY) 2853
Herdem Aslan, Onur Gonulal, Elif Can-Yilmaz, Belgin Elipek, Ozgur Baytut, Murat Tosunoglu, Ersin Karabacak, Yusuf Kurt

THE INFLUENCE OF SOIL PROPERTIES AND PLANT SPECIES' COMPOSITION ON METAL UPTAKE BY VEGETATION ON FALLOW LAND 2867
Jan Zarzycki, Agnieszka Petryk

THE EFFECT ON K, Na, AND Cl CONTENT IN STEM AND ROOT OF *AGROPYRON* SPECIES UNDER DIFFERENT SALT CONCENTRATIONS 2873
Nur Koc, Ramazan Acar

SOME MICROBIOLOGICAL PROPERTIES OF ROADSIDE SOILS EXPOSED TO TRANSPORTATION POLLUTANS IN SANLIURFA'S REGION, TURKEY 2878
Cigdem Kucuk, Onur Baysoy

INVESTIGATION OF IN VITRO GENOTOXIC EFFECTS OF MONOCROTOPHOS ON HUMAN SKIN KERATINOCYTE CELLS 2883
Abdullah A AlKahtane, Saud Alarifi, Ahmed A Al-Qahtani, Hamad Al-Yahya, Daoud Ali, Suliman Y Alomar, Mohammed S Alessia, Bader Al-dahmash, Saad Alkahtani

ASSESSMENT OF WATER-SAVING IRRIGATION DEVELOPMENT LEVEL OF A REGIONAL AREA BASED ON FUZZY COMPREHENSIVE ASSESSMENT METHOD 2891
Lujun Ding, Yuhong Liu

ANALYSIS OF SPATIAL AND TEMPORAL WATER POLLUTION PATTERNS IN TERZI POND (KASTAMONU/TURKEY) BY USING MULTIVARIATE STATISTICAL METHODS 2900
Ekrem Mutlu, Arzu Aydin-Uncumusaoglu

INHIBITORY EFFECT OF NATURAL ZEOLITE AND ITS CHITOSAN COMPOSITES ON CADMIUM-CONTAMINATED SOILS 2913
Na Yi, Yaoguo Wu, Sihai Hu

ACOUSTICAL ENVIRONMENT DESIGN OF THE LECTURE HALL BASED ON THE IMPROVED ACOUSTIC INDEX ANALYSIS 2922
Ziqing Tang, Fenghua Lu

LAND USE CONVERSION EFFECTS TRIGGERED BY TEA PLANTATION ON LANDSLIDE OCCURRENCE AND SOIL LOSS IN NORTHEASTERN ANATOLIA, TURKEY 2933
Sezgin Hacisalihoglu, Selcuk Gumus, Ugur Kezik

AIRBORNE FUNGI IN OUTDOOR AIR OF RIYADH CITY, KINGDOM OF SAUDI ARABIA 2943
Abd El-Rahim M A El-Samawaty, Mohamed A Yassin, Mohamed A Abdel-Wahab

THE ECOTOXICOLOGICAL EFFECTS OF ZNO-TiO2 NANOCOMPOSITE IN *CHODATODESMUS MUCRANULATUS* 2951
Betul Yilmaz-Ozturk, Yesim Daglioglu

PERFORMANCE OF HERBICIDE SPRAYING METHODS AT DIFFERENT APPLICATION VOLUMES IN MAIZE 2963
Ali Bolat, Ali Bayat, Ozcan Tetik, H Ali Karaagac, Ibrahim Cerit, Ugur Sevilmis

DUST EXPOSURE IN FOAMING WORKSHOP, CASE OF THE HOME APPLIANCE INDUSTRY IN ALGERIA 2968
Hakima Rebbah, Amina Akachat, Krim Louhab

STUDY ON IDENTIFICATION TO PATHOGENS OF WOODS CANKER, GENETIC DIFFERENTIATION RESEARCH TO ITS MAIN SPECIES VALSA MALI AND RAPID DETECTION TO PRIMARY INFECTION SOURCE OF *V. MALI* IN XINJIANG 2978
Kaifa Guo, Benchun Xiang, Sifeng Zhao, Cailan Wu

INVESTIGATION OF THE NATURAL CAT AND DOG DETOX PRODUCTS ON RATS 2985
Musa Yavuz, Elif Rabia Sanli

SYNTHESIS, STRUCTURE INVESTIGATION, SPECTRAL PROPERTIES AND IN VITRO ANTIOXIDANT EVALUATION OF NEW 1-(3-METHYL-3-MESITYL)-CYCLOBUTYL-2-(5-THIOPHEN-4-ETHYL-2H-[1,2,4]TRIAZOL-3-YLSULFANYL)-ETHANONE 2992
Cahit Orek, Kamiran Sarac, Akif Evren Parlak, Pelin Koparir, Semra Turkoglu, Metin Koparir

EVALUATION OF THE PHYSICOCHEMICAL CHARACTERISTICS AND CHLOROPHYLL-A CONTENT OF LAKE YENICAGA, BOLU 3006
Savas Kilic, Z Arzu Becer

STATISTICAL AND SPATIAL ANALYSES OF THE MANGANESE CONCENTRATIONS IN THE SHALLOW GROUNDWATER OF THE URBAN AREA OF SUZHOU, ANHUI PROVINCE AND ITS ENVIRONMENTAL IMPLICATIONS 3013
Sun Linhua, Cheng Chen

EFFICIENT REGENERATION AND *AGROBACTERIUM TUMEFACIENS* MEDIATED GENETIC TRANSFORMATION OF POTATO (*SOLANUM TUBEROSUM* L.) 3020
Hussein Abdullah Ahmed, Surendra Barpete, Guray Akdogan, Gulsum Aydin, Cengiz Sancak1, Sebahattin Ozcan

SPATIOTEMPORAL ANALYSIS OF ANTARCTIC SNOWMELT CHANGES USING MICROWAVE RADIOMETER DATA (1978-2015) 3028
Xingdong Wang, Cheng Wang, Bin Li

EFFECT OF LOCUST BEAN (*CERATONIA SILIQUA* L.) EXTRACT WASTE ON CLOGGING OF IN-LINE EMITTERS 3035
Servet Tekin

MECHANISM OF ADSORBING URANIUM BY ORGANIC MATTER IN PADDY SOIL NEAR URANIUM MINE TAILING POND 3043
Jingying Chen, Zumin Qiu, Bai Gao

INFLUENCE OF DISINFECTANT ADDED TO DRINKING WATER ON QUAIL GROWTH PERFORMANCE AND EGG QUALITY 3051
Ali Karabayir, Mustafa Ogutcu, Nazan Arifoglu

GROWTH RESPONSE OF URBAN WEEDS IN SINGLE AND MULTI-METAL CONTAMINATED SOIL, CHINA 3059
Kan-kan Shang, Jie Wang, Gilles Vincent

THE EFFECTS OF DIFFERENT COMBINATION OF COMBINED FERTILIZER DOSES ON SOME AGRONOMIC CHARACTERISTICS OF TURF MIXTURE 3068
Mustafa Yilmaz

TOXIC EFFECT OF ATRAZINE HERBICIDE ON THE HEMATOLOGICAL INDICES OF SNOW CARP (*SCHIZOTHORAX PLAGIOSTOMUS*): AN INDIGENOUS FISH SPECIES OF ECONOMIC IMPORTANCE. 3075
Farman Ali, Muhammad Qayash Khan, Muhammad Zubair Anjum, Irfan Khattak

INFLUENCE OF DIFFERENT PRIMING MATERIALS ON GERMINATION OF SORGHUM HYBRIDS (*SORGHUM BICOLOR* L. MOENCH. X *SORGHUM SUDANENSE* STAPH.) SEEDS 3081
Negar Ebrahim Pour Mokhtari, Hasan Yavuz Emeklier

DETERMINATION OF YIELD PERFORMANCE OF EARLY AND MAIN SEASON POTATO COMMERCIAL CANDIDATE VARIETIES 3087
Ercan Ozkaynak, Yasemin Orhan, Tugba Simşek

SUPPLY RESPONSE OF MAIN LEGUMES IN TURKEY BY VECTOR ERROR CORRECTION APPROACH 3094
R Figen Ceylan

UPTAKE OF URANIUM BY PLANTS GROWING AROUND AN OLD URANIUM MILL TAILING IN NORTHEAST CHINA 3102
Dong Yan, Kuke Ding, Yingxue He, Li Fan, Rui Zuo, Xiaoyan Jiang

PREDICTING SITE INDEX FOR ORIENTAL SPRUCE (*PICEA ORIENTALIS* L. (LINK)) USING ECOLOGICAL FACTORS IN THE EASTERN BLACK SEA, TURKEY 3107
Ismet Yener, Lokman Altun

THE EFFECTS OF ACARICIDE DIPPING METHODS ON BULB MITE [*RHIZOGLYPHUS ECHINOPUS* (FUMOUZE & ROBIN) (ACARI: ASTIGMATA)] THAT HARMFULL ON GARLIC 3117
Cihan Cilbircioglu, Sultan Cobanoglu

EFFECTS OF DIFFERENT KIND OF SOURCES IN NOISE EXPOSURE: ANTALYA AS A CASE STUDY 3124
Nesimi Ozkurt, Deniz Sari, Samet Feyyaz Hamamci, Melike Nese Tezel, Muhammet Erdol, Mustafa Ece, Nazli Yalcindag, Nese Yugruk-Akdag

PROBLEMS MEASURED AND EVALUATED OF IRRIGATED AGRICULTURAL AND NON-IRRIGATED AGRICULTURAL SOILS 3133
Ahu Alev Abaci-Bayan

ARBUSCULAR MYCORRHIZAL FUNGI IN *CYNODON DACTYLON* (L.) PERS. (BERMUDA GRASS) FROM TEMPERATE BLACK SEA COASTAL REGIONS 3140
Sahin Palta

PROTECTIVE EFFECT OF ELLAGIC ACID AGAINST CARBON TETRACHLORIDE (CCl4) – INDUCED OXIDATIVE BRAIN INJURY IN RATS 3148
H Turan Akkoyun, Aydin Sukru Bengu, Aykut Ulucan, Mahire Bayramoglu-Akkoyun, Okan Arihan

STUDY ON THE CHARACTERISTICS AND UTILIZATION OF A TRICLOPYR BUTOXYETHYL ESTER DEGRADING BACTERIUM, *LACTOBACILLUS BUCHNERI* TBE-6 3156
Jiang-wei Zhu, Yan Zhao, Xiao-lou Li, Wei-hong Chen, Rong Huang

FERTILITY VARIATION AND GENE DIVERSITY BASED ON CONE AND SEED PRODUCTION IN A CLONAL SEED ORCHARD OF *PINUS NIGRA* ARNOLD 3162
Zafer Kaya, Halil Baris Ozel

THE EFFECT OF MIXING *SOLIDAGO CANADENSIS* L. SOIL WITH THAT OF NEIGHBOURING *IMPERATA CYLINDRICAL* (L.) P. BEAUV. ON NITROGEN TRANSFORMATIONS 3166
Liya Zheng, Bangliang Deng, Qian Liu, Xiang Zheng, XiaoFeng Xu, ShuLi Wang, LiJun Huang, Xiaomin Guo, Dekui Niu

THE EFFECTS OF ORGANIC AMENDMENTS ON CADMIUM UPTAKE OF SPINACH (*SPINACIA OLERACEA L.*) AND PLANT GROWTH UNDER CADMIUM TOXICITY 3174
Sibel Boysan-Canal, Mehmet Ali Bozkurt, Selma Kipcak

PLASMA IRISIN AND HEAT SHOCK PROTEIN 70 LEVELS IN PRIMARY RAYNAUD'S PHENOMENON AND SYSTEMIC SCLEROSIS 3180
Nevzat Gozel, Ahmet Karatas, Meltem Yardim, Mesude Seda Kinaci, Ramazan Ulu, Fatih Demircan, Faruk Kilinc, Fethi Ahmet Ozdemir, Suleyman Aydin, Suleyman Serdar Koca

EFFICACY OF HOT WATER AND CHEMICAL SEED TREATMENTS ON BACTERIAL SPECK OF TOMATO IN TURKEY 3185
Sumer Horuz, Aysegul Ocal, Yesim Aysan

EFFECTIVENESS OF VARIOUS ATTRACTANTS FOR MEDITERRANEAN FRUIT FLY, CERATITIS CAPITATA (WIEDEMANN) (DIPTERA: TEPHRITIDAE) ON POMEGRANATE FRUITS IN TURKEY 3191
Nihat Demirel, Ahmet Emin Yildirim, Gamze Kilic

DETERMINATION OF THE EFFECT OF SOME ORGANIC AND ORGANO-MINERAL FERTILIZERS ON TOTAL PHENOLIC, FLAVONOID AND ANTHOCYANIN CONTENT OF BOGAZKERE (VITIS VINIFERA L.) GRAPES 3199
Gultekin Ozdemir

THE VARIABLE OF LEAF MICROMORPHOGICAL CHARACTERS ON GROWN IN DISTINCT CLIMATE CONDITIONS IN SOME LANDSCAPE PLANTS 3206
Mehmet Cetin, Hakan Sevik, Nurcan Yigit, Halil Baris Ozel, Burak Aricak, Tugrul Varol

TOWARD AN INTEGRATED SAFE AND SUSTAINABLE FOOD SYSTEM 3212
Sule Turhan, Erkan Rehber, Burcu Erdal, Hasan Vural

© by PSP Volume 27 – No. 5/2018 pages 2612-2628 Fresenius Environmental Bulletin

REVIEW

NATIONAL AMBIENT AIR QUALITY STANDARDS AND GUIDELINES: A GLOBAL REVIEW

Sabah A Abdul-Wahab[1,*], Amani Alnahdi[2], Ali Elkamel[2], Emmanuel Ikhile[2]

[1]Department of Mechanical and Industrial Engineering, College of Engineering, Sultan Qaboos University, Muscat, Sultanate of Oman
[2]Department of Chemical Engineering, University of Waterloo, Waterloo, Ontario, Canada

ABSTRACT

The air quality limits and levels play a key role for effective and useful air quality management. Ambient air quality standards perform as a recommendation for what air pollutions levels are generally safe for most human begins. In this paper, we identify national ambient air quality standards and guidelines for include particulate matter (PM_{10}, $PM_{2.5}$), sulphur dioxide (SO_2), nitrogen dioxide (NO_2), carbon monoxide (CO), lead (Pb), and ozone (O_3) in different countries and organizations. These national ambient air quality standards covered a verity of averaging times and taken from literature reviews and inquiring international official databases.

KEYWORDS:
Ambient air quality, Atmospheric pollutants, Guidelines, Standards

INTRODUCTION

Suspended fine particulate matter, sulphur dioxide (SO_2), nitrogen dioxide (NO_2), carbon monoxide (CO) and ozone (O_3) are considered to be the major pollutants by many countries and organizations [1-5]. Setting air quality limits and thresholds for these pollutants is very essential in protecting public health.

Ambient air quality standards are essential for air quality management. To protect people and the environment from harm, designing ambient air quality standards that control concentrations level of air pollutants is required. The assurance of the air quality standards comes through Laws and regulations governing air quality [4, 5]. In fact, it is a challenging task to precisely set a standard for an air pollutant, which requires inputs from two main sources including observations of the short-term and long-term impact of environmental pollutants and specific experiments under controlled conditions. Ambient air quality standards are sometimes different for the same air pollutant that is due to that different organizations have independently evaluated the evidence on the same air pollutant [4, 5].

In this paper, we investigate the ambient air quality standards through official publications, relevant responsible government documents, and literature surveys. However, several nations do not have air quality standards at all and sometimes we face difficulties to report the standard due to the language issues. As we mentioned earlier, there is significant difference in the ambient air quality standards implemented by different countries. This results in presenting only a total of fifty countries and organizations as shown in Table 1. It is worth noting that World Health Organization's (WHO) recommendations for air quality is well accepted for many countries [5, 6]. For instance, Singapore has standards that are generally adopted from the WHO guidelines [7].

AMBIENT AIR QUALITY STANDARDS

World. The World Health Organization (WHO). The *WHO Air quality guidelines* (AQGs) are proposed to offer global guidance for avoiding any health effects caused by air pollution [8]. The first guidelines issued by WHO was in 1979 which focused on sulphur dioxide and particulate matter [9]. A comprehensive ambient air quality guideline that include the carbon monoxide (CO), lead, nitrogen dioxide (NO_2), ozone (O_3), sulphur dioxide (SO_2) and Total Suspended Particulate (TSP) matter was published in 1987 by WHO European Office [10]. The first update to the WHO guidelines was published in 2000 [11-13] where TSP was replaced by $PM_{2.5}$ and PM_{10}, annual average for NO_2 was introduced, and O_3 range values were replaced by an 8-hour average. The most recent update to WHO guidelines was published in 2005 [13]. The most significant changes in WHO 2005 compared to WHO 2000 are as follows:

- For CO: not considering CO where there was a plan for including it in the WHO indoor air guidelines [14].

- For SO_2: the 24-hour guideline value was decreased by over six times (from 125 to 20 μg/m^3), but the annual value was stopped and a 10-minute value introduced.
- For $PM_{10,2.5}$: numerical guidelines were provided [15].

The 2005 *WHO Air quality guidelines* for SO_2 in the ambient atmosphere are 500 μg/m^3 as a 10-minute average concentration and 20 μg/m^3 as a 24-hour average concentration. The 8-hour averaging time for O_3 is 100 μg/m^3. The SO_2 standards include 1-hour and annual averaging times that set to be 200 μg/m^3 and 40 μg/m^3 respectively. The standard concentration for PM_{10} based on 24-hour average is 50 μg/m^3 and based on annual average is 20 μg/m^3. Finally, the standard values for $PM_{2.5}$ are 25 μg/m^3 and 10 μg/m^3 based on 24-hour and annual average times respectively.

Oceania. Australia. The National Environment Protection Council (NEPC) prepared Australia's first national ambient air quality standards as part of the National Environment Protection Measure for Ambient Air Quality (NEPM-AAQ) in 1998 [16, 17]. In 2003, the NEPM recommended standards for $PM_{2.5}$ [18]. The NEPM-AAQ standards were legally required to be met by the year 2008. The NEPC established a framework and method for setting new air quality standards in 2009 [19]. The NEPM-AAQ standard for CO in an 8-hour averaging time is 10 mg/m^3. NO_2 should not exceed 225 μg/m^3 per 1-hour and 56 μg/m^3 per year. The standards limits for SO_2 in 1-hr/24-hr/year are 524/210/52 μg/m^3. O_3 has a limit of 200 μg/m^3 for every one hour measurement. The PM_{10} is restricted to 50 μg/m^3 per day while $PM_{2.5}$ is limited to 25 μg/m^3 per day and 8 μg/m^3 per year. Finally, Pb should not exceed 0.5 μg/m^3 in one -year averaging time.

Europe Union. Many European Union (EU) Directives have been established for evaluating environmental air quality in EU member countries. This is done by the European Commission (EC) that is the executive body of the European Union responsible for proposing legislations for EU members [20, 21]. The first EU legislation on ambient air quality standard was issued in 1980, Directive 80/779/EEC, which was based on two main pollutants including SO_2 and TSP [22]. Two years later, EU established a new legislation, Directive 82/884/EEC, for limiting the value for lead in the air [23]. Nitrogen dioxide concentration limit came into force in 1985 through directive 85/203/EEC [24]. In 1992, EU issued a standard limit for ozone under legislation No. EC Directive 92/72/EEC [25]. The first comprehensive ambient air quality standard was introduced in 1996 namely, the European Air Quality Framework Directive (Directive 96/62/EC) [26]. Many European Union (EU) Directives in the period from 1996 to 2008 were established [27-30]. However, in 2008, the new Air Quality Directive (2008/50/EC) entered into force in which merged four existing Directives into a single Directive on air quality with no change to existing air quality objectives [31-32]. The New Air Quality Directive specifies a concentration limit of 10 mg/m^3 for CO in 8-hour averaging times. The 8-hours limit for O_3 is 120 μg/m^3. The NO_2 standard value for 1-hour is 200 μg/m^3 and for annual averaging times is 40 μg/m^3. The hourly and daily concentration level for SO_2 should not exceed 350 μg/m^3 and 80 μg/m^3 respectively. For PM_{10}, the standard values are 50 μg/m^3 based on 24-hour and 40 μg/m^3 based on annual average times. $PM_{2.5}$ has a limit of 25 μg/m^3 in one year averaging time. Finally, the annual averaging times for Pb is 0.5 μg/m^3.

Asia. Bangladesh. The first set of national ambient air quality standards was issued in 1997 by the Department of Environment (DOE) under Environment Conservation Rules [33]. In July 2005 World Bank-Funded Air Quality Management Project3 (AQMP) proposed some modifications to the established air quality standards. In South Asia, Bangladesh considered to be one of the first countries to establish $PM_{2.5}$ in its air quality standards [34]. Bangladesh specifies a CO 8-hour standard of 10 mg/m^3 and 1-hour standard of 40 mg/m^3. The averaging times for SO_2 based on 24-hour and annual measurement times are with standard values of 365 μg/m^3 and 80 μg/m^3 respectively. Ambient concentrations of O_3 range from 157 μg/m^3 based on 8-hour averages to 235 μg/m^3 based on 1-hour averages. The annual averaging times for NO_2 and Pb are 100 μg/m^3 and 0.5 μg/m^3 respectively. The standard concentration for PM_{10} based on 24-hour average is 150 μg/m^3 and based on annual average is 50 μg/m^3. Finally, the 24-hours and annual averages for $PM_{2.5}$ are set to be 65 μg/m^3 and 15 μg/m^3.

Bhutan. Bhutan has been able to establish its own set of ambient air quality standards in 1999 through the National Environment Commission's (NEC) [35, 36]. The shortcoming of this standard is that it is adopted straight out of WHO standards without taking into consideration the realistic relevance to Bhutan. Furthermore, this standard is not implemented due to the lack of appropriate monitoring equipment and human resources [37]. In 2003, however, NEC had established a Bhutan Air Quality Network under the project funded by Asian Development Bank (ADB). The recommended air quality standard for Bhutan is divided into three areas including, industrial, residential, and sensitive areas. The standard specifies the CO limit values for the industrial areas as 10 mg/m^3 per 1-hour and 5 mg/m^3 per 8-hours, for residential areas as 4 mg/m^3 per 1-hour and 2 mg/m^3 per 8-hours, for

sensitive areas as 2 mg/m^3 per 1-hour and 1 mg/m^3 per 8-hours. Bhutan standards share similar values for both NO_2 and SO_2 for all industrial, residential, and sensitive areas where the 24-hours average is 120 μg/m^3 and the annual average is 80 μg/m^3. The daily maximum allowed values for PM_{10} is 150 μg/m^3 for industrial areas, 100 μg/m^3 for residential areas, and 75 μg/m^3 for sensitive areas where the annual maximum allowed values is 120 μg/m^3 for industrial areas, 60 μg/m^3 for residential areas, and 50 μg/m^3 for sensitive areas. Finally, the Pb concentration levels for the industrial areas are 1.5 μg/m^3 per daily and 1 μg/m^3 annually, for residential areas are 1 μg/m^3 daily and 0.75 μg/m^3 annually, for sensitive areas are 0.75 μg/m^3 daily and 0.5 μg/m^3 annually.

Cambodia. In Cambodia, several ministries contribute during the process of issuing the air quality standards including The Ministry of Environment (MoE), Ministry of Health (MoH) and Ministry of Industry (MoI), and Mine and Energy (MIME) [38,39]. The first set of ambient air quality standards in Cambodia was established in July 2000. The Cambodian standard for CO in 8-hour averaging time is 20 mg /m^3 and in 1-hour averaging time is 40 mg/m^3. For SO_2, three averaging times specified for the Cambodian standards including 1-hour, 24-hour and annual; and the standard values are 500 μg/m^3, 300 μg/m^3 and 100 μg/m^3 respectively. The 1-hour averaging time for O_3 is 200 μg/m^3. The standard concentration for NO_2 based on 1-hour average is 300 μg/m^3 and based on 24-hours average is 100 μg/m^3. Finally, the 24-hours averaging times for Pb is set to be 5 μg/m^3. The Cambodian's standard does not consider PM_{10} or $PM_{2.5}$.

China. The air quality standards of China were first established 1996 and revised in 2000 by the State Environmental Protection Administration (SEPA) of China [40-41]. The China's air quality standards are divided into three grades based on the area [43,44]. Grade 1 is for protected areas, such as natural conservation areas and historical sites, Grade 2 is for residential commercial areas, and Grade 3 is for industrial areas. The concentration levels for CO based on 24-hours averaging times are 4 mg/m^3 for Grades 1 and 2 and 6 mg/m^3 for Grade 3. The NO_2 maximum limits based on 1-hr/24-hr/annual averaging times for Grade 1 are 120/80/40 μg/m^3 and for Grades 2 and 3 are 240/120/80 μg/m^3. Grade 1 area has limited values for SO_2 of 150 μg/m^3 based on 1-hour average, 50 μg/m^3 based on 24-hour average, and 20 μg/m^3 based on annual average. Grade 2 standards are not restricted in SO_2 as in Grade 1 where the limited values for 1-hour, 24-hours, and annual averages are 500 μg/m^3, 150 μg/m^3, and 60 μg/m^3 respectively. Grade 3 standards for SO_2 are 700/250/100 μg/m^3 based on 1-hr/24-hr/annual. The 1-hours average limits for O_3 are 160 μg/m^3 for Grade 1 and 200 μg/m^3 for Grades 2 and 3. Finally, PM_{10} standards for Grade 1 are 50 μg/m^3 for 24-hr and 40 μg/m^3 annually, for Grade 2 are 150 μg/m^3 for 24-hr and 100 μg/m^3 annually, and for Grade 3 are 250 μg/m^3 for 24-hr and 150 μg/m^3 annually.

Hong Kong. The ambient air quality standard in Hong Kong (Special Administrative Region, SAR) was established in 1987 under the Air Pollution Control Ordinance (APCO) [45-47]. The Environmental Protection Department (EPD) [48] under the Environment Bureau of the Hong Kong SAR Government is responsible for setting the air quality standards. Hong Kong set a standard for CO in 8-hour averaging times as 10 mg/m^3 and 1-hour as 30 mg/m^3. The SO_2 standards include 1-hour, 24-hour and annual averaging times, which set to be 800 μg/m^3, 350 μg/m^3 and 50 μg/m^3 respectively. The 1-hour averaging time for O_3 is 240 μg/m^3. Again, three averaging times for NO_2 including 1-hour, 24-hour and annual and the standard values are 300 μg/m^3, 150 μg/m^3 and 80 μg/m^3 respectively. The standard concentration for PM_{10} based on 24-hour average is 180 μg/m^3 and based on annual average is 55 μg/m^3. Finally, the 3-months averaging times for Pb is set to be 1.5 μg/m^3. In 2007, the Government proposed new Air Quality Objectives based on the acknowledgement of the World Health Organization (WHO) which add SO_2 (350 μg/m^3 for 10-minute), NO_2 (200 μg/m^3 for 1-hour and 40 μg/m^3 for annual); and Pb (0.5 μg/m^3 for annual). Also, adopting the concentration targets set out under WHO Interim Target (IT2) for PM_{10} (100 μg/m^3 for 24-hour and 50 μg/m^3 for annual); and finally adopting the concentration targets set out under WHO IT1 for SO_2 (125 μg/m^3 for 24-hour) and update $PM_{2.5}$ (75 μg/m^3 for 24-hour and 35 μg/m^3 for annual), and the IT for O_3 (160 μg/m^3 for 8-hour). In January 2012, the Hong Kong Government update of the proposed new Air Quality Objectives (AQOs) and expected that the update will take effect in 2014 [48].

India. The first ambient air quality standards in India was issued in 1982 [49]. The Central Pollution Control Board (CPCB) reported the national ambient air quality standards in 1994 which uses different set of standards according to the area prescribed (i.e., industrial, residential, and sensitive areas) [49]. Again in 2009, Ministry of Environment and Forests (MoEF) updated the air quality standards where it placed uniform standards for residential and industrial areas [50]. The concentration levels for all pollutants are similar for industrial, residential, and sensitive areas except for SO_2 and NO_2 as annual averaging times that set to be 50 μg/m^3 for residential and industrial areas and 20 μg/m^3 for sensitive areas for SO_2 as well as 40

μg/m^3 for residential and industrial areas and 30 μg/m^3 for sensitive areas for NO_2. The standard for CO in 8-hour averaging times is 20 mg/m^3 and in 1-hour as 40 mg/m^3. Both SO_2 and NO_2 standards for 24-hour averaging times is set to be 80 μg/m^3. The allowed concentration levels for O_3 range from 100 μg/m^3 based on 8-hour averages to 180 μg/m^3 based on 1-hour average. The standard concentration for PM_{10} based on 24-hour average is 100 μg/m^3 and based on annual average is 60 μg/m^3. For $PM_{2.5}$, the standard values are 60 μg/m^3 and 40 μg/m^3 based on 24-hour and annual average times respectively. Finally, the 24-hours and annual averages for Pb are set to be 1 μg/m^3 and 0.5 μg/m^3 respectively.

Indonesia. The Government Regulation or Peraturan Pemerintah (PP) of the Republic of Indonesia first established the national ambient air quality standard in Indonesia in 1999. The Ministry of Environment (MoE) allows provincial governments to set ambient air quality standards that are stricter than or at least equivalent to the national standards [51,52]. The national standard for CO in 8-hour averaging times is 10 mg/m^3 and in 1-hour as 30 mg/m^3. The SO_2 standards include 1-hour, 24-hour and annual averaging times that set to be 900 μg/m^3, 365 μg/m^3 and 60 μg/m^3 respectively. Three averaging times for NO_2 including 1-hour, 24-hour and annual and the standard values are 400 μg/m^3, 150 μg/m^3 and 100 μg/m^3 respectively. The concentration levels for O_3 are 50 μg/m^3 for 24-hour averaging times and 235 μg/m^3 for 1-hour average. The standard concentration for PM_{10} based on 24-hour average is 150 μg/m^3. Finally, the annual averaging times for Pb is 1 μg/m^3.

Iran. In Iran, the Department of Environment (DOE) is responsible for prevention of Air Pollution since 1973 [53]. The government of Iran is considering the air pollution seriously after realizing that Tehran is one of the worst cities in the world in terms of air pollution, according to data collected by the Air Quality Control Company (AQCC) and the DOE. The national air quality standard for Iran specifies the limit for CO as of 10 mg/m^3 every 8-hour averaging time. The annual NO_2 standard is 100 μg/m^3 and the daily SO_2 standard is 365 μg/m^3. Finally, the daily PM_{10} limit is 260 μg/m^3.

Japan. Japanese Ministry of the Environment (MoE) enacted the Air Pollution Control Act in 1968 and established the first ambient air quality standard for SO_2 [54, 55]. The standard values for SO_2 in one hour averaging time is 282 μg/m^3 (0.1 ppm) and in 24 hours averaging time is 110 μg/m^3 (0.04 ppm). In 1978 the standard for NO_2 was added where the limited daily value is set to be 120 μg/m^3 (0.06 ppm). The maximum allowed values for CO in 1-hour and 8-hours averaging times are 12.3 mg/m^3 (10 ppm) and 24.7 mg/m^3 (20 ppm), respectively. For PM_{10}, the daily average values shall not exceed 100 μg/m^3, and annual values shall not exceed 200 μg/m^3. The environmental quality standard for $PM_{2.5}$ was introduced in 2009 where the 24 hours standard is set to be 35 μg/m^3 and the annual standard is set to be 15 μg/m^3.

Korea. The Environmental Preservation Act in Korea issued Air Quality Preservation Act in 1990, which now referred to as the 1990 Clean Air Conservation Act [56]. The first air quality standards for Korea was established in 1978 and then revised in 1983, 1991, 1993, 2001, 2007 and 2009 [57]. The Ministry of Environment (MoE) is responsible drafting, reviewing and approving the air quality standards. The CO standards for averaging times 1-hour and 8-hours are 28, 625 μg/m^3 and 10,305 μg/m^3 respectively. The SO_2 standard value for 1-hour is 392 μg/m^3, for 24-hour is 131 μg/m^3, and for annual averaging times is 52 μg/m^3. For NO_2, the allowed value for 1-hour averaging time is 188 μg/m^3, for 24-hour is 113 μg/m^3 and for annual is 56 μg/m^3. O_3 are limited to 196 μg/m^3 for 1-hour averaging time and 118 μg/m^3 for 8-hours average. For PM_{10}, the standard values are 100 μg/m^3 based on 24-hour and 60 μg/m^3 based on annual average times. Finally, the annual averaging times for Pb is 0.5 μg/m^3.

Kuwait. Kuwait Environment Public Authority (KEPA) issued new/revised air quality regulations on March 2012 [58,59]. KEPA is responsible for mandating strict controls to meet the ambient air quality standards. Ambient air quality within Kuwait should be under control by applying Kuwait Ambient Air Quality Standards. The CO standards are 30 mg/m^3 for 1-hour average and 10 mg/m^3 for 8-hours average. For NO_2, the daily allowed value is 200 μg/m^3 while the annual limit is 40 μg/m^3. The daily average limit for SO_2 is 20 μg/m^3 and its hourly limit is 75 μg/m^3. The O_3 has a limit of 100 μg/m^3 per 8 hours. The maximum daily limits for PM_{10} and $PM_{2.5}$ are 150 μg/m^3 and 35 μg/m^3 respectively, while the annual limit for them are 90 μg/m^3 and 15 μg/m^3 respectively. Finally, Pb has an annual limit of 0.5 μg/m^3.

Malaysia. The Department of Environment in Malaysia formulated a set of air quality guidelines called the Recommended Malaysian Air Quality Guidelines (RMG) in 1989 [60]. DoE then established the Malaysian Air Quality Index (MAQI) based on RMG, in 1993 [61]. The Malaysian's standards for CO are 35 mg/m^3 based on 1-hour average and 10 mg/m^3 based on 8-hours average. The NO_2 guidelines are specified as 320 μg/m^3 for 1-hour average and as 90 μg/m^3 annually. The 1-hour and 24-hours averages for SO_2 are 350 μg/m^3 and 105 μg/m^3 respectively. For O_3, the 1-hour limit

is 200 μg/m^3 and the 8-hours limit is 120 μg/m^3. The daily average limit for PM_{10} is 150 μg/m^3 and the annual average limit is 50 μg/m^3. Finally, the Pb concentration level based on the Malaysia standard is restricted to 1.5 μg/m^3 for 3 months average times.

Mongolian. The Mongolian national ambient air quality standards were established in 1998 through Mongolian Agency of Standardization and Metrology [62-64]. The Mongolian national standard for 24-hour NO_2 concentration is 40 μg/m^3. For SO_2, the standard limit is 30 μg/m^3 on a daily average. The 1-hours averaging time for O_3 should not exceed 120 μg/m^3. Finally, the daily average for Pb is 1 μg/m^3.

Nepal. In 2003, His Majesty's Government (HMG) established Nepal's national ambient air quality standards [64]. Ministry of Science and Technology (MoST) is in charge of the national ambient air quality standards. Nepal has ambient air quality standards for PM_{10} as 120 μg/m^3 for 24-hour. For CO, the standard is 10 mg/m^3 for 8-hour and 10 mg/m^3 for 15-minutes. The 24-hours and annual averaging times for NO_2 are set to be 80 μg/m^3 and 40 μg/m^3 respectively. The SO_2 concentration levels are limited to 70 μg/m^3 for 24-hour and 50 μg/m^3 for annual averaging times. Lastly, Pb has not to exceed 0.5 μg/m^3 annually.

Oman. Ministry of Environment and Climate Affairs (MECA) is the responsible Ministry for air quality in Sultanate of Oman. Since there are no national Omani standards for ambient air quality, MECA recommends applying the of USEPA's National Ambient Air Quality (NAAQ) [66]. Currently, MECA in the process of developing a preliminary developing Omani Ambient Air Quality (OAAQ) Standard, which is considering a daily averaging time for NO_2, SO_2, and PM_{10} as 112, 125, and 125 μg/m^3 respectively. The 8-hour averaging time for CO is limited to 6 mg/m^3 and for O_3 is limited to 120 μg/m^3. This standard also indicates the limit for hydrocarbon non-methane (HCNM) for 3 hours averaging time as of 160 μg/m^3.

Pakistan. Although, Pakistan lacks standards for ambient air quality [67], researchers start to review other standards including, the World Health Organization air quality guidelines, standards established by the Eastern Mediterranean and Southeast Asian countries, in order to propose the national ambient air quality standard for Pakistan [68, 69]. The draft National Air Quality Standards for Pakistan supposed to be effective 2009 and 2012 [69]. Both proposals share the same limit values for all pollutants except PM, O_3, and Pb. The proposed standards limit values for CO are 10 mg/m^3 for 1-hour average and 5 mg/m^3 for 8-hours average. The daily and annual average limits for SO_2 are 80 μg/m^3 and 40 μg/m^3. NO_2 daily average level is 120 μg/m^3 while the annual average limit is 20 μg/m^3. The 1-hour averaging time for O_3 is 180 μg/m^3 as of 2009 and 130 μg/m^3 as of 2012. The PM_{10} standards are 250 μg/m^3 for 24-hr and 200 μg/m^3 annually as of 2009 and 150 μg/m^3 for 24-hr and 120μg/m^3 annually as of 2012. The $PM_{2.5}$ maximum limits based on 1-hr/24-hr/annual averaging times for 2009 are 25/40/25 μg/m^3 and for 2012 are 15/35/15 μg/m^3. Finally, the concentration levels for Pb are 2 μg/m^3 for 24-hr and 1.5 μg/m^3 annually as of 2009 standards and 1.5 μg/m^3 for 24-hr and 1 μg/m^3 annually as of 2012 standard.

Philippine. The Presidential Decree (PD) in Philippine issued the first air quality standards in 1978 [70]. Then, the Department of Natural Resources (DENR) Administrative Order (DAO) updated the standards in 1992 as known as the national air quality guidelines values (NAAQGV) [71]. The NAAQGV for CO is 10 mg/m^3 as 8-hours averaging times and 35 μg/m^3 as 8-hours. For SO_2, NAAQGV is set to be 180 μg/m^3 as 24-hr averaging times and 80 μg/m^3 annually. The NO_2 concentration level is limited to 150 μg/m^3 for 24-hour. The maximum levels for O_3 range between 60 μg/m^3 for 8-hour and 140 μg/m^3 for 1-hour average times. PM_{10} has NAAQGV as 140 μg/m^3 for 24-hr and 140 μg/m^3 annually. The 3-months and annual averages for Pb are 1.5 μg/m^3 and 1 μg/m^3 respectively.

Qatar. The State of Qatar has paid attentions to the air quality through regulations and implementation of standards by Supreme Council for Environment and Natural Reserves (SCENR) [72]. In 2002, the Qatar Government published the executive regulations (Law No. 30/2002) related environmental protection and standards related to ambient air quality became legally binding [73]. These standards defined the maximum authorized values for CO as 40 mg/m^3 based on 1-hour averaging period. The maximum permissible level for NO_2 in 1-hour is 400 μg/m^3, in 24-hours is 150 μg/m^3 and in 1-year is 100 μg/m^3. For SO_2, the allowed value in one day is 365 μg/m^3 and in one year is 80 μg/m^3. The daily and annual averaging times for PM_{10} are 150 μg/m^3 and 50 μg/m^3 respectively. Finally, the 3-months averages for Pb is 1.5 μg/m^3.

Saudi Arabia. In Saudi Arabia, Presidency of Meteorology and Environment (PME) is responsible for the protection of the environment and the development of environmental protection standards [74]. PME recently issued national ambient air quality standards that were effectuated in 2012. The standard recommends limit values for CO are 40 mg/m^3 for 1-hour average and 10 mg/m^3 for 8-hours average. For NO_2, the 1-hour average is limited to

660 μg/m^3 and 100 μg/m^3 annually. The concentration level for SO_2 in 1-hour is 730 μg/m^3, in 8-hours is 365 μg/m^3, and in 1-year is 80 μg/m^3. O_3 has limited values for 1-hour and 8-hours as 150 μg/m^3 and 150 μg/m^3 respectively. The maximum allowed values for PM_{10} and $PM_{2.5}$ per day are 340 μg/m^3 and 35 μg/m^3, and per year are 80 μg/m^3 and 15 μg/m^3. Lastly, Pd is restricted to 0.5 μg/m^3 annually.

Singapore. The National Environment Agency (NEA) is a legal board formed in July 2002 which responsible for implementing environmental policies [75]. The National Energy Efficiency Committee (NEEC) is actively engaged in Singapore's clean air. The Singapore legislated standards for air pollutants are adopted for US EPA Primary air quality standards and WHO air quality guidelines. The one-hour concentration level of CO is limited to 40 mg/m^3 while the 8-hour level is 10 mg/m^3. The hourly limit for NO_2 is 188 μg/m^3 and the annual limit is 100 μg/m^3. For SO_2, the 1/24/annual averaging times are 196/365/80 μg/m^3. The O_3 is limited to 235 μg/m^3 per hour and 147 μg/m^3 per 8-hour averaging times. The daily and annual averaging times for $PM_{2.5}$ are 35 μg/m^3 and 15 μg/m^3 respectively, while the PM10 daily limit is 150 μg/m^3.

Sri Lanka. In Sri Lanka, the first set of national ambient air quality standards were established in 1994 through Gazette Extraordinary and the Central Environmental Authority (CEA) that is responsible for implementing the standard [76]. The first revision of the air quality standard was in 2008 by Ministry of Environment and Natural Resources (ME&NR). Sri Lanka has national ambient air quality standards for CO as 1-hour with the value of 30 mg/m^3 and as 8-hours with value of 10 mg/m^3. The NO_2 standards for 1-hour are set to be 250 μg/m^3 and 100 μg/m^3 for 8-hour. The 1-hour standard for SO_2 is 200 μg/m^3 and the 24-hours averaging times standard is 80 μg/m^3. The O_3 has a limit of 200 μg/m^3 based on 1-hour averaging time. The 24-hours standard for PM_{10} is 100 μg/m^3 and for $PM_{2.5}$ is 50 μg/m^3 where the annually averaging times for PM_{10} is 50 μg/m^3 and for $PM_{2.5}$ is 25 μg/m^3.

Thailand. Thailand established the first national ambient air quality standards (NAAQS) in 1981 where Ministry of Natural Resources and Environment (MNRE) and the Pollution Control Department (PCD) contributed to the drafting, reviewing and proposing of NAAQS. Including the promulgation of the 8-hours average standard for O_3 and the proposal of the PM_{10} were proposed during revision of the 1981 standard in 2007 [57,77,78]. The current NAAQS of Thailand indicates that the NO_2 level should not exceeded 319.16 μg/m^3 in 1-hour average. The 1-hour average for CO is 34.350 μg/m^3 and the 8-hours average is 10305 μg/m^3. For SO_2, three averages are considered where the 1-hour average is 784.8 μg/m^3, the 24-hours average is 313.92 μg/m^3 and the annual average is 104.64 μg/m^3. The O_3 concentration level at 1-hour average is 196.2 μg/m^3 and the 8-hours average is 137.34 μg/m^3. PM_{10} should not exceed 120 μg/m^3 in 24-hours averaging time and 50 μg/m^3 annually. Finally, Pb standard is 0.5 μg/m^3 as 1-month averaging time.

Vietnam. Tieu Chuan VietNam (TCVN) established the air quality standard in Vietnam in 1995 [57]. Provincial Departments of Science, Technology and Environment (DOSTE) is responsible for developing and issuing standards relating to environmental issues including the air quality standard. Some revisions to national ambient air quality standards were taken in 2005 and 2009. The VietNam's standard specifies that the CO concentration level in 1-hour is set to be 30 mg/m^3, in 8-hours is 10 mg/m^3 and in 24-hours average is 5 mg/m^3. The NO_2 and SO_2 concentration levels for 1-hour, 8-hours and annual averaging times are 200 μg/m^3, 100 μg/m^3, 40 μg/m^3 and 350 μg/m^3, 125 μg/m^3, 50 μg/m^3 respectively. The concentration levels for O_3 are 180 μg/m^3 for 1-hour, 120 μg/m^3 for 24-hour averaging times and 80 μg/m^3 for 1-hour average. PM_{10} has a concentration level as 150 μg/m^3 and 50 μg/m^3 for 24-hours and annual averages. Finally, Pb has an annual average of 0.5 μg/m^3.

Afghanistan. Afghanistan has not established any national ambient air quality standards. The Government is still in the process of adoption of standards [57].

Bahrain. Although, the Bahrain Government set up air monitoring equipment in each of Bahrain's five governorates, however; no national standards are issued but these data are compared ambient air quality standards [73].

Lao PDR. The Lao PDR government currently does not consider any air pollutants standards for any of the air pollutants. One of the reasons for why air pollutants has been compiled to date is that the government reported to United Nation UN is the lack of resources [57].

Africa. Egypt. The ambient air quality standard was first issued in 1994 under the Executive Regulations of the Environmental Law (no 4/1994). The Environmental Information and Monitoring Program (EIMP) under the Environmental Quality Sector-Egyptian Environmental Affairs Agency [79] issued this standard. The 1994 standards specify a limit for CO concentration level as of 1-hour with the value of 30 mg/m^3 and as 8-hours with

value of 10 mg/m^3. The maximum annual/day/hour allowable limits for SO_2 are 60/150/350 μg/m^3. The daily and hourly limits for NO_2 are 150 μg/m^3 and 400 μg/m^3 respectively. The maximum allowable limits for O_3 is 120 μg/m^3 per hour and 200 μg/m^3 per 8-hour. The daily limit for PM_{10} is set to be 70 μg/m^3. Finally, the Pb concentration level is limited to 1 μg/m^3 per year.

Tunis. The Ministry of Environment and Sustainable Development in Tunis has established standards regarding the main pollutants [80]. Due to the lack of any official documents, the establishing year for this standard could not be presented. The standard restricted the concentration levels for CO in 1 hour to be 40 mg/m^3 and in 8 hours to be 10 mg/m^3. NO_2 concentration level should not exceed 660 μg/m^3 based on one hour averaging time and 200 μg/m^3 annually. The daily and annual limits for SO_2 are 80 μg/m^3 and 365 μg/m^3 respectively. O_3 is restricted to 235 μg/m^3 every one hour. For PM_{10}, the daily average values should not exceed 260 μg/m^3, and annual values should not exceed 80 μg/m^3. The Pb daily limit is 2 μg/m^3.

Ghana. Regulations for issuing national environmental standards for ambient air quality in Ghana was first introduced in 2000, under The Environmental Protection Agency Act, (Act 490) [81]. The Ghana's standards for ambient air quality are divided into two main limits based on the area protected including, Industrial and Residential areas. Both the Industrial and Residential standards for CO are 30 mg/m^3 in 1-hour and 10 mg/m^3 in 8-hour averaging times. The Industrial standard for NO_2 is 400 μg/m^3 based on one year average. The SO_2 maximum concentration levels based on 1-hr/24-hr/annual averaging times for Industrial standard are 900/150/80 μg/m^3 and for Residential standards are 700/100/50 μg/m^3. PM_{10} limit for both Industrial and Residential standards is 70 μg/m^3 based on 24-hour averaging times. Finally, the annual limit for Pb in both standards is 2.5 μg/m^3.

Tanzania. The National Environmental Standards Committee of Tanzania Bureau of Standards proposed the first national ambient air quality standards in 2007 [82, 83]. In this standard, CO has a concentration limit of 30 mg/m^3 in 1-hour period and 10 mg/m^3 in 8-hours averaging times. The NO_2 concentration level should not exceed 120 μg/m^3 within 8-hour averaging times and should not exceed 150 μg/m^3 on a daily average. The maximum levels in daily and yearly averaging times for SO_2 are 125 μg/m^3 and 50 μg/m^3 respectively. Finally, the Pb concentration level is 1.5 μg/m^3 in one day period.

Senegal. The Senegal Government issued their first national ambient air quality standards in 2001 under the Senegalese Norm NS 05-062, which specifies limit values for ambient air pollution concentration [84]. The Senegal's standard limits the CO concentration level to be 30 mg/m^3 in 24-hours average. The O_3 concentration level at 8-hour average is 120 μg/m^3. The maximum allowed level for NO_2 in 1-hour is 200 μg/m^3 and in 1-year is 40 μg/m^3. For SO_2, the allowed value in one day is 125 μg/m^3 and in one year is 50 μg/m^3. The daily average limit for PM_{10} is 260 μg/m^3 and its yearly limit is 25 μg/m^3. The Pb annual limit is 2 μg/m^3.

South African. In 2004, The National Framework for Air Quality Management in South Africa established the air quality objectives under Air Quality Act (Act No. 39 of 2004) [85]. The standard recommends limit values for NO_2 are 200 μg/m^3 for 1-hour average and 40 mg/m^3 for annual average. The concentration level for O_3 is 120 μg/m^3 for 8-hour period. For SO_2, three averages are measured where the 1-hour average is 350 μg/m^3, the 24-hours average is 125 μg/m^3 and the annual average is 50 μg/m^3. The daily and annual averaging times for $PM_{2.5}$ are 65 μg/m^3 and 25 μg/m^3 respectively, while daily and annual limits the PM10 are 120 μg/m^3 and 50 μg/m^3 respectively.

North America. Canada. The Canadian Government issued two official standards including National Ambient Air Quality Objectives (NAAQOs) and Canada-Wide Standards (CWS). In mid 1970s, the NAAQOs were issued under the Canada's foremost federal environmental law, the Canadian Environmental Protection Act (CEPA). The NAAQOs is consider to be a federal standard, however provincial governments have their own air quality standards that often differ from the federal objectives [86]. The NAAQO specifies maximum desirable, acceptable, and tolerable concentration levels for SO_2, NO_2, CO, O_3, and PM [87,88]. The NAAQOs maximum acceptable levels are considered here in this research. The 1-hour and 8-hour standards for CO are 35 mg/m^3 (13 ppm) and 15 mg/m^3 (5 ppm). The 1-hour averaging time for NO_2 is 400 μg/m^3 (213 ppb), the daily limit is 200 μg/m^3 (106 ppb), and the annual limit is 100 μg/m^3 (53 ppb). For SO_2, three averaging times specified for the NAAQO standards including 1-hour, 24-hour and annual and the standard values are 875 μg/m^3 (334 ppb), 300 μg/m^3 (115 ppb) and 60 μg/m^3 (23 ppb) respectively. Finally, the maximum acceptable levels for O_3 are set to be 160 μg/m^3 (82 ppb) for 1-hour averaging times, and 50 μg/m^3(25 ppb) for 8-hour averaging times. The Canada-wide Standards was first issued in 2000 by the Canadian Council of Ministers of the Environment (CCME), for all provinces except Québec, for $PM_{2.5}$ and O_3 [89]. The CWS standard for $PM_{2.5}$ is 30 μg/m^3 based on 24-hour averaging time and to be met by 2010. The CWS for O_3 of 128 μg/m^3 (65 ppb) based on 8-

hours averaging time and to be achieved by 2010 as well. In 2010, a new Canadian Ambient Air Quality Standards (CAAQS) was proposed as part of comprehensive air management system for Canada [90, 91]. The CAAQS is proposed to replace the existing Canada-wide Standards by strengthening standards for $PM_{2.5}$ and O_3, and ambient goals to be achieved by 2015 and 2020 (slight difference between 2015 and 2020 standards). The CAAQS limit for $PM_{2.5}$ is 28 μg/m^3 as a 24-hours averaging time and 10 μg/m^3 per year, and to be achieved by 2015. The CAAQS for O_3 based on 8-hours averaging time is set to be 124 μg/m^3 (63 ppb) and to be achieved by 2015.

Mexico. In Mexico, air quality guidelines and regulations has been established the federal level since 70's by Mexico's Environmental and Natural Resources Ministry, Secretaría de Medio Ambiente y Recursos Naturales (SEMARNAT) [92]. The first official Mexican standards that control maximum concentrations of environmental pollutants were issued 1993 [93]. Since then, there were no any changes to the first official standards [94]. The Mexican's national standard for CO over 8-hours average is 57 mg/m^3 and over 1-hour average is 13 mg/m^3. The NO_2 concentration level should not exceed 100 μg/m^3 in one year and 395 μg/m^3 in one hour averaging times. The maximum allowed level for SO_2 in 1-hour is 524 μg/m^3, in 8-hours is 288 μg/m^3, and in 1-year is 66 μg/m^3. The O_3 has a limit of 157 μg/m^3 in one hours and 216 μg/m^3 in 1 hours averaging times. The 24-hours standards for PM_{10} and $PM_{2.5}$ are 120 μg/m^3 and 65 μg/m^3 respectively, where their annually averaging times are 50 μg/m^3 and 15 μg/m^3. The Pb standard is 0.5 μg/m^3 as 3-month averaging time.

United States. United States Environmental Protection Agency (EPA) is the Federal Department that is responsible for ambient air quality standard. The National Ambient Air Quality Standards (NAAQS) was the first air quality standard that was issued in 1970 under the federal law of Clean Air Act (CAA) [95]. Two types of NAAQS are set by EPA including, primary standards (for public health) and secondary standards (for public welfare). Several modifications were applied to NAAQS such as the addition of Pb in1977 and removal of hydrocarbons in 1983. Other alterations to the NAAQS include the replacement of total suspended particulates (TSP) by PM_{10} in 1987 and the addition of $PM_{2.5}$ in 1997. In terms of changes in the maximum allowable level of pollutants since 1970 NAAQS standards to the current one, we refer reader to National ambient Air Quality Standards [96] for further details. However, we will mention the current NAAQS as of 2013 as well as the difference between the primary and secondary standards. The NAAQS primary standard for CO in 8-hour averaging time is 10 mg/m^3 and in 1-hour averaging time is 40 mg/m^3. For NO_2, the primary standard in 1-hour average is limited to 190 μg/m^3 and the primary and secondary standard is 100 μg/m^3 annually. The 1-hour averaging time for SO_2 in the primary standard is 190 μg/m^3 and the 3-hour averaging time for that secondary standard is 1300 μg/m^3. The NAAQS for PM_{10} and $PM_{2.5}$ are identical for primary and secondary in the daily averaging time, which set to be as 35 μg/m^3 and 15 μg/m^3 respectively. The annual averaging time for $PM_{2.5}$ in the primary standard is 12 μg/m^3 and in the secondary standard is 15 μg/m^3. The O_3 concentration level at 8-hour average is 150 μg/m^3 for both primary and secondary standards. Finally, the Pb concentration level for both primary and secondary standards is 0.15 μg/m^3 in 3-months.

Latin America. Argentina. Argentina has several environmental regulations similar to other countries. Different standards are exist for each level of government including standards for the city of Buenos Aires (ordenanza 39.025 of 1983), standards for the Province of Buenos Aires (law 11.459 of 1993), and standards for all the Nation (law 20.284 of 1973) [94, 97]. In this paper, we will mention the National Air Quality Standards in Argentina. The national standards limit the CO to be 11 mg/m^3 in 8-hour averaging times and 57 mg/m^3 in 1-hour averaging time. The standard concentration for NO_2 based on 1-hour average is 847 μg/m^3 and based on 24-hours average is 282 μg/m^3. The maximum level can be reached in SO_2 based on 1-hour averaging times is 1620 μg/m^3, based on 8-hour is 780 μg/m^3, and based on 3-months averaging times is 80 μg/m^3. Finally, the concentration level of 200 μg/m^3 is the maximum allowed level for O_3 in 1-hour averaging times.

Bolivia. The year of 2008 in Bolivia approved new rules on air quality by the Bolivian Institute Standardization and Quality (IBNORCA) [94, 98, 99]. Bolivian standards specify a CO 8-hour standard of 10 mg/m^3 and 1-hour standard of 40 mg/m^3. The one-hour O_3 concentration level should not exceed 236 μg/m^3. For NO_2, the standard for 1-hour period is 400 μg/m^3 and the standard for 8-hour period is 150 μg/m^3. The maximum levels for daily and yearly averaging times in SO_2 are 365 μg/m^3 and 80 μg/m^3 respectively. Finally, PM_{10} should not be above 150 μg/m^3 in 24-hours and 50 μg/m^3 in one year averaging times.

Brazil. The standards for air quality were approved in 1990 by the National Environment Council (CONAMA) which is the Brazilian agency in charged with ambient air quality policies [100]. Similar to US NAAQS, CONAMA air quality standard is divided into primary standards which human health would be impacted, and secondary

standards which related to area other that than in the primary. The primary standard is the most applicable for Brazil, yet states can designate air quality criteria within their territory. Henceforth, we will consider the primary standards for the pollutants of our interest in this research. The CONAMA standard for CO in 8-hour averaging times is 10 mg/m^3 and in 1-hour as 40 mg/m^3. The 24-hour and annual averaging times for SO_2 are 365 μg/m^3 and 80 μg/m^3 respectively. For NO_2, the allowed value for 1-hour averaging time is 320 μg/m^3 and for the annual averaging time is 100 μg/m^3. Finally, the concentration levels for O_3 are 160 μg/m^3 for 1-hour averaging times.

Chile. In 1996, The National Commission for the Environment, "la Comisión Nacional del Medio Ambiente" (CONAMA) as part of Law no 19.300 has participated into the process of issuing a number of environmental regulations including air quality standards and emission [94, 101]. Chile's national ambient air quality standards as reported in Joanne and Sanchez [94] and Baldasano et al. [102] set the maximum level of CO in 8-hour averaging times as 10 mg/m^3 and 1-hour as 30 mg/m^3. The hourly and annually averaging time for NO_2 should not exceed 400 μg/m^3 and 100 μg/m^3 correspondingly. For SO_2, the allowed value in one day is 250 μg/m^3 and in one year is 80 μg/m^3. The 8-hour averaging time for O_3 is 120 μg/m^3. The standard concentration for PM_{10} based on 24-hour average is 150 μg/m^3 and based on annual average is 50 μg/m^3. For $PM_{2.5}$, the standard values are 50 μg/m^3 and 20 μg/m^3 based on 24-hour and annual average times respectively.

Colombia. The first air quality standard in Colombia as the legally allowable concentration of contaminate materials in the air was defined in 1995 by the Ministry of Environmental, Housing, and Territorial (MAVDT) under Decree No. 948/1995 and 601/2006 [103]. Colombia's national ambient air quality standards sets the CO concentration limits to 10 mg/m^3 based on 8-hour and 40 mg/m^3 based on 1-hour averaging times [74,82]. The maximum acceptable levels for O_3 are set to be 120 μg/m^3 for 1-hour averaging times and 80 μg/m^3 for 8-hour averaging times. For NO_2, the permissible concentration for 1-hour averaging time is 200 μg/m^3, for 24-hour is 150 μg/m^3 and for annual is 100 μg/m^3. For SO_2, the daily average value is set to be 250 μg/m^3, and annual value is set to be 80 μg/m^3. The daily maximum allowed values for PM_{10} and $PM_{2.5}$ are 100 μg/m^3 and 50 μg/m^3, and the annual values are 50 μg/m^3 and 25 μg/m^3.

Costa Rica. In 1996, a law specifying air quality standard was enacted by the Congress under legal act of Decree 30.221 [94, 102, 104]. This standard limits the CO_2 concentration level to be 10 mg/m^3 per 8-hours and 40 mg/m^3 per 1-hour averaging times. The O_3 concentration level is set to be 160 μg/m^3 every one hour. The NO_2 standard for 1-hour averaging time is 400 μg/m^3 and for one year period is 100 μg/m^3. The daily and yearly concentration levels for SO_2 should not be above 365 μg/m^3 and 80 μg/m^3, correspondingly. Finally, the concentration levels of 150 μg/m^3 and 50 μg/m^3 are the maximum allowed levels for PM_{10} in 24-hour and 1-year averaging times respectively.

Ecuador. One policy established in 2003 by the Ecuadorian Government is called La Norma Ecuatoriana de Calidad del Aire (NECAA) [94, 102, 105]. The primary objective of these air pollution level standards is to protect the health of the citizens of Ecuador, maintain a healthy environment, and to protect Ecuador's ecosystems. Ecuador's standard limits the CO concentration levels in 1-hour to be 40 mg/m^3 and in 8-hour to be 10 mg/m^3. O_3 concentration levels should not exceed 160 μg/m^3 in one hour and 120 μg/m^3 in 8-hours averaging times. For NO_2, the daily concentration level is set to be 150 μg/m^3 and the yearly level is set to be 100 μg/m^3. Finally, the daily limits for PM_{10} and $PM_{2.5}$ are 150 μg/m^3 and 65 μg/m^3 respectively, while the annual limits for them are 50 μg/m^3 and 15 μg/m^3 respectively.

El Salvador. The Ministry of Environment in El Salvador proposed technical standards on air quality in 2000 under Law No. DECREE 40/2000 [94, 102, 104]. This standard has CO limits of 40 mg/m^3 in 1-hour and 10 mg/m^3 in 8-hour averaging times. The hourly limit for O_3 is 235 μg/m^3 and the 8-hours limit is 120 μg/m^3. The concentration levels for NO_2 are 150 μg/m^3 for 24-hour averaging times and 100 μg/m^3 for 1 year. For SO_2, the daily allowed value is 365 μg/m^3 and in one year is 80 μg/m^3. The standard concentration level for PM_{10} based on 24-hour average is 150 μg/m^3 and based on annual average is 50 μg/m^3. The 24-hours standard for $PM_{2.5}$ is 65 μg/m^3 and the annual standard is 15 μg/m^3.

Jamaica. Jamaican Natural Resources Conservation Authority (NRCA) issued the first national Jamaican Ambient Air Quality Standards (JAAQS) in 1996 [106, 107]. Later in 2006 [106], The National Environment and Planning Agency (NEPA) proposed an Ambient Air Quality Guideline Document to provide support and information for implementing the JAAQS under the Natural Resources Conservation Authority (NRCA) [108]. The national Jamaican Ambient Air Quality Standards (JAAQS) [94, 102] recommends that CO concentration levels should not exceed 10 mg/m^3 in 8-hour and 40 mg/m^3 in 1-hour. The one hour concentration levels for O_3 and NO_2 are limited to 235 μg/m^3 and 100 μg/m^3 respectively. The SO_2 stand-

ard value for 1-hour is 700 μg/m^3, for 24-hour is 365 μg/m^3, and for annual averaging times is 80 μg/m^3. PM_{10} has a limit of 150 μg/m^3 in 24-hour and a limit of 50 μg/m^3 in 1-year. Lastly, Pd is restricted not to exceed 2 μg/m^3 daily.

Nicaragua. The first Nicaragua Air Quality Standard has been approved 2001 by Ministry Environment and Natural Resources (MARENA) under law 290 (NTON 05 012 02) [94,102,109]. MARENA formulates environmental quality standards and monitoring compliance to ensure that air quality is satisfactory for environment in general and the welfare and health of the population. The Nicaragua Air Quality Standard restricts the concentration levels on CO to be 40 mg/m^3 per 1-hour and to be 10 mg/m^3 per 8-hours. The O_3 levels are not supposed to exceed 235 μg/m^3 in one hour and 160 μg/m^3 in 8-hours averaging times. For NO_2, the 1-hour standard is 400 μg/m^3 and the 8-hour standard is 100 μg/m^3. The daily average limit for SO_2 is 265 μg/m^3 and its yearly limit is 80 μg/m^3. For PM_{10}, the daily average values should not exceed 150 μg/m^3, and annual values should not exceed 50 μg/m^3. Finally, the concentration levels for Pb are 1.5 μg/m^3 for 3-months and 0.5 μg/m^3 annually.

Puerto Rico. Puerto Rico usually applies US (Federal) laws including US environmental laws such as the Clean Air Act (CAA) [110, 111]. The Puerto Rico Public Policy Environmental Act (Law 416/2004) established an administrative agency the Puerto Rico's Environmental Quality Board (PREQB), which sets out regulations and guidelines for the environmental protection of the island. Among these regulations is the standard for ambient air quality established by EQB in Regulations on the Control of Air Pollution. The PREQB standard [74, 82] specify the CO limit as of 10 mg/m^3 based on 8-hour period and as of 40 mg/m^3 based on 1-hour averaging times. The one-hour averaging time for O_3 is limited to 235 μg/m^3 and the 8-hours limit is 147 μg/m^3. For NO_2, the hourly average time is limited to 188 μg/m^3 and 100 μg/m^3 annually. For SO_2, the daily and annual standard values are 367 μg/m^3 and 79 μg/m^3 respectively. The daily PM_{10} limit is 260 μg/m^3. Finally, the daily and annual standard values for $PM_{2.5}$ are 35 μg/m^3 and 15 μg/m^3 respectively.

Peru. The Government of Peru established the "Regulations for National Air Quality Standards" in 2001 through the Supreme Decree 074 by The Ministry of Health, through the General Directorate of Environmental Health (DIGESA) [94, 112]. The Peru standards set maximum permissible levels of CO as 30 mg/m^3 every one hour and 10 mg/m^3 every 8-hours averaging time. The 8-hours standard for O_3 is set to be 120 μg/m^3. For NO_2, the 1-hour averaging time is limited to 200 μg/m^3 and the 1-year period is set to be 100 μg/m^3. SO_2 has a daily limit of 80 μg/m^3. The daily and annual averaging times for PM_{10} are 150 μg/m^3 and 50 μg/m^3 respectively, while the PM_{10} daily limit is 50 μg/m^3. Finally, the monthly averaging time for Pb is 1.5 μg/m^3.

Republic of Dominican. In 2003, the Ministry of the Environment and Natural Resources in Dominican Republic (SEMARENA) issued the environmental standard on air quality and air emissions control throw Resolution No. 10-2003 [113]. The SEMARENA standard limits the concentration levels of CO to not exceed 40 mg/m^3 per one hour and 10 mg/m^3 per 8-hours [74]. The 1-hour standard for O_3 is limited to 250 μg/m^3 and the 8-hours standard is set to be 160 μg/m^3. The 1-hour, 24-hours and annual averaging times for NO_2 are set to be 400 μg/m^3, 150 μg/m^3 and 100 μg/m^3 respectively. The hourly average limit for SO_2 is 450 μg/m^3, the daily average limit is 150 μg/m^3 and its hourly limit is 100 μg/m^3. The standard concentration for PM_{10} based one day average time is 150 μg/m^3 and based on annual average time is 50 μg/m^3. Finally, the daily and annual averages for $PM_{2.5}$ are set to be 65 μg/m^3 and 15 μg/m^3 respectively.

Venezuela. The Ministry of Environment and Natural Resources in Venezuela established standards for the improvement of air quality and prevention and control of air pollution in 1995 (Decree No. 638) [114]. This Decree specifies the limit concentration of a pollutant in the ambient air acceptable to protect health and the environment [94, 115]. These standards air quality limits are set for the CO as of 35 mg/m^3 based on 1-hour averaging times and 10 based on 8-hours period. The 1-hour averaging time for O_3 is 200 μg/m^3 and the 8-hours averaging time is 160 μg/m^3. The concentration level for NO_2 in 1-hour is 367 μg/m^3, in 8-hours is 300 μg/m^3, and in 1-year is 100 μg/m^3. For SO_2, the allowed value for 24-hour is 365 μg/m^3 and for annual is 80 μg/m^3. Finally, the daily average limit for PM_{10} is 150 μg/m^3 and its yearly limit is 50 μg/m^3.

TABLE 1A
Summary of International Ambient Air Quality Standards (µg/m³).

Area	Country / Organization	$PM_{2.5}$		PM_{10}		SO_2			NO_2			O_3			CO (mg/m³)			Pb	
		24h	1yr	24h	1yr	1h	24h	1 yr	1 h	24h	1yr	1h	8h	24h	1 h	8h	24h	24h	1yr
World	WHO	25	10	50	20	500[d]	20		200		40		100						
Europe	EU	-	25	50	40	350	125	-	200	-	40	-	120	-	-	10	-	-	0.5
Asia	Bangladesh	65	15	150	50	-	366	78	-	-	100	235	157	-	40	10	-	-	0.5
	Bhutan																		
	Industrial	-	-	200	120	-	120	80	-	120	80	-	-	-	10	5	-	-	-
	Mixed	-	-	100	60	-	80	60	-	80	60	-	-	-	4	2	-	-	-
	Sensitive	-	-	75	50	-	30	15	-	30	15	-	-	-	2	1	-	-	-
	Cambodia	-	-	-	-	500	300	100	300	100	-	200	-	-	40	20	-	5	-
	China 1																		
	Grade I	-	-	50	40	150	50	20	120	80	40	160	-	-	10	-	4	-	1
	Grade II	-	-	150	100	500	150	60	240	120	80	200	-	-	10	-	4	-	1
	Grade III	-	-	-	-	700	250	100	240	120	80	200	-	-	20	-	6	-	1
	China 2																		
	Grade I	-	-	-	-	150	50	20	200	80	40	-	-	-	10	-	4	-	-
	Grade II	-	-	250	150	500	150	60	200	80	40	-	-	-	10	-	4	-	-
	Hong Kong																		
	HK1	-	-	-	-	800	350	80	300	150	80	240	-	-	30	10	-	-	-
	HK SAR	75	35	180	55	-	125	-	200	-	40	-	160	-	-	-	-	-	0.5
	India																		
	Area 1	60	40	100	60	-	80	50	80	40	50	180	100	-	4	2	-	-	0.5
	Area 2	60	40	100	60	-	80	20	80	30	20	180	100	-	4	2	-	-	0.5
	Indonesia	-	-	150	-	900	365	60	400	150	100	235	-	50	30	10	-	-	1
	Iran	-	-	260	-	210	-	-	-	100	-	280	-	160	-	50	10	-	-
	Japan	35	15	100	200	282	113					-	-	-				-	-
	Korea	-	-	100	50	393	131	52	188	113	56	196	118	-	29	10	-	-	0.5
	Kuwait	-	-	150	90	800	500	-	200	100		160			40	9	-	2	1.5
	Malaysia	-	-	150	50	350	105	-	320	-	90	200	120	-	35	10	-	-	1.5[a]
	Mongolia	50	25	150	50		30	10	85	40	30	120	100	-	-	-	-	-	-
	Nepal	-	-	120	-	-	70	50	-	80	40	-	-	-	-	10	-	-	0.5
	Oman	35	15	150	-	130[b]	-	-	-	-	100				40	-	-		
	Pakistan																		
	2009	40	25	250	200		120	80	-	80	40	180	-	-	10	5	-	-	0.5
	2012	35	15	150	120		120	80	-	80	40	130	-	-	10	5	-	-	-
	Philippines	-	-	150	60	-	180	80	-	150	-	140	60	-	35	10	-	-	1
	Qatar	-	-	150	50	-	365	80	400	150	100	-	-	-	40	-	-	1.5[a]	-
	Saudi Arabia	35	15	340	80	730	365	80	660		100	235	157	-	40	10	-	-	0.5
	Singapore	35	15	150	-	196	365	80	188	-	100	235	147		40	10	-	-	-
	Sri Lanka	50	25	100	50	200	80	-	250	100	-	200	-	-	30	10	-	-	-
	Thailand	-	-	120	50	784	314	104	319	-	-	196	137	-	34	10	-	1.5[c]	-
	Viet Nam	-	-	150	50	350	125	50	200	100	40	180	120	80	30	10	5	1.5	0.5

[a]: 3 months
[b]: 3 hours
[c]: 1 month
[d]: 10 minutes

TABLE 1B
Summary of International Ambient Air Quality Standards (µg/m³).

Area	Country/ Organization	$PM_{2.5}$		PM_{10}		SO_2			NO_2			O_3			CO (mg/m³)			Pb	
		24 h	1yr	24 h	1 yr	1 h	24h	1 yr	1 h	24 h	1 yr	1h	8 h	24h	1 h	8 h	24h	24 h	1 yr
Africa	Egypt	-	-	70	-	350	150	60	400	150	-	200	120	-	-	-	-	-	1
	Tunisia	260	80	-	-	-	365	80	660	-	200	235	-	-	40	10	-	2	-
	Ghana																		
	Industrial	-	-	70	-	900	150	80	-	-	400	-	-	-	30	10	-	-	2.5
	Residential	-	-	70	-	700	100	50	-	-	-	-	-	-	30	10	-	-	2.5
	Tanzania	-	-	-	-	-	100	60	120[d]	150	-	-	-	-	30	10	-	1.5	-
	Senegal	-	-	260	80	-	125	50	200	-	40	-	120	-	-	-	30	-	2
	South Africa	65	25	120	50	350	125	50	200	-	40	-	120	-	-	-	-	-	0.5
North America	Canada																		
	NAAQO	-	-	-	-	875	300	60	400	200	100	160		50	35	15	-	-	-
	CWS	30	-	-	-	-	-	-	-	-	-	-	128	-	-	-	-	-	-
	CAAQS	28	10	-	-	-	-	-	-	-	-	-	124	-	-	-	-	-	-
	Mexico	65	15	120	50	524	288	66	395	-	100	216	157	-	-	13	-	1.5[e]	-
	United State																		
	Primary	35	12	150	-	196	-	-	190	-	100	-	150	-	40	10	-	1.5[e]	-
	Secondary	35	15	150	-	-	1300[g]	-	-	-	100	-	150	-	-	-	-	1.5[e]	-
Latin America	Argentina	-	-	-	-	2620	780[d]	80[e]	847	282	-	200	-	-	57	11	-	-	-
	Bolivia	-	-	150	50	-	365	80	400	150	-	236	-	-	40	10	-	-	-
	Brazil	-	-	-	-	365	-	80	320	-	100	160	-	-	40	10	-	-	-
	Chile	50	20	150	50	-	250	80	400	-	100	-	120	-	30	10	-	-	-
	Colombia	50	25	100	50	-	250	80	200	150	100	120	80	-	40	10	-	-	-
	Costa Rica	-	-	150	50	-	365	80	400	-	100	160	-	-	40	10	-	-	-
	Ecuador	65	15	150	50	-	350	80	-	150	100	160	120	-	40	10	-	-	-
	El Salvador	65	15	150	50	-	365	80	-	150	100	235	120	-	40	10	-	-	-
	Jamaica	-	-	150	50	700	365	80	100	-	-	235	-	-	40	10	-	2[e]	-
	Nicaragua	-	-	150	50	-	365	80	400	-	100	235	160	-	40	10	-	1.5[e]	0.5
	Puerto Rico	35	15	150	-	-	367	79	188	-	100	235	147	-	40	10	-	-	-
	Pure	50	-	150	50	-	80	-	200	-	100	-	120	-	30	10	-	1.5[f]	-
	Rep. Dominican	65	15	150	50	450	150	100	400	300	100	250	160	-	40	10	-	-	-
	Venezuela	-	-	150	50	-	365	80	367	300	100	200	160	-	35	10	-	-	-
Oceania	Australia	25	8	50	-	524	210	52	225	-	56	200	-	-	-	10	-	-	0.5

[d]: 8 hours
[e]: 3 months
[f]: 1 month
[g]: 3 hours

REFERENCES

[1] Duman-Yuksel, U. (2015) Assessment of the Air Quality in Ankara, Turkey. Fresen. Environ. Bull. 24, 986-996.

[2] Demir, S., Saral, A., Išik, D., Akyildiz, A., Levent Kuzu, S., Mert, S., Demir, G. and Goncaloğlu, B.I. (2011) Characterization of Ambient Volatile Organic Compounds and their Diurnal Variations in Istanbul, Turkey. Fresen. Environ. Bull. 20, 2951-2958.

[3] Vicente, A.B., Sanfeliu, T., Jordan, M.M. and Pardo, F. (2013) PM10 Air Quality Assessment in an Industrialized Area of the Mediterranean Basin. Proposal for an Air Quality Plan. Fresen. Environ. Bull. 22, 870-878.

[4] Nikolaou, K. (2002) Comparative Evaluation of the Air Quality in Athens and Thessaloniki versus EC New Standards. Fresen. Environ. Bull. 11, 426-431.

[5] Dimitroulopoulou, C. and Ziomas, I.C. (2012) State of Air Quality in Greece. Fresen. Environ. Bull. 21, 3202-3211.

[6] Zhang, Q., He, K. and Huo, H. (2012) Policy: Cleaning China's Air. Nature. 484(7393), 161-162.

[7] Branco, P.T.B.S., Alvim-Ferraz, M.C.M., Martins, F.G. and Sousa, S.I.V. (2014) Indoor Air Quality in Urban Nurseries at Porto City: Particulate Matter Assessment. Atmospheric Environment. 84, 133-143.

[8] WHO. (2016) Air Quality and Health. Available from: http://www.who.int/mediacentre/factsheets/fs313/en/.

[9] WHO. (1979) Sulfur Oxides and Suspended Particulate Matter. World Health Organization, Geneva.

[10] WHO. (1987) Air Quality Guidelines for Europe World Health Organization Regional Publication, European Series No. 23. Air Quality Guidelines for Europe World Health Organization Regional Publication. Available from: http://www.who.int/mediacentre/factsheets/fs313/en/.

[11] Air Quality Guidelines for Europe. (2000) World Health Organization, Regional Office for Europe, Copenhagen. Available from: http://www.euro.who.int/__data/assets/pdf_file/0005/74732/E71922.pdf.

[12] Air Quality Guidelines. (2000) World Health Organization, Geneva. Available from: http://www.euro.who.int/__data/assets/pdf_file/0005/74732/E71922.pdf.

[13] WHO. (2006) Air Quality Guidelines: Global Update 2005: Particulate Matter, Ozone, Nitrogen dioxide, and Sulfur dioxide. World Health Organization, Copenhagen, Denmark. Available from: http://www.euro.who.int/__data/ assets/ pdf_file/0005/78638/E90038.pdf.

[14] WHO. (2010) WHO Guidelines for Indoor Air Quality: Selected Pollutants. World Health Organization, Geneva, Switzerland. Available from: http://www.euro.who.int/__data/ assets/pdf_file/0009/128169/e94535.pdf.

[15] Morawska L. (2010) Adverse Health Effects to Air Pollution and Guidelines to Prevent them. Air Quality and Climate Change. 44, 16-18. Available from: https://getinfo.de/app/Adverse-health-effects-to-air-pollution-and-guidelines/id/BLSE%3ARN267684766.

[16] AAQ NEPM. (1998) National Environmental Protection Council (NEPC). Available from: http://www.comlaw.gov.au/Details/C2004H03935.

[17] Spickett, J., Katscherian, D. and Harris, P. (2013) The role of Health Impact Assessment in the Setting of Air Quality Standards: An Australian Perspective. Environmental Impact Assessment Review. 43, 97-103.

[18] Hill, R. (1999) Annual Report to the National Environment Protection Council on the Implementation of the National Environment Protection (National Pollutant Inventory) Measure for the Commonwealth. NEPC Annual Report. 1998, 99, 143-45.

[19] NEPC. (2008) Review of the National Environment Protection Measure for the National Pollutant Inventory. Adelaide: National Environment Protection Council.

[20] EU. (2008) Air Quality Standards. Available from: http://transportpolicy.net/index.php?title=EU:_Air_Quality_Standards.

[21] European Commission. (2017) Air Quality Existing Legislation. Available from: http://ec.europa.eu/index_en.htm.

[22] Council of the European Union (1980) Council Directive 80/779/EEC on Air Quality Limit Values and Guide Values for Sulphur dioxide and Suspended Particulates. Official Journal L, 15 July 1980. 229, 0030-0048. Available from: http://eurlex.europa.eu/LexUriServ/LexUriServ.do?uri=CONSLEG:1980L0779:19911223:EN:PDF.

[23] Council of the European Union (1982) Council Directive 82/884/EEC on a Limit Value for Lead in the Air. Off. J. Eur. Comm., NL 378:31-12. Available from: http://eur-lex. europa.eu/LexUriServ/LexUriServ.do?uri=CONSLEG:1982L0884:19911223:EN:PDF.

[24] Council of the European Union (1985) Council Directive 85/203/EEC on Air Quality Standards for Nitrogen Dioxide. European Community Environment Legislation, 7 March 1985. Available from: http://eur-lex.europa.eu/LexUriServ/LexUriServ.do?uri=CONSLEG:1985L0203:19911223:EN:PDF.

[25] EU. (1992) Official Journal of the European Communities No. 92/72/EEC: Official Journal of the European Communities. Available from: http://eur-lex.europa.eu/LexUriServ/LexUriServ.do?uri=CELEX:31992L0072:EN:HTML.

[26] Council of the European Union (1996) Council Directive 96/62/EC on Ambient Air Quality Assessment and Management (The Framework Directive). Official Journal of the European Communities. 21. Available from: http://eur-lex.europa.eu/LexUriServ/LexUriServ.do?uri=CELEX:31996L0062:EN:HTML.

[27] EC. (1999) Council Directive 1999/30/EC relating to Limit Values for Sulphur dioxide, Nitrogen dioxide and Oxides of Nitrogen, Particulate Matter and Lead in Ambient Air. Off. J. Eur. Communities L 22 April 1999. 163:29-6.

[28] EC. (2000) Council Directive 2000/69/EC relating to Limit Values for Benzene and Carbon monoxide in Ambient Air. Official Journal of the European Communities, Brussels, 13.

[29] EC. (2002) Directive 2002/3/EC of the European Parliament and of the Council.

[30] EC. (2005) Directive 2004/107/EC of the European Parliament and of the Council relating to Arsenic, Cadmium, Mercury, Nickel and Polycyclic Aromatic Hydrocarbons in Ambient Air. Off. J. Eur. Union L. 23, 3-16.

[31] EC. (2008) Directive 2008/50/EC of the European Parliament and of the Council on Ambient Air Quality and Cleaner Air for Europe. Off. J Eur. Union L. 152, 1-44.

[32] Gemmer, M., Xiao, B. (2013) Air quality legislation and standards in the European Union: Background, status and public participation. Advances in Climate Change Research. 4, 50-59.

[33] DoE and UNEP. (2001) Regional Resource Centre for Asia and the Pacific (RCCAP). Bangladesh State of the Environment Report.

[34] CAI-Asia. (2006) Country Synthesis Report on Urban Air Quality Management, Bangladesh. Discussion Draft, December 2006.

[35] World Bank (2008) Bhutan: Country Environmental Safeguard Review. Report No. 43785-BT. South Asia Region.

[36] National Environment Commission (1999) Institutionalizing and Strengthening of the Environmental Assessment Process in Bhutan: Reference Document, National Environment Commission.

[37] Asian Development Bank and the Clean Air Initiative for Asian Cities (CAI-Asia) Center. (2006) Country Synthesis Report on Urban Air Quality Management, Bhutan, Discussion Draft, December 2006.

[38] Asian Development Bank (2004) Cambodia country environmental analysis. Cambodia country environmental analysis.

[39] Asian Development Bank and the Clean Air Initiative for Asian Cities (CAI-Asia) Center. (2006) Country Synthesis Report on Urban Air Quality Management, Cambodia, Discussion Draft, December 2006.

[40] Florig, H.K., Song, G. (2000) Industry Reporting of Air Pollution Emissions in China. http://www.andrew.cmu.edu/user/kf0f/Emissions_Reporting_slides_3-00.pdf.

[41] Streets, D.G. and Waldhoff, S.T. (2000) Present and Future Emissions of Air Pollutants in China: SO_2, NO(x), and CO. Atmospheric Environment. 34(3), 363-374.

[42] Fei, Y., Ahmad, N., Holfelt, I. (2002) Technical Assistance for Prevention and Control of Dust and Sandstorms in Northeast Asia. ADB. 13.http://www.unccd.int/Lists/SiteDocumentLibrary/Publications/dustsandstorms_northeastasia.pdf.

[43] Good, M.L. (2004) CEO Endorsement of ADB/GEF Capacity Building to Combat Land Degradation Project in the Peoples Republic of China (PRC).

[44] People's Republic of China. (2006) Country Synthesis Report on Urban Air Quality Management. http://cleanairinitiative.org/portal/taxonomy/term/23.

[45] Hong Kong Productivity Council (2009) Public consultation on Air Quality Objectives Review launched. Available from: http://www.info.gov.hk/gia/general/200907/23/P200907230082.htm.

[46] Asian Development Bank and the Clean Air Initiative for Asian Cities (CAI-Asia) Center. (2006) Country Synthesis Report on Urban Air Quality Management, Hong Kong, Discussion Draft, December 2006. Available from: http://cleanairinitiative.org/portal/system/files/ documents/overview_0.pdf.

[47] Environmental Protection Department (2006) A Proposal for Reviewing the Air Quality Objectives and Developing a Long Term Air Quality Strategy. Available from: http://www.epd.gov.hk/epd/english/boards/advisory_council/files/ACE_Paper_14-2006.pdf.

[48] EPD. (2017) Air Quality Objectives. Available from: http://www.epd.gov.hk/epd/english/ environmentinhk/air/air_quality_objectives/ air_quality_objectives.html.

[49] CAI-Asia. (2006) Country Synthesis Report on Urban Air Quality Management, Discussion Draft, India, December 2006. Available from: http://cleanairinitiative.org/portal/system/files/ documents/india_0.pdf.

[50] MEF. (2013) Ministry of Environment and Forests (MEF), Government of India. Annual Report 2011-2012. Available from: http:// envfor.nic.in/publication-reports/annual-report/annual-report-2012-2013.
[51] Asian Development Bank and the Clean Air Initiative for Asian Cities (CAI-Asia) Center (2006) Indonesian. Country Synthesis Report on Urban Air Quality Management. Discussion Draft. December 2006. Available from: http://cleanairinitiative.org/portal/system/files/documents/indonesia_0.pdf.
[52] Indonesian Multi-sectoral Action Plan Group (2002) Indonesian. Vehicle Emissions Reduction. Integrated Vehicle Emission Reduction Strategy for Greater Jakarta. ADB. Available from: http://cleanairinitiative.org/portal/ system/files/presentations/36530_recurso_0.pdf.
[53] Asadollah-Fardi, G. (2008) Air quality management in Tehran. 19. Available from: https://www.zotero.org/groups/theasthmafiles/items/itemKey/DCBQHHTB.
[54] MOE (2009) Japan. Air Quality Standards. Available from: http://transportpolicy.net/ index.php?title=Japan:_Air_Quality_Standards.
[55] MOE (2009) Environmental Quality Standards in Japan - Air Quality [MOE]. http://www.env.go.jp/en/air/aq/aq.html.
[56] Haq, G., Jinhan, W., Kim, C., Vallack, H. (2002) Benchmarking urban air quality management and practice in major and mega cities of Asia, Stage 1. Air Pollution in Themegaci Ties of Asia (APMA) Project. Korea Environment Institute, Seoul, South Korea. Available from: http://www.unep.org/PDF/APMA_Benchmarking_report.pdf.
[57] Ambient Air Quality Standards in Asia Survey Report, Clean Air Initiative for Asian Cities (CAI-Asia) Center (2009) Available from: http://cleanairinitiative.org/portal/system/files/AQ_Standards_Report_Draft_2_Dec_FINAL.pdf.
[58] Al-Hamad, K.K., Nassehi, V. and Khan, A. R. (2008) Using a Simulation Tool to Model the Ground Level Concentrations of Green House Gases Emitted by Flaring in Petroleum Production in Kuwait Oilfields. American Journal of Environmental Sciences. 4(5), 420-438.
[59] Al-Hamad K.K., Nassehi, V., Khan, A.R. (2010) Methane and other Hydrocarbon Gas Emissions Resulting from Flaring in Kuwait Oilfields. Inter J Civil Environ Eng. 2010:2-1.
[60] Yahaya, N., Ali, A, Ishak, F. (2006) Air Pollution Index (API) and the Effects on Human Health: Case Study in Terengganu City, Terengganu, Malaysia. In: The International Association for People-Environmental Studies (IAPS) Conference. September 2006. Alexandria, Egypt.
[61] Asian Development Bank and the Clean Air Initiative for Asian Cities (CAI-Asia) Center (2006) Malaysia. Country Synthesis Report on Urban Air Quality Management. Discussion Draft. December 2006. Asian Development Bank and the Clean Air Initiative for Asian Cities (CAI-Asia) Center.
[62] Bayarlkhagva, M. (2008) Air pollution issues and air quality management practice in Ulaanbaatar City. Available from: http://www.etd.ceu.hu/2008/e05bam01.pdf.
[63] MASM. (1998) Mongolian Agency of Standardization and Metrology, Mongolian National Standard. Ambient Air Quality. General Requirements. MNS 4585:1998. Ulaanbaatar.
[64] Asian Development Bank and the Clean Air Initiative for Asian Cities (CAI-Asia) Center (2006) Mongolia. Country Synthesis Report on Urban Air Quality Management, Discussion Draft, December 2006. Asian Development Bank and the Clean Air Initiative for Asian Cities (CAI-Asia) Center 2006.
[65] Asian Development Bank and the Clean Air Initiative for Asian Cities (CAI-Asia) Center (2006) Nepal. Country Synthesis Report on Urban Air Quality Management, Discussion Draft, December 2006. Asian Development Bank and the Clean Air Initiative for Asian Cities (CAI-Asia) Center.
[66] HMR Environmental Engineering Consultants (2010) Environmental Impact Assessment for Solar-II Independent Power Project. Project No. HMR/2826.
[67] Document of the World Bank. (2006) Report No. 36946-PK. Pakistan. Strategic Country Environmental Assessment. Volume I: Main Report.
[68] Aziz, J.A. (2006) towards establishing air quality guidelines for Pakistan. Eastern Mediterranean Health Journal. 12, 886.
[69] Colbeck, I., Nasir, Z.A. and Ali, Z. (2010). The State of Ambient Air Quality in Pakistan-A Review. Environmental Science and Pollution Research. 17(1), 49-63.
[70] UN (2009) Philippines Country Profile: Clean Air for Smaller Cities in the Association of Southeast Asian Nations (ASEAN) Region 2009.

[71] The Department of Natural Resources (DENR) (1993) Administrative Order (DAO) No.14 and No.14a: Revised Air Quality Standards of 1992, Revising and Amending the Air Quality Standards of 1978. Available from: http://goo.gl/mRZ8al.
[72] UN (2007) Qatar: United Nations Division for Sustainable Development-Commission on Sustainable Development. National Information. Available from: http://www.un.org/esa/ agenda21/natlinfo/countr/qatar/pastThematicProfiles.htm.
[73] AFED (2011) Air Quality - Arab Forum for Environment and Development. Available from: http://afedonline.org/Report2011/PDF/En/Full-eng.pdf.
[74] MEPA (2012) Kingdom of Saudi Arabia National Environmental Standard Ambient Air Quality, Presidency of Meteorology and Environment. 2012. Available from: http://www.pme.gov.sa/en/En_EnvStand19.pdf
[75] Asian Development Bank and the Clean Air Initiative for Asian Cities (CAI-Asia) Center (2006) Singapore 2006: Country Synthesis Report on Urban Air Quality Management, Discussion Draft, December 2006. Asian Development Bank and the Clean Air Initiative for Asian Cities (CAI-Asia) Center 2006.
[76] Asian Development Bank and the Clean Air Initiative for Asian Cities (CAI-Asia) Center (2006) Sri Lanka 2006: Country Synthesis Report on Urban Air Quality Management. Discussion Draft. December 2006. Asian Development Bank and the Clean Air Initiative for Asian Cities (CAI-Asia) Center 2006.
[77] National Legislative Assembly (2010). The Enhancement and Conservation of National Environment Quality Laws in Thailand.
[78] Asian Development Bank and the Clean Air Initiative for Asian Cities (CAI-Asia) Center (2010) Thailand 2010: Country Synthesis Report on Urban Air Quality Management. Discussion Draft. ADB. Asian Development Bank (ADB) and Clean Air Initiative for Asian Cities (CAI-Asia) Center 2010.
[79] Egypt State of Environment and Egyptian Environmental Affairs Agency (2013) Egyptian Air Quality Limits Values. Available from: http://www.eeaa.gov.eg/eimp/limit%20values.html.
[80] Chemingui, M.A., Thabet, C. (2011) Trade Liberalization, Local Air Pollution, and Public Health in Tunisia: Assessing the Ancillary Health Benefits of Pollution Abatement Policy.
[81] GNIP (Ghana National Implementation Plan) (2007) National Implementation Plan of the Stockholm Convention on Persistent Organic Pollutants. Environmental Protection Agency of Ghana 2007.
[82] East Africa Community (2011) East Africa Community Thematic Area 2 – Environmental Regulations and Standards, 2011.
[83] The Environmental Management (Air Quality Standards) Regulations (2007). The Environmental Management Act (CAP. 191).
[84] Sivertsen, B., Guerreiro, C., Ly, I. (2010) Air quality standards for Senegal. Kjeller (NILU OR 49/2010).
[85] South African National Standards (SANS). (2011) South African National Standard, Ambient Air Quality – Limits for Common Pollutants. SANS 1929:2011. Standards South Africa, Pretoria.
[86] Wood, J. (2012) Canadian Environmental Indicators: Air Quality. Studies in Environmental Policy.
[87] Government of Canada (2013) Environment Canada - Canadian Ambient Air Quality Standards.
[88] Shepherd, M., McMillan, A. (1998) Canadian National Ambient Air Quality Objectives: Process and Status. In Emerging Air Issues for the 21st Century: The Need for Multidisciplinary Management: Proceedings of an International Specialty Conference Jointly Sponsored by the Air & Waste Management Association, the Association of Professional Engineers, Geologists and Geophysicists of Alberta, and the Alberta Society of Professional Biologists, September 22-24, 1997, Calgary, Alberta, Canada. 78, 15.
[89] Canadian Council of Ministers of the Environment (2007) Guidance document on achievement determination Canada-wide standards for particulate matter and ozone 2007.
[90] Canadian Council of Ministers of the Environment (2010) Comprehensive air management system: a proposed framework to improve air quality management. Canadian Council of Ministers of the Environment, Winnipeg.
[91] Taylor, E., Brook, J.R., Moran, M., Stieb, D.M., Angle, R.P., Karman, D., Krzyzanowski, J., McMillan, A., Stevens, S., Young, J. (2014) The Future of Air Quality Management. Air Quality Management. 379-388.
[92] Instituto Nacional de Ecología y Cambio Climático. (2015) Supporting National Planning of Short-lived Climate Pollutants in Mexico.
[93] Secretary of Health (2017) Mexico: Air Quality Standards - Transportpolicy.net.
[94] Joanne, G., Sanchez, S. (2013) Air Quality in Latin America: An Overview - Clean Air Institute.

[95] US (1970) Clean Air Act Extension of 1970, Public Law 91-604, 84 Statutes 1676, 1970-12-31.
[96] Department of Ecology (2017) National Ambient Air Quality Standards, Washington State Department of Ecology. Available from: http://www.ecy.wa.gov/programs/air/sips/pollutants/naaqs.htm.
[97] Conte Grand, M. (2000) Public Environmental Expenditures in Argentina during the 90's. Available from: http://www.ucema.edu.ar/publicaciones/download/documentos/169.pdf.
[98] U.S. EPA (2012) Our Nation's Air: Status and Trends through 2010. EPA-454/R-12-001.
[99] Melgarejo Pomar, I.G., Soria Sánchez, R., Orozco, D., Villanueva, W. (2010) Functional respiratory Study, in Traffic Agents of Bolivian police, in the Cities of La Paz and El Alto. Exposed to Environmental Pollution. BIOFARBO 18, 31.
[100] CONAMA–Conselho Nacional do Meio Ambiente. (2010) Brazil publishes its first national on-road vehicles emission inventory. Available from: http://www2.mma.gov.br/sitio/.
[101] Government of Chile (2003) Environmental standards. Taught under the law Environmental Base No. 19.300. National Environment Commission. Available from: http://cmsdata.iucn.org/downloads/pumalin_en.pdf.
[102] Baldasano, J.M., Valera, E. and Jiménez, P. (2003) Air Quality Data from Large Cities. Science of the Total Environment. 307(1-3), 141-165.
[103] Rubiano, D.R. (2011) Environmental Law in Colombia. Kluwer Law International.
[104] Tosun, J. (2013) Environmental Policy Change in Emerging Market Democracies: Eastern Europe and Latin America compared. University of Toronto Press.
[105] Kuniholm I. (2011) Air Pollution in Cuenca, Ecuador. /Air-Pollution-in-Cuenca.pdf.
[106] National Environment and Planning Agency. (2006) Natural Resources Conservation Authority Ambient Air Quality Guideline Document.
[107] The National Environment and Planning Agency (NEPA) (2010) The Jamaica Air Quality Management Programme (JAQMP). The Jamaica Air Quality Management.
[108] Excell C. (2003) The Enforcement of Planning Laws in Jamaica, Paper submitted to the National Environment and Planning Agency Judicial Symposium. Available from: http://www.nepa.gov.jm/symposia_03/Others/199_3300.pdf.
[109] The Nicaragua Gazette 211 (2001) Technical Standard Air Quality, Technical Committee on Air Quality Standard. The Nicaragua Gazette Supplement. NTON 05 012-02. 2001.
[110] Puerto Rico Environmental Quality Board (2011) Lead Infrastructure SIP Requirements of Clean Air Act Section 110a (2). Air Quality Area, Commonwealth of Puerto Rico Office of the Governor Puerto Rico Environmental Quality Board, Proposal. Available from: http://nepis.epa.gov/Exe/ZyNET.exe/91.
[111] Puerto Rico Environmental Quality Board. (2016) Nitrogen Dioxide Infrastructure SIP Requirements of Clean Air Act Section 110(a) (2). Commonwealth of Puerto Rico Office of the Governor Puerto Rico Environmental Quality Board, Proposal. Available from: http://www2.pr.gov/agencias/jca/Docum.
[112] Ministry of the Environment (2001) Decreto Supremo Nº 074-2001-PCM: Regulation of National Standards of Air Quality. Lima: Presidency of the Council of Ministers.
[113] Ministry of the Environment and Natural Resources (SEMARENA) (2008) National Implementation Plan of the Stockholm Convention in the Dominican Republic, Santo Domingo, Dom Rep.
[114] Ministry of the Environment (1995) Rules on Air Quality and Air Pollution Control. Decree No. 638. 1995.
[115] Arrocha, A., Octavio, K.H., Sanhueza, E., Cedeno, A.L. (1991) Baseline Air Quality Evaluation for the Venezuelan Orinoco bitumen belt. In SPE Health, Safety and Environment in Oil and Gas Exploration and Production Conference. Available from: http://www.researchgate.net/researcher/2010208759_A_Arrocha/

Received: **31.01.2016**
Accepted: **16.07.2016**

CORRESPONDING AUTHOR

Sabah A Abdul-Wahab
Department of Mechanical and Industrial Engineering, College of Engineering,
Sultan Qaboos University,
Muscat – Sultanate of Oman

e-mail: sabah1@squ.edu.om.

© by PSP Volume 27 – No. 5/2018 pages 2629-2634 Fresenius Environmental Bulletin

EVALUATION OF THE RECREATIONAL POTENTIAL OF KUTAHYA URBAN FOREST

Mehmet Cetin[1,*], Hakan Sevik[2], Ugur Canturk[3], Cansel Cakir[1]

[1]Kastamonu University, Faculty of Engineering and Architecture, Department of Landscape Architecture, 37150, Kastamonu, Turkey
[2]Kastamonu University, Faculty of Engineering and Architecture, Department of Environmental Engineering, 37150, Kastamonu, Turkey
[3]Kastamonu University, Institute of Science and Technology, Program of Landscape Architecture, 37150, Kastamonu, Turkey

ABSTRACT

Kutahya urban forest has an important historical value and great potential because of its outstanding natural and cultural heritage. It is an area that can make an important contribution to the entire region. But in order to do so, making long-term plans for the area and its surroundings, creating the necessary infrastructure, and promoting it locally and internationally are required. This study deals with the recreational tourism resources of Kutahya urban forest that include its historical, cultural, and natural landscape to determine its potential classification in terms of values that can be a source of tourism activity and are intended to be mapped. For this purpose, the value of the tourism resources that constitute Kutahya urban forest's values such as maps, photos, and surveys were evaluated in light of data collected as a result of work done in the area and of existing and potential recreational activities. Then the appropriate fields for the specified activities creating a digital base were determined. During the evaluation and processing of data, they were used to map the ArcGIS program. In conclusion, Kutahya urban forest's recreational resources including its historical, cultural, and ecological values were identified and mapped.

KEYWORDS:
GIS, Recreational potential, sustainable, Urban forest, Kutahya

INTRODUCTION

Natural resources are vital to human life. However, especially in the last century, the irresponsible use of natural resources has become one of the most alarming problems threatening nature and the environment. Therefore, global warming, climate change, air pollution, the irresponsible use of water resources, and the sustainable use of natural resources in all areas have been brought to the agenda [1-8]. For centuries, people have been inspired by nature, and tourism activities have been carried out to see different natural landscapes. In particular, urban tourism is the hippest form of tourism in recent years. Visiting urban areas, swimming, water sports, and hiking have been quite attractive for people, and millions of people have started to carry out tourism activities in this manner to forget, albeit for a while, problems in the city and to participate in natural and cultural activities, desiring to make it even more valuable. Natural, cultural, and historic sites are seen with great interest. However, the intensive use and increasing interest in the area also brings the risk of damage, so establishing the right balance between the protection and the use of these areas is of paramount importance [9-14].

Removing the environment and wildlife conservation from the forefront and the importance of recreational from tourism, this process has increased and continues to increase. Recreational tourism focuses on unusual properties, promoting natural and cultural areas, and providing a positive contribution in many areas. Areas where recreational tourism is applied become the center of attraction. Recreational tourism activities are carried out with a general awareness in the use of the natural environment. Besides holding activities for the protection of natural and cultural values for economic use, to adjust the balance between protection and use is the sine qua non of sustainable tourism, and it can be achieved through the natural and cultural aspects of sustainability in the field of the foreground and environmentally sensitive recreational tourism, as well as aesthetic, recreational, or cultural activities that protect delicate ecosystems. Education can be brought in the forefront as awareness [15-20].

Ensuring cooperation among the local population is one of the most important requirements for planning in the tourism sector. In the long term, natural resources, tourism, alternative tourism, recreational tourism, and nature tourism are becoming an important choice based on sustainable use. In this study, the natural and cultural aspects of urban areas are intended to reveal the potential of recreational tourism in Kutahya urban forest districts.



FIGURE 1
Kutahya urban forest height analysis

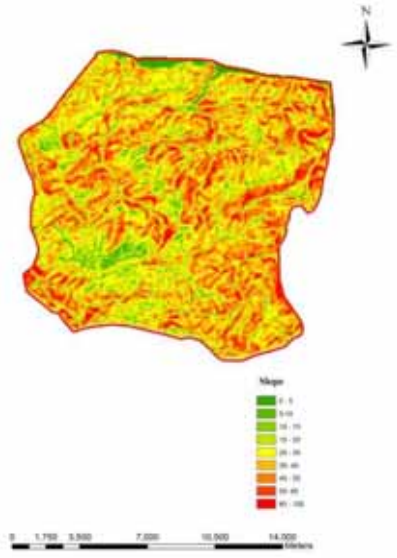


FIGURE 2
Kutahya urban forest slope analysis

MATERIALS AND METHODS

The study material includes Kutahya urban forest districts. The geographic location of Kutahya urban forest districts with rich natural and cultural areas are found between the coordinates 39°25' north latitude and 29°59' east longitude.

Located in urban areas in the West Aegean Region, Kutahya urban forest town is a mountainous and rugged terrain. The average altitude is around five meters in the central district. It is 121 km from the city center through the district [21, 22].

Temperatures in winter fall as much as 5 degrees and in summer around 30 degrees. The beach continues to increase toward the interior upgrade. With a mild climate, during winter season on the beach, the altitude of the large amount of snow in the inner part is over 1000 meters. Winter rain is experienced in urban areas, while inland, snow is seen. The summers are hot and arid.

While old houses are made of wood, because of the concrete forest district, new homes are now made of wood and brick. In indigenous places, slate stones are used in the roof.

Our district is full of natural beauty for tourism due to take place on the beach. It has unique landscapes that combine the water and the forest, the green and blue intertwining.

In the study, geological, hydrological, topographical, and soil maps were obtained. Then the climate of the region and flora and fauna information were collected. The obtained data can be fed into computers belonging to the area with the help of ArcGIS maps, and the data is processed on the maps.

During the fieldwork in the study area, surveys, opportunities, and constraints were determined by considering various pieces of information regarding the local population. SWOT was used in analyzing the obtained data, and these data were evaluated using maps. All the data and created maps of areas suitable for recreational tourism were evaluated to develop an alternative to the current use of the area's strengths and weaknesses in terms of recreational tourism, and threats and opportunities were identified.

RESULTS

The urban areas, forest areas, forest openings, potential areas for accommodation, and recreational facilities in the Kutahya urban forest districts are rather limited. Landscape, urban areas, nature and culture, vegetation and wildlife, geological and hydrological conditions, and soil have values in Kutahya urban forest. Given the topographical features of the Kutahya urban forest districts, the slope of the high woodlands and narrow urban strip limit the number of suitable areas for construction.

The geological, geomorphological, and geological structures of the soil groups in the region have interesting features, such as urban and mountain formations. The height and slope analysis of Kutahya urban forest area shown in Figure 1 and 2, and the soil groups are shown in Figure 3. Different geomorphological character movements in the valley are characterized by ridges and peaks. This geomorphological structure creates an extraordinary natural landscape with lush forests.

The Aegean Sea climate prevails in the region. Summers are hot, and winters are usually mild. Adequate rainfall is experienced in all seasons. The number of visitors per day during the tourist season ranges from 15,000 to 20,000. During this period, the following activities can be done: hiking, camping, photo safari, trekking, cycling, and amateur fishing.

Many recreational activities, such as botanical tourism and air sports, are also offered. The Kutahya urban forest survey was conducted to determine the protection of the urban area in the protection-use balance and to determine the level of awareness. The SWOT analysis was conducted, and the opportunities that may be encountered in the future, as well as the current strengths and weaknesses and threats identified in the area, are shown in Table 1.

Areas under recreational tourism activities in the study area, urban tourism, historical sites, bird observation areas, natural monuments, springs, rivers, canyons, bike tours, hiking, photo-jeep safari, camping, rock climbing, cave, winter tourism hunting-fishing, paragliding, wind, water, surf, cultural, and thermally processed tourism maps are shown in Figure 4.

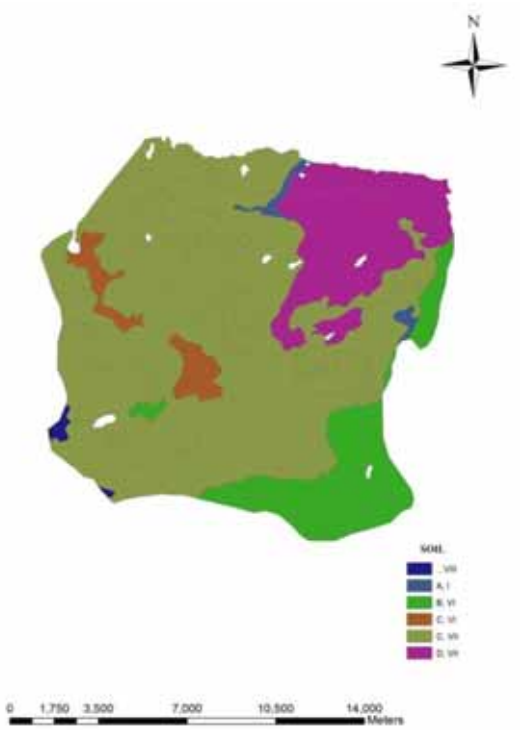


FIGURE 3
Kutahya urban forest soil groups

TABLE 1
SWOT analysis for determining the recreational tourism potential of the Kutahya urban forest District

	Weaknesses:
Strengths:	People unconsciously using natural resources
Protection of the natural character of the urban areas	Lack of social awareness about the urban areas
Protection of the natural character of the forest areas	Shortage of qualified personnel
Historical and cultural values	Lack of imagination and target recognition
Applicability of different recreational tourism activities in all seasons	Apparent lack of eligibility criteria for recreational tourism activities in different environmental, economic, and social problems
Climate and geomorphology	
Unique urban areas in terms of beauty and cultural landscapes	Uncontrolled access and lack of an institutional structure to control recreational tourism activities
Urban tourism, swimming, water sports, cave tourism, hiking, mountain sports, photo safaris, bird and butterfly watching, nature walks, and many other activities such as study tours	Defensive awareness being an underdeveloped tourism
	Lack of control
	Lack of infrastructure and superstructure
	Lack of adequate studies on flora and fauna
	Lack of accommodation
Opportunities:	**Threats:**
Kutahya's growing demand for recreational tourism	Increase in pressure and threat of extinction of biodiversity in recreational tourism
Preservation of natural and cultural landscape values	
Different geographical structures	Destruction of flora and fauna in protected areas
Local awareness of nature conservation, national and global awareness of development opportunities	Extinction of endemic species and rise of their economic value as a result of the illegal smuggling trade
A wide range of leisure and tourism activities	Unplanned expansion
Transport facilities and consequently long-distance travel opportunities	Use exceeding carrying capacity
	Solid waste pollution
Rich flora and fauna and natural structure	Air and water pollution
Landscape beauty	Natural and cultural texture corruption
recreational tourism being considered an alternative type of tourism	Uncontrolled and unconscious ecotourism that cause loss of life
Growing interest in recreational tourism issues worldwide	Monotony in recreational tourism activities, implementation of similar activities everywhere
Increase in the quality and quantity of natural areas protected by law	Natural areas of investment that cause excessive use

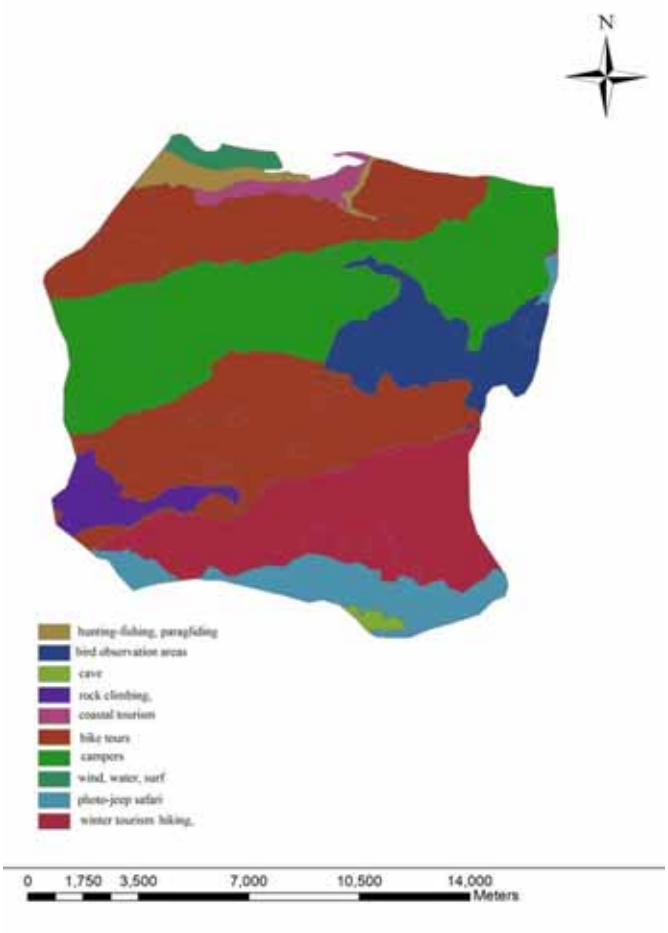


FIGURE 4
Potential Kutahya urban forest recreational tourism map

CONCLUSIONS AND DISCUSSION

Once it is known enough to become one of the most important tourist areas in the town of Kutahya, even the Aegean Sea will take its rightful place in tourism. Enough accommodation is needed so there is no reason to eliminate openness to tourists. There are those rare places where natural beauty remains intact in their natural state. On weekends, families can come and go easily, although there are tea gardens and recreational areas where they can have a picnic in Kutahya and the surrounding counties that are not known. Although it has the same features as our other urban districts, because it has not been introduced that much, Kutahya urban forest is not known.

For the development and economic growth of countries, the importance of sustainable tourism activities with an ecological approach is great. Sustainable recreational tourism can be achieved only with a proper approach to the ecological characteristics of tourism development and management plan. To set up recreational tourism strategy in the area of tourism and recreational activities, there is a need to organize and have a good planning. The study area has quite a high tourism potential in terms of tourism and recreation. Kutahya urban forest's scarce resources and assets allow different tourism activities in different seasons.

The Kutahya urban forest District's beach, historical sites, photography, bird watching, adventure and sports tourism, historical and cultural tourism, wildlife tours, caves, camping, picnic activities, horse riding, cycling, and rich recreational tourism activities such as fishing have a potential.

Kutahya urban forest's regulations on the urban forest area for recreational tourism has a significant potential. However, the routes for many activities and lack of contacts and facilities are a major problem. The solution to these problems and the use of the potential of the region, as well as the process involved, can provide important economic contributions to the region.

Kutahya urban forest is rich in vegetation, and the mountain tourism potential is high in the region. In the area of botanical gardens, arboretum structures that promote the region's biodiversity can make an important contribution to increase the public's awareness and so on. In addition, the area contains interesting examples of different geological and geomorphological structures. In terms of biodiversity, this area may be of interest to enthusiasts and researchers in particular.

Areas suitable for various activities are shown in Figure 4. This map of recreational tourism infrastructure, site selection, planning, design, transportation, management of solid waste pollution, and sewage systems can be used in accommodation facilities and the natural environment and can also be utilized for taking measures to protect wetlands.

In addition, historical and cultural tourism resources have been identified and are again shown in Figure 4. A forest area, an ideal area for the observation of wild animals, offers substantial opportunities for wildlife tours. Ideal plateau areas for wildlife tours are also shown in Figure 4. The use of these fields also needs to be done with trained guides and an orientation on plants.

There are problems in the area of transport, especially in regional transport, which as to be available and seamless. In addition, the area is very safe, and people are very hospitable. Promotion should be done in this regard. Also, at the entrance to the urban forest of Kutahya urban forest, information about important areas in the region must be available, and promotion should be done by putting up maps. Also, the introduction of the place should be done at the national and international levels.

ACKNOWLEDGEMENTS

The study has been supported by The Scientific and Technological Research Council of Turkey (TUBITAK) during the 2209-A-2016/1 period (University Students Domestic Research Projects Support Program) working on projects numbered 1919B011601370. We sincerely thank TUBITAK 2209-A-2015/2.

Furthermore, Ugur Canturk's Master Thesis in Kastamonu University, Institute of Science, Program of Landscape Architecture conducted one of part of this research. He sincerely thanks to his advisor's Assist. Prof. Dr. Mehmet Cetin and Kastamonu University.

Author Contributions. Mehmet and Hakan conceived and designed the experiments, Ugur and Cansel performed the experiments. Ugur and Mehmet analyzed the data, Cansel, Mehmet and Hakan contributed reagents/materials/analysis tools, Cansel and Mehmet wrote the paper.

Conflict of Interest. The authors declare no conflict of interest.

REFERENCES

[1] Cetin, M., Zeren, I., Sevik, H., Cakir C., Akpinar, H. (2018) A study on the determination of the natural park's sustainable tourism potential. Environmental Monitoring Assessment. 190(3), 167.

[2] Cetin, M., Topay, M., Kaya L.G., Yilmaz, B. (2010) Efficiency of bioclimatic comfort in landscape planning process: case of Kutahya. Turkish Journal of Forestry. 1(1), 83-95.

[3] Maple, L.C., Eagles, P.F.J., Rolfe, H. (2010) Birdwatchers' specialization characteristics and National Park Tourism Planning. Journal of Ecotourism. 9(3), 219-238.

[4] Cetin, M. (2015) Determining the bioclimatic comfort in Kastamonu City. Environmental Monitoring Assessment. 187(10), 640.

[5] Cetin, M. (2016) Changes in the amount of chlorophyll in some plants of landscape studies. Kastamonu University, Journal of Forest Faculty. 16(1), 239-245.

[6] Cetin, M., Sevik, H. (2016) Evaluating the recreation potential of Ilgaz Mountain National Park in Turkey. Environmental Monitoring and Assessment. 188(1), 52.

[7] Cetin, M, Sevik, H. (2016) Assessing Potential Areas of Ecotourism through a Case Study in Ilgaz Mountain National Park. (Chapter 5). In: Butowski, L. (ed.) Tourism - From Empirical Research Towards Practical Application. ISBN:978-953-51-2281-4. InTech. 81-110.

[8] Cetin, M., Adiguzel, F., Kaya, O., Sahap, A. (2018) Mapping of bioclimatic comfort for potential planning using GIS in Aydin. Environment, Development and Sustainability. 20(1), 361-375.

[9] Nouri, J., Danehkar, A., Sharifipour, R. (2008) Evaluation of ecotourism potential in the Northern Coastline of the Persian Gulf. Environmental Geology. 55, 681-686.

[10] Kaya, L.G., Cetin, M., Doygun, H. (2009) A holistic approach in analyzing the landscape potential: Porsuk Dam Lake and its environs, Turkey. Fresen. Environ. Bull. 18, 1525-1533.

[11] Ngoka, P.C. (2013) Capacity and levels of utilization of tourism potentials of Yankari and Cross River National Parks – implications for optimistic ecotourism development in Nigeria. African Journal of Hospitality, Tourism and Leisure. 2(4), 1-12.

[12] Cetin, M. (2016) A change in the amount of CO_2 at the center of the examination halls: case study of Turkey. Studies on Ethno-Medicine. 10(2), 146-155.

[13] Cetin, M. (2016) Determination of bioclimatic comfort areas in landscape planning: A case study of Cide Coastline. Turkish Journal of Agriculture-Food Science and Technology. 4(9), 800-804.

[14] Cetin, M. (2016) Sustainability of urban coastal area management: A case study on Cide. Journal of Sustainable Forestry. 35(7), 527-541.
[15] Cetin, M. (2015) Evaluation of the sustainable tourism potential of a protected area for landscape planning: a case study of the ancient city of Pompeipolis in Kastamonu. International Journal of Sustainable Development & World Ecology. 22(6), 490-495.
[16] Cetin, M. (2015) Using GIS analysis to assess urban green space in terms of accessibility: case study in Kutahya. International Journal of Sustainable Development & World Ecology. 22(5), 420-424.
[17] Cetin, M. (2015) Consideration of permeable pavement in landscape architecture. Journal of Environmental Protection and Ecology. 16(1), 385-392.
[18] Powell, R.B., Ham, S.H. (2008) Can ecotourism interpretation really lead to pro-conservation knowledge, attitudes and behaviour? Evidence from the Galapagos Islands. Journal of Sustainable Tourism. 16(4), 467-489
[19] Cetin, M., Sevik, H., Saat, A. (2017) Indoor air quality: The samples of Safranbolu Bulak Mencilis Cave. Fresen. Environ. Bull. 26, 5965-5970
[20] Cetin, M. (2017) Change in amount of chlorophyll in some interior ornamental plants. Kastamonu University Journal of Engineering and Sciences. 3(1), 11–19.
[21] T.C. Municipality. T.C. Kutahya Municipality, (2017) http://www.kutahya.bel.tr/, (Accessed: 18/05/2017)
[22] T.C. District Governorship. T.C. Kutahya District Governorship. (2017) http://www.kutahya.gov.tr/, (Accessed: 18/05/2017)

Received: **09.09.2017**
Accepted: **25.02.2018**

CORRESPONDING AUTHOR

Mehmet Cetin
Kastamonu University,
Faculty of Engineering and Architecture,
Department of Landscape Architecture,
37150, Kastamonu – Turkey

e-mail: mcetin@kastamonu.edu.tr

© by PSP Volume 27 – No. 5/2018 pages 2635-2641 Fresenius Environmental Bulletin

SPECTROPHOTOMETRIC MEASUREMENTS OF RHODAMINE B AS A DYE TRACER FOR BRINE OUTFALL LABORATORY EXPERIMENTS

Naim Sezgin[1], Emin Ahmet Yesil[2], Mehmet Altun[2], Ugur Emre Temelli[3], Semih Nemlioglu[1,*]

[1]Istanbul University, Faculty of Engineering, Department of Environmental Engineering, 34320 Avcilar, Istanbul, Turkey
[2]Istanbul University, Faculty of Engineering, Department of Chemistry, 34320 Avcilar, Istanbul, Turkey
[3]Istanbul University, Vocational School of Technical Sciences, Property Protection and Security Department, Civil Defense and Fire Fighting Program, 34320 Avcilar, Istanbul, Turkey

ABSTRACT

Rhodamine B (RhB) as a dye tracer is widely used both in laboratory scale and *in-situ* studies about determination of wastewater plumes' movement and their dilution characteristics in marine environments. RhB added salt (mainly NaCl) water solutions are used on brine outfall laboratory physical model experiments. Some of the experiments in laboratory tanks can be conducted via taking samples inside the discharged brine jets. Taken samples can be measured by optical methods such as ultraviolet-visible spectrophotometry for determination of dye tracer concentrations and dilution levels. However, absorbance specifications of a dye tracer, like RhB, might be affected by high concentrations of NaCl in discharge solutions.

This study, aimed at determining the effect of variable NaCl concentration, which represents the discharged solutions, on prepared with RhB as a dye tracer which are diluted with distilled water in the laboratory. Absorbance levels of variable dilutions of source discharge solution were obtained and their differences were compared with different levels of NaCl concentrations. In order to decrease the experimental errors for tap water used in lab scale dye tracer studies, a mathematical expression for Salinity (S)-Absorbance (I)/Concentration(c) relation was suggested in the studied range for salinity 30-100 ppt.

KEYWORDS:
Brine outfall, Dye tracer, Rhodamine B, UV-visible spectrometry

INTRODUCTION

Water-soluble dyes have been used for ages. Early types of natural dyes were stable and nontoxic. However, most of them have been replaced by synthetic dyes, because of their limited availability, low yield, and increased cost [1, 2]. Since their first synthesis in the 1850s, synthetic dyes have slowly been popularized by virtue of advantages such as easy use, low cost, high yield, high stability, and abundant varieties [3]. Dyes have been used with the large-scale industries such as textile, leather, paper, and printing industries. Also, dyes are increasingly used as a tracer dye in wastewater discharge research both *in-situ* and laboratory scale experimental studies [4, 5]. Common goals of a tracer study on marine outfall system include the measurement of the dilution factor, the estimation of the dispersion field, the measurement of transportation field of the effluent discharge, and its transport model calibrations [6]. During such experimental studies, fluorescent dyes can mostly be selected as ideal tracer dyes, because they remain clear at even low concentrations they are transparent quantitatively and optically measurable. In addition, they have ionic character, thus they can be measured with ion-selective electrodes and by conductometry [7].

A tracer may be defined as any substance which can demonstrate the course of process and can be measured. Tracers to be used in water can be derived from natural or artificial processes. There are several fluorescent dyes that have been suggested for use in outfall tracer studies. Among these include, Acid Red 50 and Acid Yellow 73 [8], Uranine, Pyranine, Eosin, Sulfo-Rhodamine, and Na Naphthionate [9], red Rhodamine WT dye and Saturn Yellow Day-Glo fluorescent paint [10, 11]. Rhodamine derivatives (Rhodamine B, Rhodamine WT, Rhodamine 6G) are popular tracers and Rhodamine B (RhB) are used in laboratory experiments, while Rhodamine WT is used *in situ* experiments [12], and Rhodamine 6G is used in laser-induced fluorescence (LIF) [13]. A fluorescent dye must be water soluble, fluorescent in a wavelength range distinguishable from background, non-toxic to humans, inexpensive and commercially available, stable with respect to photochemical decay, resistant to adsorption onto silt particles, and easy to handle [14].

RhB ($C_{28}H_{31}ClN_2O_3$), which is a rhodamine derivative, is a green crystal or reddish-violet powder that turns bluish-red when dissolved in water-soluble compound [15]. The dilute solutions of RhB are strongly fluorescent—and because of the fact that

RhB is a chloride salt, it is a traceable substance in aqueous environment not only by optical but also by chemical methods. On the other hand, if there are some impurities such as metals, they can easily make complexes with dyes [16, 17] and the wavelength of maximum absorption might shift.

RhB is commonly used in many aquatic environments such as ocean, sea, lake, and stream as a tracer in wastewater dispersion in environmental engineering applications [18], outfall performance tests both in laboratory [19] and in-site applications. Simulated wastewater discharges can be domestic, industrial, or thermal effluents. Laboratory tests of outfalls can include photographic inspections of simulated wastewater jets' trajectories originated from a singular port or multi-port outfall diffusers. In this kind of experimental studies, especially the shape of jets, concentration distribution of the wastewater jets in cross-sectional area, and jet interactions are inspected. On the other hand, in many cases, discharged and receiving waters are artificially prepared from tap water.

In order to determine the local dilution of dense wastewaters discharged into the sea (local dilution = c_0/c, where c_0 is source pollutant concentration, c is local pollutant concentration), laboratory studies are usually performed with RhB tracer and physical models with down-scale. After the tracer dye concentration is set to c_0 in physical laboratory models, amount of dilution of the simulated wastewater jet discharged into a receiving water body (mainly tap water is used) in a laboratory tank can be determined by precisely measuring the local concentration, c, in the jet. The physical model is realized by the discharge of stock solution representing the wastewater containing NaCl at definite concentrations in order to provide the high density and RhB is added and prepared with the same water sample and they are put into the physically modeled experimental tank altogether. There should be many holes to deliver the RhB into the tank. Water samples are taken at definite positions, in order to determine the local dilution conditions of the dense wastewater jet, while the distribution is observed in the experimental tank. The dilution values of these wastewater samples are determined with UV-Vis spectrophotometry, by measuring the concentration of RhB. However, since copious amounts of water are used in these type of discharge experiments, tap water instead of distilled water is used. Both tap water and increasing salinity concentrations will make the absorbances measured with UV-Vis spectrophotometry different. These differences will affect the determinations of dilutions of RhB trace solution added to saline, both of which are discharged in the experimental tank. Therefore, to remove these differences and to measure RhB plus NaCl stock solution concentrations more efficiently, concentration–absorbance calibration curves are needed. In this study, the difference of RhB absorbances, which were measured with UV-Vis spectrophotometry, were investigated by considering the water sources used for the physical modeling experiments.

MATERIALS AND METHODS

Materials. Rhodamine B (RhB) was used as a dye-purchased from commercial suppliers, Merck. Absorbance values of all solutions were measured on Perkin Elmer Lambda 35 UV-Vis Spectrophotometer (Norwalk, USA) with 1400 µL Hellma quartz cuvette.

Method. 0.05 g/L (1,046 x10^{-4} M) RhB stock solution was prepared for use in the analysis. Maximum wavelength of absorbance that will be adopted was determined by use of this stock solution (λ = 553 nm, Fig. 1) and by use of Beer-Lambert Law. Then, 0.1 mL of stock solution was taken into test tubes and diluted 10, 25, 40, 50, 65, 80, 90, 100 times separately with distilled and tap water. Absorbance values of solutions were measured at 553 nm in a spectrophotometer.

Setting of Salinities. NaCl was weighed and put into test tubes to be 30, 60, 75, 90, 100 ppt ratio of the mass of solution and the new stock solution was prepared providing specified salinity of total mass of solution to be 20 g. Then, separately and respectively diluted with distilled and tap water for 10, 25, 40, 50, 65, 80, 90, 100 times. Absorbance values of solutions were measured at 553 nm in a spectrophotometer.

RESULTS AND DISCUSSION

Firstly the maximum absorbance values were determined for aqueous RhB solutions (dissolved in distilled water) at 0.005, 0.002, 0.001, and 0.0005 g/L concentrations. The maximum wavelengths were found according to the dilution factor at λ=553nm, and 554nm. According to these results, maximum absorbance values and the optimum wavelength was λ=553 nm for solutions prepared with distilled water—then the spectra were generated as seen in Figure 1.

Experiments with distilled water. RhB solutions prepared with distilled water at 0.0005 – 0.005 g/L and containing salinity concentrations of S = 30-100 ppt were applied to UV-Vis spectrophotometry and the obtained absorbance values (I) are given in Table 1. The absorbance values in Table 1 show that increasing salinity also increases the absorbance values.

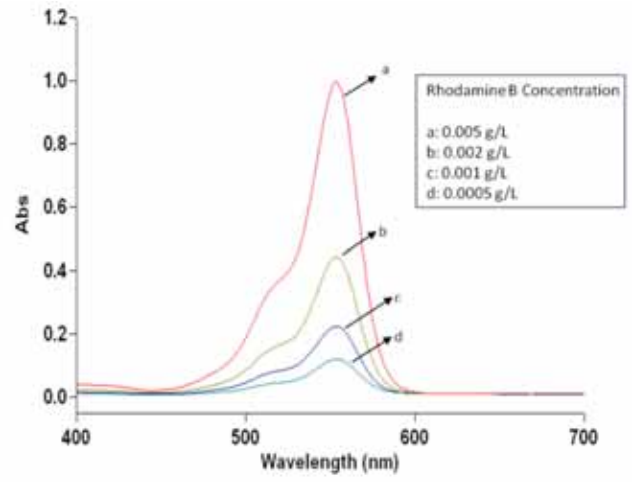


FIGURE 1
UV-Vis spectra for various RhB concentrations prepared with distilled water.

TABLE 1
Absorbance variations of various RhB and sodium chloride solutions prepared with distilled water.

RhB Concentration c (g/L)	I (Abs) S (ppt) 30	S (ppt) 60	S (ppt) 75	S (ppt) 90	S (ppt) 100
0.00050	0.1190	0.1198	0.1290	0.1373	0.1340
0.00056	0.1498	0.1522	0.1578	0.1450	0.1497
0.00063	0.1755	0.1699	0.1658	0.1784	0.1785
0.00077	0.1801	0.1939	0.2074	0.1996	0.2020
0.00100	0.2280	0.2513	0.2513	0.2556	0.2550
0.00125	0.3005	0.3173	0.3128	0.3410	0.3320
0.00200	0.4450	0.4990	0.4915	0.4815	0.4890
0.00500	0.9959	1.1356	1.1783	1.2184	1.2295

TABLE 2
Absorbance variations of various RhB and sodium chloride solutions prepared with tap water.

RhB Concentration c (g/L)	I (Abs) S (ppt) 30	S (ppt) 60	S (ppt) 75	S (ppt) 90	S (ppt) 100
0.00050	0.12007	0.12233	0.12613	0.13233	0.13153
0.00056	0.13750	0.14177	0.14427	0.14653	0.14730
0.00063	0.14520	0.15223	0.15633	0.15960	0.16183
0.00077	0.19753	0.20130	0.21193	0.21597	0.21970
0.00100	0.22047	0.22723	0.23830	0.25653	0.26113
0.00125	0.31837	0.31200	0.32757	0.34160	0.34870
0.00200	0.51807	0.51870	0.53137	0.54000	0.55267
0.00500	1.04077	1.17473	1.20967	1.24437	1.26647

Experiments with Tap Water. RhB concentrations between 0.0005-0.005 g/L were prepared with tap water. The different average absorbance values (I) at S=30-100 ppt salinity concentrations are gave in Table 2. Results show that tap water-prepared solutions have higher absorbances with increasing salinity. When compared with Table 1, these absorbances were higher. This can be attributed to the increase of the ionic strength [20, 21]. In addition, the tap water content used in the experiments were published in Istanbul Water and Sewerage Administration (ISKI) website [22], and given in Table 3.

Difference of Absorbance. In this work, separate RhB concentration (c) and Absorbance (I) graphs were prepared for data obtained with distilled water and tap water. For each of these graphs, separated c-I calibration curves were plotted. By using calibration curve equations and salinity concentrations, a new graph was generated from salinity (S), absorbance (I) and RhB concentrations (c) to show the relationship among them (Figure 2). In Figure 2, both distilled water, and tap water S-I/c values were used to obtain the trend-lines. These trend-lines show a linear relationship between salinity concentration and absorbance/RhB concentration. In addition, Figure 2 shows that distilled water and tap water trend-lines are parallel to each other, and tap water I/c values are greater than those of tap water. The main theme of this work was accepted as the mathematical expression of the tap water trend-line having

S, I, and c values. Therefore, by using the recommended equation used in the UV-Vis spectrophotometric measurements which are related to the salinity concentrations and RhB concentrations, tap water-based calibration curves was obtained. Equation 1 gives the mathematical expression obtained by linear regression.

$$\frac{I}{c} = 0.5641S + 203.2 \qquad (1)$$

In Equation 1, I is absorbance (Abs), c is the concentration of RhB (g/L), S is salinity concentration (ppt).

The recommended mathematical expression was used to estimate the absorbance values for each salinity concentration. The experimental and theoretical absorbance values are shown in Figure 3. When the graphs in Figure 3 are examined, it is revealed that the recommended mathematical expression and experimental values are highly harmonious to each other. In Tables 1 and 2, the given absorbance values show that distilled water-originated values are less than those of tap water. Figure 4 shows the comparison between experimental absorbance values and mathematical expression absorbance values. The high success of the suggested absorbance prediction mathematical expression can be seen with the experimental tap water results and that the mathematical expression predictions are close to y=x line.

TABLE 3
Tap water characteristics in Buyukcekmece, Istanbul (adopted from ISKI, June 2016) [14].

Parameter name	Average Values	Parameter name	Average Values
Primary Standards (Disinfection By-Products), µg/L		**Secondary Standards Aesthetic Standards (mg/L)**	
Total Trihalomethanes	76.4	Chloride	80
Bromate	< 2.0	Color (PC units)	< 2.0
Primary Standards (Inorganic Chemicals), mg/L		Copper	0.001
Aluminum	0.142	Iron	0.012
Arsenic	0.0006	Manganese	<0.002
Boron	0.072	Taste-Odor Causing Geosmin	4.8
		Compounds ng/LMIB	1.2
Nickel	0.002	pH	7.38
Barium	0.065	Sulfate	91.9
Cadmium	<0.0001	Total Dissolved Solids	357
Chromium	<0.0002	Zinc	<0.001
Bromide	0.05		
Fluoride	0.223		
Cyanide	<0.02	**Additional Parameters (mg/L)**	
Lead	<0.0003	Calcium	63.9
Mercury	<0.0001	Hardness as ($CaCO_3$)	214
Nitrate	1.1	Magnesium	15.0
Selenium	<0.0003	Potassium	4.6
Silver	0.00003	Sodium	49.2
Antimony	<0.0002	Residual Chlorine	1.47
Beryllium	<0.0001	Ammonia	<0.03

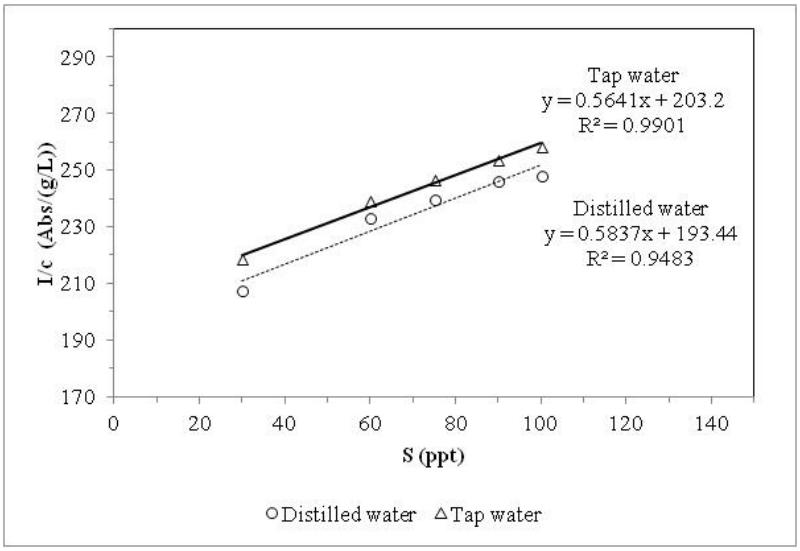
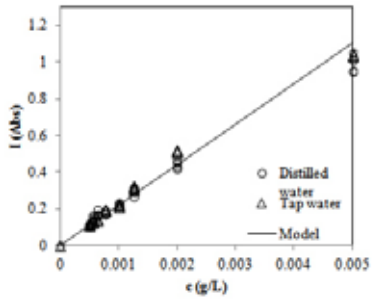
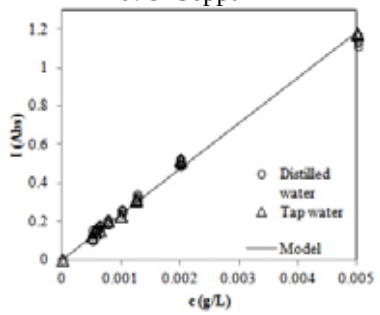


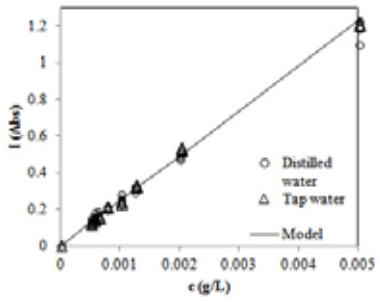
FIGURE 2
Calibration curves.



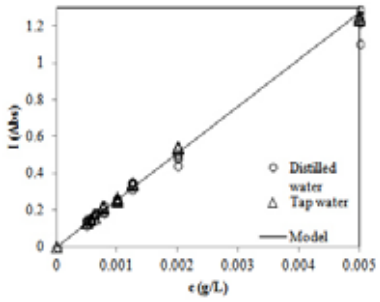
a. S=30ppt



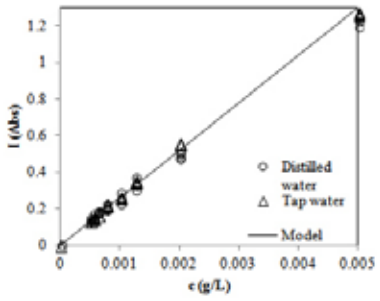
b. S=60ppt



c. S=75ppt



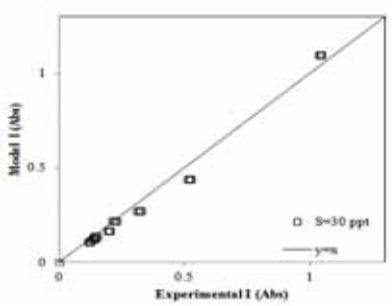
d. S=90ppt



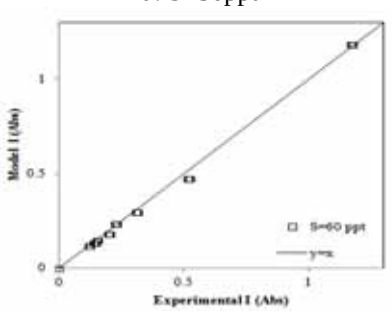
e. S=100ppt

FIGURE 3

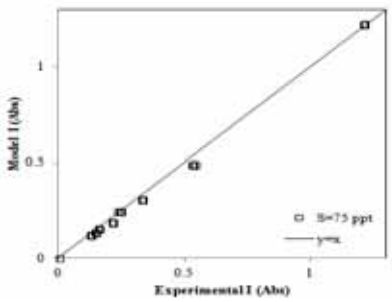
Comparisons for tap water equation results *vs* experimental data sets of distilled water and tap water.



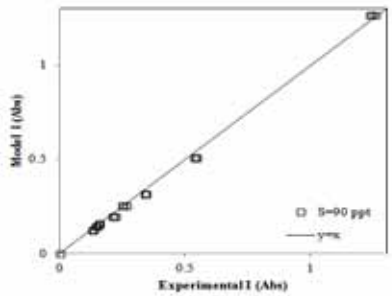
a. S=30ppt



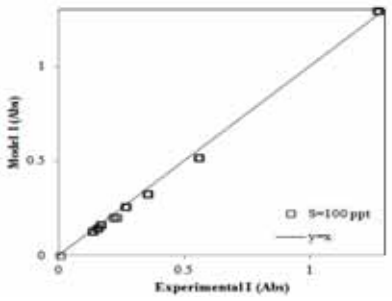
b. S=60ppt



c. S=75ppt



d. S=90ppt



e. S=100ppt

FIGURE 4

Absorbance comparison of experimental *vs* equation results for tap water and salinity.

CONCLUSIONS

Tracers are used in the physical modeling experiments carried out in the laboratory scale to determine the initial dilution capacities of plants where dense wastewater is discharged to the sea. The accuracy of dilution factors of wastewater jet in the receiving ambient depends on the sensitive measurement of dye tracers. In laboratory experiments, some margin of error is present up to a defined level. For real project designs, the margin of error values is used as a security factor. A low margin of error is important in the construction of more economical designs. High accuracy in the experimental results in the physical modeling studies for sea outfall system designs means that the selected security factor will be low. Therefore, the accuracy of experimental studies is highly important. For physical modeling, experimental studies use RhB for tracing dye and brine (NaCl) is used to obtain dense wastewater. The stock solution as the source of wastewater and water samples taken at definite points of the experiment tank is used in spectrophotometric measurements to see the concentration of RhB. With this way, different RhB concentrations produce the RhB concentration – Absorbance (c-I) calibration curve and the samples taken from the experimental study will give absorbance (I) values. These measurements will give the RhB concentrations, and therefore, the dilution values of the wastewater in the receiving environment are obtained. Different concentrations of RhB solutions used to generate the calibration curve are most commonly prepared with distilled water with no salt content. However, generally tap water is used to prepare NaCl and high concentration of RhB stock solutions along with the receiving environment water. Since different water sources are used in the preparation of calibration curve and experimental solutions, the accuracy investigation of measured absorbance values is important. In this study, the change of RhB absorption, measured with spectrophotometry, in used water sources of the experimental studies are investigated by including salinity concentrations. For this purpose, both RhB, and NaCl solutions were prepared and distilled water and tap water were used as water sources; the c-I calibration curves were generated. The c-I measurements at 30-100 ppt salinity were compared and there were differences in measurements. These differences are caused by both the concentration of NaCl and the constituents of tap water. In solutions where tap water was used, increasing NaCl concentrations gave a linear I/c line. In addition, in order to decrease the experimental errors for tap water used in the lab scale dye tracer studies, a mathematical expression for S-I/c relation was suggested in the studied range. With the recommended mathematical equation, the amount of salinity effect on the c-I calibration curve could be predicted for tap water condition in the range of 30-100 ppt. According to the result of this study, by referring to salinity, the absorbance difference between solutions prepared with distilled water and tap water will guide researchers to the application of laboratory experiments of brine outfall systems in the forthcoming studies.

ACKNOWLEDGEMENTS

This work was supported by Scientific Research Project Coordination Unit of Istanbul University. Project number: 26561.

REFERENCES

[1] Mondal, P.K., Ahmad, R., Usmani, S.Q. (2010) Anaerobic Biodegradation of Triphenylmethane Dyes in a Hybrid UASFB Reactor for Wastewater Remediation. Biodegradation. 21, 1041

[2] Qi, Z.-P., Liu, Q., Zhu, Z.-R., Kong, Q., Chen, Q.-F., Zhao, C.-S., Liu, Y.-Z., Miao, M.-S., Wang, C. (2016) RhB Removal from Aqueous Solutions Using Loofah Sponge and Activated Carbon Prepared from Loofah Sponge. Desalination Water Treatment. 57, 29421.

[3] Tiwari, D., Kim, W., Kim, M., Prasad, S.K., Lee, S.-M. (2015) Organo-Modified Sericite in the Remediation of Phenol Contaminated Waters. Desalination Water Treatment. 53, 446.

[4] Khan, T.A., Nazir, M., Khan, E.A. (2013) Adsorptive Removal of RhB from Textile Wastewater Using Water Chestnut (*Trapa Natans* L.) Peel: Adsorption Dynamics and Kinetic Studies. Toxicological and Environmental Chemistry. 95, 919

[5] Nemlioglu, S., Sezgin, N. (2014) Water Depth Effects on Initial Dilution of Horizontally Discharged Cold Water from an Elevated Outfall. International Journal of Global Warming. 6(2-3), 284.

[6] Lillie, R.D. (1977) Conn's Biological Stains. (Ed.- Lillie, R.D.). Williams & Wilkins, Baltimore, Md, U.S.A.

[7] Gabrovsek, F., Kogovsek, J., Kovacic, G., Petric, M., Ravbar, N., Turk, J. (2010) Recent Results of Tracer Tests in the Catchment of the Unica River (SW Slovenia). Acta Carsologica. 39 (1), 27.

[8] Carvalho, J.B., Roberts, P.J.W., Roldao, J. (2002) Field Observations of Ipanema Beach Outfall. Journal of Hydraulic Engineering. 128(2), 151.

[9] Magal, E., Weisbrod N., Yakirevich, A., Yechieli, Y. (2008) The Use of Fluorescent Dyes in Highly Saline Groundwater. Journal of Hydrology. 358, 124.

[10] Adams, E.E., Stolzenbach, K.D., Lee, J.-J., Funk, D. (1998) Deposition of Contaminated Sediments in Boston Harbor Studied Using Fluorescent Dye and Particle Tracers, Estuarine. Coastal and Shelf Science. 46, 371.
[11] Roberts, P.W.C., Hunt, D., Mickelson, M.J., Tian, X. (2011) Field and Model Studies of The Boston Outfall. Journal of Hydraulic Engineering. 137(11), 1415.
[12] Hunt, C.D., Mansfield, A.D., Mickelson, M.J., Albro, C.S., Geyer, W.R., Roberts, P.J.W. (2010) Plume Tracking and Dilution of Effluent from the Boston Sewage Outfall. Marine Environmental Research. 70(2), 150.
[13] Gungor, E., Roberts, P.J.W. (2009) Experimental Studies on Vertical Dense Jets in a Flowing Current. Journal of Hydraulic Engineering. 135(11), 935.
[14] Budavari, S. (Ed.) (1989) The Merck Index an Encyclopedia of Chemicals, Drugs, and Biologicals. Merck & Co., Inc., Rahway, N.J., U.S.A.
[15] Gurr, E. (1971) Synthetic Dyes in Biology, Medicine and Chemistry. Academic Press, London, England.
[16] Abril, J.M., Abdel-Aal, M.M., Al-Gamal, S.A., Abdel-Hay, F.A., Zahar, H.M. (2000) Marine Radioactivity Studies in The Suez Canal, Part II: Field Experiments and a Modelling Study of Dispersion. Coastal and Shelf Science. 50, 503.
[17] Bayat, C., Nemlioglu, S., Altuncu, F.F., Berkun, M. (2003) Experimental Scaling Originated Differences in Cold Water Outfall Design. Mesaep & Secotox 12th International Symposium on Environmental Pollution and its Impact on Life in the Mediterranean Region, Poster No. A58, Antalya, Turkey.
[18] Grace, R.A. (1978) Marine Outfall Systems Planning, Design and Construction. Prentice-Hall, Inc., Englewood Cliffs, New Jersey, U.S.A.
[19] Roberts, P.J.W., Toms, G. (1987) Inclined Dense Jets in Flowing Current. Journal of Hydraulic Engineering, ASCE. 113(3), 323.
[20] Stoll, M.H.C., Bakker, K., Nobbe, G.H., Haese, R.R. (2001) Continuous-Flow Analysis of Dissolved Inorganic Carbon Content in Seawater. Analytical Chemistry. 73, 4111.
[21] Qin, X., Liu, F., Wang, G. (2015) Adsorption of Humic Acid from Aqueous Solution By Hematite: Effects of pH and Ionic Strength. Environmental Earth Sciences. 73, 4011.
[22] Iski, Istanbul Water Quality Report (July 2016) Retrieved from: Http://Www.Iski.Gov.Tr, Istanbul, 2016.

Received: **28.04.2017**
Accepted: **31.01.2018**

CORRESPONDING AUTHOR

Semih Nemlioglu
Istanbul University,
Faculty of Engineering,
Department of Environmental Engineering,
34320 Avcilar, Istanbul

e-mail: snemli@istanbul.edu.tr

© by PSP Volume 27 – No. 5/2018 pages 2642-2648 Fresenius Environmental Bulletin

COCONUT OIL-LOADED CHITOSAN NANOPARTICLES FOR THE TREATMENT OF ACNE VULGARIS: CYTOTOXICITY, ANTIBACTERIAL ACTIVITY, AND ANTIBIOFILM PROPERTIES

Rabia Cakir-Koc[1,*], Yasemin Budama-Kilinc[1], Zeynep Kaya[1], Buse Berber Orcen[1,2], Ezgi Ucarkus[2]

[1]Yildiz Technical University, Faculty of Chemical and Metallurgical Engineering, Department of Bioengineering, Istanbul, Turkey
[2]Nanomik Biotechnology Co., Istanbul, Turkey

ABSTRACT

Acne vulgaris is a skin disease that affects 79%–95% of the adolescent population in western societies. The bacterial agent *Propionibacterium acnes* may colonize sebum-rich follicles, and *Staphylococcus aureus* and *Staphylococcus epidermidis* can be isolated from skin lesions. Hundreds of medicinal plant extracts and oils have been investigated *in vitro* for antibacterial activity against acne vulgaris. However, new approaches are under development for topical delivery of herbal oils as there is a need for novel and more efficient drug-delivery systems. Considering the attractive properties and advantages of chitosan nanoparticles (NPs), we aimed to develop coconut oil-loaded chitosan NPs and to identify their antibacterial effects, antibiofilm properties, and toxicity profile.

Coconut oil-loaded chitosan NPs were prepared using the ionic gelation method based on the interactions between positively-charged chitosan and coconut oil. The NP size was analyzed with a Zetasizer and investigated for antibacterial and antibiofilm effects against *P. acnes*, *S. aureus, S. epidermidis*, and a mixed culture. The toxicity of the developed formulations was studied with the XTT method using L929 fibroblast cells.

These novel chitosan-encapsulated coconut oil NPs showed good antibacterial and antibiofilm effects and are potent candidates for the treatment of acne vulgaris.

KEYWORDS:
Nanoparticle, Chitosan, Coconut Oil, Acne Vulgaris

INTRODUCTION

Acne vulgaris (generally called acne) is a skin disease [1] affecting 79%–95% of the adolescent population in western societies [2]. Acne is an inflammatory disease resulting from *Propionibacterium acnes* colonization in sebum-rich follicles [1]. *Staphylococcus aureus* and *Staphylococcus epidermidis* are other bacterial agents that can be isolated from pustular and nodulocystic skin lesions [3].

Systemic and epicutaneous antimicrobial agents and antibiotics have also been used for several decades. However, antibiotics may be ineffective against antibiotic-resistant bacteria and biofilm formation [4]. Biofilms are defined as communities of single- or multi-bacterial species attached to biological or non-biological surfaces [5, 6]. Bacterial cells within biofilms have certain advantages, such as resistance to antibiotics, chemicals, UV damage, and other unfavorable environmental conditions [7]. *P. acnes* can cause serious skin infections due to biofilm formation. Antibiotics used for treating acne can be ineffective against *P. acnes* biofilms [8]. Novel approaches to replace conventional acne treatments are under wide development [1] due to the limitations of current treatments, including inefficacy against antibiotic-resistant bacteria and biofilm formation.

Coconut oil, an antibacterial herbal oil, has been tested against different microorganisms [9] due to its unique chemical composition of fatty acids (lauric and capric acid), sugars, vitamins, minerals, amino acids, and phytohormones. Coconut oil contains vitamin E and antibacterial compounds and is used to cure and prevent acne and to treat acne scars and blemishes [10]. It is also an effective and safe skin moisturizer and softener [11]. For the topical delivery of herbal oils, new approaches are being developed as there is a need for novel and more efficient drug-delivery systems [12].

Nanodelivery systems for the treatment of wounds and other cutaneous disorders provide a high surface area-to-volume ratio. NPs with dimensions of 1–1000 nm exhibit properties different from those of their macroscale counterparts, including enhanced solubility, bioavailability, permeability, penetration, and retention of active compounds on the outer skin layer [13, 14]. NPs also have the ability to protect and transport drug molecules to specific targets, thus decreasing drug degradation and adverse effects [15]. Chitosan, a natural nontoxic biopolymer derived from the deacetylation of chitin, has been

widely studied as a nanocarrier. In addition to antimicrobial and antifungal properties, the small size and quantum effects of chitosan NPs make them very attractive for drug-delivery applications [16]. Only few studies have studied chitosan as a nanocarrier against acne [17], and there are none specifically on chitosan-encapsulated coconut oil NPs for the treatment of acne. Considering the attractive properties and advantages of both coconut oil and chitosan NPs, we aimed to develop coconut oil-loaded chitosan NPs and to identify the antibacterial, antibiofilm, and toxicity properties of this novel formulation.

MATERIALS AND METHODS

Preparation of coconut oil-loaded chitosan NPs. Coconut oil-loaded chitosan NPs were prepared according to a modified version of the methods reported by Calvo et al. and Yoksan et al. [18, 19]. Chitosan NPs were synthesized by ionotropic gelation of chitosan with tripolyphosphate (TPP, 7758-29-4, Sigma–Aldrich) anions. Chitosan solution (0.25% [w/v]) (75%–85% degree of deacetylation, 9012-76-4, Sigma–Aldrich) was mixed with 2.5-mg chitosan and 1% (v/v) aqueous acetic acid solution at 60°C for 45 min using magnetic stirrer. Coconut oil (140 µg) was then added to Tween 80 (hydrophilic–lipophilic balance [HLB] 15.9, 1.5%) as a surfactant and stirred at room temperature for 2 h to obtain a homogeneous mixture. Then, chitosan NPs were spontaneously synthesized by the dropwise addition of the chitosan solution to TPP solution during magnetic stirring (110×g, 2 h) at room temperature. The suspension was filtered through 0.45-µm pore-size filters.

Preparation of chitosan NPs. Chitosan NPs were synthesized using the same method without coconut oil. Briefly, the chitosan solution was prepared in an aqueous acetic acid solution [1% (v/v)]; then, Tween 80 (HLB 15.9, 1.5%) was added as a surfactant, and the solution was stirred at room temperature for 2 h to obtain a homogeneous mixture. Chitosan NPs were spontaneously fabricated with the dropwise addition of 5 mL of the chitosan solution to 6 mL of TPP solution under magnetic stirring (110×g, 2 h) at room temperature; these were then filtered through 0.45-µm pore-size filters.

Zetasizer analysis of coconut oil-loaded chitosan NPs. The average particle size and size distribution (polydispersity index [PDI]) of the particles were measured based on the dynamic light scattering (DLS) technique. A Zetasizer Nano ZS (Malvern Instruments, UK) instrument equipped with a 4.0-mV He–Ne laser (633 nm) was used at 25°C. Next, the samples were filtered in phosphate-buffered saline (PBS) by using 0.22-µm pore size filter.

Transmission electron microscopy analysis. The solution of coconut oil-loaded chitosan NPs was placed directly into an ultrasonic bath at room temperature for 1–2 min; then, two drops of the solution were deposited on a Formvar-coated, carbon-supported copper grid. Thereafter, TEM imaging was performed with a JEOL JEM 1400 Plus at 80 kV.

Bacterial strains and culture. *P. acnes* 6919 was kindly provided from the Anadolu University, Eskisehir, Turkey. *S. aureus* ATCC 25923 and *S. epidermidis* ATCC14990 were kindly provided from the Yeditepe University, Istanbul, Turkey. All strains were cultivated in enriched thioglycollate broth (HiMedia, M738) at 37°C for 24 h. Thioglycollate medium was used for this experiment because it supports the growth of both aerobic and anaerobic microorganisms.

Determination of antibacterial activity and minimum inhibitory concentration (MIC). The antibacterial activity and MIC values of chitosan NPs, coconut oil, and coconut oil-loaded chitosan NPs were determined against the tested microorganisms by the broth microdilution method with some modifications [20]. Briefly, 100 µL of the microorganisms to be tested (*P. acnes, S. aureus, S. epidermidis*, and the mix culture) containing 0.5 Mc Farland at the final concentration was added to 96-well plates. Next, 100 µL of thioglycollate medium (HiMedia, M738) enriched with diluted extracts from stock solutions (140 µg coconut oil in 11 mL, 2.5 mg chitosan in 11 mL, and 140 µg coconut oil + 2.5 mg chitosan in 11 mL) was added to 96-well plates with different dilutions (50%, 25%, 12.5%, 6.5%, and 3.125%) and incubated at 37°C for 24 h. Ampicillin (Thermo Fisher, 11593027) was used as a positive control. After incubation, the MIC of each extract was spectrophotometrically measured at a wavelength of 600 nm (Multiskan Go Microplate Spectrophotometer, Thermo Fisher Scientific). The lowest concentration of extract that visibly inhibited the microbial growth was considered as the MIC. For anti-biofilm studies, sub-MIC concentrations of these three extracts were selected. Percent viability was estimated with the following formula:

$$\%\,\text{viability} = \frac{\text{absorbance of sample}}{\text{absorbance of control}} * 100$$

Determination of antibiofilm activity. A biofilm-formation assay was performed using the microdilution method as described previously with some modifications [21]. Overnight cultures of all strains (*P. acnes, S. aureus,* and *S. epidermidis)* and the mix culture were diluted 1:100 with thioglycollate medium. Various volumes of diluted cultures were added to 96-well plates. To determine the impact of the various extracts on biofilm formation, chitosan NPs (2.5 mg chitosan in 11 mL), coconut oil (140 µg coconut oil in 11 mL), and coconut oil-

loaded chitosan NPs (140 µg coconut oil and 2.5 mg chitosan in 11 mL) were added to culture suspensions in different dilutions (25%, 12.5%, and 6.25%), and the final volume of the wells was adjusted to 100 µL. Thioglycollate medium was used as the negative control. The microplates were incubated at 37°C for 24 h without shaking. After incubation, the culture suspensions removed from the wells and microplates were washed three times with distilled water. The biofilm was visualized by staining with 125 µL of 0.1% crystal violet (Merck, 1159400025) for 10 min. The microplates were washed with distilled water three times to remove the excess stain. After the microplates had dried, crystal violet was dissolved with 125 µL of 10% acetic acid, and the measurements were performed at 590-nm wavelength.

Determination of cytotoxicity. The L929 cell line was used to determine the cytotoxicity of chitosan NPs, coconut oil, and coconut oil-loaded chitosan NPs. Briefly, the cells were cultured in DMEM-F12 medium (supplemented with 10% fetal bovine serum and penicillin–streptomycin) and incubated at 37°C in 5%CO_2. After 3–4 days, the cultured cells were detached by trypsinization and counted with a hemocytometer.

The L929 cells were seeded (10,000 cells/well) in 96-well flat-bottom microplates with 100 µL of medium. They were incubated for 24 h at 37°C for attachment to the well bottom. Different dilutions (25%, 18%, 12%, and 6.5%) of chitosan NPs (2.5 mg chitosan in 11 mL), coconut oil (140 µg coconut oil in 11 mL), and coconut oil-loaded chitosan NPs (140 µg coconut oil and 2.5 mg chitosan in 11 mL) were added and incubated for another 24 h. The media containing chitosan or NPs were then aspirated, and 100 µL of 2,3-bis-(2-methoxy-4-nitro-5-sulfophenyl)-2H-tetrazolium-5-carboxanili-de (XTT) solution in fresh medium was added to the wells at a concentration of 0.5 mg/mL (with 7.5 µg/mL phenazine methosulfate). The pla-tes were incubated for 3 h at 37°C, and the optical density was measured at 450 nm using a multi-plate reader (Thermo Labsystems Multiskan Ascent 354 Microplate Photometer).

RESULTS

The preparation of chitosan NPs was based on an ionic gelation interaction between positively-charged chitosan and coconut oil. Empty chitosan NPs were also synthesized for a comparison of effects on cells. Particle size, surface charge, and PDI are important considerations in the design of delivery systems for bioactive compounds. In theory, the most ideal NPs have the smallest size, highest surface charge, and lowest PDI [22].

The size and size distribution of chitosan NPs and coconut oil-loaded chitosan NPs were analyzed using the Zetasizer. In the size distribution profile, a typical batch of chitosan NPs had a mean diameter of 37.93 nm and a narrow size distribution (PDI). The size of coconut oil-loaded chitosan NPs was approximately 11.08 nm with a PDI of 0.124. TEM images of coconut oil-loaded chitosan NPs clearly showed spherical structure (Figure 1).

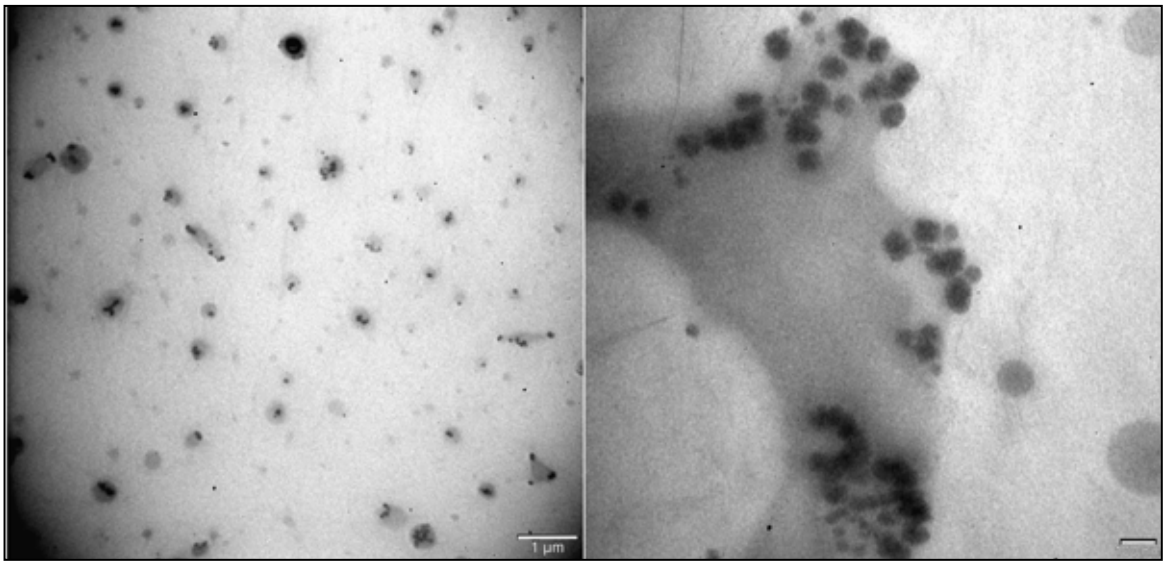


FIGURE 1
TEM images of coconut oil-loaded chitosan NPs.

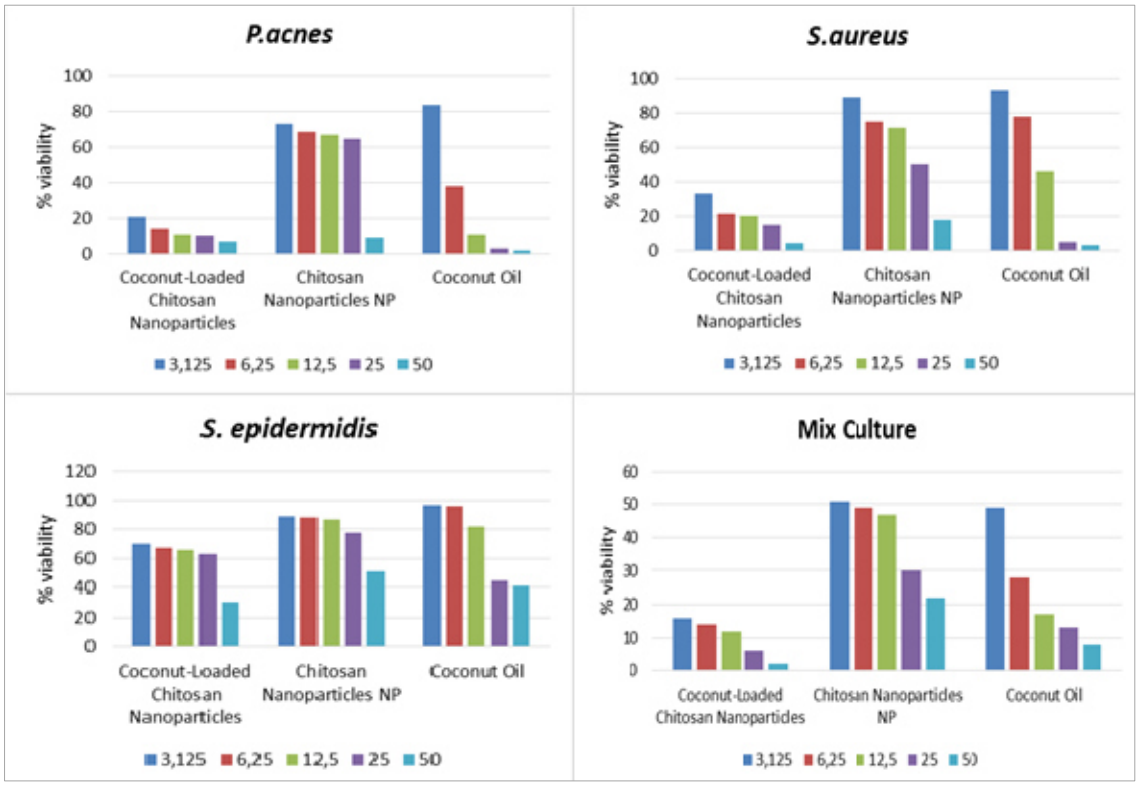


FIGURE 2
Antibacterial effects of coconut oil and of chitosan NPs with or without coconut oil

Coconut oil, chitosan NPs, and coconut oil-loaded chitosan NPs were analyzed with the Zetasizer, and the morphology of the loaded NPs was observed on TEM. All results indicated that the loaded NPs were formed successfully. Then, the antibacterial and antibiofilm effects of coconut oil-loaded chitosan NPs were analyzed. The *in vitro* results of the antibacterial activity tests of chitosan, coconut oil, and coconut oil-loaded chitosan NPs are shown in Figure 2. The highest concentration of chitosan showed a strong antibacterial activity against *P. acnes* (9% viability), *S. aureus* (18% viability), and the mixed bacterial culture (22% viability). However, at lower concentrations, the antibacterial activity of chitosan was decreased. Chitosan did not show significant antibacterial activity against *S. epidermidis* (51% viability). Coconut oil showed significant antibacterial activity against all tested bacterial species, except for *S. epidermidis* (41% viability). Particularly against the mixed culture, coconut oil showed antibacterial activity even at lower concentrations. Coconut oil-loaded chitosan NPs showed relatively strong antibacterial activity against *P. acnes* (7% viability), *S. aureus* (4% viability), *S. epidermidis* (31% viability), and the mixed culture (2% viability). In addition, coconut oil-loaded chitosan NPs decreased the concentration of *S. epidermidis* more than the two other groups.

Chitosan decreased biofilm formation of all tested pathogens, albeit not significantly. As seen in Figure 3, the highest concentration of coconut oil decreased biofilm formation in all tested groups, except for *S. aureus*; however, the lower concentrations showed no significant anti-biofilm activity. Coconut oil-loaded chitosan NPs showed high antibiofilm activity, particularly against *S. aureus* with 6.25% and 12.5% dilutions.

After determining the antibacterial and antibiofilm effects of coconut oil and of NPs with or without coconut oil, the fibroblast toxicity profile was assayed with the XTT method.

As seen in Figure 4, chitosan NPs had no toxic effect on fibroblast cells. Coconut oil showed a low degree of toxicity, but chitosan encapsulation prevented such toxicity. There were no adverse effects on fibroblasts from chitosan-encapsulated coconut oil NPs at any of the studied concentrations.

The results showed that chitosan NPs had good antibacterial and antibiofilm effects at non-toxic concentrations.

DISCUSSION

For the first time in the literature, this study has shown the antibacterial and antibiofilm effects of coconut oil-loaded chitosan NPs. These NPs demonstrated excellent antibacterial and antibiofilm effects at non-toxic concentrations.

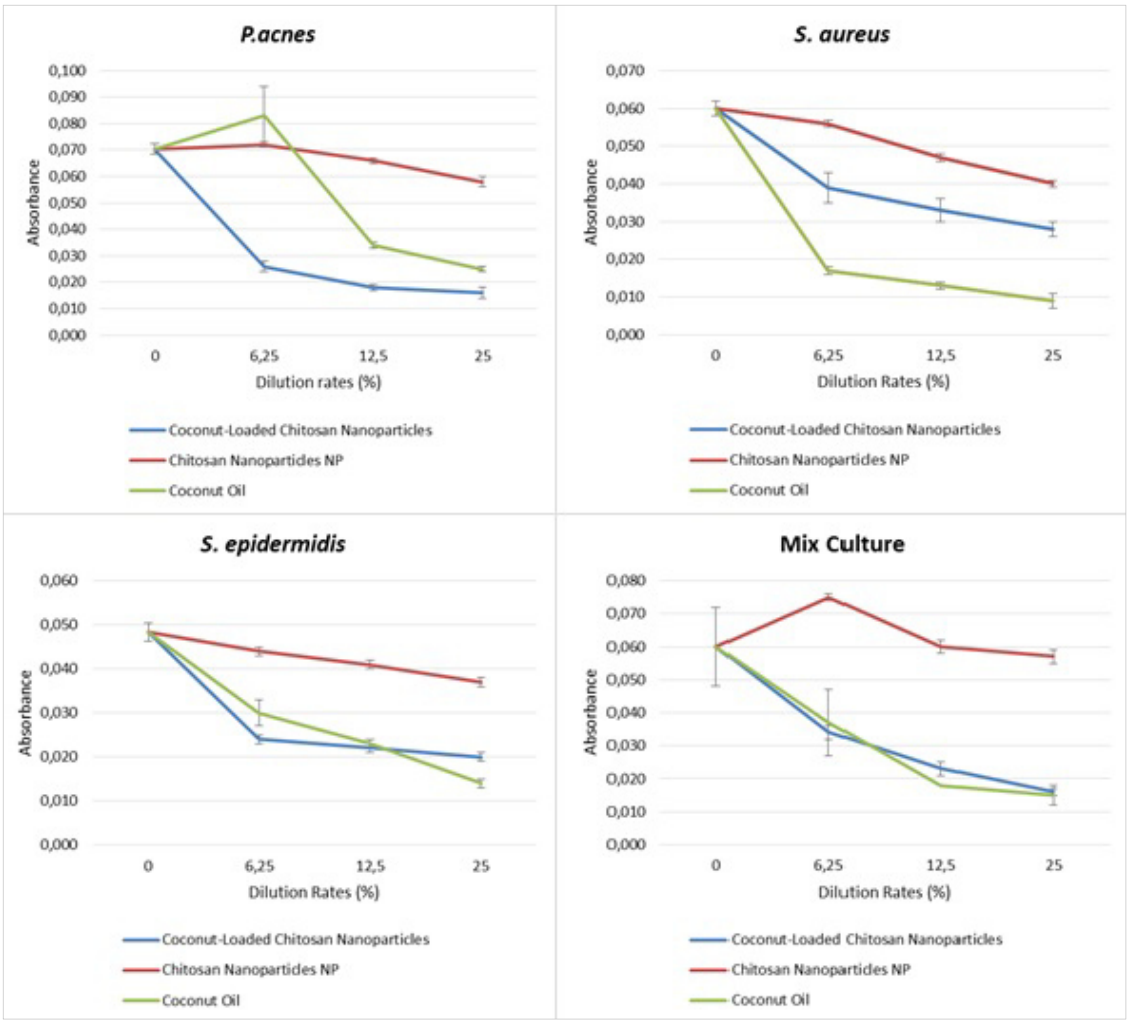


FIGURE 3
Biofilm formation of bacteria exposed to coconut oil and to chitosan NPs with or without coconut oil.

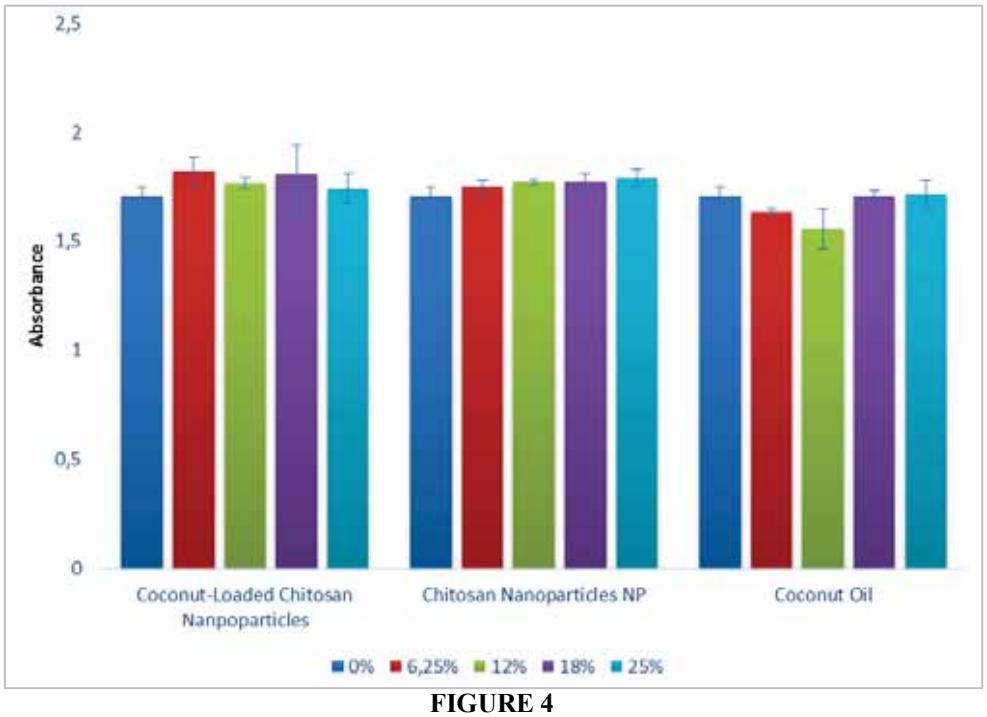


FIGURE 4
Toxicity of coconut oil and of chitosan NPs with or without coconut oil against L929 fibroblast cells

The antibacterial, antifungal, antiviral, and antiparasitic effects of coconut oil have been reported in several previous studies. Like many medicinal plants, coconut shows excellent antibacterial activity against life-threatening infections [9]. In our study, coconut oil used alone showed strong antibacterial effects, particularly against *P. acnes* and *S. aureus*. *S. aureus* and *P. acnes* are known to be primarily responsible for acne [3], and defenses against these bacteria are important for the treatment of this condition. Effects against *S. epidermidis* were also observed; however, they were not as strong as the effects in the mixed culture. The mixed culture was prepared as a model for acne vulgaris by including the common bacteria involved in acne [3].

A biofilm is defined as a community of bacteria enclosed in an extracellular matrix [23]. Little is known about the antibiofilm effects of coconut oil in the literature. Our results showed that coconut oil displays antibiofilm effects against selected bacteria separately as well as in mixed cultures. The antibacterial and antibiofilm effects of coconut oil make it a very attractive candidate for the treatment of acne vulgaris. Herein, to increase its efficacy and to provide a delivery system, coconut oil was encapsulated in a chitosan biopolymer of nanodimensions. The antibacterial properties of chitosan biopolymers are well known, and their antibiofilm properties have also been shown in a few studies [23, 24]. The present study showed that nano-sized empty chitosan NPs displayed antimicrobial and antibiofilm effects. These effects were weaker than those of coconut oil; however, when coconut oil is encapsulated in chitosan, the total antibacterial effect is significantly increased. At the lowest dilution, the percent viability of *P. acnes*, *S. aureus*, and mixed culture exposed to chitosan-encapsulated coconut oil NPs was approximately 20%.

This increased effect may be caused by a synergistic relationship between coconut oil and chitosan. Another factor may be the nanodimensions of the formulation as it is known that NPs provide greater efficacy against bacterial cells as a result of the quantum-size effect. NPs may be adsorbed, thus disrupting the bacterial membrane. Taken together, nanotechnology makes novel approaches possible for efficient drug-delivery strategies, including for dermatological diseases. Many NP-based formulations are currently commercially available for cosmetic purposes [15].

Chitosan is a well-known biocompatible polymer; however, to our knowledge, the toxicity of chitosan-encapsulated coconut oil NPs has not been previously studied. Therefore, we evaluated the toxicity of our newly developed chitosan-based coconut oil NPs and found no toxicity against fibroblast cells.

These novel chitosan-encapsulated coconut oil NPs, owing to their strong antibacterial and antibiofilm effects, may be a good candidate for the treatment of acne vulgaris. Effective and non-toxic concentrations may be used directly as acne treatments or as additives in anti-blemish cosmetic products.

REFERENCES

[1] Yang, D., Pornpattananangkul, D., Nakatsuji, T., Chan, M., Carson, D., Huang, C.M., Zhang, L. (2009) The antimicrobial activity of liposomal lauric acids against Propionibacterium acnes. Biomaterials. 30, 6035-6040.

[2] Cordain, L., Lindeberg, S., Hurtado, M., Hill, K., Eaton, S.B., Brand-Miller, J. (2002) Acne vulgaris: a disease of Western civilization. Archives of dermatology. 138, 1584-1590.

[3] Hassanzadeh, P., Bahmani, M., Mehrabani, D. (2008) Bacterial resistance to antibiotics in acne vulgaris: An in vitro study. Indian journal of dermatology. 53, 122.

[4] Høiby, N., Bjarnsholt, T., Givskov, M., Molin, S., Ciofu, O. (2010) Antibiotic resistance of bacterial biofilms. International journal of antimicrobial agents. 35, 322-332.

[5] Hall-Stoodley, L., Costerton, J.W., Stoodley, P. (2004) Bacterial biofilms: from the natural environment to infectious diseases. Nature reviews microbiology. 2, 95-108.

[6] O'Toole, G., Kaplan, H.B., Kolter, R. (2000) Biofilm formation as microbial development. Annual Reviews in Microbiology. 54, 49-79.

[7] de la Fuente-Núñez, C., Reffuveille, F., Fernández, L., Hancock, R.E. (2013) Bacterial biofilm development as a multicellular adaptation: antibiotic resistance and new therapeutic strategies. Current opinion in microbiology. 16, 580-589.

[8] Coenye, T., Peeters, E., Nelis, H.J. (2007) Biofilm formation by Propionibacterium acnes is associated with increased resistance to antimicrobial agents and increased production of putative virulence factors. Research in microbiology. 158, 386-392.

[9] DebMandal, M., Mandal, S. (2011) Coconut (Cocos nucifera L.: Arecaceae): In health promotion and disease prevention. Asian Pacific journal of tropical medicine. 4, 241-247.

[10] Kapoor, S., Saraf, S. (2011) Topical herbal therapies an alternative and complementary choice to combat acne. Res J Med Plant. 5, 650-659.

[11] Gediya, S.K., Mistry, R.B., Patel, U.K., Blessy, M., Jain, H.N. (2011) Herbal plants: used as a cosmetics. J Nat Prod Plant Resour. 1, 24-32.

[12] Jackson, J.E., Kopecki, Z., Cowin, A.J. (2013) Nanotechnological Advances in Cutaneous Medicine. J Nanomater. 2013, 8p.

[13] Jadhav, N., Powar, T., Shinde, S., Nadaf, S. (2014) Herbal nanoparticles: A patent review. Asian journal of Pharmaceutics. 8.

[14] Ganesan, P., Choi, D.-K. (2016) Current application of phytocompound-based nanocosmeceuticals for beauty and skin therapy. International journal of nanomedicine. 11, 1987.
[15] Jackson, J.E., Kopecki, Z., Cowin, A.J. (2013) Nanotechnological advances in cutaneous medicine. J Nanomater. 2013, 16.
[16] Qi, L., Xu, Z., Jiang, X., Hu, C., Zou, X. (2004) Preparation and antibacterial activity of chitosan nanoparticles. Carbohydrate research. 339, 2693-2700.
[17] Ridolfi, D.M, Marcato, P.D., Justo, G.Z., Cordi, L., Machado, D., Durán, N. (2012) Chitosan-solid lipid nanoparticles as carriers for topical delivery of tretinoin. Colloids and Surfaces B: Biointerfaces. 93, 36-40.
[18] Calvo, P., Remunan-Lopez, C., Vila-Jato, J., Alonso, M. (1997) Novel hydrophilic chitosan-polyethylene oxide nanoparticles as protein carriers. Journal of Applied Polymer Science. 63, 125-132.
[19] Yoksan, R., Jirawutthiwongchai, J., Arpo, K. (2010) Encapsulation of ascorbyl palmitate in chitosan nanoparticles by oil-in-water emulsion and ionic gelation processes. Colloids and Surfaces B: Biointerfaces. 76, 292-297.
[20] Zgoda, J., Porter, J. (2001) A convenient microdilution method for screening natural products against bacteria and fungi. Pharmaceutical Biology. 39, 221-225.
[21] Zhang, J., Rui, X., Wang, L., Guan, Y., Sun, X., Dong, M. (2014) Polyphenolic extract from Rosa rugosa tea inhibits bacterial quorum sensing and biofilm formation. Food Control. 42, 125-131.
[22] Bulmer, C., Margaritis, A., Xenocostas, A. (2012) Production and characterization of novel chitosan nanoparticles for controlled release of rHu-Erythropoietin. Biochemical engineering journal. 68, 61-69.
[23] Tan, Y., Leonhard, M., Moser, D., Schneider-Stickler, B. (2016) Antibiofilm activity of carboxymethyl chitosan on the biofilms of non-Candida albicans Candida species. Carbohydrate polymers. 149, 77-82.
[24] Carlson, R.P., Taffs, R., Davison, W.M., Stewart, P.S. (2008) Anti-biofilm properties of chitosan-coated surfaces. Journal of Biomaterials Science. Polymer Edition. 19, 1035-1046.

Received: **27.10.2017**
Accepted: **20.02.2018**

CORRESPONDING AUTHOR

Rabia Cakir-Koc
Yildiz Technical University,
Davutpasa Campus,
Faculty of Chemical and Metallurgical Engineering,
Department of Bioengineering,
Davutpasa Street,
34210 Esenler, Istanbul – Turkey

e-mail: rabiacakir@gmail.com

© by PSP Volume 27 – No. 5/2018 pages 2649-2653 Fresenius Environmental Bulletin

THE EFFECTS OF OLIVE MILL WASTEWATER IN FOUR ADSORBENTS ON GERMINATION CHARACTERISTICS OF WHEAT (*TRITICUM AESTIVUM* L.)

Ilkay Yavas*

Adnan Menderes University, Kocarli Vocational High School, Department of Crops and Animal Production, Aydin, Turkey

ABSTRACT

Olive mill wastewater (OMWW) has been a significant environmental problem in countries producing them. Therefore a randomized parcel design with two factors was set up during the germination period to assess effects of different adsorbent materials on OMWW phytotoxicity on wheat (*Triticum aestivum* L.) growth parameters. The different concentrations of OMWW and perlite, zeolite, fine sand and volcanic tuff as adsorbent are used materials. The best germination percentage and seedling growth were found in control and OMWW at 25% concentration respectively. Results of germination studies showed that at 25% concentrations of OMWW along with application of perlite, zeolite, fine sand and volcanic tuff increased the germination (%), germination index, seedling length, root length and shoot length of the crop. The results indicated that 100, 75, and 50% OMWW were very phytotoxic and completely prohibited seed germination. In our other studies examining the effects of adsorbent dose; phytotoxicity decreased significantly by the 25 % OMW dilution, and along with adsorbents (0.8 g) as results of removing the phenols and other phytotoxic organic compounds. In conclusion, the zeolite and volcanic tuff can be used at 0.8 g and 0.5 g doses to reduce the negative effects of 50% and 25% OMWW respectively.

KEYWORDS:
Adsorbents, germination percentage, wheat, Olive mill wastewater, seedling growth

INTRODUCTION

There are about 750 million olive tree species in the world, 98% of them living in the Mediterranean region. Main producers of olive oil are Spain, Italy, Greece, Turkey, Tunisia, Portugal, Morocco, and Algeria. Olive mill waste water (OMWW) is a violet-dark brown up to black liquid which is caused by polyhenols that contains high percentage of water, organic acids mineral nutrients, phenols, pectins and sugars. Therefore its high phenol, lipid and organic acid concentrations they are phytotoxic materials [1, 2] and becoming enormous problems for crops, aquatic life, environment and human health in the Mediterranean region [3, 4, 5, 6, 7, 8, 9].

On the other hand the high potassium, nitrogen, phosphorus, calcium, magnesium, and iron levels in OMWW are favourable for soil fertility. Thus, addition of this matter can accelerate leaching of Na^+, reduce the electrical conductivity, and enhance water infiltration, waterholding capacity, and aggregate stability especially in sodic soils [7].

It was indicated that adsorbent material using with low cost and high metal binding capasity is a suitable method to waste water such as olive mill and, different absorbent materials are used for decontamination of soil and water [10]. Kocadaglı et al. [8] showed that resin can be a suitable adsorbent material for removal of phenolic compounds in OMWW.

This investigation focused on some adsorbents such as perlite, zeolite, fine sand and volcanic tuff materials. We aimed to reduce the phytotoxic compounds produced by OMWW using with these materials and assess seed germination and seedling growth of *Triticum aestivum* L. during the germination and seedling period.

MATERIALS AND METHODS

Materials. This research was conducted at Kocarli Vocational High School's laboratory located at the Adnan Menderes University in Turkey. Experimental plots were arranged in randomized parcel design with two factors and five replicates. Germination tests were conducted with wheat seed (*Triticum aestivum* L.) with as control along with 4 different concentrations (25%, 50%, 75% and 100%) of treated oil mill wastewater (factor 1). Twenty five healty wheat seeds were placed on filter papers installed in petri plates and incubated for 7 days in dark conditions 25 ^oC. Ten milliliter of tap water was placed in petri plate for the control treatment, instead of oil mill wastewater (OMWW). OMWW used as liquid was obtained from olive oil

mill in the Aydin province. The seeds were sown 4 various growing adsorbents (perlite, zeolite, fine sand and volcanic tuff as factor 2). In other experiment, OMWW, adsorbents and three different doses (0.3 g, 0.5 g, 0.8 g) of adsorbents were only evaluated for germination pertentage. The zeolite used in this study was obtained from the mines of Manisa-Gördes located in Aegean District of Turkey.

Methods. After the two days period, the observations of seeds were recorded daily up to 5 days. At the end of the 7th day, a number of growth parameters such as root length, shoot length, seedling growth length phytotoxicity index, phytotoxicity (%) and tolerance index were measured.

Germination (%): Germination was defined by radical emergence [11] as follows;

Germination (%) =[total number of seeds germinated/total number of seeds sown] x 100

The following charactersitics were determined according to [12]. Root length (cm) was measured from the tip of the primary radicle to the base of hypocotyl. Shoot length (cm) was measured from the base of the primary leaf to the base of the hypocotyl. Seedling growth length (cm) was calculated by adding the root length and shoot length.

Phytotoxicity index (PI): It was estimated using equation; PI = 1 – RLT/RLC

RLT= Root length in the treated seeds

RLC= Root length in the control treatment.

PI values changes from 0 to 1, in which higher value means a negative (toxic) effect and a lower value means a positive (stimulatory) effect.

The main objective of this study was to evaluate the effect of different adsorbent materials on olive mill wastewater (OMWW) phytotoxicity of wheat (*Triticum aestivum* L.) growth parameters during the germination and seedling period.

Statistical analysis was performed by the SPSS statistical programme, and means were separated by use of LSD test at $p<0.05$.

RESULTS AND DISCUSSION

Effects of OMWW at different dilutions on root length, shoot length, tolerance index, phytotoxicity index and phytotoxicity of wheat was significant (Table 1).

The examined characteristics decreased as OMWW concentrations increased. Higher concentrations (75% and 100%) of OMWW were inhibitory of germination percentage. The seeds showed higher root and shoot length at control than at different concentrations of OMWW in *Triticum aestivum* plants. These results are in line with that obtained by Singh et al. [13]. In a related study, Wins and Murugan [14] observed that higher root and shoot length at 25 % of textile mill effluent than control after 96 hours in *Vigna mungo* plants. These results are similar to those of [11] who considered the root length was higher in 25% Blue water (BW): 75% Oil mill watewater (OMW). Phytotoxicity index (PI) was significantly higher up to 25% doses of OMWW. These results proved that OMWW was very phytotoxic to wheat. Besides Mycin et al. [15] stated that the toxicity of the sugar mill effluent increased gradually with the increase of percentage of phytotoxicity values. Similar results were observed for *Leucaena leucocephala* by Al-Tabbal et al. [11]. Rusan et al. [11] in their experiment on effect of OMWW on seed germination found that, at 25 % OMWW concentrations enhanced dry weight, shoot length and root length, germination percentage and phytotoxicity index. The tolerance index value decreased with increase in the OMWW concentrations. Similarly Mycin et al. [15] found that the tolerance index decreased with increase in the 5% of sugar mill effluent in cowpea plants.

The root length, shoot length, tolerance index, phytotoxicity index and phytotoxicity of wheat were significantly affected by growing medium (Table 2).

While OMWW combined with perlite and zeolite showed better root length and shoot length respecively. Kelepesi and Tzortzakis [7] also found that similar results using OMWW. The highest tolerance index values obtained from zeolite (0.266). Perlite and volcanic tuff gave similar results. The lowest tolerance index was found at fine sand medium. Similar trends were observed on phytotoxicity and phytotoxicity index in wheat. Killi and Erol [16] in their experiment to evaluate seed germination and seedling growth based vegetation waster also found similar results.

The effect of OMWW on seedling growth length was found to be statistically significant with treament at various concentrations of OMWW as well as between different medium. The seedling growth length was also increased at lower concentrations of OMWW (Table 3).

The results of the data was 2 zero counts which were observed at the 75% and 100% OMWW levels. The values were increased with control conditions and thereafter they declined gradually towards high concentrations of OMWW. Mixing adsorbents into the growing medium resulted in increased seedling length. The highest seedling growth length values were generally obtained from the combination of 25% OMWW with zeolite and volcanic tuff after control conditions.

The germination percentage of wheat was significantly affected by growing medium and adsorbent doses (Table 4). Increasing levels of adsorbents in growing media were effective in seed germination of wheat. The adding of some adsorbents (perlite and zeolite) gave higher values at different OMWW conditions.

TABLE 1
Effects of different treatment of OMWW on root and shoot length, tolerance index, phytotoxicity index and phytotoxicity

Treatment	Root length (cm)	Shoot length (cm)	Tolerance index	Phytotoxicity index	Phytotoxicity (%)
Control	10.27 a	4.490 a	-	-	-
25% OMWW	3.289 b	4.093 b	0.321 a	0.680 b	67.990 b
50% OMWW	1.833 c	2.397 c	0.178 b	0.823 a	82.340 a
75% OMWW	0.0 d	0.0 d	0.0 c	0.0 c	0.0 c
100% OMWW	0.0 d	0.0 d	0.0 c	0.0 c	0.0 c
LSD	0.054	0.053	0.003	0.003	0.287

TABLE 2
Effects of different adsorbent on root and shoot length, tolerance index, phytotoxicity index and phytotoxicity

Medium	Root length (cm)	Shoot length (cm)	Tolerance index	Phytotoxicity index	Phytotoxicity
Perlite	5.063 a	3.564 c	0.249 b	0.751 b	75.090 b
Zeolite	5.427 b	3.991 a	0.266 a	0.734 c	73.660 c
Fine Sand	4.871 c	3.389 d	0.230 c	0.770 a	77.080 a
Volcanic Tuff	5.161 d	3.687 b	0.251 b	0.749 b	74.830 b
LSD	0.065	0.059	0.007	0.007	1.016

TABLE 3
Effects of different concentrations of OMWW and different adsorbent on seedling length

Treatment	Adsorbents			
	Perlite	**Zeolite**	**Fine Sand**	**Volcanic Tuff**
Control	14.440 a	15.460 a	14.260 a	14.900 a
25% OMWW	7.264 b	8.054 b	6.814 b	7.398 b
50% OMWW	4.178 c	4.738 c	3.726 c	4.276 c
75% OMWW	0.0 d	0.0 d	0.0 d	0.0 d
100% OMWW	0.0 d	0.0 d	0.0 d	0.0 d
LSD	0.112			

TABLE 4
Effects of different concentrations of OMWW and different adsorbent on germination percentage

	Perlite			**Zeolite**			**Fine Sand**			**Volcanic Tuff**		
OMWW (%)	**0.3g**	**0.5g**	**0.8g**	**0.3g**	**0.5g**	**0.8g**	**0.3g**	**0.5g**	**0.8g**	**0.3g**	**0.5g**	**0.8g**
Control	94.6a	94.9a	95.1a	94.5a	95.4a	96.1a	91.9a	92.3a	95.4a	95.1a	95.3a	96.5a
25	22.7b	33.1b	34.1b	69.8b	71.1b	74.1b	27.3b	28.9b	31.0b	69.5b	71.5b	76.0b
50	19.0c	19.6c	28.0c	63.5c	69.4c	71.3c	24.1c	28.1b	28.0c	64.5c	71.2b	72.8c
75	0.0d	0.0d	0.0d	0.0d	0.0d	0.0d	0.0d	0.0d	0.0d	0.0d	0.0c	0.0d
100	0.0d	0.0d	0.0d	0.0d	0.0d	0.0d	0.0d	0.0d	0.0d	0.0d	0.0c	0.0d
LSD	1.57											

Ogboi et al. [17] in their experiment on influence of palm oil mill effluent (POME) on seed germination found that, germination rate at the first two days after planting, zero germination was recorded. At the 4rd day after planting, 100% germination was observed in POME application while 65 % germination was recorded in non-POME application. Dash [18] found that, seed germination efficiency and vigor index of rice and wheat was increased progressively with increasing doses of domestic waste water up to 50% and thereafter it decreased. Results indicated that growing media (100 % zeolite, 100 % perlite) had similar influences on the germination percentage, height, stem diameter, and fresh weight of cucumber seedlings. Besides zeolite, turf, and perlite mixture affect seedling improvement [19]. Seed germination percentage for green gram and mustard decreased with increasing sugar industry concentrations. At lower dilutions (75%) the seeds showed positive effect on germination and seedling growth [20]**.** Germination percentage of kidney bean was higher at control, followed by 50% and 25% respectively. Germination percentage and seedling growth were inhibited at 100% concentration of POME at 24 hrs. The root and shoot length were decreased with increasing

palm oil mill effluent (POME) concentration as compared to that of control These results are in line with those obtained by [13]. Muscolo et al. [21] mentioned that low concentrations of OMWW didn't reduce seed germination and seedling growth. Dilution with water at a high ratio reduced OMW phytotoxicity.

CONCLUSION

The results of the study showed that the raw oil mill wastewater directly affects the wheat germination percentage and other growth parameters. The results of germination percentage showed germination (%) higher than 50% only for control, 25% and 50% treatments. Therefore apply of OMWW (at 25% and 50%) may be used for germination and seedling production. OMWW can be used in agricultural practices after proper dilutions. For, 75 % and 100% OMWW treatment showed 0% germination (%) and it's proved that 75% and 100% concentrations of treated OMWW not safely used for agricultural purposes because of its high toxicity level. Therefore they should not be applied presowing due to lowering germination percentage. If it dilutes, salt content can be reduced. Thus germination problem can be eliminated. The using zeolite and volcanic tuff were efficient in reducing the detrimental effects of OMWW. Therefore it has a significant impact on germination and seedling growth. They will be effective at the seedling stage because of increasing N content of seedling adhere to the root. The study suggests that the OMWW can be used safely for wheat, only after dilution and mixing with zeolit or volcanic tuff at 0.8 g and 0.5 g doses.

REFERENCES

[1] Ozden, A. and Dios-Palomares, R. (2015) Environmental, quality and technical efficiency in olive oil industry. A metafrontier comparison between Turkey and Spain. Fresen. Environmen. Bull. 24, 4353-4363.

[2] Vaizoğullar, A.L., Ugurlu, M., Ayyildiz, A., Yilmaz, S.I. and Chaudhary, A.J. (2017) TiO2, WO3, and V2O5, Supported on Activated carbon: Preparation, Structural and Catalytic Behaviour in Photocatalytic Treatment of Phenol and Lignin from Olive Mill Wastewater. Fresen. Environ. Bull. 26, 3529-3541.

[3] Tsagaraki, E., Lazarides, H.N. and Petrotos, K.B. (2007) Olive Mill Wastewater Treatment. In: Oreopoulou, V. and. Russ, W. (Eds.) Utilization of By-products and Treatment of Waste in the Food Industry. Springer Science + Business Media, New York. 133-157.

[4] Mebirouk, M., Sbail, L., Lopez, M. and Gonzalez, J. (2007) The absorption of polyphenols from olive oil mill wastewaters by sawdust and biodegradation by the fungus Phanerochaetae chrysosporium. Grasas Y Aceites. 58(4), 366-371.

[5] Leouifoudi, I., Zyad, A., Amechrouq, A., Oukerrou, M.A., Mouse, H.A. and Mbarki, M. (2014) Identification and characterisation of phenolic compounds extracted from Moroccan olive mill wastewater. Food Science and Technology. 34(2), 249-257.

[6] Otles, S. and Selek, I. (2012) Treatment of Olive Mill Wastewater and the Use of Polyphenols Obtained After Treatment. International Journal of Food Studies. 1, 85-100.

[7] Kelepesi, S. and Tzortzakis, N.G. (2009) Olive Mill Wastes-A Growing Medium Component for Seedling and Crop Production of Lettuce and Chicory. International Journal of Vegetable Science. 15, 325-339.

[8] Kocadaglı, T., Ataç Mogol, B. and Gökmen, V. (2014) Removal of Phenolic Compounds from Olive Mill Wastewater by Adsorbent Resins. Desalination and Water Treatment. 52(13-15), 2875-2885.

[9] PROSODOL (2012) Strategies to improve and protect soil quality from the disposal of Olive Oil Mill Wastes in the Mediterranean region: Results and Achievements of a 4-year demonstration project. What to consider; What to do. Doula, M.K., Kavvadias, V., Komnitsas, K., Tinivella, F., Moreno-Ortego, J.L., Sarris, A. (Eds.) LIFE07 ENV/GR/000280.

[10] Azmat, R., Akhter, Y., Ahmed, T. and Qureshi, S. (2010) Treatment of Cr+3 contaminated soil by solid tea wastage; A study of physiological processes of Vigna radiata. Pakistan Journal of Botany. 42(2), 1129-1136.

[11] Al-Tabbal, J.A., Ammary, B.Y., Al-Zboon, K.K. and Al-Zou'By, J. (2015) Effect of treated industrıal wastewater reuse on the germination and seedling growth of Leucaena leucocephala. Proceedings of the 14th International Conference on Environmental Science and Technology. Rhodes, Greece. 3-5 September 2015.

[12] Rusan, M.J., Albalasmeh, A.A., Zuraiqi, S. And Bashabsheh, M. (2015) Evaluation of phytotoxicity effect of olive mill wastewater treated by different technologies on seed germination of barley (Hordeum vulgare L.). Environmental Science and Pollution Research International. 22(12), 9127-35.

[13] Singh, R.P., Embrandiri, A., Ibrahim, M.H. and Singh, P. (2013) Effect of different Palm Oil Mill Effluent (POME) concentrations on Seed Germination, Seedling Growth and physiological response of Kidney bean (Phaseolus vulgaris). Journal of Environmental Science and Sustainability (JESS). 1(3), 97-102.

[14] Wins, J.A. and Murugan, M. (2010) Effect of Textile Mill Effluent on Growth and Germination of Black Gram-Vigna mungo (L.) Hepper. International Journal of Pharma and Bio Sciences. 1(1), 1-7

[15] Mycin, T.R. (2014) Use of sugar mill effluent for irrigation: an evaluative study on the response of germination and growth of cow pea Vigna unguiculata (L.) Walp. Asia Pacific Journal of Research. I(XVIV), 44-55.

[16] Killi, F. and Erol A. (2006) Effects of by-product of the olive oil mill process on germination and early seedling growth of grasspea (Lathirus sativus L.), common vetch (Vicia sativa L.) and hairy vetch (Vicia villosa Roth) seeds. Journal of Environmental Biology. 27(2), 207-210.

[17] Ogboi, E., Kperegbeyi, I., Nmor, EI and Odeh, H.O. (2010) The performance of maize (Zea mays) in soil contaminated with palm oil mill effluent (POME) in South, South Central Nigeria. African Journal of General Agriculture. 6(1), 19-24.

[18] Dash, A.K. (2012) Impact of Domestic Waste Water on Seed Germination and Physiological Parameters of Rice and Wheat. International Journal of Recent Research and Applied Studies. 12(2), 280-286.

[19] Yılmaz, E., Sonmez, I. and Demir, H. (2014) Effects of Zeolite on Seedling Quality and Nutrient Contents of Cucumber Plant (Cucumis sativus L. cv. Mostar F1) Grown in Different Mixtures of Growing Media. Communications in Soil Science and Plant Analysis. 45, 2767-2777.

[20] Shenkani, K., Sam Manohar Das, S. (2015) Impact of coir retting effluent on seed germination and seedling growth of green gram and mustard. European Journal of Biotechnology and Bioscience. 3(11), 43-46.

[21] Muscolo, A., Sidari, M., Mallamaci, C. and Attina, E. (2010) Effects of olive mill wastewater on seed germination and seedling growth. Terrestrial and Aquatic Environmental Toxicology. 4(1), 75-83.

Accepted: 14.08.2017
Received: 18.01.2018

CORRESPONDING AUTHOR

Ilkay Yavas
Adnan Menderes University,
Kocarli Vocational High School,
Department of Crops and Animal Production,
Aydin – Turkey

e-mail: iyavas@adu.edu.tr

© by PSP Volume 27 – No. 5/2018 pages 2654-2661 Fresenius Environmental Bulletin

GLOBAL TRENDS AND PERFORMANCES OF CELLULOSE MATERIALS DEGRADATION RESEARCH

Zhanying Liu[1], Yaping Yan[2], Qiuping Zhang[2], Shuli Zhang[3], Qunhui Wang[4], Jianguo Liu[2,*]

[1]Department of Chemical Engineering, Inner Mongolia University of Technology, Inner Mongolia 010051, China
[2]Department of Environmental Engineering, Inner Mongolia University of Technology, Inner Mongolia 010051, China
[3]Environmental Monitoring Center of Inner Mongolia, Inner Mongolia 010011, China
[4]Department of Environmental Engineering, Beijing University of Science and Technology, Beijing 100083, China

ABSTRACT

As a renewable biomass energy resource, cellulose materials are an important solution to global energy scarcity. In this study, bibliometric analysis was used for the statistical evaluation of research trends in cellulose degradation. In this study, the research articles indexed in SCI-EXPANDED from the ISI Web of Science database published from 1996 to 2013 were investigated. The results indicate that number of scientific papers published on cellulose degradation increased significantly from 1996-2013, and that America dominated research output through this period. Among all institutes involved in this field, the University of Tokyo, Japan, had the largest production. The majority of research on cellulose degradation is related to biotechnology, energy, environment and materials engineering. The three most popular journals in this area, in descending order of most cellulose degradation papers published, are *Bioresource Technology*, *Carbohydrate Polymers*, and *Journal of Applied Polymer Science*. In addition, keyword analysis revealed that biomass, biodegradation, pyrolysis, fermentation and enzymolysis have been research hotspots from 1996-2013.

KEYWORDS:
cellulose materials, degradation, bibliometrics, research trends, energy resource

INTRODUCTION

Cellulose materials exist widely in nature and are commonly used in a variety of industrial processes As the energy crisis and related environmental problems become increasingly severe, utilization of cellulose materials to produce high value-added resources (ethanol, biogas, lactic acid, etc.) has become one of the hot areas of research to maintain sustainable industrial development [1,2,3,4]. Since a majority of cellulose is wrapped by complex structures consisting of hemicellulose and lignin, its efficient degradation becomes key to the utilization of cellulose materials. There has therefore been a large contingent of research performed worldwide focusing on efficient degradation of a variety of cellulose materials [5, 6]. Studies in this field started in late 1960s. Khan and Trottierwere, in 1978, the first to degrade cellulose through anaerobic degradation technology [7]. Since then, different degradation technologies have been studied and applied to the cellulose material recycling process [8, 9, 10, 11]. More and more disciplines, including biotechnology, environmental science, energy and fuel science, polymer materials and medicine have been involved in this area and it is evident that cellulose degradation has become an interdisciplinary field [12, 13, 14, 15].

The literature can reflect the results of scientific research. By analyzing the literature, we can systematically evaluate the significance of the results in a particular research field, reveal research trends and determine the regional distribution of research efforts [16]. Bibliometric methods have been applied to different topics, such as rehabilitation [17], adsorption technology [18], and aerosols [19].

In recent years, a large number of articles related to cellulose degradation have been published annually. However, reports on its development and research trends are relatively few. In this paper, a bibliometric technique was used to analyze research trends in cellulose degradation in order to provide a basis for a better understanding of the present state of global cellulose degradation research.

DATA SOURCES AND METHODS

ISI Web of Science is the world's largest and most comprehensive academic information resource. In this study, articles related to cellulose degradation were queried based on the topic "(fibrin or cellulose) and (degradation or degrade or degrading or degradable or degradative or degradability or degraded or degrades or degradations)" based on the ISI Web of Science database. A total of 10193 articles were retrieved and 9623 of which were published from 1996-2013. Microsoft Excel 2007 software was used to collate and statistically analyze article information including document types, languages, countries, institutes, authors, citations, reference numbers, page

numbers, subject categories, and journals, based on the method used by Ho [20]. Keyword analysis was carried out to obtain the research trends in this field.

RESULTS AND DISCUSSION

Document Type and Language. There were 9 document types found in a total of 10193 publications during 1996-2013. Article (87.11%) is the dominant document type, followed by review (4.31%), meeting abstract (2.23%), note (1.42%), editorial (0.89%), letter (0.92%), correction (0.78%), reprint (0.78%), correction addition (0.65%), news item (0.61%), and discussion (0.41%). Non-articles were discarded from further analysis.

Among the 9623 articles, 9344 (97.1%) were published in English, followed by Germany (64), French (38), Chinese (28), Russian (26), Japanese (26), Portuguese (18), Spanish (14), Polish (9), Czech (5), Korean (4), Serbian (2), Turkish (2), Hungarian (1), and Croatian (1). This may not purely be because English is the dominant language in cellulose degradation research, but may also be because most journals in the ISI database are published in English.

Trend of Production. Research on cellulose degradation increased rapidly in the 21st century, with annual publications surging from 368 in 2002 to 1069 in 2012. As shown in Figure 1, annual publications on cellulose degradation kept relatively stable prior to 2007, but subsequently rapidly increased. This may be explained by an unprecedented increase in global energy demand making resource utilization and energy regeneration of cellulose materials a crucial global research topic.

Table 1 shows the characteristics of cellulose degradation related articles during 1996-2013. The average number of references increased from 30 in 1996 to 40 in 2013; the average number of authors per article also increased from 3.9 to 4.4. Paper length remained relatively stable at an average of 8.5 pages per article. The average number of institutes and countries involved increased from 1.5 to 2.2 and 1.1 to 1.2, respectively, implying a strengthening in international and inter-institutionary cooperation.

Contributions of Institutes and Countries. Contributions of different countries were estimated by the affiliation of at least one author of the articles. Articles originating from England, Scotland, Wales and Northern Ireland were reclassified as being from the United Kingdom (UK), and publications from Hong Kong were combined with those of mainland China. Among the 9623 articles, 294 (3.1%) articles were published by one author, and the other 9329 (96.9%) articles were published by two or more authors. The top 10 most productive countries together with their total number of publications, independent publications, first author publications, and corresponding author publications are listed in Table 2. The USA published a total of 1659 (17.23%) articles from 1996-2013, which almost doubled that of the second most productive country, China. The numbers of articles published over this period by China, Japan, Germany and France are all above 400, and cooperative publications accounted for 2%, 11%, 19% and 21% of the total publications of each respective country. The number of cellulose degradation related articles from a country may reflect the urgency of energy demand, concern for environmental pollution, as well as the scientific capabilities of that country.

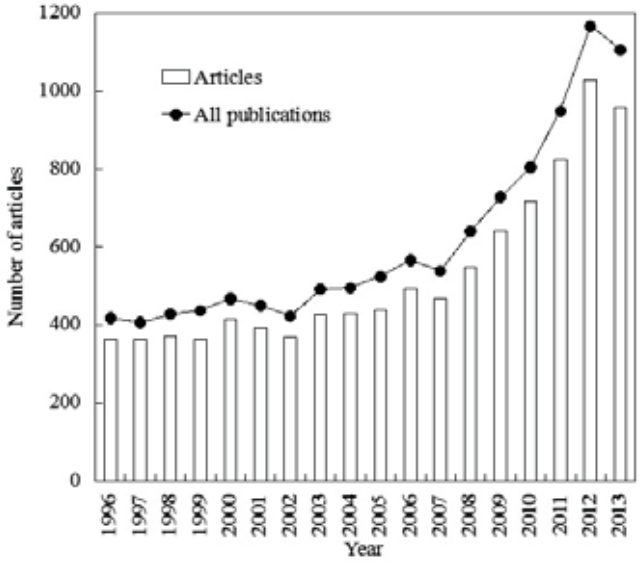


FIGURE 1
Number of SCI publications referring to cellulose degradation from 1996 to 2013

TABLE 1
Basic characteristics of publications from 1996 to 2013

Year	TP	AU/TP	NR/TP	PG/TP	NC/TP	NI/NP
1996	364	4.0	30	8.0	1.1	1.5
1997	363	4.1	30	7.8	1.1	1.6
1998	372	4.0	31	8.6	1.2	1.6
1999	364	4.0	30	8.4	1.2	1.7
2000	416	4.0	33	8.6	1.2	1.7
2001	392	3.9	30	8.1	1.1	1.8
2002	368	4.1	29	8.2	1.2	1.8
2003	428	3.9	31	8.7	1.2	1.6
2004	431	4.0	31	8.6	1.2	1.8
2005	439	4.0	31	8.8	1.2	1.8
2006	493	4.4	32	8.4	1.2	1.9
2007	469	4.0	33	8.6	1.2	1.8
2008	548	4.1	33	8.5	1.2	1.8
2009	643	4.1	34	8.4	1.2	1.8
2010	718	4.1	35	8.5	1.2	1.9
2011	826	4.1	36	8.8	1.2	2.1
2012	1029	4.0	39	9.1	1.2	2.2
2013	960	4.0	40	9.2	1.2	2.2
Total	9623					
Average		4.1	33	8.5	1.2	1.8

* TP: total publications; AU/TP: average number of authors per article; PG/TP: average number of pages per article; NR/TP: average number of references per article; NC/TP: average number of countries involved per article; NI/TP: average number of institutes involved per article.

TABLE 2
Top 10 most productive countries/territories from 1996 to 2013

Country	*TP*	*TP R (%)*	*SP R (%)*	*FP R (%)*	*RP R (%)*	*%C*
USA	1659	1 (17.23)	1 (17.18)	1 (16.32)	1 (16.83)	18
China	864	2 (8.97)	2 (10.72)	2 (10.93)	2 (10)	2
Japan	857	3 (8.9)	3 (9.59)	3 (8.52)	3 (8.78)	11
Germany	488	4 (5.07)	4 (4.99)	4 (5.12)	4 (4.96)	19
France	415	5 (4.31)	6 (4.13)	5 (4.18)	5 (4.26)	21
India	397	6 (4.12)	5 (4.66)	6 (4.01)	6 (4.1)	7
Italy	310	7 (3.22)	8 (3.25)	8 (2.95)	7 (3.19)	17
Brazil	302	8 (3.14)	7 (3.35)	7 (2.98)	8 (3.15)	12
UK	298	9 (3.09)	12 (2.68)	9 (2.84)	47 (0.25)	29
Canada	296	10 (3.07)	9 (2.86)	10 (2.82)	9 (3)	24

*TP: total publications; TPR (%): Rank and percentage of total publications; SPR (%): Rank and percentage of independent publications; FPR (%): Rank and percentage of first author publications; RPR (%): Rank and percentage of statistical corresponding author publications; C (%): percentage of cooperative publications in total publications.

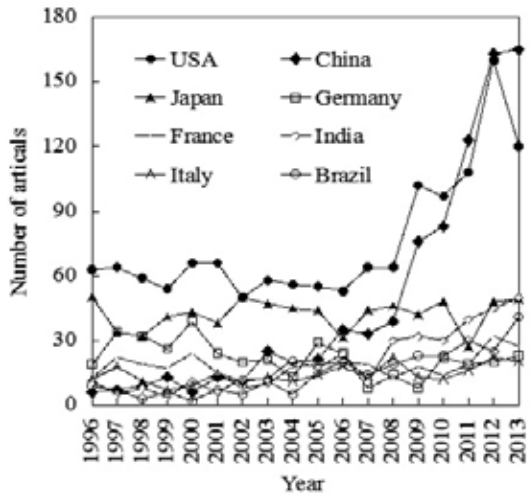


FIGURE 2
The yearly publication outputs of the top 8 most productive countries from 1996 to 2013

The annual numbers by publications of the top 8 most productive countries during 1996-2013 are shown in Figure 2. The number of publications by the USA and China increased rapidly since 2006. China published the least articles amongst the 8 countries prior to 1998, but from 2006 to 2010 became the world's second biggest contributor to this field, only after the USA.

Contributions of different institutes were analyzed by the affiliations of at least one author of the articles. Among the 9623 articles, 564 (5.9%) were published independent of other institutes, and 9059 (94.1%) were inter-institutionary publications. The 9623 articles were submitted by 3804 different institutes, among which 2447 (64.3%) institutes published only one article and 492 (12.9%) published two articles. As shown in Table 3, 8 out of the top 15 most productive institutes are from China, 3 are from the USA, 2 are from Japan and one each is from Rus-

sia, Brazil, and France. Chinese Academy of Sciences, University of Tokyo, and South China University of Technology were the top three most productive institutes. However, since the Chinese Academy of Science has branches in many cities, a different ranking would be generated if the articles were divided between the branches. Shandong University, China, and Cornell University, USA, published the most independent articles. Chinese Academy of Sciences carried out more collaborative research. University of Tokyo, Japan was home to the most corresponding authors besides Chinese Academy of Sciences, indicating its long history in cellulose degradation research. Based on the above analysis, it is evident that the USA, China, and Japan possess more power in cellulose degradation research, which is relative to the national resource demand and policies on development and utilization of new energies in these countries. The top 3 most productive institutes in cellulose degradation research from China from 1996-2013 were Chinese Academy of Sciences (169), South China University of Technology (74) and China Agricultural University (73), ranking 1, 3 and 4 in the world, respectively. This indicates that the technology and research reserves of China are close to those of developed countries (Table 3).

Distribution of Subject Categories And Journals. According to the classification of subject categories in ISI Journal Citation Reports (JCR), the 9623 articles were distributed in 158 subject categories. As shown in Figure 3, the top 6 subject categories containing the most articles are chemistry (1201, 12%), biotechnology & applied microbiology (1046, 11%), biochemistry & molecular biology (962, 10%), agriculture (878, 9%), materials science (741, 8%), and engineering (685, 7%). The top 10 most productive journals in this field from 1996-2013 are listed in Table 4. These top 10 journals accounted for 16.5% of total publications. Based on the above analysis, cellulose degradation is closely related to biological, chemical, agricultural, materials, and engineering industries. Among them, biotechnology and applied microbiology are important methods used after cellulose degradation, indicating that degradation

TABLE 3
Top 15 most productive institutes from 1996 to 2013

institutes	*TP*	*TP R (%)*	*SP R (%)*	*CP R (%)*	*FP R (%)*	*RP R (%)*
Chinese Acad Sci, China	169	1 (1.09)	5 (0.89)	1 (1.71)	1 (0.99)	1 (1.03)
Univ Tokyo, Japan	74	2 (0.6)	9 (0.71)	4 (0.71)	3 (0.58)	2 (0.75)
S China Univ Technol, China	74	3 (0.58)	2 (1.06)	2 (0.75)	7 (0.44)	12 (0.42)
China Agr Univ, China	73	4 (0.52)	3 (1.01)	3 (0.74)	3 (0.58)	6 (0.61)
INRA, France	68	5 (0.45)	5 (0.89)	5 (0.64)	5 (0.52)	3 (0.69)
Kyoto Univ, Japan	62	6 (0.42)	87 (0.18)	6 (0.62)	2 (0.6)	4 (0.65)
Univ Sao Paulo, Brazil	59	7 (0.39)	9 (0.71)	7 (0.56)	6 (0.45)	5 (0.62)
Shandong Univ, China	55	8 (0.36)	1 (1.24)	9 (0.49)	8 (0.43)	16 (0.37)
Sichuan Univ, China	54	8 (0.36)	6(0.82)	8 (0.55)	11 (0.37)	13 (0.4)
Russian Acad Sci, Russia	51	10 (0.35)	9 (0.71)	11 (0.48)	8 (0.43)	7 (0.52)
Univ Calif Davis, USA	48	11 (0.34)	9 (0.71)	14 (0.44)	17 (0.31)	9 (0.47)
Beijing Forestry Univ, China	48	13 (0.31)	7(0.79)	9 (0.49)	14 (0.34)	18 (0.35)
USDA ARS, USA	48	14 (0.3)	25 (0.35)	13 (0.47)	14 (0.34)	8 (0.48)
Zhejiang Univ, China	47	15 (0.29)	4 (0.91)	11 (0.48)	16 (0.33)	17 (0.36)
Cornell Univ, USA	46	16 (0.28)	2 (1.06)	16 (0.4)	10 (0.4)	9 (0.47)

TP: total publications; TPR (%): Rank and percentage of total publications; SPR (%): Rank and percentage of independent publications; CP R (%): Rank and percentage of cooperative publications; FPR (%): Rank and percentage of first author publications; RPR (%): Rank and percentage of corresponding author publications.

TABLE 4
Top 10 most productive journals on cellulose degradation from 1996 to *2013*

Journal	TP	IF	Subject category
Bioresource Technology	298	4.75	Agricultural Engineering; Biotechnology & Applied Microbiology; Energy & Fuels
Carbohydrate Polymers	223	3.479	Chemistry, Applied; Chemistry, Organic; Polymer Science
Journal of Applied Polymer Science	194	1.395	Polymer Science
Cellulose	151	3.476	Materials Science, Paper & Wood; Materials Science, Textiles; Polymer Science
Polymer Degradation and Stability	148	2.77	Polymer Science
Applied And Environmental Microbiology	147	3.678	Biotechnology & Applied Microbiology
Journal Of Analytical And Applied Pyrolysis	122	2.56	Chemistry, Applied
Thrombosis and Haemostasis	110	6.094	Hematology; Peripheral Vascular Disease
Applied Microbiology and Biotechnology	96	1.349	Biotechnology & Applied Microbiology
Thrombosis Research	96	2.406	Hematology; Peripheral Vascular Disease

TP: total publications; IF: based on JCR 2013.

of cellulose is an important technology for mitigating energy crises and environmental pollution. About 26.3% of articles on cellulose degradation from China were published in journals listed Table 4. 2 of the 10 journals listed in Table 4 are from China, and their impact factors are relatively low.

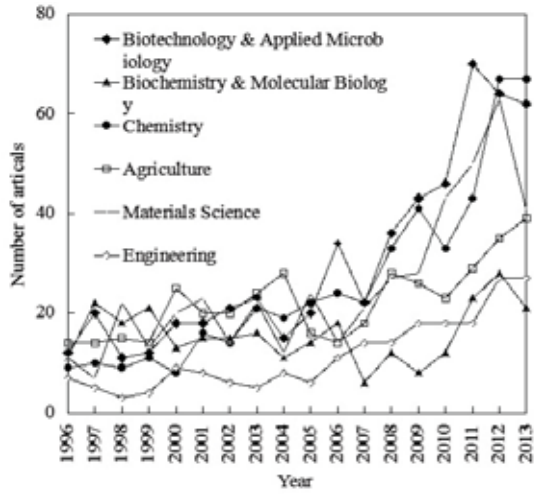


FIGURE 3
The top 6 most productive subjects within cellulose degradation *research from 1996 to 2013*

Distribution of Author Keywords. Statistical analysis of keywords can help researchers find scientific research trends in a particular field. Bibliometric methods concerning author keywords analysis can only be found in recent years, so using the author keywords to analyze research trends is much more infrequent. In this study, a total of 15062 keywords were listed by authors from 1996-2013 in the cellulose degradation field. Author keywords appeared in articles referring to cellulose degradation were calculated and ranked by total 18-year and three 6-year sub-periods (Table 5). By analysis of these keywords, it could be concluded that cellulose degradation can be classified into many subject categories. For example, "biodegradation" and "fermentation" were related to biological engineering; "kinetics," "pyrolysis," and "fibrinolysis" were related to chemical engineering; and "mechanical properties", "d-dimer", and "lignocellulose" were related to material science.

By analyzing the top 25 most frequently used author keywords, we can roughly draw the research trends of each sub-period. Except for search terms like "degrad*", "cellulose", and "fibrin*", other keywords including "biodegradation", "pyrolysis", "thermal degradation", "fermentation", "endoglucanase", "xylanase", and "beta-glucosidase" were frequently used, indicating that the main methods for cellulose degradation are biodegration, pyrolysis, fermentation, and enzymolysis. During the study period, the rankings of some author keywords changed dramatically. For instance, "biodegradation" and "thermal degradation" ranked 23 and 22 during 1996-2001, respectively, and increased to 6 and 11 during 2008-2013. This suggests that biodegradation and thermal degradation have gradually become research hotspots. On the contrary, enzymatic hydrolysis, which ranked 8 during 1996-2001, had declined to 101 during 2008-2013, indicating that enzymatic hydrolysis has matured as a research technology in this field.

TABLE 5
Top 30 most frequently used author keywords from 1996 to 2013

author keywords	*96-13 TP*	*96-13 R (%)*	*96-01 R (%)*	*02-07 R (%)*	*08-13 R (%)*
Cellulase	279	4 (3.18)	3 (2.95)	4 (3.02)	3 (3.48)
Fibrinolysis	235	2 (3.73)	16 (1.31)	5 (2.48)	2 (6.63)
Lignin	204	3 (3.24)	2 (3.12)	3 (3.06)	3 (3.48)
Degradation	159	5 (2.53)	4 (2.74)	2 (3.4)	10 (1.62)
Cellulose Degradation	116	6 (1.84)	18 (1.26)	9 (1.8)	6 (2.32)
Biodegradation	101	7 (1.6)	23 (0.99)	6 (1.99)	6 (1.97)
Kinetics	98	8 (1.56)	13 (1.53)	7 (1.95)	15 (1.24)
Mechanical Properties	96	9 (1.52)	5 (2.68)	10 (1.75)	87 (0.46)
Fibrin	93	10 (1.48)	25 (1.04)	18 (1.12)	7 (2.11)
Pyrolysis	89	11 (1.41)	10 (1.81)	8 (1.85)	42 (0.75)
D-Dimer	87	12 (1.38)	65 (0.49)	24 (0.92)	5 (2.44)
Hemicellulose	85	13 (1.35)	21 (1.15)	12 (1.46)	14 (1.41)
Thermal Degradation	85	13 (1.35)	22 (1.04)	13 (1.36)	11 (1.75)
Xylanase	80	15 (1.27)	7 (1.91)	24 (0.92)	20 (1.08)
Coagulation	78	17 (1.24)	52 (0.6)	17 (1.22)	9 (1.74)
Endoglucanase	76	18 (1.21)	30 (0.82)	11 (1.7)	20 (1.08)
Fibrinogen	75	19 (1.19)	65 (0.49)	24 (0.92)	8 (1.95)
Hydrolysis	69	20 (1.1)	13 (1.53)	14 (1.26)	53 (0.62)
Enzymatic Hydrolysis	66	21 (1.05)	8 (1.86)	20 (1.07)	101 (0.41)
Fermentation	57	22 (0.91)	27 (0.93)	21 (0.97)	32 (0.83)
Purification	57	22 (0.91)	30 (0.82)	18 (1.12)	39 (0.79)
Biomass	56	24 (0.89)	80 (0.58)	60 (0.47)	12 (1.46)
Lignocellulose	55	25 (0.87)	19 (1.2)	32 (0.83)	50 (0.66)
Xylan	55	25 (0.87)	30 (0.82)	21 (0.97)	32 (0.83)
Biodegradation	54	27 (0.86)	15 (1.48)	52 (0.63)	57 (0.58)

TP: total publications; R (%): Rank (percentage of total publications).

TABLE 6
Top 30 most frequently used keywords plus from 1996 to 2013

Keyword plus	96-13 TP	96-13 R (%)	96-01R (%)	02-07 R (%)	08-13 R (%)
degradation	1911	1 (20.65)	1 (3.89)	1 (5.75)	1 (11.28)
cellulose	1481	2 (16)	2 (2.24)	2 (4.12)	2 (9.81)
purification	454	3 (4.91)	3 (1.51)	3 (1.33)	7 (2.18)
lignin	435	4 (4.7)	7 (0.8)	4 (1.16)	5 (2.8)
hydrolysis	427	5 (4.61)	9 (0.67)	7 (0.88)	4 (3.17)
biomass	420	6 (4.54)	51 (0.3)	16 (0.66)	3 (3.6)
wood	371	7 (4.01)	22 (0.48)	6 (0.89)	6 (2.72)
expression	334	8 (3.61)	4 (1.04)	5 (1.13)	16 (1.51)
fermentation	324	9 (3.5)	13 (0.58)	9 (0.83)	8 (2.12)
kinetics	287	10 (3.1)	20 (0.51)	9 (0.83)	10 (1.78)
enzymes	272	11 (2.94)	22 (0.48)	11 (0.78)	11 (1.73)
behavior	262	12 (2.83)	164 (0.13)	14 (0.69)	9 (2.04)
water	251	13 (2.71)	43 (0.32)	12 (0.75)	13 (1.67)
acid	240	14 (2.59)	16 (0.56)	22 (0.61)	20 (1.43)
decomposition	235	15 (2.54)	66 (0.27)	12 (0.75)	14 (1.61)
mechanism	232	16 (2.51)	16 (0.56)	8 (0.86)	32 (1.08)
identification	218	17 (2.36)	24 (0.46)	15 (0.68)	23 (1.25)
system	211	18 (2.28)	30 (0.41)	16 (0.66)	25 (1.24)
trichoderma-reesei	200	19 (2.16)	27 (0.42)	21 (0.62)	29 (1.15)
polysaccharides	194	20 (2.1)	33 (0.38)	24 (0.57)	27 (1.18)
cellulases	194	20 (2.1)	19 (0.53)	38 (0.41)	27 (1.18)
bacteria	194	20 (2.1)	13 (0.58)	26 (0.49)	34 (1.03)
pyrolysis	192	23 (2.07)	73 (0.25)	49 (0.37)	18 (1.48)
pretreatment	191	24 (2.06)	264 (0.09)	68 (0.28)	12 (1.7)
binding	190	25 (2.05)	8 (0.69)	16 (0.66)	55 (0.71)
fibers	188	26 (2.03)	126 (0.16)	55 (0.35)	15 (1.52)
growth	183	27 (1.98)	12 (0.59)	25 (0.56)	44 (0.82)
model	178	28 (1.92)	36 (0.36)	19 (0.64)	37 (0.96)
wheat-straw	172	29 (1.86)	204 (0.11)	40 (0.4)	21 (1.37)
enzymatic-hydrolysis	172	29 (1.86)	126 (0.16)	102 (0.22)	16 (1.51)

TP: total publications; R (%): Rank (percentage of total publications

Distribution of Keywords Plus. 'Keywords Plus' were generated independently of the title or author keywords, describing the article's contents with greater depth and variety. As additional search terms, keywords plus are usually more concerned about novel research directions than the mature directions in the field [21, 22]. For example, the word "biomass", which represents the resource utilization direction of cellulose materials, ranked 51 during 1996-2001, surged to 16 during 1998-2003 then ranked 3 during 2008-2013. By 2008 much cellulose degradation research had adopted "biomass" techniques [23, 24, 25]. This is due to the fact that the increasing demand for new energy because of energy crises in recent years has made studies on cellulose degradation to produce high value-added products a hot topic. As shown in Table 6, the most frequently studied cellulose-based materials were straw and wood, because these two materials are extensively available and inexpensive, which meets the great demand for raw materials to produce new energy [26].

Analysis of Research Hotspots. By comprehensively analyzing the distribution of two keyword types (author keywords and keyword plus), we summed the research hotspots on cellulose degradation into three categories: materials engineering, chemical engineering and biological engineering, especially enzymolysis-related researches. Generally, hotspots of biological engineering were biodegradation, cellulases and bacteria related research. Each hotspot was supported by a single word or a word cluster. For example, degradation was supported by "biodegradation", "thermal degradation", "pyrolysis", and "enzymatic hydrolysis". The supporting words of "cellulases" were "cellulose", "xylanase", "enzymes", and "trichoderma-reesei". "Bacteria", "growth", "biodegradation", and "fermentation" comprised the supporting word cluster of bacteria. Hotspots of materials engineering were classified into two sub-groups. One was raw materials-related research, whose supporting word cluster included "biomass", "wood", "wheat-straw", "fibers", "lignocellulose", "lignin", and "hemicellulose". The other was material property-related research, whose supporting words contained "mechanical properties", "binding", "mechanism", and "coagulation". Chemical engineering related research was supported by "pretreatment", "acid", "purification", "decomposition", "pyrolysis", "polysaccharides", and "expression".

Generally, the above mentioned hotspots can be reflected by certain highly cited articles. Taking degradation-related research for example, Zhang and Lynd [27] reviewed the enzymatic hydrolysis by

noncomplexedcellulase enzyme systems, emphasizing on the development of aggregated understanding incorporating substrate features as well as concentration and multiple cellulase components. Pääkkö and Viikari [28] adopted enzymatic hydrolysis combined with mechanical shearing and high-pressures to research homogenization for nanoscale cellulose fibrils and strong gels.

CONCLUSIONS

A bibliometric technique was used to analyze the literature related to cellulose degradation based on the ISI web of science database, and research trends during 1996-2013 in this field were obtained. The results show that along with the development of the world economy, the emergence of energy crises and increasing concern over environmental pollution, research on degradation of cellulose-based material has attracted widespread attention from more and more countries, institutes, and researchers. Among them, the Chinese Academy of Sciences and the University of Tokyo were the largest contributors. The dominant subject categories include biology, chemistry, agriculture, and materials engineering; keywords analysis shows that biodegradation, pyrolysis, fermentation, and enzymolysis have become hotspots in current cellulose degradation research. Two kinds of cellulose degradation technology: "biodegradation" and "thermal degradation" have gradually become focal points of this field. Meanwhile, the degradation of cellulosic materials to produce high value-added energy has also become a hot topic. The research hotspots can be classified into three subjects: materials engineering, chemical engineering and biological engineering (especially enzyme-related research). These changes bear a historical background. With the rapid development of modern technology and growing global energy depletion, energy produced from cellulose-based substances is under increasingly strong demand. As costs decrease, we expect that an efficient low-cost celloluse degradation technology will be developed in the near future.

ACKNOWLEDGEMENTS

This work was supported by the Inner Mongolia Autonomous Region Natural Science Foundation under Grant (number 2015BS0509); The National Natural Science Foundation of China under Grant (number 21666028); and The Inner Mongolia Autonomous Region science and technology major projects.

REFERENCES

[1] Sun, Y. and Cheng, J.Y. (2002) Hydrolysis of lignocellulosic materials for ethanol production: a review. Bioresource Technology. 83(1), 1 – 11.

[2] Sun, F.B. and Chen, H.Z. (2008) Enhanced enzymatic hydrolysis of wheat straw by aqueous glycerol pretreatment. Bioresource Technology. 99(14), 6156 – 6161.

[3] Singhvi, M., Joshi, D., Adsul, M., Varma, A., Gokhale, D. (2010) D-(-)-Lactic acid production from cellobiose and cellulose by Lactobacillus lactis mutant RM2-24. Green Chemistry. 12(6), 1106 – 1109.

[4] Chen, W.H., Tu, Y.J., Sheen, H.K. (2011) Disruption of sugarcane bagasse lignocellulosic structure by means of dilute sulfuric acid pretreatment with microwave-assisted heating, Applied Energy. 88(8), 2726 – 2734.

[5] Divya Nair, M.P., Padmaja, G., Moorthy S.N. (2011) Biodegradation of cassava starch factory residue using a combination of cellulases, xylanases and hemicellulases. Biomass Bioenergy. 35(3), 1211 – 1218.

[6] Foston, M. and Ragauskas, A.J. (2010) Changes in the Structure of the Cellulose Fiber Wall during Dilute Acid Pretreatment in Populus Studied by H-1 and H-2 NMR. Energy & Fuels. 24(10), 5677 – 5685.

[7] Khan, A.W. and Trottier T.M. (1978) Effect of sulfur-containing compounds on anaerobic degradation of cellulose to methane by mixed cultures obtained from sewage sludge, Applied & Environmental Microbiology. 35(6), 1027 – 1034.

[8] Liu, C.Z. and Cheng, X.Y. (2010) Improved hydrogen production via thermophilic fermentation of corn stover by microwave-assisted acid pretreatment. International Journal of Hydrogen Energy. 35(17), 8945 – 8952.

[9] Moilanen, U. and Viikari, L. (2010) Enzymatic modification of lignin for enhanced hydrolysis. Journal of Biotechnology. 150(6), 574 – 575.

[10] Zheng, M., Li, X., Li, L., Yang, X., He, Y. (2009) Enhancing anaerobic biogasification of corn stover through wet state NaOH pretreatment. Bioresource Technology. 100(21), 5140-5145.

[11] Liu, Y., Yu, P., Song, X., Qu, Y.B. (2008) Hydrogen production from cellulose by co-culture of Clostridium thermocellum JN4 and Thermoanaerobacterium thermosaccharolyticum GD17. International Journal of Hydrogen Energy. 33(12), 2927 – 2933.

[12] Abdel-Rahmana, M.A., Yukihiro, T., Sonomoto, K. (2011) Lactic acid production from lignocellulose derived sugars using lactic acid bacteria Overview and limits. Journal of Biotechnology. 156(4), 286 – 301.
[13] Quye, A., Littlejohn, D., Pethrick, R.A., Stewart, R.A. (2011) Investigation of inherent degradation in cellulose nitrate museum artefacts. Polymer Degradation and Stability. 96(7), 1369 – 1376.
[14] Chen, Y., Li, G., Yang, F., Zhang, M.S. (2011) Mn/ZSM-5 participation in the degradation of cellulose under phosphoric acid media. Polymer Degradation and Stability. 96(5), 863 – 869.
[15] Ben, M.M., Majdoub, H., Bataille, I., Roudesli, M.S., Hassine, M., Ajzenberg, N., Chaubet, F., Maaroufi, R.M. (2009) Polysaccharides from the skin of the ray Raja radula. Partial characterization and anticoagulant activity. Thrombosis Research. 123(4), 671 – 678.
[16] Cimmino, M.A., Maio, T., Ugolini, D., Borasi, F., Mela, G.S. (2005) Trends in otolaryngology research during the period 1995–2000: a bibliometric approach. Otolaryngol Head Neck Surg. 132(2), 295 – 302.
[17] Tesio, L., Gamba, C., Capelli, A., Franchignoni F.P. (1995) Rehabilitation: the Cinderella of neurological research-a bibliometric study. Italian Journal of Neurological Sciences. 16(7), 473 – 477.
[18] Ho, Y.S. (2007) Bibliometric analysis of adsorption technology in environmental science. Journal of Environmental Protection Science. 1(1), 1 – 11.
[19] Xie, S.D., Zhang, J., Ho, Y.S. (2008) Assessment of world aerosol research trends by bibliometric analysis. Scientometrics. 77(1), 113-130.
[20] Ho, Y.S. (2008) Bibliometric analysis of biosorption technology in water treatment research from 1991 to 2004. International Journal of Environment & Pollution. 34(1-4), 1-13.
[21] Garfield, E. (1990a) Keywords plus—Isis breakthrough retrieval method.1. Expanding your searching power on current-contents on diskette. Current Contents. 32, 5 – 9.
[22] Garfield, E. (1990b) Keywords-plus takes you beyond title words.2. Expanded journal coverage for current contents- on-diskette includes social and behavioral-sciences. Current Contents. 33, 5-9.
[23] Frostegard, A. and Baath, E. (1996) The use of phospholipid fatty acid analysis to estimate bacterial and fungal biomass in soil. Biology and Fertility of Soils. 22(1), 59-65.
[24] Laurance, W.F. and Laurance, S.G. (1997) Biomass collapse in Amazonian forest fragments. Science. 278(5340), 1117-1118.
[25] Lee, J. (1997) Biological conversion of lignocellulosic biomass to ethanol. Journal of biotechnology. 56(1), 1-24.
[26] Feamside, P.M. (1997) Wood density for estimating forest biomass in Brazilian Amazonia. Forest ecology and management. 90(1), 59 – 87.
[27] Zhang, Y.H. and Lynd, L.R. (2004) Toward an aggregated understanding of enzymatic hydrolysis of cellulose: noncomplexedcellulase systems. Biotechnology and Bioengineering. 3088(7), 797 – 824.
[28] Pääkkö, M., Ankerfors, M., Kosonen, H., Nykänen, A. (2007) Tenzymatic hydrolysis combined with mechanical shearing and high-pressure homogenization for nanoscale cellulose fibrils and strong gels. Biomacromolecules. 8(6),1934 – 1941.

Received: **27.04.2016**
Accepted: **24.02.2018**

CORRESPONDING AUTHOR

Jianguo Liu
Department of Environmental Engineering,
Inner Mongolia University of Technology,
Inner Mongolia 010051 – China

e-mail: jgliu_yxc@163.com.

© by PSP Volume 27 – No. 5/2018 pages 2662-2670 Fresenius Environmental Bulletin

INTEGRATING GIS TO DETERMINE THE SPATIAL DISTRIBUTION OF PRINCIPAL COMPONENTS AND THE SOURCES OF HEAVY METALS IN FARMLAND SOILS NEAR MINING AREA IN TONGLING, CHINA

Hong Jiang[1], Jingru Nie[1], Shanshan Fan[1], Guoqing Yin[1], Youhua Ma[1,*], Tiezheng Ma[1], Qiang Wang[1], Rungui Shi[2]

[1]Institute of Resources, Environment and Information Technology, Anhui Agricultural University, Hefei, 230036, China
[2]Anhui Agricultural Ecological Environment Station, Hefei, 230001, China

ABSTRACT

This study was performed to determine the status of heavy metal contamination in agricultural soil near the mining area in Tongling County, Anhui Province, China. Soil samples (490) were collected from farmland across the county, and contents of Cr, Pb, Cd, As, Hg, Cu, Zn, and Ni, were measured. Multiple statistical analyses (MSA), including correlation analysis, principal components analysis (PCA), and clustering analysis, in combination with GIS, have identified clearly the sources of these pollutants. Results showed that ratio of exceeding the background levels for Cd, Zn, and Cu was 100%, 75.10% and 71.43%, respectively. The average content of Cr and Hg was lower than their respective background level. This study showed that soil contents of Pb, Cd, and Cu were greatly affected by human activities; and the exogenous contamination had very minimal influence on soil Ni content. The 8 heavy metals were divided into four principal components according to the spatial distribution of soil contents across Tongling. The first principal component (PC1) is comprised of Pb, As, Zn and Cu, and the major sources of contaminants were from mining, milling, smelting industrial activities. The second principal component (PC2) contains Cr and Ni; the contents of these two metals were basically influenced by soil parent materials from lacustrine sediments and recent Youngtze river alluvium. The third principal component (PC3) has Cd. Soil Cd content was greatly affected by human activities involving a complex set of sources but mainly from mining and irrigation with contaminated water. The fourth principal component (PC4) has Hg which mainly came from air precipitation.

KEYWORDS:
Farmland Soil, Heavy Metal, Sources of Pollution, Tongling

INTRODUCTION

Soils are vital to humans because they provide the major resources for agricultural production and the sustainable development. According the most recent survey by the Ministry of China Environmental Protection and Ministry of Land and Resources, the national soil quality situation in China is not optimistic. Among the most serious problems, is that the quality of agricultural lands continuously declines and over 19.4% of farmland soil contains heavy metals far above the standard levels [1].

Soil heavy metal pollution has engrossed a great attention all over the world [2, 3]. Tongling is known as 'The ancient capital of copper and modern copper production base in China'. The history of copper smelting in this area is dated back to about 3500 year ago during the Shan-Chou Dynasty. Many scholarly studies have been performed to identify the negative effects of heavy metals from various aspects, and the associated environmental geochemistry properties in Tongling [4-6]. These studies mostly were performed in designated mining areas, or around a few watersheds. Because of the limited smaller number of sampling sites, none of these studies were able to provide insight information on heavy metal pollution in agricultural soil as a whole across the county.

In many of these related studies, GIS has been used when assessing the soil heavy metal pollution situation, and, together with the principal component analysis (PCA) method, to predict the sources of contamination. Still, there is an urgent need to identify the relationship and common properties among multiple species of heavy metals in agricultural soil.

In this study, we have collected top soil samples from farm lands in Tongling County. Soil contents of 8 heavy metals including Cr, Pb, Cd, As, Hg, Cu, Zn, Ni, were measured. Then GIS and multivariate statistical analysis were performed to identify the pollution sources and distribution of these heavy metals in soils across the region.

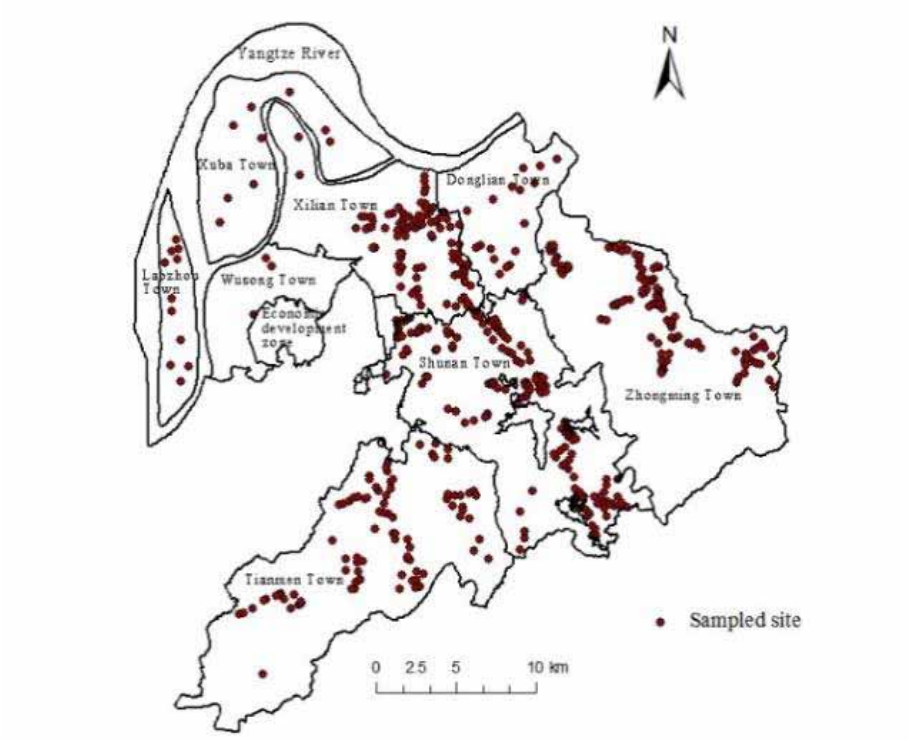


FIGURE 1
Location of soil sample collection sites in Tongling farmland soils near mining area

MATERIALS AND METHODS

Description of the study area. Tongling sits on the south bank of the lower reaches of Yangtze River in southern Anhui province, China. Geographically, the county spreads from 117°42'00" to 118°10'6" E, and 30°45'12" to 31°07'56" N. Tongling is on the Iron-copper Minerogenetic Belt on Yangtze River, where the land has a favorable metallogenic condition rich in mineral resources. It is well known for metallurgy non-ferrous metal copper mines. The geological structure in this area is very complex and therefore soils are formed from various parent materials.

Sample collection and analysis. A soil sampling map covering every major crop species and soil types was drawn using the GPS accurate positioning system in reference to the present land use map, and soil type map in the study area. Soil sampling spots were chosen on farmlands which were suspected to be contaminated by industrial and mining pollution and irrigated with polluted water. A soil sample was collected per 10 hectare of contained farm land. For the non-contained soil, a soil sample was taken every 200 hectare of farm land. Soil samples were taken at the 0-20cm depth, and a total of 490 soil samples were collected (Fig. 1). These soil samples represent each type of soils of major crop fields.

The content of As, Hg was determined using atomic fluorescence spectroscopy on a GB/T22105-2008. The content of Cd, Pb, Cr, Cu, Zn, Ni was analyzed using atomic absorption spectroscopy on a NY/T1613-2008. Analysis of parallel double samples was included for each soil sample. A full-range quality control and monitoring system was implemented for blank and treated samples during sample loading and the analytical procedures.

Data analysis. The descriptive statistics, correlation analysis, and principal components analysis (PCA) of heavy metal content were conducted using SPSS 20.0. Exploratory data analysis and the space Kriging interpolation were carried out using the geostatistical analyst module in ArcGIS 9.3.

RESULTS AND ANALYSIS

Soil heavy metal element contents. Soil contents of the eight heavy metals were measured and then compared to the background levels [7] in Tongling area and the soil environmental quality for agricultural land with the second grad of criteria (GB15618-1995 in China). As shown in Table 1, according to the rate of exceeding the national standard level, the 8 heavy metals were ranked as Cd>Cu>Zn>Ni>As>Cr>Hg>Pb. According to the rate of exceeding the background level, they were arranged in a descending order as Cd>Zn>Cu>Ni>Pb>As>Cr>Hg. Between the two types of comparison analysis, Cd, Cu, Zn, Ni did

not change their position relative to other heavy metals. However, for the other heavy metals, there are some discrepancies between the background level in Tongling and the criterial level in the national standards. Consequently, the relative ranking of these metals differed when compared in the two systems. For instance, the national criterial level of Pb and Cr is four-fold higher than the background level in Tongling, therefore the two metals were placed at a lower end of the rank in the former system.

Similar results were also reported in a former study [8] of heavy metal contents in Shanghai agricultural soil. According to the average soil content levels, six heavy metals (excluding Hg and Cr) were all above the background levels. These results indicate that the agricultural soils in Tongling area were invaded by exogenous heavy metals. The CV of Cd and Cu is > 1, which indicates that the two heavy metals differ greatly in spatial distribution. Presumably, human activities should have some influences on soil accumulation of these two heavy metals.

Correlation analysis of soil heavy metals. As shown in Table 2, based on the Pearson correlation coefficient, the higher value (> 0.5) among Zn, Pb and As indicates a strong linear relationship among the three heavy metals. In other words, these three heavy metals should come from the same pollution sources. For the pairs of Cu and Zn, Cu and As and Cr and Ni, there is still to a lesser degree of correlation, these results indicate the some of the contamination sources should be the same for the two metals in each group.

The principal components of heavy metals in soil. As shown in Table 3, the 8 heavy metals were placed in four significant principal components which account for 76% of the total variation in the spatial distribution in the study area. The eigenvalues of PC1-3 is above 1, and for the PC4, the eigenvalues of the rotation matrix is also greater than 1. Analysis of the component loading matrix clearly indicates that Pb, As, Cu and Zn belong to PC1, Cr and Ni to PC2, Cd to PC3, and Hg to PC4. Additionally, Cu has some loading value on PC3, Cd has some loading value in PC1 and PC2, and Hg has some loading value in PC1. These results indicate that these heavy metals have multiple and complex instead of single pollution sources. A similar situation was reported by Zheng Y M et al. [9].

TABLE 1
Descriptive statistical analysis of soil heavy metals on agricultural land near mining area in study area

Heavy metals	Cr	Pb	Cd	As	Hg	Cu	Ni	Zn
Highest soil content (mg kg^{-1})	591.0	605.5	11.792	91.71	0.697	1065.7	72.4	909.4
Lowest soil content (mg kg^{-1})	25.0	16.6	0.108	2.97	0.017	16.6	11.4	52.3
Average soil content (mg kg$^{-1)}$	87.1	73.9	1.315	15.47	0.140	67.0	29.4	139.7
SE (%)	58.57	67.83	1.89	11.49	0.074	92.71	8.20	85.71
CV	0.67	0.92	1.44	0.74	0.53	1.38	0.28	0.61
BL	88.56	47.79	0.086	12.44	0.25	32.15	24.71	85.58
ERB (%)	30.20	47.75	100	43.88	5.92	71.43	66.53	75.10
SSG	250	250	0.30	30	0.30	50	40	200
ERS (%)	2.86	2.45	82.86	8.77	2.65	32.86	13.67	17.96

Note: SE, Standard error; CV, coefficient of variation; BL, Background level for heavy metals in Tongling; ERB, exceeding rate above the background level; SSG, the second grad soil quality standard for heavy metal contents; ERS, exceeding rate above SSGS level.

TABLE 2
Pearson's correlation coefficient of soil heavy metal concentrations in study area

	Cr	Pb	Cd	As	Hg	Cu	Ni	Zn
Cr	1							
Pb	-0.011	1						
Cd	0.232**	0.185**	1					
As	0.029	0.582**	0.203**	1				
Hg	-0.004	0.313**	0.019	0.160**	1			
Cu	-0.039	0.186**	0.150**	0.300**	0.122**	1		
Ni	0.253**	-0.097*	-0.005	0.094*	-0.121**	-0.118**	1	
Zn	0.021	0.771**	0.234**	0.723**	0.233**	0.418**	0.083	1

Note : * Metals are significantly correlated at p = 0.05 level (two-tails); ** Metals are significantly correlated at p = 0.01 level (two-tails)

TABLE 3
Principal component analysis of soil heavy metal concentrations in study area

Total variance explained									
Component	Initial Eigenvalues			Extraction Sums of *Squared Loadings*			Rotation Sums of *Squared* Loadings		
	Sum	Variance %	Cumulative %	Sum	Variance %	Cumulative %	Sum	Variance %	Cumulative %
1	2.759	34.483	34.483	2.759	34.483	34.483	2.578	32.230	32.230
2	1.377	17.211	51.694	1.377	17.211	51.694	1.232	15.398	47.628
3	1.004	12.556	64.250	1.004	12.556	64.250	1.223	15.283	62.912
4	0.941	11.767	76.018	0.941	11.767	76.018	1.049	13.106	76.018
5	0.789	9.857	85.875						
6	0.608	7.594	93.469						
7	0.374	4.679	98.148						
8	0.148	1.852	100.000						

Components matrix a				
Heavy metals	1	2	3	4
Cr	0.053	0.756	0.247	0.332
Pb	0.836	-0.108	-0.146	0.157
Cd	0.360	0.396	0.677	-0.033
As	0.819	0.098	-0.211	-0.150
Hg	0.385	-0.297	0.027	0.766
Cu	0.505	-0.171	0.331	-0.426
Ni	-0.013	0.712	-0.532	-0.067
Zn	0.923	0.040	-0.159	-0.102

(1) In PC1, the loading value of Pb, As, Zn ad Cu is 0.836, 0.819, 0.923 and 0.505, respectively. In the correlation analysis, these four metals have a very high correlation coefficient. Together these results indicate that the four heavy metals share the same pollution sources. Pb, Cu and Zn mainly accumulate in soil due to air precipitation [10, 11]. Previously, it was found that the effects of air precipitation on heavy metal pollution also varied among functional regions [12]. Tongling has a very aggressive mining industry. Those mining and smelting industrial activities may have caused more serious air precipitation compared to traffic. Results from this study agree with a study by Wang Y Q [13].

The coefficient of variation (CV) of Pb, As, Zn and Cu, and the rate exceeding the background levels are all very high. The CV of Pb and Cu is 0.92 and 1.38, and the content of Cu and Zn in more than 70% soil samples is above the background level. Based on these results, soil accumulation of these heavy metals was primarily caused by air precipitation from mining and smelting industrial activities.

Additionally, several studies have found that Hg and Cd in air mainly come from mining and metallurgical operations [14, 15]. These can help to explain the loading of Cr and Hg in PC1, thus validating the conclusion that Cd and Hg in soil came from air precipitation [16].

(2) In PC2, Cr and Ni have a relatively high loading value each at 0.756 and 0.712, respectively. The average content of Cr did not rise to above the background level, Ni was slightly higher than the background level with the smallest CV (0.28) compared to the other 7 heavy metals. These results indicate that human activity had a very minimal influence on soil Ni accumulation whereas the heavy metal should mainly come from natural factors [17-19].

(3) PC3 mainly represents Cd with a proportion of variance of 12.556%. Thus, Cd in the agricultural soil should come from a complex source. Cr also showed some loading values in PC1 and PC2. The CV of Cd is as high as 1.44, and it has a 100% in the rate exceeding background level, 82.26% higher than the national second grad criteria level. These results indicate that Cd pollution in agricultural lands in Tongling has become a wide-spread problem [20].

In nature, Cd can only be found in some ore species. The heavy metal is released in large amount during mining in the area. Additionally, human activities such as irrigation with polluted water and fertilizer, all have some influences on the elevated level of exchangeable Cd in soil [21, 22]. It can be summarized that the Cd pollution in Tongling agricultural soil is a result of many factors including the position of ore layers, industrial and mining activities, fertilizer, and irrigation with polluted water.

Cu has some loading in the PC3, indicating that the accumulation of this metal was affected by air-precipitation, milling and mining, the position of the ore body, and agricultural irrigation [23, 24].

(4) PC4 mainly explains soil Hg, with a variance contribution rate of 11.767%. In the study area, the average level of Hg was lower than the background level (which is already very low at 5.92) in Tongling area. These results show that these farmland soil Hg was not influenced by exogenous pollutant sources. However, the higher CV (0.53) together with the loading in PC1 indicate that on a smaller

scale, Hg was affected by human activity, such as air precipitation due to mining, but the overall pollution level remained low [25-27].

Cluster analysis. A dendrogram was constructed using clustering analysis of the normalized data (Fig. 2). Pb, Zn and As were clustered into first group, Cr and Ni in the second, Cu and Cd in the third, and Hg in the fourth group. These clustering analysis results not only validated the PCA analysis, they also demonstrated that Cd and Cu accumulation in the farmland soil was affected by a multiple set of factors, consequently, the pollution sources for these heavy metals need to be investigated more comprehensively.

Analysis of sources of soil heavy metal pollutants. As shown in Table 4, PC1 and PC4 both fit into the spherical model. The PC2 and PC3 fit into index model and Gaussian's model. In these models, ME and the absolute value of NME are both close to nil (0); RMSE is similar to NME; and NRMSE value is around 1. It is apparent that these theoretical models meet the basic requirements [28], and thus they were used to simulate the spatial distribution of soil heavy metals in this study.

When measured by the nugget effects, PC4 had the highest value of 0.91 which indicates that the spatial distribution of this metal was absolutely affected by random factors. The nugget effect value was 0.65 and 0.51 for PC1 and PC3, respectively, which indicate that heavy metals in these two components have a medium-level spatial correlation relationship, and furthermore they were affected by natural and random factors. The smaller nugget effect (0.25) of PC2 indicates that natural factors had a bigger influence on metals in this component. In general, these properties of variance in spatial distribution measured by the nugget effects of each component agree with the results of descriptive statistics, PCA and clustering analysis.

The spatial distribution of the major principal components in Tongling area was described in Fig. 3. Then a soil parent material distribution map (Fig 4) was used to corroborate with the sources of heavy metals as described above in PCA analysis.

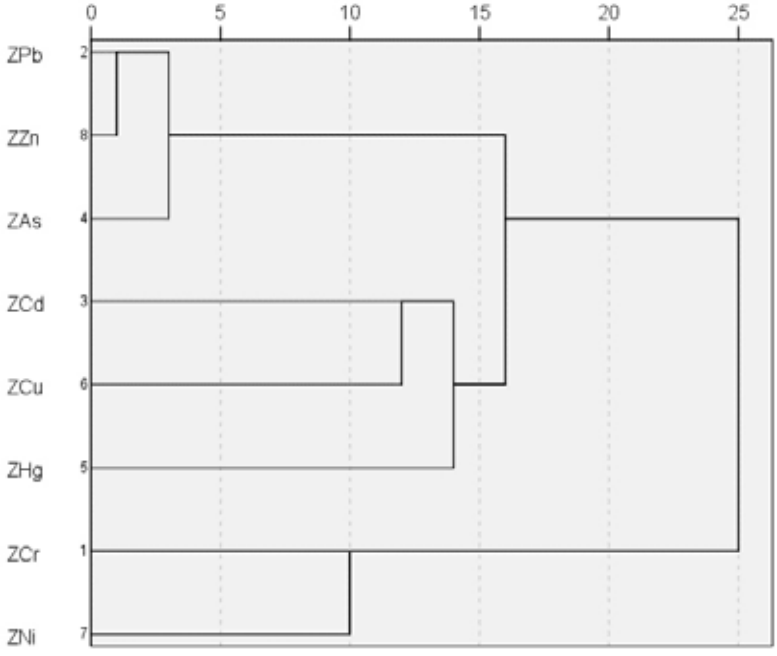


FIGURE 2
Cluster tree of soil heavy metals in study area

TABLE 4
The semivariance fitting of soil heavy metals in study area

	Model	NV	NE	ME	RMSE	ASE	NME	NRMSE
PC1	Spherical	1.32	0.65	-2.18E-03	1.420	1.228	-2.37E-03	1.068
PC2	Exponential	0.35	0.25	-3.25E-03	0.861	0.815	-2.64E-03	1.067
PC3	Gaussian	0.47	0.51	-7.3E-04	0.821	0.769	-9.93E-04	1.067
PC4	Spherical	0.77	0.91	1.34E-02	0.901	0.909	1.46E-02	0.9898

Note: NV, nugget value; NE, nugget effect; ME, mean error; RMSE, root mean squared error; ASE, average squared error; NME, Normalized mean error; NRMSE, normalized root mean square error

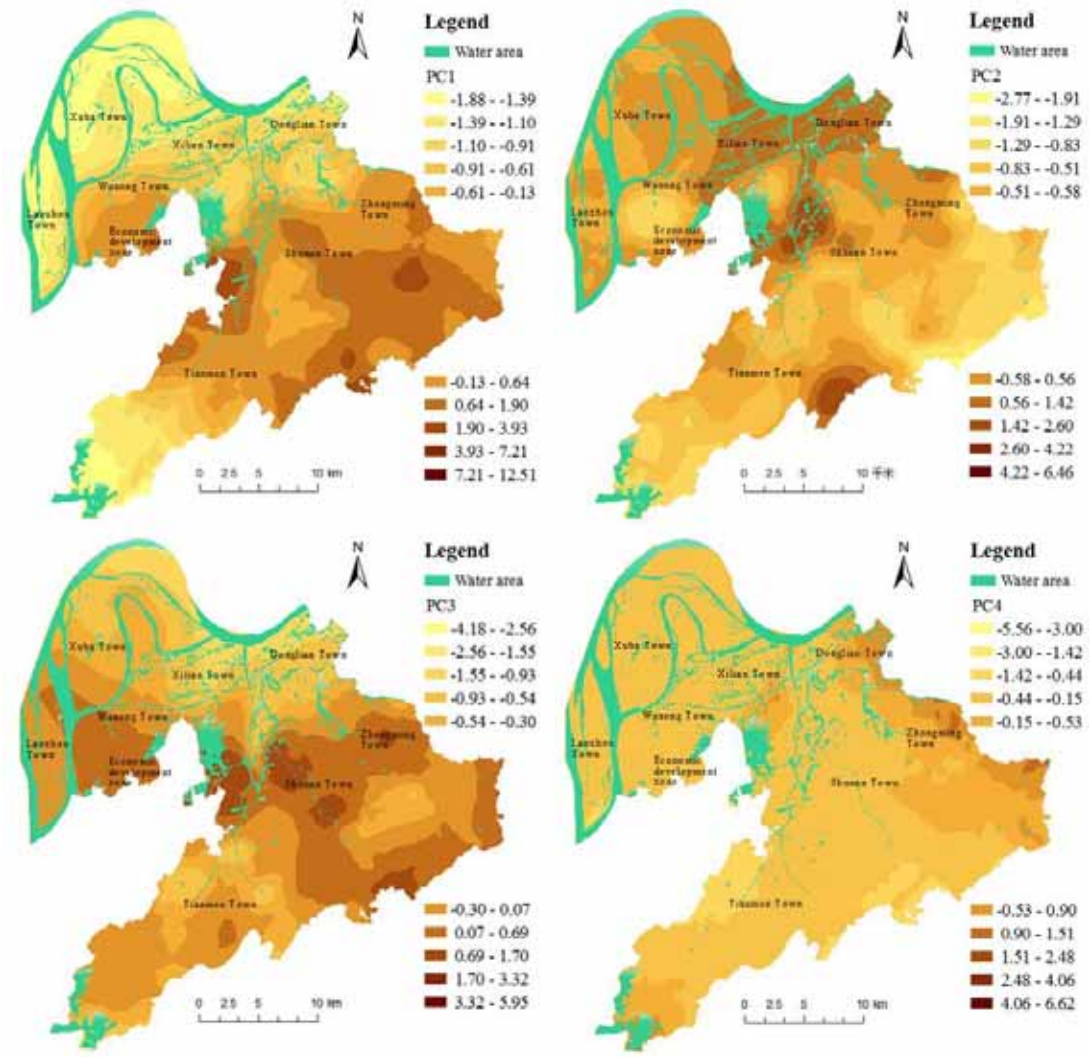


FIGURE 3
Spatial distribution of principal components of soil heavy metals in study area

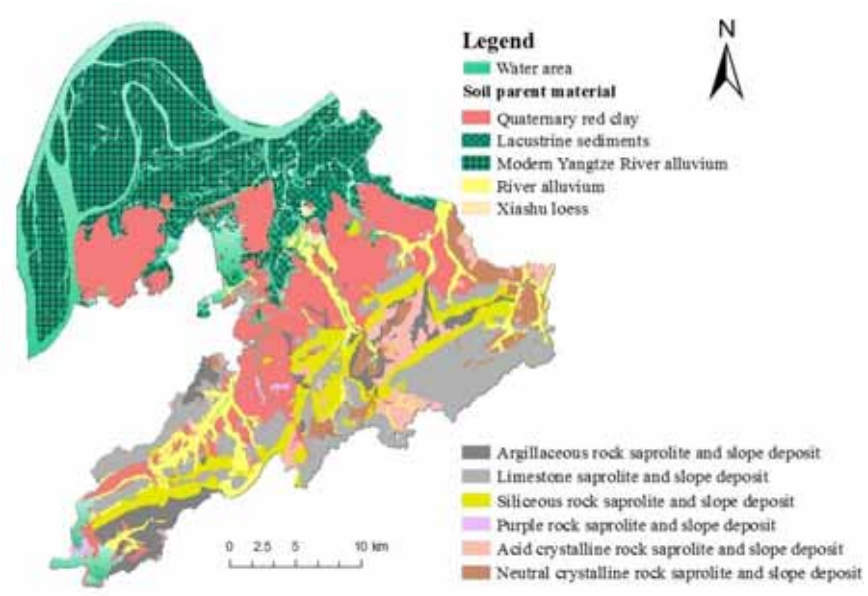


FIGURE 4
Spatial distribution of soil parent materials in study area

(1) PC1 spatial distribution properties and sources of pollutants. PC1 mainly represents Pb, As, Cu Zn. The high value areas were localized to three spots, in west of Shun'an, southeast of Zhongming, and east of Tianmen. The pattern of soil contamination of these heavy metals has a central hot spot which then spread out spherically into surrounding areas. These results indicate that these heavy metals were introduced into soil through human activities [29-31].

The high value area in west of Shun'an occurred in places where all the copper, gold and limonite mines and mining milling factories were located. The high value areas near southeast Zhongming matched to the area with lead-zinc mines, Pyrites ore, and active mining and milling companies. The high value area in east of Tianmen also was localized to an area having several mining factories and copper ore mines. Therefore, Pb and Zn pollution in agricultural soil in Tongling is connected to gold lead and zinc mining and milling [22, 32].

The pollution origin of As was associated with the pyrite mining area. The pollution sources of Cu were not able to separate from copper-iron and gold mining beds. Even though the distribution of these mines had some influences on accumulation of heavy metals in soil, the major causes of the enrichment of these heavy metals should be from mining, milling and smelting and the 'Three Wastes' discharged from these factories. Based on the spatial distribution of PC1, the high value areas in the east of Tianmen, and Zhongming tended to spread out in northwest direction along the river. These results indicate that irrigation with polluted water was the major cause for the high heavy metal content in agricultural soil [33]. In PC1, the content of Pb, As, Zn and Cu in soils was found to have some degree of correlation with raw ore layers. These heavy metals may have also entered soil through air precipitation. Cu accumulation in soil was also caused through irrigation by the local farmers.

(2) PC2 spatial distribution properties and the cause of pollution. Cr and Ni were placed in PC2. The high value spots were found on the alluvial plain of Yangtze River north of Tongling. Soil parent materials in this northern area are basically comprised of modern Yountze river alluvium and lacustrine sediments. The shape of the landscape nearly overlapped with the high value region of PC2, and it was distantly separated from other soil parent materials. These results indicate that soil Cr and Ni were mainly regenerated from the parent materials in Yountze river alluvium and lacustrine sediments.

The additionally two high value areas were located in Shun'an and Tianmen. Soil in the former area is rich in limonite. There are several studies showing that soil enrichment of Ni occurs in the presence of limonite. In Shun'an where three rivers confluence, water was polluted by acidic waste water from mining, industrial waste and municipal sewage. Cr and Ni may have entered soil through irrigation [23, 32]. Tianmen has a large number of mining, milling and metallurgy non-ferrous metal factories. These industrial and mining activities all have contributed to the enrichment of Cr and Ni in local soil. Therefore, for Cr and Ni in PC2, the major sources of pollutants include soil parent materials, followed by limonite and discharge of industrial waste water and irrigation with polluted water.

(3) PC3 spatial distribution properties and causes of pollutants. PC3 mainly reflects Cd. The high value area spread out widely into the surrounding areas from the Economic Zone in Zhongming. In Shun'an, elevated soil Cd level was identified along rivers. On the west side of the county there is a high value area which overlaps with PC1.

According to the survey data in the Economic Development Zone, a metallurgy non-ferrous metal factory was identified as the most likely source of Cd pollution. Zhongming is located in the vicinity of pyrite mine layers. Around the town there are many mining, smelting and commercial foundry. These factories have big influences on the emission of Cd and its accumulation in soil. In Shun'an, the high value area has a strong correlation with mining beds of pyrite, gold, lead, and zinc. They are also strongly correlated with the location of several mining, and milling factories. The high value areas on the two river banks spread out gradually, which supports the conclusion that irrigation has a significant impact on soil Cd accumulation. In west Shun'an, a large portion of the high value area overlapped with PC1. In those mines nearby Shun'an, minerals have weathered completely which occurred mainly near the rock-soil interface [21, 22, 25]. Additionally, frequent acid rain together with very low soil pH results in formation of exchangeable Cd in soil. Cd leaching into the waste acidic water when discharged during mining and ground water, would enter soil through irrigation and then bind onto soil colloids. Mining and milling also produce dust, and precipitation from of the metallurgical Cd-bearing dust also adds Cr into soil. In summary, the sources of Cd in Tongling are very complex. The enrichment of the heavy metal in soil is a result under influences of polluted air, water and soil.

(4) PC4 spatial distribution properties and causes of pollutants. PC4 has only Hg. No obvious high-value spots were found on the spatial distribution map. In other words, the heavy metal did not show accumulation in areas of dense mineral deposits and industrial and mining activities. There was no correlation between soil Hg content and soil parent materials either. This heavy metal was only found along the border of Zhongming. These results suggest that soil Hg should be influenced by random

factors, which concurs with the conclusion from the PCA analysis as described above. The Hg content of ore in the mining areas in this area is rather low [23] and sediment of dust in air might be the major source of this heavy metal leading to the accumulation of the heavy metal in soil.

CONCLUSIONS

(1) The overall situation of soil heavy metal concentration in Tongling County can be summarized as: soil content of Cd was the highest reaching a 100% exceeding rate against the background level, followed by Zn and Cu at 75.10% and 71.43%, respectively. The average level of Cr and Hg across the county was lower than the background level in the area.

(2) Soil content of Pb, Cd, Cu showed a characteristic big variation across sampling sites (with higher CV). These results suggest that these heavy metals were affected greatly by human activities. Additionally, soil contents of these two metals differed greatly in farmlands across the county. Soil Ni content varied very slightly among the sampling sites, which indicates that exogenous sources had made very minimal influences on this heavy metal.

(3) In the study area, Pb, As, Zn and Cu were clustered in PC1. Contents of these heavy metals were correlated with the position of the ore-containing layers in Tongling. The major source of these pollutants came from mining, milling and smelting industrial activities. Soil Cu content was also influenced by irrigation with polluted water.

(4) Cr and Ni are placed in PC2. The major pollution sources were identified to be the soil parent materials in lake sediments and modern Youngtze river alluvium and irrigation.

(5) Cd is the only metal in PC3. The source of this pollutant is very complicated, which involves in the ore-bearing layers of Pyrites, the 'Three Wastes" discharged from manufactories and mines as the major sources of pollutants. In particularly, irrigation with acidic waste water and precipitation of mining dust should have the greatest influence on Cd accumulation.

(6) Hg, as the component of the PC4, was found to be strongly influenced by small-scale human activities. But in general soil content of this metal is very low, and accumulation in certain areas is more likely due to air precipitation.

REFERENCES

[1] Ministry of Environmental Protection and Ministry of Land and Resources. (2014) National survey of soil pollution bulletin. Environmental Education. 6, 8-10.

[2] Uncumusoglu, A.A., Sengul, U. and Akkan, T. (2016) Environmental contamination of heavy metals in the Yaglidere Stream (Giresun), southeastern Black Sea. Fresen. Environ. Bull. 25, 5492-5498.

[3] Mazur, Z., Radziemaka, M., Fronczyk, J. and Jeznach, J. (2015) Heavy metal accumulation in bioindicators of pollution in urban areas of northeastern Poland. Fresen. Environ. Bull. 24, 216-223.

[4] Wang, S.H. (2012) The environmental geochemistry investigation of heavy metal elements in the Shizishan mining area, Tongling, Anhui Province. M.S. Dissertation. Nanjing University.

[5] Ye, H.M., Yuan, X.Y. and Zhao, J. (2012) Spatial migration and environmental effects of heavy metals in river sediments from in the Tongling mining area, Anhui province. China Environmental Science. 32, 1853-1859 (in Chinese).

[6] Li, R.Z., Xu, J.J., Jiang, Y.M., Chen, J. and Ding, G Z. (2012) Fraction distribution and ecological risk assessment of soil heavy metals in the riparian zone of Huixi stream in Tongling City. Research of Environmental Sciences. 26, 88-96 (in Chinese).

[7] China Environmental Monitoring Station (1990) Chinese soil element background values. China Environmental Science Press, Beijing.

[8] Meng, F., Liu, M. and Shi, T.G. (2008) Evaluation on environmental quality of heavy metals in agricultural soils of Shanghai. Environmental Science. 29, 428-433.

[9] Zheng, Y.M., Chen, T.B. and He, J.Z. (2008) Multivariate Geostatistical Analysis of Heavy Metal in Top soils from Beijing, China. Soils Sediments. 8, 51–58.

[10] Martin, L. (2001) Urban land use influences on heavy metal fluxes and surface sediment concentrations of small lakes. Water Air Soil Poll. 126, 363–383.

[11] Nicholson, F.A., Smith, S.R., Alloway, B.J., Carlton-Smith, C. and Chambers, B.J. (2003) An inventory of heavy metals inputs to agricultural soils in England and Wales. Sci Total Environ. 311, 205–219.

[12] Li, S.Q., Yang, J.L., Ruan, X.L. and Zhang, G.L. (2014) Atmospheric deposition of heavy metals and their impacts on soil environment in typical urban areas of Nanjing. China Environmental Science. 34, 22-29.

[13] Wang, Y.Q. (2014) Pollution assessment and source apportionment of heavy metals in soils around XinQiao Mining Area in Tongling, Anhui Province. M.S. Dissertation, Hefei University of Technology.

[14] Streets, D.G., Hao, J.M., Wu, Y., Jiang, J.K., Chan, M., Tian, H.Z. and Feng, X.B. (2005) Anthropogenic mercury emissions in China. Atmos. Environ. 39, 7789–7806.
[15] Yin, H.Q., Zhou, T.F., Chen, Y.N., Chen, F.R., Yuan, F. and Li, X.L. (2011) Pollution character of Cd in dust fall of Tongling City and its effect on soil. Geological Review. 57, 218-222.
[16] Lu, A.X., Wang, J.H., Qin, X.Y., Wang, K.Y., Han, P. and Zhang, S.Z. (2012) Multivariate and geostatistical analyses of the spatial distribution and origin of heavy metals in the agricultural soils in Shunyi, Beijing, China. Science of the Total Environment. 425, 66-74.
[17] Facchinelli, A., Sacchi, E. and Mallen, L. (2001) Multivariate statistical and GIS-based approach to identify heavy metal sources in soils. Environmental Pollution. 114, 313-324.
[18] Cai, L.M., Xu, Z.C., Bao, P., He, M., Dou, L., Chen, L.G., Zhou, Y.Z. and Zhu, Y.G. (2015) Multivariate and geostatistical analyses of the spatial distribution and source of arsenic and heavy metals in the agricultural soils in Shunde, Southeast China. Journal of Geochemical Exploration. 148, 189–195.
[19] Kumar, A. and Maiti, S.K. (2015) Assessment of potentially toxic heavy metal contamination in agricultural fields, sediment, and water from an abandoned chromite-asbestos mine waste of Roro hill, Chaibasa, India. Environmental Earth Sciences. 74, 2617-2633.
[20] Bai, X.Y., Yuan, F., Zhou, T.F., Li, X.L., Zhang, X., Fan, Y., Chen, X.R., Chen, Y.N. and Chen, F.R. (2008) The determination of geochemical abnormity of soil Cd in Tongling mining area using multifractal method. Bulletin of Mineralogy, Petrology and Geochemistry. 27, 306-310.
[21] Zhang, X., Zhou, T.F., Yuan, F., Shi, X.L., Fan, Y. and Liao, X.N. (2004) Speciation and bioavailability of cadmium in Tongling mining soils. Ecology and Environment. 13, 572-574.
[22] Yin, H.Q., Chen, F.R., Chen, X.R., Chen, Y.N., Jia, S.J., Wang, X.Y. (2010) Assessment of heavy metal pollutions to the soils in Tongling City, Anhui. Journal of Safety and Environment. 10, 98-102. Zhang, X. (2005) Geochemical characteristics and environmental effects of heavy metal elements releasing and migrating in Tongling mine area, Anhui Province. M.S. Dissertation. Hefei University of Technology.
[23] Yin, H.Q., Zhou, T.F., Zhang, X., Yuan, F., Li, X.L., Chen, Y.N., Chen, X.R., Chen, F.R. and Jia, S.J. (2009) Pollution characteristics of copper element in dustfall of Tongling City in Anhui Province. Journal of Jilin University (Earth Science Edition). 39, 734-738.
[24] Bai, X.Y., Yuan, F., Li, X.L., Zhou, T.F., Zhang, X., Chen, X.R., Chen, Y.N., Chen, F.R. and Jia, S.J. (2008) Spatial variance and pollution analysis of soil heavy metals in Tongling mining area, South China. Earth Science Frontiers. 15, 256-263.
[25] Lin, Y.S., Song, Y.Q. (2013) Research Advances on Heavy Metal Pollution in Tongling city. Science& Technology Information. 21, 137-139.
[26] Yang, X.F. (2007) A current research on heavy metal pollution to the soil and rice in the farmland in Tongling mining district. M.S. Dissertation. Hefei University of Technology.
[27] Liu, Y.L., Zhang, L.J., Han, X.F., Zhuang, T.F., Shi, Z.X. and Lu, X.Z. (2012) Spatial variability and evaluation of soil heavy metal contamination in the urban- transect of Shanghai. Environmental Science. 33, 599-605.
[28] Sun, L.H., Gui, H.R., Xu, D.S. and Huang, S.L. (2012) Heavy metal pollution in rural area of China: a case study of pond sediments from Sixian County, northern Anhui Province. Fresen. Environ. Bull. 21, 263-268.
[29] Mamat, Z., Yimit, H., Ji, R.Z.A. and Eziz, M. (2014) Source identification and hazardous risk delineation of heavy metal contamination in Yanqi basin, northwest China. Science of the Total Environment. 493, 1098-1111.
[30] Alam, N., Ahmad, S.R., Qadir, A., Ashraf, M.I., Lakhan, C. and Lakhan, V.C. (2015) Use of statistical and GIS techniques to assess and predict concentrations of heavy metals in soils of Lahore City, Pakistan. Environmental Monitoring and Assessment. 187, 636.
[31] Zhou, T.F. (2012) Environmental geochemistry and pollution remediation of heavy metal elements in Tongling mining area. Geological Publishing House, Beijing.
[32] Li, Y.X., Gao, H.C., Mo, L., Kong, Y.H. and Lou, I. (2013) Quantitative assessment and source apportionment of metal pollution in soil along Chao River. Desalination and Water Treatment. 51, 4010-4018.

Received: **07.07.2016**
Accepted: **05.03.2017**

CORRESPONDING AUTHOR

Youhua Ma
Anhui Agricultural University
Hefei, 230036 – China

e-mail: yhma2020@qq.com

© by PSP Volume 27 – No. 5/2018 pages 2671-2682 Fresenius Environmental Bulletin

NUMERICAL SIMULATION OF THE HYDRODYNAMIC EFFECTS OF AN ARTIFICIAL ISLAND

Xiaofeng Guo, Chuhan Chen*, Junjian Tang

Third Institute of Oceanography, State Oceanic Administration, Xiamen 361005, China

ABSTRACT

This study simulated the hydrodynamic effects prior to and after the construction of Quanzhou Bay Artificial Island using a semi-implicit Lagrangian–Eulerian finite difference method. Triangular meshes were used to refine mesh in the sea area surrounding the island in the model. To increase the accuracy of the simulation, the minimum mesh length was set to approximately 5 m. The simulation results indicated that during the falling tide, the flow velocities at the front of the berths on the west end and on the south side of the island increased by 0.2–0.4 m/s, and flow velocity in the main navigation channel between south Shihu and Dazhui Island decreased by 0.05–0.2 m/s. During the rising tide, the flow velocities at the front of the southwest end and south side of the island increased by 0.1–0.4 m/s, and the flow velocity in the main navigation channel between south Shihu and Dazhui Island decreased by 0.05–0.1 m/s. After construction, sediment concentrations decreased in the main navigation channel on the south side of Quanzhou Bay, in the channel to the north of the island, and in the marine space west of Baiyu. The waters between the Shihu Port area and the island underwent erosion and siltation within a range of -20–20 cm/a, which indicated slight sedimentation. The change of the movement rule of tidal current and sediment will reduce the tidal prism and self-purification capacity of bay and thus affect the structures and functions of the marine ecosystem.

KEYWORDS:
Numerical simulation, Lagrangian–Eulerian finite difference, Triangular mesh, Quanzhou Bay artificial island

INTRODUCTION

An artificial island is a multi-purpose, manmade offshore structure in shallow water. Artificial islands can serve as deepwater ports, offshore airports, floating towns, or as bases for activities such as offshore oil and gas development, seabed mineral exploitation, aquatic product processing, and waste disposal. Rapid economic development has significantly increased sea space utilization and resulted in the increasing construction of artificial islands [1]. Artificial island construction creates new coastlines; changes submarine topography; influences the hydrodynamic environment, e.g., via seabed erosion or siltation of the surrounding marine area; and reduces the tidal prism and self-purification capacity of bays [2]. Hence, in addition to guaranteeing the structural stability of artificial islands, construction projects should analyze the potential influences of construction on the surrounding marine environment [3-4], and develop appropriate preventive measures to significantly mitigate potential adverse effects on the environment [1].

The hydrodynamic impact of an artificial island project can be studied using numerical simulation methods [5-8]. The present study used a semi-implicit Lagrangian–Eulerian finite difference method and triangular or quadrilateral meshes [9-10] with a 5 m minimum mesh length to determine the tidal current field adjacent to the island [11-12] and simulate the hydrodynamic effects of island construction on a marine area. The impact of artificial island construction on the marine environment was then assessed based on the prediction of the hydrodynamic effects [13].

INTRODUCTION OF AREA AND PROJECT UNDER STUDY

Quanzhou Bay. Quanzhou Bay is located off the southeastern coast of Fujian Province (Figure 1). It is surrounded by Huian County to the northeast, Quanzhou City to the northwest, and Jinjiang City and Shishi City to the southwest, and it is adjacent to the Taiwan Strait to the east. A mouth-bar development (Xiesha Shoal) is located at the bay front, which opens to the southeast, where Dazhui Island and Xiaozhui Island cross the middle of the entrance. With its wide mouth, winding shorelines, and alternating headlands, Quanzhou Bay is characterized by regular semi-diurnal tides with a mean range of 4.27 m. The bay has reciprocating tidal currents that are relatively stable. Currents flow into the bay at high tide and flow back out at low tide. Waves in Quanzhou Bay are mainly mixed waves formed by wind waves in the NNE–NE and SSW directions and surges from the SE direction. Historical measurements have yielded a monthly average wave height of 0.7–1.1 m and an average wave period of 3.7–4.2 s. Quanzhou Bay is a semi-closed bay joined by the

Jinjiang River and Luoyang River. Its sediment is mainly transported by runoff from the Jinjiang River and via tidal currents at high tide. The average sediment concentration during middle tide is lower than that during spring tide but higher than that during neap tide. The suspended sediments in different parts of Quanzhou Bay are categorized as fine-grained sediments, with an average median particle diameter of approximately 0.01 mm. Sediment samples collected from Quanzhou Bay include coarse sand, medium-coarse sand, medium sand, medium-fine sand, medium sand, clayey sand, and sandy clay.

Project under Study. Quanzhou Bay Artificial Island is located on the Xiesha Shoal in the middle of the bay mouth. It extends from east to the west and is primarily parallel to tidal currents (Figure 2). The maximum length of the artificial island is 4,446 m from east to west and 800 m from south to north. The enclosed land area is 323 hm^2. To reduce local deflecting flow and backflow at the corners of the eastern and western coastlines, a diverging opening was created on the west tip of the artificial island. The western coastline is deflected 14° clockwise, and an arc flow adjustment occurs along the east bank for protection, with a 100–700 m wide tidal channel remaining between the artificial island and Dazhui Island [14]. Twelve 50,000 ton multi-functional berths are planned for the southern coastline [15].

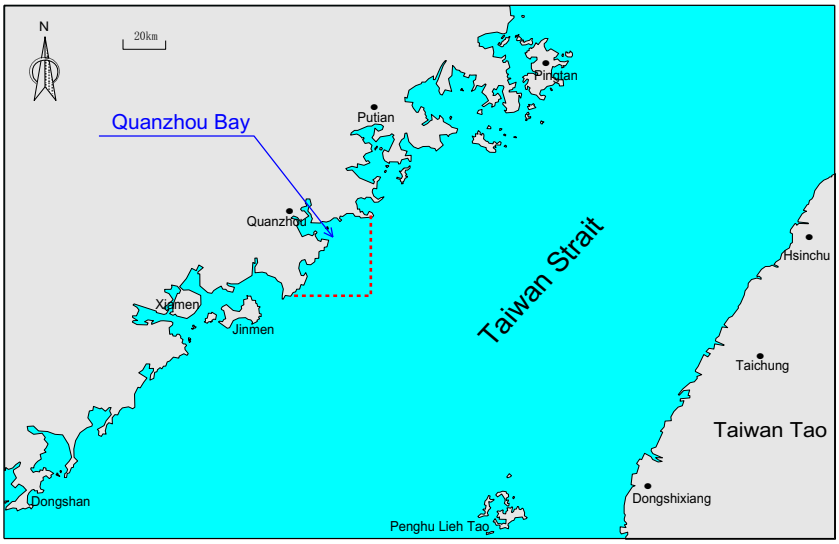


FIGURE 1
Geographical location of Quanzhou Bay

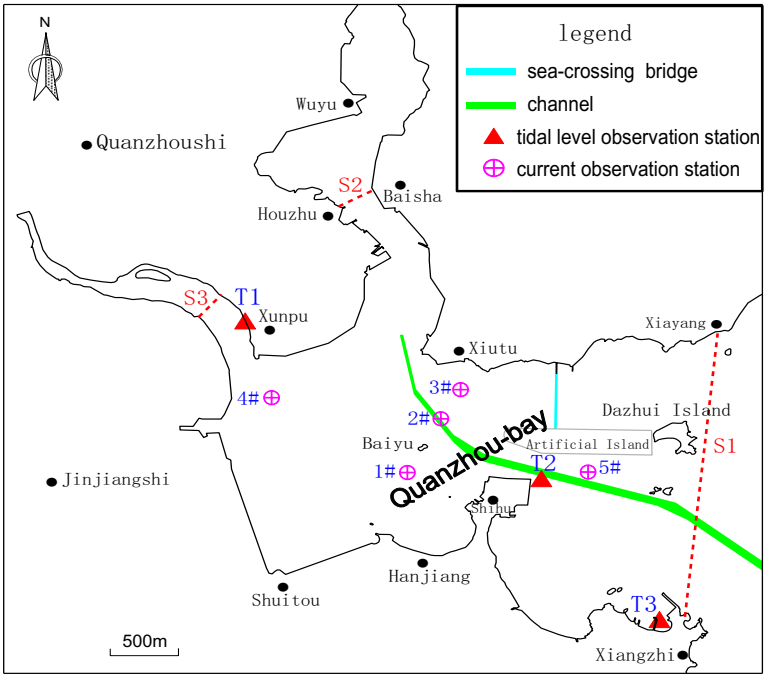


FIGURE 2
Locations of the Quanzhou Bay artificial island and the hydrological observation stations

MATERIALS AND METHODS

Model Control Equations. Two-dimensional (2D) shallow water equations in plane rectangular coordinates were used to simulate the tidal current field, which was the basis for solving the sediment and water exchange fields. The 2D transport equations of mean suspended sediment and seabed deformation equations [16] were derived from the sediment transport equations originally developed by Dou [17] under the combined influence of waves, tides, and the dynamic diffusion effect. Mass transport equations were used for the water exchange field, whereas the corresponding equations for the tidal current field, sediment field, and water exchange field were as follows:

$$\frac{\partial \eta}{\partial t}+\frac{\partial}{\partial x}(Hu)+\frac{\partial}{\partial y}(Hv)=0 \quad (1)$$

$$\frac{\partial u}{\partial t}+u\frac{\partial u}{\partial x}+v\frac{\partial u}{\partial y}=-g\frac{\partial \eta}{\partial x}+fv-ru+A_x\left(\frac{\partial^2 u}{\partial x^2}+\frac{\partial^2 u}{\partial y^2}\right) \quad (2)$$

$$\frac{\partial v}{\partial t}+u\frac{\partial v}{\partial x}+v\frac{\partial v}{\partial y}=-g\frac{\partial \eta}{\partial y}-fu-rv+A_y\left(\frac{\partial^2 v}{\partial x^2}+\frac{\partial^2 v}{\partial y^2}\right) \quad (3)$$

$$\frac{\partial HS}{\partial t}+\frac{\partial HuS}{\partial x}+\frac{\partial HvS}{\partial y}+\alpha\omega_s(S-S_*)=\frac{\partial}{\partial x}\left(HD_x\frac{\partial S}{\partial x}\right)+\frac{\partial}{\partial y}\left(HD_y\frac{\partial S}{\partial y}\right) \quad (4)$$

$$\gamma'\frac{\partial \eta_s}{\partial t}=\alpha\omega_s(S-S_*) \quad (5)$$

$$\frac{\partial(HC)}{\partial t}+\frac{\partial(HuC)}{\partial x}+\frac{\partial(HvC)}{\partial y}=\frac{\partial}{\partial x}\left(HK_x\frac{\partial C}{\partial x}\right)+\frac{\partial}{\partial y}\left(HK_y\frac{\partial C}{\partial y}\right) \quad (6)$$

where x and y are plane rectangular coordinates; t is time; H is water depth ($H = d+\eta$); d is the water depth beneath the mean water level; η is the water level; u and v are the directional components in the x and y directions, respectively; $u=(1/H)\int_{-h}^{\eta}u'dz$ and $v=(1/H)\int_{-h}^{\eta}v'dz$ are the average flow velocities integrated over the water depth; g is gravitational acceleration; f is the Coriolis parameter; r is the bottom friction coefficient, which equals $r=g\sqrt{u^2+v^2}/c_n^{\,2}H$; $c_n=H^{1/6}/n$ is the Chézy coefficient; n is the roughness coefficient of the seabed; Ax and Ay are the viscosity coefficients of horizontal movements; S is the vertical mean sediment concentration; ω_s is the settlement velocity of suspended sand particles; D_x and D_y are sediment dispersion coefficients in the x and y directions, respectively; $\gamma'=1750d_{50}^{0.183}$ is the dry density of suspended sediment [18]; α is the settlement probability of suspended sediment particles; η_s is the erosion and siltation thickness associated with suspended sediment; C is the water body concentration; and K_x and K_y are the water body diffusion coefficients in the x and y directions, respectively. S_*, which is the sand-carrying capacity under the combined influence of waves and tides, can be calculated using the following equation [19-20]:

$$S_*=\alpha\frac{\gamma\gamma_s}{\gamma_s-\gamma}\left(\frac{V^3}{C^2h\omega}+\beta\frac{H^2}{hT\omega}\right) \quad (7)$$

where γ and γ_s are the bulk densities of water and sand, respectively, ω is the settling velocity, C is the Chézy coefficient, h is the water depth, and V is the tidal velocity. The annual average wave height of Quanzhou Bay H is 0.9 m, and the average wave period T is 4.0 s.

Equations (1) – (6) were solved using Vincenzo Cassulli's semi-implicit finite difference method [21- 27], which uses non-structural triangular or quadrilateral orthogonal meshes for modeling. Each side of the triangular (or quadrilateral) mesh was the boundary of another triangular (or quadrilateral) mesh. The central lines of adjacent meshes were perpendicular to the boundary sides [28-29]. Implicit finite difference components in equations were selected to solve the model, and the Lagrangian–Eulerian method was used to decompose the transport and horizontal viscosity components. Thus, the time step of the solution was not limited by the CFL condition and could be amplified in comparison with the time steps used in other methods. This method ensured the stability of the solution [26].

When the model is applied to artificial island construction, smaller sides can be used for the meshes, and the time step can be longer (20 s). This treatment ensures the stability of the solution and improves the computational efficiency. Minimum mesh sides of 5 m were used in this study. Coastal waters have wide tidal areas that are submerged when the tide rises and emerge when the tide falls. In the modeling computation, beach exposure was treated as a dynamic boundary condition [30]. A non-flow passing technique was used in the model to automatically assess and treat the dry-wet elements, sides, and nodes [24].

Boundary and Definite Conditions. Boundary and Definite Conditions of the Tidal Current Field. Coastal line is a solid boundary, and the flow velocity in the normal direction is zero. However, a tidal flat is a variable boundary, and the water level of the open boundary of the tidal current field is based on the tide level of the tidal current field in the Taiwan Strait [31].

Boundary and Definite Conditions of the Sediment Field.

A. Boundary conditions:

Shore boundary: $\frac{\partial S}{\partial n}=0$ (where n is the normal direction of the shore boundary)

Water boundary:

Computational domain of inflow:

$S(x,y,t) = S_{in}(x,y,t)$, where S_{in} is the measured value of sediments at the water boundary.

Computational domain of outflow: $\frac{\partial(HS)}{\partial t} + \frac{\partial(HUS)}{\partial x} + \frac{\partial(HVS)}{\partial y} = 0$

The values assigned at the open boundary of the suspended sediment field are as follows: 0.44 kg/m^3 is the sediment concentration at the mouth of the Jinjiang River; 0.03 kg/m^3 (spring tide), 0.02 kg/m^3 (middle tide), and 0.012 kg/m^3 (neap tide) were the sediment concentrations in the open sea at the eastern open boundary of the construction site; and 0.03 kg/m^3 (spring tide), 0.02 kg/m^3 (middle tide), and 0.012 kg/m^3 (middle tide) were the sediment concentrations in the open sea at the southern open boundary of the construction site.

B. Initial condition:

$$S(x,y,0) = S_0(x,y)$$

Boundary and Definite Conditions of the Water Exchange Field.

Condition of shore boundary: $\frac{\partial c}{\partial n} = 0$, where *n* is the normal direction of the shore boundary.

Conditions of open boundary are calculated by $\frac{\partial c}{\partial t} + u\frac{\partial c}{\partial x} = 0$ and $\frac{\partial c}{\partial t} + v\frac{\partial c}{\partial y} = 0$ during the falling tide. The concentration at the boundary during a rising tide was zero.

Computational Domain and the Associated Identification of the Model. Computational domain includes the marine space east of Weitou and south of Chongwu. The meshes of the marine space near the Quanzhou Bay construction site were refined. The maximum mesh length was 1,000 m, and the minimum mesh length was 5 m. The overall number of mesh nodes was approximately 20,000, with approximately 40,000 meshes. The coastline was a solid boundary. The flow velocity in the normal direction was zero [32]. The open fluid boundary of the open sea included two cross-sections. One control point, the SE point, was located at the southeast corner of the computational marine space. The line connecting the SE point and Weitou was south of the open boundary section, whereas the line connecting the SE point and Chongwu was to the east. The water depth of the open boundary was based on the tide level of the tidal current field in the Taiwan Strait.

Tidal level and tidal current data were collected from flow measurements of the 2009 spring tide and from real data on tidal level synchronization. The hydrological observation stations are shown in Figure 2. Tidal level stations were located at Xunpu, Shihu, and Xiangzhi, and there were five tidal current and sediment stations. Stations 1 through 3 were located on both sides of the artificial island, Station 4 was located at the Jinjiang River estuary on the southeastern side of Xunfu, and Station 5 was located at the edge of the main navigation channel on the south side of the construction site.

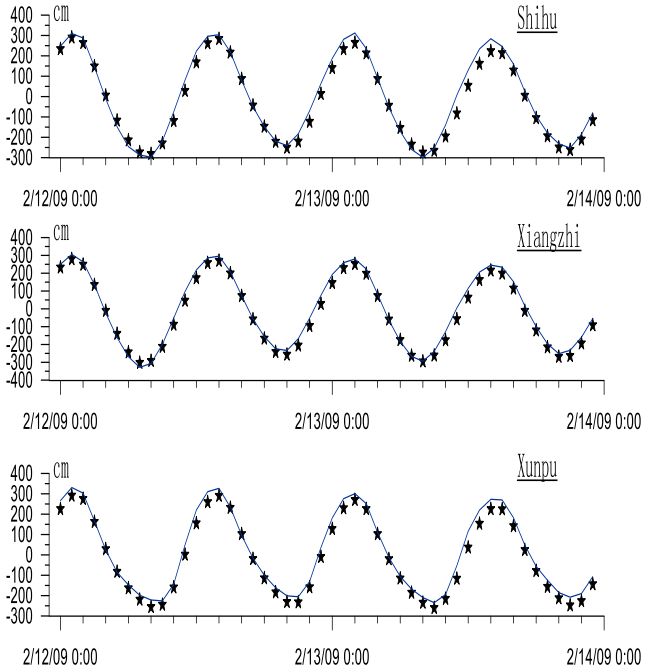


FIGURE 3

Simulated and measured values collected during flow monitoring at tidal level stations

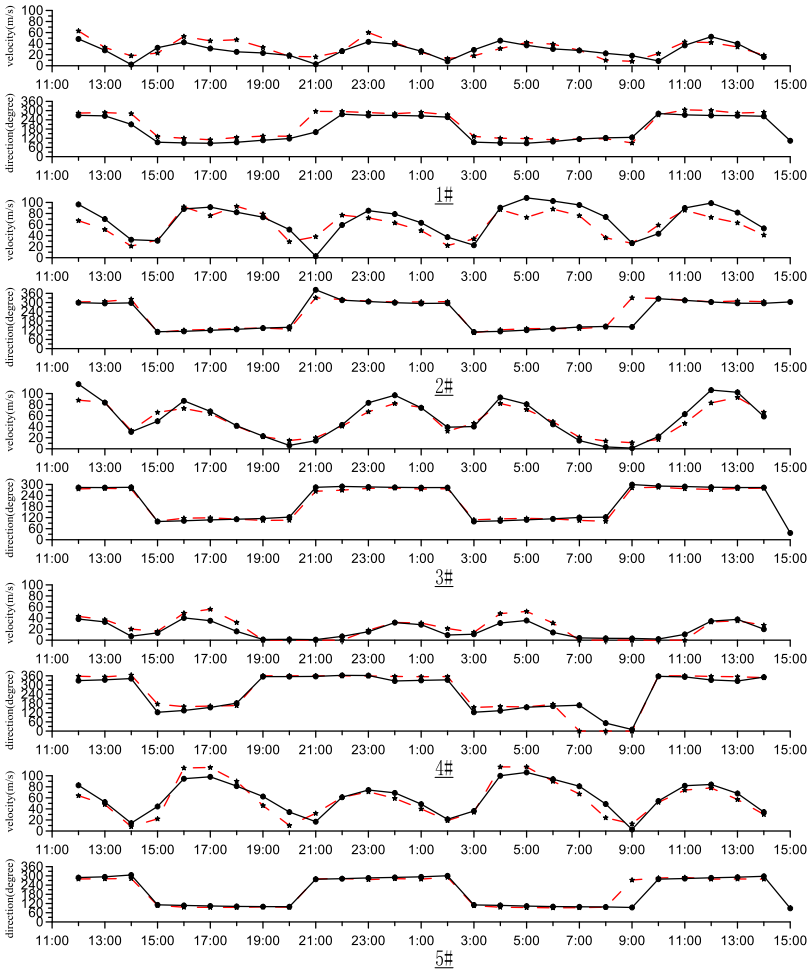


FIGURE 4
Simulated and measured verification curves from tidal current stations

Figure 3 shows the computational and observed tidal levels at spring tide from the Xunfu, Shihu, and Xiangzhi temporary tidal level stations in February 2009. The computational and observed values exhibited satisfactory agreement based on the tidal curves. Figure 4 shows the curves of simulated and observed values at tidal current stations No. 1 through 5 in February 2009. In general, the computational values matched the observed values of flow velocity and direction. Figure 5 shows the variations in sediment concentration curves over time at hydrology and sediment stations No. 1 through 5 for the spring tide in February 2009. The sediment concentration values observed at various stations were similar to the computed and vertically averaged sediment concentrations. Hence, the numerical simulation results suggested that the model satisfactorily reflected the tidal sediment movement in Quanzhou Bay and that the model could be used for construction analysis.

RESULTS AND DISCUSSION

Numerical Simulation of the Tidal Current and Sediment. Summary of the Numerical Simulation Plan. This simulation included a status quo plan and a construction plan as follows.

(1) The status quo plan refers to the pre-construction plan, i.e., the current coastline and water depth scenarios in Quanzhou Bay.

(2) The construction plan for the Quanzhou Bay Artificial Island project was executed based on the pre-construction plan, and the minimum distance between the east coast of the artificial island and the west tip of Dazhui Island was 100 m.

Simulation Results of the Status Quo Plan. The flow velocity in Quanzhou Bay was high near the deep trough and low in shallow areas. At high tide, the flow velocity near the construction site was low. The rapid falling stage exposed part of the coastal shallows. There were two main ebb currents. The ebb currents of the Houzhu navigation channel flowed east and outward via the Xiesha north channel and converged with the Jinjiang River to the east of Baiyu. They then continued eastward via the Shihu channel to outer Quanzhou Bay via the Dazhuimen and Xiaozhuimen navigation channels. The ebb currents associated with Xiesha Shoal flowed southeast into the deep trough south of Dazhui Island. Low tide exposed the shallow areas along the coastline of Xiutu and the large shallows on both sides of Xiesha and Shihu while water continued

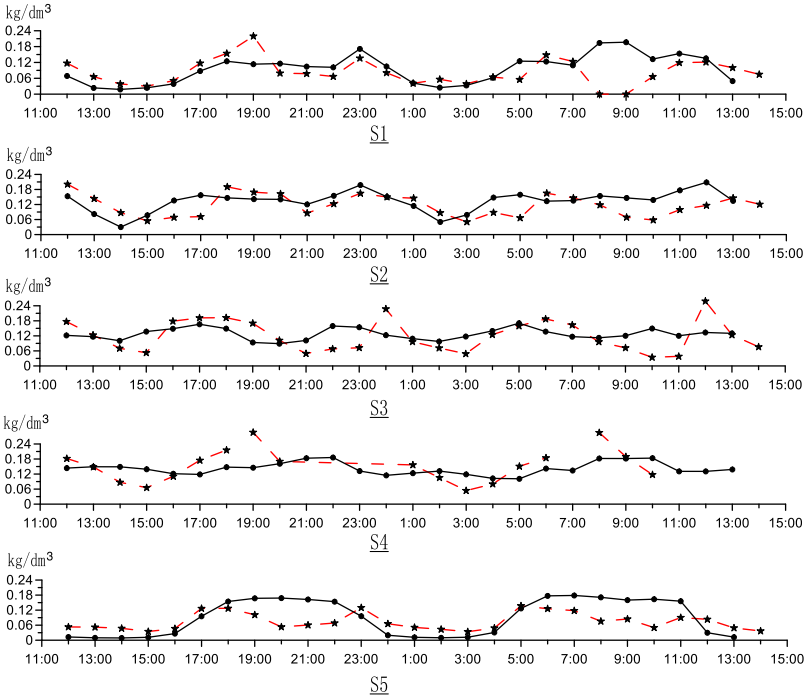


FIGURE 5
Process curves of measured and simulated average vertical sediment concentrations from sediment stations

to flow through a trough in the middle of Xiesha. The tidal direction in Quanzhou Bay during the rapid rising stage was opposite that of the ebb tide. The rising tide consisted of two streams to the south and north of Xiesha. One stream flowed along and into the north channel of Dazhui Island, whereas the other flowed along the Dazhuimen and Xiaozhuimen navigation channels into the Shihu navigation channel (south channel). The flow velocity of the current in the north channel was slightly higher than that in the south channel. After flowing through Shihu-Xiutu, the current fanned out, with the north branch flowing into the Houzhu navigation channel and the west branch entering the Jinjiang River estuary.

The frontier waters along the northwest-west coast of Dazhui Island were shallow, allowing water to only flow at high tide. The tidal current weakened before reaching the shallow area, with the flow direction varying greatly. The flood and ebb currents at the southwest beach frontier of Dazhui Island were reciprocating currents. The flood currents south of Dazhui Island flowed northwest to Xiesha Shoal, and the ebb currents from Xiesha Shoal flowed southeast and converged with the mainstream ebb current south of Dazhui Island, which was tranquil.

Figure 6 shows the isogram distribution of the average flow velocity during rising and falling tides prior to construction. Additionally, Figure 6 shows that the flow velocity in Quanzhou Bay was high in the southern and northern channels and low in shallow areas. At ebb tide, the flow velocity in the Xiesha northern channel was approximately 0.4–0.8 m/s, the average flow velocity in the deep trough at the Shihu frontier was approximately 0.8–1.0 m/s, and the flow velocity in the deep trough to the south of Dazhui Island was approximately 0.6–0.8 m/s. At rising tide, the flow velocities of the currents in the Xiesha north channel were slightly higher than those of the ebb currents, but in other areas, the average flow velocities during the rising tide were lower than those of the ebb currents.

The sediment field in Quanzhou Bay was mainly formed by suspended sediment transport and bed load movement under tidal dynamics and wave action. Figure 7 shows the annual sedimentation intensity distribution near the construction site along the current coastline. The figure shows that the annual sedimentation intensity in the Xiesha north channel was approximately 5–20 cm/a. Sediment erosion and siltation occurred in the Xiesha waters, and the sediment erosion intensity was 0–10 cm/a, whereas the sedimentation intensity was 5–20 cm/a. The annual sedimentation intensity in the Shihu harbor district, where the Shihu main navigation channel is located, was approximately 10 cm/a. The annual sedimentation intensities in the waterways connected to the adjacent Dazhui and Xiaozhui Islands were 2–10 cm/a, indicating that sedimentation in Quanzhou Bay occurred along the main navigation channel and the Xiesha south and north channels.

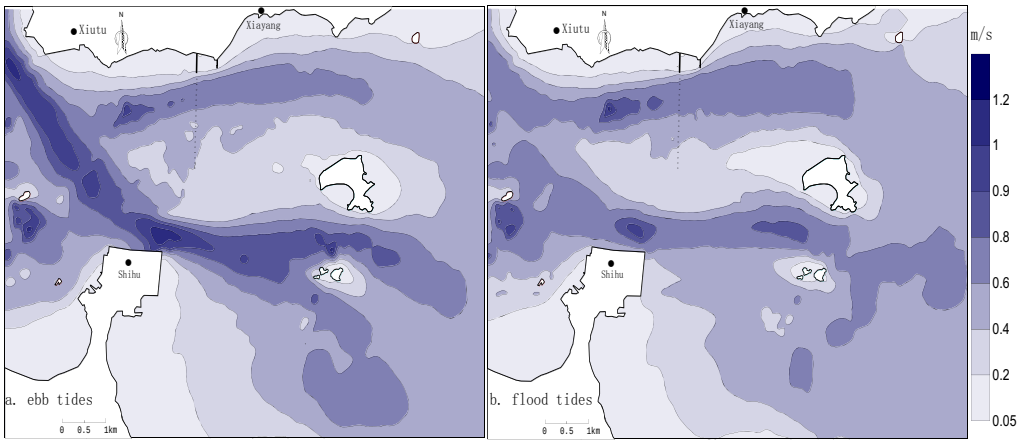


FIGURE 6
Average flow velocity distribution of spring tide in the construction site prior to construction

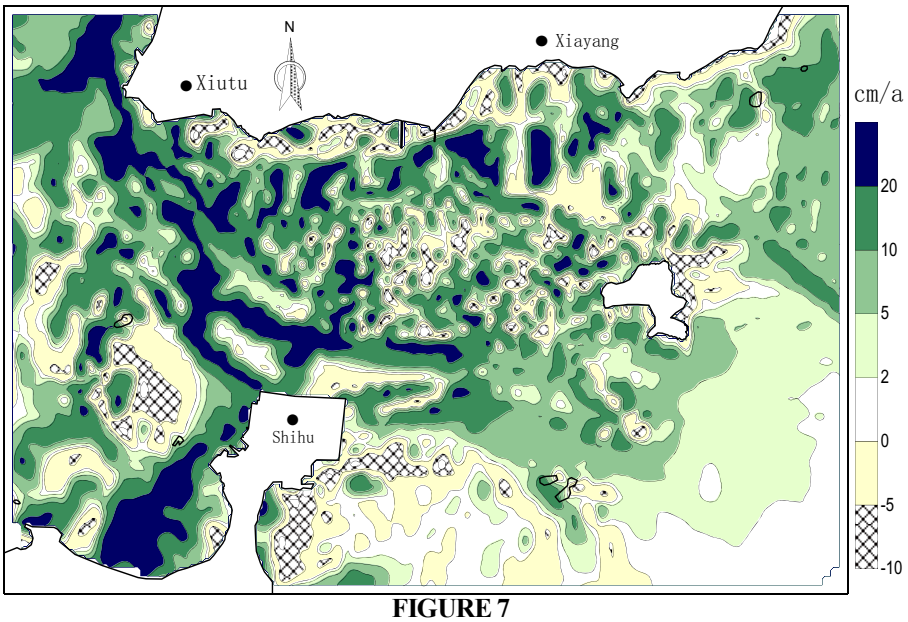


FIGURE 7
Annual sediment intensity sistribution in the sea area of the construction site prior to construction

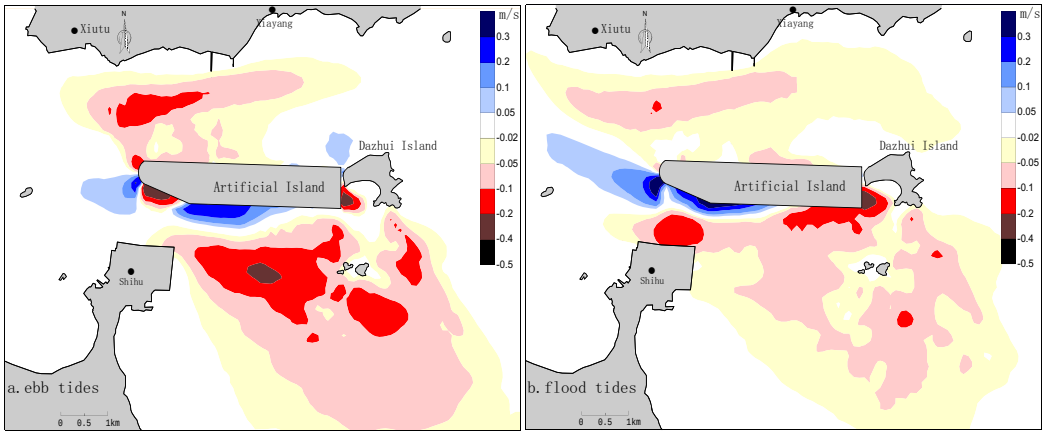


FIGURE 8
Comparison of average flow velocity prior to and after construction

Simulation Results of the Construction Plan. Figure 8 shows the isogram distribution of flow velocity variations during the rising and falling tides prior to and after construction. The figure shows the following results:

(1) After the southwestern and eastern coastlines of the artificial island were optimized, no reflow occurred in the frontier waters on the southwest side of the island during the rapid falling stage, and weak reflow was observed near low tide. Additionally, almost no reflow occurred in the frontier waters off the protected east bank at ebb tide.

(2) Following island construction, the flow velocities near the western tip and southern berth frontiers increased by 0.2–0.4 m/s at ebb tide, and the flow velocity in the main navigation channel from Shihu to southern Dazhui Island decreased by 0.05–0.2 m/s. At high tide, the flow velocities near the southwest end and southern frontier of the artificial island increased by 0.1–0.4 m/s, and the flow velocity in the main navigation channel from Shihu to south Dazhui Island decreased by 0.05–0.1 m/s. In addition, the flood and ebb currents in the north channel of the artificial island decreased by 0.02–0.1 m/s.

Annual isogram curves of the sediment intensity variation were used to compare the variations in the annual suspended sediment intensities near the construction site prior to and after construction. The annual suspended sediment intensity at nodal points prior to construction was subtracted from the intensity after construction, as shown in Figure 9. Sediment concentrations decreased in the main navigation channel south of Quanzhou Bay, the north channel of the artificial island, and the sea area west of Baiyu during construction, indicating that the artificial island helped regulate outward sediment transport from the bay. Sediment scouring and silting within -20–20 cm/a occurred in the waters between the Shihu harbor district and the artificial island, and minor siltation was observed.

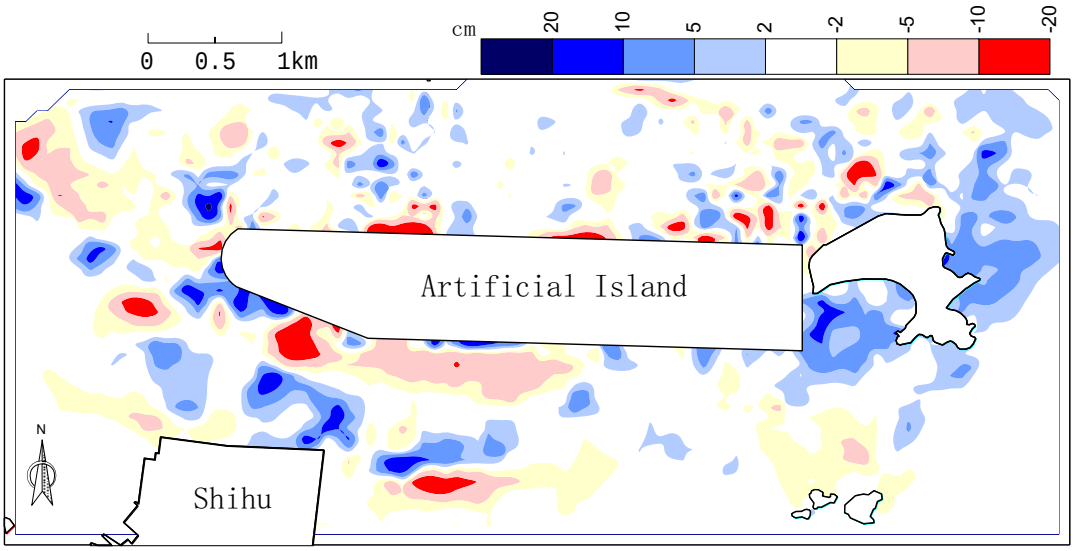


FIGURE 9
Comparison of annual sedimentation intensity prior to and after construction

TABLE 1
Comparison of tidal flows by section during rising and falling tides in a tidal cycle after the construction of the artificial island

Stage	Falling tide ($\times 10^8$ m^3)			Rising tide ($\times 10^8$ m^3)		
	S1 Section	S2 Section	S3 Section	S1 Section	S2 Section	S3 Section
Prior to construction	Spring tide	6.268	0.448	0.291	6.157	0.451	0.206
	Middle tide	4.860	0.306	0.213	4.766	0.301	0.147
	Neap tide	3.348	0.252	0.182	3.280	0.256	0.119
	Average	4.825	0.335	0.229	4.734	0.336	0.157
After construction	Spring tide	6.138	0.448	0.291	6.025	0.451	0.206
	Middle tide	4.757	0.306	0.213	4.658	0.301	0.147
	Neap tide	3.270	0.252	0.182	3.210	0.256	0.119
	Average	4.722	0.335	0.229	4.631	0.336	0.157
	Increase/decrease	-0.104	0	0	-0.103	0	0
	Percentage	-2.1	0	0	-2.2	0	0

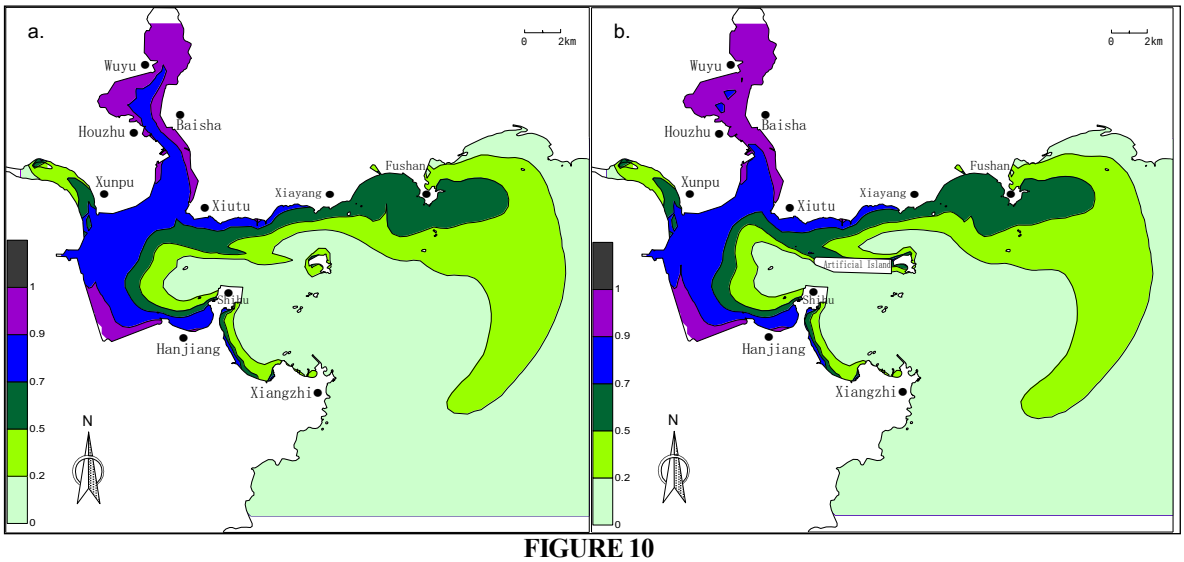


FIGURE 10
Characteristic concentration distribution of water exchange at high tide (a. prior to construction and b. after construction)

Variations in the Tidal Prism Prior to and After Construction. The tidal prism is a key indicator that represents the vitality of a semi-closed bay. Tidal prism variations generally reflect changes in tidal current characteristics and can affect the sediment discharge, water exchange capacity, and environmental capacity of the bay. This study determined the tidal prism by calculating the fluxes through different sections [33]. The sectional flows of rising and falling tides represented the integrals of sectional velocity fluxes during these tides. In the planned analog computation, the S1 section from Xiangzhi–Dazhui Island and Xiaozhui Island–north coast, the S2 section from Houzhu, and the S3 section from the Jinjiang River estuary were used to compute the flows associated with spring, modest, and neap tides in the tidal cycle. The S1, S2, and S3 sections are shown in Figure 2. Table 1 compares the sectional flows between the rising and falling tides in a tidal cycle prior to and after construction. After construction, the average flows of falling and rising tides in section S1 were 4.722×10^8 m^3 and 4.631×10^8 m^3, respectively; thus, they decreased by 1.040×10^7 m^3 and 1.030×10^7 m^3, or by approximately 2.1% and 2.2%, compared with the volumes observed during the status quo plan. The flows of rising and falling tides in sections S2 and S3 remained unchanged. These observations indicated that the construction of Quanzhou Bay Artificial Island had no significant impact on the tidal prism of the bay.

Numerical Simulation of Water Body Exchange Prior to and After Construction. To calculate the water exchange in a specific area, we assumed that water was evenly distributed inside and outside the research area. The initial concentration of water was c=1 in the specific area and c=0 outside the specific area. During the water exchange process, the concentration within the specific area gradually became 0<c<1 (the average concentration after mixing) [34-35]. In each calculation step, the average "concentration" $\bar{c}$ is computed within the specific area as follows:

$$\bar{c} = \frac{\sum c_i V_i}{V_0} \tag{8}$$

where c_i is the concentration of the ith mesh node at a given time, V_i is the water body volume in the ith node, and V_0 is the total volume of the water body in the bay. The cumulative time was also calculated.

When $\bar{c}$=0.5 (where $\bar{c}$ is the average value in a tidal cycle), the corresponding time is the half-life time.

Based on the water exchange within and outside of Quanzhou Bay with the S1 section serving as the boundary, the water outside the bay was new, whereas the water in the bay was original, as shown in Figure 2. Specifically, water to the west of S1 was original, water to the east of S1 was new, and water flowing into the Jinjiang River estuary was new. At high tide, water outside Quanzhou Bay passed through the S1 section and flowed into the bay. Thus, mixing intensity was high near the mouth of the bay and low distant from the bay mouth. At low tide, water within the bay was transported beyond the bay mouth to areas outside the bay.

The simulation of water exchange showed that the half-life of water off the coastline of Quanzhou Bay was 113 hours prior to construction and 111 hours after construction. This result indicated that the half-life of water prior to and after construction changed minimally and that construction of the artificial island had little impact on the water exchange

in Quanzhou Bay. Figure 10 shows the concentration distribution at high tide prior to and after island construction. The figure shows that after construction, the isoline of concentrations lower than 0.2 in the water west of the artificial island extended further toward the inner bay. This result was attributed to the increase in flow velocity during rising and falling tides in the water west of the artificial island, which increased the water body exchange in pertinent local waters.

CONCLUSION

This study used a refined mesh method to simulate the hydrodynamic effects of constructing an artificial island and obtained the local tidal current field and the sediment erosion and siltation field adjacent to the construction site. The results indicated that during falling tide, the flow velocities at the front of the berths on the west end and south side of the artificial island increased by 0.2–0.4 m/s, and the flow velocity in the main navigation channel from south Shihu to Dazhui Island decreased by 0.05–0.2 m/s. During the rising tide, the flow velocities at the front of the southwest end and south side of the artificial island increased by 0.1–0.4 m/s, and the flow velocity in the main navigation channel from south Shihu to Dazhui Island decreased by 0.05–0.1 m/s. After construction, sediment concentrations decreased in the main navigation channels to the south and north of the artificial island and in the marine space west of Baiyu. Moreover, erosion and siltation occurred within -20–20 cm/a in the waters between the Shihu Port area and the artificial island, indicating slight sedimentation. After construction, the water semi-exchange cycle in Quanzhou Bay changed by less than 2%, which suggested that the project had little influence on the water exchange inside and outside of Quanzhou Bay. Predicting the effects of a project on marine hydrodynamics is the basis of marine environment assessment and engineering design. This study simulated the construction of an artificial island and explored how to precisely determine the effects of the artificial island on the marine environment. In future work, monitoring data will be assessed after the completion of the project, and the simulation results will be validated to further improve the model parameters [36].

ACKNOWLEDGEMENTS

This study was supported by the Natural Science Foundation of Fujian Province (grant no. 2012J05075) and the Xiutu Artificial Island of Quanzhou Bay Environmental Impact Assessment (grant no. ZX-2014-027).

This report presents our original and unpublished work, which has not been and will not be submitted elsewhere until we receive your final decision. The authors declare that there are no conflicts of interest.

REFERENCES

[1] Lin, Y. and Wu, J. (2008) Discussion on the numerical analysis of the influence of construction of artificial island project upon the marine environment. Guangdong Shipbuilding. 29(1), 16-20.

[2] Martin-Short, R., Hill, J., Kramer, S.C., Avdis, A., Allison, P.A. and Piggott, M.D. (2015) Tidal resource extraction in the Pentland Firth, UK: Potential impacts on flow regime and sediment transport in the Inner Sound of Stroma. Renewable Energy. 76, 596-607.

[3] Gerristsen, H., Sutherland, J., Delgaard, R., Sumer, M., Fortes, C.J.E.M., Sierra, J.P., and Schmidtke, U. (2011) Composite modelling of the interactions between beaches and structure. Journal of Hydraulic Research. 47(S1), 2-14.

[4] Li, M. and Shi, Z. (2006) Numerical Modeling Study of Tidal Flow for Construction of An Artificial Island on Xitaiyangsha Shoal at Rudong, Jiangsu Province. China Harbour Engineering. 3, 1-4.

[5] Lu, Y. and Dong, Z. (2002) The influence of sea reclamation works at estuary with strong tide upon hydrodynamic environment. The Ocean Engineering. 20(4), 17-25.

[6] Qin, H., Ni, J. and Li, Y. (2002) Coastline selection for land reclamation of bay based on mathematical model of sediment. Journal of Sediment Research. 3, 92-100.

[7] Qin, H., Ni, J. and Liang, L. (2002) Shoreline choices for land reclamation of bay based on hydrodynamic Model. Journal of Hydrodynamics. 17(1), 92-100.

[8] Wang, X. and Sun, C. (2000) Numerical study of the influence of marine reclamation land upon hydrodynamic environment of Jiaozhou Bay. Marine Environmental Science. 19(3), 55-59.

[9] Chen, C., Liu, H. and Beardsley, E.C. (2003) An unstructured, finite-volume, three-dimensional, primitive equation ocean model: application to coastal ocean and estuaries. Journal of Atmospheric and Oceanic Technology. 20(1), 159-185.

[10] Zhu, J. (2003) Numerical Computation Method and Numerical Model of Ocean. Beijing: China Ocean Press. 326p.

[11] Fang, W., Li, K., Zhang, G. (2008) Analysis of Interaction of Environmental Factors of Beach Engineering with Artificial Islands. China Harbour Engineering. 3, 15-17

[12] Guo, L., Yang, S. (2009) Influence of artificial island construction on hydrodynamics in waters around Rudong. Journal of Waterway and Harbor. 5, 342-346
[13] Li, P., Xie, G., Chen, X., Jiang, M. (2008) The Application of Numerical Simulation Method in Marine Environmental Impact Assessment. Journal of Hainan Normal University (Natural Sciences). 21, 200-207
[14] Xie, S. (1995) The progress of artificial island design. Coastal Engineering. 14(1), 1-7
[15] Third Institute of Oceanography, State Oceanic Administration. (2011) Regional sea utilization plan of Xiutu Artificial Island of Quanzhou Bay. Xiamen: Third Institute of Oceanography, State Oceanic Administration. 226p.
[16] Guomo, G., Allsop, W. and Takahashi, S. (2010) Scaling wave impact pressures on vertical walls. Coastal Engineering. 57(6), 604-609.
[17] Dou, G. (1999) E-exploration of Sediment Incipience Velocity. Journal of Sediment Research. 6, 1–9.
[18] Whitehouse, R.J., Harris, J., Mundon, T. and Sutherland, J. (2010) Scour at offshore structures. In: Proceedings of the Fifth International Conference on Scour and Erosion (ICSE-5). San Francisco: ASCE Publications, 1-12.
[19] Lu, Y., Ji, R. and Zuo, L. (2009) Morphodynamic responses to the deep water harbour development in the Caofeidian sea area, China's Bohai Bay. Coastal Engineering. 56(8), 831-843.
[20] Zhang, X., Dou, X., Wang, X., Wang, H., Zhao, X., and Xu, X. (2012) 3D numerical modelling of local scour processes around spur dikes in tidal rivers. Advances in Water Science. 23(2), 222-228.
[21] Casulli, V. and Cattani, E. (1994) Stability, accuracy and efficiency of a semi-implicit method for three-dimensional shallow water flow. Computer Math Applic. 27(4), 99-112.
[22] Casulli, V. and Cheng, R.T. (1992) Semi-implicit finite difference methods for three-dimensional shallow water flow. International Journal for Numerical in Fluids. 15(6), 629-648.
[23] Casulli, V. and Zaolli, P.A. (1998) A three-dimensional semi-implicit algorithm for environmental flows on unstructured grids. In: Proceedings of Conference on Numerical Methods for Fluid Dynamics. Oxford: University of Oxford, 57-70.
[24] Ji, R., Lu, Y. and Zuo, L. (2008) Research on the process of flow and sediment dynamics under coastal engineering of island. Advances in Water Science. 19(5), 640-649.
[25] Oliveria, A. and Baptista, A.M. (1995) A comparison of integration and interpolation Eulerian-Lagrangian methods. International Journal of Numerical Methods in Fluids. 21(3), 183-204.
[26] Tang, J., Chen, C. and Wen, S. (2011) Numerical Simulation of Tidal Flow Field for Quanzhou Bay Sea-Crossing Bridge. In: Proceedings of the Fifteenth Session of the Chinese Marine (Coastal) Engineering Symposium, ed. Chinese Ocean Engineering Society. Beijing: Marine Press, 159-166.
[27] Zhang, Y., Baptista, A.M. and Myers, E.P. (2004) A cross-scale model for 3D baroclinic circulation in estuary–plume–shelf systems: I. Formulation and skill assessment. Continental Shelf Research. 24(18), 2187-2214.
[28] Chen, Y., Lin, B. and Lin, J. (2014) Modelling tidal current energy extraction in large area using a three-dimensional estuary model. Comput. Geosci. 72, 76-83.
[29] Neill, S.P., Jordan, J.R. and Couch, S.J. (2012) Impact of tidal energy converter (TEC) arrays on the dynamics of headland sand banks. Renewable Energy. 37, 387-397.
[30] Bray, M.S., Ahmadian, R. and Falconer, R.A. (2016) Impact of representation of hydraulic structures in Modelling a Severn barrage. Comput. Geosci. 89, 96-106.
[31] Rayson, M.D., Gross, E.S. and Fringer, O.B. (2015) Modeling the tidal and sub-tidal hydrodynamics in a shallow, micro-tidal estuary. Ocean Model. 89, 29-44.
[32] Legrand, S., Deleersnijder, E., Delhez, E. and Legat, V. (2007) Unstructured, anisotropic mesh generation for the Northwestern European continental shelf, the continental slope and the neighbouring ocean. Cont. Shelf Res. 27, 1344-1356.
[33] Ahmadian, R., Falconer, R. and Bockelmann-Evans, B. (2012) Far-field modelling of the hydro-environmental impact of tidal stream turbines. Renewable Energy. 38, 107-116.
[34] Ji, R., Xu, Q. and Mo, S. (2012) Influence of Hong Kong-Zhuhai-Macao Bridge artificial island upon flow and sediment dynamics environment. Advances in Water Science. 6, 842-850.
[35] Lu, M., Sun, Z. and Sun, D. (2011) Numerical research on the influence of artificial island upon water environment of bay. The Ocean Engineering. 29(3), 88-95.
[36] Guo, X., Wang, C. Chen, C. and Tang, J. (2014) Numerical Simulation of Suspended Sediment Transport During Construction of Meizhou Bay Peak Tail Reclamation Project. Journal of Applied Oceanography. 33, 125–132.

Received: **02.12.2016**
Accepted: **29.01.2018**

CORRESPONDING AUTHOR

Chuhan Chen
Third Institute of Oceanography,
State Oceanic Administration,
Xiamen 361005 – P.R. China

e-mail: chenchuhan@tio.org.cn

© by PSP Volume 27 – No. 5/2018 pages 2683-2689 Fresenius Environmental Bulletin

OPTIMIZATION OF PHOTODEGRADATION OF o-TOLUIDINE IN WATER WITH NANO SPHERICAL $CoFe_2O_4$ / COPPER SLAG AS A CATALYST

Rezvan Zeynolabedin, Kazem Mahanpoor*

Department of Chemistry, Arak Branch, Islamic Azad University, Arak, Iran

ABSTRACT

In the present work, precipitation method has been used to stabilize $CoFe_2O_4$ on Copper Slag(CS). $CoFe_2O_4$/Copper Slag catalysts have been characterized by SEM, XRD and BET surface area analysis. process done in Circulate Packed Bed Photo Reactor (CPBPR). Optimum process conditions were determined for the removal of O-toluidine from water using Taguchi fractional design. Three controllable factors containing pH, o-toluidine concentration and H_2O_2 concentrations at three levels were identified for each factor. The optimum conditions were found to be as follows pH= 10, O-toluidine concentration = 20(mg/l) and H_2O_2 concentrations =150(ppm). In optimum conditions a first order reaction to k= 0.0387 min^{-1} was observed for the photocatalytic degradation of o-toluidine in water by UV+H_2O_2/ $CoFe_2O_4$/Copper Slag.

KEYWORDS:
$CoFe_2O_4$/Copper Slag, Photodegradation, Taguchi, o-toluidine

INTRODUCTION

One of the most important sources of water pollutants are organic materials and these compounds are found in industrial wastewater. Aromatic amines are one of the most toxic and hazardous substances and Ortho toluidine is one of these compounds that are widely used in rubber and dye industrial. Ortho toluidine is known as a cause of urinary bladder cancer [1, 2]. In view of environmental aspects, it is essential to remove the o-toluidine to desired concentration on wastewater.

Different techniques such as adsorption, ozonation, photocatalytic degradation and thermal decomposition exist for the removal of environmental pollutants [3-6].

These methods have problems such as formation of solid pollution, relatively high cost and a long time to remove contaminants [3, 4]. Advanced oxidation processes (AOPs), including new methods that do not have these problems [5-7].

The use of heterogeneous photocatalytic oxidation techniques for wastewater treatment has been the subject of a wide range of investigations. The mechanism constituting heterogeneous photocatalytic oxidation processes has been discussed extensively in the literature [6-10].

Irradiation of semiconductors like TiO_2, Fe_2O_3, ZnO in fixed to various supports, in water containing organic pollutants, creates a redox environment, which is effectively able to destroy these pollutants.

$CoFe_2O_4$, the most stable Ferrite under ambient conditions, is widely used in catalysts, sensors, water treatment [11-13].

Photocatalytic activity is strongly dependent on the transport and separation efficiencies of photo-generated electrons and holes in the photocatalysts. However, free charge carriers (free electrons and holes) can be trapped or scattered by various kinds of random defects, resulting in increasing recombination probability [8-10].

Therefore, promoting the separation of photo-generated electrons and holes will facilitate the photocatalytic process.

There is a wide range of applications of Taguchi method, from engineering and agriculture to chemistry [14, 15]. The using of the Taguchi method of the ordinary experimental design methods, in addition to keeping the experimental cost at a lowest level, is that it minimizes the product diversity response while keeping the average response on objective. Another benefit is that optimal experimental conditions can be used in the real environment [16].

In the present work is stabilized $CoFe_2O_4$ on the copper slag. Precipitation method has been used to stabilize $CoFe_2O_4$ on the copper slag.

In this study was determined optimum process conditions for the removal of o-toluidine from water using Taguchi fractional design.

In this research, four controllable factors (pH, o-tolouidine concentration and H_2O_2 concentrations) were used in the optimization of the removal of o-toluidine.

The four parameters were set at four levels to observe the main effects.

MATERIALS AND METHODS

Materials. In this study, Or-tolouidine (C_7H_9N), Cobalt nitrate (Co $(NO_3)_2.6H_2O$) and Iron nitrate (Fe $(NO_3)_3.9H_2O$) salt and other materials was provided from Merck Company (Germany). Copper Slag including Al_2O_3(2%), SiO_2(34.5%), FeO (51.3%), CaO (6.5%), MgO (4.6%), CuO (0.7%) and undetectable materials (0.4%) (Analyzed by XRF) purchased from the Iranian company of Messbareh. The pH values were adjusted desired level using dilute NaOH and H_2SO_4.

Preparation of $CoFe_2O_4$ immobilized on Copper Slag. For the preparation of $CoFe_2O_4$, 50 ml 0.25 M Cobalt nitrate solutions were added to the 50 ml 0.5 M Ferric nitrate solution, then the prepared solution was poured into the 250 ml flask refluxes and 100 ml 2M molar urea solutions (as the precipitating agent to release hydroxyl ions slowly during the reaction) was added to this solution and reflux in the hot water bath to 12 hours. All reflux was performed at 90° C in nitrogen atmosphere. After completing the process, precipitate was confirmed. After filtering and washing with distilled water the precipitates were placed inside an oven at 110 °C to dry. To form $CoFe_2O_4$ catalyst, this dried deposition was put into the furnace at a temperature of 550 °C to 6 hours. Copper slags were used as the basis of the above catalyst. Copper slags were washed several times by dilute H_2SO_4 and dilute NaOH solutions, after which they were rinsed with doubly distilled water and dried at 120°C. Copper slags were mixed with a large amount $CoFe_2O_4$, this mixture was put into the furnace at a temperature of 550 °C to 6 hours. The catalyst is completely stuck to the base and catalyst $CoFe_2O_4$ / Copper slag was prepared.

Apparatus. Figure 1 shows the schematic diagram of the equipment. The Circulate Packed Bed Reactor (CPBR). Total volume of 1 liter and effective volume of reactor was 0.3 liter. One UV lamp with a power of (15 W, Philips) was placed directly inside the reactor and around the UV lamp was filled with catalyst.

The photocatalytic process, the reactor CPBR was filled with 70 grams of catalyst $CoFe_2O_4$ / Copper slag. The different volume levels of Hydrogen peroxide were added to the o-toluidine solution. The solution pH was adjusted to diluted sodium hydroxide or sulfuric acid. The resulting solution was transferred to the storage tank and send in to the reactor by using a water pump.

XRD analysis of the samples was done using a XRD stoe-stidy-mp model (German). The morphologies of the photocatalyst were taken by using a Mira 3-XMU (USA) scanning electron microscope (SEM).

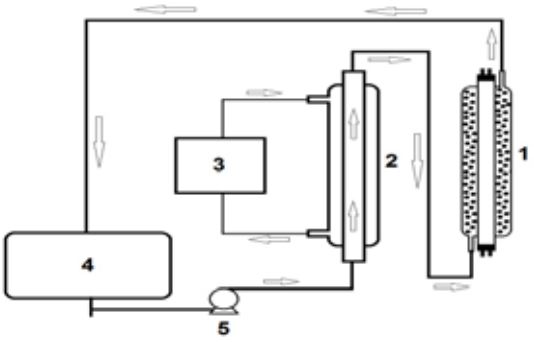


FIGURE 1
Schematic view of apparatus: 1- Reactor (CPBR), 2- Heat exchanger, 3-Thermo bath 4- Storage tank, 5- Water pump

Procedures. For the photodegradation of o-toluidine, a solution containing knew concentration of o-toluidine and H_2O_2 was prepared. The solution pH values were adjusted to desired level using dilute NaOH and H_2SO_4 (the pH values were measured with Horiba M12 pH meter). The degree of photodegradation (X) as a function of time is given by equation 1:

$$X = \frac{COD_0 - COD}{COD_0} \quad (1)$$

Where COD_0 and COD are the Chemical Oxygen Demand of o-toluidine solution to t = 0 and t, respectively.

For determination of optimal condition used Taguchi experimental design. This method includes the following steps:

1- The variables affecting the test results will be determined

2- Levels of each variable is identified separately (interaction between variables to be considered)

3- Choose the suitable orthogonal array (OA) and the assignment of process parameters to the orthogonal array

4- Required experiments are performed based on the (OA)

5- Calculate the performance statistics

6- Experimental result analysis is done using ANOVA statistics and performance

The study was done to determine the optimal process conditions for removing o-toluidine from aqueous solution. Optimal conditions were determined by Taguchi experimental design with Qualitek-4 software. Effect of experimental parameters on the removal of o-toluidine and their levels are given in (Table 1).

TABLE 1
Experimental parameters and their levels

Factors	Level 1	Level 2	Level 3
A) pH	4	7	10
B) o-toluidine concentration(ppm)	20	40	60
C) H_2O_2 concentration(ppm)	50	100	150

TABLE 2
Experimental plan table

Experiments No	A	B	C
1	1	1	1
2	1	2	2
3	1	3	3
4	2	1	2
5	2	2	3
6	2	3	1
7	3	1	3
8	3	2	1
9	3	3	2

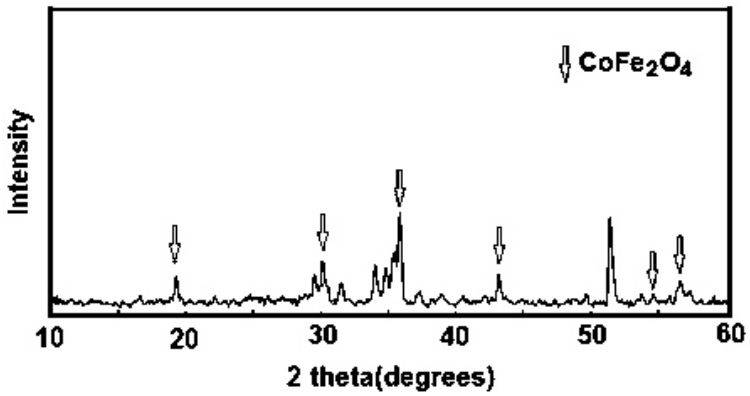


FIGURE 2
The XRD patterns of photocatalyst $CoFe_2O_4$ / CS

The orthogonal array experimental design method was selected to determine experimental plan, as seen Table 2 [16].

In order to see the effects of noise sources remove o-toluidine, each test was repeated three times at same conditions. Optimize function statistics were chosen as indicators. Three classes of function statistics, bigger are better, smaller are better and nominal are the better. In this research, the function statistics bigger is the better was used to define optimal conditions [16].

The bigger are better function statistics was given by equation 2.

$$SN_L = -10\log\left(\frac{1}{n}\sum_{i=1}^{n}\frac{1}{Y_i^2}\right) \quad (2)$$

Where SNs are function statistics, n the number of repetition done for an experimental combination, and Yi the function value of ith experiment.

In Taguchi experimental design method, the experiment corresponding to optimum experimental conditions might not have been done during the alltime of the experimental stage. In such cases, the function amount corresponding to optimum test conditions can be predicted by utilizing the balanced characteristic of OA. For this, the additive model may be used equation 3 [16]:

$$Y_i = \mu + X_i + e_i \quad (3)$$

Where μ is the overall mean of performance values; X_i the fixed effect of the parameter level combination used in ith experiment and e_i the random error in ith experiment.

RESULTS AND DISCUSSION

Characterization of photocatalyst. After preparation of Photocatalyst $CoFe_2O_4$ based on Copper slag, identification was performed by XRD

and SEM devices. The corresponding powder X-ray diffraction (XRD) pattern provides further crystallinity and phase information on the obtained $CoFe_2O_4$ (Figure 2). The observed peak positions are consistent with the characteristic peaks reported for $CoFe_2O_4$ in the literature [17].

Moreover, the mean size of the synthesized Nano-spherical are calculated from the peak broadening in the XRD pattern by using the Debye–Scherrer formula [17]. The average size of $CoFe_2O_4$ Nano-spherical are 96 nm.

The morphology of the ferrite powders was investigated by SEM. In the Figure 3 are presented the SEM micrographs. As shown that in this Figure the structural of the $CoFe_2O_4$ are Spherical shape and $CoFe_2O_4$ Nano-spherical particles have loaded on the surface of copper slag.

Determination of optimum operational parameter on the photodegradation of o-toluidine. The removal of o-toluidine process of the synthetic wastewater was investigated in different experimental conditions (according Table 2). To determine the optimum conditions for the removal of o-toluidine in the solutions, o-toluidine concentration, pH and H_2O_2 concentration were investigated, respectively. The reaction conditions in which the effect of parameters investigated. The experimental results are given in (Table 3). The degrees of the influences of parameters on the performance statistics are given at the graphs in (Figure 5).

The numerical value of the maximum point in each graph marks the best value of particular parameter.

Photocatalyst mechanism is for this reason that ultraviolet radiation to the semiconducting oxides; electrons are transferred from the valance Bond to conduction Bond. On this transition, is created the holes in the valance Bond and is created electrons additional in the conduction bond. Dissolve oxygen molecules in water are extra electrons from the conduction bond and after doing some reaction there to bring hydroxide radical. On the other hand, the water molecules and the hydroxide ions after reaction to several holes (created in the valance bond) is created hydroxide radicals. Finally, hydroxide radicals with organic pollutants such as o-toluidine react and causes the breakdown and failures and to convert them into minerals. This mechanism is summarized in Figure 4 [6-10].

Catalytic activity of $CoFe_2O_4$/CS after being stabilized on the copper slag increases, and to justify it is assumed that the hydroxide radicals are available for the reaction with the o-toluidine absorbed on the surface of copper Slag.

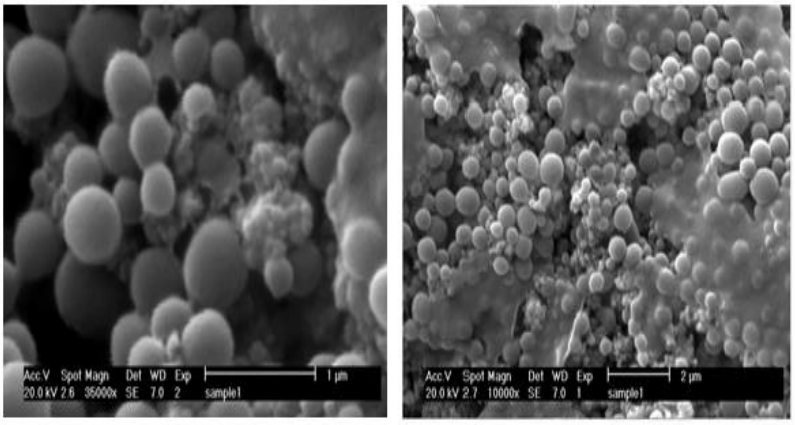


FIGURE 3
SEM images of $CoFe_2O_4$ / CS

TABLE 3
Experimental result of an orthogonal array of L_9

Exp No	X_1(%)	X_2(%)	X_3(%)	Average	S/N	St Dev
1	53.25	53.42	53.12	53.2633	50.9811	0.15044
2	56.31	56.26	59.18	57.2500	30.6928	1.67162
3	62.84	63.15	62.76	62.9167	49.6982	0.20599
4	69.14	69.37	69.02	69.1767	51.7977	0.17786
5	75.58	75.42	75.58	75.5267	58.2508	0.09238
6	50.47	50.51	50.55	50.5100	62.0263	0.04000
7	91.86	91.86	91.96	91.8933	64.0369	0.05774
8	72.78	73.67	73.35	73.2667	44.2182	0.45081
9	59.50	59.55	59.50	59.4067	49.1792	0.20648

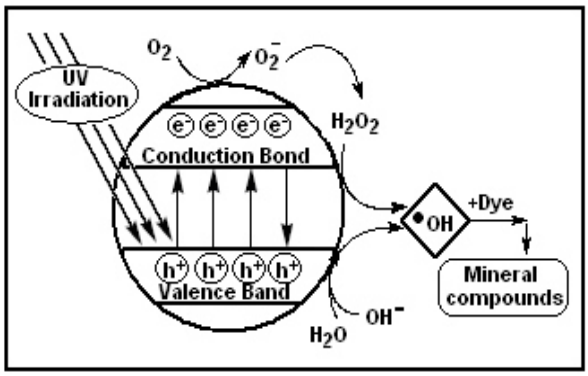


FIGURE 4
General mechanism of the photocatalysis

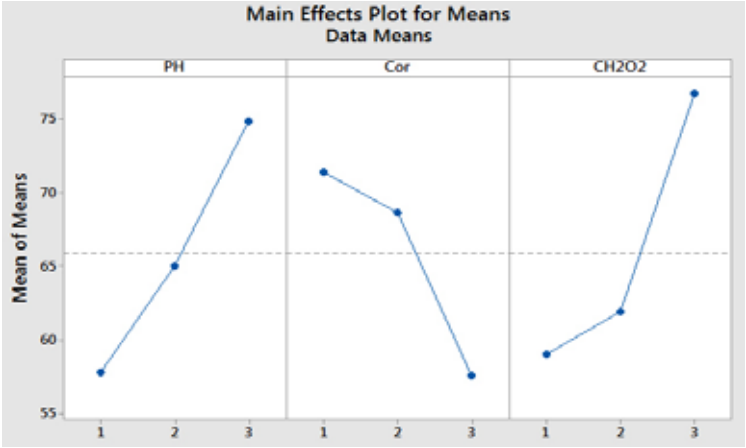


FIGURE 5
Main Effects Plot for Means

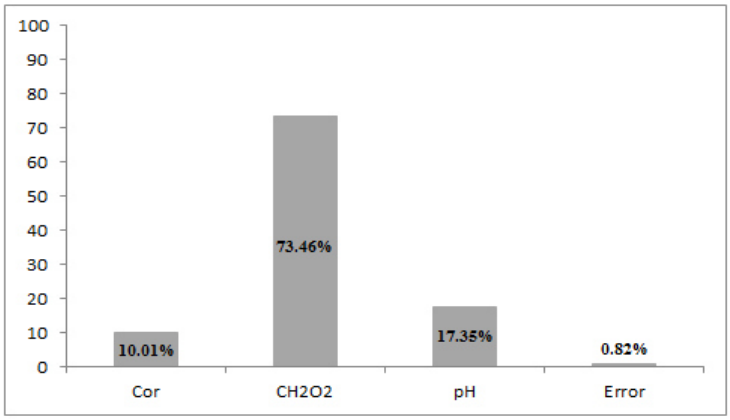


FIGURE 6
Effect of parameters on photocatalytic decomposition of o-toluidine

As show in Figure 5, photocatalytic decomposition of o-toluidine better dons in alkaline solution. The reaction to hydroxide ions and holes makes hydroxide radicals (h^+_{VB} + OH^- → •OH). In alkaline solution are formed more hydroxyl radicals, so effectively can destroy the o-toluidine molecules. thus, the photodegradation efficiency increases to the alkaline to o-toluidine photodegradation.

As seen in Figure 5, when H_2O_2 concentration increased, the decomposition rate will increase. The formation rate of hydroxyl radical from H_2O_2 was increased from two ways. First, H_2O_2 symmetry breaking by illumination would also produce hydroxyl radicals (Equation 4). Second, the reduction of hydrogen peroxide at the conduction band would produce hydroxyl radicals (equation 5) [6-10].

$$H_2O_2 + h\upsilon \longrightarrow 2OH^\bullet \quad (4)$$

$$H_2O_2 + photocatalyst(e_{CB}^-) \longrightarrow photocatalyst + OH^\bullet + OH^- \quad (5)$$

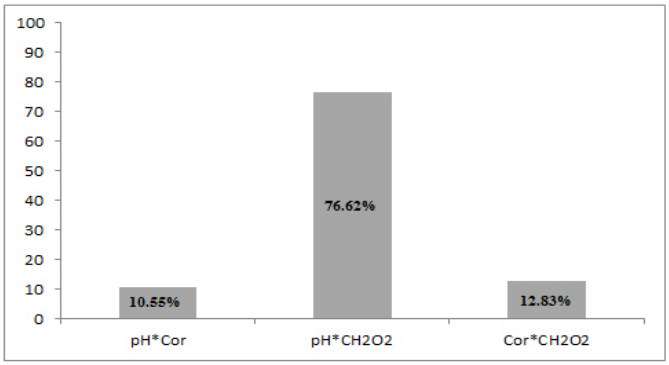


FIGURE 7
Effect of each parameter on other variables

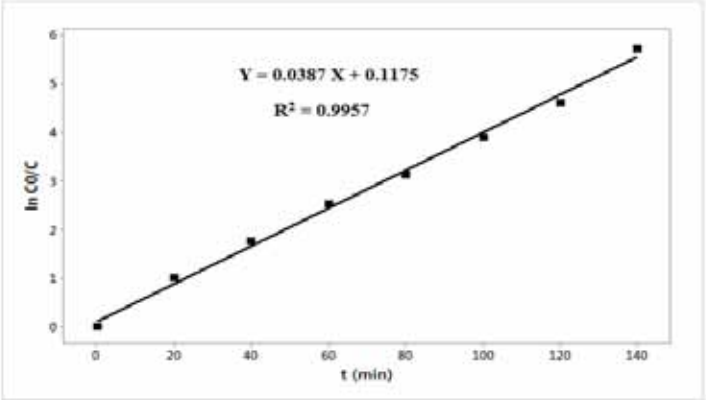


FIGURE 8
Kinetic plot of pseudo-first order photocatalytic degradation of o-toluidine in optimal condition. (pH= 10; H_2O_2 concentrations=150(ppm), and initial o-toluidine concentration=20(ppm)

As shown in Figure 6, H_2O_2 concentration is the most effective parameters on the photocatalytic decomposition of o-toluidine

In Figure 7, the effect of each of the variables on other variables defined. Interaction of o-toluidine concentration and concentration of hydrogen peroxide on each other is the highest value. The optimum conditions were found to be as follows: pH=10; H_2O_2 concentrations=150 (ppm); and o-toluidine =20 (ppm).

Kinetics of photocatalytic degradation of o-toluidine. Photocatalytic decomposition reaction kinetics of o-toluidine shows good agreement with the kinetic of pseudo-first-order reaction model reaction. In the for our semi batch system, kinetic integral equation of pseudo-first-order relationship between concentration(C) and time (t) is as follows equation 6 [18]:

$$[\ln(\frac{COD_0}{COD})] = k_{app}t \quad (6)$$

Where k_{app} is the apparent pseudo-first-order rate constant (that is affected by o-toluidine concentration), and t the reaction time.

A plot of ln (COD_0/COD) versus t for optimal condition of photo catalytic degradation of o-toluidine is shown in Figure 8.

CONCLUSIONS

Physical and chemical characterization of supported photocatalyst were determined by SEM, XRD and BET techniques. According to the literature, the results demonstrated that produced $CoFe_2O_4$/CS has sufficient properties as a photocatalyst for degradation of o-toluidine. Here, Taguchi design method was used to optimize the parameter values for obtaining desired characteristics. Various factors affecting the degradation process were analyzed and optimized pH, H_2O_2 concentration have been shown to be highly influential upon the photocatalytic degradation of o-toluidine. In optimal conditions (pH=10, H_2O_2 concentrations=150 (ppm) and initial o-toluidine concentration=20(ppm)) that analyzed by Taguchi method, determined kinetics of photocatalytic decomposition reaction. Pseudo-first-order models reaction

good agreements with experiment data on to photocatalytic degradation of o-toluidine reaction.

ACKNOWLEDGEMENTS

The authors would like to gratefully acknowledge members of the Research Laboratory of Islamic Azad University, Arak branch, Arak, Iran.

REFERENCES

[1] Ferlay, J., Parkin, D.M., Steliarova-Foucher, E. (2010) Estimates of cancer incidence and mortality in Europe in 2008. European journal of cancer. 46(4), 765–781.

[2] Gaber, K., Harreus, U.A., Matthias, C., Kleinsasser, N.H., Richter, E. (2007) Hemoglobin adducts of the human bladder carcinogen o-toluidine after treatment with the local anesthetic prilocaine. Toxicology. 229(1–2), 157–164.

[3] Prabu, S.L., Suriyaprakash, T.N.K., Kumar, J.A. (2011) Wastewater Treatment Technologies. A Review. Pharma Times. 43(5), 55-62.

[4] Topare, N.S., Attar, S.J., Manfe, M.M. (2011) Sewage/Wastewater Treatment Technologies: A Review. Scientific Reviews Chemical Communications. 1(1), 18-24.

[5] Winkler, C.A., Fletcher, C.J.M., Hinshelwood, C.N. (1934) The Thermal Decomposition of Propionic Aldehyde. Proceedings of the Royal Society of London. Series A. 146, 345- 356.

[6] Parsons, S. (2004) Advanced oxidation processes for water and wastewater treatment. IWA Publishing Company, London.

[7] Aguado, J., Grieken, R.V., LMunoz, M.J., Marugan, J. (2006) A comprehensive study of the synthesis, characterization and activity of TiO_2 and mixed TiO_2/SiO_2 photocatalysts. Applied Catalysis A: General. 312, 202–212.

[8] Nikazar, M., Gholivand, K., Mahanpoor, K. (2007) Using TiO_2 supported on Clinoptilolite as a catalyst for photocatalytic degradation of azo dye Disperse yellow 23 in water. Kinetics and Catalysis. 48, 214-220.

[9] Ajmal, A., Majeed, I., Malik, R.N., Idriss, H., Nadeem, M.A. (2014) Principles and mechanisms of photocatalytic dye degradation on TiO_2 based photocatalysts: a comparative overview. RSC Advances. 4, 37003-37026.

[10] Chong, M.N., Jin, B., Chow, C.H.K., Saint, C. (2010) Recent developments in photocatalytic water treatment technology: A review. Water research. 44, 2997-3027.

[11] Sadri, F., Ramazani, A., Massoudi, A., Khoobi, M., Azizkhani, V., Tarasi, R., Dolatyari, L., Min, B.K. (2014) Magnetic $CoFe_2O_4$ Nanoparticles as an Efficient Catalyst for the Oxidation of Alcohols to Carbonyl Compounds in the Presence of Oxone as an Oxidant. Bull. Korean Chem Soc. 35, 2029-2032.

[12] Ye, D., Xu, Y., Luo, L., Ding, Y., Wang, Y., Liu, X. (2012) $LaNi_{0.5}Ti_{0.5}O_3/CoFe_2O_4$-based sensor for sensitive determination of paracetamol. Journal of Solid State Electrochemistry. 16, 1635–1642.

[13] Goldman, A. (1993) Modern Ferrite Technology. Marcel Dekker Inc. Publication Company, New York

[14] K-Roy, R. (2001) Design of experiments using the Taguchi approach. 16 steps to product and process improvement. John Wiley & Sons Hoboken NJ Publication Company, New York

[15] Singh, H. (2012) Taguchi optimization of process parameters: A review and case study. International Journal of Advanced Engineering Research and Studies. 1, 39-41.

[16] Ross, P.J. (1998) Taguchi techniques for quality engineering. McGraw-Hill Publication Company, New York.

[17] Sathiya, S., Parasuraman, K., Anbarasu, M., Balamurugan, K. (2015) FT-IR, XRD, and SEM Study of $CoFe_2O_4$ Nanoparticles by Chemical Co-Precipitation Method. Nano Vision. 5, 133-138.

[18] Shokri, A., Mahanpoor, K., Soodbar, D. (2016) Degradation of 2-Nitrophenol from Petrochemical Wastewater by UV/$NiFe_2O_4$/Clinoptilolite Process. Fresen. Environ. Bull. 25, 500-508.

Received: **06.12.2016**
Accepted: **19.02.2018**

CORRESPONDING AUTHOR

Kazem Mahanpoor
Department of Chemistry,
Arak Branch,
Islamic Azad University,
Arak – Iran

e-mail: k-mahanpoor@iau-arak.ac.ir

© by PSP Volume 27 – No. 5/2018 pages 2690-2696 Fresenius Environmental Bulletin

TRACE METALS IN VEGETABLE PLANTS (*ALLIUM CEPA* L., *CAPSICUM ANNUM* L. *LYCOPERSICON ESCULENTUM* MILL. AND *BETA VULGARIS* L.) FROM THE ZETA VALLEY OF MONTENEGRO

Sladjana Krivokapic, Dragana Petrovic*

Faculty of Natural Sciences and Mathematics, University of Montenegro, G. Washington Street, P. O. Box 5455, 81000 Podgorica, Montenegro

ABSTRACT

Total concentrations of copper (Cu), zinc (Zn), chromium (Cr), cadmium (Cd), lead (Pb) and nickel (Ni) were determined in the soil and four vegetable plants from the Zeta valley of Montenegro. The results obtained indicate that in the soil, generally contaminated with Ni and Cr (215.6 mg kg^{-1}; 196.6 mg kg^{-1}), the concentrations of both elements often exceeded soil quality guidelines. The distribution of metals in vegetables decreases in the following order: Zn> Cu> Cr > Pb > Ni > Cd. The concentrations of Zn, Cu and Cd were highest in the fruit of *Beta vulgaris* L. and the concentrations of Cr and Ni in the fruit of *Capsicum annum* L, while the concentration of Pb was almost the same in all species. The mean value of the Metal pollution index (MPI) was the highest in the fruit of *Beta vulgaris* L. and *Capsicum annum* L., followed by *Lycopersicon esculentum* Mill. and then *Allium cepa* L. In general, it can be concluded that the concentrations of trace metals in the four vegetable plants were below the limits set by Codex general standard for contaminants and toxins in food and feed and do not constitute a health hazard for consumers.

KEYWORDS:
Trace metal, vegetables, soil, contamination, metal pollution index

INTRODUCTION

The effects of air, water and soil pollution by heavy metals are different and are first manifested through plants, as the most sensitive part of the food chain: plants-animals-man.

The presence of heavy metals in soil usually comes from anthropogenic sources. Increased concentrations can result in the accumulation of metals in agricultural crops, clearing the way for further transport up the food chain. Precisely applied agrochemical measures in order to improve yields are one of the ways of introducing heavy metals into the soil [1]. Many heavy metals are essential micronutrients (Cu, Zn) for plants, because they are involved in numerous metabolic processes as constituents of enzymes and other proteins. However, they can become toxic if their concentration is higher than a specific critical point, as they can propagate a range of interactions at the cellular and the molecular level [2, 3]. Heavy metals such as Cd and Pb have been shown to have carcinogenic, mutagenic and teratogenic effects [4, 5]. Uptake from the soil and the distribution of metals in the above ground parts of vegetables depends on a variety of factors: the chemical characteristics of the metal, the plant species in question and the environmental conditions [6]. Metal distribution in plants is quite heterogeneous and controlled by genetic, environmental and toxic factors. The dynamics of heavy metals in plant-soil interactions depends mainly on the levels of soil contamination and plant species [7, 8].

Numerous investigations of heavy metals in vegetables and their corresponding soils have been conducted in recent years [9-16].

The primary purpose of this study was to obtain quantitative information on the concentration of trace metals (Cu, Zn, Cr, Cd, Pb and Ni) in the fruit of four vegetable plants: *Allium cepa* L., *Capsicum annum* L., *Lycopersicon esculentum* Mill. and *Beta vulgaris* L. from the Zeta Valley of Montenegro. The following points were considered: a. variations in metal concentrations between species; b. variations in metal levels from one sampling site to another and c. the determination of the average of the Metal Pollution Index (MPI) at the different sampling sites for all the selected species.

MATERIALS AND METHODS

Sample collection. The samples of plant material and soil were taken from five different locations from the Zeta Valley during the summer of 2013. A description of the sampling sites and their positions is given in Table 1.

The samples were mainly collected to the south-west of the Aluminium Factory in Podgorica (Figure 1).

These sites were selected along a gradient from the pool of red mud within the factory. In this area, north-easterly winds blow that transport particles of red mud to the south-west of the factory.

Analytical methods. (1) Metal analysis. In the laboratory, the plant material was washed thoroughly using deionized water and dried at 75 °C for 48 hours. The dry samples were ground into a fine powder and homogenized in an electrical mill. The prepared samples (0.5 g) were mineralized by the Milestone Microwave Ethos 1, with a mixture of HNO_3 and H_2O_2 (3:1). After digestion, the solution was diluted using deionized water to a final volume of 50 ml.

The soil samples were first air-dried and then in an oven at 75 °C for 48 hours. The dry soil samples were ground in an agate mortar and sieved through a 1.5 mm sieve. Approximately 0.5 g of the sample was mineralized using microwave digestion with a mixture of HCl and HNO_3 (3:1). After mineralization, the solutions were diluted by 2M HNO_3 to a final volume of 100 ml.

The concentrations of the metals (in relation to Cu, Zn, Cr, Cd, Pb, Ni) in the plant and soil samples were determined by using an inductively coupled plasma optic emission spectroscopy (ICP-OES) technique on the Spectro Acros instrument. The working standards for the measurement of the elements were prepared on the Sigma Aldrich for solutions of 1000 mg dm^{-3} each. The reliability of the analytical method was evaluated by the analysis of certified standard reference materials NCS DC73348 (Bush Branches and Leaves) and NCS DC70312 (Tibet sediment) from the China National Analysis Center for Iron and Steel, Beijing. All the results are expressed on their dry weight basis.

(2) Calculation of the Metal Pollution Index (MPI). To compare the total content of the metals at the different sampling sites, the Metal Pollution Index was used. This was obtained using the equation [17, 18].

$MPI = (Cf_1 \times Cf_2 \ldots\ldots Cf_n)^{1/n}$

where Cf is the concentration of the metal in the sample 1-n.

Statistical analysis. The experimental data were analyzed using the statistical software program Statistica 7.1. (StatSoft Inc., 2006). The comparison of the metal concentrations by species or sampling areas was performed using a One-way ANOVA with the value of $p < 0.05$. The correlations between the metal concentrations in the plant and in the soil samples were evaluated using the Pearson correlation coefficient.

TABLE 1
Description and position of the sampling sites

Location	Description	Latitude and Longitude
T1	Botun (south of the Aluminium Factory)	42° 38' 24"N ; 19° 21' 00"E
T2	Botun (south of the Aluminium Factory)	42° 37' 81"N ;19° 20' 45"E
T3	Botun (south of the Aluminium Factory)	42° 38' 37"N ;19° 19 '69"E
T4	Inflow of the River Morača (south of the Aluminium Factory)	42° 38' 34"N ;19° 19' 16"E
T5	Dajbabe (north of the Aluminium Factory)	42° 40' 09"N ; 19 °22'70" E

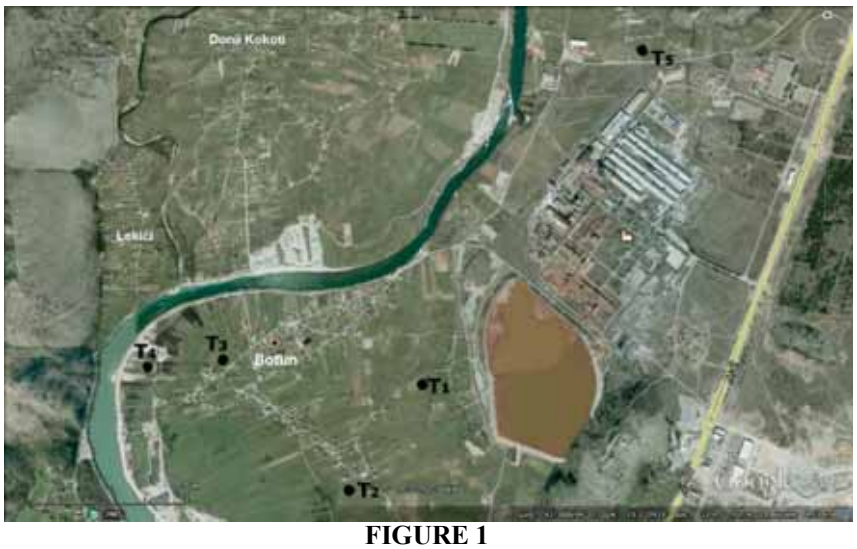


FIGURE 1
Map of the sampling sites

TABLE 2
The minimum and maximum concentrations, average concentrations ± standard deviation and coefficient of variance of metals in soil

Metal	Min-max (mg kg^{-1})	Average ± SD	Cv (%)
Cu	28,8-35,3	31,36±2,31	7,36
Zn	46,6-67,1	59,54±7,28	12,23
Cr	83,4-196,6	153,5±37,64	24,51
Cd	0,068-0,596	0,243±0,211	87,09
Pb	8,4-21,7	14,32±4,03	28,19
Ni	84,0-215,8	173,8±46,32	26,63

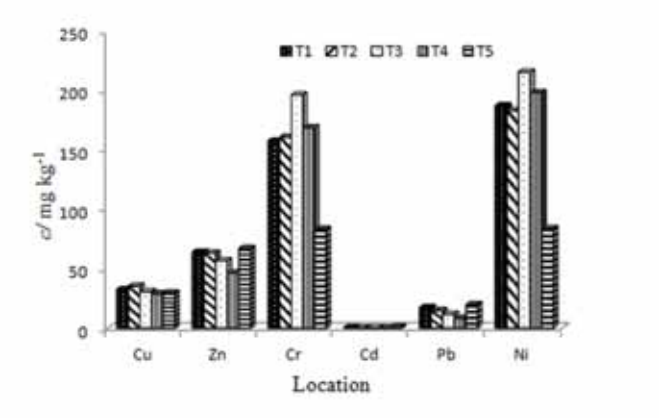


FIGURE 2
Distribution of Cu, Zn, Cr, Cd, Pb and Ni concentrations in the soil

RESULTS AND DISCUSSION

Distribution of metals in soils and plants. Mean concentration values for metals analysed in the soil are given in the Table 2.

The metal distribution in the soil by the locations used in this research is given in the Figure 2.

The maximum concentrations were recorded for Ni and Cr (215.8 mg kg^{-1},196.6 mg kg^{-1}) at location T3, while the minimum concentration was registered for Cd (0.068 mg kg^{-1}) also at location T3. Zn, Cu and Pb concentrations by location in this research were significantly more even. The values of the metal concentrations in the soil at all the sampling sites decrease in the following order: Ni> Cr >Zn >Cu>Pb> Cd. Analyses show that the content of metals at the studied locations differs significantly.

Similar distributions are noticeable for Cr and Ni on the one hand, with maximum concentrations registered at location T3, as well as for Cd, Zn and Pb on the other, with maximum concentrations registered at location T5. It is very important to note that the Ni and Cr concentrations at all the studied locations were above the MAC for soil according to the world standards [19].

The results of the analysis of the metal content in the fruit of the agricultural crops covered by the study are given in the Figure 3.

Significant differences can be noted in their content depending on the species, metal and the location from which the plant material was sampled.

The metal distribution in the fruit of all four plant species decreases in the following order: Zn > Cu > Cr > Pb > Ni > Cd. Of all the metals analysed, the highest concentration was registered for Zn in the fruit of the species *Beta vulgaris* L. (4.62 mg kg^{-1}) at location T3 and lowest for Cd (0.005 mg kg^{-1}) in the fruit of the species *Capsicum annum* L. at location T2. The extremely high concentrations of Cr and Ni in the soil did not have a significant effect on their content in the fruit of all four of the plant species studied.

The comparison of the metal content in all four of the selected agricultural crops showed that the maximum concentrations of Cu, Zn and Cd were registered in the fruit of the species *Beta vulgaris* L., while the maximum concentrations for Ni and Cr were registered in the fruit of the species *Capsicum annum* L. Pb concentrations in all four species was almost equal at all the locations studied (Pb < 0.05 mg kg^{-1}). The minimum concentrations for most of the metal analyses were registered in the fruit of the species *Allium cepa* L. (Cr, Ni) and the fruit of the species *Lycopersicon esculentum* Mill. (Cu, Zn). The same trend of concentrations for Cu, Zn, Pb and Cd was recorded in the species *Allium cepa* L. (Cu- 0.437 mg kg^{-1}; Zn- 1.229 mg kg^{-1}; Cd-0.020 mg kg^{-1}) and the species *Lycopersicon esculentum* Mill. (Cu- 0.744 mg kg^{-1}; Zn- 1.495 mg kg^{-1}; Cd-0.318 mg kg^{-1}) in the paper of Maksimović et al. [13] who took their samples from a number of locations in the Republic of Serbia. Mirecki et al. [7] was recorded

some higher concentrations for Cu, Zn, and Cd in the species *Allium cepa* L. (Cu $_{(mg\ kg^{-1})}$ - 1.25 ± 0.10; Zn $_{(mg\ kg^{-1})}$ - 6.82 ± 0.64; Cd $_{(mg\ kg^{-1})}$ - 0.06 ± 0.01) and the species *Beta vulgaris* L. (Cu $_{(mg\ kg^{-1})}$-3.88 ±0.48; Zn $_{(mg\ kg^{-1})}$ - 16.05 ± 1.55; Cd$_{(mg\ kg^{-1})}$- 0.16 ± 0.02) from unpolluted area-Leposavic, in south of Serbia .

Reaves and Chaney [20] demonstrated that low plant-available Zn in the soil promotes Cd uptake. The results of this study also suggest that the bioavailability of Cd is different for different food sources. This indicates that the food that is nutritionally marginal with respect to Zn has much higher risk of containing more Cd. Therefore, we compared the Zn/Cd ratio in all the vegetable plants (Table 3).

The Zn/Cd ratio was the highest in the fruit of *Capsicum annum* L. (239.66) and lower in *Beta vulgaris* and *Allium cepa* L. (142.74; 132.15). The lowest Zn/Cd ratio was recorded in the fruit of *Lycopersicon esculentum* Mill. (70.89). There were significant differences between *Capsicum annum* L. and *Lycopersicon esculentum* Mill.cultivars with respect to Zn/Cd concentration. Maksimović *et al.* [13] found a similar Zn/Cd ratio in the species *Lycopersicon esculentum* Mill. (68.29), while in the species *Allium cepa* L., the Zn/Cd ratio was somewhat lower (93.16).

The concentration of all the metals analysed, except Pb, in all four species varies significantly by location. It was noted that the maximum metal concentrations for all four plant species were recorded at locations T1, T3 and T5, as well as that the concentrations of all the metals analysed in the fruit of all four species were below the maximum allowable concentrations (MAC) for vegetables, according to the world standards [19].

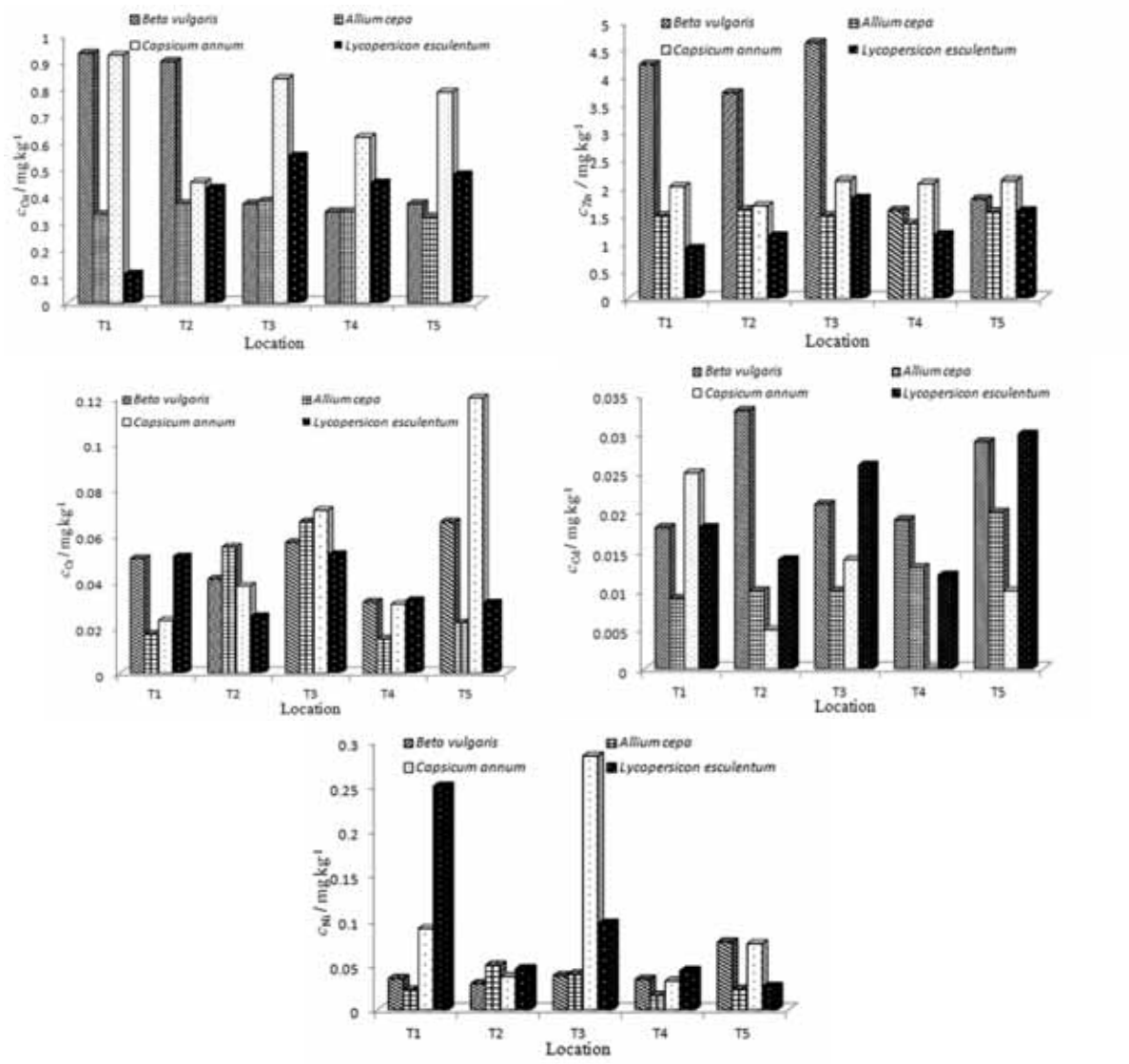
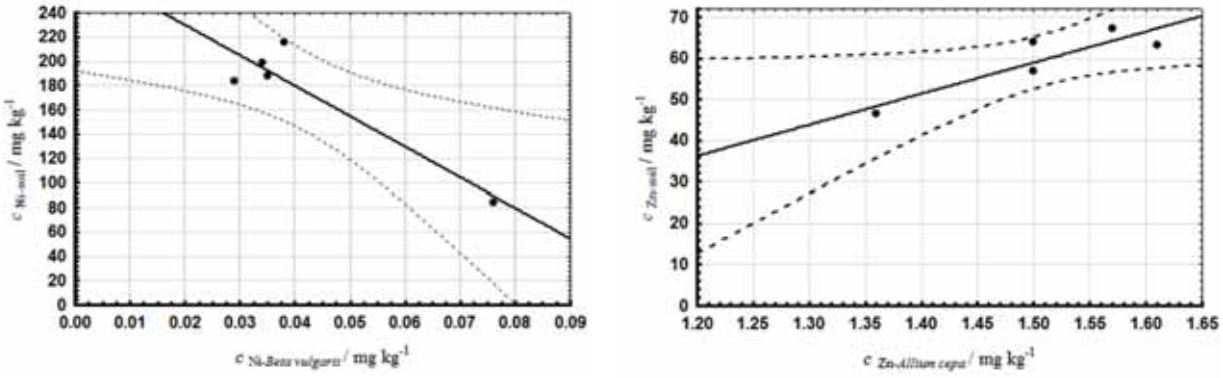


FIGURE 3
Distribution of Cu, Zn, Cr, Cd and Ni concentration in the fruit of the investigated species at all studied locations.

TABLE 3
Descriptive statistics of the concentrations of Cu, Zn, Cr, Cd, Pb, Ni and Zn/Cd ratios in the four vegetable plants.

	Concentration (mg kg^{-1})						
Allium cepa	Cu	Zn	Cr	Cd	Pb	Ni	Zn/Cd
Mean	0.348	1.508	0.035	0.012	<0.05	0.030	132.15
Std. Dev	0.023	0.085	0.021	0.004		0.012	34.57
Coef.Var.	6.65	5.65	60.66	32.50		42.11	26.17
Beta vulgaris							
Mean	0.582	3.192	0.049	0.024	<0.05	0.042	142.74
Std. Dev	0.272	1.253	0.0121	0.005		0.017	71.18
Coef.Var.	46.78	39.27	24.86	24.72		40.21	49.87
Capsicum annum							
Mean	0.722	2.010	0.056	0.011	<0.05	0.103	239.66
Std. Dev	0.168	0.169	0.035	0.007		0.092	121.53
Coef.Var.	23.37	8.41	63.48	62.83		89.66	50.71
Lycopersicon esculentum							
Mean	0.404	1.334	0.038	0.020	<0.05	0.092	70.89
Std. Dev	0.152	0.331	0.011	0.006		0.082	17.51
Coef.Var.	37.75	24.84	29.12	34.64		88.74	24.71



(a) **(b)**

FIGURE 4
The values of the Pearson's correlation coefficient (p < 0,05) between:
a. concentrations of Ni in the soil and the fruit of *Beta vulgaris* L.(r= -0,92; p<0,05)
b. concentrations of Zn in the soil and the fruit of *Allium cepa* L.(r= 0,88; p<0,05)

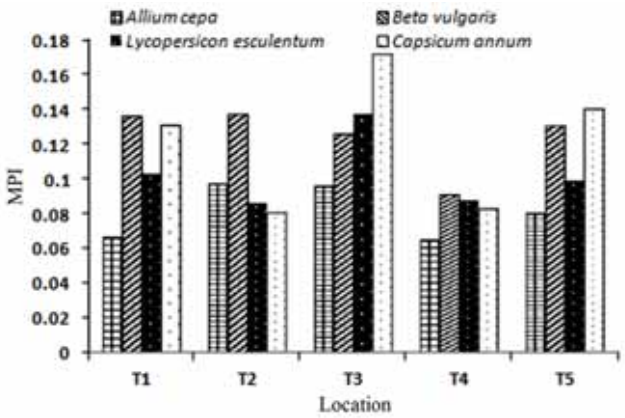


FIGURE 5
The values of the Metal Pollution Index (MPI) for each sampling site

The results of the correlation analysis (using Pearson's correlation coefficient, $p<0.05$) between the metal content in the soil and the fruit of all four agricultural crops (Figure 4), show the existence of a highly significant positive correlation ($r=0.88$; $p<0.05$) between the Zn content in the soil and the fruit of the species *Allium cepa* L., as well as a highly significant negative correlation between the Ni content in the soil and the fruit of the species *Beta vulgaris* L. ($r=-0.92$; $p<0.05$), which points to the fact that a high Ni concentration in the soil has no significant effect on the Ni content in the fruit of the species *Beta vulgaris* L.

Metal Pollution Index (MPI). The average value of the Metal Pollution Index (MPI) was highest in the fruit of *Beta vulgaris* L. and of *Capsicum annum* L. (0.123 and 0.120, respectively) (Figure 5).

The average value of the MPI in the fruit of *Allium cepa* L. was considerably lower. Sharma *et al.* [11] found the highest value of the MPI in *Beta vulgaris* L. (2,82). Maksimovic et al. [13] registered similar values for the MPI in *Allium cepa* L. and *Lycopersicon esculentum* Mill. (0.269 and 0.166, respectively).

The concentration of most of the metals varied significantly depending on the location of the sampling sites. Figure 5 clearly shows that, for all the species studied, the MPI was the highest in those samples taken from the locations at T1, T3 and T5.

CONCLUSION

In general, it can be concluded that the concentrations of trace metals in four vegetable plants were below the limits set by the Codex general standard for contaminants and toxins in food and feed and do not constitute health hazards for consumers [19]. The distribution of metals in vegetables decreases in the following order: Zn> Cu > Cr > Pb > Ni > Cd. The concentrations of Zn, Cu and Cd were the greatest in the fruit of *Beta vulgaris* L. and of Cr and Ni in the fruit of *Capsicum annum* L, while the concentration of Pb was almost the same in all the species.

Since this research has shown that the maximum concentrations of metals in the soil were registered for Ni and Cr, and that their concentrations in most of the locations studied in this research were above the maximum allowable concentrations, in accordance with global standards, particular attention should be paid in the upcoming period to the biomonitoring of the quality and suitability of the soil for plant production in these areas.

ACKNOWLEDGEMENTS

This work was supported by the Ministry of Science of the Montenegro (through the project Application of Bioassays to test the Cause-effect relationship between Environmental Pollutants and the Level of Toxicity of the soil of the Zeta Plain and the sediments of Lake Skadar).

REFERENCES

[1] Petrovic-Gegic, A., Vojinovic-Miladinov, M., Cehmajster, K. and Ileš, F. (2007) Absorption of essential and toxic elements in various fruit and vegetable sorts in the flooded area the Tisa river. Chemical Industry. 61, 321-325.

[2] Baldisserotto, C., Ferroni, E., Anfuso, E., Pagnoni, A., Fasulo, M.P. and Pancaldi, S. (2007) Responses of *Trapa natans* L. Floating laminae to high concentrations of manganese. Protoplasma. 231, 65-82.

[3] Pandey, N., Pathak, G.C., Pandey, D.K. and Pandey, R. (2009) Heavy metals, Co, Ni, Cu, Zn and Cd, produce oxidative damage and evoke differential antioxidant responses in spinach. Brazilian Journal of Plant Physiology. 21, 103-111.

[4] Trichopoulos, D. (1997) Epidemiology of cancer. In: De Vita, V.T. (Ed.) Cancer: Principles and Practice of Oncology. Lippincott Company, Philadelphia, 231-258.

[5] Radwan, M.A. and Salama, A.K. (2006). Market basket survey for some heavy metals in Egyptian fruits and vegetables. Food and Chemical Toxicology. 44, 1273-1278.

[6] Khairiah, T., Zalifah, M.K., Yin, Y.H. and Aminah, A. (2004) The uptake of heavy metals by fruit type vegetables grown in selected agricultural areas. Pakistan Journal of Biological Sciences. 7, 1438-1442.

[7] Mirecki, N., Agič, R., Šunić, Lj., Milenković, L. and Ilić, S.Z. (2015) Transfer factor as indicator of heavy metals content in plants. Fresen. Environ. Bull. 24, 4212-4219.

[8] Mmolawa, K.B., Likuku, A.S. and Gaboutloeloe, G.K. (2011) Assessment of heavy metal pollution in soils major roadside areas in Botswana. African Journal of Environmental Science and Technology. 5, 186-196.

[9] Camazano, M., Martin, M. and Lavenzo, L. (1994) Lead and cadmium in soils and vegetables from urban gardens of Salamanca (Spain). Science of the Total Environment. 146, 163-168.

[10] Mohamed, A.E., Rashed, M.N. and Mofty, A. (2003) Assessment of essential and Toxic elements in some kinds of vegetables. Ecotoxicology Environmental Safe. 55, 251-260.

[11] Sharma, R.K., Agrawal, M. and Marshall, F.M. (2008) Heavy metal (Cu, Zn, Cd and Pb) contamination of vegetables in urban India: A case study in Varanasi. Environmental Pollution. 154, 254-263.
[12] Chao, W., Xiao-Chen, L., Li-Min, Z., Pei-Fang, W. and Zhi-Yong, G. (2007) Pb, Cu, Zn and Ni concentrations in vegetables in relation to their extractable fractions in soils In Suburban Areas of Nanjing, China. Polish Journal of Environmental Studies. 16, 199-207.
[13] Maksimovic, I., Putnik-Delić, M., Ilin, Ž. and Mirosavljević, M. (2012) Essential (Cu and Zn) and trace (Pb and Cd) heavy metal loads in onion and potato. Agroknowledge Journal. 13, 113- 122.
[14] Manojlovic, M. and Singh, B.R. (2012) Trace elements in soils and food chains of the Balkan region. Acta Agriculture Scandinavia. 62, 673-695.
[15] Papa, S., Bartoli, G., Alvarez-Romero, M., Mottola, S. and Fioretto, A. (2017) Trace metals accumulation in *Fragaria ananassa* and its possible use as a bioaccumulator. Fresen. Environ. Bull. 26, 475-482.
[16] Qiang L., Jingshuang, L., Fengguo, D. and Yanlong, S. (2017) Assessment of heavy metal pollution in agricultural soils from suburban vegetable fields under different planting time. Fresen. Environ. Bull. 26, 3542-3549.
[17] AMA (Agencia de Medio Ambiente de Andalucia, Spain) (1992) Determinining the pesticide content in waters and metal content in living organisms. Ed. AMA, Seville, 55-67.
[18] Usero, J., Gonzalez, R.E. and Gracia, I. (1996) Trace metals in the bivalve mollusc *Chamelea gallina* from the Atlantic coast of southern Spain. Marine Pollution Bulletin. 32, 305-310.
[19] Codex Alimentarius Commission. (2010) Joint FAO/WHO Food Standards Program. Codex General Standard for Contaminants and Toxins in Food and Feed (Codex Stan 193-1995). Adopted 1995. Revised 1997, 2006, 2008, 2009, Amended 2010. p. l, 26, 27.
[20] Reaves, P.G. and Chaney, R.L. (2008) Bioavailability as an issue in risk assessment and management of food cadmium. Science of the Total Environment. 398, 13-19.

Received: **21.12.2016**
Accepted: **06.02.2018**

CORRESPONDING AUTHOR

Dragana Petrovic
Faculty of Natural Sciences and Mathematics,
University of Montenegro,
G. Washington Street, P. O. Box 5455,
81000 Podgorica – Montenegro

e-mail: draganap2104@gmail.com

© by PSP Volume 27 – No. 5/2018 pages 2697-2702 Fresenius Environmental Bulletin

DETERMINATION OF CYTOTOXIC EFFECTS OF PROCHLORAZ AND TRALKOXYDIM IN BARLEY (*HORDEUM VULGARE* L.) ROOTS

Selda Metin-Kir, Filiz Vardar*, Meral Unal

Marmara University, Faculty of Arts and Sciences, Department of Biology, 34722, Goztepe, Istanbul, Turkey

ABSTRACT

The effects of prochloraz (fungicide) and tralkoxydim (herbicide) on the root morphology, root growth, mitotic index and chromosomal behaviour were analysed in a non-target plant, barley (*Hordeum vulgare* L.). The commercial and higher doses of prochloraz (40, 80 and 120 µM) and tralkoxydim (50, 100 and 150 µM) were applied to barley roots up to 60-h. Some morphological defects such as grey regions and tumours occurred on the root tips of barley treated with the prochloraz and tralkoxydim, respectively. Besides the root elongation and mitotic indices were inhibited by the treatment with the two pesticides time and dose dependently. Various types of mitotic aberrations such as chromosome bridges, stickiness, laggards, monopolarity, c-mitosis, abnormal metaphase and anaphase were observed in prochloraz and tralkoxydim treated barley root tips. Based on our results, tralkoxydim is more toxic to barley roots in comparison to prochloraz. In conclusion, the two pesticides, prochloraz and tralkoxydim may be harmful to non-target organisms even their commercial and higher concentrations.

KEYWORDS:
Chromosomal abnormalities, Fungicide, Herbicide, Mitotic index, Root growth.

INTRODUCTION

Pesticide has been defined as any substance or mixture of substances used to prevent, control, repulse, reduce or damage any pest, including insects, snails, nematodes, rodents, weeds, fungi and bacteria [1, 2]. Although pesticides have been used for a long time, their widespread usage began after World War II with the introduction of DDT (dichlorodiphenyltrichloroethane), BHC (beta-hexachlorocyclohexane), 2,4-D (2,4-dichlorophenoxyacetic acid), dieldrin, endrin, and aldrin [2]. Contemporary agribusiness involves broad use of pesticides for qualified yield and it is definite that the application of pesticides will be increased in the near future [3].

While the pesticides have provided to repel or control the pests, they can be toxic to not-target organisms through contaminating soil, water and air. Pesticides can interact with algae, fungi, animals and plants from the water resources and soil penetrating to the food chain causing serious harmful effects in animals and humans. Plants which are one of the essential base components of the ecosystems undertake an important role to evaluate the effects and chain reactions of pesticides in the environment being sessile organisms [3, 4].

One of the imidazole fungicides is prochloraz and it is extensively used within horticulture and agriculture against a wide range of diseases affecting cereals, field crops, fruit and many other crops [5]. Tralkoxydim is a cyclohexane herbicide for use in wheat, barley, rye and triticale against grassy weeds [6]. According to the literature most of the attention has been paid to economic return including seed production, yield quantity and quality [7, 8]. In the present paper, root morphology, root growth, mitotic index and chromosome aberrations were evaluated to detect the toxic damage of prochloraz and tralkoxydim in one of the non-target organism barley (*Hordeum vulgare* L.) roots.

MATERIALS AND METHODS

Barley (*Hordeum vulgare* L. cv. Efes) seeds were obtained from The Field Crops Central Research Institute (Ankara-Turkey). Similar-sized seeds were surface-sterilized with freshly prepared 1% sodium hypochlorite solution for 5 min. After rinsing, the seeds were left for one night in deionized water for imbibition. Seeds were germinated on moistened filter paper with or without prochloraz (IUPAC - N-propyl-N-[2-(2,4,6-trichlorophenoxy)ethyl] imidazole-1-carboxamide) and tralkoxydim (IUPAC - 2-[1-(ethoxyamino)propylidene]-5-(2,4,6-trimethylphenyl) cyclohexane-1,3-dione) in Petri dishes. Stock solutions of prochloraz (40, 80, 120 µM) and tralkoxydim (50, 100, 150 µM) were prepared according to commercial application doses and their folds. Deionized water was used for the control group. Relative primary root length of

control and treated groups was measured by 12-h periods up to 60 h. For better comprehension the germinated seedlings, which reached 1 cm root elongation, were chosen at 12 h to precede the treatment.

Control and 60 h treated groups of barley roots were fixed in acetic-alcohol (1:3, v/v) for 24-h and stored in 70% ethanol at +4ºC. The standard Feulgen technique applied to the Al treated roots has been adapted and modified from Vardar et al. [9]. The root tips were hydrolyzed in 5 N HCl at room temperature for 25 min. After hydrolysis roots were transferred to basic fuchsin for 2-h in the dark. Squash preparations were performed in 2% aceto-orcein. In each treatment, ten well-spread preparations were chosen and approximately 5000 cells were scored for mitotic analysis including mitotic index (MI) and scoring of aberrant cells. MI was calculated as the ratio of the number of dividing cells to the total number of cells. The mitotic analysis was completed with KAMERAM software, assisted by a KAMERAM colour camera and an Olympus BX-51 light microscope. Thirty seeds were used for each experiment. All experiments were repeated three times and results were evaluated statistically. All the experimental data were subjected to Duncan's post-hoc HSD using SPSS with 95% ($p<0.05$) significance of differences between means.

RESULTS AND DISCUSSION

Barley is one of the important cereals that has been bred for centuries and is considered as essential nutrition in animal fodder, a source of fermentable material for beer and certain distilled beverages, and a component of various health foods [10]. The yield quantity and quality of barley has been limited due to different types of pests. To eliminate the potential pests, various types of pesticides are used. On application of pesticides the growth and development of barley as being a non-target organism might be affected unfavourably [11]. In this context, we aimed to display the possible toxic effects of different doses of prochloraz (herbicide) and tralkoxydim (fungucide) in barley roots.

The average root lengths of prochloraz and tralkoxydim treated barley roots were measured by 12-h intervals up to 60-h. Prochloraz application stimulated the root elongation in all concentrations up to 24-h period with regard to controls. Although there was no significant difference between control and 40 µM prochloraz treatment, the root elongation inhibited in 80 µM and 120 µM concentrations after 48-h. While the root elongation decreased by 17.2% in 120 µM prochloraz application at the end of the 60-h, no significant difference was determined in 40 µM and 80 µM in contrast to control (Table 1). On the other hand tralkoxydim applications also caused alterations in barley root growth. Even if 50 µM tralkoxydim application stimulated the root growth, it was inhibited slightly in 100 and 150 µM concentrations after 24-h in compare to control. Furthermore all of the treatments started to inhibit the root elongation after 36-h with respect to controls. It was reduced by 38.4% in 50 µM, 40.7% in 100 µM and 41.6% in 150 µM tralkoxydim application after 60-h (Table 2).

Moreover prochloraz and tralkoxydim treatments caused some morphological alterations on barley roots. In prochloraz treatment grey regions on roots were distinctive in compare to controls (Figure 1). Similarly tralkoxydim treatment induced tumour formations in the barley roots significantly (Figure 2).

Mitotic index is a significant parameter to evaluate the percentage of mitotic cells. For better comprehension the mitotic index and chromosomal abnormalities were evaluated by Feulgen procedure. The frequency of dividing cells in meristematic cells of root tips was found to decrease after prochloraz and tralkoxydim treatment at 60-h with regard to control. This result is evidenced by the ratio of the cells in different mitotic phases. The data revealed that while the ratio of interphase increased distinctively, the different mitotic phases (metaphase, anaphase and telophase) decreased in barley roots with increasing concentrations of prochloraz and tralkoxydim at 60-h (Table 3).

TABLE 1
The effects of prochloraz on the root elongation of barley (*H. vulgare*). All of the data are significantly different from each other according to Duncan test for independent samples at P<0.05. Values represent means ±SD

Treatment time (h)	Root elongation (mm)			
	Control	40 µM	80 µM	120 µM
12	1.00 ±0.0	1.00 ±0.0	1.00 ±0.0	1.00 ±0.0
24	1.77 ±0.23	2.59 ±1.56	2.40 ±0.22	2.14 ±0.19
36	6.14 ±0.58	6.09 ±0.42	5.80 ±0.43	5.06 ±0.49
48	10.07 ±0.77	10.16 ±0.17	9.79 ±0.52	7.81 ±0.63
60	14.23 ±0.80	14.39 ±0.73	14.28 ±0.67	11.79 ±0.68

TABLE 2
The effects of tralkoxydim on the root elongation of barley (*H. vulgare*). All of the data are significantly different from each other according to Duncan test for independent samples at P<0.05. Values represent means ±SD

Treatment time (h)	Root elongation (mm)			
	Control	50 µM	100 µM	150 µM
12	1.00 ±0.0	1.00 ±0.0	1.00 ±0.0	1.00 ±0.0
24	2.95 ±0.32	3.35 ±0.23	2.7 ±0.19	2.86 ±0.16
36	5.4 ±0.49	4.67 ±0.24	4.41 ±0.26	4.94 ±0.18
48	8.68 ±0.58	6.29 ±0.23	6.04 ±0.22	6.17 ±0.19
60	11.52 ±0.86	7.1 ±0.21	6.83 ±0.19	6.73 ±0.17

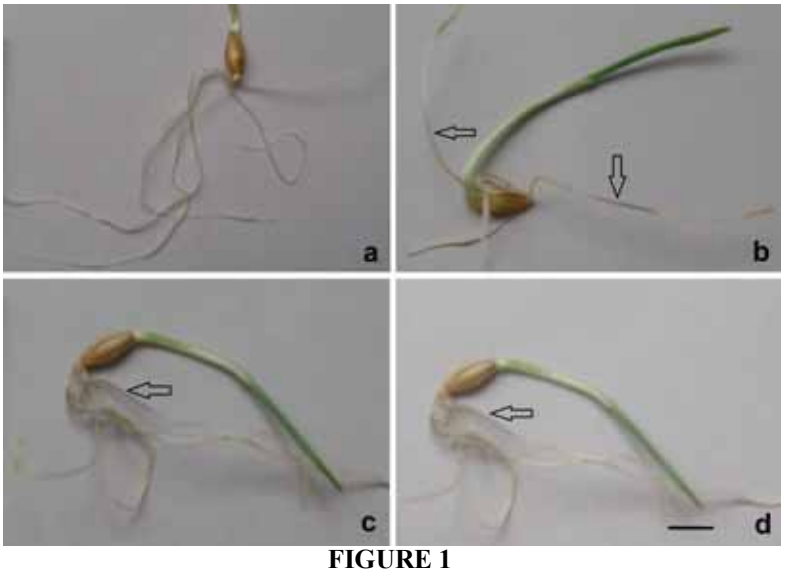


FIGURE 1
Morphological view of control and prochloraz treated fresh barley roots showing grey regions (arrows). The bar (1 cm) in d also applies to a-c

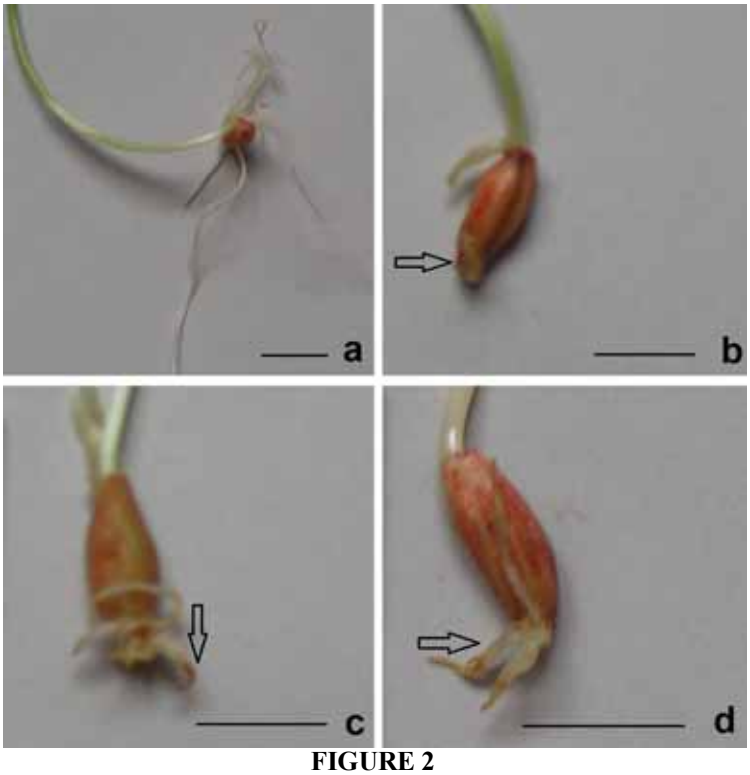


FIGURE 2
Morphological view of control and tralkoxydim treated fresh barley roots showing tumour formations (arrows). The bar (1 cm) in d also applies to a-c

TABLE 3

The effects of prochloraz and tralkoxydim on the different phases of mitosis in barley (*H. vulgare*) roots after 60-h. All of the data are significantly different from each other according to Duncan test for independent samples at P<0.05. Values represent means ±SD

% of Cells in Different Mitotic Phases	Prochloraz				Tralkoxydim		
	Control	40µM	80µM	120µM	50 µM	100µM	150µM
Interphase	88.12 ±1.86	91.39 ±1.29	95.6 ±0.52	94.94 ±0.65	94 ±2.63	94.55 ±0.46	96.76 ±0.58
Prophase	7.91 ±1.43	4.96 ±0.7	2.31 ±0.44	2.95 ±0.61	2.29 ±0.48	3.31 ±0.32	2.12 ±0.45
Metaphase	2.75 ±0.96	1.14 ±0,23	0.54 ±0.16	0.6 ±0.10	0.62 ±0.16	1.18 ±0.07	0.44 ±0.18
Anaphase	1.91 ±0.89	2.18 ±0.59	1.49 ±0.3	0.98 ±0.18	0.35 ±0.09	0.32 ±0.07	0.31 ±0.04
Telophase	0.21 ±0.12	0.36 ±0.24	0.06 ±0.04	0.52 ±0.2	0.68 ±0.12	0.47 ±0.11	0.31 ±0.09

TABLE 4

The effects of prochloraz and tralkoxydim on the mitotic index and chromosomal behaviours of barley (*H. vulgare*) roots after 60-h. All of the data are significantly different from each other according to Duncan test for independent samples at P<0.05. Values represent means ±SD

	Prochloraz				Tralkoxydim		
	Control	40µM	80µM	120µM	50 µM	100µM	150µM
Total cell	5423	6130	5010	6046	5860	7220	5870
Dividing cell	612	464	219	310	219	383	184
Mitotic index (%)	11.87 ±1.86	8.65 ±1.27	4.39 ±0.52	5.06 ±0.65	3.86 ±0.55	5.86 ±0.39	3.23 ±0.58
Monopolarity	-	8	17	12	2	2	8
Stickiness	-	16	7	22	17	5	16
Laggard	-	-	6	10	-	-	-
Bridges	-	4	5	21	3	1	2
c-mitosis	-	17	10	41	9	9	18
Abnormal metaphase	-	23	57	57	20	9	44
Abnormal anaphase	-	28	32	42	12	7	9
Total abnormality	-	1.57 ±0.51	2.67 ±1.38	3.39 ±1.17	1.08 ±0.13	0.46 ±0.08	1.65 ±1.18

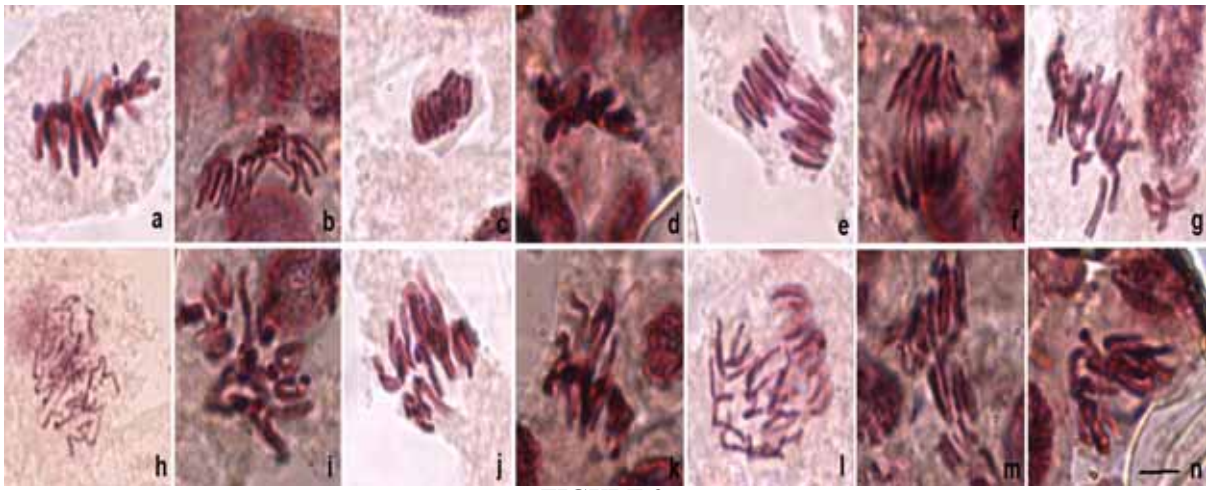


FIGURE 3

Mitotic abnormalities in barley roots after prochloraz and tralkoxydim treatments. a, c, e, g, h, j, l. 120 µM procloraz treatment; b, d, f, g, i, k, m, n. 150 µM tralkoxydim treatment. a, b. Monopolarity; c, d. Stickiness; e, f. Bridges; g. Laggards; h, i. C-mitosis; j, k. Abnormal metaphases; l, m. Abnormal anaphases; n. Abnormal mitosis. The bar (100 µm) in n also applies to a-m

The mitotic index was 11.87% in the control barley root tips. It was reduced by 27.1% in 40 µM, 63% in 80 µM and 57.4% in 120 µM prochloraz treatment at 60-h. According to the results the higher concentrations (80-120 µM) reduced the mitotic index by 60% approximately leading to intensive toxicity. Furthermore the mitotic index was decreased by 67.5% in 50 µM, 50.6% in 100 µM and 72.8% in 150 µM tralkoxydim treatment at 60-h. These results can be considered as the commercial and higher doses of tralkoxydim are strikingly toxic on mitotic index. Our results also indicated that tralkoxydim is more toxic to barley roots in comparison to prochloraz.

Mitotic observations in the prochloraz and tralkoxydim treated root tip cells revealed various

types of chromosomal abnormalities (Figure 3). Most of the aberrations were characterized by monopolarity, chromosome stickiness, laggards, anaphase bridges, c-mitosis and abnormal appearance at metaphase and anaphase. Laggards were only seen in the application of 80 µM and 120 µM prochloraz. The most frequently occurred abnormal metaphase and anaphase were obvious for both prochloraz and tralkoxydim. The frequency of cells with chromosomal abnormalities increased with increasing dose of prochloraz treatments. Although the total chromosomal aberration ratio showed fluctuations with increasing doses of tralkoxydim, the possible fact of lower abnormalities may be inhibition of mitotic index.

Several researchers examined the effects of pesticides in many aspects. Coşkun [12] stated that decis (insecticide) caused sticky chromosomes in *Allium cepa* roots with increasing doses. A similar process was performed by Ateeq et al. [13]. The researchers treated *A. cepa* roots with 3 different herbicides (2,4-D, butachlor, pentachlorophenol). According to their results the herbicides affected the root morphology and caused tumours. Although the mitotic index values was similar with respect to control in butachlor treatment, 2,4-D and pentachlorophenol reduced the mitotic indices. Moreover, Türkoğlu [14] examined the genotoxic effects of chlorfenvinphos (insecticide) and fenbuconazole (fungicide) by evaluating mitotic index and chromosomal aberrations on the roots of *A. cepa*. The researcher indicated that the both pesticides decreased the mitotic indices, while the chromosomal aberrations increased. In one of the latest researches the genotoxic effects of carbendezim (fungicide) on the roots of *A. cepa* were determined [15]. According to the results carbendezim caused several chromosomal aberrations and decreased mitotic indices time and dose dependently. Consistent with our results different types of pesticides induced reduced mitotic index and increased chromosomal abnormalities.

Cytological abnormalities in plants represent as a significant monitoring procedure for the evaluation of environmental chemicals/mutagens that may cause a genetic damage [16]. Furthermore determination of mitotic index and chromosomal behaviour reveals whether or not a particular chemical can cause breaks in chromosomes, leading to detect parts of the chromosome being deleted, added, or rearranged. The term of clastogen is the general name of the chromosome breaks. Clastogenity is a form of mutagenesis, and can lead to carcinogenesis [13, 17]. Most of the toxicity researches performed with many types of pesticides has shown that plant chromosomes exhibit different types of aberrations some of which are specific for different pesticides. It has been noted that there is an excellent correlation between chromosome abnormalities recorded in roots and those observed in mammalian cells. It can be suggested that several higher plants provide specific and important systems for monitoring and evaluating the effects of chemicals/mutagens [16].

CONCLUSION

Based on our results, tralkoxydim caused significant toxicity even in the commercial doses. Although the commercial dose of prochloraz (40 µM) revealed slight toxicity, in the highest concentrations (80 and 120 µM) the toxicity was more severe. According to WHO [18] prochloraz and tralkoxydim are in Class III, which contains slightly hazardous pesticides. It has been widely known that the impact rate of the pesticides depends on their type, dose and application period. Moreover developmental, morphological, biochemical and physiological conditions of the plants are also very important criterions for their interaction [19]. It can be concluded that prochloraz and tralkoxydim may be harmful to non-target organisms even their commercial and higher concentrations. The presented study will help to understand potential impacts of prochloraz and tralkoxydim being a potential risk to humans and other life forms. Our results may also assist in terms of use and control of pesticides as the reduction of its harmful adverse effects in both environmental and agricultural systems.

REFERENCES

[1] Bolognesi, C. (2003) Genotoxicity of pesticides: A review of human biomonitoring studies. Mutation Research. 543, 251−272.
[2] Cooper, J. and Dobson, H. (2007) The benefits of pesticides to mankind and the environment. Crop Protection. 26, 1337−1348.
[3] Maksymiv, I. (2015) Pesticides: Benefits and hazards. JPNU Science Journal. 2, 70−76.
[4] Aktar, M.W., Sengupta, D. and Chowdhury, A. (2009) Impact of pesticides use in agriculture: Their benefits and hazards. Interdisc Toxicology. 2, 1-12.
[5] Vinggaard, A.M., Hass, U., Dalgaard, M., Andersen, H.R., Bonefeld-Jørgensen, E., Christiansen, S., Laier, P., Poulsen, M.E. (2006) Prochloraz: an imidazole fungicide with multiple mechanisms of action. International Journal of Andrology. 29, 186−92.
[6] Devine, M.D., Harren, J.C., Abrams, S.R. and Gusta, L.V. (1995) Effect of drought stress, abscisic acid, and abscisic acid analogues on the efficacy of diclofop-methyl and tralkoxydim. Journal of Plant Growth and Regulation. 14, 77−84.

[7] Nan, Z.B., Skipp, R.A. and Long, P.G. (1991) Use of fungicides to assess the effects of root disease: Effects of prochloraz on red clover and microbial populations in soil and roots. Soil Biology and Biochemistry. 23, 743−750.
[8] O'Donovan, J.T., Harker, K.N., Clayton, G.W., Newman, J.C., Robinson, D. and Hall, L.M. (2001) Barley seeding rate influences the effects of variable herbicide rates on wild oat. Weed Science. 49, 746−754.
[9] Vardar, F., İsmailoğlu, I. İnan, D, and Ünal, M. (2011) Determination of stress responses induced by aluminum in maize (*Zea mays* L. Karadeniz Yıldızı). Acta Biologica Hungarica. 62, 156−170.
[10] Bartlett, J.G., Alves, S.C., Smedley, M., Snape, J.W. and Harwood, W.A. (2008) High-throughput *Agrobacterium*-mediated barley transformation. Plant Methods. 4, 1−12.
[11] Kaya, S., Pirinççi, İ. and Bilgili, A. (2002) Veterinerlikte Toksikoloji [Toxicology in Veterinary medicine]. Medisan Press. Turkey.
[12] Coşkun, E.E. (1992) *Allium cepa* L. kök meristem hücrelerinde Decis'in (İnsektisit) etkileri [The effects of Decis (Insecticide) in the root meristem cells of *Allium cepa* L.] Master Thesis. Ege University, İzmir, Turkey.
[13] Ateeq, B., Farah, M.A., Ali, M.N. and Ahmad, W. (2002) Clastogenicity of pentachlorophenol, 2,4-D and butachlor evaluated by *Allium* root tip test. Mutation Research. 514, 105−113.
[14] Türkoğlu, Ş. (2012) Determination of genotoxic effects of chlorfenvinphos and fenbuconazole in *Allium cepa* root cells by mitotic activity, chromosome aberration, DNA content, and comet assay. Pesticide Biochemistry and Physiology. 103, 224−230.
[15] Selvaraju, S., Vasanth, M., Rajarajan, R., Muralidharan, R. and Raghupathy, V. (2015) Genotoxic effects of carbendezim (fungicide) on the root apical meristems of *Allium cepa* L. Research Journal of Pharmacognosy and Phytochemistry. 7, 29−33.
[16] Nilan, R.A. and Vig, B.K. (1976) Plant Test Systems for Detection of Chemical Mutagens. In: Hollaender, A. (Ed.) Chemical Mutagens; Principles and Methods for Their Detection. Plenum Press. New York.
[17] Grant, W.F. (1978) Chromosome aberrations in plants as a monitoring system. Environmental Health Perspectives. 27, 37−43.
[18] Nemli, Y. (1983) Yabani Otlar [Wild Weeds], Ege University Press. İzmir, Turkey.
[19] World Health Organization (WHO) (2004) Recommended classification of pesticides by hazard and guidelines to classification. World Health Organization, Geneva, Switzerland.

Received: **30.12.2016**
Accepted: **09.11.2017**

CORRESPONDING AUTHOR

Filiz Vardar
Marmara University,
Faculty of Arts and Sciences,
Department of Biology,
34722, Göztepe, İstanbul – Turkey

e-mail: filiz.vardar@gmail.com

© by PSP Volume 27 – No. 5/2018 pages 2703-2716 Fresenius Environmental Bulletin

REMEDIATION OF A URANIUM-CONTAMINATED GROUNDWATER USING THE PERMEABLE REACTIVE BARRIER TECHNIQUE COUPLED WITH HYDROXYAPATITE-COATED QUARTZ SANDS

Weimin Zhang, Yadan Guo*, Zhiping Pan, Yiran Li, Hua Zeng

State Key Laboratory Breeding Base of Nuclear Resources and Environment, East China University of Technology, 418 Guanglan Road, Nanchang, 330013, P. R. China

ABSTRACT

Treatment of uranium-contaminated groundwater remains a challenge for environmental scientists worldwide. In this study, a permeable reactive barrier (PRB) was coupled with hydroxyapatite-coated quartz sands to treat uranium-contaminated groundwater. The effects of quartz sand particle size, hydroxyapatite coating amount, and velocity and initial concentration of uranium on the removal of U(VI) from an aqueous solution was investigated by dynamic column tests, so as to determine the optimal conditions for uranium removal. The adsorption process was studied using a dynamic adsorption model. Results showed that when the diameter of quartz composite sand was 0.6–1.18 mm, the adsorption capacity of the composites reached the maximum of 6.26 mg/g. The Thomas and Yoon–Nelson models suitably described the influence of quartz sand diameter on the adsorption of U(VI) by the PRB. The equilibration adsorption capacities of the PRB for U(VI) estimated by the Thomas and Yoon–Nelson models were 5.62 and 5.88 mg/g, respectively. This study indicates that the combination of the PRB technique and hydroxyapatite-coated quartz sands is efficient and promising for uranium removal from groundwater.

KEYWORDS:
Permeable reactive barrier (PRB), groundwater, uranium, hydroxyapatite

INTRODUCTION

Groundwater contaminated with heavy metals such as lead can pose a serious threat to drinking water supply systems and ecosystem health [1, 2]. Radionuclide contamination also threatens aquatic life and human health due to its potential toxic and carcinogenic effects. Therefore, developing highly efficient methods for the removal of radionuclides from aqueous solutions has become an issue of great concern. Treatment of groundwater contaminated with uranium remains a challenge for environmental scientists worldwide [3, 4]. Several technologies [5-7] exist for the remediation of U(VI)-contaminated groundwater, and are broadly categorized as chemical treatment technologies, biological treatment technologies and physical–chemical treatment technologies. Compared with other technologies, permeable reactive barriers (PRBs), with a reactive media emplaced to separate contaminants from groundwater, may create a passive treatment system (based on factors including: reactivity, permeability, environmental compatibility, availability, cost, and long-term stability) are a passive remediation technology that offer a cost-effective alternative to the conventional pump and treat (P&T) systems for remediating contaminated groundwater [8, 9].

It was first proposed as an in-situ remediation in 1982 by U.S. Environmental Protection Agency. Various reactive media have been used in various studies [10-12], these include zero-valent iron (ZVI), activated carbons, zeolites, lime and other alkaline materials, apatite, transformed red mud, oxides, sodium dithionite and combination of reactive materials. ZVI is the most widely used material filled in PRBs, however, it is expensive and increases the overall cost of the entire remediation engineering. In this study, PRB was composed of hydroxyapatite-coated quartz sands to treat a groundwater contaminated with uranium. The particle size of quartz sand, hydroxyapatite coating amount, velocity and initial uranium concentration were considered in the removal of U(VI) in the aqueous solution by dynamic column tests. The optimal experimental conditions were determined and analyzed using a dynamic adsorption model.

METHODOLOGY

Methods. The breakthrough curves show the performance of PRB dynamic columns. The breakthrough time of the breakthrough curve influences the dynamic column of PRB. The time that the effluent concentration of uranium (C_t) is 10 percent of the

initial influent concentration (C_0) is called the breakthrough point; the time that the effluent concentration of uranium (C_t) is about of 95 percent of the influent initial concentration (C_0) is called "post consumption" [13], that is, through the end point. Once the reaction of the PRB dynamic column has been defined, the breakthrough curve is generally a function of C_t/C_0 to time or volume [14, 15]. The calculation equation of the effluent total volume flow V_{eff} at the breakthrough end point is:

$$V_{eff} = 24 \times 60 \times Qt_{total} \quad (1)$$

where, Q is the flow rate (mL/min), and t_{total} is the total outflow time (min) when the adsorption equilibrium is reached.

When the initial concentration and flow rate of uranium is defined, the calculation equation of saturated adsorption capacity q_{total} is [16, 17]:

$$q_{total} = \frac{Q \times 24 \times 60}{1000} \int_{t=0}^{t=total} C_{ad} dt \quad (2)$$

where C_{ad} is the removal concentration of uranium (VI) solution (mg/L).

The adsorption capacity of uranium q_{eq} (mg/g) when the dynamic column of PRB equilibrium is reached and the equation is:

$$q_{eq} = \frac{q_{total}}{m} \quad (3)$$

In the equation, m is the dry weight (g) of the reaction material in the dynamic column of PRB. The calculation formula for the total amount of the adsorbed m_{total} mass flowing through the dynamic column of PRB is:

$$m_{total} = \frac{24 \times 60 \times C_0 \times Q \times t_{total}}{1000} \quad (4)$$

The calculation equation of the total adsorption percentage(Y), that is the removal rate of uranium in the dynamic column of PRB is:

$$Y(\%) = \frac{q_{total}}{m_{total}} \times 100 \quad (5)$$

RESULTS AND DISCUSSION

Effect of quartz sands particle size in the composite materials on the removal of U(VI) by dynamic absorption. Fig. 1 is a schematic diagram of quartz sands particle size in the composite materials on the removal of U(VI) by a dynamic PRB absorption column. As shown in Fig. 1, the dielectric materials in the third part of the four PVC column are (a) ranged from 0.15 to 0.3 mm hydroxyapatite-coated quartz sands, (b) ranged from 0.3 to 0.6 mm hydroxyapatite-coated quartz sands, (c) ranged from 0.6 to 1.18 mm hydroxyapatite-coated quartz sands, (d) ranged from 1.18 to 2.36 mm hydroxyapatite-coated quartz sands, respectively. When the influent concentration of uranium solution was 3 mg/L, the flow rate was 6 ml/min, pH was 4.01, the color of the third part of PVC column gradually turned from white to yellow. The effect of quartz sand particle size on U(VI) adsorption by dynamic PRB absorption column is shown in Fig. 2. The size of reaction medium quartz sand is the greatest, the specific surface area is the smallest, the penetration time is the shortest, and column consumption occurs the fastest. When the condition of influent concentration of uranium sand in composite materials is gradually increased from 0.15-0.3 mm to 0.6-1.18 mm, the breakthrough point of PRB dynamic column breakthrough curves moved to the right, while the upward slope of breakthrough curve slowed down.

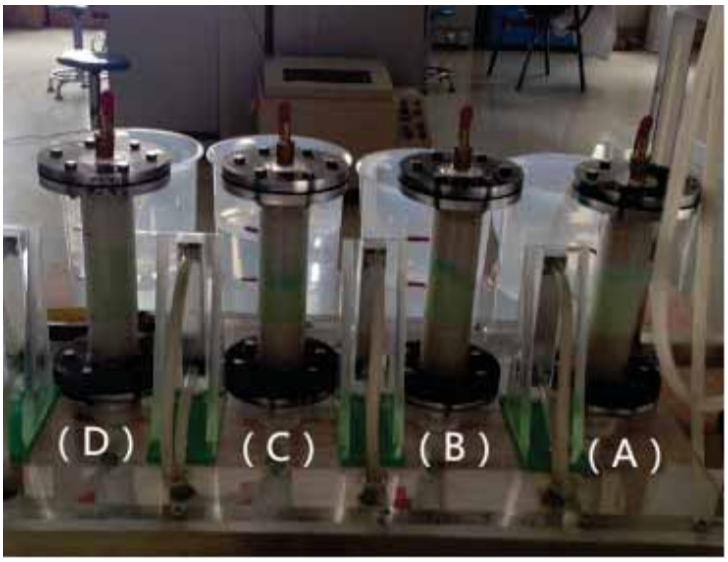


FIGURE 1
Effect of quartz sands particle size on the removal of U(VI) by dynamic PRB absorption column test schematic diagram

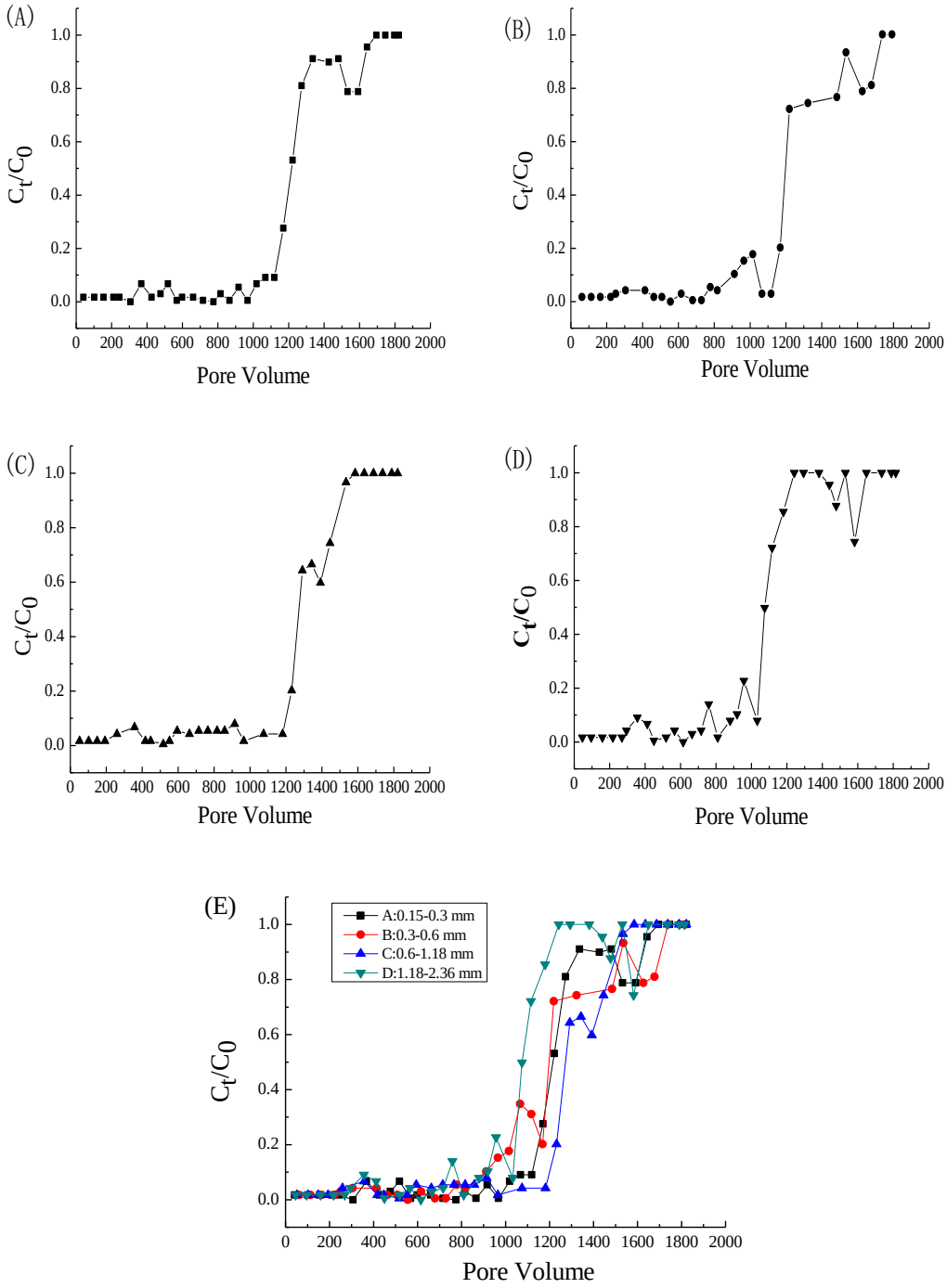


FIGURE 2
Effect of quartz sands particle size on the breakthrough curve of dynamic PRB absorption column used for U(VI) adsorption

TABLE 1
Parameters of quartz sands particle size on the breakthrough curve of dynamic PRB absorption column used for U(VI) adsorption

C_0	Q	Quartz sand diameter	t_{total}	m_{total}	q_{total}	q_{eq}	V_{eff}	Y
mg/L	mL/min	mm	d	mg	mg	mg/g	mL	%
3	6	0.15–0.3	33	855.36	595.16	5.95	285120	69.58
3	6	0.3–0.6	34	881.28	614.16	6.14	293760	69.69
3	6	0.6–1.18	31	803.52	626.37	6.26	267840	77.95
3	6	1.18–2.36	34	881.28	509.81	5.10	293760	57.85

The penetration curve parameters of quartz sands particle size on the breakthrough curve of dynamic PRB absorption column for U(VI) adsorption were calculated and are shown in Table 1. The maximum adsorbing capacity of composite materials used for uranium(VI) adsorption is 5.95 mg/g, 6.14 mg/g, 6.26 mg/g, 5.10 mg/g for quartz sands in the corresponding composite materials from the ranges from 0.15 to 0.3 mm, 0.3 to 0.6 mm, 0.6 to 1.18 mm and 1.18 to 2.36 mm, respectively. Thus, it could be seen that the adsorbing capacity of composite materials used for uranium(VI) adsorption increased first and then decreased with increasing quartz sand particle size in composite materials. This is because quartz sand of larger particles sizes provided less adsorption sites for PRB dynamic column [18-20], thus shortening the contact time. As can be seen from Table 1, with increasing composite particle size from 0.15–0.3 mm to 0.6–1.18 mm, the removal rate of the uranium solution in the PRB dynamic column increased from 69.58% to 77.95%.



FIGURE 3
Effect of hydroxyapatite dosage on the removal of U(VI) by dynamic PRB absorption column test schematic diagram

Effect of hydroxyapatite dosage in composite materials on the breakthrough curve of dynamic adsorption of uranium(VI). Fig. 3 shows the color change of the U(VI) contained dielectric materials before (Fig. 3(1)) and after (Fig. 3(2)) treatment. The proportion of hydroxyapatite and quartz sands in the third part of dielectric materials of the four PVC columns are (a) 0.0157, (b) 0.0118, (c) 0.0094, (d) 0.0079, respectively. When the influent concentration of uranium solution was 3 mg/L, the flow rate was 6 ml/min, and pH was 4.01, the color of the dielectric materials in PRB dynamic column turned from white to yellow. Fig.4 shows the effect of hydroxyapatite dosage on the breakthrough curve of dynamic PRB absorption column used for U(VI) adsorption. In Fig. 4, the reaction medium for the ratio of hydroxyapatite and quartz sands is 0.0079. As can be seen from Fig. 4, the penetration point of PRB dynamic column breakthrough curve moves to the left, indicating that the cycle the penetration curve used shortens as the ratio of hydroxyapatite and quartz sands in composite materials gradually increases from 0.0157 to 0.0079.

The parameters of hydroxyapatite dosage on the breakthrough curve of dynamic PRB absorption column used for U(VI) adsorption have been calculated and are shown in Table 2. When the ratio of hydroxyapatite and quartz sands in composite materials are 0.0157, 0.0118, 0.0094, and 0.0079, the maximum adsorbing capacity of composite materials used for U(VI) adsorption were 9.67 mg/g, 8.97 mg/g, 8.74 mg/g and 7.52 mg/g, respectively. Thus, as the amount of hydroxyapatite in the composite increased, the adsorption capacity of the composite materials also increased gradually. We added lesser amounts of quartz sand when the size of quartz sands was all the same, because the surface of quartz sand could provide better contact with hydroxyapatite solution in the process of preparation. Therefore, hydroxyapatite coating in composite materials is beneficial for the enhancement of adsorption capacity to uranium(VI). From Table 2, the removal rate of uranium in PRB dynamic column increased from 69.8% to 81.3% with increasing the ratio of hydroxyapatite and quartz sands from 0.0079 to 0.0157. Therefore, the ratio of dielectric material of hydroxyapatite and quartz sands used in follow-up test is 0.0157 is appropriate.

Effect of flow rate on the dynamic adsorption of U(VI). Figure 5 is a test schematic diagram of U(VI) removal using a dynamic PRB absorption column. The figures to the left and right show the reaction column before and after the reaction, respectively. The reaction dielectric materials in the three columns in Fig. 5 are hydroxyapatite-coated quartz sands of size 0.6–1.18 mm (the ratio of the hydroxyapatite to quartz sands is 0.0157). We studied the effect of different flow rates (3 mL/min, 6 mL/min, and 9 mL/min) on U(VI) removal for an influent uranium solution concentration on 3 mg/L and a pH of 4.01. Figure 6 shows the effect of flow rate on the breakthrough curve of the dynamic PRB absorption column used for U(VI) adsorption. As shown in Fig. 6, when the flow rate increases gradually from 3 mL/min to 9 mL/min, the point of penetration on the penetration curve moves to the left.

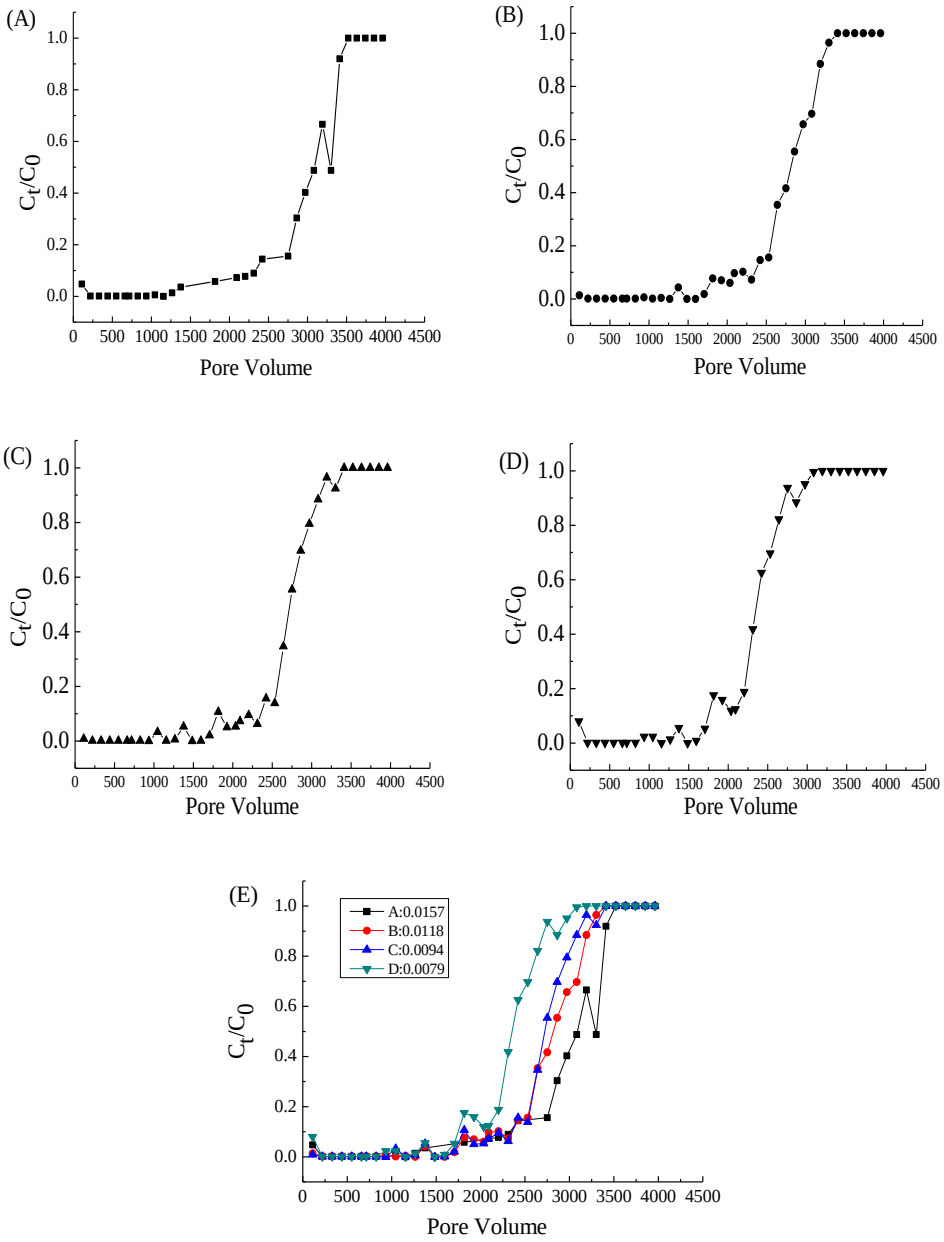


FIGURE 4
Effect of hydroxyapatite dosage on the breakthrough curve of dynamic PRB absorption column used for U(VI) adsorption

TABLE 2
Parameters of hydroxyapatite dosage on the breakthrough curve of dynamic PRB absorption column used for U(VI) adsorption

C_0	Q	Hydroxyapatite: quartz sand	t_{total}	m_{total}	q_{total}	q_{eq}	V_{eff}	Y
mg/L	mL/min		d	mg	mg	mg/g	mL	%
3	6	0.0157	64	1664.82	1353.45	9.67	570240	81.30
3	6	0.0118	62	1612.79	1256.36	8.97	570240	77.90
3	6	0.0094	62	1612.79	1222.99	8.74	570240	75.83
3	6	0.0079	58	1508.74	1053.17	7.52	570240	69.80

This is because the flow velocity is lower, the contact time of uranyl ion and the adsorbent is longer.

Table 3 presents the calculated parameters of the breakthrough curve dynamic column for U(VI) adsorption. When the flow rate is 3 mL/min, 6 mL/min, and 9 mL/min, the corresponding composite maximum of U(VI) is 11.76 mg/g, 10.67 mg/g, and 7.92 mg/g. When the flow velocity increases gradually from 3 mL/min to 9 mL/min, the removal rate of the uranium solution reduces from 69.8% to



FIGURE 5
Effect of flow on the removal of U(VI) using the dynamic PRB absorption column test: A schematic diagram

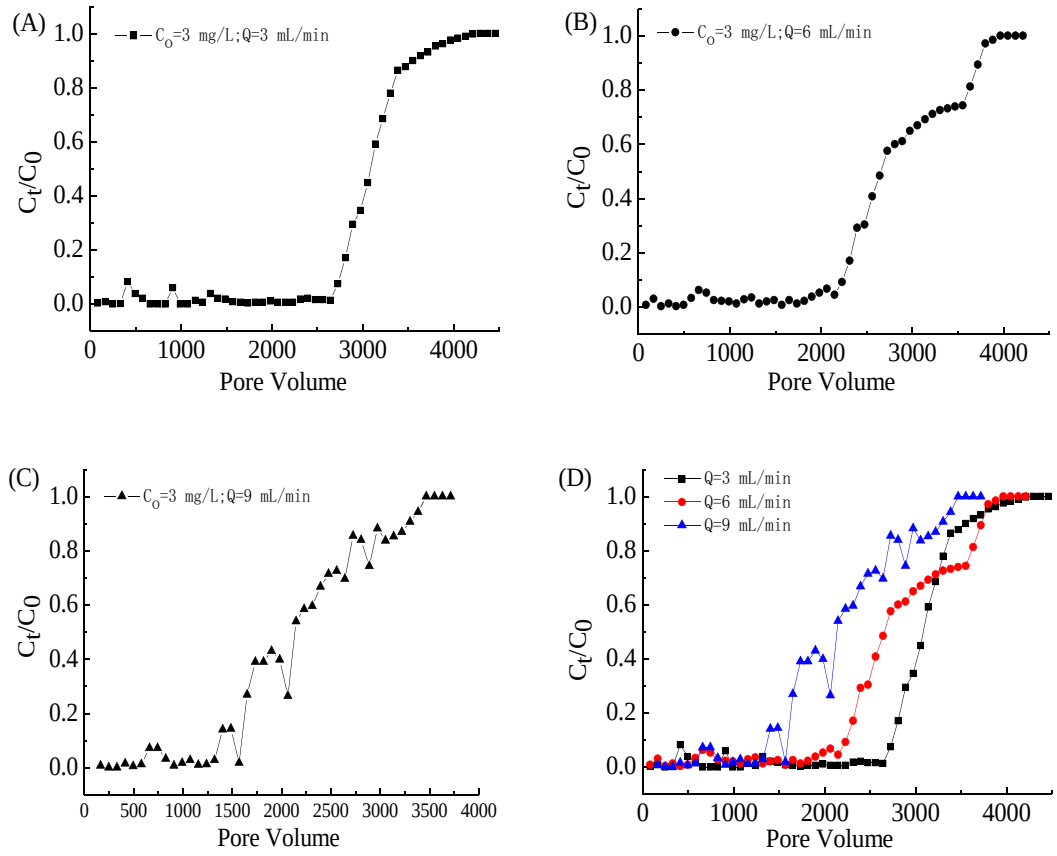


FIGURE 6
Effect of flow on the breakthrough curve of dynamic PRB absorption column used for U(VI) adsorption

TABLE 3
Flow parameters on the breakthrough curve of the dynamic PRB absorption column used for U(VI) adsorption

C_0	Q	t_{total}	m_{total}	q_{total}	q_{eq}	V_{eff}	Y
mg/L	mL/min	d	mg	mg	mg/g	mL	%
3	3	156	2021.76	1411.1	11.76	673920	69.8
3	6	72	1866.24	1280.32	10.67	622080	68.6
3	9	43	1671.84	950.94	7.92	557280	56.88

56.88%. Thus, higher flow velocities are unfavorable for U(VI) removal by the composite materials.

Curve fitting model. The flow curve is usually utilized for the PRB dynamic column adsorption test. Laboratory-scale dynamic column adsorption

experiments typically rely on a series of simple mathematical models, which could provide relatively accurate design parameters for the project of laboratory adsorption but more accurate information is required at expanded scales applications. In this work, the Thomas and Yoon–Nelson models were used to simulate the lm-prb dynamic column adsorption process, so as to provide reliable design parameter data for further practical applications.

Thomas' model. Thomas' model is based on the Langmuir kinetics equation. It is an idealized model that assumes no axial diffusion. It is used to calculate saturated adsorption capacity and the adsorption rate constant of the lm-prb dynamic column. The following expression applies.

$$\frac{C_t}{C_0} = \frac{1}{1+\exp\left[\frac{k_{Th}}{Q}\left(q_0 m - C_0 v\right)\right]} \quad (6)$$

In equation (6), k_{Th} is Thomas' rate constant (L/d mg), q_0 is the amount of U (VI) absorbed by unit mass at the equilibration time (mg/g), Q is the column flow rate (L/d), C_0 is the initial concentration of the uranium solution (mg/L), Ct is the outflow concentration of the uranium solution (mg/L), *v* represents the volume of the solution passing through the dynamic column (L), and m is the dosage of the composite materials in the prb dynamic column (g).

(1) Effect of quartz sand particle size in composite materials on the dynamic adsorption of U (VI). Using equation (6), the plot for V versus C_t/C_0 is drawn (Fig. 7). The calculated parameters, k_{Th}, q_0, and phase sequence, are presented in Table 4. Since the value of the correlation coefficient R^2 is greater than 0.95, the Thomas model can well describe the removal of U(VI) by the dynamic PRB absorption column. Based on the assumption made by the Thomas model, the internal diffusion and external diffusion in the adsorption process are considered as inessential steps. When the initial U(VI) concentration is 3 mg/L and the flow rate is 6 mL/min, the adsorption capacities are 5.20 mg/g, 5.23 mg/g, 5.62 mg/g, and 4.64 mg/g for quartz sand particle sizes of 0.15–0.3 mm, 0.3–0.6 mm, 0.6–1.18 mm, and 1.18–2.36 mm, respectively. When the particle size of

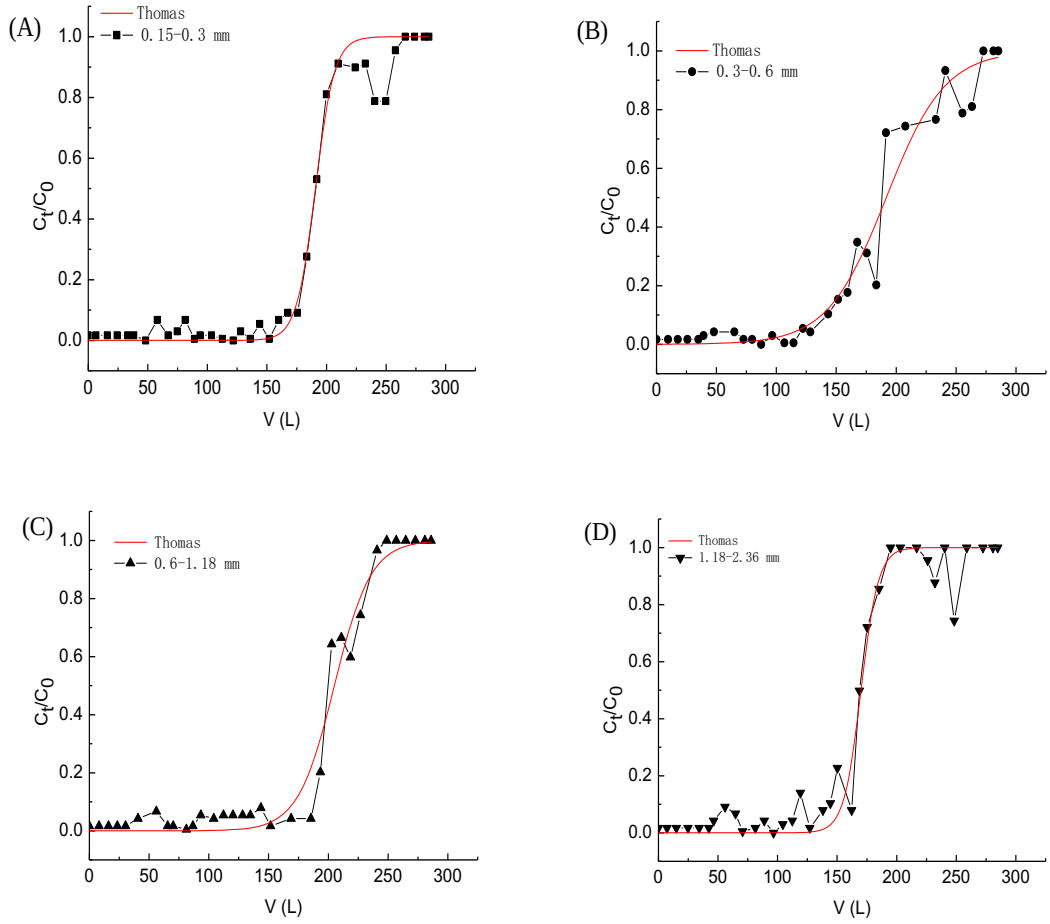


FIGURE 7
Effect of quartz sand particle size on the removal of U(VI) by the dynamic PRB absorption column as per Thomas' model

TABLE 4
Parameters of quartz sand particle sizes as per Thomas' model

Initial U(VI) concentration	Flow rate	Quartz sands particle size	Thomas		R^2
C_0	Q		K_{Th}	q_0	
(mg/L)	(mL/min)	(mm)	(L/dmg)	(mg/g)	
3	6	0.15–0.3	0.36	5.20	0.9777
3	6	0.3–0.6	0.12	5.23	0.95876
3	6	0.6–1.18	0.22	5.62	0.97606
3	6	1.18–2.36	0.40	4.64	0.96834

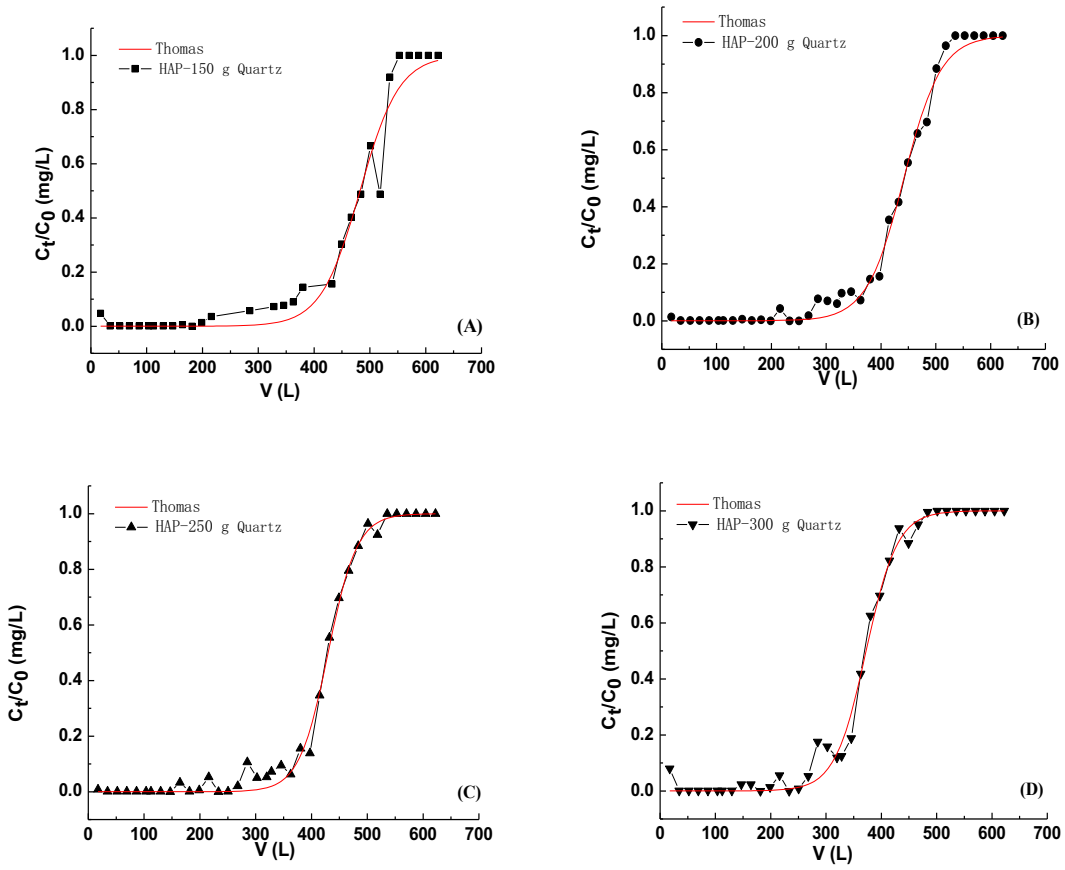


FIGURE 8
Effect of hydroxyapatite dosage on U(VI) removal by the dynamic PRB absorption column as per Thomas' model

TABLE 5
Parameters pertaining to hydroxyapatite dosage as per Thomas' model

Initial U(VI) concentration	Flow rate	Hydroxyapatite: quartz sand particle	Thomas		R^2
C_0	Q		K_{Th}	q_0	
(mg/L)	(mL/min)		(L/dmg)	(mg/g)	
3	6	0.0157	0.08	10.34	0.97083
3	6	0.0118	0.09	9.47	0.99310
3	6	0.0094	0.11	9.21	0.99398
3	6	0.0079	0.10	7.98	0.99196

quartz varies from 0.6–1.18 mm, the calculated maximal U(VI) absorption capacity is 5.62 mg/g, which is close to the measured adsorption capacity (6.26 mg/g).

(2) Effect of hydroxyapatite dosage on U(VI) removal due to the dynamic adsorption capacity of the composite material. Using equation 6, the plot for V versus Ct/C_0 is drawn (Fig. 8). The calcu-

lated parameters, k_{Th}, q_0, and other correlation coefficients, are presented in Table 5. The table shows that the correlation coefficient R^2 is greater than 0.971, and thus, Thomas' model can well describe the removal process of U(VI) by the dynamic PRB absorption column. For an initial U(VI) concentration of 3 mg/L and a flow rate of 6 mL/min, the adsorption capacity is 10.34 mg/g, 9.47 mg/g, 9.21 mg/g, and 7.98 mg/g when the ratio of quartz to hydroxyapatite is 0.0157, 0.0118, 0.0094, and 0.0079, respectively. The maximal U(VI) absorption capacity is obtained when the ratio of quartz to hydroxyapatite is 0.0157, and this value is close to the measured adsorption capacity (9.67 mg/g).

(3) Effect of flow rate on the removal of U(VI) by dynamic adsorption capacity of composite material. The curve of V versus Ct/C_0 was drew based on the formula 6, which is shown in Fig. 9. The calculate k_{Th}, q_0 and other correlation coefficients are summarized in Table 6. As shown in Table 6, the correlation coefficient R^2 value is greater than 0.972, which means the Thomas model can better describe the effect of velocity on the U(VI) removal by the PRB dynamic column. When the initial concentration of U(VI) is 3 mg/L, the flow rates were 3 mL/min, 6 mL/min and 9 mL/min, the corresponding maximum adsorption amount of U(VI) were 12.11 mg/g, 10.98 mg/g and 8.50 mg/g. When the flow rate was 3 mL/min, the maximum saturated adsorption capacity was 12.11 mg/g, which was close to the measured adsorption capacity (11.78 mg/g). Therefore, the effect of flow velocity on the performance of PRB dynamic column adsorption of U(VI) can be processed with Thomas model.

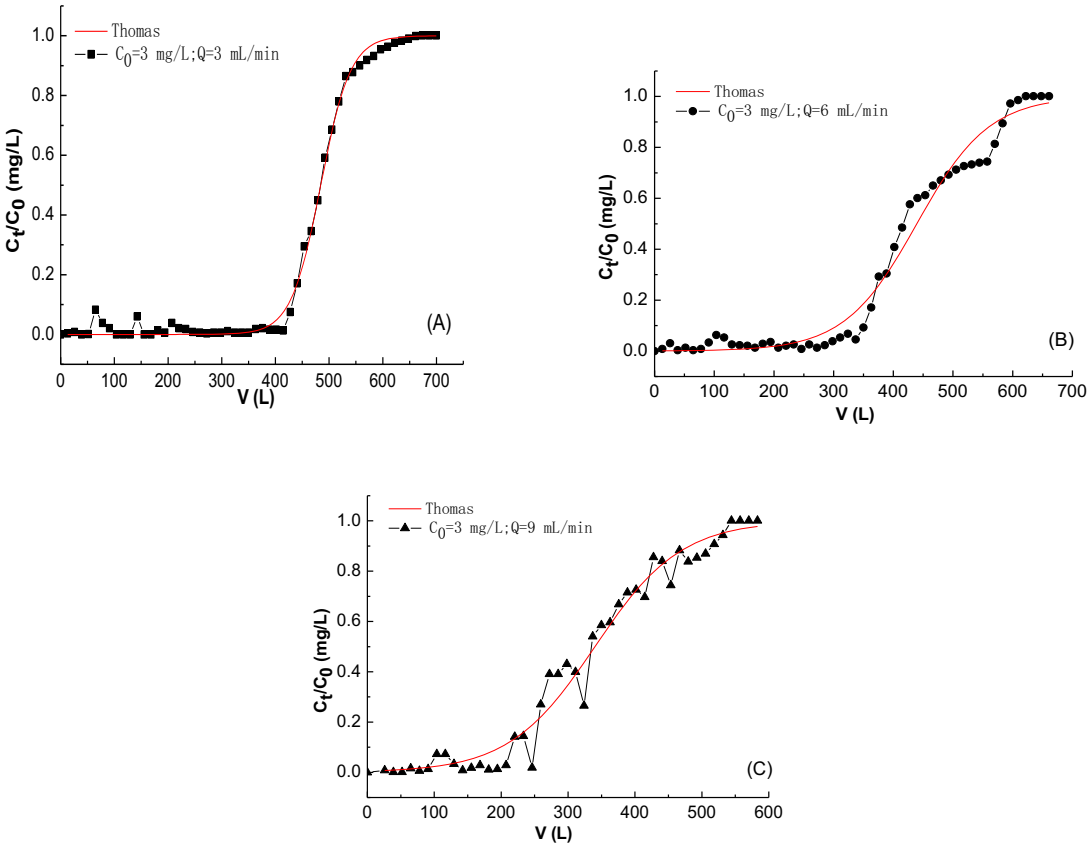


FIGURE 9
Effect of flow rate from Thomas model on the removal of U(VI) by dynamic PRB absorption column

TABLE 6
Parameters of flow from Thomas model on the curve of dynamic PRB absorption column used for U(VI) adsorption

Initial U(VI)concentration	Flow rate	Thomas		R^2
C_0	Q	K_{Th}	q_0	
(mg/L)	(mL/min)	(L/dmg)	(mg/g)	
3	3	0.05	12.11	0.99654
3	6	0.05	10.98	0.97869
3	9	0.08	8.50	0.9729

Analysis of the Yoon–Nelson model. Yoon and Nelson [19] jointly established an adsorption probability model, which is a semi-empirical gas adsorption model. This model is primarily based on the assumption that the rate of decrease in adsorption and the probability of adsorbate adsorption are proportional to the probability of adsorbent penetration. The advantages of this model are that it is simpler than other models and does not require detailed characterization data (such as adsorbent and fixed bed). By using this model, the time required to achieve the initial concentration can be calculated and the complete breakthrough curve can be predicted. The expression for the Yoon-Nelson model is:

$$\frac{C_t}{C_0} = \frac{1}{1+\frac{1}{\exp\left[k_{YN}\left(kt-\tau k\right)\right]}} \quad (7)$$

$$q_0 = \frac{C_0 Qt - \int_0^t CeQdt}{m} \quad (8)$$

where k_{YN} is the rate constant (min^{-1}); t is the breakthrough time of the PRB column used in this study (d); τ is the time required for 50% adsorbate breakthrough (d); C_0 is the initial concentration of the uranium solution (mg/L); C_t is the concentration of uranium in the outflow solution (mg/L); and Q is the flow rate (mL/min).

(1) The effect of quartz sand particle size on the adsorption of uranium (VI). According to equations 7 and 8, the curve of breakthrough time (t) versus C_t/C_0 was plotted (shown in Fig. 10). The calculated parameters (K_{YN}, τ, and q_0) and correlation coefficients are listed in Table 7. As shown in Table 7, all the correlation coefficients (R^2) are higher than 0.956. This suggests that the Yoon–Nelson model can describe the effect of quartz sand particle size on (VI) removal in the PRB dynamic column in a better manner. When the initial concentration of the U(VI) solution was 3 mg/L, the flow rate was 6 mL/min, and the quartz sand diameters were 0.15–0.3 mm, 0.3–0.6 mm, 0.6–1.18 mm, and 1.18–2.36 mm, the saturated adsorption capacities of the corresponding composite for uranium (VI) were 5.57 mg/g, 5.88 mg/g, 529 mg/g, and 5.02 mg/g, respectively. When the grain size of composite quartz sand was 0.3–0.6 mm, the maximum saturation adsorption capacity (5.88 mg/g), which is close to the measured adsorption capacity (6.14 mg/g), was achieved.

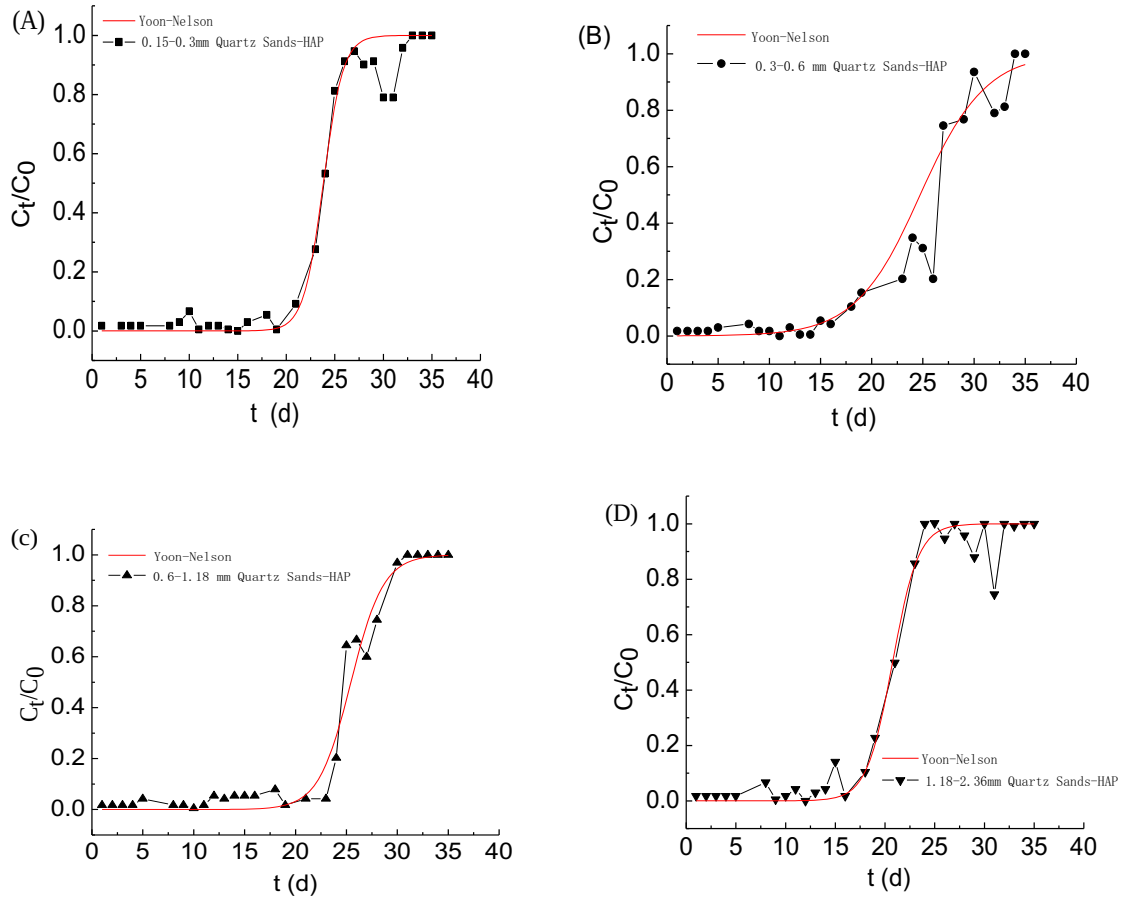


FIGURE 10
Effect of quartz sand particle size from the Yoon–Nelson model on the removal of U(VI) in the dynamic PRB absorption column

TABLE 7
Parameters of hydroxyapatite dosage from the Yoon–Nelson model on the curve of the dynamic PRB absorption column used for U(VI) adsorption

Initial concentration	Flow rate	Particle size	Yoon–Nelson model			R^2
C_0	Q		$K_{yn}\times10^{-4}$	τ	q_0	
(mg/L)	(mL/min)	(mm)	(min^{-1})	(d)	(mg/g)	
3	6	0.15–0.3	6.81	23.8	5.57	0.97648
3	6	0.3–0.6	2.48	24.0	5.88	0.95566
3	6	0.6–1.18	3.82	25.6	5.29	0.96688
3	6	1.18–2.36	5.36	20.8	5.02	0.97944

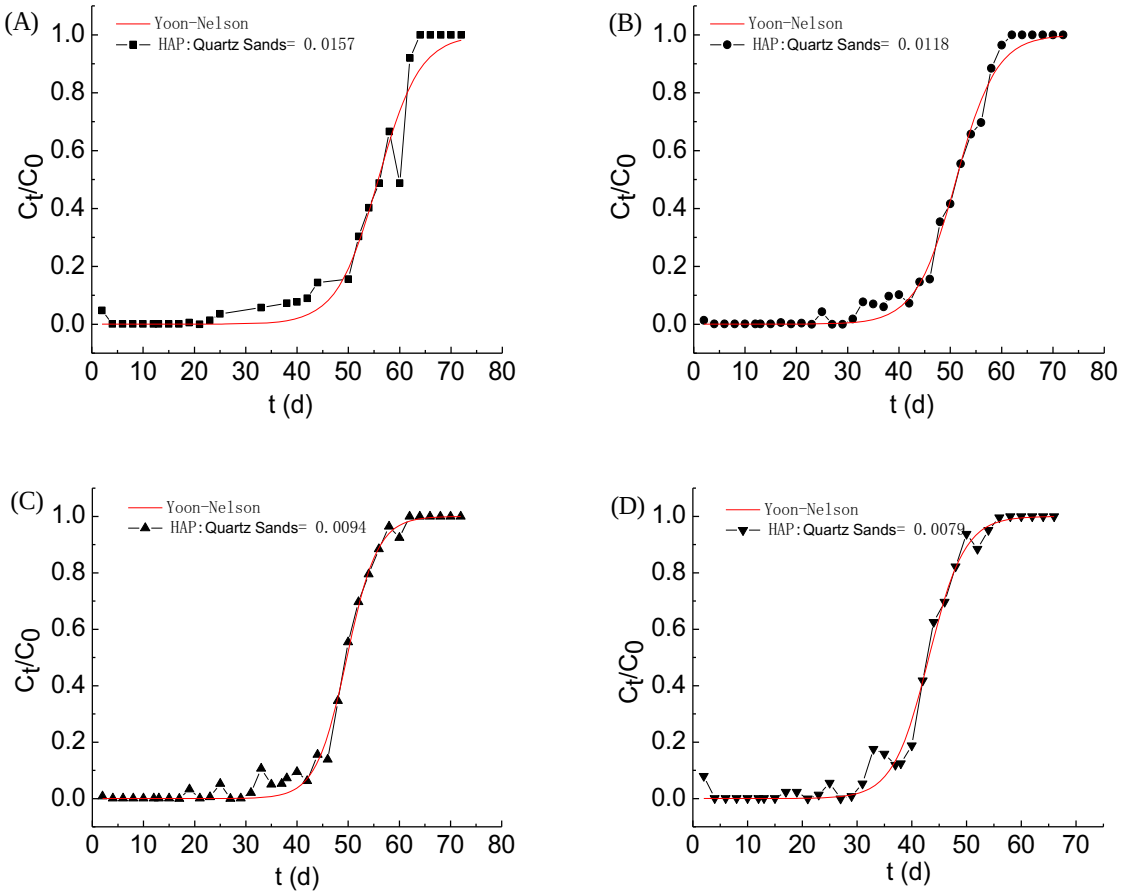


FIGURE 11
Effect of hydroxyapatite dosage from the Yoon–Nelson model on the removal of U(VI) in the dynamic PRB absorption column

TABLE 8
Parameters of hydroxyapatite dosage from the Yoon–Nelson model on the curve of the dynamic PRB absorption column used for U(VI) adsorption

Initial concentration	Flow rate	hydroxyapatite dosage	Yoon–Nelson model			R^2
C_0	Q		$K_{yn}\times10^{-4}$	τ	q_0	
(mg/L)	(mL/min)		(min^{-1})	(d)	(mg/g)	
3	6	0.0157	1.71	55.8	8.51	0.97083
3	6	0.0118	1.76	51.1	7.45	0.9931
3	6	0.0094	2.31	49.7	7.21	0.99398
3	6	0.0079	2.13	43.1	5.25	0.97042

(2) The effect of amount of coating in composite materials on the adsorption of uranium (VI). The curve of breakthrough time (t) versus Ct/C_0 was drawn according to equations 7 and 8 and is shown in Fig. 11. The calculated parameters (K_{YN}, τ, and q_0) and the correlation coefficients are listed in Table 8. As shown in Table 8, the correlation coefficients (R^2) were higher than 0.970. This indicates that the Yoon–Nelson model can describe the effect of hydroxyapatite coating amount on U(VI) removal in the PRB dynamic column in a better manner. When the initial concentration of the U(VI) solution

was 3 mg/L and the flow rate was 6 mL/min, the proportion of hydroxyl phosphorus limestone and quartz sand were 0.0157, 0.0118, 0.0094, and 0.0079 respectively. Furthermore, under these conditions, the saturated adsorption capacities of the corresponding composites for uranium (VI) were 8.51 mg/g, 7.45 mg/g, 7.21 mg/g, and 5.25 mg/g, respectively. When the ratio of hydroxyapatite to quartz sand was 0.0157, the highest saturated adsorption capacity was 8.51 mg/g, which is close to the measured adsorption capacity (9.67 mg/g).

(3) Effect of flow rate on the dynamic adsorption of U(VI). The curve of breakthrough time (t) versus C_t/C_0 was plotted according to equations 7 and 8 (shown in Fig. 12). The calculated parameters (K_{YN}, τ, and q_0) and correlation coefficients are listed in Table 9. As shown in Table 9, the correlation coefficients (R^2) were higher than 0.972, indicating that the Yoon–Nelson model can describe the flow behavior in the PRB dynamic column used for U(VI) removal. When the initial concentration of the U(VI) solution was 3 mg/L and the composite filling was consistent, the saturated adsorption capacities for uranium (VI) were 11.43 mg/g, 10.02 mg/g, and 7.92 mg/g at flow rates of 3 mL/min, 6 mL/min, and 9 mL/min, respectively. When the flow rate was 3 mL/min, the maximum saturated adsorption capacity was 11.43 mg/g. This value is close to the adsorption capacity (11.78 mg/g) obtained in the experiment.

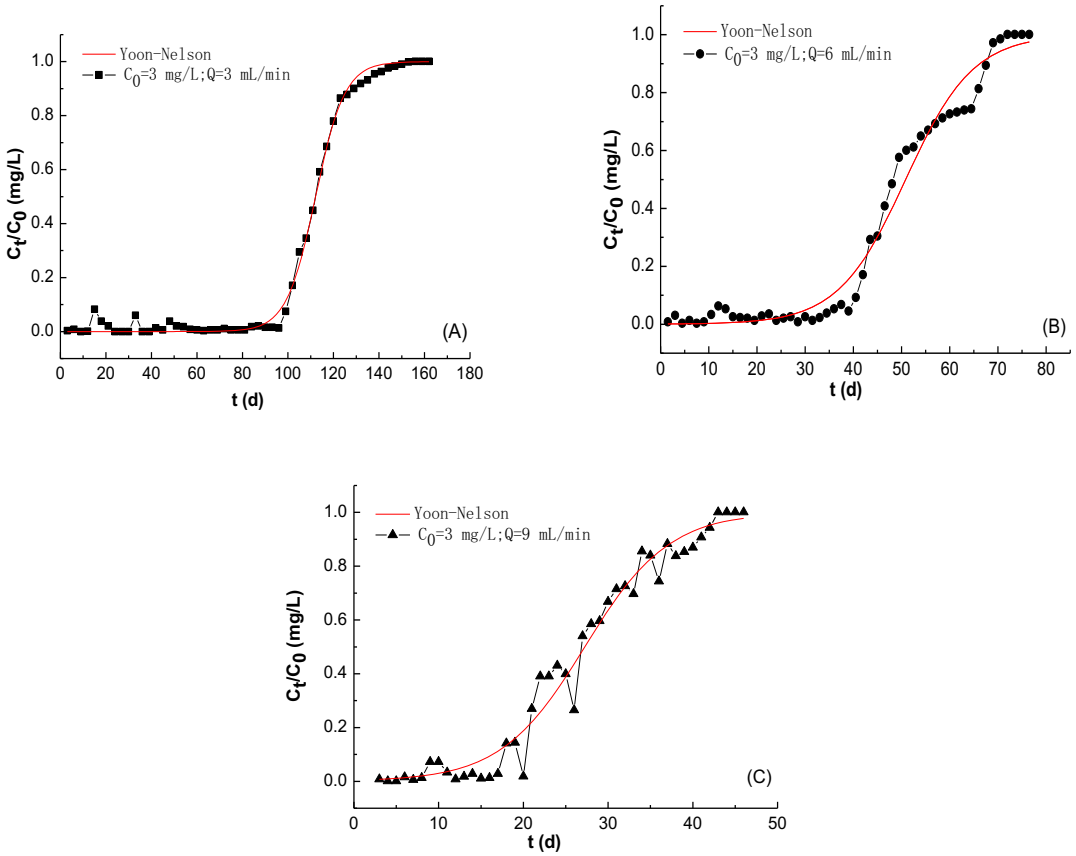


FIGURE 12
Effect of flow from the Yoon-Nelson model on the removal of U(VI) in the dynamic PRB absorption column

TABLE 9
Parameters of flow obtained from the Yoon–Nelson model on the curve of the dynamic PRB absorption column used for U(VI) adsorption

Initial concentration	Flow rate	Yoon–Nelson			R^2
C_0	Q	$K_{yn}\times10^{-4}$	τ	q_0	
(mg/L)	(mL/min)	(min^{-1})	(d)	(mg/g)	
3	3	1.0839	112.14	11.43	0.99654
3	6	0.992	50.86	10.02	0.97869
3	9	1.4027	27.25	7.92	0.9729

CONCLUSIONS

Through this research, we can draw the following conclusions:

(1) The particle size of quartz sand in the composite material significantly influenced its adsorption performance for U(VI) removal. The adsorption capacity of the composite materials increased initially and subsequently decreased with increase in quartz sand particle size. The maximum U(VI) adsorption capacity (6.26 mg/g) was achieved when the diameter of quartz sand was 0.6–1.18 mm. The saturated adsorption capacities calculated with the Thomas and Yoon–Nelson models were 5.62 and 5.88 mg/g respectively. Both these models are suitable for describing the influence of quartz sand diameter on the U(VI) removal efficiency in PRB dynamic experiments.

(2) It was observed that the amount of hydroxyapatite coating in the composite material influenced the dynamic adsorption of U(VI) significantly. As the amount of hydroxyapatite in the composites increased, their adsorption capacity also increased gradually. When the ratio of hydroxyapatite to quartz sand was 0.0157, the maximum adsorption capacity of the composite was 9.67 mg/g. The Thomas and Yoon–Nelson models can describe the influence of hydroxyapatite coating amount on U(VI) removal in the PRB dynamic column. Furthermore, the simulated adsorption capacity based on the above two models were 10.34 and 8.51 mg/g, respectively.

(3) The flow rate influences the dynamic adsorption performance of the materials for U(VI) removal significantly. As flow rate increased, the adsorption capacity of the composites decreased gradually. When the flow rate was 3 mL/min, the maximum adsorption capacity of the composite was up to 11.76 mg/g. The adsorption capacities obtained with the Thomas and Yoon–Nelson models were 12.11 and 1.143 mg/g, respectively, which are very close to measured results.

ACKNOWLEDGEMENTS

This work was supported by the National Natural Science Foundation of China (41562011), the Science Funds of the Education Office of Jiangxi, China (KJLD13054), the Natural Science Foundation of Jiangxi, China (20171BAB213019), State Key Laboratory Breeding Base of Nuclear Resources and Environment, East China University of Technology, China (Z201406) and International Atomic Energy Agency Coordinated Research Project (IAEA No. 21122).

REFERENCES

[1] Franklin, O.N., Jolanta, K.M., Grzegorz, M., Tomasz, K. (2015) Geochemical modelling for predicting the long-term performance of zeolite-PRB to treat lead contaminated groundwater. J. Contam. Hydrol. 177-178, 76-84.

[2] Huang, G., Liu, F., Yang, Y., Kong, X., Li, S., Zhang, Y. and Cao, D. (2015) Ammonium-nitrogen-contaminated groundwater remediation by a sequential three-zone permeable reactive barrier (multibarrier) with oxygen-releasing compound (ORC)/clinoptilolite/spongy iron: column studies. Environ. Sci. Pollut. Res. 22, 3705-3714.

[3] Su, H.C. (2012) The study on the modification of corn straw and its adsorption properties of six Cr ions. Shandong University, Jinan.

[4] Thomas, H.C. (1944) Heterogeneous ion exchange in a flowing system. J. Am. Chem. Soc. 66, 1466-1664.

[5] Ahmad, A.A. and Hameed, B.H. (2010) Fixed-bed adsorption of reactive azo dye onto granular activated carbon prepared from waste. J. Hazard. Mater. 175, 298-303.

[6] Baek, K.W., Song, S.H., Kang, S.H., Rhee, Y.W., Lee, C.S., Lee, B.J., Hudson, S., Hwang, T.S. (2007) Adsorption kinetics of boron by anion exchange resin in packed column bed. J. Ind. Eng. Chem. 13(3), 452-456.

[7] Bortone, I., Di Nardo, A., Di Natale, M., Erto, A., Musmarra, D. and Santonastaso, G.F. (2013) Remediation of an aquifer polluted with dissolved tetrachloroethylene by an array of wells filled with activated carbon. J. Hazard. Mater. 260, 914-920.

[8] Mumford, K.A., Rayner, J.L., Snape, I., Stark, S.C., Stevens, G.W. and Gore, D.B. (2013) Design, installation and preliminary testing of a permeable reactive barrier for diesel fuel remediation at Casey Station, Antarctica. Cold Reg. Sci. Technol. 96, 96-107.

[9] Obiri-Nyarko, F., Grajales-Mesa, S.J. and Malina, G. (2014) An overview of permeable reactive barriers for in situ sustainable groundwater remediation. Chemosphere. 111, 243-259.

[10] Liu, Y.Y., Mou, H.Y., Chen, L.Q., Mirzad, Z.A. and Liu, L. (2015) Cr(VI)-contaminated groundwater remediation with simulated permeable reactive barrier (PRB) filled with natural pyrite as reactive material: Environmental factors and effectiveness. J. Hazard. Mater. 298, 83-90.

[11] Fan, Z.L., Zha, H.P., Li, S., Qiao, H.H., (2013) Dynamic adsorption of copper and zinc cations on ethylenediamine-grafted silica gel. Chinese Journal of Applied Chemistry. 30(01), 93-98.

[12] Zhou, D., Li, Y., Zhang, Y., Zhang, C., Li, X., Chen, Z., Huang, J., Li, X., Flores, G. and Kamon, M. (2014) Column test-based optimization of the permeable reactive barrier (PRB) technique for remediating groundwater contaminated by landfill leachates. J. Contam. Hydrol. 168, 1-16.
[13] Kundu, S., Kavalakatt, S.S., Pal, A., Ghosh, S.K., Mandal, M., Pai, T. (2004) Removal of arsenic using hardened paste of Portland cement: batch adsorption and column study. Water Res. 38, 3780-3790.
[14] Han, R.P., Zou, L.N., Zhao, X., Xu, Y.F., Xu, F., Wang, Y. (2009) Characterization and properties of iron oxide-coated zeolite as adsorbent for removal of copper(II) from solution in fixed bed column. Chem. Eng. J. 149, 123-131.
[15] Aksu, Z., Gönen, F. (2004) Biosorption of phenol by immobilized activated sludge in a continuous packed bed: prediction of breakthrough curves. Process Biochem. 39, 599-613.
[16] Xianfeng, H., Xutao, Z. and Qingfang, Z. (2011) The study on the dynamic adsorption of Ni (II) by the clay of the concave and convex. Chemical and Biological Engineering. 28(6), 56-60.
[17] Fangwen, L., Xiaoai, W. and Zhongjian, S. (2009) The dynamic adsorption of methylene blue in water by iron coated porous ceramics. J. Environ. Eng. 3(3), 385-390.
[18] Zou, W., Zhao, L., Zhu, L. (2013) Adsorption of uranium(VI) by grapefruit peel in a fixed-bed column: experiments and prediction of breakthrough curves. J. Radioanal. Nucl. Chem. 295(1), 717-727.
[19] Yoon, Y.H., Nelson, J.H. (1984) Application of gas adsorption kinetics I. A theoretical model for respirator cartridge service life. Am. Ind. Hyg. Assoc. J. 45, 509-516.
[20] Baral, S.S., Das N., Ramulu, T.S., Sahoo, S.K., Das, S.N., Roy Chaudhury, G. (2009) Removal of Cr(VI) by thermally activated weed Salvinia cucullata in a fixed-bed column. J. Hazard. Mater. 161. 1427-1435.

Received: **09.01.2017**
Accepted: **10.02.2018**

CORRESPONDING AUTHOR

YaDan Guo
State Key Laboratory Breeding Base of
Nuclear Resources and Environment,
East China University of Technology,
418 Guanglan Road,
Nanchang, 330013 – P.R. China

e-mail: guoyadan88@163.com

© by PSP Volume 27 – No. 5/2018 pages 2717-2723 Fresenius Environmental Bulletin

DETERMINATION OF NATURAL RADIOACTIVITY LEVELS OF CONCRETE CORE AND CEMENTS IN ESKISEHIR AREA

Ugur Emre Temelli*

Istanbul University, Vocational School of Technical Sciences, Property Protection and Security Department, Civil Defense and Fire Fighting Program, 34320, Avcilar, Istanbul, Turkey

ABSTRACT

People spend large part of their daily lives inside the building where they are exposed to environmental factors—natural radioactivity. Cement is a building material of reinforced concrete structures; therefore, determination of the natural radiation level of cement is important for human health. Natural radio activity levels of raw material sources affect radioactivity level of cement which in turn affect the radioactivity level of concrete in structures. High amount of natural radioactivity can be expected in thorium-rich soils such as Eskisehir, Turkey.

In this study, fifteen concrete core samples from Eskisehir, and five cement samples collected from Bilecik-Eskisehir-Ankara area. The levels of natural radioactivity (^{226}Ra, ^{232}Th, and ^{40}K) were measured using gamma-ray spectrometry, and some of the radiological parameters were calculated. The mean activity concentrations of ^{226}Ra, ^{232}Th, and ^{40}K were 13.2, 15.4, and 212.6 Bq kg^{-1} in concrete core samples, and 30.6, 21.3, and 247.2 Bq kg^{-1} in cement, respectively. The mean radium equivalent activities (Ra_{eq}) were calculated as 54.5 and 80.2 Bq kg^{-1} for concrete and cement samples, respectively. All Ra_{eq} values in the studied samples were found to be lower than the criterion limit of 370 Bq kg^{-1}. The mean Representative Level Index (RLI) values of concrete and cement samples were lower than the upper limit for RLI but higher than worldwide mean values. According to RLI results, concrete and cement can be considered as non-harmful to human.

KEYWORDS:
Specific Radioactivity, Concrete, Cement, Eskisehir, Public Health

INTRODUCTION

Human are exposed to naturally occurring radioactivity emitted from radioactive nuclides. The radionuclides such as Potassium-40 (^{40}K), uranium-238 (^{238}U) and thorium-232 (^{232}Th) are always present in the Earth's crust. When building raw materials from such sources are used in construction, human beings are exposed to radioactivity [1]. The rate of radioactivity in the buildings depends on the activity concentrations of radionuclides in the construction materials, amount of used materials and the type of building [2].

Concrete and cement are important materials for the construction of buildings and they are used almost in all the residential buildings. Concrete is obtained by mixing cement, sand and water [3]. These concrete materials can have naturally occurring radionuclides whose activity concentrations depend on the location from where the raw materials were sourced. The emitted radioactivity from raw materials of concrete leads to some radiation exposure of inhabitants in the buildings. Depending on the level of radioactivity, some reverse effect can occur to living human beings in the buildings. Consequence, knowledge of radioactivity of some building materials such as concrete and cement is important for human safety. The criterion limit of radium equivalent is 370 Bq kg^{-1} in building materials as recommended by Nuclear Energy Agency [4]. Table 1 shows the recommended maximum levels of radium equivalents for building materials [5].

Eskisehir is located in the northwestern Turkey, Figure 1. According to the Population Registration System, 2013 of Turkey, Eskisehir population is 799,724 and is the twenty-fifth most populous city of Turkey [6]. Eskisehir, which is defined as the gateway to the west of Central Anatolia, is one of the well-developed city in addition to transportation convenience, energy facilities, suitable agricultural structure and rich mineral resources in Turkey. Recently, due to these factors, the rate of urbanization and the number of buildings built in Eskisehir are on constant rise.In this study, the activity concentrations of natural radionuclides of ^{226}Ra, ^{232}Th and ^{40}K, and radiological parameters were determined to assess the radiation risk associated with the concrete core from Eskisehir and cements samples around Eskisehir (Eskisehir, Bilecik, and Ankara), because of high amount of natural radioactivity expected in thorium-rich soils located in Eskisehir, Turkey.

TABLE 1
Recommended limits for building materials [5]

Ra_{eq}	(Bq kg^{-1})	Class	Recommendation
<370		1	Good for homes
370-740		2	Good for industries
740-2220		3	Good for roads and bridges
2220-3700		4	Good only for use in foundations of non-residential
>3700		5	Not to be used for construction of any type



FIGURE 1
Locations of concrete and cement sampling area in Turkey

MATERIALS AND METHODS

Sample collection and preparation. In this study, to measure the natural radioactivity levels of building concrete core and cement samples in Eskisehir, a total of 20 samples (15 concrete core, 5 cement) were collected from buildings in different parts of Eskisehir for concrete core, and local market in Eskisehir, Bilecik and Ankara cities for cement samples.

The concrete core samples were first pulverized, homogenized and sieved by a sieve of 2 mm grid mesh before measurement of activity concentration [7, 8]. Cement samples were used without any prior processing (such as pulverization, homogenization and sieving) because they were in a powder form. All concrete core and cement samples were dried in a temperature-controlled furnace at 110 ºC for 20-24 h until constant weight was obtained, ensuring complete removal of moisture from the samples. The weighted samples were kept in a plastic container of 250 cm^3, and hermetically sealed for 4 weeks. This process was done to ensure secular equilibrium of ^{238}U and ^{232}Th in the sample with their respective daughters [9]. The natural radioactivity levels of present radionuclide in the samples were measured using a gamma-ray spectrometry with a high purity Germanium (HPGe) detector [10]. All measurements were duplicated and presented data sets were given as calculated mean values.

Gamma spectrometry measurements. Gamma spectrometric measurements of the concrete core and cement samples were done using a high resolution HPGe (High Purity Germanium) detector. This detector was manufactured by Canberra Inc. and it has an active volume of 451 cm^3. Background gamma rays were shielded using the cylindrically shaped lead of 100 mm thick [11]. The back ground spectra were collected and for 20,000 seconds for each sample and the counts were subtracted from the respective region of interest [12]. The main obstacle to widespread use of detectors has been the non-linearity of its response to ionizing charged particles, therefore a detailed is necessary for the nuclear species to be detected over a whole energy range [13]. The energy calibration was done by measuring mixed standard sources with well-defined energies within the energy range of interest usually 200 keV to 3000 keV mixed gamma ray standard, which were obtained from International Atomic Agency in Vienna Australia. The 1460.8 keV gamma line was used to directly estimate ^{40}K, while 609.3 keV gamma line from 214Bi and 1764.5 KeV from 214Bi was used to determine ^{238}U activities and 583.19 keV from 208Tl was used to determine the activity of ^{232}Th [14]. The gamma spectroscopy was done by a computer based program, which matches gamma energies at various levels to a library of possible isotopes [15]. The activity concentration in Bq kg-1 (A) in the environmental samples was obtained as follows:

$$A = \frac{N_p}{e \times \eta \times m} \qquad (1)$$

where, Np is (cps) sample-(cps) background, e is the abundance of the γ-peak in a radionuclide, η is the measured efficiency for each gamma-ray peak observed for the same number of channels either for the sample or the calibration source and m is the sample mass in kilograms.

RESULTS AND DISCUSSION

Specific radioactivity concentrations of concrete core and cement samples. The activity concentrations and some radiological parameters of ^{226}Ra, ^{232}Th and ^{40}K in concrete and cement samples are shown in Table 2. According to Table 2, mean activity concentration of ^{226}Ra, ^{232}Th and ^{40}K were measured as 13.23, 15.41 and 212.63 Bqkg^{-1} for concrete samples and 30.68, 21.38 and 247.20 Bq kg^{-1} for cement samples, respectively. The mean concentration values of radionuclides in concrete and cement were found to be lower than the corresponding worldwide mean values, which are 35, 30 and 400 Bq kg^{-1}for ^{226}Ra, ^{232}Th and ^{40}K, respectively [14]. As given in table 2, the maximum specific activity values of ^{226}Ra, ^{232}Th and ^{40}K in concrete samples were measured as 25.00, 38.00 and 490.00 Bq kg^{-1} in CS06 sample, respectively. ^{232}Th and ^{40}K activity concentrations were measured higher than worldwide mean values. For cement samples, maximum activity values of ^{226}Ra, ^{232}Th and ^{40}K were 44.00 (CEM2), 32.00 (CEM1) and 340.00 (CEM1) Bq kg^{-1}, respectively. ^{226}Ra (CEM2) and ^{232}Th (CEM1) activity concentrations were found higher than worldwide mean values.

Radium equivalent activity. Radium equivalent activity (Ra_{eq}) for both concrete and cement was calculated using Equation 2. The radium activity is a very useful index commonly used to determine the total activities of ^{226}Ra. ^{232}Th and ^{40}K. The Ra_{eq} [16, 17].

$$Ra_{eq} = A_{Ra} + 1.43A_{Th} + 0.077A_K \quad (2)$$

where A_{Ra}, A_{Th} and A_K are the specific activities of ^{226}Ra, ^{232}Th and ^{40}K respectively, in Bq kg^{-1}. In the definition of the radium equivalent, it is assumed that 10 Bq kg^{-1} of ^{226}Ra, 7 Bq kg^{-1} of ^{232}Th and 130 Bq kg^{-1} of ^{40}K each produce an equal gamma-ray dose rate [18,19]. The calculated values of Ra_{eq} for concrete and cement samples are presented in Table 2. The mean radium equivalent activities were calculated as 54.57 and 80.29 Bqkg^{-1} for concrete and cement samples, respectively. All values of Ra_{eq} in the studied samples were found to be lower than the criterion limit of 370 Bq kg^{-1} [4]. The calculated radium equivalent values and some radiological index of some country of the world for concrete and cement samples are given in Table 3 and 4 [20]. The Ra_{eq} values that are presented in this study were found to be lower than the mean values of world country in Table 3 and 4.

TABLE 2
The activity concentrations and radiological parameters of concrete and cement samples

Sample ID	Activity concentration (Bq kg^{-1})			Ra_{eq} (Bq kg^{-1})	RLI (Bq kg^{-1})	Absorbed dose rate (D_R) (nGy h^{-1})	Annual effective dose rate (H_R) (mSv y^{-1})
	^{226}Ra	^{232}Th	^{40}K				
Concrete Sample							
CS01	12.4	15.9	305	58.62	0.45	53.30	0.07
CS02	6.8	9.6	109	28.92	0.21	25.54	0.03
CS03	6.8	8.7	82	25.56	0.19	22.39	0.03
CS04	14.05	18	273	60.81	0.46	54.57	0.07
CS06	25	38	490	117.07	0.87	104.00	0.13
CS07	21	21	193	65.89	0.48	57.86	0.07
CS08	15	13.9	290	57.21	0.43	52.29	0.06
CS09	10.2	16.6	319	58.50	0.45	53.16	0.07
CS10	24	27	278	84.02	0.62	74.02	0.09
CS11	3.7	5	34	13.47	0.10	11.62	0.01
CS12	20	20	250	67.85	0.50	60.40	0.07
CS13	17.5	15.1	137	49.64	0.36	43.67	0.05
CS14	12.2	12.1	336	55.38	0.43	51.41	0.06
CS15	2.3	2.8	17	7.61	0.05	6.56	0.01
CS16	18.5	20	272	68.04	0.50	60.78	0.07
Min	2.30	2.80	17.00	7.61	0.05	6.56	0.01
Mean	13.23	15.41	212.63	54.57	0.41	48.77	0.06
Max	25.00	38.00	490.00	117.07	0.87	104.00	0.13
SD	7.10	8.76	128.83	27.72	0.21	24.74	0.03
CV	0.51	0.54	0.57	0.51	0.51	0.51	0.51
Limit				370.00	1.00	84.00 (world average)	0.48 (world average)
Cement Sample							
CEM1	17.4	32	340	89.34	0.66	78.41	0.10
CEM2	44	12.3	142	72.52	0.51	65.37	0.08
CEM3	32	24	234	84.34	0.61	74.56	0.09
CEM4	30	20	266	79.08	0.58	70.88	0.09
CEM5	30	18.6	254	76.16	0.56	68.38	0.08
Min	17.40	12.30	142.00	72.52	0.51	65.37	0.08
Mean	30.68	21.38	247.20	80.29	0.58	71.52	0.09
Max	44.00	32.00	340.00	89.34	0.66	78.41	0.10
SD	9.44	7.28	71.16	6.66	0.06	5.12	0.01
CV	0.31	0.34	0.29	0.08	0.10	0.07	0.07
Limit				370.00	1.00	84.00 (world average)	0.48 (world average)

TABLE 3
The activity concentrations and radiological parameters of some country concrete [20]

Sample ID	Activity concentration (Bq kg^{-1})			Ra_{eq} (Bq kg^{-1})	RLI (Bq kg^{-1})	Absorbed dose rate (D_R) (nGy h^{-1})	Annual effective dose rate (H_R) (mSv y^{-1})
	^{226}Ra	^{232}Th	^{40}K				
Australia	15.00	41.00	200.00	89.03	0.32	74.90	0.09
Bangladesh	36.60	49.40	250.00	126.49	0.45	108.01	0.13
Brazil	21.90	25.3	42.00	61.31	0.21	51.34	0.06
Cuba	24.50	12.00	595.00	87.48	0.34	83.34	0.10
Czech Republic	21.10	17.40	404.00	77.09	0.29	70.87	0.09
Germany	30.00	23.00	450.00	97.54	0.37	88.90	0.11
Italy	22.00	16.00	237.00	63.13	0.23	56.80	0.07
Jordan	38.00	6.00	138.00	57.21	0.20	52.60	0.06
Lithuania	32.00	17.00	426.00	89.11	0.33	82.22	0.10
Malaysia	85.00	52.00	322.00	184.15	0.65	161.16	0.20
Netherlands	14.00	16.00	130.00	46.89	0.17	40.88	0.05
Norway	28.00	36.00	650.00	129.53	0.49	117.36	0.14
Pakistan	27.00	21.00	240.00	75.51	0.28	67.14	0.08
Rep. of Korea	26.40	39.10	596.00	128.21	0.48	114.98	0.14
Romania	69.00	77.00	918.00	249.80	0.92	221.62	0.27
Sweden	47.00	80.00	577.00	205.83	0.75	177.40	0.22
United States	27.00	11.00	350.00	69.68	0.26	64.94	0.08
Min	14.00	6.00	42.00	46.89	0.17	40.88	0.05
Mean	33.21	32.12	383.82	108.12	0.40	96.14	0.12
Max	85.00	80.00	918.00	249.80	0.92	221.62	0.27
SD	18.59	22.87	227.80	56.97	0.21	49.59	0.06
CV	0.56	0.71	0.59	0.53	0.52	0.52	0.52
Limit				370.00	1.00	84.00 (world average)	0.48 (world average)

TABLE 4
The activity concentrations and radiological parameters of some country cement [20, 21]

Sample ID	Activity concentration (Bq kg^{-1})			Ra_{eq} ((Bq kg^{-1})	RLI (Bq kg^{-1})	Absorbed dose rate (D_R) (nGy h^{-1})	Annual effective dose rate (H_R) (mSv y^{-1})
	^{226}Ra	^{232}Th	^{40}K				
Australia	51.80	48.10	114.70	129.41	0.45	109.74	0.13
Austria	26.70	14.20	210.00	63.18	0.23	56.98	0.07
Bangladesh	62.30	59.40	329.00	172.58	0.61	148.98	0.18
China	50.00	30.00	140.00	103.68	0.36	90.20	0.11
Cuba	22.80	10.60	467.00	73.92	0.28	70.00	0.09
Czech Republic	26.50	20.70	306.00	79.66	0.29	71.63	0.09
Finland	40.20	19.90	251.00	87.98	0.32	78.95	0.10
Germany	15.10	22.90	325.00	72.87	0.27	65.08	0.08
Italy	42.00	66.00	369.00	164.79	0.59	140.76	0.17
Jordan	43.21	11.23	265.12	79.68	0.29	73.32	0.09
Jordan	45.07	11.42	226.40	78.83	0.28	72.14	0.09
Jordan	49.10	13.47	111.91	76.98	0.27	68.94	0.08
Lithuania	31.00	13.00	172.00	62.83	0.23	56.58	0.07
Malaysia	81.40	59.20	303.50	189.43	0.67	164.29	0.20
Netherlands	27.00	19.00	230.00	71.88	0.26	64.14	0.08
Norway	29.60	18.50	259.00	76.00	0.28	68.30	0.08
Pakistan	36.50	28.10	214.90	93.23	0.33	81.68	0.10
Rep. of Korea	34.50	19.40	241.00	80.80	0.29	72.36	0.09
Romania	64.00	27.00	281.00	124.25	0.44	111.06	0.14
Spain	48.30	32.30	316.30	118.84	0.43	105.27	0.13
Sudan	16.60	13.20	107.20	43.73	0.16	38.37	0.05
Sudan	24.00	13.60	91.90	50.52	0.18	44.39	0.05
Sudan	19.50	12.30	101.10	44.87	0.16	39.56	0.05
Sudan	25.90	16.80	176.30	63.50	0.23	56.41	0.07
Sudan	19.80	10.60	90.60	41.93	0.15	37.12	0.05
Turkey	33.00	16.70	239.00	75.48	0.55	68.01	0.08
Min	15.10	10.60	90.60	41.93	0.15	37.12	0.05
Mean	37.15	24.14	228.42	89.26	0.33	79.01	0.10
Max	81.40	66.00	467.00	189.43	0.67	164.29	0.20
SD	16.20	16.18	96.05	39.05	0.14	33.13	0.04
CV	0.44	0.67	0.42	0.44	0.44	0.42	0.42
Limit				370.00	1.00	84.00 (world average)	0.48 (world average)

Indices and some radiological parameters of concrete and cement samples. The calculated Representative Level Index (RLI) and radiological parameters such as absorbed dose rate (D_R) and annual effective dose rate (H_R) are given in Table 2. The RLI which is used to estimate the level of gamma radioactivity associated with different concentration of certain specific radionuclides is determined with Eq. 3 [4, 22-24].

$$RLI = \frac{1}{150}A_{Ra} + \frac{1}{100}A_{Th} + \frac{1}{1500}A_K \quad (3)$$

where A_{Ra}, A_{Th}, and A_K are the average activity concentrations of ^{226}Ra, ^{232}Th, and ^{40}K, respectively. The mean values RLI for concrete and cement samples were 0.41 and 0.58 Bq kg^{-1}, respectively. The maximum RLI values were 0.87 Bq kg^{-1} (CS06) for concrete samples and 0.66 Bq kg^{-1} (CEM1) for cement samples. The mean RLI values of concrete and cement samples were lower than the upper limit for RLI but higher than worldwide mean values as shown in Table 3. The upper limit of RLI is 1 [24]—therefore, RLI results of these samples of concrete and cement are not harmful to humans.

For calculation of the absorbed dose rates in indoor air (D_R) and the corresponding annual effective doses (H_R) from ^{226}Ra, ^{232}Th, and ^{40}K in concrete and cement samples, formulas recommended by UNSCEAR [13] and the European Commission [24] were used. In the UNSCEAR [13] and EC reports, the dose conversion coefficients were calculated for the center of a standard room. The dimensions of this room were 4 m x 5 m x 2.8 m. The thickness of the walls, floors and ceiling and the density of the structure were 20 cm and 2350 kg m^{-3} (concrete), respectively. The D_R formula is given as Eq. 4;

$$D_R(nGy\ h^{-1}) = 0.92A_{Ra} + 1.1A_{Th} + 0.08\ A_K \quad (4)$$

where A_{Ra}, A_{Th}, and A_K are the specific activities of ^{226}Ra, ^{232}Th, and ^{40}K respectively, in Bq kg^{-1}. According to UNSCEAR, the external exposure rates from terrestrial gamma radiation of population-weighted average of global absorbed dose rate in air is 84.00 nGy h^{-1}. For D_R values comparison, this global average value was accepted as a reference in this study.

The effective dose rate is determined as follows:

$$H_R(mSv\ y^{-1}) = D_R \times 8766 \times 0.2 \times 0.7 \times 10^{-6} = D_R \times 0.00123 \quad (5)$$

where D_R(nGy h^{-1}) is stated by Eq. (4). The global mean value of H_R is 0.48 mSv y^{-1} which is taken from UNSCEAR [13] as a comparison limit.

Absorbed gamma dose rates (D_R) in the indoor air for concrete samples varies between 6.5 and 104.0 nGy h^{-1}. The mean value of D_R is 48.7nGyh^{-1}. Except for only one concrete sample (CS06), all of other concrete sample values remained lower compared to the global average of 84.00 nGy h^{-1}. On the other hand cement sample values were between 65.3 and 78.4 nGy h^{-1}; these results are lower than the reference value for D_R parameter.

Annual effective dose rate (H_R) values were between 0.01 and 0.13 mSv y^{-1} (mean is 0.06 mSv y^{-1}) for concrete samples, and 0.08 and 0.10 mSv y^{-1} (mean is 0.09 mSv y^{-1}) for cements samples. All of H_R values of for both concrete and cement samples are very low when they compared with global reference value.

CONCLUSIONS

The natural radionuclide content of the ^{226}Ra, ^{232}Th, and ^{40}K in concrete core samples from Eskisehir, and cement samples from around Eskisehir region in Turkey were evaluated in this study. All measurements were performed by gamma-ray spectroscopy method. The results of this study could be helpful about evaluation of the exposures and the radiation doses of the natural radioactive element ingredients in concrete core and cement in the related region, which is a thorium-rich territory.

The mean activity concentrations of ^{226}Ra, ^{232}Th, and ^{40}K were 13.2, 15.4, and 212.6 Bq kg^{-1} in concrete core samples, and 30.6, 21.3, and 247.2 Bq kg^{-1} in cement, respectively. The mean concentration values of radionuclides in concrete and cement were lower than the corresponding worldwide mean values, which are 35, 30 and 400 Bq kg^{-1}for ^{226}Ra, ^{232}Th, and ^{40}K, respectively. The maximum specific activity values of ^{226}Ra, ^{232}Th, and ^{40}K in concrete samples were measured as 25.00, 38.00 and 490.00 Bq kg^{-1} in CS06 sample, respectively. ^{232}Th, and ^{40}K activity concentrations were higher than worldwide mean values. For cement samples, maximum activity values of ^{226}Ra, ^{232}Th, and ^{40}K were found 44.00 (CEM2), 32.00 (CEM1) and 340.00 (CEM1) Bq kg^{-1}, respectively. ^{226}Ra (CEM2) and ^{232}Th (CEM1) activity concentrations were higher than worldwide mean values.

The mean radium equivalent activities were calculated as 54.5 and 80.2 Bq kg^{-1} for concrete and cement samples, respectively. All values of Ra_{eq} in the studied samples were lower than the criterion limit of 370 Bq kg^{-1}. This study clearly shows that Ra_{eq} values are lower than the mean values of world countries.

The mean values RLI for concrete and cement samples were 0.4 and 0.5 Bq kg^{-1}, respectively. The maximum RLI values were found to be 0.8 Bq kg^{-1} (CS06) for concrete samples and 0.6 Bq kg^{-1} (CEM1) for cement samples. The mean RLI values of concrete and cement samples were lower than the upper limit for RLI but higher than worldwide mean values. The upper limit of RLI is 1, thus Eskisehir's concrete and cement can be considered as non-harmful

to human beings.

Concrete absorbed gamma dose rates, D_R for indoor air for varied between 6.5 and 104.0 nGy h^{-1} with a mean value of 48.7 nGy h^{-1}. Except for only one concrete sample (CS06), all concrete samples values were lower compared to the global average of 84.00 nGy h^{-1}. On the other hand cement sample values were between 65.3 and 78.4 nGy h^{-1}, which are below the reference value for D_R parameter. Annual effective dose rate (H_R) values were between 0.01 and 0.13 mSv y^{-1} (mean is 0.06 mSv y^{-1}) for concrete samples, and 0.08 and 0.10 mSv y^{-1} (mean is 0.09 mSv y^{-1}) for cements samples. All of H_R values of for both concrete and cement samples are very low when compared with global reference value. Especially for a thorium-rich region, the results of the present study are valuable for evaluation of such site about radioactive pollution levels and comparison between concrete and cement relations concerning building material sources.

ACKNOWLEDGEMENTS

The researcher acknowledges TAEK, Cekmece Nuclear Research, and Training Center, Istanbul, Turkey for carrying out sample measurements.

REFERENCES

[1] Ademola, J.A. and Oguneletu, P.O. (2005) Radionuclide content of concrete building blocks and radiation dose rates in some dwellings in Ibadan, Nigeria. Journal of Environmental Radioactivity. 81, 107-113.

[2] Mustonen, R. (1985) Methods for evaluation of radiation from building materials. Radiation Protection Dosimetry. 7, 235-238.

[3] Farai, I.P. and Ademola, J.A. (2005) Radium equivalent activity concentrations in concrete building blocks in eight cities in Southwestern Nigeria. Journal of Environmental Radioactivity. 79, 119–125.

[4] NEA-OECD (1979) Exposure to radiation from natural radioactivity in building materials. Report by NEA group of Experts of the Nuclear Energy Agency OECD, Paris, France.

[5] Oresegun, M.O. and Babalola, A.I. (1988) Annual indoor dose burden estimates in dwellings built in Nigeria with radioactive U–Th rich tailings. Proceedings of an International Conference on Radiation Protection in Nuclear Energy, 2, 18–22 April 1988, IAEA, Vienna, Austria, 159–166.

[6] TUIK (Türkiye Istatistik Kurumu) (2014) Seçilmiş Göstergelerle Eskişehir 2013, Yayın No. 4212, ISSN 1307-0894. (in Turkish).

[7] Awodugba, A.O., Adelabu, J.S.A., Awodele, M.K. and Ishola, G.A. (2007) Material and the end product from West African Portland cement plc, Ewekoro, southwestern part of Nigeria. Indoor and Built Environment. 16, 569.

[8] Mollah, A.S., Ahmad, G.U., Hussain, S.R. and Rahman, M.M. (1986) The natural radioactivity of some building materials used in Bangladesh. Health Physics. 50, 849–851.

[9] Schotzing, V. and Debertin, K. (1983) Photon emission probabilities per decay of 226Ra and 232Th equilibrium with their daughter products. International Journal Applied Radiation Isotopes. 34, 533-538.

[10] Ajayi, O.S. and Ajayi, I.R. (1999) Survey of environmental gamma radiation levels of some areas of Ekiti and Ondo State, Southwestern part of Nigeria. Nigeria Journal of Physics. 11, 17-21.

[11] Islam, M.N., Alam, M.N., Mustafafa, M.N., Saddiqua, N., Miah, N.M.H., Chowdbury, M.I., Shah, S.H., Ali, L. and Roy, P.K. (1990) Characteristics of shielding arrangement for a HPGe detector designed and fabricated locally. Chittagong University Studies, part II. Science. 14(2), 105-111.

[12] Tchokossa, P. (2006) Radioactivity in food materials in Delta area and River State, Nigeria. PhD thesis. Obafemi Awolowo University, Ile Ife.

[13] United National Scientific Committee on the Effects of Atomic Radiation (UNSCEAR) (2000) Sources and Risks of Ionizing Radiation. Report to the General Assembly with annexes. New York, United Nations

[14] Ayinmode, B.O., Famakinwa, R.O. and Ajayi, J.O. (2012) Assessment of natural radioactivity in concrete block, extruded clay brick, and mud brick taken from Ogbomoso, Southwestern, Nigeria. Anadolu University Journal of Science and Technology –A 12(1), 23- 29.

[15] Krieger, R. (1981) Radioactivity of construction materials. Betonwerk Fertigteil Techn. 47, 468–473.

[16] Beretka, J. and Mathew, P.J. (1985) Natural radioactivity of Australian building materials, industrial wastes and by-product. Health Phys. 48, 87-95.

[17] Krisiuk, E.M., Tarasov, S.I., Shamov, V.P., Shlak, N.I., Lisachenko, E.P. and Gomslsky, L.G. (1971) A Study of Radioactivity in Building Materials. Research Institute of Radiation Hygeine Leningrad

[18] Stranden, E., (1976) Some aspects on radioactivity of building materials. Phys. Norv.

[19] United National Scientific Committee on the Effects of Atomic Radiation (UNSCEAR) (2010) Sources and Effects of Ionizing Radiation. 2008 Report to the General Assembly with annexes, New York, United Nations.

[20] Sam, A.K. and Abbas, N. (2001) Assessment of radioactivity and the associated hazards in local and imported cement types used in Sudan. Radiat. Prot. Dosim. 93(3), 275–277
[21] Altun, M., Sezgin, N., Nemlioglu, S., Karakelle, B., Can, N., Temelli, U.E. (2017) Natural radioactivity and hazard-level assessment of Portland cements in Turkey. J. Radioanal. Nucl. Chem. 314, 941–948
[22] Abbady, A.G.E. (2004) Estimation of radiation hazard indices from sedimentary rocks in Upper Egypt. Appl. Radiat. Isot. 60, 111–114.
[23] Alam, M.N., Chowdhury, M.I., Kamal, M., Ghose, S., Islam, M.N., Mustafa, M.N., Miah, M.M.H., and Ansary, M.M. (1999a) The ^{226}Ra, ^{232}Th and ^{40}K activates in beach sand minerals and beach soils of Cox's bazaar, Bangladesh. J. Environ. Radioact. 46, 243–250.
[24] EC (European Commission) (1999) Radiation Protection, 112- Radiological Protection Principles Concerning the Natural Radioactivity of Building Materials. Directorate-General Environment. Nuclear Safety and Civil Protection

Received: **06.04.2017**
Accepted: **09.02.2018**

CORRESPONDING AUTHOR

Ugur Emre Temelli
Istanbul University,
Vocational School of Technical Sciences,
Property Protection and Security Department,
Civil Defense and Fire Fighting Program,
34320, Avcilar, Istanbul – Turkey

e-mail: etemelli@istanbul.edu.tr

© by PSP Volume 27 – No. 5/2018 pages 2724-2734 Fresenius Environmental Bulletin

TRANSPOSON MUTAGENESIS AND CLONING ANALYSIS OF *MamZ* GENE IN *MAGNETOSPIRILLUM GRYPHISWALDENSE* MSR-1

Lei Zhou[1], Ruixue Guo[1], Sha Wu[1], Junjie Xu[1], Minghua Xiong[1], Ying Li[2], Feng Li[1,*], Guangli Wang

[1]College of Life Science, Huaibei Normal University, Huaibei, Anhui 235000, China
[2]State Key Laboratories for Agro-biotechnology and College of Biological Sciences, China Agricultural University, Beijing 100193, China

ABSTRACT

A magnetosome-deletion mutant strain of *Magnetospirillum gryphiswaldense* MSR-1, known as NM7, was obtained by means of a mini-Tn5 *lac Z2* transposon insertion in conjugation experiments. A 4642-bp fragment containing a mini-Tn5 *lac Z2* in NM7 was cloned through the sequential steps of digestion, self-ligation, and transformation, followed by complete sequencing. The results showed that this fragment contained two putative ORFs, designated ORF1 and ORF2, and the mini-Tn5 *lac Z2* was inserted into the ORF2 sequence encoding the MamZ protein by using the BLAST program in NCBI. Experiments and software analysis indicated that the MamZ protein might possess both the iron transport and ferric-ion reduction capabilities, both of which activities participate in magnetosomes biometabolism in *M. gryphiswaldense* MSR-1.

KEYWORDS:
Magnetospirillum gryphiswaldense, magnetosome biosynthesis, protein expression, functional analysis, major facilitator superfamily

INTRODUCTION

Magnetospirillum gryphiswaldense MSR-1 is a member of a widespread group of Gram-negative magnetotactic bacteria (MTB) exhibiting genetic polymorphisms. Most of these bacteria are obligate micro-aerobic motile prokaryotes that navigate along geomagnetic field lines and swim to a favorable habitat [1]. MTB cells usually contain intracellular, nanoscale, membrane-bound magnetic particles, termed "magnetosomes," that consist of iron oxide or iron sulfide crystals aligned in cytoplasmic chain-like structures. These magnetosomes are synthesized via a biomineralization process under precise genetic control and they direct bacterial movement toward micro-aerobic zones [2].

Several aspects of applied magnetosome biochemistry have been clarified, such as obtaining high chemical purity, crystal morphology and excellent immobilization [3-5]. The properties of these particles are of particular interest for biomagnetics and bionics. Although magnetosomes are important for theoretical research and have potential value in that area, they have not been widely applied for commercial purposes owing to the low level of magnetosome production during cell development.

Hence, in order to increase magnetosome production, it is necessary to clarify the function of related proteins or genes associated with magnetosome biosynthetic mechanisms [6-14]. The discovery of the magnetosome island (MAI), containing conserved genes for its production, has allowed for a broader examination of the evolution and conservation of magnetosome formation, including membrane biogenesis, iron uptake, magnetite biomineralization, and magnetosome chain regulation in magnetotactic bacteria. In order to obtain a large amount of mutants, classic transposon mutagenesis methods have been adopted for decades, in order to acquire target genes in cells. For example, a non-magnetic strain, NMA21, and two magnetosome-deletion mutants — all generated by mini-Tn5 transposon mutagenesis — demonstrated the relationship between the ORFs and magnetosome biosynthetic mechanisms [15-17]. Although some aspects of genes associated with magnetosome biosynthesis have been confirmed, detailed molecular analysis and discovery of their exact functions in magnetosome formation require further investigation [8-11].

In this study, the transposon insertion method was adopted to seek functional genes. A mutant strain of *M. gryphiswaldense* MSR-1, denoted "NM7," was isolated, and a complete fragment was cloned from the insertion site by mini-Tn5 *lac Z2* transponson mutagenesis. Experiments and sequence analysis showed that the MamZ protein may play a significant role in magnetosome formation in *M. gryphiswaldense* MSR-1.

MATERIALS AND METHODS

Strains and culture conditions. Herein, the strains and plasmids used are listed in Table 1. The growth medium (per liter) contained the following:

0.5 g K_2HPO_4, 0.6 g NH_4Cl, 0.1 g yeast extract, 2 mL sodium lactate, 0.1 g $MgSO_4 \cdot 7H_2O$, 0.05 g sodium thioglycolate, 5 mL mineral element solution and 100 μM ferric citrate. Each 100 mL infusion bottle contained a 10% inoculation in 45 mL of medium and was cultivated for 15 h at 120 rpm and 30 °C.

The non-magnetic mutant, NM7, was inoculated into selective medium, which had the same components as the growth medium but without ammonium chloride and yeast extract. In addition, sodium glutamate was used instead of sodium lactate and 5 μg / mL kanamycin was added.

Escherichia coli (*E. coli*) were cultured in Luria–Bertani (LB) medium overnight at 200 rpm and 37 °C. Additionally, the antibiotics, Kanamycin and Ampicillin were added to the medium in order to isolate resistant strains containing recombinant plasmids.

Conjugation of both M. gryphiswaldense MSR-1 and *E. coli* UQ3022. *M. gryphiswaldense* MSR-1 and *E. coli* UQ3022 were cultivated and harvested when they reached logarithmic phase. A 0.9-mL sample of *M. gryphiswaldense* MSR-1 and a 0.3-mL sample of *E. coli* UQ3022 were mixed in a 1.5-mL tube. The cells were then washed twice and resuspended with 50 μL selective medium after discarding the supernatant. The mixtures were spread on a sterilizing filter membrane attached to the solid selective medium for 10-h conjugation and sealed. Subsequently, the filter membrane was transferred to a 1.5-mL tube with 0.8 mL selective medium and shock blended. A 100-μL mixture of the solid selective medium containing 5 μg / mL kanamycin was aspirated for use in inoculation and in screening non-magnetic mutants, because *E. coli* UQ3022 cannot grow with glutamate as carbon source.

Screening for non-magnetic mutants in conjugants. Discrete colonies on solid selective medium were transferred to serum bottles containing 8 mL selective medium at 30 °C for 48 h. Cells positive for magnetism were detected by using a magnet attached to the infusion bottle. Any non-magnetic mutants selected by this procedure were observed with a transmission electron microscope (TEM) (Technai G2 F20, Tecnai Corp., Hillsboro, Oregon, USA) at 20 kV.

Isolation of the fragment flanking mini-Tn5 lac Z2 in mutant NM7. The genomic DNA of NM7 was extracted by a rapid bacterial genomic DNA isolation kit (Sangon Biotech Co., Shanghai, China) and digested with restriction endonuclease *Bam*HI, which has no restriction site within mini-Tn5 *lac Z2*. The digestion was performed in a 20-μL system that contained 2 μL genomic DNA, 2 μL buffer and 16 μL ddH_2O for 4 h at 35 °C. After digestion, 3–5 kb fragments were recovered by agarose gel electrophoresis. The fragments were then self-ligated and transformed into *E. coli* UQ3021, cultivated on solid LB medium containing 5 μg / mL kanamycin. When discrete colonies developed on the plate, the plasmids were extracted and sequenced using a pair of primers provided by Sangon Corporation: primer 1 (5´-AAC AAG CCA GGG ATG TAA CG-3´) and primer 2 (5´-CAG CAA CAC CTT CTT CAC GA-3´).

TABLE 1
Strains and plasmids utilized in this study

Strains / plasmids	Relevant genotype and description	Source
Strains		
M. gryphiswaldense MSR-1	Wild type	Provided by China Agricultural University
M. gryphiswaldense NM7	Non-magnetic mutant of *M. gryphiswaldense* MSR-1	This work Laboratory collection
E. coli DH 5α	The host for recombinant plasmid lacZα complement	Laboratory collection
E. coli BL21	The host for expression vectors	Laboratory collection
E. coli UQ3022	BW20767/pRL27; Km^r	Provided by China Agricultural University
E. coli UQ3021	DH5α/ λ pir	Provided by China Agricultural University
Plasmids		
pMD-18T	2.69 kb cloning and sequencing vector, Amp^r	TAKARA
pMD187	pMD18-T containing *MamZ* fragments at the sites of *Bam*H I, *Eco*R I, Amp^r	This work
pGEX-KG	Expression vector with the GST tag protein, pBR322 origin, Amp^r, $LacI^q$	Laboratory collection
pGEX1877	The vector pGEX-KG containing *MamZ* fragment, at the sites of *Bam*H I, *Eco*R I, Amp^r	This work
pRL27	Contains mini-Tn5 transposon（oriR6K）delivery vector; Km^r	Provided by China Agricultural University

Construction and expression of pGEX-KG 1877. In wild type *M. gryphiswaldense* MSR-1, the ORF2 fragment was amplified by PCR using a pair of specific primers: primer 1 (5´-TT GGA TCC ATG CCG AAG AGC GGT AAA-3´) and primer 2 (5´-TT GAA TTC TTA GCC GAT TCG CAG GGC-3´). The process was carried out as follows: (1) 95 °C for 5 min; (2) 30 cycles of 95 °C for 30 s, 45 °C for 30 s, and 72 °C for 90 s; and (3) 72 °C for 10 min. The amplified fragments were extracted and cloned into the pMD18-T easy vector to yield pMD187 for sequencing. Additionally, the two target fragments digested from pMD187 and pGEX-KG, were isolated and ligated together to construct the expression vector pGEX-KG 1877. Meanwhile, the recombinant plasmid pGEX-KG 1877 was transformed into *E. coli* BL21 and induced by Isopropyl β-D-1-thiogalactopyranoside (IPTG) for 2 h, 4 h, or 6 h to determine protein expression by polyacrylamide gel electrophoresis (SDS-PAGE).

Functional analysis for the proteins encoded by the ORFs. Whole cloning fragments and the proteins encoded by the ORFs were analyzed with DNAman and identified by using the BLAST program in NCBI. TMpred software was used to confirm the transmembrane domains of the whole proteins, and the ExPASy Server (http://www.expasy.org/resources) was used to analyze the protein hydrophobicity and to perform a tertiary structure simulation.

RESULTS

Screening conjugants for mutant strains. A non-magnetic mutant containing the mini-Tn5 *lac Z2* transposon was screened out from conjugants and designated as *M. gryphiswaldense* NM7. Magnetotaxis of NM7 in liquid medium was absent; it formed no black magnetic cell spot at the position of the magnet after 12 hours (Fig. 1), and NM7 cells contained no magnetosomes detectable by TEM (Fig. 2). These results demonstrate that the mini-Tn5 *lac Z2* might be interfering with processes related to magnetosome formation in MSR-1, thus leading to the absence of magnetosomes in NM7 cells.

Cloning and analysis of the whole cloning fragment. With the hypothesis that the absence of magnetotaxis in the non-magnetic mutant NM7 might be the result of the mini-Tn5 *lac Z2* transposon insertion, experiments were conducted to investigate the fragment related to the formation of magnetosomes. A 4642-bp fragment was obtained by recovering the NM7 genomic digestion fragments from 3 to 5 kb, which were self-ligated and transferred into UQ3021 as described above. Afterward, this 4642-bp fragment was analyzed using BLAST in NCBI, demonstrating that it consisted of two ORFs and that there was a 17-bp overlap between ORF1 and ORF2. The mini-Tn5 *lac Z2* was inserted into ORF2 between 2173 and 2174 bp (Fig. 3), which was registered at GenBank (Accession No. AM085146). The homology analysis indicated that this cloning fragment had high homology with *M. magneticum* AMB-1. The fragment had 85% identity with a 3.6-kb fragment containing the gene of the predicted cell division–related GTPase from *M. magneticum* AMB-1. Moreover, it had 81% identity with the approximately 800-bp fragment containing the predicted methyl-accepting chemotaxis protein from base-pairs 27 to 830.

Functional analysis of the proteins encoded by the ORFs. The proteins encoded by the ORFs were analyzed using the BLAST program in NCBI. Results showed that the protein encoded by ORF1 was similar to the MamE and Mams proteins from *M. gryphiswaldense* MSR-1. It exhibited 85% identity with the protein amb1017 from *M. magneticum* AMB-1 and 47% identity with MamX from the magnetite-containing magnetic vibrio. The amino acid sequence transcribed by ORF2 demonstrated that it was the MamZ protein controlled by the gene operon mamXY in the magnetosome island. The MamZ protein has 92% identity with the permease of the major facilitator superfamily (MFS) from *M. magneticum* AMB-1, 44% identity with MamH from *M. gryphiswaldense* MSR-1, and 40% identity with MamZ from *Magnetovibrio blakemorei*. Notably, all of these proteins belong to the major facilitator superfamily (MFS), a large family of transmembrane transporters that utilize electrochemical gradients to drive transport, or else, function as co-transporters.

Meanwhile, in an analysis for ferric reductase activity, the entire amino acid sequence transcribed by MamZ presented 45% identity with the ferric reductase transmembrane protein from *Burkholderia* sp. Y123 [18], 44% identity with the ferric reductase from *Comamonas testosterone* CNB-2 [19], 37% identity with the ferric reductase transmembrane subunit from *Candidatus koribacter versatilis* Ellin 345 [20], 41% identity with the ferric reductase domain-containing transmembrane protein from *Burkholderia* spp. CCGE1002 [21], 42% identity with the ferric reductase transmembrane protein from *Rubrivivax gelatinosus* IL 144 [22], and 42% identity with ferric reductase domain from *Ralstonia syzygii* R 24 [23]. However, when these ferric-reductase transmembrane proteins were compared with the relevant portion of the MamZ protein, high homology with the displayed proteins was observed (Fig. 4).

The ExPASy Server was used to analyze protein hydrophobicity and tertiary structure for MamZ. With respect to its structure as a transmembrane protein, the functionally important amino acids possessed strong hydrophobicity throughout the cell membrane (Fig. 5). Additionally, the Z-scores for

Cβinteraction (–6.72), all-atom interaction (–5.71), salvation (–6.21), and torsion (–5.16) indicated that the MamZ protein had a low QMEAN Z-score (–8.43), suggesting that it may be a membrane protein with transmembrane domains, as previously described (Fig. 6) [24].



FIGURE 1
Detection of the magnetotaxis of wild type MSR-1 and non-magnetic mutant NM7 by growth in liquid medium. The arrow shows the black magnetic cell spot coalesced by placement of a magnetic disk, which is absent in NM7.

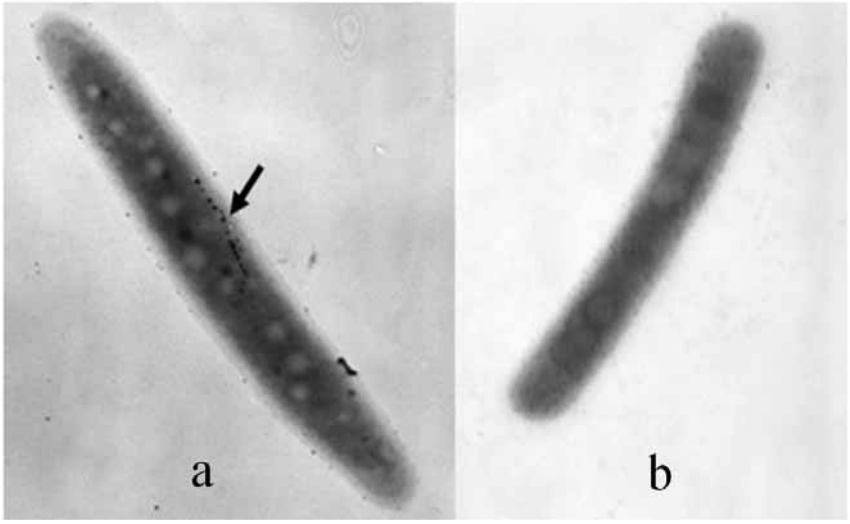


FIGURE 2
TEM images of the magnetosomes in MSR-1 and NM7 cells. (a) MSR-1; (b) NM7. The arrow indicates magnetosome position in MSR-1.

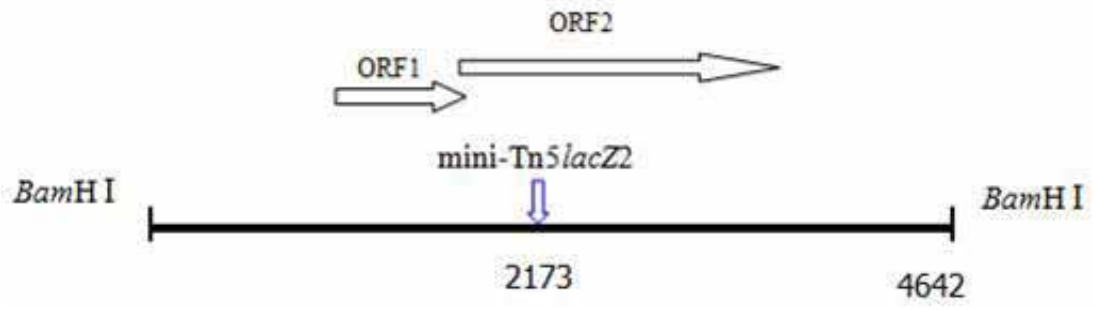


FIGURE 3
Arrangement of ORFs and location of the mini-Tn5 insertion site within the OFR-2 sequence of the 4642-bp fragment.

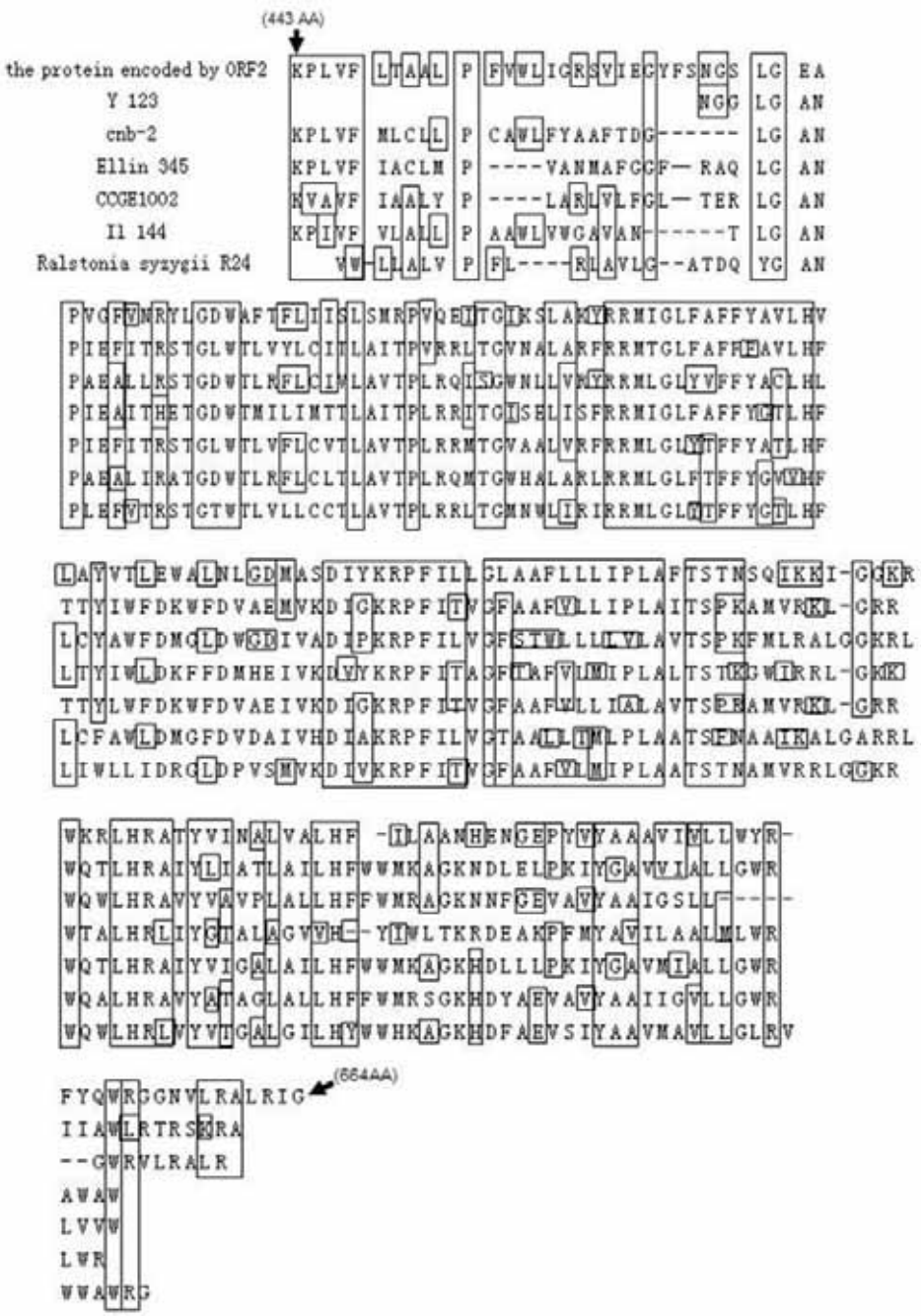


FIGURE 4
The amino acids from residue positions 433 to 644 of MamZ compared with other ferric reductases.

TMpred software and BLAST program were used to analyze the transmembrane domains of the MamZ protein. Results indicated that this protein contains seventeen transmembrane domains and three putative conserved domains as: CD06174, PRK05419 and COG2717. Zigzag fluctuation above and below zero degrees of the transmembrane domains indicated the helical structures of the MamZ protein shown in Fig. 7. Most transmembrane domains are embedded in the membrane, with especially the amino acids at the positions of approximately 220, 430 and 580, showing strong protrusion. The conserved CD06174 domain, belonging to the major facilitator superfamily (MFS) can transport substrates such as ions, sugar phosphates and amino acids into cells. Moreover, both the conserved COG2717 domain and the conserved PRK 05419 domain belong to the ferric reductase superfamily (FRS) that can reduce trivalent iron into divalent iron in *E. coli*. These predictions appear to indicate that the MamZ protein contains both iron transport and reduction capabilities relevant to the process of magnetosome biometabolism in *M. gryphiswaldense* MSR-1.

Expression of the MamZ protein in E. coli BL21. MamZ protein analysis with DNAStar software and the ExPASy Server showed that the molecular weight of the protein was approximately 70 kD and the projected isoelectric point occurred at approximately pH 9.6. For further analysis, the recombination plasmid pGEX-KG 1877 was introduced into *E. coli* BL21 and induced for 0, 2, 4, or 6 hours and subsequently assessed by PAGE. Fig. 8 shows that the induced proteins appeared at the 70 kD position, which gradually became darker over time. This darkening could indicate increased expression of the MamZ protein in cells. However, whether this phenomenon was caused specifically by the MamZ protein will need to be verified in future work.

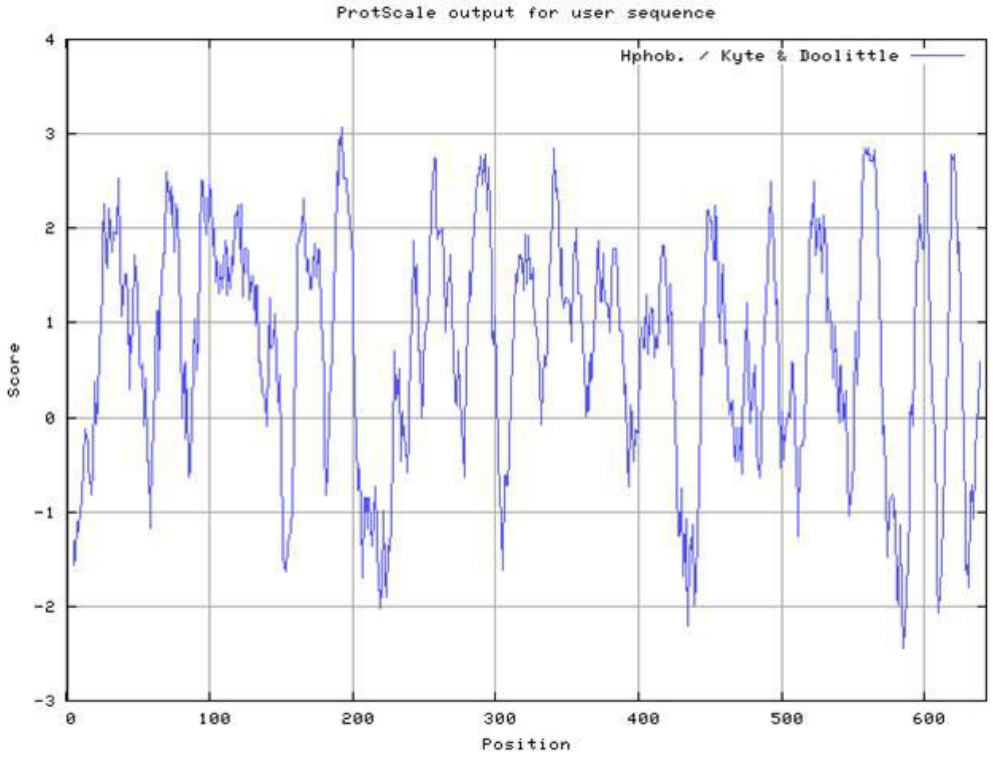


FIGURE 5
Hydrophobic analysis of the MamZ protein

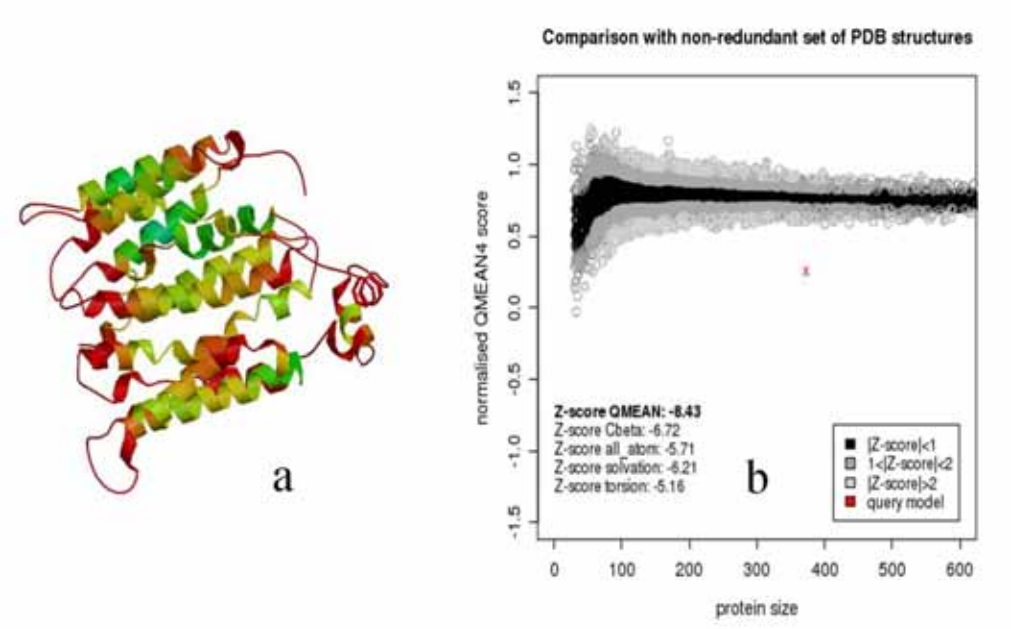


FIGURE 6
(a) the predicted three-dimensional structure simulation range from amino acid residues 58 to 430 of MamZ; (b) the QMEAN Z-scores of the MamZ protein.

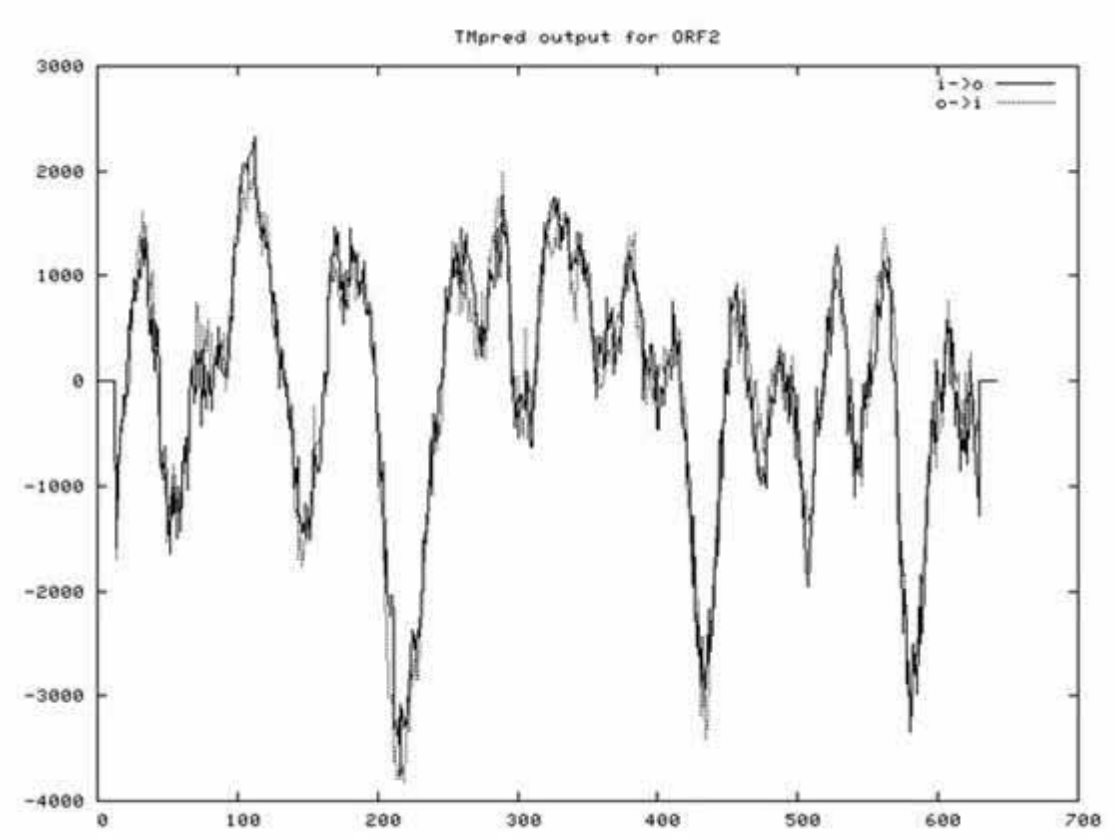


FIGURE 7
Transmembrane domains of the MamZ protein.

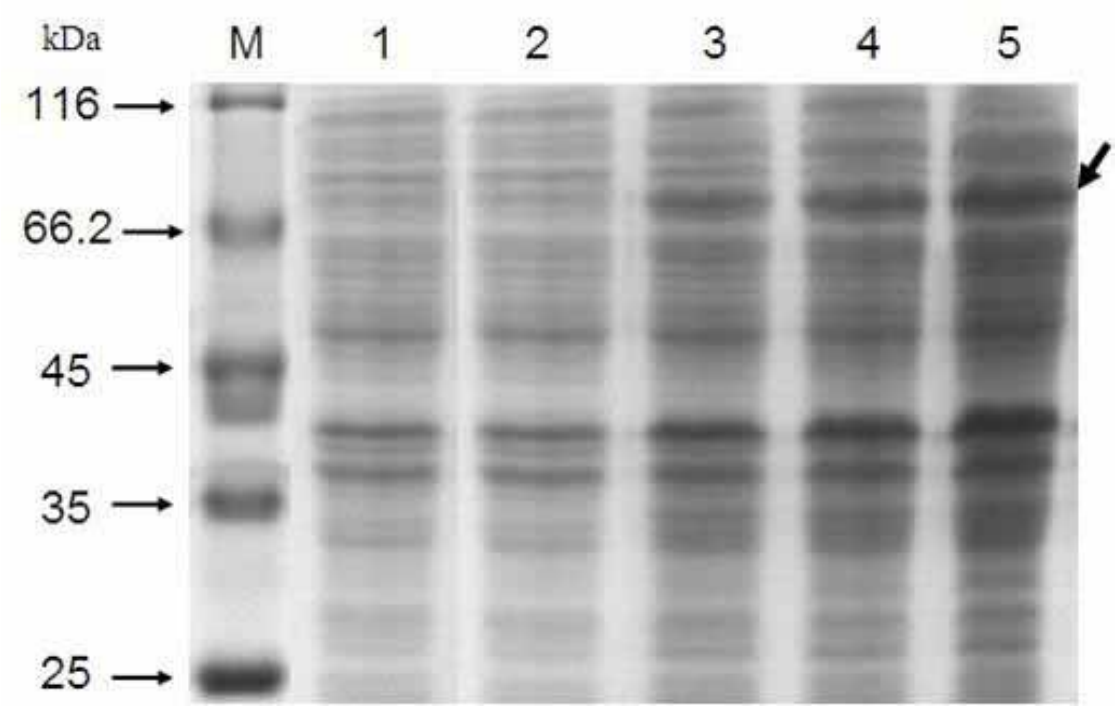


FIGURE 8
PAGE. Lane M : protein markers; Lane 1 : total protein in *E. coli* BL21 cells containing pGEX-KG prior to induction; Lane 2 : total protein in *E. coli* BL21 cells containing pGEX-KG 1877 prior to induction; Lanes 3-5 : the total protein in *E. coli* BL21 cells containing pGEX-KG 1877 induced by IPTG for 2, 4, or 6 hours, respectively. The arrow shows the position of protein expression at approximately 70 kDa.

DISCUSSION

The non-magnetic mutant, NM7 was screened out using a mini-Tn5 *lac Z2* transposon insertion in conjugation experiments, and the entire 4642-bp fragment sequences flanking mini-Tn5 in NM7 were cloned. The entire sequence contains two ORFs; the mini-Tn5 *lac Z2* was inserted into the ORF2 fragment encoding the MamZ protein. It appears that the MamZ protein may exhibit both transport and reducing activities relevant to magnetosome biosynthesis in *M. gryphiswaldense* MSR-1.

Analysis of the MamZ protein using NCBI program indicated that the protein contains the following three putative conserved domains: CD06174, COG2717 and PRK05419. The conserved domain CD06174 in GlpT belongs to the MFS, which comprises a large and diverse group of secondary transporters that facilitate transport of a variety of substrates such as ions, sugar phosphates, and amino acids across cytoplasmic or internal membranes [25]. In *E. coli*, glycerol-3-phosphate (G3P) plays a significant role in glycolysis and phospholipid biosynthesis. The secondary membrane transporter GlpT serves as an organic phosphate/inorganic phosphate antiporter that is involved in organic phosphate (G3P) uptake by exporting an inorganic phosphate out of the cytoplasm to complete the exchange of organic and inorganic phosphates [26-28]. Similarly, the MamZ protein may act as an antiporter that functions in ferric ion absorption via the uptake of organic iron (ferric citrate) into the cytoplasm. However, to confirm this functionality, evidence is still needed to clarify whether the system has the ability to export an inorganic ferric ion, as is the case in *E. coli*.

The conserved domains, COG2717 and PRK05419, belong to the ferric reductase family (FRS), members of which contain a common ferric reductase transmembrane component such as that found in both yeast and in the respiratory burst oxidase from mouse-ear cress. For example, the Frp1 protein, containing the conserved domain COG2717 from *Schizosaccharomyces pombe*, exhibits a ferric reductase component that is required for cell-surface ferric reductase activity, during ferric ion uptake that participates in electron transport from cytoplasmic NADPH to ferric ions. Additionally, the heme acts as an intermediate in trivalent iron reduction during this process [29]. Furthermore, the *frp1* mutants from *S. pombe* are deficient in ferric iron uptake, as described by Takegawa et al. [30]. Another transmembrane-spanning protein, YedZ, is anchored to the membrane by a heme-containing transmembrane subunit that contains the conserved domain PRK05419 in *E. coli* [31]. The results of this study indicate that some of the YedZ homologues encoded in magnetotactic bacteria could combine protein transporter and electron-transfer activities that exhibit the requisite conserved histidyl residues within their transmembrane domains, and which, therefore, might function in heme binding [32]. Because the MamZ protein contains both these conserved domains, we predict that the conserved domain of PRK05419 might have the ability to use heme binding as an auxiliary function to complete the reduction of ferric ions that interact with the conserved domain COG2717. Nevertheless, in *M. gryphiswaldense* MSR-1, extracellular ferric iron must first be reduced to the ferrous state during iron uptake. The MamZ protein is likely equipped with the abilities to transport ferric ions into cells and reduce them to the ferrous state directly through an electron transport chain to simultaneously complete both iron transport and reduction. Consequently, this should lead to a higher cellular free ferrous-ion concentration. However, to avoid ferrous-ion toxicity, the divalent metal ions are restricted to the membrane-bound magnetic particles through the efflux of ferric ion from the cytoplasm.

Bazylinski, DA *et al*. have proposed a model for the biosynthetic mechanism of magnetosome formation in MTB and have demonstrated that *M. gryphiswaldense* MSR-1 is able to transport ferric ions into the cytomembrane by siderophores, using the same mechanism as MV-1 or MS-1, and that the ferric irons might be reduced to the ferrous form during their transport [33]. For the magnetosome biosynthesis mechanisms in *M. gryphiswaldense* MSR-1, we hypothesized that two major methods of energy generation exist during this process. One could use oxygen as the electron acceptor and the other could alternatively use ferric ions, with both mechanisms either alternating or occurring simultaneously. When high ambient oxygen concentrations exist, *M. gryphiswaldense* MSR-1 usually uses oxygen as an electron acceptor to generate energy, but if ferric ions predominate, MSR-1 could switch to them as electron acceptors. Additionally, within a certain, possibly limited range of oxygen concentrations, the two possible mechanisms might co-exist simultaneously. However, in a micro-aerobic environment, the electrons were transferred to ferric acceptors by ferric reductases in an electron transport chain, and the generated ferrous ions would be transported into cells accompanied by liberation of energy [34, 35]. In this case, to acquire more energy, the concentration of ferrous ions was approximately 10- to 100-times higher in MSR-1 cells than in other non-magnetotactic bacteria [36, 37]. Due to the toxicity of the higher concentration of ferrous ions and the subsequent inhibition of ferric reductase activity, energy production can be lessened. Other studies indicate that magnetosome vesicles will be formed by cell membrane invagination in response to the pressure of a higher ferrous ion concentration [38, 39]. The excess ferrous ions were transported into magnetosome vesicles by transferrins, and formed magnetosomes by redox, hydration, and dehydration mecha-

nisms. As a result, the toxic ferrous ions were transformed into nontoxic magnetosomes, which could be used as an iron source or as an energy reserve. Notably, the process of ferrous-ion transfer is driven by concentration gradients eliminating the necessity for consumption of ATP or GTP. This mechanism might provide an explanation for the following three research findings: (1) why the low production of magnetosomes was associated with both the interruption of electron transfer by respiratory chain inhibitors and the inhibition of ferric reductase activity under a micro-aerobic condition [39, 40]; (2) why there is little effect on magnetosome biosynthesis when certain gene sequences of the ferrous transporter were knocked out [41]; and (3) why the utilization of ferric ions in MSR-1 is 70-times faster than in *E. coli* during magnetosome formation [39, 42-44]. These conditions illustrate that ferric ions act as electron acceptors during the process of electron transport in a micro-aerobic environment, thereby creating a high ferrous ion concentration, which leads to the coupling of magnetosome vesicle synthesis with the invagination of the cell membrane. Ultimately, magnetosomes were assembled when the ferrous ions were transferred into magnetosome vesicles by transferrins.

Additionally, the transmembrane-domain and hydrophobic analysis of the MamZ protein indicated that, throughout its structure, this protein might well be a transmembrane protein. And simultaneously, compared with other ferric reductases, MamZ has a high homology with genes associated with the ferric reductase process in biometabolism.

In conclusion, the MamZ protein may play a significant role in this metabolic pathway, in that it might be responsible for the transit of trivalent iron into cells coupled with ferric ion reduction, ultimately resulting in cell membrane invagination to form membrane-bound, nanoscale magnetic particles. We suspect that the MamZ protein may have both transporter and reductase functionalities during magnetosome biosynthesis.

Herein, the MamZ protein with a molecular weight of nearly 70 kD has reported, but there still need more inveatigation of this protein by western blotting as well as its complex crystal structure. In the further work, the protein will be purified with a GST tag in pGEX-KG and the precise structure will be explored with X-ray diffraction, which might provide more information on magnetosome particles biosynthetic mechanism in *M. gryphiswaldense* MSR-1.

ACKNOWLEDGEMENTS

This work was supported by grants from the Chinese National Natural Science Foundation (30940001), Provincial Natural Science Foundation of Anhui (1208085MC40), Key Foundation of Science and Technology of Huaibei City (070114), and the Innovation Team of Scientific Research Platform of Anhui Province, China. No. KJ2015TD001.

REFERENCES

[1] Blakemore, R. (1975) Magnetotactic bacteria. Science (New York, NY). 190(4212), 377-9.

[2] Bazylinski, D.A., Frankel, R.B. (2003) Biologically controlled mineralization in prokaryotes. In: Dove, P.M., DeYoreo, J.J., Weiner, S. (eds.) Reviews in Mineralogy and Geochemistry. Biomineralization. 54, 217-248.

[3] Sun, J., Jiang, W., Li, Y., Zhang, Y., Li, J. (2007) The magnetosomes of magnetotactic bacteria may be used as drug-carriers for targeted therapy. Microbiology-Beijing. 34(1), 165.

[4] Matsunaga, T.K.S. (1987) Use of magnetic particles isolated from magnetotactic bacteria for enzyme immobilization. Appl Microbiol Biotechnol. 26, 328-32.

[5] Tang, T., Zhang, L.F., Gao, R., Dai, Y.P., Meng, F.C., Li, Y. (2012) Fluorescence imaging and targeted distribution of bacterial magnetic particles in nude mice. Appl Microbiol Biotechnol. 94(2), 495-503.

[6] Kornig, A., Dong, J., Bennet, M., Widdrat, M., Andert, J., Muller, F.D., Schuler, D., Klumpp, S., Faivre, D. (2014) Probing the mechanical properties of magnetosome chains in living magnetotactic bacteria. Nano Lett. 14(8), 4653-9.

[7] Rahn-Lee, L., Byrne, M.E., Zhang, M., Le Sage, D., Glenn, D.R., Milbourne, T., Walsworth, R.L., Vali, H., Komeili, A. (2015) A genetic strategy for probing the functional diversity of magnetosome formation. PLoS Genet. 11(1), e1004811.

[8] Li, Y., Sabaty, M., Borg, S., Silva, K.T., Pignol, D., Schüler, D. (2014) The oxygen sensor MgFnr controls magnetite biomineralization by regulation of denitrification in Magnetospirillum gryphiswaldense. BMC Microbiol. 14(1), 153.

[9] Rawlings, A.E., Bramble, J.P., Walker, R., Bain, J., Galloway, J.M., Staniland, S.S. (2014) Self-assembled MmsF proteinosomes control magnetite nanoparticle formation in vitro. P Natl Acad Sci. 111(45), 16094-9.

[10] Raschdorf, O., Plitzko, J.M., Schüler, D., Müller, F.D. (2014) A tailored galK counterselection system for efficient markerless gene deletion and chromosomal tagging in Magnetospirillum gryphiswaldense. Appl Environ Microb. 80(14), 4323-30.

[11] Lohße, A., Borg, S., Raschdorf, O., Kolinko, I., Tompa, É., Pósfai, M., Faivre, D., Baumgartner, J., Schuler, D. (2014) Genetic dissection of the mamAB and mms6 operons reveals a gene set essential for magnetosome biogenesis in Magnetospirillum gryphiswaldense. J Bacteriol. 196(14), 2658-69.

[12] Kanetsuki, Y., Tanaka, T., Matsunaga, T., Yoshino, T. (2013) Enhanced heterologous protein display on bacterial magnetic particles using a lon protease gene deletion mutant in Magnetospirillum magneticum AMB-1. J Biosci Bioeng. 116(1), 65-70.

[13] Yoshino, T., Matsunaga, T. (2006) Efficient and stable display of functional proteins on bacterial magnetic particles using Mms13 as a novel anchor molecule. Appl Environ Microb. 72(1), 465-71.

[14] Raschdorf, O., Müller, F.D., Pósfai, M., Plitzko, J.M., Schüler, D. (2013) The magnetosome proteins MamX, MamZ and MamH are involved in redox control of magnetite biomineralization in Magnetospirillum gryphiswaldense. Mol Microbiol. 89(5), 872-86.

[15] Wahyudi, A.T., Takeyama, H., Okamura, Y., Fukuda, Y., Matsunaga, T. (2003) Characterization of aldehyde ferredoxin oxidoreductase gene defective mutant in Magnetospirillum magneticum AMB-1. Biochem Bioph Res Co. 303(1), 223-9.

[16] Li, F., Li, Y., Jiang, W., Wang, Z.F., Li, J.L. (2009) Cloning and functional analysis of the sequences flanking mini-Tn5 in the magnetosome-deleted mutant NM21 of Magnetospirillum gryphiswaldense MSR-1. Chinese Sci Bull. 54(9), 1522-8.

[17] Li, F., Li, Y., Jiang, W., Wang, Z.F., Li, J.L. (2005) Cloning and functional analysis of the sequences flanking mini-Tn5 in the magnetosomes deleted mutant NM4 of Magnetospirillum gryphiswaldense MSR-1. Sci China Life Sci. 48(6), 574-84.

[18] Lim, J.S., Choi, B.S., Choi, A.Y., Kim, K.D., Kim, D.I., Choi, I.Y., Ka, J.O. (2012) Complete Genome Sequence of the Fenitrothion-Degrading Burkholderia sp Strain YI23. J Bacteriol. 194(4), 896.

[19] Ma, Y.F., Zhang, Y., Zhang, J.Y., Chen, D.W., Zhu, Y.Q., Zheng, H.J., Wang, S.Y., Jiang, C.Y., Zhao, G.P., Liu, S.J. (2009) The Complete Genome of Comamonas testosteroni Reveals Its Genetic Adaptations to Changing Environments. Appl Environ Microb. 75(21), 6812-9.

[20] Ward, N.L., Challacombe, J.F., Janssen, P.H., Henrissat, B., Coutinho, P.M., Wu, M., Xie, G., Haft, D.H., Sait, M., Badger, J., Barabote, R.D., Bradley, B., Brettin, T.S., Brinkac, L.M., Bruce, D., Creasy, T., Daugherty, S.C., Davidsen, T.M., DeBoy, R.T., Detter, J.C., Dodson, R.J., Durkin, A.S., Ganapathy, A., Gwinn-Giglio, M., Han, C.S., Khouri, H., Kiss, H., Kothari, S.P., Madupu, R., Nelson, K.E., Nelson, W.C., Paulsen, I., Penn, K., Ren, Q., Rosovitz, M.J., Selengut, J.D., Shrivastava, S., Sullivan, S.A., Tapia, R., Thompson, L.S., Watkins, K.L., Yang, Q., Yu, C., Zafar, N., Zhou, L., Kuske, C.R. (2009) Three Genomes from the Phylum Acidobacteria Provide Insight into the Lifestyles of These Microorganisms in Soils. Appl Environ Microb. 75(7), 2046-56.

[21] Ormeno-Orrillo, E., Rogel, M.A., Chueire, L.M.O., Tiedje, J.M., Martinez-Romero, E., Hungria, M. (2012) Genome Sequences of Burkholderia sp Strains CCGE1002 and H160, Isolated from Legume Nodules in Mexico and Brazil. J Bacteriol. 194(24), 6927.

[22] Nagashima, S., Kamimura, A., Shimizu, T., Nakamura-Isaki, S., Aono, E., Sakamoto, K., Ichikawa, N., Nakazawa, H., Sekine, M., Yamazaki, S., Fujita, N., Shimada, K., Hanada, S., Nagashima, K.V. (2012) Complete Genome Sequence of Phototrophic Betaproteobacterium Rubrivivax gelatinosus IL144. J Bacteriol. 194(13), 3541-2.

[23] Remenant, B. (2011) Phylotype IV strains of Ralstonia solanacearum, R. syzygii and the blood disease bacterium form a single genomic species despite their divergent life-styles. PLoS One. 6, e24356.

[24] Benkert, P., Biasini, M., Schwede, T. (2011) Toward the estimation of the absolute quality of individual protein structure models. Bioinformatics. 27(3), 343-50.

[25] Law, C.J., Maloney, P.C., Wang, D.N. (2008) Ins and Outs of Major Facilitator Superfamily, Antiporters. Annu Rev Microbiol. 62, 289-305.

[26] Lemieux, M.J., Huang, Y.F., Wang, D.N. (2004) Glycerol-3-phosphate transporter of Escherichia coli: Structure, function and regulation. Res Microbiol. 155(8), 623-9.

[27] Elvin, C., Hardy, C., Rosenberg, H. (1985) Pi exchange mediated by the GlpT-dependent sn-glycerol-3-phosphate transport system in Escherichia coli. J Bacteriol. 161(3), 1054-8.

[28] Huang, Y., Lemieux, M.J., Song, J., Auer, M., Wang, D.-N. (2003) Structure and mechanism of the glycerol-3-phosphate transporter from Escherichia coli. Science. 301(5633), 616-20.

[29] Roman, D.G., Dancis, A., Anderson, G.J., Klausner, R.D. (1993) The fission yeast ferric reductase gene frp1+ is required for ferric iron uptake and encodes a protein that is homologous to the gp91-phox subunit of the human NADPH phagocyte oxidoreductase. Mol Cell Biol. 13(7), 4342-50.
[30] Takegawa, K., Iwaki, T., Fujita, Y., Morita, T., Hosomi, A., Tanaka, N. (2003) Vesicle-mediated protein transport pathways to the vacuole in Schizosaccharomyces pombe. Cell Struct Funct. 28(5), 399-417.
[31] Loschi, L., Brokx, S.J., Hills, T.L., Zhang, G., Bertero, M.G., Lovering, A.L., Weiner, J.H., Strynadka, N.C. (2004) Structural and biochemical identification of a novel bacterial oxidoreductase. J Biol Chem. 279(48), 50391-400.
[32] Von Rozycki, T., Yen, M.-R., Lende, E., Saier, Jr. M. (2003) The YedZ family: possible heme binding proteins that can be fused to transporters and electron carriers. J Mol Microb Biotech. 8(3), 129-40.
[33] Bazylinski, D.A., Frankel, R.B. (2004) Magnetosome formation in prokaryotes. Nat Rev Microbiol. 2(3), 217-30.
[34] Lesuisse, E., Casteras-Simon, M., Labbe, P. (1996) Evidence for the Saccharomyces cerevisiae ferrireductase system being a multicomponent electron transport chain. J Biol Chem. 271(23), 13578-83.
[35] Matsunaga, T., Okamura, Y., Fukuda, Y., Wahyudi, A.T., Murase, Y., Takeyama, H. (2005) Complete genome sequence of the facultative anaerobic magnetotactic bacterium Magnetospirillum sp. strain AMB-1. DNA Res. 12(3), 157-66.
[36] Blakemore, R., Maratea, D., Wolfe, R. (1979) Isolation and pure culture of a freshwater magnetic spirillum in chemically defined medium. J Bacteriol. 140(2), 720-9.
[37] Matzanke, B.F., Müller, G.I., Bill, E,. Trautwein, A.X. (1989) Iron metabolism of Escherichia coli studied by Mössbauer spectroscopy and biochemical methods. Eur J Biochem. 183(2), 371-9.
[38] Grass, G., Otto, M., Fricke, B., Haney, C.J., Rensing, C., Nies, D.H., Munkelt, D. (2005) FieF (YiiP) from Escherichia coli mediates decreased cellular accumulation of iron and relieves iron stress. Arch Microbiol. 183(1), 9-18.
[39] Schüler, D., Baeuerlein, E. (1996) Iron-limited growth and kinetics of iron uptake in Magnetospirillum gryphiswaldense. Arch Microbiol. 166(5), 301-7.
[40] Liu, J., Ding, Y., Jiang, W., Tian, J., Li, Y., Li, J. (2008) A mutation upstream of an ATPase gene significantly increases magnetosome production in Magnetospirillum gryphiswaldense. Appl Microbiol Biot. 81(3), 551-8.
[41] Rong, C., Huang, Y., Zhang, W., Jiang, W., Li, Y., Li, J. (2008) Ferrous iron transport protein B gene (feoB1) plays an accessory role in magnetosome formation in Magnetospirillum gryphiswaldense strain MSR-1. Res Microbiol. 159(7), 530-6.
[42] Frost, G., Rosenberg, H. (1973) The inducible citrate-dependent iron transport system in Escherichia coli K12. BBA-Mol Basis Dis. 330(1), 90-101.
[43] Hancock R.W., Hantke, K. and Braun, V. (1977) Iron transport in Escherichia coli K-12. 2, 3-Dihydroxybenzoate-promoted iron uptake. Arch Microbiol. 114, 231-9.
[44] Winkelmann, G. (1991) Specificity of iron transport in bacteria and fungi. In: Winkelmann, G. (ed.) CRC Handbook of microbial iron chelates. Boca Raton: CRC Press, 366.

Received: **25.04.2017**
Accepted: **28.12.2017**

CORRESPONDING AUTHOR

Feng Li
College of Life Sciences,
Huaibei Normal University,
235000, Huaibei – China

e-mail: rx2500@163.com

© by PSP Volume 27 – No. 5/2018 pages 2735-2742 Fresenius Environmental Bulletin

PROGRESS IN THE BIODEGRADATION OF CHLORONICOTINYL INSECTICIDE ACETAMIPRID

Qianqian Yang[2], Yiran Wang[1], Guangli Wang[1,*], Feng Li[1]

[1]College of Life Science, Huaibei Normal University, Huaibei, Anhui 235000, China
[2]College of Chemistry and Materials Science, Huaibei Normal University, Huaibei, Anhui 235000, China

ABSTRACT

A member of the neonicotinoid class of systematic broad-spectrum insecticides, Acetamiprid (ACE) has been extensively used in agriculture, and because of its massive application, adverse effects on ecology and the environment have also been increasing. These effects include the contamination of water and soil and the disruption of biogeochemical cycles, and their impact has led to an increasing trend toward research involving available microbial methods for ACE degradation. This review summarizes progress in research on microbiological degradation of ACE, including organisms capable of degrading ACE, pathways for ACE biodegradation, ACE's behavior in soil, and the effect of environmental conditions on soil ACE degradation, as well as the prospects for ACE elimination. In addition, we review a broader spectrum of knowledge regarding the biodegradation of ACE, and we attempt to place this information into context with the most recent and sometimes surprising research results.

KEYWORDS:
Biodegradation, Acetamiprid, Soil, Neonicotinoid Insecticide

INTRODUCTION

Acetamiprid(ACE),((E)-N1-[(6-chloro-3-pyridyl)methyl]-N2-cyano-N1-methylacetamidine), a member of the group of chloropyridinyl neonicotinoids, has been considered to be a favorable choice for controlling insects, given its activity against numerous sucking and biting insect pests, including aphids, whiteflies, thrips, leaf miners, beetles, some lepidopteran species [1], and fleas on dogs and cats [2, 3]. As a neonicotinoid insecticide, ACE acts as an agonist at the nicotinic acetylcholine (Ach) receptors of insects' central nervous system synapses, but at high levels that accumulate at nicotinic synapses-and similarly to over-accumulation of Ach at such synapses-blocks neurotransmission, thus interfering with stimulus conduction, leading to obstruction of nervous system pathways and to insect paralysis and eventual death.

On the basis of the advantages of ACE—including high selectivity, perceived relative environmental safety, and efficient inhibition in sucking and biting pest insects—it is widely used in agriculture, worldwide. However, this extensive application of such neonicotinoids has provoked a major problem, that is, their exertion of extreme toxic effects on non-target economical insects such as honeybees and silkworms [4], the acute sublethal treatment of ACE on the behavior of the honeybee (Apis mellifera)was studied and indicated ACE could affected physiology or behavior of honeybee through locomotor activity, sucrose gustatory sensitivity, water responsiveness, and olfactory learning and memory[5]. Furthermore, the accumulation of ACE in soil can also result in serious concerns about inhibition of soil respiration and phosphatase activity [6]. Moreover, in recent years, ACE residues in crops are receiving considerable attention with respect to their potential toxicity to humans [7, 8], with the publication of reports regarding headaches, dizziness, nausea, vomiting, and other symptoms after the inhalation of ACE as a pesticide [9-11]. These reports have promoted active investigations into methods for the biotransformation of neonicotinoids, particularly because ACE remains stable, even under submerged conditions, and is not affected by field capacity nor levels of submerged moisture. Bioremediation of ACE pollution is therefore recognized as a cost-effective and reliable method of removal. More generally, microbial degradation is considered to be an efficient "green" solution for eliminating environmentally polluting chemicals [12, 13]. Therefore, it is essential to study the microbiological degradation of ACE, both in terms of its biology and its application to environmental remediation.

This review presents an overview of recent advances in the microbiological degradation of ACE through pure culture microorganisms, as well as pathways for the degradation of ACE, behavior of ACE in soil, effects of environmental conditions on the degradation of ACE in soil, and research into prospects for the bioremediation of ACE-contaminated ecosystems.

Organisms capable of degrading ACE. In recent years, ACE residues in crops have been

receiving considerable attention due to their potential toxicity to humans. There are, of course, many research reports describing the metabolism of ACE, and a number of microorganisms capable of degrading neonicotinoids have been identified. For example, one previous study examined the elimination of ACE from a liquid medium by the white-rot fungus *Phanerochaete sordida* YK-624 [10] and reported that, after 15 days of incubation, 45% and 30% of ACE was eliminated under ligninolytic and non-ligninolytic conditions, respectively. In addition, the bacteria *Stenotrophomonas maltophilia* CGMCC 1.1788 and *Rhizopus* sp. have also been reported to metabolize ACE via N-demethylation to IM 2-1 [9-11]. Further, the bacteria *Pigmentiphaga* sp. ACE-1, *Pseudoxanthomonas* sp. ACE-7, *Ochrobactrum* sp. D-2, D-12, *Rhodococcus* sp. BCH2, and *Stenotrophomonas* sp. THZ-XP, and the yeast *Rhodotorula mucilaginosa* IM-2 metabolize ACE via the proposed N-deacetylation, C-demethylation, or oxidative cleavage of the N-cyanoimine group to IM-1-4, which is further metabolized by *Rhodococcus* sp. BCH2 to IC-0 or by *R. mucilaginosa* IM-2, *Rhodotorula mucilaginosa* R1 and *Pigmentiphaga* sp. D-2 to IM1-3 [14]. In addition, it is notable that a new functional strain, AC, reformed through protoplast fusion of *Pseudomonas* sp. CTN(chlorothalonil)-4 and *Pigmentiphaga* sp.strain AAP-1, could synchronously enhance the degradation efficiency of ACE and CTN [15]. Moreover, beyond the aforementioned organisms, there are also some other strains that can bio-transform ACE; are shown in the following table (Table 1).

Metabolic Pathways of ACE Biodegradation in Microorganisms. Many studies of the metabolites of the microorganisms in table 1 have been performed to verify the environmental fate of ACE, and a variety of analytical techniques have been applied for analyzing its biodegradation based on distinct properties of metabolites, such as the UV-Vis absorption spectra, Thin layer chromatography (TLC) analyses, High Performance Liquid Chromatography (HPLC), Liquid Chromatography-Mass Spectrometry (LC-MS) for IM1-4, Gas Chromatography-Mass Spectrometer (GC-MS), Nuclear Magnetic Resonance (NMR) Spectra, FTIR spectrum, High-resolution electro spray ionization mass spectra (HR-ESI-MS) and so on. Consequently, about five main types of ACE metabolites have been detected and identified during ACE biotransformation by pure culture strains or soil microbial consortia. This, in turn, led to the elaboration, in many of the studies, of various ACE-degradation pathways.

TABLE 1
Summary of microorganisms capable of biodegrading ACE

Microorganisms	Metabolic product	Phylogenetic group	Reference
Pseudomonas sp. strain FH2	ND	γ-Proteobacteria	[6]
Rhodotorula mucilaginosa strain IM-2	IM1-3, IM1-4	Urediniomycetes	[11]
Stenotrophomonas maltophilia CGMCC 1.1788	IM2-1	γ-Proteobacteria	[9]
Pigmentiphaga sp. strain AAP-1	IM1-4	β-Proteobacteria	[16]
Pichia guilliermondii W1	ND	Saccharomycetes	[11]
Rhizopus sp.	IM2-1, IM1-3, IM1-4, IM2-3	Mucormycotina	[11]
Phanerochaete sordida YK-624	IM2-1	Agaricomycetes	[10]
Stenotrophomonas sp. THZ-XP	IM1-4	γ-Proteobacteria	[17]
Rhodotorula mucilaginosa R1	IM1-3	Urediniomycetes	[10]
penicillium sp. X1	ND	Eurotiomycetes	[11]
Rhodococcus sp. BCH2	IM1-4 and IC 0	Actinobacteria	[4]
Pseudoxanthomonas sp. AAP-7	IM1-4	γ-Proteobacteria	[18]
Pigmentiphaga sp. D-2	IM 1-3 and IM1-4	β-Proteobacteria	[19]
Ochrobactrum sp. D-12	IM1-4	α-Proteobacteria	[20]
Ensifer meliloti CGMCC 7333	IM1-2, IM1-4	α-Proteobacteria	[14]
Fusant-AC	ND		[15]

i. ACE served as both carbon and energy source during ACE biodegradation.
ii. The abbreviations listed under the "Metabolic product" column of the table are the same as those referred to in figure 1; ND = not determined.

The metabolic pathway for ACE degradation has been studied in apple, cabbage, carrots, cotton, honeybee, mice, spinach, and soil bacteria [21, 22]. There are five main metabolic pathways to biodegrade ACE. First, we observed that six recently isolated strains metabolized ACE via the proposed C-demethylation, oxidative cleavage, or N-deacetylation of the N-cyanoimine group to 1-(6-chloropyridin-3-yl)-N-methylmethanamine (IM-1-4), which is further metabolized by *Rhodococcus sp.* BCH2 to 6-chloronicotinic acid (IC-0) based on UV-Vis absorption spectra analysis, FTIR, (HPLC) and GC–MS results [4] or by *R. mucilaginosa* IM-2 to N'-[(6-chloropyridin-3-yl)methyl]-N-methylacetamide (IM-1-3) by HR-ESI-MS)analysis [10]. The second metabolic pathway involves N-demethylation to form (E)-N-[(6-chloro-3-pyridyl)-methyl]-N-cyano-acetamidine (IM2-1) from ACE biodegradation, which was associated with *Phanerochaete sordida* YK-624 and *Stenotrophomonas maltophilia* CGMCC 1.1788 according to HPLC-MS/MS and NMR Spectra analysis results, [9, 10]. It is interesting to note that the strain *Pigmentiphaga* sp. D-2 utilized the third and fourth pathway of ACE degradation, and the metabolites were identified in terms of the HPLC-ESI-MS analysis results as N′-cyano-N-methyl-N-(pyridin-3-ylmethyl)imidoformamide, IM-1-4 and IM-1-3, respectively [19]. The fifth and final pathway was proposed by Zhou et al. (2014) [14]; they indicated that the nitrogen-fixing bacterium *Ensifer meliloti* CGMCC 7333 with its nitrile hydratase (NHase) specifically transformed the neonicotinoid insecticide ACE to its (N-carbamoylimine derivate) IM-1-2 by means of HPLC, LC-MS and NMR analysis. Interestingly, the unstable IM-1-2 could not be further degraded by this nitrogen-fixing bacterium, but was instead hydrolyzed to the derivate ACE-NH through the N-carbamoylimine group; the ACE-NH was further converted to the derivative ACE-NH_2. Subsequently, ACE-NH_2 was cleaved to the major metabolite IM-1-4 [14]. It is worthwhile to note that this is the only article which reported and thoroughly described NHase, with respect to cloning the responsible genes involved in the degradation pathway, and this study has improved the understanding of the corresponding enzymatic biochemical mechanism of ACE biotransformation. Moreover, all the products proposed above are less toxic than ACE, which suggested that the method of microbiological ACE degradation is essential for environmental protection. The related metabolic pathways of ACE biodegradation are shown in detail in figure 1.

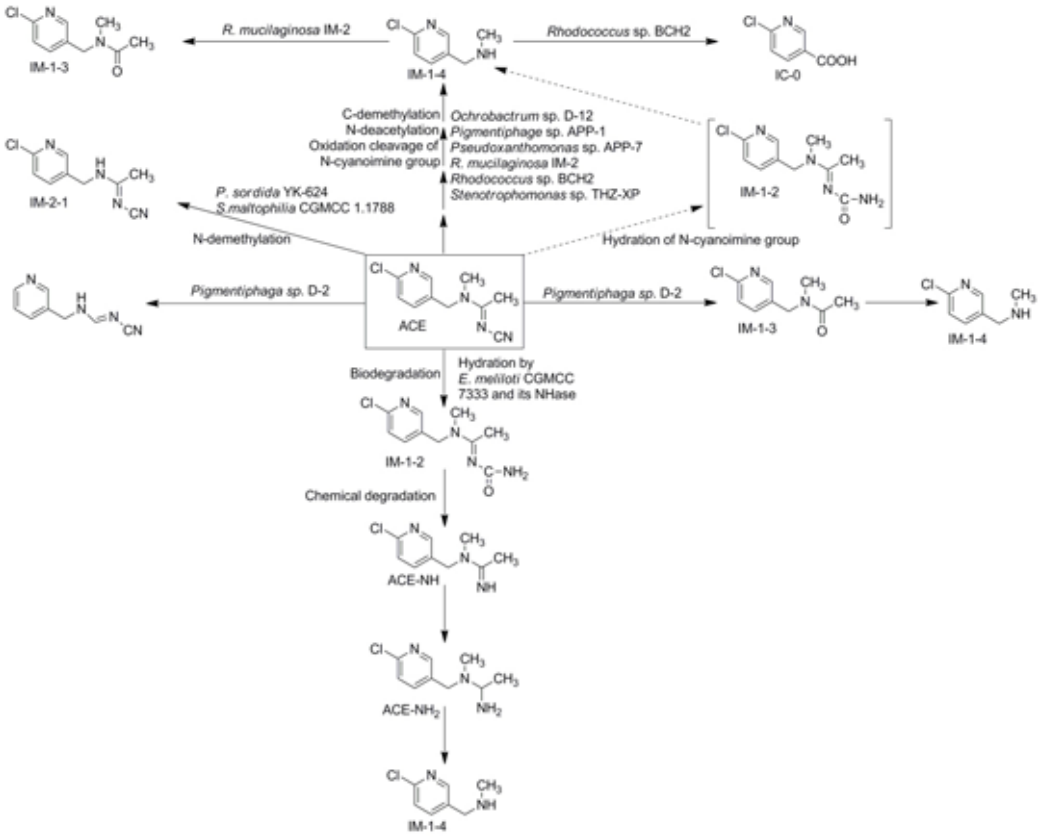


FIGURE 1

Proposed metabolic pathways of ACE metabolism in microorganisms. Abbreviations denote the following: IM-1-4 (1-(6-chloropyridin-3-yl)-N-methylmethanamine) [4, 11, 14, 16-18, 20]; IC-0 (6-chloronicotinic acid) [4]; IM2-1 ((E)-N-[(6-chloro-3-pyridyl)-methyl]-N-cyano-acetamidine) [9, 10]; IM-1-2 (N-carbamoylimine derivate) [14]; IM-1-3 (N′-[(6-chloropyridin-3-yl)methyl]-N-methylacetamide) [11, 19].

Behaviors of ACE in soil. There have been many reports concerning the effects of pesticides on soil enzyme activities, studies that demonstrate differences in the responses of soil enzymes to pesticides [23-25]. Yang et al. (2004) found mefenacet strongly inhibited soil urease activity in a concentration-dependent manner, but stimulated phosphatase activity; by contrast, quinclorac could inhibit proteinase, hydrogen peroxidase, phosphatase, and urease activities, which demonstrated that the higher the concentration of applied pesticides, the more significant the inhibition observed to these enzyme activities, and the longer time necessary to recover to the level of controls [26]. Unfortunately, in the case of ACE, there is only a relatively small amount of available information about the influence of this new pesticide on soil enzyme activities and soil respiration [6]. Yao et al. (2006) indicated that a normal field (0.5 mg kg^{-1} dried soil) dose of ACE would not pose a threat to soil enzymes, but could potentially pose a threat to soil respiration. However, when ACE concentration was increased (5 mg kg^{-1} and 50 mg kg^{-1} dried soil), the threat to soil phosphatase and respiration increased, and the enzyme activities in soil treated with these high concentrations of ACE were dramatically ($P < 0.05$) lower than control after incubation [6]. Actually, the effects of this pesticide on soil is generally a long-term process, closely related to other soil characteristics, such as the presence of other pesticides, physico–chemical characteristics of soil, heavy metal concentrations and other factors.

Taken together, these studies imply a well-known and quite intimate set of connections between soil characteristics and ACE behaviors—the efficiency of ACE degradation may be, directly or indirectly, strongly influenced by the composition of the surroundings. For example, soil adsorption might reduce the concentration of ACE in contact with microorganisms; this is important because ACE is stable to hydrolysis at environmental temperatures, and biodegradation is reported to be the most significant mechanism for its dissipation from soil.

Given these observations, it is noteworthy that a bacterial strain capable of effectively degrading ACE has been isolated from soil and characterized by authors. Consequently, it is conceivable that these identified microorganisms, which could degrade ACE efficiently in soil, would both decrease the concentration of ACE, and could subsequently provoke additional changes in soil. For example, diminishment in ACE toxicity would affect the behavior of soil enzymes[26]; moreover, some changes caused by the metabolites of ACE affecting soils' biological and biochemical properties might influence the structure of soil; and, in addition, these metabolites might act as growth factors for certain other soil microbes or as inhibition factors for certain soil enzymes.

Furthermore, the potential human toxicity of the residues present in the environment has been considered an essential problem and has been discussed in many studies [27, 28]. In the study of Cavas T et al. (2012) [27], CaCo-2 cells, a validated *in vitro* model for the human intestinal epithelium, were selected for experiments, and these studies demonstrated the *in vitro* cytotoxicity and genotoxicity of technical grade ACE on CaCo-2 cells. Zhang et al. [28] and Samiran et al. [29] investigated the effects of ACE on mice and Wistar rats, and they noted that ACE had deleterious effects on male reproductive function and suppressed both cell mediated immune response and the antibody-forming ability of lymphocytes in female Wistar rats, acting potentially through its metabolites, which induced oxidative stress. In addition, based on liquid chromatography with tandem mass spectrometry (LC–MS/MS), Marin A et al. (2004) [30] also clarified the human hazards of ACE by assessing the exposure of greenhouse workers to ACE. Most of these papers reported that pesticide residues pose one of the major environmental health problems due to their potential adverse effects on non-target organisms, and suggested that ACE should, therefore, be used in a restricted and cautious manner to protect animals and other organisms. In contrast, Bibhuti et al. (2012) [31] indicated that ACE produced significant elevation in only three enzymes, with no significant effect observed on total plasma protein, blood cholinesterase, lactate dehydrogenase, and five additional enzymes. That study also revealed that ACE at recommended concentration is a mild-risk insecticide in buffalo calves. Taken together, the available studies therefore suggest that far more research is needed to clearly understand the influence of ACE residues on soil and other organisms.

Effect of environmental conditions on the degradation of soil ACE. ACE is a chloronicotinoid insecticide, and its residues in crops are receiving considerable attention due to their potential toxicity to humans; hence, many articles have reported investigations of microbial ACE degradation under different conditions of laboratory-reared soil. ACE could be degraded more quickly by microbes from soil and mixed microbial enrichment culture. One of these studies clarified that the half life of ACE was 5.0 d in unsterilized soil, 8 times shorter than in sterilized soil [32]. It wasreported that the half-life values of ACE in chili (*Capsicum annum L.*) were in the range2.24–4.84 days[8]. But in contrast with the controls, several bacteria and fungi have been reported to be capable of degrading ACE more slowly. *Pseudomonas* sp. FH2 was reported to degrade 53.3%–96.7% of ACE in different media within 14 days [6], the white-rot fungus *Phanerochaete sordida* YK-624 was reported to transform 45% and 30% of ACE within 15 days under lig-

ninolytic and non-ligninolytic conditions, respectively[10]. In the study of Gupta S et al. (2008), residues of ACE in soil dissipated with half-lives of 11.1 days under UV light and 19.1 days under sunlight, respectively [33]. And Zhou et al. [14] described that the newly identified nitrogen-fixing bacterium *Ensifer meliloti* CGMCC 7333 could degrade 65.1% of ACE in 96 h, with a half-life of 2.6 days rather than controls that was not incubated. To summarize, the degradation of ACE was obviously influenced by environmental conditions.

ACE degradation in soil primarily depends upon the species and numbers of microbes with the required degrading ability in the contaminated soil. It is well known that the degradation of ACE in soil was induced by microorganisms, and the factors that affect microbial activity could cause some difference with respect to its degradation in soil. Moreover, temperature and pH also play an essential role in its degradation. Wang et al. (2010) [20] demonstrated that degradation of ACE occurred at 25–35 °C and pH 6–8, whereas Yang et al. (2013) [19] clarified that the optimal conditions for ACE degradation occurred at temperatures ranging from 30 °C to 45 °C and pH values ranging from 5 to 10. In addition, the effect of initial pesticide concentration on biodegradation is also an important parameter that reveals the correlation between cell biomass and biodegradation rate [4]. In the study of Phugare S et al. (2013), the researchers indicated that the biodegradation rate was 85% for 50 mg L^{-1} ACE concentration, with the degradation rate decreased to 14% at 250 mg L^{-1} in comparison with the controls. Wang et al. (2013) [20] also illustrated that high concentration would inhibit degradation.

Beyond these parameters, there are also many other physicochemical factors that can affect the efficiency of ACE degradation, such as metal ions, light, and the presence of other co-subrates. It was found that K^+, Ca^{2+} and Co^{2+} enhanced the biodegradation of ACE, while ACE degradation was significantly inhibited by Zn^{2+}, Fe^{2+}, Cu^{2+} and Ni^{2+} compared with the controls [16]. Moreover, in another study the researchers demonstrated that adding additional glucose or ammonium chloride would delay ACE biodegradation [20], but that enhanced degradation occurred with extra glucose or ammonium nitrate, which could be regarded as a second carbon or nitrogen source to be co-metabolized [18]. It is notable that photolysis is also an efficient way to eliminate ACE in the environment, some studies under sunlight and UV-light revealed that ACE is unstable to light, especially UV wavelengths [33, 34], so some substances coexist could influenced its efficiency, like photocatalysts (such as TiO_2 and Degussa P25), the surfactants (such as sodium dodecylbenzene sulfonate and Tween-80) [34, 35] . Finally, some other reports indicated that a matrix or matrices present in soil may also slow down the removal process [36]. Beyond the aforementioned factors, some others could affect degradation of ACE were summarized in the following table 2.

TABLE 2
Summary of factors in soil that can influence ACE elimination

Parameters	Descriptions	Reference
Temperature	Range of 30-37°C	
Metal ions	K^+,Ca^{2+},Co^+,Zn^{2+},Fe^{2+},Cu^{2+}, Ni^{2+},Mg^{2+},Al^{3+},Mn^{2+}	[16]
pH values	Range of 3-11	
Initial concentrations	Range of 50-600 mg.L^{-1}	[4, 16]
Carbon sources	Sucrose, glucose, yeast extract	[18, 20,10]
Nitrogen sources	NH_4Cl, $(NH_4)_2SO_4$, $NaNO_3$, NH_4NO_3	[4, 17, 18, 20]
Matraix	Woodchip biochar	[36]
Light	Sunlight, UV-light	[33,37]
Oxidative stress	SOD, CAT	[4]
Bacterial communities	Phyllospher microbes	[38]
Surfactants	SDBS, CTAB, Tween-80	[34]
Photocatalysts	TiO_2, Degussa P25	[35]

Genes Responsible for the ACE Biodegradation. Currently, many studies have reported various pathways involved in the biodegradation of ACE. However, only a little about genes was reported to be responsible for the ACE elimination. The nitrile hydratase (NHase) gene was cloned from the Nitrogen-Fixing Bacterium Ensifer meliloti CGMCC 7333, which coded a cobalt-type NHase composed of an a-subunit, b-subunit, mediated the hydration of ACE to metabolites IM-1-2 [14]. In fact, the NHase has been reported for hydrolyzing nitrile to the corresponding amide by amidase [39]. Interestingly, CGMCC 7333 NHase catalyzed the hydration of ACE to IM-1-2, whereas IM-1-2 was not further degraded by CGMCC 7333 and would be converted to ACE-NH due to chemical hydrolysis, ACE-NH was then transformed to ACE-NH2, which was subsequently cleaved to IM-1-4 (Fig. 1) [14] Actually, the Ensifer meliloti CGMCC 7333 was isolated from THI(Thiacloprid)-contaminated soil, which has the same N-cyanoimine group as ACE and also belongs to neonicotinoid insecticides. These presentations above would elucidate that the same structural components correspond to chemical compounds are hydrolyzed by the same enzyme or metabolized by the same microbes.

Besides, cytochrome P450-enzyme-system was also involved in the N-demethylation of ACE accompanied with some degrading strains. It has been reported that cytochrome P450 in white-rot fungi was essential in degrading various obstinate aromatic compound, such as the *Phanerochaete sordida* YK-624, which was related to catalyze demethylation and detoxification of ACE. Another

studies indicated that the hydroxylation of ACE by *Stenotrophomonas maltophilia* CGMCC 1.1788 could proceed neonicotinoid insecticide imidacloprid (IMI). However, cytochrome P450 in the same *S. maltophilia* CGMCC 1.1788 demethylize ACE, and the activity of enzymes in cytochrome P450-enzyme-system was promoted by adding reduced nicotinamide adenine dinucleotide (NADH) but was critically inhibited through the increase of piperonyl butoxide (PB)[9, 40].

DISCUSSION

ACE belongs to the chloropyridinyl neonicotinoid class of systemic broad-spectrum insecticides, which has been widely applied in controlling insects for crop protection, and for this reason, the biotransformation of ACE has garnered significant attention from the research community. There are about 15 types of microorganisms isolated and identified from contaminated agricultural soil that are able to use ACE as sole carbon and energy source, as well as nitrogen source for growth. This body of research additionally established that fungi can also degrade neonicotinoid compounds, such as the white-rot fungus *Phanerochaete sordida* YK-624 [10] and the yeast *Rhodotorula mucilaginosa* IM-2 [11]. Moreover, many metabolites have been produced in soil biogeochemical cycles or in other diverse ecosystems, but do not provide ideal conditions for the bioremediation of ACE; and some products like IC-0 are more readily dissolved in water leading to secondary pollution, although most metabolites are less toxic than ACE itself.

Therefore, new strategies for mitigating ACE contamination should be developed on the basis of previous studies, especially directed at isolating and identifying new strains or stable microbial communities that can absolutely eliminate ACE or its potentially harmful metabolic byproducts. The high ability of fusant-AC strain to CTN and ACE degradation were verified, which implied a potential role of fusant strains in the development of novel strategies for the bioremediation of ACE contaminated environments. Beyond these prospective studies are those focused on the genome, because there is limited knowledge regarding key genes or enzymes in ACE degradation. For example, Wilkinson et al. (1972)[41] indicated that ACE is biotransformed in the honeybee by Phase I enzymes, mainly by mixed function oxidases that convert ACE into more polar metabolites that are more readily excreted; NHase from CGMCC 7333 and P450-enzyme-systems-mediated demethylation was responsible for the biotransformation of ACE [9, 14]. These sparse studies remind us that cloning the genes involved in the degradative pathway may help to understand the corresponding enzymatic biochemical mechanism of ACE biotransformation. In other ways, photocatalysts and surfactants were also found to catalyze the photodegradation of ACE under the condition of oxygen and light[34,35]. To sum up, all descriptions above suggest that probable mechanisms in various aspects could be responsible for the elimination of ACE, which indicated more attention should be paid to this research area.

ACKNOWLEDGEMENTS

This work was supported by grants from the Chinese National Natural Science Foundation (31100083, 41501304), the Foundation for Young Talents in College of Anhui Province, the Natural Science Foundation from Educational Commission of Anhui Province (KJ2015A049), Provincial Natural Science Foundation of Anhui (1508085MC49), The Open Project Program of the Collaborative innovation center of modern bio-manufacture Anhui university(BM2015010), and the Innovation Team of Scientific Research Platform of Anhui Province, China. No. KJ2015TD001.

REFERENCES

[1] Jeschke, P., Nauen, R. (2007) Thiamethoxam: A Neonicotinoid Precursor Converted to Clothianidin in Insects and Plants. Synthesis and Chemistry of Agrochemicals VII. American Chemical Society. 948, 51-65.

[2] Arther, R.G., Cunningham, J., Dorn, H., Everett, R., Herr, L.G., Hopkins, T. (1997) Efficacy of imidacloprid for removal and control of fleas (Ctenocephalides felis) on dogs. American journal of veterinary research. 58, 848-850.

[3] Jacobs, D.E., Hutchinson, M.J., Fox, M.T., Krieger, K.J. (1997) Comparison of flea control strategies using imidacloprid or lufenuron on cats in a controlled simulated home environment, American journal of veterinary research. 58, 1260-1262.

[4] Phugare, S.S., Jadhav, J.P. (2013) Biodegradation of Acetamiprid by Isolated Bacterial StrainRhodococcussp. BCH2 and Toxicological Analysis of Its Metabolites in Silkworm (Bombax mori). CLEAN - Soil, Air, Water. 43, 296-304.

[5] El Hassani, A.K., Dacher, M., Gary, V., Lambin, M., Gauthier, M., Armengaud, C. (2008) Effects of sublethal doses of acetamiprid and thiamethoxam on the behavior of the honeybee (Apis mellifera). Archives of environmental contamination and toxicology. 54, 653-661.

[6] Yao, X.H., Min, H. (2006) Isolation, characterization and phylogenetic analysis of a bacterial strain capable of degrading acetamiprid. Journal of environmental sciences (China). 18, 141-146.

[7] Pramanik, S.K., Bhattacharyya, J., Dutta, S., Dey, P.K., Bhattacharyya, A. (2006) Persistence of Acetamiprid in/on Mustard (Brassica juncea L.). Bulletin of environmental contamination and toxicology. 76, 356-360.
[8] Sanyal, D., Chakma, D., Alam, S. (2008) Persistence of a neonicotinoid insecticide, acetamiprid on chili (Capsicum annum L.). Bulletin of environmental contamination and toxicology. 81, 365-368.
[9] Chen, T., Dai, Y.J., Ding, J.F., Yuan, S., Ni, J.P. (2008) N-demethylation of neonicotinoid insecticide acetamiprid by bacterium Stenotrophomonas maltophilia CGMCC 1.1788. Biodegradation. 19, 651–658.
[10] Wang, J., Hirai, H., Kawagishi, H. (2011) Biotransformation of acetamiprid by the white-rot fungus Phanerochaete sordida YK-624. Appl Microbiol Biotechnol. 93, 831-835.
[11] Dai, Y.J., Ji, W.W., Chen, T., Zhang, W.J., Liu, Z.H., Ge, F., Yuan, S. (2010) Metabolism of the Neonicotinoid Insecticides Acetamiprid and Thiacloprid by the Yeast Rhodotorula mucilaginosa Strain IM-2. J Agric Food Chem. 58, 2419–2425.
[12] Arora, P.K., Sasikala, C., Ramana Ch, V. (2012) Degradation of chlorinated nitroaromatic compounds. Appl Microbiol Biotechnol. 93, 2265-2277.
[13] Fan, X., Liu, X., Huang, R., Liu, Y. (2012) Identification and characterization of a novel thermostable pyrethroid-hydrolyzing enzyme isolated through metagenomic approach. Micro-bial cell factories. 11, 33.
[14] Zhou, L.Y., Zhang, L.J., Sun, S.L., Ge, F., Mao, S.Y., Ma, Y., Liu, Z.H., Dai, Y.J., Yuan, S. (2014) Degradation of the neonicotinoid insecticide acetamiprid via the N-carbamoylimine derivate (IM-1-2) mediated by the nitrile hydratase of the nitrogen-fixing bacterium Ensifer meliloti CGMCC 7333. Journal of agricultural and food chemistry. 62, 9957-9964.
[15] Wang, G., Zhu, D., Xiong, M., Zhang, H., Liu, Y. (2016) Construction and analysis of an intergeneric fusion from Pigmentiphaga sp. strain AAP-1 and Pseudomonas sp. CTN-4 for degrading acetamiprid and chlorothalonil. Environmental science and pollution research international. 23(13), 13235-44.
[16] Wang, G., Yue, W., Liu, Y., Li, F., Xiong, M., Zhang, H. (2013) Biodegradation of the neonicotinoid insecticide Acetamiprid by bacterium Pigmentiphaga sp. strain AAP-1 isolated from soil. Bioresource technology. 138, 359-368.
[17] Tang, H.Z., Li, J., Hu, H.Y., Xu, P. (2012) A newly isolated strain of Stenotrophomonas sp. hydrolyzes acetamiprid, asynthetic insecticide. Process Biochemistry. 47, 1820–1825.
[18] Wang, G., Zhao, Y., Gao, H., Yue, W., Xiong, M., Li, F., Zhang, H., Ge, W. (2013) Cometabolic biodegradation of acetamiprid by Pseudoxanthomonas sp. AAP-7 isolated from a long-term acetamiprid-polluted soil. Bioresource technology. 150, 259-265.
[19] Yang, H., Wang, X., Zheng, J., Wang, G., Hong, Q., Li, S., Li, R., Jiang, J. (2013) Biodeg-radation of acetamiprid by Pigmentiphaga sp. D-2 and the degradation pathway. International Biodeterioration & Biodegradation. 85, 95-102.
[20] Wang, G., Chen, X., Yue, W., Zhang, H., Li, F., Xiong, M. (2013) Microbial degradation of acetamiprid by Ochrobactrum sp. D-12 isolated from contaminated soil. PloS one. 8, e82603.
[21] Brunet, J.L., Badiou, A., Belzunces, L.P. (2005) In vivo metabolic fate of [14C]-ace-tamiprid in six biological compartments of the honeybee, Apis mellifera L. Pest management science. 61, 742-748.
[22] Ford, K.A., Casida, J.E. (2006) Chloropyridinyl neonicotinoid insecticides: diverse molecular substituents contribute to facile metabolism in mice. Chemical research in toxicology. 19, 944-951.
[23] Gianfreda, L., Sannino, F., Violante, A. (1995) Pesticide effects on the acttivity of free, innobilized and soil invertase. Soil Biol Eio&w. 27, 1201-1208.
[24] Megharaj, M., Singletona, I., Kookanab, R., Naidu, R. (1999) Persistence and effects of fenamipphos on native algal populations and enzymatic activities in soil. Soil Biology and Biochemistry. 31, 1549-1553.
[25] Sannino, F., Fianfreda, L. (2001) Pesticide influence on soil enzymatic activities. Chenosphere. 45, 417-425.
[26] Lu, Z.M., Min, H., Ye, Y.F. (2004) Short-Term Influence of Herbicide Quinclorac Oil Activities in Flooded Paddy Soils Enzyme. Pedosphere. 14(1), 71-76.
[27] Çavaş, T., Çinkılıç, N., Vatan, Ö., Yılmaz, D., Coşkun, M. (2012) In vitro genotoxicity evaluation of acetamiprid in CaCo-2 cells using the micronucleus, comet and γH2AX foci assays. Pesticide Biochemistry and Physiology. 104, 212-217.
[28] Zhang, J.Q., Wang, Y., Xiang, H.Y., Li, M.X., Li, W.H., Ma, K.G., Wang, X.Z., Zhang, J.H. (2011) Oxidative Stress: Role in Acetamiprid-Induced Impairment of the Male Mice Reproductive System. Agricultural Sciences in China. 10(5), 786-796.
[29] Mondal, S., Ghosh, R.C., Mate, M.S., Karmakar, D.B. (2009) Effects of Acetamiprid on Immune System in Female Wistar Rats. Proc zool Soc. 62(2), 109–117.

[30] Marin, A., Martinez Vidal, J.L., Egea Gonzalez, F.J., Garrido Frenich, A., Glass, C.R., Sykes, M. (2004) Assessment of potential (inhalation and dermal) and actual exposure to acetamiprid by greenhouse applicators using liquid chromatography-tandem mass spectrometry, Journal of chromatography B. Analytical technologies in the biomedical and life sciences. 804, 269-275.

[31] Ranjan, B., Dumka, V.K., Ola, A.K., Rampal, S. (2012) Effect of Oral Subacute Exposure of Acetamiprid on Some Biochemical Parameters in Buffalo Calves. Proceedings of the National Academy of Sciences, India. Section B: Biological Sciences. 83, 59-63.

[32] Liu, Z., Dai, Y., Huang, G., Gu, Y., Ni, J., Wei, H., Yuan, S. (2011) Soil microbial degradation of neonicotinoid insecticides imidacloprid, acetamiprid, thiacloprid and imidaclothiz and its effect on the persistence of bioefficacy against horsebean aphid Aphis craccivora Koch after soil application. Pest management science. 67, 1245-52.

[33] Gupta, S., Gajbhiye, V.T., Gupta, R.K. (2008) Effect of light on the degradation of two neonicotinoids viz acetamiprid and thiacloprid in soil. Bulletin of environmental contamination and toxicology. 81, 185-189.

[34] Xie, G.H., Lv, J.X., Liu, G.G., Sun, D.Z. Zheng, L.Q., (2008) Effects of surfactants on the kinetics of acetamiprid photolysis. Reaction Kinetics and Catalysis Letters. 95, 289-299.

[35] Khan, A., Haque, M. M., Mir, N. A., Muneer, M., Boxall, C. (2010) Heterogeneous photocatalysed degradation of an insecticide derivative acetamiprid in aqueous suspensions of semiconductor. Desalination. 261, 169-174.

[36] Yu, X.Y., Mu, C.L., Gu, C., Liu, C., Liu, X.J. (2011) Impact of woodchip biochar amendment on the sorption and dissipation of pesticide acetamiprid in agricultural soils. Chemosphere. 85, 1284-1289.

[37] Pitam, S., Mukherjee, I., Kumar, A. (2013) Evaluation of environmental fate of acetamiprid in the laboratory. Environ Monit Assess. 185, 2807-2816.

[38] Zhou, Y., Xiong, W.Q., Li, W.J., Xu, J.F, Wang, W., Chen, X. (2011) Phyllosphere bacterial communities associated with the degradation of acetamiprid in Phaseolus vulgaris. African Journal of Biotechnology. 10, 3809-3817.

[39] Kobayashi, M., Shimizu, S., (2000) Nitrile hydrolases. Current Opinion in Chemical Biology. 4, 95–102.

[40] Dai, Y.J., Chen, T., Ge, F., Yu, H., Yuan, S., Zhu, F.F. (2007) Enhanced hydroxylation of imidacloprid by *Stenotrophomonas maltophilia* upon addition of sucrose. Appl Microbiol Biotechnol. 74, 995–1000.

[41] Wilkinson, C. F. & Brattsten, L. B. (1972) Microsomal Drug Metabolizing Enzymes in Insects, Drug Metabolism Reviews. 1, 153-227.

Received: **25.04.2017**
Accepted: **28.12.2018**

CORRESPONDING AUTHOR

Guangli Wang
College of Life Sciences,
Huaibei Normal University,
235000, Huaibei – China

e-mail: wanf-3344@163.com

© by PSP Volume 27 – No. 5/2018 pages 2743-2750 Fresenius Environmental Bulletin

STATUS AND PREDICTION OF NO_2 AS AN AIR POLLUTANT IN ISFAHAN, IRAN

Masoud Masoudi*, Soraya Gerami

Department of Natural Resources and Environmental Engineering, Shiraz University, Iran.

ABSTRACT

In the present study, air quality analyses for Nitrogen dioxide (NO_2) were conducted in Isfahan, Iran. The measurements were taken in three different locations to prepare average data in the city. The averages concentrations were calculated for every 24 hours, each month and each season. Results showed that the highest concentration of Nitrogen dioxide occurs generally in morning and night while the least concentration occurs in the afternoon and mid-night. Monthly concentrations of the Nitrogen dioxide showed highest value in March. The seasonal concentrations showed the least amounts in spring while the highest in winter. Then Relations between the air pollutant and some meteorological parameters were calculated statistically using the daily average data. The temperature (min, max), precipitation, Wind Direction (max), Wind Speed (max) and Evaporation were considered as independent variables. The level relationships between concentration of pollutant and meteorological parameters were expressed by multiple linear equations for both annual and seasonal conditions using SPSS software. RMSE test showed that among different prediction models, stepwise model is the best option. Results showed that quantities of NO_2 in different seasons and whole year could be estimated by climate parameters. Results also indicated that relations between the NO_2 and meteorological parameters are stronger than whole year during the seasons.

KEYWORDS:
NO_2, Air pollution, Meteorological Parameters, Regression model.

INTRODUCTION

Air sustains life. But the air we breathe is not pure. It contains a lot of pollutants and most of these pollutants are toxic [1, 2, 3, 4, 5]. While developed countries have been making progress during the last century, air quality has been getting much worse especially in developing countries air pollution exceeds all health standards. For example, in Lahore and Xian (china) Dust is ten times higher than health standards [1]. Nitrogen dioxide (NO_2) is one of the seven conventional (criteria) pollutants (including SO_2, CO, particulates, hydrocarbons, nitrogen oxides, O_3 and lead). These pollutants produce the highest volume of pollutants in the air and the most serious threat for human health and welfare. Concentration on these pollutants, especially in cities, has been regulated by Clean Air Act since 1970 [6].

Some Properties of Nitrogen dioxide (NO_2) are: reddish brown gas, formed as fuel burnt in car, strong oxidizing agent and forms Nitric acid in air. Its Sources are divided to two parts: 1) natural emissions including forest fires, volcanoes, bacteria in soil, lightening, etc. 2) anthropogenic activity including motor vehicle emissions and power generation. Fuel combustion increases NO_2 production. Half of emission of HC and NOx in cities is by Motor vehicles.

Nitrogen oxides (NO_x) include different forms of oxides of nitrogen. NO_2 generally derives from emissions of NO (in high temperature). About 95% of Nitrogen oxides are emitted as NO and 5% as NO_2. Other oxides are N_2O, N_2O_3 and N_2O_5 which are not so important in air pollution. Among NO_x, NO_2 lead to respiratory problems and therefore NO_2 is the most important of the oxides of nitrogen.

The presence of pollutants in the atmosphere, causes a lot of problems, thus the study of pollutant' behaviour is necessary [7]. Some of the main health effects of NO_2 as follow: lung and heart problems, NO_2 poisoning, asthma, lowered resistance to infection. Other effects include on plants and materials such as damages of leaves, retard photosynthesis activity, cause chlorosis, damages on various textile fibers, multiplying the photochemical smog problems and damages of acid rain.

Status of pollutants concentration and effects of meteorological and atmospheric parameters on these pollutants compose the base of following studies: Ho and Lin [8] studied semi-statistical model for evaluating the NO_x concentration by considering source emissions and meteorological effects. Street level of NO_x and SPM in Hong Kong has been studied by Lam et al [9] in a study, the relationship between monitored air pollutants and meteorological factors, such as wind speed, relative humidity ratio and temperature, was statistically analyzed, using SPSS. According to the results obtained through multiple linear regression analysis, for some months there was a

moderate and weak relationship between the air pollutants like PM level and the meteorological factors in Trabzon city [10].

Mandal [11] has shown the progressive decrease of air pollution from west to east in Kolkata. Statistical modelling of ambient air pollutants in Delhi has been studied by Chelani [12]. Abdul-Wahab and Al-Alawi [13] developed a neural network model to predict the tropospheric (surface or ground) ozone concentrations as a function of meteorological conditions and various air quality parameters. The results of this study showed that the artificial neural network (ANN) is a promising method for air pollution modelling. The observed behavior of pollution concentrations to the prevailing meteorological conditions has been studied for the period from June 13 to September 2, 1994, for the Metropolitan Area of Sao Paulo [14]. Results show low concentrations associated with intense ventilation, precipitation and high relative humidity. While high values of concentrations prevailed due to weak ventilation, absence of precipitation and low relative humidity for some pollutants. Also for predicting CO, Sabah et al. [15] used a statistical model.

Elminir [16] mentioned dependence of air pollutants on meteorology over Cairo in Egypt. The results hint that, wind direction was found to have an influence not only on pollutant concentrations but also on the correlation between pollutants. As expected, the pollutants associated with traffic were at highest ambient concentration levels when wind speed was low. At higher wind speeds, dust and sand from the surrounding desert was entrained by the wind, thus contributing to ambient particulate matter levels. It was also found that, the highest average concentration for NO_2 and O_3 occurred at humidity $\leq 40\%$ indicative for strong vertical mixing. For CO, SO_2 and PM_{10} the highest average concentrations occurred at humidity above 80%. In another research, data on the concentrations of seven air pollutants (CH_4, NMHC, CO, CO_2, NO, NO_2 and SO_2) and meteorological variables (wind speed and direction, air temperature, relative humidity and solar radiation) were used to predict the concentration of ozone in the atmosphere using both multiple linear and principal component regression methods [17]. Results showed that while high temperature and high solar energy tended to increase the day time ozone concentrations, the pollutants NO and SO_2 being emitted to the atmosphere were being depleted. However, the model did not predict the night time ozone concentrations as precisely as it did for the day time. Asrari et al. [7] studied effect of meteorological factors for predicting CO. Also variations in concentration of CO in different times have been shown in this study.

Li et al. [18] presented the spatial and temporal variation of Air Pollution Index (API) and examined the relationships between API and meteorological factors during 2001–2011 in Guangzhou, China. Relationships were found between API and a variety of meteorological factors. Temperature, relative humidity, precipitation and wind speed were negatively correlated with API, while diurnal temperature range and atmospheric pressure were positively correlated with API in the annual condition. Yoo et al. [19] mentioned that all of the pollutants showed significant negative correlations between their concentrations and rain intensity due to washout or convection. The relative effect of the precipitation on the air pollutant concentrations is estimated to be: $PM_{10} > SO_2 > NO_2 > CO > O_3$, indicating that PM_{10} was most effectively cleaned by rainfall.

Wang *et al.* [20] studied on air quality in Chongqing, the largest mountainous city in China. From 2002 to 2012, statistical analysis of SO_2, PM_{10} and NO_2 concentrations is conducted. The analysis of Pearson correlation indicated that concentrations of SO_2, PM_{10} and NO_2 were positively correlated with atmospheric pressure, but negatively with temperature and wind speed. The analysis of Multi-Pollutant Index (MPI) showed that air quality in Chongqing was serious.

The climatology of tropospheric ozone at Irene was investigated using SHADOZ network data to assess the correlation between the observed seasonal ozone enhancement and meteorological factors [21]. A multiple linear regression model was used to provide seasonal correlation between ozone and temperature and relative humidity. All seasons display strong regression coefficients between ozone and temperature. Similar trends are also observed for relative humidity and ozone concentrations in autumn, spring and summer.

Statistical modelling of ozone in Shiraz and PM_{10} in Tehran were studied by Masoudi et al. [22, 23]. According to the results obtained through multiple linear regression analysis, for seasonal and annual conditions there were significant relationships between ozone and PM_{10} levels and the meteorological factors in both cities.

The present study exhibits diurnal, monthly and seasonal variations of concentration of NO_2 and also a statistical model that is able to predict its amount. This is based on multiple linear regression technique. Multiple Regression estimates the coefficients of the linear equation, involving one or more independent variables that best predict the value of the dependent variable (NO_2 in this study). So, large statistical and graphical software package (SPSS, Software Package of Social Sciences, V. 20) as one of the best known statistical packages has been used [24].

MATERIALS AND METHODS

Study Area. The research area, Isfahan, capital of Isfahan Province, is one of the biggest cities in the central part Iran (Fig. 1) located around 32° 38' N and 51° 40' E and the elevation is about 1590 m above the mean sea level. It has semi-arid climate

with four distinct seasons. Residential population was 1,834,000 in 2011. Isfahan is built on the banks of the Zayandeh-rud River. There are a lot of cars in city and many factories and industrials place around the city. Because of these problems Isfahan is one of the most polluted cities in Iran. Hence a need was felt to carry out an ambient air quality analysis in this city.

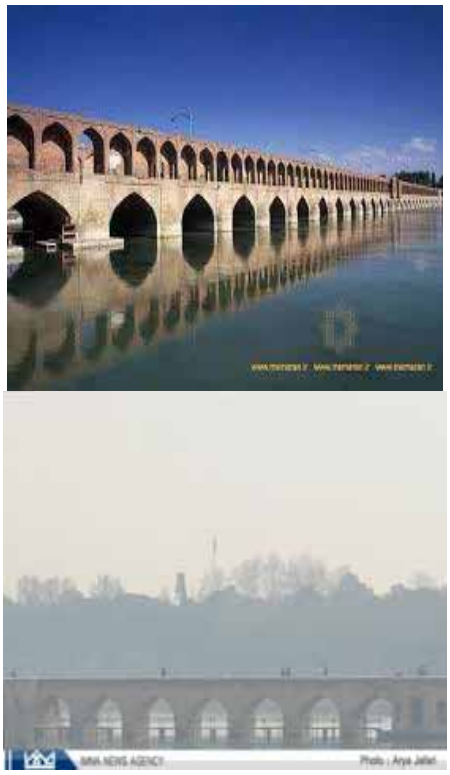


FIGURE 1
Two photographs from the same place in Isfahan showing impacts of dust pollution during recent years (left one in clean condition and right one in worse condition).

Data and methodology. Three available sampling stations in the city called, Azadi, Bozorg-mehr and Laleh, belong to Environmental Organization of Iran were selected to represent different traffic loads and activities.

The sampling has been performed every 1hour daily for each pollutant during all months of 2010 and 2011. Among the measured data in the three stations Nitrogen dioxide was chosen. Then the averages were calculated for every hour, each month and each season for the three stations by Excel. Finally averages of data at three stations were used to show air pollution situation as diurnal, monthly and seasonal graphs of concentration of Nitrogen dioxide in the city.

Studying correlation of Nitrogen dioxide and metrological parameters of synoptic station of city was the next step. The metrological parameters studied include: temperature (min, max), precipitation, Wind Direction (max), Wind Speed (max) and Evaporation.

In the next step, daily average data at three stations in 2011 was considered as dependent variable for statistical analysis while daily data of meteorological parameters during this year were selected as independent variables in SPSS programme and the multiple regression equations showed that the concentration of Nitrogen dioxide on the kind of meteorological parameters and also give an idea about the levels of these relations. The relationship between the dependent variables and each independent variable has been considered for linear technique. The significant values in output are based on fitting a single model. Also linear regression equation was made for different seasons maybe show those relationships which are not observed using annual data.

The model for predicting Nitrogen dioxide was determined using two multiple regression modelling procedures of 'enter method' and 'stepwise method'. In 'enter method' all independent variables selected are added to a single regression model. In 'stepwise' which is better, all variables can be entered or removed from the model depending on the significance. Therefore only those variables which have more influence on dependent variable are observed in a regression model.

RESULTS AND DISCUSSION

In Figs. 2, 3 and 4, the diurnal, monthly and seasonal variations in concentration of Nitrogen dioxide have been presented. As shown in fig. 2 the high concentration of Nitrogen dioxide occurs in the morning and night. High traffic during these times may be responsible for this high concentration. Monthly concentration of the Nitrogen dioxide shows the highest values in March and the least amounts in June and July (Fig. 3). Seasonal concentration of Nitrogen dioxide showed the highest values in winter and the least in spring (Fig. 4). Unfortunately, all graphs showed that the concentrations of the Nitrogen dioxide are upper than Primary Standards of Nitrogen dioxide recommended by National Ambient Air Quality Standards (NAAQS) of Iran (21 ppb), protecting human health. These results are almost in good agreement other results obtained in other cities like Shiraz [25], Tehran [26] and Ahvaz [27].

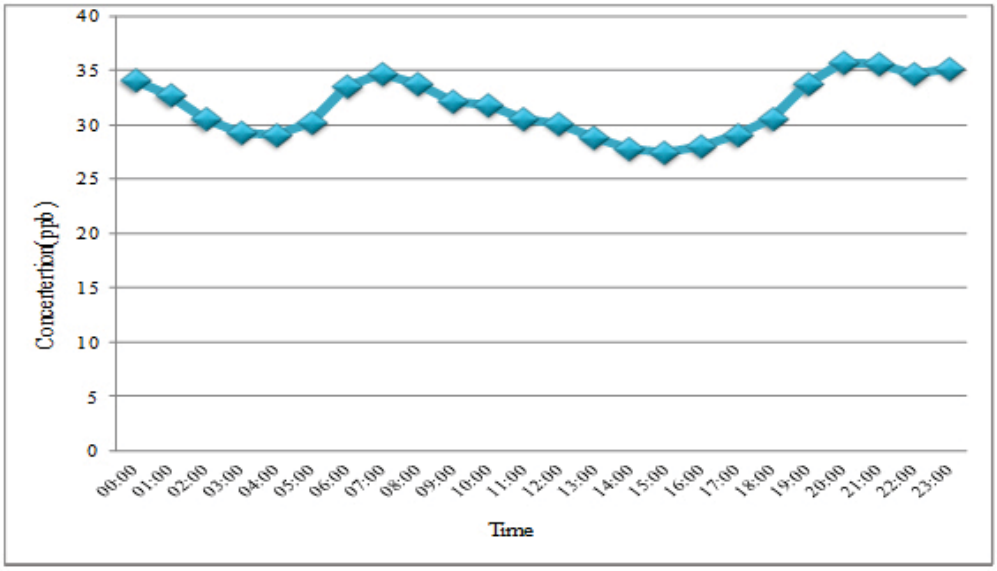


FIGURE 2
Diurnal variation of Nitrogen dioxide concentration in Isfahan.

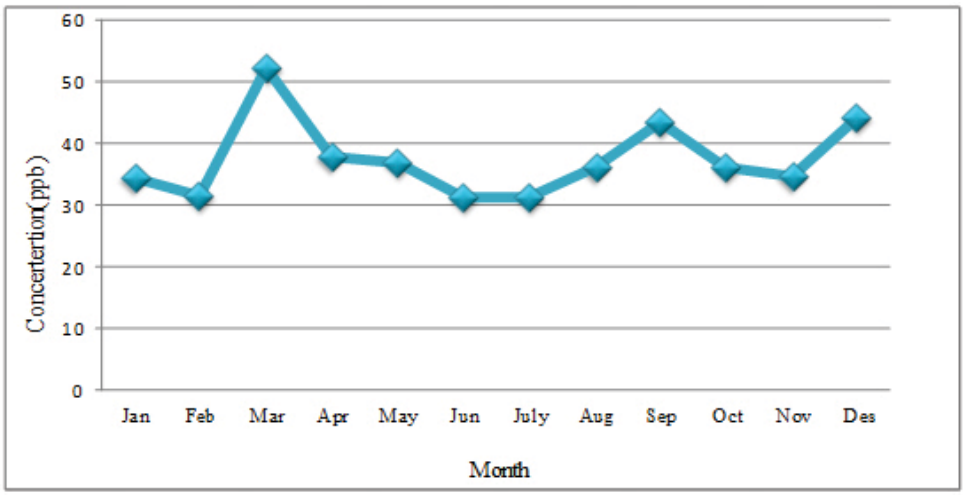


FIGURE 3
Monthly variation of Nitrogen dioxide concentration in Isfahan.

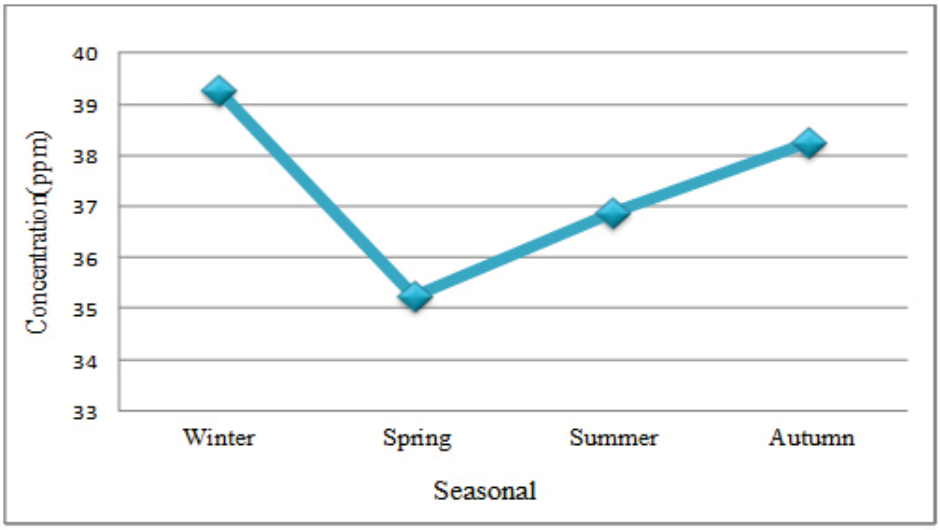


FIGURE 4
Season variation of Nitrogen dioxide concentration in Isfahan.

TABLE 1
Correlation between air pollutants and Nitrogen dioxide.

	CO	O_3	NOx	PM_{10}	SO_2
Pearson Correlation	-.128**	.562**	.675**	-.409**	-.143**
Sig. (2-tailed)	.018	.000	.000	.000	.008
N	344	344	344	344	344

Table 1 shows the relationships between Nitrogen dioxide and other air pollutants. For example the concentration of Nitrogen dioxide shows negative correlation with PM_{10} and SO_2 while it shows positive correlation with O_3 and NO_x. NO_2 like most of pollutants is increased when traffic and industrial activity are increased while PM_{10} in this city, which its main source is detached, soils from western neighbors like Iraq. These results are almost in good agreement with other results regarding Nitrogen dioxide assessment in other Iranian cities like Shiraz [25], Tehran [26] and Ahvaz [27].

Correlation coefficients significant at the 0.05 level are identified with a single asterisk (significant), and those significant at 0.01 level are identified with two asterisks (highly significant).

Table of analysis of variance (Table 2) shows both regressions of 'enter' and 'stepwise' methods for annual condition are highly significant, indicating a significant relation between the different variables.

In Tables 3 the coefficients of Nitrogen dioxide pollution model and regression lines for both enter and stepwise methods in annual condition are presented. Regression coefficients, standard errors, standardized coefficient beta, t values, and two-tailed significance level of t have been shown in the Tables.

TABLE 2
Tables of analysis of variance for both regressions of 'enter' (a) and 'stepwise' (b) methods for annual condition.

Analysis of variance (a)

Model	Sum of Squares	df	Mean Square	F	Sig.
Regression	3093.106	6	515.518	5.688**	.000
Residual	23385.068	258	90.640		
Total	26478.173	264			

Predictors: (Constant), Rain, Wind direction (max), Wind speed (max), Temperature (max), Temperature (min) and Evaporation.
Dependent Variable: Nitrogen dioxide

Analysis of variance (b)

Model	Sum of Squares	df	Mean Square	F	Sig.
Regression	2679.737	2	1339.868	14.751**	.000
Residual	23798.437	262	90.834		
Total	26478.173	264			

Predictors: (Constant), Wind speed (max), Temperature (max)
Dependent Variable: Nitrogen dioxide

TABLE 3
Coefficients of Nitrogen dioxide pollution model and regression lines for both enter (a) and stepwise (b) methods for annual condition.

Coefficients (a)

Model	Unstandardized Coefficients		Standardized Coefficients	t	Sig.
	B	Std. Error	Beta		
(Constant)	45.616	3.512		12.988	.000
Evaporation	.660	.342	.229	1.930	.055
Temperature $_{max}$	-.346	.221	-.288	-1.565	.119
Temperature $_{min}$	-.336	.271	-.217	-1.244	.215
Rain	-.002	.331	.000	-.006	.995
Wind direction $_{max}$	.002	.006	.020	.311	.756
Wind speed $_{max}$	.449	.221	.129	2.031	.043

Dependent Variable: Nitrogen dioxide

Coefficients (b)

Model	Unstandardized Coefficients		Standardized Coefficients	t	Sig.
	B	Std. Error	Beta		
(Constant)	46.163	2.340		19.724	.000
Temperature $_{max}$	-.358	.071	-.298	-5.071	.000
Wind speed $_{max}$	.485	.205	.139	2.369	.019

Dependent Variable: Nitrogen dioxide

The linear regression equations show that the Nitrogen dioxide pollution depends on the meteorological parameters and also give an idea about the levels of relations. The linear model equations after using 'enter method' and 'stepwise method' for annual condition are:

Nitrogen dioxide amount (ppb) using 'enter method' for annual condition = 45.616 + (.660) Evaporation + (-.346) Temperature $_{max}$ + (-.336) Temperature $_{min}$ + (-.002) Rain + (.002) Wind direction $_{max}$ + (.449) Wind speed $_{max}$ R= .342 (significant at 0.01)

Nitrogen dioxide amount (ppb) using 'stepwise method' for annual condition = 46.163 + (-.358) Temperature $_{max}$ + (.485) Wind speed $_{max}$
R= .318 (significant at 0.01)

Results of linear regression model show that Temperature $_{max}$ have reverse effect on concentration of Nitrogen dioxide. So that when these parameters increase, the concentration of Nitrogen dioxide decreases. While, when Wind speed $_{max}$ increases, the concentration of Nitrogen dioxide significantly increases (Table 3b). Other meteorological parameters show different effects on Nitrogen dioxide amounts although these results are not significant. For example rainfall has reverse effect on concentration of Nitrogen dioxide (Table 3a). These results are almost in good agreement with other results regarding Nitrogen dioxide measurements in other Iranian cities like Shiraz [25], Tehran [26] and Ahvaz [27] and other regions [14, 16, and 18]. Actually some of these events happen in real condition. Increasing in rainfall, and temperature (inversion happens in low temperatures) usually decrease most of air pollutants [7].

The values and significance of R (multiple correlation coefficients) in both equations show capability of them in predicting Nitrogen dioxide amount. The amount of Adjusted R^2 in both equations is almost 0.10 showing that different parameters used can calculate almost 10% variability of Nitrogen dioxide. This result indicates for predicting most of air pollutants like Nitrogen dioxide, we should take into consideration consumption of fossil fuel especially Motor vehicles. Half of emission of (VOC) Hydrocarbons and NOx in cities is by Motor vehicles. The automobile exhaust produces 75% of total air pollution. It releases poisonous gases of CO (77%), NOx (8%) and Hydrocarbons (14%) [1]. On the other hand, R in enter method (0.34) is equal to stepwise method (0.32), showing no difference. Therefore, second equation based on stepwise method can be used to predict Nitrogen dioxide in the city instead of using first equation which needs more data. On the other hand, no difference between the two R values indicates that the excluded variables in second equation have less effect on measuring of Nitrogen dioxide in the city.

Beta in Table 3 shows those independent variables (meteorological parameters) which have more effect on dependent variable (Nitrogen dioxide). The beta in the both Table 3 shows a highly significant effect of some variables like temperature compared to other meteorological parameters for measuring the Nitrogen dioxide which is close to the results of Shiraz [25], Tehran [26] and Ahvaz [27].

Parameter Sig (P-value) from Table 3 shows amount of relation between Nitrogen dioxide and meteorological parameters. For example, Table 3a shows Wind speed $_{max}$ has higher effect than other parameters on Nitrogen dioxide.

On the other hand, in Table 4 the linear regression equations of Nitrogen dioxide amount are presented for both enter and stepwise methods for different seasonal condition. Almost all of the models except summer models are significant. Stepwise methods show those meteorological parameters which are most important during these seasons for estimating the pollution. Among the models, autumn models have the highest R which these results for different seasonal condition differ a little from the results of Tehran [26] and Shiraz [25]. R amounts in spring, winter and autumn models are higher than in annual models, also indicating that relations between the pollutant and meteorological parameters are stronger than whole year during these seasons.

TABLE 4
Nitrogen dioxide amount (ppb) using two methods of enter and stepwise for different seasonal condition.

season	Enter method	R	Stepwise method	R
Spring	= 61.402 + (.019) Evaporation + (-.160) Temperature $_{max}$ + (-1.162) Temperature $_{min}$ + (-.196) Rain + (-.020) Wind direction $_{max}$ + (.321) Wind speed $_{max}$	.624 (0.01 significant)	= 61.044 + (-1.304) Temperature $_{min}$ + (-.018) Wind direction $_{max}$	.614 (significant at 0.01)
Summer	= 28.095+ (.072) Evaporation + (.416) Temperature $_{max}$ + (-.586) Temperature $_{min}$ + (-.783) Rain + (-.001) Wind direction $_{max}$ + (.603) Wind speed $_{max}$	.244 (not significant at 0.05)	-	Not prepared by software showing no significance relationship
Autumn	= 52.479 + (.087) Evaporation + (-.957) Temperature $_{max}$ + (.775) Temperature $_{min}$ + (-.103) Rain + (-.001) Wind direction $_{max}$ + (-.526) Wind speed $_{max}$	.640 (significant at 0.01)	= 51.797 + (-.905) Temperature $_{max}$ + (.747) Temperature $_{min}$ + (-.549) Wind speed $_{max}$	.639 (significant at 0.01)
Winter	= 61.402 + (.019) Evaporation + (-.160) Temperature $_{max}$ + (-1.162) Temperature $_{min}$ + (-.196) Rain + (-.020) Wind direction $_{max}$ + (.321) Wind speed $_{max}$	.624 (significant at 0.01)	= 61.044 + (-1.304) Temperature $_{min}$ + (-.018) Wind direction $_{max}$	.614 (significant at 0.01)

To test which annual model is better to use, RMSE (Root Mean Square of Error) is calculated for different linear models of enter and stepwise. Predicted amounts using the different annual models for 25 days during 2011 are calculated and compared with observed data during those days using RMSE equation:

$$\mathrm{RMSE} = \sqrt{\frac{\sum_{i=1}^{n}(O_{obs} - O_{pre})^2}{n}}$$

O_{obs}: observed NO_2 value

O_{Pre}: predicted NO_2 value using model

The values of RMSE in both linear models of enter and stepwise is equal (16) show capability of stepwise model in predicting NO_2 amount compared to enter model due to easy calculation. This result which is the same as the other results [25, 26, and 27] indicate for predicting most of air pollutants like Nitrogen dioxide, we may take into consideration only linear models of stepwise which need less data compared to enter model and also its calculation is easier than other models. Results showed that quantities of NO_2 in different seasons and whole year could be estimated by climate parameters. Results also indicated that relations between the NO_2 and meteorological parameters are stronger than whole year during the seasons.

Actually it shows that NO_2 levels during the seasons may have larger peaks of NO_2 than whole year. The findings of the current study should be considered with its limitations.

CONCLUSIONS

In the current research air quality analyses for Isfahan, are conducted for NO_2. Isfahan is one of the most polluted cities in Iran. Hence a need was felt to carry out an ambient air quality analysis in this city. Results show there is significant relationship between NO_2 and some meteorological parameters. Based on these relations, different multiple linear regression equations for NO_2 for annual and seasonal conditions were prepared. Results show among different prediction models, stepwise model is the best option. Results also showed that quantities of NO_2 in different seasons and whole year could be estimated by climate parameters. Results also indicated that relations between the NO_2 and meteorological parameters are stronger than whole year during the seasons. Also different variations in concentration during day, months and seasons were observed. Unfortunately, all graphs showed that the concentrations of the Nitrogen dioxide are upper than Primary Standards of Nitrogen dioxide recommended by National Ambient Air Quality Standards (NAAQS) of Iran. According to the obtained model, if conditions of this present study do not change, life will be impossible in the future years owing to the increasing proportion of pollutants. Therefore, as far as possible, some strategies like reduction in the number of imported vehicles and the proportion of distance travelled by vehicles etc. can be applied to implement the pollution reduction [28, 29, and 30].

ACKNOWLEDGEMENTS

The authors are thankful to the Organization of Environment in Iran, for providing the data, for this risk assessment work.

REFERENCES

[1] Sharma, B.K. (2001) An Introduction to Environmental Pollution. Krishna Prakashan Media (P) Ltd. 1.

[2] Majidnezhad, V.A. (2014) Novel Hybrid Method for Vocal Fold Pathology Diagnosis Based on Russian Language. J. Air and Data Min. 2, 141.

[3] Fleischer, N.L., Merialdi, M., Van Donkelaar, A., Vadillo-Ortega, F., Martin, R.V., Betran, A.P. (2014) Outdoor Air Pollution, Preterm Birth, And Low Birth Weight: Analysis of The World Health Organization Global Survey on Maternal and Perinatal Health. Environ. Health Perspect. 122, 425.

[4] Asghari Esfandani, M., Nematzadeh, H. (2016) Predicting Air Pollution in Tehran: Genetic Algorithm and Back Propagation Neural Network. J. Air and Data Min. 4, 49.

[5] Khader, Y., Abdelrahman, M., Abdo, N., Awad, S., Al-Sharif, M., Elbetieha A. (2016) Exposure to Air Pollution and Pregnancy Outcomes in The East Mediterranean Region: A Systematic Review. Int. J. Pediatr. 4, 1255.

[6] Cunningham, W.P., Cunningham, M.A. (2002) Principles of Environmental Science Inquiry and Applications. Mcgraw Hill Company. 1.

[7] Asrari, E., Sen, P.N., Masoudi, M. (2007) Status of Carbon Mono Oxide in Tehran City- Iran. Pollut. Res. 26, 531.

[8] Ho, L.C., Lin, W.Y. (1994) Semi-Statistical Model for Evaluating the Effects Of Source Emissions And Meteorological Effects On Daily Average No_x Concentrations In South Taiwan. Atmos. Environ. 37, 2051.

[9] Lam, G.C.K, Leong, D.Y.C, Niewiadomski. (1997) Street Level Concentration of No_x And Suspended Particulate Matter in Hong Kong. Atmos. Environ, 93, 1.

[10] Cuhadaroglu, B., Demirci, E. (1997) Influence of Some Meteorological Factors On Air Pollution in Trabzon City. Energy and Buildings. 25, 179.

[11] Mandal, S. (2000) Progressive Decrease of Air Pollution Level from West to East at Calcutta. Indian J. Environ. Protect. 20, 6.
[12] Chelani, A.B. (2001) Statistical Modeling of Ambient Air Pollutants in Delhi. Water, Air and Soil Pollut. 1326, 315.
[13] Abdul-Wahab, S.A., Al-Alawi, S.M. (2002) Assessment and Prediction of Tropospheric Ozone Concentration Levels Using Artificial Neural Networks. Environ Modell Softw. 17, 219.
[14] Sánchez-Ccoyllo, O.R., Andrade, M.F. (2002) The Influence of Meteorological Conditions on The Behavior of Pollutants Concentrations in São Paulo, Brazil. Environ. Pollut. 116, 257.
[15] Sabah, A., Al-Rubiei, R., Al-Shamsi, A. (2003) A Statistical Model for Predicting Carbon Monoxide Levels. Int J Environ Pollut. 19, 209.
[16] Elminir, H.K. (2005) Dependence of Urban Air Pollutants on Meteorology. Sci Total Environ. 350, 225.
[17] Abdul-Wahab, S.A., Bakheit, C.S., Al-Alawi, S.M. (2005) Principal Component and Multiple Regression Analysis in Modelling of Ground-Level Ozone And Factors Affecting Its Concentrations. Environ Modell Softw. 20, 1263,.
[18] Li, L., Qian, J., Ou, C.Q., Zhou, Y.X., Guo, C., Guo, Y. (2014) Spatial and Temporal Analysis of Air Pollution Index and Its Timescale-Dependent Relationship with Meteorological Factors in Guangzhou, China, 2001–2011. Environ. Pollut. 190, 75.
[19] Yoo, J.M., Lee, Y.R., Kim, D., Jeong, M.J., Stockwell, W.R., Kundu, P.K., Oh, S.M., Shin, D.B., Lee, S.J. (2014) New Indices for Wet Scavenging of Air Pollutants (O_3, Co, No_2, So_2, And Pm_{10}) By Summertime Rain. Atmos. Environ. 82, 226.
[20] Wang, S.M., Yu, H., Song, L., Xie, Y., Zhu, Q. (2015) Air Quality in A Mountainous City: A Case Study in Chongqing, China. Fresen. Environ. Bull. 24, 2699.
[21] Mulumba, J.P., Venkataraman, S., Afullo, T.J.O. (2015) Modeling Tropospheric Ozone Climatology Over Irene (South Africa) Using Retrieved Remote Sensing and Ground-Based Measurement Data. J. Remote Sens. Gis. 4, 1.
[22] Masoudi, M., Ordibeheshti, F., Rajaipoor, N., Sakhaei, M. (2016) Status and Preparation of Prediction Models for Ozone As An Air Pollutant In Shiraz, Iran. Pollut. 2, 387.
[23] Masoudi, M., Sakhaei, M., Behzadi, F., Jokar, P. (2016) Status of Pm_{10} As an Air Pollutant and Its Prediction Using Meteorological Parameters in Tehran, Iran. Fresen. Environ. Bull. 25, 2008.
[24] Kinnear, P.R. (2002) Spss For Windows Made Simple Release 10. Psychology Press. 1.
[25] Ordibeheshti, F., Rajai Poor, N. (2014) Study of Air Pollution and Its Relationship with Meteorological Parameters in Shiraz City. Project of B.Sc. Degree in Shiraz University. 1.
[26] Masoudi, M., Behzadi, F., Sakhaei, M. (2014) Status and Prediction of Ozone As An Air Pollutant In Tehran, Iran. Ecology Environment and Conservation. 20, 775.
[27] Asadifard, E. (2013) Study of Air Pollution and Its Relationship with Meteorological Parameters in Ahvaz City. Project of B.Sc. Degree in Shiraz University. 1.
[28] Najafpoor, A.A., Hosseinzadeh, A., Allahyari, S., Javid, A.B., Esmaily H. (2014) Modeling of Co And Nox Produced by Vehicles in Mashhad, 2012. Environmental Health Engineering and Management Journal. 1, 45.
[29] Motesaddi, S., Nowrouz, P., Alizadeh, B., Khalili, F., Nematin, R. (2015) Sulfur Dioxide Aqi Modeling by Artificial Neural Network in Tehran Between 2007 and 2013. Environmental Health Engineering and Management Journal. 2, 173.
[30] Omidi, Y., Goudarzi, G., Heidari, A.M., Daryanoosh, S.M. (2016) Health Impact Assessment of Short- Term Exposure to No2 In Kermanshah, Iran Using AirQ Model. Environmental Health Engineering and Management Journal. 3, 91.

Received: **13.05.2017**
Accepted: **31.12.2017**

CORRESPONDING AUTHOR

Masoud Masoudi
Department of Natural Resources and
Environmental Engineering,
Shiraz University – Iran

e-mail: masoudi@shirazu.ac.ir

© by PSP Volume 27 – No. 5/2018 pages 2751-2760 Fresenius Environmental Bulletin

FUNGI COLONIZING CHRYSANTHEMUMS PLANTS CULTIVATED IN THE FIELD IN DIFFERENT PROTECTION SYSTEMS

Marek Kopacki[1,*], Stanislaw Parafiniuk[2], Barbara Skwarylo-Bednarz[1]

[1]Department of Plant Protection and Quarantine, University of Life Sciences, Leszczynskiego 7, 20-069 Lublin, Poland
[2]Department of Machinery Exploitation and Management of Production Processes, University of Life Sciences Gleboka 28, 20-612 Lublin, Poland

ABSTRACT

The aim of our investigation was to evaluate three fungicides for their antifungal activity against fungi occurring on chrysanthemum plants using two types of nozzles: standard RS-MM 110 03 and ejector type ID 120 03 C.

Studies of three years (2007-2009) were conducted at Czesławice in the south-east of Poland. The objects of research were the plants of cultivar Tripoli Dark. The following agents were used for protection: Dithane NeoTec 75 WG, Sumilex 500 SC and Amistar 250SC. Observations were carried out in October in each year. Diseased plants were collected for mycological analysis. Plants with symptoms of stem and root rot, leaves yellowing and wilt were noticed on the investigated plantations. The results of mycological analysis showed that chrysanthemum plants were colonized by *Fusarium* spp., *Sclerotinia* spp. and *Alternaria* spp. Among isolated fungi *Alternaria alternata*, *Fusarium oxysporum, Fusarium avenaceum* and *Sclerotinia sclerotiorum* predominated among pathogenic species. The best health status and the lowest number of colonies were noticed on plants protected by azoksystrobine with both types of nozzles.

KEYWORDS:
Chrysanthemum, root and stem rot diseases, ejector nozzles

INTRODUCTION

Chrysanthemum (*Chrysanthemum grandiflorum* Ramat. /Kitam.) is one of the most beautiful and the oldest flowering plants commercially grown in different parts of the world. There has been constant demand for chrysanthemum flowers from European market. However, it is difficult to get good quality exportable blooms, higher yields and long lasting postharvest life of the cultivars under open and cover conditions. The beauty of chrysanthemums is spoiled by many soil-borne and air-borne pathogens. Necrotic lesions on roots, stems and leaves and wilt are the most common symptoms of the diseases [1]. The most important factors responsible for these symptoms are the diseases like grey mould [2]. Among the diseases Alternaria leaf blight caused by *Alternaria alternata* is one of the most destructive disease, commonly prevailing in almost all chrysanthemum growing [3]. Septoria leaf spot has a wide geographical distribution, including the Asian, American and European regions [4]. The situation is similar with white rust (CWR) caused by *Puccinia horiana* [5, 6]. Recommended fungicides are often effective but windy weather weakens their effectiveness. In Poland the pesticides should be applied with wind less than 4 m/sec and that is why attempts are being made to improve the effectiveness of spraying and looking for a modern method of application [7, 8]. The main goal in pest-management research is to improve pesticide application technology for its effective action and rapid dissipation from crop tissuses [9].

Effectiveness of spraying depends largely on technique which was used for doing it. In practice of plant protection different types of nozzles are used. In field spraying flat-stream standard nozzles are used most frequently. With higher work pressure they give small and very small droplets which perfectly cover the spraying surface but are prone to drifting. The second kind of tested nozzles were air-ejector nozzles. These nozzles generate a lot of aerated droplets which are less prone to drifting and to a lesser extent cover the spraying surface. Nowadays on the labels of pesticides there is information on parameters of doing spraying and recommended spectrum of droplets [10, 11].

The aim of investigation was to determine the influence of the fungicides sprayed by means of standard and thick drop nozzles on the healthiness of the cv. Tripoli Dark and to estimate the fungal communities colonising the chrysanthemums grown in the field in Czeslawice, Lublin region.

MATERIALS AND METHODS

Experimental design and management. The experiment was conducted at the Agricultural Research Station in Czeslawice, Lublin region, Poland (51°18'23''N 22°16'02''E). The experiment was conducted in a randomized complete blocks design with four replicates where block was the random effect. The chrysanthemum plants were planted in the field in mid May in 60 × 60 spacing. The experimental combination consisted of 36 plants of each cultivar (9 plants in 4 replicates). Chrysanthemum cultivar Tripoli Dark received three levels of fungicide treatments: (1) – non treated control and (2)- three fungicide applications with use of standard RS-MM 110 03 (Marian Mikołajczyk) sprayers and (3) - three fungicide applications with use thick drop nozzles ID 120 03 (Lechler). Fungicide was applied starting 6 weeks after planting and repeated every 14 days thereafter. Three products were used: Dithane NeoTec 75 WG, Sumilex 500 SC and Amistar 250 SC (Table 1).

Weather parameters. Weather parameters, measured at Meteorological Station, were achieved from the Laboratory of Agrometeorology (Czesławice Meteorology Station).

Effectiveness of fungicides. The healthiness of plants was estimated at the blooming period in October using McKinney's formula [12]. Effectiveness of fungicide was estimated using Abbot's formula [13]: S=(A-B)/A x 100% (S- effectiveness, A - diseases index in the control object, B - diseases index in the object with protection).

The results were statistically tested with ANOVA using Statistica 10 software (StatSoft) [14].

Mycological analysis of plants. During flowering (end of October), 6 randomly selected chrysanthemum plants were sampled from each plot. The diseased plants (roots, stems and leaves) were analyzed in laboratory. Plant material was precleaned, rinsed with running water for 20 minutes and then surface disinfected with for 1 minute. Disinfected plant material was rinsed 3 times in distilled water. Next, 3 mm fragments were placed on mineral medium in Petri dishes [16]. For each experimental treatment 10 dishes with plant material, 10 plant fragments, were prepared and incubated in the thermostat at 20–22ºC for 7 days in darkness. The obtained fungal colonies were transferred to potato dextrose medium (PDA, Difco) and identified to the species with the available monographs.

RESULTS

Weather. Weather conditions in 2007–2009 were very favourable for the development of fungal diseases (Tab. 2). Average precipitation per month from May to the end of October in 2007, 2008, 2009 was 22,6 to 125,8mm respectively (according to Czeslawice Meteorology Station).

Effectiveness of fungicides. Study in the field. Several symptoms were observed on diseased plants: yellowing (Fig. 1) and necrosis of leaves (Fig. 2), stem and root rot (Fig. 3) and tracheomycosis. Weather conditions in 2007–2009 were very favourable for the development of grey mould and alternariosis (Tab. 2). The highest mean effectiveness of fungicides in 2007 was noticed for Amistar 250 SC with thick drops nozzles (29%) and the lowest one for Dithane NeoTec 75WG with standard nozzles (17%). In 2008 the highest mean effectiveness of fungicides was noticed for Amistar 250 SC with thick drops nozzles (65%) and the lowest one for Sumilex 500SC with standard nozzles (23%). The highest mean effectiveness of fungicides in 2009 was noticed for Amistar 250 SC with standard nozzles (27%) and the lowest one for Amistar 250 SC with thick drops nozzles (10%) (Tab. 3). Effectiveness of fungicides for the tested fungicides varied statistically and its values depended on pesticides and weather conditions (Tab. 2).

TABLE 1
Active ingredients of fungicides used in investigation

Combination	Formulation	Active ingredient	Producer	Dose (%)
Control	-	-	-	-
Dithane NeoTec 75 WG	WG	mancozeb	Dow AgroSciences Polska	0,2
Dithane NeoTec 75 WG- ID	WG	mancozeb	Dow AgroSciences Polska	0,2
Sumilex 500 SC	SC	procymidone	Sumi-Agro Poland	0,1
Sumilex 500 SC - ID	SC	procymidone	Sumi-Agro Poland	0,1
Amistar 250 SC	SC	azoksystrobine	Syngenta Polska Sp. z o.o.	0,1
Amistar 250 SC - ID	SC	azoksystrobine	Syngenta Polska Sp. z o.o.	0,1

Pressure of spray amounted to 3 bars and working speed was 4 km/h

TABLE 2
Average monthly temperature (°C) and rainfall in months (mm).

Year	Average monthly temperature (°C)					Sum of rainfall in months (mm)				
	V	VI	VII	VIII	IX	V	VI	VII	VIII	IX
2007	14.9	18.2	18.8	18.8	13.0	46.4	85.1	70.0	31.4	105.1
2008	12.5	16.8	18.4	18.6	12.1	103.8	30.2	77.1	55.1	78.2
2009	12.7	15.9	19.6	18.3	15.2	72.2	125.8	55.6	57.5	22.6
Multiannual mean for 1951–2005	13.0	16.2	17.8	17.7	12.6	57.7	65.7	83.5	79.2	51.6



FIGURE 1
Yellowing of leaves of chrysanthemum and first necrotic spots



FIGURE 2
Necrotic spots on leaves of chrysanthemum



FIGURE 3
Decaying of basal stems

TABLE 3
Effectiveness of fungicides.

Combination	Year of research					
	2007		2008		2009	
	ID	Eff	ID	Eff	ID	Eff
Control	45,250a*	-	81,500a	-	21,000a	-
Dithane NeoTec 75WG	32,500ab	17	71,750c	24	16,500a	20
Dithane NeoTec75WG -ID	34,250ab	22	74,250bc	56	18,750a	11
Sumilex 500 SC	35,000ab	20	82,000a	23	17,250a	17
Sumilex 500 SC - ID	36,750ab	25	78,000ab	61	17,250a	17
Amistar 250 SC	21,750ab	21	58,000d	47	15,250a	27
Amistar 250 SC - ID	20,750b	29	57,500d	65	18,500a	10
HSD	24,182		4,9861		11,458	

* values marked with the same letters (a, b, c...) within columns do not significantly differ at 5% error

The results of three-year investigation showed that the type of atomizer had no effect on the populations of chrysanthemum pathogens. We saw the differences between monitored fields where we didn't carry out the security plants and fields where was this operation. On the monitored fields all plants had diseases symptoms. The chemical preparation which used have influence on this illness. The best was Amistar 250 SC chemical preparation especially in 2008. More effective was Amistar 250 SC and Sumilex 500 SC preparations which used in thick drops nozzles ID" with broad-spectrum of drops. Where we used Dithane NeoTec 75 WG preparation and standard RS-MM nozzles all plants were infect with lots of symptoms. Because we didn't have enough parameters we must continue more investigation about effectiveness protection at use of different kinds of nozzles.

To define the degree of covering plants with fungicide when doing plant spraying with two kinds of nozzles, water sensitive papers were placed on plants on the upper part. After spraying the papers were scanned and the obtained image was analysed. The image analysis was done with the use of Image-Pro Premier 3D. The degree of covering the water sensitive papers was defined in percentage. The diameter of droplets which fell on the plants was measured and the number of droplets which were on the analysed surface was defined. Percentage share in particular fractions of droplets in eight size intervals was defined. Average results from eight measurements for each kind of nozzles were presented in Table 1 [15].

TABLE 4
The degree of covering the sprayed surface with the use of two kinds of spraying nozzles.

	Average sample from RS- MM 110 03	Average sample from Lechler ID 120 03
Sample surface area [mm^2]	1000,00	1000,00
Droplets surface area [um^2]	4968647,25	1168369,53
Degree of covering [%]	49,19	22,81
Number of droplets [pcs.]	360	199

TABLE 5
The average degree of covering the sprayed surface in 8 size intervals of droplets for two kinds of tested nozzles.

Range	Average sample from RS- MM 110 03			Average sample from Lechler ID 120 03		
	Droplets surface area	% sample area	Number of droplets	Droplets surface area	% sample surface	Number of droplets
[um]	[um2]	[%]	[pcs.]	[um2]	[%]	[pcs.]
0-49	105411,26	1,04	226	168755,84	1,67	85,33
50-99	312333,04	3,09	65	662774,30	6,56	48,17
100-249	1261450,60	12,49	53	911738,46	9,03	28,00
250-399	1184517,21	11,73	12	404589,92	4,01	4,33
400-599	707590,34	7,01	3	120516,02	1,19	0,67
600-999	388391,50	3,85	1	359321,23	3,56	32,67
1000-1499	173218,61	1,71	1	0,00	0,00	0,00
1500 i pow.	835734,68	8,27	1	0,00	0,00	0,00

To measure the degree of covering water sensitive papers were used. The papers were attached to leaves of sprayed plants. On each paper the area of 1000 mm2 surface was analysed. On the basis of the image analysis of the measured surface it was stated that droplets generated by standard atomizers RS MM gave the average degree of covering 49,19% of the spayed surface and the number of these droplets was 360 pieces. Whereas, with the same parameters of spraying, the average degree of covering with droplets generated by air-ejector atomizers was 22,81% and the number of droplets was 199.

Analysing the average degree of covering the sprayed surface in 8 size intervals of droplet trace for two kinds of tested nozzles (tab. 2) it was stated that standard nozzles generated the most droplets from the size interval from 0 to 49 um. Average uniformity of these droplets was 226 pieces, while these droplets covered only 1,04% of the tested area. The largest degree of covering for standard nozzles was occupied by droplet traces from the size interval 100-249 um (12,49%) and 250-399 um (11,73%) for which the number of droplet traces was respectively 53 and 12 pieces. In another size intervals of droplet traces their number was little 1-3 but their degree of covering was quite considerable and they occupied almost the half of the area covered by droplet traces. It was caused by the fact that traces of largest droplets joined together creating the uniform surface.

Air-ejector nozzles also in the largest number generated droplets whose trace was in the interval from 0 to 49 um. The number of these droplet traces was 85 pieces and the surface covered with them occupied 1,67% of the analysed area. The largest percentage participation of the covered area was occupied by droplet traces from the interval 100-249 um. The number of these traces was 28 pieces. A quite considerable number of droplet traces in this type of nozzles was occupied by traces from the range 600-999um, their average number was 33 pieces and the area which they occupied was 3,56% of the analysed surface. In this type of nozzle there was no signs of droplets bigger than 1000 um.

The analysis of the image of the sprayed surface with two kinds of nozzles showed that standard nozzles give higher degree of covering and traces of particular droplets join together in bigger areas; whereas air-ejector nozzles give a smaller degree of covering and the number of droplets generated at these nozzles is smaller.

Mycological analysis of plants. In 2007–2009 from roots, as the result of mycological analysis, 1456 fungal colonies belonging to 17 species were isolated. The predominating species were *Alternaria alternata*, *Fusarium* spp., *Botrytis cinerea* and *Sclerotinia sclerotiorum* (Tab. 6). More colonies were obtained in autumn than in summer. From stems were isolated 1689 fungal colonies belonging to 20 species (Tab. 7). In 2007–2009 from leaves

1140 fungal colonies belonging to 18 species were isolated (Tab. 8).

A. alternata, *Fusarium* spp. and *S. sclerotiorum* predominated among fungi which are regarded as pathogenic. The occurrence of indiwidual species of *Fusarium* depended on the used fungicides. *F. oxysporum* was isolated frequently from all plant organs especially from plants treated by azoksystrobine with both types of nozzles. Numerous colonies of *F. avenaceum* were obtained every year especially from chrysanthemum roots and stems treated with mancozeb, procymidone and azoksystrobine. *A. alternata* occurred on all plants but more frequently on plants treated with mancozeb and procymidone. *S. sclerotiorum* colonised frequently leaves and stems. Also three other fungi: *C. obtusisporum*, *R. solani* and *S. chrysanthemella* were isolated frequently. *Rhizoctonia. solani*, *S. sclerotiorum*, *B. cinerea* and *C. destructans* colonised the plants very rarely.

TABLE 6
Fungi colonizing roots of chrysanthemum.

Year	Fungus species	Control	Dithane		Sumilex		Amistar		Total (%)
			S	ID	S	ID	S	ID	
	Alternaria alternata (Fr.) Keiss.	58	56	41	21	12	12	16	216 (38)
	Botrytis cinerea Pers. ex Fries.	16							16(3)
	Cylindrocarpon destructans (Zins.) Sch.	6		4					10(2)
	Epicoccum nigrum Link	14	8	11	1				34(6)
	Fusarium avenaceum (Corda ex Fries) Sacc.	13	14	2	6	4	2	2	43(7)
07	*Fusarium equiseti* (Corda) Sacc.	21				12			33(6)
	Fusarium oxysporum Schlecht.	6	4	8	4	2	2	12	38(7)
	Gliocladium catenulatum Gill. et Abb..	10				1			11(2)
	Mucor mucedo Mich. Ex St.-Am.	11							11(2)
	Penicillium expansum Link ex S.F.Gray	22					1	2	25(4)
	Thanatheporus cucumeris Kühn	21	11	1		1			34(6)
	Sclerotinia slerotiorum (Lib.) de By	21	11						32(6)
	Trichoderma harzianum Rifai	2	14				1	1	18(3)
	Trichoderma koningii Oud.	14	1	2		1	14	18	50(8)
	total	235	119	69	32	33	32	51	571
	Alternaria alternata (Fr.) Keiss.	13		29	12	41	22	31	148 (24)
	Aspergillus niger van Tieghem			11			4	34	49(8)
	Botrytis cinerea Pers. ex Fries.				5	23		8	36(6)
	Epicoccum nigrum Link	3		23				21	47(8)
	Fusarium avenaceum (Corda ex Fries) Sacc.	3		2	4	12	8	22	51(8)
	Fusarium culmorum (Smith) Sacc.	3		14					17(3)
08	*Fusarium equiseti* (Corda) Sacc.				2	2			4 (1)
	Fusarium oxysporum Schlecht.	6		6	2	14	6	31	65 (11)
	Mucor mucedo Mich. Ex St.-Am.				7	12			19 (3)
	Penicillium expansum Link ex S.F. Gray	6		3			4	12	25 (4)
	Sclerotinia slerotiorum (Lib.) de By					12	2	32	46 (8)
	Trichoderma harzianum Rifai			2	11	5	6	21	45 (7)
	Trichoderma koningii Oud.	3					4	14	21 (3)
	Verticillium dahliae Kleb.						14	22	36 (6)
	total	37		90	43	121	70	248	609
	Alternaria alternata (Fr.) Keiss.	11	7	6			2	2	28(10)
	Botrytis cinerea Pers. ex Fries.	2							2(1)
	Cylindrocarpon destructans (Cooke&Hark.)	4	7		11		4	2	28(10)
	Epicoccum nigrum Link						6		6(2)
	Fusarium avenaceum (Corda ex Fries) Sacc.	4		6		4	4	4	22(8)
	Fusarium equiseti (Corda) Sacc.	2							2(1)
09	*Fusarium oxysporum* Schlecht.	13	13	26	7	18	2	18	97(35)
	Gliocladium catenulatum Gill. et Abb..		7						7(3)
	Penicillium expansum Link ex S.F.Gray	1				8		6	15(5)
	Penicillium nigricans (Bain.) Thom			6					6(2)
	Stemhyllium botryosum Wallr.	4			2				6(2)
	Thanatheporus cucumeris Kühn	4	3		8	8	17	8	48(17)
	Trichoderma harzianum Rifai	2							2(1)
	Trichoderma koningii Oud.			2			5		7(3)
	total	47	37	46	28	38	49	40	276

TABLE 7
Fungi colonizing stems of chrysanthemum.

Year	Fungus species	Control	Dithane		Sumilex		Amistar		Total (%)
			S	ID	S	ID	S	ID	
	Alternaria alternata (Fr.) Keiss.	67	18	2	41	32	8	2	170(31)
	Aspergillus niger van Tieghem	4			3				7(1)
	Botrytis cinerea Pers.ex Fries.	18	14						32(6)
	Cladosporium cladosporioides (Fres.) deVries	2				2	2		6(1)
	Cylindrocarpon destructans (Cooke&Hark.)	2	4						6(1)
	Chaetomium cochlioides Palliser		2	14	2				18(3)
	Fusarium avenaceum (Corda ex Fries) Sacc.	2	2	9	3	4	2	1	23(4)
07	*Fusarium culmorum* (Smith) Sacc.		3						3(1)
	Fusarium equiseti (Corda) Sacc.	8		2	14			2	26(5)
	Fusarium oxysporum Schlecht.	12	4	2	2	4	1		25(5)
	Fusarium sporotrichioides Scherb.	2				2			4(1)
	Gliocladium catenulatum Gill. et Abb..	14				3		2	19(3)
	Penicillium verrucosum Dierckx	13	14		4		2		33(6)
	Phoma chrysanthemicola Hollos	4							4(1)
	Thanatheporus cucumeris Kühn	8	3			2		1	14(3)
	Sclerotinia slerotiorum (Lib.) de By	42	31	16	10	3	1		103(19)
	Trichoderma harzianum Rifai	18	12	2		2	13	1	48(8)
	Truncatella angustata (Pers.ex Lk) Hughes	4	2				2		8(1)
	total	220	109	47	79	54	31	9	549
	Alternaria alternata (Fr.) Keiss.	27		17	11	12	18	39	124(20)
	Botrytis cinerea Pers.ex Fries.	-		12	-	18	7	7	44 (7)
	Epicoccum nigrum Link	2		-	-	13	-	-	15 (2)
	Fusarium avenaceum (CordaexFries) Sacc.	3		-	19	13	19	21	75 (12)
	Fusarium culmorum (Smith) Sacc.	2		-	-	19	-	-	21 (3)
08	*Fusarium equiseti* (Corda) Sacc.	-		12	-	-	-	-	12 (2)
	Fusarium oxysporum Schlecht.	11		18	-	14	9	27	79 (12)
	Mucor mucedo Mich.Ex St.-Am.	-		7	-	-	-	21	28 (4)
	Penicillium expansum Link ex S.F.Gray	-		-	23	-	-	13	36 (6)
	Sclerotinia slerotiorum (Lib.) de By	-		17	-	29	14	28	88 (14)
	Trichoderma harzianum Rifai	-		22	13	11	-	19	65 (10)
	Verticillium dahliae Kleb.	14		-	-	23	13	-	50 (8)
	total	59		105	66	152	80	175	637
	Alternaria alternata (Fr.) Keiss.	4	5	9	7	46	9	3	83(17)
	Botrytis cinerea Pers.ex Fries.	12					2		14(3)
	Cylindrocarpon destructans (Zins.) Sch.	11	13				8		32(6)
	Epicoccum nigrum Link				11	6			17(3)
09	*Fusarium avenaceum* (Corda ex Fries) Sacc.	4	34	19	23	4	12	10	106(21)
	Fusarium culmorum (Smith)Sacc.	11	3			32	18		64(13)
	Fusarium equiseti (Corda)Sacc.					2	2		4(1)
	Fusarium oxysporum Schlecht.	12		9	2	2	19	4	48(9)
	Gliocladium catenulatum Gill. et Abb..				3			2	5(1)
	Penicillium nigricans (Bain.) Thom	2		4	2		2		10(2)
	Thanatheporus cucumeris Kühn	19			5	4	2	11	41(8)
	Stemhyllium botryosum Wallr.	4							4(1)
	Trichoderma harzianum Rifai			10			21		31(6)
	Trichoderma koningii Oud.	12		2		8	13	9	44(9)
	total	91	55	53	53	104	108	39	503

DISCUSSION

The results of investigations showed the effect of tested fungicides on the health status of chrysanthemums. During the time of experiment the statistically significant differences were observed despite rather low disease index. Probably with stronger infection pressure it would be possible to observe the greater differences in the effectiveness of tested fungicides with the application of various drop nozzles [17]. The results proved that *Fusarium* spp., *S. sclerotiorum* and *R. solani* were most probably the cause of diseases of chrysanthemum grown in the field. The populations of these fungi differed between years and seasons what was probably due to weather conditions as the high humidity of soil favours the development of these species [18, 19]. *F. oxysporum* is known as the pathogen of chrysanthemum in many countries [20]. Also *F. avenaceum* is regarded by some researches as the cause of stem and root rot, as well as flower blight [21]. *R. solani*, isolated mostly from roots and stems, was observed also in other countries as the cause of stem rot and leaves spot [22]. *S. sclerotiorum* causes rots of many crops under conditions of high humidity. Such conditions occur under covers, especially in autumn. The pathogen has a great importance in many countries, especially in Asia [23].

TABLE 8
Fungi colonizing leaves of chrysanthemum.

Year	Fungus species	Control	Dithane		Sumilex		Amistar		Total (%)
			S	ID	S	ID	S	ID	
	Alternaria alternata (Fr.)Keiss.	14	12	2	23	3	12	8	74(27)
	Alternaria chrysanthemi Simmons & Crossier	10		1					11(4)
	Botrytis cinerea Pers.ex Fries.	53	4					1	58(21)
	Epicoccum nigrum Link	6	13		3	1	1		24(8)
	Fusarium avenaceum (CordaexFries)Sacc.	4	2	2	2	1	3	1	15(5)
07	*Fusarium oxysporum* Schlecht.	8							8(3)
	Gliocladium catenulatum Gillman & Abbot			3				4	7(2)
	Penicillium expansum Link ex S.F.Gray	11	12	2					25(9)
	Thanatheporus cucumeris Kühn	3							3(1)
	Septoria chrysanthemella Sacc.	2					2		4(1)
	Stemphyllium lycopersici (Enjoji) W.Yam.	4	14	2					20(7)
	Trichoderma koningii Oud.	13	11	3		2	2	3	34(12)
	total	128	68	15	28	7	20	17	283
	Alternaria alternata (Fr.)Keiss.	4		25	-	11	-	31	71(16)
	Botrytis cinerea Pers.ex Fries.	-		13	2	8	-	12	35(8)
	Cladosporium cladosporioides (Fres.) deVries	6		31	-	-	-	17	54(13)
	Fusarium avenaceum (Corda ex Fries) Sacc.	-		7	-	-	12	16	35(8)
	Fusarium equiseti (Corda) Sacc.	5		-	2	-	8	4	19(5)
	Fusarium oxysporum Schlecht.	2		6	-	-	5	18	31(7)
	Mucor mucedo Mich.Ex St.-Am.	4		6	-	16	21	12	59(14)
08	*Penicillium nigricans* (Bain.) Thom	-		-	-	9	3	14	26(6)
	Sclerotinia slerotiorum (Lib.) de By			12	-	-	-	31	43(10)
	Trichoderma harzianum Rifai	6		11	3	-	3	-	23(5)
	Trichoderma koningii Oud.	8		-	-	-	-	27	35(8)
	total	35		111	7	44	52	182	431
	Alternaria alternata (Fr.) Keiss.	35	23	34	12	23	12	8	147(35)
	Aspergillus niger van Tieghem	2			4			1	7(2)
	Botrytis cinerea Pers.ex Fries.	4	6	6	5		2		23(5)
	Cylindrocarpon destructans (Zins.) Sch.		3						3(1)
	Epicoccum nigrum Link	10	9		4	4	11	10	48(11)
09	*Fusarium avenaceum* (Corda ex Fries) Sacc.	4	2		16	2	12	10	46(11)
	Fusarium culmorum (Smith) Sacc.	4					2		6(1)
	Fusarium oxysporum Schlecht.	14	4		2	2	11	9	42(10)
	Penicillium expansum Link ex S.F.Gray	21			2				23(5)
	Penicillium verrucosum Dierckx	2		4					6(1)
	Septoria chrysanthemella Sacc.	14	2	12		4			32(8)
	Trichoderma koningii Oud.	12		24	4			3	43(10)
	total	122	49	80	49	35	50	41	426

P. chrysanthemicola, B. setariae and *S. chrysanthemella*, known for their pathogenicity to chrysanthemum [24, 25], were not isolated frequently from analysed plants.

A. alternata is regarded very often as weak pathogen but its importance for health status of many crops is increasing recently. In Poland this species was not connected with chrysanthemum diseases while in China it caused considerable losses in chrysanthemum production [26]. Numerous populations of *A. alternata* obtained in our investigations suggest further studies on its pathogenicity to chrysanthemum.

Frequently isolated antagonistic fungi, like *Trichoderma* sp. or *Chaetomium* sp., have a great influence on healthness of chrysanthemum plants due to the reduction of pathogenic fungi number, especially in the soil [27].

It should be observed that with the application of standard as well as ejector nozzles, the health status of plants was the best when the azoxystrobine was used. Only in 2009 the disease index in this combination did not differ from the control. The effectiveness of azoxystrobine as the active ingredient is known for many years [28]. This fungicides has also a positive effect on the physiological processes in leaves [29]. During our experiment, the colour of leaves on the plots treated with azoxystrobine was of darker green. However, too often application of this active ingredient might cause the resistance of fungi [30]. The inconsiderable effect of nozzles might be due to the weather conditions during the experiment and the low infection pressure of pathogens on the tested plants.

REFERENCES

[1] Kopacki, M., Wagner, A. (2006) Effect of some fungicides on mycelium growth of *Fusarium avenaceum* pathogenic to chrysanthemum (*Dendranthema grandiflora* Tzvelev). Agronomy Research. 4, 237-240

[2] Sugawara, K., Chikuo, Y., Hagiwara, H., Rzutu, S. (2000) Occurrence of gray mold caused by *Botrytis cinerea* on osteospermum, yellow kosmos and swamp chrysanthemum. Annual Report of the Society of Plant Protection of North Japan. 51, 119-121.

[3] Arum Kumar, G.S., Kamanna, B.C., Benagi V.I. (2011) Management of chrysanthemum leaf blight caused by Alternaria alternata (Fr.) Keissler under field condition. Plant Archives. 11(1), 553-555.

[4] Azimi-Motem, H., Osipyan, L.L. (2009) Taxonomic notes on the genus Septoria of several ornamental plants in Iran. Biolog. Journal of Armenia. 3(61), 10-15.

[5] Velasco, R.G., Mejia, E.Z., Martinez, R.I.R., Mir, S.G.L., Simpson, J.K., Davila, G.F. (2005) Antagonismo de *Cladosporium* sp. contra *Puccinia horiana* Henn. causante de la roya blanca del crisantemo (*Dendranthema grandiflora* Tzvelev). Revista Mexicana de Fitopatologia. 23(1), 79-86.

[6] Bonde, M.R., Murphy, C.A., Bauchan, G.R., Luster, D.G., Palmer, C.L., Nester, S.E., Revell, J.M., Berner, D.K. (2015) Evidence for Systemic Infection by Puccinia horiana, Causal Agent of Chrysanthemum White Rust, in Chrysanthemum. Phytopathology. 105, 91-98.

[7] Doruchowski, G. (2013) Challenges and advances in pesticide application technology. Communications in agricultural and applied biological sciences. 78(2), 3-5.

[8] Subr, A.K., Sawa, J., Parafiniuk, S. (2015) Practical deviation in sustainable pesticide application process. Agriculture and Agricultural Science Procedia. 7, 241-248.

[9] Gamliel, A. (2010) Application aspects of integrated pest management. Journal of Plant Pathology. 92(4-Suppl.), 23-26.

[10] Nuyttens, D., De Schampheleire, M., Verboven, P., Brusselman, E., Dekeyser, D. (2009) Droplet size and velocity characteristics of agricultural sprays. Trans. ASABE. 52(5), 1471−1480.

[11] Hewitt, A.J. (1998) The importance of nozzle selection and droplet size control in spray application. The North American Conf. Pest. Spray Drift Manag. Portland, Univ. Maine. March 29 - April 1, 1998, 75–85.

[12] Parafiniuk, S., Kopacki, M. (2012) Biological efficacy of the chemical chrysanthemums protection with the use of fine and coarse droplets. Journal of Central European Agriculture. 13(3), 554-559.

[13] Jańczak, C., Pawlak, A. (2004) Susceptibility of the Esprit hybrid rye cultivar. Biul IHAR. 221, 287-295.

[14] Frątczak, E., Pęczkowski, M., Sienkiewicz, K. (2005) Statystyka od podstaw z systemem SAS wersja 9.1. SGH Warszawa. 115-135.

[15] Thacker, J.R.M., Hall, F.R. (1991) The effects of drop size and formulation upon the spread of pesticide droplets impacting on water-sensitive papers. Journal of Environmental Science and Health, Part B Pesticides, Food Contaminants, and Agricultural Wastes. 26(5-6), 631-651.

[16] Kopacki, M., Wagner, A. (2003) Health status of garden mums *(Dendranthema grandiflora* Tzvelev*)* in Lublin region. Sodininkyste ir Darzinikyste (Horticulture and Vegetable Growing). 22(3), 89-90.

[17] Foque, D., Nuyttens, D. (2011) Effects of nozzle type and spray angle on spray deposition in ivy pot plants. Pest Management Science. 67(2), 199-208.

[18] Chauhan, S., Tandon, M.P., Bhargava, V. (1996) Annual recurrence of fusaria in the rhizosphere of ornamental crops grown in different soils of Allahabad. Philipp. J. Sci. 125(4), 301-303.

[19] Horst, R.K., Nelson, P.E. (1997) Compendium of Chrysanthemum diseases. APS Press: St. Paul, 62p.

[20] Singh, P.K., Kumar, V. (2014) Fusarium Wilt of Chrysanthemum – Problems and Prospects. Plant Pathology & Quarantine. 4(1), 34–44.

[21] Kopacki, M., Wagner, A., Michałek, W. (2016) Pathogenicity of Fusarium oxysporum, Fusarium avenaceum and Sclerotinia sclerotiorum and their effect on photosynthetic activity of chrysanthemum plants. Acta Sci. Pol.-Hortorum Cultus. 15(3), 59-70

[22] Alam, M., Sattar, A., Abdul-Khaliq Samad A., Khanuja, S.P.S. (2006) A root rot and wilt disease of pyrethrum (*Chrysanthemum cinerariaefolium*) caused by *Rhizoctonia solani* AG-4 in the north Indian plains. Plant Pathology. 55, 301.

[23] Alvarez-Castellanos, P.P., Bishop Ch., D., Pascual-Villalobos, M.J. (2001) Antifungal activity of the essential oil of flowerheads of garland chrysanthemum (*Chrysanthemum coronarium*) against agricultural pathogens. Phytochemistry, 57(1), 99-102

[24] Bartyńska, M. (1998) Grzyby zasiedlające chore rośliny złocienia wielkokwiatowego (*Dendranthema grandiflora* Tzvelev). Zesz. Nauk. AR Krak. 333, 671-674.

[25] Verkley, G.J.M., Quaedvlieg, W., Shin, H.-D., Crous, P.W. (2013) A new approach to species delimitation in Septoria. Studies in Mycology. 75, 213–305.

[26] Xu, G.J., Chen, S.J., Chen, F.D. (2009) Isolation and Identification of Alternaria sp. Causing Black Spot in Chrysanthemum (*Dendranthema×grandiflorum*). Jiangsu. J. Agric. Sci. 25, 752.
[27] Song, W.L., Dai, C.C., Liu, X.Z., Cai, X.Z. (2010) The effect of different endophytic fungi on Chrysanthemum morifolium output and quality. Zhong Yao Cai. 33(1), 4-7.
[28] Wong, F.P., Wilcox, W.F. (2001) Comparative Physical Modes of Action of Azoxystrobin, Mancozeb, and Metalaxyl Against Plasmopara viticola (Grapevine Downy Mildew). Plant Dis. 85, 649-656.
[29] Włodarek, A., Sobolewski, J., Robak, J. (2016) Possibilities of integrated protection against Alternaria leaf spot (Alternaria spp.) of Chinese cabbage using three different groups of plant protection products. Progress in Plant Protection. 56, 150-154.
[30] Mavroeidi, V.I., Shaw, M.W. (2005) Sensitivity distributions and cross-resistance patterns of Mycosphaerella graminicola to fluquinconazole, prochloraz and azoxystrobin over a period of 9 years. Crop Protection. 24, 259–266.

Received: **10.06.2017**
Accepted: **10.02.2018**

CORRESPONDING AUTHOR

Marek Kopacki
University of Life Sciences in Lublin
Departament of Plant Protection and Quarantine
ul. Leszczynskiego 7,
20-069 Lublin – Poland

e-mail: marekkopacki01@gmail.com

© by PSP Volume 27 – No. 5/2018 pages 2761-2767 Fresenius Environmental Bulletin

COMPARISON OF ANTIBIOTIC SENSITIVITY RATIO OF *ESHERICHIA COLI* AND *KLEBSIELLA PNEUMONIAE* STRAINS ISOLATED FROM VARIOUS CLINICAL SPECIMENS IN INTENSIVE CARE UNIT

Nur Ceyhan-Guvensen[1,*], Dilek Keskin[2], Funda Sankur[3]

[1]Mugla Sitki Kocman University, Faculty of Sciences, Department of Biology, Mugla, Turkey
[2]Adnan Menderes University, Cine Vocational High School, Aydin, Turkey
[3]Mugla Sitki Kocman University Research Hospital, Mugla, Turkey

ABSTRACT

A retrospective analysis of the widely used antibiotics all susceptibility testing results from *Esherichia coli* and *Klebsiella pneumoniae* cultured from clinical specimens Muğla Sıtkı Koçman University Educatioan and Research hospital (January to December in 2015) was performed. The new BD PHOENIX automated microbiology system (Becton Dickinson Diagnostic Systems, Sparks, Md.) is designed for automated rapid antimicrobial susceptibility testing and identification of clinically relevant bacteria. Minimum Inhibitory Concentration (MIC) results previously obtained in recent clinical isolates with well-defined in isolates with well-characterized resistance mechanisms with the microdilution method were re-interpreted for the susceptible, intermediate and resistant categories using the 2012 EUCAST breakpoints. Clinical samples are most commonly isolated from tracheal aspirates, wound site, blood, mucus, abcess, catheter, urine samples, throat and nose cultures. *E.coli* isolates were highly resistant to Ciprofloxacin (CIP), Cefepime (FEP), and Aztreonam (ATM) 47%, %47 and 40% respectively. Unlike *K.pneumoniae* isolates were highly resistant to Ampicillin/Sulbactam (SAM), ATM and FEP 58%, 53% and 50% respectively. Both of the bacteria showed the highest sensitivity rate to Amikacin (AN) 98% and 90% *E.coli* and *K.pneumoniae* respectively. Out of the 60 *E.coli* strains 34 (57%) isolates showed Multiple Antibiotic Resistance (MAR) two to ten antibiotics. Out of the 60 *K.pneumoniae* strains 38 (63%) isolates showed MAR two to ten antibiotics. Considering the antibiogram, AN and Meropenem (MEM) should be preferred drugs for *K. pneumoniae* and *E.coli* infection isolated from clinical samples.

KEYWORDS:
Esherichia coli, *Klebsiella pneumoniae*, antibiotic sensitivity, clinical specimens, intensive care unit

INTRODUCTION

Antibiotic resistance in Gram-negative bacteria is a major threat to public health [1-4]. Patients with non-severe infections caused by multidrug-resistant bacteria are subject to in-hospital intravenous therapy because there are no effective oral drugs available. Resistance to empirical antibiotic therapy results in delayed appropriate antibiotic treatment for severe infections, which is associated with increased mortality, prolonged hospital stay and higher costs [5-7]. Further, resistance challenges the achievements of modern medicine, including advanced surgery and immunosuppressive treatment, which are dependent on effective antibiotics.

Escherichia coli and *Klebsiella pneumoniae* are two important members of Gram-negative rods (Enterobacteriaceae), which belongs to a part of human gastrointestinal normal flora [8-10]. These organisms are substantial human pathogens which lead to a wide spectrum of hospital and community-acquired infections such as urinary tract infection (UTI), septicemia, pneumonia, peritonitis, meningitis, etc. [11, 12]. In the lack of appropriate treatment of infections by these organisms, noticeable morbidities and mortalities will occur [13].

The aim of this study was to determine the characteristics and patterns of antibiotic resistance among isolates of *Escherichia coli* and *Klebsiella pneumoniae* recovered from clinical specimens in Muğla

MATERIALS AND METHODS

Bacterial isolates. Ethical approval is was taken before study. Because of retrospective analysis, we did not patient approval. 60 *Escherichia coli* and 60 *Klebsiella pneumoniae* were isolated from clinical specimens from intensive care unit of internal medicine in Muğla Sıtkı Koçman University Education and Research hospital. Bacterial isolates were identified to level of species and subspecies by using the morphological and traditional biochemical

tests and automatic diagnostic systems currently present in the market and commonly used for AST (Antimicrobial Susceptibility Testing) in clinical laboratories will therefore have to incorporate these criteria in their instruments to meet the needs of European microbiology laboratories according to standard methods described by [14-16]. All isolates were obtained from patients at intensive care units. In total, 120 *Escherichia coli* and *Klebsiella pneumoniae* were isolated from various clinical samples and detected by the PHOENIX (Becton Dickinson, USA) at the microbiology laboratory of our hospital between from January to December 2015.The PhoenixTM Automated Microbiology System (BD Diagnostics, Sparks, MD, USA) is designed for the rapid bacterial identification at the species level and determination of AST of clinically significant human bacterial pathogens [17].

Antibiogram profile of *Escherichia coli* and *Klebsiella pneumoniae.* Minimum Inhibitory Concentration (MIC) results previously obtained in recent clinical isolates with well-defined in isolates with well-characterized resistance mechanisms with microdilution method were re-interpreted for the susceptible, intermediate and resistant categories using the 2012 EUCAST breakpoints. Ten different antibiotics were used.

Multiple Antibiotic Resistance (MAR) index. For all isolates, we calculated the MAR index values (a/b, where a represents the number of antibiotics the isolate was resistant to, b represents the total number of antibiotics the isolate tested against). A MAR index value ≥ 0.2 is observed when isolates are exposed to high risk sources of human or animal contamination, where antibiotics use is common; in contrast a MAR index value <or = 0.2 observed when antibiotics are seldom or never used [18-19].

RESULTS AND DISCUSSION

Resistance pattern results. The results of resistance pattern of *E.coli* isolates in our locality to antimicrobial agents showed that the 60 *E.coli* and 60 *K.pneumoniae* strains tested against ten antimicrobial agents in Table 1. *E.coli* isolates were highly resistant to Ciprofloxacin (CIP), Cefepime (FEP), and Aztreonam (ATM) 47%, %47 and 40% respectively. Unlike *K.pneumoniae* isolates were highly resistant to Ampicillin/Sulbactam (SAM), Aztreonam (ATM) and Cefepime (FEP) 58%, 53% and 50% respectively. Both of the bacteria showed the highest sensitivity rate to Amikacin (AN) 98% and 90% *E.coli* and *K.pneumoniae* respectively.

In our study, when we compared to resistance of CIP, *E.coli* isolates showed high antibiotic resistance with 47% CIP. Unlike *K.pneumoniae* isolates showed resistance to CIP with 18%. Many researchers were reported resistance rate to CIP *E.coli* and *K.pneumoniae* [20-22]. Our results were similiar to Giray et al. (2012) [23] who also reported that Ciprofloxacin resistance rate to *E.coli* was 47%.

In this study, resistance of FEP *E.coli* and *K.pneumoniae* 47% and 50% respectively. Many researchers were reported resistance rate to FEP *E.coli* and *K.pneumoniae* [24-27]. Our results were similiar to previous researchers.

When it comes to resistance of ATM *K.pneumoniae* isolates showed high resistance to ATM with 53%. Unlike *E.coli* isolates showed resistance to ATM with 40%. Many researchers were reported resistance rate to ATM *E.coli* and *K.pneumoniae* [25-33]. Our results were similiar to Sabir et al. (2014) [33] who also reported that ATM resistance rate to *E.coli* was 44.8%.

In our study, resistance of Norfloxacin (NOR) were *E.coli* with 35% and *K.pneumoniae* with 32%. Many researchers were reported resistance rate to NOR *E.coli* and *K.pneumoniae* [34-36].Our results were similiar to previous researchers.

TABLE 1
Antibiotic resistance pattern of *E.coli* and *K.pneumoniae* isolated from clinical specimens in intensive care unit.

Antibiotics	*E.coli*			*K.pneumoniae*		
	R	**I**	**S**	**R**	**I**	**S**
CIP	28(47%)	-	32(53%)	23(18%)	1(2%)	36(60%)
FEP	28(47%)	2(3%)	30(50%)	30(50%)	1(2%)	29(48%)
ATM	24(40%)	-	36(60%)	32(53%)	-	28(47%)
NOR	21(35%)	-	39(65%)	19(32%)	1(2%)	40(67%)
CXM	20(33%)	1(2%)	39(65%)	28(47%)	1(2%)	31(52%)
SAM	18(30%)	14(23%)	28(47%)	35(58%)	5(18%)	20(33%)
TZP	6(10%)	4(7%)	50(83%)	14(23%)	7(12%)	39(65%)
AMC	5(8%)	8(13%)	47(78%)	13(22%)	9(15%)	38(63%)
MEM	3(5%)	2(3%)	55(92%)	15(25%)	3(5%)	42(70%)
AN	1(2%)	-	59(98%)	6(10%)	-	54(90%)

Abbrevations; CIP; Ciprofloxacin, FEP; Cefepime, ATM; Aztreonam, NOR; Norfloxacin, CXM; Cefuroxime sodium, SAM; Ampicillin/Sulbactam; TZP;Tazobactam/Piperacillin, AMC; Amoxicillin/Clavulanic Acid, MEM; Meropenem, AN; Amikacin, -; No result.

TABLE 2
Number of clinical samples and MAR Index 60 *E.coli* and *K.pneumoniae* strains.

Clinical Samples in Intensive Care Unit	*E.coli*		*K.pneumoniae*	
	Number of Isolates	MAR	Number of Isolates	MAR
Urine	37	0(13isl), 0,1(4isl), 0,2(7isl), 0,3(1), 0,4(2isl), 0,5(3isl), 0.6(4isl), 0,7(1), 0,8(2isl)	35	0(9isl), 0,1(4isl), 0,2(3isl), 0,3 (3isl), 0,4(3isl), 0,5(1isl), 0,6 (5isl), 0,7(3isl), 0,8(1isl), 0,9(2isl), 1(1isl)
Tracheal aspirate	6	0(1), 0,1(1isl), 0,5(2isl), 0,6(1isl), 0,7(1isl)	10	0(4isl), 0,2(2isl), 0,3(1isl), 0,4(1isl), 0,5(1isl), 0,8(1isl)
Blood	4	0,3(2isl), 0,4(2isl)	5	0(2isl), 1(1isl), 0,5(1isl), 0,9(1isl)
Gaita	1	0,4	-	
Vagen	6	0(2isl), 0,1(3isl), 0,2(1isl)	2	0(1isl), 0,5(1isl)
Abces	4	0(1isl), 0,1(1isl); 0,2(1isl); 0,3(1isl)	2	0(1isl), 0,5(1isl)
Wound	1	0,3(1isl)	3	0,1(1isl), 0,8(1isl),1(1isl)
Periton	1	0,3(1isl)	-	
Throat	-	-	1	0,4(1isl)
Mucus	-	-	2	0,4(1isl), 0,7(1isl)

MAR, Multiple Antibiotic Resistance Index, isl; isolates, -; No result.

When we compared to resistance of Cefuroxime sodium (CXM) *K.pneumoniae* isolates showed high resistance to CXM with 47%, but *E.coli* isolates showed resistance of CXM with 33%. Many researchers were reported resistance rate to CXM *E.coli* and *K.pneumoniae* [30, 37]. Our results were similiar to previous researchers.

In this study, *K.pneumoniae* resistance (58%) of SAM were higher than *E.coli* (30%). Many researchers were reported resistance rate to SAM *E.coli* and *K.pneumoniae* [38-42]. Our results were similiar to Tsakris et al. (1997) [42] who also reported that SAM resistance rate to *E.coli* was 32.1% .

When we compared to resistance of Tazobactam/Piperacillin (TZP), *K.pneumoniae* (23%) isolates showed more resistance than *E.coli* (10%). Many researchers were reported resistance rate to TZP *E.coli* and *K.pneumoniae* [43, 44]. Our results were similiar to Tsakris et al. (1997) [42] who also reported that TZP resistance rate to *E.coli* was 10.5%.

When it comes to resistance of Amoxicillin/Clavulanic acid (AMC), *K.pneumoniae* (22%) isolates showe more resistance than *E.coli isolates* (8%). Many researchers were reported resistance rate to AMC *E.coli* and *K.pneumoniae* [45-47]. Our results were similiar to previous researchers.

In this research, Meropenem (MEM) and AN were the most sensitive antibiotics to both of the isolates. While percentage of MEM sensitivity was 92% and 70% *E.coli* and *K.pneumoniae* respectively. Many researchers were reported resistance rate to MEM *E.coli* and *K.pneumoniae* [36, 48-50]. Our results were similiar to Sohail et al. (2015) [51] who also reported that MEM resistance rate to *E.coli* was 3%.

In our study, sensitivity rate of AN were *E.coli* with 98% and *K.pneumoniae* with 90%. Many researchers were reported resistance rate to AN *E.coli* and *K.pneumoniae* [23,31,52-54]. Manikandan and Amsath (2013) [55] reported that the highest susceptibility pattern of bacterial isolates from respiratory tract infection showed to AN like our study.

MAR index results. Out of the 60 *E.coli* strains 34 (57%) isolates showed MAR two to ten antibiotics. 17 (28%) isolates showed no antibiotic resistance especially isolated from urine samples. Out of the 60 *K.pneumoniae* strains 38 (63%) isolates showed MAR two to ten antibiotics. Both of the bacteria, 17 (28%) isolates showed no antibiotic resistance especially isolated from urine samples. The MAR indices give an indirect suggestion of the probable source(s) of the organism. The results were given Table 2. Some researchers have reported MAR rate to *E.coli* from 2% to 97% [56-58]. MAR is considered as a good tool for risk assessment. This also gives an idea of the number of bacteria showing antibiotic resistance in the risk zone in the study's routine susceptibility testing. This MAR index also recommended that all isolates, somehow, originated from the environment where antibiotics were over used% [59]. Notably, MAR indices for the clinical isolates of *E. coli* were generally lower than *Klebsiella pneumoniae* isolates recovered from same conditions (Table 2).

CONCLUSIONS

High antibiotic resistance of *K. pneumoniae* and *E.coli* towards commonly used antibiotics are the major reasons for prolonged infections, increased hospitalization, increased cost of therapy and enhanced morbidity and mortality rates. *K. pneumoniae* and *E.coli* was found to be most sensitive to AN and MEM. Considering the antibiogram, AN and MEM should be preferred drugs for *K. pneumoniae* and *E.coli* infection isolated from clinical samples. MAR indices for the clinical isolates of *E.*

coli were generally lower than *K. pneumoniae* isolates recovered from same conditions. The findings in present the study suggest that there is an urgent need for constant monitoring of susceptibility of pathogens in different populations to commonly used antimicrobial agents. The data of this study may be used to determine trends in antimicrobial susceptibilities, to formulate local antibiotic policies and overall to assist clinicians in the rational choice of antibiotic therapy to prevent misuse, or overuse, of antibiotics.

REFERENCES

[1] Kraker, M.E., Wolkewitz, M., Davey, P.G., Koller, W., Berger, J., Nagler, J., Icket, C., Kalenic, S., Horvatic, J., Seifert, H., Paniara, O., Argyropoulou, A. (2011) Burden of antimicrobial resistance in European hospitals: excess mortality and length of hospital stay associated with bloodstream infections due to *Escherichia coli* resistant to third-generation cephalosporins. Journal of Antimicrobial Chemotheraphy. 66, 398-407.

[2] Miyakis, S., Pefanis, A., Tsakris, A. (2011) The challenges of antimicrobial drug resistance in Greece. Clinical Infectıous Diseases. 53, 177-184.

[3] Ceyhan-Güvensen, N., Keskin, D., Sankur, F. (2017) Antibiotic resistance ratio of *Acinetobacter baumannii* against to ten antibiotics and multidrug resistance index in clinical isolates. Fresen. Environ. Bull. 26, 8316-8320.

[4] Rossi, F. (2011) The challenges of antimicrobial resistance in Brazil. Clinical Infectious Diseases. 52, 1138-1143.

[5] Schwaber, M.J., Carmeli, Y. (2007) Mortality and delay in effective therapy associated with extended-spectrum beta-lactamase production in Enterobacteriaceae bacteraemia: a systematic review and meta-analysis. Journal of Antimicrobial Chemotheraphy. 60, 913-920.

[6] Schwaber, M.J., Navon-Venezia, S., Kaye, K.S., Ben-Ami, R., Schwartz, D., Carmeli, Y. (2006) Clinical and economic impact of bacteremia with extended- spectrum-beta-lactamase-producing Enterobacteriaceae. Antimicrob Agents Chemother. 50, 1257-1262.

[7] Alharbi, N.S., Khaled, J.M., Kadaikunnan, S., Mothana, R., Alobaidi, A.S., Salmen, S. (2016) Evaluation of an efficiency of alcoholic extracts isolated from *Lagenaria siceraria* (Molina) against some antibiotic resistant clinical microorganisms. Fresen. Environ. Bull. 25, 3251-3256.

[8] Paterson, D.L., Ko, W.C., Von Gottberg, A., Mohapatra, S., Casellas, J.M., Goossens, H., Mulazimoglu, L., Trenholme, G. (2004) Antibiotic therapy for *Klebsiella pneumoniae* bacteremia: implications of production of extended-spectrum betalactamases. Clinical Infectious Diseases. 39, 31-37.

[9] Ayatollahi, J., Vahidi, A., Shahcheraghi, S.H., Bagheripour, A., Lotfi, M., Lotfi, M., Lotfi, S.R. (2013) Investigating the resistance of *Escherichia coli* against some selected antimicrobials in Bam. Jundishapur Journal of Microbiology. 6(8), 7407-7411.

[10] Dormanesh, B., Dehkordi, S.F, Hosseini, S., Momtaz, H., Mirnejad, R., Hoseini, M.J., Yahaghi, E., Tarhriz, V., Khodaverdi Darian, E. (2014) Virulence factors and o-serogroups profiles of uropathogenic *Escherichia coli* isolated from Iranian pediatric patients. Iran Red Crescent Med J. 16(2), 125-132.

[11] Atmani, S.M., Messai, Y., Alouache, S. (2015) Virulence characteristics and genetic background of ESBL-producing *Klebsiella pneumoniae* isolates from wastewater. Fresen. Environ. Bull. 24, 103–112.

[12] Allocati, N., Masulli, M., Alexeyev, M.F., Di Ilio, C. (2013) *Escherichia coli* in Europe: an overview. Internatioanl Journal of Environmental Research Public Health. 10(12), 6235–54.

[13] Russo, T. (2003) Medical and economic impact of extraintestinal infections due to *Escherichia coli*: focus on an increasingly important endemic problem. Microbes Infectious. 5(5), 449–56.

[14] Cappuccino, J.G., Sherman, N. (2004) Microbiology: A Laboratory Manual. 7th Edn. Pearson Education (Singapore). Indian Branch, New Delhi, 544.

[15] Gunasekaran, P. (2000) Laboratory Manual in Microbiology. New Age. International, New Delhi, 320.

[16] MacFaddin, F.J. (2000) Biochemical tests for identification of medical bacteria. 3rd Edn. Philadelphia, USA, 912p.

[17] O'Hara, C.M. (2005) Manual and automated instrumentation for identification of *Enterobacteriaceae* and other aerobic gram-negative bacilli. Clinical Microbiology Reviews. 18, 147-162.

[18] Krumperman, P.H. (1985) Multiple antibiotic resistance indexing of *Escherichia coli* to identify high-risk sources of fecal contamination of foods. Applied and Environmental. Microbiology. 46, 165– 170.

[19] Matyar, F., Kaya, A., Dinçer, S. (2008) Antibacterial agents and heavy metal resistance in Gram-negative bacteria isolated from seawater, shrimp and sediment in Iskenderun Bay, Turkey. Science Total and Environment. 407, 279-285.

[20] Aiyegoro, O.A., Igbinosa, O.O., Ogunmwonyi, I.N., Odjadre, E.E., Igbinosa, O.E., Okoh, A.I. (2007) Incidence of urinary tract infections (UTI) among children and adolescents in lIe-Ife, Nigeria. African J. Microbiol. Res. 12, 013–019.

[21] Turnidge, J., Bell, J., Biedenbach, J., Jones, R.N. (2002) Pathogen occurrence and antimicrobial resistance trends among urinary tract infection isolates in the Asia-Western Pacific Region: report from the SENTRY Antimicrobial Surveillance Program, 1998– 1999. International Journal of Antimicrobial Agents. 20, 10-17.

[22] Mansouri, S., Shareif, S., Ahmad, K. (2002) Antimicrobial resistance pattern of *E. coli* causing urinary tract infections and that of human faecal flora in southeast of Iran. Iran Medical Journal. 8, 123-128.,

[23] Giray, B., Ucar, F.B., Aydemir, S.S. (2012) Characterization of uropathogenic *Escherichia coli* strains obtained from urology outpatient clinic of Ege Medical Faculty in Izmir. Turk J Med Sci. 42(1), 1328-1337.

[24] Kumarasinghe, G., Chow, C., Tambyah, P.A. (2001) Widespread resistance to new antimicrobials in a university hospital before clinical use. International Journal of Antimicrob Agents. 18(4), 391-393.

[25] Iqbal, M., Patel, I.K., Shah, S.H., Ain, Q., Barney, N., Kiani, Q., Rabbani, K.Z., Zaidi, G., Mehdi, B. (2002) Susceptibility patterns of *Escherichia coli*: prevalence of multidrug-resistant isolates and extended spectrum beta-lactamase phenotype. Journal of Pakistan Medical Association. 52(9), 407-411.

[26] Ashgar, A.H. (2006) Frequency and anti-microbial susceptibility patterns of bacterial pathogens isolated from septisemic patients in Makkah hospitals. Saudi Medical Journal. 27(3), 361-367.

[27] Albayrak, N., Kaya, S. (2009) Extended spectrum beta lactamases production and antimicrobial resistance ratio of the *Escherichia coli and Klebsiella pneumoniae* strains isolated from various clinical specimens. Turkish Society of Microbiology Journal. 39, 16–21.

[28] Gonlugur, U., Bakici, M.Z., Akkurt, I., Efeoglu, T. (2004) Antibitic susceptibility patterns among respiratory isolates of Gram negative bacilli in a Turkey university hospital. BMC Microbiol. 4, 1–5.

[29] Cho, S.H., Lim, Y.S., Park, M.S., Kim, S.H., Yeon-Ho Kang, Y.H. (2011) Prevalence of antibiotic resistance in *Escherichia coli* fecal isolates from healthy persons and patients with diarrhea. Public Health Res Perspect. 2(1), 41-45.

[30] Rashid, M., Rakib, M.M., Hasan, B. (2015) Antimicrobial-resistant and ESBL producing *Escherichia coli* in different ecological niches in Bangladesh. Infection Ecology and Epidemiology. 5, 26712.

[31] Shilpa, K., Thomas, R., Ramyashree, A. (2016) Isolation and Antimicrobial sensitivity pattern of *Klebsiella pneumoniae* from sputum samples in a tertiary care hospital. International Journal of Biomedical and Advance Research. 7(2), 053-057.

[32] Ruh, E., Gazi, U., Guvenir, M., Suer, K., Cakır, N. (2016) Antibiotic resistance rates of *Pseudomonas aeruginosa, Acinetobacter bau-mannii* and *Klebsiella pneumoniae* isolated from a university-affiliated hospital in North Cyprus. Turk Hij Den Biyol Derg. 73(4), 333-344.

[33] Sabir, S., Anjum, A.A., Ijaz, T., Ali, M.A., Khan, M.R., Nawaz, M. (2014) Isolation and antibiotic susceptibility of *E. coli* from urinary tract infections in a tertiary care hospital. Pakistan Journal of Medical Science. 30(2), 389–392.

[34] Karki, T., Truuaslu, K., Mikellsaaar, M. (2001) Antibiotic susceptibility patterns of community- and hospital-acquired *Staphylococcus aureus* and *Escherichia coli* in Estonia. Scand J Infect Dis. 33, 333–338.

[35] Ay, S., İşeri, L.A., Duman, B. (2003) Antibiotic susceptibilities of gram negative microorganisms isolated from urine samples. İnönü Üniv Tıp Fak Derg. 10(2), 59-62.

[36] Amin, A., Ghumro, P.B., Hussain, S., Hameed, A. (2009) Prevalence of antibiotic resistance among clinical isolates of *Klebsiella pneumoniae* isolated from a Tertiary Care Hospital in Pakistan. Malaysian Journal of Microbiology. 5(2), 81-86.

[37] Hatzaki, D., Poulakou, G., Katsarolis, I., Lambri, N., Souli, M., Deliolanis, I., Nikolo-poulos, G.K., Lebessi, E., Giamarellou, H. (2012) Cefditoren: Comparative efficacy with other antimicrobials and risk factors for resistance in clinical isolates causing UTIs in outpatients. BMC Infectious Diseases. 12, 228-234

[38] Davis, G.S., Waits, K., Nordstrom, L., Weaver, B., Aziz, M. (2015) Intermingled *Klebsiella pneumoniae* populations between retail meats and human urinary tract infections. Clinical Infectious Diseases. 61(6), 892-899.

[39] Toroglu, H., Avan, D. Keskin. (2013) Beta-Lactamases production and antimicrobial resistance ratio of *Pseudomonas aeruginosa* from hospitalized patients in Kahramanmaraş, Turkey. Journal of Environmental Biology. 34(4), 695-700.

[40] Abuhandan, M., Güzel, B., Oymak, Y., Çiftçi, H. (2013) Antibiotic sensitivity and resistance in children with urinary tract infection in Sanliurfa. Turkish Journal of Urology. 39(2), 106-10.
[41] Khan, A.U., Zaman, M.S. (2006) Multiple drug resistance pattern in urinary tract infection patients in Aligarh. Biomedical Research. 17(3), 179-181.
[42] Tsakris, A., Douboyas, J., Leonidas, S. (1997) High rates of resistance to piperacillin/ tazobactam among *Escherichia coli and Klebsiella pneumoniae* strains isolated in a Greek hospital. Diagnostic Microbiology and Infectious Disease. 29(1), 39-41.
[43] Yang, Q., Zhang, H., Wang, Y., Xu, Z., Zhang, G., Chen, X. (2017) Antimicrobial susceptibilities of aerobic and facultative gram-negative bacilli isolated from Chinese patients with urinary tract infections between 2010 and 2014. BMC Infectious Diseases. 17,192-199.
[44] Zarakolu, P., Hascelik, G., Unal, S. (2006) Antimicrobial suspectibility pattern of nosoco-mial gram negative pathogens: Results from mystic study in Hacettepe university adult hospital (2000-2004). Bulletin of Microbiology. 40, 147-154.
[45] Bashir, R., Zaib, N., Altaf, I., Saleem, F., Sultana, Q., Naz, S. (2016) Optimization of PCR for rapid detection of CTX-M gene in ESBL producing *Klebsiella pneumoniae* clini-cal isolates from Punjab, Pakistan. Malaysian Journal of Microbiology. 12(5), 365-369.
[46] Uzun, K., Teke, T., Yavuz, Z.G. (2006) Surveillance of antimicrobial resistance and susceptibility in bacterai isolated from pulmonart critical care. Tıp Araşt Derg. 4(3), 8-13.
[47] Kader, A.A., Kumar, A. (2004) Prevalence and antimicrobial susceptibility of extended-spectrum β-lactamase-producing *Escherichia coli* and *Klebsiella pneumoniae* in a general hospital in Saudi Arabia. Saudi Medical Journal. 25, 570–574.
[48] Yılmaz, N., Köse, Ş., Ağuş, N., Ece, G., Akkoçlu, G., Kıraklı, C. (2010) Microorganisms isolated from blood cultures of intensive care unit patients, their antimicrobial susceptibility and etiological agents in nosocomial bacteremia. Ankem Journal. 24(1), 12-19.
[49] İnan, N.U., Gurler, N. (2004) Investigation of antibiotic resistance and some virulence factors of *Escherichia coli* strains isolated from children with urinary tract infections. Ankem Journal. 18(2), 89-96.
[50] Barišić, Z., Babić-Erceg, A., Borzić, E., Zoranić, V., Klaiterna, V., Carev, M. (2003) Urinary tract infections in South Croatia: aetiology and antimicrobial resistance. International Journal of Antimicrobial Agents. 22, 61-64.
[51] Sohail, M., Khurshid, M., Saleem, H.G.M., Javed, H., Khan, AA. (2015) Characteristics and antibiotic resistance of urinary tract pathogens isolated from Punjab, Pakistan. Jundishapur Journal of Microbiology. 8(7), 1-5.
[52] Ekim, M., Kuluglu, Z., Aysev, D., Can, S. (1998) Changes in antibiotic sensitivity in urinary tract infection caused by *Escherichia coli*. Journal of the Turkish Nephrology. 3 141-144.
[53] Cetin, E.S., Demirci, M., Kaya, S., Arıdogan, B.C., Adiloglu, A.K., Goksu, Y., Gonulates, N. (2006) Antibiotic susceptibilities of *Escherichia coli, Klebsiella pneumoniae* and Enterobacter strains isolated from blood specimens. Turkish Microbiology Society Journal. 36(1), 20-24.
[54] Kumar, A.R. (2013) Antimicrobial sensitivity pattern of *Klebsiella pneumonia* isolated from pus from tertiary care hospital and issues related to the rational selection of antimicrobials. Journal of Chemical Pharmaceutical Research. 5(11), 326-331.
[55] Manikandan, C., Amsath, A. (2013) Antibiotic suspectibility of bacterial strains isolated from patients with respiratory tract ınfections. International Journal of Pure and Applied Zoology. 1(1), 61-69.
[56] Al-Mardeni, R.I., Batarseh, A., Omaish, L., Shraideh, M., Batarseh, B., Unis, N. (2009) Empirical treatment for pediatric urinary tract infection and resistance patterns of uropathogens, in Queen Alias Hospital and Prince A'lsha Military Center. Jordan. Saudi J Kidney Dis Transplant. 20, 135-9.
[57] Mathai, E., Chandy, S., Thomas, K., Antoniswamy, B., Joseph, I., Mathai, M., Sorensen, T.L., Holloway, K. (2008) Antimicrobial resistance surveillance among commensal *Escherichia coli* in rural and urban areas in Southern India. Trop Med Int Health. 13(1), 415.
[58] Al-Tawfiq, J.A. (2006) Increasing antibiotic resistance among isolates of *Escherichia coli* recovered from inpatients and outpatients in a Saudi Arabian hospital. Infectious Control Hospital Epidemiology. 27, 748-753.
[59] Paul, S., Bezbaruah, R.L., Roy, M.K., Ghosh, A.C. (1997) Multiple antibiotic resistance (MAR) index and its reversion in *Pseudomonas aeruginosa*. Letters in Applied Microbiology. 24, 169-171.

Received: **06.06.2017**
Accepted: **08.02.2018**

CORRESPONDING AUTHOR

Nur Ceyhan-Guvensen
Muğla Sıtkı Koçman University
Faculty of Sciences
Department of Biology
Muğla – Turkey

e-mail: nurceyhan@msn.com

© by PSP Volume 27 – No. 5/2018 pages 2768-2776 Fresenius Environmental Bulletin

SPATIAL ECONOMETRIC ANALYSIS OF ENVIRONMENTAL REGULATION IN CHINA

Yuanhua Yang[1,*], Guohua Niu[2], Dengli Tang [3], Mengjue Zhu[1]

[1]School of Public Management, Guangdong University of Finance and Economics, Guangzhou 510320, China
[2]Personnel Education Department, Foshan Municipal Local Taxation Bureau, Foshan, 528000, China
[3] School of Business Administration, Guangdong University of Finance and Economic, Guangzhou 510320, China

ABSTRACT

Strict environmental regulation is the foundation and guarantee of the ecological civilization in a country. Based on the data of total pollution control investment in China from 2003 to 2014, this paper uses spatial exploratory data analysis technology to analyze the temporal and spatial evolution characteristics and spatial cluster trend of regional environmental regulation in China. It is discovered that, from 2003 to 2014, the Global Moran's I values of regional environmental regulation level fluctuates between -0.0071 and 0.3599. In every year except 2010, the values are greater than 0.2. This indicates the spatial distribution of environmental regulation in China is not completely randomized. As for the spatial cluster of environmental regulation, the high-high cluster area with high environmental regulation is concentrated in the eastern part of China, covering 2, 5, 3 and 5 provinces in 2003, 2007, 2011 and 2014, respectively. The low-low cluster area with low environmental regulation is mainly distributed in the western part of China. With the passage of time, the high-high cluster area is expanding, while the low-high cluster area is gradually transforming into high-high cluster area. Finally, this paper puts forward some recommended policies on improving environmental regulation in China in light of the results.

KEYWORDS:
Regional environmental regulation, exploratory spatial data analysis technology, spatial autocorrelation

INTRODUCTION

As China's economic development enters a new normal, the country has to simultaneously deal with the slowdown in economic growth, make difficult structural adjustments, and absorb the effects of previous economic stimulus policies [1-3]. The situation calls for the transition from the environmental-unfriendly extensive development mode to the green development mode. From "we need both mountains of gold and silver and green hills and clear waters", "green hills and clear waters are better than mountains of gold and silver" to "green hills and clear waters are mountains of gold and silver", the change in slogans reflects the central government's firm resolution in and strategic emphasis on environmental protection [4, 5]. In order to further strengthen the environmental regulation in China, the local government has been actively enacting environmental laws and regulations over the years, seeking to improve the level of environmental regulation with a full-fledged system of laws and regulations. In 2014 alone, 31 local laws and regulations and 27 local government rules were formulated across the country [1]. In total, 391 local regulations and 346 local government rules are currently in effect. Apart from the development of sound laws and regulations, the local government have also strengthened the collection of sewage charges and stepped up the investment in the control of environmental pollution [6]. The country collected 2.08 billion yuan of sewage charges in 2013, and invested 902.1 billion yuan on the control of environmental pollution in 2014 [4].

In this background, what are the temporal and spatial characteristics of environmental regulation in China? Does the intergovernmental environmental regulation bear clustering characteristics? So far, scholars at home and abroad have studied the relationship between environmental regulation and FDI [2, 6-14], the competitive strategy of intergovernmental environmental regulation [1, 15-22], and the effect of environmental regulation on economic development [3, 23-29]. However, few of them have examined the development trend and spatial distribution characteristics of China's environmental regulation over the years. Aiming to fill up the gap, this paper attempts to provide the government a panorama of the status quo and spatial distribution characteristics of China's regional environmental regulation, and blaze a new trail in the improvement and perfection of the level of regional environmental regulation in China.

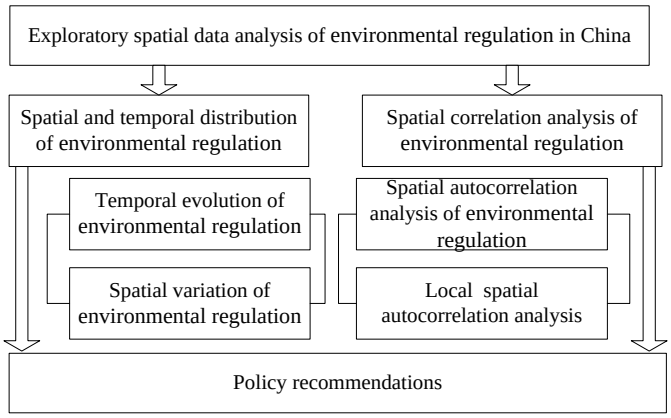


FIGURE 1
Research framework

TABLE 1
Total investment in regional pollution control in China in 2003-2014 (Unit: 100 million yuan)

Zone	2003	2004	2005	2006	2007	2008	2009	2010	2011	2012	2013	2014
Beijing	64.5	65.4	84.9	165.5	185.3	152.9	208.7	231.4	213.1	342.6	433.5	624.4
Tianjin	51.5	42.7	71.4	40.8	59.8	68.1	103.7	109.7	174.9	157.5	191.3	278.9
Hebei	75.8	91.2	121.4	132.2	170.2	208.3	248.6	370.9	623.9	486.1	490.0	455.5
Shanxi	32.0	45.0	48.5	63.2	97.0	140.9	157.8	206.9	248.5	328.2	337.2	293.2
InnerMongolia	28.0	44.3	68.0	104.8	90.5	135.0	155.2	238.9	395.9	445.1	506.8	562.3
Liaoning	88.0	118.9	129.0	145.8	125.1	163.7	204.9	206.5	376.5	683.4	347.6	271.5
Jilin	22.4	35.4	34.0	42.3	50.9	59.6	66.1	124.2	101.2	103.4	105.4	98.1
Heilongjiang	56.1	61.3	46.7	54.2	58.7	98.8	107.8	131.3	152.7	218.1	298.5	182.1
Shanghai	79.4	70.3	88.1	94.3	123.0	153.5	160.1	134.0	144.8	134.1	187.6	250.0
Jiangsu	179.4	205.0	294.3	282.7	318.2	395.9	369.9	466.4	575.8	657.1	881.0	880.6
Zhejiang	139.3	158.3	160.3	140.3	177.4	519.7	198.0	333.7	238.7	375.4	390.4	474.2
Anhui	28.0	41.3	49.3	52.0	82.4	139.0	139.2	179.9	267.5	330.2	506.0	428.7
Fujian	34.9	52.6	80.9	59.8	78.0	83.1	87.2	129.7	198.4	222.5	282.9	193.4
Jiangxi	21.6	29.6	37.1	37.5	45.5	39.2	70.4	156.5	241.2	316.1	239.6	231.2
Shandong	156.4	191.9	238.8	258.1	320.8	432.2	459.5	483.9	614.1	739.1	848.0	823.8
Henan	48.1	61.1	82.4	95.1	114.4	109.9	121.3	132.2	163.3	209.5	288.1	295.1
Hubei	31.8	44.8	62.0	67.7	64.3	90.1	150.6	146.8	259.8	285.5	252.7	316.5
Hunan	25.6	29.0	37.7	54.0	64.6	91.4	146.4	106.6	127.3	190.3	233.9	213.7
Guangdong	123.6	112.2	171.5	160.4	153.6	164.6	240.1	1416.2	332.6	260.2	351.9	303.1
Guangxi	27.5	32.0	41.4	41.2	65.5	93.0	132.3	164.1	161.5	190.5	217.8	200.4
Hainan	3.6	7.2	6.3	8.3	14.9	12.7	19.7	23.6	28.0	44.7	26.6	21.1
Chongqing	40.1	48.2	50.2	60.1	63.7	67.3	109.7	176.3	259.2	186.9	173.3	168.4
Sichuan	59.7	74.7	78.3	71.1	102.2	100.7	103.5	89.0	140.1	178.3	234.0	288.2
Guizhou	10.0	15.4	14.1	19.8	22.4	23.2	21.2	30.0	64.9	68.9	109.7	170.4
Yunnan	17.1	22.6	28.4	29.0	29.9	44.1	79.6	106.2	119.2	132.4	197.1	152.0
Shaanxi	30.8	35.7	36.5	41.0	63.8	75.5	119.1	179.2	153.3	180.6	221.7	185.4
Gansu	13.3	16.5	20.4	27.8	38.1	31.2	44.4	63.9	59.6	121.4	176.2	143.5
Qinghai	3.7	6.3	5.3	6.1	10.6	18.1	12.3	17.0	26.2	24.1	36.7	30.0
Ningxia	16.0	18.1	12.1	21.3	33.4	30.9	28.7	34.5	57.4	55.7	72.4	78.6
Xinjiang	35.6	37.8	33.5	23.3	35.2	47.7	78.2	78.4	132.7	255.1	318.7	392.4

MATERIALS AND METHODS

Theoretical Analysis Framework. The purpose of this study is to analyze the temporal and spatial distribution characteristics of environmental regulation in China based on spatial exploratory data analysis technology, and find the spatial agglomeration characteristics and changing trend of environmental regulation in China. As shown in Figure 1, the research framework consists of the following parts: First, the discussion of the spatial and temporal pattern of environmental regulation. The national and provincial temporal variation and spatial distribution of environmental regulation are depicted based on the data in China from 2003 to 2014. Second, it is the spatial correlation analysis of environmental regulation in China. The spatial autocorrelation characteristics of environmental regulation in China are explored by the theory and method of spatial autocorrelation in spatial econometrics. Finally, policy recommendations are given to enhance policy recommendations are given to enhance in China.

Research Method. In China, the environmental regulation situation varies from province to province. During the promotion of corruption governance,

it is of great importance to make rational zoning of corruption control regions, identify key regions, and take pertinent policies. Based on the theory and method of spatial autocorrelation in spatial econometrics, this paper analyzes the correlation of corruption in each region. The term spatial autocorrelation refers to analyzing the correlation of the same variable in different spatial locations. The analysis methods include global spatial autocorrelation and local spatial autocorrelation [30]. There are three possible: positive spatial autocorrelation, negative spatial autocorrelation and no spatial autocorrelation.

The theory and method of global spatial autocorrelation. Global spatial autocorrelation detects the spatial pattern of the whole research area and uses a single value to reflect the autocorrelation of the entire region. In this paper, the global spatial autocorrelation index is adopted to calculate the global spatial autocorrelation. The global spatial autocorrelation index is denoted as Global Moran's I [28]. The calculation process is given in formula (1).

$$I = \frac{n\sum_{i=1}^{n}\sum_{j=1}^{n} w_{ij}(x_i-\bar{x})(x_j-\bar{x})}{\sum_{i=1}^{n}\sum_{j=1}^{n} w_{ij}\sum_{i=1}^{n}(x_i-\bar{x})} = \frac{n\sum_{i=1}^{n}\sum_{j=1}^{n} w_{ij}(x_i-\bar{x})(x_j-\bar{x})}{S^2\sum_{i=1}^{n}\sum_{j=1}^{n} w_{ij}} \quad (1)$$

Where $s^2 = \frac{1}{n}\sum_{i=1}^{n}(x_i-\bar{x})^2$, $\bar{x} = \frac{1}{n}\sum_{i=1}^{n}x_i$

In formula (1), I is the global spatial autocorrelation index, n is the number of spatial unit data, X_i and X_j are the attribute values of the spatial units i and j, respectively, W_{ij} is the spatial weight coefficient matrix to describe the adjacency relation of each spatial unit.

The global Moran's I falls in the range of [-1,1]. When the index is greater than 0, the research area exhibits positive spatial autocorrelation in the spatial distribution, and the observable attributes are clustered; the positive correlation grows as the index approaches 1. On the contrary, when the index is smaller than 0, the research area exhibits negative spatial autocorrelation in the spatial distribution, and the observable attributes are discretized; the negative correlation grows as the index approaches -1. When the index gets close to 0, the observable attributes show no spatial autocorrelation and are randomly distributed [28].

The theory and method of local spatial autocorrelation. Local spatial autocorrelation detects the association between each spatial unit and its neighbors on a certain attribute. It can be expressed by local indicators of spatial association (LISA). According to the properties of spatial autocorrelation, this paper calculates the autocorrelation of local space by the local autocorrelation index, which is denoted as Local Moran's I [31]. The calculation process is given in formula (2).

$$I_i = \frac{(x_i-\bar{x})\sum_{j=1}^{n} w_{ij}(x_j-\bar{x})}{S^2} \quad (2)$$

Where, I_i is the local spatial autocorrelation index; n is the number of spatial unit data; X_i and X_j are the attribute values of the spatial units i and j, respectively; W_{ij} is the spatial weight coefficient matrix to describe the adjacency relation of each spatial unit.

Establishment of the spatial weight matrix. The spatial weight matrix expresses the spatial arrangement of the observable variables between different regions. The adjacent relations between several regions are often illustrated by a binary symmetric spatial weight matrix (W) [31]. The matrix is expressed as below:

$$W = \begin{bmatrix} W_{11} & W_{12} & \text{K} & W_{1n} \\ W_{21} & W_{22} & \text{K} & W_{2n} \\ \text{M} & \text{M} & \text{M} & \text{M} \\ W_{n1} & W_{n2} & \text{K} & W_{nn} \end{bmatrix} \quad (3)$$

Where, N is the total number of regions, W_{ij} is the adjacency relation between regions i and j. In this research, the weight matrix is constructed based on spatial adjacency relation. In other words, if region i and region j share common vertex or common boundary, W_{ij} is 1; otherwise, W_{ij} is 0.

Data Source. As is known to all, there is no direct indicator of "environmental regulation". The existing literatures generally measure the intensity of environmental regulation with alternative indicators. These indicators either focus on investment or performance. The investment indicators include pollution reduction cost, pollution control investment, supervision and inspection frequency, and the government's environmental expenditure; the performance indicators consist of sewage charges and major pollutant emissions. Targeted at disclosing the intensity of regional environmental regulation and analyzing the provincial investment in environmental regulation, this paper chooses to measure the level of environmental regulation by the regional investment in pollution control in reference to the practice of scholars like Li (2013) and Zhang (2016) [1, 32]. Total investment in regional pollution control in China in 2003-2014 is shown in table 1.

RESULTS

Temporal and Spatial Distribution of Regional Environmental Regulation in China. In terms of temporal distribution, the Chinese government's investment in environmental pollution control has increased year by year. From 154.41 billion yuan in 2003 to 902.11 billion yuan in 2014, the national total investment in environmental pollution has grown by nearly 5 times in the 12-year period.

Figure 2 illustrates the variation of China's total investment in regional environmental regulation in 2003-2014. As can be seen from the figure, the national total investment in environmental pollution rises slowly from 2003 to 2006, and rather rapidly from 2007 to 2013, and slows down in 2014. The overall trend of growth shows: the environmental protection awareness and the environmental regulation intensity of the Chinese government have been growing year by year with the economic development.

In terms of spatial distribution, the provinces differ significantly in the intensity of environmental regulation. Figure 3 lists the total investment in environmental regulation by different provinces of China in 2014. Jiangsu invests more money (88.06 billion yuan) in environmental pollution control than any other province in 2014, followed by Shandong (82.38 billion yuan) and Beijing (62.44 billion yuan). By total investment in pollution control, Hainan and Qinghai ranks lowest and second lowest in that year. The total investment in pollution control by Jiangsu is about 42 times that of Hainan. Hence, there is a huge gap between the provinces in the investment in environmental regulation.

Spatial Autocorrelation Analysis of Regional Environmental Regulation. (1) Global spatial autocorrelation analysis. For the purpose of exploring the spatial distribution characteristics and clustering trend of China's regional environmental regulation, the global spatial autocorrelation index I and the local spatial autocorrelation index Ii of China's regional environmental regulation in 2003-2014 are calculated by Geoda1.6.7. Table 2 presents the results of the global spatial autocorrelation indexes. The following conclusions are drawn from the table.

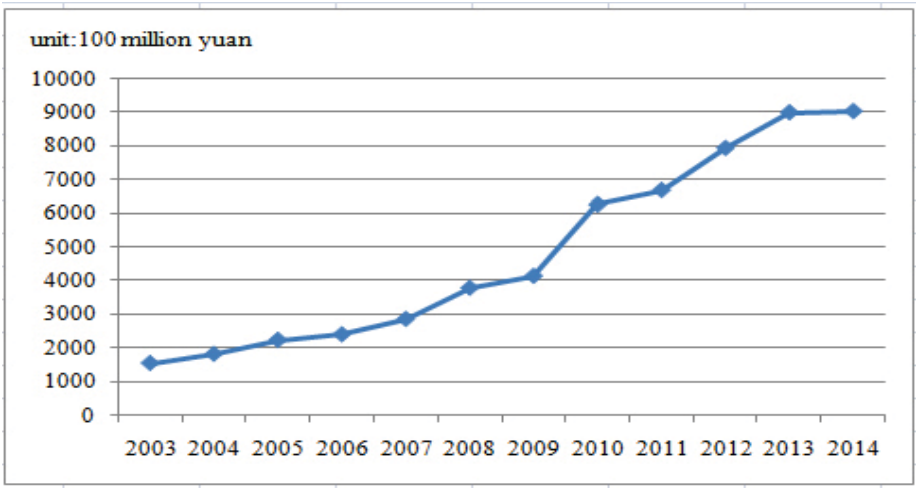


FIGURE 2
Total investment in regional environmental regulation by China in 2003-2014

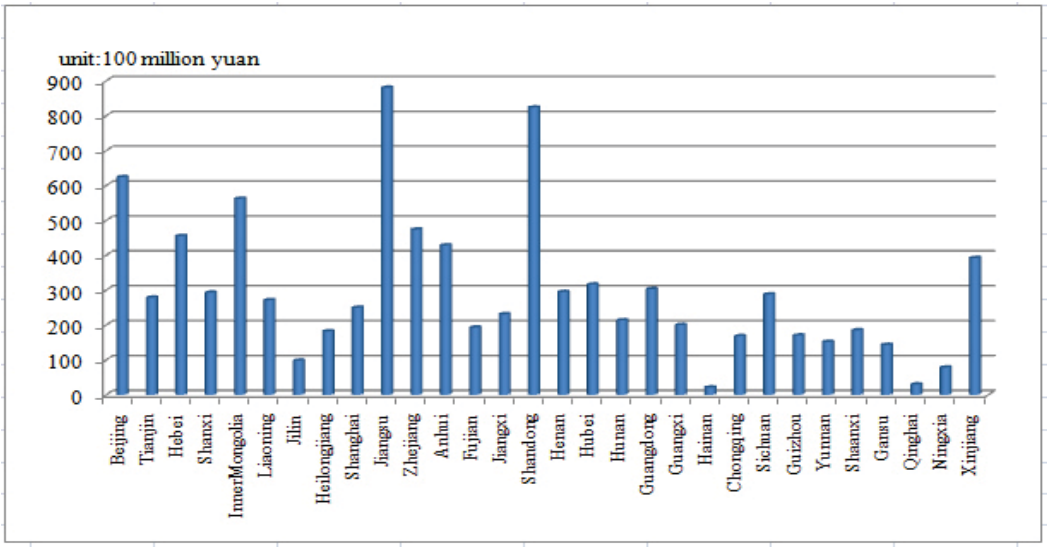


FIGURE 3
Total investment in environmental regulation by Chinese provinces in 2014

TABLE 2
Global Moran indexes of China's regional environmental regulation in 2003-2014

Years	Moran *I*	P-value	Years	Moran *I*	P-value
2003	0.270899	0.013	2009	0.309379	0.006
2004	0.273369	0.014	2010	-0.007145	0.323
2005	0.304102	0.004	2011	0.280477	0.011
2006	0.267382	0.011	2012	0.237961	0.017
2007	0.359937	0.006	2013	0.276695	0.006
2008	0.318529	0.004	2014	0.235505	0.021

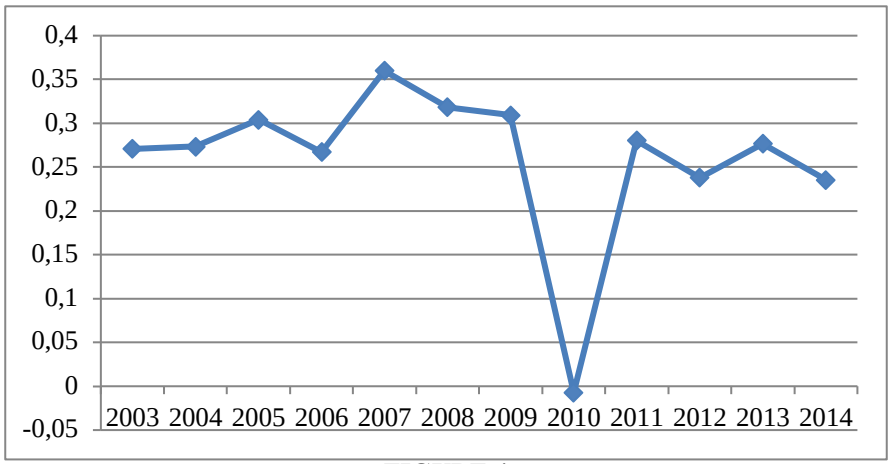


FIGURE 4
Variation of global spatial autocorrelation indexes of regional environmental regulation in China in 2003-2014

There is a significant positive spatial autocorrelation between the provinces in environmental regulation. During the 12 year observation period, 2010 is the only year for which the global spatial autocorrelation index of the total investment in provincial pollution control in China is negative; in the remaining 11 years, however, the indexes are always positive and proved acceptable in the significance test. This indicates the spatial distribution of provincial investment in pollution control in China is not completely randomized; instead, the similar values are clustered together. Since the spatial autocorrelation indexes are predominantly greater than 0, the provinces with high total pollution control investment tend to be adjacent to the provinces with high total pollution control investment, and the provinces with low total pollution control investment tend to be adjacent to the provinces with low total pollution control investment. In other words, the adjacent provinces mostly bear the "high-high" or "low-low" spatial agglomeration characteristics, and rarely the "high-low" or "low-high" spatial agglomeration characteristics.

The spatial autocorrelation of the provincial spatial regulation level is fluctuating. Figure 4 depicts the variation of the global spatial autocorrelation indexes of China's regional environmental regulation level from 2003 to 2014. It can be seen that the Global Moran's I value varies between -0.0071 and 0.3599 from 2003 to 2014. The minimum value -0.007145 appears in 2010, and the maximum value 0.359937 appears in 2007. However, the overall fluctuation is not fierce as the Global Moran's I is greater than 0.2 in every year except 2010.

(2) Local spatial autocorrelation analysis. The DeoDA software is used to calculate the local Moran's indexes of regional environmental regulation levels in 30 Chinese provinces in 2003-2014, and to obtain the Moran scatterplots of the corresponding years. Due to space limitation, 2003, 2007, 2011 and 2014 are selected as typical years for analysis. The results are shown in Figure 5.

It can be seen from Figure 5 that most Chinese provinces are distributed in the first and third quadrants of the Moran scatterplots on environmental regulation. There are 20 provinces falling into these quadrants in 2003, 23 in 2007, 19 in 2011, and 16 in 2014. Overall, 66.67%, 76.67%, 63.33% and 53.33%of the provinces are located in in the first and third quadrants of Moran scatterplots in the four years, respectively. The distribution further testifies that the regional environmental regulation in China features significant spatial autocorrelation.

Figure 6 shows the LISA agglomeration maps of China's regional environmental regulation levels in 2003, 2007, 2011 and 2014. As shown in Figure 6, China's regional environmental regulation levels

form different agglomeration areas in the local spatial distribution. The high-high agglomeration area with high environmental regulation concentrates in Jiangsu and Shanghai in 2002, Jiangsu, Shanghai, Shandong, Hebei, Beijing and Tianjin in 2007, Shandong, Hebei and Anhui in 2011, and Jiangsu, Shandong, Anhui, Hebei and Tianjin in 2014. From 2003 to 2014, the number of provinces within the high-high agglomeration area fluctuates, but the overall trend is increasing. The low-low agglomeration area with low environmental regulation is mainly distributed in Xinjiang in 2003 and 2007, Xinjiang and Sichuan in 2011, and Sichuan in 2014. The high-low agglomeration area with high environmental regulation covers Sichuan in 2007 and 2011, and Xinjiang in 2014. The low-high agglomeration area with low environmental regulation lies in Anhui in 2003 and 2007, Henan and Tianjin in 2011, and Shanghai in 2014.

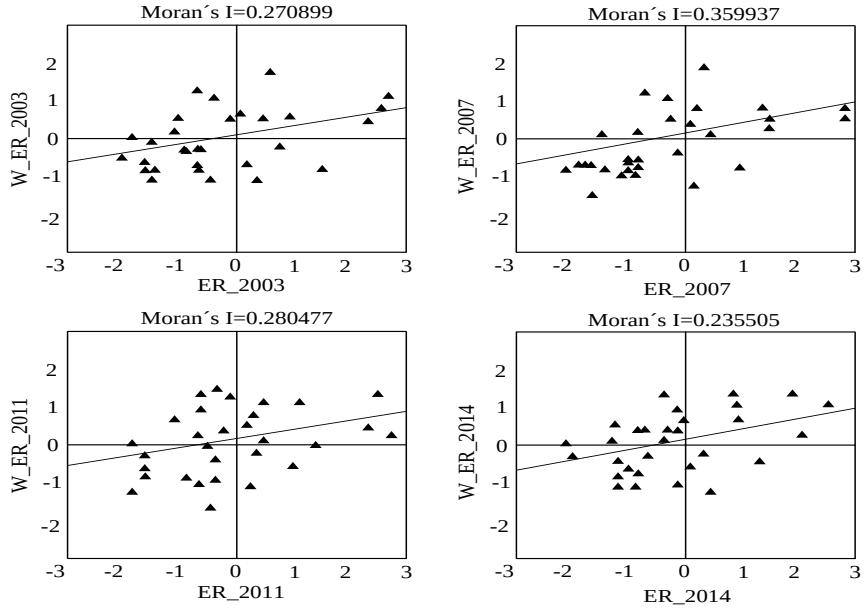


FIGURE 5
Moran scatterplots of China's regional environmental regulation levels in 2003, 2007, 2011 and 2014

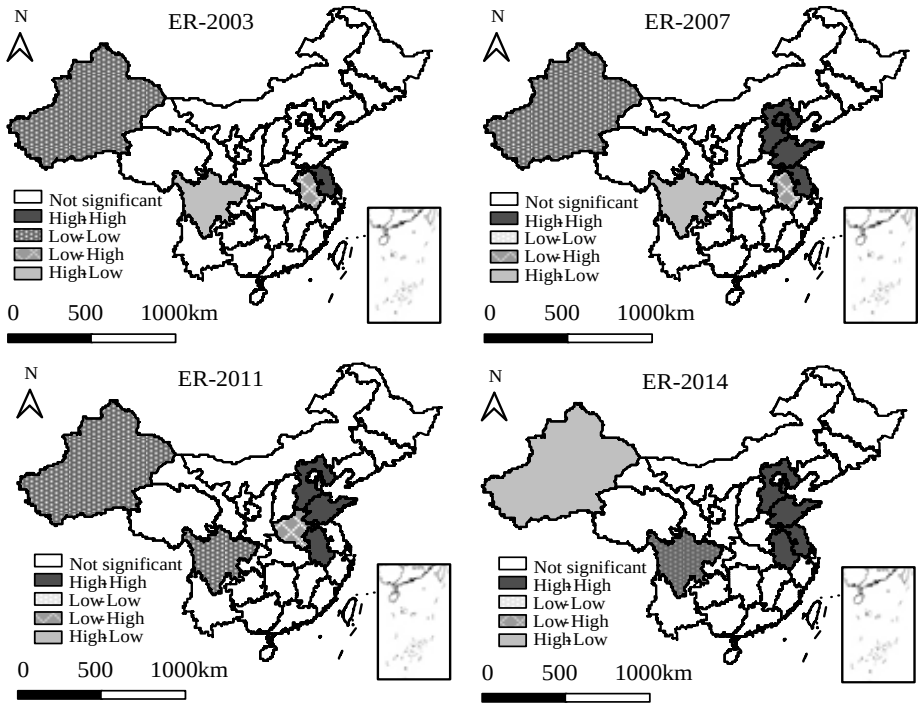


FIGURE 6
LISA cluster maps of China's regional environmental regulation levels in 2003, 2007, 2011 and 2014

For the overall spatial agglomeration of regional environmental regulation in China, the high-high agglomeration area with high environmental regulation is concentrated in the eastern part of China, covering 2, 5, 3 and 5 provinces in 2003, 2007, 2011 and 2014, respectively. The low-low agglomeration area with low environmental regulation is mainly distributed in the western part of China. With the passage of time, the high-high agglomeration area with high environmental regulation is expanding, while the low-high agglomeration area with low environmental regulation is gradually transforming into high-high agglomeration area. For example, Anhui gradually moves from the low-high agglomeration area into the high-high agglomeration area. Moreover, the low-low agglomeration area with low environmental regulation is slowly changing to high-low agglomeration area. A typical example is Xinjiang, which evolves from the low-low agglomeration area with low environmental regulation into the high-low agglomeration area with high environmental regulation.

DISCUSSION AND CONCLUSION

Based on the spatial exploratory analysis of environmental regulation in China in 2003-2010, the following conclusions can be drawn: First, in terms of temporal distribution, the Chinese government's investment in environmental pollution control has increased year by year. From 154.41 billion yuan in 2003 to 902.11 billion yuan in 2014, the national total investment in environmental pollution has grown by nearly 5 times in the 12-year period. In terms of spatial distribution, the provinces differ significantly in the intensity of environmental regulation. In 2014, Jiangsu invests more money in environmental pollution control than any other province, while Hainan makes the fewest investment in controlling environmental pollution. The total investment in pollution control by Jiangsu is about 42 times that of Hainan. Second, the spatial autocorrelation of the provincial spatial regulation level is fluctuating. From 2003 to 2014, the Global Moran's I of China's regional environmental regulation level fluctuates between -0.0071 and 0.3599. In every year except 2010, the Global Moran's I is greater than 0.2. The Moran scatterplot analysis reveals that: 20, 23, 19 and 16 regions falls into the first and third quadrants in 2003, 2007, 2011 and 2014, respectively. This indicates the spatial distribution of provincial investment in pollution control in China is not completely randomized; instead, the similar values are clustered together. Then, when it comes to the spatial agglomeration characteristics of environmental regulation, the high-high agglomeration area with high environmental regulation is concentrated in the eastern part of China, covering 2, 5, 3 and 5 provinces in 2003, 2007, 2011 and 2014, respectively. The low-low agglomeration area with low environmental regulation is mainly distributed in the western part of China. With the passage of time, the high-high agglomeration area with high environmental regulation is expanding, while the low-high agglomeration area with low environmental regulation is gradually transforming into high-high agglomeration area. For example, Anhui gradually moves from the low-high agglomeration area into the high-high agglomeration area. Moreover, the low-low agglomeration area with low environmental regulation is slowly changing to high-low agglomeration area. A typical example is Xinjiang, which evolves from the low-low agglomeration area with low environmental regulation into the high-low agglomeration area with high environmental regulation.

In view of the correlations and differences between the Chinese provinces in environmental regulation level, the author puts forward the following policy recommendations: First, the environmental regulation policies should be adjusted in a timely manner according to the temporal and spatial evolution pattern of regional environmental regulation. Facing constantly changing provincial environmental regulation situation across the country, it is unwise to stick to the same policy throughout the years. The government must note the dynamic changes in various provinces and issue balanced policies on environmental regulation. It is clearly observed in the empirical analysis that: the level environmental regulation in the eastern part of China is much higher than that in the western part the country. Hence, the Chinese government ought to further increase its investment and strike a balance between the investments on environmental pollution control in the eastern and western parts. Second, in light of the spatial distribution of provincial environmental regulation in China, the provinces within the high-high agglomeration area (the core provinces) and their neighboring provinces spend more efforts in environmental pollution control; these provinces, particularly the eastern provinces of Shandong and Hebei, should be treated as the demonstration areas of environmental pollution control, aiming to promote their experience in environmental pollution control to other provinces, and elevate the regional environmental regulation intensity across the country.

Based on the data of provincial environmental regulation in the country from 2003 to 2014, this paper explores the effective ways and makes policy recommendations for regional pollution control in China. Although it is more in-depth and inclusive than the existing research, this study is subjected to certain limitations. There are two main limitations. First, the analysis of this research is entirely based on the data from the 12 years from 2003 to 2014. Objectively speaking, the period is rather short. Second, this is only a preliminary research into the tem-

poral and spatial distribution characteristics and spatial correlation of regional environmental regulation in China with the aid of spatial exploratory analysis. Actually, the regional environmental regulation is not only under the influence of factors like economic development and geographical location, but also brings about a series of implications on the economy. In the future, more spatial measurement methods should be utilized to further study the effect of regional environmental regulation on a country's economic and regional development.

ACKNOWLEDGEMENTS

This study was supported by Guangdong Soft Science Item (No. 2016A070706008) and Foshan City Philosophy and Social Science Fund (No.2017-GJ36).

REFERENCES

[1] Zhang, H. (2017) Advances in Environmental Regulation Competition. Environmental Economics Research. 4(01), 99-112. [In Chinese].
[2] Manderson, E., Kneller, R. (2012) Environmental Regulations, Outward FDI and Heterogeneous Firms: Are Countries Used as Pollution Havens? Environmental and Resource Economics. 51(3), 317-352.
[3] Rezza, A. (2015) A Meta-analysis of FDI and Environmental Regulations. Environment and Development Economics. 20(2), 118-208.
[4] Zhang, H. (2016) A Study on the Strategic Interaction of Regional Environmental Regulation-An Explanation of the Incomplete Execution of Environmental Regulation. China Industrial Economy. 4(07), 74-90. [In Chinese].
[5] Li, G., Wang, B. (2015) Research on the Construction of Global System Quality Measurement System. Journal of Northwest Normal University. 52(4), 122-131. [In Chinese].
[6] Zhou, C., Du, Y., Peng, A. (2016) Does Environmental Regulation Affect the Location Choice of FDI in China? - Empirical Study based on Cost Perspective. World Economic Studies. 1(01), 110-120. [In Chinese].
[7] Fu, J., Li, L. (2010) FDI, Environmental Regulation and Pollution Shelter Effect: An Empirical Analysis Based on Provincial Data in China. Journal of Public Administration. 03, 65-74. [In Chinese].
[8] Zhang, Z., Zhao, G. (2012) FDI, Environmental Regulation and Technological Progress: An Empirical Analysis Based on Provincial Data in China. Quantitative Economic, Technical and Economic Research. 04, 19-32. [In Chinese].
[9] Yuan, Y., Xie, R. (2015) FDI, Environmental Regulation and Green Growth Total Factor Productivity Growth in China: An Empirical Study Based on Luenberger Index. International Trade Issues. 08, 84-93. [In Chinese].
[10] Li, Z. (2016) Regional Differences, Sources of FDI and Regulation of FDI Environment Regulation. Chinese Soft Science. 08, 89-101. [In Chinese].
[11] Zhu, P., Zhang, Z., Jiang, G. (2011) FDI and Environmental Regulation: An Empirical Study Based on Local Decentralization. Economic Research. 06, 133-145. [In Chinese].
[12] Lombard, P. (2002) The Impacts of Environmental Regulations on Industrial Activity: Evidence from the 1970 & 1977 Clean Air Act Amendments and the Census of Manufactures. Journal of Political Economy. 110(6), 1175-1219.
[13] Zhang, J., Fu, X. (2007) FDI and environmental regulations in China. Journal of the Asia Pacific Economy. 13(3), 332-353.
[14] Yang, Y., Niu, G., Tang, D. (2016) Study on the impact of environmental regulation on firm size distribution: a case study of Guangdong province. Fresen. Environ. Bull. 25, 5483-5491.
[15] Zhang, W., Zhang, L., Zhang, K. (2010) Environmental Regulation Intensity and Its Evolution in China-An Analysis Based on the Durbin Fixed Effect Model of Two-Zone System Space. Management Word. 12, 34-44. [In Chinese].
[16] Zhao, X. (2014) Environmental Regulation, Environmental Regulation Competition and Regional Industrial Economic Growth: An Empirical Study Based on Spatial Durbin Panel Model. International Trade Issues. 07, 82-92. [In Chinese].
[17] Li, S., Chu, S., Shen, C. (2014) Local Government Competition, Environmental Regulation and Regional Ecological Efficiency. World Economy. 04, 88-110. [In Chinese].
[18] Zhao, X. (2014) Local Government's Environmental Regulation Competition Strategy and Its Regional Growth Effect-Empirical Data from Urban Cities above Cities. Financial Economy. 10, 105-113. [In Chinese].
[19] Wang, Y. (2015) Research on Environmental Regulation Competition of Local Government in China Based on Spatial Panel Model. Manage Comments. 08, 23-32. [In Chinese].
[20] Say, N., Okten, SO. (2017) Integration of strategic environmental assessment into urban development plans in Turkey: case study of Adana city. Fresen. Environ. Bull. 26, 2840-2852.
[21] Bobat, A. (2017) Environmental Impact Assessment of Hydropower Projects in Turkey: Applications and Problems. Fresen. Environ. Bull. 26, 1192-1200.

[22] Yorulmaz, B., Yilmaz, F., Genc, T.O. (2015) Heavy metal concentrations in European EEL (anguilla anguilla l., 1758) From Köyceğiz-Dalyan lagoon system. Fresen. Environ. Bull. 24, 1607-1613.
[23] Dean, J.M., Lovely, M.E., Wang, H. (2005) Are foreign investors attracted to weak environmental regulations? Evaluating the evidence from China. Social Science Electronic Publishing. 90(1), 1-13. [In Chinese].
[24] Cole, M.A, Fredriksson, P.G. (2006) Endogenous Pollution Havens: Does FDI Influence Environmental Regulations? The Scandinavian Journal of Economics. 108(1), 157-178.
[25] Xu, M., Zuo, H. (2013) A Study on the Relationship between Environmental Regulation and Industrial Competitiveness under Agglomeration: A Re-examination Based on "Porter Hypothesis". China Industrial Economy. 03, 72-84. [In Chinese].
[26] Song, M., Wang, S. (2013) Analysis of Environmental Regulation，Technological Progression and Economic Growth from the Perspective of Statistical Tests. Economic Research Journal. 03, 122-134. [In Chinese].
[27] Li, B., Peng, X., Ouyang, M. (2013) Environmental Regulation, Green Total Factor Productivity and the Transformation of China's Industrial Development Mode: An Empirical Study Based on 36 Industrial Sector Data. China Industrial Economy. 04, 56-68. [In Chinese].
[28] Yuan, Y., Xie R. (2014) A Study on the Effect of Industrial Regulation on Environmental Regulation-An Empirical Test Based on China's Provincial Panel Data. China Industrial Economy. 08, 57-69. [In Chinese].
[29] Yuan, Y., Xie, R. (2016) Environmental Regulation and Industrial Green Productivity Growth: Re-examination of "Strong Potter Hypothesis". Chinese Soft Science. 8(07), 144-154. [In Chinese].
[30] Wu, H. (2015) Carbon Emission Reduction in China: Spatial and Temporal Pattern, Evolution Mechanism and Policy Suggestions - Theory and Method Based on Spatial Econometrics. Management World. 11, 3-10. [In Chinese].
[31] Li, L., Tang, D., Kong, Y., Liu, D., Yang, Y. (2016) A Study on the Impact of FDI on Urban Haze Pollution: A Case Study of the Pearl River. Management Comment. 28(6), 11-24. [In Chinese].
[32] Li, H., Zhang, J. (2015) Corruption and Firm Innovation: A Grease or Stumbling Block Relationship. Nankai Economic Research. 2(02), 24-58. [In Chinese].

Received: **29.6.2017**
Accepted: **24.01.2018**

CORRESPONDING AUTHOR

Yuanhua Yang
School of Public Management,
Guangdong University of Finance and Economics,
Guangzhou 510320 – China

e-mail: 260782245@qq.com

© by PSP Volume 27 – No. 5/2018 pages 2777-2784 Fresenius Environmental Bulletin

USE OF WATER QUALITY INDICES AS A TOOL IN WATER RESOURCES MANAGEMENT

Ireneusz Cymes*

Department of Water Resources, Climatology and Environmental Management, University of Warmia and Mazury in Olsztyn, Oczapowskiego Str. 2, 10-719 Olsztyn, Poland

ABSTRACT

The purpose of this study was to analyze the use of water quality indicators (WQIs) in assessing water quality in four river basins closed by impacts with retention reservoirs constructed on these inlets, and evaluation the application of this tool in water resource management. Water samples for determination of physicochemical parameters were collected from inflows supplying water to the reservoirs, from the reservoirs from the layers near the surface and close to the bottom. Analyses also comprised samples of treated municipal wastewater reaching two of the studies rivers at points upstream the reservoirs, and samples of waters before their inflow to the reservoirs.

Values of Water Quality Indicators were derived from 16 physicochemical parameters measured in 2004-2013. These numerous data, by means of the calculation method developed by the Canadian Council of Ministers of the Environment, were brought to single WQI values. Of key importance for the protection of water quality in rivers is the water and wastewater management carried out in river catchments. The input of treated wastewater to rivers is responsible for deterioration of the water quality class. This negative effect can be eliminated if water reservoirs are constructed below a wastewater treatment plant. Studies have shown their positive influence on the quality of water passing through such facilities, for example the CCME-WQI can rise by over 10 per cent. In consequence, the quality of water in rivers below such water bodies reached the same level as above a given WTP.

KEYWORDS:
water reservoirs, water resources, water quality, WQI

INTRODUCTION

For economy, a key element in water resources management is to make an assessment of both quantity and quality of avaliable water [1, 2, 3, 4, 5, 6, 7, 8, 9]. The WFD defines the concept of integrating water management in river basins, where the preparation and implementation of measures concerning a single ecological, hydrological and hydrogeological unit are coordinated. This approach requires international integration as water use often has a transborder character [7].

The quality of water is difficult to assess because of a large number of factors which influence it and a large number of parameters describing water characteristics. One outcome of water monitoring studies is a great wealth of analytical data, which is another obstacle to a more rapid interpretation of the results [10].

The water quality index (WQI) is a single numerical expression which inteprets the complex information on water quality represented by a large amount of data [11, 12, 13, 14, 15]. In many countries, e.g. in the USA, Canada, Spain, France, Germany, Austria, Italy and Turkey, the WQI is treated as an inseparable element of environmental monitoring used for reporting the results [5]. The WQI can be determined rapidly, and is therefore an important tool for the assessment of the quality and management of water resources [15, 16].

The objective of this research has been to use the selected WQI calculation method to assess the quality of water in watercourses supplying water to four lowland dam reservoirs. The investigations were carried out with the aim to identify the sources of pollution and to make more rational the management of water resources in the catchment basins of the watercourses supplying water to the reservoirs. Another purpose was to analyse the impact of the water reservoirs on the quality of waters which flow through them.

MATERIALS AND METHODS

Description of the Study Area and Sites. The studies were carried out in catchment basins of four rivers in northeastern Poland, in the North Masovian Lowland, in the area covered by the District of Ostrołęka and the Distrct of Przasnysz. Dam water retention reservoirs have been constructed on these rivers (Figure 1). They are situated between 52°57`36``N and 53°19`42``N latitude and 20°48`32``E and 21°43`57``E longitude.

The water reservoirs covered by this research are used for recreation: bathing, water sports, angling, family and social get-togethers, as well as a

source of water for irrigation in agriculture. The catchment basins of the reservoirs are used for farming or forestry and farming. The watercourses supplying water to the reservoirs Grodzisk Duży and Wykrot receive treated municipal wastewater and storm water. Wykrot Reservoir is divided into two parts: the main reservoir and the preliminary reservoir, which plays a protective role for the main part of the reservoir. In addition to the Rozoga River, the preliminary reservoir is supplied with water by a small stream called the Pełtówka and a drainage ditch. The analysed reservoirs belong to small and shallow water bodies: their average depth does not exceed 1.5 m, while the maximum depth is within the range of 2.0 m to 3.4 m (Table 1).

Sampling and Laboratory Analysis. Water for laboratory analyses was sampled from the watecourses supplying water to the reservoirs, from two depths of the reservoirs: near the surface and near the bottom, and from the rivers downstream from the reservoirs (Figure 1, Table 2). The analyses also comprised samples of treated wastewater discharged to the rivers above the reservoirs Grodzisk Duży and Wykrot, and water sampled from the rivers prior to the wastewater discharge point.

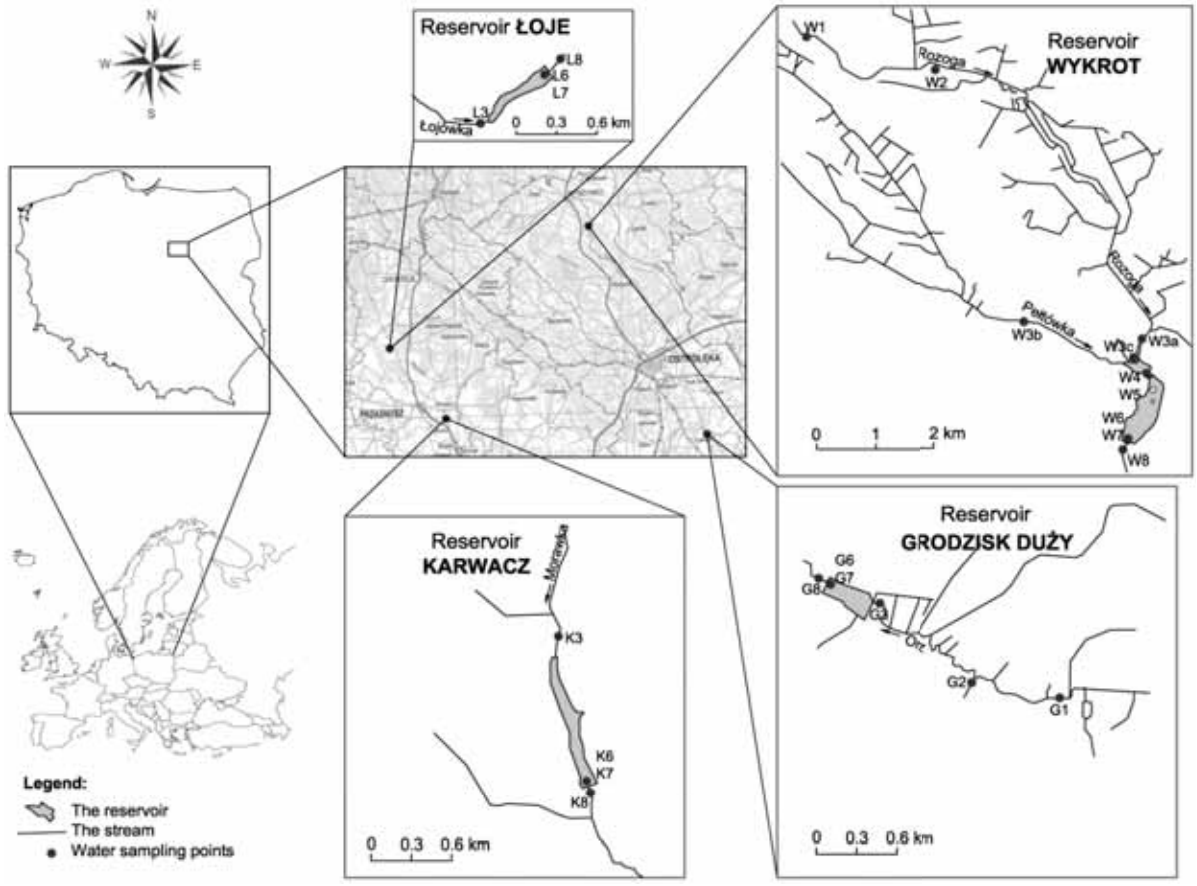


FIGURE 1
Location of the reservoirs covered by the surveys and measurement points

TABLE 1
Basic morphometric parameters of the analyzed reservoirs

Reservoir		Basin area [km^2]	Water surface area [ha]	Capacity [m^3]	Depth [m]	
					average	maximal
Grodzisk Duży		300	5.1	68 000	1.3	2.0
Karwacz		155	10.2	122 000	1.2	2.1
Łoje		6	4.6	55 000	1.2	3.3
Wykrot	preliminary	275	8.3	83 000	1.0	1.5
	main		43.7	687 000	1.5	3.4

TABLE 2
Sites of water sampling for laboratory analyses and the determinations run on samples

Sampling station	Location of a sampling site	Reservoir			
		Wykrot	Grodzisk Duży	Karwacz	Łoje
The river before a water treatment plant		W1	G1	-	-
The outflow from the treatment plant		W2	G2	-	-
Inflow into the reservoir	Rozoga	W3a	G3	K3	L3
	Pełtówka	W3b			
	drainage ditch	W3c			
Preliminary reservoir	layer at the surface	W4	-	-	-
	layer at the bottom	W5	-	-	-
Main reservoir	layer at the surface	W6	G6	K6	L6
	layer at the bottom	W7	G7	K7	L7
The outflow from the reservoir		W8	G8	K8	L8

TABLE 3
The CCME-WQI index categorization system [11]

WQI value	Water quality	Description
95-100	Excellent	Water quality is protected with a virtual absence of threat or impairment, conditions very close to natural or pristine levels
80-94	Good	Water quality is protected with only a minor degree of threat or impairment, conditions rarely depart from natural or desirable levels
65-79	Fair	Water quality is usually protected but occasionally threatened or impaired, conditions sometimes depart from natural or desirable levels
45-64	Marginal	Water quality is frequently threatened or impaired, conditions often depart from natural or desirable levels
0-44	Poor	Water quality is almost always threatened or impaired, conditions usually depart from natural or desirable levels

Water samples were taken in the years 2004-2013. The following parameters were determined in field, using a multi-parameter probe YSI 6600: pH, dissolved oxygen, electrical conductivity, total dissolved solids TDS, turbidity.

In the laboratory, the following water parameters were analysed: nitrite, nitrate, ammonia, phosphates, sulphates, chloride, sodium, potassium, calcium, magnesium in line with the methodology described in the Standard Methods [17], and total hardness – as a sum of Mg and Ca ions [18].

Calculating of Water Quality Index (WQI). The water quality index according to the Canadian Council of Ministers of the Environment: CCME-WQI was chosen for the assessment of water quality. He is calculated based on the water physicochemical characteristics referred to in the potable water quality requirements set by the WHO [19, 20, 21], as these are broadly recognisable norms, used all over the world [22].

The Canadian Council of Ministers of the Environment Water Quality Index is determined from the relationship [11, 23]:

$$CCME - WQI = 100 - \left(\frac{\sqrt{F_1^2 + F_2^2 + F_3^2}}{1.732}\right)$$

where:

F_1 – Scope - represents the percentage of variables that do not meet their objectives at least once during the time period under consideration ("failed variables"), relative to the total number of variables measured:

$$F_1 = \left(\frac{Number\ of\ failed\ variables}{Total\ number\ of\ variables}\right) \cdot 100$$

F_2 – Frequency - represents the percentage of individual tests that do not meet objectives ("failed tests"):

$$F_2 = \left(\frac{Number\ of\ failed\ tests}{Total\ number\ of\ tests}\right) \cdot 100$$

F_3 – Amplitude - represents the amount by which failed test values do not meet their objectives:

$$F_3 = \left(\frac{nse}{0.01 \cdot nse + 0.01}\right)$$

where:

nse - normalized sum of excursions - is calculated through the formula of:

$$nse = \frac{\sum_{i=1}^{n} excursion_i}{Total\ number\ of\ tests}$$

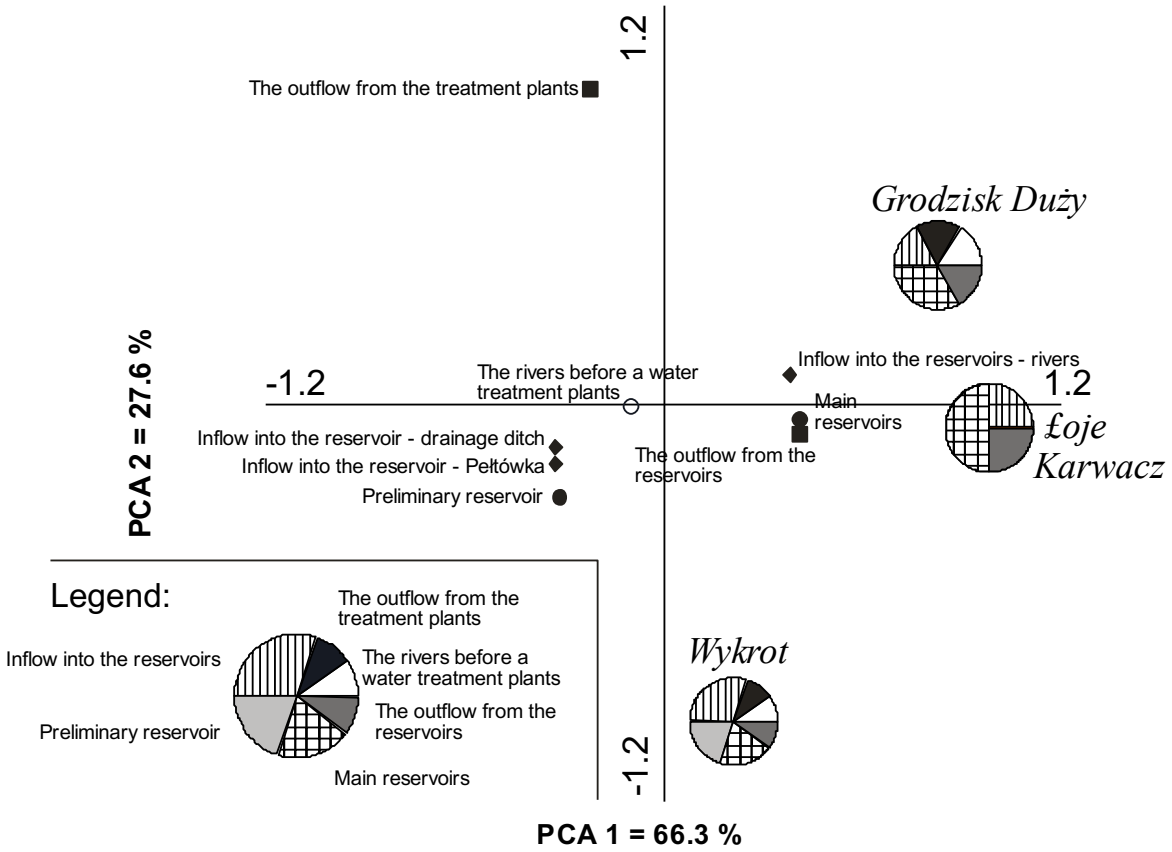
The number of times by which an individual concentration is greater than (or less than, when the objective is a minimum) the objective is termed an "excursion" and is expressed as follows:

- when the test value must not exceed the objective:

$$Excursion_i = \left(\frac{Failed\ test\ value_i}{Objective_j}\right) - 1$$

- for the cases in which the test value must not fall below the objective:

$$Excursion_i = \left(\frac{Objective_j}{Failed\ test\ value_i}\right) - 1$$



Axes	PCA 1	PCA 2	PCA 3	PCA 4	Total variance
Eigenvalues:	0.663	0.276	0.061	0.000	
Species-environment correlations:	0.556	0.414	0.477	0.392	
Cumulative percentage variance					1.000
of species data:	66.3	93.9	100.0	100.0	
of species-environment relation:	76.9	94.8	100.0	100.0	
Sum of all eigenvalues					1.000
Sum of all canonical eigenvalues					0.266

FIGURE 2
Analysis of relationship between the values of the indices CCME-WQI calculated for the water associated with the four dam reservoirs using method PCA

The quality of water is defined by comparing the calculated value of the CCME-WQI to a 100-point scale (Table 3).

Statistical analyses. Our analysis of the relationships between the research stations with regard to the structure of data, and the analysed waters depending on a sampling site, was based on the PCA method supported by the software program Canoco 4.5.

RESULTS AND DISCUSSION

The principal component analysis (PCA) served for interpretation of the data obtained from the calculations. This appraoch enabled us to diminish the number of attributes, which made it easier to notice dependences between the data that had been unobservable previously. The PCA was also applied to compare the research stations with respect to the structure of data as well as the analysed waters depending on their sampling sites. This analysis showed that the first two components were responsible for 93.9% of the variance of the original data set, where the first principal component (PCA1) represented 66.3% and the second one (PCA2) – 27.6% (Figure 2).

The PCA performed demonstrated a strong correlation in the structure of data (values of the CCME-WQI) for waters flowing into, retained and flowing out of the water reservoirs Grodzisk Duży and Wykrot, although the waters associated with the reservoir Łoje were of better quality. No such relationships were found for waters associated with the reservoirs which were fed waters through the rivers to which treated wastewater is discharged.

Waters flowing through rivers above the dam

water reservoirs built on these watercourses belonged to the water purity class called 'fair' (Table 4).

Wastewater flowing from WTPs flows to the Rozoga River above the reservoir Wykrot, and to the Orz River above the reservoir Grodzisk Duży. This wastewater belonged to the worst quality class called 'poor'. The CCME-WQI values of these waters (from 29.55 to 32.95) were approximately half the values of this index achieved for the other waters, and were not correlated with the latter (Figure 2). The influx of treated wastewater to the above rivers deteriorated the quality of river waters. The value of the CCME-WQI for the water in the Rozoga River fell down by 12.48, while decreasing by 4.5 for the Orz River waters. In both cases, a decrease in the value of the index meant that the water qualiy class changed from 'fair' to 'marginal'. A similar tendency was noted during a study on the quality of water in the Jajrood River in Iran, where the inflow of water from urbanised areas classified as 'poor' led to a decrease in the river water category from 'marginal' to 'poor' [24]. Analogously, the discharge of wastewater to Bherya Lake in India is implicated by Panduranga and Hosmani [25] as a reason why the lake water is classified as 'poor' in terms of water quality, i.e. corresponding to the CCME-WQI value of 32. A strong impact of the water and wastewater management conducted in river catchment basins is also suggested by a study completed on the Qu'Appelle River in Canada [26]. The quoted research demonstrated a considerable improvement in the river water quality, corresponding to an increase in the CCME-WQI by 26, after a new waterwater treatment plant had been constructed.

Values of the CCME-WQI for waters fed to the analysed dam reservoirs varied between 60.61 and 72.00. The worst quality waters, within the 'marginal' category, were flowing to the reservoir Grodzisk Duży from the Orz River, and to Wykrot from the Rozoga (Table 4). The preliminary reservoir Wykrot is also suplied with water classified as 'fair', which is brought through a drainage ditch and a small stream called the Pełtówka. Values of the CCME-WQI obtained for these waters were mutually correlated (Figure 2).

The water quality index values calculated for the water which has passed through the reservoirs show an unquestionably beneficial effect of these water bodies. The CCME-WQI value for water which has just flowed through the preliminary reservoir Wykrot increased by an average 14% compared to the values of this index calculated for the water reaching this water body. The water quality improves to a similar degree after water has passed through the reservoirs Grodzisk Wielki and Łoje, where the surface layer of water represented the 'good' water quality category, i.e. the highest class

TABLE 4
The values of CCME-WQI quality indicators for the analyzed water and the classification of water quality in 2004-2013

Location	CCME-WQI	Water quality
Reservoir Wykrot		
The river before a water treatment plant	76.53	Fair
The outflow from the treatment plant	29.55	Poor
Inflow into the reservoir - Rozoga	64.05	Marginal
Inflow into the reservoir - Pełtówka	69.04	Fair
Inflow into the reservoir - drainage ditch	67.30	Fair
Preliminary reservoir - layer at the surface	77.38	Fair
Preliminary reservoir - layer at the bottom	75.32	Fair
Main reservoir - layer at the surface	75.86	Fair
Main reservoir - layer at the bottom	71.92	Fair
The outflow from the reservoir	76.36	Fair
Reservoir Grodzisk Duży		
The river before a water treatment plant	65.11	Fair
The outflow from the treatment plant	32.95	Poor
Inflow into the reservoir	60.61	Marginal
Reservoir - layer at the surface	70.80	Fair
Reservoir - layer at the bottom	68.24	Fair
The outflow from the reservoir	67.01	Fair
Reservoir Karwacz		
Inflow into the reservoir	69.89	Fair
Reservoir - layer at the surface	72.54	Fair
Reservoir - layer at the bottom	68.87	Fair
The outflow from the reservoir	72.92	Fair
Reservoir Łoje		
Inflow into the reservoir	72.00	Fair
Reservoir - layer at the surface	83.52	Good
Reservoir - layer at the bottom	75.54	Fair
The outflow from the reservoir	81.31	Good

achieved by the analysed waters. Nikoo et al. [24] reported even better results. With regard to the impact of the Lytyan Dam on the Jajrood River in Iran, the quality index CCME-WQI for the water which has passed through the reservoir and dam improved by around 18 and the water quality class changed from 'poor' to 'marginal'. In another study, the water which has flowed through the dam Pucalro erected on the Elqui River in Chile was reported to have an CCME-WQI value raised from 74 before the reservoir to 95 below the dam, which corresponds to the improvement of water class from 'fair' to 'excellent' [27].

Water near the bottom in all the reservoirs was characterised by a distinctly worse quality, often falling into a lower class than the water sampled near the surface. The reason could be the enrichment of water with substances from bottom sediments via resuspension, which proceeds more intensively in shallow water bodies. This is an important feature of shallow water bodies in terms of using their water for utility purposes. Studies on the quality of water in Dobczyce Reservoir, used to supply waterworks, showed that a better quality water occurs in the surface layer outside the plant growing season, while during the plant growing season it is found at medium depths [28].

The value of the CCME-WQI for most of the water samples we analysed was within the interval of 65 to 79, which corresponds to the class named 'fair', representing waters of the quality periodically diverging from its natural or desriable quality (e.g. potable water quality). Comparable results with respect to the water quality in the Rozoga River were achieved by Grabińska et al. [29], who assessed the quality of water based on the Macrophyte River Index. The Rozoga River waters demonstrated a moderate ecological state and the water quality class III (on a five-grade scale), determined according to the physicochemical parameters. Thus, it can be concluded that method elaborated by the Canadian Council of Ministers of the Environment for calculating the WQI values is suitable for determination of the quality of surface waters in the conditions of northeastern Poland.

CONCLUSIONS

The assessment of water quality in four catchment basins located in north-eastern Poland was carried out at key points for water management using the water quality indicator developed by the Canadian Council of Ministers of the Environment [11]. Calculations were made using 16 parameters measured in 2004-2013. The numerous data available, through some uncomplicated formulas, were narrowed down to single values of the WQI. The used method has shown a high degree of comparability of water quality classifications with reports published by other authors [29].

The CCME-WQI values obtained showed that most of the analysed waters were of quality that periodically divereged from natural quality or the quality of potable water (class III on the five-grade scale). The application of water quality indices, the WQI, which simplify the water quality assessment procedure, provided us with sufficient data to draw key conclusions for the management of waters in the catchment basins of the four analysed rivers:

- Among the waters supplied to the dam reservoirs analysed, the best quality was achieved by the smallest watercourses.
- The worst water quality was determined for the treated wastewater discharged above Wykrot Reservoir into the Rozoga River, and Grodzisk Duży Reservoir into the Orz River. By discharging treated wastewater to the river, the quality of water flowing into the resevoirs supplied by these rivers deteriorated, and consequently the quality of water in the reseervoirs fell into a lower water quality class.
- With respect to the rivers to which treated wastewater was discharged, the quality of water below the reservoirs was observed to be restored to the value observed above the site of wastewater discharge.
- The water near the bottom in all the reservoirs was characterised by a distinctly worse quality, often falling into a lower water quality class, than the water sampled near the surface. This is an important feature of shallow water bodies from the point of view of water intake for household or industrial use.
- The localisation of water reservoirs on running watercourses, especially below the section where point sources of pollution exist, tends to have a positive effect on the quality of water flowing through reservoirs, although the risk of a negative impact canot be excluded, particularly when a reservoir is a shallow one, with the maximum depth of no more than 2 m.
- It was not confirmed that the runoff waters from arable fields lying on intensively cultivated sand soils were a threat to the quality of waters in the rivers or reservoirs.

ACKNOWLEDGEMENTS

The research was performed as part of a statutory grant no 20.610.012-300 executed at the Department of Water Management, Climatology and Environment Managemment, the University of Warmia and Mazury in Olsztyn, Poland.

REFERENCES

[1] Johnson, D.L., Ambrose, S.H., Bassett, T.J., Bowen, M.L., Crummey, D.E., Isaacson, J.S., Johnson, D.N., Lamb, P., Saul, M. and Winter-Nelson, A.E. (1997) Meanings of environmental terms. Journal of Environmental Quality. 26, 581-589.

[2] Khan, F., Husain, T. and Lumb, A. (2003) Water quality evaluation and trend analysis in selected watersheds of the Atlantic Region of Canada. Environmental Monitoring and Assessment. 88, 221-242.

[3] Sargaonkar, A. and Deshpande, V. (2003) Development of an overall index of pollution for surface water based on a general classification scheme in Indian context. Environmental Monitoring and Assessment. 89, 43-67.

[4] Glińska-Lewczuk, K. (2006) Effect of land use and lake presence on chemical diversity of the Łyna river system. Polish Journal of Environmental Studies. 15(2), 259-269.

[5] Ionuş, O. (2010) Water quality index - assessment method of the Motru river water quality (Oltenia, Romania). Annals of the University of Craiova, Series: Geography. 13, 74-83.

[6] Koc, J., Wons, M., Glińska-Lewczuk, K., Szymczyk, S. and Cymes, I. (2010) Fluorine concentrations in underground water intended for human consumption. Fresen.Environ. Bull. 19, 563-568.

[7] Khwakaram, A.I., Majid, S.N. and Hama, N.Y. (2012) Determination of water quality index (WQI) for Qalyasan stream in Sulaimani city Kurdistan region of Iraq. International Journal of Plant, Animal and Environmental Sciences. 2, 148-157.

[8] Obolewski, K. and Glińska-Lewczuk, K. (2013) Distribution of heavy metals in bottom sediments of floodplain lakes and their parent river - a case study of the Słupia. Journal of Elementology. 18(4), 673-682.

[9] Szejba, D., Papierowska, E., Cymes, I. and Bańkowska A. (2016) Nitrate nitrogen and phosphate concentrations in drainflow: An example of clay soil. Journal of Elementology. 21(3), 899-913.

[10] Darapu, S.S.K., Sudhakar, B., Krishna, K.S.R., Rao, P.V. and Sekhar, M.C. (2011) Determining water quality index for the evaluation of water quality of river Godavari. International Journal of Environmental Research and Application (IJERA). 1(2), 174-182.

[11] Canadian Council of Ministers of the Environment (2001) Canadian water quality guidelines for the protection of aquatic life: CCME Water Quality Index 1.0, Technical Report. In: Canadian environmental quality guidelines. Canadian Council of Ministers of the Environment, Winnipeg.

[12] Rubio-Arias, H., Contreras-Caraveo, M., Quintana, R. M., Saucedo-Teran, R. A. and Pinales-Munguia, A. (2012) An overall water quality index (WQI) for a man-made aquatic reservoir in Mexico. International Journal of Environmental Research and Public Health. 9(5), 1687-1698.

[13] Tomas, D., Cuk, R., Marie, A.S. and Mijatovic, I. (2013) Assessment of the Drava river (Croatia) by water quality index method. Fresen. Environ. Bull. 22, 904-913.

[14] Tyagi, S., Sharma, B., Singh, P. and Dobhal, R. (2013) Water Quality Assessment in Terms of Water Quality Index. American Journal of Water Resources. 1(3), 34-38.

[15] Cymes, I. and Glińska-Lewczuk, K. (2016) The use of Water Quality Indices (WQI and SAR) for multipurpose assessment of water in dam reservoirs. Journal of Elementology. 21(4), 1211-1224.

[16] Abbasi, T. and Abbasi, S.A. (2012) Water Quality Indices. Elsevier, Oxford.

[17] APHA (1992) Standard Methods for the Examination of Water and Wastewater. Water Pollution Control Federation, 15th ed. New York.

[18] Chapman, D. (ed.) (1996) Water quality assessments: a guide to the use of biota, sediments and water in environmental monitoring. 2nd ed. Chapman & Hall, London.

[19] WHO (2004) Guidelines for drinking water quality, 3rd ed. Geneva: World Health Organization. Available at: www.who.int/water_sanitation_health/dwq/GDWQ2004 web.pdf

[20] WHO (2006) Guidelines for drinking water quality, 3rd ed. Geneva: World Health Organization. Available at: www.who.int/water_sanitation_health/ dwq/gdwq3rev/en.

[21] WHO (2011) Guidelines for drinking water quality, 4rd ed. Geneva: World Health Organization. Available at: http://www.who.int/water_sanitation_health/publications/ 2011/dwq_guidelines/en.

[22] Vasanthavigar, M., Srinivasamoorthy, K., Vijayaragavan, K., Rajiv Ganthi, R., Chidambaram, S., Anandhan, P., Manivannan, R. and Vasudevan, S. (2010) Application of water quality index for groundwater quality assessment: Thirumanimuttar sub-basin, Tamilnadu, India. Environmental Monitoring and Assessment. 171(1-4), 595-609.

[23] Bharti, N. and Katyal, D. (2011) Water quality indices used for surface water vulnerability assessment. International Journal of Environmental Sciences. 2(1), 154-173.
[24] Nikoo, M.R., Kerachian, R., Malakpour-Estalaki, S., Bashi-Azghadi, S. N. and Azimi-Ghadikolaee M.M. (2011) A probabilistic water quality index for river water quality assessment: a case study. Environmental monitoring and assessment. 181(1-4), 465-478.
[25] Panduranga, M.G. and Hosmani, S.P. (2009) Water Quality Index (WQI) to Evaluate Surface Water Quality for Protection of Aquatic Life: A Case Study: Bherya Lake, Mysore, Karnataka State, India. In 13th World Lake Conference, Wuhan, China, papers s5-4.
[26] Davies, J.M. (2006) Application and tests of the Canadian water quality index for assessing changes in water quality in lakes and rivers of central North America. Lake and Reservoir Management. 22(4), 308-320.
[27] Espejo, L., Kretschmer, N., Oyarzún, J., Meza, F., Núñez, J., Maturana, H., Soto, G., Oyarzo, P., Garrido, M., Suckel, F., Amezaga, J. and Oyarzún, R. (2012) Application of water quality indices and analysis of the surface water quality monitoring network in semiarid North-Central Chile. Environmental Monitoring and Assessment. 184(9), 5571-5588.
[28] Bogdał, A., Policht-Latawiec, A. and Kołdras, S. (2015) Changes of Water Quality Indices with Depth at Drinking Water Intake from Dobczyce Reservoir. Annual Set the Environment Protection. 17(2), 1239-1258.
[29] Grabińska, A., Szymczyk, S. and Grabińska, B. (2012) The assessment of water quality of the River Omulew and Rozoga based on the macrophytes. Inżynieria ekologiczna. 38, 129-135 (in Polish).

Received: **09.08.2017**
Accepted: **10.02.2018**

CORRESPONDING AUTHOR

Ireneusz Cymes
Department of Water Resources,
Climatology and Environmental Management,
University of Warmia and Mazury in Olsztyn,
Oczapowskiego Str. 2,
10-719 Olsztyn – P oland

e-mail: irecym@uwm.edu.pl

© by PSP Volume 27 – No. 5/2018 pages 2785-2790 Fresenius Environmental Bulletin

CHEMICAL DIVERSITY OF ESSENTIAL OIL FROM LEAVES OF *ZIZIPHORA CLINOPODIOIDES* GROWING IN VAN, TURKEY

Nese Okut[1,*], Nilufer Selcuk[2], Mehmet Yagmur[3], Bunyamin Yildirim[4]

[1]Department of Field Crops, University of Yuzuncu Yil Van 65080, Turkey
[2]Department of Biology Sciences, University of Yuzuncu Yil Van 65080, Turkey
[3]Department of Field Crops, University of Ahi Evran Kirsehir 40100, Turkey
[4]Department of Field Crops, University of Igdir Igdir 76000, Turkey

ABSTRACT

Blue Mint Bush (*Ziziphora clinopodioides*) belongs to the family Lamiaceae and grows in Iran, Iraq, Central and Eastern part of Turkey. The leaves of *Ziziphora clinopodioides* L. samples were collected on the beginning of July (2010) from Koçköprü area (Van Province, Turkey) at an altitude of 1924 m and described accordingly. Hydrodistillation was used to isolate the essential oil of the plant and then 33 constituents were identified by using GC-MS. The majority presented compounds of the essential oil were Pulegone (29.31%), Menthone (21.79%), 1,8-Cineole (15.31%), β-Pinene (8.74%), Limonene (3.91%), α-Pinene (3.17%), 3-Terpinolenone (3.09%), β-Phellandrene (2.88%), respectively. Menthofurane, Isopulegone and Germacrene D are represented by low concentrations. A cluster analysis was carried on the essential oil composition of *Z. clinopodioides* to identify homogenous groups.

KEYWORDS:
Essential oil constituent, GC-MS analysis, *Ziziphora clinopodioides*, cluester analysis

INTRODUCTION

Ziziphora from to Lamiaceae spreaded in Turkey with 6 taxa belonging to *Z. clinopodioides* Lam., *Z. capitata* L., *Z. persica* Bunge., *Z. tenuior* L. and *Z. taurica* Biebspecies [1]. These have been used as a sedative, stomachic, aphrodisiac and carminative in Iranian and Turkish folk medicine.

Three chemotypes of *Z. clinopodioides* have been identified to the constituent of volatile oil, named as pulegone-rich, thymol-rich, and cineole-rich chemotypes [2]. In Turkey *Z. clinopodioides* oil is a pulegone-rich oil, composed mainly of pulegone (73%-35%), neomenthol (7%-23%), and menthone (6%-13%) [3].

Previous studies on the chemical constituent of *Z. clinopodioides* growing in Iran [4, 5, 6, 7], Turkey [8, 9, 10], Kazakhstan [11] and China [12, 13] have been reported. The chemical composition of the volatile oil from *Z. clinopodiodes* in wild form at Kermanshah province, Western Iran was examined by Shahabazi, [14]. Twenty-four components were identified in which carvacrol (64.22%), thymol (19.22%), γ-terpinene (4.63%), and p-cymene (4.86%) [14]. Mohammadreza, [15]. Z. clinopodioides Lam. samples from North of Iran and the volatile oil from plant samples was extracted and 26 components were identified. Pulegone (36.45%), piperitenone (19.12%), and menth-2-en-1-ol (5.31%) were reported as the most important components. A study by Ercisli et al, [16] on the chemical constituent of volatile oil from eight ecotypes of *Z. clinopodioides* grown in wild form at Coruh in Northeastern Turkey was determined seventeen components. The major contituents of all samples were (+)-pulegone, 1,8-cineole, limonene, menthol, β–pinene, menthone, piperitenone and piperitone.

This study, reports the chemical constituent of the essential oil of *Z. clinopodioides* at Eastern Anatolia in Turkey. The goal of current study is to illustrate the chemical compostion that can be useful in potential benefits, to provide the accessible information to help and guide future studies and to asses the potential chemotaxonomic importance of these species. Therefore, we evaluated the chemical constituent of the leaf essential oil of *Z. clinopodioides* from Turkey and compared the composition with different geographical locations.

MATERIALS AND METHODS

Plant material. The aerial parts (leaves and stems) of *Z. clinopodioides* were sampled during its flowering stage in July from Koçköprü area (Van Province, Turkey) located in the region of Eastern Turkey at an altitude of 1924 m and identified by Dr. N. Selcuk at Yuzuncu Yil University, Department of Biology Sciences, Van-Turkey. Voucher specimens were deposited at the Yuzuncu Yil University, Van, Turkey. The leaves were detached from the

stem and then dried in shade conditions as well as at the appropriate room temperature.

Preparation of essential oil. Air-dried plant materials were crushed and subjected to hydrodistillation using Clevenger-type apparatus for 3 h as suggested by European Pharmacopoeia [17]. The distillated oils were dried over anhydrous sodium sulphate and stored in an amber vial at 4 °C in the dark prior until analysis after the filtration.

Gas chromatography – mass spectrometry. Essential oils from plant were diluted 1/10 in n-hexane (v/v) before the analysis. GC/MS instrument (GCMS-QP 2010 Plus Shimadzu, Japan) fitted with built-in-Auto sampler using a Teknokroma TRB Wax capillary colomn (30m x 0.25 mm i.d., 0.25µm film thickness) was used. Injector temperature was 240 ºC. Column temperature was set from 60º to 240 ºC, temperatures held at 60 ºC during 2 min, and then gradually increased up to 240ºC at 10 ºC /min kept there for 5 minutes. As the carrier gas, helium was used and mass spectra were reported in the scan mode. The flow rate of helium was set 1 mL/min. Ionization voltage considered as 70 eV. The split ratio was set as 1:20. Ion source temperature was 200 ºC. Interface temperature was 240 ºC and mass was ranged from 40 to 350 amu (Resolution). The cut time of solvent was set 3 min. A sample of 0.1µl was used for the GS-MS analysis. The essential oil constituents were determined as a pilot study of previously sampled plant species. An then most appropriate temperature program for GC-MS was defined for analysis of the essential oils and the same program was considered for all samples. Each analysis in this experiment was repeated twice.

The preparation was analyzed to uncover of chemical components by GC-MS. For identification of the constituents, the retention time (Rt) and on computer matching against the spectra with MS-data bank (Wiley and Nist Library) was used. The relative quantity of compounds was estimated by integrating the total ion content of the individual peaks [18, 19]. For the identification of compounds, spectra above 95% was needed. The peak area measurments was used to compare the quantity of oil components

A total of 29 *Z. clinopodioides* leaf oil compositions both from the published literature and the composition from this study were considered as operational taxonomic units (OTUs). The percentage composition of 23 essential oil components [α-Pinene, Camphene, Sabinene, β-Pinene, Limonene, 1.8-Cineole, γ-Terpinene, p-Mentha-3-en-8-ol, Menthone, neo_Menthol, Menthol, Pulegone, Piperitone, Thymol, Carvacrol, Borneol, Germacrene D, isomenthol, β-caryophyllene, caryophyllene-oxide, p-Cymene, p-menthonene, piperitenone] were used to identify the chemical association between the various *Z. clinopodioides* essential oil samples by agglomerative hierarchical cluster (AHC). The XLSTAT software, version 2015.4.01 was used for clustering and the unweighted, pairgroup method with Centroid linkage clustering (UPGMC) was used a linkage criteria to spesify the distance between group of observations as a function of the pairwise distances and to develop a dendrogram for the Z. *clinopodioides* samples [20]. Chemical composition of the Z. *clinopodioides* leaves essential oils used in the cluster analysis are given in Table 1; the dendrogram of the cluster analysis is depicted in Figure 3.

RESULTS AND DISCUSSION

The chemical components were analyzed by GC-MS. In total thirty-three compounds were identified that representing 100% of the oil (Table. 1) which were extracted from essential oil of *Z. clinopodioides* leaves. The retention times and percentage compositions of identified compounds are listed in Table 1. The main components were Pulegone (29.31%), Menthone (21.79%), 1,8-Cineole (15.31%), β-Pinene (8.74%), Limonene (3.91%), α-Pinene (3.17%), 3- Terpinolenone (3.09%), β-Phellandrene (2.88%) respectively (Figure 1 and Figure 2).

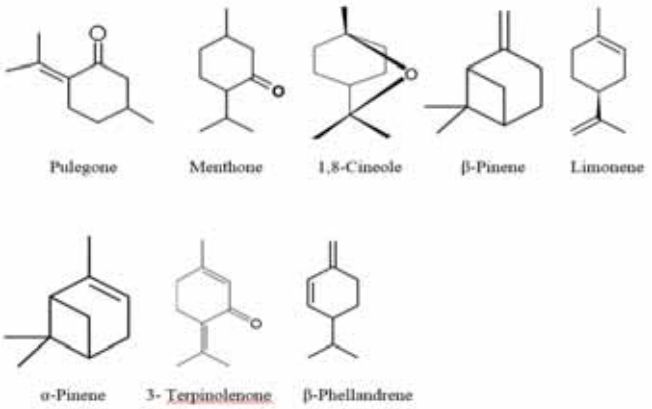


FIGURE 1
Some principals identified in the essential oil for the leaves of *Z. Clinopodioides*

TABLE 1
Chemical composition of the *Z. clinopodioides* leaves essential oils

Peak number	Component[a]	R_t(min)	Rate (%)
1	α- Pinene	3.043	3.17
2	Camphene	3.503	0.31
3	β- Pinene	4.020	8.74
4	β- Phellandrene	4.163	2.88
5	β- Myrcene	4.708	0.75
6	Limonene	5.255	3.91
7	1,8- Cineole	5.438	15.31
8	γ- Terpinene	5.926	0.18
9	Octan-3-one	6.052	0.14
10	Thymene	6.307	0.15
11	1-Octen-3-ol	8.945	0.19
12	Menthone	9.313	21.79
13	Menthofurane	9.491	0.34
14	β- Bourbonene	10.024	0.63
15	Linalool	10.253	0.21
16	Isopulegol	10.517	0.10
17	Isopulegone	10.889	0.58
18	neo-Menthol	11.067	1.23
19	Menthol	11.642	0.09
20	Pulegone	11.865	29.31
21	α- Terpineol	12.277	0.42
22	Borneol	12.338	1.05
23	Germacrene D	12.519	0.56
24	Cis Piperitone Oxide	12.674	0.88
25	p-Menth-1-en-3-one	12.763	1.80
26	β- Citrenellol	13.086	0.10
27	Myrtenol	13.488	0.13
28	3-Terpinolenone	15.093	3.09
29	cis-Jasmone	15.266	0.17
30	Cuminal	15.753	0.55
31	Eugenol	17.603	0.39
32	T hymol	17.700	0.75
33	Cembrene	18.257	0.10
Total			100

a Compounds given in order of elution for a TRB Wax capillary colomn

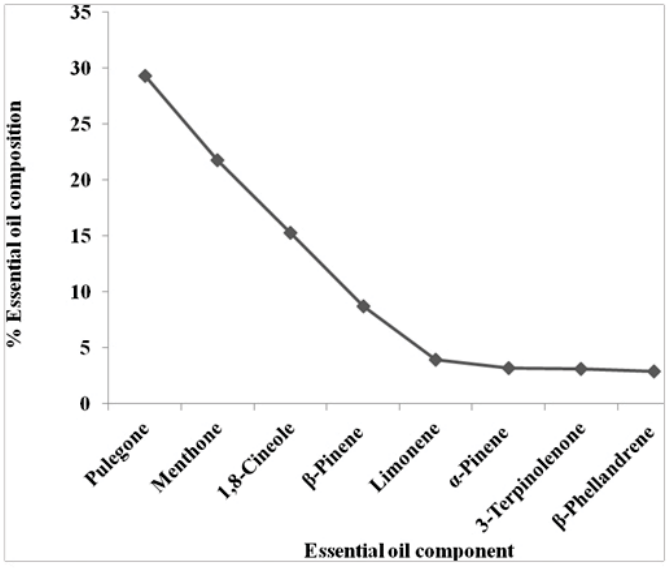


FIGURE 2
The main components rates obtained in *Z. clinopodioides* leaves essential oil

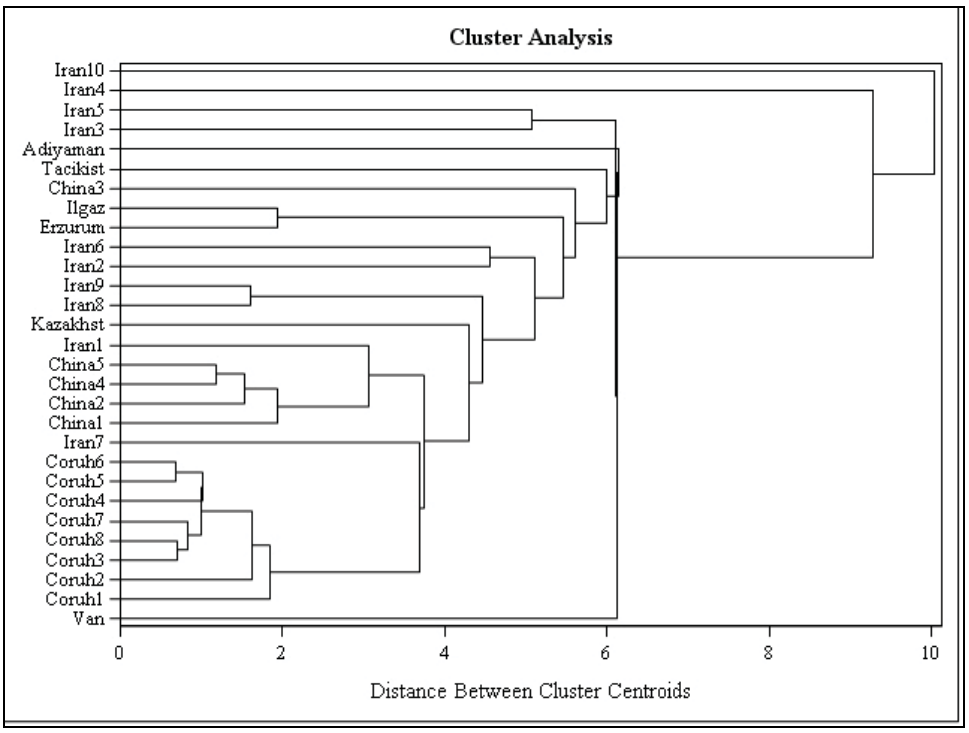


FIGURE 3
Dendrogram of agglomerative hierarchical cluster of 29 *Ziziphoraclinopodioides* leaf essential oil compositions

Enable to provide some insight into the chemotaxonomy of *Z. clinopodioides*, hierarchical cluster analysis was run on 29 different *Z. clinopodioides* essential oil samples reported in the literature as well as the current samples from Van (Turkey) (Figure 3). The cluster analysis reveals at least 26 pulegone-rich samples, a 1,8-cineole-rich sample, a thymol-rich sample and a β-caryophyllene-rich sample. The chemical composition of leaf essential oil of *Z. clinopodioides* from Van-Turkey is qualitatively similar to leaf oil from other geographical locations. The cluster analysis discloses the similarities in most of the leaf oils with the exception of three samples from Iran (#3) [5,14] (Figure 3), samples from Iran (#3 and #4) had not have thymol, Iran (#10) had not have any amount of 1,8-cineole and had very small concentration of β-pinene (%0.06). The samples from different part of Turkey had high concentration of Limonene (%6.98-10.66) after the pulegone except for Van region and they had also high concentration of 1,8-cineole (%5.67-15.31) except for Adiyaman location [9].

The major essential oil components in *Z. clinopodioides* (pulegone, limonene, 1,8-cineole, piperitenone or thymol) and piperitenone showed relevant antibacterial activity, indicating that the plant has potential use in phytotherapy. With phytochemical studies, *Ziziphora* species including *Z. clinopodioides* was found to be rich in particular for Pulegone [21, 22] which is agreement with our results. In addition the genus also has been reported to be strong antioxidant activity [22].

Our results showed some similarities with [4, 23, 10] studies about the main chemical component of *Z. clinopodioides*. In addition [24], 5 presented in a study that, *Z. clinopodioides* essential oil is used as a natural flavoring and stabilizer in food products. *Z. clinopodioides*is recommended for gastric pain. The powders of its leaves are used for giving aroma to food. The essential oil of *Z. clinopodioides*was found to be fungicidal at >1 µl/ml against *T. rubrum* and *M. gypseum* [23].

CONCLUSION

This study revealed that the leaf essential oil of *Z. clinopodioides*from Van, Turkey rich inPulegone (29.31%), Menthone (21.79%), 1,8-Cineole (15.31%), β-Pinene (8.74%), Limonene (3.91%), α-Pinene (3.17%), 3- Terpinolenone (3.09%), β-Phellandrene (2.88%) (Table 1). These components have antibacterial characteristics and can be used in making anaesthetic and antiseptic drugs and may be a commercially significant source of these phytochemicals.

REFERENCES

[1] Davis, P.H. (1982) Flora of Turkey and East Aegean Islands. University Press. Edinburgh, 7.

[2] Sharopov, F.S. and Setzer, W.N. (2011) Chemical diversity of *Ziziphora clinopodioides*: Composition of the essential oil of *Z. clinopodioides* from Tajikistan. Nat. Prod. Commun. 6, 695–698.

[3] Primo, V., Rovera, M., Zanon, S., Oliva, M. Demo, M., Daghero, J. and Sabini, L. (2001) Determinación de la actividad antibacteriana y antiviral del aceite esencial de *Minthostachys verticillata* (Griseb.) Epling. Rev. Argent. Microbiol. 33, 113–117.

[4] Sardashti, A.R., Valizadeh, J. and Adhami, Y. (2012) Chemical composition of the essential oil from *Ziziphora clinopodioids* Lam. from Iran by means of gas chromatography-mass spectrometry (GC-MS). Journal of Horticulture and Forestry. 4, 169-171.

[5] Khodaverdi-Samani, H., Pirbalouti, A.G., Shirmardi, H.A. and Malekpoor, F. (2015) Chemical composition of essential oils of *Ziziphora clinopodioides* Lam. (endemic Iranian herb) collected from different natural habitats. Indian Journal of Traditional Knowledge. 14 (1), 57-62.

[6] Amiri, H. (2009) Influence of growth phase on the essential oil composition of *Ziziphora clinopodioides* Lam. Natural Product Research. 23(7), 601–606.

[7] Masrournia, M. and Shams, A. (2013) Elemental determination and essential oil composition of *Ziziphora clinopodioides* and consideration of its antibacterial effects. Asian Journal of Chemistry. 25(12), 6553-6556.

[8] Baser, K.H.C., Sezik, E. and Tumen, G. (1991) Composition of essential oil of *Zizihora clinopodiodies* Lam. J. Ess. Oil Res. 3, 237-239.

[9] Kılıc, O. and Bagcı, E. (2013) Essential oils of three *Ziziphora* L. taxa from Turkey and their chemotaxonomy. Asian Journal of Chemistry. 25(13), 7263-7266.

[10] Ozturk, S. and Ercisli, S. (2007) Antibacterial activity and chemical constitutions of *Ziziphora clinopodioides*. Food Control. 18, 535–540

[11] Belyaev, N.F. and Demeubaeva, A.M. (1999). Chromatographic study of th composition of the essential oil of *Ziziphora clinopodioides*, a vicarious form of *Origanum vulgare*. Chemistry of Natural Compounds. 35, 52-54.

[12] Xing, S.-l., Zhang, P.-h., Ji, Q.l., Jia, H.-l. and Wang, X.-h. (2010) Essential oil compositions and antioxidant activities of two *Ziziphora* species in Xinjiang. Food Science. 31(07), 154-159.

[13] Zhoua, X., Yua, Q., Gonga, H and Tiana, S. (2012). GC-MS Analysis of *Ziziphoraclinopodioides* Essential Oil from North Xinjiang, China Natural Product Communicatioans. Vol.7, No.1, 81-82

[14] Shahbazi, Y. (2015) *Ziziphora clinopodioides* essential oil and nisin as potential antimicrobial agents against *Escherichia coli* O157:H7 in Doogh (Iranian Yoghurt Drink). Journal of Pathogens. 2015, Article ID 176024, 7p.

[15] Mohammadreza, V.R. (2008) Essential oil composition and Biological Activity of *Z. Clinopodioides* American-Eurasian J. Sustain. Agric. 2(1), 69-71.

[16] Ercisli, S., Dogan, H., Jurikova, T., Temim, E., Leto, A. and Hadziabulic, A. (2014) Chemical constitutions and antioxidant activity of *Ziziphora clinopodioides* Lam. ecotypes from Turkey. 4 International Conference on Food and Nutrition Technology. IPCBEE vol. 72. IACSIT Press, Singapore.

[17] Anonymous. (1996) European pharmacopoeia (3th Ed.). Council of Europe, Strasburg, France. 121p.

[18] Tepecik, M., Esetlili, B.C., Anac, D., Cicekli, M., Ozturk, B. (2016) Effects of different mineral fertilizers on macro nutrient content and essential oil components of lemon balm Fresen. Environ. Bull. 25, 4469-4477.

[19] Kose, Y.B., Demirci, B., Iscan, G. (2017) Volatile oil composition and biological activity of *Achillea biebersteinii* Afan. and Aachillea teretifolia Willd. Fresen. Environ. Bull. 26, 5213-5218.

[20] Rokach, L. and Oded M. (2005) "Clustering methods." Data mining and knowledge discovery handbook. Springer. US. 321-352.

[21] Baser, K.H.C. (2002). Aromatic biodiversity among the flowering plant taxa of Turkey. Pure Appl. Chem. 74, 527–545.

[22] Meral, G.E., Konyalioglu, S. and Ozturk, B. (2002) Essential oil composition and antioxidant activity of endemic *Ziziphora taurica* subsp *cleonioides*. Fitoterapia. 73, 716–718.

[23] Behravan, J., Ramezani, M., Hassanzadeh, M.K., Eskandari, M., Kasaian, J. and Sabeti, Z. (2007) Composition, Antimycotic and Antibacterial Activity of *Ziziphora clinopodioides* Lam. Essential Oil from Iran. Journal of Essential Oil Bearing Plants. 10, 339-345.

[24] Beikmohammadi, M. (2011) The evaluation of medicinal properties of *Ziziphora clinopodioides.* World Applied Sciences Journal. 12, 1635-1638.

Received: **10.8.2017**
Accepted: **23.01.2018**

CORRESPONDING AUTHOR

Nese Okut
Department of Field Crops,
University of Yuzuncu Yil
Van 65080 – Turkey

e-mail: neseokut@gmail.com

© by PSP Volume 27 – No. 5/2018 pages 2791-2799 Fresenius Environmental Bulletin

USE OF THE WATER QUALITY INDEX (CCME-WQI) IN AN EVALUATION OF THE IMPACT OF DAM RESERVOIRS ON QAULITY OF GROUNDWATER

Ireneusz Cymes*

Department of Water Resources, Climatology and Environmental Management, University of Warmia and Mazury In Olsztyn, Oczapowskiego Str. 2, 10-719 Olsztyn, Poland

ABSTRACT

The study covered four lowland dam reservoirs and groundwater in the direct catchment basins of these water bodies, situated in north-eastern Poland. The analysis of the impact of the reservoirs on water quality was supported by the method developed by the Canadian Council of Ministers of the Environment, that is the Water Quality Index based on 16 physicochemical water parameters, which were determined in 2004-2013. The groundwater in the area surrounding the reservoir Grodzisk Duży was classified as 'poor', while in the basins of the reservoirs Karwacz and Łoje it belonged to the category 'marginal', and that in the basin of Wykrot was categorised as 'fair'. The analysis showed a relationship between changes in the quality of groundwater and its distance to the shoreline of a reservoir, which was in agreement with the direction of water filtration from the basin to the reservoir. The best quality of groundwater, comparable to the quality of water in the reservoirs, was determined in piezometers most distant from the reservoirs, and the worst one – in piezometers closest to these water bodies. Despite the small distance, the quality of groundwater in the latter location was significantly worse that the quality of water retained in the reservoirs. Thus, it can be concluded that infiltration of worse quality water from the ground to the reservoirs was not intensive enough to pose a threat to the quality of water retained in these artificial water bodies, not even in ones created in easily permeable soils.

KEYWORDS:
groundwater, water quality, WQI, dam reservoirs

INTRODUCTION

Many countries across the world apply various methods to determine the quality of water. For years, attempts have been made to unify and improve water quality assessment systems. An example is the use of water quality indices. The earliest work in this area dates back to 1848, when a biological criterion was used in Germany to evaluate water quality [1]. Indices built on numerical scales were first developed in 1965 by Horton [2]. Water quality indices (WQI) are a useful tool to simplify, inform and interpret complex information about water quality, which is described by many parameters but here can be expressed by a single number [3, 4, 5, 6, 7, 8]. Many methods applied to caclulate WQI are referred to the potable water quality requirements set by the WHO [9, 10, 11], which are the standards broadly acknolwedged and used all over the world [12]. Many authors use them to assess the quality of waters in watercourses [4, 5, 7, 13, 14, 15, 16, 17, 18], natural and artificial water bodies [19, 20, 21, 22], or groundwater resources [12, 23, 24, 25, 26, 27, 28].

The objective of this research has been to apply the water quality index CCME-WQI to analyse interactions between groundwater and water retained in four lowland dam water reservoirs, situtated in north-eastern Poland.

METHODS AND MATERIALS

The study covered the groundwater resources lying in the direct catchment basin of four dam water reservoirs situated in north-eastern Poland, in the North Masovian Lowland, between the latitudes 52º57`36``N and 53º19`42``N and the longitudes 20º48`32``E i 21º43`57``E (Figure 1).

Several small watercourses had been dammed to create the four reservoirs, which now cover the following area: 4.6 ha – the reservoir Łoje, 5.1 ha - Grodzisk Duży and 10.2 ha - Karwacz. The largest one, Wykrot, is divided into two parts: the main reservoir covering 43.7 ha, and the preliminary reservoir, which is 8.3 ha in size. The average depth of the reservoirs does not exceed 1.5 m, and the maximum one is 3.4 m.

The direct catchment basin of Grodzisk Duży lies on peat soil developed on alluvial deposits, fine sands and gravels, underlain by low-plasticity sandy clays. The clays appear from the depth of 1.3-2.8 m. The geological profile in the Karwacz reservoir catchment has a similar structure. In it, the top layer consists of sands and gravel, peat and alluvial deposits are found in relief depressions, and all are underlain

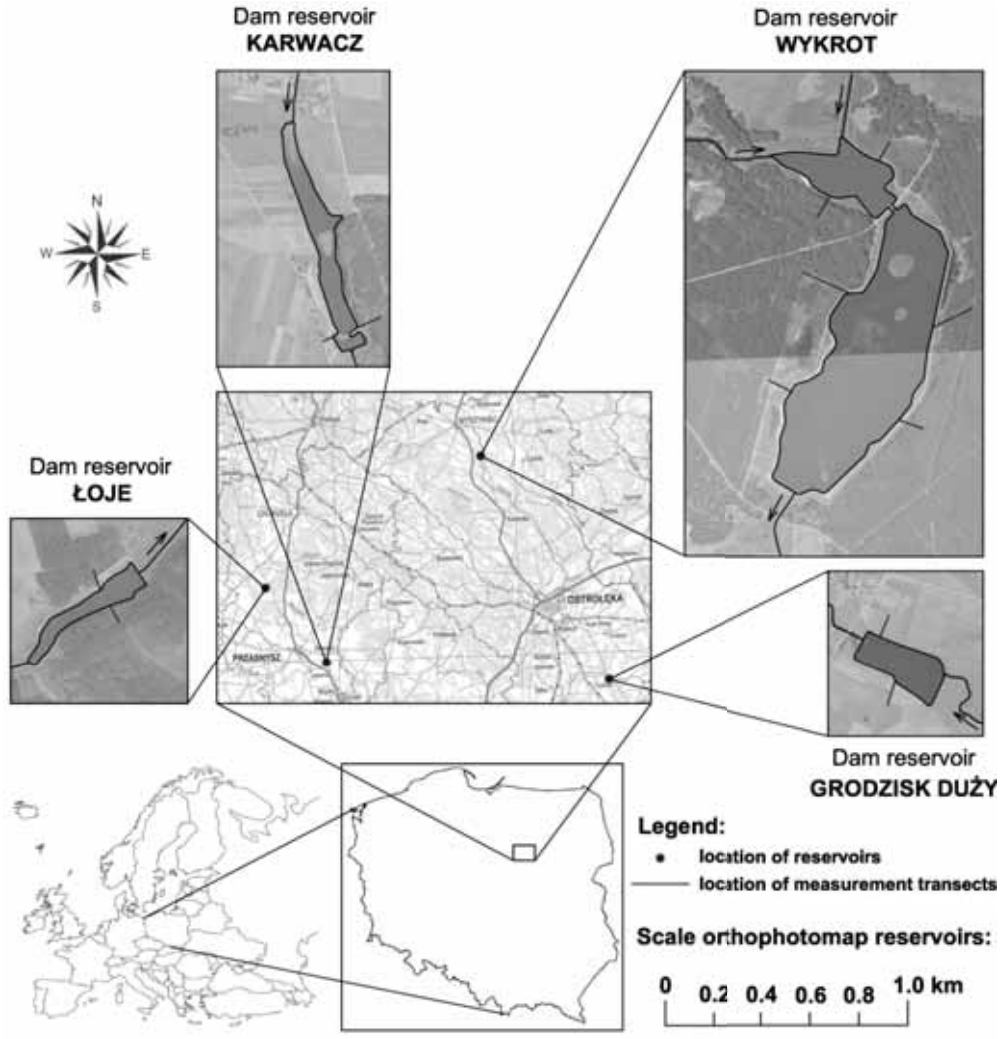


FIGURE 1
Localisation of the analysed water reservoirs and the transects along which piezometers were drilled.

by glacial till.

Around the reservoir Łoje there are fine to medium sands, moderately and well compacted, lying down to the depth of 5.5-6.0 m on low- and slight-plasticity clayely sands.

One transect, composed of 3 to 6 piezometers, whose exact location is shown in Fig. 1 was prepared for each of the analysed water reservoirs in order to make a quality assessment of groundwaters found in its direct catchment basin.

The number of piezometers depended on the land relief of a given basin and the depth at which groundwater was found – although the piezometers were drilled with a manual drill down to the depth of 6.0 m, some holes made in the catchment of Łoje reservoir remained empty during the study.

The reservoir Wykrot lies within the zone of sandur deposits accumulated on moraine clays from the North Polish Glaciation. The geological profile contains loose fine sands on medium dense fine sands to the depth of 2.0 m, while below 9.0 m there are silty clays of low plasticity and slight plasticity. Groundwater was sampled from 20 piezometers located along 3 transects: one perpendicular to the axis of the preliminary reservoir and composed of 6 piezometers, and two in the catchment of the main reservoir, one of which had 8 piezometers while the other one contained 6 piezometers.

Groundwater samples for laboratory analyses were drawn from the piezometers in 2004-2013. In field, using a multi-parameter probe YSI 6600, the following were determined: pH, dissolved oxygen, electrical conductivity, total dissolved solids (TDS) and turbidity. In the laboratory, in line with the Standard Metods [29], the following determinations were made: nitrite, nitrate, ammonia, phosphates, sulphates, chloride, sodium, potassium, calcium, magnesium. Total hardness was determined as the sum of Mg and Ca ions [30].

The quality of groundwater was assessed using the Canadian Council of Ministers of Environment Water Quality Index. This index is calculated from the formula [31, 32]:

$$CCME - WQI = 100 - \left(\frac{\sqrt{F_1^2 + F_2^2 + F_3^2}}{1.732} \right)$$

where:

F_1 – Scope - represents the percentage of variables that do not meet their objectives at least once during the time period under consideration ("failed variables"), relative to the total number of variables measured:

$$F_1 = \left(\frac{Number\ of\ failed\ variables}{Total\ number\ of\ variables}\right) \cdot 100$$

F_2 – Frequency - represents the percentage of individual tests that do not meet objectives ("failed tests"):

$$F_2 = \left(\frac{Number\ of\ failed\ tests}{Total\ number\ of\ tests}\right) \cdot 100$$

F_3 – Amplitude - represents the amount by which failed test values do not meet their objectives:

$$F_3 = \left(\frac{nse}{0.01 \cdot nse + 0.01}\right)$$

where:

nse - normalized sum of excursions - is calculated through the formula of:

$$nse = \frac{\sum_{i=1}^{n} excursion_i}{Total\ number\ of\ tests}$$

The number of times by which an individual concentration is greater than (or less than, when the objective is a minimum) the objective is termed an "excursion" and is expressed as follows:

- when the test value must not exceed the objective:

$$Excursion_i = \left(\frac{Failed\ test\ value_i}{Objective_j}\right) - 1$$

- for the cases in which the test value must not fall below the objective:

$$Excursion_i = \left(\frac{Objective_j}{Failed\ test\ value_i}\right) - 1$$

The calculated values of the CCME-WQI were referred to a 100-point scale and assigned to one of the five classes (Table 1).

TABLE 1
The CCME-WQI index categorization system [32]

Water quality	WQI value	Description
Excellent	95-100	Water quality is protected with a virtual absence of threat or impairment, conditions very close to natural or pristine levels
Good	80-94	Water quality is protected with only a minor degree of threat or impairment, conditions rarely depart from natural or desirable levels
Fair	65-79	Water quality is usually protected but occasionally threatened or impaired, conditions sometimes depart from natural or desirable levels
Marginal	45-64	Water quality is frequently threatened or impaired, conditions often depart from natural or desirable levels
Poor	0-44	Water quality is almost always threatened or impaired, conditions usually depart from natural or desirable levels

Statistical analyses were supported by the program Statistica v.10.0 PL. Homogeneous groups were identified with respect to the WQI values calculated for the groundwater found in the direct catchments of the dam reservoirs. The groups were determined with the aid of one-factor analysis of variance (ANOVA) and the Duncan's range test, at $p \leq 0.05$. The Hierarchical Clustering Analysis (HCA) approach was applied to analyse the quality of groundwater determined with the CCME-WQI, depending on the distance to a reservoir. The data set was treated by the Ward's method of linkage with the Euclidean distance as a measure of similarity. The PCA method, supported by the software programe package Canoco 4.5, was applied to analyse relationships between the original quality parameters for waters retained in the reservoirs and the groundwater found at different distance from the reservoirs.

RESULTS AND DISCUSSION

The CCME-WQI values for the water retained in the analysed water reservoirs ranged from 69.52 for the reservoir Grodzisk Duży, whose catchment is used for intensive agricultural production and which is supplied water by a river to which treated wastewater is discharged at a point above the reservoir, to 79.53 for the reservoir Łoje, fed water by a small watercourse and located in an agricultural and forest catchment (Table 2). Waters from all the reservoirs fell within the water quality class termed as 'fair'. Approximately same results were obtained by researchers who studied the quality of waters in reservoirs in other parts of the world. For example, the CCME-WQI values between 49 and 62 were calculated for the water in Lake Hawassa in Ethiopia, corresponding to the water quality class called 'marginal' [33, 34]. Slightly higher values of the CCME-WQI, within the range of 64 – 67, were achieved for the waters of the dam reservoir called Tehri in India [35], as well as for the waters of the marsh Al-Hammar in Iraq, where the CCME-WQI values ranged from 64 to 73 [36]. However, some of the analysed waters fell into the category 'poor' (values of the CCME-WQI from 34.3 to 44), and the reason was the discharge of wastewater from sewers [37]. The same cause of poor quality of waters was implicated by Panduranga Murthy and Hosmani [38], who analysed the water in Bherya Lake in India. Such bad quality of water is often responsible for diseases of aquatic organisms, including fish, which was demonstrated by Rakesh and Ammini [39], who examined waters of Chakkamkandam Lake in India. Compared to the quality of waters retained in the analysed water reservoirs, situated in north-eastern Poland, the quality of the groundwater in the catchments of these reservoirs was much worse (Table 2).

TABLE 2
Values of the CCME-WQI calculated for the years 2004-2013 for waters retained in the dam reservoirs and for groundwaters in the reservoirs' direct catchments

Reservoir	Index CCME-WQI									
	Groundwaters – off the left shore				Water in the reservoir	Groundwaters – off the right shore				Ground-waters, on average
Distance of a piezometer to the reservoir [m]	190-200	100-110	40-50	10-20		10-20	40-50	100-110	190-200	
Grodzisk Duży	-	45.05	45.85	57.10	69.52	17.73	24.76	35.04	-	37.59[a]
Karwacz	-	50.04	45.32	58.20	70.71	26.90	51.54	-	-	53.34[a]
Łoje	-	-	-	47.02	79.53	50.18	60.86	-	-	52.69[a]
Wykrot - preliminary reservoir	-	73.28	60.90	48.91	76.35	73.40	81.13	79.25	-	69.48[b]
Wykrot – main reservoir	82.58	79.25	78.29	70.89	73.89	67.94	83.73	78.83	78.09	72.46[b]
	-	76.22	61.32	65.19		36.17	83.03	72.94	-	

a, b – homogeneous groups identified by one-factor analysis of variance (ANOVA) and the Duncan's test at $p \leq 0.05$

A similar relationship was reported by Zhang et al. [40], who examined waters in the Second Songhua River basin, China, and concluded that the difference in water quality was mostly due to the higher concentrations of sodium, chlorides and nitrates in groundwater than in surface water.

The lowest value of the CCME WQI among the grounwater samples tested in this study was calculated for the ones drawn from the piezometer located 10-20 m from the reservoir Grodzisk Duży, where it equalled 17.73, whereas the highest value, 83.73, was achieved by the groundwater samples drawn at a distance of 40-50 m from the main reservoir of Wykrot. On average, the groundwater in the area around Grodzisk Duży belonged to the lowest category 'poor', the one in the catchments of Karwacz and Łoje – to the category 'marginal', and the groundwater in the catchment of Wykrot fell into the category 'fair'. High variance among the CCME-WQI values was also noted by the researchers who studied the quality of groundwater in India [41, 42], or Sri Lanca [43]. These authors underlined the negative impact of anthropogenic factors, of which farming played an important role, being responsible for high concentrations of nitrates in grounwater. This conclusion is supported by results of investigations carried out in north-eastern Poland [44, 45].

The application of a one-factor analysis of variance (ANOVA) and the Duncan's test at $p \leq 0.05$ revelaed two homogeneous groups: the first one included groundwaters of worse quality (categories 'poor' and 'marginal'), which were found in the catchments of Grodzisk Duży, Karwacz and Łoje, while the second group comprised groundwaters of better quality (category 'fair'), which appeared in the direct catchment of the reservoir Wykrot. This is the catchment dominated by forests growing on sandur sands.

The physiographic and hydrological conditions suggest that the analysed water reservoirs drain their direct catchments. The run-off water carries away certain substances from a given catchment, which means that the quality of groundwater deteriorates along the direction towards the reservoir (Figure 2). The best quality of groundwater was identified in the catchment of the reservoir Wykrot, situated on outwash sands, in piezometers located 190-200 m away from the reservoir's shoreline. These waters belonged to the catgory 'good', having the highest value of the CCME-WQI, which reached 80.34. In the dendrogram produced by the Ward's hierarchical method, they appeared in the same cluster as the waters from the reservoirs, even though the latter were classified as belonging to a lower water quality class, i,e, 'fair', as the CCME-WQI value they obtained was lower by 6.36.

The groundwaters distant by 100-110 m from the reservoir were classified as belonging to the same water quality category, although attaining a lower average value of CCME-WQI, namely 65.54. The grounwaters nearest to the reservoirs compose a separate cluster, containing waters of the lowest quality class, i.e. 'marginal'. The worst quality grounwaters occurred in the nearest vicinity of the reservoirs, that is 10-20 m away from these water bodies. Despite such a short distance, their quality was statistically significantly worse than the quality of waters retained in the reservoirs. The average values of the CCME-WQI for the compared waters were different by 22.34. Among the 16 parameters applied to calculate the CCME-WQI values, values of 13 parameters were higher for the groundwaters sampled 10-20 m from the shoreline than for the waters in the reservoirs (Table 3), and of these parameters the values of electrical conductivity and turbidity as well as the concentrations of TDS, nitrate, ammonia, phosphates, sodium and potassium were statistically significantly higher, which was confirmed by the Duncan's test at $p \leq 0.05$.

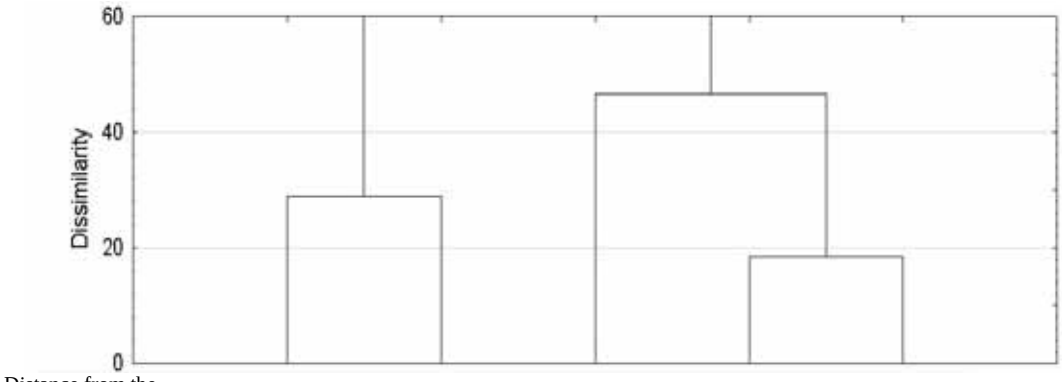


FIGURE 2
Tree diagram of cluster analysis of study sites based on value CCME-WQI, obtained by using Ward's method as linkage rule and Euclidean distances as metric for distance calculation

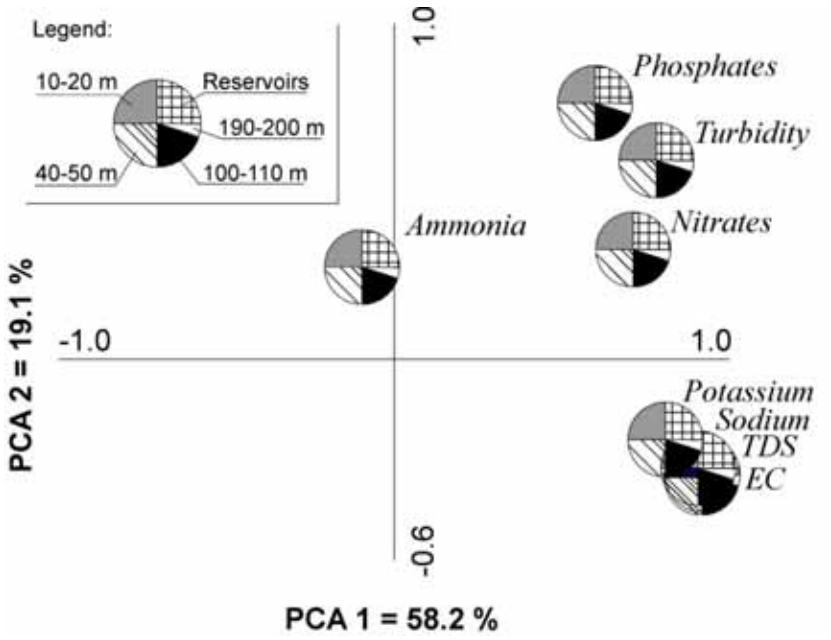
TABLE 3
Average values of the water parameters in the reservoirs and groundwaters, used to calculated the CCME-WQI

Parameter	Unit	Reserviors	Distance from the reservoirs [m]			
			10-20	40-50	100-110	190-200
Dissolved oxygen	$mg \cdot dm^{-3}$	9.46*	4.47	3.97	4.07	4.15
Electrical conductivity	$\mu S \cdot cm^{-1}$	430	589*	582	434	150
TDS	$mg \cdot dm^{-3}$	281.3	384.5*	372.3	275.7	96.9
Turbidity	NTU	6.4	68.4*	21.4	16.1	3.7
Nitrite	$mg \cdot dm^{-3}$	0.048	0.036	0.025	0.031	0.024
Nitrate	$mg \cdot dm^{-3}$	2.76	12.38*	1.89	9.46	0.59
Ammonia	$mg \cdot dm^{-3}$	0.20	4.95*	0.56	0.13	0.08
Phosphates	$mg \cdot dm^{-3}$	0.24	1.24*	0.20	0.13	0.14
Chloride	$mg \cdot dm^{-3}$	13.6	26.2	50.7	48.3	9.0
Sulfate	$mg \cdot dm^{-3}$	137.2	219.9	254.9	170.4	68.5
Magnesium	$mg \cdot dm^{-3}$	9.1	12.6	14.8	11.6	2.1
Calcium	$mg \cdot dm^{-3}$	72.6	75.9	69.9	57.4	19.4
Sodium	$mg \cdot dm^{-3}$	7.0	13.6*	18.5	15.1	6.0
Potassium	$mg \cdot dm^{-3}$	3.0	22.2*	16.4	4.0	0.6
Total hardness	$mg \cdot dm^{-3}$	81.7	88.5	84.7	69.0	21.5

* statistically significant differences between the waters in the reservoirs and groundwaters at a distance of 10-20 m from the shorelines were determined with the Duncan's test at $p \leq 0.05$

The Principal Component Analysis was carried out in order to explore the dependences between the aforementioned parameters of the waters retained in the reservoirs and the groundwaters found at different distances from these water bodies. The first two analyses (PCA 1 and PCA 2) represent 77.3% of the variance of the original data set (Figure 3). Based on the PCA results, three groups could be distinguished. The first group of water quality parameters, with strong, mutual positive correlations, demonstrates a close relationship between electrical conductivity versus TDS and the water content of the analysed metals, of which Na and K are shown in Figure 3. The second group implicates a relationship (positive correlation) between turbidity and the water content of biogenic substances, which in this analysis were represented by nitrates and phosphates. The third group comprises ammonia, which is not correlated with any of the analysed parameters.

Figure 4 shows values achieved by the parameters characteristic for each of the above groups, in the reservoir waters and in groundwaters relative to their distance to the reservoirs. The statistical analysis and visualisation of results in the diagrams, representative for the distinguished three groups of parameters applied to testing water quality, confirm the results obtained from the calculated values of the CCME-WQI. With respect to lowland water reservoirs which drain the surrounding soils, water running off from the direct catchment towards such reservoirs is enriched with substances. In consequence, the worst quality groundwaters were found in piezometers located at the shortest distance to these reservoirs. However, the infiltration of worse quality water from the ground to the reservoirs was not intensive enough to deteriorate significantly the quality of water retained in these water bodies.



Axes	PCA 1	PCA 2	PCA 3	PCA 4	Total variance
Eigenvalues:	0.582	0.191	0.124	0.060	
Species-environment correlations:	0.068	0.113	0.140	0.154	
Cumulative percentage variance					1.000
of species data:	58.2	77.3	89.7	95.8	
of species-environment relation:	20.7	39.1	57.5	68.4	
Sum of all eigenvalues					1.000
Sum of all canonical eigenvalues					0.013

FIGURE 3
Dependences between water quality parameters applied to the waters in the reservoirs and to the groundwaters at different distances from the reservoirs, analysed by PCA

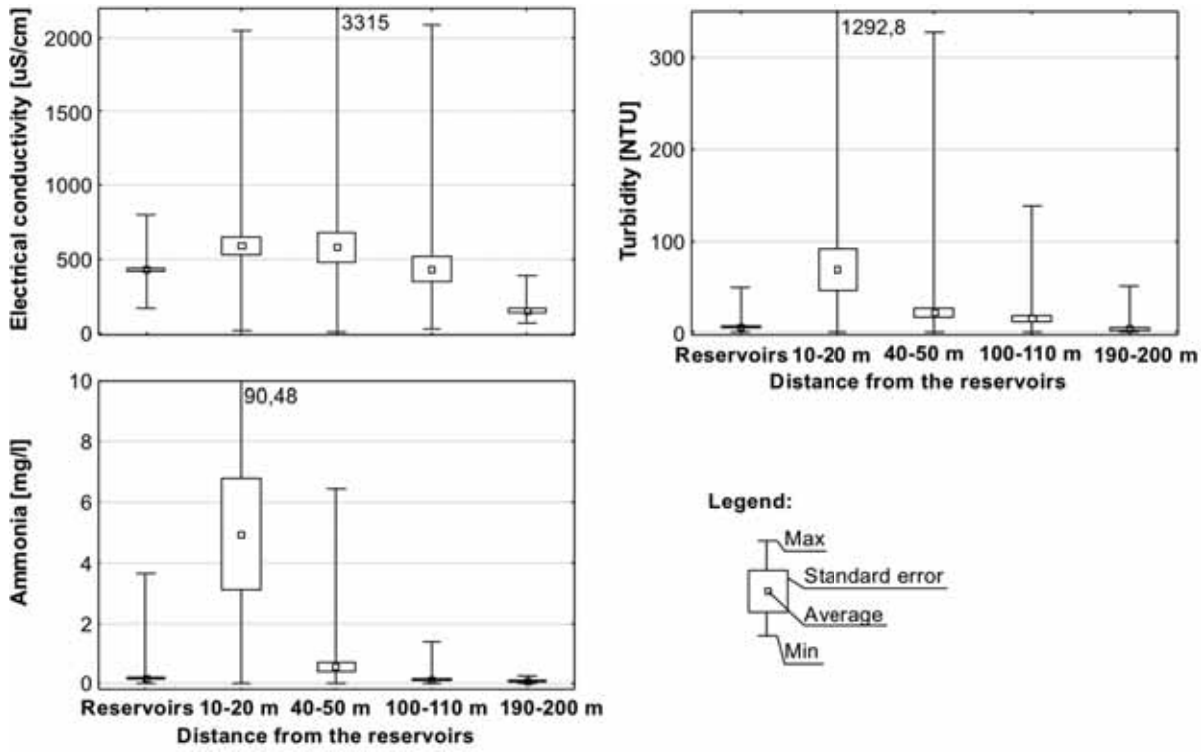


FIGURE 4
Characteristic values of EC, turbidity and ammonia in waters retained in the reservoirs and in groundwaters depending on their distance to the reservoir shorelines

CONCLUSIONS

During the performed study, the waters retained in the lowland dam reservoirs located in north-eastern Poland belonged to the category 'fair', which implicates a periodical threat to their quality. The tested groundwaters were of worse quality. The groundwaters within the area surrounding the resservoir Grodzisk Duży fell into the lowest water quality class, i.e. 'poor', while the groundwaters in the catchments of Karwacz and Łoje were classified as 'marginal', and the ones around the reservoir Wykrot were categorised as 'fair'. Best quality groundwaters were found in piezometers situated the furthest from the reservoirs. The run-off of water from the catchment towards the reservoirs was induced by their draining action, and the influx of substances with the flowing water meant that the worst quality groundwaters were detected in the nearest vicinity of the reservoirs, that is in piezometers located 10-20 m from the shorelines. Despite such short distance, their quality was much worse than the quality of waters retained in the reservoirs. Thus, it can be concluded that even in such reservoirs as Wykrot and Łoje, created on highly permeable bed (sandur sands, fine and medium sands), infiltration of groundwater to these water bodies was not intensive enough to depress the quality of water retained in these reservoirs.

ACKNOWLEDGEMENTS

The study was performed under the framework of statutory grant no 20.610.012-300, carried out at the Department of Water Resources, Climatology and Environmental Management, University of Warmia and Mazury in Olstzyn.

REFERENCES

[1] Abbasi, T. and Abbasi, S.A. (2012) Water Quality Indices. Elsevier. Berlin, Heidelberg, 1-362.
[2] Horton, R.K. (1965) An index number system for rating water quality. Journal of Water Pollution Control Federation. 37(3), 300-306.
[3] Damo, R. and Icka, P. (2013) Evaluation of Water Quality Index for Drinking Water. Polish Journal Environmental Studies. 22(4), 1045-1051.
[4] Sharma, D. and Kansal, A. (2011) Water quality analysis of River Yamuna using water quality index in the national capital territory, India (2000-2009). Applied Water Science. 1(3-4), 147-157.
[5] Khwakaram, A.I., Majid, S.N. and Hama, N.Y. (2012) Determination of water quality index (WQI) for Qalyasan stream in Sulaimani city/ Kurdistan region of Iraq. International Journal of Plant, Animal and Environmental Sciences. 2, 148-157.
[6] Miller, W.W., Joung, H.M., Mahannah, C.N. and Garrett J.R. (1986) Identification of water quality differences Nevada through index application. Journal of Environmental Quality. 15, 265-272.
[7] Darapu, S.S.K., Sudhakar, B., Krishna, K.S.R., Rao, P.V. and Sekhar, M.C. (2011) Determining water quality index for the evaluation of water quality of river Godavari. International Journal of Environmental Research and Application (IJERA). 1(2), 174-182.
[8] Tyagi, S., Sharma, B., Singh, P. and Dobhal, R. (2013) Water Quality Assessment in Terms of Water Quality Index. American Journal of Water Resources. 1(3), 34-38.
[9] WHO. (2004) Guidelines for drinking water quality, 3rd ed. World Health Organization, Geneva. Available at: www.who.int/water_sanitation_health/dwq/GDWQ2004web.pdf.
[10] WHO. (2006) Guidelines for drinking water quality, 3rd ed. World Health Organization, Geneva. Available at: www.who.int/water_sanitation_health/dwq/gdwq3rev/en.
[11] WHO. (2011) Guidelines for drinking water quality, 4rd ed. World Health Organization, Geneva. Available at: http://www.who.int/water_sanitation_health/publications/2011/ dwq_guidelines/en.
[12] Vasanthavigar, M., Srinivasamoorthy, K., Vijayaragavan, K., Rajiv Ganthi, R., Chidambaram, S., Anandhan, P., Manivannan, R. and Vasudevan, S. (2010) Application of water quality index for groundwater quality assessment: Thirumanimuttar sub-basin, Tamilnadu, India. Environmental Monitoring and Assessment. 171(1-4), 595-609.
[13] Ionuş, O. (2010) Water quality index - assessment method of the Motru river water quality (Oltenia, Romania). Annals of the University of Craiova, Series: Geography. 13, 74-83.
[14] Hamid, A., Dar, N.A., Bhat, S.U. and Pandit, A.K. (2013) Water Quality Index: A Case Study of Vishav Stream, Kulgam, Kashmir. International Journal of Environment and Bioenergy. 5(2), 108-122.
[15] Pesce, S.F. and Wunderlin, D.A. (2000) Use of water quality indices to verify the impact of Córdoba city (Argentina) on Suquía river. Water Research. 34, 2915-2926.
[16] Tomas, D., Cuk, R., Marie, A.S. and Mijatovic, I. (2013) Assessment of the Drava river (Croatia) by water quality index method. Fresen.Environ. Bull. 22, 904-913.

[17] Al-Heety, E.A.M., Turki, A.M. and Al-Othman, E.M.A. (2011) Assessment of the water quality Index of Euphrates River between Heet and Ramadi Cities, Iraq. International Journal of Basic & Applied Sciences IJBAS-IJENS. 11(6), 38-47.
[18] Parmar, K. and Parmar, V. (2010) Evaluation of water quality index for drinking purposes of river Subernarekha in Singhbhum District. International Journal of Environmental Sciences. 1(1), 77-81.
[19] Yogendra, K. and Puttaiah, E.T. (2008) Determination of Water Quality Index and suitability of an urban waterbody in Shimoga Town, Karnataka. In: Proceedings of Taal 2007: The 12th World Lake Conference. 342-346.
[20] Rubio-Arias, H., Contreras-Caraveo, M., Quintana, R.M., Saucedo-Teran, R.A. and Pinales-Munguia, A. (2012) An overall water quality index (WQI) for a man-made aquatic reservoir in Mexico. International Journal of Environmental Research and Public Health. 9(5), 1687-1698.
[21] Breabăn, I.G., Gheţeu, D. and Mădălina, P.A.I.U. (2012) Determination of Water Quality Index of Jijia and Miletin Ponds. Bulletin of University of Agricultural Sciences and Veterinary Medicine Cluj-Napoca. Agriculture. 69(2), 160-167.
[22] Cymes, I. and Glińska-Lewczuk, K. (2016) The use of Water Quality Indices (WQI and SAR) for multipurpose assessment of water in dam reservoirs. Journal of Elementology. 21(4), 1211-1224.
[23] Ketata-Rokbani, M., Gueddari, M. and Bouhlila, R. (2011) Use of Geographical Information System and Water Quality Index to Assess Groundwater Quality in El Khairat Deep Aquifer (Enfidha, Tunisian Sahel). Iranica Journal of Energy & Environment. 2(2), 133-144.
[24] Silva, M.C.R., Albuquerque, M.T.D. and Ribeiro, L. (2010) Use of water quality index to evaluate the influence of anthropogenic contamination on groundwater chemistry of a shallow aquifer, Loures valley, Lisbon, Portugal. Global Groundwater Resources and Management. 347-362.
[25] Banoeng-Yakubo, B., Yidana, S.M., Emmanuel, N., Akabzaa, T. and Asiedu, D. (2009) Analysis of groundwater quality using water quality index and conventional graphical methods: the Volta region, Ghana. Environmental Earth Sciences. 59(4), 867-879.
[26] Hatha, A.A.M., Rejith, P.G., Jeeva, S.P., Vijith, H. and Sowmya, M. (2009) Determination of groundwater quality index of a highland village of Kerala (India) using geographical information system. Journal of Environmental Health. 71(10), 51-58.
[27] Jinturkar, A.M., Deshmukh, S.S., Agarkar, S.V. and Chavhan, G.R. (2010) Determination of water quality index by fuzzy logic approach: A case of ground water in an Indian town. Water Science and Technology. 61(8), 1987-1994.
[28] Pei-Yue, L., Hui, Q. and Jian-Hua, W. (2010) Groundwater quality assessment based on improved water quality index in Pengyang County, Ningxia, Northwest China. E-Journal of Chemistry. 7(S1), S209-S216.
[29] APHA. (1992) Standard Methods for the Examination of Water and Wastewater. 15th ed. New York: Water Pollution Control Federation.
[30] Chapman, D. (ed.) (1996) Water quality assessments: a guide to the use of biota, sediments and water in environmental monitoring. (2nd ed). London: Chapman & Hall.
[31] Bharti, N. and Katyal, D. (2011) Water quality indices used for surface water vulnerability assessment. International Journal of Environmental Sciences. 2(1), 154-173.
[32] Canadian Council of Ministers of the Environment. (2001) Canadian water quality guidelines for the protection of aquatic life: CCME Water Quality Index 1.0, Technical Report. In: Canadian environmental quality guidelines. Winnipeg: Canadian Council of Ministers of the Environment.
[33] Worako, A.W. (2015) Evaluation of the water quality status of Lake Hawassa by using water quality index, Southern Ethiopia. International Journal of Water Resources and Environmental Engineering. 7(4), 58-65.
[34] Mallampati, P. and Osman, M.K. (2015) Ccme water quality index and assessment of physicochemical parameters of Lake Hawassa, Ethiopia. International Journal of Recent Scientific Research. 6(6), 7891-7894.
[35] Bhutiani, R., Khanna, D.R., Tyagi, P.K. and Tyagi, B. (2014) Application of CCME WQI to evaluate feasibility of potable water availability: A case study of Tehri dam reservoir. Environment Conservation Journal. 15(1-2), 13-19.
[36] Al-Shammary, A.C., AL-Ali, M.F. and Yonuis, K.H. (2015) Assessment of Al-Hammar marsh water by uses Canadian water quality index (WQI). Mesopotamia Environmental Journal. 1(2), 26-34.
[37] Manii, J.K. and Al-Zubaidi, A.A. (2013) Assessment of Hydrochemical Water Quality on Al Delmaj Marsh Application of the CCME WQI. Journal of Babylon University/Pure and Applied Sciences. 21(1), 270-280.
[38] Panduranga Murthy, G. and Hosmani, S.P. (2009) Water Quality Index (WQI) to Evaluate Surface Water Quality for Protection of Aquatic Life: A Case Study: Bherya Lake, Mysore, Karnataka State, India. In 13th World Lake Conference, Wuhan, China, papers s5-4.

[39] Rakesh, V.B. and Ammini, J. (2013) Evaluation of pollution status of Chakkamkandam Lake, India using water quality index. Journal of Environmental Research and Development. 7(3), 1311-1315.
[40] Zhang, B., Song, X., Zhang, Y., Ma, Y., Tang, C., Yang, L. and Wang, Z.L. (2016) The interaction between surface water and groundwater and its effect on water quality in the Second Songhua River basin, northeast China. Journal of Earth System Science. 125(7), 1495-1507.
[41] Vijaya Bhaskar, C. and Nagendrappa, G. (2008) A comparative study of ground water quality and water quality index of certain selected areas situated around Tumkur city, Karnataka. Current World Environment. 3(1), 75-82.
[42] Sarala Thambavani, D. and Uma Mageswari, T.S.R. (2013) Consumers Water Quality Indices. Journal of Applicable Chemistry. 2(2), 317-327.
[43] Mahagamage, M.G.Y.L., Chinthaka, S.D.M. and Manage, P.M. (2016) Assessment of Water Quality Index for Groundwater in the Kelani River Basin, Sri Lanka. International Journal of Agriculture and Environmental Research. 2(5), 1158-1171.
[44] Szymczyk, S. (2010) Influence of the type of soil dewatering and land use on the dynamics of concentrations and volume of nitrogen discharged from agricultural areas. Journal of Elementology. 15(1), 189-211.
[45] Szymczyk, S., Pawluczuk, J. and Stępień, A. (2010) Seasonal variability of mineral nitrogen in groundwater of hydrogenic soils. Journal of Elementology. 15(4), 713-723.

Received: **12.8.2017**
Accepted: **10.02.2018**

CORRESPONDING AUTHOR

Ireneusz Cymes
Department of Water Resources, Climatology and Environmental Management,
University of Warmia and Mazury in Olsztyn,
Oczapowskiego Str. 2,
10-719 Olsztyn – Poland

e-mail: irecym@uwm.edu.pl

© by PSP Volume 27 – No. 5/2018 pages 2800-2808 Fresenius Environmental Bulletin

DINOFLAGELLATE CYST STUDIES IN THE SEDIMENTS OF TURKISH COASTAL WATERS AND FUTURE ASPECTS

Serdar Uzar*, Hilal Aydin, Emine Erdem Yurur

Manisa Celal Bayar University, Biology Department, Faculty of Science and Arts, Campus of Martyr Prof. Dr. Ilhan Varank 45140, Manisa, Turkey

ABSTRACT

Marine organisms provide a valuable source of knowledge regarding how the marine ecosystem works. Studies of phytoplankton ecology and their dynamics offer a great opportunity for understanding these ecosystems. Dinoflagellates are a major part of marine phytoplankton and some dinoflagellates are able to produce resting cysts, which are composed of organic polymers that are highly resistant. These cysts are usually preserved very well in marine sediments. The number of studies on dinoflagellate cysts in the world's oceans is gradually increasing and these studies have become more detailed and multidisciplinary. Studies on dinoflagellate cysts in sediments have undergone a very important development in recent years, both in Turkish coastal waters as well as in the world's oceans. Here, we review the aims of the existing dinoflagellate cysts studies and summarise their results. We also give different future perspectives so as to contribute to the dinoflagellate cysts studies from Turkish coastal waters.

KEYWORDS:
Ecology, phytoplankton, dinoflagellate, resting cyst, sediment, biodiversity, indicator.

INTRODUCTION

Dinoflagellates, a highly variant group of marine phytoplankton, include a high number of harmful and toxic species [1, 2]. It is known that some dinoflagellates, as a part of their life cycle, have the ability to create a resting cyst [3]. These cysts help them survive unfavourable conditions and can be preserved in the soil sediment for an extensive period of time [4, 5]. Therefore, dinoflagellate cysts can provide historical data regarding their past occurrences. These data have been compiled via innumerable regionally-focused studies over the last century, which have greatly enhanced our understanding of sedimentary dinoflagellate cyst associations with regards to their palaeoecological significance. This abundance of worldwide studies has also enhanced our understanding of the cysts' modern biogeography, ecological affinities, and use as a proxy for sea surface conditions reconstruction [6].

Turkey has a very unique location geographically, and is surrounded by seas with different environmental features, such as the Marmara Sea, Black Sea, Aegean Sea, and Mediterranean Sea [7]. Fossil and modern dinoflagellate cysts have been researched in various samples of sediment from the Marmara Sea, Black Sea, Aegean Sea, and Mediterranean Sea [7, 8, 9]. Dinoflagellate cyst abundance and distribution were recorded horizontally from open sea areas of the Marmara Sea, Black Sea, and Aegean Sea [7, 8, 9, 10, 11, 12, 13]. Dinoflagellate cyst distributions were also investigated alongside environmental changes in recent years in these studies. Surface sediment studies (or modern dinoflagellate cyst studies) were started to offer a different perspective of the cyst distribution and have increased in different locations in the coastal waters of Turkey [14, 15, 16, 17, 18, 19, 20, 21]. Modern cyst studies have focused on cyst distribution, abundance, and relationship to environmental conditions [14, 15, 17, 18, 19, 20, 21]. Recently, cyst culture studies, and molecular and phylogenetic surveys have begun in these coastal areas as well [22, 23, 21]. Here, we aimed to provide a detailed review of dinoflagellate cyst studies in the marine sediments of Turkish coastal waters and discuss the potential of future dinoflagellate cyst surveys in Turkey with regards to global aspects.

PREVIOUS DINOFLAGELLATE CYST STUDIES FROM TURKISH COASTAL WATERS

Dinoflagellate cyst studies on sediment were completed both paleontologically and recently from Turkish coastal waters. Paleontological and fossil dinoflagellate cyst study samples were mainly collected from the open sea, whereas modern cyst studies in surface sediment were mostly collected from coastal regions of Turkey.

Although each of the dinoflagellate cyst studies in the literature provide detailed information, the dinoflagellate cysts were studied for different pur-

poses. For example, paleontological and fossil dinoflagellate cyst studies in Turkish coastal areas were mainly focused on the cyst distribution and abundance in relationship to past environmental changes and morphological traces of past environmental conditions. Dinoflagellate cyst studies from surface sediments include cyst distribution and abundance with environmental factors, potential toxic cyst distribution, cyst-theca relationships, and molecular phylogenetic links between the cysts and vegetative cells.

Fossil and paleontological dinoflagellate cyst studies from Turkish coastal waters. Over recent decades, important developments have been taking place with regards to the discipline of marine micropaleontology, which includes the emergence of micropaleontological indicators with a highly varied chemical composition and biological affinities from the world of Micropaleontology, influenced mainly by carbonate foraminifers. Organic-walled dinoflagellate cysts, which are also known as dinocysts and are among these microfossils, have recently been receiving more attention, as they seem to be quite unique and have a fascinating position in the field of micropaleontology [24].

Mudie et al. [8] investigated dinoflagellate cyst assemblages and environmental effects on cyst morphology in Late Quaternary drill cores from the Marmara Sea, Black Sea, Aegean Sea. In this paper, a quantitatively study of the connection between dinoflagellate cyst morphology and sea surface salinity was performed. Data from this study showed that dinoflagellate cysts have unusual features, such as their cruciform shape and processes being a reliable indicator of low-salinity paleoenvironments. The statistical relationship between variations in dinoflagellate cyst morphology and paleosalinity estimates was used by Mudie et al. [8] in their study.

To determine past changes in the sea surface salinity, from the Black and Marmara seas, they used fungal spores and freshwater algae with dinoflagellate cysts as an environmental indicator [7]. In their study, it was observed that the dinoflagellate cyst assemblages from the Marmara and Black seas were different than those from the Mediterranean Sea. *Polysphaeridium zoharyi*, *Operculodinium israelianum*, and *Impagidinium aculeatum*, are dinocyst species which indicate summer salinities, and are currently restricted to the Aegean and Mediterranean seas. In contrast, *S. inaequalis*, *Spiniferites cruciformis*, *Polykrikos* spp., and *Peridinium ponticum* were found in the Marmara Black seas, which have low salinity. *Quinquecuspis concreta* was present only in the Marmara Sea, which has intermediate salinity. Mudie et al. [7] pointed out that, in the Black Sea, Early Holocene dinoflagellate cyst assemblage s indicated a surface salinity lower than present, yet no clear-cut evidence has been found proving that the surface salinity had ever been as low as that of a fresh water lake.

Noah's Flood hypothesis, using dinoflagellate cysts collected from the sediments of the Black Sea, was investigated by Mudie et al. [9]. They aimed at presenting a statistical analysis of the distributions of dinocyst assemblages in relation to the surface salinity of the Marmara Gateway and eastern Mediterranean regions, as well as a detailed account of the present-day oceanography. The morphological variations of key indicator species were also provided. The results showed that autotrophic cysts with a high gonyaulacoid cyst abundance were found at a higher rate in the Aegean and Mediterranean seas, whereas the Black and Marmara seas were more abundant with heterotrophic peridinoid dinoflagellate cysts. This hypothesis was re-examined by Mudie et al. [9] using organic-walled dinoflagellate cysts, which showed moderate to high diversity and outstanding preservation in Marmara Sea Gateway sediments from the Pleistocene Holocene. Their study results supported the theory that the Black Sea had saline surface conditions and the salinity had decreased with an increase in the flow of fresh water. Evidence supporting the concept that, in the early Holocene, the Black Sea was a large fresh-water lake appropriate for farming, or that a sudden (6500-year) flood by the Black Sea, causing a 100-m high waterfall in the waters of the Mediterranean, took place at 7.5 ka has never been found. To sum up, in the Marmara Gateway, organic-walled dinocysts proved to be highly useful markers of the surface water salinity, and the results of the study definitively supports the semi-persistent overflow model, indicating an exchange of water between the Black and Marmara seas.

Mudie et al. [10] reported their initial results from the south-western Black Sea Shelf, which provides records of anthropogenic activity and decadal-scale climate changes in the Holocene. Their study results showed that dinoflagellate cyst assemblages had major changes throughout the Black Sea-Mediterranean corridor. The process length variability marked low diversity Pleniglacial-early Holocone *Spiniferites cruciformis* assemblages with conditions ranging from brackish to saline. To help understand the estimated time period of these corridor connections, the distribution of some euryhaline cysts, such as *Spiniferites bentorii* and *Spiniferites mirabilis*, were used. No palynological evidence of freshwater or catastrophic marine flooding was observed in the study samples.

A new record was presented by Marret et al. [12] from the south-western shelf of the Black Sea detailing organic-walled dinoflagellate cyst assemblages with resolution ranging from decadal to centennial. In this study, this record of high-resolution dinoflagellate cysts was analysed in detail so as to more extensively evaluate the legitimacy of the hypothesis of a catastrophic flood which has been proposed by several researchers [25, 26, 27]. The dinoflagellate cyst assemblages from the Black Sea shelf

were also compared to the recent record of the dinocysts from the Central Asian Sea. There are 2 main assemblages: the first, which is dominated by brackish species, includes freshwater algae, *Pyxidinopsis psilata*, and *Spiniferites cruciformis*, while the second, which is characterised by euryhaline species, includes *Protoperidinium ponticum*, *Brigantedinium* spp., and *L. machaerophorum*. In addition, Marret et al. [12] first reported the presence of a harmful algal bloom (HAB)-forming species from the Holocene in the Black Sea. In their study, they showed the occurrence of extremely large *L. polyedrum* cyst blooms approximately 6000–5000 years ago, and new HAB cysts within the past 2000 years.

Another study was carried out on samples from the Marmara Sea regarding Holocene hydrology and dinoflagellate cyst records by Londeix et al. [13]. The objectives of this study were to provide evidence of either the flood or outflow hypothesis regarding the reconnection of the Mediterranean and Black seas, and as well, with regards to the demise of the Fennoscandian ice sheet, to determine the sequence and timing of the events involved along with its impact on the hydrography of the Marmara and Black seas. The results showed that the Marmara Sea was slightly brackish according to late glacial dinoflagellate cyst assemblages. Prior to the end of the late glacial maximum, a strong melt water influence and flux were observed in the Marmara Sea for the first time.

Mudie et al. [11] studied dinoflagellate cysts with other non-pollen palynomorphs in the corridor of the Black Sea. In their study, the importance of dinoflagellate cysts as indicators of eutrophication and salinity in the Black Sea was summarised. Mudie et al. [11] pointed out that dinoflagellates and other non-pollen palynomorphs might be more sensitive to nutrient changes then salinity.

Dinoflagellate cysts were studied focusing on their morphological characters, such as process length in the Black Sea, by Mertens et al. [28]. The process length of *Lingulodinium machaerophorum* was chosen to understand the surface salinity changes during the Holocene Black Sea. In their study, it was shown that, after the earliest Holocene, the salinity increase was gradual, ranging between 12.3 and 17.1 psu. It was also pointed out that following an early period of low salinity caused by enhanced precipitation, large Holocene salinity fluctuations were not recorded in the salinity-proxy.

Surface sediment dinoflagellate cyst studies from Turkish coastal waters. Dinoflagellate cyst studies have become more interesting and provide more information regarding their link to the water column as a biological and physicochemical indication, due to their excellent preservation in sediment (Figure 1 and Table 1).

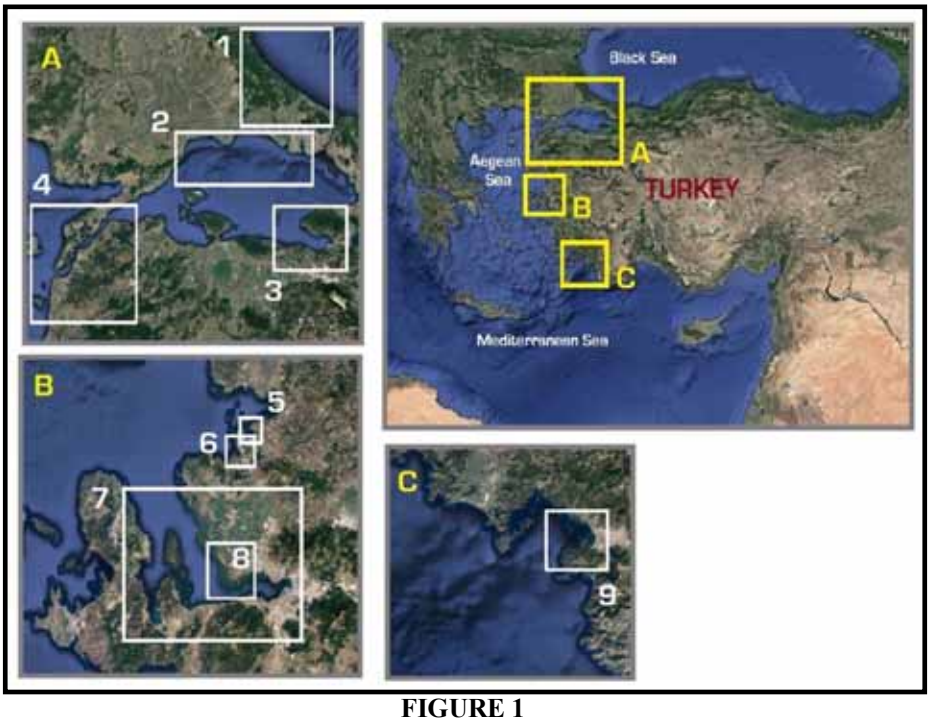


FIGURE 1

Study areas of the modern dinoflagellate cysts from Turkish Coastal Areas: 1. Black Sea; 2. Marmara Sea; 3. Gemlik Gulf (Marmara Sea); 4. Çanakkale Strait; 5. Aliağa Bay (Aegean Sea); 6. Nemrut Bay (Aegean Sea); 7. İzmir Bay (Aegean Sea); 8. Homa Lagoon (İzmir Bay, Aegean Sea); and 9. Fethiye Bay (Mediterranean Sea).

TABLE 1
Surface sediment dinoflagellate cyst study sampling areas from Turkish Coastal Areas.

	Area	References
1	Black Sea	Aydın et al. [20]
2	Marmara Sea	Aydın and Uzar [17]
3	Gemlik Gulf (Marmara Sea)	Balkıs et al. [21]
4	Çanakkale Strait	Aydın et al. [20]
5	Aliağa Bay (Aegean Sea)	Aydın et al. [19]
6	Nemrut Bay (Aegean Sea)	Aydın et al. [19]
7	İzmir Bay (Aegean Sea)	Uzar et al. [14], Aydın and Uzar [16, 17], Aydın et al. [15, 18], Mertens et al. [22], Luo et al. [23]
8	Homa Lagoon (Aegean Sea)	Aydın et al. [29]
9	Fethiye Bay (Mediterranean Sea)	Aydın and Uzar [17]

Although previous deep core sediment samples and studies have involved surface dinoflagellate cyst distribution, dinoflagellate cysts have been investigated from different surface sediments from Turkish coastal waters. Modern dinoflagellate cysts in the surface sediments were reported for the first time from İzmir Bay by Uzar et al. [14]. In their study, dinoflagellate cyst assemblages and distribution in the bay were determined. *Q. concreta*, *L. machaerophorum*, *Dubridinium caperatum*, and *Polykrikos kofoidii* were the most common cysts in the study area. Morphological details of the identified species were also provided in the study. Dinoflagellate cyst assemblages were compared with some other points from the Mediterranean Sea [30, 31] and open ocean samples by Mudie et al. [9]. In this study samples were collected mainly in inner Izmir Bay. Cysts of *Gonyaulax scrippsae*, *Protoperidinium denticulatum*, *P. nudum*, *P. obtusum*, *P. compressum*, *P. oblongum*, *P. conicoides*, *Preperidinium meunieri*, *Diplopelta parva*, *Polykrikos kofoidii*, and *P. schwartzii* were identified in sediment samples from İzmir Bay, whereas a vegetative form of these species had not been recorded previously in the phytoplankton samples from the bay.

Aydın et al. [15] presented a very detailed study about modern dinoflagellate cysts and their distributions in the surface sediments of İzmir Bay. In their study, they identified 36 types of dinoflagellate cysts and the cyst abundance was recorded as 41 to 3292 cysts g^{-1} dry weight sediment. Aydın et al. [15] reported 2 cyst species (*Gymnodinium* cf. *nolleri* and *Oblea acanthocysta*) for the first time from Aegean marine waters. The most abundant cysts in the study area were, *P. kofoidii*, *L. machaerophorum*, *G.* cf. *nolleri*, *Q. concreta*, and *O. centrocarpum*. Aydın et al. (2011) [15] observed that the dinoflagellate cyst concentrations had changed in different locations (inner, middle, and outer) of the bay. In this study, *Alexandrium affine*, *A. catanella/tamarense complex* and *A. minutum* were determined to indicate potential seedbeds for potentially toxic species outbreaks in İzmir Bay.

Aydın and Uzar [16] investigated potentially toxic cysts from sediment samples collected between 2003 and 2011 in İzmir Bay. *A. affine*, *A. catanella/tamarense* complex, and *A. minutum* type cysts were recorded as potential toxic species. *L. machaerophorum* and *O. centrocarpum* were also mentioned as the most abundant potentially toxic cyst species in the bay during the 2003 to 2011 time period.

Dinoflagellate cyst studies have been on the increase in different regional areas and locations in Turkey. Aydın and Uzar [17] added different regional areas and locations from Turkish coastal waters to investigate dinoflagellate cysts in the surface sediments. In addition to sediments from İzmir Bay, Marmara Sea and Fethiye Bay (Mediterranean), surface sediment samples were used to determine cyst distribution and abundance. In their study, a total of 40 cyst types were identified and the abundance was recorded as between 34 and 31532 cyst g^{-1} dry weight sediment from the sampling areas. *L. machaerophorum*, *P. kofoidii*, *Q. concreta*, *D. caperatum* and *S. bulloideus* were recorded as the most abundant dinoflagellate cyst species. Aydın and Uzar [17] observed that the dinoflagellate cyst assemblages were different in the Marmara Sea locations compared to those from the Aegean and Mediterranean areas. For example, *Trinovantedinium capitatum*, *Spiniferites cruciformis*, *Stelladinium abei*, *S. robustum*, *S. reidii*, *Nemathosphaeropsis sp.*, and *Tuberculodinium vancompoae* were observed only in the surface sediment samples from the Marmara Sea. This study showed that the total autotrophic cyst concentration was higher than that of the heterotrophic cysts in the study areas.

Surface sediment samples were collected from marine coastal bays and open sea areas in previous modern dinoflagellate cyst studies. Aydın et al. [29] investigated modern dinoflagellate cyst distribution in surface samples from Homa Lagoon, one of the estuarine areas in the Mediterranean. In this study, the purpose was to investigate the connection between the dinoflagellate cyst concentration and other factors (salinity, temperature, and sediment type). In

the lagoon sampling area, they identified 12 dinoflagellate cyst morphotypes and the cyst abundance found to be quite low. The following study results were pointed out: 1) The Homa Lagoon has a broad salinity and temperature range and these environmental factors could have mainly effected the dinoflagellate cyst distribution in the lagoon. 2) Autotrophic dinoflagellate cysts were observed in all of the sampling points; however, heterotrophic cysts were only observed at the station outside of the lagoon. 3) The dinoflagellate cysts were particularly distributed in clay and silty sediments. 4) Studies on dinoflagellate cyst distribution in extreme environments such as lagoons were very limited and this study was another contribution to dinoflagellate cyst studies in estuarine areas.

It is well known that dinoflagellate cyst distribution and abundance are linked to environmental changes or features in the areas. In a study by Aydın et al. [18] of İzmir Bay, 12 sediment samples were collected from different sides of the bay, where the water features are different, and used to investigate the relationship between dinoflagellate cysts and the impact of industrial pollution. Dinoflagellate cyst abundance, metal level, organic carbon, and sediment type were analysed to understand the impact of industrial pollution. In İzmir Bay, from the surface sediments collected, *L. machaerophorum*, *P. kofoidii*, *D. caperatum* showed a significant correlation in their Cd, Pb, Cu, Zn, and organic carbon levels, whereas the sediment type and dinoflagellate cyst distribution showed no significant correlation. Although the dinoflagellate cyst distribution was only investigated with an industrial pollution source, this study provided preliminary data regarding the influence of pollution sources on dinoflagellate cysts. Aydın et al. [18] pointed out that more data need to be provided to evaluate the impact of industrial pollution on dinoflagellate cyst distribution and the distribution should be studied with other pollution sources such as nutrient enrichment.

A similar based study was carried on 2 different close bays in the Aegean Sea [19]. The objective of this study was to further investigate Turkish coastal waters to learn more about the impact of industrial pollution on the dinoflagellate cyst distribution. In the Aliağa and Nemrut bays, from the 8 surface sediment samples that were collected, 42 dinoflagellate cyst types were found and the cyst concentration was between 11 and 2543 cysts g^{-1} dry weight sediment. Cyst concentrations of *G. nolleri*, *A. affine*, and *L. machaerophorum* were dominant in the study areas. In this study, the total cyst concentration and autotrophic cyst concentration indicated metal pollution in the sampling areas. The sediment structure also showed correlation with dinoflagellate cyst distribution. This study also provided excellent data regarding Turkish coastal waters, as no previously published phytoplankton studies were found for the Aliağa and Nemrut bays. In this study of Turkish coastal waters, *Ataxiodinium choane, Impagidinium sp*., and *Dubridinium sp.* were recorded for the first time.

Surface sediments were collected from 2 other different locations, the Çanakkale Strait and Black Sea, to observe the modern dinoflagellate cyst distribution [20]. The aim of their study was to provide the first data of modern dinoflagellate cysts from surfaces sediment in Çanakkale Strait and the southeastern Black Sea. The study results showed that the cyst concentration was very low compared to other locations from Turkish coastal areas. *L. machaerophorum*, *A. minutum*, and *S. bulloideus* cyst types were reported as the most dominant species in their study. Dinoflagellate cyst assemblages showed differences between the 2 locations. For example, *S. cruciformis* and *Polysphaeridinium zoharyi* were identified only at the Black Sea stations, whereas *Votadinium spinosum*, *Operculodinium israelianum*, and *Scrippsiella* spp. were only observed at the Çanakkale Strait station. In the study, it was concluded, from the surface sediments from these areas, that the dinoflagellate cyst distribution might have been affected by the local phytoplankton species, sea surface conditions (salinity and temperature), local currents, and sediment type.

Dinoflagellate cyst studies from surface sediments in Turkish coastal areas also included dinoflagellate cyst-theca relationships. Mertens et al. [22] published the first cysts-theca studies from surface sediment samples in İzmir Bay. Cysts of *Spiniferites pachydermus* were isolated form sediment samples and incubated in a laboratory environment. The results showed that the vegetative cells of *S. pachydermus* were morphologically different from the existing species. The molecular examinations and their phylogenetic relationships supported a new specimen: *Gonyaulax ellegaardiae*. In their study, a detailed morphological description was given for both *S. pachydermus* and *G. ellegaardiae*, including scanning electron microscope pictures. Similar to previous cyst-theca relationship studies, *Scrippsiella spinifera* was studied for the first time from Turkish coastal waters by Luo et al. [23]. Their study aimed to provide further information regarding the systematics and phylogeny of the species *Scrippsiella*. In surface samples from İzmir Bay, *S. spinifera* cysts were isolated and incubated. The study data were compared with different salinity areas and different *Scrippsiella* species in the samples from marine waters and brackish environments. That part of the study provided morphological and molecular phylogenetic details belonging to samples from İzmir Bay.

Balkıs et al. [21] studied dinoflagellate cysts in sediment samples from the Gemlik Gulf, Marmara Sea. The study was based on identifying dinoflagellate resting cysts, the determination of HAB species, and investigating possible seasonal changes in their production. A total of 44 dinoflagellate cyst taxa were identified dominated by *L. machaerophorum*,

O. centrocarpum, and *Selenopemphix quanta* species in the study area. In their study, some of the cysts were incubated and a vegetative form of the cysts was determined in a laboratory environment. This study provides the first seasonal dinoflagellate cyst distribution from Turkish coastal waters. Cysts of toxic species *Cochlodinium sp*. were reported for the first time from Turkish coastal waters and other cysts of HAB species were also observed in the study area, including: *Alexandrium tamarense*, *Protoceratium reticulatum*, *Heterocapsa triquetra*, *Gymnodinium catenatum/nolleri*, *Lingulodinium polyedrum*, and *Scrippsiella trochoidea*. Balkıs et al. [21] reported that an autotrophic dinoflagellate cyst species dominated over heterotrophs in species number and abundance. The dinoflagellate cyst distribution was significantly influenced by the surface temperature, dissolved oxygen, and total water depth; however, the surface salinity had the strongest impact on cyst occurrence in this study.

OVERVIEW OF EXISTING DINOFLAGELLATE CYST STUDIES AND FUTURE ASPECTS

Fossil and paleontological dinoflagellate cyst studies have been mainly focused on the Black and Marmara Sea regions and open sea sampling [7, 8, 9, 10, 11, 12, 13]. These studies provide a wide contribution to our understanding of paleoecological environmental conditions, especially the sea surface salinity of the Black Sea. Moreover, important data were added to the literature as evidence of existing theories of past salinity changes in the Black Sea. Fossil dinoflagellate cyst studies were also used as proxy to investigate marine pollution and eutrophication with past sea surface condition changes in some areas, such as the Norwegian Fjord [32], Po-River, Mediterranean [6, 33], Yellow Sea, China [34], and Canada [35]. Similar to these study areas, fossil dinoflagellate cysts can be studied in some coastal areas in Turkey where eutrophication and industrial pollution have appeared in past as well as present.

Dinoflagellate cysts indicate present environmental conditions as well as past environmental changes [36, 37]. Dinoflagellate cyst diversity, abundance of some cyst species, and autotrophic and heterotrophic cyst concentration rate have been used as ecological tools to evaluate environmental conditions [34, 36, 38]. Some results using these tools have been presented in some studies of Turkish coastal waters [18, 19]. However, more data should be collected from different coastal areas in Turkish coastal waters to understand and evaluate dinoflagellate cysts as an environmental indicator.

Modern dinoflagellate cysts in surface sediments were widely studied from different regions of Turkish coastal waters, such as İzmir Bay, Fethiye Bay, Aliağa Bay, Nemrut Bay, Gemlik Gulf, Çanakkale Strait, and the south-eastern Black Sea. In most of these studies, the dinoflagellate cyst assemblages and abundance were evaluated with previous or existing environmental data [14, 15, 17], and some of the studies discussed present environmental data [18, 19, 21]. The surface sediments allow us to gain a good understanding of the dinoflagellate cyst distribution in relation to our present environmental data. Therefore, it is necessary to provide more detailed studies, including great environmental data in some studied areas, as well as new coastal regions of Turkey. Moreover, different types of coastal regions such as bays, estuarine regions, upwelling areas, lagoons, or river mouths can also be important geographical areas used to bring more attention and present information. Freshwaters have great potential, as do marine areas, and we have very limited data from these regarding dinoflagellate cyst studies [39, 40]. Although dinoflagellate cyst composition can be very different in marine waters, freshwater dinoflagellates and their life cycle should also be monitored in detail. Therefore, maybe some freshwater areas from Turkey should be focused on to investigate fresh water dinoflagellate cysts in future.

Phytoplankton observation and monitoring can be difficult depending on a few conditions, such as the sampling method, time, and locations. Therefore, dinoflagellate cyst examinations help to observe species from local regions. Some dinoflagellate cyst studies from Turkish coastal waters have contributed to the Turkish coastal water phytoplankton check list [14, 15, 21]. From this point of view, dinoflagellate cyst studies in different areas can help us to observe phytoplankton composition in those areas. The more regions which are studied with dinoflagellate cysts, the more phytoplankton data we could generate. By providing dinoflagellate cyst data from the surface sediments of different areas, the diversity of the species among the Turkish coasts can be observed and monitored more easily. Some studies pointed out that dinoflagellate cysts can be easily transferred from one area to another by a ship's ballast water [41]. Therefore, dinoflagellate cyst studies provide a great tool for monitoring local species, invasive species, and changes in the local phytoplankton composition.

Some studies have shown that dinoflagellate cyst assemblages can change seasonally in some areas [42, 43, 44]. Balkıs et al. [21] first reported seasonal dinoflagellate cyst data from the Gemlik Gulf from Turkish coastal waters. Links between seasonal phytoplankton changes and vegetative-form dinoflagellate cysts have been well observed with sediment trap studies from the world's oceans [42, 43, 44]. Until now, there have been no sediment trap studies in Turkey; therefore, sediment trap studies can be planned to monitor dinoflagellate cysts and phytoplankton dynamics from Turkish coastal areas.

Dinoflagellate cysts have a very strong resistance under difficult conditions and can be protected for future blooms. Dinoflagellate cyst accumulation and preservation in sediment is known to be a seedbed for future blooms for the area; hence, the sand can provide early warnings about potential harmful and toxic bloom events [15, 45]. It was also reported that some dinoflagellate cysts had higher toxin content than vegetative cells [46]. Therefore, dinoflagellate cysts can be a potentially toxic source for marine environments. HAB events are frequently reported in Turkish coastal waters [47]. Dinoflagellate cyst abundances have provided a good perspective of future blooms in the İzmir Bay and Gulf of Gemlik. HAB events can cause serious damage economically and affect human health. Therefore, dinoflagellate cyst monitoring could be an effective tool in avoiding potential danger in aquatic farms and fishing locations.

Dinoflagellate cysts and their thecal form studies help us to improve our knowledge about species and their ecological needs. For example, the encystment and excystment of *L. polyedrum* have been studied under very different ecological conditions by different researchers [48, 49]. Although dinoflagellate cyst distribution relationships with environmental conditions can improve our knowledge about specific species, more individual and species-specific experiments are needed from Turkish coastal waters and other oceans. Dinoflagellate cyst culture experiments not only give information regarding species ecology, but species identification and taxonomy also provide a great contribution from these studies. Some studies provide some evidence that cyst morphology might rely on genetic material plus environmental conditions [50]. Therefore, morphological studies continue with the support of molecular phylogenetic relations. Some studies have begun to focus on cyst theca relationships with molecular data from Turkish coastal areas [22, 23]. However, further studies should be expected, especially for unknown, uncertain, and potential toxic/bloom species, such as cysts of *Alexandrium* spp. or *Scrippsiella* spp., which were reported in previous studies [14, 15, 16, 21].

There are a few studies and some data in the literature providing an understanding of dinoflagellate cysts and their distribution in Turkish coastal areas. Here, we reviewed previous studies of Turkish coastal areas and tried to create an overview regarding these dinoflagellate cyst studies. We have observed that dinoflagellate cyst studies of Turkish coastal areas have provided some preliminary data, and the complexity of the studies has increased over time. However, so much more research can be proposed for a better understanding of dinoflagellate cysts for the world's oceans.

REFERENCES

[1] Ribeiro, S., Amorim, A. (2008) Environmental drivers of temporal succession in the recent dinoflagellate cyst assemblages from a costal site in the North-East Atlantic (Lisbon Bay Portugal). Mar Micropaleontol. 68, 156-178

[2] Smayda, T., Reynolds, C.S. (2003) Strategies of marine dinoflagellate survival and some rules of assembly. J Sea Res. 49, 95–106.

[3] Head, M.J. (1996) Modern Dinoflagellate Cysts and Their Biological Affinities. In: Jansonius, J., McGregory, D.C. (Eds.) Palynology: Principles and Applications. American Association of Stratigraphic Palynologists Foundation. Salt Lake City, UT, Vol: 3, 1197-1248.

[4] Mertens, K., Takano, Y., Head, M.J., Matsuoka, K. (2014) Living fossils in the Indo-Pacific warm pool: A refuge for thermophilic dinoflagellates during glaciations. Geology. 42, 531-534.

[5] Limoges, A., Mertens, K., Carolina. R.F.A., De Vernal, A. (2015) First report of fossilized cysts produced by the benthic bysmatrum subsalsum (dinophyceae) from a shallow Mexican lagoon in the Gulf of Mexico. J Phycol. 51, 211-215.

[6] Zonneveld, K.A.F., Chen. L., El-Shanawany, R., Fischer, H.W., Hoins, M., Pittaurova, D. (2012) The use of dinoflagellate cysts to separate human-induced from natural variability in the trophic state of the Po River discharge plume over the last two centuries. Mar Poll Bull. 64, 114-132.

[7] Mudie, P.J., Rochon, A., Aksu, A.E., Gillespie, H. (2002) Dinocysts, freshwater algae and fungal spores as salinity indicators in Late Quaternary cores from Marmara and Black seas. Mar Geol. 190, 203-231.

[8] Mudie, P.J., Aksu, A.E., Yasar, D. (2001) Late Quaternary dinoflagellate cysts from the Black, Marmara and Aegean seas: variations in assemblages, morphology and paleosalinity. Mar Micropaleontol. 43, 155-178.

[9] Mudie, P.J., Rochon, A., Aksu, A.E., Gillespie, H. (2004) Late glacial, Holocene and modern dinoflagellate cyst assemblages in the Aegean, Marmara, Black Sea corridor: statistical analysis and re-interpretation of the early Holocene Noah's Flood hypothesis. Rev Palaeobot Palynol. 128, 143-167.

[10] Mudie, P.J., Marret, F., Aksu, A.E., Hiscott, R.N., Gillespie, H. (2007) Palynological evidence for climatic change, anthropogenic activity and outflow of Black Sea water during the Late Pleistocene and Holocene: centennial- to decadal-scale records from the Black and Marmara Seas. Quatern Int. 167-168, 73-90.

[11] Mudie, P.J., Marret, F., Rochon, A., Aksu, A.E. (2010) Non-pollen palynomorphs in the Black Sea corridor. Veget Hist Archae Bot. 19, 531-544.
[12] Marret, F., Mudie, P., Aksu, A., Hiscott, R.N. (2009) A Holocene dinocyst record of a two-step transformation of the Neoeuxinian brackish water lake into the Black Sea. Quatern Int. 193, 72-86.
[13] Londeix, L., Herreyre, Y., Turon, J.L., Fletcher, W. (2009) Last Glacial to Holocene hydrology of the Marmara Sea inferred from a dinoflagellate cyst record. Rev Palaeobot Palynol. 158, 52-71.
[14] Uzar, S., Aydın, H., Minareci, E. (2010) Dinoflagellate cyst assemblages in the surface sediments from Izmir Bay, Aegean Sea, Eastern Mediterranean. Sci Res Essay. 5, 285-295.
[15] Aydın, H., Matsuoka, K., Minareci, E. (2011) Distribution of dinoflagellate cysts in recent sediments from Izmir Bay (Aegean Sea, Eastern Mediterranean). Mar Micropaleontol. 80, 44-52.
[16] Aydın, H., Uzar, S. (2013) Some potentially toxic dinoflagellate cysts in recent sediments from İzmir Bay. Ege J Fish Aquat Sci. 30, 109-114.
[17] Aydın, H., Uzar, S. (2014) Distribution and abundance of modern dinoflagellate cysts from Marmara, Aegean and Eastern Seas of Turkey. J Environ Biol. 35, 413-419.
[18] Aydın, H., Yürür, E.E., Uzar, S., Küçüksezgin, F. (2015a) Impact of industrial pollution on recent dinoflagellate cysts in Izmir Bay (Eastern Aegean). Mar Poll Bull. 94, 144-152.
[19] Aydın, H., Yürür, E.E., Uzar, S., Küçüksezgin, F. (2015b) Modern dinoflagellate cyst assemblages of Aliağa and Nemrut Bay: influence of industrial pollution. Turkish J Fish Aquat Sci. 15, 543-554.
[20] Aydın, H., Balcı, M., Uzar, S., Balkıs, N. (2015c) Dinoflagellate cyst assemblages in surface sediments of southwestern Black Sea and Çanakkale Strait (Dardanelles). Fresen Environ Bull. 24, 4789-4798.
[21] Balkıs, N., Balcı, M., Giannakourou, A., Venetsanopoulou, A., Mudie, P. (2016) Dinoflagellate resting cysts in recent marine sediments from the Gulf of Gemlik (Marmara Sea, Turkey) and seasonal harmful algal blooms. Phycologia. 55, 187-209.
[22] Mertens, K., Aydin, H., Uzar, S., Takano, Y., Yamaguchi, A., Matsuoka, K. (2015) Relationship between the dinoflagellate cyst *Spiniferites pachydermus* and *Gonyaulax ellegaardiae* sp. nov. from Izmir Bay, Turkey, and molecular characterization. J Phycol. 51, 560-573.
[23] Luo, Z., Mertens, K.N., Bagheri, S., Aydın, H., Takano, Y., Matsuoka, K., McCarthy, F.M.G., Gu, H. (2016) Cyst-theca relationship and phylogenetic positions of *Scrippsiella plana* sp. Nov. and *S. spinifera* (Peridiniales, Dinophyceae). Eur J Phycol. 51, 188-202.
[24] Dale, B. (2009) Eutrophication signals of sedimentary records of dinoflagellate cyst in coastal waters. J Sea Res. 61, 103-113.
[25] Ryan, W.B.F., Pitman III, W.C. (1998) Noah's Flood: The New Scientific Discoveries about the Event that Changes History. Simon and Schuster. New York, 319p.
[26] Ryan, W.B.F., Pitman III, W.C., Major, C.O., Shimkus, K., Moskalenko, V., Jones, J.A., Dimitrov, P., Görür, N., Sakinç, M., Yüce, H. (1997) An abrupt drowning of Black Sea shelf. Mar Geol. 138, 119-126.
[27] Ryan, W.B.F., Major, C.O., Lericolais, G., Goldstein, S. (2003) Catastrophic flooding of the Black Sea. Ann Rev Earth Planet Sci. 31, 525-554.
[28] Mertens, K., Bradley, L.R., Takano, Y., Mudie, P.J., Marret, F., Aksu, A., Hiscott, R.N., Verleye, T.J., Mousing, E.A., Smyrnova, L.L., Bagheri, S., Mansor, M., Pospelova, V., Matsuoka, K. (2012) Quantitative estimation of Holocene surface salinity variation in the Black Sea using dinoflagellate cyst process length. Quatern Sci Rev. 39, 45-59.
[29] Aydın, H., Yürür, E.E., Uzar, S. (2014) Dinoflagellate cyst assemblages in surface sediments from Homa Lagoon (Izmir Bay, Eastern Aegean Sea, Mediterranean). Fresen Environ Bull. 23, 1795-1801.
[30] Giannakourou, A., Orlova, T.Y., Assimakopoulou, G., Pagou, K. (2005) Dinoflagellate cysts in recent marine sediments from Thermaikos Gulf, Greece: Effects of resuspension events on vertical cyst distribution. Cont Shelf Res. 25, 2585-2596.
[31] Montresor, M., Zingone, A., Sarno, D. (1998) Dinoflagellate cyst production at a coastal Mediterranean site. J Plank Res. 20, 2291-2312.
[32] Dale, B., Thorson, T.A., Fjellsa, A. (1999) Dinoflagellate cyst as indicators of cultural eutrophication in the Oslofjord, Norway. Estuar. Coast. Shelf Sci. 48, 371-382.
[33] Zonneveld, K.A.F., Chen, L., Möbius, J., Mahmoud, M.S. (2009) Environmental significance of dinoflagellate cysts from the proximal part of the Po-river discharge plume (off southern Italy, Eastern Mediterranean). J Sea Res. 62, 189-213.
[34] Cho, H.J., Matsuoka, K. (2001) Distribution of dinoflagellate cysts in surface sediments from the Yellow sea and East China Sea. Mar Micropaleontol. 42, 103-123.

[35] Pospelova, V., Pedersen, T.F., de Vernal, A. (2006) Dinoflagellate cysts as indicators of climatic and oceanographic changes during the past 40 kyr in the Santa Barbara Basin, southern California. Paleoceanography. 21, 1-16.
[36] Pospelova, V., Chmura, G.I., Boothman, W., Latimer, J.S. (2005) Spatial distribution of modern dinoflagellate cysts in polluted estuarine sediments from Buzzards Bay (Massachusetts, USA) embayments. Mar Ecol Prog Ser. 292, 23-40.
[37] Liu, D.Y., Shen, X.H., Di, B.P., Shi, Y.J., Keesing, J.K., Wang, Y.J., Wang, Y.Q. (2013) Palaeoecological analysis of phytoplankton regime shifts in response to coastal eutrophication. Mar Ecol Prog Ser. 475, 1-14.
[38] Liu, D., Shi, Y.J., Di, B.P., Sun, Q., Wang, Y., Dong, Z., Shao, H. (2012) The impact of different pollution sources on modern dinoflagellate cysts in Sishili Bay, Yellow Sea, China. Mar Micropaleontol. 84-85, 1-13.
[39] Tardio, M., Sangiorgi, F., Brinkhuis, H., Filippi, M.L., Cantonati, M., Lotter, A.F. (2006a) Peridinioid dinoflagellate cysts in a Holocene high-mountain lake deposits in Italy. J Paleolimnol. 36, 315–318.
[40] McCarthy, F.M.G., Mertens, K.N., Ellegaard, M., Sherman, K., Pospelova, V., Ribeiro, S., Blasco, S., Vercauteren, D. (2011) Resting cysts of freshwater dinoflagellates in southeastern Georgian Bay (Lake Huron) as proxies of cultural eutrophication. Rev Palaeobot Palynol. 166, 46-62.
[41] Lacasse, O., Rochon, A., Roy, S. (2013) High cyst concentrations of the potentially toxic dinoflagellate *Alexandrium tamarense* species complex in Bedford Basin, Halifax, Nova Scotia, Canada. Mar Poll Bull. 66, 230-233.
[42] Harland, R., Nordberg, K., Filipsson, H.L. (2004) The seasonal occurrence of dinoflagellate cysts in surface sediments from Koljö Fjord, west coast of Sweden – a note. Rev Palaebot Palynol 128, 107-117.
[43] Fujii, R., Matsuoka, K. (2006) Seasonal change of dinoflagellates cyst flux collected in a sediment trap in Omura Bay, West Japan. J Plank Res. 28, 131-147.
[44] Bringué, M., Pospelova, V., Pak, D. (2013) Seasonal production of organic-walled dinoflagellate cysts in an upwelling system: A sediment trap study from the Santa Barbara Basin, California. Mar Micropaleontol. 100, 34–51.
[45] Joyce, L.B., Pitcher, G.C., du Randt, A., Monteiro, P.M.S. (2005) Dinoflagellate cysts from surface sediments of Saldanha Bay, South Africa: An indication of the potential risk of harmful algal blooms. Harmful Algae. 4, 309-318.
[46] Dale, B., Yentscm, C.M. (1978) Red tide and paralytic shell- fish poisoning. Oceanus. 21, 41-49.
[47] Koray, T. (2004) Potentially toxic and harmful phytoplankton species along the coast of the Turkish Seas. Harmful Algae. 2002, 335-337.
[48] Okamoto, O.K., Colepicolo, C. (1998) Response of super oxide dismutase to pollutant metal stress in the marine dinoflagellate *Gonyaulax polyedra.* Compar Biochem Physiol. 119, 67–73.
[49] Okamoto, O.K., Shao, L., Hastings, J.W., Colepicolo, P. (1999) Acute and chronic effects of toxic metals on viability, encystment and bioluminescence in the dinoflagellate *Gonyaulax polyedra*. Compar Biochem Physiol. 123, 75-83.
[50] Rochon, A., Lewis, J., Ellegaard, M., Harding, I.C. (2009) The Gonyaulax spinifera (Dinophyceae) "complex": perpetuating the paradox? Rev Palaeobot Palynol. 155, 52-60.

Received: **15.8.2017**
Accepted: **20.02.2018**

CORRESPONDING AUTHOR

Serdar Uzar
Manisa Celal Bayar University,
Biology Department,
Faculty of Science and Arts,
Campus of Martyr Prof. Dr. İlhan Varank
45140, Manisa – Turkey

e-mail: uzarserdar@yahoo.com.tr

© by PSP Volume 27 – No. 5/2018 pages 2809-2817 Fresenius Environmental Bulletin

EFFECTS OF DEFICIT IRRIGATION ON PEPPER YIELD UNDER VARIOUS GREENHOUSE CONDITIONS

Waheed Ahmed Siddiqui, Zhu Mei*, LiXue Ling

Anhui Agricultural University, Department of Engineering, Hefei, 230036, Anhui Province, P.R. China

ABSTRACT

The study was carried out with the aim of determining the effects that deficit irrigation will have on pepper grown in heated and unheated in greenhouse condition. The pepper plants were grown under different water condition and data was recorded. In heated condition, water was applied efficiently as 70, 62, 48, 2% and 0% (control experiments). Under the various conditions, irrigation of the same amount was carried out at a constant rate of 4 days so that to determine how the plants would be affected by the varying conditions. Whereas, unheated greenhouse conditions, control experiments of 120, 85, 55 and 0% (control) was used to act as control gadgets in ensuring that determination of evaporation would be easy. In heated conditions, we applied water in the range of 30mm to 550mm while in unheated environment water applied ranged from 120mm to 800mm. It was noticed that under the varying conditions, considerable effects that were experienced such as yield, dry matter ration, weight, and fruit size varied significantly across all the crops grown under heated and unheated environments. Because the water sources are extremely scarce, many have gone a step further in trying to recommend treatment factors that would be used when production of pepper diminishes to a considerable rate. Variation of the amount of water applied affected production rate significantly in unheated greenhouse condition. Additionally, there were no considerable effects that were noticed on crops grown under heated conditions. The experiment revealed that the rate of irrigation does not have effects on final products which are different from crops that are grown under heated conditions.

KEYWORDS:
Efficiency of irrigation, greenhouse, heated and unheated conditions, pepper yield

INTRODUCTION

It would be difficult for various countries to efficiently meet food requirements in the future with increasing water variations. Approximately 70-89% of available water is used in food production. For efficient water use, appropriate mechanisms should be applied to ensure that there is considerable rise in the amount of products that are harvested from crops. It has been noticed that crops grown under heated greenhouse conditions give out the adequate outcome. Agronomic practices such as tillage can easily reduce the rate at which demand for water is needed [1, 22]. There have been various development schemes that were carried out in the condition of saving water used for irrigation. Deficit irrigation and partial rootzone drying are the main contributors to the growth in the required amount of pepper in varying conditions. In this chapter, we will take a controlled experiment so that we can notice and gauge the effects that heated conditions will have on pepper and how various management techniques can be used to ensure that there are maximum production and minimum adverse effects on crops. Experiment under unheated condition [2, 23].

The crop produces fruits that are in high demand in many various markets. Furthermore, the fruits of pepper possess a pleasant smell and much typical flavor making it be one of the most sought-after crop in the current world market. Pepper is one of the most valuable crops in today's world [3]. The crop produces thin and elongated fruits that are typically 25-35 centimeters long that are accompanied by dark green color. The fruits have seeds because they belong to a group of gynoid-parthenocarpic hybrid. The crops are well known for their nature of seeds that they can grow in various conditions they are exposed [4]. Additionally, the crop requires trellis and is usually cultivated in closed greenhouses, and pollination is restricted because it has the ability to modify the shape of the fruits. Moreover, cultivation of pepper in greenhouses enables efficient use of hybrids that have the potential of high yields [5]. Furthermore, there has been a significant increase in the area that pepper is planted. There were also protected environments during the past number of decades especially under vegetable and fruit production carried out in greenhouses. Greenhouse cropping system allows for a chance of obtaining a higher quality of yields as well as having the ability to reduce seasonal effects that are experienced by crops. Briefly, irrigation has been taken as one of the techniques that are used to increase production of crops [2]. Carrying out the practice in a protected environment, irrigation is considered to be one of the best techniques that increases the final output of the

crops. Also, mismanagement of the technique will finally hamper production thus leading to reduced production as well as limiting final product on farms. For one to realize excellent crop success, irrigation should be carried out before the amount of water present in the soil goes below the minimum that supports the life of the crops [6]. This practice will help in maintaining the productivity of the crops as high as possible. Proper maintenance of the amount of water present in the soil will ensure that metabolism of the crops will be held at the same level hence there will be no decreased yields of the crops. Water deficiency has been marked to be one of the leading limiting factors thus leads to obtaining high yields under protected environments as well as in various fields [7].

MATERIALS AND METHODS

To efficiently understand the effects of deficit irrigation on pepper on both heated and unheated greenhouse conditions, an experimental research was approved in the greenhouse of Faculty of Agriculture in Anhui Agriculture University, situated in Hefei city Anhui province. According to the experiments, it was noticed that pepper is an exceptional crop that is highly sensitive to deficit irrigation under varying conditions [7]. The study was mainly factorial because it was randomly randomized with the help of three irrigation treatments. The use of a tunnel measuring 9m x 48m was used to show the size used during the experiment. Considering various forms of seasons experienced in the region, summers are always taken to be dry and hot, rainy and cold are characteristics for winters [8]. The total rainfall of the experiment area was recorded as 492.45mm [5]. Experimental city climate is characterized by a subtropical monsoon type with four distinct seasons. The average annual temperature is about 15.7 °C (60.2 °F), with a high temperature of 38 °C (100 °F) in summer and a low temperature of -21 °C (69 °F) in winter was taken to show various forms through which the experiment would be undertaken.

$1-Y_a/Y_m=K_y\ (1- ET_a/ET_m)$

The soil used for the experiment was approximated to be sandy loam and the PH of the soil estimated to be around 7.89-8.06. There were physical and chemical properties of the soil that have been given in Table 1. 168 kg per hectare N, 190 kg per hectare DAP (18% N and 48% p2o5), and 200 kg per hectare KNO 3 (12% N and 45% K 2 O) of fertilizer were applied before the actual planting was done [8]. The application of pest control chemical was applied as required. The planting criteria were to ensure that the required outcome from the experiment would be easily realized in which pepper can counter any essential deficits that may arise during the process.

The seedlings were transplanted into the nursery as well as planting them with fitting separation in nursery outskirts. It was developed in common support, and moisture conditions were taken into consideration when heated, and unheated conditions were used [9]. The crops used were inundated during weight remunerated trickle water system framework.

Relationship between Decrease in Relative Use of Water and Yield Difference with Response to Drip System. Dripper separating was 38 centimeters, and it managed to have 3 Lh-1. Pepper that had ordinary water necessities of which satisfaction was a necessity, and it was used by trickle water system until when promising period that was estimated to take place in the first month was taken into bay [9]. Additionally, they were later subjected to manufactured dry spell stretch. When blossoming started, estimations of the probable amount produced by the crop were estimated. The test was done by part plot outline that contained 6 seedlings and the same that consisted of only 4 seedlings. There was also different water system supply that was in the regions of 100% water system. The main supply acted as a control experiment, and much of the work done was mainly referred to it, 60% irrigation system, 35% water system and 0% water system). In every one of the examinations, 30 allocate aggregate and 30 plants for each bundle were utilized [10].

TABLE 1
Physio-chemical properties of the field soil used during the experiment.

Soil Texture	Sandy clay loam
Grade texture	0.36
Saturation cm^3/cm^3	0.20
Capacity of the field cm^3	0.24
Wilting point cm^3	0.68
Sat. Conductivity hydraulic cm/hr	1.48
Organic matter %	2.6

TABLE 2
The relationship between the decrease in relative water use and a decrease in yield of green peppers grown under heated conditions.

Treatment of irrigation	Yield (t ha-1)	Applied water (mm)	ETa (mm)	ET_a/ET_m	Y_a/Y_m	$1-(ET_a/ET_m)$	$1-(Y_a/Y_m)$	Ky
Kl *cp*	28.4	528	524	1	1	0	0	0
K2 *cp*	27.8	398	420	0.896	0.853	0.248	0.038	0.129
K4 *cp*	5.2	268	286	0.524	0.725	0.467	0.218	1.16
K5*cp*	1.8	136	178	0.326	0.172	0.626	0.468	1.28
K6 *cp*	1.68	72	68	0.164	0.056	0.062	0.983	1.18

TABLE 3
The relationship between the decrease in relative water use and a decrease in yield of pepper grown under unheated conditions.

Treatment of irrigation	Yield (t ha-1)	Applied water (mm)	ETa (mm)	ETa/ETm	Ya/Ym	1-(ETa/ETm)	1-(Ya/Ym)	Ky
Kl *cp*	30.4	618	434	1	1	0	0	0
K2 *cp*	26.6	286	420	0.784	0.948	0.364	0.120	0.138
K4 *cp*	5.6	178	336	0.682	0.685	0.582	0.318	1.118
K5*cp*	2.4	102	164	0.236	0.186	0.728	0.564	1.38
K6*cp*	1.28	52	56	0.142	0.124	0.128	0.995	1.28

WUE was calculated as the ratio of yield (YLD) to ETa, given as WUE = YLD/ETa (t $ha^{-1}mm^{-1}$). IWUE was estimated by the following equation.

$$\text{IWUE (t ha}^{-1}\text{mm}^{-1}) = \frac{YDL - YDLx\inf d}{IRAG}$$

Where $YLD_{rainfed}$ is the yield obtained from the rainfed treatment or dryland yield, and IRGA is the seasonal irrigation amount used in millimeter. To discover contrasts that existed between various forms of treatment, different correlation measures were made utilizing the exceed expectations of 16.0 for Windows measurable programming software and the probability degrees were expressed at 0.9% likelihood. Furthermore, there was no examination of difference was made for the potential of leaves to retain the required amount of water that would help in finishing the experiment that was being performed. The work being undertaken in heated and unheated environments, it was noticed that crops showed various forms when exposed to varying amounts of water and weather conditions. Leaf water potential, as well as exact estimation of temperature possessed by the leaves, was taken into explicit consideration while creating the solutions that are needed in measuring leaf temperature. Their outcomes were given as perceptions and for providing the extra data required for efficient use of the experiment. Other forms of experiments were performed when placed in other conditions to show how crops manage to survive when soil conditions are not maintained in the same condition. Atmosphere information of the universe was analyzed for many years. The information gotten showed that in one week, crops would receive least amount of water that would not be able to support their survival. Half water system: half of the irrigation control marks. - 25% water system: 25% of the water used for irrigation - 0% was used to show that no water was applied in this test experiment.

The experiment was randomized with the block design for both forms of greenhouses irrigations schemes to be tested separately. Replications have been sent to other various sectors in which blocks of various ways have been used to ensure that there is no disturbance of the existing irrigation system. Irrigation system used for the two sets of systems has varying pan coefficients (KL *cp* ranging to 1.00).

Additionally, K2*cp*: 0.70, K3*cp* 0.65, K4*cp* 0.30, K5*cp* 0.00-acting as a control experiment for unheated condition. The amount of water used for both irrigation schemes was estimated to be the same level with those that are in varying greenhouse conditions. The amount of water used was accurately estimated using the following equation.

I = E*P* x K*cp* x P

Where:

E*p* is the cumulative evaporation when there was a 2-day irrigation practice in a constant interval. Kcp is the coefficient of pan evaporation and P was taken to be the percentage of the total wetted area. The amount of water required for irrigation was measured by the use of flow meter placed at the head of each plot. The amount of water used for irrigation was supplied from wells that were drilled from the adjacent areas. The quality of water that was used was determined by the help of expertise who helped in determining whether the quality of water used was enough for performing the experiment and get the required output that fulfils the aim of the experiment.

The water was actually taken and placed in C2S1 classes that had low risks of sodium that had minimum values of EC. Furthermore, there was no problem recorded by the amount of water that was used. The value of crop evaporation was estimated by the use of water balance equation situated and allocated by the performers of the experiment.

Evaporation noticed from crops was estimated by use of water balance equation that is stated below.

$ETc = (SWC_{10} - SWC_{tl}) + IW - D$,

The use (SWC_{10}-SWC_{tl}) was used to show the volumetric value of water content between the different dates through which valuable measurements were taken. IW and D were the total value of irrigation that was applied and the collected amount of drainage and the total amount of period under consideration. When monitoring was done, it was revealed that deep percolation was the taking place more than 0.68m below the ground and it was considered negligible. The use of Steward Model helped in determining the relationship that exists between the actual yield and ET.

RESULTS AND DISCUSSION

After planting seeds, 60mm of irrigation water was applied so that it would aid in bringing the amount of soil water to 0-58 cm of the field capacity [11]. Treatments of irrigation were started, and measurement of evaporation rate was done after first irrigation practice was performed. The total amount of water applied to both crops planted in the two irrigation conditions of heated and unheated conditions varied considerably in which 726mm in the Kl_{cp} was used for total irrigation practice for the unheated condition [12]. The use of heated condition required the application of $K1_{cp}$ of water in carrying out the treatment procedure. Minimum of 68mm of water was applied to both forms of crops in which crops were supposed to be filled with the water that would be able to support their survival under the limited water conditions and those areas where continuous supply was being undertaken. In other forms of irrigation treatment, the amount of water applied ranged from 538 and 190 mm [13]. The form of seasonal evapotranspiration experienced during the varying periods increased considerably and managed to range from 112 to 738 mm for $K5_{cp}$ and the use of $K1_{cp}$. Furthermore, there was the use of linear relationships that was observed between crop evapotranspiration (ET) and yield as much as the total amount of water that is used for irrigation. The equation that was used in determining the total amount of water that was used to realize maximum yield was $Y_a=0.346ET_c-2.328$ with the help of $R^2=0.98$, it then turned out that $Y_a=0.0256IW-1.342$ with $R^2=98$

In our study of the experiment of trying to come up with various ways to which deficit irrigation will be able to affect the form of productivity that is got out of pepper. Furthermore, the highest yield was made from heated greenhouse condition when compared to yield that was got from areas that had limited amount of production [13]. In unheated conditions, it was noticed that more water was supposed to be used to maintain continuous yield from the majority of crops

From the experiment, it was noticed that deficit irrigation had a considerable effect on the height of fruits when consideration of both conditions are taken into consideration. K2 and K3 played a crucial role in ensuring that maximum production is realized and efficient irrigation practices were placed in the last group [12]. There was the general conclusion that deficit irrigation applied to crops would not be compatible with the total reduction of bulb height. Data is shown in table 2 and 3.

The amount of water applied for both conditions varied by approximately 25% in both conditions of heated and unheated places where the accumulated results showed that there was a considerable effect that was noticed on the value of all crops under irrigation. From the results, it was noticed that there was no effect on the fruit height that would impact the market value of the plant. In both conditions, it was noticed that fruit diameter and weight had a similar response to deficit irrigation and managed to affect the production considerably in both areas and realization of maximum yield would pose a considerable variation [13]. It was also noticed that all treatments had higher values than those found in non-irrigated schemes. There was a considerable rise in dry matter value in which it was noticed that lowest and highest values were recorded at K5 and K1cp respectively. The variation can be attributed to considerable differences in fruit height and weight that was observed from the K1cp treatment than those shown in deficit treatment that was performed [14].

TABLE 4
Chemical composition of irrigation water used during the experiment.

Chemical properties	ECw (ds/m)	Na^+	Ca^+	K^+	Mg^+	Class	SAR	PH
Values	710	2.6	2.56	9.46	7.20	C_2S_1	0.86	7.18

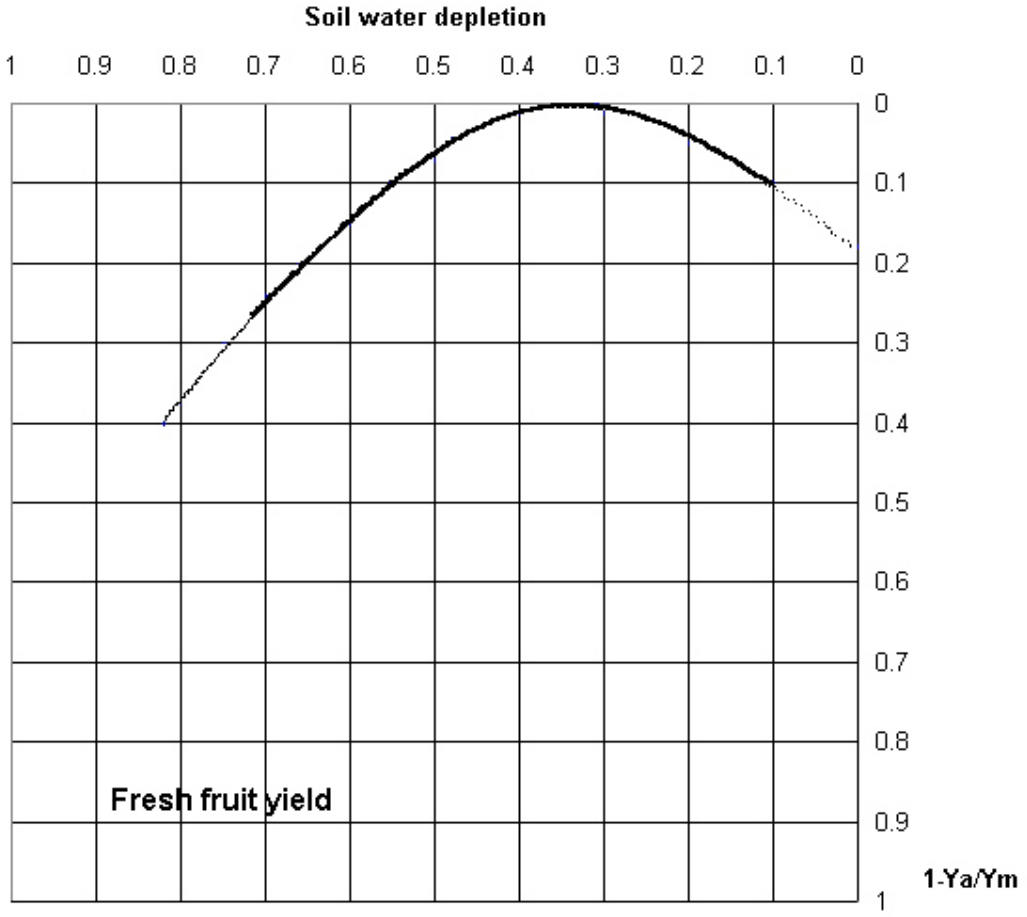


FIGURE 1
Depletion of water in the soil affects pepper production.

TABLE 5
Effects of irrigation treatments on pepper marketable parameters under heated conditions.

Irrigation treatment	Height (cm)	Diameter (cm)	Weight (kg)	Dry matter (%)	Yield (t ha^{-1})
$K1_{cp}$	18.4^{a}	26.5^{a}	1020.2^{a}	6.6^{c}	28.3^{a}
$K2_{cp}$	18.2^{a}	22.4^{a}	998.6^{a}	7.8^{c}	26.4^{a}
$K3_{cp}$	16.4^{a}	18.2^{b}	546.2^{b}	13.2^{b}	14.4^{b}
$K4_{cp}$	11.2^{b}	11.2^{c}	186.8^{c}	28.4^{a}	5.3^{c}
$K5_{cp}$	9.4^{b}	9.3^{c}	69.5^{d}	26.4^{a}	1.7^{c}
Treatment	-	-	-	-	-
Blocks	Ns	Ns	Ns	Ns	Ns

To find differentiates that existed between different types of treatment, distinctive relationship measures were made using the surpass desires of 16.0 for Windows quantifiable programming, and the likelihood degrees were communicated at 0.9% probability [15]. Besides, there was no examination of contrast was made for the capability of leaves to hold the necessary measure of water that would help in completing the test that was being conveyed [16]. The work being attempted on warmed and unheated situations, it was seen that harvests demonstrated different structures when presented to changing measures of water and climate conditions. Leaf water potential and also correct estimation of temperature controlled by the leaves was taken into clear thought while concocting the arrangements that are required in measuring leaf temperature [17]. Their results were unmistakably given as recognition and for giving the additional information required for productive utilization of the analysis [18]. Different types of examinations were done when putting in different conditions to indicate how survival of products can do when soil conditions are not kept up in a similar condition [12]. Climate data for the were dissected for a long time and the path through which

the sum of 7 days in seven days is simple in vanishing was taken as a preface in guaranteeing of water framework water entireties half water framework: half of the water system control marks. - 25% water framework: 25% of the water utilized for water system - 0% was utilized to demonstrate that no water was connected in this test [19]. The examination was randomized with the piece plan for the two types of greenhouses water systems plans to be tried independently. Replications have been sent to different segments in which squares of different ways have been utilized to guarantee that there is no aggravation of the current water system framework. Water system framework utilized for the two arrangements of frameworks has fluctuating dish coefficients [13] (Figure 2).

Crop Yield Response. The response of crop yield was represented by factor K_y that was used to indicate the linear relationship that was shown between the general decrease in relative yield [17]. There was a considerable decrease in yield concerning amount of water consumption. The factor considerably decreased when yield caused by the irrigation schemes was done as per the stipulated schedule [17]. The crop yield factor showed that in a heated condition, pepper yield was considerably higher than the ones that are found in unheated conditions. Seasonal crop response was found to range between 1.04 for all irrigation treatment done in both conditions. The value of Ky was noticed to be higher when water deficit increased thus showing that reduced amount of water used for irrigation reduces the total amount of yield that is collected from the crops [20] (Figure 1).

Water use efficiencies. IWUE and WUE considerably decreased when the amount of water applied for irrigation was reduced. The highest amount of production was realized when treatment was done for both growing conditions that took the values of pepper fruits was consumed and how values of K2 cp affected the general fruits of the experiment [7]. From the study, it was realized that irrigation that is deficit would affect the value of crops and market value. Height and diameter of the products are supposed to be taken into consideration when assembling the amount of water that is to be applied for irrigation during the varying conditions [13]. Data is shown in Table 5 and 6.

TABLE 6
Marketable parameters for irrigation effects on peppers yield under unheated conditions.

Irrigation treatment	Height (cm)	Diameter (cm)	Weight (kg)	Dry matter (%)	Yield (t ha^{-1})
$K1_{cp}$	28.4^{a}	26.5^{a}	1120.4^{a}	5.8^{c}	30.2^{a}
$K2_{cp}$	24.2^{a}	24.6^{a}	986.2^{a}	8.2^{c}	25.2^{a}
$K3_{cp}$	18.2^{a}	19.5^{b}	420.6^{b}	14.2^{b}	16.2^{b}
$K4_{cp}$	10.2^{b}	13.2^{c}	178.7^{c}	26.4^{a}	4.8^{c}
$K5_{cp}$	8.5^{b}	9.0^{c}	58.3^{d}	23.1^{a}	2.1^{c}
Treatment	-	-	-	-	-
Blocks	Ns	Ns	Ns	Ns	Ns

TABLE 7
The table shows WUE as well as IWUE values for pepper planted under drip irrigation and different treatment criteria used under heated conditions.

Irrigation treatment	Yield (t ha^{-1})	WUE (kg mm^{-1})	IWUE (kg mm^{-1})
KI_{cp}	26	3.28	3.10
$K2_{cp}$	18	3.48	3.16
$K3_{cp}$	13	3.01	2.36
$K4_{cp}$	6	2.18	1.18
$K5_{cp}$	3	1.86	0.00

TABLE 8
The table shows WUE as well as IWUE values for pepper planted under drip irrigation and different treatment criteria used under unheated conditions

Irrigation treatment	Yield (t ha^{-1})	WUE (kg mm^{-1})	IWUE (kg mm^{-1})
KI_{cp}	34	4.16	3.28
$K2_{cp}$	22	3.26	3.08
$K3_{cp}$	18	3.15	2.86
$K4_{cp}$	8	2.20	1.28
$K5_{cp}$	2	1.56	0.00

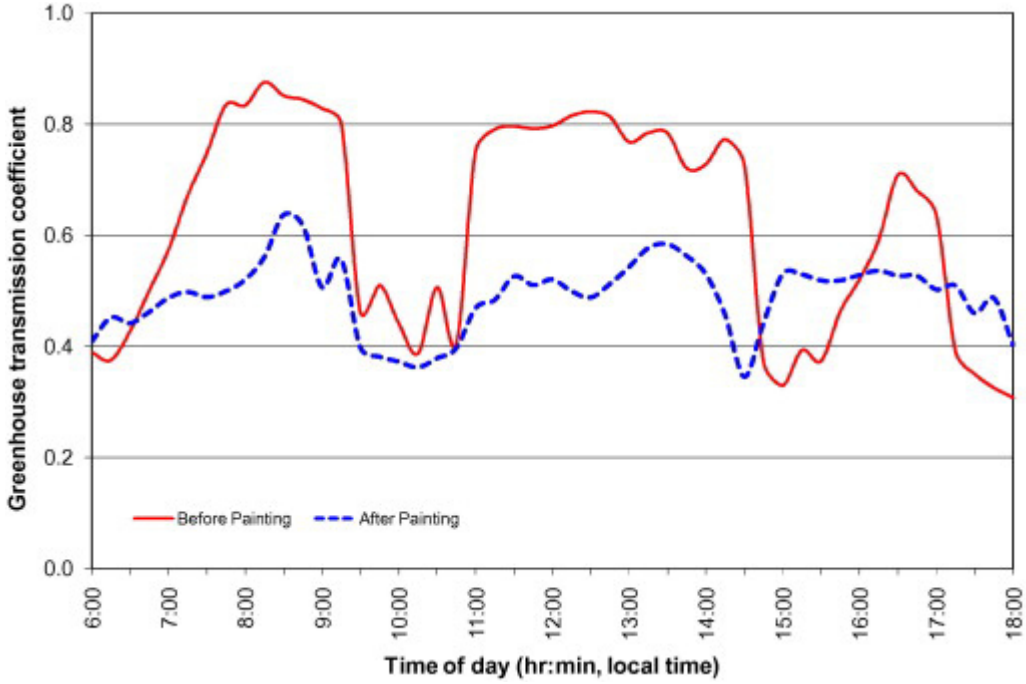


FIGURE 2
Showing how the production of pepper is influenced after and before planting.

Comparison between Heated and Unheated Greenhouse Chilies Production. Depending on the greenhouse that was used, the amount produced from different conditions varied to a great extent. It was noticed that a number of chilies produced from heated greenhouses was higher than those from unheated greenhouses [21]. The variation rose because of the varying solar radiation that is transmitted into greenhouses and the amount of water applied to each sector that is intended to cover the materials used [7]. Pepper from heated greenhouses had proper diameter, and weight thus was able to influence significantly market value. Additionally, the level of solar radiation that is carried out under protective structures that allowed protection of the planted crops thus showing considerable rise during different seasons. The vertical transmission of the applied water aide in helping crops to blossom and have the ability to determine the level of quality produced by each plant [21]. Values are shown in Table 7 and 8.

CONCLUSION

While carrying out this study, it was noticed that irrigation treatments affected crop production significantly. The yield, diameter, fruit length and dry matter ratio are one of the leading properties that have been significantly affected. Under heated conditions, it was noticed that the highest yield was obtained at treatment levels of $K1_{cp}$ in which there was the total production of 26 t ha^{-1}, and there was minimum yield obtained from $K5_{cp}$ because only two tonnes were obtained from one hectare. Furthermore, there was a significant reduction in the amount of yield realized as the amount of water applied for irrigation was reduced. The amount that was applied for each yield was significant in which every irrigation treatment resulted in higher products when compared to the use of irrigation water that was applied to a limited value thus showing scarce resources. Various greenhouse conditions reveal that water resources are scarce, treatment of $K2_{cp}$ was taken to be the most suitable because water application for pepper irrigation should be applied under specific criteria that is tended to show how much value would be realized when the correct amount of water is applied to crops. IWUE applied during the treatment period was higher, and the value of $K2_{cp}$ was realized to be higher than the value of $K1_{cp}$ as well as the use of $K3_{cp}$ which was used as the primary form of treatment criteria. The application of varying criterion used for treatment of heated condition led to indifference in production and the quality of the products thus showing that there is a considerable decrease in the amount of water applied to enhance the production rate of each part. The value that was recommended indicated that $K2_{cp}$ was the most suitable form of treatment that can be used to increase the amount of pepper that was produced from each portion. It was noticed that deficit irrigation had considerable effect on fruit height and weight. The applied amount of water had considerable effects on yield and quality of pepper. There was raise of concern in which the necessary treatment method was supposed to be used to ensure that weight, length, and diameter of the fruits was maintained constant.

REFERENCES

[1] Duffy, R. (2017) Good Agricultural Practices for greenhouse vegetable production in the South East European countries. Food and Agriculture Organization of United Nations. Rome.

[2] Sahin, U., Ekinci, M., Kiziloglu, F. M., Yildirim, E., Turan, M., Kotan, R., Ors, S. (2015) Ameliorative effects of plant growth promoting bacteria on water-yield relationships, growth, and nutrient uptake of lettuce plants under different irrigation levels. Hortscience. 50(9), 1379-1386.

[3] Sharma, H., Shukla, M.K., Bosland, P.W., Steiner, R. (2017) Soil moisture sensor calibration, actual evapotranspiration, and crop coefficients for drip irrigated greenhouse chile peppers. Agricultural Water Management. 179, 81-91.

[4] Santosh, D.T., Tiwari, K.N., Singh, V.K., Reddy, A.R.G. (2017) Micro Climate Control in Greenhouse. Int. J. Curr. Microbiol. App. Sci. 6(3), 1730-1742.

[5] Elad, Y. (2016) Cultural and Integrated Control of Botrytis spp. In: Fillinger, S., Elad, Y.(eds.) Botrytis–the Fungus, the Pathogen and its Management in Agricultural Systems. Springer International Publishing, Edition: 1st ed. 149-164

[6] Tüzel, Y., Öztekin, G.B., Tüzel, I.H., Tunali, U., Tepecik, M. (2013) Automated irrigation management of organic greenhouse tomatoes. In: II International Symposium on Organic Greenhouse Horticulture 1041. October 2013, 109-118.

[7] Fernández, M.D., López, J.C., Baeza, E., Céspedes, A., Meca, D.E., Bailey, B. (2015) Generation and evaluation of typical meteorological year datasets for greenhouse and external conditions on the Mediterranean coast. International journal of biometeorology. 59(8), 1067-1081.

[8] Gajanayake, B., Reddy, K.R., Shankle, M.W., Arancibia, R.A. (2014) Growth, developmental, and physiological responses of two sweet potato (Ipomoea batatas L.[Lam]) cultivars to early season soil moisture deficit. Scientia Horticulturae. 168, 218-228.

[9] Gallardo, M., Thompson, R.B., Fernández, M.D. (2013) Water requirements and irrigation management in Mediterranean greenhouses: the case of the southeast coast of Spain. Good Agricultural Practices for Greenhouse Vegetable Crops: Principles for Mediterranean Climate Areas. edited by FAO-AGP and ISHS-CMPC, FAO, Rome, Italy, 109-136.

[10] Bonanomi, G., Chirico, G.B., Palladino, M., Gaglione, S.A., Crispo, D.G., Lazzaro, U., Rippa, M. (2017) Combined application of photo-selective mulching films and beneficial microbes affects crop yield and irrigation water productivity in intensive farming systems. Agricultural Water Management. 184, 104-113.

[11] Ghaemi, A., Moazed, H., Rafie Rafiee, M., Broomand Nasab, S. (2016) Determining cwsi to estimate eggplant evapotranspiration and yield under greenhouse and outdoor conditions. Iran Agricultural Research. 34(2), 49-60.

[12] Liang, X., Gao, Y., Zhang, X., Tian, Y., Zhang, Z., Gao, L. (2014) Effect of optimal daily fertigation on migration of water and salt in soil, root growth and fruit yield of cucumber (Cucumissativus L.) in solar-greenhouse. PloS one. 9(1), e86975.

[13] Gruda, N., Tanny, J. (2014) Protected crops. In: Dixon, G.R., Aldous, D.E. (eds.) Horticulture: Plants for People and Places. Volume 1. Springer Netherlands. 327-405.

[14] Luvai, A.K., Gitau, A.N., Njoroge, B.N.K., Obiero, J.P.O. (2014) Effect of Water Application Levels on Growth Characteristics and Soil Water Balance of Tomatoes in Greenhouse. International Journal of Engineering Innovations and Research. 3(3), 271.

[15] López-Marín, J., González, A., Pérez-Alfocea, F., Egea-Gilabert, C., Fernández, J.A. (2013) Grafting is an efficient alternative to shading screens to alleviate thermal stress in greenhouse-grown sweet pepper. Scientia Horticulturae. 149, 39-46.

[16] Tittatelli, F., Bath, B., Ceglie, F.G., Garcia, M. C., Moller, K., Reents, H.J., Voogt, W. (2016) Soil fertility management in organic greenhouses in Europe. BioGreenhouse, Netherlands.

[17] Zikeli, S., Deil, L., Möller, K. (2017) The challenge of imbalanced nutrient flows in organic farming systems: A study of organic greenhouses in Southern Germany. Agriculture, Ecosystems & Environment. 244, 1-13.

[18] Kumari, P. (2013) Studies on water requirement for vegetable production in naturally ventilated polyhouse. Doctoral dissertation. DYSPU. Dr. Y.S. Parmar University of Horticulture & Forestry, Solan, HP, India.

[19] Koller, M., Rayns, F., Cubison, S., Schmutz, U., Messelink, G.J., Voogt, W. (2016) Guidelines for experimental practice in organic greenhouse horticulture. BioGreenhouse, Netherlands.

[20] Haapala, T., Palonen, P., Tamminen, A., Ahokas, J. (2015) Effects of different paper mulches on soil temperature and yield of cucumber (Cucumissativus L.) in the temperate zone. Agricultural and Food Science. 24(1), 52-58.

[21] Giménez, C., Gallardo, M., Martínez-Gaitán, C., Stöckle, C.O., Thompson, R.B., Granados, M.R. (2013) VegSyst, a simulation model of daily crop growth, nitrogen uptake and evapotranspiration for pepper crops for use in an on-farm decision support system. Irrigation science. 31(3), 465-477.
[22] Jin, Q., Yang, Q., Zhong, F., Zhu, L. (2017) Impact of drip irrigation and buried straw layer on the soil cultivated environment: a case study under greenhouse. Fresen. Environ. Bull. 26, 5413-5419.
[23] Zhong, F., Sheng, Q., Wang, S., Lin, B., Zhou, X.Z., Xu, R., Chen, I., Lin, Y. (2017) Precision irrigation scheduling for greenhouse tomato based on analysis of environmental characters and the Penman−Monteith model. Fresen. Environ. Bull. 26, 6938-6944.

Received: **18.8.2017**
Accepted: **09.02.2018**

CORRESPONDING AUTHOR

Zhu Mei
Anhui Agricultural University
Department of Engineering
Hefei- 230036 Anhui Province – P.R. China

e-mail: zhumei@ahau.edu.cn

© by PSP Volume 27 – No. 5/2018 pages 2818-2828 Fresenius Environmental Bulletin

STUDY OF THE RELATIONSHIP BETWEEN ECONOMIC GROWTH AND ENVIRONMENTAL QUALITY WITH THE KUZNETS CURVE IN GUANGXI, CHINA

Yuping Xu[1,2], Miao Wang[1], Man Qin[1], Huaxian Shi[2], Bowen Sui[2], Xinzhong Jia[1], Dongliang Lu[3,*]

[1]Management College of Ocean University of China, Qingdao, 266100, China
[2]Economics and Management College of Qinzhou University, Qinzhou 535099, China
[3]Guangxi Key Laboratory of Marine Disaster in the Beibu Gulf, Qinzhou University, Qinzhou 535099, China

ABSTRACT

Guangxi is located in the southern part of China, with Guangdong in the west and Beibu Bay in the north. Guangxi's per capita gross domestic product has increased with an average annual growth rate of 16.10 % from 1985 to 2014. With the rapid development of economy, the ecological environment bears considerable stress. Therefore, this study analyzed the dynamic relationship between economic development and environmental quality if Guangxi through the examination of water waste, gas waste, and solid waste using the EKC hypothesis with panel data from 1985 to 2014. Results confirm that the relationship between water waste, gas waste, and solid waste pollutants and per capita GDP were an inverted U-shaped, where the turning points at per capita GDP were 28851, 21000, and 23000 RMB, respectively, from 2008 to 2009. The scenario elucidates that the rapid growth of environmental protection investment and the strict environmental policy promote the harmonious development of economy and environment. Principal component analysis proves that the major pollutants were waste gas and solid waste in Guangxi. Therefore, the local government should strengthen the management of discharges, such as gas waste and solid waste. This study aims to provide an epitome of the conflicts and consolations between socio-economic development and environmental quality in the past as well as hints for overall management in the future.

KEYWORDS:
Environmental Kuznets curve, economic growth, environmental quality, Guangxi

INTRODUCTION

With the acceleration of social economic development and human activities, the destruction of environment has become serious worldwide, such as habitat degradation, alteration of food-web structure, and loss of biodiversity [1, 2, 3]. Much of this environment degradation has been driven by three waste discharges (water waste, gas waste, and solid waste) [4, 5, 6]. Accordingly, economic developments have generally generated negative effects on ecosystem functioning, such as soil acidification, habitat degradation, and even biodiversity [7, 8, 9]. Generally, economists have recognized that, to a certain level, social and economic developments can help improve environment quality and promote the harmonious development of economy and environment [10, 11, 12].

Notably, Guangxi has been successfully following the concept of developing the economy without damaging the environment, the so-called "win–win" strategy [13]. Therefore, the regional economic integration raises our particular interest for exploring the economic development and quality environment relationship.

Many researchers have explored the relationship between economic development and environment quality by employing the environmental Kuznets Curve [14, 15, 16, 17]. The environmental Kuznets Curve (EKC) hypothesis has, thus, acquired worldwide attention [18, 19, 20]. The EKC concept has become an independent research issue that has provoked a large body of theoretical and empirical literature [21, 22, 23]. Several existing studies on the relationship between economic growth and environmental pollutant conditions have argued that environmental degradation increases first as income increases, when income increases to a certain peak, and the environmental degradation will decreases with the increase of income assume of the inverted U-shaped relationship [24, 25]. This inverted U-shaped relationship is known as EKC in the literature. The empirical results in the literature regarding this inverse U-shaped relationship between environmental pollutants and per capita income have been based on three different channels: scale, composition, and technique efferent [22, 26, 27]. Empirical evidence confirms that the economic growth will lead to a gradual degradation of environment in its initial stages and then, after a certain level of growth, to an improvement in the environmental conditions, such as wastewater discharge, waste gas emissions, and solid waste. However, carbon dioxide has been

among the most commonly used environmental degradation indicators, and EKC hypothesis has been proven to hold mostly for carbon dioxide emissions in the literature [28]. Others have reported a U-shaped relationship [29] or even an N-shaped relationship [30]. The EKC hypothesis asserts that the different shapes have been influenced by several types of factors, such as range of year, index selection, and curvilinear forms [31, 32].

This hypothesis posits an inverted U-shaped relationship between economic growth and environmental degradation, where environmental degradation increases with economic growth but also decreases when economic growth reaches a certain point, the so-called turning point. Many studies have shown that annual income level's turning point is approximately 5000–8000$ [33, 20]. The conventional EKC has elicited many critiques. Likewise, arguments have mainly focused on the assertion that the inverted U-shaped relationship applies only to a subset of environmental measures [34, 35], for example, certain conventional pollutants, such as waste water discharge, suspended particulates, and carbon dioxide [36, 37], which also argues that the EKC pattern might exist, but not for overall environmental pressure.

Many researchers have summarized the relationships between pollution and income, with the following four scenarios: the conventional EKC, new toxics, race to the bottom, and revised EKC scenario (Fig. 1) [38, 20]. New toxins for common pollutants may have an inverted U-shaped curve, but new pollutants replacing common pollutants are emerging, with similar effect on the environment. The race to the bottom scenario posits that the reduced pollution in developed countries has been likely achieved through directing pollution-causing discharges to developing countries. Therefore, developing countries will have difficulty in reducing pollution. The revised EKC scenario has not denied the EKC curve but suggests that technological change has shifted the curve downward and to the left in the course of time [20]. The EKC scenario suggests that environmental improvements are possible in developing countries and that peak levels of environmental degradations will be low in developed countries.

Guangxi is a medium income-developing district in southern China, which has undergone remarkable economic growth over the past three decades. Similar to other developing districts, the extensive development pattern played a significant role in boosting Guangxi's economic growth and energy consumption increased by an average annual growth rate of 11 % from 1985 to 2014 and a per capital GDP average annual growth rate of 16.10 % from the Guangxi statistical yearbook. The annual growth rate of three waste discharges has gone up to at least 14.36 %, 0.54 %, and 6.06 % from 1985 to 2014 in Guangxi.

In Guangxi, linkages between three wastes and economic growth have received inconsiderable attention. Although several studies have recently tackled the issue only, these studies have only focused on carbon dioxide (CO_2) emissions [39, 40], and have ignored the importance of water waste and solid waste's effect on the environment. However, the role of the three wastes in the context of economic growth and environmental effect is fairly important.

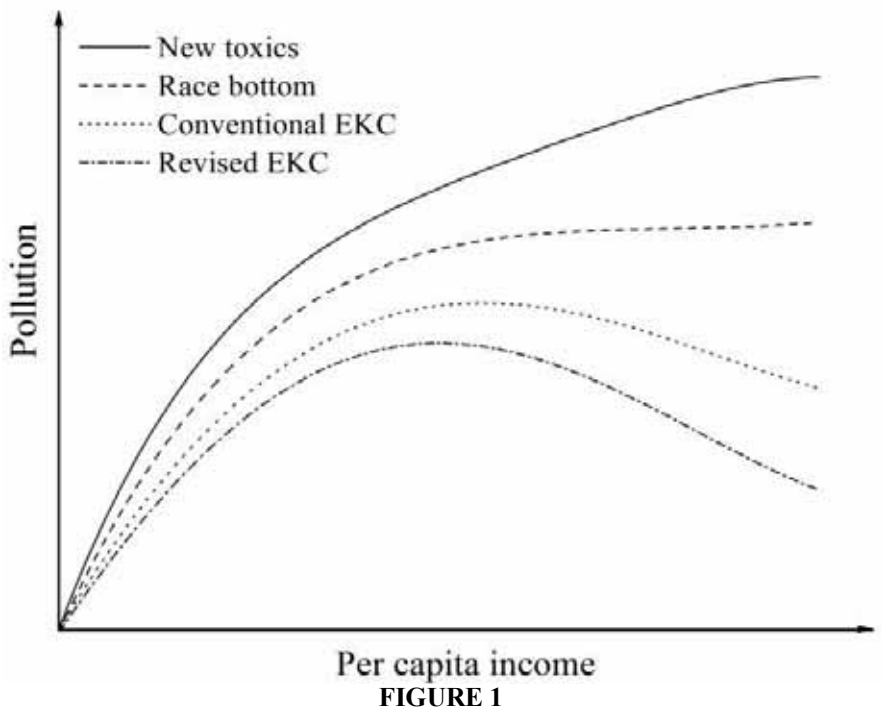


FIGURE 1
Environmental Kuznets curve (EKC) modified by [38, 20].

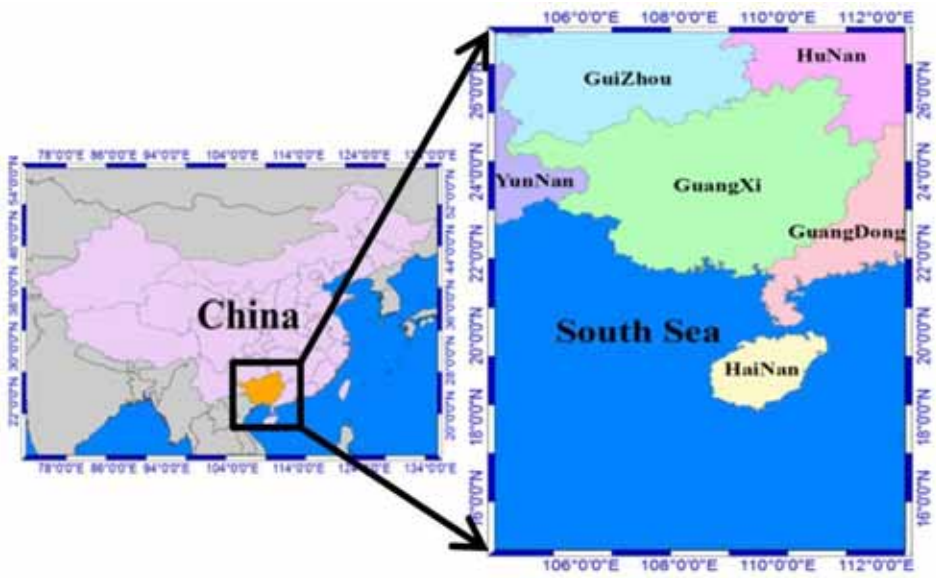


FIGURE 2
Map showing the geographical location of Guangxi

TABLE 1
Relationship between EKC and the coefficient of the model

Number	Coefficient			Explanation
	α_1	α_2	α_3	
1	0	0	0	Indicate a level relationship between $ln(C_t)$ and ln Y_t
2	>0	0	0	Indicate a monotonically increasing linear relationship
3	<0	0	0	Indicate a monotonically decreasing linear relationship
4	>0	<0	0	Indicate an inverted U-shaped relationship
5	>0	>0	<0	Indicate an inverted U-shaped relationship
6	<0	>0	0	Indicate a U-shaped relationship
7	>0	<0	>0	Indicate an inverted N-shaped relationship
8	<0	>0	<0	Indicate an N-shaped relationship

This study aims at understanding the challenges involved in the balanced development of economic growth and environmental quality in a different perspective by analyzing the relationship between the rapid economic growth and the three waste pollutants through the standard EKC mode, as well as promote Guangxi's harmonious development of economy and environment.

MATERIALS AND METHODS

Description of study area. Guangxi is located in the southern part of the China, with bordered by the Guangzhou Province on the west, the Huan Province on the south and the Yunnan Province on the east (Fig. 2), which includes 14 prefecture-level cities and 33 counties, covering an area of 236,000 km^2, 39 rivers, and with a population of over 48 million [41]. The large amount of the three wastes that polluted the environment was mainly from the industry and domestic pollution sources.

Description of study methods. Previous empirical studies on the relationship between economic growth and environmental quality have confirmed that the pollution deterioration indices can be described by parameterized models, using the per income index as an independent parameter or variable in the form of multinomial functions. In this paper, the multinomial curve model was used to analyze the relationship between environmental quality and economic growth. Equation (1) shows the reduced form model:

$$Y_t = \alpha_0 + \alpha_1 X + \alpha_2 X^2 + \alpha_3 X^3 + \mu_t \quad (1)$$

where t is the time period, Y_t is the environmental variable, X_t is per capita real GDP, and μ_t is the standard error term. Table 1 shows the relationship between EKC and the coefficient of the model.

Principal component analysis (PCA) is a multivariable analytical tool that enables the data reduction and characterization of a given poly dimensional system using the means for a small number of new variables [42]. The raw data matrix was a Z-score standardized and mid-range normalized to eliminate the effect of differing units and to ensure that each

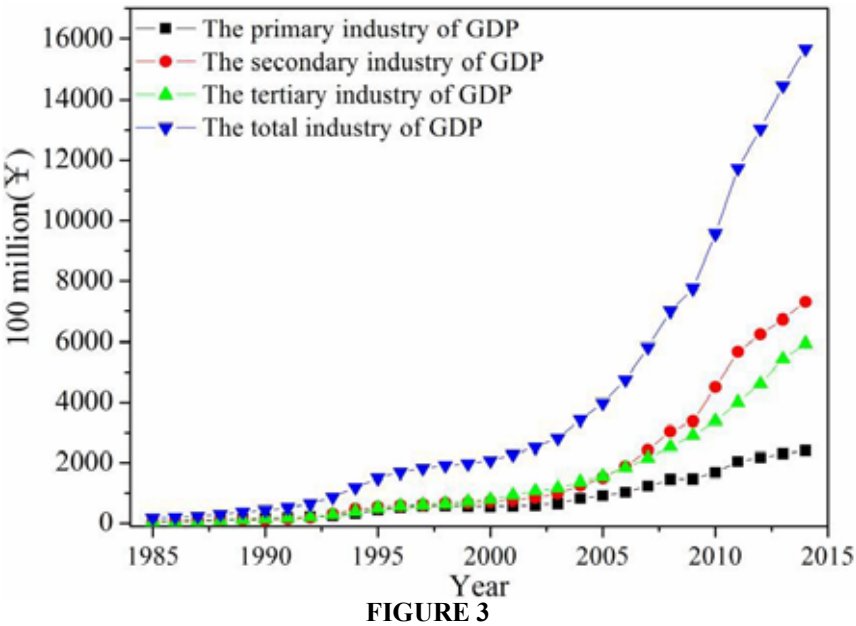


FIGURE 3
Total of GDP and three industrial sectors during various years of Guangxi

determined variable had an equal weighting in the PCA [43]. Generally, principal components (PCs) should account for approximately 75% of the total variance, and the relevant PCs were those having eigenvalues >1 [44].

The principal component analysis was used to evaluate the effect of environmental pollutant factors on the economic growth [45].

$$\ln X_t = \beta_1 \ln I_0 + \beta_2 \ln I_1 + \beta_3 \ln I_2 \quad (2)$$

where X_t is per real GDP; I_0, I_1, and I_2 are the gas waste, water waste, and solid waste; and β_1, β_2, and β_3 are the coefficients of gas waste, water waste, and solid waste, respectively. In this study, the data used are three wastes per GDP from 1985 to 2014. We used the all samples for our estimations from the Guangxi statistical yearbook. In the current study, per GDP is used as the index indicating the economic growth, the per GDP is calculated at current prices from reported of Guangxi statistical yearbook. Three indices were employed to gauge the levels of environment pollution in Guangxi, including industrial gas waste emissions, industrial water waste discharge, and industrial solid waste.

Data analysis. The normality of the data was tested by means of the Kolmogorov–Simonov test and was accepted at $p < 0.05$ using SPSS 19.0 software and Origin 9.0. A difference of synchronous data for different parameters was determined by a t-test [46] and was accepted at $p < 0.05$.

RESULTS

Economic growth of Guangxi. Guangxi was established as a bridgehead of China–ASEAN Free Trade Area in 2010. Guangxi's GDP has increased with an average annual growth rate of 17.12% from 1985 to 2014. In 2014, the total GDP reached 1567.29 billion. The per GDP is over 38,000 RMB in Guangxi, and the per capita annual income is approximately 18,000 that is significantly lower than the nation-wide average.

Base on the data of Guangxi Statistical yearbook from 1982 to 2014, the major contributing sectors to GDP growth are the secondary and the tertiary sectors of industries in Guangxi, which account for 47% and 38% of the total GDP, respectively. The primary sector of industry only accounts for 15% of the total GDP. The mainstay industries were sugar, papermaking, metallurgic, and tourist industries in Guangxi (Fig. 3).

Regression analysis on waste gas emissions. Industrial waste gas emissions (WGEs) mainly include carbon oxide (CO_X), sulfur dioxide (SO_X), and nitric oxide (NO_X). Waste gas emissions were chosen as the dependent variables in studying relations with the per GDP. For WGEs, the regression model clearly showed an inverted U-shaped (Fig. 4), and the coefficient estimate was significantly different ($p < 0.05$). The R^2 value is 0.9102. Accordingly, the fitted curve met the requirements. Table 2 exhibits the regression equation parameters.

We calculated that the turning point at per GDP is 28,851 RMB based on regression equation on waste gas as well as per GDP and occurred at the time interval between 2008 and 2009. The value of WGEs increase with the increase of per GDP when per GDP is less than 28,851 RMB, and vice versa. Currently, Guangxi has passed the turning point of the EKC. Therefore, with any further development of the economy, WGEs will also alleviate in Guangxi.

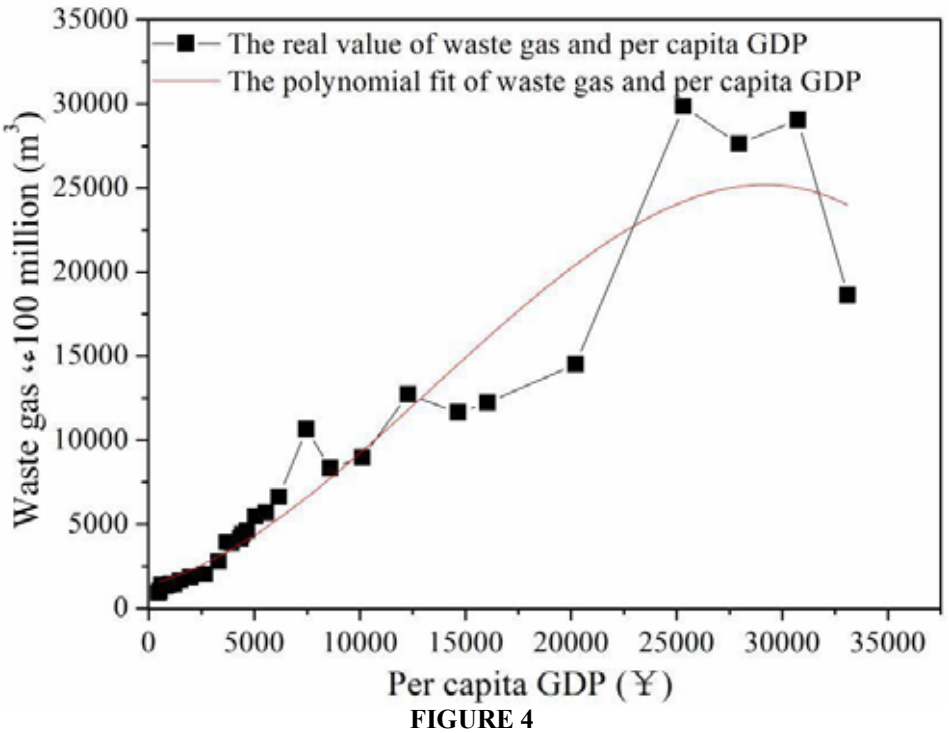


FIGURE 4
Environmental Kuznets Curve of waste gas and per GDP

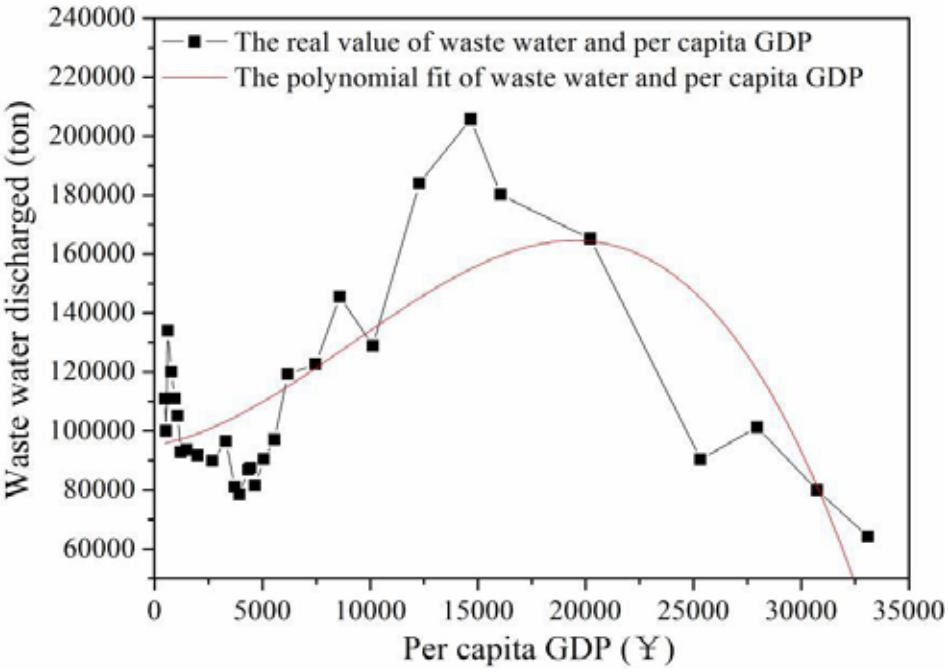


FIGURE 5
Environmental Kuznets Curve of waste water and per GDP

Regression analysis on water waste discharge. The dependent variable is the wastewater discharge (WWD). Based on regression model that shows a linkage between an inverted U-shaped in WWD and per GDP (Fig. 5), the coefficient estimate is significantly different from 0 to 0.05. The R^2 value is 0.5327. Therefore, the fitted curve meets the requirements. Table 2 presents the regression equation parameters.

From the regression equation of the WWD and per GDP, we can obtain a turning point at per GDP = 21,000, which indicates that the values of WWD begin to decrease when per GDP exceeds 21.000 RMB, and vice versa. Currently, Guangxi has passed the turning point of the EKC. Therefore, with any further development of the economy, WWD will also alleviate in Guangxi.

Regression analysis on solid waste produced. Figure 6 depicts that the regression model indicates an inverted U-shaped relation between solid wastes produced (SWP) and Per GDP. The coefficient estimate is significantly different from 0 to 0.02. The R^2 value is 0.9283. Accordingly, the fitted curve met the requirements. Table 2 shows the regression equation parameters.

From the regression equation of the SWP and Per GDP, we can obtain a turning point at per GDP = 23,000 RMB, indicating that the values of SWP begin to decrease when per GDP exceeds 23.000 RMB, and vice versa. Currently, Guangxi has passed the turning point of the EKC. Therefore, with any further development of the economy, WWD will also alleviate in Guangxi.

The estimated parameters, as the F-statistic value is significantly small and all the equations possess a high fitness R^2 of over 0.703. From the statistical aspect, therefore, the derived EKC was, thus, acceptable. Table 2 exhibits the estimated coefficient on each regression and the values of R^2 and F.

Principal component analysis. We selected various per GDP indices to analyze the effect of three waste discharges on environmental quality, per GDP, industrial water waste, industrial gas waste, and solid waste. These indices represented human activities, such as service, agricultural, and industrial processes. Spearman's rank correlation coefficient was applied to measure statistical dependence between two variables. However, without the assumption of normal distribution of two variables, the coefficient has abroad application field in statistical analysis using a monotonic function. Table 3 presents the results of Spearman's rank coefficient test.

The results of the PCA confirmed that F-1 explains the 81.9% of the total variance. Afterward, the relative roles of three pollutants in governing the per GDP was carried out using stepwise regression analysis. The regression calculation (Eq. (3)) suggests that the per GDP is controlled by the three pollutions. According to Eq. (3), the regression is positively associated with the gas waste as well as soil waste and negatively associated with the water waste.

$$\ln X_t = 0.978\ln I_0 - 0.190\ln I_1 + 0.982\ln I_2 \qquad (3)$$

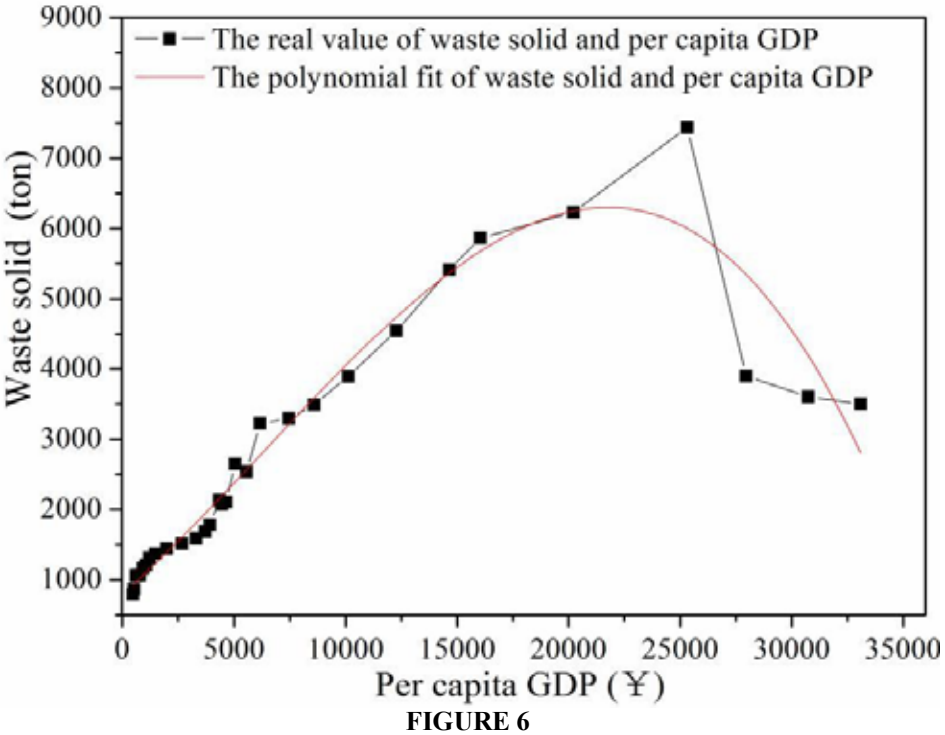


FIGURE 6
Environmental Kuznets Curve of solid waste and per capita GDP

TABLE 2
EKC parameters of three wastes and per GDP in Guangxi

Parameters	Gas waste	Water waste	Solid waste
α_0	1408	95233	790
α_1	0.3169	1.1926	0.2849
α_2	6.2089E−5	4.2511E−4	8.7604E−6
α_3	−1.5423E−9	−1.5570E−8	−4.6936E−10
R^2	0.9102	0.5327	0.9283
F	98.987	10.794	126.172
P	2.398E−14	8.683E−5	1.332E−15

TABLE 3
Spearman's correlations for per GDP and three wastes in Guangxi from 1985 to 2014

Parameters	Gas waste	Water waste	Solid waste	GDP
Gas waste	1			
Water waste	0.133[b]	1		
Solid waste	0.931[a]	0.361	1	
GDP	0.978[a]	0.081[b]	0.923[a]	1

a Correlation is significant when0 <p<0.01(two-tailed). n=30.
b Correlation is significant when0.01≤ p<0.05(two-tailed). n=30.

DISCUSSION AND POLICY IMPLICATION

Analysis results asserted that the relationship between water waste, gas waste, as well as solid waste of pollutants and per capita GDP was inverted U-shaped. The research result is of great significance to the adjustment of industrial structure, energy consumption and environment investment of Guangxi.

Industrial structure of Guangxi. The aforementioned analyses verify that the relationship between economic growth and comprehensive environmental pollution emissions from 1985 to 2014 in Guangxi is inverted U-shaped located at the right side of the inverted U-shaped. Many of scholars' literature have shown that the unhealthy industrial structure of the economy has an effect on the shape of EKC curve [47, 48]. Therefore, we can judge whether industrial structure was the reason that influenced the shape of EKC the fitting curve. The rapid economic development and reasonable industrial structure are helpful in improving the environmental quality of Guangxi. Moreover, the increased PC GDP in Guangxi was 6925% from 1985 to 2014. The total GDP of Guangxi was 1573 billion in 2014, and the average annual growth rate of GDP is 16.07%. The primary, secondary, and the tertiary sectors of industry accounted for 15%, 47%, and 38% of the total GDP, respectively (Fig. 7). The average annual growth rate of the primary, secondary, and the tertiary sectors of industry were −3.33%, 1.84, and 1.33%, respectively. From the per GDP of Guangxi and industrial structure perspective, the average annual growth was more rational rather the industrially structured, and the living standard of people was significantly improved. The change in the economy growth mode from one extension rule to another in upgrading the industry promoted the rapid development of Guangxi's economy, and the degree of industrialization has accelerated. The large number of pollutants affected the resource utilization, which led to the downward trend in the level of pollution discharges.

Energy consumption in Guangxi. With the rapid development of economy, the industrial structure should be adjusted. Note that the energy consumption only increased; however, Guangxi's energy consumption structure is constantly changing. The average annual total energy consumption has increased by 7.92 % from 1985 to 2014, and the average annual consumption growth rates of coal, oil, and electricity were 6.18%, 7.53%, and 6.54%, respectively (Fig. 8). The coal, oil, and electricity consumption changes from account for 55.3%, 13.0%, and 31.7% of the total energy consumption to 44.4%, 17.6%, and 38.0%, respectively, from 1985 to 2014. Only the technological innovation has the energy structure adjustment, and the adjustment of industrial structure promotes a series of industry development and growth. The electricity energy is developed by the means of hydro-power resources and the wind or nuclear power to make electricity. The models of energy consumption are changed, which promoted the development of green energy. Accordingly, the low consumption policies have been drawn up by the local government of the Guangxi Zhuang autonomous region that include new material, new energy, industry plans for energy conservation, and environment. The low consumption policies are entailed for function, industrialization, and modernization. People's 18th Congress emphasized the need for intensified energy and resource conservation, environment protection, and enhanced capacity for sustainable development to advance on the path of sustainable development. The local government has put forward a series of policies and measures in protecting the environment, such as straw burning prohibited in the countryside, construction, and the completion of clean energy compensation, a mechanism for ecological compensation, and the optimization of the energy consumption policies' structure.

Environment investment of Guangxi. The rapid development of industry accelerated the production capacity, which increased the total GDP and environment investment. Based on the practice in some developed countries, for the environment investment accounting for 1.5%–3% of the total GDP, the ecological and environmental qualities are effectively improved. However, the environment investment of Guangxi was approximately 1.51%–2.15% of the total GDP from 2006 to 2013 (Fig. 9). Moreover, the annual total investment in the environment

protection and ecological construction has been approximately 20 billion [49, 50]. At some time, the government of Guangxi raised the management of country domestic that became the important task for departments of government when "village cleaning project" was launched, which reduced the non-point source of three waste discharges. The rapid development of economy in recent years deteriorated, and the environment investment accounting quality of the total GDP and the amount of total environment investment hardly changed. People's 12th Congress of Guangxi Zhuang Autonomous Region has encouraged the creation of the natural ecology's picturesque scenery as the overall objective [51]. The regional policy of development priority zones is improved and used to raise considerable capital for pollution control and environmental protection, which improved the sound mechanism of the ecological civilization system. According to the EKC curve of the three wastes in Guangxi, further improvement of scientization, systematize, and legislation on the environment investment management level that promoted the environmental quality in Guangxi is promising, which also explains that the "three wastes" treatment in Guangxi is effective.

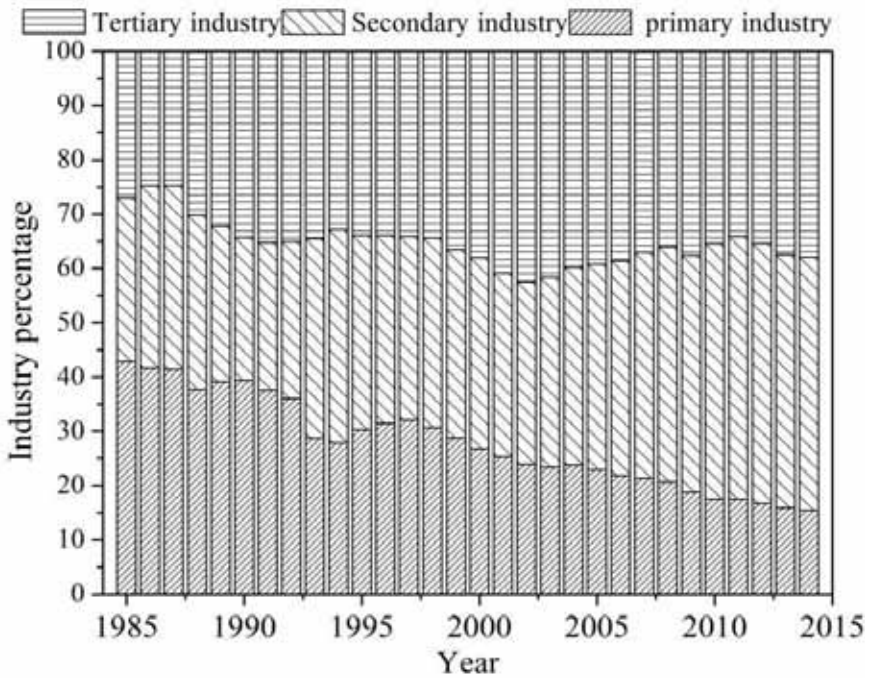


FIGURE 7
Industrial structure of Guangxi in several years

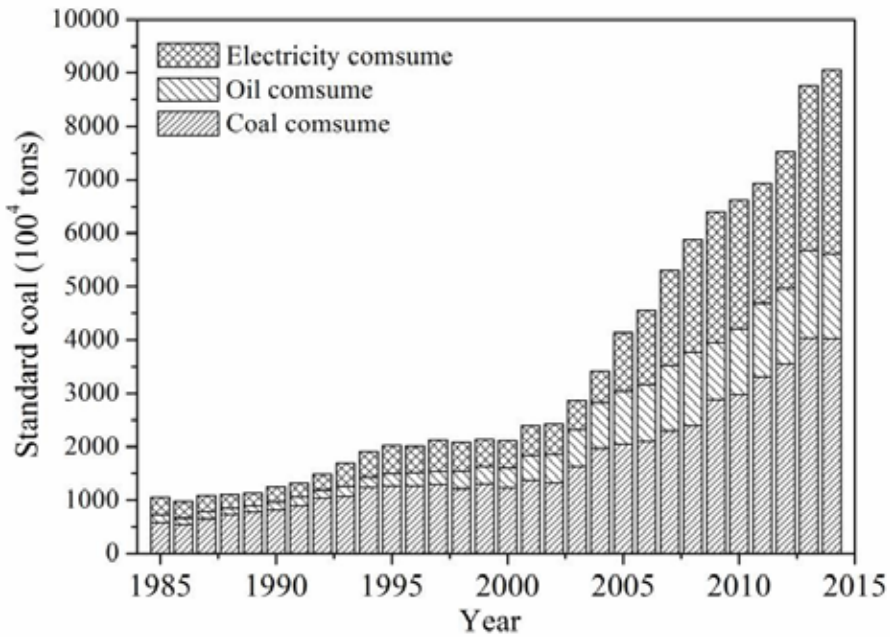


FIGURE 8
Energy consume structure of Guangxi in several years

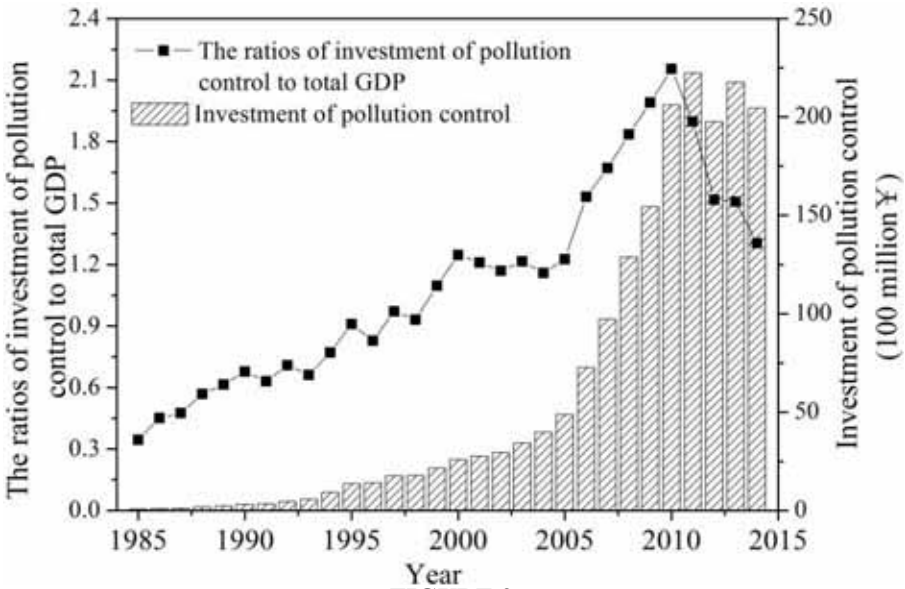


FIGURE 9
Investment of pollution control of Guangxi in several years

Evaluation of the main pollutant. Some studies have confirmed that gas waste is highly related to per capita GDP status and that many catchments in development of the industrial regional show moderately-high pollution [52, 53]. Table 3 shows that the *p* values in the water waste were larger than 0.05, therefore, we postulated that these indices have little relationship with per capita GDP and were deleted from the dataset. The *p* values in the gas waste and water waste are smaller than 0.01 and have significant differences. On the basis of the results of coefficient analysis, we proceeded with PCA to reduce the dimension of the per capita GDP indices for further statistical analysis. With the use of an orthogonal transformation, PCA converts correlated variables into linearly uncorrelated variables called principal components. The PCs correspond to the first eigenvector of the covariance matrix, which accounts for most of the variability in the data as possible, and each succeeding component in turn has the highest variance under the constraint that is orthogonal to the preceding components. The output of PCA has only one main component PCs, which accounted for 81.9% of the total variance. The three wastes discharge variables (gas waste and solid waste) had positive loadings on PCs, whereas water waste variables had negative loadings.

CONCLUSION

We examined the relationship between economic growth and environmental pollution in Guangxi, China. Over the past three decades, Guangxi has experienced rapid socio-economic development that exerted high stress on environment ecological system; thus, considerable attention has been paid to environment quality. Therefore, researchers and managers should understand the important relationship between economic growth and environmental quality.

On the basis of quantitative analysis on the long-term variation of economy and environment, we confirm that (1) the relationship between water waste, gas waste, and solid waste of pollutants and per capita GDP was inverted U-shaped from 1985 to 2014. (2) The quality of environment is improving in Guangxi, but pressure for implementing environmental still persists. Likewise, pollutions that resulted from industrial gas waste and solid waste discharges still aggravate the region. Therefore, the government should further strengthen the management and encouragement of recycling waste discharge. Furthermore, develop invigorative mechanisms to achieve a win–win combination of environmental improvement and economic growth.

This study not only helps researchers find the turning point of environmental health as a result of long-term economic development but also helps managers examine the management measures or strategies' effectiveness. Further scientific research is needed to optimize the industry structure. Moreover, interdisciplinary cooperation can significantly understand the economic growth and environmental pollution variations.

ACKNOWLEDGEMENTS

The authors would like to thank the editor and anonymous reviewers for their constructive comments on the manuscript. We are also thankful to colleagues of our lab for their assistance in data collection and analysis. We gratefully acknowledge the financial support of the Cultivation of High-quality

Talents Foundation of Qinzhou University (2016PY-SJ04). The Science and Technology Programmer of Education Department of Guangxi (2013LX160), Guangxi Key Laboratory of Marine Disaster in the Beibu Gulf (2017TS06), research start-up fund of Qinzhou University (2017KYQD218) and the Capacity Building of Guangxi "Marine Ecology Environment" Academician Workstation (Gui Science AD17129046).

REFERENCES

[1] Slocombe, D.S. (1993) Environmental planning, ecosystem science, and ecosystem approaches for integrating environment and development. Environ. manage. 17(3), 289–303.
[2] Rapport, D.J., Costanza, R., McMichael, A.J. (1998) Assessing ecosystem health. Trends. ecol. evol. 13(10), 397–402.
[3] Kandziora, M., Burkhard, B., Müller, F. (2013) Interactions of ecosystem properties, ecosystem integrity and ecosystem service indicators—A theoretical matrix exercise. Ecol. Indic. 28, 54–78.
[4] Johari, A., Ahmed, S.I., Hashim, H., Alkali, H., Ramli, M. (2012) Economic and environmental benefits of landfill gas from municipal solid waste in Malaysia. J. Renew. Sustain. Ener. Rev. 16(5), 2907–2912.
[5] Deudney, D. (1990) The case against linking environmental degradation and national security. Millennium. 19(3), 461–476.
[6] Vergara, S.E., Tchobanoglous, G. (2012) Municipal solid waste and the environment: a global perspective. Annu. Rev. Env. Resour. 37, 277–309.
[7] Yang, K., Ye, M., Xu, Q. (2003) Environmental Kuznets characteristics of municipal solid waste growth in Shanghai city. Geogr. Res. 2003, 1, 22–23. (in Chinese).
[8] Chandra, A. (2011) A deliberate inclusive policy (DIP) approach for coastal resources governance: a Fijian perspective. Coast. Manage. 39(2), 175–197.
[9] Cai, M., Liu, Y., Chen, K., Huang, D., Yang, S. (2016) Quantitative analysis of anthropogenic influences on coastal water–A new perspective. Ecol. Indic. 67, 673–683.
[10] Jiang, B., Sun, Z., Liu, M. (2010) China's energy development strategy under the low-carbon economy. Energy. 35(11), 4257–4264.
[11] Tietenberg, T.H., Lewis, L. (2016) Environmental and natural resource economics. Routledge. London, 10-11.
[12] Jebli, M.B., Youssef, S.B., Ozturk, I. (2016) Testing environmental Kuznets curve hypothesis: The role of renewable and non-renewable energy consumption and trade in OECD countries. Ecol. Indic. 60, 824–831.
[13] Stadtler, H. (2015) Supply chain management: An overview. In: Stadtler, H., Kilger, C., Meyr, H. Supply chain management and advanced planning. Springer. Berlin, Heidelberg, 3–28.
[14] Cropper, M., Griffiths, C. (1994) The interaction of population growth and environmental quality. Am. Econ. Rev. 84(2), 250–254.
[15] Mann, G.E., Lamming, G.E. (2001) Relationship between maternal endocrine environment, early embryo development and inhibition of the luteolytic mechanism in cows. Reproduction. 121(1), 175–180.
[16] Stern, D.I. (2004) The rise and fall of the environmental Kuznets curve. World. Dev. 32(8), 1419–1439.
[17] Lau, L.S., Choong, C.K., Eng, Y.K. (2014) Investigation of the environmental Kuznets curve for carbon emissions in Malaysia: Do foreign direct investment and trade matter. Energ. Policy. 68, 490–497.
[18] Ekins, P. (1997) The Kuznets curve for the environment and economic growth: examining the evidence. Environ. Plan. 29(5), 805–830.
[19] Cole, M.A. (2004) Trade the pollution haven hypothesis and the environmental Kuznets curve: examining the linkages. Ecolog. Econ. 48(1), 71–81.
[20] Liu, X., Heilig, G.K., Chen, J.M., Heino, M. (2007) Interactions between economic growth and environmental quality in Shenzhen, China's first special economic zone. Ecol. Econ. 62(3), 559–570.
[21] Grossman, G.M., Krueger, A.B. (1991) Environmental Impacts of a North American free trade agreement. NBER Working Paper 3914. NBER, Cambridge.
[22] Grossman, G.M., Krueger, A.B. (1995) Economic growth and the environment. Quarterly J. Econ. 110, 353–377.
[23] Song, T., Zheng, T., Tong, L. (2008) An empirical test of the environmental Kuznets curve in China: a panel cointegration approach. China Econ. Rev. 19(3), 381–392.
[24] Yandle, B., Vijayaraghavan, M., Bhattarai, M. (2002) The environmental Kuznets curve. A Primer, PERC Research Study. 1–2.
[25] He, J., Wang, H. (2012) Economic structure, development policy and environmental quality: An empirical analysis of environmental Kuznets curves with Chinese municipal data. Ecol. Econ. 76, 49–59.
[26] Al-Mulali, U., Saboori, B., Ozturk, I. (2015) Investigating the environmental Kuznets curve hypothesis in Vietnam. Energ Policy. 76, 123–131.
[27] Göktuğ, T.H., Bulut, Y., Demir, M. (2013) Estimating carrying capacity of Olympos Bey Mountains Coastal National Park. Fresen. Environ. Bull. 22, 3730-3738.

[28] Saboori, B., Sulaiman, J., Mohd, S. (2012) Economic growth and CO_2 emissions in Malaysia: a cointegration analysis of the environmental Kuznets curve. Energ. Policy. 51, 184–191.
[29] Kaufmann, R.K., Davidsdottir, B., Garnham, S., Pauly P. (1998) The determinants of atmospheric SO2 concentrations: reconsidering the environmental Kuznets curve. Ecol. Econ. 25(2), 209–20.
[30] Fried, B., Getzner, M. (2003) Determinants of CO_2 emissions in a small open economy. Ecol. Econ. 45(1), 133–48.
[31] Lantz, V., Feng, Q. (2006) Assessing income, population, and technology impacts on CO_2 emissions in Canada: Where's the EKC. Ecol. Econ. 57(2), 229–238.
[32] Opherk, C., Coromilas, J., Hirsch, L.J. (2002) Heart rate and EKG changes in 102 seizures: analysis of influencing factors. Epilepsy res. 52(2), 117–127.
[33] Dasgupta, S., Laplante, B., Wang, H., Wheeler, D. (2002) Confronting the environmental Kuznets curve. J. Econ. Perspect. 16, 147–168.
[34] Stern, D.I, Common, M.S., Barbier, E.B. (1996) Economic growth and environmental degradation: The Environmental Kuznets Curve and sustainable development. World. Dev. 24(7), 1151–1160.
[35] Lean, H.H., Smyth, R. (2010) CO_2 emissions, electricity consumption and output in ASEAN. Appl. Energ. 87, 1858–1864.
[36] Halicioglu, F. (2009) An econometric study of CO_2 emissions, energy consumption, income and foreign trade in Turkey. Energ. Policy. 37(3), 1156–1164.
[37] Jaunky, V.C. (2010) The CO_2 emissions-income nexus: evidence from rich countries. Energ. Policy. 39, 1228–1240.
[38] Perman, R., Stern, D.I. (2003) Evidence from panel unit root and cointegration tests that the environmental Kuznets curve does not exist. Aus. J. Agr. Resour. Ec. 47(3), 325–347.
[39] Selden, T.M., Song, D. (1994) Environmental quality and development: is there a Kuznets curve for air pollution emissions. Environ. Econ. Manage. 27(2), 147–162.
[40] Jalil, A., Mahmud, S.F. (2009) Environment Kuznets curve for CO_2 emissions: a cointegration analysis for China. Energ. Policy. 37(12), 5167–5172.
[41] Yang, L., Lam, L.T., Liu, Y. (2005) Epidemiological profile of mortality due to injuries in three cities in the Guangxi Province, China. Accident Analysis & Prevention. 37(1), 137–141. (in Chinese)
[42] Jha, R., Murthy, K.V.B. (2003) An inverse global environmental Kuznets curve. J. Comp. Econ. 31(2), 352–368.
[43] York, R., Rosa, E.A., Dietz, T. (2003) STIRPAT, IPAT and ImPACT: analytic tools for unpacking the driving forces of environmental impacts. Ecol. Econ. 46(3), 351–365.
[44] Wagner, M. (2008) The carbon Kuznets curve: a cloudy picture emitted by bad econometrics. Resour. Energ. Econ. 30(3), 388–408.
[45] Clemente, R., Dickinson, N.M., Lepp, N.W. (2008) Mobility of metals and metalloids in a multi-element contaminated soil 20 years after cessation of the pollution source activity. Environ. Pollut. 155(2), 254–261.
[46] Cohen, J. (1992) Statistical power analysis. Curr. direct. psychol. Sci. 1(3), 98–101.
[47] Dinda, S. (2004) Environmental Kuznets curve hypothesis: a survey. Ecol. Econ. 49(4), 431–455.
[48] Munasinghe, M. (1999) Is environmental degradation an inevitable consequence of economic growth: tunneling through the environmental Kuznets curve. Ecol. Econ. 29(1), 89–109.
[49] Environmental Protection Bureaus of Guangxi. (2013) The Report on Environmental Quality of Guangxi. Environmental Protection Bureaus of Guangxi. (in Chinese).
[50] Environmental Protection Bureaus of Guangxi. (2014) The Report on Environmental Quality of Guangxi. Environmental Protection Bureaus of Guangxi. (in Chinese).
[51] Guangxi Zhuang Autonomous Region Environmental Protection. (2017) The 13th Five-year Plan of Guangxi Zhuang Autonomous Region Environmental Protection. Guangxi Zhuang Autonomous Region Environmental Protection, Nanning. (in Chinese).
[52] Diao, X.D., Zeng, S.X., Tam, C.M. (2009) EKC analysis for studying economic growth and environmental quality: a case study in China. J. Clean. Prod. 17(5), 541–548.
[53] Han, X.M., Zhang, M.L., Liu, S. (2011) Research on the relationship of economic growth and environmental pollution in Shandong province based on environmental Kuznets curve. Energ. Procedia. 5, 508–512.

Received: **23.08.2017**
Accepted: **28.12.2017**

CORRESPONDING AUTHOR

Dongliang Lu
Guangxi Key Laboratory of Marine Disaster in the Beibu Gulf,
Qinzhou University,
Qinzhou 535099 – China

e-mail: ldl@qzhu.edu.cn

© by PSP Volume 27 – No. 5/2018 pages 2829-2833 Fresenius Environmental Bulletin

"NEW FINDINGS" ON *BOSTRICHUS CAPUCINUS* LINNAEUS, 1758 (COLEOPTERA: BOSTRICHIDAE) IN TURKEY

Inanc Ozgen*

Firat Univesity, Faculty of Engineering, Department of Bioengineering, 23119, Elazig, Turkey

ABSTRACT

Bostrichus capucinus (Linnaeus, 1758) (Coleoptera: Bostrichidae) is a xyllofag species that causes secondary damage in various culture plants in European countries and in Turkey. The damages caused by this species on the fig plant in Turkey and mode of damage are published for the first time with this study. Dimensions of the pupa nest of the species are also given. Furthermore*;* the species *Dendrosotinus ferrugineus* (Marshall, 1888) (Hymenoptera: Braconidae) as the new larva parasitoid of *B. capucinus* has been determined in this study. This is the first record that this species parasitizes the subspecies belonging to the Bostrychidae family. This species emerges from the cocoons of *B. capucinus* in the xylemic galleries. Moreover; both species have been determined in the fauna of Southeastern Anatolian Region and in Diyarbakır Province for the first time.

KEYWORDS:
Bostrichus capucinus, *Dendrosotinus ferrugineus*, new host, new record parasitoid, *Ficus caria*, Turkey.

INTRODUCTION

Bostrichus capucinus Linnaeus, 1758 is a widespread species found in a large area including a large part of Europe and in Turkey, Syria, Iraq and in the area from Asia to China [1, 2]. It is seen in almost every region of our country, more or less. It is found on hosts including *Castanea sativa* (=*C. vesca*,) *Quercus conferta*, *Q. ilex*, *Morus alba* and *Viburnum tinus*, and lives in dead oak, boadleaves trees, *Pinus*, hazelnut wood and timber [3, 4]. It has been reported that this species is a secondary pest. It has also been reported that this species prefers mostly the dying hazelnut wood [1]. This species is capable of causing damage in many plants including those belonging to Ericaceae, Fabaceae, Fagaceae, Moraceae, Myrtaceae, Rhamnaceae and Vitaceae families [5]. Furthermore, it has been reported that this species is a pest of *Quercus* sp., *Arbutus unedo* (L.), *Vitis vinifera* (L.) in Spain [6]. In a study carried out in Turkey aiming at determining the Xylophagous species on fig, the species belonging to the Bostrichidae family including *Xylonites praeustus* Germar, 1817, *Scobicia chevrieri* Villa, 1835, *Sinoxylon sexdentatum* Olivier, 1790, *Xyloperthella picea* Olivier, 1790 and *Schistocerus bimaculatus* has been determined, and of these species, *Scobicia chevrieri* Villa and *Sinoxylon sexdentatus* Oliver (Bostrychidae) cause significant damages on branches and stem. However, no information has been given in this study on damages caused by *B. capucinus* [7]. There are no detailed studies on the hosts of this pest in our country. There are no studies aiming at the natural enemies of the pest, and mechanical struggle is given against this pest in general. The species *Dendrosotinus ferrugineus* Marshall, 1888 emerging from the pupas of this pest however, is widespread in European countries, and is found also in Turkey in the Eastern Anatolia, Aegean and Middle Anatolia regions [8]. It has been reported in the studies carried out till now that this parasitoid parasitizes the species belonging to the Cerambycidae, Curculionidae and Scolytidae families of the Coleoptera order. In this study, the new host of *B. capucinus,* its pupa nest and parasitoid are introduced.

MATERIALS AND METHODS

The samples were collected between February 15, 2017 and March 1, 2017 in Eğil District of Turkey (Figure 1). In the study, the perennial fig tree in dying process was cut off over the root section and was divided into pieces with the help of a saw; fetched to the laboratory and was cultured. The culturing procedure was carried out between March 1, 2017 and May 15, 2017. Culture containers were checked weekly, and the emerging individuals were collected with the help of an aspirator and were prepared for diagnosis. The exit holes have been studied, pupa nests on the damaged pieces of wood have been examined and the exit holes of *B. capucinus* individuals have been photographed with stereo binocular Olympus SZX7 microscope and recorded.



FIGURE 1
The study areas in Eğil District (Turkey).

RESULTS AND DISCUSSION

Genus. *Bostrichus* Geoffroy, 1762
Bostrichus capucinus (Linnaeus, 1758)

Material. Diyarbakır Eğil (Central District) (41°9′50″N, 42°52′45″E), 1800 m. 10.04.2017, 12 exc, 17.04.2017, 4 exc., 23.04.2017, 6 exc, 29.04.2017, 2 exc. **Totally:** 24 exc. The period of the emergency of the pest is shown in Fig 2.

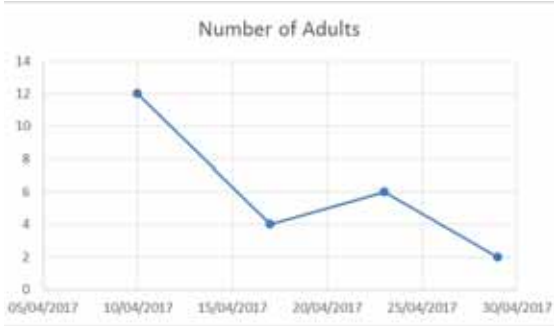


FIGURE 2
The period of the emergency of *Bostrichus capucinus* Linnaeus, 1758.

General Distribution. Europe, Sudan, Middle East, Iraq, Iran, Kazakhistan, Morocco, Algeria, Syria, Tunisia, Turkmenistan, Russia and China [1, 8, 9].

The pupa exit hole and an adult individual of *B. capucinus* are shown in Figure 3. The species exits this hole as an adult. The length of this hole is 7629 µm (7,6 mm), and the width are the widest point is 1696,89 µm (1,6 mm), while the width at the narrowest point is 1381,70 µm (1,3 mm).



FIGURE 3
Adult individual and pupa nest of *Bostrichus capucinus* L. *Dendrosotinus ferrugineus* (Marshall, 1888)

Material. Diyarbakır Eğil (Central District) (41°9′50″N, 42°52′45″E), 1800 m. 15.04.2017, 5 exc.(Figure 4).

Distribution in Turkey. Ardahan, Balıkesir, Bartın, Erzincan, Erzurum, Iğdır, Kars, Kayseri, Konya, Muğla [8].

General Distribution. West Palearctic, Armenia, Azerbaijan, Bosnia Herzegovina, France, Greece, Israel, Italy, Russia, Spain, Yugoslavia [8].

Hosts. Coleoptera, Cerambycidae: *Scobicia chevrieri* Villa & Villa, 1835, *Sinoxylon sexdentatum Olivier*, 1790. Curculionidae: *Phloeotribus scarabaeoides* Bernard, 1788. Scolytidae: *Chaetoptelius vestitus* Mulsant & Rey, 1860.



FIGURE 4
Adult *Dendrosotinus ferrugineus* Marshall, 1888.

In conclusion, the fact that *B. capucinus* damages the body of fig plant has been proven with this study for the first time. This species is seen in our country as a saproxylic species on may many culture plants with oak tree in the first place [2]. The larvae of this species is develops in *Aesculus hippocastaneum*, *Castanea vesca*, *Morus alba*, *Quercus,* and *Viburnum tinus* in Turkey [2]. It is seen that *Quercus* sp. Spreads at a distance of 250 m to orchard that study was carried out in. Furthermore, *Vitis vinifera*, *Prunus amygdali* and *Pistachio terebinthus* are widespread with commercial purposes and in wild form in the vicinity of the orchard (Figure 1). There are wide oak forests in the location of Eğil (Diyarbakır, Turkey), in which the study has been carried put. Therefore, it is considered that this species especially prefers the oak plant, and prefers fig plant as the secondary host. Studies related to the preference of this species for *Quercus* sp. Or other culture plants must be detailed in future years. The species has been harvested from the wooden tissue surrounding the stools of the plant within soils receiving and holding water in the garden. It has been observed that the pest is more spread in the fig trees planted around the gardens where humidity is greater. These findings parallel the data of the study carried out in Italy [10]. This species is also included in the red list of extinguishing species of Europe [11]. Besides, inclusion of this species is in the red list has ensured its evaluation under the indicators of biodiversity in Northern Europe [17]. Such species are indicator species especially for forest areas. In particular, *B. capucinus* species found on big dead trees has been shown as the indicator species as regards the biodiversity in forests. Intensity and number of individuals of this species have been indicated as the measure of biodiversity. Such species are very useful indicators for the landscape scale [11]. Although this species has been found on fig trees in this study, its presence in the red list and intensity of the oak trees in the vicinity of the land that the study has been carried out renders this study important as regards biodiversity. The period that the species is found in nature and determining its existing time are important for the struggle against it. This period varies in countries with different temperature and climatic characteristics. It has been reported that this species is active between April and September in the Iberian Peninsula [12]. It was found in a study of this type that this species is also active in Diyarbakır Province again between April and September. In addition, the emerging period of adults is determined by this study which was completed at the end of April (Fig 2.). Furthermore, there are no detailed studies aiming at determining of population intensity of this species. Information on the population intensity of the species is next to nothing [13]. Studies about the months that the species is found in nature and its biology must be detailed more. It was observed in this study that the species completed its existing period in the Southeastern Anatolia Region in April. This pest is known as a secondary pest, mechanical methods are important in the struggle against the pest. In general, struggle against to this species is mechanical. Cutting off the dead twigs and removing them is important in this struggle. In the studies carried out to determine the natural enemies of the pest, there is only one study reporting that the species *Cyanopterus flavator* Fabricius 1793 (Hymenoptera: Braconidae) parasitizes this species [14]. This species also emerges from the coons of *B capucinus* in xylemic galleries, like the species obtained in this study. Furthermore, the species *Chorebus* (*Phaenolexis*) *posticus* Haliday, 1839 has also been reported as the larva parasitoid of *B. capucinus* [15, 16]. The fact that, *D. ferrugineus* Marshall, 1888 species also parasitizes this pest has been reported in this study for the first time. Parasitoid had started to emerge within the first week of April, during which the pest started emerging. It has been reported in earlier studies that this species parasitizes species belonging to Cerambycidae, Curculonidae and Scolytidae families. However, there are no records showing that this species parasitizes species belonging to Bostrichidae family. This study reports that this species parasitizes the species belonging to this family. In addition, these data constitute additional data related to the initiation of existence of its natural enemies in nature. Moreover; this study is also important since it involves the first determination of the pest's natural enemy on the pest, and it includes the first record that this species parasitizes a species belonging to the Bostrichidae family. Beneficial arthropods in agriculture, mainly natural enemies are increasingly important both economically and environmentally [18, 19, 20]. Therefore, the results of this study are notable as regards the biological control against saproxylic species.

CONCLUSION

As a result, the importance of this work is given as follows:

1. This is the first study about *B. capucinus* to be harmful to fig plant.
2. In this study, it has been reported that *B. capucinus* is the secondary pest in the fig plant.
3. It was observed that *B. capucinus* exits from xylemic galleries under the climatic conditions of Southeastern Anatolia Region in April.
4. *B. capucinus* has been observed to cause more damage to figs holding water at the edge of the garden.
5. *B. capucinus* has been determined more harmful to especially in gardens near to *Quercus* sp. forests.
6. The species of *D. ferrugineus* was identified for the first time as the natural enemy of the pest.
7. This is first record that parasitization to Bostrichidae, except to Cerambycidae, Curculonidae and Scolytidae family species

ACKNOWLEDGEMENTS

I would like to extend my thanks to my gratitude to Prof. Dr. Ahmet Beyarslan (Bitlis Eren University) for identification of Braconidae species, and to Mehmet Zeki Efe (Eğil/Diyarbakır/Turkey) for material contributions.

REFERENCES

[1] Fisher, W.S. (1950) A Revision of the North American Species of Beetles Belonging to the Family Bostrichidae, United States Deparment of Agriculture. Miscallenous Publication. No: 698. 157p.
[2] Lodos, N. (1985) Türkiye'de mobilyaların önemli yeni bir zararlısı: *Bostrychus capucinus* (L) (Coleoptera: Bostrichidae). Türk. Bit. Kor. Derg. 9(3), 183-188.
[3] Nardi, G. and Ratti, E. (1995) Coleoptera Lyctidae, Bostrychidae e Anobiidae di Pantelleria e Lampedusa. In: Massa, B. (Ed.) Arthropoda di Lampedusa, Linosa e Pantelleria (Canale di Sicilia, Mar Mediterraneo). Il Naturalista siciliano 19(Suppl.), 477–492.
[4] Nardi, G. and Mifsud, D. (2015) The Bostrichidae of the Maltese Islands (Coleoptera). *ZooKeys*. 481, 69–108.
[5] Liu, L.Y., Ghahari, H. and Beaver, R.A. (2016) An annotated synopsis of the powder post beetles of Iran (Coleoptera: Bostrichoidea: Bostrichidae). Journal of Insect Biodiversity. 4 (14), 1-22.
[6] Murillo, A., and Obregon, R. (2013) Nuevas aportaciones a la fauna de Bostrichidae (Coleoptera) de la provincia de Córdoba (Andalucía, España). Boletín de la SAE Nº 21: 46-57.
[7] Akşit, T., Çakmak, İ., and Özsemerci, F., (2005) Some New Xylophagous Species on Fig Trees (*Ficus carica* cv. Calymirna L.) in Aydın, Turkey. Tuk. J. Zool. 29, 211-215.
[8] Beyarslan, A. (2005) A faunal study of the subfamily Doryctinae in Turkey (Hymenoptera: Braconidae). Turkish J. of Zoology. 39, 126-143.
[9] Simon, G. (2014) First record of *Bostrichus capucinus* (L.) (Coleoptera: Bostrichidae) in Iraq. Bulletin of the Iraq Natural History Museum. 13, 1–3.
[10] Feci, E., Manucci, M., and Palanti, S. (2013) Diagnostic evaluation of insect attack on existing timber structures: a review of some case studies. Advanced Material Research. 778, 1020-1027.
[11] Nieto, A. and Alexander, N.A. (2010) European Red List of Saproxylic Beetles. Publication Office of European Union. Luxemburg, 45p.
[12] Bahillo de la Puebla, P., López-Colón, J.I. and Baena, M. (2007) Los Bostrichidae Latreille, 1802 de la fauna íbero-balear (Coleoptera). *Heteropterus Revista de Entomologia.* 7, 147–227.
[13] Anonymous (2018) The IUCN Red List of Threatened Species. "*Bostrichus capucinus*" Date: 01.01.2018.
[14] Silva, R.P., Villar, J.P., Naves, P.,Souza, E., and Belokobylskij, S. (2012) Parasitoids of *Monochamus galloprovincialis* (Coleoptera, Cerambycidae), vector of the pine wood nematode, with identification key for the Palaearctic region. Zookeys. 251, 29-48.
[15] Yu, D.S., Achterberg, C., Horstmann, K., (2012) World Ichneumonoidea 2011. Taxonomy, biology, morphology and distribution. http://www.taxapad.com/taxapadmain.php.
[16] Gadallah, N.S., Ghahari, H., Peris-Felipo, F.J. and Fischer, M. (2015) An annotated catalogue of the Iranian Alysiinae (Hymenoptera: Braconidae). *Zootaxa.* 3974 (1), 001–028.
[17] Nilsson, S.G., Heidin, J. and Niklasson, M. (2001) Biodiversity and Its Assessment in Boreal and Nemoral Forests. Scand. J. For. Res. Suppl. 3, 10-26.
[18] Şimşek, Z. and Kondur, Y. (2017) Determination of the Natural Enemies of *Diprion pini* L. (Hymenoptera: Diprionidae) in Çankırı, Turkey. Fresen. Environ. Bull. 26, 6749-6759
[19] Aydoğdu, M., Gökalp, F.D. and Güner, U., (2017) Toxic effects of pyrethroids Lambda-Cyhalothrin and Alpha Cypermethrin on Pest *Archips rosana* (Lepidoptera: Tortricidae) and Its common parasitoid. Fresen. Environ. Bull. 26, 2436-2445.

[20] Tunca, H., Tatlı, Ş., Moran, H.H. and Özkan, C. (2016) Effects of Some Botanical Insecticides on the Egg Parasitoid *Trichogramma pintoi* Voegele, (Hymenoptera: Trichogrammatidae). Fresen. Environ. Bull. 25, 429-443.

Received: **05.09.2017**
Accepted: **06.02.2018**

CORRESPONDING AUTHOR

Inanc Ozgen
Fırat University
Faculty of Engineering
Department of Bioengineering
23119, Elazığ – Turkey

e-mail: inancozgen@gmail.com

© by PSP Volume 27 – No. 5/2018 pages 2834-2843 Fresenius Environmental Bulletin

A MODIFIED RAINFALL SIMULATOR: DESIGN PRINCIPLES, RAINFALL CHARACTERISTICS AND SIMULATION ABILITY TO NATURAL RAINS

Tugrul Yakupoglu[1,*], Nutullah Ozdemir[2], Imanverdi Ekberli[2], Elif Ozturk[3]

[1]Bozok University, Faculty of Agriculture, Department of Soil Science and Plant Nutrition, TR-66900, Yozgat, Turkey
[2]Ondokuz Mayıs University, Faculty of Agriculture, Department of Soil Science and Plant Nutrition, TR-55139, Samsun, Turkey
[2]Ondokuz Mayıs University, Faculty of Agriculture, Department of Soil Science and Plant Nutrition, TR-55139, Samsun, Turkey
[3]Minestry of Food, Agriculture and Livestock, Blacksea Agricultural Research Institute, TR-55100, Samsun, Turkey

ABSTRACT

The performance of rainfall simulators strongly depend on their construction properties and principles of operation. The most important criterion in evaluation of simulator performance is the compatibility of rainfall characteristics between simulated and natural rainfall. This study aims to (i) identify the simulator design principles (ii) determine the rainfall characteristics and (iii) measure the simulated rainfall's representative ability of the natural rainfall in the region using a laboratory drop-former simulator with limited range of motion. As a result of this study, the physical and mechanical properties of the aforementioned rainfall simulator were clearly identified. It has been shown that the intensities of the eight different rainfalls varied between 18.8-189.9 mm h^{-1}, while their kinetic energy varied between 0.208-0.290 MJ ha^{-1} mm^{-1}. The drop median values of the simulated rainfalls were between 2.26-2.38 mm and the falling drop speed varied between 6.063-6.919 m sec^{-1}. A logarithmic relationship (R^2= 0.88) have been determined between the unit kinetic energies and the intensity values of the simulated rainfall. The results suggest that the rainfall simulator can successfully represent the natural rainfall and can be used effectively in soil erosion studies.

KEYWORDS:
Erosivity, kinetic energy, rainfall intensity, rainfall simulator

INTRODUCTION

Rainfall simulators underwent a significant change in parallel with the developing technology and scientific progress since their first use in 1930s on studies involving soil erosion [1]. Through the use of rainfall simulators, different types of data can be acquired with innumerable conveniences and thereby different aspects of soil erosion can be rapidly studied. Especially from the 1980s up to now, splash erosion mechanism was identified by raindrop studies [2-3], the inherent strength of soil against erosion was significantly determined [4] and works on the effects of the physical properties of the rainfall on soil erosion made more sense [5-9].

The erosivity of natural rainfalls is directly related to raindrop size distribution, raindrop fall velocity and intensity [10, 11, 12]. Meyer identified the possible criteria for comparing the simulated rainfalls with the natural rainfalls being i) kinetic energy ii) momentum iii) the kinetic energy per unit of raindrop area iv) momentum per unit of raindrop area and v) the relationship of these parameters with the rainfall intensity [13]. First four of these parameters are calculated using the raindrop size distribution and raindrop fall velocity [14] and therefore a rainfall can be distinguished from another [15-16]. In principle, rainfall simulators can be classified as laboratory simulators and field simulators. According to their method of forming raindrops, they are classified into two groups: spraying model type and drop-former type rainfall simulators [8-17-18-26].

This study was conducted in order to (i) identify the design principles (ii) identify the rainfall characteristics and (iii) measure the ability of the simulated rainfalls to represent the regional natural rainfalls of the rainfall simulator which was modified from Erpul and Çanga [22] for the Soil and Water Conservation Laboratory at the Department of Soil Science and Plant Nutrition in Faculty of Agriculture, Ondokuz Mayis University.

MATERIALS AND METHODS

Design of the Apparatus. The rainfall simulator that is modified from Erpul and Çanga [22] and subject to this study comprises eight types of pieces, which are rainfall heads, water container, basin, water circulation set-up, adjustable inclined plane, splash-boards, erosion pans and ventilation blowers.

The detailed drawing with the original dimensions of the simulator is provided in Figure 1. Four profiles with 50 mm diameter form the frame of the simulator. Rainfall tank is placed on these profiles.

Rainfall basin forms the base of the rainfall simulator. To achieve limited range of motion, four wheels with 100 mm diameter are attached to the bottom of the simulator. To ensure the raindrops fall with a certain angle to the rainfall basin, two ventilation blowers facing each other were placed on the profiles of the simulator. Each of these ventilators blows a wind of 9 m sec^{-1} to the center of the raindrop trajectory. As rainwater, purified water is used in the simulator. This water is delivered to the rainfall unit by a 2900 rpm 0.5 HP circulation pump. Profile view of the rainfall simulator and the dimensions of the simulator frame are shown in Figure 2. According to Figure 2, the distance between the base of the rainfall tank and the base of the rainfall basin [A] is 3080 mm and the distance between the connection point of the rainfall tank to the simulator profile and the holding arm of the motor-shaft system [B] is 260 mm. The distance between the top of the erosion pan placed on the carrier plate at the center of the rainfall basin and the tips of the drop-forming drippers fitted vertically to the rainfall tank, which corresponds to the raindrop fall distance, [C] is 2710 mm.

Rainfall tank. The actual view of the rainfall tank and the scaled profile view are provided in Figure 3. Rainfall tank is a circular unit with a diameter of [A] 1000 mm and a depth of [B] 150 mm. This tank is made of 3 mm-thick sheet metal and revolves on its own axis with a speed of 1 rpm with the help of a motor-shaft system. Revolving motion occurs with the energy (220 V) provided from the regular mains electricity. There is a drainage channel with 135 mm width [C] and 80 mm depth [C] around the rainfall tank which collects and sends the excess water in the rainfall tank back to the water storage unit. Four valves, which keep water load levels in the rainfall tank fixed at different levels, are fitted to the lateral surface of the rainfall tank at a position which will contain the taps inside the drainage channel while the tank makes its circular motion. The distances of water level control valves from the rainfall unit base are 45 [E], 65 [F], 85 [G] and 105 [H] mm, respectively. 96 drop-forming drippers are placed at the base of the rainfall tank. The distance of each dripper to the rainfall tank is calculated using the equations developed by Mutchler and Moldenhauer [27] (see reference 22 for detailed calculating of distance between each dripper and tank center).

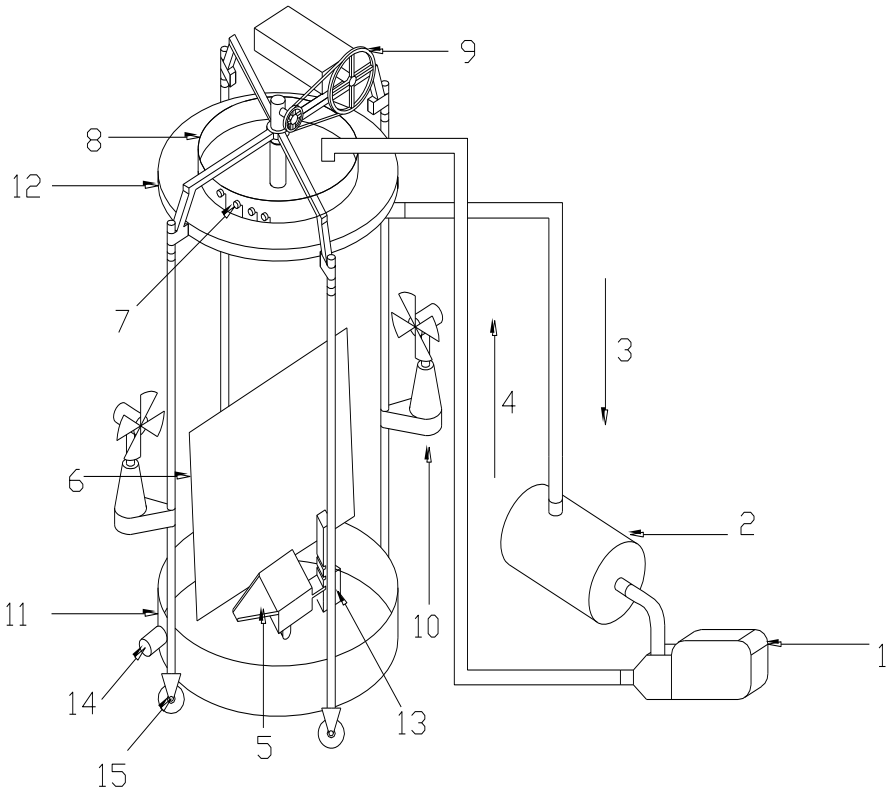


FIGURE 1
General view of rainfall simulator: (1) circulation pomp; (2) water tank with capacity 500 L; (3) water turning pipe, (4) water transport pipe; (5); erosion pan; (6) splash board; (7) water head vanes; (8) rainfall tank; (9) engine-axis system; (10) fan; (11) rain basin; (12) excess water canal; (13) table adjustable slope; (14) outlet; (15) wheel

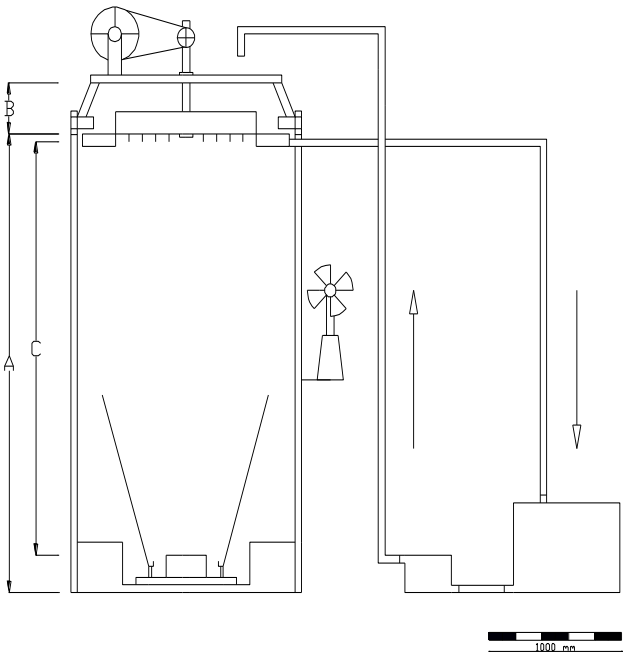


FIGURE 2
Two dimension view of simulator

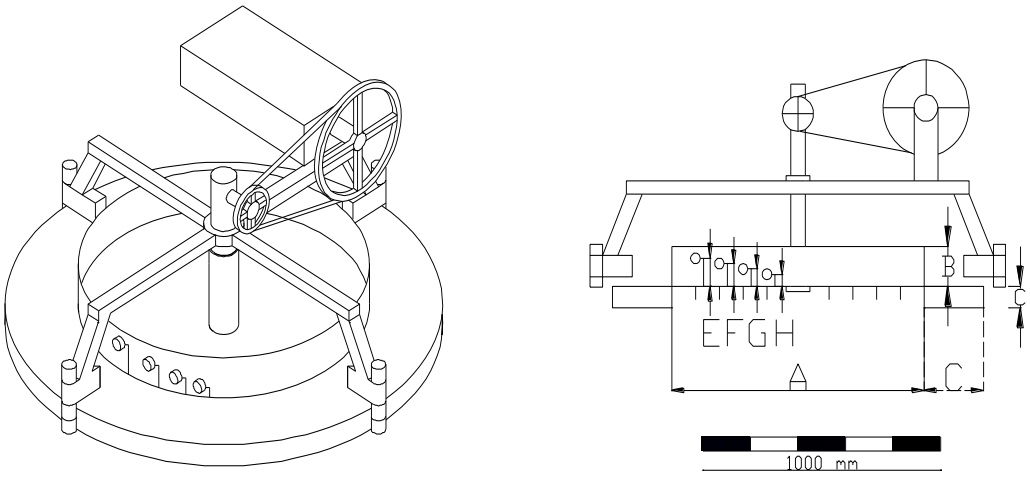


FIGURE 3
General and two dimension views of rainfall tank

Drop-forming drippers. Rain is formed via the drop-forming drippers placed vertically to the base of the rainfall unit. These circular drippers are manufactured by opening two interconnected water flow paths, one being narrower than the other, on the center of a 30 mm-long, hard plastic material. Figure 4 shows the profile view and dimensions of the drop-forming drippers. In this study, two different drippers with tip inner diameters of [A] 0.4 and 0.6 mm were used. According to Figure 4, thick water flow path inner diameter is [B] 2 mm, peak thickness is [C] 3 mm, thick water flow path length is [D] 18 mm, distance between internal and external notches is [E] 6 mm, distance between the external notch and the tip of the drop-former is [F] 6 mm, indentation length of the external notch is [G] 1.5 mm and dripper tip thickness is [H] 2.2 or 2.3 mm depending on the narrow water flow path diameter.

Rainfall basin and its equipment. Dimensions and the cross-section of the water collection trough defined as the rainfall basin is shown in Figure 5. The diameter of the rainfall basin, which is made of 1.5 mm-thick sheet metal, is [A] 1500 mm and its depth is [B] 340 mm. The center of this unit contains the adjustable inclined plane that carries the erosion pans. The incline of the plane can be adjusted to 9, 15, 22 and 30% using the attached latches. The dimension of the erosion pan is 300 x 295 x 150 mm (length-width-depth). This pan has a triangular open top coat, with a side length of 270 mm, side height of 10 mm and a mouth opening of 70 mm, collecting

the surface flow. The base of the pan contains 16 systematically placed drainage holes with a diameter of 1 mm. Two portable splash-boards are placed on both sides of the erosion pan to collect the soil that is moved by the splash. Height of the collecting surface of these splash-boards is [C] 1200 mm and width is 1400 mm. A 35 mm-wide gutter making a 20º angle to the ground can be found at the bottom corner of both splash-boards to collect the splashing soil.

Measuring methods of some rainfall properties. This study investigates some of the properties of eight different rainfalls formed by different combinations of water load and drop-former type. Purified water with a pH of 7.64 and an $EC_{25°C}$ of 8.75 µS cm^{-1}, has been used in the rainfall simulator. When the characteristics of the artificial rainfall formed by the simulator are evaluated, intensity (I_m), Christiansen uniformity coefficient (CUC), the median drop diameter (D_{50}), raindrop fall velocity (V) and unit kinetic energy (E_m) were considered. These parameters chosen as indicators are the rainfall properties that directly affect the soil erosion [28-31]. The intensity measurements were made with a Vantage PRO2 pluviometer and repeated 10 times, with the results represented in mm h^{-1}. The distribution of the rainfall within the rainfall basin was evaluated by using Christiansen uniformity coefficient and Equation 1 is used to calculate this variable [32].

$$CUC = \left(1 - \frac{I_{SD}}{I_{mean}}\right) x\ 100 \quad (1)$$

Where; *CUC*: Christiansen uniformity coefficient (%), I_{mean}: mean intensity (mm h^{-1}), I_{SD}: standard deviation in the intensity measurements.

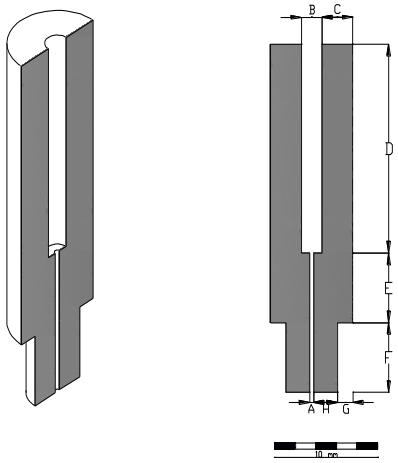


FIGURE 4
Profile and two dimension views of dripper

To obtain drop size measurements, rainfall tank was divided into 8 equal pieces and one of the 12 drop-former per piece was randomly selected to collect 100 drops from each head. This was performed for each different water load and for each of the drop-formers with different tip inner diameters. Drop volume is calculated via drop mass (Equation 2) and equivalent drop diameter was calculated (Equation 3) from here [33]. The temperature of the water delivered to the rainfall tank was measured to be 20.6 ℃ and the intensity of the water as a function of this temperature was taken as 0.99808 g cm^{-3}.

$$m = \rho V_1 \quad (2)$$

Where; *m*: drop mass (mg), ρ: drop intensity, (mg mm^{-3}), V_1: drop volume, (mm^3)

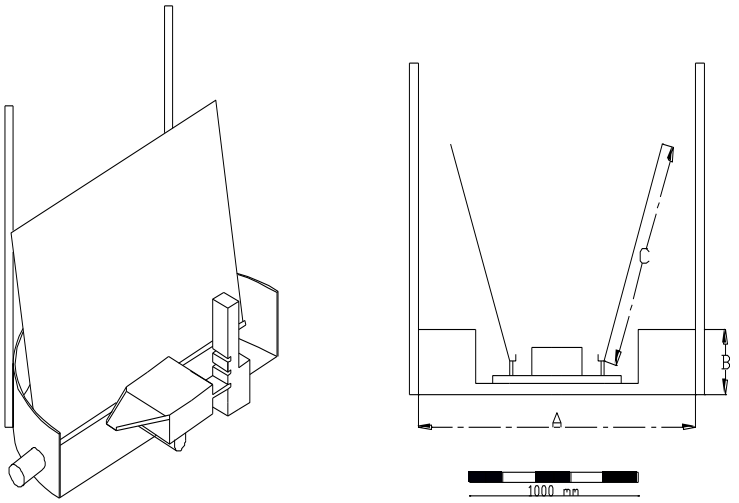


FIGURE 5
Profile and two dimension views of rainfall basin

$$V_1 = \frac{1}{6}\,\pi\, d^3 \quad (3)$$

Where; d: equivalent drop diameter (mm)

Drop fall velocity is calculated using Equation 4, the resolution of the equation was done by Runge-Kutta numerical method [34-35]. Initial drop velocities (velocity the drop has just when it leaves the head) required by this method was calculated using Equation 5 [36] and the friction coefficient was calculated using Equation 6 [37].

$$\frac{dv}{dt} = g - C_n V^2 \quad (4)$$

Where; g: gravitational acceleration (m s^{-2}), C_n: friction coefficient, V: velocity

$$v = \left(\sqrt{2\,g\,h}\right)\mu \quad (5)$$

Where; v: initial drop velocity (m s^{-1}), g: gravitational acceleration (kN m^{-2}), h: water load in the rainfall tank (cm), μ: the constant varying between 0.62-0.97 depending on the shape of the hole that water drops (= 0.85)

$$C_n = 0.4671 d^{-0.9859} \quad (6)$$

Where; d: median drop diameter (D_{50}) (mm)

The calculation of the kinetic energy transferred to soil surface by one unit of each rainfall was performed using Equation 7 [38].

$$E_m = 0.29\left[1 - 0.72e^{(-0.05I_m)}\right] \quad (7)$$

Where; E_m: Unit kinetic energy of the rainfall (MJ ha^{-1} mm^{-1}), I_m: Intensity of the rainfall (mm h^{-1})

Simulator performance. To test the simulator performance, the relationships between KE-I_m and V-D_{50} of each simulated rainfall were compared with the previous studies. Moreover, total kinetic energies of each of the 60 minute-long rainfalls by the simulator (E_T) were calculated using Equation 8 and their erosion-forming power ($R_{simulated}$) were identified by Equation 9. Here, rainfall duration of 60 minutes was chosen arbitrarily. The results obtained after these calculations were compared with the highest monthly $R_{natural}$ data obtained from the natural rainfalls in Samsun region [39].

$$E_T = E_m\, x\, I_{\square} \quad (8)$$

Where; E_T: Total kinetic energy (MJ ha^{-1}), E_m: Unit kinetic energy of the rainfall (MJ ha^{-1} mm^{-1}), I_m: Intensity of the rainfall (mm h^{-1})

$$R_{Simulated} = E_T\, x\, I_{30} \quad (9)$$

Where; $R_{simulated}$: (MJ ha^{-1} mm h^{-1}), I_{30}: Highest rainfall intensity for 30 minutes (mm h^{-1}) (Since the simulated rainfall has uniform intensity, this value is taken directly as I_m)

RESULTS AND DISCUSSION

Table 1 indicates the I_m, CUC, E_m, D_{50} and V values of eight different simulated rainfalls under various combinations of drop-former-water load. The I_m value of rainfall no.1 is 18.8 mm h^{-1}, whereas for rainfall no.8, it is 189.9 mm h^{-1}. The CUC values of the eight simulated rainfalls in terms of intensity varied between 0.73-0.94. When the E_m values of the simulated rainfalls were compared, E_m of rainfall no.1 was the lowest with 0.208 MJ ha^{-1} mm^{-1} whereas the E_m of rainfalls no. 6, 7 and 8 was the highest with 0.290 MJ ha^{-1} mm^{-1}. The D_{50} values of the simulated rainfalls varied between 2.26-2.38 mm while their V values varied between 6.063-6.919 m sec^{-1}.

The correlation between the intensity and D_{50} values of 8 different simulated rainfalls is shown in Figure 6. According to Figure 6a, in rainfalls no. 1, 2, 3 and 4 that are simulated by the drop-former with a tip inner diameter of 0.4 mm, D_{50} and I_m are inversely proportional and there is a polynomial regression (R^2= 0.79) between these two values. In rainfalls simulated by the drop-former with a tip inner diameter of 0.6 mm (rainfalls no. 5, 6, 7, and 8), D_{50} and I_m are inversely proportional while the regression is linear (R^2= 0.99) (Figure 6b).

The correlation between the I_m and V of 8 different simulated rainfalls is shown in Figure 7. While I_m and V were inversely proportional in all rainfalls, a polynomial regression (R^2= 0.99) was observed in low intensity values (rainfalls no. 1, 2, 3, and 4) (Figure 7a), and an exponential regression (R^2= 0.98) was observed in high intensity values (rainfalls no 5, 6, 7, and 8) (Figure 7b).

TABLE 1
Some physical properties of simulated rainfalls

Rain No	Inner diameter of dripper tip (mm)	Water head (mm)	[1]I_m (mm h^{-1})	[2]CUC	[3]E_m (MJ ha^{-1} mm^{-1})	[4]D_{50} (mm)	[5]V (m sn^{-1})
1	0.4	45	18.8	0.84	0.208	2.34	6.743
2		65	26.7	0.73	0.235	2.28	6.236
3		85	35.9	0.87	0.255	2.28	6.174
4		105	51.5	0.86	0.274	2.26	6.063
5	0.6	45	109.5	0.94	0.289	2.38	6.919
6		65	138.9	0.94	0.290	2.33	6.618
7		85	159.6	0.92	0.290	2.30	6.341
8		105	189.9	0.90	0.290	2.28	6.200

[1]I_m: Rainfall intensity; [2]CUC: Christiansen uniformity coefficient; [3]E_m: Rainfall kinetic energy per unit; [4]D_{50}: Mean drop value; [5]V: Drop velocity

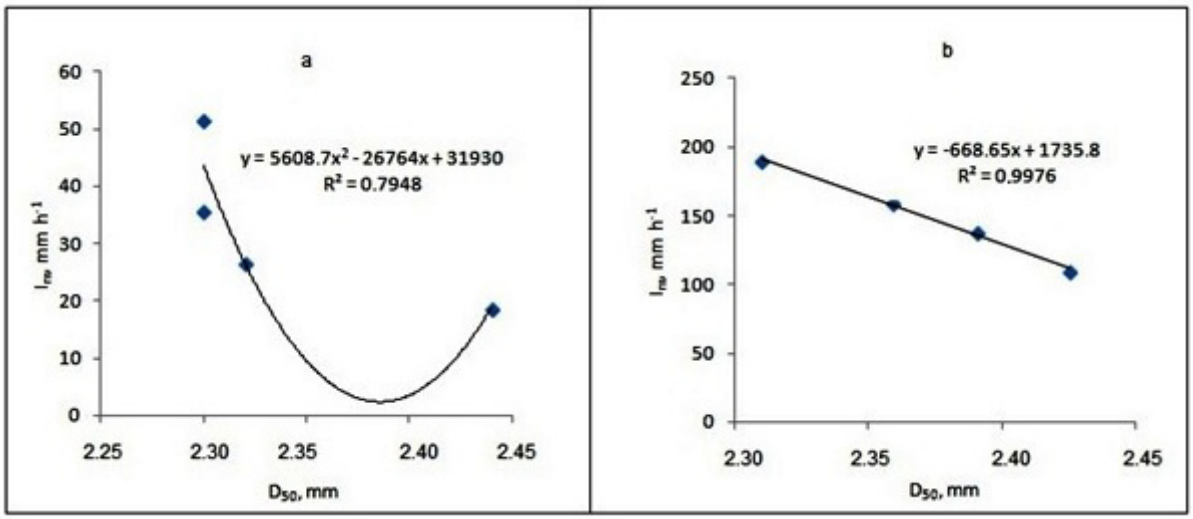


FIGURE 6
Change of D_{50} values depending I_m

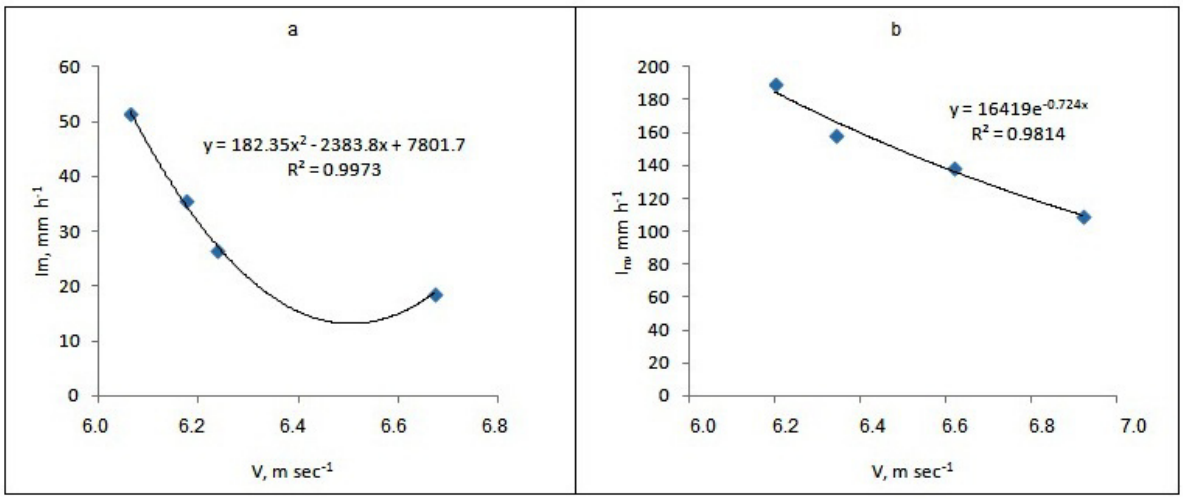


FIGURE 7
Change of V values depending I_m

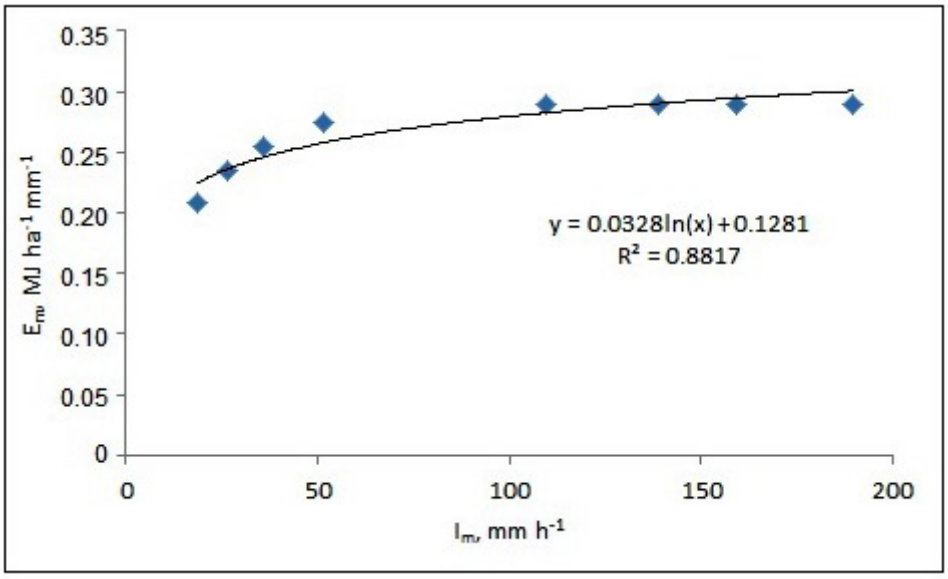


FIGURE 8
Relationship between E_m and I_m of simulated rainfalls

TABLE 2
Erosivity of simulated rainfalls ($R_{simulated}$)

	$R_{simulated}$							
Artificial rains	1	2	3	4	5	6	7	8
MJ ha^{-1} mm h^{-1}	73.5	167.5	328.7	726.7	3465.2	5595.0	7386.9	10458.0

TABLE 3
Comparison of natural and simulated rains in terms of erosivity ($R_{natural}$ data belongs to 1993-2007 years and they were taken from Erpul et al. [39])

*Months	Maximum $R_{natural}$ (MJ ha^{-1} mm h^{-1})	$R_{simulated}$ (MJ ha^{-1} mm h^{-1})	Artificial Rain No	$R_{simulated}$ / $R_{natural}$ (%)
April	426	328.7	3	77
May	659	328.7	3	50
June	473	328.7	3	69
July	97	73.5	1	76
August	275	167.5	2	61
September	222	167.5	2	75
October	371	328.7	3	89
November	881	726.7	4	82
December	42	73.5	1	175

*Measurement results are no present for January, February and March months, since rains of these months were ignored in this study because of their low negligible erosivity

The correlation between the E_m and I_m values of the simulated rainfalls is shown in Figure 8. Direct proportionality with logarithmic regression (R^2= 0.88) was found between these two values and the E_m had asymptotic value in high intensity values.

The erosivity values of the simulated rainfalls when it rained for 60 minutes ($R_{simulated}$) are shown in Table 2. The I_m was directly proportional with $R_{simulated}$, which was 73.5 the lowest and 10458.0 MJ ha^{-1} mm h^{-1} the highest.

The comparison of maximum erosivity values ($R_{natural}$) of the natural rainfalls in Samsun region between years 1993-2007 [39] and the appropriate $R_{simulated}$ values of the simulated rainfalls is shown in Table 3. It could be seen that the $R_{simulated}/R_{natural}$ value was determined higher than 50%, with the highest success rate of 89% obtained in rainfall no.3, which represents the rainfalls in October.

The results obtained in this study showed that the CUC values of the simulated rainfalls no. 1, 2, 3 and 4 (formed by the drop-former with a tip inner diameter of 0.4 mm) were lower than those of the simulated rainfalls formed by the drop-former with a tip inner diameter of 0.6 mm. This could be due to a possible lathing mistake which causes the thin waterpath within the tip inner diameter to be non-uniform.

Thomas and El Swaify obtained simulated rainfalls with a CUC value of 92% in a rather high rainfall intensity of 150 mm h^{-1}[40]. Battany and Grismer obtained a CUC value of 91.9% in a simulated rainfall with an intensity of 60 mm h^{-1} [21], whereas Cerda et al. got a CUC value of 93.3% in a simulated rainfall with 55 mm h^{-1} intensity [41]. In the simulated rainfalls with intensities 150 and 200 mm h^{-1}, Clarke and Walsh obtained CUC values of 88% and 91%, respectively [1]. If the CUC value of a simulated rainfall is higher than or equal to 70%, the rainfall intensity could be regarded as uniform [18]. All of the simulated rainfalls produced by the simulator in this study had such CUC values that they could be regarded as uniform in terms of their intensity, except the rainfall no.2 which had the lowest CUC value (0.73).

Increasing water load in the rainfall tank increased the intensity of the rainfalls produced by both types of drop-formers, however while the first rainfalls had an I_m value lower than 52.5 mm h^{-1}, rainfalls no. 5, 6, 7, and 8 had varying the I_m values between 109.6 and 189.0. This is due to the differences in tip inner diameters of the drop-former, since formation of drops with higher D_{50} values by the drippers with an inner tip diameter of 0.6 mm affects the cumulative drop volume. It was reported that rainfalls with different physical properties can be generated by changing the dripper design [22, 42] and the performance of the drop-former is dictated by the surface tension and inner frictional forces [17].

The reason the drops formed by drop-former heads with the inner tip diameter of 0.4 mm have lower D_{50} values could be because the drops fall before they get larger due to increasing water load and the surface tension at the tip of the drop does not suffice to hold the drop. Therefore, the V value decreases as the drop diameter decreases with the simultaneous increase in water load. On the other hand,

the intensity and the kinetic energy of the simulated rainfall tend to increase since the drop fall frequency increases contrarily to the decrease in the D_{50} and V values with the increasing water load. In rainfalls with high intensity, drop diameter and intensity are reported to be inversely proportioned [14] and numerous correlations between rainfall intensity and drop intensity were identified [43-46].

In studies on simulated rainfalls, it is not practical to simulate the physical properties of each individual natural rainfall in a region and form them. Therefore, many researchers suggest that using the properties of the strongest regional rainfalls as criteria to test the performance of the simulators would provide great ease [47-49]. 60-minute long rainfalls formed by the simulator are similar to natural rainfalls in terms of erosivity. Maximum intensity individual rainfalls which fall especially on April, July, October and November can be simulated by this rainfall simulator. The simulator was weak to simulate December rainfalls, and the similarity of the simulated rainfalls to some of the other months varied between 50-70%. To increase the representative ability of the simulator, changing the rainfall duration or disabling some of the drop-formers in the rainfall tank could be the solution. Thereby, total energy flow of the natural rainfall could be mimicked by the simulator. Another option to change the erosivity would be to produce tips with different inner and outer diameters for the drop-formers in the rainfall tank. However, it should be noted that the D_{50} and V values will change directly.

CONCLUSIONS

When it is considered that the majority of the total splash erosions occur due to high intensity rainfalls with short durations, especially the rainfalls no. 6, 7, 8 and regional rainfalls or total energy flows over longer periods of time can be mimicked by the simulator. Although there are disadvantages such as the frequent congestion of the drop-former heads by dust and formation of one-dimensioned drops in each rainfall by the simulator, it was concluded that the rainfall simulator subject to this study successfully represents the natural rainfalls and can be used efficiently in studies on soil erosion.

ACKNOWLEDGEMENTS

The rainfall simulator had been made to realize another scientific research (Project No. OMU-BAP/Z-501). We thank Rectorate of Ondokuz Mayis University (OMU, Samsun, Turkey) for financial supporting.

REFERENCES

[1] Clarke, M.A. and Walsh, R.P.D. (2007) A portable rainfall simulator for field assessment of splash and slopewash in remote locations. Earth Surface Processes and Landforms. 32, 2052-2069.

[2] Nearing, M.A., Bradford, J.M. and Holtz, R.D. (1986) Measurement of force vs. time relationship for waterdrop impact. Soil Sci. Soc. Am. J. 50, 1532-1536.

[3] Mermut, A.R., Luk, S.H., Römkens, M.J.M. and Poesen, J.W.A. (1997) Soil loss by splash and wash during rainfall from two loess soils. Geoderma. 75, 203-214.

[4] Sharma, P.P., Gupta, S.C. and Rawis, W.J. (1991) Soil detachment caused by rainfall. Soil Sci. Soc. Am. J. 55, 301-307.

[5] Eigel, J.D. and Moore, I.D (1983) A simplified technique for measuring raindrop size and distribution. Trans ASAE. 26, 1079-1084.

[6] Erpul, G. Gabriels, D. and Janssens, D. (2000) Effect of wind on size and energy of small simulated raindrops: a wind tunnel study. Int. Agrophysics. 14, 1-7.

[7] Li, J. and Kawano, H. (1995) Simulating waterdrop movement from noncircular sprinkler nozzles. J. Irrigation and Drainage Engineering. 121, 152-158.

[8] Sobrinho, T.A., Gomez-Macpherson, H. and Gomez, J.A. (2008) A portable integrated rainfall and overland flow simulator. Soil Use and Management. 24, 163-170.

[9] Deviren-Saygin, S. and Erpul, G. (2012) Interactive assessment of the splash erosion and aggregate breakdown mechanism for the soils of different semi-arid land uses. Geophysical Research Abstract. 14: EGU2012, 7865.

[10] Blanquies, J. Scharff, M. and Hallock, B. (2003) The design and construction of a rainfall simulator. International Erosion Control Association (IECA) 34th Annual Conference and Expo., Feb. 24-28, Las Vegas, Nevada, USA.

[11] Dunkerley, D. (2008) Rain event properties in nature and in rainfall simulation experiments: a cooperative review with recommendations for increasingly systematic study and reporting. Hydrological Processes. 22, 4415-4435.

[12] Erpul G. and Çanga, M. (2000) Comparasion of the natural rainfall with laboratory simulated rainfall. Journal of Agricultural Sciences. 6(1), 32-35.

[13] Meyer, L.D. (1965) Symposium on simulation of rainfall for soil erosion research. Trans ASAE. 8(1), 66-67.

[14] Hudson, N. (1995) Soil Conservation. B.T. Batsford Limited, London, UK.

[15] Park, S.W., Mitchell, J.K. and Bubenzer, G.D. (1982) Splash erosion modelling: Physical analyses. Trans ASAE. 25(2), 357-361.

[16] Imeson, A.C. (1977) A simple field-portable rainfall simulator for difficult terrain. Earth Surface Processes. 2, 431-436.
[17] Regmi, T.P. and Thompson, A.L. (2000) Rainfall simulator for laboratory studies. Applied Engineering in Agriculture. 16(6), 641-647.
[18] Parsakhoo, A., Lotfalian, M., Kavian, A., Hoseini, S.A. and Demir, M. (2012) Calibration of a portable single nozzle rainfall simulator for soil erodibility study in hyrcanian forests. African Journal of Agricultural Research. 7(27), 3957-3963.
[19] Grierson, I.T. and Oades, J.M. (1977) A rainfall simulator for field studies of run-off and soil erosion. Agric. Eng. Res. 22, 37-44.
[20] Moore, I.D., Hirschi, M.C. and Barfield, B.J. (1983) Kentucky rainfall simulator. Trans ASAE. 26, 1085-1089.
[21] Battany, M.C. and Grismer, M.E. (2000) Development of a portable field rainfall simulator for use in hillside vineyard runoff and erosion studies. Hydrol. Process. 14(6), 1119-1129.
[22] Erpul, G. and Çanga, M.R. (2001) Design principles of a rainfall simulator and characteristics of simulated rainfalls for soil erosion studies. Journal of Agricultural Sciences. 7(1), 75-83
[23] Paige, G.B. Stone, J.J. Smith, J.R. and Kennedy, J.R. (2003) The Walnut Gulch rainfall simulator: A computer-controlled variable intensity rainfall simulator. Appl. Eng. Agric. 20(1), 25-31.
[24] Hanke, M. Perry, D. and Kung, K.J.S. (2004) A low-intensity, high uniformity water application system. Soil Sci. Soc. Am. J. 68, 1833-1837.
[25] Parsons, A.J. and Lascelles, B. (2000) Rainfall simulation in geomorphology. Earth Surf. Proc. Land. 25(7), 679.
[26] Covert, A. and Jordan, P. (2009) A portable rainfall simulator: techniques for understanding the effects of rainfall on soil erodibility. Watershed Manage. Bull. 13, 5-9.
[27] Mutchler, C.K. and Moldenhauer, W.C. (1963) Applicator for laboratory rainfall simulator. Trans ASAE. 6, 220-222.
[28] Wischmeier, W.H. and Smith, D.D. (1978) Predicting rainfall erosion losses-A guide to conservation planning. USDA Handbook No. 537. Washington, D.C.
[29] Esteves, M. Planchon, O. Lapetite, J.M. Silvera, N. and Cadet, P. (2000) The "EMIRE" large rainfall simulator: design and field testing. Earth Surf. Proc. Land. 25, 681-690.
[30] Gabriels, D. (2006) Assessing the modified Fournier index and the precipitation concentration index for some European countries. In: Boardman, J. and Poesen, J. (eds.) Soil Erosion in Europe. Wiley, Wiltshire, 675-684.
[31] Grismer, M. (2012) Standards vary in studies using rainfall simulators to evaluate erosion. California Agriculture. 66(3), 102-107.
[32] Christiansen, J.E. (1942) Irrigation by Sprinkling. California Agriculture Experiment Station Bulletin 670. University of California, Berkley, California.
[33] Giley, J.E. and Finkner, S.C. (1985) Estimating soil detachment caused by raindrop impact. Trans ASAE. 28, 140-146.
[34] Danilina, N.I., Dubrovskaya, N.S., Kvasa, O.P., Smirnov, G.L. and Feklisov, G.I. (1976) Numeric Methods. 1st edition, in Russian Vissaya Skola, Moscow.
[35] Stillmunkes, R.T. and James, L.G. (1982) Impact energy of water droplets from irrigation sprinklers. Trans ASAE. 25, 130-133.
[36] Kuchling, F.H. (1980) Physics. 15th edition. in German. VEB Fachbuchverlag, Leipzig.
[37] Hills, D.J. and Gu, Y. (1989) Sprinkler volume mean droplet diameter as a function of pressure. Trans ASAE. 32, 471-476.
[38] Brown, L.C. and Foster, G.R. (1987) Storm erosivity using idealized intensity distributions. Trans ASAE. 30(2), 379-386.
[39] Erpul, G., Bayramin, İ., Kaya-Topçu, P. and Deviren-Saygın, S. (2009) Determination of Rainfall Energy and Intensity for Water Erosion Studies Using Long-Term Meteorological Data at National Scale in Turkey. TUBITAK Project Final Report No: CAYDAG107Y155, TUBİTAK, Ankara, Turkey. (In Turkish)
[40] Thomas, M.F. and El Swaify, S.A. (1989) Construction and calibration of a rainfall simulator. Journal of Agricultural Engineering Research. 43, 1-19.
[41] Cerda, A., Ibanez, S. and Calvo, A. (1997) Design and operation of a small and portable rainfall simulator for rugged terrain. Soil Technology, 11, 163-170.
[42] Bryan, R.B. and De Ploey, J. (1983) Comparability of soil erosion measurements with different laboratory rainfall simulators. In: De Ploey, J. (ed.) Rainfall Simulation, Runoff and Soil Erosion. Catena Supplement. 4, 33-56.
[43] Laws, J.O. and Parsons, D.A. (1943) The relations of raindrop size to intensity. Transaction of the American Geophysical Union. 26, 452-460.
[44] Assouline, S., El Idrissi, A. and Persoons, E. (1997) Modelling the physical characteristics of simulated rainfall: a comparison with natural rainfall. Journal of Hydrology. 196, 336-347.
[45] van Dijk, A.I.J.M., Bruijnzeel, L.A. and Rosewell, C.J. (2002) Rainfall intensity-kinetic energy relationship: a critical literature appraisal. Journal of Hydrology. 261, 1-23.
[46] Abd Elbasid, M.A.M., Yasuda, H. Salmi, A. and Ahmad, Z. (2011) Impact of rainfall microstructure on erosivitty and splash soil erosion under simulated rainfall. In: Godone, D. (ed.) Soil Erosion Studies. InTech, Rijeka, Croatia, 167-178.

[47] Peterson, A.E. and Bubenzer, G.D. (1986) Intake rate: sprinkler infiltrometer. In: Klute, A. (ed.) Methods of Soil Analysis. Part I, 2nd ed. Physical and Mineralogical Methods. Vol. 9, ASA, Madison, WI, 845-867.
[48] Blough, R.F., Jarrett, A.R., Hamlett, J.M. and Shaw, M.D. (1990) Runoff and erosion rates from silt, conventional and chisel tillage under simulated rainfall. Trans ASAE. 33, 1557-1562.
[49] Brodie, I. and Rosewell, C. (2007) Theoretical relationships between rainfall intensity and kinetic energy variants associated with stormwater particle washoff. Journal of Hydrology. 340, 40-47.

Received: **05.09.2017**
Accepted: **18.02.2018**

CORRESPONDING AUTHOR

Tugrul Yakupoglu
Bozok University,
Faculty of Agriculture
Department of Soil Science & Plant Nutrition
66900, Yozgat – Turkey

e-mail: tugrul.yakupoglu@bozok.edu.tr

© by PSP Volume 27 – No. 5/2018 pages 2844-2852 Fresenius Environmental Bulletin

GEOGRAPHICAL DISTRIBUTION, CHEMICAL SPECIATION AND RISK ASSESSMENT OF HEAVY METALS IN TING RIVER: THE INFLUENCE OF HEAP BIOLEACHING PLANT ON THE NEARBY RIVER

Jiankang Wen*, Mingjiang Zhang, Xingyu Liu, Xinglan Cui, Xiao Yan, Biao Wu, Bowei Chen

National Engineering Laboratory of Biohydrometallurgy, General Research Institute for Nonferrous Metals, Beijing 100088, China

ABSTRACT

The Zijin heap bioleaching plant was operated at the end of 2005. A potential risk of environmental pollution by heavy metals from heap bioleaching plant arises due to the proximity to the Ting River. In this study, a sequential extraction procedure, a geo-accumulation index and a risk assessment code were applied to separate heavy metals from sludge, assess the extent of heavy metal pollution, and evaluate potential ecological risks, respectively. Results showed that the heap bioleaching plant had influence on the distribution of S, Pb and Cu and no significant influence on the distribution of As, Fe and Cr. Most of the water samples reached the third class standard of the People's Republic of China for surface water. Most of the sludge samples was moderately polluted or moderately to strongly polluted by Cr, and unpolluted or unpolluted to moderately polluted by Cu and Pb. However, all the sludge samples were extremely polluted by Fe. Fe, Cu, Cr and part of Pb were mainly present as the relatively stable chemical speciation. Cr, Cu and Pb had no ecological risk in the upstream and high risks for nearby and downstream sites. The order of potential ecological risks was Cr > Cu > Pb.

KEYWORDS:
Heap bioleaching, heavy metals pollution, geo-accumulation index, risk assessment

INTRODUCTION

For over half a century, bioleaching has been employed to economically extract metal from certain sulfide minerals [1].This process has many advantages; it is simple, environmentally friendly and energy efficient, compared with traditional methods [2, 3]. Furthermore, bioleaching is especially suitable for low grade ore and could be broadly developed as mineral resources become increasingly scarce. In China, the first commercial heap bioleaching plant, with a capacity of 10,000 t.Cu/a, began operation at the Zijin Copper Mine at the end of 2005 [4].

In recent years, extensive efforts have been made to the study of bioleaching efficiency and mine pollution [5-8]. However, a potential risk of environmental pollution by heavy metals from heap bioleaching plant has been rarely reported. As heavy metals are non-biodegradable and accumulative in nature, elevated emissions and deposition can further enrich the metal contents in the environments, cause the surface environment pollution [9] and do harm to the human health [10].

The ZiJin Copper Mine is located in Fujian province in the southeast of China, which has richer rainfall and higher temperature than the rest of the country. Due to the particular geographic location of the Zijin Copper Mine, heavy metals could be more easily to spread from the bioleaching heap to the nearby river with rainwater. Up to now, few studies have been devoted to evaluate the pollution extent and potential ecological risk caused by heap bioleaching plant.

In river, sediments can adsorb heavy metals from water and thus lessen water pollution caused by heavy metals. Total content of heavy metals in the sludge is an indicator that provides information on the status of heavy metal accumulation (contamination). However, total content of heavy metals does not provide enough information to identify ecological risk or perform a bioavailability assessment [11]. This is because the dissolution rate of heavy metals from the sediments is different at various environmental conditions, such as pH and electric potential (Eh). Furthermore, heavy metals exist in different chemical fractions within sediments, and these different fractions have different levels of mobility, bioavailability, and potential toxicity. As a result, ecological risk and bioavailability are not merely dependent on their total contents but also on the chemical forms of heavy metals within an aquatic environment [12].

To identify pollution problems, the anthropogenic contributions should be distinguished from the natural sources. Geochemical approaches, such as the geo-accumulation index (Igeo) [13, 14] is often used to distinguish anthropogenic contributions from the natural sources. Meanwhile, the ecological risk assessment method numerous sediment quality

guidelines (SQGs), TEL (threshold effects level) and PEL (probable effects level), which were proved to be effective sediment quality guidelines are very popular methods in evaluating the ecological risk posed by heavy metals in sediments [15, 16].

In this study, the main objectives were (1) to determine pH, Eh and the total content of S, Pb, As, Cr, Cu, Fe; (2) to explain the spatial distribution and estimate the amount of different chemical speciation of heavy metals in sludge samples; (3) to explore the degree of heavy metals contamination and possible sources compared to background pollution using the geo-accumulation index (Igeo) method; (4) to assess the potential ecological risks of these heavy metals to the environment using numerous sediment quality guidelines (SQGs) method.

MATERIALS AND METHODS

Ethics statement. Permission to collect samples in the Ting River was obtained from Zijin Mining Group Co., Ltd. The field studies did not involve endangered or protected species.

Sampling sites information. Ting River near Zijin Mining heap bioleaching plant (116°21′48.5″E; 25°12′13.2″N) located in Fujian province, belongs to subtropical maritime monsoon climate, the average temperature is 18.7~21.0 degrees, the average rainfall is 1031~1369 mm.

Sample preparation and classification. 19 sludge samples (S1-S19) and 11 water samples (W1-W11) were collected using sterile plastic bottles in October of 2015 year. All the samples were stored at 4°C before determination. The spatial distribution of the sampling sites was shown in Fig. 1.

To research the effect of heap bioleaching plant on the nearby river, samples were divided into 3 groups according to their spatial distribution, and the details were shown in Table 1.

Physicochemical analysis of the samples. The pH and ORP of water samples were determined using a pH and ORP electrode. The dissolved ions of water samples were analyzed using inductively coupled plasma atomic emission spectroscopy (ICP-OES) after the samples were filtered with super membrane filters (0.2 μm pore size, Sigma-Aldrich, MO, USA) [17].

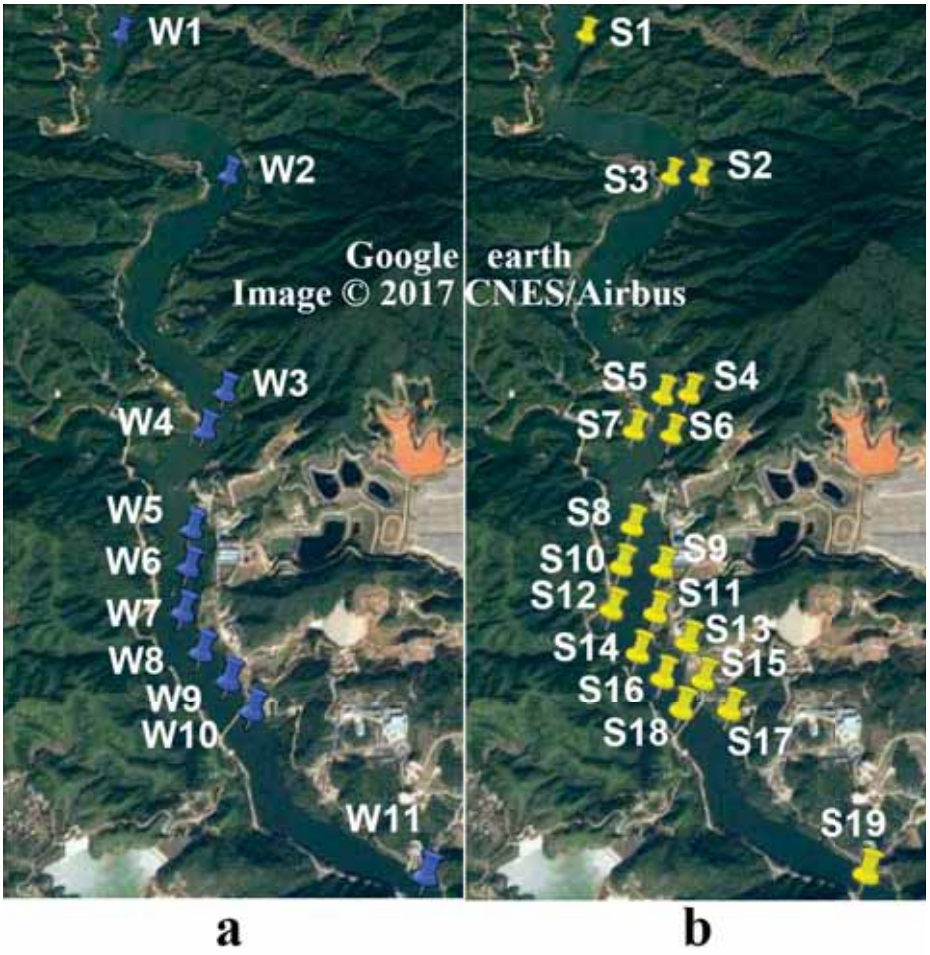


FIGURE 1
Sample collecting sites. Water samples collecting sites (a), Sludge samples collecting sites (b).

TABLE 1
Sample grouping information

Groups	Sludge samples	Water samples
Upstream	S1, S2, S3, S4, S5, S6, S7	W1, W2, W3, W4
Nearby	S8, S9, S10, S11, S12, S13, S14, S15, S16	W5, W6, W7, W8, W9
Downstream	S17, S18, S19	W10, W11

To analyze the heavy metals contents of the sludge samples, 0.5 g air-dried sludge samples were weighed, 15 mL nitric acid, 5 mL hydrochloric acid and 2 mL hydrochloric acid were added successively, heated until the liquid was evaporated completely and white smoke fumed, 5 mL deionized water was added and heated to boiling, 5 mL hydrochloric acid was added and heated to boiling, then cooled and deionized water of 10 mL was added. Water samples were filtered before analysis. All samples were analyzed using ICP [18].

To estimate the amount of different chemical speciation of heavy metals in sludge samples, the sequential extraction procedure, consisting of a series of chemical extractions, was carried out using the following steps [19-21]:

Collection of Exchangeable Fraction. 1.000 g of dry sludge sample was weighed and transferred to a 50 mL capped centrifuge bottle. 15 mL of 1 M $MgCl_2$ (pH = 7.0) was added, and the sample was mechanically shaken for 2 h. Then, it was centrifuged for 15 min at 8000 rpm, and the exchangeable fraction was collected from the supernatant.

Collection of Carbonate and Sulfide Bound Fraction. 15 mL of 1 M NaAc (pH = 5.0) was added to the residue, and it was mechanically shaken for 2 h. Then, it was centrifuged for 15 min at 8000 rpm, and the carbonate and sulfide bound fraction was collected from the supernatant.

Collection of Fe and Mn Oxide Bound Fraction. 20 mL of 0.04 M $NH_2OH{\cdot}HCl$ was added to the residue, leached for 5 h at 96 °C and shaken occasionally. Then, another 10 mL of 0.04 M $NH_2OH{\cdot}HCl$ was added, the solution was centrifuged for 15 min at 8000 rpm after cooling, and then the Fe and Mn oxide bound fraction was collected from the supernatant.

Collection of Organic Matter Bound Fraction. 3 mL (0.02 M) of HNO_3 and 10 mL of H_2O_2 (30%) was added to the residue, the pH was adjusted to 2.0 with HNO_3, and the solution was heated for 2 h at 85 °C. Then, another 3 mL of H_2O_2 was added (adjusted to pH = 5.0 with HNO_3), and the residue was maintained at 85 °C for 3 h. 5 mL of NH_4Ac (3.2 M) was added after cooling, and the residue was diluted to 20 mL with deionized water and shaken for 1 h. After that, it was centrifuged for 15 min at 8000 rpm, and the organic matter bound fraction was collected from the supernatant.

Collection of Residual Fraction. 5 mL of HF and 10 mL of $HClO_4$ were added to the residue, which was heated until the liquid was completely evaporated, and the above steps were repeated three times. Then, 1 mL of $HClO_4$ was added, and the solution was heated until the liquid was completely evaporated and white smoke fumed, following which 0.5 mL of concentrated HCl was added, and deionized water was used to adjust the solution to 25 mL.

After the sequential extraction, all the samples were filtered with super membrane filters (0.2 μm pore size, Sigma-Aldrich, MO, USA) and analyzed using ICP-OES. The river water samples were analyzed using ICP-OES directly after filtration with super membrane filters (0.2 μm pore size, Sigma-Aldrich) [22].

Statistical analysis. The pH, the dissolved copper and the dissolved ferric ion were analyzed with separately one-way ANOVA (analyses of variance). All these statistical analysis were performed using SPSS 19.0 for Windows [23]. The distribution of metal ion and microbes were analyzed by surfer 8.

Geo-accumulation index analysis. The geo-accumulation index (*I*geo) was used to assess the extent of heavy metal pollution in sediments. This index was originally introduced by Müller as follows [13, 24]:

$$I_{geo} = \log_2\left(\frac{C_n}{1.5 \times B_n}\right) \quad (1)$$

Where C_n is the measured metal concentration of n, and B_n is the geochemical background concentration of metal n. In this study, the background value of soils in Fujian Province was used as the Bn (with Cr, Cu, Fe and Pb concentrations equaling 14 $mg{\cdot}kg^{-1}$, 22.8 $mg{\cdot}kg^{-1}$, 4.24 $mg{\cdot}kg^{-1}$, 41.3$mg{\cdot}kg^{-1}$, respectively) [25]. A value of 1.5 was used as the background matrix-correction factor to account for the lithogeny effect.

Potential eco-toxicity risk assessment. The probable effect level (PEL) and the threshold effect level (TEL) were applied to assess the ecological risks from heavy metals. The PEL represents the concentration above which adverse effects are expected to occur frequently, and the TEL represents the concentrations above which the toxic effects of long-term exposure to these contaminants may be expected [15]. The toxic unit (TU), which is defined as the ratio of the determined content to the probable

effect level (PEL), was used to assess the ecological toxicity:

$$TU=C_n/PEL \quad (2)$$

Where TU is the toxic unit, Cn is the measured metal concentration of n, and PEL is the probable effect level.

Pedersen et al. (1998) proposed that the potential acute toxicity of the contaminants in a sample can be estimated as the sum of the toxic units (ΣTUs) [26].

RESULTS AND DISCUSSION

Physiochemical properties differences and spatial distribution of heavy metals in the river. Spatial distribution patterns and physiochemical properties of heavy metals in the river were shown in Fig. 2 and in Fig. 3. The pH and Eh of water samples were in the range of 6.43-7.54 and 313-324 mV, respectively. The pH and Eh of the heap bioleaching plant nearby was slightly higher ($p>0.05$) and obviously lower ($p<0.05$), respectively, than the upstream and downstream. This was opposite to the results of 2009 [18] and consistent with the data of Longjiang River dosing sites [19]. This may be related to the use of a large amount of soda lime for remediation in 2012 pollution incidents.

Previous reports showed that S, Cu, Fe, Pb, As and Cr are the main elements of Zijin copper mine [27]. Thus, these six elements were determined to verify heap bioleaching plant pollution. Soluble S concentration significantly increased in the water samples nearby heap bioleaching plant, and S content in the sludge samples also increased, comparing the downstream with the upstream. The spatial distribution of Pb in water was not significant; Cu could hardly be detected in water; however, the Pb and Cu content in downstream sludge notably increased compared with upstream sludge ($p<0.05$). The distribution of soluble S, Pb and Cu illustrated that some S, Pb and Cu migrated into the river from the heap bioleaching plant, and Pb and Cu were precipitated into the sludge due to high pH of heap bioleaching plant nearby water. The spatial distribution changes of As in water and the spatial distribution changes of Fe, Cr in sludge were not notable ($p>0.05$) along the river. Furthermore, As in sludge and Fe, Cr in water could hardly be detected, which showed that heap bioleaching plant had no significant influence on the distribution of As, Fe and Cr.

Most of the water samples reached the third class standard of the People's Republic of China for surface water (GB3838-2002) and individual water sample was above the fifth class standard of the People's Republic of China for surface water (GB3838-2002) because of As [28].

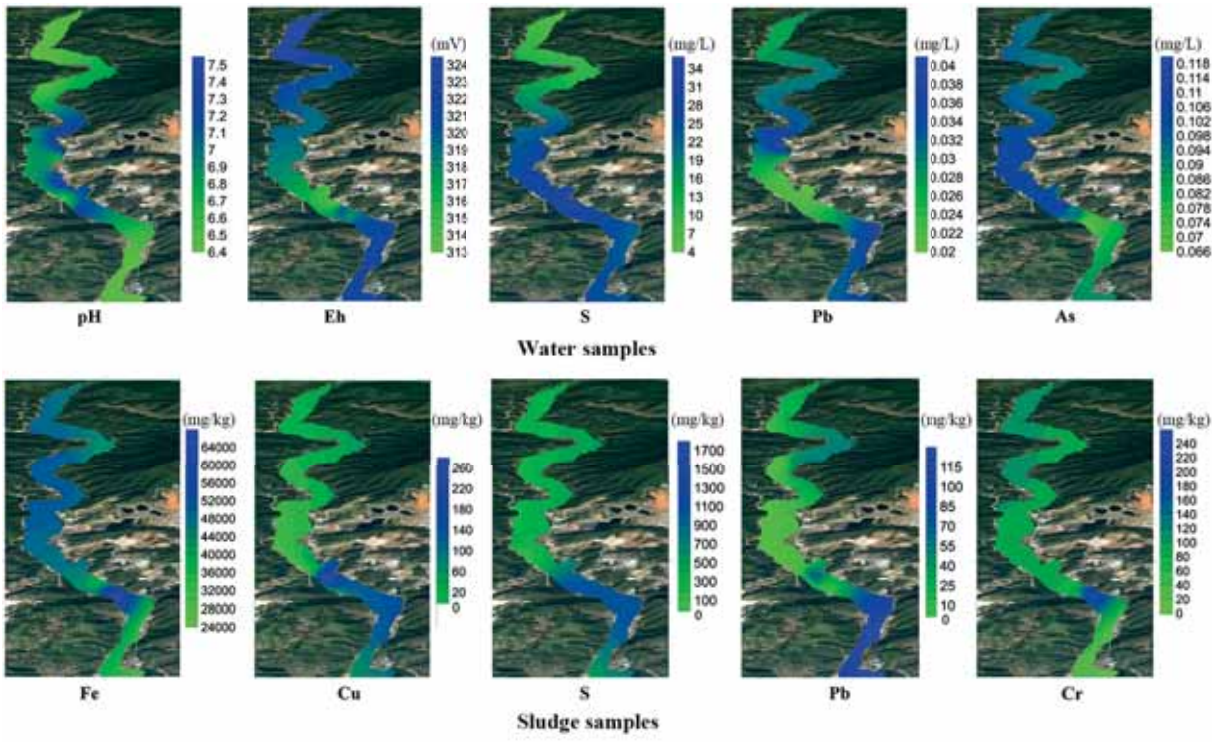


FIGURE 2
Physiochemical properties difference and spatial distribution of heavy metals in the river.

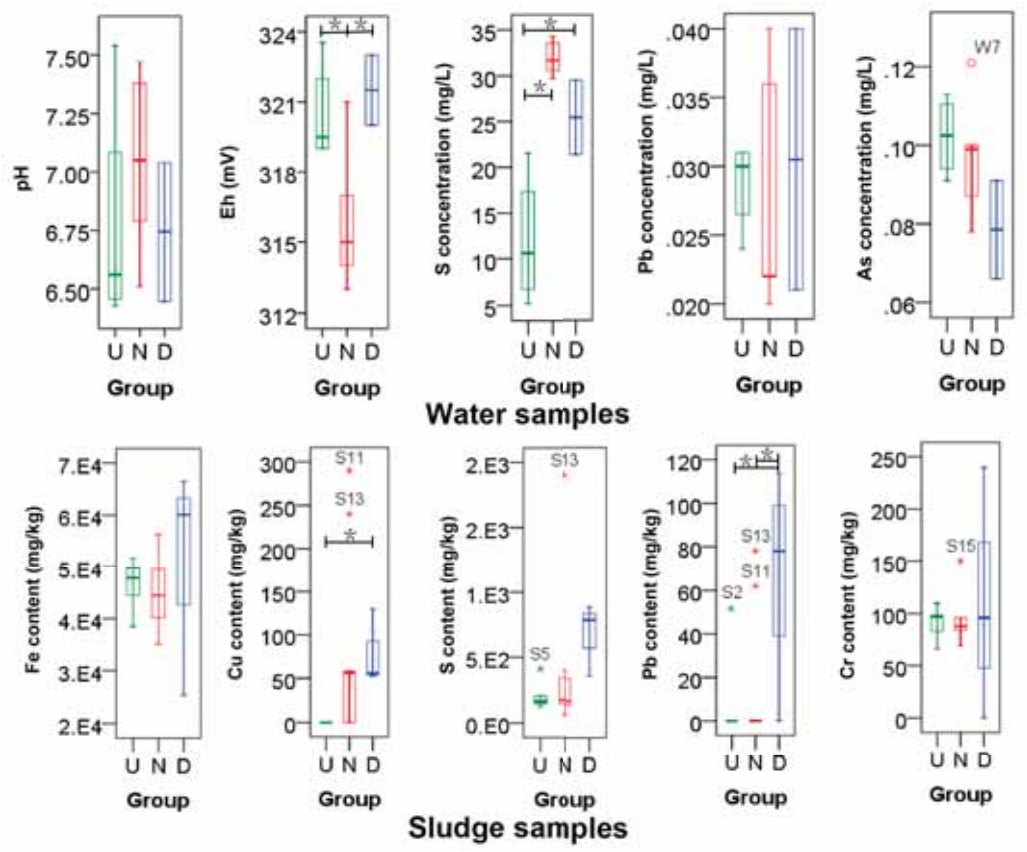


FIGURE 3
The compare of Samples' physiochemical properties in water and sludge samples. Upstream (U), nearby of the heap bioleaching plant (N), downstream (D)

Geo-accumulation index analysis and pollution assessment. The geo-accumulation index was developed by Muller based on his study on heavy metals in fluvial stream sediments [24]. It has been widely used because it takes into account the effects of the natural elements and human activities on pollution [14]. The geo-accumulation indexes of Cr, Cu, Fe and Pb were calculated in this study (Fig. 4 and Table 2). Fe had the largest geo-accumulation index, Cr came second, and the geo-accumulation indexes of Fe and Cr had no notable changes in all the sludge samples ($p>0.05$). These results indicated that the heap bioleaching plant had no obvious effect on the Fe and Cr accumulation in sludge. The geo-accumulation index differences of Cu between upstream, the heap bioleaching plant nearby and downstream were significant ($p<0.05$). The geo-accumulation indexes of Cu in upstream samples were less than 0, and it in the heap bioleaching plant nearby and downstream could reached 2.84. Most of the geo-accumulation indexes of Pb were less than 0, only a few of samples from the heap bioleaching plant nearby and downstream were more than 0 and less than 1. These results implied that the heap bioleaching plant increased the Cu and Pb content in the sludge; however, the effect on Pb was subtle.

The geo-accumulation indexes were classified into seven classes as follows: (1) unpolluted (Igeo≤0), (2) unpolluted to moderately polluted (0<Igeo≤1), (3) moderately polluted (1< Igeo≤2), (4) moderately to strongly polluted (2< Igeo≤3), (5) strongly polluted (3< Igeo≤4), (6) strongly to extremely polluted (4< Igeo≤5), and (7) extremely polluted (Igeo>5) [26]. 94.8% of Cr's geo-accumulation index ranging in 1-3 represented most of the samples was moderately polluted or moderately to strongly polluted by Cr. 84.2% of Cu and 100% of Pb's geo-accumulation indexes were below 1, representing that most of the samples were unpolluted or unpolluted to moderately polluted by Cu and Pb. 100% of Fe's geo-accumulation indexes were above 5, suggesting that all the samples were extremely polluted by Fe.

Chemical speciation of heavy metals. Fig. 5 showed that the total contents of different heavy metals in sediments and the contents of different chemical speciation depicted in different colors. Fe mainly occurred in the residue, which accounted for 98.9%±0.02%. Cu and Cr were also present as the relatively stable chemical speciation. Residue fraction, organic matter bound fraction, Fe and Mn oxide bound fraction of Cu accounted for 84.03%±0.04%, 10.48%±0.07%, 1.72%±0.02% respectively. By contrast, Cr was present as residue fraction, organic

matter bound fraction, Fe and Mn oxide bound fraction with 81.62%±4.99%, 5.63%±1.37%, 3.49%±0.85% respectively. Pb mainly was present as relatively stable residue fraction, organic matter bound fraction, accounting for 67.01%±1.45%, 7.20%±0.87%, respectively. Furthermore, Pb also occurred in the relatively unstable chemical speciation, carbonate and sulfide bound fraction, exchangeable fraction, accounting for 20.58%±0.37%, 4.19%±0.07% respectively. The relatively stable of Fe, Cu and Cr and some unstable of Pb might be the reason why Fe, Cu and Cr could hardly be detected and Pb could be detected in water [12].

The metals in the carbonate and sulfide bound fraction, exchangeable fraction are weakly bound which could equilibrate with the aqueous phase and become more rapidly bioavailable [11, 29]. When the sum of the carbonate and sulfide bound fraction percentage, exchangeable fraction percentage is less than 1%, there is no risk (NR), low risk (LR) for a range of 1–10%, medium risk (MR) for a range of 11–30%, high risk (HR) for 31–50% and very high risk (VHR) for 51–100% [12]. The sum of the carbonate and sulfide bound fraction percentage, exchangeable fraction percentage of Fe, Cu, Cr and Pb were 0.83%, 3.71%, 7.16% and 24.77%, respectively. These results indicated that Fe might have no risk even with high content; Cu and Cr had low risk; Pb had medium risk.

Ecological risk assessment of heavy metals. Concentrations of Cr, Cu and Pb were evaluated in a screening-level ecological risk assessment by comparing to PELs (Fig. 6). A toxic unit greater than 1 represents an adverse effect that is prone to occur [30]. The toxic units of Cr, Cu and Pb less than 1 in the upstream sites represented these three heavy metals had no ecological risk in the upstream. At some of the heap bioleaching plant nearby and downstream sites, some of the toxic units were more than 1, the biggest of which was 2.9. These results indicated some of the heap bioleaching plant nearby and downstream sites had high ecological risk.

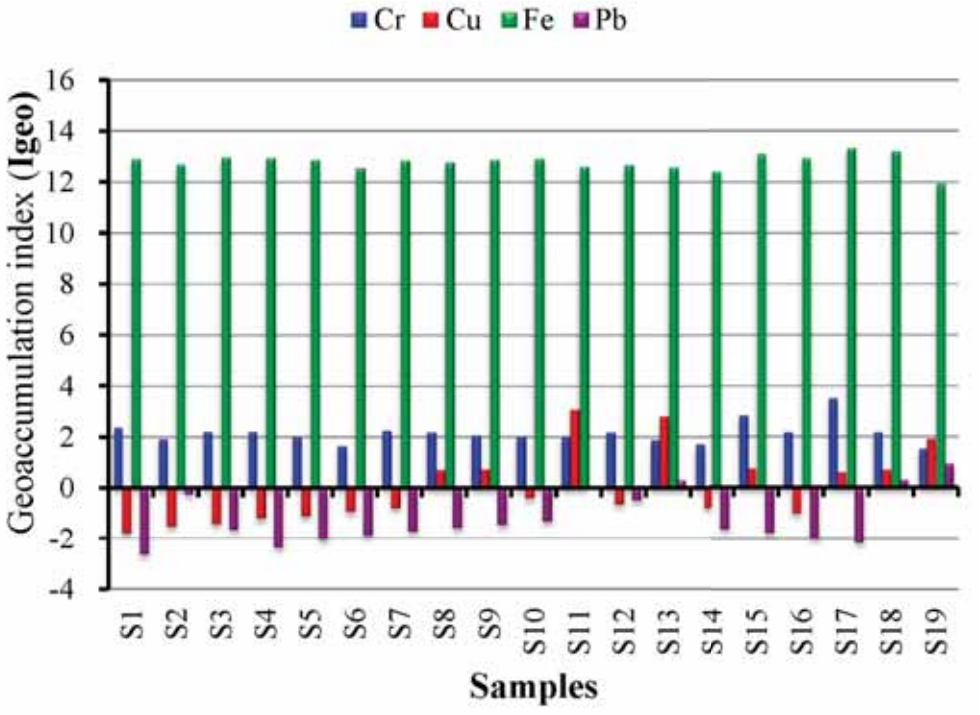


FIGURE 4
Geo-accumulation index (Igeo) of heavy metals in sludge samples

TABLE 2
Statistics of samples geo-accumulation index

Igeo	Class	Pollution Status	Cr	Cu	Fe	Pb
			%	%	%	%
<0	1	Unpolluted	0.0	57.9	0.0	78.9
0-1	2	unpolluted to moderately polluted	0.0	26.3	0.0	21.1
1-2	3	moderately polluted	31.6	5.3	0.0	0.0
2-3	4	moderately to strongly polluted	63.2	5.3	0.0	0.0
3-4	5	strongly polluted	5.3	5.3	0.0	0.0
4-5	6	strongly to extremely polluted	0.0	0.0	0.0	0.0
>5	7	extremely polluted	0.0	0.0	100.0	0.0

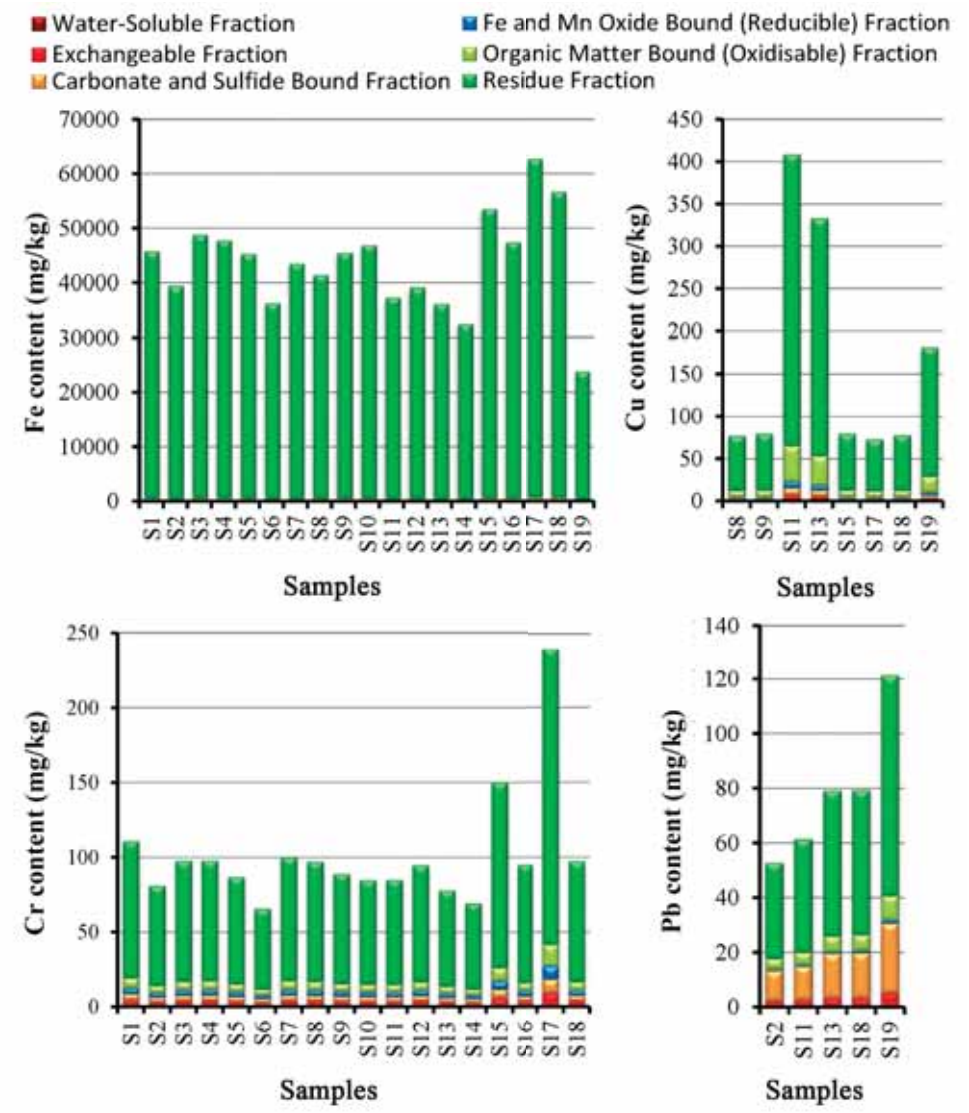


FIGURE 5
The chemical speciation of heavy metals in sludge

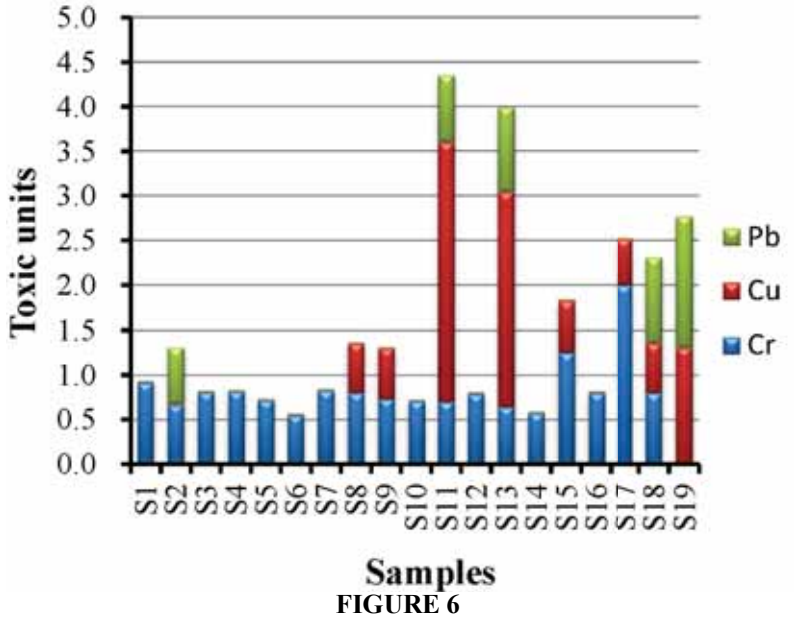


FIGURE 6
Toxic units of heavy metals in sludge sample

The sum of the toxic units more than 6 represent the potential acute toxicity of the contaminants in this sample [26], all the sum of the toxic units less 6 in this study indicated no potential acute toxicity. For these three examined heavy metals Cr, Cu and Pb, the mean value of toxic unit in all the samples were 1.51, 0.95 and 0.49, therefore, the order of potential ecological risk generally followed the pattern Cr > Cu > Pb.

CONCLUSIONS

The heap bioleaching plant had influence on the distribution of S, Pb and Cu and no significant influence on the distribution of As, Fe and Cr. Most of the water samples reached the third class standard of the People's Republic of China for surface water and individual water sample was above the fifth class standard of the People's Republic of China for surface water (GB3838-2002) because of As. Most of the sludge samples was moderately polluted or moderately to strongly polluted by Cr, and unpolluted or unpolluted to moderately polluted by Cu and Pb. However, all the sludge samples were extremely polluted by Fe. Fe, Cu, Cr and part of Pb were mainly present as the relatively stable chemical speciation. Cr, Cu and Pb had no ecological risk in the upstream and high risks for nearby and downstream sites. The order of potential ecological risks was Cr > Cu > Pb.

ACKNOWLEDGEMENTS

This work was supported by the National Natural Science Foundation of China under grant numbers U1402234, 41573074, 51574036; the nation high-level youth talents special support plan; the Guangxi scientific research and technology development plan under grants GuikeAB16380287 and GuikeAB17129025; the public welfare fund of the Ministry of Environmental Protection of People's Republic of China under grant number 201509049; Program of International S & T Cooperation 2016YFE0130700; and the fund of General Research Institute for Nonferrous metals under grant numbers 53321 and 53348.

Conflict of interest. The authors declare no conflict of interest.

REFERENCES

[1] Brierley, C., Brierley, J. (2013) Progress in bioleaching: part B: applications of microbial processes by the minerals industries. Applied Microbiology and Biotechnology. 97(17), 7543-7552.

[2] Pradhan, N., Nathsarma, K.C., Rao, K.S., Sukla, L.B., Mishra, B.K. (2008) Heap bioleaching of chalcopyrite: A review. Miner Eng. 21(5), 355-365.

[3] Zheng, H., Zhang, C., Wu, Y., Shi, P., Wang, Z., Wang, X., Li, B., Liu, J., Xie, X. (2015) Bioleaching of arsenic-containing gold ore influenced by cysteine. Fresen. Environ. Bull. 24, 379-385.

[4] Ruan, R., Wen, J., Chen, J. (2006) Bacterial Heap-Leaching: Practice in Zijinshan Copper Mine. Hydrometallurgy. 83, 77-82.

[5] Halinen, A.-K., Beecroft, N.J., Määttä, K., Nurmi, P., Laukkanen, K., Kaksonen, A.H., Riekkola-Vanhanen, M., Puhakka, J.A. (2012) Microbial community dynamics during a demonstration-scale bioheap leaching operation. Hydrometallurgy. 125–126, 34-41.

[6] Watling, H.R., Collinson, D.M., Li, J., Mutch, L.A., Perrot, F.A., Rea, S.M., Reith, F., Watkin, E.L.J. (2014) Bioleaching of a low-grade copper ore, linking leach chemistry and microbiology. Minerals Engineering. 56, 35-44.

[7] Liu, R., Liu, J., Zhang, Z., Borthwick, A., Zhang, K. (2015) Accidental Water Pollution Risk Analysis of Mine Tailings Ponds in Guanting Reservoir Watershed, Zhangjiakou City, China. International journal of environmental research and public health. 12(12), 15269-84.

[8] Koumantakis, E., Kalliopi, A., Dimitrios, K., Gidarakos, E. (2009) Asbestos pollution in an inactive mine: determination of asbestos fibers in the deposit tailings and water. Journal of hazardous materials. 167(1-3), 1080-8.

[9] Wong, C.S.C., Li, X., Thorton, I. (2006) Urban environmental geochemistry of trace metals. Environmental pollution. 142(1), 1-16.

[10] Kabir, M.I., Lee, H., Kim, G., Jun, T. (2011) Correlation assessment and monitoring of the potential pollutants in the surface sediments of Pyeongchang River, Korea. International Journal of Sediment Research. 26, 152-162.

[11] Sundaray, S.K., Nayak, B.B., Lin, S., Bhatta, D. (2011) Geochemical speciation and risk assessment of heavy metals in the river estuarine sediments--a case study: Mahanadi basin, India. Journal of hazardous materials. 186(2-3), 1837-46.

[12] Jain, C.K. (2004) Metal fractionation study on bed sediments of River Yamuna, India. Water research. 38(3), 569-78.

[13] Zhang, L., Liao, Q., Shao, S., Zhang, N., Shen, Q., Liu, C. (2015) Heavy Metal Pollution, Fractionation, and Potential Ecological Risks in Sediments from Lake Chaohu (Eastern China) and the Surrounding Rivers. International journal of environmental research and public health. 12(11), 14115-31.

[14] Song, J., Yang, X., Zhang, J., Long, Y., Zhang, Y., Zhang, T. (2015) Assessing the Variability of Heavy Metal Concentrations in Liquid-Solid Two-Phase and Related Environmental Risks in the Weihe River of Shaanxi Province, China. International journal of environmental research and public health. 12(7), 8243-62.
[15] MacDonald, D.D., Ingersoll, C.G., Berger, T.A. (2000) Development and evaluation of consensus-based sediment quality guidelines for freshwater ecosystems. Arch Environ Contam Toxicol. 39(1), 20-31.
[16] Lu, Q., Bai, J., Gao, Z., Zhao, Q., Wang, J. (2016) Spatial and Seasonal Distribution and Risk Assessments for Metals in a *Tamarix Chinensis* Wetland, China. Wetlands. 36(1), 125-136.
[17] Zhang, M., Liu, X., Li, Y., Wang, G., Wang, Z., Wen, J. (2017) Microbial community and metabolic pathway succession driven by changed nutrient inputs in tailings: effects of different nutrients on tailing remediation. Scientific reports. 7(1), 474.
[18] Liu, X., Chen, B., Chen, J., Zou, L., Zhang, M., Wen, J., Liu, W. (2016) Biogeographical distribution of acidophiles and their effects around the Zijinshan heap bioleaching plant. Chemistry and Ecology. 32(5), 419-431.
[19] Zhang, M., Huang, F., Wang, G., Liu, X., Wen, J., Zhang, X., Huang, Y., Xia, Y. (2017) Geographic distribution of cadmium and its interaction with the microbial community in the Longjiang River: risk evaluation after a shocking pollution accident. Scientific reports. 7(1), 227.
[20] Liang, D., Jun, R., Ling, T., Hua, L. (2017) Risk assessment and speciation of zn, cu, ni and cr in sewage sludge amended with attapulgite. Fresen. Environ. Bull. 26, 2066-2075.
[21] Wang, L., Wang, L.A., Zhao, X., Wang, X., Li, Y., Hu, C. (2017) Leaching characteristics and change of bioavailability of heavy metals in mswi-fly ash during various washing processes. Fresen. Environ. Bull. 26, 4542-4548.
[22] Wang, G., Liu, X., Gu, Q., Zhang, M., Zhang, X., Huang, Y., Huang, F., Wen, J. (2017) Chemical speciation of heavy metals in the sediments of longjiang river: after a cadmium spill. Desalination and water treatment. 62, 298-306.
[23] Li, J., Zheng, Y., Yan, J., Li, H., Wang, X., He, J., Ding, G. (2013) Effects of different regeneration scenarios and fertilizer treatments on soil microbial ecology in reclaimed opencast mining areas on the Loess Plateau, China. PloS one. 8(5), e63275.
[24] Muller, G. (1969) Index of geoaccumulation in sediments of the Rhine River. Geojournal. 2 108-118.
[25] Wei, F., Chen, J., Wu, Y. (1990) Background Element Values in Soils of China. Beijing, China: China Environmental Science Press. 329-493.
[26] Pedersen F., Bjørnestad E., Andersen H. V., Kjølholt J., Poll C. (1998) Characterization of sediments from Copenhagen Harbour by use of biotests. Water Science & Technology, 37(6–7), 233-240.
[27] Liu, X., Chen, B., Chen, J., Mingjiang, Z., Jiankang, W., Dianzuo, W., Renman, R. (2016) Spatial variation of microbial community structure in the Zijinshan commercial copper heap bioleaching plant. Miner Eng. 94, 76-82.
[28] The State Environmental Protection Administration, the General Administration of Quality Supervision, Inspection and Quarantine. (2002) Standard of the People's Republic of China for surface water Beijing.
[29] Ikem, A., Adisa, S. (2011) Runoff effect on eutrophic lake water quality and heavy metal distribution in recent littoral sediment. Chemosphere. 82(2), 259-67.
[30] Luo, W., Lu, Y., Wang, T., Hu, W., Jiao, W., Naile, J.E., Khim, J. S., Giesy, J. P. (2010) Ecological risk assessment of arsenic and metals in sediments of coastal areas of northern Bohai and Yellow Seas, China. Ambio. 39(5-6), 367-75.

Received: **08.09.2017**
Accepted: **14.01.2018**

CORRESPONDING AUTHOR

Jiankang Wen
National Engineering Laboratory of Biohydrometallurgy,
General Research Institute for Nonferrous Metals,
Beijing 100088 – China

e-mail: kang3412@126.com

© by PSP Volume 27 – No. 5/2018 pages 2853-2866 Fresenius Environmental Bulletin

SPECIES DIVERSITY IN LENTIC, LOTIC, MARINE AND TERRESTRIAL BIOTOPES OF GOKCEADA SALT LAKE WETLAND (CANAKKALE, TURKEY)

Herdem Aslan[1,*], Onur Gonulal[2], Elif Can-Yilmaz[3], Belgin Elipek[4], Ozgur Baytut[5], Murat Tosunoglu[6], Ersin Karabacak[6], Yusuf Kurt[6]

[1]Department of Fisheries Technology, Gokceada School of Applied Sciences, Canakkale Onsekiz Mart University, Canakkale, Turkey
[2]Faculty of Fisheries, Istanbul University, Laleli, İstanbul, Turkey
[3]Institute of Marine Sciences and Technology Dokuz Eylul Unversity, 35430, Izmir, Turkey
[4]Department of Biology, Faculty of Sciences, Trakya University, 22030, Edirne, Turkey
[5]Department of Biology, Faculty of Arts and Sciences, Ondokuz Mayıs University, 55139, Kurupelit-Samsun, Turkey
[6]Department of Biology, Faculty of Arts and Sciences, Canakkale Onsekiz Mart University, Canakkale, Turkey

ABSTRACT

This study was carried out to provide detailed information on species diversity and community structure of Gökçeada Salt Lake Wetland (brook feeding the lake, neighboring sea and terrestrial area around the wetland). Aquatic species diversity (algae, invertebrates, and fish) at 9 different stations in freshwater, brackish water and marine ecosystems, and terrestrial species diversity (plants, amphibians, reptiles, birds and mammals) in the surrounding wetland were studied seasonally in 2016. A total of 195 taxa of terrestrial vascular flora and 134 species of aquatic flora (97 species of phytoplankton, 37 species of benthic algae); a total of 23 macrobenthic invertebrate taxa from the lake and 131 invertebrate species from the sea were identified. Also, 4 fish, 14 reptiles, 3 amphibians and 71 bird species were observed in the study area. While one species of phytoplankton was determined as a new record for the Turkish aquatic flora, a total of 71 marine invertebrate species were reported for the first time in the marine fauna of Gökçeada. The obtained data will not only provide a solid basis to expand the understanding of the island's ecosystem, but also will serve as an important tool in the action plans for wetland conservation.

KEYWORDS:
Salt Lake, Gökçeada, diversity, Imbros, wetlands

INTRODUCTION

Wetlands are one of the most important ecosystems on Earth because of their rich biodiversity, natural value and economic benefits. To be able to ensure the sustainability of these ecosystems, it is essential to investigate and learn more about their ecological balance. Wetlands have a rich and specialized biodiversity due to their structures and locations between the terrestrial and aquatic areas; therefore, they serve as rich ecosystems for the inhabitants living in these areas and also provide multiple ecosystem services to humans [1]. Several previous studies have determined the biological diversity in wetlands [2-9].

Coastal lagoons have special hydrodynamic perspective and very sensitive structures [10]. They are particularly important aquatic ecosystems, usually located near a sea and relatively isolated from the sea by coastal barriers [11]. Coastal lagoons range from nearly fresh to hypersaline waters, and can be fed by freshwater from a stream or salt water from the sea. Therefore, their species diversity may change seasonally within an ecological balance. Also, any artificial influence to these sensitive areas may cause the destruction of the natural balance within those areas [10]. Incidentally, lagoons and their surrounding areas may also serve the tourism sector. Therefore, it is very hard to maintain their sustainability. For this reason, it is necessary to know their hydrobiological structures to protect their ecological balance.

In Turkey, wetlands cover more than 60,000 ha and almost 50% of those areas are located in the Mediterranean Region, followed by the Aegean Region (35%) [12]. Lagoons are targeted as marine protected areas due to the remarkable biodiversity they hold in the ecosystems as a result of the influence of both marine and terrestrial factors [13]. Many species can be ecologically and/or commercially important [14, 15]. They provide goods and services for humans besides their ecological role [16]. Thus, monitoring of these ecosystems is essential for the spatio-temporal changes in organisms and the sustainability of these areas. Determining the changes in organisms living in the aquatic system is the best method for identifying threats. The persistence of the local species and biodiversity are directly related to the protection of the wetland. In this study, the wetland system of Gökçeada Salt Lake including the reptiles, amphibians and bird

species from the surrounding terrestrial area was monitored seasonally in 2016 to determine the aquatic species diversity from the lake and the neighboring.

Gökçeada is the biggest island of Turkey, covering an area of 290 km^2, with a 95 km coastline situated on the north Aegean Sea (40°05 – 40°14 N 25°39 – 26°00 E). The southwesterly and northeasterly winds are prevalent on the island. The Gökçeada Salt Lake is also called Gökçeada Lagoon, which is on the list of Wetlands of International Importance of Turkey and a suitable habitat for bird species under conservation protection [17].

Previous studies were conducted on terrestrial vegetation, fresh and marine fauna, ornithofauna and herpetological features of Gökçeada including the Salt Lake [17-32]. But, except one study [17], none of these studies focused on determining the diversity of the species in Gökçeada Salt Lake Wetland. The Gökçeada Salt Lake Wetland has not been sufficiently protected. It is close to the settlement areas with considerable tourism pressure especially in summer months. And ecological shifts have not been explained scientifically.

This study aims to improve the overall knowledge of the species diversity of the Gökçeada Salt Lake Wetland and to provide information on spatiotemporal variation of the species in lentic, lotic, marine and terrestrial biotopes. As such, algae, plants, invertebrates (except terrestrial and semi-aquatic insects) and vertebrates were investigated. At the end of this paper, we offer some suggestions for the sustainable use and ecological management of the Gökçeada Salt Lake Wetland.

MATERIALS AND METHODS

Studied Area and Sampling Locations. The Salt Lake Wetland is located in the southeast of Gökçeada Island, in the Aydıncık region (Figure 1). The surface area of the lake is approximately 2 km^2 with an average depth of 1-2 m. The lake is connected with the sea when the southwesterly winds are strong. Overall, nine sampling stations to determine aquatic flora and fauna in the study area were selected. While one of them was chosen as lotic biotope in the stream feeding of the Salt Lake (TK1), the other four stations, located on the lake, were chosen as lentic biotope (TG2, TG3, TG4 and TG5). Four farther stations were chosen from the sea as marine biotope (TD6, TD7, TD8, and TD9) (Figure 1, Table 1). The sampling for fish was made at the same time as the sampling of marine macrozoobenthos. Terrestial plants, amphibians, reptiles and mammal specimens were observed in the wetland with an area of 6.883 hectares. While all these samplings and observations were made at the selected stations at seasonal intervals between January 2016 and December 2016, only the bird observations were conducted monthly from three regions (TB10, TB11 and TB12).

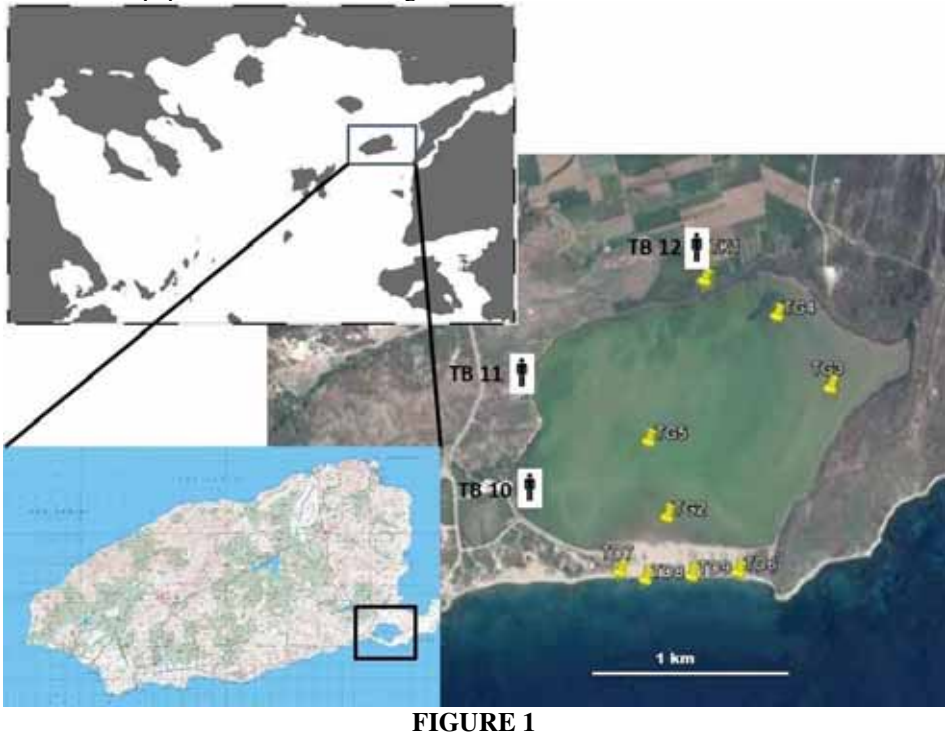


FIGURE 1
The map of sampling area

TABLE 1
Information of sampling stations (van Veen grab: VG, Plankton net: PN, Sampling bottle: SB, Beam trawl: BT, Binocular: B, Camera: C)

Station No	Biotope	Coordinate	Date	Sampling tool	Depth (m)	Station No	Biotope	Coordinate	Date	Sampling tool	Depth (m)
TK1	Stream	40 08 254 25 57 087	09.01.2016 08.05.2016 09.08.2016 13.11.2016	VG, PN, SB	0.1	**TD6**	Sea	40 07 522 25 57 171	29.02.2016 28.05.2016 02.08.2016 17.11.2016	BT, PN	1.5
TG2	Salt lake	40 07 481 25 57 231	08.01.2016 08.05.2016 09.08.2016 13.11.2016	VG, PN, SB	0.3	**TD7**	Sea	40 07 501 25 57 162	29.02.2016 28.05.2016 02.08.2016 17.11.2016	VG, PN	8.0
TG3	Salt lake	40 07 587 25 57 498	08.01.2016 08.05.2016 09.08.2016 13.11.2016	VG, PN, SB	0.3	**TD8**	Sea	40 07 433 25 57 251	29.02.2016 28.05.2016 02.08.2016 17.11.2016	BT, PN	5.0
TG4	Salt lake	40 07 652 25 57 041	08.01.2016 08.05.2016 09.08.2016 13.11.2016	VG, PN, SB	0.3	**TD9**	Sea	40 07 464 25 57 325	29.02.2016 28.05.2016 02.08.2016 17.11.2016	VG, PN	7.0
TG5	Salt lake	40 08 013 25 57 143	09.01.2016 08.05.2016 09.08.2016 13.11.2016	VG, PN, SB	1.2	**TB10**	Wetland	40 07 342 25 57 125	Every Month	B, C	-
						TB11	Wetland	40 07 421 25 57 110	Every Month	B, C	-
						TB12	Wetland	40 08 178 25 56 145	Every Month	B, C	-

Algal samplings. Water samples were taken from nine stations at depths of 0.1-8 m using a Hydro-Bios Free Flow Water Sampler (2.5 liters) to obtain the phytoplankton samples. Also, a plankton net with a 20 µm mesh size was used to evaluate the phytoplankton qualitatively, and a glass tube with a diameter of 0.8 cm and a length of 1 m was used to collect the epipelic algal samples from lentic and lotic biotopes. All phytoplankton samples were transferred into plastic bottles and fixed with 5% formalin. Before the phytoplanktonic organisms were counted, the water samples were homogenized at a low speed until the sediment was thoroughly mixed and were of uniform consistency. Three water-mounted slides for each sample were examined and living diatoms were collected at each station to obtain an estimate of the algal relative abundance [33, 34]. At least 500 algal cells were counted at 600x magnification. Permanent slides for the identification of diatoms were prepared from the same sample after boiling in a 1:1 mixture of concentrated H_2SO_4 and HNO_3. The acid-cleaned diatoms were mounted in Naphrax high refractive index medium [4]. Microscopic observations were conducted under a Prior phase-contrast inverted microscope and a Prior phase-contrast. The Lugol-fixed water samples were concentrated to 1-3 ml and then counted in the Sedgewick-Rafter chamber for the marine samples and utermohl counting chambers for the lotic and lentic phytoplankton samples under an inverted microscope [35]. New records of taxa from the Turkish Algal Flora were checked according to Aysel [36]. Furthermore, valid taxa names and arrangement of taxonomic groups were determined according to the website of [37].

Macroinvertebrates and Fish Samples. Sediment samples were taken from a total of five different sampling stations (TK1, TG2, TG3, TG4, and TG5) by van Veen Grap (15 x 15 cm^2) twice at each station. However, the sampling could not be done at the sampling station TG4 in autumn because of the drying. The obtained material was put into the plastic bottles including 70% ethanol after using a sieve. The specimens were identified from papers by [38-44]. All samples were preserved in 70% ethanol.

For the marine macrozoobenthic community sampling, we made three replicates by using a 0.1 m^2 van Veen Grab in two sampling stations (TD7 & TD9) and by using a beam trawl in the other two stations (TD6 & TD8). All sediment samples were sieved on deck through 0.5 mm size mesh and preserved in a formaldehyde seawater solution (4-5%) for further analyses. The samples were evaluated with ÇOMÜ-3 R/V and I.U Fırtına R/V. The macrozoobenthic samples were sorted and identified to the lowest possible taxonomic level (typically species level) with Olympus SZX-16 stereomicroscope and light microscope, preserved in 70% ethanol. Also, the fish species were obtained by means of the beam trawl in the marine sampling locations. WoRMS is followed here for the nomenclature of the species [45].

.**TABLE 2**
Literatures and field studies are the result of species and subtaxa list of vascular plants

APIACEAE

Apium nodiflorum (L.) Lag.

Lagoecia cuminoides L.
Oenanthe silaifolia M.Bieb.
Scandix pecten-veneris L.
Torilis arvensis (Huds.) Link subsp. *neglecta* (Spreng.) Thell.
Torilis nodosa (L.) Gaertn.

ARACEAE

Lemna minor L.

AMARYLLIDACEAE

Allium sphaerocephalon L.

ASPARAGACEAE

Ornithogalum pyrenaicum L.

ASPLENIACEAE

Asplenium obovatum Viv.

ASTERACEAE

Achillea maritima (L.) Ehrend. & Y.P.Guo

Anthemis auriculata Boiss.

Anthemis cotula L.

Anthemis tomentosa L.

Bellis perennis L.

Carduus nutans L.
Centaurea spinosa L.
Conyza bonariensis (L.) Cronquist
Cota tinctoria (L.) J.Gay ex Guss.
Crepis commutate (Spreng.) Greuter
Crepis zacintha (L.) Babc.
Filago eriocephala Guss.
Filago pygmaea L.
Filago pyramidata L.
Hedypnois rhagadioloides (L.) F.W.Schmidt subsp. *cretica* (L.) Hayek
Inula viscosa (L.) Aiton
Picnomon acarna (L.) Cass.
Scolymus hispanicus L.
Senecio vernalis Waldst. & Kit.
Sonchus oleraceus L.
Tragopogon porrifolius L. subsp. *longirostris* (Sch.Bip.) Greuter

BORAGINACEAE

Anchusa hybrida Ten.
Echium italicum L.
Heliotropium europaeum L.

BRASSICACEAE

Alyssum umbellatum Desv.

Capsella rubella Reut.

Clypeola jonthlaspi L.
Diplotaxis viminea (L.) DC.
Draba verna L.

Hirschfeldia incana (L.) Lagr.-Foss.

Nasturtium officinale R.Br.
Raphanus raphanistrum L.

CAMPANULACEAE

Legousia pentagonia (L.) Thell.

CAPRIFOLIACEAE

Valerianella discoidea (L.) Loisel.

CARYOPHYLLACEAE

Arenaria serpyllifolia L. subsp. *leptoclados* (Rchb.) Nyman
Cerastium brachypetalum Pers. subsp. *roeseri* (Boiss. & Heldr.) Nyman

Polycarpon tetraphyllum (L) L.

Silene colorata Poir.
Silene gallica L.
Spergula pentandra L.
Spergularia marina (L.) Besser

Stellaria media (L.) Vill.

Velezia quadridentata Sibth. & Sm.

CISTACEAE

Cistus creticus L.

Fumana thymifolia (L.) Spach

CONVOLVULACEAE

Calystegia sepium (L.) R.Br.

Convolvulus arvensis L.
Convolvulus elegantissimum Mill.

CRASSULACEAE

Umbilicus horizontali (Salisb.) Dandy

CYPERACEAE

Bolboschoenus maritimus (L.) Palla

Carex divisa Huds.

Carex divulsa Stokes
Cyperus capitatus Vand.

Isolepis cernua (Vahl) Roem. & Schult.

Scirpoides holoschoenus (L.) Soják

DENNSTAEDTIACEAE

Pteridium aquilinum (L.) Kuhn

EQUISETACEAE

Equisetum ramosissimum Desf.

EUPHORBIACEAE

Euphorbia chamaesyce L.
Euphorbia helioscopia L.
Euphorbia paralias L.

FABACEAE

Lathyrus annuus L.
Medicago constricta Dur.

Medicago coronata (L.) Bart.

Medicago falcata L.
Medicago marina L.
Medicago orbicularis (L.) Bartal.
Medicago polymorpha L.
Medicago rigidula (L.) All.

Melilotus albus Desr.

Ononis serrata Forssk.
Ononis viscosa L. subsp. *brevifolia* (DC.)
Trifolium angustifolium L.
Trifolium arvense L.
Trifolium campestre Schreb.
Trifolium fragiferum L. var. *pulchellum* Lange

Trifolium purpureum Lois.

Trifolium scabrum L.
Vicia hirsuta (L.) Gray
Vicia lathyroides L.
Vicia villosa Roth subsp. *eriocarpa* (Hausskn.) P.W.Ball

FAGACEAE

Quercus coccifera L.

GENTIANACEAE

Centaurium maritimum (L.) Fritsch
Centaurium tenuifolium (Hoffmanns. & Link) Fritsch

GERANIACEAE

Erodium acaule (L.) Becherer & Thell.

Erodium cicutarium (L.) L Hér.

Geranium molle L.

HYPERICAEAE

Hypericum perforatum L.

IRIDACEAE

Crocus pulchellus Herb.
Iris suaveolens Boiss. & Reut.

Romulea linaresii Parl.

JUNCACEAE

Juncus acutus L.
Juncus gerardii Loisel.

Juncus hybridus Brot.

Juncus maritimus Lam.

LAMIACEAE

Ballota acetabulosa (L.) Benth.
Lamium amplexicaule L.
Marrubium peregrinum L.
Micromeria graeca (L.) Benth. ex Reicbh.
Origanum vulgare L. subsp. *hirtum* (Link) Ietsw.
Salvia viridis L.
Stachys cretica L. subsp. *lesbiaca* Rech.f.
Teucrium chamaedrys L.
Teucrium polium L.
Teucrium scordium L. *subsp. scordioides* (Schreb.) Arcang.
Thymbra capitate (L.) Cav.

Vitex agnus-castus L.

LINACEAE

Linum bienne Mill.
Linum trigynum L.

MALVACEAE

Alcea biennis Winterl
Malva sylvestris L.

OLEACEAE

Olea europaea L.
Phillyrea latifolia L.

ORCHIDACEAE

Orchis laxiflora Lam.

OROBANCHACEAE

Bartsia trixago L.
Parentucellia latifolia (L.) Caruel
Parentucellia viscosa (L.) Caruel

PAPAVERACEAE

Fumaria kralikii Jord.

Hypecoum pendulum L.
Papaver argemone L.
Papaver rhoeas L.

PLANTAGINACEAE

Plantago coronopus L.

Plantago lagopus L.

Plantago major L. subsp. *intermedia* (Gilib.) Lange
Veronica cymbalaria Bodard
Veronica polita Fr.

POACEAE

Aegilops biuncialis Vis.

Aegilops caudata L.
Aeluropus littoralis (Gouan) Parl.
Aira elegantissima Schur subsp. *ambigua* (Arcang.) Doğan
Anthoxanthum aristatum Boiss.

Avena barbata Pott ex Link

Brachypodium distachyon (L.)
Briza maxima L.

Briza minor L.

Bromus arvensis L.

Bromus diandrus R*oth*

Bromus fasciculatus C.Presl
Bromus madritensis L.
Bromus tectorum L.
Catapodium rigidum (L.) C.E.Hubb.
Crypsis aculeata (L.) Aiton
Cynosurus echinatus L.
Dactylis glomerata L.
Elymus elongatus (Host) Runemark
Hordeum bulbosum L.
Hordeum murinum L. subsp. *leporinum* (Link) Arcang.
Imperata cylindrica (L.)
Koeleria pyramidata (Lam.)
Lagurus ovatus L.

Lolium perenne L.

Lolium rigidum Gaudich

Oryzopsis miliacea (L.)
Phragmites australis (Cav.) Trin. ex Steud.
Poa annua L.
Poa bulbosa L.

Poa trivialis L.

Polypogon maritimus Willd.
Polypogon monspeliensis (L.) Desf.
Puccinellia distans (Jacq.) Parl.
Rostraria cristata (L.)
Vulpia ciliate Dumort.

POLYGONACEAE

Polygonum patulum
Rumex acetosella L.
Rumex pulcher L.
Rumex tuberosus L.

PRIMULACEAE

Anagallis arvensis L.
Anagallis arvensis L. *var. caerulea* (L.) Gouan

PTERIDACEAE

Anogramma leptophylla (L.)

RANUNCULACEAE

Anemone coronaria L.
Ranunculus ficaria L

Ranunculus muricatus L.

Ranunculus neapolitanus
Ranunculus peltatus

ROSACEAE

Potentilla reptans L.
Rubus sanctus Schreb.
Sarcopoterium spinosum (L.) Spach

RUBIACEAE

Galium debile Dev.
Valantia muralis L.

SALICACEAE

Salix alba L.

SCROPHULARIACEAE

Verbascum sinuatum L.

TAMARICACEAE

Tamarix smyrnensis Bunge

TYPHACEAE

Typha angustifolia L.

VERBENACEAE

Verbena officinalis L.

VIOLACEAE

Viola kitaibeliana Roem. & Schult.

XANTHORRHOEACEAE

Asphodelus aestivus Brot.

TABLE 3
Phytoplankton species list in the water samples from Gökçeada Salt Lake. New record algal flora for the Turkey were marked with *.

MARINE SPECIES			
CYANOBACTERIA	*Lyrella lyroides* (Hendey) D.G. Mann in Round	**CHLOROPHYTA**	*Noctiluca scintillans* (Macartney) Kofoid
Phormidium limosum (Dillwyn) P.C. Silva	*Navicula cryptocephala* Kützing	*Halosphaera viridis* F. Schmitz	*Polykrikos kofoidii* Chatton
BACILLARIOPHYTA	*Navicula salinarum* Grunow	*Pyramimonas adriaticus* J. Schiller	*Prorocentrum compressum* (Bailey) Abé ex
Achnanthes longipes C. Agardh	*Nitzschia longissima* (Brébisson) Ralfs	**CRYPTOPHYTA**	*Prorocentrum cordatum* (Ostenfeld) Dodge
Actinocyclus normanii (Gregory) Hustedt	*Nitzschia sigma* (Kützing) W. Smith	*Rhodomonas marina* (P.A. Dangeard) Lemmermann	*Protoperidinium mediterraneum* (Kofoid) Balech
Amphora ocellata Donkin	*Podosira hormoide*s (Mont.) Kutzing	**DINOFLAGELLATA**	*Protoperidinium oceanicum* (VanHöffen) Balech
Bacteriastrum hyalinum Lauder	*Proboscia alata* (Brightwell) Sündstrom	*Amphidinium sphenoides* WüIff	*Protoperidinium pallidum* (Ostenfeld) Balech
Cerataulina pelagica (Cleve) Hendey	*Pseudo-nitzschia delicatissima* (Cleve) Heiden	*Ceratium hirundinella* (O.F. Müller) Dujardin	*Protoperidinium pellucidum* Bergh exLoeblich
Coscinodiscus perforatus Ehrenberg	*Pseudosolenia calcar-avis* (Schultze) Sundström	*Cochlodinium archimedes* (Pouchet) Lemmermann	*Protoperidinium steinii* (Jorgensen) Balech
Diploneis chersonensis (Grunov) Cleve	*Thalassionema nitzschioides* (Grunow)	*Gonyaulax scrippsae* Kofoid	*Torodinium teredo* (Pouchet) Kofoid & Swezy
Gyrosigma acuminatum (Kützing) Rabenhorst	*Thalassiothrix mediterranea* Pavillard	*Gyrodinium pingue* (Schütt) Kofoid & Swezy	*Tripos furca (*Ehrenberg) F. Gómez
Hannaea arcus (Ehrenberg) R.M. Patrick	**OCHROPHYTA**	*Gyrodinium spirale* (Bergh) Kofoid & Swezy	*Tripos macrocer-os* (Ehrenberg) F. Gómez
Hemiaulus hauckii Grunow ex Van Heurck	*Heterosigma akashiwo* (Y. Hada)	*Karenia brevis* (C.C. Davis) Gert Hansen & Ø. Moestrup	
Leptocylindrus minimus Gran	**BIGYRA**	*Katodinium fungiforme* (Anissimova) A.R. Loeblich III	
	Bicosoeca mediterranea Pavillard	*Neoceratium fusus* (Ehrenberg) F. Gomez,	

LAKE SPECIES			
CYANOBACTERIA	*Gyrosigma attenuatum* (Kützing) Rabenhors	*Plagiotropis lepidoptera* (W. Gregory) Kuntze	**CHLOROPHYTA**
Leptolyngbya fragilis (Gomont)	*Gyrosigma acuminatum* (Kützing) Rabenhorst	*Rhoicosphenia abbreviata* (C. Agardh) Lange-Bertalot	*Aegagropila linnaei* Kützing
BACILLARIOPHYTA	*Gyrosigma distortum* (W. Smith) Griffith & Henfrey	*Surirella brebissonii* Krammer & Lange-Bertalot	*Ankistrodesmus spiralis* (W.B. Turner)
Amphora ovalis (Kützing) Kützing	*Licmophora ehrenbergii* (Kützing) Grunow	***Surirella notabilis* G. Leuduger-Fortmorel***	*Chlamydomonas reinhardtii* P.A. Dangeard
Caloneis limosa (Kützing) R.M. Patrick in Patrick	*Melosira varians* C. Agardh	*Tryblionella acuta* (Cleve) D.G. Mann in Round	*Cladophora glomerata* (Linnaeus) Kützing
Cocconeis pediculus Ehrenberg	*Navicula cincta* (Ehrenberg) Ralfs in Pritchard	*Tryblionella navicularis* (Brébisson) Ralfs in Pritchard	*Closterium ehrenbergii Meneghini ex Ralfs*
Coronia decora (Brébisson) Ruck & Guiry	*Navicula cryptocephala* Kützing	*Ulnaria danica* (Kützing) Compère & Bukhtiyarova	*Closterium moniliferum Ehrenberg ex Ralfs*
Cyclotella meneghiniana Kützing	*Navicula salinarum* Grunow	*Ulnaria ulna* (Nitzsch) Compère in Jahn et al.	*Dunaliella tertio-lecta* Butcher
Cymatopleura elliptica (Brébisson) W.Smith	*Nitzschia acicularioides* Hustedt	**CHAROPHYTA**	*Oocystis elliptica* West
Encyonema minutum (Hilse) D.G. Mann	*Nitzschia communis* Rabenhorst	*Spirogyra crassa* (Kützing) Kützing	**DINOFLAGELLATA**
Entomoneis alata (Ehrenberg) Ehrenberg	*Nitzschia dissipata* (Kützing) Rabenhorst	**CRYPTOPHYTA**	*Karenia brevis* (C.C. Davis) Gert Hansen
Fragilaria capucina Desmazières	*Nitzschia nana* Grunow in Van Heurck	*Cryptomonas ovata* Ehrenberg	*Prorocentrum cordatum* (Ostenfeld) Dodge
Fragilaria crotonensis Kitton	*Nitzschia ovalis* H.J. Arnott in Cleve & Grunow	*Plagioselmis nannoplanctica* (H. Skuja) G. Novarino	**HAPTOPHYTA**
Gomphonema minutum (C. Agardh) C. Agardh	*Nitzschia sigmoidea* (Nitzsch) W. Smith	*Rhodomonas marina* (P.A. Dangeard) Lemmermann	*Phaeocystis globosa* Scherffel
Gomphonema olivaceum (Hornemann) Brébisson		*Teleaulax acuta* (Butcher) D.R.A. Hill	**OCHROPHYTA**
			Heterosigma akashiwo (Y. Hada)

Terrestrial Plant Samples. The terrestrial vascular plants around the Salt Lake were collected at spring vegetation periods. The samples were collected, photographed and identified. The specimens were kept in the Çanakkale Onsekiz Mart University, Çanakkale Botanic Garden Herbarium (CBB). In addition, herbarium samples previously collected from the site were examined in CBB and

Herbarium of Ege University Botanic Garden (EGE).

Birds, Amphibians, Reptilians and Mammals Observations. The birds in and around the lake were observed in detail under the transect work. Three binoculars (8x40, 8,20 wide angle, Meade telescope (EXT 70), Garmin GPS Etrex navigation device (Vista-HCX), and a camera (Canon 60D, Canon 7D Mark II body, Canon 300mm f2.8L IS USM super telephoto lens) were used during the observations. In the study area, species of fixed birds primarily were counted and photographed.

Amphibian, reptile and mammal specimens were captured during about 20 days in 10 excursions by two people on various dates. They were caught by net, hand or using fish traps.

RESULTS

In this study, a total of 195 taxa of terrestrial vascular flora and 134 species of aquatic flora (97 species of phytoplankton, 37 species of benthic algae); 23 macrobenthos taxa from lotic and lentic biotopes; and 131 species from marine biotope were identified. Furthermore, 4 fish, 14 reptilians, 3 amphibian and 71 bird species were observed in the study area. Although, one species of phytoplankton was found as a new record for the Turkish aquatic flora, a total of 71 marine invertebrate species were reported for the first time in the marine fauna of Gökçeada. The species lists, which were observed at the study area, are detailed in Tables 2-6.

Algae. A total of 97 phytoplankton taxa belonging to Cyanobacteria (2), Bacillariophyta (56), Bigyra (1), Chlorophyta (11), Cryptophyta (4), Dinoflagellata (21), Haptophyta (1) and Ochrophyta (1) were identified in the water samples collected from the lentic, lotic and coastal marine stations of Gökçeada Salt Lake. The list of phytoplankton species and their distributions are presented in Table 3 and Figure 2, respectively. Dominant phytoplankton groups consist of pennate diatoms, techate and atechate dinoflagellates and flagellated chlorophytes. The most abundant sampling station was TG3 (2.533.980 cellL^{-}) according to cell counts in the water samples from the lentic, lotic and coastal marine stations of Gökçeada Salt Lake (Figure 2). The lowest abundance was 1335 cellL^{-} in the TK1, whereas the most abundant systematic category was the Chlorophyta (1.431.840 cellL^{-}). Common species among the stations were *Chlamydomonas reinhardi* and *Cryptomonas ovata*. In the lotic station (TK1), the highest cell abundance was 976.540 cellL^{-} in May 2016 (Figure 2). In the coastal marine stations, the highest abundance was observed in TD7 (33.000 cellL^{-}) in February 2016. Chlorophytes and diatoms were the most abundant and common groups of coastal marine phytoplankton. A total of 37 taxa were identified from the lotic (TK1) and lentic (TG2, TG3, TG4 and TG5) sampling stations of Gökçeada Salt Lake. The most abundant and common species are *Epithemia sorex* Kützing during the first half of the sampling period and *Gyrosigma acuminatum* (Kützing) Rabenhorst during the second half.

Plants. A total of 195 taxa belonging to terrestrial vascular flora were observed in this study. While the Poaceae were represented by 36 taxa, it was followed by Asteraceae and Fabaceae with 21 taxa, Lamiaceae with 12 taxa, Caryophyllaceae with 9 taxa, Brassicaceae with 8 taxa, Apiaceae and Cyperaceae with 6 taxa, Gentianaceae, Ranunculaceae and Plantaginaceae with 5 taxa, Juncaceae and Polygonaceae with 4 taxa, Boraginaceae, Convolvulaceae, Euphorbiaceae, Rosaceae, Orobanchaceae, Papaveraceae and Iridaceae with 3 taxa, Asparagaceae, Cistaceae, Linaceae, Malvaceae, Oleaceae and Rubiaceae with 2 taxa. The other groups (Araceae, Aspleniaceae, Campanulaceae, Caprifoliaceae, Dennstaedtiaceae, Equisetaceae, Hypericaceae, Papaveraceae, Pteridaceae, Orchidaceae, Violaceae, Salicaceae, Scrophulariaceae, Tamaricaceae, Typhaceae, Verbenaceae, Xanthorrhoeaceae) were represented by only one taxa.

Macroinvertebrates. The taxonomic analysis of the invertebrate samples collected from the sea resulted in 1,205 individuals belonging to 131 species of 8 taxa (Porifera, Anthozoa, Sipuncula, Polychaeta, Crustacea, Mollusca, Bryozoa, Echinodermata) (Table 4). The seasonal distribution of the species at the sampling stations was exhibited in Figure 3a. Mollusks were the most abundant taxon (682 individuals and 64 species), followed by crustaceans (420 individuals and 45 species) and polychaetes (94 individuals and 15 species) (Figure 3b). The most abundant species were the mollusks (*Bittium latreillii, B. reticulatum* and *Sepiola rondeletii),* and grouped as "constant"; the mollusk (*Cerithium vulgatum, Mangelia callosa, Rissoa violacea, Chamelea gallina, Donacilla cornea, Lucinella divaricata*), the crustaceans (*Nototropis massiliensis, Eurydice spinigera, Cumella (Cumella) pygmaea, Clibanarius erythropus, Diogenes pugilator, Liocarcinus depurator, Philocheras trispinosus*). The polychaetes (*Sphaerosyllis* sp., *Lumbrinerides amoureuxi*) were grouped as "common" in the results of the frequency index. A total of 23 taxa belonging to benthic macroinvertebrates were determined in Gökçeada Salt Lake (lotic and lentic biotopes) (Table 4).

TABLE 4
The list of invertebrate species the study area. New record fauna for the Gökçeada island were marked with **

MARINE SPECIES			
Phylum / Species	**Phylum / Species**	**Phylum / Species**	**Phylum / Species**
Porifera	*Mangelia* sp. **	**Arthropoda**	*Nototropis guttatus*
Halichondria panicea	*Mangelia striolata* **	*Ampelisca brevicornis* **	*Nototropis massiliensis*
Anthozoa	*Manzonia crassa* **	*Ampelisca sarsi* **	*Pachygrapsus marmoratus*
Calliactis parasitica **	*Modiolula phaseolina*	*Ampelisca* sp.	*Paragnathia formica*
Mollusca	*Monophorus* sp	*Anoplodactylus petiolatus* **	*Paranthura costana* **
Alvania cimex	*Muricopsis cristata*	*Aora gracilis* **	*Perioculodes longimanus* **
Bela nuperrima **	*Musculus costulatus*	*Bathyporeia guilliamsoniana*	*Philocheras trispinosus*
Bela zonata **	*Mytilus galloprovincialis*	*Bathyporeia phaiophthalma*	*Porcellio scaber*
Bittium lacteum **	*Naticarius stercusmuscarum* **	*Chrinomid* sp	*Sphaeroma serratum* **
Bittium latreillii	*Neverita josephinia*	*Clibanarius erythropus*	*Squilla mantis*
Bittium reticulatum	*Ocinebrina aciculata* **	*Cumella pygmaea* **	*Stenosoma capito* **
Bolinus brandaris	*Peronidia albicans* **	*Deflexilodes griseus*	*Urothoe pulchella* **
Caecum sp. **	*Pisania striata*	*Dexamine spinosa*	*Thracia phaseolina* **
Caecum trachea **	*Pitar rudis*	*Diogenes pugilator*	**Bryozoa**
Cerithium vulgatum	*Raphitoma linearis* **	*Dynamene* sp.	*Cryptosula pallasiana* **
Chamelea gallina	*Rissoa* sp.	*Ericthonius brasiliensis*	*Shcizomavella* sp.
Clanculus cruciatus	*Rissoa variabilis*	*Eurydice spinigera*	Bryozoa (sp)
Conus ventricosus	*Rissoa violacea* **	*Gammarella fucicola* **	**Polychaeta**
Cuspidaria cuspidata	*Sepiola rondeletii*	*Gammarus subtypicus***	*Sphaerosyllis* sp.
Donacilla cornea	*Solen marginatus*	*Gastrosaccus sanctus* **	*Arabella iricolor* **
Donax semistriatus **	*Spisula subtruncata*	*Harpackoid* sp	*Phyllodocidae (sp).*
Donax trunculus	*Thracia phaseolina* **	*Hyale schmidti* **	*Nephtys cirrosa* **
Donax variegatus	*Tricolia pullus*	*Gammarus subtypicus* **	*Micronephthys stammeri* **
Enginella leucozona **	*Tricolia speciosa* **	*Homalopoma sanguineum* **	*Glycera* sp.
Epitonium sp.	*Tritia incrassata* **	*Hyale* sp.	*Lumbrinerides amoureuxi* **
Eulima glabra	*Tritia mutabilis* **	*Idotea balthica*	*Schistomeringos neglecta* **
Gibbula sp	*Tritia neritea* **	*Leucothoe spinicarpa* **	*Protodorvillea kefersteini*
Haliotis tuberculata	*Tritia neritea* **	*Liocarcinus depurator*	*Saccocirrus* sp.
Hiatella arctica	*Turbonilla* sp	*Lysianassa costae* **	*Spio filicornis* **
Hiatella rugosa	*Turritella communis*	*Macropodia rostrata*	*Platynereis dumerilii*
Loripes orbiculatus **	*Vexillum ebenus*	*Microdeutopus algicola*	*Fabricia* sp.
Lucinella divaricata	*Vexillum granum* **	*Microdeutopus* sp	*Pisione* sp.
Mactra stultorum **	**Echinodermata**	*Microdeutopus versiculatus* **	*Magelona mirabilis* **
Mangelia callosa **	*Echinocardium cordatum*	*Monoculodes* sp	**Spinculoid**
Mangelia costulata **		*Mysid* sp	*Aspidosiphon muelleri*

LAKE SPECIES			
Oligochaeta	**Amphipoda**	**Insecta**	
Tubifex sp.	*Gammarus* sp.	*Chironomus plumosus*	*Microtendipes chloris*
Stylaria lacustris	*Gammarus komareki*	*Stictochironomus* sp.	*Crocothemis erythraea*
Nais bretscheri	**Isopoda**	*Cricotopus bicinctus*	*Ischnura elegans*
Limnodrilus hoffmeisteri	*Idothea baltica*	*Procladius (Holotanypus)* sp.	Coenagrienidae
Dero digitata	*Asellus aquaticus*	*Chironomus riparius*	*Caenis* sp.

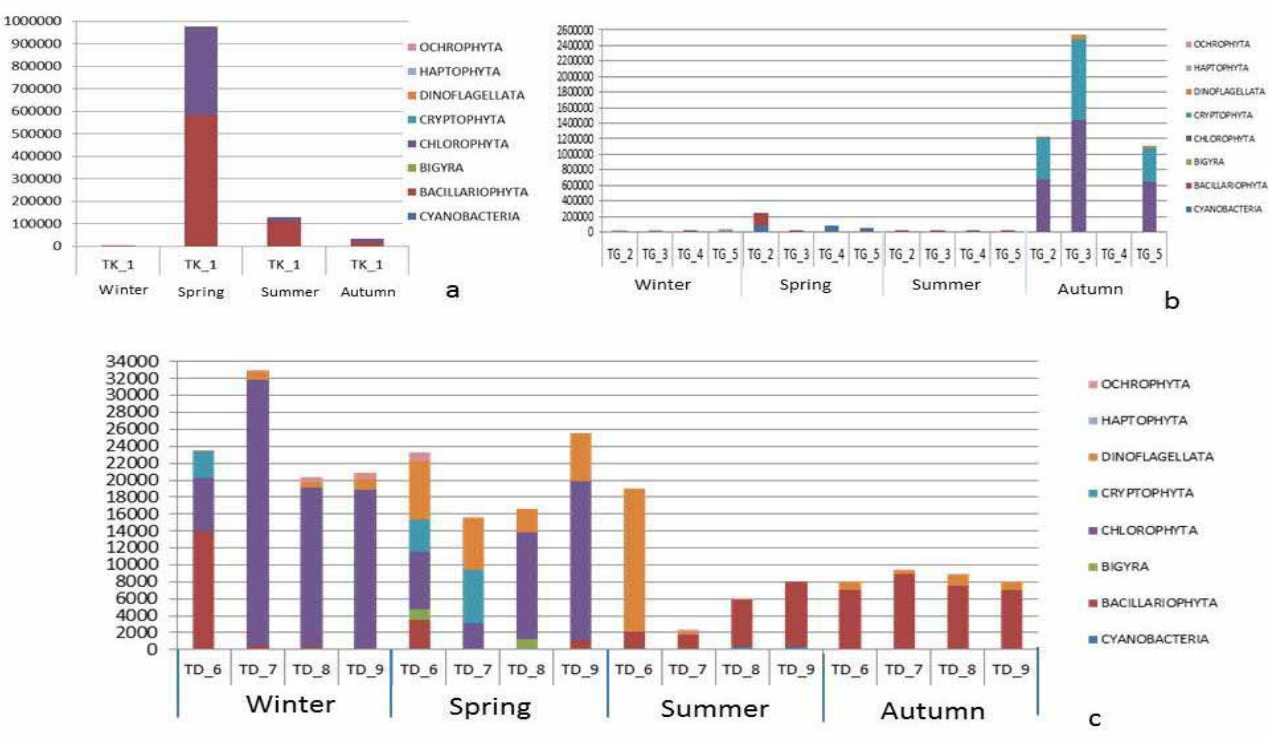


FIGURE 2
Phytoplankton abundance and variation in the water samples from the study area.
a) lotic, b) lentic, c) marine

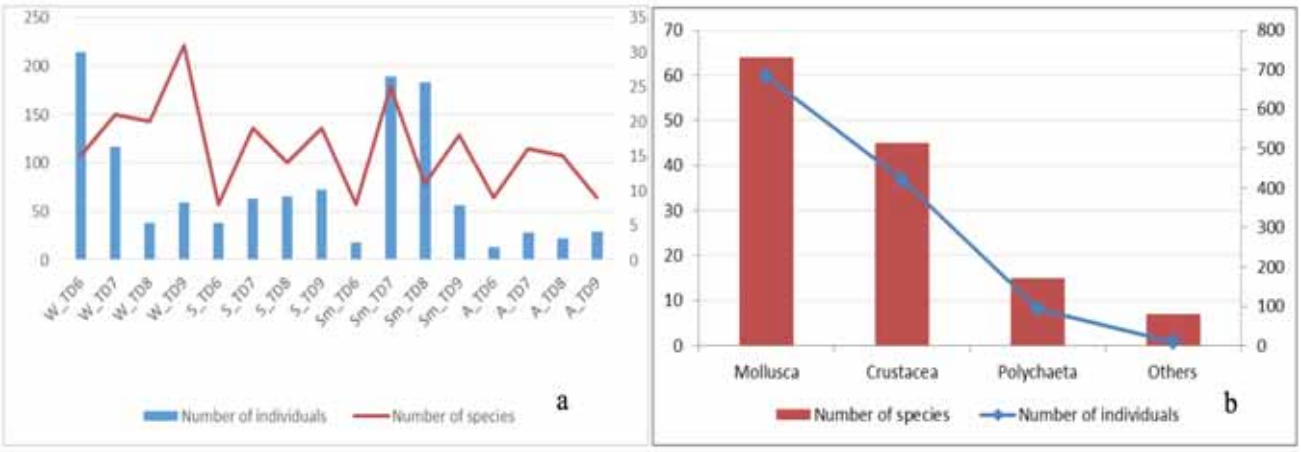


FIGURE 3
Marine macrozoobenthos a) Seasonal distribution of the individual and species numbers at the sampling stations b) The number of individual and species numbers of the marine macrozoobenthos

According to the results, we found 2 taxa in the summer sampling, 4 taxa in the winter sampling, 10 taxa in the spring sampling, 16 taxa in the autumn sampling (Table 5). We found cross-larval chironomids only in the spring sampling. At the sampling stations, station TK1 was the richest location with 15 taxa during the sampling period, followed by station TG2 with 5 taxa and stations TG4 and TG5 with 3 taxa. According to the individual site results, station TK1 was also found to be the richest (155 individuals m^{-2}) followed by the others with 22 individuals m^{-2}. The specimens belonging to Oligochaeta were found at all sampling stations in all seasons except summer. However, the group Amphipoda was found only at three stations (TG2, TG4 and TG5) and the group Isopoda was found only at stations TK1 and TG4. The larval chironomids were the most dominant group belonging to Insecta. This group was followed by Odonata and Ephemeroptera. The specimens belonging to Gastropoda were found only at station TK1 (Table 5). Although the shells of Ostracoda were recognized, they were not identified.

TABLE 5
The seasonal distributions of benthic macroinvertebrates from lotic and lentic biotopes (individuals/m2)
***diagnostik characters are damaged **juvenile forms**

SUMMER							AUTUMN					
Taxa↓	Station →	TK1	TG2	TG3	TG4	TG5	Taxa ↓	Station →	TK1	TG2	TG3	TG5
INSECTA	*Chironomus plumosus*	-	44	-	-	-	OLIGOCHAETA	*Tubifex* sp.	288**	-	-	-
	Stictochironomus sp.	66**	-	-	-	-		*Limnodrilus hoffmeisteri*	200	-	-	-
	Total	66	44	0	0	0		*Dero digitata*	88	-	-	-
SPRING							ISOPODA	*Asellus aquaticus*	2777	-	-	-
Taxa↓	Station →	TK1	TG2	TG3	TG4	TG5		Chironomidae	25**	-	-	-
OLIGOCHAETA		22*	-	-	-	-		*Chironomus plumosus*	222	-	-	-
	Stylaria lacustris	-	66	-	-	-		*Procladius (H.)* sp.	155	-	-	-
	Nais bretscheri	-	66	-	-	-		*Chironomus riparius*	22	-	-	-
AMPHIPODA	*Gammarus* sp.	-	22*	-	-	222**	INSECTA	*Microtendipes chloris*	88	-	-	-
	Gammarus komareki	-	-	-	333	-		*Crocothemis erythraea*	44	-	-	-
ISOPODA	*Idothea baltica*	-	-	-	22	-		*Ischnura elegans*	44	-	-	-
	Asellus aquaticus	44	-	-	-	-		Coenagrienidae	44**	-	-	-
INSECTA	*Chironomus plumosus*	-	-	-	-	22		*Caenis* sp.	44*	-	-	-
	Stictochironomus sp.	444	22	-	-	-	GASTROPODA	Bithyniidae	177**	-	-	-
	Cricotopus bicinctus	-	-	-	-	266		Planorbidae	200**	-	-	-
	Total	510	176	0	355	510		**Total**	4506	0	0	0
WINTER												
Taxa↓	Station →	TK1	TG2	TG3	TG4	TG5						
OLIGOCHAETA	*Tubifex* sp.	155*	-	-	-	-						
AMPHIPODA	*Gammarus* sp.	-	-	-	-	22*						
INSECTA	*Chironomus plumosus*	-	22	-	-	-						
	Stictochironomus sp.	-	-	-	22**	-						
	Total	155	22	0	22	22						

Fish. Fish samples collected from the sea (TD6 & TD8) resulted in 28 individuals belonging to four species (Table 6). *Arnoglossus laterna* had the highest individual number. Additionally, *Trachinus draco* was grouped as "common" in the results of the frequency index.

Amphibian and Reptiles. Three amphibian species were found at the Salt Lake in Gökçeada during the sampling period (Table 6). The Marsh Frog (*Pelophylax ridibundus*) has been observed in all rivers and streams around the lake at the beginning of spring and at the beginning of winter. The nightly frog (*Bufotes variabilis*), a terrestrial species, was found in the areas close to the settlements and was encountered throughout nearly the entire sampling period except winter. Tree frog (*Hyla orientalis*) was more frequently observed in vegetative wetlands, during spring and summer. Twelve reptile species (2 turtles, 3 lizards, 7 snakes) were found on the Salt Lake (Table 6). No mammals were observed.

Birds. As a result of the 12-month bird watching study, 71 bird species were identified on and around the Salt Lake (Table 6). Flamingo could not be observed in August, July and September 2016 because the Salt Lake was almost completely dry (Figure 4). Windsurfing was observed in the lake during the bird monitoring studies on April 24, 2016. On the same date, gull eggs and pups were also recorded around the lake.

DISCUSSION

Inland, marine and terrestrial ecosystems are under global pressure from human impacts in various forms, i.e. pollution, habitat degradation, urbanization, etc. A better understanding of the biodiversity is urgently needed to mitigate the human impacts through effective conservation and

TABLE 6
The list of vertebrate species observed Gokceada Salty Lake Wetlands and around biotopes and their IUCN Status (NE: Not Evaluated, DD: Data Deficient, LC: Last Concern, NT: Near Threatened, VU: Vulnarable, EN: Endangered)

Family / Species	IUCN	Family / Species	IUCN	Family / Species	IUCN	Family / Species	IUCN
(PISCES)		*Platyceps najadum* (Eichwald, 1831)	LC	**(AVES)**		**Muscicapidae**	
Bothidae		*Malpolon insignatus* (Geoffroy 1809)	LC	**Podicipedidae**		*Ficedula parva* (Bechstein, 1792)	LC
Arnoglossus laterna (Walbaum. 1792)	LC	*Zamenis situla* (Linnaeus, 1758)	LC	*Podiceps cristatus* (Linnaeus, 1758)	LC	*Ficedula semitorquata* (Homeyer, 1885)	LC
Gobiidae		*Natrix natrix* Linnaeus, 1758	LC	**Phalacrocoracidae**		*Erithacus rubecula* (Linnaeus, 1758)	LC
Deltentosteus quadrimaculatus (Valenciennes. 1837)	NE	**Scolopacidae**		*Phalacrocorax aristotelis* (Linnaeus, 1761)	LC	*Luscinia megarhynchos (Brehm, 1831)*	LC
Trachinidae		*Calidris alba* (Pallas, 1764)	LC	**Ardeidae**		*Oenanthe oenanthe* (Linnaeus, 1758)	LC
Trachinus draco Linnaeus. 1758	LC	*Calidris minuta* (Leisler, 1812)	LC	*Egretta garzetta* (Linnaeus, 1766)	LC	*Oenanthe hispanica* (Linnaeus, 1758)	LC
Rajidae		*Calidris alpina* (Linnaeus, 1758)	LC	*Ardea alba* Linnaeus, 1758	LC	**Turdidae**	
Raja radula Delaroche. 189	EN	*Gallinago gallinago* (Linnaeus, 1758)	LC	*Ardea cinerea* Linnaeus, 1758	LC	*Turdus merula* Linnaeus, 1758	LC
(AMPHIBIA)		*Numenius arquata* (Linnaeus, 1758)	NT	**Phoenicopteridae**		*Turdus pilaris* Linnaeus, 1758	LC
Bufonidae	DD	*Tringa totanus* (Linnaeus, 1758)	LC	*Phoenicopterus ruber* Linnaeus, 1758	LC	**Paridae**	
Bufotes variabilis (Pallas, 1769)		*Tringa nebularia* (Gunnerus, 1767)	LC	**Anatidae**		*Cyanistes caeruleus* (Linnaeus, 1758)	LC
Hylidae		**Laridae**		*Cygnus cygnus* (Linnaeus, 1758)	LC	*Parus majör* Linnaeus, 1758	LC
Hyla orientalis Bedriaga, 1890	LC	*Larus audouinii* Payraudeau, 1826	LC	*Tadorna ferruginea (Pallas, 1764)*	LC	**Laniidae**	
Ranidae		*Larus michahellis* J.F. Naumann, 1840	LC	*Tadorna tadorna* (Linnaeus, 1758)	LC	*Lanius collurio* Linnaeus, 1758	LC
Pelophylax ridibundus (Pallas, 1771)	LC	**Columbidae**		*Anas penelope* Linnaeus, 1758	LC	**Corvidae**	
(REPTILIA)		*Streptopelia turtur* (Linnaeus, 1758)	VU	*Anas platyrhynchos* Linnaeus, 1758	LC	*Garrulus glandarius* (Linnaeus, 1758)	LC
Geoemydidae		**Meropidae**		*Aythya ferina* (Linnaeus, 1758)	VU	*Corvus monedula* Linnaeus, 1758	LC
Mauremys rivulata (Valenciennes, 1833)	-	*Merops apiaster* Linnaeus, 1758	LC	**Accipitridae**		*Corvus cornix* (Linnaeus, 1758)	LC
Testudinidae		**Picidae**		*Circus aeruginosus* (Linnaeus, 1758)	LC	*Corvus corax* Linnaeus, 1758	LC
Testudo graeca Linnaeus, 1758	VU	*Dendrocopos syriacus* (Ehrenberg, 1833)	LC	**Haematopodidae**		**Sturnidae**	
Lacertidae		**Sylviidae**		*Haematopus ostralegus* Linnaeus, 1758	NT	*Sturnus vulgaris* Linnaeus, 1758	LC
Ophisops elegans Ménétries, 1832	-	*Acrocephalus scirpaceus* (Herman, 1804)	LC	**Recurvirostridae**		**Passeridae**	
Gekkonidae		*Sylvia cantillans* (Pallas, 1764)	LC	*Himantopus himantopus* (Linnaeus, 1758)	LC	*Passer domesticus* (Linnaeus, 1758)	LC
Hemidactylus turcicus (Linnaeus, 1758)	LC	*Sylvia melanocephala* (Gmelin, 1789)	LC	*Recurvirostra avosetta* Linnaeus, 1758	LC	**Fringillidae**	
Anguidae		*Sylvia curruca* (Linnaeus, 1758)	LC	**Charadriidae**		*Fringilla coelebs* Linnaeus, 1758	LC
Pseudopus apodus (Pallas, 1775)	LC	*Sylvia communis* Latham, 1787	LC	*Charadrius dubius* Scopoli 1786	LC	*Chloris chloris* (Linnaeus, 1758)	LC
Typhlopidae		*Sylvia atricapilla* (Linnaeus, 1758)	LC	*Charadrius hiaticula* Linnaeus, 1758	LC	*Carduelis carduelis* (Linnaeus, 1758)	LC
Xerotyphlops vermicularis (Merrem, 1820)	-	*Phylloscopus collybita (Vieillot, 1817)*	LC	*Charadrius alexandrinus* Linnaeus, 1758	LC		
Boidae		**Emberizidae**		*Pluvialis apricaria* Linnaeus, 1758	LC		
Eryx jaculus (Linnaeus, 1758)	LC	*Emberiza cirlus* Linnaeus, 1766	LC	*Pluvialis squatarola* (Linnaeus, 1758)	LC		
Colubridae		*Emberiza hortulana* Linnaeus, 1758	LC	**Troglodytidae**			
Dolichophis caspius (Gmelin, 1789)	-	*Emberiza schoeniclus* (Linnaeus, 1758)	LC	*Troglodytes troglodytes* (Linnaeus, 1758)	LC		
		Emberiza calandra	LC				

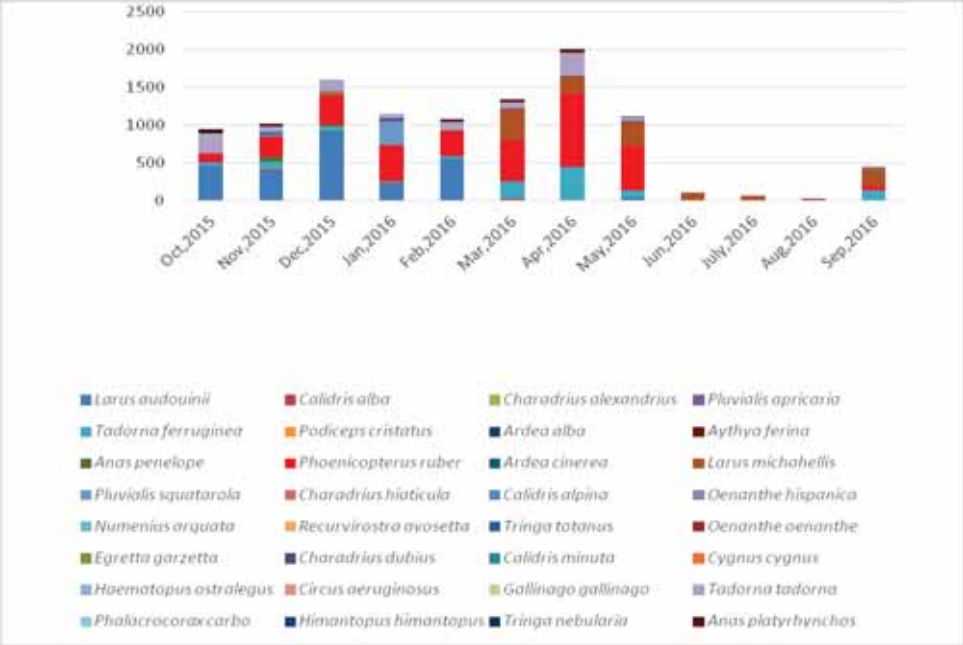


FIGURE 4
The abundance of the aquatic birds observed montly in the study area

management actions. The wetlands are the most significant ecosystems on Earth in respect to their natural function and economic benefits. Despite their natural and economic importance, they have faced detrimental human impacts throughout the last century in Turkey [46]. The Gökçeada Salt Lake Wetland encounters multiple serious problems such as increased human interaction, especially during summer, from surfing activities that result in physical and some environmental impacts. Assessing the state of the area's biodiversity gives us the ability to understand the actual situation of the wetlands and the dimension of threats the species are facing. Monitoring of the biodiversity is essential to emphasize the importance of these areas. The main point of this study is to describe the present state of the biodiversity of Gökçeada Salt Lake Wetlands.

In this study, while a total of 195 terrestrial vascular plant taxa were identified from Gökceada Salt Lake Wetland and its surroundings, 97 taxa were identified in the phytoplankton of lentic (TG2, TG3, TG4 and TG5), lotic (TK1) and coastal marine stations of Gökçeada Salt Lake. This aquatic flora belongs to Cyanobacteria (2), Bacillariophyta (56), Bigyra (1), Chlorophyta (11), Cryptophyta (4), Dinoflagellata (21), Haptophyta (1) ve Ochrophyta (1). In the lotic station, the most abundant phytoplankton groups were chlorophyes and diatoms, while chlorophytes and cryptophytes were dominant in lentic stations. Chlorophytes and dinoflagellates in the first half of the year and the diatoms in the second half were the most abundant groups of coastal marine phytoplankton. Benthic algae consisted of 37 taxa from the lotic and lentic sampling stations of Gökçeada Salt Lake. Among those taxa, the most abundant and common species were the species *E. sorex* in the first half of the sampling period and *G. acuminatum* in the second half. Benthic algal composition of the Salt Lake included the common diatom species, which are resistant to the dramatic salinity variations and eutrophic conditions. This is the first study including a detailed benthic algal flora (37 taxa) of the Gökçeada Salt Lake, although Bassler-Veit et al., [31] observed four epizoic *Cocconeis placentula* varieties on the shells of *Loxoconcha elliptica* Brady.

Macroinvertebrates are reported as an important group of organisms, which are found in sediment beneath the water column and act as key components in any aquatic ecosystem [9]. Furthermore, the invertebrate communities of the Salt Lake wetlands are more diverse than expected [47]. In this study of the aquatic invertebrates, a total of 23 macrobenthic species from lotic and lentic biotopes and 131 species from the marine biotope were identified. The station TK1 was found to be the richest location with 15 taxa during the sampling period while the highest taxa were found in the autumn sampling with 16 taxa found in the lake. Oligochaeta was found predominantly at the station TK1, related to its freshwater feature. *Gammarus komareki,* Amphipoda, usually known from unpolluted water resources, was not found in the station TK1. In this study, Isopoda was presented by the species *Asellus aquaticus,* commonly known from freshwater ecosystems, and the species *Idothea baltica,* known from brackish waters. Chironomidae was a dominant group in the lake with 5 taxa. Two species *Chironomus plumosus* and *C. riparius* are known as indicator species for eutrophic ecosystems [48]. The low individual numbers belonging to

Odonata and Ephemeroptera supported the findings on organic loads. In this study, we observed only two species belonging to Odonata nymphs (*Crocothemis erythraea* and *Ischnura elegans*) and two taxa belonging to Ephemeroptera (Coenagrienidae and *Baetis* sp.). The other specimens belong to popular indicator groups for wetland ecosystems like Plecoptera and Trichoptera, which were not observed in the sampled aquatic ecosystem. These groups are known from nonpolluted areas. The results belonging to the benthic macro invertebrates in the lake show that the organic load entering the lake should be controlled. In the previous Gökçeada Salt Lake study, three Gastropod species (*Hydrobia ulvae, Bittium latreilli,* and *Bittium* sp.) and two Bivalve species (*Cerastoderma glaucum, Scrobicularia plana*) were reported [31]. In our current study, only two taxa belong to Gastropoda (Bithynidae and Planorbiidae) are being reported. Many shells of Ostracoda were observed in the study area, but they were not evaluated quantitatively.

Viaroli et al. [49] emphasizes the lack of information comprising the relationship between river–wetland connectivity as a driver of zooplankton and macroinvertebrate communities. This study includes macroinvertabrates but zooplankton could not be studied which are often neglected in wetland studies [49]. Also, Brraich and Kaur [9] indicate that moderately polluted wetlands affect the occurrence of benthic macroinvertebrates.

Gönülal and Güreşen [24] reported 685 marine species from Gökçeada Island, except Peracarida and Polychaeta groups. Although only 131 species were found in this study due to the small sampling area and small tools, 71 species of them are newly recorded for marine fauna of Gökçeada Island.

In addition, 4 fishes, 12 reptilian species and 3 amphibian species were observed in the study area. According to the literature [26-29], 14 reptile species (3 turtles, 3 lizards, 8 snakes) are known from Gökçeada. But, 2 of those reptile species, *Emys orbicularis, Montivipera xanthina* species are not found in Salt Lake. A total of 143 bird species [30] and 178 bird species [32] were reported in Gökçeada. There is no detailed ornithological study at the Salt Lake. In this study, 71 bird species were observed during the sampling period. In fact, flamingos can be observed all year (except during the lake's dry season). However, human activities such as hunting, surfing and mud baths have negative effects on this area, preferred by flamingos. Almost 50 dead flamingos were also recorded during the bird watching.

Sulaiman et al. [8] reported that bird abundance and diversity is fundamentally affected by attributes of wetland size and type. Datry et al. [50] mentioned that the habitat mosaics, including the lotic, lentic and terrestrial, should make scientists responsible for integrating the concepts, understanding these ecosystems and managing them. In this sense, this study contributes to this opinion and includes marine wetland habitats. This study builds upon the central concept in ecology of disturbance, which is widely known to affect from populations to ecosystems [52].

Even though the present study reported a rich biodiversity despite the current human impacts in the Gökçeada Salt Lake, the area urgently needs protection through an effective conservation and management due to its importance to the island's biodiversity. Pollution may lead to the elimination of some macrobenthos while some may remain abundant due to higher tolerance to new conditions. Coastal areas have a high value in terms of biodiversity. Furthermore, these areas have a great appeal for tourism with potential for "eco-tourism." Therefore, wetlands are in a difficult situation stuck between ecological and management processes. Pérez-Ruzafa et al. [11] recommend developing close contact between researches and municipalities. Consequently, the composition of the communities in Gökçeada Salt Lake Wetland is a reflection of the health of the overall area. We hope this information can be used to design further strategies on conservation and management programmes. For a sustainable ecosystem, a management plan will be necessary in light of scientific wetlands research. As a conclusion, wetlands which are known as the most sensitive areas for biological diversity in the world, need to be protected by humans.

ACKNOWLEDGEMENTS

This research has been financially supported by TUBITAK (Project No: 115Y457). The authors wish to thank Bekir Bektas and Ozan Guresen who helped for sampling.

REFERENCES

[1] Verones, F., Pfister, S., van Zelm, R., Hellweg, S. (2017) Biodiversity impacts from water consumption on a global scale for use in life cycle assessment. The International Journal of Life Cycle Assessment. 22(8), 1247-1256.

[2] Anbuchezhian, R., Rameshkumar, G., Ravichandran, S. (2009) Macrobenthic composition and diversity in the coastal belt of Thondi, southeast coast of India. Global J. Environ. Res. 3(2), 68–75.

[3] Sharma, C., Rawat, J. S., (2009) Montoring of aquatic macroinvertebrates as bioindicator for assessing the health of wetlands: A case study in the central Himalayas, India. Ecol. Indic. 9, 118–128.

[4] Ahmadi, R., Mohebbi, F., Hagigi, P., Esmailly, L., Salmanzadeh, R. (2011) Macroinvertebrates in the wetlands of the Zarrineh estuary at the south of Urmia Lake (Iran). Int. J. Environ. Res. 5(4), 1047–1052.
[5] Hazarika, L.P. (2013) Diversity indices of macroinvertebrates in the Satajan Wetland of Lakhimpur District, Assam. Ann. Biol. Res. 4(8), 68–72.
[6] Jurua, K.T., Pagel, I.A., Tavares, V.E., Sosinski, L.T.W. (2014) Structure and composition of the benthic macroinvertebrate community on wetland and irrigated rice cultivation. Acta Limnologica Brasiliensia. 26(3), 229-234.
[7] Patial, P., Hassan, M.A., Mishra, A.P. (2015) Macrobenthic diversity during pre and post drought period of floodplain wetlands in Vaaishali district of Bihar. Int. J. Appl. Biol. Pharm. Technol. 6(2), 294–298.
[8] Sulaiman, I.M., Abubakar, M.M., Ringim, A.S., Apeverga, P.T., Dikwa, M.A. (2015) Effects of wetlands type and size on bird diversity and abundance at the Hadejia-Nguru wetlands, Nigeria. International J. of Research Studies in Zoology. 1(1), 15-21.
[9] Brraich, O.S., Kaur, R. (2017) Temporal composition and distribution of benthic macroinvertebrates in wetlands. Current Science. 112(1), 116-125.
[10] Çamur-Elipek, B., Kırgız, T. (2011) The Evaluation of Some Limnological Features of the Lagoon Lakes in European Part of Turkey. In: Biology, Man-agement and Environmental Impact (Editor: Friedman, A.G.) Nova Science Publishers, Inc. Hauppauge, N.Y., USA, 493 pp.
[11] Pérez-Ruzafa, A., Marcos, C., Pérez-Ruzafa, I.M. (2011) Mediterranean coastal lagoons in an ecosystem and aquatic resources management context. Physics and Chemistry of the Earth Parts AB, 36, 160–166.
[12] Yerli, S. (1999) Türkiye Lagünlerine Genel Bir Bakış. In: Demirsoy, A. (Ed.) Genel ve Türkiye Zoocoğrafyası. Ankara, Türkiye, Metaksan press., 465-474.
[13] Sıvacı, E. R., Çankaya, E., Kılınç, S., Dere, Ş. (2008) Seasonal assessment of epiphytic diatom distribution and diversity in relation to environmental factors in a karstic lake (Central Turkey). Nova Hedwigia. 86(1-2), 215-230.
[14] Williams, M. (1990) Wetlands: A Threatened Landscape. Cambridge and Oxford, England, Blackwell Press. 432 pp.
[15] Görmez, K. (1997) Çevre Sorunları ve Türkiye. Ankara, Turkey, Gazi Kitabevi Press, 88p.
[16] Arı, Y. (2006) The Ramsar Convention on Wetlands: A Critical Review. Doğu Coğrafya Dergisi, 11(15), 275-302.
[17] Anonymous (2012) Gökçeada Lagoon. T.C. Ministry of Forest and Water Affairs. General Directorate of Nature Conservation and Natioanal Parks. Department of Sensitive Areas. Çanakklae, Turkey, Çanakkale Branch Office Press. 88p.
[18] Seçmen, Ö., Leblebici, E. (1978) Gökçeada ve Bozcaada Adalarının Vejetasyon ve Florası II-Flora Bitki. 5(3), 271-368.
[19] Gülen, D. (1985) The species and distribution of the group Podocopa (Ostracoda-Crustacea) in the fresh waters of western Anatolia. Istanbul Üniversitesi Fen Fakültesi Mecmuasi (B). 50, 65-80.
[20] Balık, S., Ustaoğlu, M.R. (1993) A preliminary investigation on freshwater fauna of Gökçeada (Imroz) Island. Biologia Gallo-Hellenica, 20(1), 299-303.
[21] Özkan, N. (2006) The larval Chironomidae (Diptera) fauna of Gökçeada (Imbroz). G.U. Journal of Science. 19(2), 69-75.
[22] Ketmaier, V., Pirollo, D., De Matthaeis, E., Tiedemann, R., Mura, G. (2008) Large-scale mitochondrial phylogeography in the halophilic fairy shrimp Phallocryptus spinosa (Milne-Edwards, 1840) (Branchiopoda: Anostraca). Aquatic Sciences. 70(1), 65-76.
[23] Mura, G., Özkütük, S.R., Aygen, C., Cottarelli, V. (2011) New data on the taxonomy and distribution of anostracan fauna from Turkey. J. Biol Res-Thessalon. 15, 17-23.
[24] Gönülal, O., Güreşen, S.O. (2014) A list of macrofauna on the continental shelf of Gökçeada Island (northern Aegean Sea) with a new record (Gryphus vitreus Born, 1778) (Brachiopoda, Rhynchonellata) for the Turkish seas. Journal of Black Sea/Mediterranean Environment. 20(3), 228-252.
[25] Isinibilir Okyar, M., Martell, L., Topçu, E.N., Yilmaz, I.N., Piraino, S. (2015) First inventory of the shallow-water benthic hydrozoan assemblages of Gökçeada Island (northern Aegean Sea). Italian Journal of Zoology. 82(2), 281-290.
[26] Başoğlu, M., Baran, İ. (1980) Türkiye Sürüngenleri, Kısım II: Yılanlar. Bornova, İzmir, Ege Üniv. Fen-Fak. Press. 218p.
[27] Baran, İ. (1981) Kuzey Ege Denizi, Marmara Denizi ve Karadeniz'deki adalarımızın herpeto faunasının taksonomik ve ekolojik araştırılması. Doğa Bil. Der. 5, 155-162.
[28] Broggi, M.F. (1999) Notizen zur herpetofauna der Ägäisinsel Gökçeda. Herpetozoa, 12(1-2), 73-78.
[29] Habiboğlu, K. Çiçek, K., Tok, C.V. (2016) A case of melanism in the Grass snake, Natrix natrix (L., 1758) (Reptilia: Colubridae) from Gökçeada (Imbros) Turkey. Biharean Biologist. 10(1), 60-61.

[30] Sevim, İ. (2007) Observations on bird populations and habitat relations of islands in Çanakkale (Master Thesis). 18 Mart University, Çanakkale, Turkey.
[31] Bassler-Veit, B., Barut, I.F., Meric, E., Avsar, N., Nazik, A., Kapan-Yeşilyurt, S., Yildiz, A. (2012) Distribution of microflora, meiofauna, and macrofauna assemblages in the hypersaline environment of northeastern Aegean Sea coasts. J. Coast. Res. 29(4), 883-898.
[32] Samsa, Ş. (2014) Gökçeada'nın kuşları. In: Öztürk, B., Pazarkaya, Y. (Eds.) Gökçeada Doğa ve Kültür Varlıkları. İstanbul, Turkiye, pp. 155-180.
[33] Round, F.E. (1953) An investigation of two benthic algal communities in Malharm Tarn, Yorkshire. Jour. of Ecol. 41, 174–197.
[34] Sládečkova, A. (1962) Limnological investigation methods for the periphyton (aufwsuchn) community. Bot. Rev. 28, 286–350.
[35] Guillard, R.R.Y. (1978) Counting slides. In: Sournia, A. (Ed.) Phytoplankton manual. Paris, France, UNESCO Press. 182-189.
[36] Aysel, V. 2005. Check-List of the Freshwater Algae of Turkey. Journal of the Black Sea/Mediterranean Environment, 11(1),1-124.
[37] Guiry, M.D. & Guiry, G.M. 2018. AlgaeBase. World-wide electronic publication, National University of Ireland, Galway. http://www.algaebase.org; searched on 27 February 2018.
[38] Brinkhurst, R.O., Jamieson, B.G.M. (1971) Aquatic Oligochaeta of the World. Toronto, Canada, University of Toronto Press. 860p.
[39] Karaman, G.S., Pinkster, S. (1977a) Freshwater *Gammarus* species from Europe, North Africa and adjacent regions of Asia (Crustacea, Amphipoda) Part I *Gammarus pulex*-group and related species. Bijdr Dierkd. 47, 1-97.
[40] Karaman, G.S., Pinkster, S. (1977b) Freshwater *Gammarus* species from Europe, North Africa and adjacent regions of Asia (Crustacea, Amphipoda) Part II *Gammarus roeseli*-group and related species. Bijdr Dierkd. 47, 165-196.
[41] Karaman, G.S., Pinkster, S. (1987) Freshwater *Gammarus* species from Europe, North Africa and adjacent Regions of Asia (Crustacea-Amphipoda) Part III *Gammarus balcanicus*-group and related species. Bijdragen Tot de Dierkunde. 57, 207-260.
[42] Wetzel, M.J., Kathman, R.D., Fend, S.V., Coates, K.A. (2000) Taxonomy, systematics, and ecology of freshwater Oligochaeta. In: Workbook prepared for North American Benthological Society Technical Information Workshop, 48th Annual Meeting, Keystone Resort, CO., 120p.
[43] Çamur, B., Kırgız, T. (2000) Freshwater Isopod Species (Crustacea) in Turkish Thrace and Their Distribution. Turkish Journal of Zoology, 24, 17-22.
[44] Hacet, N., Çamur-Elipek, B., Kırgız, T. (2009) A study on the Odonate larvae of Turkish Thrace: with larval identification keys to the considered taxa. Journal of the Entomological Research Society. 12(2), 57-74.
[45] WoRMS (2017) World Register of Marine Species. Available. Retrieved from http://www.marinespecies.org.
[46] Karadeniz, N., Tırıl, A., Baylan, E. (2009) Wetland management in Turkey: problems, achievements and perspectives. African Journal of Agricultural Research. 11, 1106-1119.
[47] Jones, S.M., Pinder, A.M., Sim, L.L., Halse, S.A. (2009) Evaluating the conservation significance of inundated basin wetlands within the Avon Natural Resource Management region: Stage Three Assessment Method. Prepared for the Avon Catchment Council by the Department of Environment and Conservation, Perth.
[48] Armitage, P.D., Cranston, P.S., Pinder, L.C.V. (1995) The Chironomidae: Biology and Ecology of Non-Bitting Midges. London, England, Chapmann and Hall Press. 572p.
[49] Viaroli, P., Bartoli, M., Vymazal, J. (2016) Preface: Wetlands biodiversity and processes—tools for conservation and management. Hydrobiologia. 774(1), 1-5.
[50] Datry, T., Larned, S. T., Tockner, K. (2014) Intermittent rivers: a challenge for freshwater ecology. BioScience. 64(3), 229-235.
[51] Epler, J.H. (2001) Identification manual for the larval Chironomidae (Diptera) of North and South Carolina. Crawfordwille press. 53p.
[52] Rosset, V., Ruhi, A., Bogan, M. T., Datry, T. (2017) Do lentic and lotic communities respond similarly to drying? Ecosphere. 8(7), e01809.

Received: **18.9.2017**
Accepted: **12.02.2018**

CORRESPONDING AUTHOR

Herdem Aslan
Department of Fisheries Technology,
Gokceada School of Applied Sciences,
Canakkale Onsekiz Mart University,
Canakkale – Turkey

e-mail: asherdem@comu.edu.tr

© by PSP Volume 27 – No. 5/2018 pages 2867-2872 Fresenius Environmental Bulletin

THE INFLUENCE OF SOIL PROPERTIES AND PLANT SPECIES' COMPOSITION ON METAL UPTAKE BY VEGETATION ON FALLOW LAND

Jan Zarzycki[1,*], Agnieszka Petryk[2]

[1]Department of Environmental Engineering and Land Surveying, University of Agriculture in Krakow, 30-059 Krakow, Poland
[2]Department of Public Economy and Administration, Cracow University of Economics, 31-510 Krakow, Poland

ABSTRACT

Soils located in the Jaworznicko-Chrzanowski Industrial District in Southern Poland have been contaminated with heavy metals due to mining and processing of non-ferrous metals. The aim of the study was to evaluate the uptake of copper, cadmium, zinc and lead by vegetation on fallow land as a function of soil parameters and species composition of plant communities. The research revealed no correlation between bioaccumulation factor and botanical composition. The main soil parameters affecting the bioaccumulation factor depended on the metal and these were as follows: organic matter and soil reaction for cadmium, organic matter and electrolytic conductivity for lead and soil reaction for copper. The content of the metal in the soil did not affect the bioaccumulation factor only in the case of cadmium. It was the single significant factor in the case of zinc. No impact of granulometric fraction on the bioaccumulation factor was observed.

KEYWORDS:
bioaccumulation factor, vegetation, heavy metals, fallow land

INTRODUCTION

In recent decades, there has been a significant increase in awareness of toxic effects of heavy metal soil contamination on human health and ecosystem functioning [1, 2]. In contrast to organic contaminants, heavy metals cannot be degraded and thus remain in the soil [3]. In addition, metals accumulate in the food web [4]. There are many areas that were contaminated in the past, and the removal of such contaminants is extremely difficult or even impossible, especially when it applies to vast areas [2]. Therefore, the assessment of soil contamination with heavy metals is currently being addressed by the institutions involved in environmental protection [5, 6]. A variety of methods utilised to determine the absorbable metal content in the soil have been developed [1, 7]. However, the metal content itself does not provide full information on mobility or bioavailability, and therefore it is not sufficient to assess the degree of toxicity of these metals because that is the result of numerous geochemical and biological dependences [8, 9, 10]. The use of plants as bioindicators of bioavailability is an approach that takes into account all the factors. The ability of different plant species to uptake metals in the soil is diverse. For this reason, most research on metals' uptake by plants applies to individual species as indices [11, 12, 13]. The differentiation of metal content in plants is tremendous and depends on the plant species, the metal as well as the soil and climate conditions. Because of the considerable diversity of individuals in heavy metal uptake [14, 15] within the population, samples based on a small number of tested subjects might not reflect the actual influence of heavy metals on the population [16]. On the other hand, some studies did not take into account species composition at all [17, 18], which may be a considerable oversimplification. The current study adopted a different approach. Owing to the occurrence of many species with different contributions in species' composition in the studied area, and also allowing for the variability of response of individual species to soil parameters, we analysed the metals' uptake by vegetation treating the plant community as a whole, having regard to the contribution of individual species and species groups in vegetation. This approach enabled an averaged comprehensive examination of the impact of soil parameters on the absorption of heavy metals by plants.

Studies on absorption of heavy metals in relation to the content of these elements in the soil usually take place in sites where the metal content exceeds the values occurring in the natural environment by a factor of hundreds [10, 13]. Such sites, however, cover a relatively small area and can undergo remediation or may constitute protected areas due to the specific flora and fauna [19, 20]. In many regions, however, the contents of heavy metals in the soil exceed, but to a lesser extent, the permissible values. These sites typically cover larger areas and could potentially be used for agricultural purposes. The region where the research was conducted has a significant amount of fallow soil contaminated to different degrees with heavy metals. The main aim of the study was to draw up a model of heavy metal

transfer in soil–plant systems including soil parameters and species composition of the plant community to assess the degree of the risk of releasing heavy metals accumulated in the soil of former arable fields.

Numerous studies have found no significant correlation between the metal content in the soil and the soil properties with metal content in plants [8, 9, 21, 22]. In addition, the analyses based on the data used in this study showed only a weak correlation in the case of copper [23, 24, 25, 26]. Therefore, to assess the metal uptake by plants, the bioaccumulation factor (BF), which was calculated as the content of the element in the aboveground parts of plants to the total content of the element in the soil, was applied [27].

MATERIALS AND METHODS

The municipality of Trzebinia, a part of the Jaworznicko-Chrzanowski Industrial District, located in Southern Poland, was the studied area. There are deposits of non-ferrous metals in the region that are associated with the presence of carbonate Triassic rocks—ore-bearing dolomites [19]. Since the Middle Ages, they have been intensively exploited by mining and processing of ores of non-ferrous metals [28]. As a result, on the surface, several sites with a high metal content appeared. Some of these sites have been forested and some exist as disused heaps. However, many of them have been converted into meadows, pastures and arable land [29]. At the end of the 20th century, most of the arable land became fallow and the process of secondary succession began.

For the survey, former arable lands of a similar, not advanced, succession stage were selected. There, 83 research plots of 25 m^2 area each were located (5 m × 5 m). Four samples of soil material from the depth of 0–20 cm were collected from every plot. Then, they were mixed to form a collective sample. The analysis of every plot involved the determination of granulometric composition using a modified Braun–Blanquet scale to estimate plant cover. In addition, a sample of the aboveground vegetation biomass was collected combining samples from four subplots of 0.25 m^2 each.

The granulometric composition of the soil was assessed with the use of the aerometric Casagrande method modified by Prószyński. Soil aicidity (pH) was determined after extraction in water and 1 M KCl with the use of a potentiometric method. Electrolytic conductivity of the soil was established with the use of a conductometric method and the content of organic matter in soil was assessed by its annealing using the modified Tiurin method. The determination of the total content of cadmium, lead, copper and zinc in the soil was performed with the use of atomic absorption spectrometry after mineralization in a mixture of nitric(V) and chloric(VII) acids in the ratio 3:1. Vegetation samples were dry mineralized with dissolution and the contents of cadmium, lead, zinc and copper were determined by atomic absorption spectrometry. All samples were air dried and values relate to the air dry weight content.

Before the statistical analyses, variables that did not meet the condition of normality were subjected to logarithmic transformation or Bliss transformation ($y = \arcsin\sqrt{x}$) in the case of the percentage (the share of soil fractions and plant groups). Multiple regression was used to identify the major factors affecting the metals' uptake by a plant and also to create model transfer of heavy metals in soil–plant systems by taking into account the total metal content in the soil, soil pH in KCl, electrolytic conductivity of the soil, organic matter content and granulometric composition of the soil. Calculations were performed using Statistica 10 software. The diversity assessment of species composition of the vegetation was based on Detrended Correspondence Analysis (DCA), which was conducted using CANOCO ver. 4.5 software [30] as well as on the contribution of species groups divided into monocotyledonous and dicotyledonous plants.

RESULTS AND DISCUSSION

The species composition was dominated by ruderal species typical of grasslands and fallow lands [31]. DCA showed no significant correlation between species composition of vegetation on the plot and BFs for metals calculated for the plot (Table 1). There was also no significant effect ($p > 0.05$) of monocotyledonous and dicotyledonous plants' contribution to BF of any of the metals tested (Table 1). The comparison of results obtained for collective samples of biomass should, however, be carried out in plant communities of a similar nature as heavy metals' uptake in diverse communities can be significantly different [18]. For that reason, the analysis of collective samples of vegetation seemed justified.

The general physico-chemical properties of the soil (Table 2) were discussed by Petryk [23]. The content of cadmium was in the range 0.90–43.5 mg kg^{-1} (Table 2) and in many samples exceeded the permissible content of the metal in the soil (<5 mg kg^{-1}) in Poland [32]. It was, however, much lower than in the remains of historical mining sites located nearby, which reached the value of 1464 mg kg^{-1} [13].

The copper content in the soil in only one sample (177.4 mg kg^{-1}) exceeded the permissible value [32]. For this reason, it should be stated that the tested soils are not contaminated with this element [26]. The mean value amounted to 19.73 mg kg^{-1} (Table 2) with the standard for soils in Poland <100 mg kg^{-1} [32]. Really high values of Cu soil content, such as 8087 mg kg^{-1} have been reported from the

area near a Cu smelter in Slovakia [33].

Soils in the study area were considerably contaminated with lead [25]. The average lead content was 204.24 mg kg^{-1} (Table 2), while the norm for Poland is <100 mg kg^{-1}, however, the contamination of soils in the vicinity of smelters can be much higher, e.g. in northern France 4480 mg kg^{-1} [34] or the Czech Republic 4660 mg kg^{-1} [35]. Very high contamination with lead reaching even the value of 22265 mg kg^{-1} was found in the old heaps nearby [13].

The greatest range of variation among the analysed elements was found for zinc and fluctuated within the range 82.26–4594 mg kg^{-1} (Table 2) and in the case of 47 samples exceeded the permissible value of 350 mg kg^{-1} [24]. However, the content of Zn in the vicinity of smelters can be much higher, e.g. in Belgium it was 20476 mg kg^{-1} [36]. The maximum value found in postmining heaps in this region amounted to 171 790 mg kg^{-1} [13].

TABLE 1
Pearson correlation coefficient between bioconcentration factor (BF) and the first four DCA axes and the share of plant groups

					Plant group	
	AX1	AX2	AX3	AX4	Monocotyledonous	Dicotyledonous
BF_{Cd}	-0.1161	-0.3916	-0.0763	-0.0532	-0.17	-0.05
BF_{Pb}	-0.2034	-0.2104	-0.1428	-0.0558	-0.13	0.02
BF_{Zn}	-0.2007	-0.3323	-0.1937	-0.1546	-0.21	0.04
BF_{Cu}	-0.1514	-0.2988	-0.0424	-0.2610	-0.22	-0.11

TABLE 2
Physico-chemical parameters of soil and plant heavy metal contents

Variable	Min.	Lower quartile	Median	Mean	SD	Upper quartile	Max.	Variation coefficient
Organic Mat. (%)	1.33	2.86	3.75	3.82	1.44	4.54	8.10	37
pH_{KCl}	4.4	5.4	6.0	5.92	0.67	6.5	7.0	11
EC (µS cm^{-1})	32	91.3	165	175.5	98.0	234.1	464	55
Sand (%)	19	56	72	68.4	19.4	84	95	28
Silt (%)	3	11	16	22	16.6	29	74	75
Clay (%)	0	5	8	9.5	6.5	13	37	67
Total soil Cd (mg kg^{-1})	0.9	2.8	3.9	6.2	6.4	6.7	43.5	104
Total soil Pb (mg kg^{-1})	19.3	72.5	130.6	204.2	203.8	258.1	924.2	99
Total soil Zn (mg kg^{-1})	82.3	243.7	449.5	722.0	802.2	883.6	4594.0	111
Total soil Cu (mg kg^{-1})	2.6	7.9	13.0	19.7	23.8	21.8	177.4	120
Total plant Cd (mg kg^{-1})	0.15	0.45	0.76	1.09	1.31	1.29	10.20	119
Total plant Pb (mg kg^{-1})	0.62	1.32	1.65	1.93	1.11	2.29	7.60	57
Total plant Zn (mg kg^{-1})	15.6	34.4	58.3	71.8	42.0	100.9	217.0	58
Total plant Cu (mg kg^{-1})	1.36	2.46	3.06	3.45	1.40	4.30	7.40	40

TABLE 3
Bioconcentration factors—ratios between metal concentrations in plant and total metal concentrations in the soil

Variable	Minimum	Lower quartile	Median	Mean	SD	Upper quartile	Maximum	Variation coeficient
BF_{Cd}	0.03	0.08	0.15	0.27	0.28	0.37	1.36	103
BF_{Pb}	0.00	0.01	0.01	0.02	0.01	0.02	0.09	82
BF_{Zn}	0.01	0.06	0.11	0.23	0.28	0.26	1.58	125
BF_{Cu}	0.04	0.12	0.21	0.33	0.29	0.47	1.36	89

TABLE 4
Pearson correlation coefficient between bioconcentration factor and environmental variables

	CS_{Cd}	CS_{Pb}	CS_{Zn}	CS_{Cu}	M_{org}	pH_{KCl}	EC	Soil fraction		
								sand	silt	clay
BF_{Cd}	-0.48**	-0.34**	-0.47**	-0.46**	-0.56**	-0.56**	-0.60**	0.31**	-0.23**	-0.42**
BF_{Pb}	-0.67**	-0.71**	-0.70**	-0.33**	-0.56**	-0.50**	-0.47**	0.19	-0.09	-0.37**
BF_{Zn}	-0.61**	-0.54**	-0.70**	-0.43**	-0.63**	-0.72**	-0.74**	0.33**	-0.23**	-0.50**
BF_{Cu}	-0.33**	-0.14	-0.30**	-0.81**	-0.48**	-0.34**	-0.53**	0.50**	-0.46**	-0.44**

CS = Total metal concentration in soil (mg kg^{-1})

The median of BF for all the heavy metals was less than 1 (Table 3). The lowest value was calculated for lead. This is associated with low mobility of the element and with emergence of a variety of plant adaptations to limit the uptake of highly toxic metals that are unnecessary in metabolism [37]. The BF for the other metals were at a significantly higher but approximate level. The BF values were slightly lower than in the research carried out by other authors [17, 21, 38, 39] but fell into the same order of magnitude.

On the basis of Pearson's simple correlation, it was found that the BF was substantially correlated with most of the soil parameters considered except for the correlation between the BF of lead and the content of fractions of sand and silt (Table 4).

Most of the tested soil parameters were mutually correlated, and therefore multiple regression was utilised to determine the factors that significantly affected the uptake of metals by plants (Table 5) The models best described the relationship for copper (the coefficient of determination $R^2 = 0.71$) whereas for cadmium the relationship was the weakest ($R^2 = 0.45$). The developed models revealed that for all metals apart from cadmium, the total metal content in the soil was crucial. It was the only significant factor in the case of zinc. Depending on the metal, the influence of soil pH, electrolytic conductivity and organic matter on plant metal concentration was found. The share of granulometric fractions of soil was not included in the model. However, the granulometric composition may influence BF indirectly by affecting the other soil parameters.

TABLE 5
Multicorrelation models for the estimation of bioconcentration factors. In the model, only parameters with significance $p < 0.05$ were presented

Metal	Model	R^2	Significance
Cadmium	BF_{Cd} = - 0,40·Morg – 0,61·pH	0.45	0,000
Lead	BF_{Pb} = - 0,61·Morg + 0.54· EC – 0,53·C_S	0.62	0.000
Zinc	BF_{Zn} = - 1,20 – 0.37·C_S	0,70	0.000
Copper	BF_{Cu} = - 0.40·pH – 0.68·C_S	0,71	0.000

CS = Total metal concentration in soil (mg kg^{-1})

The research results confirmed the generally observed relationships between the uptake of heavy metals by plants and metal content in the soil and the impact of soil parameters. The increased BF is associated with low soil pH, lower content of metal in the soil [27, 40] and lower organic matter content. General relationships are not always accurately reflected in the research results of different authors. In many models of soil–plant systems, significance for only some parameters was found. Niesiobędzka's studies [17] demonstrated negative correlations between BF and soil reaction for copper but for the organic matter content the correlation was positive or negative depending on the region from which the sample had been collected. In turn, for lead, a positive or negative correlation with soil reaction was found. The importance of individual soil parameters may differ and depends on the plant species. Boshoff et al. [12] found that clay content in the soil had an impact on the uptake of cadmium and lead by a nettle, and the lack of such a relationship for zinc and in the case of grasses for all studied metals. On the other hand, Tack and Verloo [8] proved the influence of clay on the zinc content in nettle and the lack of such a reaction for lead, cadmium and copper.

CONCLUSIONS

The content of heavy metals in plants is a useful measure in numerous studies on bioavailability of trace metals but it must be analysed and interpreted in relation to other data, such as the concentration of the metal in the soil, the soil parameters, the type of plants or the production of biomass. The BF describes the efficiency of heavy metals' uptake by plants far better than the metal content in the plant. The BFs of cadmium, lead, copper and zinc in the vegetation of fallow land were not related to the species' composition of vegetation. Therefore, in the assessment of bioavailability of heavy metals in multispecies community of a similar type. collective samples of plant material may be utilised. Based on multiple regression, it was found that the principal soil factors affecting the BF values depended on the metal analysed. For cadmium, these were organic matter and soil pH, for lead they were organic matter and electrolytic conductivity and for copper, soil reaction. The content of the metal in the soil did not affect the BF only in the case of cadmium, and in the instance of zinc it was the single significant factor. No effect of granulometric fractions on BF was observed. The soil parameters and species composition of the vegetation did not explain unequivocally the possibility of heavy metals' uptake by plants. In each case, another parameter could be the primary factor responsible for the process. It seems that for a given metal it is not possible to develop a universal model that would represent all the parameters that affect the bioavailability of the element. Such models can only be useful locally.

ACKNOWLEDGEMENTS

The research was realized within the Project DS-3337, financed from the research grant allocated by the Polish Ministry of Science and Higher Education.

REFERENCES

[1] Szyczewski, P., Siepak, J., Niedzielski, P. and Sobczyński, T. (2009) Research on heavy metals in Poland. Pol. J. Environ. Stud. 18(5), 755-768.

[2] Kabata-Pendias, A. (2010) Trace elements in soils and plants. CRC Press, Boca Raton, London, New York, Washington, DC.

[3] Babin-Fenske, J.J. and Anand, M. (2010) Terrestrial insect communities and the restoration of an industrially perturbed landscape: assessing success and surrogacy. Restor. Ecol. 18, 73-84.

[4] Gall, J.E., Boyd, R.S. and Rajakaruna, N. (2015) Transfer of heavy metals through terrestrial food webs: a review. Environ. Monit. Assess. 187(4), 201.

[5] Kördel, W., Bernhardt, C., Derz, K., Hund-Rinke, K., Harmsen, J., Peijnenburg, W., Comans, R. and Terytze, K. (2013) Incorporating availability/bioavailability in risk assessment and decision making of polluted sites Germany as example. J. Hazard. Mater. 261, 854-862.

[6] Harmsen, J. and Naidu, R. (2013) Bioavailability as a tool in site management. J. Hazard. Mater. 261, 840-846.

[7] Melo, V.F., Batista, A.H., Gilkes, R.J. and Rate, A.W. (2016) Relationship between heavy metals and minerals extracted from soil clay by standard and novel acid extraction procedures. Environ. Monit. Assess. 188, 668.

[8] Tack, F. and Verloo, M. (1996) Metal contents in stinging nettle (Urtica dioica L) as affected by soil characteristics. Sci. Total. Environ. 192, 31-39.

[9] Smolders, E., Oorts, K., van Sprang, P., Schoeters, I., Janssen, C.R., McGrath, S.P. and McLaughlin, M.J. (2009) Toxicity of trace metals in soil as affected by soil type and aging after contamination: using calibrated bioavailability models to set ecological soil standards. Environ. Toxicol. Chem. 28, 1633-1642.

[10] Remon, E., Bouchardon, J.L., Le Guedard, M., Bessoule, J.J., Conord, C. and Faure, O. (2013) Are plants useful as accumulation indicators of metal bioavailability? Environ. Pollut. 175, 1-7.

[11] Malizia, D., Giuliano, A., Ortaggi, G. and Masotti, A. (2012) Common plants as alternative analytical tools to monitor heavy metals in soil. Chem. Cent. J. 6(2), S6.

[12] Boshoff, M., De Jonge, M., Scheifler, R. and Bervoets, L. (2014) Predicting As, Cd, Cu, Pb and Zn levels in grasses (Agrostis sp. and Poa sp.) and stinging nettle (Urtica dioica) applying soil-plant transfer models. Sci. Total. Environ. 493, 862-871.

[13] Wójcik, M., Sugier, P. and Siebielec, G. (2014) Metal accumulation strategies in plants spontaneously inhabiting Zn-Pb waste deposits. Sci. Total. Environ. 487, 313-322.

[14] Devetakovic, J., Stankovic, D., Ivetic, V., Sijacic-Nikolic, M., Maksimovic, Z. (2016) Potential of different European white elm (Ul-mus laevis Pall.) genotypes for phytoextraction of heavy metals. Fresen. Environ. Bull. 25, 4318-4323.

[15] Orcen, N. (2017) Stomatal parameters and growth responses of Nicotiana and *Atriplex* to Cd, Pb and Cd – Pb -contaminated soil. Fresen. Environ. Bull. 26, 6340-6345.

[16] Ernst, W.H.O., Verkleij, J.A.C. and Vooijs, R. (1983) Bioindication of a surplus of heavy metals in terrestrial ecosystems. Environ. Monit. Assess. 3(3-4), 297-305.

[17] Niesiobędzka, K. (2012) Transfer of copper, lead and zinc in soil-grass ecosystem in aspect of soils properties in Poland. B. Environ. Contam. Tox. 88(4), 627-633.

[18] Roggeman, S., van den Brink, N., Van Praet, N., Blust, R. and Bervoets, L. (2013) Metal exposure and accumulation patterns in free-range cows (Bos taurus) in a contaminated natural area: Influence of spatial and social behavior. Environ. Pollut. 172, 186-199.

[19] Jędrzejczyk-Korycińska, M. (2009) Obszary dawnej eksploatacji złóż cynkowo-ołowiowych - ich bogactwo florystyczne a możliwości ochrony. Problemy Ekologii Krajobrazu. 24, 71-80.

[20] Szarek-Łukaszewska, G. and Grodzińska, K. (2011) Grasslands of a Zn-Pb post-mining area (Olkusz Ore-bearing Region, S Poland). Polish Botanical Journal. 56(2), 245-260.

[21] Lopes, C., Herva, M., Franco-Uria, A. and Roca E (2012) Multicorrelation models and uptake factors to estimate extractable metal concentrations from soil and metal in plants in pasturelands fertilized with manure. Environ. Pollut. 166, 17-22.

[22] Jusufi, K., Stafilov, T., Vasjari, M., Korca, B., Halili J., Berisha, A. (2017) Measuring the presence of heavy metals and their bioavailability in potato crops around Kosovo`s power plants. Fresen. Environ. Bull. 26, 1682-1686.

[23] Petryk, A. (2016) Assessment of the content of heavy metals in plants and soil in the area of the Trzebinia municipality, Poland 1 Cadmium. Infrastructure and Ecology of Rural Areas. IV(1), 1243-1256.

[24] Petryk. A. (2016) Assessment of the content of heavy metals in plants and soil in the area of the Trzebinia municipality, Poland 2 Zinc. Infrastructure and Ecology of Rural Areas. IV(3), 1581-1592.

[25] Petryk, A. (2016) Assessment of the content of heavy metals in plants and soil in the area of the Trzebinia municipality, Poland 3 Lead. Infrastructure and Ecology of Rural Areas. IV(3), 1689-1702.
[26] Petryk, A. (2016) Assessment of the content of heavy metals in plants and soil in the area of the Trzebinia municipality, Poland 4 Copper. Infrastructure and Ecology of Rural Areas. IV(4), 1711-1721.
[27] Mirecki, N., Agič, R., Šunić, L., Milenković, L., Ilić, Z.S. (2015) Transfer factor as indicator of heavy metals content in plants. Fresen. Environ. Bull. 24, 4212-4219.
[28] Godzik, B. and Woch, M. (2015) History of mining in the Olkusz region. In: Godzik, B. (ed.) Natural and historical values of the Olkusz Ore-bearing Region. Szafer Institute of Botany, Polish Academy of Sciences, Kraków. 29-36.
[29] Stefanowicz, A.M., Woch, M.W. and Kapusta, P. (2014) Inconspicuous waste heaps left by historical Zn-Pb mining are hot spots of soil contamination. Geoderma. 235-236, 1-8.
[30] ter Braak, C.J.F. and Smilauer, P. (2002) Canoco Reference manual and CanoDraw for Windows users guide: Software for Canonical Community Ordination (version 45). Microcomputer Power (Ithaca NY USA)
[31] Petryk, A. (2016) Species composition of vegetation cover in the fallow lands in the area of the Trzebinia municipality. Infrastructure and Ecology of Rural Areas. IV(2), 1399-1409.
[32] Journals of Laws (Dziennik Ustaw) (2002) Nr 165. poz.1359. Rozporządzenie Ministra Środowiska z dnia 4 października 2002 r. w sprawie standardów jakości gleb i jakości ziemi. http://isap.sejm.gov.pl/DetailsServlet?id=WDU20021651359.
[33] Bigalke, M., Weyer, S., Kobza, J. and Wilcke, W. (2010) Stable Cu and Zn isotope ratios as tracers of sources and transport of Cu and Zn in contaminated soil. Geochim. Cosmochim. Ac. 74, 6801-6813.
[34] Denaix, L., Semlali, R.M. and Douay, F. (2001) Dissolved and colloidal transport of Cd, Pb, and Zn in a silt loam soil affected by atmospheric industrial deposition. Environ. Pollut. 113, 29-38.
[35] Rieuwerts, J.S., Farago, M.E., Cikrt, M. and Bencko, V. (2000) Differences in lead bioavailability between a smelting and a mining area. Water, Air Soil Pollut. 122, 203-229.
[36] Nachtegaal, M., Marcus, M.A., Sonke, J.E., Vabgronsveld, J., Livi, K.J.T., van der Lelie, D. and Sparks, D.L. (2005) Effects of in situ remediation on the speciation and bioavailability of zinc in a smelter contaminated soil. Geochim. Cosmochim. Ac. 69, 4649-4664.
[37] Broyer, T.C., Johnson, C.N. and Paull, R.E. (1972) Some aspects of lead in plant nutrition. Plant. Soil. 36, 301-313.
[38] Efroymson, R.A., Sample, B.E. and Suter, G.W. (2001) Uptake of inorganic chemicals from soil by plant leaves: regressions of field data. Environ. Toxicol. Chem. 20, 2561-2571.
[39] Malinowska, E., Sosnowski, J., Jankowski, K. (2017) Accumulation of some heavy metals by herb plants growing in fields with ponds. Fresen. Environ. Bull. 26, 2156-2162.
[40] Cule, N., Vilotic, D., Nesic, M., Veselinovic, M., Drazic, D., Mitrovic, S. (2016) Phytoremediation potential of Canna indica L. in water contaminated with lead. Fresen. Environ. Bull. 25, 3728-3733.

Received: **21.9.2017**
Accepted: **24.01.2018**

CORRESPONDING AUTHOR

Jan Zarzycki
Faculty of Environmental Engineering and Land Surveying
University of Agriculture in Krakow
30-059 Kraków – Poland

e-mail: j.zarzycki@ur.krakow.pl

© by PSP Volume 27 – No. 5/2018 pages 2873-2877 Fresenius Environmental Bulletin

THE EFFECT ON K, Na, AND Cl CONTENT IN STEM AND ROOT OF *AGROPYRON* SPECIES UNDER DIFFERENT SALT CONCENTRATIONS

Nur Koc*, Ramazan Acar

Selcuk University, Faculty of Agriculture, Department of Field Crops, Konya, Turkey

ABSTRACT

Salinity is a predominant problem in many arid regions of the world. Plant development in these regions is negatively affected by the high salt ion concentrations which have accumulated in the rhizosphere. This research aimed to determine the effects various salt concentrations (Control, 5, 10 and 15 EC dS m^{-1} NaCl) have on three species of wheatgrass [crested wheatgrass *(Agropyron cristatum),* desert wheatgrass (*A. desertorum),* and tall wheatgrass (*A. elongatum*)] located in the Central Anatolian drought rangelands. The K%, Na% and Cl% content in the stems and the roots of these *Agropyron* species were determined at each stage of growth until seed production. The potassium uptake increased with salt application, most especially for the tall wheatgrass species. The maximum Na% content recorded (i.e. 0.51%) was in the stem of tall wheatgrass at a salt concentration of 10 EC dS m-1 NaCl; the minimum Na% recorded was for crested wheatgrass (i.e. 0.06 %) in the control group. It was determined that tall wheatgrass was more tolerant to salinity in regard to the other *Agropyron* species. Furthermore, with respect to literature, results indicated desert wheatgrass to be a much more salt tolerant species.

KEYWORDS:
Salinity, Crested Wheatgrass [*Agropyron cristatum* (L.) Gaernt], Dessert Wheatgrass [*A. desertorum* (Fisch. ex Link) Schult], Tall Wheatgrass [*A. elongatum* (Host) P. Beauv.]

INTRODUCTION

About 1.5 million ha of Turkey's soils have salinity and alkalinity problems. One-third of these salt affected areas are located in the Konya Closed Basin [1, 2]. Salinity, which is often seen in arid and semi-arid regions, causes decreases in quality and yield in crops by negatively affecting their growth and development. A high influx of available salt ions due to an excess of dissolved salts in the rhizosphere, is one of the main reasons for salt stress seen in plants [3]. Under salt stress, the high salt concentrations in the soil compete with other available plant nutrients in the solution for uptake. This leads to insufficient uptake of vital plant nutrients causing not only, adverse morphological and physiological changes, but also causes plant nutrient deficiencies [4]. For this reason, it is crucial to determine salt tolerant plants which can obtain significant yields under high salinity conditions and can provide an economic yield in these areas [5].

Agropyron species can naturally grow in areas having salinity problems such as those of the Central Anatolian drought rangelands [6]. The *Agropyron* genus show a variety of salt tolerant species which differ in their forage value [7, 8]. While there is research which has focused on the salt ion accumulation in the whole plant under varying salt concentrations, research which has concentrated instead on salt ion uptake and accumulation (e.g. K, Na, Cl, etc.) in plant parts like the root, stem, young and older leaves, provides a more comprehensive understanding of salt ion distribution and tolerance under varying salinity conditions [9, 10, 11, 12, 13, 14, 15]. Therefore, this research was carried out with the aim of investigating alterations in uptake of K, Na, and Cl of the root and stem of three *Agropyron* species: tall wheatgrass, desert wheatgrass, and crested wheatgrass, and their growth at different salt concentrations.

MATERIALS AND METHODS

In this study, seeds of tall wheatgrass, desert wheatgrass, and crested wheatgrass were used. Trials were conducted in the Plant Breeding Greenhouse Department of Field Crops of the Faculty of Agriculture at Selcuk University. Seeds were planted in pots with three replications in a Completely Randomized Design on the 21st of October 2015. The dimensions of the pots were 30 x 30 cm, and in each pot six plants were grown. Turf was used as the planting medium, and had a pH 5.5-6.5; a fertilizer ratio of 0.30 g l^{-1}; a N content 30-70 mg l^{-1}; a P_2O_5 content of 30-70 mg l^{-1} and K_2O content of 40-80 mg l^{-1}. The turf had a degree of dissociation between H2-H8; a porosity weight of 96 %, a moisture content between 40 and 50 %, and an Electrical Conductivity between 0.12 and 0.22 dS m^{-1}.

The first irrigation with salt concentrations [i.e. control (0 dS m^{-1} NaCl), 5, 10 and 15 dS m^{-1} NaCl] was made on the 3rd of December 2015 when tillering occurred in the three *Agropyron* species. Once per week, one liter salt concentration solutions were given to each *Agropyron* species. While the harvest date of crested wheatgrass and desert wheatgrass occurred on the 16th of May 2016, because of tall wheatgrass's late maturation (i.e. until the grain filling period), the harvest time occurred much later (i.e. 22nd of June 2016). During the harvest date, the crop root and stem were harvested separately. The content of K, Na, and Cl of the root and stem were determined as a percent.

ELEMENTAL ANALYSIS

Determination of K and Na. 0.2 mg of dry plant matter was weighed and placed into a plastic liner tube. 5 ml of HNO_3 and 2 ml of H_2O_2 were added to each tube. The digesting process was done in the MARSX Press Microwave. Once fragmented the material was transferred to a 50mL plastic tube, and ultra-distilled water was added until a volume of 20 ml was obtained. Afterwards, the solution was filtered and each sample transferred to be analyzed using ICP-AES [13, 16].

Determination of Cl. 0.10 g of dry granulated plant matter was weighed and placed into a plastic tube. 25 ml of ultra-distilled water was added and the sample was later shaken for 10 minutes in a rinsing machine. Samples were subsequently centrifuged using the N-Biotek Combi-Shaker (NB-101MT) at 4000 cycles per min. Following centrifuging, 20 ml aliquot from the supernatant was place into a porcelain capsule and 1 ml of the indicator potassium chromate was added. Samples were titrated with a standard silver nitrate ($AgNO_3$) solution until a visible reddish-brown coloration appeared. Blank samples for comparison were prepared using only ultra-distilled water. The Cl % was calculated using the formula below [17].

$$\text{Cl Extracted From Plant (\%)} = \frac{\text{S} - \text{B}}{\text{A}} X\ 100$$

S: Amount of Standard $AgNO_3$ Solution Used in Sample Titration (ml)
B: Amount of Standard $AgNO_3$ Solution Used in Blank Titration (ml)
A: Amount of Plant Sample (mg)

All averages were grouped and the statistical analysis of all parameters investigated was done by using the statistical software package MSTAT-C.

TABLE 1
Mean values and each group's results belonging to K (%), Na (%) and Cl (%) content in the stems and the roots of *Agropyron* species under different salt concentration

Agropyron Species	Salt Concentrations (EC dS m^{-1} NaCl)	The Content in Roots			The Content in Stems		
		K (%)	Na (%)	Cl (%)	K (%)	Na (%)	Cl (%)
A. cristatum **(Crested Wheatgrass)**	Control	0,97 ^{C}	0,16 ^{K}	0,29 ^{G}	1,13 ^{H}	0,06 ^{L}	0,18 ^{G}
	5	1,01 ^{B}	0,20 ^{H}	0,44 ^{E}	1,34 ^{F}	0,11 ^{J}	0,18 ^{G}
	10	**1,17** ^{A}	0,31 ^{F}	0,44 ^{E}	1,30 ^{G}	0,26 ^{E}	0,50 ^{B}
	15	0,70 ^{G}	0,38 ^{C}	0,18 ^{I}	1,38 ^{E}	0,38 ^{D}	0,17 ^{H}
	Mean	**0,96** ^{A}	**0,26** ^{B}	**0,34** ^{C}	**1,28** ^{B}	**0,20** ^{B}	**0,26** ^{B}
A. desertorum **(Desert Wheatgrass)**	Control	0,89 ^{D}	0,19 ^{I}	0,56 ^{C}	0,85 ^{L}	0,09 ^{K}	0,26 ^{E}
	5	0,71 ^{G}	0,27 ^{G}	0,48 ^{D}	1,12 ^{I}	0,12 ^{I}	0,20 ^{F}
	10	0,56 ^{I}	0,36 ^{D}	0,18 ^{I}	1,03 ^{J}	0,20 ^{G}	0,20 ^{F}
	15	0,50 ^{J}	0,17 ^{J}	**0,73** ^{A}	0,98 ^{K}	0,21 ^{F}	0,19 ^{F}
	Mean	**0,67** ^{C}	**0,25** ^{C}	**0,49** ^{A}	**1,00** ^{C}	**0,16** ^{C}	**0,21** ^{C}
A. elongatum **(Tall Wheatgrass)**	Control	0,87 ^{E}	0,20 ^{H}	0,19 ^{H}	1,66 ^{D}	0,15 ^{H}	**0,68** ^{A}
	5	0,55 ^{I}	0,35 ^{E}	0,18 ^{I}	**2,56** ^{A}	0,45 ^{C}	0,45 ^{C}
	10	0,74 ^{F}	0,63 ^{B}	0,43 ^{F}	2,12 ^{C}	**0,51** ^{A}	0,30 ^{D}
	15	0,68 ^{H}	**0,69** ^{A}	0,58 ^{B}	2,23 ^{B}	0,49 ^{B}	0,19 ^{F}
	Mean	**0,71** ^{B}	**0,47** ^{A}	**0,35** ^{B}	**2,15** ^{A}	**0,40** ^{A}	**0,41** ^{A}
Means	Control	**0,91** ^{A}	**0,19** ^{D}	**0,34** ^{D}	**1,21** ^{D}	**0,10** ^{D}	**0,38** ^{A}
	5	**0,76** ^{C}	**0,28** ^{C}	**0,37** ^{B}	**1,68** ^{A}	**0,23** ^{C}	**0,28** ^{C}
	10	**0,82** ^{B}	**0,43** ^{A}	**0,35** ^{C}	**1,48** ^{C}	**0,32** ^{B}	**0,33** ^{B}
	15	**0,63** ^{D}	**0,41** ^{B}	**0,50** ^{A}	**1,53** ^{B}	**0,36** ^{A}	**0,18** ^{D}
	Overall Mean	**0,78**	**0,33**	**0,39**	**1,48**	**0,25**	**0,29**
CV (%)		**0,10**	**0,14**	**0,12**	**0,11**	**0,15**	**0,13**

LSD Salt concentrations (0.01)**:0.001; LSD** Agropyron species (0.01)**:0.011; LSD** Salt concentrations X Agropyron species (0.01)**: 0.002**

RESULTS AND DISCUSSIONS

Mean values and each group's results were given in Table 1. The maximum potassium content (i.e. 1.17 % K) in root was found at a salt concentration of 10 EC dS m^{-1} in crested wheatgrass. Maximum potassium content (i.e. 2.56 % K) in stem was found at a salt concentration of 5 EC dS m^{-1} salt in tall wheatgrass. While root K content decreased as salt dosage increased, the stem's K uptake however, showed a positive linear relationship amongst the three *Agropyron* species and was particularly evident for tall wheatgrass. Zhao et al. [11], Naidoo et al. [12] and Niu et al. [15] observed a decrease in K uptake with increasing salt concentrations, however our results showed an opposite effect. The three *Agropyron* species used in this research showed increases in K content with increasing salt concentrations, and this may partly be due to potassium being an essential macro element in plant water balance [18]. Potassium affects osmotic pressure in the cell by keeping water in the cell; thus, increases the plants ability to survive under stress conditions (Figure 3) [19].

Increasing salt concentration led to an increase in Na content in *Agropyron*'s root, except when the highest level of salt was applied to desert wheatgrass (Figure 1). The *Agropyron* species having the maximum Na uptake (i.e. 0.51% Na) in the stem was tall wheatgrass grown at 10 EC dS m^{-1} NaCl. Our results showed a similarity to Culha and Cakırlar [20] who stated that Na uptake in the cell was increased as the amount of NaCl given to plant increased (Figure 2).

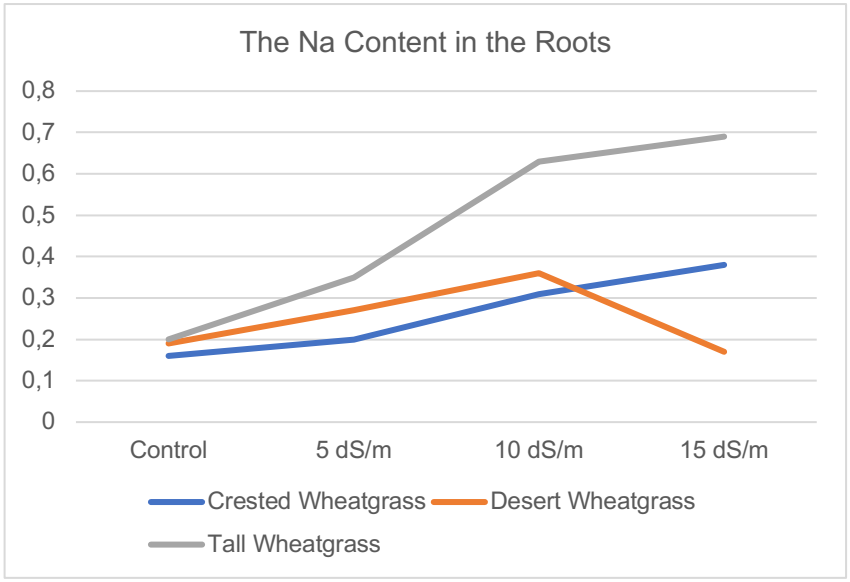


FIGURE 1
The Na content in the roots of *Agropyron* species

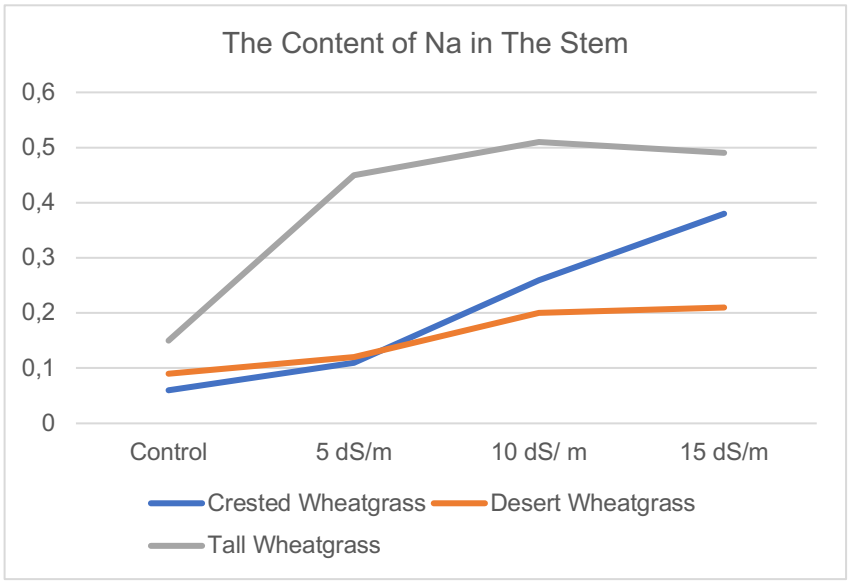


FIGURE 2
The Na content in the stems of *Agropyron* species

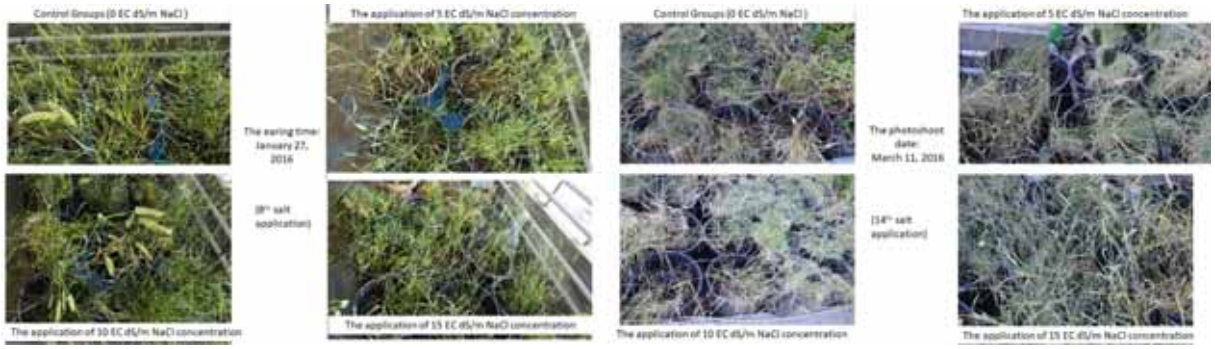


FIGURE 3
Photos belonging the research.

It was determined that desert wheatgrass grown at the highest salt concentration (15 EC dS m^{-1} NaCl) had the highest Cl content of 0.73 %. Strogonov [21] noted that toxic substances having Cl were accumulated first in the underground parts of plants in saline soils. In consideration of our findings, it can be stated that plants tried to block occurring chlorine toxicity by limiting translocation of Cl to the stems and instead accumulating chlorine in their roots.

CONCLUSIONS

Research demonstrated that forage sources such as desert wheatgrass and tall wheatgrass can be grown in salinity conditions up to 15 EC dS m^{-1} and crested wheatgrass can be grown in salinity levels at 10 EC dS m^{-1}. Thus, irrigation water which contains up to 5 EC dS m^{-1} NaCl could be recommend if the aim is for obtaining seeds from these species.

The areas of our country having the greatest salinity problem are mostly seen in rangelands. Hence, in regards to low-quality irrigation water these issues are of great concern. We recommend that plant breeding programs should emphasize on salt tolerant plants and forage crops and classify them according to their salt tolerant levels. Thus, an economic yield will be obtained in these regions as well as decrease in negative effects of salinity.

ACKNOWLEDGEMENTS

This research is financially supported by Selcuk University Coordinating Office of Academic Staff Training Program (OYP) under grant no 2015-ÖYP-078. This study has been prepared from Nur Koc's M. Sc. Thesis.

REFERENCES

[1] Topraksu. (1978) Turkiye Arazi Varlıgı. Ankara, Topraksu Genel Mudurlugu Toprak Etudleri ve Haritalama Daire Baskanligi: 55.

[2] Kanber, R. Cullu, M.A. Kendirli, B. Antepli, S. and Yilmaz, N. (2005) Sulama, drenaj ve tuzluluk. Turkiye Ziraat Muhendisligi VI. Teknik Kongresi, 3-7.

[3] Kacar, B. Katkat, V. and Ozturk, S. (2013) Bitki Fizyolojisi. Nobel Yayinları. Ankara- Turkey 493-497.

[4] Taban, S. and Katkat, A.V. (2000) Effect of salt stress on growth and mineral elements concentrations in shoots and roots of maize plants. Tarım Bilimleri Dergisi. 6(2), 119-122.

[5] Ozturk, A. (2004) Tuzluluk ve sodyumlulugun oluşumu, bitki ve topraga etkileri. Sulanan Alanlarda Tuzluluk Yonetimi Sempozyumu. 20-1.

[6] Acar, R. Koc, N. Celik S.A. and Direk, M. (2016) The Some Grasses Forage Crops Grown in Arid Rangeland of The Central Anatolian and Properties of These Plants. 3rd International Conference on Sustainable Agriculture and Environment. September 26-28, 2016. Warsaw, Poland, 347-350.

[7] Dewey, D.R. (1960) Salt Tolerance of Twenty-five Strains of Agropyron. Agronomy Journal. 52 (11), 631- 635.

[8] Sedivec, K.K. Tober, D.A. and Duckwitz, W.L. (2010) Grasses for the Northern Plains: Growth Patterns, Forage Characteristics and Wildlife Values. Volume II-Warm-Season. The NDSU Extension Service, North Dakota.

[9] Greenway, H. and Rogers, A. (1963) Growth and ion uptake of Agropyron elongatum on saline substrates, as compared with a salt-tolerant variety of Hordeum vulgare. Plant and Soil. 18(1), 21-30.

[10] Ueng, R. Lindauer, I.E. and Buss, W.R. (1994) Some Physiological Variations of Agropyron smithii Rydb. (Western Wheatgrass) At Different Salinity Levels. The Great Basin Naturalist, 54(2), 182-188.

[11] Zhao, J. Zhi, D. Xue, Z. Liu, H. and Xia, G. (2007) Enhanced salt tolerance of transgenic progeny of tall fescue (Festuca arundinacea) expressing a vacuolar Na+/H+ antiporter gene from Arabidopsis. Journal of plant physiology. 164(10), 1377-83.

[12] Naidoo, G. Somaru, R. and Achar, P. (2008) Morphological and physiological responses of the halophyte, Odyssea paucinervis (Staph) (Poaceae), to salinity. Flora Morphology, Distribution. Functional Ecology of Plants. 203(5), 437-47.
[13] Yorgancilar, M. and Yegin, Z.G. (2012) The effect of different salt concentrations on the root and stem nutrient contents of pea (Pisum sativum L. cv. Jofs). Journal of Food, Agriculture & Environment. 10(1), 605-7.
[14] Kılıc, U. Yurtseven, S. Boğa, M. and Aydemir, S. (2015) Farkli toprak tuzluluk duzeylerinin bazi bugdaygil yem bitkilerinin in vitro gaz uretimi ve yem değerleri uzerine etkisi. Toprak Bilimi ve Bitki Besleme Dergisi. 3(1), 9-15.
[15] Niu, S.Q., Li, H.R., Pare, P.W., Aziz, M., Wang, S.M., Shi, H.Z., Li, J., Han, Q.Q., Guo, S.Q., Li, J., Guo, Q., Ma, Q., Zhang, J.L. (2016) Induced growth promotion and higher salt tolerance in the halophyte grass Puccinellia tenuiflora by beneficial rhizobacteria. Plant Soil. 407(1-2), 217-230.
[16] Kacar, B. and Inal, A. (2010) Bitki Analizleri. Nobel yayinevi, Ankara. 247-248, 271.
[17] Johnson, C. and Ulrich, A. (1959) Analytical methods for use in plant analysis. California Agricultural Experiment Station. Bull. 766, 11.
[18] Kacar, B. and Katkat, V. (2007) Bitki Besleme. Nobel Yayinları, Ankara. 299-603.
[19] Armstrong, D.L. (1998) Potassium Reduces Stress from Drought, Cool Soils, and Compaction. Better Crops. 82(3), 34-36.
[20] Culha, S. and Cakırlar, H. (2011) Tuzlulugun Bitkiler Uzerine Etkileri ve Tuz Tolerans Mekanizmalari Afyon Kocatepe Universitesi Fen ve Muhendislik Bilimleri Dergisi. 11(2), 11-34.
[21] Strogonov, B. (1971) Bitkilerde Tuz Toleransinin Fizyolojik Temelleri. Izmir. Ege Universitesi Matbaası. 6-7.

Received: **02.10.2017**
Accepted: **24.01.2018**

CORRESPONDING AUTHOR

Nur Koc
Department of Field Crops,
Faculty of Agriculture,
Selcuk University, 42250,
Selcuklu, Konya – Turkey

e- mail: nurkoc@selcuk.edu.tr

© by PSP Volume 27 – No. 5/2018 pages 2878-2882 Fresenius Environmental Bulletin

SOME MICROBIOLOGICAL PROPERTIES OF ROADSIDE SOILS EXPOSED TO TRANSPORTATION POLLUTANS IN SANLIURFA'S REGION, TURKEY

Cigdem Kucuk*, Onur Baysoy

Harran University, Faculty of Arts and Science, Department of Biology, 63300 Sanliurfa, Turkey

ABSTRACT

This study investigated the effect of traffic pollutants of roadside on soil microbiological activities in Turkey's south-eastern border. The soil samples were taken from different crossroad of Şanlıurfa-Diyarbakır, Şanlıurfa-Gaziantep, Şanlıurfa-Mardin and Şanlıurfa-Akçakale where traffic is intensive. Soil samples were taken from different distances from the roadside, i.e., 1, 10, 50, 100, 150 and 250 m. Microbial respiration, catalase and urease enzyme activities, concentration of Cd and Pb, numbers of total bacteria, fungi and actinomycetes were evaluated in soil samples. According to the results of the study, exhaust gaseous causes a damage on the soil biological activities. The farther down the road, the numbers of bacteria, fungi and actinomycetes, microbial respiration, catalase and urease enzyme activities have increased. The 250 m away from the road; cadmium and lead levels and tested soil microbiological activity were increased.

KEYWORDS:
Roadside soil, Pb, Cd, urease, catalase, microorganism number

INTRODUCTION

Since the beginning of the twentieth century, in the air and soil pollution has increase occurred due to reasons such as rapid industrialization and transition to modern agriculture, a growing population and consumption [1, 2].

The demand for increased urban and industrial sources, it has brought the environmental pollution and has been dangerous situation in the living biotic factors [3]. Besides atmospheric pollution; heavy metals emitted from the exhaust gases from traffic in urban environment has been the most important environmental contaminants in human, plant and animals. The danger of falling into the organism through the food chain is very importance [4]. Heavy metals into the food chain, accumulating in living for years has been reported to cause toxic effects to create any situations that resulted in death [2]. In parallel with the growing population in developed countries, the increase occurred in vehicular traffic has also been reported to damage the environment in ecologically [5]. The number of cars per person is increasing every day. The number of motor vehicles in Turkey were found to be 17.939.447 [6].

The environmental pollution caused of lead directly related with the increased of automobiles and vehicle traffic; tetraethyl lead released from the motor vehicle is described as formed by the burning of the gasoline [2]. Heavy metals such as Pb, Hg, Cd, Ni, Cu, Zn, C and Fe are released from gasoline vehicles and metals such as Ni, Cd, Zn are released from diesel vehicles [7, 8].

Heavy metals such as Cd, Pb, Cu, Ni, Zn released from exhaust gases from internal combustion of fuel and oil additives and engine wear have been accumulated into the environment that reported in a study conducted by Lagerweff and Specht [9] and Zhang et al. [2]. A research conducted by Lenart and Wolny-Kolade [10]; concentrations of heavy metal elements such as Cu Fe, Zn, Cd, Pb, Ni and soil microbial activities were investigated in soil samples. Researchers determined that heavy metals were significantly affected the soil pH, number of the mesophilic bacteria, total fungi, *Azotobacter* sp. and actinomycetes in soils.

Sanliurfa is one of the major intersections of the road network. This road is very important in terms of transit. This route, descend to reach the border crossing to Syria in our country's south-eastern border due to take place in the transition to Arab countries highway plays an important role in transportation. This study was undertaken to assess the catalase and urease activities of soil samples, number of total microorganisms and the concentrations of Pb and Cd of roadside soils exposed to heavy traffic pollutants.

MATERIALS AND METHODS

Soil sampling and analysis. Soil samples were collected from the 0 to 15 cm depth of soil at 4 different location (1, 10, 50, 100, 150 and 250 m far away from the roadside) of Şanlıurfa-Turkey. Main

crop produced at these soils were cotton (*Gossypium hirsitum*), maize (*Zea mays* L.) and wheat (*Triticum aestivum* L.). The mean annual temperature varied from 2.2 to 38.7 ºC. Soil sampling were analysed in the same day of sample collection in September 2015. The soil samples were passed from a sieve with 2 mm and kept at 4 ºC for microbiological analysis. Soil characteristics were determined using Standard methods [11]. Soil pH was estimated using saturated soil solution (1/2.5; soil/water). Main roads, coordinates, same soil characteristics are given in Table 1.

For the concentrations of Pb and Cd; the soil samples digested with mixture of nitric and perchloric acid (2:1, ratio) and Pb and Cd concentrations of samples were determined in their extraction solution using atomic absorption spectrophotometer [11].

Microbiological analysis. To evaluate the number of colony forming units (cfu) of soil fungi (Malt Extract Agar), bacteria (Nutrient Agar) and actinomycetes (Pochan agar); the serial dilutions (from 10^{-4} to 10^{-9} for bacteria, 10^{-1} to 10^{-6} for fungi and actinomycetes) were prepared. Microorganisms numbers were determined by a spread plate count technique [12].

Microbial respiration. Basal soil microbial respiration was measured according to Anderson [13] by $Ba(OH)_2$. $8H_2O$ + $BaCl_2$ absorption of the CO_2 produced during 24 hours incubation period. 20 g of soil samples were placed in a jar with 10 ml of BaOH. Soil respiration was trapped inside the alkaline solution and titrated using a diluted HCl solution. Data were expressed as mg CO_2-C /g dry soil [13].

Catalase activity. Catalase was evaluated according to Beck [14]. 10 ml of phosphate buffer (pH 7) and 5 ml of a 3 % H_2O_2 solution were added to 5 g of soil. The volume (ml) of O_2 released within 3 minutes at 25 ºC was measured. Three replicates of each soil sample were tested. Controls were tested in the same way, but with the addition of 2 ml of 6.5 % (w/v) NaN_3. Results were calculated on the basis of oven dry weight of soil.

Urease activity. Urease activity was measured according to Hoffmann and Teicher [15]. The 250 µl of toluene, 750 µl of citrate buffer (pH 6.7) and 1 ml of 10 % urea substrate solution were added to the 1 g sample. The samples were incubated for 3 h at 37º C. Following filtration through whatman No. 42 filter papers and sodium phenolate and sodium hypochloride were added. The released ammonium was determined at 578 nm. Three replicates of each sample were tested. The control sample without urea was prepared. Results were expressed as mg N /100 g dry sample.

Statistical analysis. The data were analysed by analysis of variance using the *TARIST* computer program. The Duncan was used the separate the means.

RESULTS AND DISCUSSION

Soil pollution is effective on sensitive microorganisms and soil biological properties [16]. Gratani et al. [17] and Lagerweff and Specht [9] suggested that the soil microbiological properties were affected by various environmental factors such as soil type, traffic, management systems of crop, fertilization, vegetation. In this study, the changes in some microbiological properties, the concentrations of Pb and Cd of roadside soils are shown in Table 2.

TABLE 1
Location and characteristics of the sampling sites

Main roads	Junction	GPS coordinates	pH	EC (ds/m)	Organic matter (%)
Şanlıurfa-Akçakale	Alpet	37º125´ N-38º809´ E	8.42	0.62	1.3
	Eyyubiye	37º128´ N-38º820´ E	8.33	0.88	1.2
	Kanalurfa	37º111´ N-38º823´ E	7.86	1.02	1.4
Şanlıurfa-Mardin	Germus	37º162´ N-38º857´ E	7.40	1.11	1.76
	Göbeklitepe	37º162´ N-38º876´ E	7.68	1.09	1.42
	Gap fidancılık	37º160´ N-38º927´ E	7.81	1.24	1.35
Şanlıurfa-Diyarbakır	Shell benzinlik	37º215´ N-38º801´ E	7.70	1.85	2.42
	Doğuş	37º227´ N-38º799´ E	7.71	1.53	1.91
	Bozova	37º250´ N-38º799´ E	7.28	1.42	1.40
Şanlıurfa-Gaziantep	Sheraton	37º151´ N-38º770´ E	7.62	1.69	1.21
	Sanayi	37º142´ N-38º734´ E	7.35	1.86	1.32
	Köprü	37º138´ N-38º717´ E	7.67	1.51	1.67

TABLE 2
Some microbiological properties and heavy metal (Pb, Cd) contents of roadside soils

Properties	The distance to the road (meter)					
	1	10	50	100	150	250
Microbial respiration (mg CO_2/g soil)	5.96 e	8.9 d	12.5 c	14.5 c	18.2 b	23.0 a
Catalase (ml O_2/g soil)	9 d	10.3 cd	10.4 cd	11.6 bc	12.5 b	14.5 a
Urease (mg N/100 g soil)	5.7 d	6.5 cd	7.2 cd	8.0 bc	9.6 b	11.8 a
Bacteria (cfu/g soil)	5.7 d	5.8 cd	6.1 bc	6.5 ab	6.6 a	6.6 a
Fungi (cfu/g soil)	4.9 b	5.4 ab	5.6 ab	5.5 ab	5.9 a	6.1 a
Actinomycetes (cfu/g soil)*	3.9 c	4.4 bc	4.8 b	4.8 b	5.3 a	5.5 a
Pb (mg/kg soil)	5.5 a	4.3 b	2.9 c	2.5 c	1.7 cd	1.2 d
Cd (mg/kg soil)	4.7 a	4.4 a	4.0 b	3.8 b	3.4 c	3.5 c

*cfu/g: The number of colony forming units of microorganism

TABLE 3
Source of variation and mean squares of changes in some microbiological properties and heavy metal (Pb, Cd) contents with soil samples

Sources of variation	df	Microbial respiration (mg CO_2/g)	Catalase (ml O_2/g soil)	Urease (mg N/100g)	Bacteria (cfu/g)	Fungi (cfu/g soil)	Actinomycetes (cfu/g soil)	Pb (mg/kg)	Cd (mg/kg)
Situation (S)	3	39.48	29.48	25.70	4.651	2.43	3.50	76.6	67.07
Error I	8	64.385	9.68	11.12	0.997	1.56	2.68	10.0	3.12
Distance (D)	5	44.86*	35.62**	59.68	1.721	1.88**	4.02	31.7	2.99*
SxD	1	2.607**	2.29	2.56	0.267	1.01	1.52	4.37	0.16
Error 2	4	2.739	3.27	4.65	0.175	0.79	0.44	2.19	0.11

*, ** – significant at the 0.05 and 0.01 probability levels, respectively

Post and Beeby [18] reported that the heavy metal contents had significant negative correlations with soil microorganism number. In general, this change has been studied by Lenart and Wolny-Koladka [10] in Cracow soils. Joshi et al. [19] reported that bacterial and fungal community has decreased due to heavy traffic density in roadside soils. The results obtained in this study. The numbers of bacteria, fungi and actinomycetes were increased with distance from the road (Table 2). Distance from the road on the number of microorganism was found to be significantly at 5 % level (Table 3).

The lead concentration in soil and plant was increased due to traffic [17, 20-22]. Gülser and Erdoğan [23] found that the sensitivity of soil enzyme activities to heavy metal pollution was significantly changed with 5, 25 and 45 m from the roadside soil samples. Our results showed that the catalase and urease activities are higher farther from the road as reported by Gülser and Erdoğan [23]. Soil catalase and urease activities were sensitive to soil biological properties [24] and soil urease, catalase, dehydrogenase activities inhibited by soil contamination caused heavy metals such as Pb, Cd, Cr, Ni [24-26]. Filipek-Mazur et al. [27] reported that the reduced dehydrogenase, catalase and arylsulfatase activities of roadside soils.

Soil microbiological properties such as catalase, urease, dehydrogenase and phosphatase enzyme activities, respiration, numbers of microorganisms are a sensitive parameter and can be used as an indicator of soil fertility and pollution [19, 23, 28, 29]. Ohya et al. [28] observed that the soil organic matter mineralization, respiration, enzyme activities, nitrification effected by heavy metals. The respiration and enzyme activities in roadside soil can be effective due to stress caused by gaseous of heavy traffic. In this study, we found that; the distance to the road was significant for all the features.

Increased heavy metal concentration in soil was negatively affected soil enzymes, respiration and microbial community and plant growth [10, 23, 25, 30]. Researchers were reported that the concentrations of heavy metals such as Pb and Cd decreased when away from the road and the number of microorganisms such as fungi, actinomycetes and bacteria increased.

Wang et al. [31] reported that the sensitivity to environmental stress of three soil enzymes was obtained as urease > invertase > catalase. Wang et al. [31] reported that the soil urease activity can be used

as an index of soil degeneration and reclamation. Catalase enzyme activity of soils inhibited by soil contamination of Pb and Cd [32].

Increase of heavy metal contents in soil was stressed and the reduced the number of microorganisms, therefore it causes the deterioration of the ecological balance [24, 30]. The urease activities varied significantly between the soil samples collected from different location in Turkey [21-23, 25, 29]. Our results showed that urease and catalase activities are lower than other researchers. In this study, the cadmium and lead contents of soils is decreases as further from the road. Microbiological activities of soils were significantly affected from the distance to the road (Table 3). Distances from the roadside, on the cadmium and lead contents of soil were found to be significant ($p<0.01$) (Table 3). Jaradad and Moman [20], Haktanır et al. [29], Onianwa and Adoghe [33], Osma et al. [34] reported that heavy metal concentrations in roadside soil have increased considerably due to heavy traffic pollution which was confirmed by our study. Also, it was reported that roadside soils along the major national road in Greece are polluted by heavy metal contaminants [35]. Yan et al. [36] reported that, the compared to cadmium and lead, the pollutant effect of cadmium to the environment is more permanent and the distance play an important role in heavy metal contamination.

CONCLUSION

The soil samples were alkaline, Pb and Cd concentrations of roadside soils not exceed the allowable limits, although heavy traffic. In all the road junction, the number of microorganisms increased as away from road. But, the activities of microbiological tested were decreased in roadside soils. This situation; microorganisms against the exhaust gaseous pollution in roadside soils can be attributed sensitive.

ACKNOWLEDGEMENTS

This work was supported by Harran University, Council of Research Project Foundation, Turkey (No 14182). Therefore, we are grateful for this funding and support of this research.

REFERENCES

[1] Guney, M., Onay, T.T. and Copty, N.K. (2010) Impact of overland traffic on heavy metal levels in highway dust and soils of Istanbul, Turkey. Environ Monit Assess. 164, 101-110.

[2] Zhang, F., Chen Zeng, X., Zhang, M., Shrestha, S., Devkota, L.P. and Yao, T. (2012) Influence of Traffic Activity on Heavy Metal Concentrations of Roadside Farmland Soil in Mountainous Areas. Int J Environ Res Public Health. 9, 1715–1731.

[3] Pagotto, C., Rémy, N., Legret M. and Le Cloirec, P. (2001) Heavy Metal Pollution of Road Dust and Roadside Soil near a Major Rural Highway. Environmental Technology. 22, 307-319.

[4] Stresty, T.V.S. and Madhava Rao, K.V. (1999) Ultrastructural alterations in response to zinc and nickel stress in the root cell of pigeonpea. Environ Exp Bot. 41, 3-13.

[5] Olukanni, D.O. and Adebiyi, S.A. (2012) Assessment of Vehicular Pollution of Road Side Soils in Ota Metropolis, Ogun State, Nigeria. International Journal of Civil & Environmental Engineering. 12, 40-46.

[6] TUIK (2013) Turkey's Statistical Yearbook 2013. www.tuik.gov.tr (in Turkish).

[7] Akbar K.F., Hale, W.H.G., Headley A.D. and Athar, M. (2006) Heavy metal contamination of roadside soils of Northern England. Soil Water Res. 4, 158–163.

[8] Bai, J., Cui, B. and Wang, Q. (2009) Assessment of heavy metal contamination of roadside soils in Southwest China. Stoch. Environ. Res. Risk Assess. 23, 341–347.

[9] Lagerweff, J.V. and Specht, A.W. (1970) Contamination of roadside soil and vegetation with cadmium, nickel, lead and zinc. J. Environ. Sci. Technol. 4, 583-586.

[10] Lenart, A. and Wolny-Kolade, K. (2013) The effect of heavy metal concentration and soil pH on the abundance of selected microbial groups within Arcelor Mittal Poland steelworks in Cracow. Bulletin of Environmental Contamination and Toxicology. 90, 85-90.

[11] Kacar, B. and Katkat, V. (2007) Plant nutrition. Nobel Publish. Ankara. ISBN: 978-975-591-834-1. 559p.

[12] Alef, K. (1995) Nutrition sterilization aerobic and anaerobic culture technique. In: Alef, K. and Nannipieri, P. (eds.) Methods in Applied Soil Microbiology and Biochemistry. Academic Press. New York, 123-133.

[13] Anderson, J.P.E. (1982) Soil respiration. In: Page, A.L. (Ed.) Methods of soil analysis, part 2, chemical and microbiological properties ASA-SSSA, Madison, Winsconsin, 831-871.

[14] Beck, T. (1971) The measurements of catalase activity. Zeitschrift f. Planzenernrung und Bodenkunde. 130, 68-81.

[15] Hoffmann, G.G. and Teicher, K. (1961) Ein Kolorimetrisches Verfahren zur Bestimmung der Urease Activitat in Boden. Z. Pflanzenernahr. Bodenk. 91, 55-63.

[16] Smejkalova, M., Mikanova, O. and Boruvka, L. (2003) Effect of heavy metal concentration on biological activity of soil microorganisms. Plant Soil Environ. 49(7), 321-326.
[17] Gratani, L., Taglioni S. and Crescente, M.F. (1992) The accumulation of lead in agricultural soil and vegetation along a highway. Chemosphere. 24, 941-949.
[18] Post, R.D. and Beeby, A.N. (1996) Activity of the microbial decomposer community in metal contaminated roadside soils. J. Appl. Ecol. 33, 703-709.
[19] Joshi S.R., Kumar, R., Bhagobaty, R.K. and Thokchom, S. (2010) Impact of pollution on microbial activities in sub-tropical forest soil of north east India. Research Journal of Environmental Sciences. 4(3), 280–287.
[20] Jaradad, Q.M. and Moman, K.A. (1999) Contamination of roadside soil, plants and air with heavy metals in Jordan: A comparative study. Turkish Journal of Chemistry. 23, 209-220.
[21] Akbulut, S and Çevik, U. (2014) Accumulation of metals in roadside soil, dust and pine needles in different characteristics traffic areas. Fresen. Environ. Bull. 23, 516-522.
[22] Leblebici, Z., Aksoy, A. and Akgül, G. (2014) Accumulation and heavy metals on potatoes (*Solanum tuberosum* L.) in the Nevşehir, Turkey. Fresen. Environ. Bull. 23, 2181-2189.
[23] Gülser, F. and E. Erdoğan, (2008) The effects heavy metal pollution on enzyme activities and basal soil respiration of roadside soils. Environ. Monit. Assess. 145, 127-133.
[24] Kızılkaya, R., Aşkın, T., Bayraklı B. and Sağlam, M. (2004) Microbiological characteristics of soils contaminated with heavy metals. European Journal of Soil Biology. 40, 95-102.
[25] Karaca, A., Naseby, D.C. and Lynch, J.M. (2002) Effect of cadmium contamination with sewage sludge and phosphate fertilizer amendments on soil enzyme activities, microbial structure and available cadmium. Biology and Fertility of Soils. 35, 428–434
[26] Murata, T., Kanoa-Koshikawa, M. and Takamatsu, T. (2005) Effects of Pb, Cu, Sb, In and Ag contamination on the proliferation of soil bacterial colonies, soil dehydrogenase activity and phospholipid fatty acid profiles of soil microbial communities. Water, Air and Soil Pollution. 164, 103-118.
[27] Filipek-Mazur, M., Tabak, M. and Gorcyca, O. (2014) Enzymatic activity of soils exposed to transportation pollutants, located along road no 957. Journal of Ecological Engineering. 15, 145-149.
[28] Ohya, H., Fujiwara, S., Komai Y. and Yamaguchi, M. (1998) Microbial biomass and activity in urban soils contaminated with Zn and Pb. Biology and Fertility of Soils. 6, 9-13.
[29] Haktanır, K., Arcak, S., Erpul G. and Tan, A. (1995) Accumulation of the vehicle-generated heavy metals on the roadside soils. Turkish Journal of Engineering and Environmental Sciences. 19, 423-431.
[30] Liu, Z., Chen, W., He, X., Huang, Y., Zhang, Y. and Ding, W. (2017) Influence of cadmium on growth and antioxidative capacity of *Weigela florida* 'red prince'. Fresen. Environ. Bull. 26, 7137-7141.
[31] Wang, Y.B., Zhang, L. and Liu, D.Y. (2003) Relationship among soil enzyme activities, vegetation state and soil chemical properties of coal cinder yard. Chin. J. Appl. Ecol. 14, 110–112.
[32] Liu, S.Q., Yang, Z.X., Wang, X.M., Zhang, X.G., Gao, R.T. and Liu, X. (2007) Effect of Cd and Pb pollution on soil enzymatic activities and soil microbiota. Front. Agric. China. 1, 85–89.
[33] Onianwa, P.C. and Adoghe, J.O. (1997) Heavy-metal content of roadside gutter sediments in Ibadan, Nigeria. Environment International. 23, 873–877.
[34] Osma, E., Özyiğit, İ.İ., Demir, G. and Yaşar, U. (2014) Assessment of some heavy metals in wild type and cultivated purlane (*Portuloca oleracea* L.) and soils in Istanbul, Turkey. Fresen. Environ. Bull. 23, 2181-2189
[35] Christoforidis, A. and Stamatis, N. (2009) Heavy metal contamination in street dust and roadside soil along the major national road in Kavala's region, Greece. Geoderma. 151, 257-263.
[36] Yan, X., Gao, D., Zhang, F., Zeng, C., Xiang, W. and Zhang, M. (2013) Relationships between heavy metal concentrations in roadside topsoil and distance to road edge based on field observations in the Quighai Tibet Plateau, China. Int. J. Res. Public Healt. 10, 762-775.

Received: **4.10.2017**
Accepted: **10.02.2018**

CORRESPONDING AUTHOR

Cigdem Kucuk
Harran University,
Faculty of Arts and Science,
Department of Biology,
63300 Şanlıurfa – Turkey

e-mail: ckucuk@harran.edu.tr

© by PSP Volume 27 – No. 5/2018 pages 2883-2890 Fresenius Environmental Bulletin

INVESTIGATION OF IN VITRO GENOTOXIC EFFECTS OF MONOCROTOPHOS ON HUMAN SKIN KERATINOCYTE CELLS

Abdullah A AlKahtane[1], Saud Alarifi[1], Ahmed A Al-Qahtani[2,3], Hamad Al-Yahya[1], Daoud Ali[1,*], Suliman Y Alomar[1], Mohammed S Alessia[4], Bader Al-Dahmash[1], Saad Alkahtani[1]

[1]Department of Zoology, Science College, King Saud University, Riyadh, Saudi Arabia
[2]Department of Infection and Immunity, Research Center, King Faisal Specialist Hospital & Research Center, Riyadh, Saudi Arabia
[3]Department of Microbiology and Immunology, Alfaisal University School of Medicine, Riyadh, Saudi Arabia
[4]Department of Biology, Science College, AI -Imam Muhammad Ibn Saud Islamic University, Riyadh, Saudi Arabia

ABSTRACT

Monocrotophos (MCP), generally famous as azodrin, is widely applied in agricultural work all over the world. However, few data is available on its short-term cytotoxic effects on human keratinocyte (HaCaT) cells. The aim of this study was to estimate toxicity and its mechanism in HaCaT cells. In this study, we found cytotoxic activity and oxidative stress produced in HaCaT cells due to exposure of MCP for 24 and 48 hours. MCP (0, 100, 300, and 600 ng/ml) produced dose and time dependent cytotoxicity in HaCaT cells, which was determined by MTT and NRU assays. MCP induced oxidative stress, demonstrated by elicits of reactive oxygen species (ROS) generations, lipid peroxides (LPO) and declination of glutathione (GSH) in HaCaT cells. Due to exposure of MCP, chromosome condensation was found in HaCaT cells, which is hallmark of apoptosis was indicated by DAPI (4', 6-diamidino-2-phenylindole). Maximum, DNA single strand breakage was found at maximum dose of MCP for 48 hour. This study suggested that MCP induce cytotoxicity and apoptosis in HaCaT cells, which is likely to be facilitated via ROS production and oxidative stress.

KEYWORDS:
MCP, HaCaT cells, MTT assay, Apoptosis, DNA damage

INTRODUCTION

Organophosphorous compounds are extensively used as acaricide, insecticide in farm, agriculture in present years, due to its biodegradability and low environmental existence. MCP [dimethyl (E)-1-methyl-2-(methyl carbomoyl) vinyl phosphate] is an essential broad-spectrum systematic organophosphate pesticide, extensively applied in Asian countries. Some researchers reported that MCP is a harmful toxicant and controls a variety of pests [1]. MCP reached to terrestrial and aquatic ecosystem due to its direct applications by spraying and runoff from agriculture land [2]. As a result of its extensive application, MCP was found in fruits, grains and surface water. Mutagenic potential of MCP has been extensively studied. It is reported to be genotoxic to bacterial species and mouse lymphoma. Many pesticides can be absorbed through the skin into the blood, and can cause toxic effects. Some chemical compounds are carcinogenic to treated animal through the induction of oxidative stress, gene mutation and cell death [3]. So, exploring of the genomic toxicity of organophosphate pesticide MCP is important for protecting human health. As many of the environmental pollutants are known or doubted carcinogens, mutagenicity assays have also been used to toxicology.

Oxidative stress occurs when ROS are generated more than it may be eliminated by cellular defense mechanisms. Upturned production of ROS in living cells can lead to destroy of carbohydrates, fat, proteins and DNA and this is the main cause of cellular alterations as a consequence cell toxicity and death occurred [4]. Genotoxic effects of xenobiotic compounds may be studied by using comet assay in vitro and in vivo which is gaining popularity over others due to it can measure minute levels of DNA fragmentation and needs less duration to complete the study [5]. Many genotoxicity bioassay including micronucleus test and comet assay [6] are used in genetic toxicology for epidemiological study and bio monitoring of aquatic ecosystems for pollutants. Therefore the current study was designed to evaluate DNA damage, cytotoxic effect of MCP on HaCaT cells.

MATERIALS AND METHODS

The DMEM media, antibiotics (100 ml) and fetal bovine serum (FBS) were purchased from Sigma Aldrich USA. MCP (dimethyl (E)-1-methyl-2-(methyl carbamoyl) vinyl phosphate) with a purity of 98% was purchased from local markets.

Cell culture and morphology of HaCaT cell lines. Human skin keratinocyte (HaCaT) cell lines were subcultured in DMEM with FBS (10%), antibiotic and antimycotic solution (1.5%) at 5% CO_2 and 95% relative humidity at 37°C. After exposure of MCP, morphological changes in HaCaT cells were observed by using an inverted microscope (Leica DMIL) for 24 and 48 hours.

MTT assay. HaCaT cells (1 x10^4/ well) in 96 well plates were cultured at 37 °C for 24 hours with various concentrations of MCP (0, 100, 300, and 600 ng/ml). After exposure, the plate was incubated with MTT solution for four hours. The purple color formazan crystal which is produced in live cells was dissolved in DMSO and read at 570 nm by using a microplate reader (Biotech, Elx 800). Data was represented as reduction of MTT in percentage comparative to the evaluated absorbance from control cells.

NRU assay. The assay was done according to Borenfreund and Puerner [7].

Determination of reactive oxygen species (ROS). Production of ROS was evaluated by fluorometric test by using with 2, 7-dichlorofluorescein diacetate (DCFH-DA). DCFH-DA is a non-fluorescent dye and it is converted into fluorescent 2,7-dichlorofluorescein product (DCF) (λ_{max} = 522 nm) in various stage. HaCaT cells were exposed to the different dose of MCP for 24 and 48 h at 37°C. HaCaT cells were incubated with 20 µM DCFH-DA after treatment. Generation of ROS was evaluated after 30 min incubation at 37 °C by using fluorimeter (Biotek FL 800×) at 485 nm (excitation wavelength) and 522 nm (emission wavelength). Intensity of DCF fluorescence is relational to the quantity of ROS produced intra cellularly. H_2O_2 (20 µM) was used as a positive control.

Mitochondrial transmembrane potential (MMP) test. Rhodamine-123 is a cationic fluorescent stain and it was used for measurement of mitochondrial membrane potential [8].

Lipid peroxidation (LPO). LPO was determined by the evaluation of malondialdehyde (MDA) level as described by Ohkawa et al. [9]. HaCaT cells were grown in 6-well plates at 4 × 10^5 cells/well and treated with various concentration of MCP (0, 100, 300, and 600 ng/ml), for 48 h. After treatment HaCaT cells were scrapped and cell lysate was prepared in ice-cold 1.15% KCl. Cell lysates (1 00 µl) were added with 8.1% SDS (200 µl), 20% acetic acid (1.5 ml) adjusted to pH 3.5 and 1.5 ml of 0.8% TBA. Solution was made 4 ml by adding distilled water and heated to 95 °C for 60 min. The mixture was added with n-butanol and pyridine (15:1, v:v) and vortex vigorously at RT. Solution was extractored at 4000 rpm for 10 minute and upper layer of solution were assembled and OD was examined at 546 nm. The concentration of MDA was determined according to a standard curve.

Glutathione (GSH). GSH was determined by according of Saldak and Lindsay method [10]. The quantity of GSH was presented as nmol/mg protein.

SOD. Activity of SOD was examined according to the method of Kono [11] using Nitro blue tetrazolium (NBT) in the presence of riboflavin.

Catalase. Catalase activity was measured using the method described by Alarifi et al. [12].

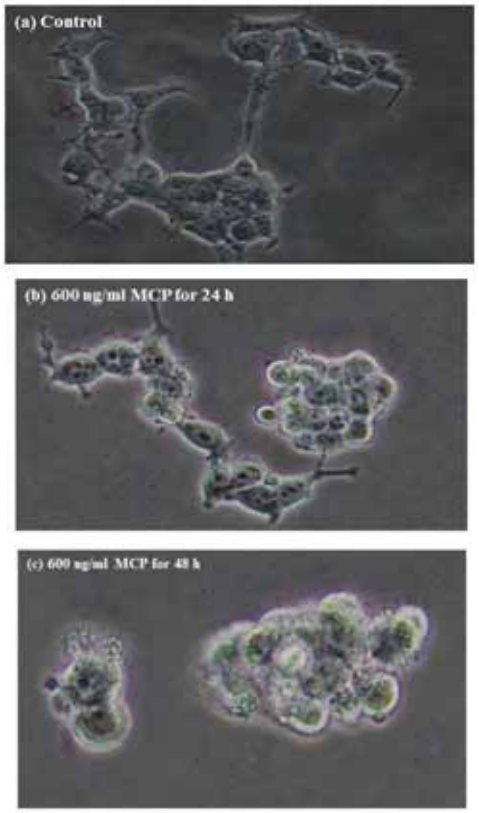


FIGURE 1
Morphology of HaCaT cells a. Control b. at 600 ng/ml of MCP for 24 h c. at 600 ng/ml of MCP for 48h.

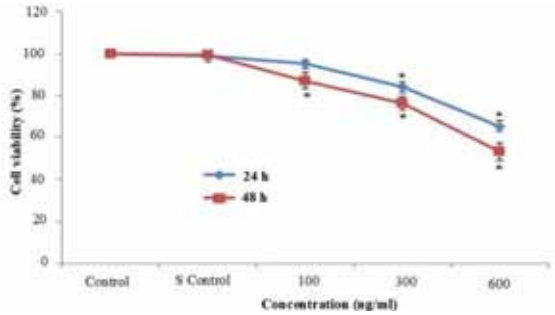
Fragmentation of chromosome in cell. Analysis of control, apoptotic and necrotic cells was done by using DAPI fluorescent dye. In this technique is depended on apoptosis produced fragmentation of nuclear and condensation. Later the exposure of MCP (0, 100, 300, and 600 ng/ml) to cells for 24 and 48 h, subsequently DAPI (10 µl) were added in cells. Later 30 min incubate; the cells were cleaned in triplicate with PBS. The chromosome condensation was observed by fluorescence images in upright microscope (Nikon Eclipse equipped with Nikon DS-Ri1 megapixel camera, Japan).

Caspase-3 assay. The activity of caspase-3 was examined according Alkahtane [13] and presented in pmol of nitroaniline /min/mg of protein.

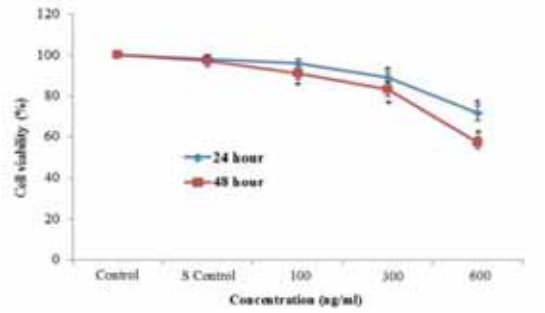
Annexin-V-FITC/PI staining for apoptosis. Annexin-V-FITC/PI staining was done by Annexin V-FITC apoptosis detection kit (Sigma, St Louis, MO, USA) as per the manufacturer's protocol. Results were analysed by FACS Diva 6.1.2 software.

Comet assay. The fragmentation of DNA was measured by comet assay as described by Singh et al., [14].

Statistical analysis. The statistical differences were determined by analysis of variance (ANOVA) and the differences were noted ($p<0.05$). The data are expressed as average for three independent experimental points.



(a)



(b)

FIGURE 2
Cytoxicity of MCP in HaCaT cells for 24 and 48 hour, as assessed by a. MTT b. NRU tests. Each value represents the mean ±SE of three expreiments *p< 0.05 vs. control

RESULTS

HaCaT cells. Fig.1 showed the comparative morphology of control and MCP treated HaCaT cells for 24 and 48 h. HaCaT cells changed into round shape and detached from surface at 600 µg/ml of MCP exposure (Fig. 1 B).

MCP induced cell death in HaCaT cells. HaCaT cells were exposed to increasing concentrations of MCP ranging from 100 to 600 ng/ml for 24 h and 48 h and cell viability was determined by MTT and NRU assays. Our results indicate that MCP induced a marked decrease in cell viability in a dose and time-dependent manner ($p < 0.05$) (Fig 2A). However, in case of NRU assay similar result was observed and cell viability was reduced at same concentration of MCP was 40% ($p<0.05$). (Fig. 2B).

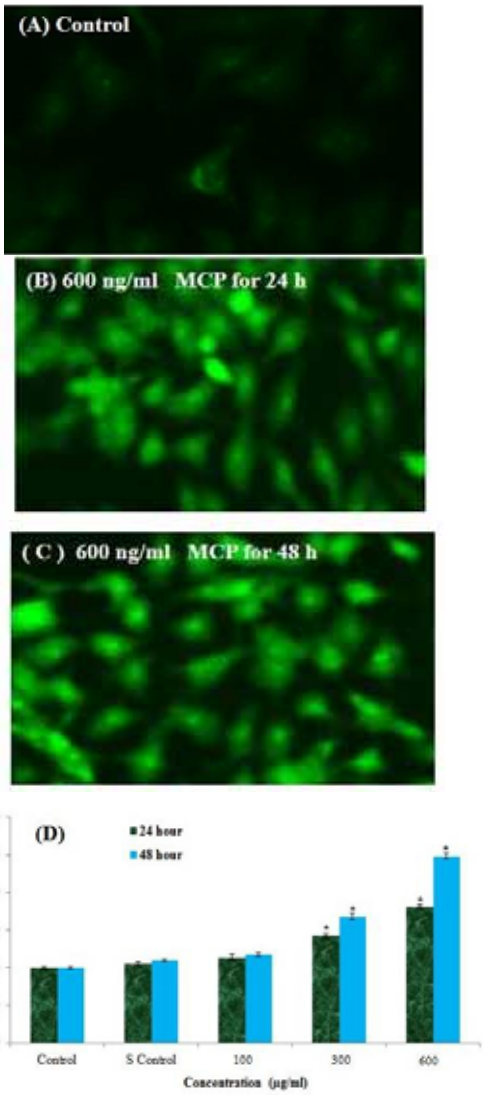


FIGURE 3
MCP induced ROS in HaCat cells. A. Control B. at 600 ng/ml of MCP for 24 h C. at 600ng/ml of MCP for 48 h D. % ROS production at various doses of MCP in HaCat cells. Images were snapped in phase contrast cum fluorescence microsope (Nikon, model 80i). Each value represents the mean± SEM of three experiments. *p <0.05 vs control

ROS generation and oxidative stress. To find out the stress in HaCaT cells due to MCP treatment, we determined the quantitative and qualitative production of fluorescent DCF (the result of DCFH oxidation by a variety of peroxides). As represented in Fig.3, present results indicated that MCP generated ROS in concentration and time dependent basis.

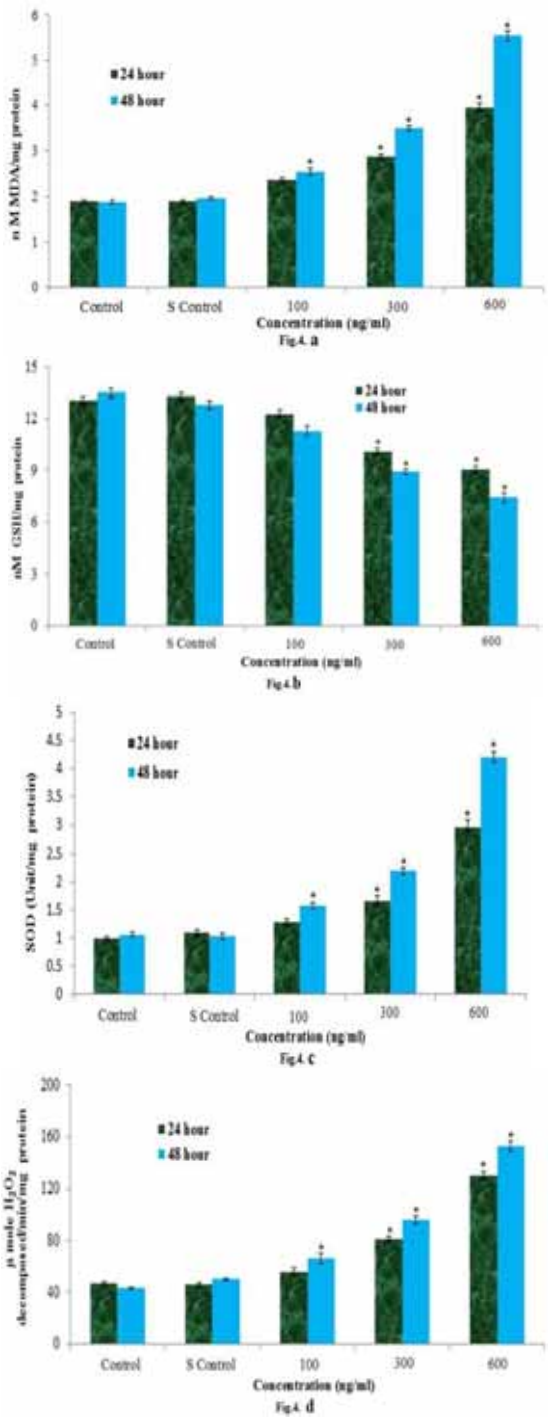


FIGURE 4
a. Levels of LPO b. GSH c. SOD d. CAT in HaCaT cells after exposure to MCP for 24 and 48 h. Each value represents the mean±SE of three experiments* p< 0.05 vs control

MCP induced LPO in model cells. Actually, later 24 and 48 h of incubation with different concentrations of MCP, the MDA levels were increased from control value (Fig.4A). Results showed that MCP induced oxidative stress were further proved by declination of GSH (Fig. 4B) and hiked level of SOD and CAT with dose and time dependent (Figs. 4 B, C and D).

MCP induced a loss of mitochondrial membrane voltage (ΔΨm). Rhodamine-123 is usually applied to make strong determination of mitochondrial membrane voltage both *in vitro* and *in situ* because ΔΨm is proportional to uptake rhodamine-123 [15] and ΔΨm changes always correlate with the apoptosis of cell. Later cell treated with above concentration of MCP, a concentration and time -dependent decrease in ΔΨm was seen ($p < 0.05$), demonstrating that mitochondria were depolarised (Fig.5).

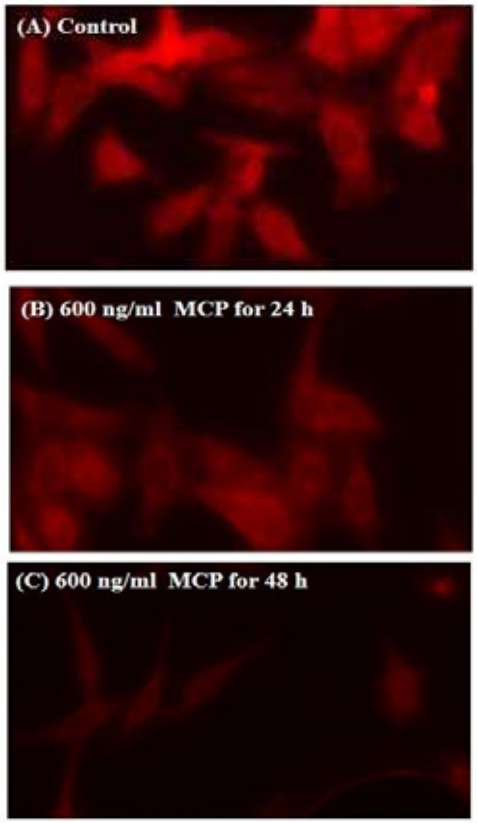


FIGURE 5
MCP induced MMP in HaCaT cells. Images of three qualitative analyses in fluorescence in microscope A.control B. 600 ng/ml for 24 h C. 600 ng/ml for 48 h.

Apoptosis detection and caspase-3 activity. Effect of MCP showed enhanced chromosome condensation which was measured by DAPI staining in HaCaT cells (Fig.6 A-C). The test is depended on morphology of nucleus, which is specific for apoptosis. The healthy cells displayed normal nuclear chromatin with blue fluorescence but apoptotic cells contain fragmented chromatin. MCP treatment showed a significant number of chromosome condensed cells as compared to control.

Flow cytometry analysis was carried out by applying Annexin-V-FITC/PI staining to find out the mechanism of cell death produced by MCP. The untreted cells were not uploaded with Annexin V-FITC and propidium iodide. But, the cells exposed to 600

ng/ml MCP for 24 and 48 h showed 32.23 and 49.5% apoptotic cells respectively (Fig.7 a-d).

To deremine the role of caspase-3 activity in MCP-produced apoptosis, HaCaT cells were pre-exposed for 2 h with the caspases inhibitor ZVAD-fmk (50 µM) before exposure to MCP at concentrations (600 ng/ml). Our finding indicated that ZVAD-fmk pre-treatment significantly prevents the cell death induced by MCP (Fig.6 D).

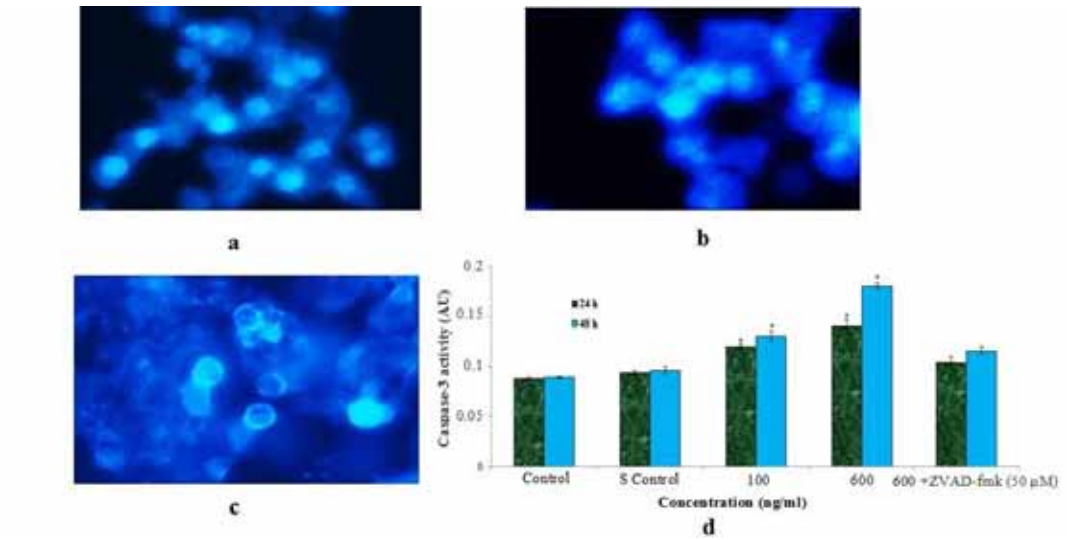


FIGURE 6

Chromosomal condensation and induction of caspase-3 activity in HaCa cells after treatment to MCP a. Control b.at 600 ng/ml MCP for 24h c. at 600 ng/ml MCP for 48 h d. Caspase-3 activity. Each value represents the mean ±SE of three experiments. *p<0.05 vs control.

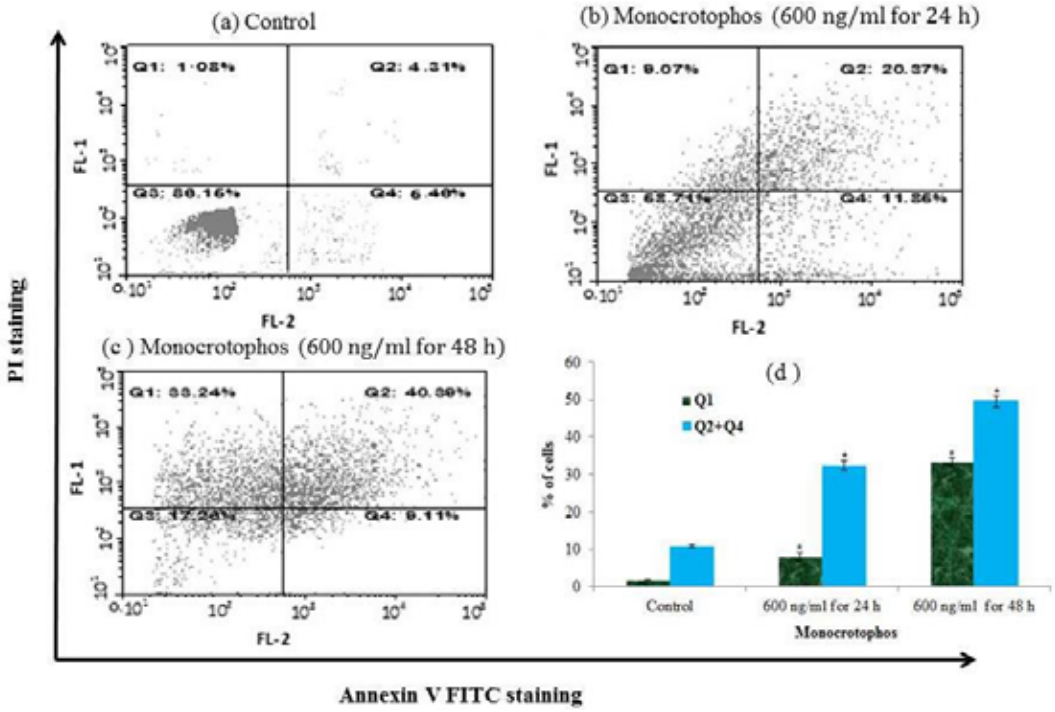


FIGURE 7

Monocrotophos (600 ng/ml) induced apoptosis in HaCaT cells. (a-d) Annexin V-FITC and PI fluorescence were measured using flow cytometer with FL-1 and FL-2 filters, respectively. Q_3, living cells (Annexin V^-/PI^-); Q_4, early apoptotic7primary apoptotic cells (Annexin V^-/PI^-); Q_2, late apoptotic7secondary apoptotic cells (Annexin V^-/PI^-). Data represent average ±SE of triplicate experiments. *p≤0.05 compared to control.

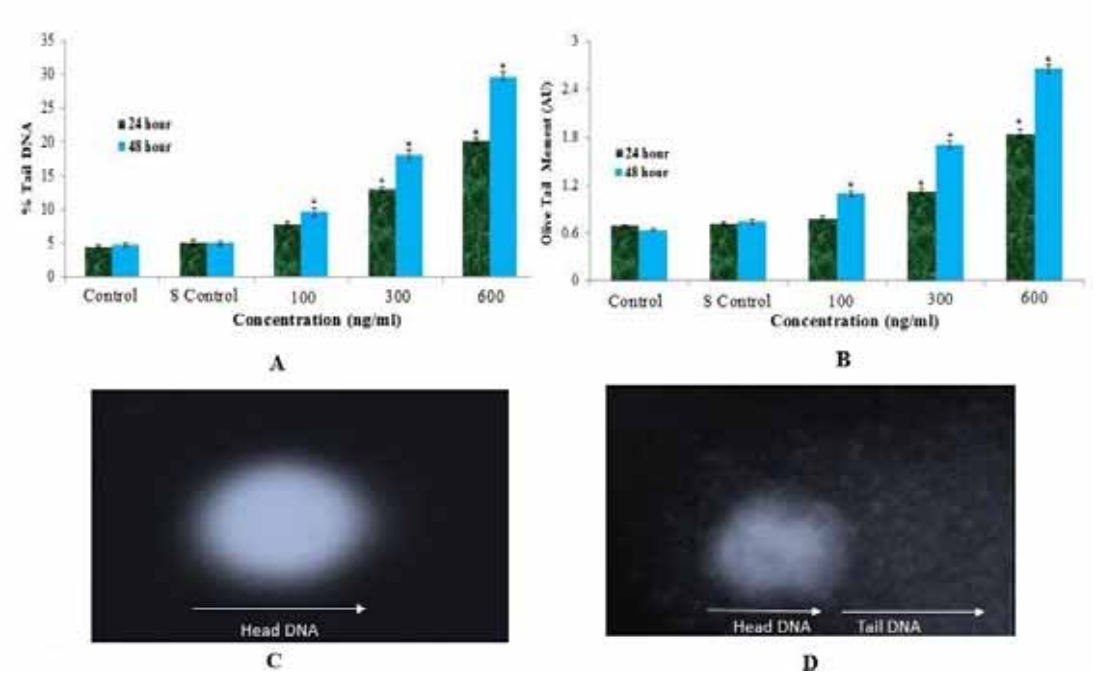


FIGURE 8

DNA impairment in HaCaT cells due to MCP A.Tail DNA(%) B. Olive tail moment C.Control cell D. at 600 ng/ml of MCP 48h. Each value represents the mean ±SE of three experiments. *p<0.05 vs control.

DNA damage. Fragmentation of DNA was measured using the comet assay, and it is a sensitive tool for measuring DNA strand breakage in individual cells [16]. The amount of DNA damage (% tail DNA and OTM) reaches about 6 and 4.5 folds to the control value after 48 h of MCP exposure at the highest concentration, respectively (Fig.8). Indeed, as shown in result MCP induced DNA damage at concentrations and time-dependent manner (Fig.8).

DISCUSSION

MCP is an organophosphate pesticide and widely used in agriculture that adversely affects nervous system. Experimental and human epidemiological data indicate that the organophosphate pesticide, such as MCP etc are being fat soluble, and it easily engrossed through intravenous, gastrointestinal tract and skin. Organophosphate insecticide can quickly absorbed through placental or blood-brain barrier as consequences disorders of the fetal organs occurred during pregnancy. In this work we have determined the mechanism of cytotoxicity in cultured HaCaT cells due to MCP exposure. Our results showed that exposure of HaCaT cells to MCP leads to cell death at concentrations (100 to 600 ng/ml) as revealed by MTT and NRU test. Taju et al. [17] has been documented that cypermethrin induced cytotoxicity in different fish cell lines.

The LPO level is determined by the balance between the generations of oxidants and elimination and scavenging of those oxidants by antioxidants [18]. Huggett et al., [19] reported that LPO is general biomarker of oxidative stress. In this study, it was shown that LPO level was increased which indicates the toxic effects of MCP exposure to HaCaT cells. The levels of LPO, SOD and CAT were found to be significantly increased, which might be associated with decreased GSH level in HaCaT cells after MCP exposure. GSH is a major antioxidant and its protective role against oxidative stress-induced toxicity in animals is well established [20]. Use of GSH and CAT as biomarkers of exposure to organic xenobiotic has gained credence in pollution bio monitoring. Decrease of GSH level by oxidants can change the redox potential of the HaCaT cell and induces a stressful and toxic effect since GSH plays a critical role in maintaining cellular redox homoeostasis. MCP induced cytotoxicity was correlated with reduction of the mitochondrial membrane potential (MMP) after 24 h and 48 h exposure. Amengual, et al., [21] had been reported that oxidative stress is involved in cell apoptosis and oxidative stresses and MMP reduction always occurred simultaneously. The generation of ROS was occurred due to exposure of MCP for 24 h. The cell organelle mitochondria is susceptible to fluctuates in the cellular redox state and changes in MMP is an important step in the initial change in mitochondria as consequence closure of mitochondrial function and cell apoptosis [22,23]. Genomic instability due to pesticides is considered the most severe possible side effects of agricultural chemicals. If a chemical interact with nuclear DNA, it induce carcinogenic and mutagenic in the treated animals. This study demonstrates that MCP significantly induced DNA damage in HaCaT cells which is agreement with the finding of Salem

et al. [24] dichlorvos induced DNA damage in HCT116 cells. Mishra et al., [25] has been reported that organophosphate insecticide (MCP and Quinalphos) induced ROS generation, oxidative stress and DNA damage *in vitro* as well as *in vivo* treatment. In the present study MCP induced apoptosis in HaCaT cells may be induction of oxidative stress accompanied by mitochondrial dysfunction and DNA fragmentation.

Apoptosis is a planned cellular death to sustain normal cellular homoeostasis, and the induction of apoptosis can be a primary pathological result that occurs diseases and tissue remodelling. So, in this study, we determined whether MCP induced apoptosis due to mechanism of toxicity. HaCaT cells treated with MCP showed apoptotic features such as chromatin condensation and apoptotic bodies, suggesting the morphological apoptotic features of HaCaT cells. The Annexin-V-FITC/PI assay showed an increase in early and late apoptosis compared with the control, upon the exposure of MCP, and the exposed cells had DNA damage (% tail DNA, OTM) a characteristic of apoptosis. Our results indicated that MCP induced caspase-3 activity, and apoptosis (Fig. 6D and Fig. 7). These data implying ROS mediate mitochondrial-dependent pathways are involved in MCP induced apoptosis. Our results also showed that MCP decreased the levels of MMP, leading to activation ofcaspase-3 for causing apoptosis.

In conclusion, the current finding suggest that cytotoxicity and DNA damaging potential of MCP due to induction of oxidative stress. As monocrotophos is extensively applied in agriculture, so precaution should be used in its handling as prolonged exposure may lead to many health problems like organ damage as well as cancer.

ACKNOWLEDGEMENTS

The authors extend their appreciation to the Deanship of Scientific Research at King Saud.

University for funding this work through Research Group no. RGP-018.

REFERENCES

[1] Corey, R.A., Moye, W.C., and Hall, W.E. (1965) Laboratory and field evaluation of S.D. 9129 as an insecticide. J Econ Entomol. 58, 658-60.

[2] Ali, D. and Kumar, S. (2008) Long-term genotoxic effect of monocrotophos in different tissues of freshwater fish Channa punctatus (Bloch) using alkaline single cell gel electrophoresis. Science of the Total Environment. 405, 345-350.

[3] Wilhelm, D., Bender, K., Knebel, A. and Angel, P. (1997) The level of intracellular glutathione is a key regulator for the induction of stress-activated signal transduction pathways including Jun N-terminal protein kinases and p38 kinase by alkylating agents. Mol. Cell. Biol. 17, 4792-4800.

[4] Valko, M., Leibfritz, D., Moncol, J., Cronin, M.T.D., Mazur, M. and Telser J. (2007) Free radical and antioxidants in normal physiological functions and human disease. Int. J. Biochem. Cell Biol. 39, 44-84.

[5] Gedic, C.M., Ewen, S.W.B. and Collins, A.R. (1992) Single cell gel electrophoresis applied to analysis of UV-C damage and its repair in human cells. Int. J Radiat. Biol. 62, 313-20.

[6] Cheung, V.V., Depledge, M.H. and Jha, A.N. (2006) An evaluation of the relative sensitivity of two marine bivalve mollusc species using the comet assay. Marine Environmental Research, 62, S301-S305.

[7] Borenfreund, E., Babich, H. and Martin-Alguacil, N. (1988) Comparisons of two in vitro cytotoxicity assays-the neutral red (NR) and tetrazolium MTT tests. Toxicology in Vitro. 2(1), 1-6.

[8] Perry S.W., Norman J.P., Barbieri J, Brown E.B. and Gelbard H.A. (2011) Mitochondrial membrane potential probes and the proton gradient: a practical usage guide. Biotechniques. 50(2), 98-115.

[9] Ohkawa, H., Onishi, N. and Yagi, K. (1979) Assay for lipid peroxidation in animal tissue by thiobarbituric acid reaction. Anal. Biochem. 95, 351-358.

[10] Sedlak, J. and Lindsay, R.H. (1968) Estimation of total, protein-bound, and non-protein sulfhydryl groups in tissue with Ellman's reagent. Anal Biochem. 25(1), 192-205.

[11] Kono, Y. (1978) Generation of superoxide radical during autoxidation of hydroxylamine and an assay for superoxide-dismutase. Archives of Biochemistry and Biophysics. 186, 189-195.

[12] Alarifi, S., Ali, D., Alkahtani, S., Siddiqui, M.A. and Ali, B.A. (2013) Arsenic trioxide-mediated oxidative stress and genotoxicity in human hepatocellular carcinoma cells. Onco Targets Ther. 6, 75-84.

[13] Alkahtane, A.A. (2015) Nanosilica exerts cytotoxicity and apoptotic response via oxidative stress in mouse embryonic fibroblasts. Toxicological and Environmental Chemistry. 97(5), 651-662.

[14] Singh, N.P., McCoy, M.T., Tice, R.R. and Schneider, EL. (1988) A simple technique for quantification of low levels of DNA damage in individual cells. Exp Cell Res. 175, 184-91.

[15] Baracca, A., Sgarbi, G., Solaini, G. and Lenaz, G. (2003) Rhodamine 123 as a probe of mitochondrial membrane potential: evaluation of proton flux through F(0) during ATP synthesis. Biochim Biophys Acta. 1606 (1-3), 137-46.

[16] Kang, C., Lee, H., Yoo, Y.S., Hah, D.Y., Kim, C. H., Kim, E. and Kim, J S. (2013) Evaluation of oxidative DNA damage using an alkaline single cell gel electrophoresis (SCGE) comet assay, and the protective effects of N-Acetylcysteine amide on zearalenone-induced cytotoxicity in CHANG liver cells. Toxicol Res. 29(1), 43-52.
[17] Taju, G., Majeed, S.A., Nambi, K.S.N., Farook, M.A., Vimal, S. and Hameed, A.S.S. (2014) In vitro cytotoxic, genotoxic and oxidative stress of cypermethrin on five fish cell lines. Pesticide Biochemistry and Physiology. 113,15-24.
[18] Filho, D.W. (1996) Fish antioxidant defenses a comparative approach. Braz. J. Med. Biol. Res. 29, 1735-1742.
[19] Huggett, R.J., Kimerle, R.A., Mehrle, P.M. and Bergman H.L. (1992) Biochemical, physiological and histological markers of anthropogenic stress, Lewis Publishers, Boca Raton, FL.
[20] Hasspielar, B.M., Behar, J.V. and DiGiulio R.T. (1994) Glutathione dependent defense in channel catfish (Ictalurus punctatus) and brown bullhead (Ameuirus nebulosus). Ecotoxicol. Environ. Saf. 28, 82-90.
[21] Amengual, J., Lobo G.P., Golczak M., Li H.N., Klimova T. and Hoppe C.L. (2011) A mitochondrial enzyme degrades carotenoids and protects against oxidative stress. FASEB J. 25, 948-959.
[22] Zamzami, N., Susin, S.A., Marchetti, P., Hirsch, T., Gomez-Monterrey I., Castedo, M. and Kroemer, G. (1996) Mitochondrial control of nuclear apoptosis. J. Exp. Med. 183, 1533-1544.
[23] Mignotte, B. and Vayssiere, J.L. (1998) Mitochondria and apoptosis. Eur. J. Biochem. 252, 1-15.
[24] Salem, I.B., Boussabbeh, M., Bacha, H. and Abid, S. (2015) Dichlorvos-induced toxicity in HCT116 cells: Involvement of oxidative stress and apoptosis. Pesticide Biochemistry and Physiology. 119, 62-66.
[25] Mishra, V., Sharma, S., Khatri, S., and Srivastava, N. (2015) Evaluation of genotoxicity of MCP and quinalphos in rats and protective effects of melatonin. Integrative Pharmacology, Toxicology and Genotoxicology. 1(1), 33-42.

Received: **21.10.2017**
Accepted: **30.12.2017**

CORRESPONDING AUTHOR

Daoud Ali
Department of Zoology
College of Science
King Saud University
BOX 2455
Riyadh 11451 – Saudi Arabia

e-mail: daudali.ksu12@yahoo.com

© by PSP Volume 27 – No. 5/2018 pages 2891-2899 Fresenius Environmental Bulletin

ASSESSMENT OF WATER-SAVING IRRIGATION DEVELOPMENT LEVEL OF A REGIONAL AREA BASED ON FUZZY COMPREHENSIVE ASSESSMENT METHOD

Lujun Ding[1,2,*], Yuhong Liu[2]

[1]Department of Civil Engineering, Sichuan College of Architectural Technology, Chengdu, China
[2]Sichuan College of Architectural Technology, Deyang, China

ABSTRACT

The objective and reasonable evaluation of the development level of regional water saving irrigation is of great practical significance for promoting the development of water resources utilization and water saving irrigation in the region. The influencing factors of the development level of water-saving irrigation are analyzed in detail, taking the 21 cities and states of Sichuan Province as evaluation units, the index system of comprehensive evaluation of regional water-saving irrigation development level is established, the fuzzy comprehensive evaluation method is used to evaluate the development level of water saving irrigation in Sichuan Province. The evaluations showed that only two regions in Luzhou and Dazhou are in good level, accounting for 9.5%, eight regions are in general, eight regions are in relatively poor, three regions are of poor, and the rations of them in all regions are 38.1 ,38.1% and 14.3%, respectively. The comprehensive evaluation result of the development level of regional water saving irrigation in Sichuan province is in general level. The results indicated that the overall development level of water saving irrigation in Sichuan is not high, and there is a huge potential in the development of regional water-saving irrigation.

KEYWORDS:
water-saving irrigation developing level, fuzzy comprehensive assessment method, index system, weight set

INTRODUCTION

China is a country badly lacking water and regional water resources uneven distribution of water for agricultural irrigation is large, agricultural irrigation water accounted for about 70% of total water consumption, effective utilization of national irrigation water coefficient is 0.53, flooding phenomenon is obvious, not only caused a great waste of water resources, and the influence of grain mu yield. Vigorously developing high efficiency and water-saving irrigation can play a great role in alleviating the shortage of water resources, expanding the area of irrigation and promoting social and economic development in China. But only to make a correct and objective water-saving irrigation comprehensive evaluation, in order to reveal the main problems are the main factors and the development of water-saving irrigation area of process restrict the development of water-saving irrigation in the scientific and effective evaluation on the development level of water-saving irrigation area development planning for regional characteristics, is of great significance for promoting the development level of water-saving irrigation[1-2].

Comprehensive evaluation of regional water saving irrigation development level is a multi level, multi index and multi factor evaluation process. In recent years, the comprehensive evaluation of water-saving irrigation has been developed from qualitative evaluation to quantitative evaluation. The construction of evaluation system has evolved from simple evaluation system to comprehensive evaluation system, and the evaluation content has evolved from single engineering benefit evaluation to multi measures comprehensive evaluation [3].

Dawit Zerihum [4] proposed that the effective utilization rate of field irrigation water, field irrigation water storage rate and irrigation uniformity should be used as indicators to evaluate the improved surface irrigation quality, and the mathematical indicators for each index were made with its influencing factors, and the relationship between the indicators was also analyzed. Lin Xingcui [5] believes in the irrigation evaluation on the ground, in addition to the water quality index, but also with water saving rate, irrigation efficiency, irrigation water productivity, irrigation cost, water-saving rate as economic evaluation index, and established a set of evaluation methods of surface irrigation system. On the basis of the concept of efficient utilization of water resources, Zhu Meiling [6] built an evaluation index system for efficient agricultural water use on the basis of the concept of efficient water use, which provided metrology tools for the evaluation of the effectiveness of the field efficient water-saving technology. Wu Jingshe [7] according to the scientific, simple, operability and targeted principles, fully consider the main factors affecting the development of water-saving irrigation, survey of experts and scholars, engaged in water-saving irrigation and manage-

ment personnel of irrigation and government decision-making production line, after inspection and correction, and finally determine the evaluation index system of comprehensive effects of water saving irrigation. Cui Yuanlai [8] analyzed the limitations of traditional irrigation efficiency index in water saving effect assessment and water resource allocation decision, and commented on the evaluation indexes under different scales. Zhang Xin [9] combines entropy theory with fuzzy matter element modeling to build a comprehensive evaluation model of fuzzy matter element agricultural water saving project based on entropy weight, but this method is prone to omission in the process of index selection and simplification. Zhang Jing-nan, Yang Luhua [10] expounded the connotation of water saving irrigation, analyzes the factors that influence the development level of water-saving irrigation, the project of water-saving and agronomic water-saving and water-saving management and three indicators belonging to thirty-four indexes of each sub index, establish the evaluation index system of the development level of water-saving irrigation. Cui Ningbo [11] established a comprehensive evaluation index system of water-saving development level of regional agriculture consists of three level two indexes, thirty-three level three indexes, using principal component analysis method to simplify it as fourteen indicators of evaluation index system, to a certain extent due to the elimination of the influence of each index on the evaluation results. The simplified index system can better evaluate the development level of agricultural water-saving irrigation area. Wang jin-guo [12] synthetically evaluates the sustainable development of water resources in seventeen provinces in northern China by using the grey clustering method. Cheng Haiying [13] proposed the neural network index optimization method of the comprehensive evaluation index system, and solved the deficiency of the existing index optimization method in the application of the nonlinear system. Lou Yuhong [14] built a comprehensive evaluation index system for the development level of water-saving irrigation. The principal component analysis method was used to simplify the evaluation index system, the set pair analysis method was applied to evaluate the development level of regional water-saving irrigation in Sichuan Province, and a scientific and reasonable evaluation result was obtained. Guo Zonglou [15] constructed an environmental impact assessment system for agricultural water conservancy, presented a comprehensive weighted evaluation model and a BP artificial neural network for comprehensive environmental impact assessment, and obtained reasonable quantitative evaluation result. Based on the membership theory of fuzzy mathematics, the comprehensive evaluation method transformed qualitative evaluation into quantitative evaluation, which not only considered the influence of various factors on the research questions, a comprehensive evaluation of the main body of the opinions, and effectively solve the fuzzy problems arising in the evaluation process, carried out a scientific quantitative treatment, combining qualitative evaluation with quantitative calculation, greatly enhanced the scientificity and effectiveness of the evaluation process. It has the characteristics of clear results and strong systematicness, and can solve the problem of fuzzy and difficult to quantify. Fuzzy comprehensive evaluation method is widely applied in expert scoring system, service quality evaluation, major risk source evaluation, project bidding evaluation, water quality evaluation, soil quality evaluation, air quality evaluation, equipment quality evaluation, software project risk assessment and other fields.

This study takes Sichuan Province as an ex-ample, constructs the comprehensive evaluation model of regional water-saving irrigation development level by fuzzy set theory, evaluates the development level of water-saving irrigation in Sichuan Province, and puts forward countermeasures for further development of water-saving irrigation in Sichuan province.

EVALUATION INDEX SYSTEM FOR THE DEVELOPMENT LEVEL OF REGIONAL WATER SAVING IRRIGATION

The Connotation of Water-Saving Irrigation and Its Influencing Factors. Water saving irrigation is a general term of various measures taken to fully and effectively utilize natural precipitation and irrigation water according to the law of crop water requirement and local water supply to obtain the best economic, social and ecological benefits of agriculture, its connotation includes rational development and utilization of water resources, water saving in distribution and distribution system, water saving in field irrigation, water management and agronomic water saving and production increasing [15]. The level of development of water saving irrigation to characterize the water efficiency of irrigation. There are many factors affecting the water saving irrigation, such as the type and scale of the irrigation area, and the natural conditions of the hydrology and geology of the irrigation area, the planting and management of the irrigation area have a great influence on the development of water saving irrigation. Water saving irrigation is not only an engineering problem, but also related to Agronomy Measures and management level. Therefore, the main factors that affect the development level of water-saving irrigation can be divided into three categories: engineering measures, agricultural measures and management measures.

Construction of Evaluation Index System for Development Level of Water-Saving Irrigation. The evaluation index system should fully

reflect the contents of water-saving irrigation construction and meet the requirements of water-saving irrigation construction. According to the principles of scientificity, practicability, comparability and representativeness, it is easy to quantify and accurately basic principles, According to the characteristics of water-saving irrigation, such as engineering, agronomy and management closely related, we have identified three thematic indicators: water-saving engineering, agronomic water saving, water saving management and so on, as well as thirty-four single indicators, which are divided into special targets, constitute the index system for evaluating the development level of water saving irrigation. The indicator system is shown in Table 1, includes nine indicators, agronomic water saving includes five indicators, and management of water saving contains twenty indicators.

TABLE 1
Index system of comprehensive evaluation model of regional water-saving irrigation development level

Aim layer	System layer	Index layer	
Comprehensive evaluation system for the development level of regional water saving irrigation	Evaluation of engineering water-saving	the proportion of saving irrigation area to effective irrigation area	
		the proportion of sprinkling irrigation area to saving irrigation area	
		utilization coefficient of Irrigate water	
		comprehensive benefit per hectare	
		seeping proof rate of main channel	
		seeping proof rate of field channel	
		irrigation water per hectare	
		water resource per capita	
		water resource develop extent	
	Evaluation of agronomic water saving	the proportion of dry seedling area to total paddy area	
		the proportion of Water saving irrigation area to total paddy area	
		crop water production rate of paddy	
		crop water production rate of wheat	
		annual income of farmer per capita	
	Evaluation of management water-savin	policies and regulations	water saving strategy
		investment mechanism	property right system reform
		technology extensive system	government support
		propaganda and education	public participation
		water-saving reward	planning and design
		engineering matching	engineering protection
		engineering classification management	the formulation of the irrigation system
		the popular rate entropy monitoring	popular rate of water measurement technique
		automatic control technology	planned water level
		measurement charge	formulation of reasonable water price

FUZZY COMPREHENSIVE EVALUATION MODEL FOR THE DEVELOPMENT LEVEL OF WATER SAVING IRRIGATION

The evaluation of the development level of regional water-saving irrigation is a comprehensive evaluation process of multi-level, multi indicators and multiple factors. The selection of evaluation methods is also important for the establishment of index system that can reflect the development level of water-saving irrigation. Multi index comprehensive evaluation is a combination of information that reflects multiple attributes of different attributes of the research object, and gets a comprehensive index, which reflects the overall situation of the evaluated object. As a common method of qualitative analysis and quantitative analysis, the fuzzy comprehensive evaluation method is generally effective, and has been widely applied in engineering technology, economic management and social life. At present, one of the difficulties of fuzzy comprehensive evaluation is how to integrate a multi index problem into a single index form scientifically and objectively, so as to achieve comprehensive evaluation in one-dimensional space. The essence of fuzzy comprehensive evaluation is how to reasonably determine the weight of these evaluation indexes [16-17].

Determination of Index Weight. Weight is the importance of evaluating the state characteristics of system state in the structure of evaluation system, or the importance of management decision-makers. It is represented by a value in interval [0, 1]. The weight not only reflects the subjective evaluation of the decision-makers, but also embodies the physical properties of the index, which is a comprehensive measure of subjective and objective. The determination of the weight of the evaluation index is directly related to the accuracy of the final evaluation result. At present, there are many kinds of methods used to calculate the weight of each index in multi index comprehensive evaluation, such as Delphi method, index method, analytic hierarchy process, product factor assignment method, entropy method and so on. In order to make the evaluation results more realistic, this paper uses analytic hierarchy process, subjective weighting and entropy weight, and objective weighting to combine the comprehensive weighting method to determine the weight of evaluation index [18].

Analytic hierarchy process. Analytic hierarchy process is a mathematical method proposed by T. L. Saaty and others in the early 1970s, which is suitable for complex problems that are difficult to be fully used in quantitative analysis. Analytic hierarchy process is a decision-making method of quantitative and qualitative, the complex problem is decomposed into various factors, determine the relative importance of the factors in the hierarchy by twenty-two ways, and then through the comprehensive judgment to determine the relative importance of various factors in the total order. When using analytic hierarchy process to analyze problems, it can be generally divided into five steps: building up a hierarchical structure model, constructing judgement matrix, assigning value, judging matrix, checking consistency, ranking single level and ranking all levels [19].

Entropy method. The use of entropy method to calculate weight can reduce the influence of human subjective factors. Entropy method according to attribute evaluation index, which is divided into incremental evaluation index and decreasing the evaluation index, the basic idea is that according to the variation of the data sequence itself affect the evaluation of the comprehensive effect caused by quantization index changes, the variability of the index generally have greater impact on evaluation the results of this method in determining the weight of the need to implement the normalization processing of each sample [20].

The multiobjective decision matrix $X=(x_{ij})_{m\times n}$ is normalized, form a new judgment matrix $B=(b_{ij})_{m\times n}$,where,

$$b_{ij} = \frac{x_{ij} - x_{\min}(j)}{x_{\max}(j) - x_{\min}(j)} \quad 1 \le i \le m,\ 1 \le j \le n \qquad (1)$$

$x_{max}(j)$—The maximum of the jth indicator in all the schemes.

$x_{min}(j)$—The minimum of the jth indicator in all the schemes.

When the entropy of the jth evaluation index is defined, there are

$$H_j = \frac{1}{\ln m}\left[\sum_{i=1}^{m} f_{ij} \ln f_{ij}\right] \quad 1 \le i \le m,\ 1 \le j \le n \qquad (2)$$

$$f_{ij} = (1 + b_{ij}) / \sum_{j=1}^{n} (1 + b_{ij}) \qquad (3)$$

Then the entropy weight of the jth evaluation index is β_j, and obtained the objective weight vector is $\boldsymbol{\beta}=(\beta_1, \beta_2, \ldots, \beta_n)$,

$$\beta_j = \frac{1 - H_j}{n - \sum_{j=1}^{n} H_j} \qquad 1 \le j \le n \qquad (4)$$

The weight values calculated by the above two methods are multiplied by the weight of the jth index, and the combined weights are obtained by normalization, the normalization formula is,

$$w_j = \frac{\alpha_j \times \beta_j}{\sum_{j=1}^{n} \alpha_j \times \beta_j} \qquad 1 \le j \le n \qquad (5)$$

Where,

w_j—Combination weight.

α_j—The weight of the jth index determined by the analytic hierarchy process.

β_j—The weight of the jth index determined by entropy weight method.

Fuzzy Comprehensive Evaluation. Fuzzy comprehensive evaluation is a method to make a comprehensive decision making use of fuzzy transformation for a certain purpose under the influence of many factors in the fuzzy environment.

Set up a set of factors. A set of factors is a set of elements that influence the various factors of the evaluation object and is recorded as $U=(u_1,u_2,\ldots,u_n)$, which $u_i(i=1, 2, \ldots, n)$ are the influence factors.

Set up a set of comments. A set of comments is a set of evaluation results made by the evaluator on the evaluation object, which is recorded as $V=(v_1, v_2, \ldots, v_m)$, which $v_i(i= 1, 2, \ldots, m)$ are the influence factors. The evaluation classification is divided into "good", "better", "general", "poor" and " relatively poor ".

Setting up the weight set of the evaluation index. In order to reflect the importance of each factor, each factor is given a corresponding weight w, get a set of weights $W=(w_1, w_2, \ldots, w_n)$.

The establishment of fuzzy evaluation matrix.

$$R=\begin{bmatrix} R_1 \\ R_2 \\ \vdots \\ R_n \end{bmatrix}=\begin{bmatrix} r_{11} & r_{12} & \cdots & r_{1m} \\ r_{21} & r_{22} & \cdots & r_{2m} \\ \vdots & \vdots & \ddots & \vdots \\ r_{n1} & r_{n2} & \cdots & r_{nm} \end{bmatrix} \quad (6)$$

Where，

R—Fuzzy judgement matrix.

r_{ij}—The membership degree of the index set relative to the comment set,$r_{ij}\in[0, 1]$.

The membership degree of index is divided into two parts: quantitative index and qualitative index. For qualitative indicators, experts can be directly scored, and membership degree can be calculated through calculation. For quantitative index, membership function of each index is calculated by membership function. Based on the characteristics of various factors affecting the development level of water saving irrigation, this paper constructs a semi trapezoid distribution membership function [20].

TABLE 2
Grading standard of assessment index of the water-Saving Irrigation development level

Classification	I	II	III	IV	V
The proportion of saving irrigation area to effective irrigation area	>55	40～55	25～40	10～25	≤10
The proportion of sprinkling irrigation area to saving irrigation area	>20	13～20	5～13	1～5	≤1
Utilization coefficient of Irrigate water	>0.6	0.5～0.55	0.45～0.5	0.40～0.45	≤0.40
Comprehensive benefit per hectare	>150	110～150	70～110	30～70	≤30
Seeping proof rate of main channel	>90	78～90	65～78	50～65	≤50
Seeping proof rate of field channel	>70	58～70	45～58	30～45	≤30
Irrigation water per hectare	＜200	400～200	600～400	800～600	≥800
Water resource per capita	>3000	1700～3000	1000～1700	500～1000	≤500
Water resource develop extent	＜10	20～10	30～20	40～30	≥40
The proportion of dry seedling area to total paddy area	>80	60～80	40～60	20～40	≤20
The proportion of Water saving irrigation area to total paddy area	>80	60～80	40～60	20～40	≤20
Crop water production rate of paddy	>1.5	1.2～1.5	1.0～1.2	0.8～1.0	≤0.8
Crop water production rate of wheat	>2.0	1.5～2.0	1.0～1.5	0.8～1.0	≤0.8
Annual income of farmer per capita	>8000	6000～8000	4000～6000	2000～4000	≤2000
Qualitative Index	9～10	7～9	5～7	3～5	0～3
Comment	good	better	general	relatively poor	poor

Fuzzy comprehensive evaluation. Fuzzy comprehensive evaluation of evaluation objects $B=W•R=(b_1, b_2, \ldots, b_n)$,the compositional operations used model $M(*, +)$,finally, according to the principle of maximum membership degree, The result of the final evaluation is to take the evaluation set element wj corresponding to $b_j=max(b_1, b_2, b_3, b_4, b_5)$.

TABLE 3
Weights of regional water saving development level comprehensive evaluation index

Aim layer	System layer	Weight	Index layer	The weight of index layer
Evaluation of the development level of water saving irrigation	engineering water-saving	0.392	the proportion of saving irrigation area to effective irrigation area	0.072
			the proportion of sprinkling irrigation area to saving irrigation area	0.086
			utilization coefficient of irrigate water	0.127
			comprehensive benefit per hectare	0.098
			seeping proof rate of main channel	0.138
			seeping proof rate of field channel	0.137
			irrigation water per hectare	0.178
	agronomic water saving	0.271	water resource per capita	0.085
			water resource develop extent	0.071
			the proportion of dry seedling area to total paddy area	0.13
			the proportion of water saving irrigation area to total paddy area	0.13
			crop water production rate of paddy	0.21
			crop water production rate of wheat	0.21
			annual income of farmer per capita	0.39
	management water-saving	0.337	investment mechanism	0.062
			government support	0.058
			policies and regulations	0.055
			engineering protection	0.052
			water saving strategy	0.053
			the formulation of the irrigation system	0.053
			planning and design	0.053
			engineering matching	0.051
			planned water level	0.049
			formulation of reasonable water price	0.051
			measurement charge	0.050
			public participation	0.049
			property right system reform	0.049
			engineering classification management	0.048
			technology extensive system	0.048
			the popular rate of water measurement technique	0.047
			water-saving reward	0.047
			propaganda and education	0.047
			the popular rate entropy monitoring	0.042
			automatic control technology	0.040

TABLE 4
Comprehensive evaluation of water saving irrigation development level in various areas of Sichuan Province

Region	Sichuan	Chendu	Mian-yang	Zi-gong	Panzhihua	Deyang	Lu-zhou	Leshan	Guang-yuan	Nanchon	Suinin
Evaluation result	general	rela-tively poor	general	gen-eral	general	general	better	rela-tively poor	general	general	rela-tively poor
Region	Guangan	Neijiang	Meishan	Dazho u	Yibin	Ziyang	Yaan	Bazhong	Aba	Ganzi	Liang-shan
Evaluation result	general	rela-tively poor	general	better	poor	poor	rela-tively poor	poor	relatively poor	rela-tively poor	rela-tively poor

EXAMPLE

Taking Sichuan Province as an example, this paper analyzes the development status of water saving irrigation in Sichuan Province, and studies the development direction and Countermeasures of water saving irrigation in Sichuan province.

Grading Standard of Evaluation Index. In the evaluation of the development level of water-saving irrigation, according to the relevant norms, standards and expert scoring forms, five level evaluation criteria were established for quantitative indicators and qualitative indicators, and the grading criteria of all indicators and corresponding comments were shown in Table 2.

Determination of Weight. Using analytic hierarchy process and entropy method of subjective and objective weights, by formula (5) to calculate the weights, the results are shown in Table 3.

Evaluation Results and Analysis. The results of comprehensive evaluation of the development level of water saving irrigation in different regions of Sichuan are shown in Table 4. From Table 4, we can see that the development level of water-saving irrigation in Sichuan is relatively poor. There is a significant difference in the development level of water-saving irrigation in different regions. Generally speaking, the development level of water-saving irrigation is not very high in all parts of Sichuan province. Sichuan Province's agricultural water-saving irrigation developing level is general，only two regions in Luzhou and Dazhou are in good level, accounting for 9.5%; eight regions are in general level，accounting for 38.1%; eight regions are in relatively poor level，accounting for 38.1%; and the other three regions such as Yibin，Ziyang and Bazhong are in poor level, accounting for 14.3%. The evaluating result accords with Sichuan Province's actual situation.

CONCLUSIONS AND SUGGESTIONS

The comprehensive evaluation of the development level of regional water-saving irrigation is a comprehensive evaluation process of multi-level, multi indicators and multiple factors. This paper systematically analyzes the influencing factors of regional water-saving irrigation development level from three aspects, namely, engineering water saving, agronomic water saving and management and water saving, constructed scientific and comprehensive evaluation system for the development level of regional water-saving irrigation, and the development level of water-saving irrigation in Sichuan has been evaluated by fuzzy comprehensive evaluation method.

1) The fuzzy comprehensive evaluation method is used to calculate the development level of water-saving irrigation in Sichuan province, the result is general. Most of the evaluation results of cities and counties are general or poor level. The results indicated that Sichuan Province's water-saving irrigation developing level is general, which proves that there is a huge potential in the development of agricultural water-saving in Sichuan province.

2) The comprehensive weight is formed by analytic hierarchy process and entropy weight, which makes up for the lack of expert's subjective experience or evaluation index sample data to determine the weight of evaluation index. The comprehensive evaluation model of regional water saving irrigation development level is used to evaluate the development level of water saving irrigation in Sichuan province, the evaluation result is basically consistent with the actual situation. It shows that the model has clear concept and simple calculation. It can provide scientific guidance for the promotion and application of regional water-saving development.

3) The fuzzy comprehensive evaluation method is used to evaluate the development level of water-saving irrigation in this paper. When the grade of evaluation belongs to the same class, it is impossible to tell where the water saving irrigation level is higher, for example, "Zigong, Panzhihua and Deyang are all general, but they can't distinguish be-

tween the three cities which have high level of development.

4) According to the results of the evaluation, Sichuan province should speed up the development of water saving, strengthen the construction of agricultural water saving project, promote the cultivation of water-saving varieties and the water-saving technology of agricultural technology, improve the effective utilization rate of irrigation water and water productivity, and improve the comprehensive agricultural water-saving technology system coordinated with engineering water saving, agronomic water saving and management and water saving, so as to promote the sustainable development of regional water resources and economic society..

REFERENCES

[1] Wang, J.-L., Wu, J.-S., Qi, X.-B., Yang, B.-Z., Zhao, H., Fan, X.-Y. (2002) Advances in water saving irrigation evaluation. Advances in water science. 13(4), 521-525.

[2] Feng, B.-Q., Cui, J. (2013) Influence analysis of irrigation area composition of well-irrigation district on irrigation water use efficiency in China. Journal of Irrigation and Drainage. 32(3), 50-53.

[3] Wu, Q.-M., Yang, L.-H., Zhai, N. (2009) The research progress on the assessment of development level of watersaving irrigation. Journal of Anhui Agricultural Sciences. 37(6), 2795-2797.

[4] Zerihum, D., Wang, Z., Rimal, S., Feyen, J., Reddy, J.M. (1997) Analysis of surface irrigation performance terms and indices. Agricultural water management. 34, 25-46.

[5] Lin, X.-C., Wang, Z., Li, Y.-N. (1996) Analysis and evaluation of irrigation quality criterion. Journal of Hydraulic Engineering. 11, 73-77.

[6] Zhu, M.-L. (2012) A Study on Agricultural Field High Efficient Water Use Evaluation Index System for Arid Oasis Irrigation District. Water Saving Irrigation. 11, 58-60+63.

[7] Wu, J.-S., Kang, S.-Z., Wang, J.-L. (2004) Study on Selection and Gradation of the Evaluation Index of Comprehensive Effects in the Water-saving Irrigation. Journal of Irrigation and Drainage. 10(23), 17-19.

[8] Cui, Y.-L., Dong, B., Li, Y.-H., Cai X.-L. (2007) Assessment indicators and scales of water saving in agricultural irrigation. Transactions of the Chinese Society of Agricultural Engineering. 23(7), 1-7.

[9] Zhang, X., Cai, H.-J. (2009) Application of fuzzy matter-element model based on coefficients of entropy in comprehensive evaluation of water-saving irrigation project investment. Journal of Water Saving Irrigation. 1, 5-7.

[10] Zhang, J.-N., Yang, L.-H., Zhai, N., Lou, Y.-H., Xing, M.-G. (2010) Assessment of water-saving irrigation level of a regional area based on fuzzy variable assessment method. Journal of Agricultural University of Hebei. 33(3), 111-119.

[11] Cui, N.-B., Zhang, Z.-P., Lou, Y.-H., Gong, D.-Z., Liu, X.-Z. (2016) Evaluation Model of Comprehensive Agricultural Water-saving Development Level Based on TOPSIS in a Regional Area. Journal of Basic Science and Engineering. 24(5), 978-994.

[12] Wang, J.-G., Zhou, Z.-F., Jin, Z.-Q. (2000) Gray Clustering Appraisal of the Sustainable Development of Water Resources in North China. Water Resources and Power. 18(3), 10-12.

[13] Cheng, H.-Y., Guo, Q., Xu, L. (2014) Neural Network-based Optimization Method of Index System. Computer Simulation. 46(2), 20-28.

[14] Lou, Y.-H., Kang, S.-Z., Cui, N.-B., Yang, H.-X., Wang, J.-Q. (2014) Application of Set Pair Analysis in the Comprehensive Water-saving Irrigation Development Level Evaluation. Journal of Sichuan University (Engineering Science Edition). 46(2), 20-28.

[15] Guo, Z.-L. (2000) Methods for Environmental Impact Assessment of Agricultural Water Conservancy Projects. Transactions of the Chinese Society of Agricultural Engineering. 16(5), 16-19.

[16] Bi, X.-L., Hong, W. (2001) Advances of composite evaluation in ecological environment. System Sciemces and Comprehensive Studies in Agriculture. 17 (2), 122-124.

[17] Jin, J.-L., Wei, Y.-M., Ding, J. (2004) Fuzzy comprehensive evaluation model based on improved analytic hierarchy process. Journal of Hydraulic Engineering. 3, 65-71.

[18] Shang, T.-C., Gao, B.-B., Li, X.-P., et al. (2009) Urban land intensive utilization valuation based on AHP and entropy method. Journal of University of Electronic Science and Technology of China(Social Sciences Edition). 11(6), 6-59.

[19] Guo, Q.-S., Dong, Z.-M., Shan, J.-Y. (2016) System Modeling. Beijing: National Defend Industry Press.

[20] Xie, J.-F., Wu, F.-Q., Sun, S.-J. (2006) Application of fuzzy comprehensive evaluation method in industry water right allocation. Haihe Water Resources. 3, 64-66.

Received: **21.10.2017**
Accepted: **06.02.2018**

CORRESPONDING AUTHOR

Lujun Ding
Sichuan College of Architectural Technology,
Deyang 618000 – China

e-mail: mddh9666@126.com

© by PSP Volume 27 – No. 5/2018 pages 2900-2912 Fresenius Environmental Bulletin

ANALYSIS OF SPATIAL AND TEMPORAL WATER POLLUTION PATTERNS IN TERZI POND (KASTAMONU/TURKEY) BY USING MULTIVARIATE STATISTICAL METHODS

Ekrem Mutlu[1,*], Arzu Aydin-Uncumusaoglu[2]

[1]Kastamonu University, Faculty of Fisheries, Kastamonu, Turkey
[2]Giresun University, Faculty of Engineering, Giresun, Turkey

ABSTRACT

This study was performed by collecting water samples at three sites of Terzi Pond in Turkey between August 2015 and July 2016. The aim was to record seasonal changes in physico-chemical parameters to identify any pollution problems, determine the pond's water quality and suitability to sustain aquatic life and classify the quality of the pond's water according to a specific set of criteria. Twenty-one physico-chemical parameters and the concentrations of seven heavy metal ions were evaluated for these purposes. Pearson correlation, hierarchical cluster analysis and principal component analysis were implemented to test the inter-relationships of all parameters and infer pollution source loads.

According to the results of the statistical analyses, it can be estimated that the pollution of the two main regions is mainly caused by nonpoint sources, such as agricultural runoff and soil leaching. In the coming years, water monitoring should be done for water management planning according to the results of these temporal and spatial scales.

KEYWORDS:
Fresh water, heavy metal, multivariate statistical analysis, principal components analysis (PCA), hierarchical cluster analysis (HCA).

INTRODUCTION

Global and regional climate changes and human activities, such as deforestation and those that increase the greenhouse effect, can lead to a degradation of the ecosystem, a reduction of biological diversity and an increase in desertification by depleting water resources and increasing the frequency and severity of droughts. In this context, in some basins the surface flow values are reduced, while in some basins short and irregular regime increases are seen.

The US National Oceanic and Atmospheric Administration and NASA Goddard Institute for Space Studies have issued reports on the dramatic and comprehensive changes in the state of the climate. According to NASA, the average temperature in the first six months of 2016 was 1.3 °C warmer than its counterpart measured during the late 19th century in the pre-industrial era [1].

In a study conducted by the European Environment Agency, water stress levels in Turkey and EU countries were determined in 2000 and 2030. According to this study, Turkey will experience water stress in excess of 40% in the inner and western regions and approximately 20–40% in the south-eastern and eastern regions. The important issues connected to the vulnerability of an area's water resources to climate change are regional differences in surface water supplies and possible flood and drought conditions, reservoir/storage and hydropower generation potential, irrigation, rehabilitation and modernisation, grid systems and groundwater [2]. Surface waters, which comprise rivers, marshes, lakes and ponds, only account for 3% of global fresh water. As the world's population grows and industry develops, fresh water resources are exposed to pollutants, such as organic and inorganic substances, nutrient salts, heavy metals, oils, petroleum derivatives, microorganisms, suspended solids, waste heat, detergents, pesticides and radioactivity, which originate from point or nonpoint sources [3, 4]. These pollutants have a toxic effect on organisms in aquatic ecosystems and are a threat to human health via the food chain. To protect existing surface water reserves in the world, it is of great importance to ensure that sustainable water management is provided at an international level, a goal that can be achieved by taking the necessary measures early on and by conducting monitoring surveys. Today, there are signs of water stress in lakes and ponds used for drinking water, agricultural irrigation, animal farming, electricity generation and recreation. To protect the fresh water reserves of the world, it is necessary to carry out relevant research, take the necessary precautions and control the implementation of sustainable water management procedures.

A pond is generally constructed with sets or embankments next to riverbeds. However, some

ponds are constructed by shifting river waters to natural beds or by transferring the water to the artificially created zone via pipes. Therefore, the aquatic ecosystem produced is a special one, and it is very important to maintain the cleanliness of the water feeding the pond. In the case of a natural pond, the components constituting the pond's environment and its ecosystem, namely, soil, flora, fauna and the ecological environment shared by aquatic organisms, should be planned. Artificial ponds have recently entered our lives and are usually user-oriented recreational structures that include both active and passive recreational items located in or near residential areas. The aim of these structures is to afford access to the refreshing effect of a body of water to individuals who are cut off from nature because of an intensive urban life [5].

The aim of this study was to determine the level of water quality and the sources of pollution of Terzi Pond. Furthermore, statistical methods have been used to facilitate the interpretation of the relationships and inter-relationships [Remark 12]. In accordance with this purpose, different multivariate statistical techniques, such as Pearson's correlation, principal components analysis (PCA) and hierarchical cluster analysis (HCA), are useful for the interpretation of complex data arrays to gain a better understanding of the ecological status and water quality of this study area [6-8]. This study will also determine the suitability of the pond water to aquatic life and will classify the quality of its waters in accordance with the inland surface water classes of Turkey's Surface Water Quality Management Regulation (SWQMR, 2015) [9].

MATERIALS AND METHODS

Sample location and sampling. Terzi Pond is located within the borders of Bozkoca Tepe Village in Kastamonu Province and is west of the Black Sea Region and south of the Isfendiyar Mountains; it has a surface area of 1100 ha and is located approximately 110 m above sea level at a distance of 39 km from Kastamonu. The pond was built in 1977 for agricultural and animal farming purposes. Owing to this pond, 0.3 km^2 (1100 acres) of land can be irrigated, with a maximum irrigation volume of 624,382 m^3. Precipitation, snowmelt and the Devrekani Stream feed the pond. In 2014, a total of 44,000 juvenile European carps (*Cyprinus carpio*) were freed in the basin for fishing purposes.

In this study, the sampling sites were determined by considering factors such as facilities, hydrological status of the pond, distance from streams and sampling points (Table 1, Figure 1).

Warm and temperate climate conditions dominate the region of Terzi Pond, and a significant level of precipitation is observed in the area. Even in the driest months, the amount of rainfall is quite high. The annual average temperature of the district is 8.8 °C, and the average annual precipitation is 621 mm. July is the hottest month of the year, with an average temperature of 18.1 °C; January is the coldest month, with an average temperature of -1.3 °C.

TABLE 1
Coordinates of sampling sites

Region	Coordinate
Site 1	41°49'11.29"N - 33°51'53.09"E
Site 2	41°39'15.79"N - 33°52'70.53"E
Site 3	41°39'16.85"N - 33°51'58.65"E



FIGURE 1
Map of the study area with the locations of the sampling sites (adapted from Google Earth).

The study started in August 2015, the water samples were collected monthly, and the study ended in July 2016. The samples were collected in 2.5 L plastic bottles that had been soaked in 5% nitric acid for 24 h and then rinsed with distilled water. For the analysis of heavy metals, water samples were collected in 1 L polyethylene bottles that had been precleaned with 50% HNO_3 and then washed thrice with deionised water and acidified with 10 ml of concentrated HNO3 per liter of water taken.

Determination of physico-chemical parameters. Among the physical parameters of water quality, dissolved oxygen (DO), electrical conductivity (EC), salinity and water temperature (WT) were measured on-site by using a YSI 556 MPS model multimeter. Other water quality parameters such as biological oxygen demand (BOD), total hardness (TH), total alkalinity (TA) and chemical oxygen demand (COD) and the concentrations of nitrite-nitrogen (NO_2^--N), nitrate-nitrogen (NO_3^--N), ammonium-nitrogen (NH_4^+-N), sulphite (SO_3^{2-}), sulphate (SO_4^{2-}), chloride (Cl^-), potassium (K^+), phosphate-phosphorus (PO_4^{3-}-P), calcium (Ca^{2+}), magnesium (Mg^{2+}) and sodium (Na^+) ions were determined in a laboratory by using the standard method [10, 11]. The concentrations of the nickel (Ni^{2+}), cadmium (Cd^{2+}), lead (Pb^{2+}), copper (Cu^{2+}), ferrous (Fe^{2+}) and zinc (Zn^{2+}) ions in water samples were determined using an inductively coupled plasma–mass spectrometry (ICP-MS) device.

The calibration curve was constructed using a certified multielement standard. The samples were prepared in triplicate and 10 readings were recorded in each parallel ICP-MS device. A blind sample prepared with 1% HNO_3 solution was taken 20 and 3 times of standard slope and LOD (detection limit), respectively, and 10 times LOQ (determination limit) were determined [12].

Data treatment and multivariate statistical analysis. The SPSS statistical package software was utilised to carry out the statistical analysis of the water analysis results. Descriptive statistical analysis, including one-way ANOVA (significance 0.01 and 0.05), was conducted for the sites and seasonal. Large differences in the mean values of the water quality parameters were evaluated by Tukey's multiple range tests [13]. Because of the non-normal distribution of the parameters, the correlation structure between variables was used as a nonparametric measure of the correlation between Pearson's correlation coefficient (r) and the variables calculated over the ranked data [14].

Additionally, the multivariate analysis of the pond water quality data set was performed by HCA [15, 16], wherein Ward's method was used as a measure of similarity [17, 18]. HCA is a combination of techniques for classifying large data sets into similarities or clusters on the basis of differences. PCA is commonly used to assess spatial and temporal variations in water quality [19]. Before implementing PCA in the present study, the Kaiser–Meyer–Olkin (KMO) test and Bartlett's tests were performed. In this study, KMO's adequacy was 0.704 for data relative to Terzi Pond. In Bartlett's test, $P = 0$ would indicate that the variables are unrelated. Analytical data were evaluated by performing HCA and PCA with standardised experimental image data for z-scale transformation to avoid misclassification due to wide differences in data densities [20, 21].

RESULTS AND DISCUSSION

The water samples were collected monthly from three sites, and the mean, standard deviation and minimum–maximum values of the water quality parameters are presented in Table 2.

According to analysis results, the mean value and standard deviation of water quality parameters were the following: DO = 9.780 ± 1.492 mg L^{-1}, salinity = 0.055 ± 0.023‰, pH 8.196 ± 0.276, WT = 13.219 ± 6.359 °C, EC = 198.241 ± 53.150 µS cm^{-1}, suspended solid (SS) matter = 4.738 ± 1.204 mg L^{-1}, COD = 2.429 ± 1.109 mg L^{-1}, BOD_5 = 1.589 ± 0.466 mg L^{-1}, $[Cl^-]$ = 3.933 ± 1.163 mg L^{-1}, $[PO_4^{3-}]$ = 0.160 ± 0.126 mg L^{-1}, $[SO_4^{2}]^-$= 46.868 ± 9.186 mg L^{-1}, $[SO_3^{2-}]$ = 0.926 ± 0.376 mg L^{-1}), $[Na^+]$ = 54.456 ± 12.991 mg L^{-1}, $[K^+]$ = 7.394 ± 3.675 mg L^{-1}, TH = 280.219 ± 21.540 mg L^{-1}, TA = 285.694 ± 21.397 mg L^{-1}, $[Mg^{2+}]$ = 42.685 ± 10.821 mg L^{-1}, $[Ca^{+2}]$ = 50.908 ± 11.252 mg L^{-1}, $[NO_2^-]$ = 0.00018 ± 0.00014 mg L^{-1}, $[NO_3^-]$ = 4.661 ± 3.019 mg L^{-1}, $[NH_4^+]$ = 0.00037 ± 0.00075 mg L^{-1}, $[Fe^{2+}]$ = 0.0006 ± 0.0012 mg L^{-1}, $[Pb^{2+}]$ = 0.5972 ± 0.4378 µg L^{-1}, $[Cu^{2+}]$ = 3.083 ± 3.281 µg L^{-1}, $[Cd^{2+}]$ = 0.183 ± 0.227 µg L^{-1}, $[Hg^{2+}]$ = 0.00074 ± 0.0012 µg L^{-1}, $[Ni^{2+}]$ = 0.528 ± 0.910 µg L^{-1} and $[Zn^{2+}]$ = 6.00 ± 6.476 µg L^{-1}.

In this study, statistically significant differences (*P>0.05*) were found between the seasons, however, no statistically significant difference (*P>0.05*) was found between the stations (Table 2).

The DO, one of the most important parameters to determine in an aquatic ecosystem, provides information on the entire correlation network within the aquatic cycle: bacterial activity, photosynthesis, availability of nutrients, stratification, etc. [22]. The DO level in Terzi Pond varied from 3.310 to 11.360 mg L^{-1}. The lowest DO level was observed at Site 2 in August, whereas the highest level was measured at Site 1 in June. The DO is in a negative, highly significant ($r \geq -0.7$) relationship at $P < 0.01$ and $P < 0.05$ with EC (r = −0.701) (Table 3). Moreover DO has, at the same level of significance, a positive significant relationship with the concentration of the Na^+ ion (r = 0.558). For aquatic life to thrive, the DO level of inland waters must not be under 5 mg L^{-1} [23]. It was concluded that this pond is suitable for aquatic life, although conditions are below optimum

during the summer (Table 2). This pond is generally a Class I (>8 mg L^{-1}) body of water in terms of DO; therefore, its water is considered clean [9].

Salinity in bodies of fresh water is a very important factor because the pond's water may be used both for human consumption (drinking) and irrigation. The salinity level of Terzi Pond ranges between 0.020‰ and 0.110‰. The lowest level of salinity was observed at Site 2 in January and February, whereas the highest level was measured at the same site in October. The salinity has a highly significant ($r \geq 0.7$) positive relationship at $P < 0.01$ and $P < 0.05$ with pH (r = 0.740), WT (r = 0.947), EC (r = 0.915), SS (r = 0.898), BOD_5 (r = 0.911), [Cl-] (r = 0.708), TH (r = 0.708) and [Mg2+] (r = 0.797) and has a significant negative relationship with DO (Table 3). This pond's salinity is low, as expected from a body of fresh water, and is suitable for aquatic life.

TABLE 2
Seasonal mean values, standard deviations and ranges (min.–max.) of water quality parameters

	Winter	Spring	Summer	Autumn	WHO [24]	Class [9]
DO (mg L^{-1})	9.943±0.594^{ab} 8.620-10.460	10.992±0.210^{c} 10.820-11.280	9.466±2.464^{ab} 3.310-11.360	8.720±0.460^{a} 8.320-9.360		**I**
Salinity (‰)	0.032±0.012^{a} 0.020-0.050	0.043±0.007^{a} 0.030-0.050	0.063±0.012^{b} 0.050-0.080	0.081±0.020^{c} 0.050-0.110		
pH	8.063±0.068^{a} 7.980-8.180	8.071±0.146^{a} 7.880-8.250	8.056±0.182^{a} 7.820-8.280	8.593±0.192^{b} 8.340-8.820	6.5-8.5	**II**
WT (°C)	6.256±3.188^{a} 3.900-10.600	9.467±2.342^{a} 6.600-12.200	17.256±3.350^{b} 12.800-20.600	19.900±3.336^{b} 15.100-23.100		**I**
EC (µS cm^{-1})	162.360±16.546^{a} 146.76-185.30	146.116±16.789^{a} 123.28-163.83	226.183±35.299^{b} 182.53-268.160	258.304±33.397^{b} 212.68-285.02	1500.0	**I**
SS (mg L^{-1})	3.567±0.878^{a} 2.640-4.700	3.883±0.653^{a} 2.980-4.360	5.642±0.311^{b} 5.240-6.020	5.858±0.597^{b} 5.040-6.360		
COD (mg L^{-1})	1.184±0.673^{a} 0.520-2.100	1.997±1.116^{a} 0.660-3.310	3.302±0.195^{b} 3.080-3.600	3.231±0.329^{b} 2.820-3.660	10.0	**I**
BOD_5 (mg L^{-1})	1.089±0.151^{a} 0.900-1.300	1.310±0.121a 1.200-1.500	1.860±0.273^{b} 1.500-2.120	2.096±0.314^{b} 1.660-2.360		**I**
Cl^-(mg L^{-1})	3.037±1.635^{a} 1.890-5.250	3.264±0.664^{a} 2.370-3.950	4.652±0.075^{b} 4.570-4.770	4.777±0.084^{b} 4.630-4.890	250.0	**I**
PO_4^{3-} (mg L^{-1})	0.068±0.043^{a} 0.030-0.128	0.103±0.096^{a} 0.035-0.238	0.135±0.043^{a} 0.092-0.196	0.334±0.093^{b} 0.208-0.420		**II**
SO_4^{2-} (mg L^{-1})	40.108±3.541^{a} 35.390-42.840	44.480±1.968^{a} 41.600-47.320	60.073±5.716^{b} 53.340-67.560	42.811±6.894^{a} 35.420-51.400	250.0	
SO_3^{2-} (mg L^{-1})	0.617±0.260^{a} 0.280-0.880	1.233±0.322b 0.840-1.680	1.192±0.151^{b} 0.980-1.390	0.662±0.227^{a} 0.440-0.980		
Na^+ (mg L^{-1})	45.103±1.185^{a} 43.690-46.640	65.487±8.849^{b} 48.640-76.400	64.103±13.182^{b} 48.340-79.140	43.129±0.718^{a} 42.060-44.180	200.0	
K^+ (mg L^{-1})	6.936±1.101^{ab} 5.540-8.180	6.673±3.955^{ab} 1.720-11.160	10.616±5.005^{b} 6.920-17.720	5.351±0.059^{a} 5.260-5.440	12.0	
TH ($CaCO_3$ mg L^{-1})	254.371±3.281^{a} 249.50-258.74	272.769±9.445^{b} 262.76-285.64	304.541±2.931^{d} 299.63-308.64	289.196±18.739^{c} 266.50-311.68		
TA ($CaCO_3$ mg L^{-1})	261.121±3.431^{a} 256.670-265.490	279.623±9.865^{b} 269.170-293.770	309.747±4.667^{c} 303.830-316.190	292.283±21.253^{b} 265.670-318.330	200	
Mg^{2+} (mg L^{-1})	33.563±9.156^{a} 25.640-45.70	33.429±3.726^{a} 30.360-38.460	52.827±5.121^{b} 46.420-58.720	50.921±2.510^{b} 47.920-53.820	50	
Ca^{2+} (mg L^{-1})	37.726±9.585^{a} 29.950-50.490	53.659±12.621^{b} 40.670-69.570	57.133±5.366^{b} 50.110-62.990	55.112±2.545^{b} 51.890-58.210	300	
NO_2^- (mg L^{-1})	0.00005±0.00002^{a} 0.00002-0.00008	0.00017±0.00007^{b} 0.00008-0.00028	0.00037±0.00015^{c} 0.00022-0.00060	0.00013±0.00004^{ab} 0.00006-0.00018		**I**
NO_3^- (mg L^{-1})	1.5933±0.74223^{a} 0.820-2.560	4.49667±2.20345^{b} 2.10-7.220	8.33556±2.77151^{b} 5.10-11.560	4.21778±0.86443^{c} 3.02000-4.860	50	**I**
NH_4^+ (mg L^{-1})	0.00023±0.00035^{a} 0.0-0.00080	0.00019±0.00021^{a} 0.0-0.00060	0.00015±0.00011^{a} 0.00004-0.00040	0.00091±0.00136^{a} 0.00-0.00310	35	**I**
Fe^{2+} (mg L^{-1})	0.0±0.0^{a} 0.0-0.0	0.00001±0.00002^{a} 0.00-0.00007	0.00013±0.00008^{a} 0.00001-0.00027	0.00222±0.00148^{b} 0.0010-0.005	0.300	**I**
Pb^{2+} (µg L^{-1})	0.38889±0.13642^{a} 0.20-0.60	0.87778±0.36667^{b} 0.50-1.50	0.78889±0.62539^{ab} 0.10-1.70	0.33333±0.19365^{a} 0.10-0.60	10	**I**
Cu^{2+} (µg L^{-1})	0.0±0.0^{a} 0.0-0.0	3.55556±3.08671^{b} 0.0-8.0	5.77778±4.05518^{b} 1.00-12.00	3.00±1.41421^{ab} 1.00-5.00	20	**I**
Cd^{2+} (µg L^{-1})	0.256±0.42459^{a} 0.0-1.0	0.10±0.0^{a} 0.10-0.10	0.156±0.08819^{a} 0.100-0.300	0.222±0.14814^{a} 0.10-0.500		**I**
Hg^{2+}(µg L^{-1})	0.00033±0.00071^{a} 0.0-0.0020	0.00±0.00^{a} 0.0-0.0	0.00056±0.00088^{a} 0.0-0.0020	0.00209±0.00161^{b} 0.00050-0.0050		**I**
Ni^{2+} (µg L^{-1})	0.333±0.707^{a} 0.0-2.0	0.111±0.333^{a} 0.0-1.0	0.111±0.333^{a} 0.0-1.0	1.556±1.130^{b} 0.0-3.0		**I**
Zn^{2+} (µg L^{-1})	0.333±0.70711^{a} 0.0-2.0	5.222±5.16667^{a} 0.0-12.0	12.444±6.67291^{b} 4.0-21.0	6.00±5.3151^{a} 0.0-13.00	10	**I**

$^{a.b.c}$ Means with different letters in the same column are statistically significant ($P<0.05$)

TABLE 3
Pearson correlation matrix among the variables

	DO	Salinity	pH	WT	EC	SS	COD	BOD_5	Cl^-	PO_4^{3-}	SO_4^{2-}
DO	1										
S	-0.596**	1									
pH	-0.605**	**0.740****	1								
WT	-0.576**	**0.947****	0.636**	1							
EC	**-0.701****	**0.915****	**0.721****	**0.941****	1						
SS	-0.537**	**0.898****	0.532**	**0.962****	**0.918****	1					
COD	-0.242	0.674**	0.191	**0.805****	0.656**	**0.833****	1				
BOD_5	-0.570**	**0.911****	0.671**	**0.940****	**0.926****	**0.887****	0.665**	1			
Cl^-	-0.396*	**0.708****	0.349*	**0.804****	**0.704****	**0.871****	**0.860****	0.590**	1		
PO_4^{3-}	-0.260	0.601**	0.472**	0.632**	0.562**	0.593**	**0.731****	0.555**	0.623**	1	
SO_4^{2-}	0.068	0.204	-0.212	0.301	0.230	0.371*	0.357*	0.345*	0.196	-0.203	1
SO_3^{2-}	0.345*	-0.052	-0.390*	-0.011	-0.166	0.047	0.154	0.053	-0.094	-0.355*	0.667**
Na^+	0.558**	-0.198	-0.637**	-0.108	-0.360*	-0.044	0.277	-0.156	0.055	-0.151	0.577**
K^+	0.357*	-0.141	-0.612**	-0.045	-0.103	0.119	0.384*	-0.070	0.133	0.026	0.601**
TH	-0.314	**0.708****	0.296	**0.796****	0.717**	**0.783****	**0.707****	**0.818****	0.539**	0.274	**0.756****
TA	-0.293	0.609**	0.242	**0.727****	0.651**	**0.718****	0.663**	**0.750****	0.496**	0.200	**0.753****
Mg^{2+}	-0.523**	**0.797****	0.453**	**0.913****	**0.863****	**0.921****	**0.820****	**0.796****	**0.890****	0.533**	0.400*
Ca^{2+}	-0.185	0.621**	0.177	**0.736****	0.530**	**0.718****	**0.837****	0.595**	**0.758****	0.476**	0.275
NO_2^-	0.194	0.163	-0.369*	0.285	0.123	0.397*	0.607**	0.235	0.399*	0.103	**0.838****
NO_3^-	0.183	0.274	-0.330*	0.424**	0.214	0.504**	**0.771****	0.328	0.545**	0.318	**0.712****
NH_4^+	-0.099	0.006	0.116	0.105	0.067	0.106	0.357*	-0.016	0.358*	0.589**	-0.437**

	SO_3^{2-}	Na^+	K^+	TH	TA	Mg^{2+}	Ca^{2+}	NO_2^-	NO_3^-	NH_4^+
DO										
S										
pH										
WT										
EC										
SS										
COD										
BOD_5										
Cl^-										
PO_4^{3-}										
SO_4^{2-}										
SO_3^{2-}	1									
Na^+	**0.710****	1								
K^+	0.512**	0.655**	1							
TH	0.450**	0.292	0.322	1						
TA	0.475**	0.316	0.317	**0.972****	1					
Mg^{2+}	-0.068	-0.025	0.058	**0.754****	**0.713****	1				
Ca^{2+}	0.294	0.387*	0.169	0.681**	0.669**	**0.721****	1			
NO_2^-	0.629**	**0.763****	**0.799****	0.651**	0.645**	0.404*	0.451**	1		
NO_3^-	0.514**	**0.746****	**0.740****	0.645**	0.617**	0.527**	0.625**	**0.924****	1	
NH_4^+	-0.382*	-0.228	-0.158	-0.234	-0.209	0.183	0.123	-0.083	0.026	1

Strong relationships (r> ± 0.700) are shown in bold.
* Correlation is significant at the 0.05 level (two-tailed), **Correlation is significant at the 0.01 level (two-tailed)

pH, one of the most important parameters determining the corrosive nature of water, is known to be positively associated with EC and TA [25]. The pH level of Terzi Pond ranges between pH 7.820 and 8.820. The lowest pH was observed at Site 1 in June, whereas the highest level was measured at Site 2 in September. This value range is similar to that observed at Sakiz Pond [26]. The pH has a highly significant ($r \geq 0.7$) positive relationship at $P < 0.01$ and $P < 0.05$ with EC ($r = 0.721$) and a negative relationship with DO ($r = -0.605$), pH ($r = -0.740$), [Na^+] ($r = -0.637$) and [K^+] ($r = -0.612$) (Table 3). This pond's pH confers to it a mildly alkaline character, thus placing this body of water in Class III (6–9); in other words, its water is considered polluted [9].

The response to sudden changes in WT depends on the tolerance of the particular organism. WT changes can cause an organism to die or migrate and affect its growth, reproduction and/or immunity. The WT of Terzi Pond ranges between 3.90 °C and 23.10 °C. The lowest temperature was measured at Site 1 in February, whereas the highest was measured at Site 2 in October. This parameter displays a highly significant ($r \geq 0.7$) positive relationship at $P < 0.01$ and $P < 0.05$ with EC ($r = 0.941$), SS ($r = 0.962$), COD ($r = 0.805$), BOD_5 ($r = 0.805$), [Cl^-] ($r = 0.804$), TH ($r = 0.796$), TA ($r = 0.727$), [Mg^{2+}] ($r = 0.913$) and [Ca^{2+}] ($r = 0.736$) and a negative significant relationship with DO (Table 3). In conclusion, Terzi Pond is suitable for aquatic life and does not have seasonal WT-based threats. Moreover, according to the inland water quality criteria of SWQMR, the pond was found to be a Class I body of water (≤25 °C) (Table 2).

For good aquaculture in fresh water, it has been determined that the EC needs to be in the 100–150 μS cm^{-1} range [27]. In a 2010 paper, Navneet Kumar et al. [28] stated that the quality of underground

drinking water could be controlled effectively by controlling water conductivity. The EC value of Terzi Pond varied between 123.280 and 285.020 µS cm^{-1}. The lowest EC level was observed in March at Site 1, whereas the highest level was measured at Site 2 in September. This parameter has a highly significant ($r \geq 0.7$) positive relationship at $P < 0.01$ and $P < 0.05$ with SS (r = 0.918), BOD_5 (r = 0.926), [Cl^-] (r = 0.704), TH (r = 0.717) and [Mg^{2+}] (r = 0.863) and a negative significant relationship with DO (Table 3). According to the classification criteria of SWQMR and WHO guidelines, as far as the EC level is concerned (<400 µS cm^{-1}), the pond is suitable for recreational uses (including those involving personal contact, such as swimming) and for animal husbandry and agricultural purposes. Furthermore, it is a Class I body of water, thus indicating that its water is considered clean (Table 2) [9, 24].

The level of SS in a pond or lake is significantly affected by the phytoplankton concentration and by the amount of flood waters reaching the basin. At high level, SS damages the sensitive tissues of fish, such as gills, and can cause damage or death to all aquatic larvae and eggs. The level of SS in this pond ranges between 2.640 and 6.360 mg L^{-1}. The lowest level was observed at Site 3 in January, whereas the highest level was measured at Site 2 in September. The level of SS has a highly significant ($r \geq 0.7$) positive relationship, at $P < 0.01$ and $P < 0.05$, with COD (r = 0.833), BOD_5 (r = 0.887), [Cl^-] (r = 0.871), TH (r = 0.783), TA (r = 0.718), [Mg^{2+}] (r = 0.921) and [Ca^{2+}] (r = 0.718), and a negative significant relationship with DO (Table 3).

COD, one of the important parameters used as a measure of water contamination by organic matter, provides the means to determine the degree of pollution due to domestic and industrial wastewater. This parameter varied between 0.520 and 3.660 mg L^{-1} in Terzi Pond. The lowest COD level was observed at Site 1 in February, whereas the highest level was measured at Site 1 in November. This parameter has a highly significant ($r \geq 0.7$) positive relationship at $P < 0.01$ and $P < 0.05$ with [Cl^-] (r = 0.860), [PO_4^{3-}] (r = 0.731), TH (r = 0.707), [Mg^{2+}] (r = 0.820), [Ca^{2+}] (r = 0.837), [NO_3^-] (r = 0.771), WT, SS and a significant negative relationship with DO (Table 3). According to the inland water quality criteria of SWQMR, the pond was found to be a Class I body of water (≤25 mg L^{-1}), thus indicating that its water is clean [9].

BOD_5 It is considered to be a sign of the level of water pollution and is the amount of dissolved oxygen required for the biochemical separation of organic compounds and for the oxidation of certain inorganic materials (e.g. iron, sulphites) [29]. The concentration of the BOD_5 in Terzi Pond, varied between 0.900 and 2.360 mg L^{-1}. The lowest value for this parameter was observed at Site 1 in January, whereas the highest level was measured at Site 2 in October. BOD_5 displays a highly significant ($r \geq 0.7$) positive relationship at $P < 0.01$ and $P < 0.05$ with TH (r = 0.818), TA (r = 0.750), [Mg^{2+}] (r = 0.796), salinity, WT, EC and SS and a negative significant relationship with DO (Table 3). Furthermore, according to the inland water quality criteria of SWQMR, the pond was a Class I (<4 mg L^{-1}) body of water in terms of BOD_5, thus indicating that its water is clean [9]. Notably, the BOD_5 value of Terzi Pond is lower than that of Borçka Lake and higher than that of Çiğdem Pond [27, 30].

Chloride ion concentration, which is generally low in natural waters, is a parameter of considerable importance for all water uses [31]. The chloride ion concentration of Terzi Pond varied between 1.890 and 5.250 mg L^{-1}. The lowest chloride concentration was observed at Site 1 in February, whereas the highest concentration was measured at Site 2 in December. Chloride ion concentration has a highly significant ($r \geq 0.7$) positive relationship at $P < 0.01$ and $P < 0.05$ with [Mg^{2+}] (r = 0.890), [Ca^{2+}] (r = 0.758), salinity, WT, EC, SS and COD and a negative significant relationship with DO (Table 3). With respect to the value of the chloride ion concentration, Terzi Pond is a Class I (≤10 mg L^{-1}) body of water, thus indicating that its water is clean [9].

In lakes and river, the phosphate ion, which is a mineral nutrient, is found in the form of inorganic phosphate, dissolved phosphate and organic particles [3]. The concentration of the phosphate ion in Terzi Pond varied between 0.030 and 0.420 mg L^{-1}. The lowest phosphate ion concentration was observed at Site 1 in February, whereas the highest level was measured at Site 2 in November. The highest phosphate ion concentration in this pond is higher than the corresponding parameter measured in Derbent and Borçka Dam Lakes, and it is lower than the same parameter measured in Işiktepe Dam Lake [32-34]. The phosphate ion concentration displays a highly significant ($r \geq 0.7$) positive relationship at $P < 0.01$ and $P < 0.05$ with COD (r = 0.731) and a negative significant relationship with DO (Table 3). According to the SWQMR, the pond is a Class III (<0.65 mg L^{-1}) body of water in terms of phosphate ion concentration, thus indicating that its water is polluted. For the trophic classification system with regard to lakes, ponds and reservoirs, Terzi Pond was determined to be oligotrophic (<10 TP µg L^{-1}) [9].

Sulphate ion concentration has a very important role in phytoplankton development, which is of great importance in the biological cycle of natural waters. An increase in sulphate ion concentration in the aquatic environment signals that the environmental pollution load is increasing. The sulphate ion concentration of Terzi Pond varied from 35.390 to 67.560 mg L^{-1}. The lowest sulphate concentration was observed at Site 1 in December, whereas the highest concentration was measured at Site 2 in June. The acceptable limit of this parameter for aquatic organisms is 90 mg L^{-1} [35]. The highest sulphate ion concentration in Terzi Pond is much lower than the

corresponding parameter measured in Derbent Lake and higher than the same parameter measured in the Oyun Reservoir [33, 36]. Sulphate ion concentration displays a highly significant ($r \geq 0.7$) positive relationship at $P < 0.01$ and $P < 0.05$ with TH ($r = 0.756$), TA ($r = 0.753$) and [NO_2^-] ($r = 0.838$) and a negative significant relationship with pH and [PO_4^{3-}] (Table 3).

Sulphite ion concentration in Terzi Pond ranged between 0.280 and 1.680 mg L^{-1}. The lowest sulphite ion concentration was observed at Site 3 in December, whereas the highest concentration was measured at Site 2 in April. Sulphite ion concentration displays a highly significant ($r \geq 0.7$) positive relationship at $P < 0.01$ and $P < 0.05$ with the concentration of the sodium ion ($r = 0.710$) and a negative significant relationship with salinity, pH, WT, EC, [Cl^-] and [PO_4^{3-}] (Table 3). In conclusion, with respect to the level of the sulphite ion, it was found that this pond is suitable for aquatic life and that there are no seasonal threats to it. The pond was found to be a Class I (≤2 mg L^{-1}) body of water in terms of sulphite ion concentration, thus indicating that its water is clean [9].

The presence of dissolved sodium ions in the water in excess of the limit is a limiting factor for the growth and development of the algae.

The sodium ion concentration of Terzi Pond ranged between 42.060 and 79.140 mg L^{-1}. The lowest sodium ion concentration was observed at Site 3 in October, whereas the highest concentration was measured at Site 2 in June. Sodium ion concentration displays a highly significant ($r \geq 0.7$) positive relationship at $P < 0.01$ and $P < 0.05$ with [NO_2^-] ($r = 0.763$), [NO_3^-] ($r = 0.746$) and [SO_3^{2-}] and a negative significant relationship with salinity, pH, WT, EC, SS, BOD_5 and [PO_4^{3-}] (Table 3).

Potassium salts are among the inorganic salts that confer taste to water, and they play an important role in the development of herbal organisms. At the same time, the presence of potassium ions in water also accelerates the development of plankton, thus contributing to the food chain. In Terzi Pond, potassium ion concentration varied from 1.720 to 17.720 mg L^{-1}. The lowest potassium ion concentration was observed at Site 3 in March, whereas the highest concentration was measured at Site 2 in June. Potassium ion concentration displays a highly significant ($r \geq 0.7$) positive relationship at $P < 0.01$ and $P < 0.05$ with [NO_2^-] ($r = 0.799$) and [NO_3^-] ($r = 0.740$) and a negative significant relationship with salinity, pH, WT, EC and BOD_5 (Table 3).

The TH of water originates from the presence in water of calcium and magnesium bicarbonate, calcium and magnesium chloride, calcium and magnesium nitrate and limited amounts of salts of ferrous, aluminium and strontium ions [37]. The TH of Terzi Pond varied from 249.50 to 311.680 $CaCO_3$ mg L^{-1}. The lowest TH was observed at Site 1 in December, whereas the highest level was measured at Site 2 in September. The TH displays a highly significant ($r \geq 0.7$) positive relationship at $P < 0.01$ and $P < 0.05$ with TA ($r = 0.972$), [Mg^{2+}] ($r = 0.754$), salinity, WT, EC, SS, COD, BOD_5 and [SO_4^{2-}] and a significant negative relationship with DO (Table 3).

The TA of Terzi Pond varied between 256.670 and 318.330 $CaCO_3$ mg L^{-1}. The lowest TA level was observed at Site 1 in December, whereas the highest level was measured at Site 2 in September. This parameter displays a highly significant ($r \geq 0.7$) positive relationship at $P < 0.01$ and $P < 0.05$ with [Mg^{2+}] ($r = 0.713$), WT, SS, BOD_5, [SO_4^{2-}] and TH and a significant negative relationship with DO (Table 3).

The magnesium ion is present in all natural waters. It is a component of chlorophyll, and no ecosystems exist that are free of this ion; therefore, magnesium is a very important element for life [38]. The magnesium ion concentration in Terzi Pond ranged from 25.640 to 58.720 mg L^{-1}. The lowest magnesium ion concentration was observed at Sites 1 and 2 in February, whereas the highest concentration was measured at Site 2 in July. Magnesium ion concentration displays a highly significant ($r \geq 0.7$) positive relationship at $P < 0.01$ and $P < 0.05$ with [Ca^{2+}] ($r = 0.721$), salinity, WT, EC, SS, COD, BOD_5, [Cl^-], TH and TA and a significant negative relationship with DO, [SO_3^{2-}] and [SO_4^{2-}] (Table 3).

The presence of calcium and magnesium cations in water increases the permeability of land to the water itself. Therefore, the concentrations of these two ions are important parameters in determining ponds suitable for irrigation purposes. In Terzi Pond, the concentration of the calcium ion varied from 29.950 to 69.570 mg L^{-1}. The lowest calcium ion concentration was observed at Site 1 in February, whereas the highest concentration was measured at Site 2 in May. According to Pearson's correlation, the calcium ion concentration displays a highly significant ($r \geq 0.7$) positive relationship at $P < 0.01$ and $P < 0.05$ with WT, SS, COD, [Cl^-] and [Mg^{2+}].

The nitrogen-containing compounds widely existing in natural waters are nitrites, nitrates, ammonium salts and organic nitrogen species [39]. The concentration of the nitrite ion in Terzi Pond was found to vary between 0.00002 and 0.00060 mg L^{-1}. The lowest concentration was observed at Site 1 in January, whereas the highest concentration was determined at Site 2 in June. The nitrite ion concentration displays a highly significant ($r \geq 0.7$) positive relationship at $P < 0.01$ and $P < 0.05$ with [NO_3^-] ($r = 0.924$), [Na^+] and [K^+] (Table 3). In conclusion, it was found that this pond is suitable for aquatic life. This pond's mean nitrite concentration was found to be within the limits of a Class I (≤0.01 mg L^{-1}) body of water, thus indicating that its water is clean [9].

The nitrate ion is nontoxic for most aquatic organism; however, high concentrations of nitrate ions (>10 mg L^{-1}) can result in the over-fertilisation of ponds, which may lead to harmful algae blooms that

adversely affect the taste and odour of the water. Furthermore, as the over-fertilised algae start dying, decomposing mats of algae can deplete the oxygen supply in the pond, causing high fish mortality. The nitrate ion concentration in Terzi Pond was found to vary between 0.820 and 11.560 mg L^{-1}. The lowest concentration of nitrate was observed at Site 1 in February, whereas the highest concentration was determined at Site 2 in June. The concentration of the nitrate ion displays a highly significant ($r \geq 0.7$) positive relationship at $P < 0.01$ and $P < 0.05$ with COD, $[Na^+]$, $[K^+]$ and $[NO_2^-]$ (Table 3). In conclusion, according to the inland water quality criteria of SWQMR, the pond was found to be a Class III (≤20 mg L^{-1}) body of water in terms of nitrate ion concentration, thus indicating that its water is polluted [9].

The ammonium ion is insignificantly toxic to organisms living in an aquatic medium. However, it transforms into ammonium at high pH and temperature, thus becoming toxic to fish and other organisms [31]. The ammonium ion concentration in Terzi Pond was found to vary between 0 and 0.00310 mg L^{-1}. The lowest concentration of the ion was observed at all sites in January, February, March and September, whereas the highest concentration was determined at Site 2 in November. The concentration of the ammonium ion displays a negative significant relationship at $P < 0.01$ and $P < 0.05$ with DO, $[SO_3^{2-}]$, $[SO_4^{2-}]$ and $[NO_2^-]$ (Table 3). According to the inland water quality criteria of SWQMR, the pond was found to be a Class I (<0.2 mg L^{-1}) body of water in terms of ammonium ion concentration, thus indicating that its water is clean [9].

The ferrous ion is very important for the aquatic environment because iron is used for the secretion of many enzymes required for the growth and survival of autotrophic bacteria. The concentration of the ferrous ion in Terzi Pond was found to range between 0.0 and 0.0050 µg L^{-1}. The lowest concentration of this ion was observed at all sites in January, February, March and April, whereas the highest concentration was determined at Site 1 in October. The ferrous ion concentration displays a highly significant ($r \geq 0.7$) positive relationship at $P < 0.01$ and $P < 0.05$ with $[Hg^{2+}]$ (r = 0.837) and a significant negative relationship with $[Pb^{2+}]$ (-r = 0.225) (Table 3). According to the inland water quality criteria of SWQMR, the pond was a Class I (≤300 µg L^{-1}) body of water in terms of ferrous ion concentration, thus indicating that its water is clean [9].

Sources of heavy metal ions such as Cu^{2+}, Cd^{2+}, Zn^{2+} and Pb^{2+} in fresh water are generally anthropogenic [40]. The mean lead ion concentration in Terzi Pond was found to range between 0.10 and 1.70 µg L^{-1}. The lowest concentration of the lead ion was observed at all sites in September, whereas the highest concentration was determined at Site 2 in June. The concentration of the lead ion displays a highly significant ($r \geq 0.7$) positive relationship at $P < 0.01$ and $P < 0.05$ with $[Cu^{2+}]$ (r = 0.836) and $[Zn^{2+}]$ (r = 0.741) and a significant negative relationship with $[Cd^{2+}]$ (−r = −0.256), $[Hg^{2+}]$ (−r = 0.256) and $[Ni^{2+}]$ (−r = 0.039) (Table 4). According to the inland water quality criteria of SWQMR, the pond was a Class I (≤10 µg L^{-1}) body of water in terms of lead ion concentration, thus indicating that its water is clean [9].

The concentration of copper ions in water is the most important indicator of metal toxicity [41]. The value of this parameter in Terzi Pond was found to range between 0 and 12.0 µg L^{-1}. The lowest concentration of copper ions was observed at all sites in December, whereas the highest concentration was determined at Sites 1 and 2 in June. Furthermore, evidence indicates that the concentration of copper ions in the Yağlıdere stream is highest during the spring [42]. The concentration of this heavy metal ion displays a highly significant ($r \geq 0.7$) positive relationship at $P < 0.01$ and $P < 0.05$ with $[Zn^{2+}]$ (r = 0.944) and a significant negative relationship with $[Cd^{2+}]$ (−r = −0.236) and $[Hg^{2+}]$ (−r = 0.162) (Table 4). According to the inland water quality criteria of SWQMR, the pond was found to be a Class I (≤20 µg L^{-1}) body of water in terms of copper ion concentration, thus indicating that its water is considered clean [9].

The concentration of cadmium ions, one of the most toxic pollutants, in uncontaminated natural waters is generally below 1 µg L^{-1}. The cadmium ion concentration in Terzi Pond varied from 0 to 1.00 µg L^{-1}. The lowest concentration of Cd^{2+} was observed at all sites in January, whereas the highest concentration was determined at Sites 1 and 2 in December. The highest value for this parameter in this pond is higher than its counterpart in Çiğdem Pond [31]. The concentration of this metal ion displays a significant positive relationship at $P < 0.01$ and $P < 0.05$ with $[Hg^{2+}]$ (r = 0.391), $[Ni^{2+}]$ (r = 0.265) and $[Fe^{2+}]$ and a significant negative relationship with $[Zn^{2+}]$ (r = −0.217), $[Pb^{2+}]$ and $[Cu^{2+}]$ (Table 4). Although the concentration of the cadmium ion in this study reaches the limit for toxicity, the pond was found to be a Class I (≤2 µg L^{-1}) body of water in terms of cadmium ion concentration on the basis of the inland water quality criteria of SWQMR, thus indicating that its water is clean [9].

The biological functions of mercury and its components are unknown; they are not found in living organisms because they are potentially dangerous metals. The concentration of Hg^{2+} in Terzi Pond was found to range between 0 and 0.0050 µg L^{-1}. The lowest value was observed at all sites in the first seven months of the year, whereas the highest concentration was determined at Site 2 in October. The concentration of this ion displays a highly significant ($r \geq 0.7$) positive relationship at $P < 0.01$ and $P < 0.05$ with $[Fe^{2+}]$ (r = 0.837), $[Ni^{2+}]$ and $[Cd^{2+}]$ and a negative significant relationship with $[Zn^{2+}]$ (−r = −0.170), $[Pb^{2+}]$ and $[Cu^{2+}]$ (Table 4). According to the inland water quality criteria of SWQMR, the pond was found to be a Class I (≤0.1 µg L^{-1}) body of

water in terms of mercury ion concentration, thus indicating that its water is clean [9].

The concentration of nickel ions in Terzi Pond was found to range between 0 and 3.0 μg L^{-1}. The lowest concentration was observed at Sites 1 and 2 in January, February, March, April, July and August, whereas the highest concentration was observed at Site 1 in November. The nickel ion concentration in this pond is higher than that observed in Çiğdem Pond [31]. The concentration of nickel ions displays a significant positive relationship at $P < 0.01$ and $P < 0.05$ with [Fe^{2+}] (r = 0.654), [Cu^{2+}], [Cd^{2+}] and [Hg^{2+}] and a significant negative relationship with [Pb^{2+}] (−r = −0.039) (Table 4). According to the inland water quality criteria of SWQMR, the pond was a Class I (≤20 μg L^{-1}) body of water in terms of nickel ion concentration, thus indicating that its water is clean [9].

The amount of zinc ion found in fresh water as a consequence of the natural overflow of minerals is low (<20 μg L^{-1}), but zinc ion concentration in water contaminated by industrial sources can exceed 100 μg L^{-1}. The Zn^{2+} concentration in Terzi Pond was found to range between 0 and 21.0 μg L^{-1}. The lowest concentration of zinc ions was observed at all sites in January, February and March, whereas the highest concentration was observed at Site 2 in June. The value of this parameter displays a highly significant (r ≥ 0.7) positive relationship at $P < 0.01$ and $P < 0.05$ with [Pb^{2+}] (r = 0.741), [Cu^{2+}] (r = 0.944), [Zn^{2+}] and [Ni^{2+}] and a significant negative relationship with [Cd^{2+}] (r = −0.217) and [Hg^{2+}] (r = −0.170) (Table 4). According to the inland water quality criteria of SWQMR, Terzi Pond was found to be a Class I (≤200 μg L^{-1}) body of water in terms of zinc ion concentration, thus indicating that its water is considered clean [9].

Statistical analyses on the data obtained from 36 samples collected monthly from three sites were conducted. An HCA was performed on the basis of seasonal mean values and site mean values of 28 parameters. According to the HCA performed on the mean values of the various parameters calculated per each sampling site, it was determined that Sites 1 and 3 have similar characteristics in terms of pollution load; therefore, their pollutant sources are similar. The pollutant sources of these sites include the businesses (facilities and recreational areas) located around Site 1 and the water flow into the pond for Site 3 (Figures 1 and 2).

On the basis of the results of the HCA performed on the seasonal mean values of the parameters, the seasonal differences are clustered (Figure 3). Between the two main clusters, the cluster dominated by winter draws attention. A second cluster consists of summer, autumn and spring. It was also determined that the inter-seasonal transition occurs during the spring months [16, 43].

TABLE 4
Pearson correlation matrix among the concentrations of heavy metal ions

	Fe^{2+}	Pb^{2+}	Cu^{2+}	Cd^{2+}	Hg^{2+}	Ni^{2+}	Zn^{2+}
Fe^{2+}	1						
Pb^{2+}	-0.225	1					
Cu^{2+}	0.012	**0.836****	1				
Cd^{2+}	0.014	-0.256	-0.236	1			
Hg^{2+}	**0.837****	-0.382*	-0.162	0.391*	1		
Ni^{2+}	0.654**	-0.039	0.148	0.265	0.448**	1	
Zn^{2+}	0.027	**0.741****	**0.944****	-0.217	-0.170	0.242	1

**. Correlation is significant at the 0.01 level (2-tailed).
*. Correlation is significant at the 0.05 level (2-tailed).

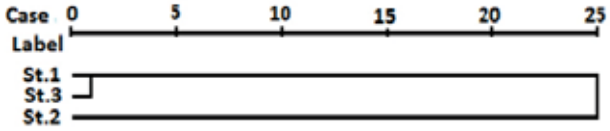


FIGURE 2
Dendogram (obtained using the Ward Method) showing clusters of variables (St.: Site)

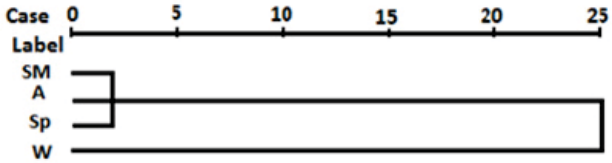


FIGURE 3
Dendogram (obtained using the Ward Method) showing clusters of variables (A: Autumn, Sm: Summer, Sp: Spring and W: Winter)

TABLE 5
Varimax rotated factor matrix for the whole data set

Variable	PC 1	PC 2	PC 3	PC 4
Eigenvalues	11.591	8.213	3.317	1.36
Variance (%)	37.865	29.961.	14.431	5.174
Cumulative (%)	37.865	67.826	82.257	87.431
	Factor loadings (varimax normalised)			
WT	**0.977**	0.104	0.128	0.070
BOD_5	**0.968**	0.025	-0.006	-0.135
EC	**0.967**	-0.112	.085	0.081
Salinity	**0.960**	-0.045	0.107	-0.047
SS	**0.936**	0.202	0.120	0.177
Mg^{2+}	**0.864**	0.222	0.128	0.336
TH	**0.816**	0.427	-0.341	-0.008
TA	**0.743**	0.434	-0.392	0.078
Hg^{2+}	**0.722**	-0.370	0.278	-0.116
Cl^-	**0.702**	0.306	0.369	0.462
pH	**0.702**	-0.566	0.178	-0.082
COD	**0.698**	0.585	0.345	0.140
DO	**-0.642**	0.442	-0.029	-0.207
Ca^{2+}	**0.631**	0.472	0.100	0.268
Fe^{2+}	**0.605**	-0.230	0.545	-0.447
Cu^{2+}	0.165	**0.956**	0.154	-0.097
NO_3^-	0.328	**0.927**	0.010	0.029
Zn^{2+}	0.178	**0.923**	0.261	-0.004
NO_2^-	0.236	**0.905**	-0.203	0.073
Pb^{2+}	-0.279	**0.881**	0.076	-0.124
Na^+	-0.185	**0.869**	-0.256	-0.004
K^+	-0.074	**0.831**	-0.127	-0.037
SO_4^{2-}	0.338	**0.627**	-0.597	-0.013
SO_3^{2-}	-0.003	**0.615**	-0.584	-0.137
Ni^{2+}	0.230	-0.047	**0.914**	0.028
NH_4^+	-0.028	0.059	**0.819**	0.198
PO_4^{3-}	0.545	0.165	**0.771**	-0.162
Cd^{2+}	0.199	-0.262	0.122	**0.762**

Extraction Method: Principal Component Analysis.
Rotation Method: Varimax with Kaiser Normalisation.

In a PCA that included 4 components, 28 physico-chemical parameters were classified. In the PCA, the factor loadings were classified as 'strong', 'moderate' or 'weak', corresponding to absolute loading values above 0.75, in the 0.75–0.50 range or in the 0.50–0.30 range, respectively [21]. Analysis results are reported in Table 5. According to Hair et al. [44], the selection of the number of principal components to be retained is also supported by the number of principal components occurring before a clear break in the scree plot (Figures 4 and 5).

Components with eigenvalues > 1 were acquired, accounting for 87.43% of the total variance in the surface water dataset (Table 5). The first PC, accounting for 37.86% of the total variance, has strong positive loading on WT, BOD_5, EC, salinity, SS, [Mg^{2+}], TH and TA; moderate positive loading on [Hg^{2+}], [Cl^{--}], pH, COD, [Ca^{2+}] and [Fe^{2+}]; and weak positive loading on [PO_4^{3-}]. It also has negative and weak loading on DO. It is remarkable that BOD_5, EC, salinity, SS, [Mg^{2+}], TH and TA have a high correlation with the parameters directly influenced by the WT. This analysis singles out the same parameters characterised by having an inverse relationship with DO that have been highlighted in the HCA (Figure 5). The natural source of the agents that modify the state of the pond, giving rise to the interconnection of parameters just alluded to, is the catchment of flowing runoffs and soil leaching. A flow into the pond of various compounds from this natural source may be the basis of the observed changes in the physico-chemical variables and ion concentrations that were the focus of this study [6].

The second PC, accounting for 29.96% of the total variance, has strong positive loading on [Cu^{2+}], [NO_3^-], [Zn^{2+}], [NO_2^-], [Pb^{2+}], [Na^+] and [K^+] and moderate positive loading on COD, [SO_3^{2-}] and [SO_4^{2-}]. It has a negative and weak loading on pH. This factor represents the contribution of nonpoint pollution sources from agriculture and from ions originating from the soil or rock structure. In particular, this factor represents the influences from nonpoint sources such as agricultural runoff, atmospheric deposition, basin geology and soil structure. In the area of Terzi Pond, farmers use nitrogenous fertilisers, which undergo nitrification processes [16,

45]. Therefore, contamination arising from nutrients to heavy metals and ions indicate the level of pollution in this pond.

The third PC, accounting for 14.43% of the total variance, has strong positive loading on [NH_4^+], [Ni^{2+}] and [PO_4^{3-}], moderate positive loading on [Fe^{2+}], and moderate negative loading on [SO_3^{2-}] and [SO_4^{2-}]. This evidence highlights the influence of agricultural runoff from the soil because nitrogenous fertilisers are extensively used in this region. Phosphorus compounds from the area's rock and soil structure washed by the surface stream is the main source of the phosphorus that reaches the pond. Therefore, the main source for this element is basin geology and soil structure [46, 47].

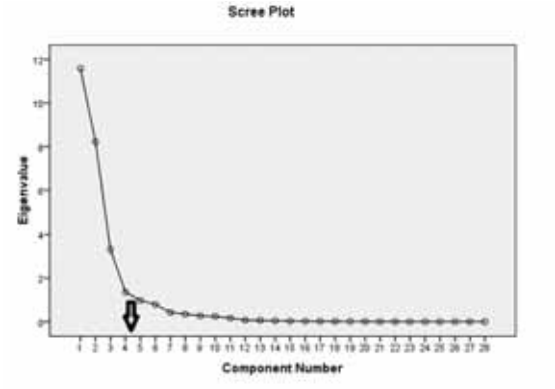


FIGURE 4
Component plot.

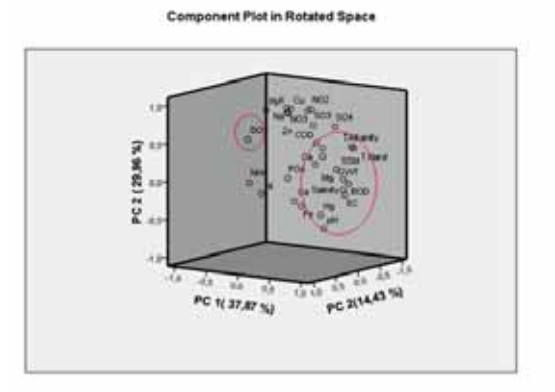


FIGURE 5
Scree plot for the principal component model of the monitoring data.

The fourth PC, accounting for the lowest variance, 5.17%, has moderate positive loading on [Cd^{2+}]. The lack of industrial facilities in the study area indicates that the only cadmium ion source is fertiliser use. The widespread use of cadmium-containing materials results in a significant level of cadmium ion contamination. The fact that pond water is being used for irrigation is a concern. Cadmium ion has the highest water solubility among heavy metal ions; thus, it is characterised by a high rate of diffusion in nature. Cadmium is not required for human life; however, owing to the high solubility of Cd^{2+} in water, this element is taken up by biological systems and by plant and aquatic organisms in the mentioned ionic form.

CONCLUSION

In this study, analytical data obtained from water samples collected at 3 different sites of Terzi Pond for 12 months were analysed by multivariate statistical methods to determine the quality of the water and whether the pond's water is suitable for aquatic life. It has been determined that Terzi Pond has aquatic life and that the quality of the pond's water is appropriate to sustain aquatic life for the time being. Analysis made and statistical tests show that conservation of water quality is only possible if; control of chemical fertilizers used in agricultural areas around the pond, inhibition of pH change, preventing domestic and animal wastes from reaching the pond, also depends on regular monitoring.

In many countries, water pollution is caused by the uncontrolled use of agricultural fertilisers, and the 'best environmental practice' principle should be applied to minimise out-of-source water pollution. Terzi Pond is categorised as oligotrophic in terms of trophic level according to TP and TP ratios. Most of the analytical parameters evaluated in this study lie within the limits set for a body of water characterised by clean water, according to SWQMR and WHO guidelines. However, the values of some of the parameters are typical of contaminated water. The pH and the concentrations of nitrate, phosphate and sulphate ions lie outside the desirable limits for both aquatic life and use of the pond water for drinking and irrigation purposes.

When we examine the levels of heavy metals (in ionic form), no risk is present, according to SWQMR and WHO guidelines. The results of the PCA are compared with the four main sources obtained and the results obtained from the results of individual evaluation of each parameter are verified as the result of the presence of nonpoint sources in the pond. The results obtained with HCA are similar to those obtained via ANOVA analysis of seasonal mean values. Measures should be taken on the basis of Turkey's SWQMR to preserve and improve the water quality of the pond. In the future, research should provide for the development of nonsource pollution, nonintegrated pollution, modelling and monitoring, which is caused by non-agricultural production. On the basis of the results obtained from a statistical analysis, the monitoring of highly-related parameters may then be made in such studies. We believe that this approach will provide time and economic convenience.

REFERENCES

[1] WMO. (2016) Global climate breaks new records January to June 2016. World meteorological organization: https://public.wmo.int/en/media/press-release/global-climate-breaks-new-records-january-june-2016.

[2] UNFCCC. (2013) Turkey's Fifth National Communication under UNFCCC's Report.

[3] Egemen, Ö. and Sunlu, U. (1996) Su kalitesi. Ege Üniversitesi, Su Ürünleri Fakültesi. Yayın no:14, Bornova, İzmir.

[4] Akkan, T. (2017) An Assessment of Linear Alkylbenzene Sulfonate (Las) pollution in Harşit Stream, Giresun, Turkey. Fresen. Environ. Bull. 26, 3217-3221.

[5] Güneş, A. and Gülgün, B. (2007) İzmir, Buca Gölet ve Buca Yedi Göller Suni Gölet Çevresi Rekreasyon Alanlarının Peyzaj Mimarlığı Açısından İrdelenmesi ve Geliştirilmesi Üzerine Bir Araştırma. Ege Üniversitesi. Ziraat Fakültesi Dergisi. 44(2), 81-91.

[6] Simeonov, V., Stratis, J.A., Samara, C., Zachariadis, G., Voutsa, D., Anthemidis, A., Sofoniou, M. and Kouimtzis, T. (2003) Assessment of the surface water quality in Northern Greece. Water Research. 37(17), 4119-4124.

[7] Kazi, T.G., Arain, M.B., Jamali, M.K., Jalbani, N., Afridi, H.I., Sarfraz, R.A., Baig, J.A. and Shah, A.Q. (2009) Assessment of water quality of polluted lake using multivariate statistical techniques: A case study. Ecotox. Environ. Safe. 72, 301–309.

[8] Aydin Uncumusaoğlu, A. and Akkan, T. (2017) Assessment of Yağlidere Stream Water Quality Using Multivariate Statistical Techniques Pol. J. Environ. Stud. 26(4), 1715-1723.

[9] SWQMR. (2015) Regulation on the surface water quality management. Number of official gazette: 29327.

[10] APHA. (2005) Standard methods for the examination of water and wastewater. American Public Health Association. Washington. 21st ed. 1082p.

[11] Anonymous. (1998) Standard methods for the examination of water and wastewater. American Public Health Association. 7th Edition. Washington, USA.

[12] Şengül, Ü. (2016) Comparing determination methods of detection and quantification limits for aflatoxin analysis in hazelnut. Journal of Food and Drug Analysis. 24(1), 56-62.

[13] Parinet, B., Lhote, A. and Legube, B. (2004) Principal component analysis: an appropriate tool for water quality evaluation and management application to a tropical lake system. Ecol Model. 178, 295-311.

[14] Wunderlin, A.D., Díaz, M.D.P., Amé, M.V., Pesce, F.S., Hued, A.C. and Bistoni, M.D.L.Á., (2001) Pattern recognition techniques for the evaluation of spatial and temporal variations in water quality. A case study: Suquía River basin (Córdoba-Argentina). Water Res. 35, 2881–2894.

[15] Singh, K.P., Malik, A., Mohan, D. and Sinha, S., (2004) Multivariate statistical techniques for the evaluation of spatial and temporal variations in water quality of Gomti River (India) - a case study. Water Res. 38, 3980–3992.

[16] Shrestha, S. and Kazama, F. (2007) Assessment of surface water quality using multivariate statistical techniques: A case study of the Fuji River Basin, Japan. Environmental Modelling and Software. 22(4), 464-475.

[17] Zhao, Y., Xia, X.H., Yang, Z.F. and Wang, F. (2012) Assessment of water quality in Baiyangdian Lake using multivariate statistical techniques. Procedia Environmental Sciences. 13, 1213 – 1226.

[18] Omo-Irabor, O.O., Olobaniyi, S.B., Oduyemi, K. and Akunna, J. (2008) Surface and ground water quality assessment using mutivariate analytical methods: a case study of the Western Niger Delta, Nigeria. Phys Chem Earth. 33, 663-673.

[19] Ouyang, Y. (2005) Evaluation of river water quality monitoring stations by principal component analysis. Water Res. 39, 2621-2635.

[20] Kannel, P.R., Lee, S., Kanel, S.R. and Khan, S.P. (2007) Chemometric application in classification and assessment of monitoring locations of an Urban River System. Analytica Chimica Acta. 582(2), 390-399.

[21] Liu, C., Lin, K. and Kuo, Y. (2003) Application of factor analysis in the assessment of groundwater quality in a Blackfoot Disease area in Taiwan. Science of the Total Environment. 313(1-3), 77-89.

[22] Yılmaz Öztürk, B. and Akköz, C. (2014) Investigation of water quality of Apa Dam Lake (Çumra-Konya) and according to the evolution of PCA. Biological Diversity and Conservation. 7(2), 136-147.

[23] Atay, D. and Pulatsü, S. (2000) Su kirlenmesi ve kontrolu. Faculty of Agriculture, Ankara University. Publication Nr.1513, Ankara.

[24] Gorchev, H.G. and Ozolins, G. (2011) WHO guidelines for drinking-water quality. WHO Chronicle. 38(3), 104–108.

[25] Gupta, D.P. and Sunita Saharan, J.P. (2009) Physiochemical Analysis of Ground Water of Selected Area of Kaithal City (Haryana) India. Researcher. 1(2), 1-5.

[26] Mutlu, E. and Kurnaz, A. (2017) Determination of seasonal variations of heavy metals and physicochemical parameters in Sakız Pond (Kastamonu-Turkey). Fresen. Environ. Bull. 26, 2807-2816.
[27] Eryılmaz, H., İpek, Ş.İ. and Yalçın Çelik, B. (2012) Investigation of water quality of Borçka Dam Lake (Artvin). Dumlupinar Üniversitesi, Fen Bilimleri Enstitüsü Dergisi. 33, 1-8
[28] Nisbet, M. and Verneaux, J. (1970) Compo-santes chimiques des eaux courantes. Discus-sion et proposition de classes en tant que bases d'interpretation des analyses chimiques. Annales De Limnologie. 6(2), 161- 190
[29] Kumar, N. and Sinha, D. K. (2010) Drinking water quality management through correlation studies among various physicochemical parameters: A case study. International Journal of Environmental Sciences. 1(2), 253-259.
[30] Patil, P.N., Sawant, D.V. and Deshmukh, R.N. (2012) Physico-chemical parameters for testing of water, A review. International Journal of Environmental Sciences. 3(3), 1194-1207.
[31] Kurnaz, A., Mutlu, E., and Aydin Uncumusaoglu, A. (2016) Determination of water quality parameters and heavy metal content in surface water of Çiğdem Pond (Kastamonu/Turkey). Turkish Journal of Agriculture - Food Science and Technology. 4(10), 907-913.
[32] Ünlü, A., Çoban, F. and Tunç, M.S. (2008) Investigation of Lake Hazar water quality according to physical and inorganic chemical parameters. Gazi Üniversitesi. Mühendislik Mimarlık Fakültesi Dergisi. 23, 119-127.
[33] Taş, B. (2006) Investigation of water quality of Derbent Dam Lake (Samsun). Ekoloji. 60, 1-6.
[34] Bilgin, A. (2015) Evaluation of Borçka Reservoir water quality by a multivariate statistical method. Celal Bayar Üniversitesi, Fen Bilimleri Dergisi. 11(2), 287-293.
[35] Küçükyılmaz, M., Örnekci, G., Uslu, A., Özbey N., Şeker, T., Birici, N., Yildiz, N. and Koçer, M. (2014) Water quality of Işıktepe Dam Lake (Maden, Elazığ). Yunus Araştırma Bülteni. 2, 55-63.
[36] Mutlu, E. and Aydın Uncumusaoğlu, A. (2016) Physicochemical Analysis of Water Quality of Brook Kuruçay. Turkish Journal of Agriculture, Food Science and Technology. 4(11), 991-998.
[37] Mustapha, M.K. (2008) Assessment of the water quality of Oyun Reservoir, Offa, Nigeria, using selected physico-chemical parameters. Turkish Journal of Fisheries and Aquatic Sciences. 8, 309-319.
[38] Güler, İ. and Çobaoğlu, Z. (1997) Su kirliliği, Çevre Sağlığı Temel Kaynak Dizisi. No: 43. 1. Baskı. 92 s. Ankara. ISBN 975-7572-60-8.
[39] Balcı, N.Ç., Karagüler, N.G., Yelboğa, E. and Vardar, N. (2009) Biogeochemical processes controlling metal dissolution and deposition: A case study: Biogeochemistry at Maslak pond. ITU 1. Tıbbi Jeoloji Çalıştayı, 30 october–1 november 2009, Ürgüp Bld., Kültür Merkezi, Ürgüp/ Nevşehir
[40] Taş B. (2011) Gaga Gölü (Ordu, Türkiye) Su Kalitesinin İncelenmesi. The Black Sea Journal of Sciences. 1(3), 43-61.
[41] Weisz, M., Polyak, K., and Hlavay, J. (2000) Fractionation of elements in sediment samples collected in rivers and harbors at Lake Balaton and its catchment area. Microchemical Journal. 67(1–3), 207–217.
[42] Bilgin Yıldırım, H. (2016) Tatlısu Ekosistemlerinde Ağır Metaller, Ankara
[43] Aydin Uncumusaoglu, A., Sengul, U. and Akkan, T. (2016) Environmental contamination of heavy metals in the Yağlıdere Stream (Giresun), Southeastern Black Sea. Fresen. Environ. Bull. 25, 5492-5498.
[44] Muangthong, S. and Shrestha, S. (2015) Assessment of surface water quality using multivariate statistical techniques: case study of the Nampong River and Songkhram River, Thailand. Environmental Monitoring and Assessment. 187(9), 548.
[45] Hair, J.F., Black, W.C., Babin, B.J. and Anderson, R.E. (2009) Multivariate Data Analysis, 7th ed. Prentice Hall. Upper Saddle. NJ 07458, ISBN-10; 0138132631 |ISBN-13: 97801381326 37, 116-120.
[46] Vieira, J.S., Pires, J.C., Martins, F.G., Vilar, V.J., Boaventura, R.A. and Botelho, C.M. (2012) Surface water quality assessment of Lis River using multivariate statistical methods. Water, Air, & Soil Pollution. 223, 5549-5561.
[47] Aydin Uncumusaoğlu, A. (2018) Statistical assessment of water quality parameters for pollution source identification in Bektaş Pond (Sinop, Turkey). Global Nest Journal. 20(1), 151-160.

Received: **25.10.2017**
Accepted: **12.02.2018**

CORRESPONDING AUTHOR

Ekrem Mutlu
Kastamonu University,
Faculty of Fisheries,
Kastamonu – Turkey

e-mail: ekrem-mutlu@hotmail.com

© by PSP Volume 27 – No. 5/2018 pages 2913-2921 Fresenius Environmental Bulletin

INHIBITORY EFFECT OF NATURAL ZEOLITE AND ITS CHITOSAN COMPOSITES ON CADMIUM-CONTAMINATED SOILS

Na Yi, Yaoguo Wu*, Sihai Hu

School of Natural and Applied Sciences, Northwestern Polytechnical University, Xi'an 710072, China

ABSTRACT

Remediation of Cd-contaminated soils has attracted considerable attention in recent years, especially in China. In order to investigate the inhibitory effect of zeolite and its chitosan composites, a pot experiment was carried out. We evaluated the effects of the addition of zeolite and its chitosan composites with different amounts and particle sizes on the soil pH, *Brassica juncea* dry weight, the amount of Cd extraction by *Brassica juncea* and bioavailable changing in soils. The results of this study indicated that, zeolite and its composites can increase soil pH and reduce the biological effectiveness of heavy metals in certain extent. The dry weight of *Brassica juncea* increased with increasing particle size of chitosan composites, whereas zeolite alone had no obvious regularity on dry weight. With an amendment dosage of 50 g per pot, the highest *Brassica juncea* dry weight could be achieved. Increasing particle size of zeolite and its chitosan composites resulted in decreased the Cd uptake by *Brassica juncea*; the Cd uptake decreased with increasing amendment dosage from 25 to 100 g. At a dosage of 100 g per pot, the Cd uptake was lowest. Lowest uptake rates were found for CS-Z-2000, followed by CS-Z-1250, CS-Z-800, Z-2000, CS-Z-325, Z-2000, Z-1250, Z-800, and Z-325, decreasing by 15.34, 14.40, 11.66, 10.27, 10.23, 9.30, 8.85, and 8.46%, respectively. The effect of zeolite-chitosan composites increased with the decreasing of particle sizes. Besides, the Cd uptake by *Brassica juncea* decreased with increasing dosage from 25 to 100 g per pot. Similarly, at the dosages of 100, 100, 50, 50, 100, 50, 100, 100 g/pot, the soil bioavailable Cd content decreased by 23.25, 22.17, 17.05, 14.61, 16.82, 12.96, 11.19, and 9.61%, respectively, compared to the control. The results clearly show that remediation efficiency was better than the treatments without added chitosan.

KEYWORDS:
Cd contamination, Remediation, Zeolite, Chitosan, *Brassica juncea*

INTRODUCTION

Cadmium (Cd) is one of the most common heavy metals in polluted environments and has a high activity in soil. Studies estimate that the area of soil contaminated with Cd covers about 1.3×10^5 ha and accounts for 1/5 of the total farmland area in China [1]. And more than 11 provinces and 25 districts are subjected to Cd-contaminated soil. In 2007, the direct economic loss from farmland metal pollution reached $ 3.2 billion as calculated by the Ministry of Land and Resource in China [2]. Unlike organic contaminants, heavy metals are not degraded in the environment and can accumulate in soils and sediments [3]. The high ability of Cd transfer from paddy soil to rice grain can cause diseases in animals and humans through the food chain, primarily affecting the kidneys, especially the proximal tubular cells [4]. Cd is not essential element for humans, and Cd contamination can cause various diseases and inhibit growth by impacting the enzymatic activity of amino acid decarboxylase, histamine, amylase, and peroxidase, and so on. In addition, it can impede the metabolism of copper, cobalt, zinc, and other trace elements. Therefore, the removal of Cd from polluted environments requires urgent clarification, and numbers of suitable methods have been investigated. *In situ* immobilization (e.g. immobilization by chemical amendments and phytostabilization) has been used to remedy Cd-contaminated soil [5, 6]. The *in situ* immobilization of metal elements by natural or synthetic additives such as alkaline compounds [7, 8], phosphate compounds [9], and clay minerals [10, 11] has been considered as a promising alternative to the currently available remediation methods because of its low-cost, low-impact and easy implementation [11-13]. Clay minerals [14] have been proposed and tested for in-situ immobilization of heavy metals in degraded soils because of their availability and low cost [15]. Clay is a potential metal chelator due to its relatively large internal and surface area and strong adsorption ability; it can effectively immobilize heavy metals in the soil and thereby prevent them from being absorbed by plants and humans. Zeolite, as a type of clay mineral, has received considerable attention as a natural adsorbent to remove heavy metals from soil. Recently, it has been reported that

zeolite could serve as an *in situ* alternative material for remediating soils contaminated with Cd through immobilization due to the capability of adsorbing heavy metals owing to its porous structure, more negative charges and a high cation exchange capacity on its surface [16-19].

The safe and low-cost recycling of various by-products and amendments in agriculture is crucial to ensure an environmentally and economically sound practice [20]. There is an increasing demand for new, applicable, and economy efficiency amendments for the remediation of Cd-contaminated soils. Of these, the use of chitosan (CS) has been described as a promising "green" and environmentally-friendly method of metal adsorption. CS is the N-deacetylated produce of chitin, which is a byproduct of shellfish processing. Due to the presence of large numbers of anmio- (NH_2-) and hydroxyl- (OH-) groups on chitosan, it has a high affinity for metal ions [21-22]. Guo et al. [24]and Shaheen et al. [20] have investigated Cd^{2+} adsorption by chitosan and reported satisfactory results. Although numbers of studies have evaluated the inhibitory effect of natural zeolite on Cd-contaminated soil, the impact of zeolite-chitosan composites on Cd-contaminated soils has not been clearly illustrated.

Cruciferae canola was a kind of plant with strong absorption characteristics and enrichment ability of heavy metal [25]. *Brassica juncea* was selected as the experimental species because of short life stage, high biomass and the hyperaccumulation ability to heavy metal [26]. It has great potential applications in phytoremediation. In this study, we investigated the effect of zeolite and its chitosan composites on Cd-contaminated soil. As indicator plant, we chose *Brassica juncea* and conducted pot experiments using three different amendment dosages and four different particle sizes. The evaluated parameters were soil pH, *Brassica juncea* dry weight, Cd uptake of *Brassica juncea*, and bioavailable Cd content.

MATERIALS AND METHODS

Materials. Zeolite was obtained from the Zhongchuan mineral powder processing plant, Lingshou, Hebei province, China. Industrial grade chitosan was obtained from Guangzhou Shengxun chemical industry co., LTD; it had the following properties: yellowish-white powder with 100 meshes, 93% degree of deacetylation, and a molecular weight of 2×10^6.

Experiment arrangement. This experiment was carried out in a greenhouse located in Yangling, Shaanxi Province, China. Surface soil (0-20 cm depth) was collected from the greenhouse in which phosphate has been applied to the soil over 30 years. Prior to physical and chemical analyses, the soil samples were passed through a 20-mm mesh sieve to remove gravel. The soil was classified as loess soil; physical and chemical properties are listed in Table 1. The pH was measured with a pH Meter (FE28-Meter, Mettler Toledo instrument co., LTD, China) in a 1:5 (w/w) soil-H_2O slurry. Soil organic matter content was determined using the potassium dichromate-outside heating method [27]. Bioavailable Cd was extracted for two hours at room temperature with DTPA (DPTA-TEA-$CaCl_2$, pH=7.3) buffer solution. Heavy metal content was determined using flame atomic absorption spectrophotometer (Z-2000, Hitachi, Japan).

Different dosages (25, 50, and 100 g) and particle sizes (325, 800, 1250, 2000 mesh) zeolite and its chitosan composites (the application ratio of chitosan was 6% in chitosan composites. CS-Z-325, CS-Z-800, CS-Z-1250, CS-Z-2000) were well mixed with 5 kg of Cd-contaminated soil before packed into respective pots. A control treatment without amendment, containing only Cd-contaminated soil, was also prepared. Then, all of the soil samples were incubated for one month.

TABLE 1
Properties of the experimental soil. Values represent means±standard deviation (n=3).

Parameter	units	Value
Soil type		Heavy loam
pH (soil:H_2O=1:5)		7.81±0.12
total nitrogen	g kg^{-1}	1.69±0.05
Olsen phospate	mg kg^{-1}	303.65±8.47
Available potassium	mg kg^{-1}	722.78±14.12
Soil organic matter	g kg^{-1}	36.15±1.16
Cd	mg kg^{-1}	1.55±0.04
Bioavailable Cd[a]	mg kg^{-1}	0.29±0.03
Fe	%	3.11±0.21
Cu	mg kg^{-1}	24.63±1.98
Zn	mg kg^{-1}	69.58±3.48
Ca	%	4.79±0.22
Mg	%	1.28±0.03

[a]: extracted for 2h at room temperature with DTPA (DTPA-TEA-$CaCl_2$, pH=7.3) buffer solution

TABLE 2
The pH value of different amendments

Amendments	CS	Z-325	Z-800	Z-1250	Z-2000	CS-Z-325	CS-Z-800	CS-Z-1250	CS-Z-2000
pH	7.823	8.356	9.471	9.574	8.882	8.411	8.823	9.065	9.164

TABLE 3
The pH value effect of the soil samples treated with different particle sizes and dosage amendments

Amendments	Added contents of different amendments (g/pot)			
	0	25	50	100
Z-325	7.786	7.823	7.786	7.819
Z-800	7.786	7.825	7.842	7.864
Z-1250	7.786	7.814	7.802	7.798
Z-2000	7.786	7.810	7.800	7.833
CS-Z-325	7.786	7.813	7.812	7.797
CS-Z-800	7.786	7.826	7.821	7.801
CS-Z-1250	7.786	7.814	7.803	7.790
CS-Z-2000	7.786	7.792	7.802	7.795

Seedlings of *Brassica juncea* were cultured in the middle of the greenhouse. The cultivation area was covered with polyethylene plastic film to maintain moisture before seeds germination. After three weeks, three equally sizes seedlings (10 cm in height) were transplanted into each pot on October 15, 2015. Soil water was maintained at 60%WHC by adding tap water daily.

Sampling pretreatment and metal analysis. After three months, all *Brassica juncea* plants were harvested. The samples were rinsed with tap water to remove surface soil and subsequently washed with deionized water and dried of surface water. The fresh samples were weighed subsequently oven dried at 105°C for 30 min, then at 70°C until constant weight. The dried *Brassica juncea* samples were crushed and ground to a fine powder using a high-speed universal pulverizer (FW100, Zhongxing Weiye instrument co., LTD, China) and stored in plastic bags until analysis.

All soil samples were pretreated with the same method prior to analysis. For analysis, 0.5 g of the dried plant material was placed into a 100 mL beaker covered with a funnel. We then added 15 mL of solution containing 87% of concentrated HNO_3 and 13% of concentrated $HClO_4$ (v/v) [28]. The sample was digested at 50-80°C overnight, followed by 180°C for 8 h to near dryness and allowed to cool. The digested solution was diluted with 2% (v/v) HNO_3 to a volume of 25.0mL before filtration. The concentration of Cd in the digested plant sample was determined using a flame atomic absorption spectrometer at a wavelength of 228.8nm.

Statistical analysis. Statistical analysis was performed using SigmaPlot 12.5, Excel 2010 and Origin 9.0 software. One-way ANOVA and multiple comparisons were used to compare the difference in the dry weight of individual *Brassica juncea*, the Cd uptake of *Brassica juncea* and the bioavailable Cd content. Significant levels of 0.01 and 0.05 were used. All the results are the average of the three repeat tests.

RESULTS AND DISCUSSION

Effects of different amendments on soil pH. Soil pH was one of the important factors in heavy metal adsorption because it affected the biological effectiveness of heavy metal ions. Table 2 shows the pH values of zeolite and its chitosan composite with different particle sizes. All amendments showed an alkaline pH, significantly affecting soil pH upon application. This, in turn, can reduce the biological effectiveness of heavy metals in certain extent [29]. The pH value effect of soil sample treated with different particle sizes zeolite and it chitosan composites are shown in Table 3. Heavy metal adsorption varied with changing soil pH values. At a low soil pH, there was competitive adsorption between heavy metals and H^+ ions in the soil, impeding heavy metal adsorption [30]. Soil pH also affected adsorption in the treatments with different particle sizes and amendment dosages (Table 3). With an increased amendment dosage (ranging from 25 to 100 g), pH had no obvious regularity. Because the buffer capacity is one of the important properties of the soil [31]. And there was an important reason that the pH value of soil was essentially alkaline.

Effects of particle sizes and amendment dosage on *Brassica juncea* dry weight. The impacts of particle size of zeolite and its chitosan composites on *Brassica juncea* dry weight are shown in Table 4. We used the analysis of variance (ANOVA) to compare the *Brassica juncea* dry weight between with different treatments. Based on the ANOVA results, there was no significant difference between different amendment dosages and particle sizes. *Brassica juncea* dry weight was higher for all amendments with different particle sizes compared to the control. Zeolite had no obvious regularity on *Brassica juncea* dry weight. However, the effect of zeolite-chitosan

composites on *Brassica juncea* dry weight increased with increasing particle size. The interior and exterior-specific surface areas of amendments were increased, and the effect of Cd-contaminated soil was weakened with increasing particles size. With an amendment dose of 100 g per pot, individual *Brassica juncea* dry weights compared with control treatment increased by 15.50, 16.76, 17.64, and 21.45%, respectively. The higher dry weights in chitosan composites-treated soils might be attributed to the introduced chitosan and increased soil pH [20]. Chitosan has a large amount of amino and hydroxyl groups with a high affinity for Cd ions, making it highly suitable for Cd removal [32-35].

In terms of the effect of different dosage amendments on *Brassica juncea* dry weight was increased, as the dose of amendments from 0 to 50 g per pot. From 50 to 100 g per pot, *Brassica juncea* dry weight has no significant change. This suggested that, the adsorption reached equilibrium. Cd-contaminated soil can significantly reduce soil pH, negatively impacting crop growth and development [35]. The addition of zeolite and its chitosan composites can significantly improve soil pH and lower cadmium activity in the soil [37]. Thereby, adverse soils conditions are alleviated and the impact of excessive soil cadmium on the growth of *Brassica juncea* is lowered. The above described results can explain the higher dry weight values with the addition of zeolite and its chitosan composites. In terms of economic considerations, a dosage of 50 g per pot achieved the best results.

Effects of particle size and amendment dosage on the Cd uptake by *Brassica juncea.* Table 5 shows the effect of particle size and amendment dosage on the Cd uptake by *Brassica juncea*. Based on the ANOVA result, there was no significant difference between different particle sizes in terms of the Cd uptake. With a dosage of 50-100 g/pot, there was a significant difference between the treatments using chitosan composites compared with the control treatment. The lower the content of Cd in the *Brassica juncea*, the better the effect of the amendment fixed Cd. The Cd uptake of *Brassica juncea* was lower than control samples treated with all amendments from the Table 5. The addition of amendments has passivation effect on Cd-contaminated soil. With the increase of the particle sizes of zeolite and its chitosan composites, we observed a decrease in the Cd uptake by *Brassica juncea*, possibly because of an

TABLE 4
The dry weight effect of different particle sizes and dosage amendments

Amendments	The dry weight of individual *Brassica juncea* (g) (the dry weight of aboveground parts)			
	0 (g/pot)	25 (g/pot)	50 (g/pot)	100 (g/pot)
Z-325	23.87±2.34 Aa	24.34±1.41 Aa	26.23±1.48 Aa	26.35±0.76 Aa
Z-800	23.87±2.34 Aa	24.73±1.21 Aa	26.93±1.75 Aa	26.25±1.34 Aa
Z-1250	23.87±2.34 Aa	25.59±2.79 Aa	26.27±2.95 Aa	26.38±1.43 Aa
Z-2000	23.87±2.34 Aa	23.82±3.08 Aa	25.97±1.41 Aa	26.15±1.24 Aa
Z-CS-325	23.87±2.34 Ab	23.88±0.85 Ab	27.47±1.62 Aa	27.57±1.39 Aa
Z-CS-800	23.87±2.34 Aa	24.65±1.71 Aa	27.56±1.55 Aa	27.87±1.47 Aa
Z-CS-1250	23.87±2.34 Aa	25.02±2.11 Aa	27.97±1.42 Aa	28.08±1.35Aa
Z-CS-2000	23.87±2.34 Ab	25.28±0.69 Ab	28.42±1.45 Aa	28.99±0.45 Aa

Different lowercase letters indicate statically different values (the dry weight effect of individual *Brassica juncea*) within different dosage according to Fisher LSD test ($p<0.05$). Different uppercase letters indicate significantly different values (in the same column) between different amendments according to Fisher LSD test ($p<0.05$).

TABLE 5
The Cd content of *Brassica juncea* on the soil treated with different particle sizes and dosages amendments

Amendments	The Cd content ($mgkg^{-1}$) (the Cd content of aboveground parts)			
	0 (g/pot)	25g (g/pot)	50g (g/pot)	100g (g/pot)
Z-325	3.097±0.249Aa	3.067±0.099 Aa	2.936±0.069Aa	2.835±0.145Aa
Z-800	3.097±0.249Aa	3.024±0.132Aa	2.849±0.061Aa	2.823±0.009 Aa
Z-1250	3.097±0.249Aa	2.965±0.141Aa	2.831±0.202Aa	2.809±0.232Aa
Z-2000	3.097±0.249Aa	2.952±0.282Aa	2.861±0.093Aa	2.779±0.119Aa
Z-CS-325	3.097±0.249Aa	2.944±0.070Aa	2.837±0.029Aa	2.781±0.066Aa
Z-CS-800	3.097±0.249Aa	2.950±0.050Aab	2.750±0.062Ab	2.736±0.078Ab
Z-CS-1250	3.097±0.249Aa	2.937±0.103Aab	2.756±0.141Abc	2.651±0.073Ab
Z-CS-2000	3.097±0.249Aa	2.923±0.063Aab	2.673±0.127Ab	2.622±0.035Ac

Different lowercase letters indicate statistically different values (dosage effect) within different dosage according to Fisher LSD test ($p<0.05$). Different uppercase letters indicate significantly different values (in the same column) between different particle sizes amendments according to Fisher LSD test ($p<0.05$).

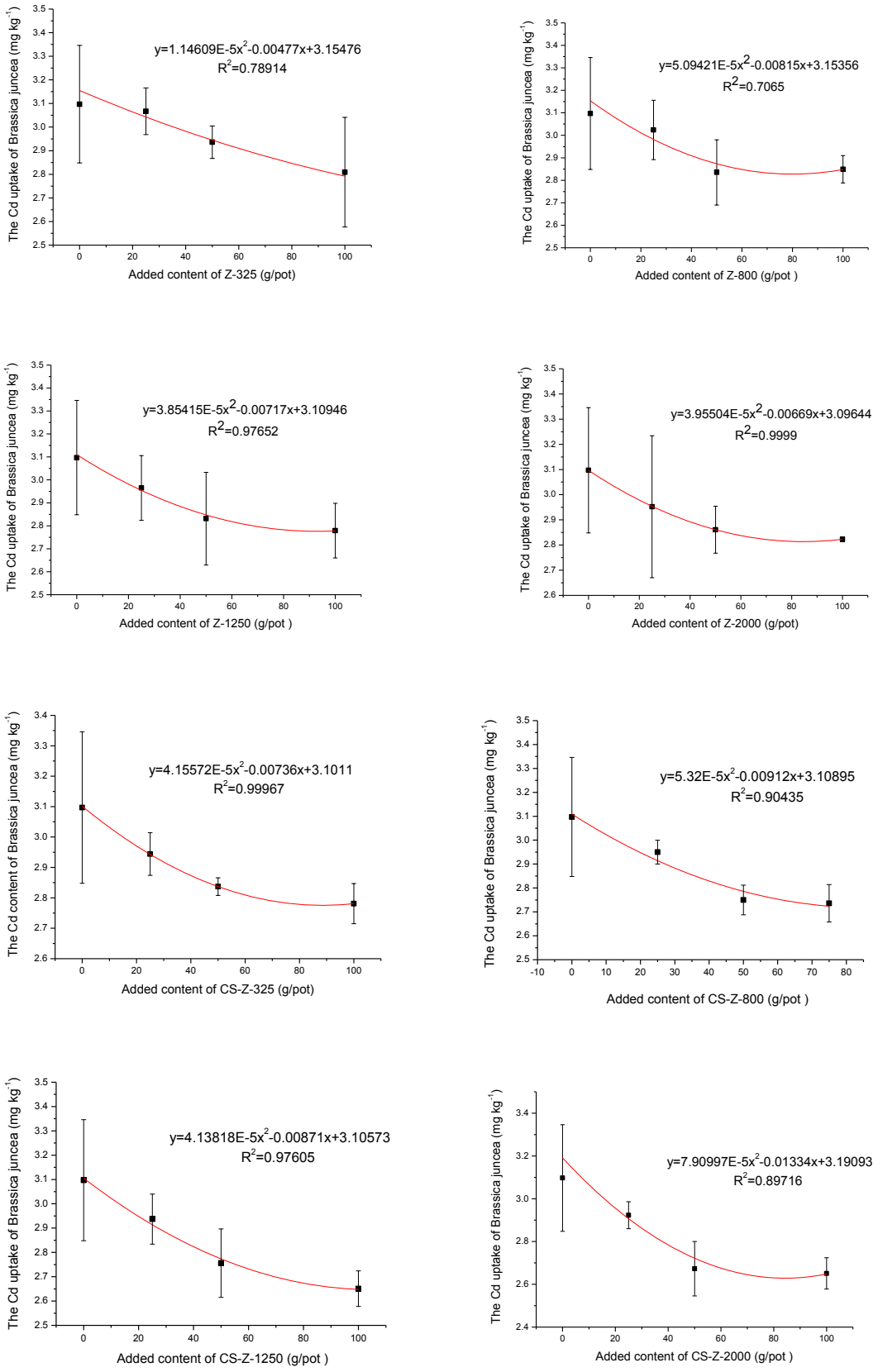


FIGURE 1
Regression curves between Cd uptake by Brassica juncea and added amount of different soil amendments

increase of surface area and, consequently, adsorption sites of the amendments with increasing particle size. Besides, the Cd uptake in the treatments with added zeolite-chitosan composites was lower than in the treatments with natural zeolite. This suggests the presence of more active sites and a synergy effect of adsorption with the introduction of chitosan.

In terms of amendment dosage, Cd uptake decreased with increasing dosage from 25 to 100 g per pot. With a dosage of 100 g per pot, Cd uptake was lowest. Lowest uptake rates were found for CS-Z-2000, followed by CS-Z-1250, CS-Z-800, Z-2000, CS-Z-325, Z-1250, Z-800, and Z-325, decreasing by 15.34, 14.40, 11.66, 10.27, 10.23, 9.30, 8.85, and 8.46%, respectively. It means that the effect of the fixed Cd of the amendment followed by CS-Z-2000, CS-Z-1250, CS-Z-800, Z-2000, CS-Z-325, Z-1250, Z-800, and Z-325. The passivation effect of the zeolite-chitosan composite was better than the effect of natural zeolite. With increasing, chitosan contents also increased, raising the numbers of amino and hydroxyl function groups on the main chain of chitosan, which act as chelation sites and have a high affinity for cadmium ions [38, 39]. The primary mechanisms of metal immobilization by soil amendments are adsorption, cation-exchange, precipitation, and surface complexation [40]. Of these, complexation is the major, most stable, and irreversible process [41].

In order to understand the effect regularities of Cd uptake by *Brassica juncea* through adding different soil amendments, the regression equations and the corresponding correlation curves were fitted and are shown in Figure 1 (amendment dosage as independent variable and Cd uptake as dependent variable).

The correlation coefficient of samples treated with chitosan was higher (R^2>0.89) than that in samples without chitosan. The relationship between Cd uptake and the addition of different amendments followed a reverse "parabola" type function (Figure 1). With an amendment dosage of 50-100 per pot, Cd uptake of *Brassica juncea* was lowest. This suggested that amendments have better remedy capacity to Cd-contaminated soil. Hence 50-100 g per pot amendments can be used for preliminary dosage to repair Cd polluted soil. To sum up, the dosage of various amendment treated with Cd polluted soil is appropriate for 50-100g/pot. The amendment can reduce by 10.27% the Cd uptake by *Brassica juncea* at least. In this case, Z-CS has well potential for reducing Cd uptake by *Brassica juncea*.

Effects of particle size and amendment dosage on the bioavailable Cd content. According to the ANOVA results (Table 6), particle size and amendment dosage significantly impacted the bioavailable Cd. With increasing particle size and dosage, the bioavailable Cd significantly decreased. And the bioavailable Cd content of soil amended with chitosan was lower than that of soil without the addition of chitosan. With the particle sizes of CS-Z-2000, CS-Z-1250, CS-Z-800, CS-Z-325, CS-2000, CS-1250, CS-800, and CS-325 and dosages of 100, 100, 50, 50, 100, 50, 100, 100 g/pot, respectively, soil bioavailable Cd content decreased by 23.25, 22.17, 17.05, 14.61, 16.82, 12.96, 11.19, and 9.61%, respectively, compared to the control. These results suggest that the introduction of chitosan effectively inhibits Cd in contaminated soils.

CONCLUSION

In this study, we investigated the inhibitory effect of zeolite and its chitosan composites on Cd-contaminated soils by evaluating soil pH, *Brassica juncea* dry weight and Cd content and bioavailable soil Cd. Our results show that using chitosan in Cd removal might be a viable alternative. In treatments with added chitosan, the inhibitory effect on Cd was significantly higher compared with treatments using only zeolite.

Although all amendments were alkaline, soil pH did not change considerably due to the intrinsic pH buffer of the soil. *Brassica juncea* dry weight increased with increasing particle size of the zeolite-chitosan composites; however, zeolite alone did have

TABLE 6
The contents of bioavailable Cd content in the soil treated with different amendments

Amendments	The bioavailable Cd content (mg kg^{-1})			
	CK	25g	50g	100g
Z-325	1.759±0.054Aa	1.711±0.023Ab	1.636±0.057Abc	1.590±0.027Ac
Z-800	1.759±0.054Aa	1.671±0.039ABCb	1.609±0.058Ab	1.562±0.051ACb
Z-1250	1.759±0.054Aa	1.653±0.049ABCDb	1.531±0.042BCc	1.573±0.038ABc
Z-2000	1.759±0.054Aa	1.689±0.033ABb	1.463±0.036CDb	1.520±0.034BCDb
Z-CS-325	1.759±0.054 Aa	1.630±0.032BCDb	1.568±0.016ABb	1.502±0.032CDb
Z-CS-800	1.759±0.054 Aa	1.611±0.037CDb	1.459±0.029CDb	1.482±0.052Dc
Z-CS-1250	1.759±0.054 Aa	1.591±0.031DEb	1.409±0.046Db	1.369±0.032Eb
Z-CS-2000	1.759±0.054 Aa	1.533±0.039Eb	1.392±0.032Dbc	1.350±0.030Ec

no obvious regularity on dry weight. In terms of economic considerations, a dosage of 50 g per pot achieved the best results. *Brassica juncea* dry weight was higher with the addition of soil amendments (irrespective of particle size) compared to the control. However, dry weight was higher with the addition of the zeolite-chitosan composites with increasing particle size and increased by 6.70, 11.27, 13.45 and 14.87%, respectively. With an amendment dosage of 50 g per pot, highest *Brassica juncea* dry weight could be achieved. Increasing particle size of zeolite and its chitosan composites resulted in decreased Cd uptake by *Brassica juncea*; the Cd uptake decreased with increasing amendment dosage from 25 to 100 g. At a dosage of 100 g per pot, the Cd uptake was lowest.

ACKNOWLEDGEMENTS

The financial support extended to the projects by Ministry of Agriculture of the People's Republic of China (no. 201203045), the National Natural Science Foundation of China (no. 40872164, 41502240), Key Laboratory of Groundwater Contamination and Remediation, China Geological Survey (CGS) & Hebei Province (no. KF201610), and China Geological Survey Project (no. 12120114056201).

REFERENCES

[1] Rafiq, M.T., Aziz, R., Yang, X., Xiao, W., Rafiq, M.K., Ali, B. and Li, T. (2014) Cadmium phytoavailability to rice (Oryza sativa L.) grown in representative Chinese soils. A model to improve soil environmental quality guidelines for food safety. Ecotoxicology and Environmental Safety. 103, 101-107.

[2] Li, G., Qiu, J. and Yin, C. (2009) Study on calculating losses of cropland degradation. Chinese Agricultural Science Bulletin. 25, 230-235.

[3] Lu, H.P., Li, Z.A., Fu, S.L., Méndez, A., Gascó, G. and Paz-Ferreiro, J. (2015) Combining phytoextraction and biochar addition improves soil biochemical properties in a soil contaminated with Cd. Chemosphere. 119, 209-216.

[4] Sun, Y.B., Sun, G.H., Xu, Y.M., Liu, W.T., Liang, X.F. and Wang, L. (2016) Evaluation of the effectiveness of sepiolite, bentonite, and phosphate amendments on the stabilization remediation of cadmium-contaminated soils. Journal of Environmental Management. 166, 204-210.

[5] Peng, J.F., Song, Y.H., Yuan, P., Cui, X.Y. and Qiu, G.L. (2009) The remediation of heavy metals contamination sediment. Journal of Hazardous of Materials. 161, 633–640.

[6] Sun, Y.B., Sun, G.H., Xu, Y.M., Wang, L., Liang, X.F., Lin, D.S. and Hu, F.Z. (2013) Assessment of natural sepiolite on cadmium stabilization, microbial communities and enzyme activities in an acidic soil. Environmental Science and Pollution Research. 20, 3290–3299.

[7] He, Y.B., Huang, D.Y., Zhu, Q.H., Wang, S., Liu, S.L., He, H.B., Zhu, H.H. and Xu, C. (2017) A three-season field study on the in-situ remediation of Cd-contaminated paddy soil using lime, two industrial by-products, and a low-Cd-accumulation rice cultivar. Ecotoxicology and Environmental Safety. 136, 135-141.

[8] Lee, S.S., Lim, J.E., Abd EI-Azeem, S.A.M., Choi, B.S., Oh, S.E., Moon, D.H. and Ok, Y.S. (2013) Heavy metal immobilization in soil near abandoned mines using eggshell waste and rapeseed residue. Environmental Science & Pollution Research. 20, 1719-1726.

[9] Li, R.D., Zhao, W.W., Li, Y.L., Wang, W.Y. and Zhu, X. (2015) Heavy metal removal and speciation transformation through the calcination treatment of phosphorus-enriched sewage sludge ash. Journal of Hazardous of Materials. 283, 423-431.

[10] Liang, X.F., Han, J., Xu, Y.M., Sun, Y.B., Wang, L. and Tan, X. (2014) In situ field-scale remediation of Cd polluted paddy soil using sepiolite and palygorskite. Geo-derma. 235-236, 9-18.

[11] Sun, Y.B., Li, Y., Xu, Y.M., Liang, X.F. and Wang, L. (2015) *In situ* stabilization remediation of cadmium (Cd) and lead (Pb) co-contaminated paddy soil using bentonite. Applied Clay Science. 105-106, 200-206.

[12] Ghosh, U., Luthy, R.G., Cornelissen, G., Werner, D. and Menzie, C.A. (2011) In-situ sorbent amendments: a new direction in contaminated sediment management. Environmental Science & Technology. 45, 1163–1168.

[13] Garau, G., Castaldi, P., Santona, L., Deiana, P. and Melis, P. (2007) Influence of red mud, zeolite and lime on heavy metal immobilization, culturable heterotrophic microbial populations and enzyme activities in a contaminated soil. Geoderma. 142, 47–57.

[14] Liang, X.F., Han, J., Xu, Y.M., Sun, Y.B., Wang, L. and Tan, X. (2014) In situ field-scale remediation of Cd polluted paddy soil using sepiolite and palygorskite. Geoderma. 235-236, 9-18.

[15] Zhou, Q.X. and Song, Y.F. (2004) Principles and Methods of Contaminated Soil Remediation. Science Press. Beijing, China.

[16] Oste, L.A., Lexmond, T.M. and Van Riemsdijk, W.H. (2002) Metal immobilization in soils using synthetic zeolites. Journal of Environmental Quality. 31, 813–821.

[17] Mahabadi, A.A., Hajabbasi, M.A., Khademi, H. and Kazemian, H. (2007) Soil cadmium stabilization using an Iranian natural zeolite. Geoderma. 137, 388-393.

[18] Sanchez, A.G., Alastuey, A. and Querol, X. (1999) Heavy metal adsorption by different minerals: application to the remediation of polluted soils. The Science of Total Environment. 242, 179–188.
[19] Motsi, T. Rowson, N.A. and Simmons, M.J.H. (2009) Adsorption of heavy metals from acid mine drainage by natural zeolite. International Journal of Mineral Processing. 92, 42–48.
[20] Shaheen, S.M. and Rinklebe, J. (2015) Impact of emerging and low cost alternative amendments on the (im)mobilization and phytoavailability of Cd and Pb in a contaminated floodplain soil. Ecological Engineering. 74, 319-326.
[21] Cui, C., He, M., Chen, B.B. and Hu, B. (2014) Chitosan modified magnetic nanoparticles based solid phase extraction combined with ICP-OES for the speciation of Cr (III) and Cr (VI). Analytical Methods. 6, 8577-8583.
[22] Eladlani, N., Dahmane, E.M., Rhazil, M., Taourirte, M. and Habibi, Y. (2014) Complexation of chromium (III) ions with chitosan and its derivatives, nanoparticles and whiskers. Fresen. Environ. Bull. 23, 3278-3285.
[23] Wu, Y.G., Zhang, Y.J., Qian, J., Xin, X., Hu, S.H., Zhang, S. and Wei, J.G. (2017) An exploratory study on low-concentration hexavalent chromium adsorption by Fe(III)-cross-linked chitosan beads. The Royal Society Open Science. 4(11), 170905.
[24] Guo, Z., Hu, X. and Ao, Y.S. (2009) Effect of chitosan on the available contents and vertical distribution of Cu^{2+} and Cd^{2+} in different textural soils. Journal of Hazardous Materials. 167, 1148-1151.
[25] Ebbs, S.D., Lasat, M.M., Brady, D.J., Cornish, J., Gordon, R. and Kochian, L.V. (1997) Phytoextraction of cadmium and zinc from a contaminated soil. Journal of Environmental Quality. 26, 1424-1430.
[26] Ebbs, S.D. and Kochian, L.V. (1998) Phytoextraction of Zinc by oat (Avena sativa), barley (Hordeum vulgare), and Indian mustard (Brassica juncea). Environmental Science and Technology. 32, 802-806.
[27] Shao, M. (2009) Determination of soil organic matter under different digestion methods. Journal of Liaoning Agricultural College. 11, 36-38.
[28] Ji, P.H., Sun, T.H., Song, Y.F., Ackland, M.L. and Liu, Y. (2011) Strategies for enhancing the phytoremediation of cadmium-contaminated agricultural soils by Solanum nigrum L. Environmental Pollution. 159, 762-768.
[29] Zhang, Q., Li, J.M., Xu, M.G., Song, Z.G. and Zhou, S.W. (2006) Effect of amendments on bioavailablility of cadmium and zinc in compound contaminated red soil. Journal of Agro-Environment Science. 25, 861-865.
[30] Lv, L.L., Jin, M.Y., Li B.W. and Xie, J.Z. (2009) Study on remediation of the soil contaminated with Cadmium by applying four minerals. Journal of Agricultural university of Hebei. 32, 1-5.
[31] Maria, V.G., Juan M.P.G., Gema, A.S., Jose M.R.M., Carlos, V.A. and Cesar, G.L. (2015) Effects of the buffering capacity of the mobilization of heavy metals. Equilibrium and kinetic. Chemosphere. 131, 78-84.
[32] Guo, Z., Hu, X. and Ao, Y.S. (2009) Effect of chitosan on the available contents and vertical distribution of Cu^{2+} and Cd^{2+} in different textural soils. Journal of Hazardous Materials. 167, 1148-1151.
[33] Borsagli, F.G.L.M., Mansur, A.A.P., Chagas, P., Oliverira, L.C.A. and Mansur, H.S. (2015) *O*-carboxymethyl functionalization of chitosan: Complexation and adsorption of Cd (II) and Cr (VI) as heavy metal pollutant ions. Reactive and Functional Polymers. 97, 37-47.
[34] Li, M.L., Zhang, Z.Q., Li, R.H., Wang, J.J. and Ali, A. (2016) Removal of Pb (II) and Cd (II) ions from aqueous solution by thiosemicarbazide modified chitosan. International Journal of Biological Macromolecules. 86, 876-884.
[35] Zeng, L.X., Chen, Y.F., Zhang, Q.Y., Guo, X.M., Peng, Y.N., Xiao, H.J., Chen, X.C. and Luo, J.W. (2015) Adsorption of Cd (II), Cu(II) and Ni(II) ions by cross-linking chitosan/rectoritenano-hybrid composite microspheres. Carbohydrate Polymers. 130, 333-343.
[36] Wang, Y.Q., Xiao, L.Z., Li, S.Y., Guo Y. and Cai X.D. (2010) Effects of compound pollution of Pb and Cd on soil and physiological and biochemistrical characteristics of rice leaves. Chinese Agricultural Science Bulletin. 26, 369-373.
[37] Jin, M.Y. (2007) A study on remedying the soil contaminated with cadmium and lead by applying four mineral materials. Shijiazhuang: Agricultural University of Hebei, 18-20.
[38] Huang, R.H., Yang, B.C., Liu, Q. and Liu, Y.P. (2014) Simultaneous adsorption of aniline and Cr (VI) ion by activated carbon/chitosan composite. Journal of applied polymer. 131, 1-9.
[39] Tripathi, N., Choppala, G. and Singh, R.S. (2016) Evaluation of modified chitosan for remediation of zinc contaminated soils. Journal of Geochemical Exploration. 128, 180-184.
[40] Yong, S.O., Oh, S.E., Ahmad, M., Hyun, S., Kim, K.R., Moon, D.H., Lee, S.S., Lim, J., Jeon, W.T. and Yang, J.E. (2010) Effect of natural and calcined oyster shells on Cd and Pb immobilization in contaminated soils. Environmental Earth Sciences. 61, 1301-1308.
[41] Muzzarelli, R.A.A. (1977) Industrial Production and Application. Chitin, Pergamon Press, Oxford, England, 207p.

Received: **26.10.2017**
Accepted: **25.02.2018**

CORRESPONDING AUTHOR

Yaoguo Wu
School of Natural and Applied Sciences,
Northwestern Polytechnic University,
Xi'an, Shaanxi, 710072 – China

e-mail: wuygal@nwpu.edu.cn

© by PSP Volume 27 – No. 5/2018 pages 2922-2932 Fresenius Environmental Bulletin

ACOUSTICAL ENVIRONMENT DESIGN OF THE LECTURE HALL BASED ON THE IMPROVED ACOUSTIC INDEX ANALYSIS

Ziqing Tang, Fenghua Lu*

College of Architecture and Civil Engineering, Taiyuan University of Technology, 030024, Taiyuan, China

ABSTRACT

Aiming at the strong uncertainty and experiential feature of acoustical environment design of the lecture hall, there are quite a few interference factors for the traditional acoustic indicator in the measurement and analysis of sound environment. This paper proposes an improved acoustic index analysis based on the rotational diffusion model and MLS pulse integral algorithm, and through comparative experiments, it proves that this method has a higher correct rate in the detection of acoustic indexes. In order to further verify the reliability of the improved algorithm and its guidance to the acoustic environmental design, this paper chooses a university's auditorium lecture hall as the object of sound environment design. In the shape design, reverberation time control, sound absorption measurement, computer-aided sound field predication and analysis of the measured acoustic effects, the improved acoustic index analysis method is applied. Then, this paper compares the prediction results in the design of sound environment and the measurement results in the actual use of the hall, and comparison results show that the improved acoustic index analysis method proposed in this paper is feasible, and has strong practicability. Compared with the traditional method, the improved method can enhance the accuracy of analysis and prediction, which has strong practical significance.

KEYWORDS:
Acoustic index analysis, architectural acoustic environment design, reverberation time control, sound absorption measurement, computer-aided acoustic prediction.

INTRODUCTION

The sound environment design of lecture halls is one of the hot topics in architectural acoustics [1]. Generally, auditorium lecture halls cover a relatively large and are complex internally. Coupled with the impact of construction and other factors, there is great difference between the design goal and the actual effect of the hall [2]. Under the influence of many factors, it is more difficult to develop the design plan of the acoustic environment of lecture halls, which makes the acoustic design have strong uncertainty and empirical features [3]. So far, lecture halls' sound environment design has been divided into theoretical guidance and practical measurement. Through the theory guidance, the original version is designed, and then in the process of practice, by measuring the acoustic environment indexes, the design scheme can be continuously improved and optimized [4]. Theoretical guidance in the first version of the design plays the leading role, and reliable theoretical guidance can determine the formation of the program, the subsequent construction and the final actual results. Theoretical guidance usually includes design of the building's sound field and acoustic index analysis which complement each other. First, it is the theoretical design of the sound field, and then through the experimental method, the acoustic index is analyzed [5]. Therefore, the sound field prediction and theoretical calculation in engineering design are of major significance, which can influence the building acoustic environment design greatly [6]. In the current situation, the architectural sound field design and the analysis of acoustic indexes are separated and the analysis method of acoustic indexes is influenced by many factors, so the analysis effect is poor, and the index's support to the design of sound field is not enough.

Based on this, this paper explores and discusses the theories in the design stage from the traditional method of the absorption coefficient and the absorption structure in detail, and proposes an improved acoustic index analysis method. This method constructs the rotational diffusion model to substitute the traditional static model, and uses the Maximum length sequence (MLS) pulse integral algorithm to replace the traditional interrupt sound source algorithm. Through the comparative test, this paper verifies the feasibility and effectiveness of the improved acoustic index analysis method. In the subsequent simulation design, through the sound environment simulation of the lecture hall of a university, it uses the improved method for theoretical analysis and respectively constructs architectural sound field design and acoustic analysis. Then, in the actual use of the

hall, various indicators are measured and the measurement results are compared with the simulation design results at the beginning. The results' comparison can reflect the architectural acoustic design situation and the accuracy of the analysis results obtained through the improved acoustic index analysis method.

EXPERIMENTAL

Improved acoustic index analysis method. Prediction and calculation of acoustic indexes are the core contents of the architectural acoustic engineering design process. Therefore, the detection accuracy of acoustic indexes is very important, because the error of the traditional calculation method is common in engineering practice and often subject to the complex factors of the actual environment of buildings, which makes the detection more difficult. So, in the sound environment simulation and research of complex scenes such as lecture halls, using the improved acoustic index analysis method can enhance the prediction accuracy and efficiency of acoustic indexes, so as to enhance the sound environment simulation's accuracy and robustness, which has practical guidance significance for the simulation of acoustic environment. The acoustic index analysis and improvement are mainly in the selection of sound field absorption coefficient and the measurement of acoustic structure indexes. In this paper, the two important indexes are analyzed theoretically and experimentally, so as to achieve an improved acoustic index analysis method.

Traditional acoustic index analysis method. In order to control the acoustic effect of the large building, reasonable design and configuration of the sound absorption structure is one of the most important means. In the sound absorption structure, sound absorption coefficient is the fundamental basis of measurement and calculation in the sound prediction process. In the sound absorption structure design using traditional methods, sound absorption coefficient usually adopts empirical data and is obtained through the query of operation manual or data. In fact, empirical data has its specific architectural environment situation, so simply by drawing on the sound absorption coefficient will bring greater errors. Even with the same kind of acoustic material, due to the difference in the production materials, process, and installation of the architectural design and changes in environmental factors, there will have a relatively large difference. Suppose that there are j independent sound sources in the acoustic environment and each source and sensor go through the combined measurement for N times, the repeated deviation of the sound absorption coefficient is shown in the following formula [7]:

$$\eta = \frac{1}{M}\sum_{j=1}^{M}\frac{\sigma_j}{\alpha_j} \quad (1)$$

Among them, σ_j is the standard deviation between the j-th sound source and the N-th combined measurement of the sensor, while α_j is the average value of the N-th combined measurement value. For the sake of simplicity, the spatial bias of the measured values of the sound absorption coefficient is:

$$\mu = \frac{\sigma}{\alpha} \quad (2)$$

Among them, σ is the standard deviation between M sound sources and the sum of the N combined measurements of the sensor, while α is the average value of the sum of the N combined measurements. In the design and construction of the acoustic environment, η and μ are the two main parameters influencing the sound absorption coefficient. Therefore, the acoustic coefficient should not be selected by checking the existing experiential value directly, but should through practical and strict measurement on site, in order to promote the accuracy and robustness of large-scale building's sound field design.

Improved acoustic index analysis method. In the measurement of acoustic structure, sound absorption coefficient is one of the most critical indicators. The sound absorption coefficient measurement usually has the reverberation chamber method and the standing wave tube method [8]. In the two kinds of methods, the reverberation room method is less influenced by environmental factors. In contrast, due to the vertical incidence of the standing wave tube method into the sound absorption coefficient, this method has higher demands on the environment and is usually affected by environmental factors. Therefore, in the index measurement of acoustic structure, the reverberation chamber method is used for the measurement of incidence absorption coefficients without rules. According to the indoor acoustic characteristics, the amount of low frequency sound section with poor sound wavelengths in indoor normal mode is relatively small; the measurement of the reverberation time is influenced by the uneven sound field which leads to poor uniformity of measurement results, and there is a measurement deviation in space. In addition, since the random signal used in the measurement cannot generate a stable stimulation for all modes within the frequency band, this will lead to different test results of each mode under the excitation state, resulting in repeated measurement errors finally. To sum up, by reducing the sound unevenness factors and increasing random signals' stability, the measuring accuracy of the reverberation chamber can be improved. In this paper, to reduce uneven factors of the sound field, a rotational diffusion model is introduced, and the MLS

pulse integral algorithm is applied to enhance the stability of random signals.

(1) Rotational diffusion model [9]: in the calculation and prediction of each frequency band's reverberation time of the large-scale construction's halls using the traditional Sabine formula, the fixed diffusion model is often used. However, the rotational diffusion model has obvious advantages in increasing the reverberation room's diffusion degree. The model can carry out confusion processing on the boundary conditions in the interior sound field from temporal and spatial aspects, so as to destroy the stability of the standing wave of the sound field boundary. This characteristic of the rotational diffusion model can fully inspire more modes.

For studying the spatial deviation and repeated deviation of the rotational diffusion model on the reverberation chamber measurement, this paper conducts deviation test through practical experiments. There are 2 sound sources in the reverberation chamber of the experiment, which are located in the two opposite walls of the reverberation chamber respectively; 6 test sensors are evenly distributed in the three-dimensional space of the reverberation chamber, and there are 18 independent measurement decay curves in space. Table 1 shows the specific coordinate value of the sound source's location and the actual test sensor.

In the experiment, the measurements under two conditions, including the diffusion model stillness and the diffusion model rotation, are conducted respectively in the reverberation chamber. The iterative results of the repeated deviation and spatial deviation of the sound absorption coefficient measurement are shown in Figure 1.

The experimental results show that the use of the rotational diffusion model has little effect on the measurement of repeated deviation, and significantly improves the space deviation. In addition, at the time that the sound field is in the low frequency band, the influence reaches the maximum. In fact, this is because the number of modes in the room with low frequency is relatively small, which leads to a larger reverberation time deviation in different measuring points. The rotational diffusion model by disrupting the standing wave modal distribution can solve the problem of the small number of models in low frequency, so as to enhance the measurement accuracy of sound absorption coefficient in both low and high frequency range.

(2) MLS pulse integration algorithm [10]: in the traditional algorithm, the interrupt sound source method uses broadband noise as the excitation signal, while the difference of modal stability leads to different excited states of measurement modes at each time, making the repeated error accumulate gradually. If MLS pulse integration algorithm is adopted, it can improve the instability of the modal excitation state. This algorithm is a periodic pseudo-random excitation signal, which can be generated by the longest linear feedback's shift register. The frequency of this excitation signal is relatively flat, which can be used for system response analysis. In order to compare the differences and similarities of the interrupt sound source method and MLS pulse integral algorithm, this paper measures the sound absorption coefficient in the reverberation chamber using the two algorithms respectively. The iterative results of the repeated deviation and the spatial deviation are given in Figure 2.

The experimental results show that the MLS pulse integral algorithm can obtain a very small repeat deviation, so it can play a key role in the improvement of repeated deviations of measurement. Instead, in the spatial deviation, the two algorithms have quite similar results. According to the above model and the comparative experiments of the improved model, it can be seen that in the measurement process within the reverberation chamber, using rotational diffusion model and MLS pulse integral algorithm can improve the spatial deviation and repeated deviation. In the simulation of the actual lecture hall sound environment, the acoustic analysis index using the two schemes can enhance the accuracy of acoustic prediction results.

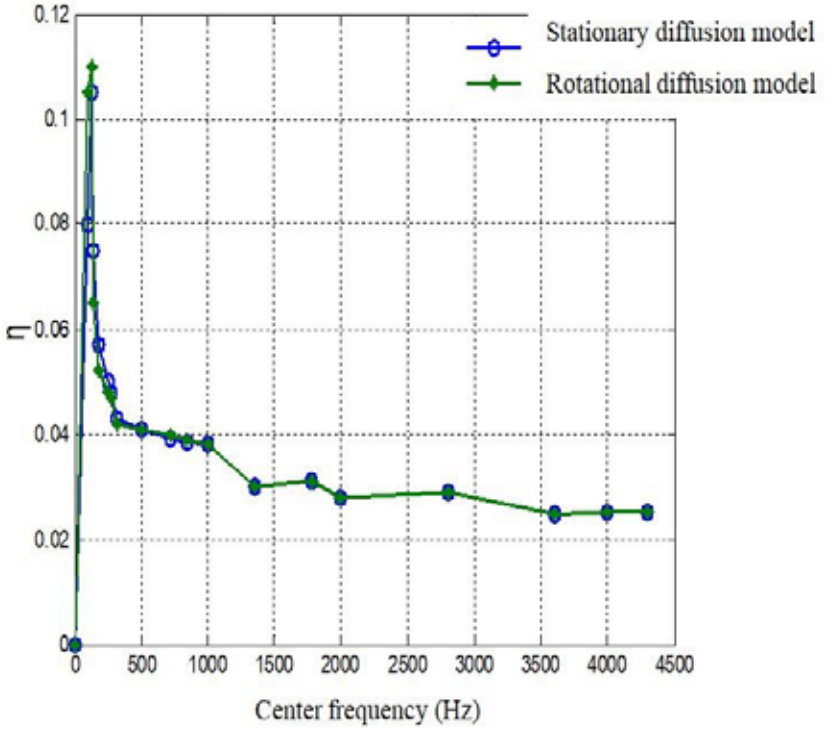
RESULTS AND DISCUSSION

Acoustic environment simulation of lecture halls. For the simulation research of the acoustic environment in lecture halls using the improved acoustic index analysis, this paper chooses a university's lecture all as the object of analysis. Through the application of the improved acoustic index analysis, this paper conducts shape design, reverberation time control and sound absorption measurement, computer-aided sound field prediction and the measured acoustic effect analysis for the simulation design.

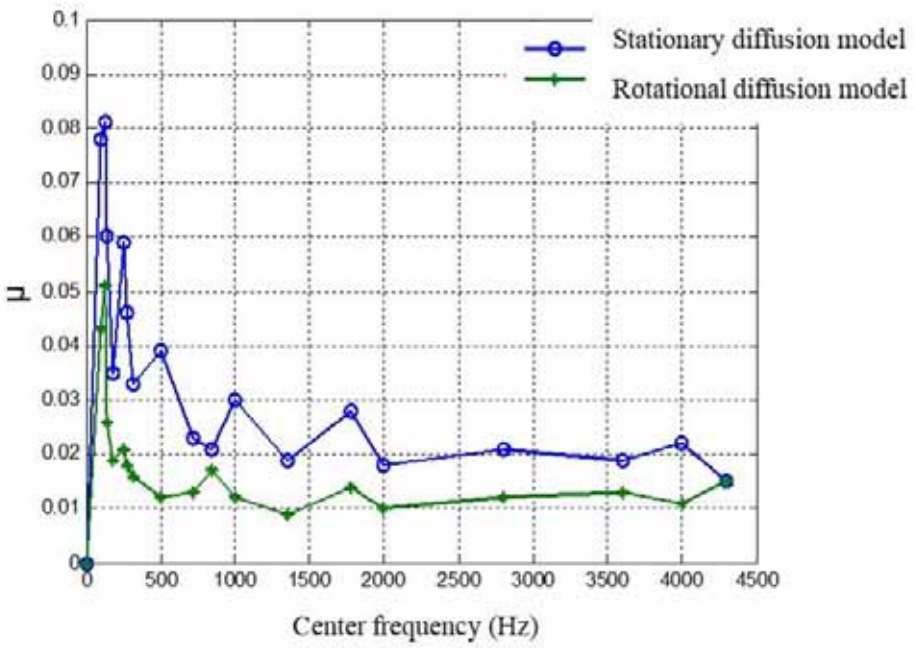
Shape design of architectural acoustic environment. The lecture hall's construction area is usually over 50 thousand square meters, with a volume of more than 2.5 cubic meters, so it belongs to an over-large object in the architectural acoustic environment design [11]. In fact, because the lecture hall is usually used for holding meetings, presenting shows and other application scenarios, its acoustic design is very difficult. Figure 3 gives the floor plan of the lecture hall.

TABLE 1
Coordinate value of sensors and sound source locations

Coordi-nate (m)	Measuring point 1	Measuring point 2	Measuring point 3	Measuring point 4	Measuring point 5	Measuring point 6	Sound source a	Sound source b
x	1.2	1.1	1.4	4.8	4.6	3.0	5.8	5.8
y	3.0	6.0	1.1	3.5	2.0	1.4	7.2	0
z	1.5	1.4	3.7	1.7	3.2	1.8	0	0

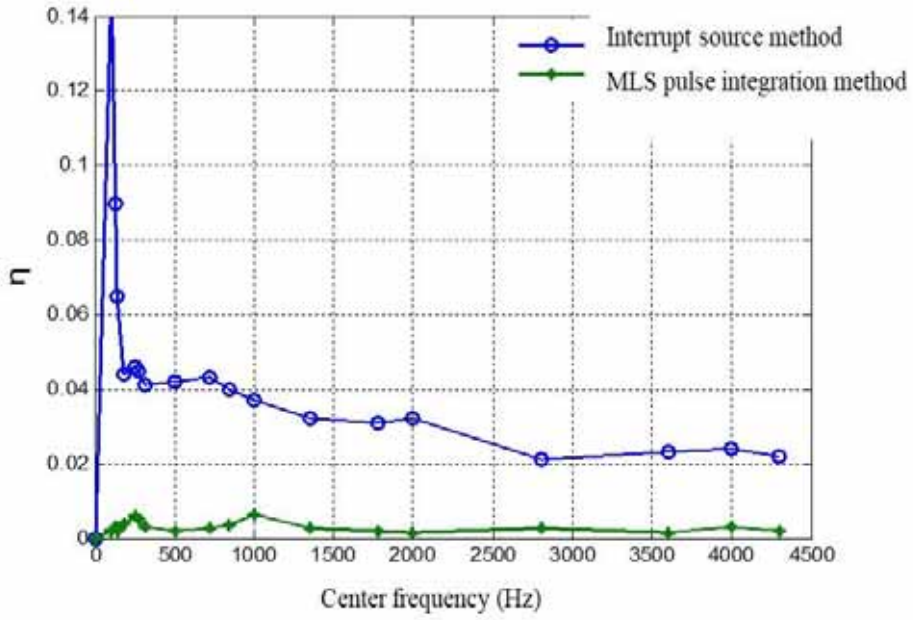


(a) Repeated deviation of the two diffusion models

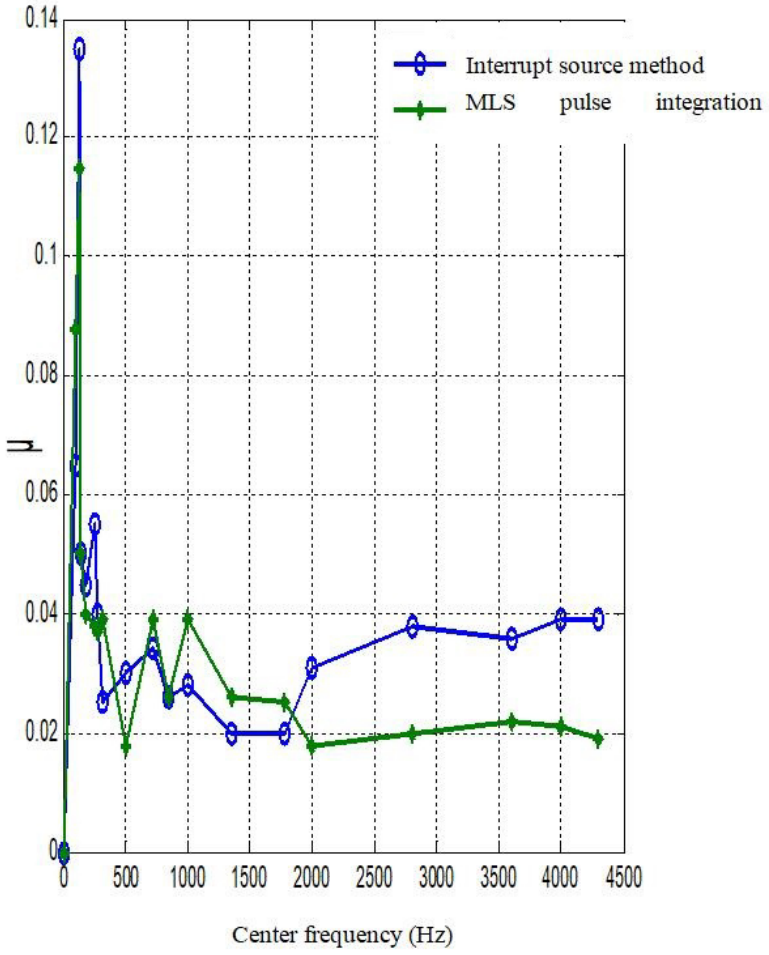


(b) Spatial deviation of the two diffusion models

FIGURE 1
Iterative result of the repeated deviation and spatial deviation of two kinds of models



(a) Repeated deviations of two different algorithms



(b) Spatial deviations of two different algorithms

FIGURE 2

Iterative results of repeated deviations and spatial deviations of two different algorithms

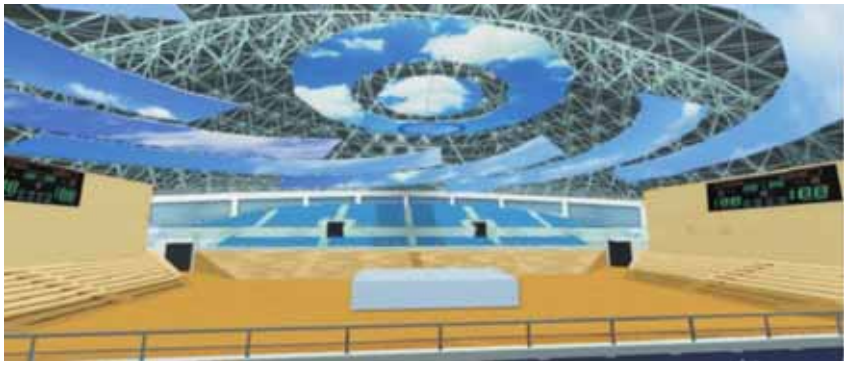


FIGURE 3
Floor plan of the lecture hall in a university

The design principles of the lecture hall include: make full use of direct sound and provide enough loudness for the audience; make the audience get enough loudness and early unilateral reflection sound field through the sound reflection control. This kind of sound reflection mode can provide a more realistic sense of space [12]; achieve the suitable evenness degree of sound field through appropriate diffusion treatment; and finally avoid the body conformation with bad sound defects in the design process. In the lecture hall, the proscenium arch is designed to be in a large horn shape extending to the auditorium. The side wall should be divided into a plurality of arc-shaped reflective surfaces whose tilt angles should increase from top to bottom. The horn-shaped stage and the side wall's reflective surfaces can provide more early lateral reflection sound field to the front seats, lifting the sound quality of the front zone of the lecture hall. The ceiling is divided into a flat plate and seven arc-shaped plates from front to back, and the arc-shaped plates with different angles are used to evenly reflect the sound from different angles to the audience. The final flat plate of the ceiling should decline in overall and its tilt angle should be reduced to reflect the sound to the back wall, so as to avoid the interference of multiple sound reflections on the front row. The surface of the arc-shaped railings in the hall goes through diffusion treatment, in order to avoid the defects produced by sound focusing. The railing's inclination degree is generally designed to be 12 degrees to supplement the early sound reflection in the central area.

Reverberation time control and sound absorption measurement. In general, the lecture hall is used for holding meetings and presenting shows. Its reverberant sound field range is generally in the intermediate frequency with an interval of [500Hz, 1000Hz], while the reverberation time is usually 1.2 seconds, and the whole frequency curve of the reverberation time is relatively stable. The lecture hall has a large space, which brings many interference factors on the prediction of sound field in the design stage. According to the estimation of Yilin formula, it can be seen that the absorption quantity of the university's lecture hall is 3792 square meters. Since the absorption quantity demand is high, it is needed to use a large area of sound-absorbing materials and structures to complete the sound-absorbing design. In the architectural acoustic environment design, the key of the reverberation time control lies in frequency characteristics, and because the frequency characteristic of the hall is relatively flat, different sound absorption structures should be designed to deal with the quantity of sound absorption in a variety of frequencies. In general, the venue of the lecture hall type uses porous sound absorption materials, including centrifugal sound absorption glass wool and cotton felt. For the sound absorption quantity adjustment of individual frequency bands, it is realized through special calculation and design of resonate sound absorption structure of different perforation rates and cavities. By filling the cavities with sound-absorbing cottons, the sound absorption frequency band and coefficient can be enlarged [13].

For the wall in the outer side of the stage and the side wall, arc-shaped reflection plate must be designed, in order to complete the sound absorption control through the perforated resonance sound absorption structure of arched reflection plates. Due to continuous changes in the perforated sound absorption board's back cavity of the arc structure of the reflection plates, the structure can increase the expansion of the sound absorption frequency range. The design of the side wall and the back wall of the auditorium uses different percentages of perforation and concave-convex, interlaced slot resonance as the sound absorption structure.

The stage area's quality requirement is relatively high: regard clarity as the standard; need to reduce the feedback pressure generated in the echo inhibition process of the sound amplifying system. The absorption on the stage generally adopts polyester fiber sound-absorbing panel and glass wool board covered by the steel screen to form the strong absorption design. In the design stage for the orchestra, the wall facing the stage uses slot resonance as the sound-absorbing material in order to control the reverberation time. For the wall facing the audience

area, considering the acoustic field's echo, the absorption processing cannot be conducted, in order to provide necessary sound radiation for the seating area [14]. In this structure, the concave-convex part uses different perforation rates and the perforation resonance sound absorption material structure. The sound absorbing material on the ceiling is the new material GRG with a light weight and high strength. Due to the reverberation time control's certain requirements on the absorption quantity, in the acoustic diffusion, there should also be appropriate sound absorption processing on the ceiling. The seven arc-shaped plates on the ceiling adopt the diffusion design, and the perforation rate of the last four plates is 16%, and the back cavity changes continuously. The last plate is designed with GRG material with a perforation rate of 8.4%.

After the completion of the reverberation time control and sound absorption material and structure design, it is needed to conduct sound absorption measurement in the reverberation chamber in which all acoustic materials and structures in the lecture should be measured actually. The measurement uses the improved acoustic index analysis based on the rotational diffusion model and the MLS pulse integral algorithm to enhance the accuracy of the measurement process. To ensure the robustness of measurement, this paper adopts the average value of the results of the 100 measurements as the final measurement result.

Computer-aided sound field prediction. In the primary stage of the architectural sound field design, through the Yilin formula, the absorption quantity of each frequency band is estimated [15]. It is also needed to conduct computer-aided sound field prediction on the design scheme through the visual sound source method and the sound ray tracing method [16]. Computer-aided prediction of sound field usually uses the ODEON7.0 software designed by the Technical University of Denmark. In the prediction of sound field, firstly, modeling software is used to carry out the 3D modeling of the university's lecture hall in real ratio. Figure 4 gives the 3D modeling results. After modeling, the sound-absorbing material data actually measured in the reverberation chamber is substituted into the model for sound field analysis. In the analysis, the three-dimensional spherical wave reflection is simulated, and this reflection method is even and relatively rich. In the predication, the average reverberation time and speech transmission index STI are calculated, and Figure 5 gives the cumulative distribution of the two parameters respectively. The predication result shows that the frequency characteristic of average reverberation time is straight, which can basically meet the acoustic design purpose. From the relationship between the STI standard provided by ODEON and subjective impression, when STI>0.6, the corresponding sound prediction results can reach the excellent standard. From the accumulation curve of STI, it can be seen that the STI index of more than 75% of the sound field designed in this paper belongs to "excellent", and the minimum value of the whole region is 0.575.

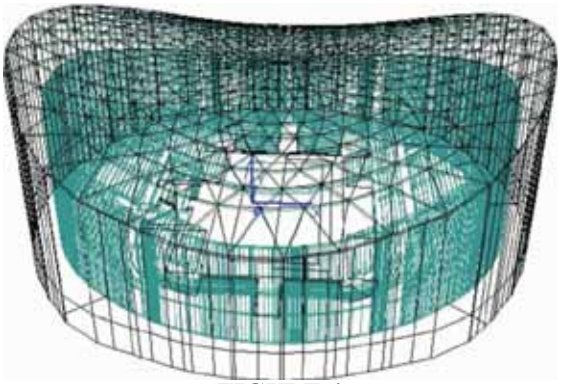
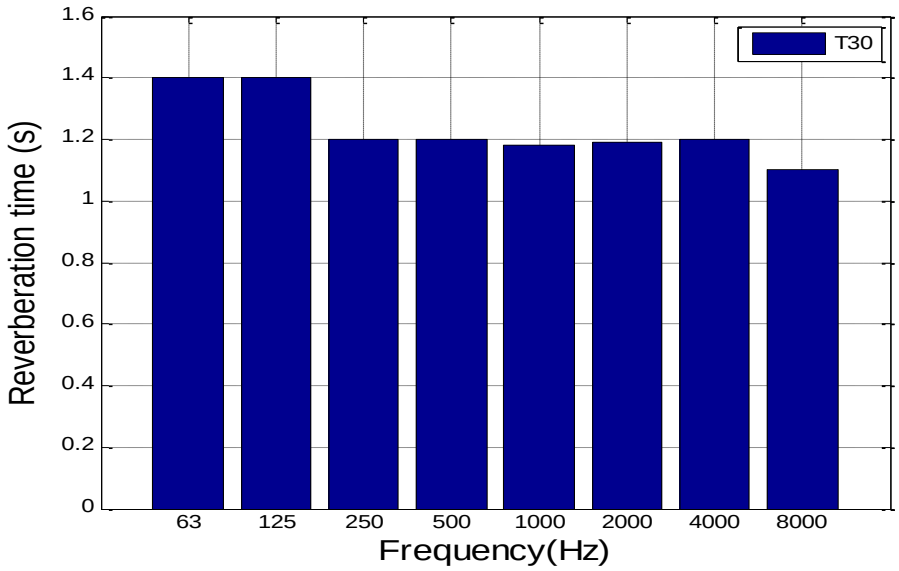


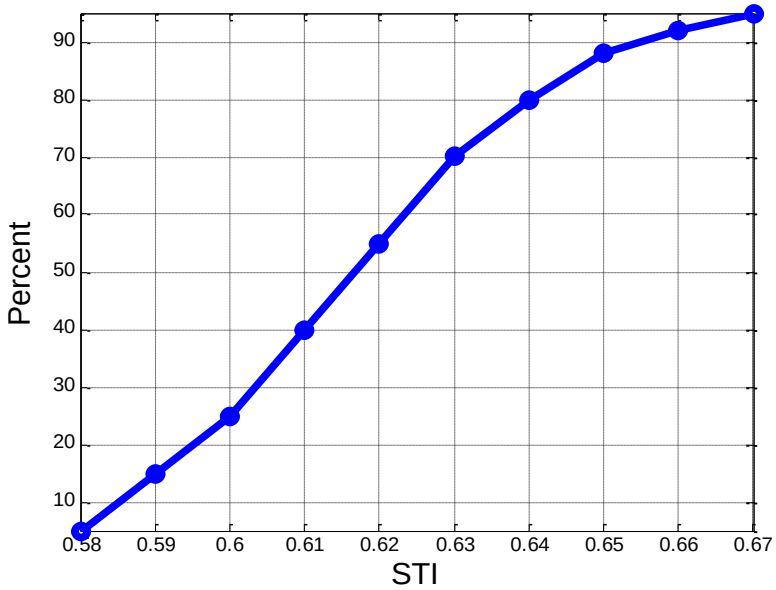
FIGURE 4
3D modeling results of the lecture hall of a university

From computer-aided sound prediction results, it can be seen that the sound field designed in this paper has no obvious defects in acoustic indicators; the frequency characteristics of various points of the reverberation time can reach the expected design range; and the sound field's uneven effect is relatively good. The statistical results of STI indexes are good, and the indexes predicated reflect the excellent sound quality in the audience hall. Predication results of the main frequency band of acoustic reflection show that reflected sound has the outstanding effect in the front row, but the effect in the rear seats is slightly lacking. In addition, through modeling analysis by ODEON, it shows that the defects such as a bad sense of echo do not appear in the overall model.

Measured acoustic effect analysis. After the completion of construction, it is also needed to base on whether the characteristics of the reverberation time of the middle-term measurement and evaluation reaches the expected objective to determine whether to adjust the design scheme. In the middle-term measurement, for the reverberation time characteristic measurement, 8 main measurement points are selected, and 2 measurement points in the second floor seating area are chosen. Through test, the average reverberation time curve is shown in Figure 6 (a). In order to test the uniformity, altogether 39 test points are selected, including the 2nd, 11th, 16th and 21st row of the auditorium and the 4th and 9th row of seats in the second floor. Test results are given in Table 2. In addition to the sound field test, 5 monitoring points are selected to test the background noise, and the test results are given in Figure 6 (b).



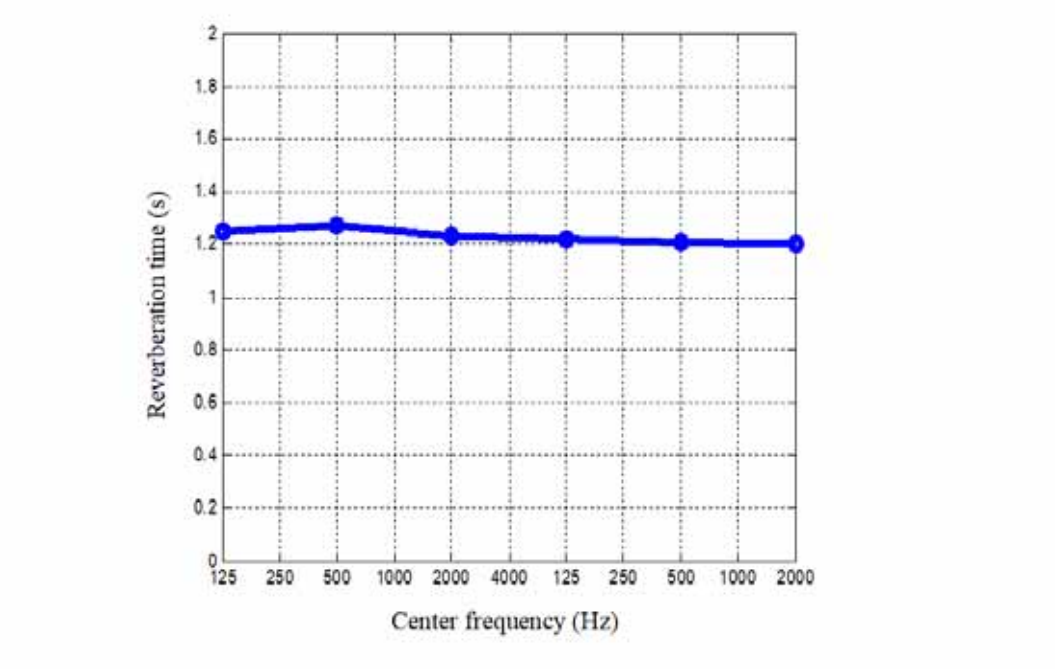
(a) Computer simulation of average reverberation time



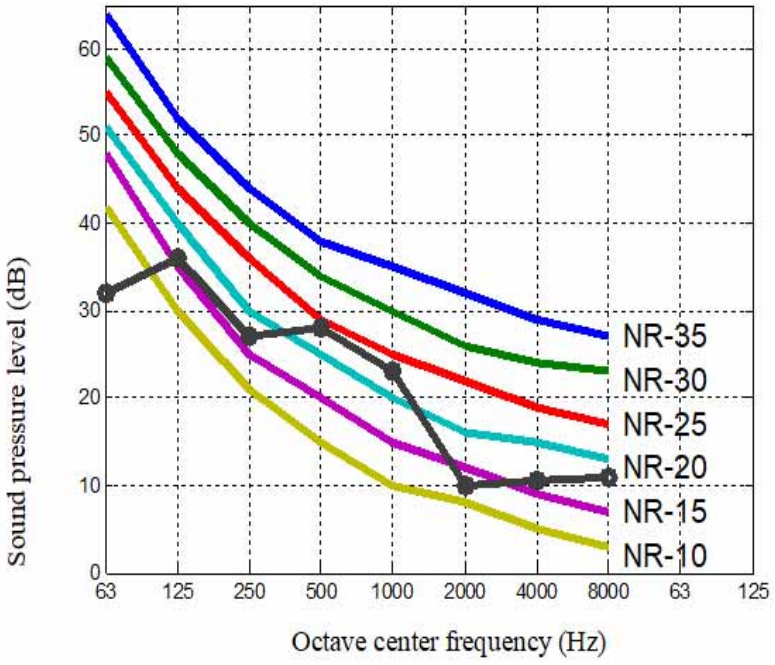
(b) STI accumulation distribution

FIGURE 5
Average reverberation time and cumulative distribution map of STI

From the mid-term test report, it can be seen that the high frequency part of the reverberation time curve is stable, while the low frequency part has some improvement, which can effectively guarantee the sound field's clarity and fullness. The reverberation time of 500Hz and 1000Hz reaches the expected design value of 1.2s, and the reverberation time can be controlled in a certain range. The uniformity of the first floor's seats is no more than 3.5dB, while that of the second floor's seats is no more than 4.2dB, so the whole uniformity of the audience seats is relatively good; the sound field design performs relatively well in size and reflection control; and the background noise test also reaches the expected requirements. The actual listening test on site shows that there are no obvious defects like echo, trembling voice and sound focusing in the lecture hall as a whole. From theoretical guidance and actual measurement results, it is found that the acoustic design project of the lecture hall of a university in this paper achieves the desired purpose, and the proposed improved acoustic index analysis method has good effectiveness and practical application ability in the accuracy of sound prediction, which can enhance the architectural acoustic prediction's robustness and practicality.



(a) Measured frequency characteristic curve of the reverberation time



(b) Measured frequency characteristic curve of the background noise

FIGURE 6
Average reverberation time and background noise test results

TABLE 2
Uniformity test results of the lecture hall in a university

Center frequency	The 2nd row	The 11th row	The 16th row	The 21st row	The 4th row in the second floor	The 9th row in the second floor
1k Hz	1.1 dB	3.1 dB	2.9 dB	2.3 dB	4.1 dB	4.2 dB
4k Hz	1.6 dB	3.4 dB	3.1 dB	2.8 dB	3.9 dB	3.9dB

CONCLUSIONS

There is a strong uncertainty and empirical feature in the sound environment design of lecture halls, and usually it is affected by many factors, resulting in the continuous optimization and updating of sound environmental design plans in the using process, consuming a lot of manpower and material resources. This paper from the theory research firstly analyzes the problems of the traditional acoustic index analysis method, including low accuracy and insufficient robustness, and puts forward a kind of improved acoustic index analysis method based on the rotational diffusion model and MLS pulse integral algorithm. The experimental result shows that this method can improve the accuracy and robustness in architectural acoustics prediction and measurement. Then, choosing a university's lecture hall as the research object, this paper conducts its body type design, reverberation time control and sound absorption measurement, computer-aided acoustic field prediction and the measured acoustic effect analysis. This thesis adopts the improved acoustic index analysis algorithm for the prediction of sound field, and compares the predication results with the mid-term actual results of the sound field. Compared with the actual results, the prediction results of sound field indicate that the proposed algorithm has a relatively strong feasibility and high accuracy. In the design and simulation of acoustic field in the future, more factors should be taken into account to build a more comprehensive sound environment design suitable for lecture halls.

REFERENCES

[1] Jalil, N.A.A., Din, N.B.C. and Daud, N.I.M.K. (2014) A Literature Analysis on Acoustical Environment in Green Building Design Strategies. Applied Mechanics & Materials. 471, 138-142.

[2] Elkhateeb, A.A. (2012) The acoustical design of the new lecture auditorium, Faculty of Law, Ain Shams University. Ain Shams Engineering Journal. 3(3), 219-235.

[3] Gu, X.A. and Wang, L. (2012) Research on the Requirement of Acoustical Environment in the Waiting Hall of High-Speed Railway Elevated Station. China Railway Science. 33(4), 120-125.

[4] Valente, D.L., Plevinsky, H.M., Franco, J.M., Heinrichsgraham, E.C. and Lewis, D.E. (2012) Experimental investigation of the effects of the acoustical conditions in a simulated classroom on speech recognition and learning in children. Journal of the Acoustical Society of America. 131(1), 232-246.

[5] Shin, B.S. (2014) Acoustic measurements based on a soundscape analysis in an open-plan classroom in a primary school. Journal of the Acoustical Society of America. 135(4), 2148.

[6] Liu, Z., Xu, W., Zhai, X., Qian, C., Chen, X. (2017) Feasibility and performance study of the hybrid ground-source heat pump system for one office building in Chinese heating dominated areas. Renew. Energ. 101, 1131-1140.

[7] Radosz, J. (2013) Research Papers: Global Index of the Acoustic Quality of Classrooms. Archives of Acoustics. 38(2), 159-168.

[8] Reeder, D.B., Bryan, C.L., Everett, K.R., Batteen, M.L., Guest, A.A. (2011) Quantitative ocean characterisation: Acoustically analogous environments. Journal of Operational Oceanography. 4(1), 3-12.

[9] Good, C.E., Glean, A.A., Vignola, J.F. (2013) A design of an impedance tube for teaching acoustic material properties and laboratory techniques. Journal of the Acoustical Society of America. 133(5), 3364-3366.

[10] Bian, L., Wang, Q. (2013) Influence of the particle size and volume fraction on micro-damage of the composites. Archive of Applied Mechanics. 83(3), 445-454.

[11] Fabre, J.P. (2007) Integrated signal excess as a metric for environmental acoustic assessment. Journal of the Acoustical Society of America. 122(5), 2942-2946.

[12] Chin-Bing, S.A., Warn-Varnas, A.C., King, D.B. (2007) A feed-back algorithm using ocean acoustic modeling to improve shallow water soliton simulations. Journal of the Acoustical Society of America. 122(5), 3004.

[13] Liang, Y. (2015) Satisfaction with Economic and Social Rights and Quality of Life in a Post-Disaster Zone in China: Evidence from Earthquake-Prone Sichuan. Disaster Medicine and Public Health Preparedness. 9(2), 111-118.

[14] Liu, Z., Li, H., Liu, K., Yu, H., Cheng, K. (2017) Design of high-performance water-in-glass evacuated tube solar water heaters by a high-throughput screening based on machine learning: A combined modeling and experimental study. Sol. Energy. 142, 61-67.

[15] Moleti, A., Sisto, R. and Tognola, G. (2005) Otoacoustic emission latency, cochlear tuning, and hearing functionality in neonates. Journal of the Acoustical Society of America. 118(1), 1576-84.

[16] Lei, B., Rahman, S.A. and Song, I. (2014) Content-based classification of breath sound with enhanced features. Neurocomputing. 141(4), 139-147.

Received: **30.10.2017**
Accepted: **06.02.2018**

CORRESPONDING AUTHOR

Fenghua Lu
College of Architecture and Civil Engineering,
Taiyuan University of Technology,
030024 Taiyuan – China

e-mail: lufenghua888@126.com

© by PSP Volume 27 – No. 5/2018 pages 2933-2942 Fresenius Environmental Bulletin

LAND USE CONVERSION EFFECTS TRIGGERED BY TEA PLANTATION ON LANDSLIDE OCCURRENCE AND SOIL LOSS IN NORTHEASTERN ANATOLIA, TURKEY

Sezgin Hacisalihoglu*, Selcuk Gumus, Ugur Kezik

Karadeniz Technical University, Faculty of Forestry, 61080 Trabzon, Turkey

ABSTRACT

Tea plants are usually grown in areas susceptible to landslides and most of the tea plantations are transformed from forestlands in Turkey. There are interrelations between soil properties and landslide occurrence. Soil characteristics are effective on the formation of landslides in combination with other factors while landslides significantly affect important soil properties such as organic matter and bulk density. This study was carried out in 15 landslides occurred in tea (*Camellia sinensi*s) plantations area in the Gundogdu region. Soil samples were taken from tea plantation and forest area that adjacent of landslides. Different soil depths (0-20 cm and 20-50 cm) and soil properties, clay type and soil loss quantities were investigated under the same slope and slope length conditions. As a result, significant negative changes have been determined in soil characteristics such as organic matter, pH, bulk density, saturated hydraulic conductivity and saturation (P<0.05). This is the fact especially where the forest areas were converted into tea fields in over time. The same negative situation was also determined in average soil loss amounts (P<0.001). Annual average soil loss was determined 85.73 t/ha/yr in areas with tea plantations, whereas this value was found to be 18.41 t/ha/yr in the forested areas. The common clay type in the field was determined as kaolinite and the soil texture was classified as sandy to sandy loam.

KEYWORDS:
Camellia sinensis, *Alnus glutinosa*, Landslide, Soil Loss, ABAG

INTRODUCTION

Landslides are natural disasters that cause loss of life and property caused by natural conditions and anthropogenic effects [1] Geographical structure, geometric change, surface and ground water, temperature changes, earthquakes and vibrations and plant cover are the main natural factors affecting the landscape, while the land use plays an important role among the artificial factors [2]. Inappropriate land use can also affect landslide formations and soil characteristics and soil loss in the unit area [3].

In general, there is a bilateral relationship between landslide formations and soil properties. The factor "*K*", which is determined by the soil properties and which is a component of the soil loss equations, is considered as a parameter that affects the erodibility of the soil [4] and is a factor triggering the landslide. Atterberg limits (including clay content and type), liquid limit (LL), plasticity index (PI) [5], spatial distribution of soil properties [6] and soil engineering properties [7-8] have considerable influence in the formation of shallow landslide. The role of soil properties on landslide formation can be observed more clearly by means of structures such as road constructions [9]. In addition, landslide formation significantly affects the physical, chemical and biochemical quality parameters of soil [10-11-12]) and soil loss in the unit area [13]. More importantly, landslides are among the most important events that limit plant development by destroying the soil in terms of plant nutrients [10].

When land use and landslide interrelation are examined, the conversion of forest areas to agricultural lands is at the top of the risk factors effecting the landslides and soil loss. Geometrical changes of landslides have been investigated with photogrammetric techniques in Rize province, where also this research has been conducted, between 1973 and 2002, and it has been reported that landslides are increasing because of converting forest areas to the tea fields [14]. Changes in land use between 1994 and 2009 in Messina (Italy) were examined using digitized aerial photographs and it was found that with the decrease in forest areas and the increase in rangelands, agriculture areas and residential areas is increasing the landslide risk [15]. Likewise, these effects can occur over the many years or even for a short period of only 10 years [16]. It is stated that 80% of the landslide risk factor can be explained by using cellular methods using GIS methods [17]. Climate factors mainly the rainfall play an important role in the formation and characterization of landslides [18]. For this reason, there are devastating landslides in the Americas, the North Atlantic Basin, the Taiwan island, and Japan [19].

Factors affecting the landslide were compared with factor analysis [20], and as a result, lithology, slope and vegetation were reported as the main factors affecting the landslide. The occurrence characteristic of the landscapes is considered as an important factor determining the damage grade [21]. Several useful models based on hydrology, topography, geology and soil characteristics have been developed to determine the general occurrence risk of landslides [22].

When the areas where the tea plantations located are evaluated in terms of the risk of landslide, social, economic and ecological conditions are among the basic parameters affecting the landslide. Tea is one of the most consumed beverages [23] and the growing world population is increasing the need for tea production [24]. Geo-ecological problems are increasing as the socio-economic situation of the local people living in the rural area is improved with tea production. Even in areas where the world's best tea (qualitative and quantitative) is produced, it has been necessary to conversion of forest areas to tea field [25]. Because, the natural forest areas easily meet the conditions of the ecological environment of the tea species [26]. It is known that the root structure of the trees increases slope stability by hydrological and mechanical effects [27]. For this reason, conversion of the deforestation areas into weak rooted tea plantations triggers the formation of landslides. According to FAO [24], tea production in the world in the last 10 years is dramatically increasing and China, India, Kenya, Sri Lanka and Turkey are among the top 5 tea producing countries. Tea production areas in these countries should be evaluated in terms of landslide risk.

Most of the landslides in Turkey (64.33%) occur in the autumn when the precipitation is intense [28] and the landslides are in the first place with 45% share in natural disaster order. The Rize region is the first in the order of landslide events [29]. In Gundogdu (Rize) 2010, 13 people lost their lives. This study was carried out in Gundogdu (Rize) region, which is among the landslide susceptible regions due to topographic, geological, vegetative and climatic conditions. In 15 landslide areas within the tea plantations (*Camellia sinensis*) which was transformed from forest areas and in adjacent forested areas. Under the same slope and slope length conditions, the soil characteristics and soil loss quantities were examined.

MATERIALS AND METHODS

Study area. The study area is placed in the Eastern Black Sea Region of Turkey in the Gundogdu, Rize (41° 02′ 48″ **N** 40° - 36′ 32″ **E**) (Figure 1). Study area is approximately 5 km far away from center of the Rize province (Fig. 1). The study area is topographically very rugged and has high slope gradient. Because of the high slope gradients, the streams are flowing fast (concentration times are short). In recent years, many hydroelectric power plants have been built on these rivers. The forests that cover the valley slopes form a belt parallel to the sea. Gundogdu, which is placed in the eastern border of the central district, was built on a flat and scattered plain. Slope gradient is somewhere around 50-60%. In the Black Sea Region, mountains are generally parallel to the coast (east - west direction), but there are also north, south and east and west slopes in Gundogdu.

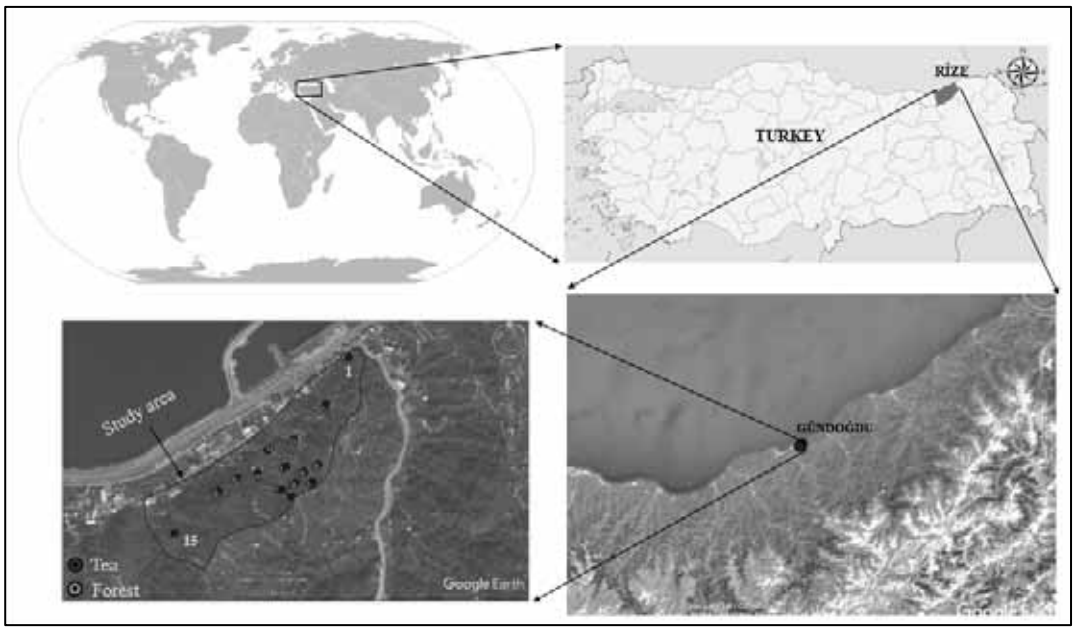


FIGURE 1
Study area and sample points

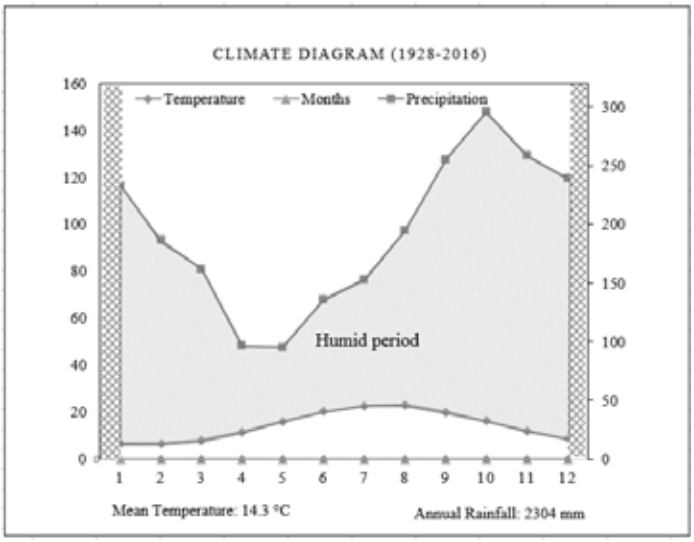


FIGURE 2
Walter climate diagram of research area

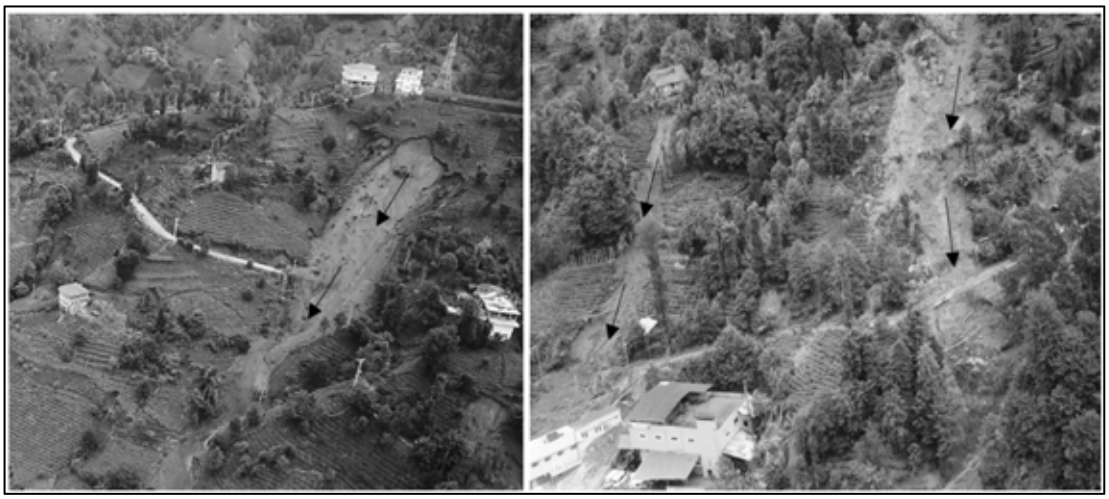


FIGURE 3
Landslide areas and nearby forest areas in the study site.

According to the climate data of the last 88 years, the average annual temperature is 14.3ºC and the annual total precipitation is 2304 mm. Most of rainfall occurs in autumn and according to Walter et al. [30] climate diagram, there is no water shortage in this region throughout to year (Figure 2). In addition, the study area is classified as "*very humid*" according to Aydeniz climate classification, "*wet*" according to DeMartonne and "*A, very humid*" according to Thornthwaite method [31].

In the study area, many landslides were occur ranging from past to present. However, by the year 2010 on August one of the most severe landslides occurred and 13 people death due to heavy rainfall (approximately 166 mm/m^2) which lasted for 6 hours continuously in Gundogdu town and neighboring villages. In this area where the landslides are seen intensively, approximately 48 ha of tea and forest land was selected as the study area. 15 landslide areas (Figure 1) and 15 forest areas adjacent to each landslide area (Figure 3) were investigated in this study area. In general, landslides with shallow heel characteristics have an average slope of 50% and an average length of 60 meters. Altitude is varying between 15m - 228m asl. and the main aspect extends from the North to the Northwest. In the study area, andesitic and basaltic lava, tuff, breccia and anglomeras are seen as main rocks. Below the main rock is an impermeable kaolinite clay layer. The soil in tea and woodland areas has a sandy and sandy loam texture. This creates sensitive conditions from the geologic point of view. All of the tea fields have been converted from the forest area in the past (50-60 years ago) in this region. In the forest area, dominant native species is alder and rarely distributed oriental beech, Anatolian chestnut, lime and hornbeam. In the understory, there is exist Rhododendron genus with grass and a single annual plant like fragaria and lichens.

Data collection. Soil Sampling. Soil profiles were opened, and soil samples were taken from the tea fields and the adjacent forest areas where the landslides happened. In the opened profiles, samples were taken from two depth levels. Topsoil samples were taken from 0-20 cm and subsoil samples were taken from 20-50 cm samples. A total of 60 soil samples from two soil depth were collected (30 from forests and 30 from tea fields).

The soil properties such as surface stoniness (%), slope gradient (%), aggregate class etc. are determined separately at each sampling point [32]. Permeability and the other hydro-physical soil properties are described according to Saxton et al. [33], the soil texture was determined by the Bouyoucos [34] hydrometer method and the organic matter content by the Walkley-Black, wet oxidation method [35]. To determine the liquid limit and plastic index in both tea plantation and forest area and the structure of clay minerals were determined according to ASTM [36] standards developed by Casagrande [37].

Soil Loss Predicting with the ABAG (Allgemeine Boden Abtrags Gleichung). In this study, to estimate of soil loss, ABAG is the international version (where the values are turned in to metric system and adapted to the European conditions) of the simulation model USLE (Universal Soil Loss Equation) was used based on Schwertmann et al. [38] model. This model is used at a global level to determine soil loss by erosion.

$$A = K \, x \, R \, x \, LS \, x \, C \, x \, P \qquad (1)$$

where A is the average annual soil loss (t/ha per year), *K* the soil erodibility factor, *R* the rainfall erosivity factor, *LS* slope and slope length factor, *C* the cover management factor and *P* is the supporting practice factor. Climate erosivity is represented by R and can be estimated from the rainfall intensity and amounts data which were taken from Dogan and Gucer [39]. The soil erodibility monograph has been used to predict the K value [38].

In soil loss equation, *C* (plant closure factor; forest:0.01, tea plantation:0.05), *P* (protection measure, for forest and tea: 1.0), R (precipitation coefficient; for forest and tea: 400) and *LS* (slope and slope length factor; for forest and tea: 21.63) values are fixed at all points under the same land use condition. However, the "*K*" factor have different values at all points. The main slope (*S*) was accepted as 50% and the slope length (*L*) as 60 meters.

Statistical methods. Analyzed soil properties and soil loss quantities at the tea plantation and forest area were tested using the SPSS program (version 23.0 software package, Institute Inc., Chicago, IL, USA, 2016). Soil loss and other soil properties were compared one another depend on land use type (tea plantation and forest area) by Independent Samples T-Test (Student's t-test) for normally distributed values and by Mann-Whitney U-test for nonparametric values and results are expressed as means ± SE (Standard error). Pearson's correlation coefficient was searched to examine the relation between normally distributed analyzed and measured soil variables. Spearman's correlation coefficient was used for non-normal distributed values. Statistical significance was defined as P was <0.05 and <0.01 and P<0.001.

RESULTS AND DISCUSSION

The result of the conversion of forest land to tea plantations in the study area, the amount of soil loss in the unit area increased about 4.5 times over 50-60 years (Figure 4). The soil loss amounts in the forest area was determined as 18.41 t/ha/yr, which was 85.73 t/ha/yr in tea plantations (Table 1). Compared with a study in an Indian region [40] where similar rainfall amounts are measured, the amount of soil loss in forest areas is in the moderate erosion class while the amount of soil loss in the tea plantation areas is in the high erosion class. In another study, the amount of annual soil loss was reported as 100-200 t/ha/year in a tea plantation with less than 40% coverage [41]. In Sri Lanka, Abeygunawardena and Samarakoon [42] estimated the soil loss amounts in a tea plantation about 43 t/ha/yr according to USLE. Hewawasam [43] reported that the soil loss amount in a weakly managed seedling tea plantation could be up to 52 t/ha/yr, and in a degraded forest area 25 t/ha/yr.

Under normal conditions, it is expected that the most erosion will be in agriculture area compared to pasture and forest area due to land use type [44]. However, sometimes land and soil conditions can affect the expected amount of soil erosion in the opposite direction. In a study using the *MPSIAC* model, the highest soil loss amounts were found in the forest area (14.05 t/ha/yr), then in the pasture area (11.02 t/ha/yr) and at least in the agricultural area (10.61 t/ha/yr) [3].

Moreover, in this study "*K*" factor one of the main component of soil loss equation was not significantly changed (Table 1) according to land use groups. And also, *R, LS* and *P* factor were used as the same value in both forest and tea plantation area. Already this region is located in sensitive areas in terms of landslides due to high precipitation and slope gradient. But "C" was the main factor that affected the soil loss amounts if soil loss amounts compared depend on land use type. Overall, in this study it was determined that there is a very important relationship between soil loss and organic matter, bulk density (Fig. 5). The studies carried out support this knowledge [44-45-46-47]. The other measured correlation relations are given in Table 2.

TABLE 1
Mean values of some soil properties depend on land use group (n=30, mean ± SE)

Variables	Forest	Tea Plantation	P value
Sand %	74.57±1.22	73.33±1.65	*NS*
Silt %	14.57±1.30	13.00±1.26	*NS*
Clay %	10.57±0.78	13.67±1.43	*NS*
Organic Matter %	5.67±0.45	3.09±0.27	*P<0.001*
pH (H_2O)	5.31±0.11	4.86±0.12	*P<0.01*
Field Capacity (FC) %	20.88±0.90	20.37±1.24	*NS*
Wilting Point (WP) %	12.16±1.20	10.63±0.89	*NS*
Saturation %	50.8±1.80	46.19±0.73	*P<0.05*
Available Water Holding Capacity (AWHC) mm/cm	0.98±0.06	0.97±0.08	*NS*
Saturated Hydraulic Conductivity (SHC, cm/hr)	7.53±0.58	4.93±0.55	*P<0.01*
Bulk Density (gr/cm^3)	1.29±0.03	1.45±0.02	*P<0.001*
K Factor	0.213±0.005	0.198±0.009	*NS*
Soil loss (A, t/ha/year)	18.41±0.48	85.73±3.68	*P<0.001*



FIGURE 4
Effects of land conversion on soil loss amount

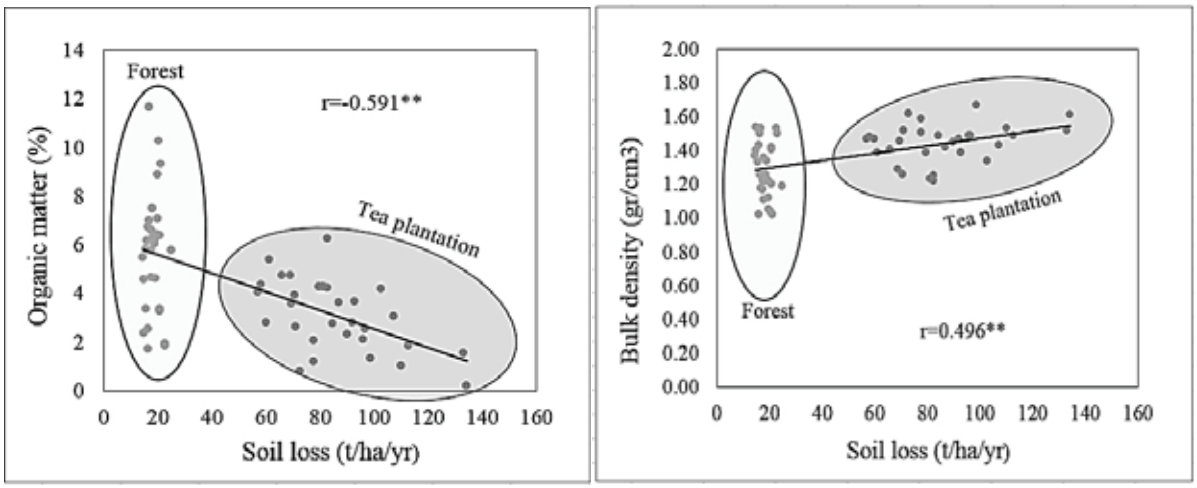


FIGURE 5
Soil parameters highly correlated with soil loss in study area (*P*<0.001, n=60)

TABLE 2
Pearson's correlation coefficients among measured and calculated the variables (n=60)

Soil Characteristics	Sand	Silt	Clay	OM	pH	FC	WP	Saturation	AWHC	SHC	BD	K_Factor	A_Soil_Loss
Sand (%)	1												
Silt (%)	-.638(**)	1											
Clay (%)	-.564(**)	-.262(*)	1										
OM (%)	-.198	.311(*)	-.068	1									
pH (%)	.118	.039	-.206	.026	1								
FC (%)	-.457(**)	.044	.555(**)	.536(**)	-.240	1							
WP (%)	-.265(*)	-.217	.589(**)	.200	-.083	.421(**)	1						
Saturation (%)	-.090	.362(**)	-.269(*)	.710(**)	-.041	.428(**)	-.431(**)	1					
AWHC (%)	-.090	.160	-.038	.405(**)	-.167	.754(**)	-.001	.537(**)	1				
SHC (cm/hr)	.431(**)	.276(*)	-.853(**)	.340(**)	.184	-.450(**)	-.424(**)	.436(**)	-.086	1			
BD (gr/cm^3)	-.017	-.321(*)	.349(**)	-.859(**)	.009	-.470(**)	.008	-.819(**)	-.602(**)	-.552(**)	1		
K_Factor	-.111	.725(**)	-.640(**)	-.083	.228	-.477(**)	-.478(**)	.080	-.077	.494(**)	-.052	1	
A_Soil_Loss (t/ha/yr)	-.071	.109	-.009	-.591(**)	-.223	-.253	-.310(*)	-.300(*)	-.067	-.214	.496(**)	.171	1

** Correlation is significant at the 0.01 level (2-tailed). * Correlation is significant at the 0.05 level (2-tailed).

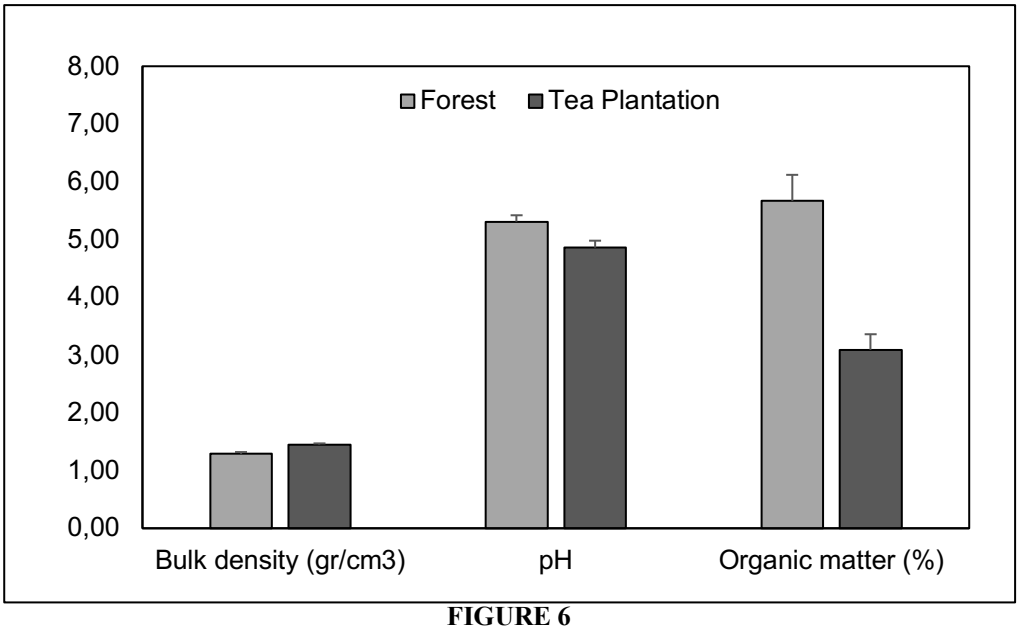


FIGURE 6
Land conversion effects on some important soil quality indicator

Landslides significantly affect the physical, chemical and biochemical properties of the soil), together with causing significant loss of life and property [48-12]. In the study area, organic matter, pH and bulk density, which are important soil quality indicators, were significantly affected because of the conversion of natural forest areas to the tea plantations (approximately within a half century period) (Table 1 and Fig. 6). Abad et al. [49] reports that physical-chemical properties such as the amount of organic matter, pH and bulk density are significantly affected by land use change (agriculture, forest, rangeland) Cheng et al. [10] have reported in their work that landslides are changes the pH and organic carbon values significantly. Also, Ollauri and Mickovski [50] reported that shallow landslides change the bio-physical diversity in the unit area. In their study, Donnini et al. [51] reported that landslides significantly increase the road network and restoration costs.

Soil properties and especially soil texture is shown as one of the main factors affecting landslide and soil loss [52-5]. Although sandy soils have good drainage and water drainage conditions [53], encountering a clay layer such as kaolinite and illite near the surface can cause to slip and collapse on the ground [54]. Similarly, in our study area, it is easier to mass move the soil due to the impermeable kaolinite clay layer just above the main rock. Studies have shown that high clay content increases the landslide with factors such as precipitation and slope

[55], and this appears to be manifest especially in shallow landslides [56].

Determination of *Atterberg limits* provides important information about the clay content of the soil, the potential for water retention and the sensitivity of the soil to the landslide. The average liquid limit in tea plantations in our study area was 50.55% and the plastic index was 18.55% (n=2). In the forested area, the liquid limit was 54.95% and plastic index was 20.25% (n = 2). Mugagga et al. [57] reported in their study that the liquid limit values changed between 47-53.5% and the plastic index values varied between 23.8-33%, which affected the landslide susceptibility. Many useful models based on hydrology, topography, geology and soil characteristics have been developed to determine the risk of landslides [22]. However, when considering the global socio-economic situation of tea plants [23]. It is clear that models should be developed that take into account socio-economic facts. Because of the increase in demand for tea, new production areas are needed [25]. This causes natural vegetation like forests to be destroyed and the land to become more susceptible to natural disasters such as landslides.

Tea production in the world and in Turkey continues to increase with each passing year [24]. However, tea production areas are increasing, forest areas are decreasing, and landslide risk is increasing in regions where tea production is concentrated [14]. This creates a landslide risk due to land use. In Turkey, 13 494 landslides and 2 956 rock fallings have been recorded in the last 50 years. Only the total number of people affected by these two types of natural disasters is 78 767 [29]. Shallow landslides are reported to be triggered by short-term heavy rainfall [58]. This type of precipitation is frequently encountered in our study area. These precipitation, along with slope and soil characteristics, are among the main factors affecting landslide formation. The infiltration of surface waters into the soil by uncontrolled flow through the slope causes the pressure of the ground water to increase [59]. For this reason, excessive rainfall should be collected in certain channels to prevent infiltration into the soil. Through these channels it must be passed to the surface flow and removed from the area in a controlled manner. This situation is great importance in terms of slope stability where area is sensitive to landslide. For this reason, excessive rainfall should be collected in certain channels to prevent infiltration into the soil. Through these channels it must be passed to the surface flow and removed from the area in a controlled manner. This situation is of great importance in terms of slope stability in landslide risk areas.

The destruction of natural forests and their conversion into different forms of land use is one of the most important factors that cause soil structure deterioration and it makes to increase shallow landslides [60]. Along with the forests, the formation, distribution and circulation of the water are modified; water quality is regulated, precipitation-flow relationship is regulated, and stream flow regime is regulated by reducing soil loss caused by water erosion [61]. However, the risk of landslide is also reduced. For this reason, forests are used as the most effective means to control soil and water erosion [62-63]. The roots of the trees in the forests mechanically increase the slope stability [27] and in the other hand, interception reduces the surface flow [64-65]. The trees in the environment reduce transpiration by absorbing the soil water and contribute to the balance conditions with the root structure [61]. Tree species are also reported to be effective on slope stability [66]. Early warning systems can also be a guide for estimating potential landslide areas. Tofani et al. [67] developed an early warning system (*MUSE*) using an appropriate modeling system for shallow landslides.

CONCLUSIONS

In this study, soil amounts and some important soil parameters were significantly affected owing to conversion of natural forest cover to tea plantation overtime in Eastern Black Sea region with high rainfall. It has been determined that the most important soil loss equation component affecting landslides in the unit area was C factor. Therefore, in areas with suitable ecological conditions for tea cultivation, appropriate protective measures must be taken to protect the ecological balance and reduce the risk of landslides. The risk of landslide can be reduced by developing excess water discharging systems to reduce the damage of rainfall which is the most important factor that triggers the landscape. For this reason, the positive contribution of the forest trees to the slope stability in the tea cultivation areas should be exploited by using species such as alder, beech, chestnut, hornbeam and linden which are the native species of the region. However, areas damaged by landslides should be remedied as soon as possible. In these areas, topsoil should be improved by adjusting *C/N* (Carbon/Nitrogen) ratios first [13]. Later, deep-rooted vegetation can be used. In addition, early warning systems should be developed with high accuracy to prevent human deaths and other hazardous conditions.

ACKNOWLEDGEMENTS

This work was supported by Scientific Research Projects Coordination Unit of Karadeniz Technical University. Project number 2010.113.001.14. The authors would like to thank to the Governor of Rize and to the Regional Directorate of Meteorology for climate data and photos. Also, a special thanks to the Prof. Dr. Canturk Gumus for their scientific supports.

REFERENCES

[1] Tseng, C.M., Lin, C.W., Hsieh, W.D. (2017) Landslide susceptibility analysis by means of event-based multi-temporal landslide inventories. Nat. Hazards Earth Syst. Sci. Discuss. 3, 1137-1173.

[2] Ranjbar, M., Ahmadi, H. (2013) Analyzing the Factors Affecting Occurrence of Landslide in NAVROUD Basin using AHP Model (Tälesh City - Iran). Advances in Environmental Biology. 7, 3188 - 3197.

[3] Heshmati, M., Arifin, A., Shamshuddin, J., Majid, N.M., Ghaituri, M. (2011) Factors affecting landslides occurrence in agro-ecological zones in the Merek catchment, Iran. Journal of Arid Environments. 75, 1072 -1082.

[4] Vopravil, J., Janeček, M., Tippl, M. (2007) Revised Soil Erodibility K-factor for Soils in the Czech Republic. Soil & Water Res. 2, 1-9.

[5] Kitutu, M.G., Muwanga A., Poesen, J., Deckers J.A. (2009) Influence of soil properties on landslide occurrences in Bududa district, Eastern Uganda. African Journal of Agricultural Research. 4, 611-620.

[6] Fan, L., Lehmann, P., Dani, O. (2015) Effects of Spatial Variability of Soil Properties on the Triggering of Rainfall-Induced Shallow Landslides. Geophysical Research Abstracts. 17, 8738 - 2015.

[7] McKenna, J.P.M., Santi, P.M., Amblard, X., Negri, J. (2011) Effects of soil-engineering properties on the failure mode of shallow landslides. Landslides. 9(2), 215-228.

[8] Jeong, S., Lee, K., Kim, J., Kim, Y. (2017) Analysis of rainfall-induced landslide on unsaturated soil slopes. Sustainability. 9, 1280.

[9] Turk, Y. (2017) The Effect of Soil Properties on Landslides along Forest Road. Eur J Forest Eng. 3, 1-6.

[10] Cheng, C.H., Hsiao, C.S., Huang, Y.S., Hung, C.Y., Pai, C.W., Chen, C.P., Menyailoc, O.V. (2016) Landslide-induced changes of soil physicochemical properties in Xitou, Central Taiwan. Geoderma. 265, 187-195.

[11] Błońska, E., Lasota, J., Piaszczyk, W., Wiecheć, M., Klamerus, A. (2017) The effect of landslide on soil organic carbon stock and biochemical properties of soil. J Soils Sediments. 1-11. https://doi.org/10.1007/s11368-017-1775-4.

[12] Eyndea, E.V., Dondeynea, S., Isabiryeb, M., Deckersa, J., Poesena, J. (2017) Impact of landslides on soil characteristics: Implications for estimating their age. Catena. 157, 173-179.

[13] Rosser, B., Ross, C. (2011) Recovery of pasture production and soil properties on soil slip scars in erodible siltstone hill country, Wairarapa, New Zealand. New Zealand Journal of Agricultural Research. 54, 23-44.

[14] Karsli, F., Atasoy, M., Yalcin, A., Reis, S., Demir, O., Gokceoglu, C. (2009) Effects of land-use changes on landslides in a landslide-prone area (Ardesen, Rize, NE Turkey). Environ Monit Assess. 156, 241-255.

[15] Reichenbach, P., Busca, C., Mondini, A.C., Rossi, M. (2014) The Influence of Land Use Change on Landslide Susceptibility Zonation: The Briga Catchment Test Site (Messina, Italy). Environmental Management. 54, 1372-1384.

[16] Chen, C.Y., Huang, W.L. (2013) Land use change and landslide characteristics analysis for community-based disaster mitigation. Environ Monit Assess. 5, 4125-4139.

[17] Suzen, M.L., Doyuran, V. (2004) Data driven bivariate landslide susceptibility assessment using geographical information systems: a method and application to Asarsuyu catchment, Turkey. Engineering Geology. 71, 303-321.

[18] Yu, F.C., Chen, T.C., Lin, M.L., Chen, C.Y., Yu, W.H. (2006) Landslides and Rainfall Characteristics Analysis in Taipei City during the Typhoon Nari Event. Natural Hazards. 37, 153-167.

[19] Ren, D. (2015) Changes in Extreme Precipitation in a Future Warming Climate. (Chapter 7). In: Storm-triggered Landslides in Warmer Climates. ISBN 978-3-319-08518-0 (eBook). Springer. Cham. 155-207.

[20] Kavzoglu, T., Sahin, E.K., Colkesen, I. (2010) Production of landslide susceptibility map by GIS based multi-criteria decision analysis method: example of Trabzon province. Remote sensing and GIS symposium. (3. UZAL-CBS). Gebze Institute of Technology. 11-13 October 2010, Kocaeli.

[21] Glastonbury, J., Fell, R. (2008) Geotechnical characteristics of large slow, very slow, and extremely slow landslides. Canadian Geotechnical Journal. 45, 984 -1005.

[22] Van Westen, C.J., Castellanos, E., Kuriakose, S.L. (2008) Spatial data for landslide susceptibility, hazard, and vulnerability assessment: An overview. Engineering Geology. 102, 112-131.

[23] Mukhopadyay, M., Bantawa, P., Das, A., Sarkar, B., Bera, B., Ghosh, P.D., Mondal, T.K. (2012) Changes of growth, photosynthesis, and alteration of leaf antioxidative defence system of tea (*Camellia sinensis* L.) O. Kuntze) seedling under aluminum stress. Biometals. 25, 1141-1154.

[24] FAO (2017) Production quantities of Tea by Country. http://www.fao.org/faostat/en/#data/QC/visualize.

[25] Tirkey, L.P., Gardner, J.S. (2006) The geo-ecological and socio-economic implications of tea estate closures in Darjeeling, Indian Himalaya. International symposium towards sustainable livelihoods and Ecosystems in mountainous regions. Chiang Mai, Thailand.

[26] Shoubo, H. (1991) A study on the ecological climates of some famous tea growing areas in high mountainous regions of China. Chinese Geographical Science. 1, 121-128.
[27] Gyssels, G., Poesen, J., Bochet, E., Li, Y. (2005) Impact of plant roots on the resistance of soils to erosion by water: a review. Progress in Physical Geography. 29, 189-217.
[28] Ozturk, K. (2002) Landslides and its effects on Turkey. G.Ü. Gazi Eğitim Fakültesi Dergisi. 22(2), 35-50.
[29] Gokce, O., Ozden, S., Demir, A. (2008) Spatial and Statistical Distribution of Disasters in Turkey. Disaster Information Inventory, Ministry of Public Works and Settlement General Directorate of Disaster Affairs, Disaster Survey and Damage Assessment Department, Ankara.
[30] Walter, H., Harnickell, E. and Mueller-Dombois, D. (1975) Climate-diagram maps of the individual continents and the ecological climatic regions of the earth. Berlin: Springer-Verlag.
[31] MGM (Turkish State Meteorological Service). (2017) Weather Classification of Turkey, Gumushane City. Available online: https://www.mgm.gov.tr/iklim/iklim-siniflandirmalari.aspx?m=GUMUSHANE.
[32] Kartieranleitung, B.K. (1994) Bodenkundlische. 4. Auflage, E. Schweizerbart Verlagsbuchhandlung, Hannover.
[33] Saxton, K.E., Rawls, W.J., Romberger, J.S., Papendick, R.I. (1986) Estimating generalized soil-water characteristics from texture. Soil Sci. Soc. Amer. J. 50(4), 1031.
[34] Bouyoucos, G.J. (1962) Hydrometer method improved for making particle size analyses of soils. Agronomy Journal. 54, 464.
[35] Allison, L.E. (1965) Organic Carbon: Walkley-Black Method. In: Methods of Analysis. Agronomy Monographs No: 9, Part 2. American Society Agronomy, Madison, Wisconsin, USA, 1367-1378.
[36] ASTM (American Society for Testing and Materials) (1991) Annual Book of ASTM Standarts. D4318 Standard Test Methods for Liquid Limit. Plastic Limit, and Plasticity Index of Soils, 18p.
[37] Casagrande, A. (1936) Characteristics of Soils Affecting the Stability of Slope and Earth fill. Journal of the Boston Society of Civil Engineers, 257-276.
[38] Schwertmann, U., Vogl, W., Kainz, M. (1990) Bodenerosion durch Wasser: Vorhersage des Abtrags und Bewertung von Gegenmassnahmen. Ulmer Verlag, Stuttgart.
[39] Dogan, O., Gucer, C. (1976) The causes of water erosion - formation and universal equation and determination of soil losses. Ministry of Rural Affairs. Ankara.
[40] Bera, A. (2017) Assessment of soil loss by universal soil loss equation (USLE) model using GIS techniques: case study of Gumti River Basin, Tripura, India. Model. Earth Syst. Environ. 3, 29.
[41] Herath, G. (2001) Estimating the user cost of soil erosion in tea smallholdings in Sri Lanka. Australasian Journal of Regional Studies. 7(1), 97-111.
[42] Abeygunawardena, P., Samarakoon, S.M.M. (1993) Economics of Upper catchment management for irrigation development: The case of Mahaweli Project in Sri Lanka. Asian Journal of Agricultural Economics. 5, 45-54.
[43] Hewawasam, T. (2010) Effect of land use in the upper Mahaweli catchment area on erosion, landslides and siltation in hydropower reservoirs of Sri Lanka. J. Nat. Sci. Foundation Sri Lanka. 38, 3-14.
[44] Hacisalihoglu, S., Misir, M., Misir, N., Yucesan, Z., Oktan, E., Gumus, S., Kezik, U. (2017) The effects of land use change on soil loss and Carbon stock amounts. Fresen. Environ. Bull. 26, 6007- 6016.
[45] Olson, K.R., Kaisi, M.A., Lal, R., Cihacek, L. (2016) Impact of soil erosion on soil organic carbon stocks. Journal of Soil and Water Conservation. 71, 61A-67A.
[46] Jankauskas, B., Jankauskienė, G., Fullen, M.A. (2007) Relationships between soil organic matter content and soil erosion severity in Albeluvisols of the Žemaičiai Uplands. Ekologija. 53, 21- 28.
[47] Jepsen, R., Roberts, J., Lick, W. (1997) Effects of bulk density on sediment erosion rates. Water, Air and Soil Pollution. 99, 21-31.
[48] Rosser, B., Dellow, S., Haubrock, S., Glassey, P. (2017) New Zealand's National Landslide Database. Landslides. 14(6), 1949-1959.
[49] Abad, J.R.S., Khosravi, H., Alamdarlou, E.H. (2014) Assessment the effects of land use changes on soil physicochemical properties in Jafarabad of Golestan province, Iran. Bull. Env. Pharmacol. Life Sci. 3, 296-300.
[50] Ollauri, A.G., Mickovski, S.B. (2017) Shallow landslides as drivers for slope ecosystem evolution and biophysical diversity. Landslides. 14, 1699 –1714.
[51] Donnini, M., Napolitano, E., Salvati, P., Ardizzone, F., Bucci, F., Fiorucci, F., Santangelo, M., Cardinali, M., Guzzetti, F. (2017) Impact of event landslides on road networks: a statistical analysis of two Italian case studies. Landslides. 14, 1521-1535.
[52] Bogner, C., Bauer, F., Trancon, Y., Widemann, B., Viñan, P., Balcazar, L., Huwe, B. (2014) Quantifying the morphology of flow patterns in landslide-affected and unaffected soils. Journal of Hydrology. 511, 460-473.

[53] Fonseca, L.A.M., Lani J.L., Filho E.I.F., Santos G.R.D., Ferreira W.P.M., Santos A.M.R.T. (2017) Variability in soil physical properties in landslide-prone areas. Acta Scientiarum. Agronomy. Maringá. 39, 109-118.
[54] Dhruba, P.S. (2000) Aspects of erosion and sedimentation in the Nepalese Himalaya. PhD thesis. ITC Dissertation No. 77. University of Ghent, Belgium. 265p.
[55] Knapen, A., Kitutu, M.G., Poesen, J., Breugelmans, W., Deckers, J., Muwanga, A. (2006) Landslides in a densely populated county at the footslopes of Mount Elgon Uganda: Characteristics and causal factors. Geomorphol. 73, 149 - 165.
[56] Meisina, C. (2006) Characterisation of weathered clayey soils responsible for shallow landslides. Nat. Hazards Earth Syst. Sci. 6, 825- 838.
[57] Mugagga, F., Kakembo, V., Buyinza, M. (2012) A characterisation of the physical properties of soil and the implications for landslide occurrence on the slopes of Mount Elgon, Eastern Uganda. Nat Hazards. 60(3), 1113-1131.
[58] Martelloni, G., Segoni, S., Fanti, R., Catani, F. (2012) Rainfall thresholds for the forecasting of landslide occurrence at regional scale. Landslides. 9, 485 - 495.
[59] Morgan, R.P.C. (2005) Soil Erosion and Conservation. 3rd ed. Blackwell Publishing, UK.
[60] Vergani, C., Chiaradia, E.A., Bassanelli, C., Bischetti, G.B. (2014) Root strength and density decay after felling in a silver Fir-Norway spruce stand in the Italian alps. Plant Soil. 377, 63 - 81.
[61] Chang, M. (2003) Forest Hydrology: An introduction to water and forests. CRC Press, Taylor &Francis Group, Boca Raton, FL, 373p.
[62] Chang, M., Roth, F.A., Hunt, E.V. (1982) Sediment production under various forest-site conditions. In: Walling, D.E. (Ed.) Recent Developments in the Explanation and Prediction of Erosion and Sediment Yield. Proceedings of the Exeter Symposium. IAHS, Exeter, U.K., 13-22.
[63] Cotrone, V. (2016) The Role of Trees and Forests in Healthy Watersheds. Green Industry. Penn State Extension. http://extension.psu.edu/plants/green-industry/landscaping/culture/the-role-of-trees-and-forests-in-healthy-watersheds.
[64] Baumgartner, A. (1967) Energetic bases for differential vaporization from forest and agricultural lands. International Symposium on Forest Hydrology. Sopper, W.H. and Lull, H.W. (Eds.) Pergamon Press. Elmsford, NY, 381–390.
[65] Verstraeten, W.E. (2005) Comparative analysis of the actual evapotranspiration of Jlemish forest and cropland using the soil water balance model WAVE. Hydrol. Earth Syst. Sci. 9, 225-341.
[66] Watson, A., Marden, M., Rowan, D. (1995) Tree species performance and slope stability. In: Vegetation and slopes. Thomas Telford, London, 161-171.
[67] Tofani, V., Bicocchi, G., Rossi, G., Segoni, S., D'Ambrosio, M., Casagli, N., Catani, F. (2017) Soil characterization for shallow landslides modeling: a case study in the Northern Apennines (Central Italy). Landslides. 14, 755–770.

Received: **30.10.2017**
Accepted: **06.02.2018**

CORRESPONDING AUTHOR

Sezgin Hacisalihoglu
Karadeniz Technical University,
Faculty of Forestry,
61080 Trabzon – Turkey

e-mail: sezgin@ktu.edu.tr

© by PSP Volume 27 – No. 5/2018 pages 2943-2950 Fresenius Environmental Bulletin

AIRBORNE FUNGI IN OUTDOOR AIR OF RIYADH CITY, KINGDOM OF SAUDI ARABIA

Abd El-Rahim M A El-Samawaty[1,2], Mohamed A Yassin[1,2,*], Mohamed A Abdel-Wahab[1]

[1]Botany and Microbiology Department, Faculty of Science, King Saud University, Riyadh, Saudi Arabia
[2]Agricultural Research Center, Plant Pathology Research Institute, Giza, Egypt

ABSTRACT

This is a qualitative and quantitative study of the culturable airborne fungi at different districts of the fast growing Riyadh city. Airborne fungi were surveyed in outdoor environment using portable personal volumetric air sampler. One cubic meter of air was sampled from 12 sampling points at each district. A total of 552 air samples were collected from 46 districts in Riyadh city and analyzed. After incubation and identification, concentrations of airborne fungi were calculated as CFU/m^3. A total of 2735 colony forming unit (CFU) were isolated which belong to 102 fungal species representing 35 genera. The most common genus was *Aspergillus* that collected from all studied sites and represented by 19 species. *Cladosporium* and *Emericella* were frequent genera, while *Penicillium*, *Alternaria*, *Ulocladium*, *Cochliobolus*, *Rhizopus*, *Paecilomyces*, *Nattrassia* and *Fusarium* were common genera. Fungal communities recorded from the 46 districts were classified into three distinct groups: (1) Districts with less than 20 CFU/m^3. These districts are newly established urban suburbs that are with new buildings, wide clean streets and with low populations. (2) Districts ranged between 128 and 157 CFU/m^3. These districts represent the old Riyadh city. These districts are very crowded with narrow streets and low levels of hygiene and housing. *Aspergillius niger* dominated the fungal communities at these districts. (3) Districts ranged between 20 and 100 CFU/m^3. These districts are intermediate in size, age, population density and standard of livings. *Cladosporium*, *Aspergillus flavus*, *A. niger*, and *Emericella* dominated the fungal communities at those districts.

KEYWORDS:
Anamorphic fungi, Microbiology of outdoor air, Middle East, Molds, Tropical fungi.

INTRODUCTION

Air sampling of microorganisms is a popular method of conducting microbial examinations. These results can be related to a concentration expressed in colony forming units per cubic meter of air. In the environment spores of molds may become airborne and are therefore ubiquitous. They can enter indoor areas either by passive ventilation or by ventilation systems. The relative humidity and/or the moisture content of the materials determine that to what extent different micro-organisms are able to grow on indoor or outdoor materials [1]. Infections by molds are very rare, but persons with an immunodeficiency are especially susceptible to fungal infections. In addition, food stuffs, house plants and flower pots, house dust, pets and their bedding, textiles, carpets, wood material and furniture stuffing, occasionally release spores of *Alternaria*, *Aspergillus*, *Botrytis*, *Cladosporium*, *Penicillium*, *Scopulariopsis* into the air. To systematically evaluate the relationship between airborne fungi and adverse health effects, the fungal concentrations, types and their relative frequencies in both indoor and outdoor air need to be known [2].

Air-borne fungi and pollen grains are well known in the etiology of respiratory allergic diseases such as asthma and allergic rhinitis. Fungi are one of the most important components of bioaerosols. Fungi can cause public health hazards. Exposure to fungi has been reported to cause irritations, infections, allergies and toxic effects [3]. Sources of microbes in air include: soil, water, plant vegetation and their remains, animals and humans. The concentration of airborne spores of fungi varies according to geographical areas, vegetations, landscape, land usage, latitude, time of the day, season of the year, condition of the surrounding areas (e.g. parks, gardens, etc.) and climatic conditions (e.g. temperature, humidity) [4, 5]. Temperature had a positive effect on total fungal concentration [6]. O'Gorman and Fuller (2008) [7] found positive correlations between relative humidity with *Penicillium* and *Aspergillus* species. However, *Cladosporium* spore concentration increased as relative humidity decreased [8]. Reyes et al. (2009) [9] found positive correlations between relative humidity with *Cladosporium* and *Alternaria*. Changes in wind speed significantly affected spore concentration especially when other climatic factors were optimal [10]. *Alternaria* and *Cladosporium* species are considered clinically the causative allergenic agents for most patients [11]. *Alternaria alternata* is consid-

ered to be one of the most important aeroallergens in the United States [12] and Europe [13].

Presence of several airborne fungi in the air is associated with risk to human health because they are either pathogenic or can cause sensitivities due to prolonged exposure [14]. In particular, *Aspergillus, Penicillium, Cladosporium, Alternaria* and others are responsible for many human health problems such as irritations, allergies, asthma, respiratory tract disorders and toxicosis [15-17]. Fungal spores may enter human body directly via inhalation of contaminated dust particles or indirectly via ingestion of contaminated foods and water. Many responses such as irritation, allergies, vomiting, diarrhea, hemorrhage, convulsions and sometimes death could attribute to exposure to fungal spores or their metabolites [18]. Nearly 10% of people worldwide have fungal allergy [19]. Distributions of fungal spores over any given region can be helpful in identifying associations between fungal sensitivity and clinical prevention of seasonal allergic diseases [20]. The current study aims to give an overview of airborne fungi and their concentrations in Riyadh city. This study represents the first study that covers the whole city with representatives from old districts with busy districts to newly established suburbs with a low population density.

MATERIALS AND METHODS

Site description. Riyadh is the capital and largest city of Saudi Arabia. Its urban area covers 2435 square kilometers with a population of more than five million peoples. Riyadh city is one of the world's fastest growing cities, and its population has risen steadily with a yearly rate at 4.2% during the period 1990 to 2004 (Riyadh Development Authority, Riyadh city population estimates 2004). Riyadh is a busy city with about 6 million traffic trips daily. The elevation of the city 606 m. It consists mainly of old commercial buildings known as the heart of the city.

The weather in Riyadh is hot and dry. Temperatures in the summer, which lasts from May to September, normally range between 35°C and 45°C during day time. Winters are mild with cold, windy nights. The overall climate is arid, but the city receives a fair amount of rain in March and April. It is also known to have many dust storms. The dust is often so thick that visibility is less than 10 m. The flat, sandy Arabian Desert covers most of Riyadh.

Collection of samples, fungal isolation and statistical analyses. Forty-six districts were chosen randomly in Riyadh city. These districts represent: (1) The busy down town with high population, very busy streets and low levels of hygiene and housing and (2) Newly established suburbs with new buildings, wide clean streets and with low populations. One cubic meter of air was sampled in 12 sampling points in each district at 1.5 m from the ground using portable air sampler (SAS (Surfair Air System) Hi VAC, Bioscience International PBI, Via Novara, 8920153 Milano). A total of 552 air samples were collected from the 46 districts from April to June 2010.

Samples were collected using the air sampler sucked air through the orifice at the top and impinged successively onto Petri plates containing 15 ml of potato dextrose agar (PDA). After exposure, the Petri plates were incubated for 3–5 days at 28±2°C for proper growth of fungal colonies to render identification. Only few fungal colonies may require more than 6 days for growth and maturation. Obtained fungal colonies were sub-cultured to new PDA plates, incubated for a further period at 27±1°C, and then purified. Identification of fungi was carried out by Assiut University Mycological Centre (AUMC). Similarity between fungal communities recorded from the 46 districts was compared using hierarchical cluster analyses, IBM SPSS version 19 software package (SPSS Inc., Chicago).

RESULTS

A total of 2735 colonies forming unit (CFU) were isolated from 552 air samples collected from 46 random sites over Riyadh city (Table 1). Isolated fungi belong to 102 fungal taxa representing 35 genera (Table 2). The most common genus was *Aspergillus* that collected from all studied sites and represented by 19 species. *Cladosporium* and *Emericella* were frequent genera, while *Penicillium*, *Alternaria*, *Ulocladium*, *Cochliobolus*, *Rhizopus*, *Paecilomyces*, *Nattrassia* and *Fusarium* were common genera (Table 3, Figure 1). *Aspergillus* species and their teleomorphs generally dominated old districts of the city with high population density and with busy streets. Of which, *Aspergillus niger* generally dominated old crowded districts with low levels of hygiene and housing. Dematiaceous hyphomycetes and their teleomorphs (i.e. *Alternaria*, *Cochliobolus* and *Drechslera*), *Paecilomyces* and *Penicillium* generally dominated the newly established urban suburbs that are with new buildings, wide clean streets and with low population density. The genus *Cladosporium*, *Aspergillus flavus* and *A. niger* dominated the medium size districts with average population density and busy streets (Figure 1).

Three sites with more than 128 CFU/m^3 were recorded namely: Al-Aziziyyah, Al-Manfuha and Al-Mansuriyah with 157, 152 and 128 CFU/m^3 respectively. The three sites are located in the heart of the Riyadh city and it is called the old Riyadh city. These three districts are with high population density, with busy narrow streets and low levels of

hygiene. While less than 20 CFU/m^3 were recorded from five sites namely: Al-Narjis, Al-Yasmin, As-Suwaidi, Al-Urayja (West) and Dharat Laban. These five districts are newly established urban suburbs that are with new buildings, wide clean streets and with low populations. The other 36 districts were with intermediate CFU (Table 2).

Hierarchical clustering analysis based on similarity between fungal communities at the 46 districts using IBM-SPSS v19 have produced five groups (Figure 2). These groups are briefly explained in the following paragraphs:

TABLE 1
The forty-six studied districts in Riyadh city.

	District name	CFU/m^3	Total species per site	The most common fungus
1.	Al-Janadria	55	12	*Cladosporium sphaerospermum*
2.	Al-Thomamah	44	14	*Cladosporium cladosporioides*
3.	Al-Hamra	60	10	*Cladosporium sphaerospermum*
4.	King Abdullah	35	7	*Aspergillus niger*
5.	King Abdulaziz	40	9	*Aspergillus flavus*
6.	Al-Rabwah	50	11	*Emericella nidulans*
7.	Al-Andalus	58	11	*Cladosporium sphaerospermum*
8.	Al-Manar	45	10	*Aspergillus flavus*
9.	Al-Naseem (East)	49	12	*Aspergillus flavus*
10.	Al-Nahdhah	44	14	*Aspergillus niger*
11.	Al-Narjis	12	12	*Paecilomyces* sp.
12.	Al-Yasmin	18	12	*Aspergillus flavus*
13.	Al-Rabie	41	11	*Alternaria alternata*
14.	Al-Falah	41	13	*Cladosporium cladosporioides*
15.	Al-Taawun	75	14	*Aspergillus niger*
16.	Al-Masif	56	15	*Aspergillus flavus*
17.	Al-Mursalat	56	13	*Cladosporium cladosporioides*
18.	King Fahd	70	22	*Emericella nidulans*
19.	Al-Muhammadiyya	42	13	*Alternaria alternata*
20.	Al-Nakheel	52	11	*Emericella nidulans*
21.	King Saud University	41	10	*Aspergillus flavus*
22.	Al-Khuzama	65	16	*Aspergillus flavus*
23.	Al-Rahmaniyya	75	13	*Aspergillus niger*
24.	Al-Raid	48	10	*Cochliobolus spicifer*
25.	Umm Al-Hamam (West)	46	16	*Aspergillus niger*
26.	Al-Sulaymaniyyah	91	11	*Aspergillus flavus*
27.	Al-Takhassusi	101	16	*Cladosporium sphaerospermum*
28.	Al-Olayya	59	11	*Aspergillus niger*
29.	Umm Al-Hamam (East)	75	7	*Emericella nidulans*
30.	Al-Ma'athar	98	17	*Aspergillus niger*
31.	Al-Sharafiyah	51	12	*Aspergillus ustus*
32.	Al-Nasriyyah	57	22	*Aspergillus flavus*
33.	Al Badiyah	45	15	*Aspergillus niger*
34.	As-Suwaidi	19	6	*Aspergillus niger*
35.	Al-Shifa	24	11	*Emericella nidulans*
36.	Al-Urayja (West)	6	5	*Ulocladium chartarum*
37.	Hijrat Laban	27	12	*Alternaria alternata*
38.	Dharat Laban	16	5	*Emericella quadrilineata*
39.	Dubbat	81	10	*Cladosporium cladosporioides*
40.	Al-Wazarat	99	18	*Aspergillus niger*
41.	Al-Murabba	95	14	*Aspergillus flavus*
42.	Al-Dirah	70	15	*Cladosporium cladosporioides*
43.	Al-Manfuha	152	22	*Aspergillus niger*
44.	Al-Mansuriyah	128	17	*Aspergillus niger*
45.	Al-'Aziziyyah	157	21	*Aspergillus niger*
46.	Al-Khaldiyah	66	17	*Cladosporium sphaerospermum*

TABLE 2
Fungi recorded from outdoor air in Riyadh City.

No.	Recorded Fungi	No. of P.S.	Mean of F %	No.	Recorded Fungi	No. of P.S.	Mean of F %
1.	*Acremonium roseolum*	2	1.77	52.	*Fusarium succisae*	1	0.12
2.	*Acremonium strictum*	2	1.38	53.	*Fusarium tricinctum*	1	1.46
3.	*Acrophialophora fusispora*	1	0.49	54.	*Fusarium verticilliodes*	1	0.24
4.	*Alternaria alternate*	24	16.22	55.	*Gonatobotryum apiculatum*	2	0.57
5.	*Alternaria chlamydospora*	4	1.06	56.	*Humicola* sp.	1	0.41
6.	*Alternaria* sp.	12	7.4	57.	*Leptosphaeria coniothgrium*	6	1.36
7.	*Arthrinium phaeospermum*	1	0.22	58.	*Neofusicoccum mangiferae*	9	5.83
8.	*Aspergillus aegyptiacus*	1	0.36	59.	*Nigrospora oryzae*	3	1.17
9.	*Aspergillus asprescens*	5	3.03	60.	*Paecilomyces baarnensis*	2	0.25
10.	*Aspergillus candidus*	4	2.96	61.	*Paecilomyces griseoviridis*	1	0.10
11.	*Aspergillus clavato-flavus*	1	0.35	62.	*Paecilomyces lilacinus*	1	0.33
12.	*Aspergillus clavatus*	1	0.16	63.	*Paecilomyces* sp.	2	1.31
13.	*Aspergillus deflectus*	4	1.71	64.	*Paecilomyces variotii*	8	4.12
14.	*Aspergillus flavipes*	1	0.38	65.	*Papulaspora immersa*	4	1.27
15.	*Aspergillus flavus*	38	51.82	66.	*Penicillium aurantiogresum*	7	2.03
16.	*A. flavus* var. *columnaris*	3	1.3	67.	*Penicillium brevicompactum*	1	0.13
17.	*Aspergillus fumigatus*	16	6.66	68.	*Penicillium chrysogenum*	21	15.95
18.	*A. fumigatus* var. *elleptcus*	1	0.10	69.	*Penicillium citrinum*	3	1.42
19.	*Aspergillus niger*	45	76.92	70.	*Penicillium corylophilum*	5	2.78
20.	*Aspergillus ochraceus*	16	6.84	71.	*Penicillium crustosum*	1	0.20
21.	*Aspergillus parasiticus*	2	1.10	72.	*Penicillium gresiofulvum*	1	1.25
22.	*Aspergillus* sp.	1	0.85	73.	*Penicillium herquei*	1	0.71
23.	*Aspergillus sydowii*	13	8.75	74.	*Penicillium janthinellum*	1	0.16
24.	*Aspergillus terreus*	3	1.09	75.	*Penicillium lividum*	1	0.60
25.	*Aspergillus ustus*	11	7.42	76.	*Penicillium miniolutum*	1	0.06
26.	*Aspergillus versicolor*	2	0.50	77.	*Penicillium ochrochloron*	4	2.57
27.	*Circinella muscae*	1	0.36	78.	*Penicillium oxalicum*	3	1.32
28.	*Cladosporium cladosporioides*	26	34.08	79.	*Penicillium* sp. 1	2	0.54
29.	*Cladosporium globisporum*	2	0.77	80.	*Penicillium* sp. 2	1	0.55
30.	*Cladosporium herbarum*	5	2.55	81.	*Penicillium* sp. 3	7	2.08
31.	*Cladosporium sphaerospermum*	15	28.61	82.	*Penicillium spinulosum*	1	0.65
32.	*Cochliobolus austrialiensis*	11	5.89	83.	*Phoma eupyrena*	2	0.77
33.	*Cochliobolus lunatus*	9	3.04	84.	*Phoma fimeti*	1	0.11
34.	*Cochliobolus spicifer*	18	8.81	85.	*Pithomyces sacchari*	3	0.70
35.	*Corynoascus sepedonium*	1	0.41	86.	*Quambalaria cyanescens*	2	0.51
36.	*Curvularia pallescens*	1	1.26	87.	*Rhinocladiella aquaspersa*	1	0.55
37.	Dark sterile mycellium	5	4.26	88.	*Rhizopus* sp.	20	13.59
38.	*Drechslera australiensis*	5	3.45	89.	*Scopulariopsis brevicaulis*	1	0.51
39.	*Drechslera biseptata*	4	1.5	90.	*Scopulariopsis carbonaria*	2	0.74
40.	*Emericella heterothallica*	3	1.01	91.	*Scytalidium dimidiatum*	1	0.59
41.	*Emericella nidulans*	37	39.98	92.	*Setosphareria rostrata*	1	0.29
42.	*Emericella quadrilineata*	10	7.53	93.	*Stachybotrys chartarum*	2	0.72
43.	*Emericella rugulosa*	1	0.25	94.	*Stachybotrys ramose*	1	0.33
44.	*Emericella* sp.	1	1.54	95.	*Stemphyllium botryosum*	2	0.35
45.	*Emericella variecolor*	4	1.04	96.	*Syncephalastrum racemosum*	3	1.06
46.	*Fusarium chlamydosporum*	2	1.01	97.	*Talaromyces* sp.	7	4.23
47.	*Fusarium oxysporum*	1	0.24	98.	*Trichoderma pseudospermum*	5	2.29
48.	*Fusarium sambucinum*	1	0.14	99.	*Ulocladium atrum*	18	6.83
49.	*Fusarium scirpi*	2	1.34	100.	*Ulocladium botrytis*	9	2.9
50.	*Fusarium semitectum*	2	0.51	101.	*Ulocladium chartrum*	9	7.43
51.	*Fusarium solani*	1	0.81	102.	*Ulocladium consortiale*	6	3.84

No. of P.S. = Number of positive sites Mean of F. % = Mean of Frequency %

Group 1. These 10 districts are newly established urban suburbs with low population density. CFU/m^3 recorded from these districts was less than 50. The most common fungi recorded from these districts were *Alternaria*, *Aspergillius*, *Cochiobolus*, *Drechslera*, *Emericella*, *Paecilomyces*, and *Penicillium*.

Group 2. These 12 districts are medium in size, age and population density. CFU/m^3 recorded from these districts ranged between 35 and 70. The most common fungi recorded were *Aspergillus flavus*, *A. niger* and *Emericella*.

Group 3. These 7 districts are medium in size, age and population density. CFU/m^3 recorded from these districts ranged between 44 and 70. The genus *Cladosporium* dominated the fungal communities at these 7 districts.

TABLE 3
Genera recorded during the present study

Genus	No of collections	%
Aspergillus	1044	38.2
Cladosporium	413	15.1
Emericella	283	10.3
Penicillium	193	7
Alternaria	151	5.5
Ulocladium	91	3.3
Cochliobolus	90	3.2
Rhizopus	64	2.3
Paecilomyces	55	2
Neofusicoccum	48	1.7
Fuarium	32	1.2
Dark sterile mycelium	21	0.8
Trichoderma	20	0.7
Drechslera	17	0.6
Stachybotrys	19	0.6
Acremonium	16	0.5
Leptosphaeria	8	0.3
Nigrospora	10	0.3
Papulaspora	9	0.3
Phoma	7	0.2
Scopulariopsis	7	0.2
Scytalidium	5	0.2
Acrophialophora	4	0.1
Circinella	4	0.1
Gonatobotryum	3	0.1
Pithomyces	4	0.1
Rhinocladiella	3	0.1
Stemphylium	3	0.1
Syncephalastrum	4	0.1
Talaromyces	3	0.1
Arthrinium	2	0.07
Corynoascus	2	0.07
Humicola	2	0.07
Quambalaria	2	0.07
Setosphaeria	2	0.07
Cochliobolus	1	0.03
Curvularia	1	0.03



FIGURE 1
Map of Riyadh city showing the 46 studied districts along with the name of the most common fungus at each district.

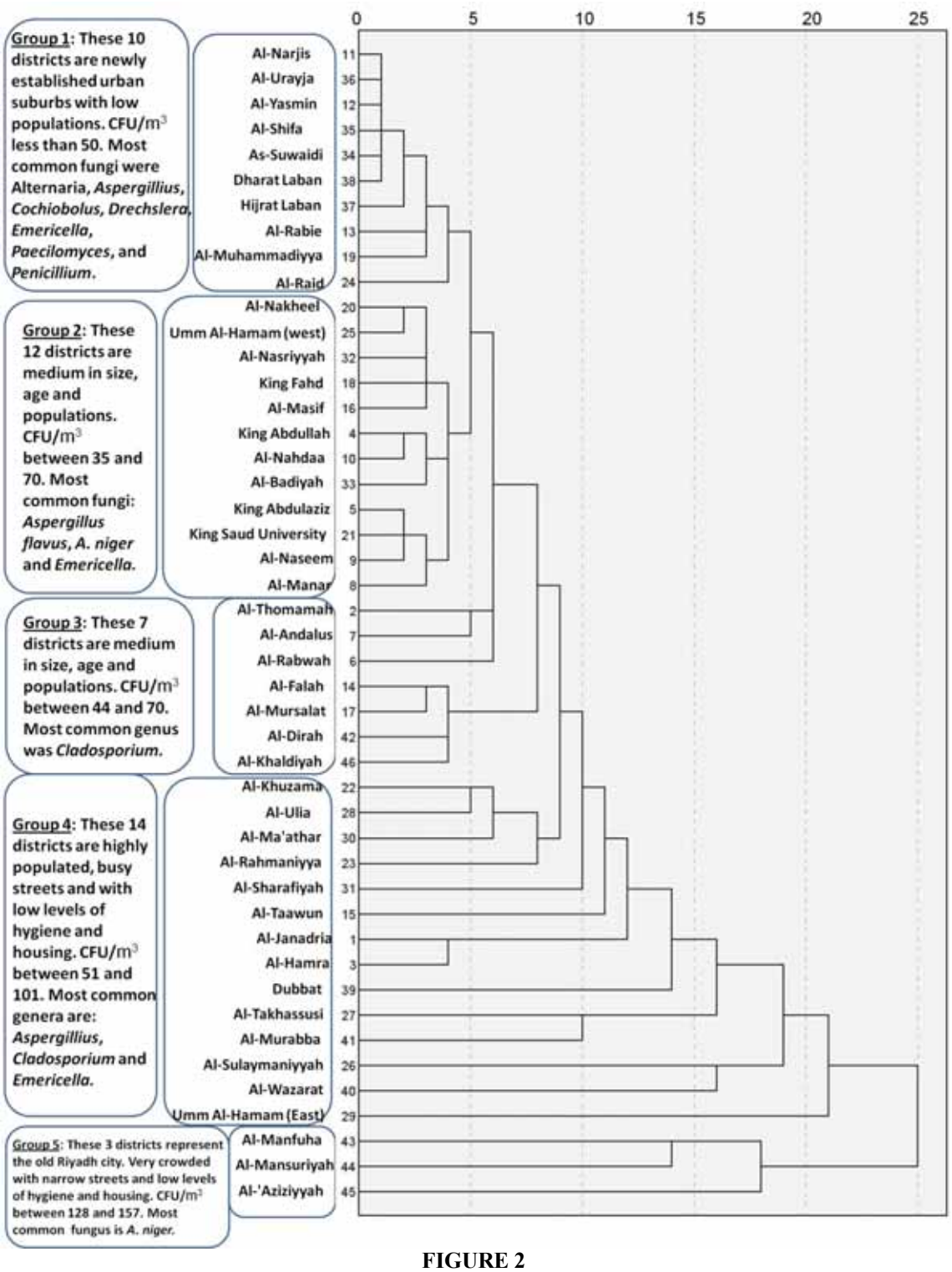


FIGURE 2
Dendogram generated from distance cluster analyses based on similarity between fungal communities at the 46 studied districts in Riyadh city using IBM-SPSS v19.

Group 4. These 14 districts are highly populated with busy streets and with low levels of hygiene. CFU/m^3 recorded from those districts ranged between 51 and 101. The most common genera recorded at these districts were *Aspergillius*, *Cladosporium*, and *Emericella.*

Group 5. These three districts represent the old Riyadh city. These districts are very crowded with narrow streets and low levels of hygiene and housing. CFU/m^3 recorded from these districts ranged between 128 and 157. *Aspergillius niger* dominated the fungal communities at the three districts.

DISCUSSION

This study showed that districts with high population density and busy streets and with low living standard of life have higher airborne fungal counts than those in newly established districts with low population density, new buildings and less busy streets. Yassin and Almougatea (2010) [21] studied the airborne fungi in Kuwait and found similar results, where higher counts of fungal spores were detected as the level of hygiene or standard of housing dropped. Recorded airborne fungal counts in the present study are generally lower than those reported from different parts of the world. Kawasaki et al. (2010) [22] recorded higher counts of fungi in railway stations in Tokyo, Japan. They recorded fungal counts ranged between 20 and 795 CFU/m^3 in the above ground sites. Shelton et al. (2002) [23] studied airborne fungi in buildings and outdoor environments across the United States. They recorded a mean of 930 CFU/m^3 from outdoor air samples. The lower counts of airborne fungi recorded from outdoor air of Riyadh city might be because: (1) desert weather of the city with low humidity. (2) low density of population in general.

Aspergillus flavus, *A. niger*, *Cladosporium* and *Emericella* dominated the outdoor air in Riyadh city. These results are in harmony with previous studies. Al-Suwaine et al. (1999) [24] studied the airborne fungi of the outdoor air at two sites in Riyadh city. They found higher spore concentration in Al-Batha site (highly populated site) than Al-Ulia site (low populated site). *Cladosporium* dominated the fungal community of the two studied site at that time. *Cladosporium* was the most frequent genus in outdoor and indoor air of Kuwait, Jordan and the United States [2, 21, 23]. *Aspergillus* was the most common genus during the present study and represented by 19 species. Of which several species have the ability to produce mycotoxins, e.g. *A. flavus* produced B1, G1 and G2 aflatoxins [25]. *Aspergillus* and *Penicillium* fungi were abundant genera in both outdoor and indoor conditions [26]. Congestion and accumulation of moldable organic materials in the garbage of big cities could results in accumulative of fungal spores in the air.

The current study revealed the existence of a rich population of airborne fungi in the outdoor air of Riyadh city which varied in quantity of fungal spore count and species composition from district to district within the city. However, it must be considered that the culture methods used revealed only a portion of the airborne microorganisms because some fungi cannot grow at all in culture media due to competition with other fungi or other factors [2]. Future studies should include molecular methods in order to determine non-culturable fungi present in the air.

CONCLUSION

Airborne fungi counts in outdoor air of Riyadh city ranged between 6 and 150 CFU/m^3 and this generally lower than those recorded from other parts of the world e.g. Japan and the United States of America. Higher counts of culturable airborne fungal spores (between 128 and 150 CFU/m^3) were recorded from highly populated districts of Riyadh city and dominated by *Aspergillus niger*. Newly established districts with low populations and high standards of life have low airborne fungal spore counts (less than 20 CFU/m^3) and dominated by dematiaceous hyphomycetes other than *Cladosporium*, e.g. *Alternaria*, *Cochliobolus* and *Drechslera.*

ACKNOWLEDGEMENTS

The authors would like to extend their sincere appreciation to the Deanship of Scientific Research at King Saud University for its funding this Research Group No (RG-298).

REFERENCES

[1] Dhanasekaran, D., Selvamani S., Panneerselvam, A., Thajuddin, N. (2009) Isolation and characterization of actinomycetes in Vellar Estuary, Annagkoil, Tamil Nadu. African Journal of Biotechnology. 8, 4159-4162.

[2] Abu-Dieyeh, M.H., Barham, R., Abu-Elteen, K., Al-Rashidi, R., Shaheen, I. (2010) Seasonal variation of fungal spore populations in the atmosphere of Zarqa area, Jordan. Aerobiologia. 26, 263–276.

[3] Mohammadi, P., Krumbein, W. (2008) Biodeterioration of ancient stone materials from the Persepolis monuments (Iran). Aerobiologia. 24, 27-33.

[4] Gioulekas, D., Balafoutis, C., Damialis, C., Papakosta, D., Gioulekas, G., Patakas, D. (2004) Fifteen years' record of airborne allergenic pollen and meteorological parameters in Thessaloniki, Greece. International Journal of Biometeorology. 48, 128–136.

[5] Mitakakis, T., O'Meara, T., Tovey, E. (2005) The effect of sunlight on allergen release from spores of the fungus *Alternaria*. Grana. 42, 43–6.

[6] Aydogdu, H., Asan, A. (2008) Airborne fungi in child day care centers in Edirne City, Turkey. Environmental Monitoring and Assessment. 147, 423–444.

[7] O'Gorman, C.M., Fuller, H.T. (2008) Prevalence of culturable airborne spores of selected allergenic and pathogenic fungi in outdoor air. Atmospheric Environment. 42, 4355–4368.
[8] Oliveira, M., Ribeiro, H., Delgado, J.L., Abreu, I. (2009) The effects of meteorological factors on airborne fungal spore concentration in two areas differing in urbanisation level. International Journal of Biometeorology. 53, 61-73.
[9] Reyes, E.S., de la Cruz D.R., Merino E.S., Sánchez, J.S. (2009) Meteorological and agricultural effects on airborne *Alternaria* and *Cladosporium* spores and clinical aspects in valladolid (Spain). Ann Agric Environ Med. 16, 53–61.
[10] Sakiyan, N., Inceoglu, O. (2003) Atmospheric Concentrations of Cladosporium and Alternaria Spores in Ankara and the Effects of Meteorological Factors. Turkish Journal of Botany. 27, 77–81.
[11] Dreborg, S., Agrell, B., Foucard, N., Kjellman, M., Koivikko, A., Nilsson, S. (1986) A double-blind, multicenter immunotherapy trial in children, using a purified and standardized *Cladosporium herbarum* Preparation I. Clinical Results. Allergy. 41, 131–140.
[12] Miles, R.M., Parker, J.L., Jones, R.T., Dahalberg, M.J., Yunginger, J.W. (1983) Studies on *Alternaria* allergens. IV. Biologic activity of purified *Alternaria* fraction. Journal of Allergy and Clinical Immunology. 71, 36–39.
[13] Huffman, D., Kozak, P., Gillman, S., Cummins, L., Gallup, J. (1981) Isolation of spore specific allergens from *Alternaria*. Ann Allergy. 46, 310–315.
[14] Griffin, D. (2007) Atmospheric Movement of Microorganisms in Clouds of Desert Dust and Implications of Human Health. Clinical Microbiology Reviews. 20, 459–477.
[15] Adhikari, A., Sen, M.M., Gupta-Bhattacharya, S., Chanda, S. (2004) Airborne viable, nonviable, and allergenic fungi in a rural agricultural area of India: a 2-year study at five outdoor sampling stations. Science of The Total Environment. 326, 123–141.
[16] Alrajhi, A.A., Enani, M., Mahasin, Z., Al-Omran, K. (2001) Chronic invasive aspergillosis of the paranasal sinuses in immunocompetent hosts from Saudi Arabia. The American Journal of Tropical Medicine and Hygiene. 65, 83–86.
[17] Bush, R.K. and Prochnau, J.J. (2004) *Alternaria*-induced asthma. The Journal of Allergy and Clinical Immunology. 113, 227–234.
[18] Menetrez, M.Y., Foarde, K.K. (2004) Emission exposure model for the transport of toxic mold. Indoor Built Environment. 13, 75–82.
[19] Pasanen, A.L., Lappalainen, S., Pasanen, P. (1996) Volatile organic metabolites associated with some toxic fungi and their mycotoxins. Analyst. 121, 1949-1953.
[20] Hedayati, M.T., Pasqualotto, A.C., Warn, P.A., Bowyer, P. and Denning, D.W. (2007) *Aspergillus flavus*: human pathogen, allergen and mycotoxin producer. Microbiology. 153, 1677–1692.
[21] Yassin, M.F., Almouqates S. (2010) Assessment of airborne bacteria and fungi in an indoor and outdoor environment. International Journal of Environmental Science and Technology. 7, 535-544.
[22] Kawasaki, T., Kyotani T., Ushiogi T., Izumi Y., Lee H., Hayakawa T. (2010) Distribution and identification of airborne fungi in railway stations in Tokyo, Japan. Journal of Occupational Health. 52, 186–193.
[23] Shelton, B.G., Kirkland, K.H., Flanders, D.W., Morris, G.K. (2002) Profiles of Airborne Fungi in Buildings and Outdoor Environments in the United States. Applied Environmental Microbiology. 68, 1743-1753.
[24] Al-Suwaine A.S., Bahkali, A.H., Hasnain, S.M. (1999) Seasonal incidence of airborne fungal allergens in Riyadh, Saudi Arabia. Mycopathologia. 145, 15-22.
[25] El-Samawaty, A.M.A., Bahkali, A.H.A., Abd-Elsalam, K., El-Naggar, M.A., Yassin, M.A. (2012) Aflatoxigenic Aspergillii in outdoor air of Riyadh city. Fresen. Environ. Bull. 21, 2587–2593.
[26] Codina, R., Fox, R.W., Lockey, R.F., DeMarco, P., Bagg, A. (2008) Typical levels of airborne fungal spores in houses without obvious moisture problems during a rainy season in Florida, USA. Journal of Investigational Allergology and Clinical Immunology. 18, 156-162.

Received: **01.11.2017**
Accepted: **10.01.2018**

CORRESPONDING AUTHOR

Mohamed A Yassin
Botany and Microbiology Department
Faculty of Science
King Saud University
Riyadh, 11451 – Saudi Arabia

e-mail: mohamdyassin@gmail.com

© by PSP Volume 27 – No. 5/2018 pages 2951-2962 Fresenius Environmental Bulletin

THE ECOTOXICOLOGICAL EFFECTS OF ZNO-TIO_2 NANOCOMPOSITE IN *CHODATODESMUS MUCRANULATUS*

Betul Yilmaz-Ozturk[1,*] Yesim Daglioglu[2]

[1]Eskisehir Osmangazi University Central Research Laboratory Application and Research Center, Eskisehir, Turkey
[2]Ordu University Faculty of Arts & Science, Department of Molecular Biology and Genetics, Ordu, Turkey

ABSTRACT

Chodatodesmus mucranulatus, which is green algae with a single cell, has been used in order to determine the toxicity and characterization of the $(ZnO\text{-}TiO_2)_{NCM}$. The algal cells were exposed to $(ZnO\text{-}TiO_2)_{NCM}$ for 72 hours in order to evaluate the photosynthetic activity, bioaccumulation and reactive oxygen species (ROS). The chlorophyll (Chl) an amount increased generally in the control group and treated groups depending on the exposure concentration and varying-time. The Chl b amount showed a constant increase with all treated groups of the $(ZnO\text{-}TiO_2)_{NCM}$ depending on the exposure time-varying. The amount of carotenoid in the groups exposed to $(ZnO\text{-}TiO_2)_{NCM}$ was considerably reduced and could not be calculated. There are very important differences between the treated groups and control groups in $(ZnO\text{-}TiO_2)_{NCM}$ in 72 hours exposure of *Chodatodesmus mucranulatus* in terms of ROS activity ($p<0.01$). There is a difference at an important level between treated groups of Zn particles and Ti particles ($P<0.01$).

KEYWORDS:
$(ZnO\text{-}TiO_2)_{NCM}$, nanocomposite, acute toxicity, bioaccumulation, algal cells, oxidative stress.

INTRODUCTION

Nanoparticles (NPs) represent a new class of important materials**.** NPs are commercially produced and nanotechnology market is expected to reach hundreds of billions of dollars by 2025 [1]. In one of these nanoparticle groups, there are the metal and metal oxide NPs. Metal and metal oxide NPs constitute a large deal of the growing nanotechnology market and are made from silver, gold, copper, nickel, cobalt zinc and titanium [2]. Metal oxide NPs are used in purifying water, medicine, cosmetics and engineering and in similar large areas [3]. ZnO NPs are initial materials for electronic applications, transparent UV protective films and chemical sensors [4]. In addition, they are also used as UV filters in solar protectors [5]. Titanium dioxide (TiO_2) NPs are the most frequently-used group of nanomaterials that are known as catalysts and adsorbents [6]. They are used as catalysts in sterilization and as water purifying adsorbent in chemical engineering [7, 8, 9], in developing self-cleaning surfaces [6] and in solar energy cells [10], in cosmetics, paints, food additives and construction materials and in production materials that are used for air, soil and water decontamination [11, 12, 13]. TiO_2 and ZnO NPs have a feature of large UV spectrum attenuation. For this reason, it is used in applications like protecting human skin against UV radiation in sunrays [14]. Exhibiting various properties doped zinc oxide also has varieties with different morphology. ZnO has many applications to TiO_2 [15]. To add to zinc, TiO_2 is selected because it becomes stable over time and has thermal cycling properties, shortly because it exhibits excellent moisture sensing properties [16, 17]. In composite materials, the formation of interface regions changes the electronic states. However, in the case of an integrated nanocomposite (NCM), a shape of the organization and pattern of each component and is determined the physicochemical properties and performance of this NCM [18]. The zinc oxide–titanium dioxide nanocomposite materials $[(ZnO\text{-}TiO_2)_{NCM}]$ is used to ensure a more effective charge isolation, extending the life of charge carriers and developing interfacial charge transfer [19]. With these usage areas, they can have unexpected effects on living organisms and in the environment [20]. The metal oxide nanoparticles in the form of produced and household waste end up in natural water [21] and the relations of the NPs with the aquatic organisms are less known [22]. With this study conducted on algal cells which are the bioindicator organisms of the aquatic environment, a contribution will be provided to the understanding of this relationship. Because of the algae constitute the basis of the food chain, any change in their density, biomass and population affect the whole food chain [3]. In aquatic environments, green algal cells constitute the main source of the necessary biomass that is necessary for animals in high ecologic trophic level. Because of the bioaccumulation of metallic contaminators and flame retardants, the algal cells are used as the bioindicator species for aquatic ecosystem health [23, 24, 25]. In addition, the reactions of the algae against toxic chemicals are various [26]. As measuring the

pigments in algal cells is easy, they are used frequently in measuring the stress levels [27].

In this study, *Chodatodesmus mucranulatus*, which is single-cell green algae, has been used in order to determine the toxicity and characterization of the $(ZnO\text{-}TiO_2)_{NCM}$. The algal cells were exposed to $(ZnO\text{-}TiO_2)_{NCM}$ for 72 hours in order to evaluate photosynthetic activity, amounts of bioaccumulation and formation of reactive oxygen species (ROS). In addition, with the reduction of the $(ZnO\text{-}TiO_2)_{NCM}$ to nanosize, the comparison of the reply of the algae cells to toxicity and bioaccumulation became possible.

MATERIALS AND METHODS

Preparing of $(ZnO\text{-}TiO_2)_{NCM}$. $(ZnO\text{-}TiO_2)_{NCM}$ were used in toxicology experiments. TiO_2 (titanium dioxide) (%99.0 pure) was obtained in pure anatase from Sigma-Aldrich, Germany $(ZnO\text{-}TiO_2)_{NCM}$ composites were synthesized in the chemistry laboratory of Karadeniz Technical University Faculty of Science.

ZnO was loaded into the TiO_2 photocatalyst with a 1% ratio. 10 g TiO_2 catalyst and 10 ml water were mixed to have a slurry. 0.3355 g ZnO was added to the slurry and was calcinated at 400 °C for 6 hours. Then it was cooled in a desiccator and stored in a closed dark bottle (Table 1).

Characterization of $(ZnO\text{-}TiO_2)_{NCM}$ suspensions. For SEM analysis, the (ZnO-TiO2)NCM stock solution was prepared at a concentration of 10 mL-1 with ultra-pure water. Test solutions were prepared by diluting this concentration. The surface of (ZnO-TiO2)NCM was observed with SEM (JEOL JSM 5600 LV). To view the particle surface was examined plating with gold and drying after the solution was diluted by 1000 ppb (Figure 1).

Algal cultures medium. The test organism *Chodatodesmus mucranulatus* was collected from freshwater (from Apa Dam Lake in Konya, Turkey), isolated and pure culture was grown according to the procedure given by Rippka [28], on BG-11 medium [$NaNO_3$, 15; K_2HPO_4, 0.4; $MgSO_4$. $7H_2O$, 0.75; $CaCl_2$. $2H_2O$, 0.36; citric acid, 0.06; iron (III) ammonium citrate, 0.06; Na_2-EDTA, 0.01; Na_2CO_3, 0.2 g/L, 1 ml; trace elements solution, (H_3BO_3, 61; $MnSO_4$. H_2O, 169; $ZnSO_4$.$7H_2O$, 287; $CuSO_4$. $5H_2O$, 2.5; $(NH_4)_6Mo_7O_{24}$. $4H_2O$, 12.5 mg/L) pH: 6.8] commonly used for growing blue-green algae in flasks. This medium contains only trace amounts of metal ions and allows rich growth.

The cells were grown in sterile shake flasks containing 100 ml of BG-11 [28]. The cultures were grown under the cool white fluorescent light intensity of 3000 lux at 25 °C, in 12 h–12 h light–dark cycle and were incubated for 15–20 days in an incubator which is suitable for photosynthesis (Figure 2a). With the obtained algae later on species, identification was realized by using morphological and molecular methods. After an intensive culturing of green algae, the DNA isolations were performed by using a DNA isolation Kit (Qiagen). Genomic DNA was stored at –20 °C prior to being used as template in polymerase chain reaction (PCR). Internal transcribed spacer sequence (ITS) was used for molecular phylogenetic analyses of green algae. For the amplification of ITS gene, the universal primer set (ITS1, 5'- TCCGTAGGTGAACCTGCGG-3'; ITS4, 5'-TCCTCCGCTTATTGATATGC-3') was used as described by Hanen et al. [29]. For all amplifications, 25 µL PCR mixtures were prepared as follows: template DNA 1 µL, 0.3 µL of Taq polymerase (Promega, Go-Taq Flexi DNA polymerase), 1 µL dNTP mix (Amresco), 2.5 µL PCR buffer (Promega, Go-Taq Green Buffer), 1 µL of each primer in final concentration, and 18.2 µL ddH_2O. The PCR products were electrophoresed on 1 % agarose gel prepared in 1X Tris-acetate-EDTA (TAE) buffer. Amplification of genomic DNA was performed with 35 PCR cycles; for the nested amplifications, 15 to 20 cycles were used. Prior to amplification, the DNA was denatured for 2 min at 95°C; after amplification, an extension step for 10 min at 72 °C was included. Cycling parameters were 95°C for 30 s, 55 °C for 30 s, and 72 °C for 1 min. After a successful PCR, the products were sent to a company (Refgen, Ankara, Turkey) where sequencing service was purchased. Then, the chromatograms were carefully examined if there were any mistakes due to the software and the final sequence reads were generated. The final gene sequences were used to find any similarity between our sequences and sequences from the databases using the Basic Local Alignment Search Tool (BLAST) (http://www.ncbi.nlm.nih.gov/BLAST). 18s rRNA gene sequence belongs to the Chlorophyta, purchased from REFREGEN (METU-Teknokent), were set through the use of the BLAST (http://www.ncbi.nlm.nih.gov/BLAST) analysis, and through the use of MEGA 5.1 Bootstrap test of phylogeny (neigboorjoining) program, the phylogenetic tree has been formed.

TABLE 1
Loading the catalyst particle size calculated by the Bragg equation.

Catalysts	FWHM (β)	Radyan (R)	2-Theta	D (particle size, nm)
TiO_2	0.197°	$3.43x10^{-3}$	25.580	44.01
(%1) ZnO-TiO_2	0.180°	$3.14x10^{-3}$	25.253	45.2

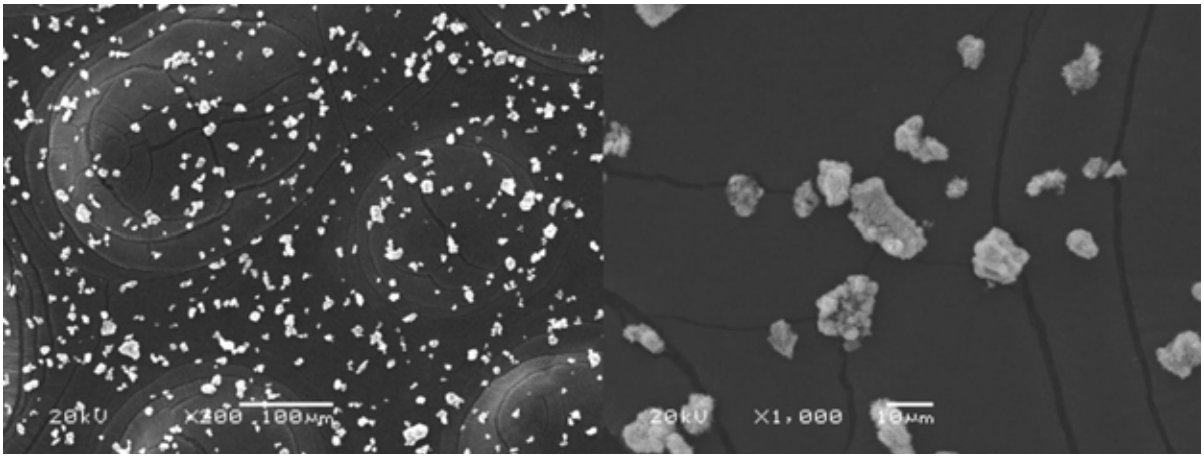


FIGURE 1
Scanning electron microscopy of $(ZnO\text{-}TiO_2)_{NCM}$

$(ZnO\text{-}TiO_2)_{NCM}$ treating method. Previous studies have provided information on the choice of bioassays. However, there is a deficiency on integrating toxicity data between different tools and models [30].

In this study, the test method was modified and applied. Stock solutions of the $(ZnO\text{-}TiO_2)_{NCM}$ were prepared with dispersions in deionized water. Afterwards, this solution, after having been vortexed for 20 seconds, was sonicated with ultra-sonic water bath (Bandelin, sonorex, Berlin, Germany) for 40 minutes in order to increase the dispersion of the stock solutions of $(ZnO\text{-}TiO_2)_{NCM}$ and to allow for their maximum dispersion in water. Following all of these stages, the test concentrations determined through preliminary studies were prepared by being diluted from the stock solution. The test solutions prepared were put within a more experimental media called BG-11 medium.

In order to perform the study for exposure to *Chodatodesmus mucranulatus* $(ZnO\text{-}TiO_2)_{NCM}$ 90 ml of BG-11 medium containing about the cell number 10^6 and 10 ml of the test, the solutions were added into a 200 ml of conical flask. The exposure studies were performed in an orbital shaker to avoid the formation of aggregation at the motionless environment of NPs and to provide the desired constant heat and natural conditions of the algae. The speed of the shaker was set in the way that the cells would be unharmed and that it would prevent the formation aggregation of the particle (85 rpm). The experimental conditions were set for 25 °C, 12-hour-daylight and 12-hour-dark atmosphere. After the experiment was set up, 2 ml sample was taken from each concentration after 24, 48 and 72 hours. Cell count and pigment measurement were performed in these samples. The exposure study was carried out in 3 repetitions, independent of each other.

Determination of photosynthetic activity and pigment contents. Algae were extracted with 80% (v/v) acetone and determined according to the method of [31]. In brief, 2 ml algae cultures were centrifuged at 2000 rpm speed, then the supernatant was discarded and the samples were added 80% (v/v) acetone and placed at 4°C during 24h. According to the following formulas, light absorption values of supernatant were measured with spectro photometer (Hach-Lange brand DR 2800) at 663, 646 and 470 nm [32].

Chlorophyll *a* (Chl a) $=12.21A_{663}\text{-}2.81A_{646}$,

Chlorophyll *b* (Chl b) $=20.13A_{646}\text{-}5.03A_{663}$

Carotenoids $=(1000A_{470}\text{-}3.27$ Chl a-104 Chl b)/229

Bioaccumulation Experiments. *Chodatodesmus mucranulatus* was exposed to $(ZnO\text{-}TiO_2)_{NCM}$ (0.1, 0.01 and 0.001 mg/L) until 72 hours. Subsequently, $(ZnO\text{-}TiO_2)_{NCM}$ bioaccumulation analysis was performed via ICP-MS (Perkin Elmer Elan DRC-e, Massachusetts, USA) device. For this process, the algae, after having been filtered from GF/C Whatman filter papers at room temperature, were dried up in the incubator at 105 °C during 5 h. The dried samples were put into 100 ml beakers, and by adding 1 g of 12 ml HNO_3-$HClO_4$ (1:1) onto them, they were exposed to wet composition while being heated in a fume hood. After the 'almost-dry' beakers had been cooled, 2 ml of concentrated $HClO_4$ was added into them, after which it was heated over a small flame until getting dried up once again. Later on, 1 g and 5 ml of concentrated HNO_3 acid were first added to the solution process and after it was volatilized, concentrated HCl was added and was heated until it almost dried up. The beaker contents were soaked with 1 ml of concentrated HCl a day later and were solubilized in 50 ml bidistilled water, after which they were filtered through the black band filter paper and washed up.

The filtrated fluids were collected in 100 ml volumetric flasks along with the wash water and were then finalized and shaken by means of 25 ml of water [33]. The amount of $(ZnO\text{-}TiO_2)_{NCM}$ accumulations were determined in these sample solutions

prepared in this way for the measurement process along with their standard solutions and the Inductively Coupled Plasma-Mass Spectrometry (ICP-MS).

Analysis of SEM and TEM. For SEM images, *Chodatodesmus mucranulatus* cells (about $5x10^7$ cell/ml) were collected by centrifugation after being $(ZnO\text{-}TiO_2)_{NCM}$-exposed for 72 hours. These cells were collected to falcon tube containing Phosphate Buffer Sodium (PBS) was centrifuged at 1000 g for 10 minutes and washed 2 times. And then, cells prepared in 0.1 M PBS was taken up in 2.5% glutaraldehyde. After 1 overnight (4 °C) cells were detected washing with buffer and taken up in 1% osmium tetroxide was subjected to secondary fixation. After these processes are passed 50%, 70%, 90% and 100% with ethanol. Images were taken up after sample coating with gold (Figure 2b). After osmium tetroxide stage algae cells were buried in the agar and dyed. Then alga cells have become ready to examine for TEM (JEOL JEM 1220) (Figure 2 c, 2 d).

Determination of reactive oxygen species (ROS) formation. Cellular oxidative stress reactive oxygen species (ROS) formation was measured using the cell permeable indicator 20,70-Dichloro-dihydrofluorescein diacetate (H2DCFDA) [6]. Cellular esterases hydrolyze the probe to the non-fluorescent 20,70-dichlorodihydrofluorescein (H2DCF), which is better retained in the cells. In the presence of ROS and cellular peroxidases, H2DCF is transformed to the highly fluorescent 20,70-dichlorofluorescein (DCF). (ZnO-TiO2)NCM treatment and control was treated with 5 mM of H2DCFDA in1 ml of solution. The DCF fluorescence was measured using an excitation wavelength of 485 nm and an emission wavelength of 530 nm. All the fluorescence data were collected using a fluorescence plate reader. Samples were diluted 9 times with potassium phosphate buffer (pH 7.8). Then, homogenization and centrifugation were performed (20 min, 10.000 rpm), the supernatant was removed.

Statistical Analyses. All experiments were independently repeated three times and the data were recorded as the mean value with standard deviation. In order to determine the significant differences between ANOVA, Tukey and single direction variance analysis differences between treated groups and control groups SPSS18 package was used. All data analyses were assessed based on 0.05 and 0.01 significance.

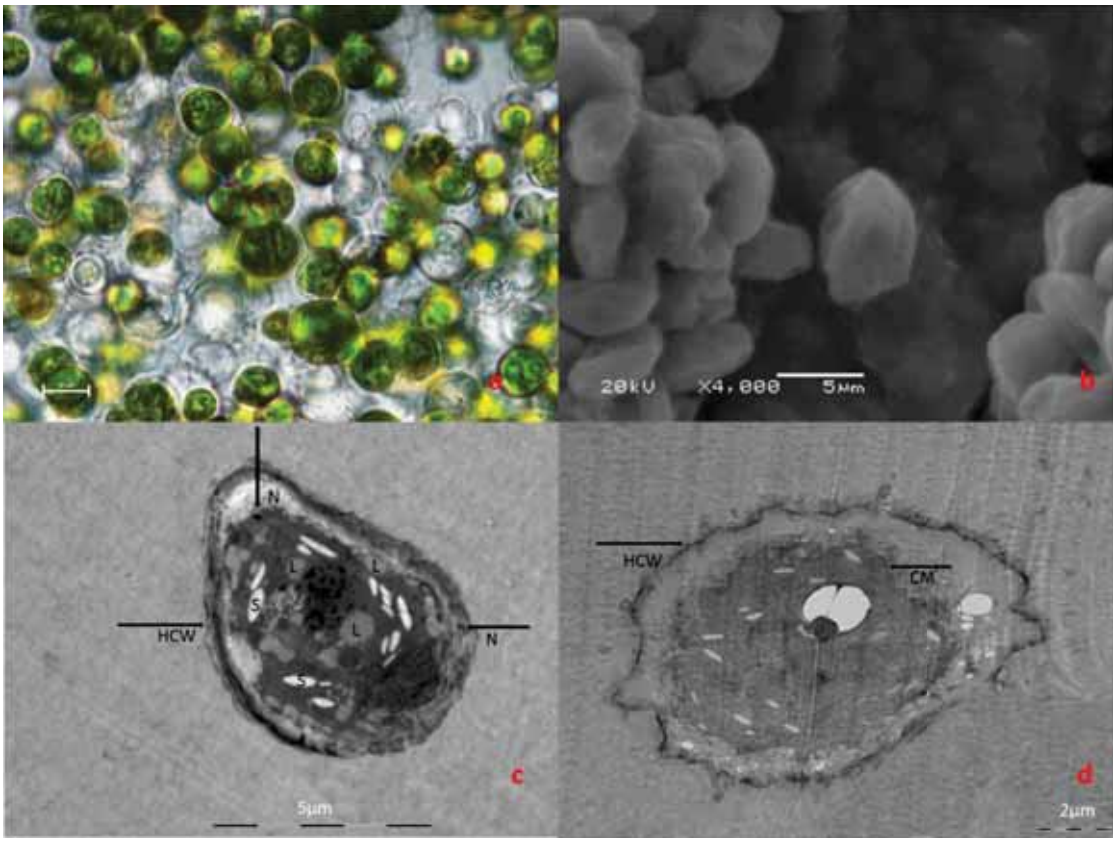


FIGURE 2

a) Light micrographs of the young and mature vegetative *Chodatodesmus mucranulatus* cells. b) SEM images of *Chodatodesmus mucranulatus* cells after exposure to $(ZnO\text{-}TiO_2)_{NCM}$ for 72 h c) TEM image of *Chodatodesmus mucranulatus* cells after exposure to $(ZnO\text{-}TiO_2)_{NCM}$ for 72 h d) damaged cell N $(ZnO\text{-}TiO_2)_{NCM}$ L lipid, S starch, HCW cell wall, Nc nucleus, CM cytoplasmic membrane

RESULTS

The Effect of $(ZnO\text{-}TiO_2)_{NCM}$ on photosynthetic activity of Chodatodesmus mucranulatus. Our example of green algae isolated from Apa Dam Lake is located in a sequence of 1168/1328 base pairs, according to partial 18S rRNA results at http://www.ncbi.nlm.nih.gov/ internet address. According to this sequence, the species belonging to the Sphaeropleales ordo was identified as 97% *Chodatodesmus mucranulatus*. The access number is KR261935. The effect of *Chodatodesmus mucranulatus* fresh water algae exposure to $(ZnO\text{-}TiO_2)_{NCM}$ depending on the time-varying exposures (24, 48 and 72 h) on chlorophyll *a* (Chl a), chlorophyll *b* (Chl b) and carotenoid pigment density are given in Fig. 3, 4 and 5.

As it is observed in Fig. 3, the Chl a amount increased generally in the control group and treated groups depending on the exposure concentration and varying-time. This increase is more when compared with that of the control group, especially in 0.001 mg/L at 72 h, the Chl a amount increased in 2.8 times more than the initial amount. Another interesting situation in the 0.001 mg/L $(ZnO\text{-}TiO_2)_{NCM}$-exposure group is that the Chl a amount decreased in 24th h; however, there was a constant increase in 0.1 mg/L and 0.01 mg/L depending on the time-varying exposures. When these data are considered in a general sense, it is observed that the Chl a amount increased with the decreasing concentrations of $(ZnO\text{-}TiO_2)_{NCM}$. In 0.1 mg/L (the highest exposed group) the Chl a amount decreased in 72th h; however, in this condition, it was still more than the initial Chl a amount. According to the ANOVA test results, there were no meaningful differences according to the Chl a amount ($p>0.05$); however, there was a meaningful difference detected depending on time ($p<0.05$).

The Chl b amount indicated a constant increase depending on all exposed groups (0.1, 0.01 and 0.001 mg/L) of the $(ZnO\text{-}TiO_2)_{NCM}$ depending on the time-varying exposures. Only in 0.1 mg/L, which is the highest treated group, in 72 h of exposure, this value decreased; however, this decrease was still more than the initial Chl b amount. Again, with the increase in the exposed group, the Chl b amount increased in the general sense. The Chl b amount increased in 4, 5.7 and 12.7 times more for 0.001 mg/L; 13 times more for 0.01 mg/L; 6, 9.3 and 6 times more in 0.1 mg/L, respectively depending on the time-varying exposures (24, 48 and 72 h) (Figure 4). According to the ANOVA test, there was no meaningful difference ($p>0.05$) in terms of the Chl b amount; however, there was a meaningful difference depending on the exposure time ($p<0.05$).

The carotenoid amount in *Chodatodesmus mucranulatus*, which was exposed to $(ZnO\text{-}TiO_2)_{NCM}$, increased depending on time-varying exposures in the control group; however, the amount of carotenoid in the $(ZnO\text{-}TiO_2)_{NCM}$-exposed groups considerably reduced and could not be calculated (Figure 5). The carotenoid value was only calculated at the 72 hours of the 0.1 mg/L exposed group and at the 24 hours of the 0.01 mg/L exposed group. According to the ANOVA test, no meaningful difference was detected ($p>0.05$).

The Bioaccumulation amount of $(ZnO\text{-}TiO_2)_{NCM}$ in *Chodatodesmus mucranulatus*. With the increasing concentration of $(ZnO\text{-}TiO_2)_{NCM}$ also increased the accumulation amount of zinc (Zn) and titanium (Ti) particles in *Chodatodesmus mucranulatus.* There are no clear differences between the treated groups. In the control group, trace amounts of Zn were encountered, but no Ti was observed. There is a difference at an important level between the exposed groups of Zn ($p<0.01$). This difference is observed mostly in the 0.1 mg/L. The differences of these treated group among themselves are given in Figure 6 as follows. There is a difference between the Ti and Zn $(ZnO\text{-}TiO_2)_{NCM}$-exposed groups at an important level ($p<0.01$).

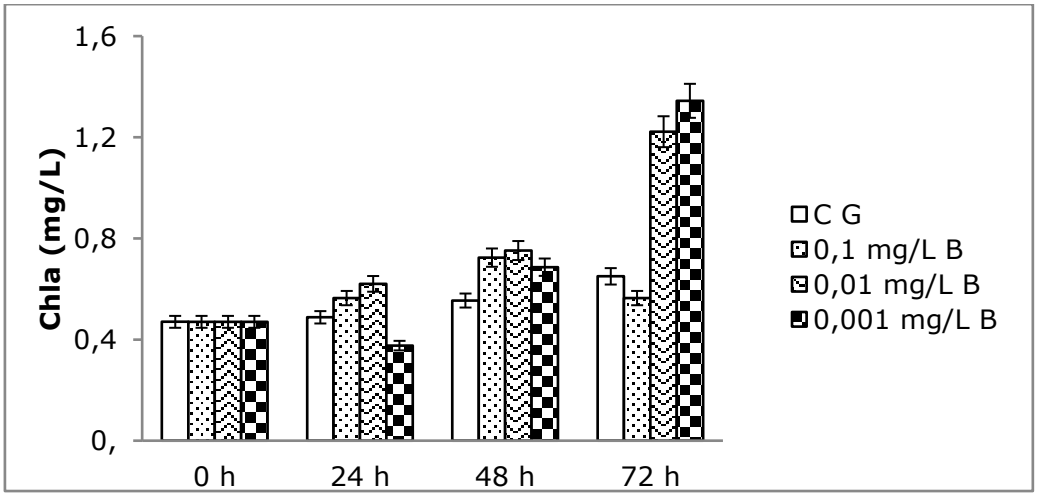


FIGURE 3
The Chlorophyll a content of *Chodatodesmus mucranulatus*

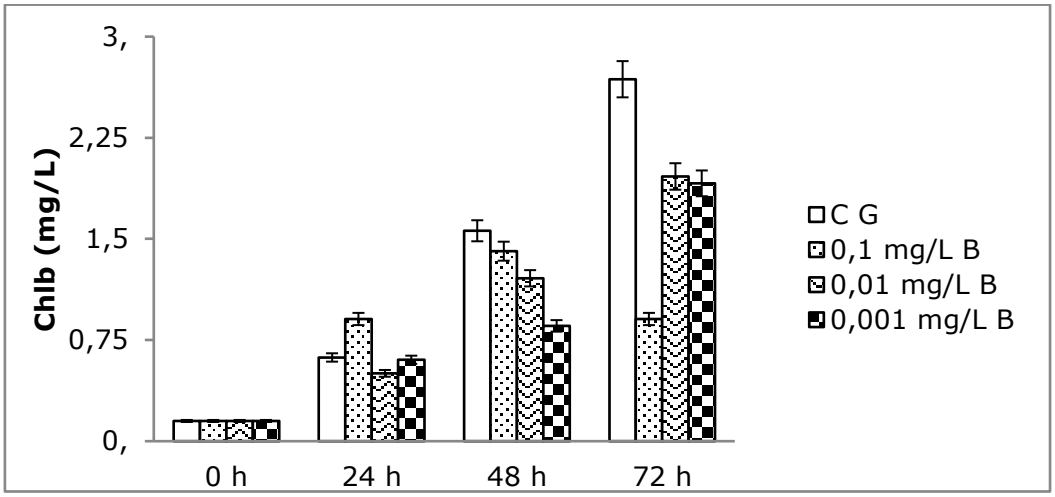


FIGURE 4
The Chlorophyll b content of *Chodatodesmus mucranulatus*

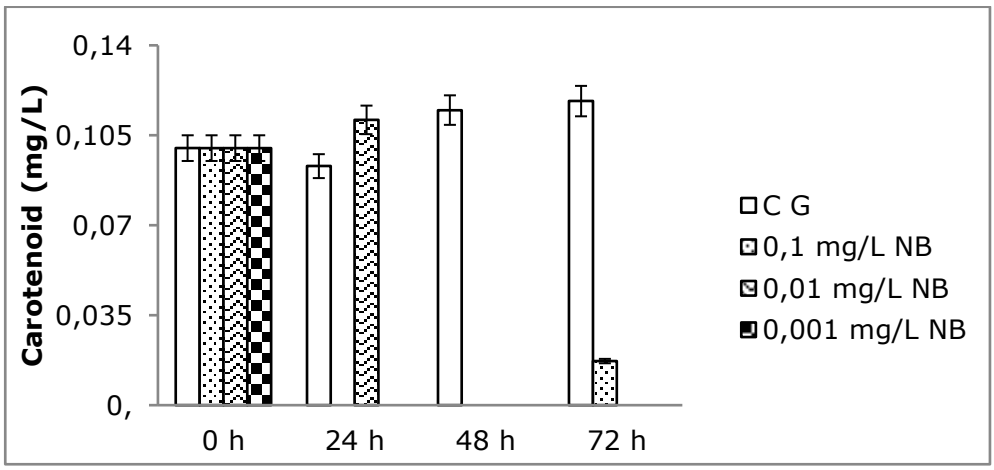


FIGURE 5
The Carotenoid content of *Chodatodesmus mucranulatus*

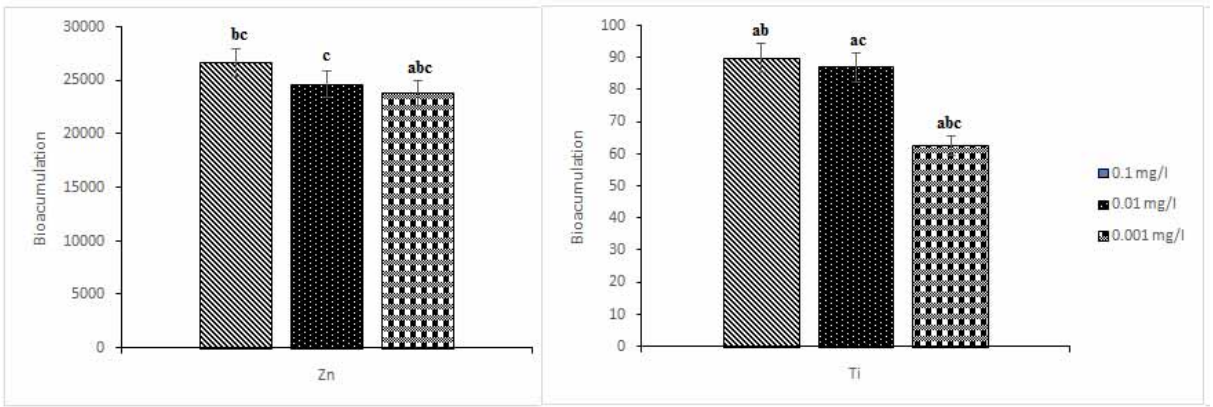


FIGURE 6
The Bioaccumulation of Zn and Ti Particles in the algal cells for 72 hours

This difference is formed in 0.1 mg/L treated group of both Zn and Ti. When the comparison amount of Zn and Ti accumulated in *Chodatodesmus mucranulatus* is evaluated, it was observed that 385 times more Zn accumulated in 0.001 mg/L; 283 times in 0.01 mg/L; 297 times more in 0.1 mg/L. When these results are considered, it is observed that the Zn intake increased much more with the increasing concentration of $(ZnO\text{-}TiO_2)_{NCM}$ when compared with the titanium (Figure 6).

Reactive oxygen species production (ROS) after exposure to $(ZnO\text{-}TiO_2)_{NCM}$. There are very important differences between the treated groups and control groups in *Chodatodesmus mucranulatus* ($p<0.01$). There are significant differences between treated groups and control groups in ROS activity after *Chodatodesmus mucranulatus* exposure to $(ZnO\text{-}TiO_2)_{NCM}$ for 72 hours. This difference was observed in $(ZnO\text{-}TiO_2)_{NCM}$ 0.1 mg/L exposed group at the highest level. When we compared treated group and the control group, the ROS level was observed as being high in all treated algal cell suspensions (Figure 7). Briefly, the ROS activity in algae increased with the increasing concentration of $(ZnO\text{-}TiO_2)_{NCM}$. However, the ROS activity was observed as fairly low at the lowest exposed group (0.001 mg/L) and was nearly close to that of the control group.

DISCUSSION

Because NPs have unique characteristics such as physicochemical, optical, reactive and electrical properties, they interact with organisms and potentially exhibit toxicity [34, 35]. In many studies, the interaction of the nanoparticle with the organism is known by the presence of cell aggregation. For instance; under nano-ZnO and TiO_2 treatment, in algae cells were observed large nanoparticle aggregates showing that they inhibit the growth of algae due to reduced light and nutrient uptake in algal cells, including nanoparticle aggregates [35]. Large aggregates of TiO_2 entrapping in almost all algal cells were observed [21]. As mentioned above, NPs tend to exhibit different aggregation behaviors depending on the chemical environment. The characterization of the medium used for toxicity assays is particularly important [36, 37]. Therefore, nanoparticle characterization should be performed. In the present research, the potential toxic effect of $(ZnO\text{-}TiO_2)_{NCM}$ changes in the contents of photosynthetic pigments, bioaccumulation, and ROS which were characterized in order to provide a better understanding $(ZnO\text{-}TiO_2)_{NCM}$ toxicity in *Chodatodesmus mucranulatus*. The characterization of $(ZnO\text{-}TiO_2)_{NCM}$ used in the test was an important understanding the potential toxic effects of this nanocomposite on algae. Used SEM for characterization, the SEM image in Figure1 shows that the $(ZnO\text{-}TiO_2)_{NCM}$ are irregular spheres and 45 nm in size. In a sterile BG-11 medium, a specific liquid growth medium was used for the cultivation and maintenance of *Chodatodesmus mucranulatus*. The medium supports the growth of photoautotrophic blue-green algae. Bluegreen algae are optimal for maintenance in exposure at the period of 24-hours [38]. In the aquatic ecotoxicity tests, the test substances should be in aqueous phase and the stock solution should be homogeneous. Because the test solutions are used by diluting the stock solution. There are basically three approaches to stirring, dispersants and sonication to make a homogeneous stock solution of the NPs test substance [39]. In the study, the reason of using sonication instead of stirring can be possibly the deforming of NPs if dispersants are used [40]. The toxicity of the nanoparticle, which changes in shape and size as a result of deformation, may vary [41]. Prolonged stirring has little evidence that the suspension NPs will remain the same after stirring has stopped [39, 42]. In addition, sonication control is not necessary at the end of the sonication. There is no risk of producing ROS due to the sonication [39].

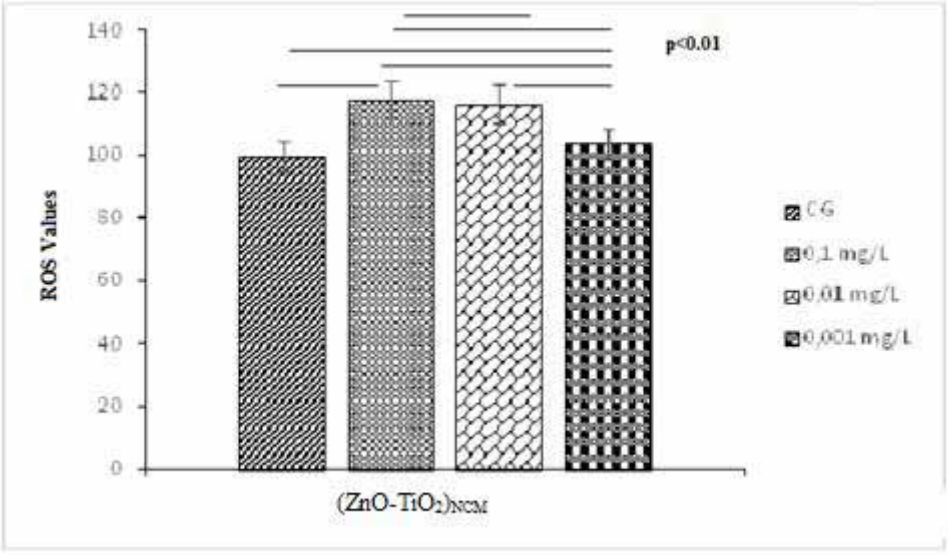


FIGURE 7
The ROS values of $(ZnO\text{-}TiO_2)_{NCM}$ within the algae cells after 72 hours.

The toxic effect of pollutants on algae is usually assessed by phytotoxicity tests based on growth inhibition. Because growth inhibition is a global parameter, we assume that other parameters can change before this parameter. Oxygen emissions and pigment contents (Chl a, Chl b and carotenoids) were found to be reliable estimates of contaminant toxicity [43]. In addition, it has been noted that measurement of plant fluorescence is a simple, rapid and sensitive evaluation method for photoinhibition and pollutant effects on plants [31, 44]. Chl a is more sensitive to photodegradation than other photosynthetic pigments as electron donor to the photosynthetic electron transport chain due to its role in the light harvesting complex and the PSII reaction center [45, 46]. Carotenoids which have more than 600 varieties are pigments found in plants, microorganisms, and animals. They are secondary pigments in plants and have very important biological effects. Among the most prominent effects are antioxidant (non-enzymatic), provitamin effect, anticancer effect, skin protective effect and so on. In addition, they have many roles in oxidative stress tolerance in plant metabolism. It was recorded by [47] carotenoids successfully extinguish triplet-state photosensitizers, singlet oxygen, and peroxy radicals. In some toxicity studies, carotenoids as antioxidant effects have been determined to increase levels under heavy metal stress in many plants, such as *Phyllanthus amorous*, *Vigna mungo* (L.) *Hepper* (black lentils), *Hordeum vulgare* (barley), and it have been suggested that increases are due to their stress defense activities [48, 49, 50]. This study, pigment analysis in treated *Chodatodesmus mucranulatus* showed that chl a, chl b and carotenoid content were changed by $(ZnO\text{-}TiO_2)_{NCM}$ comparing to the control group. The amount of Chl a and Chl b increased as the exposure time in all treated groups increased. Chl b indicated an increase in prolonged exposure time with respect to Chl a, indicating that Chl a is more susceptible to the pollutant. Carotenoids are not usually counted for in treated groups (only could be calculated for a 0.01mg/L concentration for 24 hours). When we looked at the pigment activities, it was noted that the $(ZnO\text{-}TiO_2)_{NCM}$ had no toxic effect. Because the content of Chl a and Chl b pigments is increased compared to the control group. Since carotenoids have antioxidant activity, it is expected that a number of carotenoids will increase in the face of toxic effects. However, the amount of carotenoid was reduced in the groups exposed to $(ZnO\text{-}TiO_2)_{NCM}$, although the amount of carotenoid increased, as the exposure time in the control group increased. We found contrary to results the previous studies that were conducted on the pigment content of the NPs. Some of which are the one conducted by [34] and *Chlamydomonas reinhardtii* was exposed to TiO_2 NPs, the Chl b and carotenoid content changed with the pigment analysis when compared with the control group. The Chl b and content decreased by the TiO_2 at first but then increased in a great deal. There is no important change when compared with the control group with Chl a content. The Chl a / Chl b rate increased in the 24 hours exposured, however, this rate decreased at 48, 72 and 96 h. Oukarroum et al. [51] by conducted a study on *Chlorella vulgaris* and *Dunaliella tertiolecta* exposed to AgNPs (from 0.01 to 10 mg/L) for 24 h. They reported that the total chlorophyll content decreased 34% and 51% rates for 1 and 10 mg/L in *Chlorella vulgaris* [35], the toxicity of metal oxide NPs (Al_2O_3, SiO_2, ZnO ve TiO_2) was studied in green algae *Chlorella sp*. There was no meaningful toxicity in nanoparticle Al_2O_3, SiO_2, and TiO_2 (DJ3, rutile). On the other hand, the Nano-ZnO and nano-TiO_2 (HR3, anatase) inhibited the algae growth greatly. Franklin et al. [52] examined the comparative toxicity of nanoparticle ZnO, bulk ZnO, and $ZnCl_2$ in fresh water algae *Pseudokirchneriella subcapitata*. The total Zn concentrations and ZnO (nano-ZnO_{powder} and nano-$ZnO_{dispersant}$) nanoparticle chronic toxicity is similar to bulk ZnO and $ZnCl_2$ statistically and the growth inhibition changes between LC_{50} values from 49 to 69 μg Zn/L for 72 h. Aruoja et al. [21] by conducted a study on the toxicity of CuO, ZnO and TiO_2 NPs on *Pseudokirchneriella subcapitata* micro algae and reported that the ZnO NPs were more toxic than the CuO and TiO_2 [53]. ZnO-TiO_2 NPs test concentrations showed a distinct toxic effect as the result of the study. The test concentrations determined for TiO_2 were carried out at 0.001, 0.01, 0.1 and 1 mg/L. In addition, they also reported that in the toxicity of the NPs that included metal, the solubility not their interiorizing property was important. Likewise, when Dağlıoğlu and Öztürk [54] exposed green algae (*Desmodesmus multivariabilis*) to $(ZnO\text{-}TiO_2)_{NCM}$, pigment content and ROS level was found effect in the algal cell. Accordingly, it has a positive effect on chlorophyll and carotenoid, depending on the duration of exposure. Also, At the ROS level, as the $ZnO\text{-}TiO_2)_{NCM}$ concentration increased, the ROS level increased.

In the aquatic environment are thought to cause accidental release during the production, transportation, and disposal of NPs and NPs originating from consumer products As a result, these particles cause damage to the aquatic organisms and, through the food chain, become a dangerous class of substances for humans [55]. This has been confirmed by recent studies that aqueous suspensions of many NPs are toxic to green algae [56] copepods [42, 57] crustaceans [42, 58] and fish [53, 59]. In this study, SEM images of aggregates of suspended $(ZnO\text{-}TiO_2)_{NCM}$ were observed. At the same time, it appears that this aggregate $(ZnO\text{-}TiO_2)_{NCM}$ has passed to *Chodatodesmus mucranulatus* cells (Figure 2). The accumulation amounts of Zn and Ti particles in the $(ZnO\text{-}TiO_2)_{NCM}$ are separately evaluated. Accordingly, the amount of Zn accumulation is much greater than that of Ti, and the amount of accumulation in both particles increases as the concentration increases. ZnO

NPs form large aggregates and these aggregates accumulate in the water column. Barhoumi and Dewez [23] conducted a study on superparamagnetic iron oxide to evaluate the NPs (SPION) toxicity, exposed the *Chlorella vulgaris* cells to Fe_3O_4 (SPION-1), $Co_{0.2}Zn_{0.8}Fe_2O_4$ (SPION-2) and $Co_{0.5}Zn_{0.5}Fe_2O_4$ (SPION-3) in the concentration range of 12.5 - 400 μg mL^{-1} for 24, 48 and 72 h. They reported that the soluble Fe, Co and Zn amounts in the medium depended on the exposure duration, SPION compound, and the time of the concentration. The Fe content increased in the algae biomass for SPION-1, SPION-2, and SPION-3, with the exposure to Fe, Co and Zn accumulated SPION concentration and exposure time; and contributed to the toxic effect in the algae cells. The free metal ion suspensions are important sources of toxicity for the growth speed of aquatic microorganisms [21, 52].

Reactive oxygen species (ROS), which are produced in the thylakoid membrane during photosynthesis and hydrogen peroxide, the species of ROS, has been suggested to be the predominant species in algae [60]. High ROS level may lead to cell structure damages (Halliwell and Gutteridge 1999). Our study observed ROS formation in *Chodatodesmus mucranulatus* of the $(ZnO\text{-}TiO_2)_{NCM}$-exposed. Therefore, it may be claimed that the oxidative stress formation potential of $(ZnO\text{-}TiO_2)_{NCM}$ is related directly with the concentration exposed groups. In addition, the $(ZnO\text{-}TiO_2)_{NCM}$-exposed algae may lead to toxic damage because it produces ROS. Chen et al. [34] conducted a study in which *Chlamydomonas reinhardtii* was exposed to TiO_2 NPs, and calculated the malondialdehyde (MDA) content which is an oxidative stress parameter. According to this situation, the MDA increased after the 4th hour of the exposure. After the 8th hour of the exposure, on the other hand, it reached maximum level. Barhoumi and Dewez [23] by detected the ROS formation per living cell by exposing the *Chlorella vulgaris* superparamagnetic iron oxide (SPION) NPs for 72 hours. The cell liveliness decreased at an important level when compared with the control group with 50 µg mL^{-1}. In addition, the ROS production in alive cells increased depending on the SPION types [Fe_3O_4 (SPION-1), $Co_{0.2}Zn_{0.8}Fe_2O_4$ (SPION-2) and $Co_{0.5}Zn_{0.5}Fe_2O_4$ (SPION-3)] and concentrations.

CONCLUSION

The sensitivity of $(ZnO\text{-}TiO_2)_{NCM}$-exposed *Chodatodesmus mucranulatus* was examined. According to the results, it has a positive effect on Chlorophyll *a* and Chlorophyll *b* pigments in $(ZnO\text{-}TiO_2)_{NCM}$-exposed algae; and the amount of these chlorophylls increased constantly depending on the time-varying exposure. It stopped generally in the carotenoid pigment. As for bioaccumulation; different amounts of $(ZnO\text{-}TiO_2)_{NCM}$ accumulation were observed within the algae cells. The accumulation of 0.1 mg/L $(ZnO\text{-}TiO_2)_{NCM}$ concentration is more than the other exposed groups which suggest that NPs have physicochemical properties different from the ordinary chemicals. Also, it was observed that the $(ZnO\text{-}TiO_2)_{NCM}$ formed ROS in algae.

ACKNOWLEDGEMENTS

The $(ZnO\text{-}TiO_2)_{NCM}$ used in this research was obtained Prof. Dr. Münevver Sökmen from Konya Food and Agricultural University.

REFERENCES

[1] Fingar, C.T. (Ed.) (2009) Global trends 2025: A transformed world. DIANE Publishing. Washington D.C.

[2] Griffitt, R.J., Hyndman, K., Denslow, N.D., Barber, D.S. (2008) Comparison of molecular and histological changes in zebrafish gills exposed to metallic nanoparticles. Toxicological Sciences. 107(2), 404-415.

[3] Pendashte, H., Shariati, F., Keshavarz, A., Ramzanpour, Z. (2013) Toxicity of zinc oxide nanoparticles to Chlorella vulgaris and Scenedesmus dimorphus algae species. World Journal of Fish and Marine Sciences. 5(5), 563-570.

[4] Meulenkamp, E.A. (1998) Synthesis and growth of ZnO nanoparticles. The Journal of Physical Chemistry B. 102(29), 5566-5572.

[5] Serpone, N., Dondi, D., Albini, A. (2007) Inorganic and organic UV filters: Their role and efficacy in sunscreens and suncare products. Inorganica Chimica Acta. 360(3), 794-802.

[6] Fujishima, A., Rao, T.N., Tryk, D.A. (2000) Titanium dioxide photocatalysis. Journal of photochemistry and photobiology C: Photochemistry Reviews. 1(1), 1-21.

[7] Meng, X., Dadachov, M., Korfiatis, G.P., Christodoulatos, C. (2005) U.S. Patent No. 6,919,029. Washington, DC: U.S. Patent and Trademark Office.

[8] Pena, M.E., Korfiatis, G.P., Patel, M., Lippincott, L., Meng, X. (2005) Adsorption of As (V) and As (III) by nanocrystalline titanium dioxide. Water Research. 39(11), 2327-2337.

[9] Strigul, N., Vaccari, L., Galdun, C., Wazne, M., Liu, X., Christodoulatos, C., Jasinkiewicz, K. (2009) Acute toxicity of boron, titanium dioxide, and aluminum nanoparticles to Daphnia magna and Vibrio fischeri. Desalination. 248(1-3), 771-782.

[10] Shipway, A.N., Katz, E., Willner, I. (2000) Nanoparticle arrays on surfaces for electronic, optical, and sensor applications. Chem Phys Chem. 1(1), 18-52.

[11] Aitken, R.J., Chaudhry, M.Q., Boxall, A.B.A., Hull, M. (2006) Manufacture and use of nanomaterials: current status in the UK and global trends. Occupational Medicine. 56(5), 300-306.
[12] Choi, H., Stathatos, E., Dionysiou, D.D. (2006) Sol–gel preparation of mesoporous photocatalytic TiO_2 films and TiO_2/Al_2O_3 composite membranes for environmental applications. Applied Catalysis B: Environmental. 63(1-2), 60-67.
[13] Esterkin, C.R., Negro, A.C., Alfano, O.M., Cassano, A.E. (2005) Air pollution remediation in a fixed bed photocatalytic reactor coated with TiO_2. AIChE Journal. 51(8), 2298-2310.
[14] Maier, T., Korting, H.C. (2005) Sunscreens–which and what for? Skin Pharmacology and Physiology. 18(6), 253-262.
[15] Yadav, V.K., Oury, F., Suda, N., Liu, Z.W., Gao, X.B., Confavreux, C., Klemenhagen, K.C., Tanaka, K.F., Gingrich, J.A., Guo, X.E., Tecott, L.H., Mann, J.J., Hen, R., Horvath, T.L., Karsenty, G. (2009) A serotonin-dependent mechanism explains the leptin regulation of bone mass, appetite, and energy expenditure. Cell. 138(5), 976-989.
[16] Jain, M.K., Bhatnagar, M.C., Sharma, G.L. (2000) Humidity sensing properties of MgO doped ZrO_2-TiO_2 ceramic. Indian J. Pure Appl. Phys. 38, 710-713.
[17] Yadav, B.C., Shukla, R.K., Bali, L.M. (2005) Sol-gel processed TiO_2 films on U-shaped glass-rods as optical humidity sensor. Indian Journal & Pure Applied. Physics. 43, 51-55.
[18] Dodd, A., McKinley, A., Saunders, M., Tsuzuki, T. (2006) Mechanochemical synthesis of nanocrystalline SnO_2–ZnO photocatalysts. Nanotechnology. 17(3), 692-698.
[19] Dhanalakshmi, D., Manimegalai, K. (2013) Antibacterial activity of leaf and seed extracts of Delonix regia and Achyranthus aspera against selected bacterial strains. Int. J. Pharm. Med. & Bio. Sc. 2(2), 5-31.
[20] Handy, R.D., Owen, R., Valsami-Jones, E. (2008) The ecotoxicology of nanoparticles and nanomaterials: current status, knowledge gaps, challenges, and future needs. Ecotoxicology. 17(5), 315-325.
[21] Aruoja, V., Dubourguier, H.C., Kasemets, K., Kahru, A. (2009) Toxicity of nanoparticles of CuO, ZnO and TiO2 to microalgae *Pseudokirchneriella subcapitata*. Science of the total Environment. 407(4), 1461-1468.
[22] Kahru, A., Dubourguier, H.C., Blinova, I., Ivask, A., Kasemets, K. (2008) Biotests and biosensors for ecotoxicology of metal oxide nanoparticles: a minireview. Sensors. 8(8), 5153-5170.
[23] Barhoumi, L., Dewez, D. (2013) Toxicity of superparamagnetic iron oxide nanoparticles on green alga *Chlorella vulgaris*. BioMed research international. 2013(2013), 1-11.
[24] Douville, M., Jean, K., Houde, M. (2016) Multitrophic aquatic toxicity of emerging brominated and phosphorus flame retardants. Fresen. Environ. Bull. 25, 3265-3271.
[25] Gonçalves, A.M., de Figueiredo, D.R., Pereira, M.J. (2005) A low-cost methodology for algal growth inhibition tests using three freshwater green algae. Fresen. Environ. Bull. 14, 1192-1195.
[26] Boyle, T.P. (1984) The effect of environmental contaminants on aquatic algae. In: Shubert, L.E. (ed.) Algae as ecological indicators. New York: Academic Press, 237-256.
[27] Stevenson, R.J., Bothwell, M.L., Lowe, R.L. (Eds.) (1996) Algal ecology: Freshwater benthic ecosystem. Academic Press, Inc., San Diego.
[28] Rippka, R. (1988) Isolation and purification of cyanobacteria. Methods in enzymology. 167, 3-27.
[29] Van Hannen, E.J., Fink, P., Lürling, M. (2002) A revised secondary structure model for the internal transcribed spacer 2 of the green algae Scenedesmus and Desmodesmus and its implication for the phylogeny of these algae. European Journal of Phycology. 37(2), 203-208.
[30] Manfra, L., Onorati, F., Tornambé, A., Maggi, C., Nonnis, O., Gabellini, M. (2013) Worst Case Method, Qualitative Assessment and Quantitative Assessment to Interpret Toxicity Data. Fresen. Environ. Bull. 22, 895-903.
[31] Lichtenthaler, H.K, Wellburn, A.R. (1983) Determinations of total carotenoids and chlorophyll a and b of leaf extracts in different solvents. Biochemical Society Transactions (London). 63, 591–592.
[32] Shi, D., Zheng, X., Li, L., Lin, W., Xie, W., Yang, J., Chen, S., Jin, W. (2013) Chlorophyll deficiency in th maize longated mesocotyl2 mutant is caused by a defective heme oxygenase and delaying grana stacking. PloSone. 8(11), e80107.
[33] EPA Method 200.7(1994) Determination of metals and trace elements in water and wastes by inductively coupled plasma-atomic emission spectrometry, Revision 4.4, EMMC Version. Methods for the Determination of Metals in Environmental Samples-Supplement I, EPA/600/R-94-111.
[34] Chen, L., Zhou, L., Liu, Y., Deng, S., Wu, H., Wang, G. (2012) Toxicological effects of nanometer titanium dioxide (nano-TiO_2) on *Chlamydomonas reinhardtii*. Ecotoxicology and Environmental Safety. 84, 155-162.

[35] Ji, J., Long, Z., Lin, D. (2011) Toxicity of oxide nanoparticles to the green algae *Chlorella* sp. Chemical Engineering Journal. 170(2-3), 525-530.
[36] Behra, R., Krug, H. (2008) Nanoecotoxicology: Nanoparticles at large. Nature nanotechnology. 3(5), 253.
[37] Christian, P., Von der Kammer, F., Baalousha, M., Hofmann, T. (2008) Nanoparticles: structure, properties, preparation and behaviour in environmental media. Ecotoxicology. 17(5), 326-343.
[38] Stanier, R.Y., Kunisawa, R., Mandel, M., Cohen-Bazire, G. (1971) Purification and properties of unicellular blue-green algae (order Chroococcales). Bacteriological reviews. 35(2), 171.
[39] Crane, M., Handy, R.D., Garrod, J., Owen, R. (2008) Ecotoxicity test methods and environmental hazard assessment for engineered nanoparticles. Ecotoxicology. 17(5), 421.
[40] Ham, H.T., Choi, Y.S., Chung, I.J. (2005) An explanation of dispersion states of single-walled carbon nanotubes in solvents and aqueous surfactant solutions using solubility parameters. Journal of Colloid and Interface Science. 286(1), 216-223.
[41] Wei, C., Zhang, Y., Guo, J., Han, B., Yang, X., Yuan, J. (2010) Effects of silica nanoparticles on growth and photosynthetic pigment contents of Scenedesmus obliquus. Journal of Environmental Sciences. 22(1), 155-160.
[42] Oberdorster, E., Zhu, S., Blickley, T.M., McClellan-Green, P., Haasch, M.L. (2006) Ecotoxicology of carbon-based engineered nanoparticles: effects of fullerene (C-60) on aquatic organisms Carbon. 44, 1112–20.
[43] Wang, W.C., Freemark, K. (1995) The use of plants for environmental monitoring and assessment. Ecotoxicology and environmental safety. 30(3), 289-301.
[44] Ralph, P.J., Burchett, M.D. (1998) Photosynthetic response of Halophila ovalis to heavy metal stress. Environmental Pollution. 103(1), 91-101.
[45] Rontani, J.F., Grossi, V., Faure, R., Aubert, C. (1994) "Bound" 3-methylidene-7, 11, 15-trimethylhexadecan-1, 2-diol: a new isoprenoid marker for the photodegradation of chlorophyll-a in seawater. Organic Geochemistry. 21(2), 135-142.
[46] Rontani, J.F. (2001) Visible light-dependent degradation of lipidic phytoplanktonic components during senescence: a review. Phytochemistry. 58(2), 187-202.
[47] Sanghera, G.S., Malhotra, P.K., Sidhu, G.S., Sharma, V.K., Sharma, B.B., Karan, R. (2013) Genetic engineering of crop plants for enhanced antioxidants activity. International Journal of Advanced Research Technology. 2(5), 428-458.
[48] Foyer, C.H., Souriau, N., Perret, S., Lelandais, M., Kunert, K.J., Pruvost, C., Jouanin, L. (1995) Overexpression of glutathione reductase but not glutathione synthetase leads to increases in antioxidant capacity and resistance to photoinhibition in poplar trees. Plant physiology. 109(3), 1047-1057.
[49] Büyük, İ., Soydam-Aydın, S., Aras, S. (2012) Bitkilerin stres koşullarına verdiği moleküler cevaplar. Turkish Bulletin of Hygiene & Experimental Biology/Türk Hijyen ve Deneysel Biyoloj. 69(2), 97-110.
[50] Loreto, F., Pinelli, P., Manes, F., Kollist, H. (2004) Impact of ozone on monoterpene emissions and evidence for an isoprene-like antioxidant action of monoterpenes emitted by Quercus ilex leaves. Tree Physiology. 24(4), 361-367.
[51] Oukarroum, A., Bras, S., Perreault, F., Popovic, R. (2012) Inhibitory effects of silver nanoparticles in two green algae, Chlorella vulgaris and Dunaliella tertiolecta. Ecotoxicology and Environmental Safety. 78, 80-85.
[52] Franklin, N.M., Rogers, N.J., Apte, S.C., Batley, G.E., Gadd, G.E., Casey, P.S. (2007) Comparative toxicity of nanoparticulate ZnO, bulk ZnO, and $ZnCl_2$ to a freshwater microalga (*Pseudokirchneriella subcapitata*): the importance of particle solubility. Environmental Science & Technology. 41(24), 8484-8490.
[53] Özkan, Y., Irende, İ., Akdeniz, G., Kabakçi, D., Sökmen, M. (2015) Evaluation of the Comparative Acute Toxic Effects of TiO_2, Ag-TiO_2 and ZnO-TiO_2 Composite Nanoparticles on Honey Bee (*Apis mellifera*). International Environmental Application and Science. 10(1), 26-36.
[54] Dağlıoğlu, Y., Yılmaz Öztürk, B. (2017) Effect of concentration and exposure time of ZnO-TiO2 nanocomposite on photosynthetic pigment contents, ROS production ability, and bioaccumulation of freshwater algae (*Desmodesmus multivariabilis*). Caryologia. 1-11.
[55] Zhu, X., Zhu, L., Lang, Y., Chen, Y. (2008) Oxidative stress and growth inhibition in the freshwater fish *Carassius auratus* induced by chronic exposure to sublethal fullerene aggregates. Environmental Toxicology and Chemistry. 27(9), 1979-1985.
[56] Hund-Rinke, K., Simon, M. (2006) Ecotoxic effect of photocatalytic active nanoparticles (TiO_2) on algae and daphnids (8 pp). Environmental Science and Pollution Research. 13(4), 225-232.
[57] Templeton, R.C., Ferguson, P.L., Washburn, K.M., Scrivens, W.A., Chandler, G.T. (2006) Life-cycle effects of single-walled carbon nanotubes (SWNTs) on an estuarine meiobenthic copepod. Environmental Science & Technology. 40(23), 7387-7393.

[58] Zhu, X., Zhu, L., Chen, Y., Tian, S. (2009) Acute toxicities of six manufactured nanomaterial suspensions to Daphnia magna. Journal of Nanoparticle Research. 11(1), 67-75.
[59] Griffitt, R.J., Weil, R., Hyndman, K.A., Denslow, N.D., Powers, K., Taylor, D., Barber, D.S. (2007) Exposure to copper nanoparticles causes gill injury and acute lethality in zebrafish (*Danio rerio*). Environmental Science & Technology. 41(23), 8178-8186.
[60] Pinto, E., Sigaud-kutner, T., Leitao, M.A., Okamoto, O.K., Morse, D., Colepicolo, P. (2003) Heavy metal–induced oxidative stress in algae. Journal of Phycology. 39(6), 1008-1018.

Received: **01.11.2017**
Accepted: **18.02.2018**

CORRESPONDING AUTHOR

Betul Yilmaz-Ozturk
Eskişehir Osmangazi University
Central Research Laboratory Application
and Research Center,
Eskisehir – Turkey

e-mail: byozturk@ogu.edu.tr

© by PSP Volume 27 – No. 5/2018 pages 2963-2967 Fresenius Environmental Bulletin

PERFORMANCE OF HERBICIDE SPRAYING METHODS AT DIFFERENT APPLICATION VOLUMES IN MAIZE

Ali Bolat[1,*], Ali Bayat[2], Ozcan Tetik[3], H Ali Karaagac[1], Ibrahim Cerit[1], Ugur Sevilmis[1]

[1]Eastern Mediterranean Agricultural Research Institute, Adana, Turkey
[2]Çukurova University, Department of Agricultural Machinery Adana, Turkey
[3]Biological Control Research Institute, Adana, Turkey

ABSTRACT

Novel spray nozzles with high penetration efficiency and low drifting rates have been developed in recent years and exists on nozzle market. To determine efficiencies of these new products on weed control in grain maize production we tested Standard flat fan nozzle, Air induction nozzle, Even flat fan nozzle, Air induction under leaf banding nozzle and Row application kit with standard flat fan nozzle at three different herbicide application volume of 200 l.ha-1, 300 l.ha-1 and 400 l.ha-1. Foramsulfuron active ingredient herbicide has sprayed on maize at post-emergence stage. Efficiency levels of each methods has been determined via pesticide coverage rates, weed control efficiency and maize grain yields. As a result, row application kit with standard flat fan nozzle 400 l.ha-1 application volume achieved the best results based on coverage rates (89.2% in year 2013, 80.3% in year 2014), weed control efficiency (85.3% in year 2013, 88,0% in year 2014), and maize grain yields (1267.5 kg.da-1 in year 2013 and 1303.5 kg.da-1 in year 2014). Row application kit with standard flat fan nozzle is the suggestible method for effective weed control in maize cultivation.

KEYWORDS:
Herbicide, spraying, Weed control, Maize

INTRODUCTION

As in many crop species, weeds are a main yield reducing factor in maize production. Yield reductions reasoning from weeds in maize production may reach up to 49% [1]. Herbicides are one of the most important advances in agriculture [2]. Pesticide usage in agriculture has increased in last decade which increased its affect in human health and environment [3]. Maize farmers may apply herbicides at pre-sowing, pre-emergence or post-emergence periods while the most effective time is post-emergence period [1, 4]. Without herbicide sprayings, average yield losses sourced from weed competition may reach 17% in the worldwide in maize cultivation [5]. Turkish maize farmers generally use hollow cone spray nozzles which consist of a hole on the circular plate, a turbulence part and strainer for herbicide sprayings. But this type of nozzles are more suitable for insecticide applications than herbicide applications due to small droplets sizes (<100 µm) [6]. With small droplet sizes which are mostly drift prone, pesticides can not concentrate on targets enough, loss of chemicals increase and inefficiencies occur in herbicide applications. These conditions increases herbicide doses and application numbers. Increased pesticide usage also results in increased production costs and environmental contamination. Nowadays, usage of standard XR type nozzles on sprayer boom are recommended for herbicide applications. Standard XR type flat fan nozzles perform well to control weeds under laboratory conditions but same performance doesn't appear under field conditions due to droplets high drifting rates. To solve this problem, a few companies developed novel air induction nozzles which provide less drift prone droplets by producing bigger droplets with air bubbles in and can be adopted to conventional boom sprayers. Air induction into the nozzles with liquids produces bigger droplets which increases dropping speed and reduces drifts with these systems [7]. Both broadcast spraying or spraying just banded surface area options exists. More target oriented applications also reduce contaminated surface area and increase success of pesticide applications [8]. Homogeneous distribution of chemicals on the band is an important parameter effecting the success of applications [9]. To obtain this, flat XR nozzle types can be used. In recent years, systems with multi nozzles on one band is increasingly preferred compared to systems with single nozzle on one band. Equipments spraying herbicides to the bottom part of the canopy which are targeting the root zone also exists. These systems spray herbicides to the root zone with a nozzle attached on a boom extending down to the soil surface which also sprays chemicals with an angle. By this method, weeds on the plant rows may be sprayed with very high coverage rates [10]. Another equipment for band applications is multi nozzle type arrangements. By this method, both spraying from top and from two side parts may

be provided. With this specification, multi type nozzles distribute chemicals better with high coverage rates [11]. Sprayed application volumes may be up to 600 l.ha^{-1} in Turkey. High volume applications on low leaf area indexed crops results with more runoff droplets from leaves. This negative effect increases soil contamination, environmental risks and production costs [12]. Because of this, it is important to determine appropriate volume for spraying maize for weed control. Targets of this research are:

1. To determine the droplet coverage rates for all spraying methods,
2. To determine the weed control efficiency of methods and compare with control,
3. To measure the yield increases obtained with different application methods compared to control (no herbicide application).

MATERIALS AND METHODS

Spraying equipment and application methods. Field trials of the research were conducted in 2013 and 2014 years in Cukurova Region of Turkey. Five different herbicide spraying methods were tested. Tested methods were: (1) Standard Flat fan spraying nozzle (XRN: XR11003, Lechler Co.), (2) Air induction nozzles (AIN: IDN120025, Lechler Co.), (3) Even Flat fan nozzles (EFN: TP4002E, Lechler Co.), (4) Air induction nozzles with under leaf banding application (UBN: AIUB8502, Lechler Co.) and (5) Row application kit (RAK: XR8002, Lechler Co.). XRN and AIN methods was applied as broadcast application thus EFN, UBN and RAK methods sprayed on bands. Applications was carried out with a modified boom sprayer with 800 litter tank capacity and containing 4 different handmade 2.5 meter long detachable spraying booms. Same application boom was used for broadcast applications of XRN and HEM methods. For this aim, nozzles were located on the boom with 50 cm spaces. While nozzle spaces on booms for band applications were 70 cm. Booms was manufactured only one nozzle per band in EFN method, 2 nozzles per band in UBN method.

Booms containing canopy underneath air induction nozzles in UBN method had 70 cm spacing and distance between two nozzles on one band was equal to band width (35 cm). In RAK method one of three nozzles was located on top to spray top of the plants and other two located on right and left sides of plants with 45º angle. By this way all plant canopy has been sprayed.

Spraying volumes was diversified to 200, 300 and 400 l.ha^{-1} for each method. A post-emergence herbicide (Foramsulfuron) applied with doses given in label instructions (150g.ha^{-1} granule and 2000 ml.ha^{-1} Mero). An anemometer (Pocket Wind IV) located on spraying height measured 35.1°C air temperature and 1.2 m.s^{-1} wind speed while sprayings was applied. Sprayer operation parameters for methods are given in Table 1.

Nozzle outputs given in Table 1 was measured three times and liquid produced by each nozzle in one minute time period was determined. Tractor speed was calculated in relation with target liquid volumes. The equation used to calculate application volumes for XRN and AIN methods are given in Equation 1.

$$N=600.Q/V.B \quad (1)$$

Where; N, Application volume (l.ha^{-1}); V: Speed (km.h^{-1}); B, Swath; Q, Noozle output (l.min^{-1})

Nozzle outputs in band applications (EFN, UBN and RAK) was calculated via Equation 2.

$$N=600.q/V.b \quad (2)$$

Where; N, Application volume (l.ha^{-1}); q, Total noozle output per (l.min^{-1}); V, Speed (km.h^{-1}); b, band width (m)

Experimental design. P 3394 (Pioneer) maize (*Zea Mays*) variety was used. Each parcel was 28 m^2 (10mx2.8m) and each block contained 6 parcels. Each application volume tested in 6 blocks and 24 parcels in total 12 blocks and 72 parcels.

5 meters space in-between blocks and 3 meters space between parcels to secure applications from superposition. Each block contained one control (no chemical containment) parcel.

Meteorological conditions were measured with an anemometer (Pocket Wind IV). The average air temperature was to 35.7 ° C and average wind speed was 1.6 km.h^{-1}. In the experimentation field, P 34N24 (Pioneer) type of maize have been planted.

TABLE 1
Sprayer operating conditions for the tested methods

Methods	Pressure (bar)	Nozzle output (l.min^{-1})	Sprayer speed (km·h^{-1})*		
			200 l·ha^{-1}	300 l·ha^{-1}	400 l·ha^{-1}
XRN	2	0.92	5.4	3.6	2.5
AIN	2	0.95	5.4	4.0	2.9
EFF	2	0.76	3.2	2.2	1.4
UBN	2	1.45	6.1	4.0	2.9
RAK	2	1.57	6.5	4.3	3.2

*To achieve the targeted application rates for different methods, sprayer speed was adjusted

Determination of herbicide coverage rates and droplet characterization. 10 different random points defined on middle two plant rows in each parcel and 26X52 mm dimensioned water-sensitive papers (WSP- Syngenta) located on these points to determine chemical coverage rates. These papers scanned in 600 dpi resolution and saved as JPEG files. These images processed by an image procession programme (Image Tool 5.0) and percent coverage rates (%) were calculated by dividing stain areas on WSP to WSP area projected to spray.

To make a sense of drift potential and droplet uniformity of spray, characteristics droplet diameters such as $Dv_{0.1}$, $Dv_{0.5}$ and $Dv_{0.9}$ of nozzles were in measured in the Lab conditions by using a laser measurement device (Malvern Spraytec -Open Spray).

The size and/or volume distribution of droplets in a spray is typically expressed by the size versus the cumulative volume percent. Droplet size distribution of all nozzle types were determined in same pressure (2 bar) during 60 second periods. Relative span factor (R) was determined for homogeneity coefficients of droplet sizes of each nozzles by using the following equation (Equation 3).

$$R = Dv_{0.9} - Dv_{0.1} / Dv_{0.5} \quad (3)$$

Where; R: Relative span factor; $Dv_{0.9}$, 90 percent of spray volume is in droplet size smaller than this value; $Dv_{0.1}$, 10 percent of spray volume is in droplets size smaller than this value; $Dv_{0.5}$, Volume median diameter (%50 of the volume).

Determination of weed control efficiency. To evaluate the performance of the spraying methods planed in this research weeds were counted in wooden frames located on 6 different points on middle 2 rows in each parcel to determine weed control efficiency. Each frame covered 0.15 m^2 (0.3m X 0.5m) and weed counted total surface area was 1.2m^2.

To determine percent efficiency, application parcels were compared with control and calculations were made via "Abbott" formula (Equation 4).

$$\%BE = (WNC - WNAP / WNC) * 100 \quad (4)$$

Where; BE, Biological efficiency; WNC, Weed number control; WNAP, weed number in parcels.

Determination of maize grain yields. Two middle lines of plots harvested to calculate yields at crop maturity.

Statistical analysis. Statistic program JUMP 5.0 has been used to analyze grain yields, herbicide coverage rates and weed control efficiencies. Analysis has been done based on randomized strip block design and averages of significant factors compared via LSD tests.

RESULTS AND DISCUSSION

The measurements and calculations of droplet size characteristics are given in Table 2.

As shown in the Table 2, the highest $Dv_{0,5}$ were obtained from AIN at 451,2 µm and the lowest $Dv_{0,5}$ were obtained from UBN at 149,4 µm. Considering the $Dv_{0.5}$ value measured at the same pressure of the nozzle used, it can be said UBN methods will be included more drift-prone droplets that mean higher drift potential. Proximity of "R value" to 1 means better droplet uniformity for any spray pattern. Considering particle size distribute in spray pattern of methods, Relative Span data were ranged from 0.66 to 1.63 where the best relative span data was obtained from AIN and UBN respectively.

Herbicides coverage rates on WSP targets obtained from each method and statistical groups containing LSD tests for years 2013 and 2014 are given in Table 3.

As shown in Table 3, the highest coverage rates were obtained from RAK method with 400 $l.ha^{-1}$ application volume (89.2%) in year 2013 and XRN method with same application volume followed it (68.4%). In the second year of the research (2014), similar to previous year's results, the highest coverage rate (80.3%) achieved from RAK method with 400 $l.ha^{-1}$ application volume and XRN method with same application volume (69.9%) followed it. In a study informed that increasing numbers of nozzles at band sprayings results with increased coverage rates [12]. This study gave the parallel results, where RAK method with 3 nozzles gave the highest coverage rates. Weed control efficiency values obtained from each method and statistical groups containing LSD tests for years 2013 and 2014 are given in Table 4.

TABLE 2
Droplet size distribution for each methods

Methods	Pressure (bar)	$Dv_{0,1}$ (µm)	$Dv_{0,5}$ (µm)	$Dv_{0,9}$ (µm)	Relative Span (R)
XRN	2	90.3	186.5	395.7	1.63
AIN	2	213.3	451.2	758	1.20
EFF	2	185	428.5	748.1	1.31
UBN	2	81.3	149.4	266.3	1.23
RAK	2	135.8	188.6	262	0.66

TABLE 3
Herbicide coverage rates (%) based on methods and application volumes

Methods	Coverage Rates (%)					
	Year 2013			Year 2014		
	200 l·ha^{-1}	300 l·ha^{-1}	400 l·ha^{-1}	200 l·ha^{-1}	300 l·ha^{-1}	400 l·ha^{-1}
XRN	42.1 ab	57.0 a	68.4 b	29.5 b	55.0 a	69.9 b
AIN	31.3 c	43.3 b	61.6 bc	27.1 b	41.5 b	58.5 cd
EFN	37.5 c	54.8 a	56.6 c	29.9 b	57.7 a	60.6 c
UBN	43.3 ab	51.7 a	57.4 c	43.8 a	54.1 a	52.8 d
RAK	47.2 a	55.7 a	89.2 a	49.3 a	59.8 a	80.3 a
Lsd	6.4*	8.2**	8.9*	10.7**	10.8**	6.4*

*: the values shown with the same letters on the column are not significant in the level of p<0.01
**: the values shown with the same letters on the column are not significant in the level of p<0.05

TABLE 4
Mean control efficiencies of methods and application volumes (%)

Methods	Control Efficiency (%)					
	Year 2013			Year 2014		
	200 l·ha^{-1}	300 l·ha^{-1}	400 l·ha^{-1}	200 l·ha^{-1}	300 l·ha^{-1}	400 l·ha^{-1}
XRN	33.2 d	62.7 b	79.9 b	60.1 a	66.7 ab	74.8 bc
AIN	44.2 bc	62.2 b	67.1 b	39.4 b	64.4 ab	72.1 c
EFN	51.9 b	60.0 b	70.0 b	50.8 ab	62.4 b	69.8 c
UBN	42.2 cd	64.4 b	71.0 a	40.8 b	70.8 ab	81.2 ab
RAK	61.8 a	77.1 a	85.3 a	50.4 ab	73.2 a	88.0 a
Lsd	9.4*	5.7*	7.9*	16.7*	9.2*	8.0*

*: the values shown with the same letters on the column are not significant in the level of p<0.01

TABLE 5
Yield differences compared to control parcels based on used methods and application volumes (%)

Methods	Yield Differences Compared to Control Parcels (no herbicide) (%)					
	Year 2013			Year 2014		
	200 l·ha^{-1}	300 l·ha^{-1}	400 l·ha^{-1}	200 l·ha^{-1}	300 l·ha^{-1}	400 l·ha^{-1}
XRN	18.8	19.3	21.3	10.4	11.3	24.9
AIN	16.9	17.2	20.2	12.9	16.1	18.4
EFN	11.7	19.7	18.6	9.2	15.6	18.3
UBN	14.0	20.2	21.6	18.6	23.3	27.1
RAK	19.8	23.5	29.2	13.3	23.6	30.3

Weed control efficiency values ranged between 33.2 to 85.3 % in the year 2013 (Table 4). RAK method with 400 l.ha^{-1} application volume gave the highest control efficiency rate and XRN method followed this with 400 l.ha-1 application volume (79.9%). As shown in Table 4, all the methods operating with 200 l.ha^{-1} application volume achieved lower weed control efficiency then the other application volume used in the research. Considering the effect shape of the herbicide sprayed in the research, it can be say that this is an expected result so that the efficiency of herbicide used was depending on coverage rate on weeds.

In the year 2014, weed control efficiency values ranged between 39.5 to 88.0%. RAK method with 400 l. ha^{-1} application volume gave statistically best results based on control efficiency similar to previous year results and UBN method with 400 l. ha^{-1} application volume was in the same statistical group with 81.2% control efficiency value.

Rates of yield increases compared to control parcels obtained from each method in year 2013 and 2014 by field trials are given in Table 5.

As represented in Table 5, in the highest yield increase obtained from RAK method with 400 l.ha^{-1} application volume (29.2%) compared to control parcels and 300 l.ha^{-1} application volume (23.5%) with same method followed it.

In year 2014, the highest yield increase obtained from RAK method with 400 l.ha^{-1} application volume (30.3%) compared to control parcels and UBN method with 400 l.ha^{-1} application volume (27.1%) followed it. Increasing application volumes resulted with increased yields in both years. Those mean that the higher coverage rates

provide higher weed control and consequently higher yields in maize production.

Band applications were more effective compared to broadcast applications for weed fight in maize. Increasing application volumes resulted with better results. RAK method at 400 $l.ha^{-1}$ application volume gave highest scores based on coverage rates, weed control efficiency and crop yield increases. Usage of this method in maize to fight with weeds will increase maize yields.

ACKNOWLEDGEMENTS

This research was funded by General Directorate of Agricultural Research and Policies (TAGEM) as TAGEM-BS-12/12-03/03-01 project number. The authors thank to TAGEM for their contribution to the project.

REFERENCES

[1] Dogan, M.N., Unay, A., Boz, O. and Albay, F. (2004) Determination of Optimum Weed Control Timing in Maize (Zea mays L.). Turkish Journal of Agriculture and Forestry. 28, 349-354.

[2] Sabanci, K., Aydin, C. (2016) Image Processing Based Intelligent Spraying Robot for Weed Control. Fresen. Environ. Bull. 25, 5305-5312.

[3] Pike, D.R., Mcglamery, M.D. and Knake, E.L. (1991) A Case Study of Herbicide Use. Weed Technology. 5(3), 639-646.

[4] Berzsenyi P., Bonis, B. and Arendas, T. (1995) Investigations About the Effects of Some Factors Influencing the Efficacy of Post-emergence Weed Control in Maize (Zea mays L.). Dang Quoc Lap, Agricultural Research Institute of The Hungarian Academy of Sciences. 9th EWRS Symposium Budapest, 257 – 264.

[5] Oerke, E.C. and Dehne, H.W. (2004) Safeguarding production –loses in major crops and the role of crop protection. Crop Protection. 23, 275-285

[6] Bolat, A. and Bayat, A. (2015) Drift Potential of Some New Types of Spray Nozzles in Different Wind Conditions. Environmentally friendly agriculture and forestry for future generations. XXXVI Ciosta CIGR V Conference.

[7] Bayat, A., Bolat, A. Soysal, A., Gullu, M., Sarihan, H. (2010) Efficiency of Different Spray Application Methods in Second Crop Maize. 23RD Annual Conference on Liquid Atomization and Spray Systems, Brno, Czech Republic, September 2010.

[8] Coates, W. (1996) Spraying Technologies for Cotton Deposition and Efficacy. Applied Engineering in Agriculture. 12(3), 287-296.

[9] Gunel, H. and Ozturk, I. (2007) Bant İlaçlaması ve Direk İlaçlama Yapan Üniteler ve Kullanım Alanları. Atatürk Üniversitesi Ziraat Fak. Derg. 38(1), 91-95.

[10] Moomaw, R.S. and Martin, A.R. (1986) Band Application of Herbicides. Cooperative Extension Service Institute of Agriculture and Nature Resources University of Nebraska – Lincoln.

[11] Grisso, R., Ozkan, H.E., Hofman, V., Womac, A., Wolf, R., Hoffman, W.C., Williford, C., Walco, T. (2000) Pesticide Application Equipment. Chapter 29.

[12] Edwards, C.A. (2013) Environmental pollution by pesticides. Vol. 3. Springer Science & Business Media.

[13] Tessier, M.C., Leroux, G.D. (2000) Banded Herbicide Application. Implementation benefits Conditions for Success. Saint Laurent Vision 2000.

Received: **08.11.2017**
Accepted: **13.02.2018**

CORRESPONDING AUTHOR

Ali Bolat
Eastern Mediterranean Agricultural
Research Institute,
Adana – Turkey

e-mail: bolat.ali@tarim.gov.tr

© by PSP Volume 27 – No. 5/2018 pages 2968-2977 Fresenius Environmental Bulletin

DUST EXPOSURE IN FOAMING WORKSHOP, CASE OF THE HOME APPLIANCE INDUSTRY IN ALGERIA

Hakima Rebbah[1,2,*], Amina Akachat[1], Krim Louhab[2]

[1]Research Unit Materials, Processes and Environment, UR-MPE, Faculty of engineering, University M'Hamed Bougara, Boumerdes, Algeria
[2]Food Technology Research Laboratory, Faculty of engineering, University M'Hamed Bougara, Boumerdes, Algeria

ABSTRACT

The framework of the present paper was to evaluate the exposure to dust pollution and aerosols of the polyurethanes foam intended for the thermal insulation of refrigerators.

Based upon the worker`s complaints and investigations done in collaboration with occupational physicians; four testing stations were set up to evaluate the air quality at the gates injection (GI), tanks injection (TI), tank cleaning (TC), and the workshop atmosphere (WA). Two sampling techniques were used. The first was to use the rotary cup individual sensor flow dust of 10 l/min (CIP 10), with three fractions selectors; alveolar, thoracic and inhalable to evaluate the weight concentration. The second technique was using impregnated filters to sample and analyze the identified aerosols.

For the samples taken in the (TC) station using the (CIP10), the results have shown that the air in the worker`s breathing area contains 2.6 mg/m^3 for the alveolar fraction, 1.33 mg/m^3 for the thoracic fraction and 5.33 mg/m^3 for the inhalable fractions. In the (WA) station we have got 3.3 mg/m^3 for the alveolar fraction; 8.6 mg/m^3 for the thoracic fraction and 7.33 mg/m^3 for the inhalable fraction. The qualitative analysis of the aerosols through the filter sampling has confirmed the presence of the 4,4-Methylene diphenyl diisocyanate (4,4-MDI) in the workshop atmosphere.

This research confirmed through the obtained results that operators are exposed permanently during their working hours to both pollutions dust and aerosols of 4,4-MDI.

KEYWORDS:
Dust pollution, polyurethane industry, CIP 10, aerosols, 4,4-MDI.

INTRODUCTION

Polyurethanes are polymers produced by the reaction between isocyanates containing reactive groups (NCO) and polyols [1]. The polyurethanes (PU) are widely used such as in the manufacture of antimicrobial polyurethane for applications addressing surgical infections and improving patient's life's as confirmed by several studies [2, 3, 4]. The other reference is the development of new polyurethanes which have transformed the footwear industry [5].

Related to this paper; researches have confirmed that these rigid polyurethane foams are good thermal insulators and used in nearly all freezers and refrigerators worldwide [6, 7].

From an industrial hygiene standpoint, the sprayed polyurethane foam presents the highest MDI exposure for workers in all MDI applications [8] and lead to several health risks as highlighted by the results of the following researches:

- Acute dermal contact with MDI has induced dermatitis and eczema in workers which occur during handling of paints components, paint mixing and application of sprayed polyurethane foam based on isocyanates [9, 10].
- MDI may cause sensitization and asthma [11, 12, 13].
- The inhalation of isocyanates was the cause of the Bhopal disaster in India (1984) that took the life of 3787 workers and the list has significantly increased the years after the accident [14].
- A study conducted in eleven polyurethane foam manufacturing plants in England revealed a major increase in mortality among the employees due to inhalation of MDI [15]. The same situation is observed at a steel foundry [16].
- A research conducted in 37 car body shops indicated that despite air quality controls and the use of the personal protective equipment; workers are still exposed to a significant amount of isocyanates [17].

Upon this, it`s highly recommended that MDI exposure threshold must be kept to a minimum rate in the workplace. Most of industrialized countries recommends to not exceed the threshold of 0.005 ppm as an average exposure [18, 19].

The monitoring of the indoor air quality breathed by individuals, is critical regardless the place as this would avoid health problems that can be caused by the indoor air quality, as confirmed by the study of Cetin [20] conducted in caves visited by thousands of tourists each year. The study of Kotzias [21] shows that air quality certification of buildings

is as important as to the energy performance certification.

MATERIALS AND METHODS

Materials. The CIP 10 with cups equipped by rotating heads of alveolar, thoracic and inhalable was used to sample the dust inhaled by workers attached to their torso in different defined positions. The samples were taken for periods of 15min to assess short-term pollution, and for 120min to evaluate long-term pollution. The process of dust sampling on CIP 10 is performed according to the French norm (NF X 43-257) [22]. The CIP 10 speed [23] has been adjusted manually using the strobe (EUROSAP-LM, MAO.475) and a digital tachometer (CHAUVIN ARNOUX C.A 27). The sampling rate of the filter was measured using the soap bubble electronic flowmeter (Mina-Buck Calibrator 0,1-3 l/min).

The thermo hygrometer (HANNA.HI 8564) was used to measure the temperature and the humidity in the workshop due to their influence on the dust levels and the concentrations of MDI in the workplace [24].

An analytical balance (Kern ALS 220-4) was used to weight the cup sampling. Reagents were used to prepare the filters for the sampling of aerosols. For filter`s preparation we used, -1-(2-methoxyphenyl) – peperazine 97%, acetonitril 98 %, sodium acetate 98 %, sulfuric acid 99 %, and diphenylmethane-4,4-diisocyanate 98 %, as well as distilled water to get a suitable polyurethane foam for the dust sampling.

Methods. Dust weight analysis. Air samples in various locations have been taken in the R1 workshop at the ENIEM (National Company of the Home Appliance Industries of Tizi-Ouzou). The concerned items were: gates injection (GI), tanks injection (TI), tank cleaning (TC) and the workshop atmosphere (WA). At the end of each series of sampling and after weighing the cups, the amount of dust is calculated according to the following formulas:

$$M_m = M_{mf} - M_{mi}$$

$$M_t = M_{tf} - M_{ti}$$

$$\boldsymbol{M = M_m - M_r\ (mg)}$$

Calculation of the air volume aspirated in 15 and 120min. Suction rate of the CIP 10 is 10 l/min and the volume of air aspirated in 15min is 150L. The volume of air aspirated in 120min is 1200L, therefore, the different concentrations of the collected dust were defined for the four working positions. The concentration of the collected dust was calculated using the following correlation:

$$\boldsymbol{C\ (mg/m^3) = (C_x - C_b)\ \frac{v}{V}\ \frac{M_1}{M_2}}$$

MDI concentration. Three stations were selected for MDI aerosols samples; near the injection pump of MDI (a_1), injection gate (a_2) and workshop atmosphere (a_3). The sampling aerosols using CIP10 equipped with a filter has been carried out according to the procedure of PUSCASU [25].

A volume of 60L was collected on the filter compared to the average exposure value (AEV) of MDI estimated to 0.1 mg/m^3 according to the INRS [26].

The sealing tape is checked using the method described in Annex 3 of the technical sheet MétroPol 002 of INRS [27].

To prepare the standard solution that was used for the filters treatment before processing the sampling; a quantity of 50mg derivative is dissolved in 100ml of methanol, then quantities of the initial solution obtained are diluted in acetonitrile to cover a concentration of 0.01 to 5 g/ml. Isocyanates react with 1- (2méthoxyphényl) -péperazine, on the filter to form the corresponding ureide derivatives. This derivative is then quantified by liquid chromatography.

RESULTS AND DISCUSSION

Temperature and humidity in the workshop. Given the influence of climate parameters on the particles concentration [28, 29], we have considered the humidity and the temperature in the R1 workshop, as the sampling progresses.

Figure 1 illustrates a significant presence of humidity in the R1 workshop during the hot periods of the year up to 71.5%. It also shows that the temperature reaches 21.8 °C. An important presence of humidity will highly contribute to reduce the suspension of dust and consequently their concentration, as confirmed by the researches of Han and Qian [30, 31].

Figure 2 shows a lower humidity during the cold periods of the year, within the range of 39% to 45%, and an average temperature of 18.6 °C. This increase the dust suspension in the workshop which justify the high rate of pollution by particles checked at R1 workshop particularly during the peak of activities which increase the risk of worker`s exposure to this pollution given the time they spend in their workstations which is about 08 hours a day.

Dust concentration in the workshop R1 according to the sampling periods. The results of the dust weight analysis in various positions based on sampling periods (15 and 120 min) are shown in the figures 3 & 4.

Figure 3 shows that the alveolar and inhalable fractions are detected in the GI station for the short and mid-term sampling. On other hand, the thoracic fraction is detected only at short-term sampling with a low concentration of 0.09 mg/m^3.

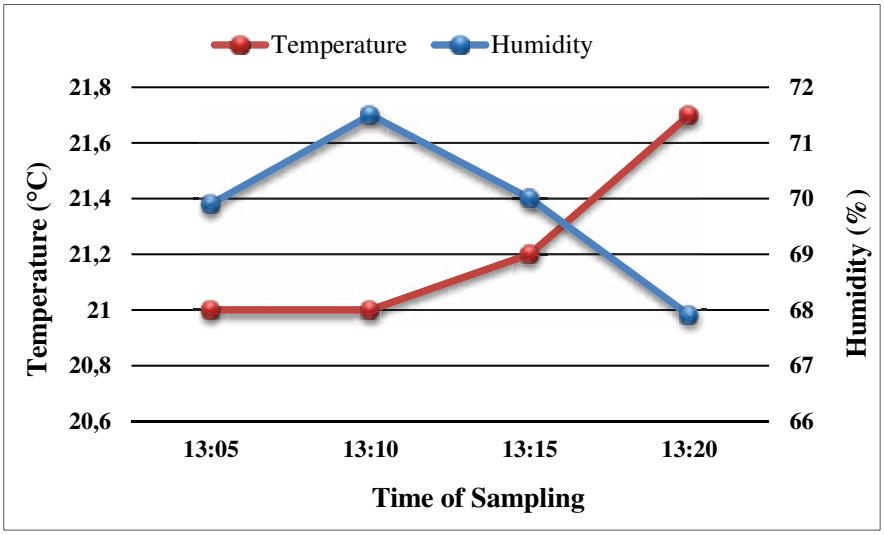


FIGURE 1
Temperature and humidity in the workshop atmosphere at hot period

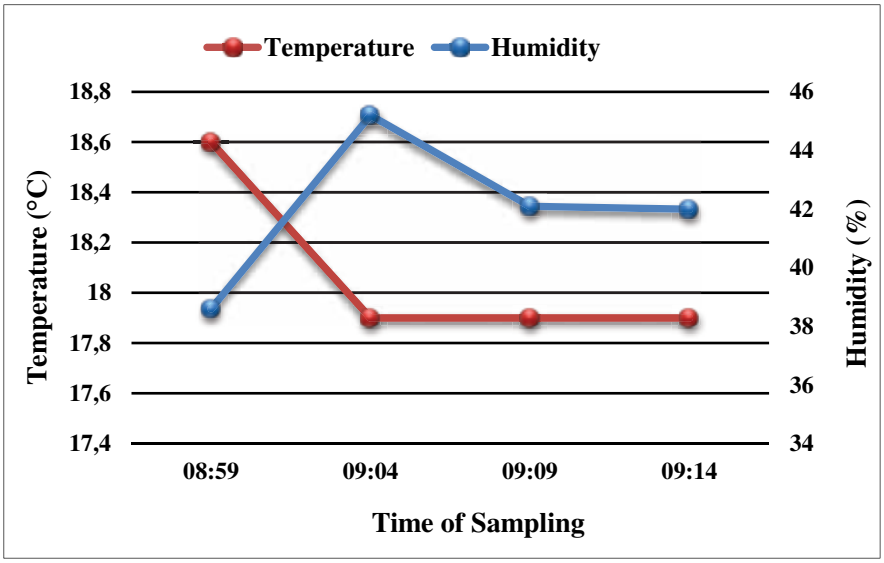


FIGURE 2
Temperature and humidity in the workshop atmosphere at cold period

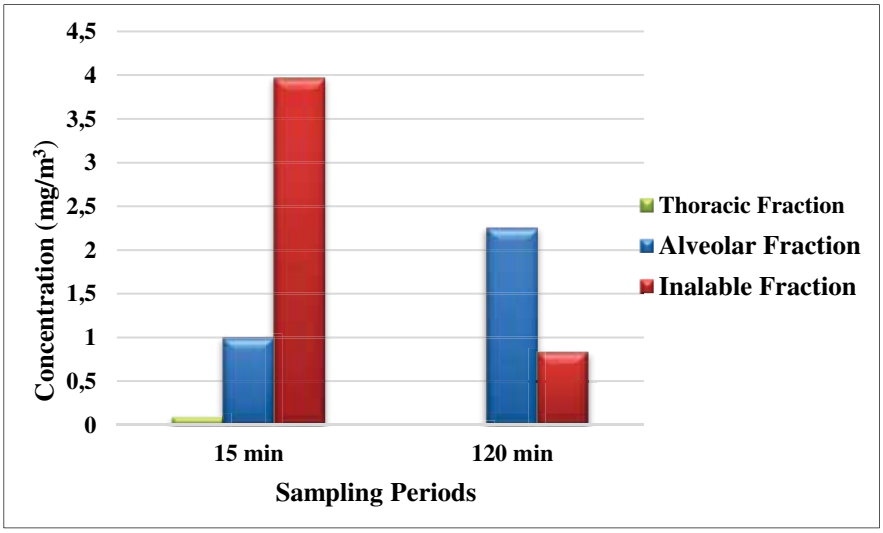


FIGURE 3
Dust concentration in GI post for 15 and 120mn of sampling.

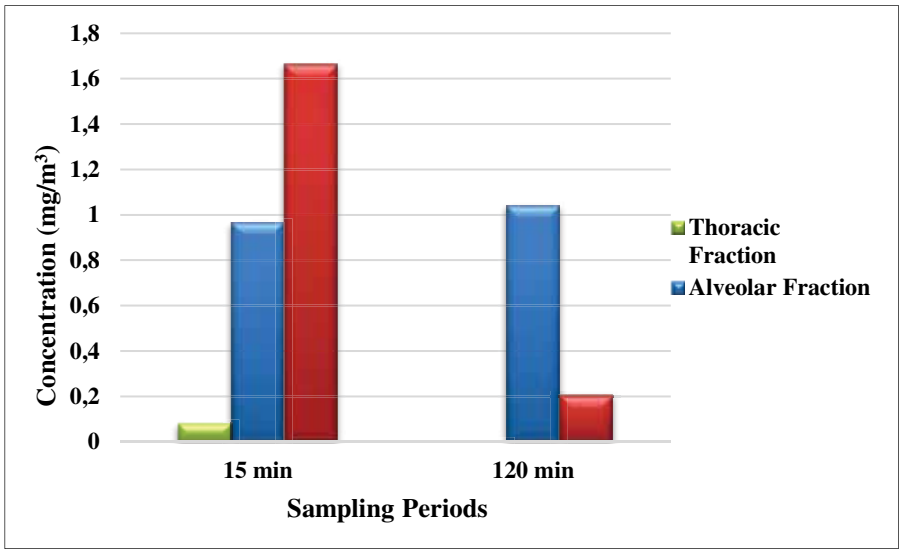


FIGURE 4
Dust concentration in TI post for 15 and 120mn of sampling

The value of the alveolar fraction has exceeded the exposure limit value (ELV) of 2 mg/m^3 recommended by the INRS [26] for mid-term sampling which increases the risk of worker`s exposure to these particles as they penetrate deep down to the pulmonary alveoli with a low possibility of removal. It has been demonstrated that it is the finer PM fraction that has the most acute effects on human health [32], especially for vulnerable people as shown by the work of Stamatelopoulou [33].

Figure 3 shows in addition that the concentration of dust collected at mid-term sampling is lower than the one collected at short-term, this is due to the fact that some of these particles stuck in the inner walls of the CIP10 as shown by the studies of James and Demange [34, 35]. The high-speed rotation of the CIP 10 (7000 rpm) re-entrained the particles at the exit of the CIP10 for the long sampling time, therefore, the results are similar to the literature work [36]. This difference can also be explained by the number of dilutions which is 8 times bigger in the mid-term sampling than the short-term.

The Figure 4 shows that the three fractions; alveolar, thoracic and inhalable are detected in TI station. The thoracic fraction is not detected for the mid-term sampling, this is due to the low concentration of this fraction in this station as this has not reached the detection threshold of the CIP10.

The values of the alveolar and inhalable fractions respectively 1.04 mg/m^3 and 0.205 mg/m^3 for mid-term sampling didn`t exceed the ELV of 2 mg/m^3 and 5 mg/m^3 [26], nevertheless, this does not exclude the risk of exposure of the workers to this pollution and the possibility of developing occupational diseases that can be caused by these particles even at low concentrations, as they are kept and accumulated by the respiratory system along the employee's career, provoking the pulmonary overload phenomenon as confirmed by the study of Churg and Nikula [37, 38].

In Figure 5 we have noticed that TC station got a dust exposure with the three fractions; alveolar, thoracic and inhalable, for the short-term sampling. For the mid-term sampling the thoracic fraction is not detected in this station.

The alveolar and inhalable fractions are detected in the TC post in mid-term sampling respectively with low concentrations of 0.205 mg/m^3 and 0.12 mg/m^3 which didn't exceed the ELV, however, this expose the ENIEM workers occupying this position to the risk of occupational diseases caused by the dust pollution knowing the important amount of time they spend in the same position during their career which is about 20 to 30 years of exposure [39].

Figure 6 shows that the dust pollution with the three fractions; alveolar, thoracic and inhalable are found in WA station with high concentration for the inhalable fraction 0.825 mg/m^3. The detected concentrations at mid-term sampling are lower than those taken at short-term one.

The results of the samples confirmed that the air in the workshop R1 presents a dust pollution in all the surface not only near the point of emissions of these particles in the related stations, as their low density allow them to move throughout all the workshop area, therefore, exposing the workers of this workshop increase the risk of developing respiratory diseases, particularly occupational asthma.

To review the dust concentration results in the workshop R1 upon the sampling periods, we have recapitulated the values we have got at the various stations in the Table 1.

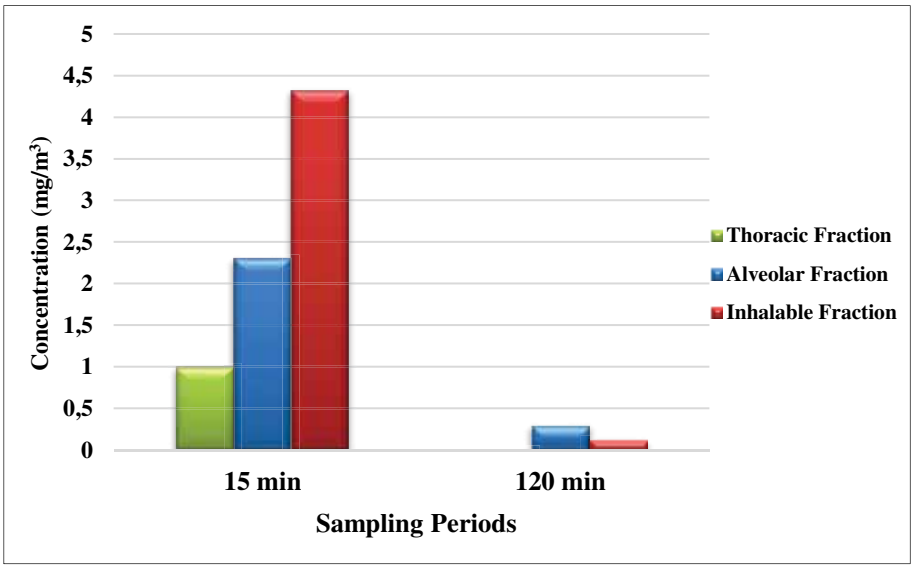


FIGURE 5
Dust concentration in TC post for 15 and 120mn of sampling

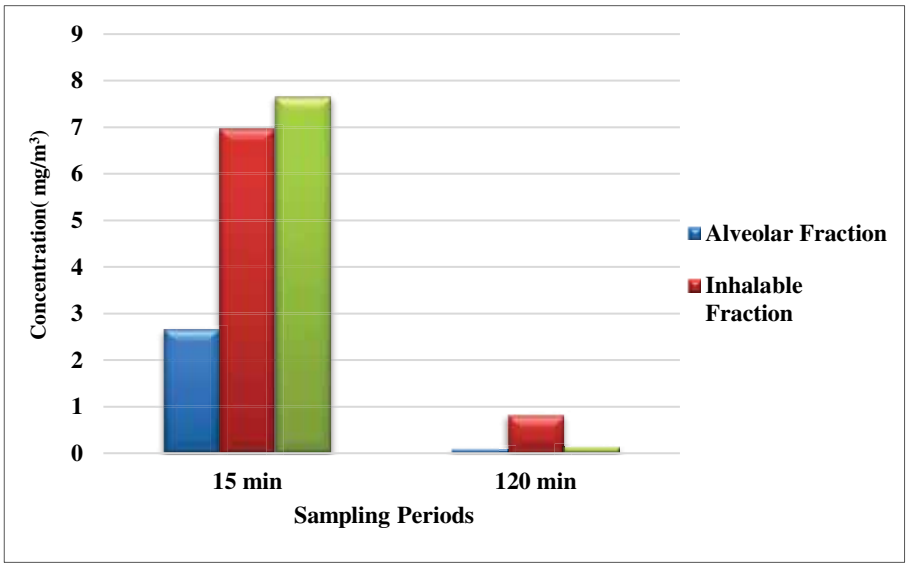


FIGURE 6
Dust concentration in WA post for 15 and 120mn of sampling

TABLE 1
Dust concentrations (mg/m^3), in the workshop R1 upon the sampling periods

	Alveolar fraction		Thoracic fraction		Inhalable fraction	
	(15 mn)	(120 mn)	(15 mn)	(120 mn)	(15 mn)	(120 mn)
Gates Injection	0.995	**2.250**	0.090	0.000	3.965	0.830
Tanks Injection	0.965	1.040	0.080	0.000	1.665	0.205
Tanks Cleaning	2.300	0.285	0.995	0.000	4.315	0.120
Workshop Atmosphere	2.650	0.080	7.650	0.120	6.965	0.825

Dust concentration in the workshop R1 according to the sampling stations. After the comparison done among the values of the dust concentrations taken in the workshop R1 upon the sampling periods, we have evaluated the exposure of the workers as per the work stations, thus, we considered the values of the concentrations taken at mid-term sampling since it is the fraction that represents the long-term exposition for dust pollution, and then we have analyzed the results for each fraction.

Alveolar fraction. Figure 7 shows that the alveolar fraction is detected in the four defined positions with a considerable rate of 1.88 mg/m^3 in WA position**.** This is due to the position of the sampling point which is located next to other work stations

that emanates dust during the whole working day leading to the displacement of the particles emanating from all the posts of the workshop R1 as well as their accumulation due to the absence of a ventilation system that will displace the dust to outdoor of the workspace, or a vacuum system that will allow the pollution aspiration from the source of it`s emanation. The dust can also come from outside the workshop due to the influence of the external environment on the air inside the building as shown by the works of Sabaziotos [40].

The dust concentration of 1.85 mg/m^3 in TC is also important for alveolar fraction. The result can be explained by the nature of the station which is in a massive production system, where the cleaning of tanks is done at each output of the molds; and also, due to the location of the station TC in the workshop which is close to the other positions that emanates dust.

Thoracic fraction. Figure 8 shows that the thoracic fraction is detected only in the WA station with a quite low concentration of 0.66 mg/m^3. This amount is due to the low rate of this fraction in the workshop R1 which has not reached the detecting threshold of CIP 10. Knowing that this fraction is responsible of the occupational asthma, even at low concentrations, we can confirm that the workers are exposed for an important risk of developing this disease over their career.

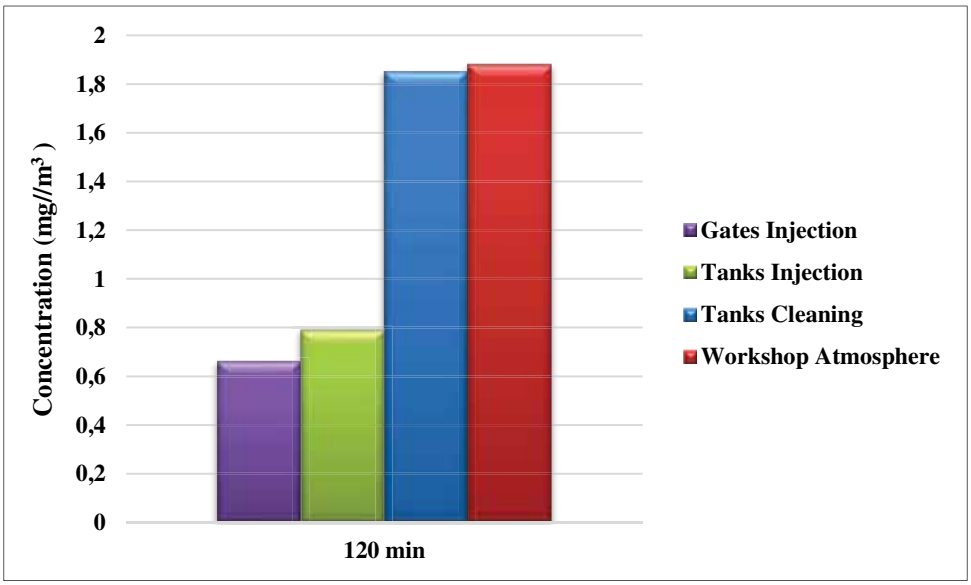


FIGURE 7
Alveolar dust concentration in, GI, TI, TC and WA for 120mn of sampling

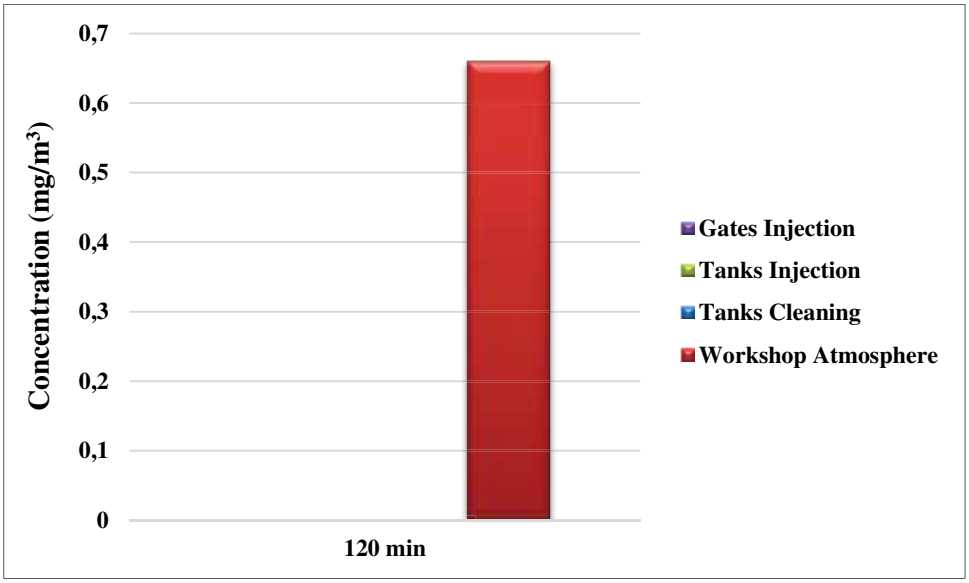


FIGURE 8
Thoracic dust concentration in, GI, TI, TC and WA for 120mn of sampling

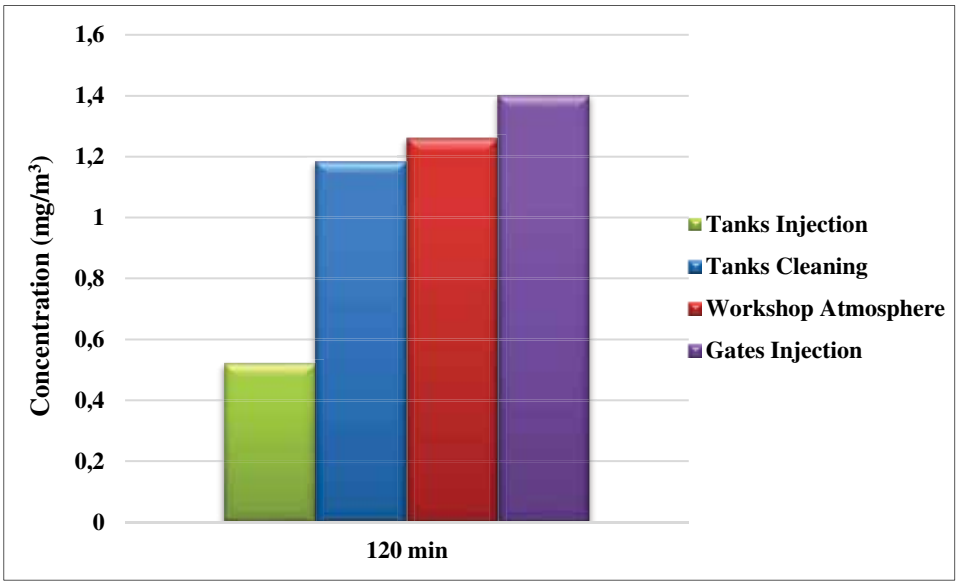


FIGURE 9
Inhalable dust concentration in, GI, TI, TC and WA for 120mn of sampling.

TABLE 2
Dust concentrations (mg/m^3), in the workshop R1 upon the sampling stations

	Gates Injection (120 mn)	Tanks Injection (120 mn)	Tanks Cleaning (120 mn)	Workshop Atmosphere (120 mn)
Alveolar fraction	0.660	0.790	1.850	1.880
Thoracic fraction	0.000	0.000	0.000	0.660
Inhalable fraction	1.400	0.520	1.183	1.260

Inhalable fraction. Figure 9 shows that the inhalable fraction is present in the four sampling stations, with a higher concentration at the GI one with 1.4 mg/m^3. Several parameters can influence the rate of the inhalable dust pollution in this station due to:

- The nature of the post where the scouring of the PU foam is made overflowing around the mold, hence the permanent emanation of the dust at this post,
- The absence of the suction of the dust released at the source,
- The climate conditions in the workshop, for example in the case of low humidity, as shown by the measurements in Figure 2, this will generate the accumulation of particles in the air of the workshop which will increase their concentration.

Upon the dust weight analysis results in the workshop R1, we can confirm that the four positions concerned indicates a dust pollution, including the three fractions, alveolar, thoracic and inhalable, with recorded peaks for the workshop atmosphere position, therefore, we can highlight that excessive exposure of workers to considerable particles pollution even at low concentrations can cause respiratory disease due to the significant exposure time to this pollution.

To review the dust concentration results in the workshop R1 upon the sampling stations, we have recapitulated the values we have got in the Table 2.

SAMPLING ON FILTER

HPLC results analyses. To evaluate the aerosol pollution in the R1 workshop, we have proceeded to the sampling in three stations with the filter at the isocyanate injection pump station (a_1), the GI (a_2) and in the WA (a_3). We have analyzed the results with the High Performance Liquid Chromatography (HPLC). The Figure 10 indicate the results of the isocyanates injection pump station of the MDI.

From the calibration curves, we derived the concentrations from the sampling stations a_1, a_2, and a_3 in order to build the MDI concentrations histogram of Figure.11.

Figure 11 shows a significant presence of MDI in the three positions identified with a major concentration in position a_1 with 13.25 10^3 mg/m^3, extremely exceeding the ELV of 0.1 mg/m^3, proposed by INRS [26]. This is due to the defective condition of the pump, resulting in considerable losses of this material in vapor form, so an immediate renewal of the injection pump will be of considerable improvement to worker`s health.

Knowing that MDI is the major cause of occupational asthma as shown in the study [41], we can highlight upon our results that workers are exposed to a significant risk of respiratory disease given the amount of inhaled aerosols along the working day.

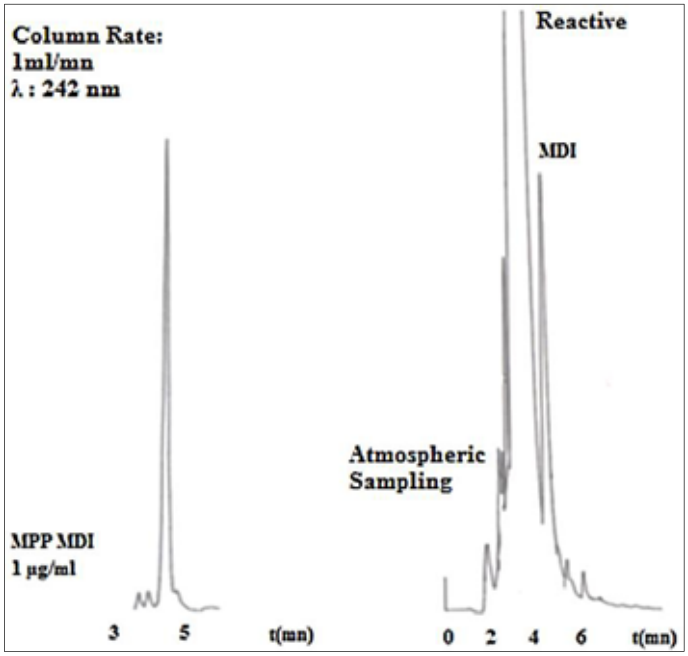


FIGURE 10
HPLC of the alveolar fraction in MDI injection pump (a_1).

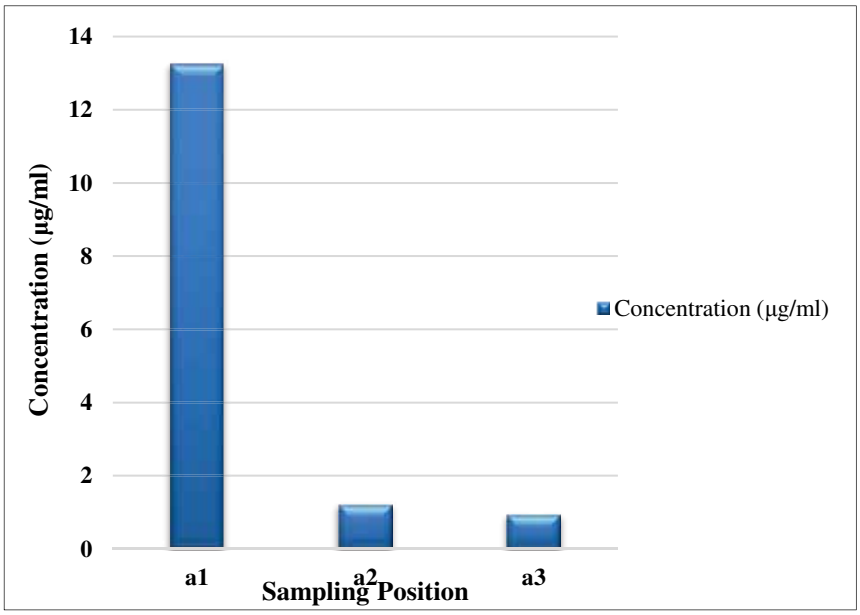


FIGURE 11
MDI concentration based on sampling stations.

CONCLUSION

Throughout this study we have evaluated the dust weight analysis by particle size classes, and characterized MDI vapor in the air of the foaming workshop R1 in a household appliance industry.

The results we have got confirmed that the three fractions; alveolar, thoracic and inhalable are present in the breathing zone of workers and in the workshop's atmosphere with various concentrations, which explains the worker`s complaints.

The results of aerosol characterization by HPLC confirmed that aerosols sampling in the workshop includes MDI, sensitizing and irritant causing occupational asthma, this was confirmed by the Zatout and Tibiche Clinical Study [42], which concluded that ENIEM workers developed respiratory diseases caused by their exposure to these aerosols, particularly for foam injectors.

Considering these results, we confirm that in the R1 workshop, workers are exposed to dust pollution and aerosols containing MDI, this is definitely

an alert to raise awareness about the risks for workers that are being excessively exposed to these substances, therefore, it`s urgent that ENIEM initiate a remedial work plan to improve the working conditions of employees.

ACKNOWLEDGEMENTS

We are grateful to the staff of ENIEM Tizi-Ouzou who contributed while carrying out this study, particularly to the workers of the workshop R1.

REFERENCES

[1] Trinca, R.B., Abraham, G.A. and Felisberti, M.I. (2015) Electrospun nanofibrous scaffolds of segmented polyurethanes based on PEG, PLLA and PTMC blocks: Physico-chemical properties and morphology. Mater. Sci. Eng. 56, 511–517.

[2] Francolini, I. and Piozzi, A. (2016) Antimicrobial polyurethanes for intravascular medical devices. Advances in Polyurethane Biomaterials. (1st Edition) Elsevier, Amsterdam, 349–385.

[3] Xu, L.C. and Siedlecki, C.A. (2016) Antibacterial polyurethanes. Advances in Polyurethane Biomaterials. (1st Edition) Elsevier, Amsterdam, 247–284.

[4] Qu, W.Q., Xia, Y.R., Jiang, L.J., Zhang, L.W. and Hou, Z.S. (2016) Synthesis and characterization of a new biodegradable polyurethanes with good mechanical properties. Chin. Chem. Lett. 27(1), 135–138.

[5] Orgiles-Calpena, E., Aran-Ais, F., Torro-Palau, A.M., Montiel-Parreno, E. and Orgiles-Barcelo, C. (2016) Synthesis of polyurethanes from CO2-based polyols: A challenge for sustainable adhesives, Special Issue on Adhesion, Surface Preparation and Adhesive Properties. Int. J. Adhes. Adhes. 67, 63–68.

[6] Mahmood, N., Yuan, Z. and Schmidt, J. (2015) Preparation of bio-based rigid polyurethane foam using hydrolytically depolymerized Kraft lignin via direct replacement or oxypropylation. European Polymer Journal. 68, 1-9.

[7] Septevani, A.A., Evans, A.C.D., Annamalai, P.K. and Martin, J.D. (2017) The use of cellulose nanocrystals to enhance the thermal insulation properties and sustainability of rigid polyurethane foam. Industrial Crops and Products. 107, 114-121.

[8] Booth, K.B., Cummings, B., and Karoly, W.J., Mullins, S., Robert, W.P., Spence, M., Lichtenberg, F.W. and Banta, J. (2009) Measurements of Airbone Methylene Diphenyl Diisocyanate (MDI) Concentration in the U.S. Workplace. J. Occup. Env. Hyg. 6(4), 228-238.

[9] Henriks-Eckerman, M.L., Mäkelä, E.A., Laitinen, J., Ylinen, K., Suuronen, K., Vuokko, A. and Sauni, R. (2015) Role of dermal exposure in systemic intake of methylenediphenyl diisocyanate (MDI) among construction and boat building workers. Toxicol. Lett. 232(3), 595–600.

[10] Bello, D., Sparer, J., Redlich, C.A., Ibrahim, K., Stowe, M.H. and Liu, Y. (2007) Slow curing of aliphatic polyisocyanate paints in automotive refinishing: A potential source for skin exposure. J. Occup. Env. Hyg. 4, 406-4011.

[11] Parod, R.J. (2014) Diphenylmethane diisocyanate (MDI), 4,4'-, Reference Module in Biomedical Sciences. Encyclopedia of Toxicology. (3rd Edition) Elsevier, Amsterdam, 1–5.

[12] Buyantseva, L.V., Liss, G.M., Ribeiro, M., Manno, L.C.E. and Tarlo, S.M. (2011) Reduction in diisocyanates and non-diisocyanate sensitizer-induced occupational asthma in Ontario. J. Occup. Environ. Med. 53(4), 420-426.

[13] Whittaker, S.G. and Reeb-Whitaker, C. (2009) Characterizing the health and safety needs of the collision repair industry. J. Occup. Env. Hyg. 6, 273-282.

[14] Varma, D.R. and Mulay, S. (2009) Methyl Isocyanate: The Bhopal Gas. Handbook of Toxicology of Chemical Warfare Agents. (2st Edition) Elsevier, Amsterdam. 293–312.

[15] Sorahan, T. and Nichols, L. (2002) Mortality and cancer morbidity of production workers in UK flexible polyurethane foam industry: updated findings, 1958-98. Occup. Environ. Med. 59(11), 751-758.

[16] Carino, M. (1997) Occupational asthma, death and diphenylmethane diisocyanates. Food and Chemical Toxicology. 35(6), 635–636.

[17] Sparer, J., Stowe, M.H., Bello, D., Liu, Y., Gore, R.J. and Youngs, F. (2010) Isocyanate Exposures in Autobody Shop Work: The SPRAY Study. J. Occup. Env. Hyg. 570-581

[18] Roberge, B., Aubin, S., Ostiguy, C. and Lesage, J. (2013) Guide de prévention pour une utilisation sécuritaire des isocyanates. Démarche d'hygiène du travail. RG-764, IRSST (Canada). 82-83.

[19] Roberge, B. and Aubin, S. (2013) Les isocyanates en milieu de travail : évaluation et prévention. IRSST (Canada).

[20] Cetin, M., Sevik, H., and Saat, A. (2017) Indoor air quality: the samples of Safranbolu Bulak Mencilis Cave. Fresen. Environ. Bull. 26, 5965-5970.

[21] Kotzias, D. and Pilidis, G. (2017) Building design and indoor air quality - experience and prospects. Fresen. Environ. Bull. 26, 323-326.

[22] NF X 43-257-. (1988) Air des lieux de travail, Prélèvement individuel de la fraction inspirable de la pollution particulaire (France).

[23] Personal dust sampler CIP 10, (1994) Instruction manuel. ARELCO. Fontenay-sous-bois. France.
[24] Schaeffer, J.W., Sargent, L.M., Sandfort, D.R. and Brazile, W.J. (2013) A comparison of Two Sampling Methods for the Detection of Airborne Methylene Bisphenyl Diisocyanate. J. Occup. Env. Hyg. 10, 213-221.
[25] Puscasu, S., Aubin, S., Van Tra, H. and Gagné, S. (2014) Adaptation of CIP10 for the sampling of 4,4'-methylene diphenyl diisocyanate aerosols. Anal. Methods. 6, 1101-1107.
[26] Courtois, B. (2008) Valeurs limites d'exposition professionnelle aux agents chimiques en France, Aide-Mémoire Technique, ED 984, INRS.
[27] Concentration pondérale d'un aérosol. (2009) Fiche 002. In : MetroPol. Métrologie des polluants. INRS, (www.inrs.fr/metropol/).
[28] Biglari, H., Geravandi, S., Mohammadi, M.J., Porazmey E.J., Chuturkova, R.Z., Khaniabadi, Y.O., Goudarzi, G., Mohammadi, B. and Yari, A.R. (2017) Relationship between air particulate matter and meteorological parameters. Fresen. Environ. Bull. 26, 4047-4056.
[29] Ni, P., Bai, L., Wang, X., Jin, H. and Xi, G. (2018) Effect of window ventilation and air cleaner purification on indoor pm2.5 emission and air exchange rate under haze weather. Fresen. Environ. Bull. 27, 210-214.
[30] Yunlong, H., Yongmei, H. and Fuping, Q. (2011) Effects of air temperature and humidity on particle deposition. Chem Eng Res Des. 89(10), 2063-2069.
[31] Jing, Q., Peccia, J. and Ferro, A.R. (2014) Walking-induced particle resuspension in indoor environments. Atmos. Environ. 89, 464–481.
[32] Schwartz, J. (2004) Air pollution and children's health. Pediatr. 113, 1037-1043.
[33] Stamatelopoulou, S., Saraga, D., Asimakopoulos, D., Vasilakos, C. and Maggos, T. (2017) The link between residential air quality and children's health. Fresen. Environ. Bull. 26, 162-176.
[34] Demange, M., Gendre J.C., Hérvé-Bazin, B., Carton, B. and Peltier, A. (1990) Aerosol avaluation difficulties due to the particle deposition on filter holder inner walls. Ann. Occup. hyg. 34(4), 399-403.
[35] James, H.V. (2005) Health related aerosol measurement: a review of existing sampling criteria and proposals for new ones. J. Environ. Monit. 7, 1037-1053.
[36] Vincent, J.H. (1989) Aerosol Sampling-Science and Practice. J. Wiley & Sons Inc. New York, USA.
[37] Churg, A., Brauer, M., Del Carmen Avila-casado, M., Fourtul, T.I., and Wright, J.L. (2003) Chronic exposure to high levels of particulate air pollution and small airway remodeling. Environ Health Perspect. 111(5) 714-718.
[38] Nikula, K-J., Vallyathan, V., Green, F-H. and Hann, F.F. (2001) Influence of exposure concentration or dose on the distribution of particulate material in rat and human lungs. Environ Health Perspect. 109(4) 311-318.
[39] Zatout, A., Mezdad, A., Ameur lamara, M., Dahleb, M., Tibiche, A., Touahria, G., Fraga, S. and Boudia, H. (2009) Asthme professionnel lié aux isocyanates chez le personnel de l'atelier moussage. ENIEM, Tizi – Ouzou, 8éme Congrès Maghrébin de santé et de sécurité au travail le 5éme Congrès National de STMT, La première rencontre Tuniso - Française de Santé au Travail.
[40] Sabaziotis, V., Galinos, K., Missia, D., Kalimeri, K.K., Tolis, E.I. and Bartzis, J.G. (2017) Indoor air quality in residences at the city of Kozani, Greece: effects of the house location. Fresen. Environ. Bull. 26, 255-262.
[41] Lemiere, C., Ameille, J., Boschetto, P., Labrecque, M. and Pralong J-A. (2012) Occupational Asthma: New Deleterious Agents at the Workplace. Clin Chest Med. 33(3), 519-530.
[42] Tibiche, A. and Zatout, A. (2014) Etude de l'asthme professionnel aux isocyanates dans une usine de fabrication de produits électroménagers à Tizi-Ouzou, Algérie. Revue Française d'Allergologie. 54(3), 285.

Received: **09.11.2017**
Accepted: **10.02.2018**

CORRESPONDING AUTHOR

Hakima Rebbah
Research Unit Materials,
Processes and Environment, UR-MPE,
Faculty of engineering,
University M'Hamed Bougara,
Boumerdes – Algeria

e-mail: rebbah_umbb@yahoo.com

© by PSP Volume 27 – No. 5/2018 pages 2978-2984 Fresenius Environmental Bulletin

STUDY ON IDENTIFICATION TO PATHOGENS OF WOODS CANKER, GENETIC DIFFERENTIATION RESEARCH TO ITS MAIN SPECIES VALSA MALI AND RAPID DETECTION TO PRIMARY INFECTION SOURCE OF *V. MALI* IN XINJIANG

Kaifa Guo, Benchun Xiang, Sifeng Zhao*, Cailan Wu

Key Laboratory at Universities of Xinjiang Uygur Autonomous Region for Oasis Agricultural Pest Management and Plant Protection Resource Utilization, Shihezi University, Shihezi, 832003, China

ABSTRACT

In order to clarify the pathogen species of woods canker of shelterbelt and economic forests in Xinjiang and clarify pathogenicity differentiation and genetic diversity of its main species Valsa mali.

A total of 281 isolates were obtained from woods canker come from 17 kinds of hosts in Xinjiang, all isolates are anamorph, and pathogenicity of these isolated were tested according to Koch's rule. These isolates were identified as 5 species, they are Valsa mali (anamorph:Cytospora mali), Valsa sordida (anamorph: Cytospora chrysosperma), Valsa macolica (anamorph: Cytospora schulzeri), Leucostoma niveum (anamorph: Cytospora nivea) and Cryptosphaeria pullmanensis (anamorph: Cytosporina pullmanensis) respectively. The V. mali and V.sordida are main pathogens of economic forest and shelter forest, respectively.

KEYWORDS:
Xinjiang, Wood canker, pathogen identification, Valsa mali, Rapid detection

INTRODUCTION

The risk for pest and disease damage is related to the probability of occurrence and the behaviour of populations of damaging agents [1-3], which is in turn influenced by the forest stand composition and management. Indeed, the occurrence of most pests and pathogens largely depends on stand density, the presence of host trees, the abundance of non-host trees, and other stand characteristics, such as stand composition and age structure [4,5]. Mixed stands consisting of site-adapted species may be more resistant to pests and diseases compared to monocultures [6,7]. Indeed, a focal tree's vulnerability to predation or parasitism can be altered by the identity, diversity, and abundance of its neighbouring species [8]. This phenomenon, also called associational resistance [9], can be explained by the resource concentration theory [10], i.e., the resources are more concentrated in monocultures and thus more easily found by pathogenic fungi or insect herbivores. Yet, the results of studies on the relation between tree species diversity and crown damage are not consistent and depend on the environmental conditions [11]. In mixed stands, populations of specialized herbivores may be reduced, but generalist herbivores and heteroecious fungal pathogens [12] can be positively affected. Tree species diversity seems to have less effect than tree species composition. For instance, herbivore damage was less when mixed forests were comprised of taxonomically or phylogenetically more distant tree species or when the host tree species were surrounded by a higher proportion of non-host tree species [13]. The associational resistance in a certain neighbourhood may also change through time, e.g., between seasons, from year to year, or as the trees get older [14]. However, most studies on the effect of tree species diversity on the resistance of trees to pests and diseases have been done in mature forests. Only few studies have focused on the young stages of forest development. Yet, the young stages of forest development, especially the particularly vulnerable regeneration stage, are important in determining the character of the trees and the stand in the later stages of forest development [15].

In this study, a wide range of samples were collected from shelterbelts and economic forests in the northern and southern Xinjiang, China. The samples were isolated in the laboratory and their isolates were obtained. The pathogenicity, morphological characteristics, ITS sequence, β-Tubulin sequence Identification. From the perspective of morphology and molecular biology, the species of pathogenic fungi in economic forest and shelter forest in Xinjiang were systematically discussed.

MATERIALS AND METHODS

Rotting samples. (1) economic forest garden: 2012 ~ 2015 in Xinjiang, southern Xinjiang, pear,

walnut, red dates, apricots and other economic trees on the collection of typical rot symptoms bark and dead branches. The main symptoms of the collection of samples: the initial bark surface of the water-like, slightly raised from the spot, with wine distress; late lesions dry shrinkage, the formation of dark brown necrotic lesions; dry spots appear black spots Of the black spots, in the case of wet and rain, easy to produce yellow to red conidia angle. The typical symptoms of decay were easily found at the branches and pruning sites of the trees. The number of samples and isolates collected from the samples was shown in Table 1.

(2) Shelterbelt: Bark and dead branches with typical rot disease symptoms were collected from trees such as poplar, willow, locust, The main symptoms of the sample collection: the initial bark surface reddish brown or yellowish brown, water-like lesions, irregular; late lesions dry shrinkage, the formation of dark brown necrotic lesions; dry spots appear on the lesion Black protruding black spots, in the case of wet and rain, easy to produce yellow to red conidia angle. The typical symptoms of decay were easily found at the branches and pruning sites of the trees. The number of samples and isolates collected from the samples was shown in Table 1.

Medium. Potato dextrose agar medium (PDA): potato 200 g, glucose 20 g, agar powder 15 g, add distilled water 1 000 mL;

Potato Glucose Medium (PD): 200 g of potato, 20 g of glucose, 1 mL of distilled water;

Water agar medium (WA): agar 15 g, add distilled water 1 000 mL.

Drugs and reagents. (1) 1 mol / LTris-HCI buffer (pH 7.5): 121.1 g Tris base was dissolved in 800 mL of distilled water, cooled to room temperature, adjusted to pH 7.5 with concentrated HCl, adjusted to pH 7.5, 1 L, autoclave.

(2) 0.5 mol / L EDTA buffer (pH 8.0): 186.1 g sodium diethoxide diacetate was dissolved in 800 mL of distilled water and adjusted to pH 8.0 with 10 mol / L NaOH under vigorous stirring. To 1 L, autoclave.

(3) DNA extract: 200 mM Tris HCl pH 7.5, 250 mM NaCl, 25 mM EDTA, 0.5% SDS (4) TE buffer (pH 8.0): 0.5 mol / L Tris-HCl (pH 8.0) mol / L EDTA (pH 8.0).

(5) 10x TBE stock solution: 54 gTris, 27.5 g boric acid, 20 mL 0.5 mol / L EDTA (pH 8.0), add distilled water to 1 L. Use 0.5x TBE solution for electrophoresis.

(6) EB solution (10mg / mL): 10 mg ethidium bromide dissolved in 1 mL of distilled water, mixed at room temperature after dark preservation. EB is a teratogenic agent and must be handled with care.

Inoculation with branches. Collection 1 a healthy healthy fresh arrow Yang, Xinjiang Yang, willow, Populus, locust tree, Elaeagnus angustifolia and other protection forest branches, harvest 1 a healthy fresh apple, pear, red dates, walnuts, apricots and other branches of the economic fruit orchard branches, the branches cut into 20 cm small, first rinse with tap water, dry and then used or put 4 ℃ freezer.

Pathogenicity of rotting bacteria. The pathogenicity determination was carried out by in vitro shoot inoculation. The specific steps of pathogenicity determination are:

(1) Select 1 a Health Healthy fresh arrows Yang, Xinjiang Yang, willow, Populus, Huai tree, Elaeagnus angustifolia and other protective forest branches; collection 1 a healthy fresh apple, pear, red dates, walnuts, apricots and other branches of economic forest orchard Branches, the branches cut into 20 cm small section;

(2) branches with alcohol after the surface wipe, with 1.0% HClO soak 5 min, and finally rinse with sterile water, air-dried, with plastic wrap will be moisturizing cotton wool wrapped at both ends of the branches;

(3) The isolates were cultured on PDA medium and cultured in incubator at 28 ℃ for 3 days. After incubation for 3 days,

(4) will be in vitro branches of the skin after scalding, picking the bacteria inoculated in the scald area, with the silk surface close to the site of the burns, and wrapped with plastic wrap;

(5) the seeds after inoculation into a sterile filter paper moisturizing tray, plastic wrap wrapped tray for moisturizing, placed in the light incubator at 26 ℃ to observe the symptoms of disease.

Each strain was inoculated with three branches, each of which was inoculated with two branches. Respectively, at 4 d, 10 d and 20 d after inoculation

Observe, record the incidence of in vitro branches, and the re-separation of the site of the disease.

Morphological identification of pathogens. Observation of culture characteristics. The test strains were inoculated on PDA plates and incubated in an incubator at 28 ℃ for 3 days.

The strains were tested for colony morphology, color, texture, mycelial growth and other traits.

Morphological observation of spheroids. The conidia formed after induction of the in vitro shoots were sliced with slices of slices, crossed and slit as thin as possible, placed on a glass slide containing sterile water, and covered with coverslips. Under the biological microscope, the morphological features of the longitudinal and transverse sections were observed and the size of the conidia was measured and recorded and photographed.

Identification of pathogens. Mycelium culture. The test strains were inoculated on PDA plates and placed in 28 ℃ incubator for 3 days.

Genomic total DNA extraction. (1) scrap a small amount of rotting mycelia to 1.5 mL centrifuge tube, add DNA extract 500 μL, electricity

Grinding the grinding rod, grinding, grinding full, at room temperature for 2 h;

(2) After centrifugation at 12 000 rpm after standing for 6 min, remove the supernatant 350 μL into the new centrifuge tube;

(3) add 350 μL of isopropyl alcohol, mix and let stand for 10 min;

(4) 10 000 rpm centrifugal 10 min, discard the supernatant, add 70% ethanol rinse precipitation 2 to 3 times, 8 000

rpm centrifuged 2 min to remove ethanol, dry for 10 min;

(5) After adding 40 μL TE solution, dissolve at -20 ° C.

rDNA-ITS, β-Tubulin gene. PCR reaction system: PCR TaqMix 12.5 μL, 10 μmol / L ITS1 / Beta-2a 1 μL, 10 μmol / L ITS4 / Beta-2b 1 μL, genomic DNA 0.5 μL, ddH2O 10 μL to final volume 25 μL.

Amplification of ITS fragments: PCR amplification of rDNA-ITS was performed using universal primers ITS1 (5'-TCCGTAGGTGAACCTGCGG-3 ') and ITS4 (5'-TCCTCCGCTTATTGATATGC-3'). The reaction conditions were as follows: denaturation at 94 ℃ for 5 min; denaturation at 94 ℃ for 30 s, annealing at 55 ℃ for 30 s, extension at 72 ℃ for 40 s, and 30 cycles at 72 ℃. After completion of the reaction, the PCR reaction product was detected by 10 g / L agarose gel electrophoresis.

Amplification of the beta-Tubulin fragment: Amplification of the [beta] -tubulin sequence using primers bt-2a (5 & apos; -GTAACCAAATCGGTGCTGCTTTC, -3 & apos;) and bt-2b (5 & apos; -ACCCTCAGTGTAGTGACCCTTGGC-3 & apos; The reaction conditions were as follows: 94 ℃ pre-denaturation 5 min; denaturation at 94 ℃ for 30 s, annealing at 58 ℃ for 30 s, 72 ℃ for 40 s, 30 cycles; After completion of the reaction, the PCR reaction product was detected by 10 g / L agarose gel electrophoresis.

PCR product was purified. PCR products were used to purify the PCR products. The specific steps were as follows:

(1) cut the agar gel gel with the target strip, cut the gel as much as possible, add the sol liquid PG according to the weight ratio of 1: 3 (ie 100 mg glue to 300 μL solution)

(2) 55 ℃ water bath, water bath during the oscillation to help dissolve, so that the plastic block completely dissolved;

(3) The solution was added to the adsorption column of the collection tube while 200 μL of Buffer PS was added and allowed to stand for 5 min

After centrifugation at 12 000 rpm for 2 min, pour the waste liquid and place the adsorption column into the collection tube.

(4) Add 500 μL Buffer PG to the adsorption column, allow to stand for 5 min and centrifuge at 12 000 rpm for 1 min.

To the waste liquid, the adsorption column and then into the collection tube;

(5) Add 600 μL Buffer PW to the adsorption column. After standing for 5 min, centrifuge at 12 000 rpm for 1 min,

(6) repeat step 5;

(7) centrifugation at 12 000 rpm for 2 min to remove residual ethanol;

(8) Place the adsorption column in a new centrifuge tube for 10 min at room temperature to completely dry the ethanol in the adsorption column.

(9) Add 30 μL Buffer EB (Buffer EB pH 8.5, preheated with 50 ° C) at the center of the adsorption column

Set aside for 10 min;

(10) 12 000 rpm centrifugation 2 min, centrifuge tube is purified DNA, stored at -20 ℃ standby.

The purified PCR reaction product was sequenced. Sequence analysis of rDNA-ITS and β-tubulin gene and construction of phylogenetic tree. The ITS, β-Tubulin sequences obtained from each test strain were identified by RTASTn program in GenBank.

Download the homologous sequences separately. ClustalX 2.0 was used to align the sequences, and the data set was manually adjusted with BioEdit 7.0.1 to remove the larger sequences and the missing bases at both ends. Using the MEGA 5 software, the phylogenetic tree was constructed using the maximum parsimony (MP), and the phylogenetic tree was tested by bootstrap. And the branches and branches of the phylogenetic tree were analyzed comprehensively to determine the fungi species represented by the branches, and the species and composition of the tested strains were identified.

RESULTS AND DISCUSSION

Statistics on the Species and Isolated Pathogens of Different Forest Species in Xinjiang economic forest and shelter forest rot disease is more serious, from Xinjiang, north and south Xinjiang collected a total of 17 kinds of forest rot. The isolates were isolated and 321 isolates were isolated. In this paper, 199 isolates were collected from pear trees, apple trees, walnut trees, jujube trees, almonds, almond and almond and other economic forest trees. The isolates were collected and isolated from the trees such

as the arrows Yang, Xinjiang Populus, Populus, Willow, Elm and other shelters Separate 122, see Table 1.

TABLE 1
The isolated result of pathogens of Valsa canker in Xinjiang

Classification	Host	Number of the isolates
Economic forest	Pyrus	103
	Pyrus	12
	Prunus armeniaca	12
	Zizyphus jujube	3
	Juglans	23
	Malus	41
	Amygdalus communis	1
	Prunus L	1
	C*rataegus pinnatifida*	3
Shelterbelt	*Populus euphratica*	14
	Populus nigra L.	35
	Ulmus pumila	9
	Salix matsudana	24
	Morus alba	3
	Sophora japonica	6
	Elaeagnus angustifolia	4
	Populus alba L.	27
Total	17 species	321

Isolation and culture of pathogens of protection forest rot disease. The main afforestation trees of Xinjiang Shelterbelt are Xinjiang Populus, Salisbury, Willow, Elm, Populus, Elaeagnus angustifolia and so on. A total of 122 isolates were isolated from Xinjiang Shelterbelt, of which 108 were rotting strains, and 108 strains were all clonal Cytospora fungi. 108 isolates were identified by morphological and molecular biology as four types: C. chrysosperma (sexual type: V. Sordida), C. mali (sexual type: V. Mali), C. nivea (sexual type: L. Niveum), C. pullmanensis (sexual type: C. pullmanensis). The number of strains was 84, 13, 3 and 8 respectively, accounting for 77.78%, 12.04%, 2.78% and 7.41% of the number of rotting bacteria respectively. The results showed that the main species of rotavirus in Xinjiang were C chrysosperma (sexual type: V. sordida).

Among them, 35 species of V.sordida, C. pullmanensis, V. mali and L. niveum were identified, and the proportion was 81.36%, 10.17%, 5.08% and 3.39% respectively. The results showed that there were four species of V. sordida, C. pullmanensis, V. mali and L. niveum, which were 87.5%, 4.17%, 4.17% and 4.17% respectively. There were 14 strains of ordida, C. pullmanensis and V. mali, which were 78.57%, 7.14% and 14.29% respectively. Six isolates and 1 rotting bacteria were isolated from locust trees and mulberry trees respectively. V. mali.

Isolation and identification of pathogens of economic forest rot disease. A total of 199 isolates were isolated from Xinjiang Orchard, and 173 isolates were identified as rot fungi, and 173 isolates were all clones of Cytospora. Morphological identification identified 173 rot fungi as C. mali, C. chrysosperma, C. sul., C. nivea (sex: L. niveum) were 149, 14, 9 and 1 strains, accounting for 86.13%, 8.09%, 5.20% and 0.58% of the rotting bacteria. Among them, 39 isolates and 114 strains were obtained from apple and pear trees. The main species were V. mali, which accounted for 94.77% of rotting bacteria, followed by V. malicola and V. sordida, accounting for 3.92% and 1.31 % Of the rotting isolates obtained from walnut in southern Xinjiang were identified as V.sordida, and two isolates were obtained from walnut in northern Xinjiang, one from L. niveum and V. sordida. From jujube and apricot 3 isolates and 1 isolate were identified and identified as V. mali. Three strains of rotting bacteria isolated from Hawthorn trees in the middle of Shihezi University were identified as V. malicola.

Pathogenicity test result. The isolates were isolated from the leaves of the trees, such as apple, pear, walnut and other economic trees and arrows, Xinjiang Yang, willow and other protective forest branches, can make inoculated branches of the disease, and appear with the outdoor Symptoms of the same lesion.

Among them, the strains identified on the economic forest were inoculated in the economic forest branches, and the spotted inoculum was expanded and rounded. The lesion is brown, the surface shrinkage, there is distiller's grains taste, at the same time in the inoculation site xylem color brown, inoculated about 20 d, the lesion surface appears black conidia; inoculated pear tree branches, (Figure 1A, B, C), and the black conidia was present at about 20 days after inoculation.

The isolates were isolated from Xinjiang, Salix psammophila, Populus euphratica and Populus euphratica. The fifth day of inoculation began to appear in the watery, slightly oval. Lesions gradually spread along the wound, the lesion surface bark shrinkage. Health at the junction of the health of the organization sometimes cracks, and sometimes there will be a black "line" appears. About 20 days after inoculation, the surface of the lesion has a small black dots, that is, conidia. In the appropriate humidity conditions, there is a yellow curl-like conidia angle overflow (Figure 1D, E, F, G, H).



FIGURE 1
Canker symptoms on stems after inoculation in vitro
Note:A-G. malus, Pyrus, Juglans, Populus alba L., Salix matsudana, Populus euphratica, Elaeagnus angustifolia, Populus nigra L.

Morphological characteristics of different rotting pathogens. Cytospora mali (sexual type is Valsa mali). The colony was randomly arranged on the surface of the colony, white to gray, 0.8 to 2.5 mm in diameter, and yellow conidia at the later stage of growth (Fig. 2A, B). Sub-seat buried in the bark, slightly protruding, dark brown, spherical to ellipsoid, diameter 0.6 ~ 1.2 mm; orifice 1, with the top plate with the high; sporulation body cavity (locule), each cavity has (3.0 ~ 4.0) × (0.75 ~ 1.0) μm (Fig. 3A, B, C). The cells were of the same size as the cells.

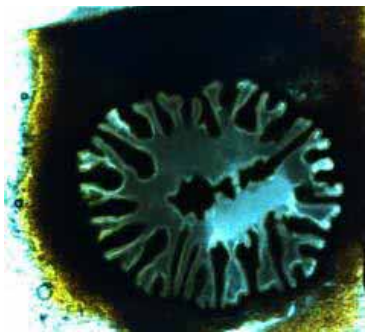


A (front)



B (Back)

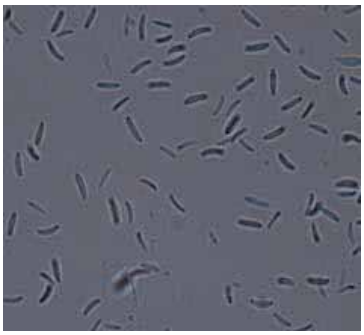
FIGURE 2
Colony characteristics of C. mali (teleomorph: V. mali) on PDA



A



B



C

FIGURE 3
Morphologic characteristics of C. Mali (teleomorph: V. mali)
Note:A –B, horizontal and longitudinal section through conidioamata. C, conidiospore

CONCLUSION

Forest rot disease in Xinjiang is more serious, especially apple trees, pear, walnut and other economic trees and poplar, willow and Populus euphratica and other protective trees, rot disease hinder the healthy development of Xinjiang's agriculture and forestry production. In this study, 321 diseased samples were collected from 17 forest host plants in Xinjiang, and 281 rot pathogens were isolated and identified as all anamorph. Five species of these rot pathogens were identified by morphological characteristics, ITS sequence and β-Tubulin gene sequence. They were Valsamali (Cytospora mali), Valsa sordida (Cytospora chrysosperma), Valsamacolica Schulzeri, Leucostoma niveum (Cyclospora nivea) and Cryptosphaeria pullmanensis (Cyclosporina pullmanensis). Among them, V. mali is the main species that endangered the rot of diseased forest in Xinjiang and V. sordida is the major species that endanger the protection forests in Xinjiang.

The biological characteristics and pathogenicity of V. mali from apple tree in Xinjiang Province showed that the virulence of V. mali different color strains in Xinjiang was different, and the virulence of yellowish and milky white strains was stronger than that of white strains. Pathogenicity of V. mali pathogen in Xinjiang is mainly caused by moderate pathogenicity and weak pathogenicity. Strong virulent strains were not found. Pathogenic differentiation was found in V. mali, a pathogen of apple tree rot in Xinjiang. V. mali can cause pathogenicity on different host trees, and there are also differences in pathogenicity between different host trees. V. mali can cross-infect the host trees. This study revealed the diversity, complexity and pathogenic differentiation of the V. mali population in apple tree rot pathogen in Xinjiang.

ACKNOWLEDGEMENTS

This paper is supported by Youth Science and Technology Innovation Funds of Xinjiang Production and Construction Corps (Grant No. 2014CB002).

REFERENCES

[1] Hambäck, P.A., Inouye, B.D., Andersson, P., Underwood, N. (2014) Effects of plant neighborhoods on plant-herbivore interactions: resource dilution and associational effects. Ecology. 95, 1370-1383.

[2] Hambäck, P.A., Beckerman, A. (2003) Herbivory and plant resource competition: a review of two interacting interactions. Oikos. 1, 26-37.

[3] Jactel, H., Nicoll, B.C., Branco, M., Gonzalez-Olabarria, J.R., Grodzki, W., Långström, B., Moreira, F., Netherer, S., Orazio, C., Piou, D., Santos, H., Schelhaas, M.J., Tojic, K., Vodde, F. (2009) The influences of forest stand management on biotic and abiotic risks of damage. Ann. For. Sci. 66, 1-18.

[4] Barbosa P., Hines, J., Kaplan, I., Martinson, H., Szczepaniec, A., Szendrei, Z. (2009) Associational resistance and associational susceptibility: having right or wrong neighbors. Annu. Rev. Ecol. Evol. Syst. 40, 1-20.

[5] Vehviläinen, H., Koricheva J., Ruohomaki, K. (2007) Tree species diversity influences herbivore abundance and damage: meta-analysis of long-term forest experiments. Oecologia. 152, 287-298.

[6] Jactel, H., Brockerhoff, E.G., Duelli, P. (2005) A test of the biodiversity-stability theory: meta-analysis of tree species diversity effects on insect pest infestations, and re-examination of responsible factors. In: Scherer-Lorenzen, M., Körner, C., Schulze, E.-D. (Eds.) Forest Diversity and Function: Temperate and Boreal Systems. Springer, 235–262.

[7] Liu, Z., Li, H., Liu, K., Yu, H., Cheng, K. (2017) Design of high-performance water-in-glass evacuated tube solar water heaters by a high-throughput screening based on machine learning: A combined modeling and experimental study. Sol. Energy. 142, 61-67.

[8] Spiecker, H. (2003) Silvicultural management in maintaining biodiversity and resistance of forests in Europe—temperate zone. J. Environ. Manage. 67, 55-65.

[9] Underwood, N., Inouye, B.D., Hambäck, P.A. (2014) A conceptual framework for associational effects: when do neighbors matter and how would we know? Q. Rev. Biol. 89, 1-19.

[10] Tahvanainen, J.O., Root, R.B. (1972) The influence of vegetational diversity on the population ecology of a specialized herbivore, Phyllotreta cruciferae (Coleoptera: Chrysomelidae). Oecologia. 10, 321-346.

[11] Root, R. (1973) Organization of a plant-arthropod association in simple and diverse habitats: the fauna of collards (Brassica oleracea). Ecol. Monogr. 43, 95-124.

[12] Koricheva, J., Vehviläinen, H., Riihimäki, J., Ruohomäki, K., Kaitaniemi, P., Ranta, H. (2006) Diversification of tree stands as a means to manage pests and diseases in boreal forests: myth or reality? Can. J. For. Res. 36, 324-336.

[13] Liu, Z., Xu, W., Zhai, X., Qian, C., Chen, X. (2017). Feasibility and performance study of the hybrid ground-source heat pump system for one office building in Chinese heating dominated areas. Renew. Energ. 101, 1131-1140.

[14] Castagneyrol, B., Jactel, H., Vacher C., Brockerhoff, E.G., Koricheva, J. (2014) Effects of plant phylogenetic diversity on herbivory depend on herbivore specialization. J. Appl. Ecol. 51, 134-141.
[15] Montagnini, F., González-Jiménez, E., Porras-Salazar, C., Rheingans, R. (1995) Mixed and pure forest plantations in the humid neotropics: a comparison of early growth, pest damage and establishment costs. Commonw. For. Rev. 74, 306-314.

Received: **09.11.2017**
Accepted: **10.01.2018**

CORRESPONDING AUTHOR

Sifeng Zhao
Key Laboratory at Universities of Xinjiang Uygur Autonomous Region for Oasis Agricultural Pest Management and Plant Protection Resource Utilization,
Shihezi University,
Shihezi, 832003 – China

e-mail: lijiazhuo889@hotmail.com

© by PSP Volume 27 – No. 5/2018 pages 2985-2991 Fresenius Environmental Bulletin

INVESTIGATION OF THE NATURAL CAT AND DOG DETOX PRODUCTS ON RATS

Musa Yavuz[1,*], Elif Rabia Sanli[2]

[1]Suleyman Demirel University, Faculty of Agriculture, Animal Science Department, Isparta, Turkey
[2]Suleyman Demirel University, Graduate School of Natural and Applied Science, Isparta, Turkey

ABSTRACT

Pets are constantly taking toxic substances from the air, soil, water or feed. These toxic substances affect all organs and cause many important health problems. These toxins need to be removed from the body of the animals. Detoxification (detox) is a process of disposing of toxic substances by converting them into non-toxic substances. There are new detoxification products for cats and dogs made from aromatic plant extracts. There are many herbal products used in the traditional medicine field and considered to have detox effect, but these products may contain some substances that may have adverse effects also. The purpose of this project was to investigate the safety of these products on animal health. In this experiment, forty rats were randomly assigned to five groups (control, 20% cat detox, 100% cat detox, 20% dog detox, 100% dog detox). Water intake was increased 7-11% in detox groups when compared to control group except 20% cat detox group which was similar to the control group. The rats were healthy from the beginning to the end and animals had no complication. According to our result, 100% cat detox or 100% dog detox products could be consumed daily up to 100% without any adverse affect.

KEYWORDS:
Herbal detox, additives, cat, dog

INRODUCTION

Pets are constantly taking toxic substances (pesticides, detergents, dyestuffs, etc.) from the air, soil, water, dust or food, and these toxic substances affect all organs in the body especially the skin, liver and kidneys [1]. Detoxification (detox) is a process of disposing of toxic substances by converting them into non-toxic substances. Detox processing is a complex process in which many enzymes actively participates [2]. The most important organs for the detox process are the liver and intestines. There are two phases during the detox process [3]. In phase I, cytochrome P450 enzymes, which contain many enzymes, play an active role [3, 2]. These enzymes activate toxic substances by subjecting them to different chemical reactions such as oxidation and hydrolysis. In addition, these reactions carry the resultant free radicals which have carcinogenic properties. In the phase II., activated chemicals become harmless and water-soluble by binding to substances such as glucuronic acid, sulphate, glycine, glutamine, taurine, ornithine and glutathione in the liver with different enzymes after that they are excreted through urine or biliary bile ducts [3]. There is a need for nutrients (amino acids, vitamins, minerals and plant active glycosides and phalavonoids, etc.) that will accelerate detoxification if intoxicants are taken or accumulated intensively [2].

There are new products made from additives containing aromatic plant extracts for cats and dogs. There are many herbal products used in the traditional medicine field and considered to have detox effect, but these products may contain some substances that may have adverse effects also. The purpose of this project to investigate safety of these product uses on animal health.

MATERIALS AND METHODS

Detox Products. *heyLove Cat Detox* and *heyLove Dog Detox* products provided by ATY Grup Yem San. ve Tic. A.Ş., Istanbul, Turkey. *heyLove Cat Detox* contains aqueous extracts of *Valerian officinalis* root, *Carlina Marianum* root, *Nasturtium officinale, Arctium lappa, Linum usitatissimum, Rheum rhabarbarum, Ulmus, Taraxacum officinale, Equisetum telmateia, Achillea millefolium* and *Astragalus Canadensis*, and *heyLove Dog Detox* contains aqueous extracts of *Lens cullinaris, Carlina Marianum root, Nasturtium officinale, Arctium lappa, Linum usitatissimum, Rheum rhabarbarum, Ulmus, Taraxacum officinale, Equisetum telmateia, Gypsophila paniculata and Astragalus canadensis*.

Animals and Groups. Twenty four weeks old, fourty male Wistar albino rats (343.8±47 g; Mehmet Akif Ersoy University Veterinary Faculty Laboratory Animal experiment Unit, Burdur, Turkey) were housed (22 C, with lights off for 12 h) in a fully accredited Animal Care facility, approval of the

Mehmet Akif Ersoy University ethics committee protocols no: 93773921-237. In Experiments, forty rats were randomly assigned to twenty shoebox cages and each cage had two rats. Rats were provided with wood shaving bedding in the shoebox cages. Cages were changed weekly for cleaning purposes. Individual rats were identified using indelible red and blue mark on tail. They were maintained ad libitum on standard laboratory chow with water and water additives. The standard rat pellet feed were purchased from commercial company (Korkuteli Yem Gıda Santic A.Ş., Antalya, Turkey). The rat feed nutrition were analyzed. Cat detox and Dog detox additives and commercial standard water was used instead of tap water for animal water requirements. Water was given to rats with the measurable bottle. Water and feed consumption were checked daily and animals were weighted weekly. Feed and water intakes' values were converted to g/ 100 g body weight per day to minimize the effect of the animal weights.

Each cage randomly assigned to five groups; a) Control group received only water, b) 20% Cat Detox group received 80% water and 20% Cat Detox, c) 100% Cat Detox received 100% Cat Detox, d) 20% Dog Detox group received 80% water and 20% Dog Detox, e) 100% Dog Detox received 100% Dog Detox. The groups were designed based on the products recommended level and the highest level to see whether it has any adverse effect on the animals.

Blood Sampling. An adult rat has a circulating blood volume of about 6% of the body weight and up to 10% of the circulating blood volume could be taken on a single occasion from a normal healthy animal without any adverse effect [4]. Rats were sedated with isoflurane. At Day 1 and Day 56, blood was collected from cardiac puncture for serum chemistry. Day 28, one ml of blood was collected from retro-orbital sinus for serum chemistry. Urea, Creatinine, Alanine aminotransferase (ALT) and Aspartate aminotransferase (AST), Gamma-glutamyl transferase (GGT), Glucose, Lactate dehydrogenase (LDH) were analyzed [5] at Mehmet Akif Ersoy University, Veterinary Faculty Laboratory, Burdur, Turkey.

Necropsy and Pathological Test. Under anesthesia euthanasia was performed by cervical dislocation method. Euthanized animals were immediately subjected to necropsy to check the anatomical location of the abdominal, thoracic and pelvic cavities and organs inside. Assessment of liver tissues was based on the evaluation criteria of [6]. When kidney tissues are examined; Mohan [7] considered the criteria for a study of renal toxic injury.

Statistics. Data were analyzed by using a commercially available statistical software package [8]. The means of the groups were compared through Duncan's multiple range tests after all data were subjected to Analysis of Variance (one way-ANOVA). The means of two groups were compared by Paired-sample t-test. $P<0.05$ were regarded as statistically significant.

RESULTS AND DISCUSSION

Rats were fed a diet containing soybean meal, corn, barley, alfalfa, wheat bran, full fat soybean, vegetable oil, marble dust, di calcium phusphate, pellet binders, toxin binders, minerals, D.L. Methionin and vitamin E. The rat feed was standard diet for the Animal Care facility which is purchased from private company with 90% DM, 24% CP, 6.84% CF and 4.33% EE.

The rats were healthy from the beginning to the end. Four animals were lost in the first day after the cardiac puncture blood collection. The animals were replaced next day. Later on, only two animals were lost with normal cause of death. There were no sign of disease or complication on them.

The rats body weight gain, feed and water intake were shown in Table 1, 2 and 3. The body weights' differences were not significant between the groups or within the groups. Average rats' body weight gain was 0.31 g/day. The body weight gain should be small because the selected rats were mature and they were fed with high protein diet.

Rats had ad-libitum feed and water. Feed and water intake may be effected by age, health status, sex, weather etc. In this situation, the treatment should affect the feed and water intake because all the animals had similar condition. In general rats can eat feed 5 g/100 g body weight/day and drink water 10 ml/100 g body weight/day [4]. There were no differences among the groups for feed intakes. Cat detox 20% group had the highest 9.88±3.23 g feed intake on the other hand dog detox 20% group had the lowest 7.65±0.83 g feed intake.

There were differences ($P<0.05$) among the groups for water intake at 42 days (Table 3). 100% cat detox and dog detox 20% group had the highest 12.4±1.33 and 13.3±1.80 ml water intake, respectively. On the other hand control and 20% cat detox group had the lowest water intake. All the detox groups had higher water intake levels except 20% cat detox group when compared to control group. At day 56, water intake levels were not significant ($P<0.055$). The detox products increased water intake of the rats except 20% cat detox group. First 28 days, water consumption was higher for all the groups after that it was lowered. Water intake seems to be effected by the blood collection at 0 and 28 days for all the groups. 100% cat detox group had higher water intake and water intake values were not different within the group. Water consumption usually effected by the feed intake, temperature, and an-

imal metabolism. Since decreased water intake lowers the feed intake and general health and animal performance for animal health. The results of 100% detox groups shown that animals consumed detox products without decreasing body weight gain, feed intake and water consumption throughout the whole research.

TABLE 1
Rat Live Body Weight Measurement for All the Groups

	Groups					
Days	Control	20% Cat detox	100% Cat detox	20% Dog detox	100% Dog detox	
7	349±61.50	346±50.71	333±56.42	347±48.78	344±20.69	NS
14	358±59.75	350±50.27	351±53.01	356±48.00	354±17.22	NS
21	358±56.01	346±44.78	348±51.87	353±33.88	355±22.55	NS
28	364±58.12	350±45.42	354±50.63	358±33.61	360±25.44	NS
35	376±58.79	362±45.11	365±53.50	364±39.63	368±27.11	NS
42	378±58.14	363±46.11	370±52.15	366±37.14	374±23.06	NS
49	380±58.42	366±41.51	375±51.29	364±37.13	371±27.52	NS
56	380±56.67	370±40.34	383±49.41	367±34.53	377±26.90	NS
Mean Value	368±56.22	357±43.59	360±51.27	359±37.84	363±25.18	
	NS	NS	NS	NS	NS	

NS= Not significant.

TABLE 2
Rat Feed Intake Levels (g/ 100 g Body Weight Per Day) for All the Groups

	Groups					
Days	Control	20% Cat detox	100% Cat detox	20% Dog detox	100% Dog detox	
7	7.94±1.32	12.3±4.69	8.93±1.11a.b	7.06±1.19	8.13±1.69	NS
14	7.51±1.19	11.9±4.21	9.58±1.37a.b	7.76±0.68	8.45±1.73	NS
21	9.06±1.07	10.8±3.56	9.62±0.89a.b	8.38±1.06	8.98±1.56	NS
28	8.84±0.82	10.8±2.71	9.92±1.99b	8.44±0.68	9.01±0.98	NS
35	8.09±0.99	8.41±2.54	8.71±1.13a.b	7.50±0.54	8.07±1.26	NS
42	8.00±1.39	8.41±2.65	7.91±0.31a	7.65±0.54	8.18±0.95	NS
49	7.59±0.75	8.13±1.09	7.82±0.22a	7.05±0.49	7.63±0.67	NS
56	7.46±0.53	8.34±2.25	7.88±0.32a	7.31±0.43	8.22±1.08	NS
Mean Value	8.06±1.08	9.88±3.23	7.91±0.35	7.65±0.83	8.35±1.22	
	NS	NS	P<0.05	NS	NS	

NS= Not significant. [a,b,c] within the column scientifically significant at P<0.05.

TABLE 3
Rat Water Intake levels (g/ 100 g Body Weight Per Day) for All the Groups

	Groups					
Days	Control	20% Cat detox	100% Cat detox	20% Dog detox	100% Dog detox	
7	bc12.4±2.03	abc12.4±0.39	12.9±0.98	12.9±0.54	bc13.9±0.49	NS
14	bc12.6±0.65	bc12.7±0.60	14.0±1.32	13.1±0.94	c14.5±1.04	NS
21	c13.6±1.18	c13.3±0.94	14.4±1.00	14.1±1.14	c14.4±1.53	NS
28	c13.4±0.55	c13.6±1.46	14.4±1.20	14.5±1.85	bc13.8±1.15	NS
35	ab11.7±0.87	abc12.0±1.16	12.8±2.53	13.5±1.39	ab12.1±1.49	NS
42	ab11.0±0.72A	a10.7±0.95A	12.4±1.33AB	13.3±1.80B	a11.8±0.56AB	P<0.05
49	ab11.4±0.72	ab11.3±0.76	13.0±1.39	12.7±1.42	a11.6±1.91	NS
56	a10.7±0.47	a10.8±1.35	12.0±0.26	12.9±1.39	a11.8±1.26	NS
Mean Value	12.1±1.36	12.0±1.41	13.2±1.49	13.4±1.34	13.0±1.61	
	P<0.01	P<0.01	NS	NS	P<0.01	

NS= Not significant. [a,b,c] within the column scientifically significant at P<0.05 or P<0.01. [A,B,C] within the line scientifically significant at P<0.05 or P<0.01.

TABLE 4
Rat Serum Urea Levels During Different Time Periods

	Control	20% Cat detox	100% Cat detox	20% Dog detox	100% Dog detox	
Days			Urea (*10.7-22 mg/dL)			
0	42.13±5.57	40.57±4.75	42.00±3.46	42.50±7.78	43.00±4.14	NS
28	42.88±3.76	41.57±3.26	42.00±3.79	41.13±1.73	42.38±3.81	NS
56	41.14±6.39	40.15±5.34	44.00±3.83	40.50±4.84	43.43±4.04	NS
Mean Value	42.09±4.98	40.76±4.34	42.77±3.64	41.37±5.21	42.91±3.84	
	NS	NS	NS	NS	NS	

NS= Not significant. *23-47 weeks of age male rats' serum chemistry [9].

TABLE 5
Rat Serum Creatinine Levels During Different Time Periods

Days	Control	20% Cat detox	100% Cat detox	20% Dog detox	100% Dog detox	
			Creatinine (*0.5-0.8 mg/dL)			
0	b0.54±0.04	b0.53±0.03	b0.53±0.04	ab0.51±0.04	a0.51±0.02	NS
28	b0.54±0.03	b0.54±0.02	b0.55±0.02	b0.54±0.02	b0.54±0.03	NS
56	a0.48±0.03ABC	a0.46±0.02A	a0.47±0.02AB	a0.49±0.03BC	a0.50±0.02C	P<0.05
Mean Value	0.52±0.04	0.51±0.04	0.51±0.04	0.52±0.03	0.51±0.03	
	P<0.01	P<0.01	P<0.01	P<0.05	P<0.01	

NS= Not significant. ^{a,b,c} within the column scientifically significant at P<0.05 or P<0.01. ^{A,B,C} within the line scientifically significant at P<0.05 or P<0.01. *23-47 weeks of age male rats' serum chemistry [9].

Blood parameters. The serum urea levels are shown in Table 4. The normal serum urea levels should be 10.7-22 mg/dL. Our results were two times higher than maximum normal blood level. Feed crude protein level (26%) was higher for this age group. Over all the groups were similar for the blood urea levels.

It has been reported that increases in serum creatinine levels are associated with renal failure, heart failure, obesity, and that their decline is not a clinical etiology. While the values in the study were within normal limits, time-dependent intra-group differences were determined. On day 56, when compared to day 0, the values decreased over the time (Table 5). At day 0, blood was collected from heart of the animals. This may have been the reason for higher creatinine levels at 0 day.

Studies have reported that stress first affects the heart, stomach, lungs and kidneys as well as the liver. Increases in liver enzyme levels associated with the stress have been shown. Additional AST is released into the bloodstream, higher AST shows that a body tissue or an organ (the heart/ liver) is diseased/ damaged. When the serum AST and ALT levels were evaluated, it was found that all the values were in the normal limits and there was no significant difference between the groups on the days 0, 28 and 56 (Table 6. and 7.). Significant differences within the groups due to sampling days were observed. At the 0 day, AST level was higher because the blood was collected with cardiac puncture from rat heart. The second time, the AST levels were within the range because blood was collected from retro-orbital sinus. The decrease in intake values at 28th and 56th days may be related to the decrease in stress during manipulation of animals, the increase in experience of working team over time, and the adaptation of animals to handlers.

When the serum GGT levels were evaluated, it was found that all the values (1.38-2.88 IU/L) were in the normal limits (0.0-3.0 IU/L) and there were no significant difference between the groups on the days 0, 28 and 56.

At day 0, between the groups glucose levels had no difference (P<0.051) in Table 8. When the serum glucose levels were evaluated, there were significant differences between the groups on the days 28 and 56. The dog detox 20% group had the highest 161.71±25.23 mg/dL glucose levels. On the other hand glucose levels were different between dog detox 20% group and dog detox %100 group. Over all animals glucose levels were seem to be high or in a border level (92-138 mg/dL). All the animals were treated humanly and isoflurane was used lower the pain during handling; however, animals may have stressed out. As we know that stress can increase the levels of cortisol which can make blood sugar rise. When we take differences between 0 and 56 day values of all the groups, control, 20% cat detox, 100% cat detox, 20% dog detox and 100% dog detox had 19, -6, 4, 5 and -7 mg/dL differences, respectively. It seems to be detox groups were less affected by the stress.

TABLE 6
Rat Serum AST Levels During Different Time Periods

Days	Control	20% Cat detox	100% Cat detox	20% Dog detox	100% Dog detox	
			AST (*57-144 IU/L)			
0	c135.03±17.85	b136.76±35.39	b160.16±39.59	b161.86±54.62	b134.0±27.68	NS
28	b108.00±20.61	a115.50±16.51	a104.46±10.15	a116.82±10.42	b118.20±19.39	NS
56	a87.41±11.37	a82.39±12.28	a100.84±34.77	a113.62±34.65	a94.46±17.33	NS
Mean Value	107.89±25.11	111.55±32.07	117.8±38.27	129.42±41.39	114.81±26.30	
	P<0.01	P<0.01	P<0.01	P<0.05	P<0.01	

NS= Not significant. [a,b,c] within the column scientifically significant at P<0.05 or P<0.01. *23-47 weeks of age male rats' serum chemistry [9].

TABLE 7
Rat Serum ALT Levels During Different Time Periods

Days	Control	20% Cat detox	100% Cat detox	20% Dog detox	100% Dog detox	
			ALT (*26-97 IU/L)			
0	75.38±11.82	b76.38±13.64	a83.00±10.88	75.00±11.78	b75.50±13.64	NS
28	68.00±9.89	b74.57±11.96	ab75.29±6.45	76.13±9.40	ab71.75±11.42	NS
56	60.38±13.04	a53.71±11.10	b67.57±8.30	63.75±13.26	a58.88±14.41	NS
Mean Value	67.91±13.04	68.59±15.71	75.28±10.50	71.47±12.47	68.70±14.57	
	NS	P<0.01	P<0.05	NS	P<0.05	

NS= Not significant. [a,b,c] within the column scientifically significant at P<0.05 or P<0.01. *23-47 weeks of age male rats' serum chemistry [9].

TABLE 8
Rat Serum Glucose Levels During Different Time Periods

Days	Control	20% Cat detox	100% Cat detox	20% Dog detox	100% Dog detox	
			Glucose (*92-138 mg/dL)			
0	139.00±20.70b	b150.88±16.18	130.14±19.46	164.62±29.05	b154.12±22.17b	NS
28	ab135.62±15.0AB	a128.86±12.68AB	139.00±14.54BC	151.75±17.38C	a120.75±11.41A	P<0.01
56	b157.67±13.77BC	ab144.43±16.40AB	134.29±12.16A	169.00±27.62C	b146.71±14.99AB	P<0.05
Mean Value	142.86±18.74	141.82±17.30	134.65±15.06	161.79±25.23	140.26±21.92	
	NS	P<0.05	NS	NS	P<0.01	

NS= Not significant. [a,b,c] within the column scientifically significant at P<0.05 or P<0.01. [A,B,C] within the line scientifically significant at P<0.05 or P<0.01. *23-47 weeks of age male rats' serum chemistry [9].

TABLE 9
Rat Serum LDH Levels During Different Time Periods

Days	Control	20% Cat detox	100% Cat detox	20% Dog detox	100% Dog detox	
			LDH (*105-652 mg/dL)			
0	b1580.8±513.8	1351.0±736.7	b1667.0±189.2	1430.0±809.0	1150.8±336.6	NS
28	a781.50±243.68	758.71±214.37	a655.86±348.49	698.57±203.35	862.12±333.64	NS
56	a1062.60±354.30	753.67±423.45	a538.83±229.68	920.88±491.21	692.00±413.17	NS
Mean Value	1101.1±479.30	964.50±563.74	938.21±571.22	1012.2±611.12	887.90±391.09	
	P<0.01	NS	P<0.01	NS	NS	

NS= Not significant. [a,b,c] within the column scientifically significant at P<0.01. **23-47 weeks of age male rats' serum chemistry [9].

When the serum LDL levels were evaluated, it was found that all the values were over the normal limits at day 0 and there were no significant difference between the groups on the days 0, 28 and 56 (Table 9.). At the 0 day, LDH levels were higher because the blood was collected with cardiac puncture from rat heart and also certain medications (alcohol, anesthetics, aspirin) may raise LDH levels [10]. The animals were sedated anesthetics (isoflurane) with longer time in first blood collection and less in the second time. The results of the LDH levels were higher at 0 days than 28 days. Rats' complete blood counts (CBC) results were within the range of normal blood parameters and were similar between the groups.

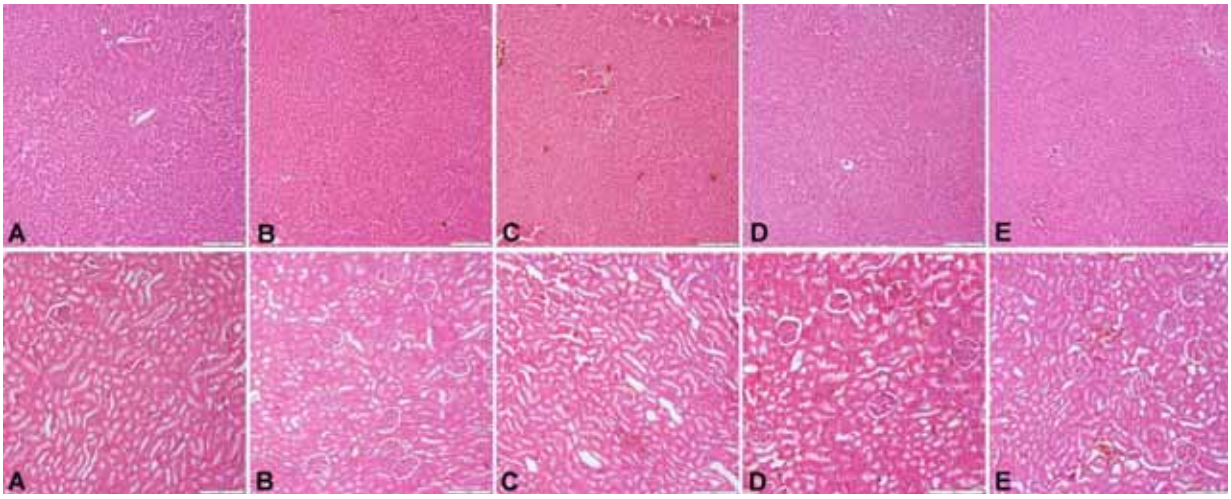


FIGURE 1
Rat Liver and Kidney Tissues Pictures for All Groups
First line shows liver tissues and second line shows kidney tissues. A: Control, B: 20% Cat detox, C: 100% Cat detox, D: 20% Dog detox and E: 100% Dog detox

Pathological Test Results. No visible pathologic disorder was observed in liver and kidney tissues due to color, shape size and cross-section of the rats' organs in Figure 1. Liver tissues were compared with the control group, taking into account all evaluation criteria. None of the study groups had any pathologic status in the liver. Fatty liver (Steatozis) was not encountered in degenerative and toxic conditions. These data were supported by the Oil Red - O dye used in the determination of fat vacuoles in tissues. The findings of mild dissociation and passive convulsions in the remnant cords seen in some animals were not considered because they were considered to be artefacts formed by the anesthetic agents used during euthanasia. No significant pathologic findings were found in kidney tissue that could document damage when compared with the control group according to the determined criteria.

CONCLUSION

Consumption of cat detox and dog detox products had no adverse effect on body weight gain, feed intake and water intake of the rats. Water intake was increased 7-11% in detox groups when compared to control group, except 20% cat detox group which was similar to the control group.

The research showed that blood parameters were not affected by the treatments; however, some blood parameters were changed because of the handling, management procedure and the diet. The rats' blood collection was made with cardiac puncture which is similar to surgery. This affected animal blood parameters significantly.

No visible pathologic disorder was observed in liver and kidney tissues due to color, shape, size and cross-section of the rats' organs among the groups.

The rats were healthy from the beginning to the end and animals had no complication. According to our results, 100% cat detox or 100% dog detox products could be consumed daily up to 100% without any adverse effect by the animals. Further investigation is needed to see effect of detox products in different situations of the animals.

ACKNOWLEDGEMENTS

We would like to thank to people who helped (Vet. Zeki EROL, Phd. Student Vet. Aysegül AVSAR for taking care of the animals, Prof. Dr. Ozlem OZMEN and Assoc. Dr. Zafer OZYILDIZ for pathological examination and Prof. Dr. Metin SEZER for statistical analyses) in this research. This research was part of the master thesis supported by ATY Grup Yem San. ve Tic. A.Ş., Istanbul, Turkey.

REFERENCES

[1] Rosenberg, J., Nicas, M. and Yomashiro, Y. (2016) Understanding Toxic Substances. University of California, Davis.
[2] Liska, D.J. (1998) The Detoxification Enzyme Systems. Alternative Medicine Review. 3(3), 187-198.
[3] Percival, M. (1997) Phytonutrients & Detoxification. Clinical Nutrition Insights. 5(2), 1-4.
[4] Perret-Gentil, M.I. (2016) Rat Biomethodology. Laboratory Animal Resources Center, The University of Texas at San Antonio.
[5] Gesan Chem 200. (2016) Gesan Chlinical Chemistry Autoanalyzer. Gesan Production, Campobello di Mazara (TP) ITALY

[6] Matsuzawa, N., Takamura, T., Kurita, S., Misu, H., Ota, T., Ando, H., Yokoyama, M., Honda, M., Zen, Y., Nakanuma, Y., Miyamoto, K. and Kaneko, S. (2007) Lipid-Induced Oxidative Stress Causes Steatohepatitis in Mice Fed an Atherogenic Diet. Hepatology. 46(5), 1392-403.
[7] Mohan, I.K., Khan, M., Shobha, J.C., Naidu, M.U.R., Prayag, A., Kuppusamy, P. and Kutala, V.K. (2006) Protection against cisplatin-induced nephrotoxicity by Spirulina in rats. Cancer Chemother Pharmacol. 58, 802–808.
[8] IBM Corp. Released (2013) IBM SPSS Statistics for Windows, Trial Version 22.0. Armonk, NY: IBM Corp. SPSS.
[9] Giknis, M.L.A. and Clifford, C.B. (2006) Clinical Laboratory Parameters for Crl:CD(SD). Charles River Laboratories.
[10] Pagana, K.D. and Pagana, T.J. (2014) Mosby's Manual of Diagnostic and Laboratory Tests. Fifth Edition. Mosby, an imprint of Elsevier Inc. St. Louis, Missouri.

Received: **10.11.2017**
Accepted: **24.01.2018**

CORRESPONDING AUTHOR

Musa Yavuz
Suleyman Demirel University,
Agricultural Faculty,
Animal Science Department,
East Campus 32260 Isparta – Turkey

e-mail: musayavuz@sdu.edu.tr

© by PSP Volume 27 – No. 5/2018 pages 2992-3005 Fresenius Environmental Bulletin

SYNTHESIS, STRUCTURE INVESTIGATION, SPECTRAL PROPERTIES AND IN VITRO ANTIOXIDANT EVALUATION OF NEW 1-(3-METHYL-3-MESITYL)-CYCLOBUTYL-2-(5-THIOPHEN-4-ETHYL-2H-[1,2,4]TRIAZOL-3-YLSULFANYL)-ETHANONE

Cahit Orek[1,2], Kamiran Sarac[3], Akif Evren Parlak[4], Pelin Koparir[5], Semra Turkoglu[6,*], Metin Koparir[1]

[1]Firat University, Faculty of Science, Department of Chemistry, 23119, Elazig, Turkey
[2]Kastamonu University, Research and Application Center, 37100, Kastamonu, Turkey
[3]Bitlis Eren University, Faculty of Architecture Engineering, Department of Metallurgy and Material Engineering, 43400, Bitlis, Turkey
[4]Firat University, Environmental Protection and Control Program, Keban Vocational School of Higher Education, 23100, Elazig, Turkey
[5]Department of Chemistry, Forensic Medicine Institute, TR-44000, Malatya, Turkey
[6]Firat University, Faculty of Health Sciences, 23119, Elazig, Turkey

ABSTRACT

The spectral analysis of 1-(3-Methyl-3-mesityl)-cyclobutyl-2-(5-thiophen-4-ethyl-2H-[1,2,4] triazol-3-ylsulfanyl)-ethanone **(3)** is carried out using the FT-IR, FT-NMR and UV–Vis spectra of the compound with the help of quantum computations by density functional theories. The recording of the FT-IR (4000 – 400 cm^{-1}) spectra is done in solid phase, while the ^{1}H and ^{13}C NMR spectra and the UV spectrum (200-400 nm) are respectively recorded in the DMSO phase and the ethanol phase. According to the generated results, the reproduction of the crystal structural parameters and theoretical vibrational frequencies can be successfully achieved by the refined geometries. Furthermore, there is consistency between the ^{1}H and ^{13}C NMR chemical shift values and the data from the experiment. The different conformers of the compound and their minimum energies are studied by potential energy surface scan, using DFT//B3LYP/cc-pVDZ method. As the energy difference between the conformers was very small. To account for the chemical reactivity and site selectivity of the molecules, molecular electrostatic potential (MEPS) map has been plotted. The in vitro antioxidant activity of the newly synthesized compound was measured and found to exhibit significantly higher antioxidant activity.

KEYWORDS:
1,2,4-Triazole, FT-IR, DFT, Antioxidant activity, Fukui descriptors

INTRODUCTION

1,2,4-triazole is a significant nucleus found in many compounds. More than 35 compounds having this nucleus are presented into the market. 1,2,4-triazole nucleus, which is stable to metabolism, functions as an important pharmacophore by interacting at the active site of a receptor as hydrogen bond acceptor and as a donor. Its polar nature allows the triazole nucleus to increase the solubility of the ligand and the pharmacological profile of the drug can be considerably improved by the triazole. According to the literature survey, based on the type of substituent, 1,2,4-triazole derivatives possessing diverse biological activities, such as antimicrobial [1, 2] and antitumor [3] properties. The other ones also show anti-inflammatory [4], antioxidant [5], anticonvulsant [6], antiviral [7] and analgesic [8] activities. On the other hand, cyclobutane derivatives can be used as starting materials for the synthesis of both acyclic and cyclic systems. Derivatives of 3-substituted cyclobutanecarboxylic acid exhibit anti-inflammatory and antidepressant activity [9, 10] as well as liquid crystal properties [11].

Density functional theory (DFT) is widely used to study electronic properties, molecular structure, chemical reactivity and hydrogen bonding of pharmaceutical compounds [12–14]. Among all of the approaches, the exchange–correlation energy is the major point in the DFT; accordingly, the approximate nature of the exchange–coordination energy functional has a straight effect on the certainty of DFT. The DFT procedures are imaginative perspective of the exchange–coordination energy. Hence, in the many theoretical researches DFT methods were regularly used [15, 16].

In this study, we synthesized 1-(3-Methyl-3-mesityl)-cyclobutyl-2-(5-thiophen-4-ethyl-2H-[1,2,4]triazol-3-ylsulfanyl)-ethanone(**3**) and tried to examine the energetic and structural properties of 1,2,4-triazole compound, based on density functional theory calculations. Also, it is very useful to refer to a comparison of the theoretical and experimental spectra in order to make correct assignments

and understand the basic c.s.-molecular structure relationship. Besides the characterization of the title compound, the antioxidant activities of the 1-(3-Methyl-3-mesityl)-cyclobutyl-2-(5-thiophen-4-ethyl-2H-[1,2,4]triazol-3-ylsulfanyl)-ethanone, was investigated.

EXPERIMENTAL

Synthesis and physical properties. The Fourier transform infrared (FT-IR) spectra were recorded with Perkin-Elmer spectrum one FT-IR spectrophotomer. Electrotermal 9100 was used to determine the melting point. The hydrogen nuclear magnetic resonance (^{1}H-NMR) and carbon-13 nuclear magnetic resonance (^{13}C-NMR) spectra were taken on Bruker ascend 400 NMR spectrometer operating at 400 MHz for ^{1}H and 100 MHz for ^{13}C NMR compound were dissolved in deuterated dimethyl sulfoxide (DMSO-d_6) and chemicals were purchased from Merck. The ultraviolet (UV) spectrum of the compound was recorded on a Schimadzu UV-1700 spectrometer in ethanol solvent. The reactions for the synthesis shown in Fig. 1.

For the synthesis **3**, a solution of 0.445 g (2 mmol) of 2-chloro-1-(3-Methyl-3-mesityl-cyclobutyl)-ethanone was dissolved in 30 mL of dry acetone containing 2 mmol K_2CO_3. To this solution, 0.421 g (2 mmol) of 4-ethyl-5-(2-thienyl)-2,4-dihydro-3H-1,2,4-triazole-3-thione in 20 mL dry acetone was added dropwise in 1h period at room temperature with stirring. The resulting solid was collected by filtration, dried and recrystallized from ethyl alcohol. Yield 70%; m.p. 120-122 ºC.

Computational methods. Becke's three parameter technique was combined with the Lee, Yang and Parr non-local functions to create a functional approach (B3LYP) [17, 18] that was applied alongside the cc-pVDZ [19, 20] basis set to optimize the geometry of **3** whilst avoiding symmetry restrictions in the potential energy surface (PES). The optimized geometry used in determining the vibrational IR frequency was at an identical theoretical level. For purposes of stimulation of the UV-Visible spectrum, the technique of time dependent-DFT (TD-DFT) [21, 22] was used within the context of B3LYPat the geometry of **3** that had been previously subjected to optimization. Furthermore, the combined approach of B3LYP and cc-pVDZ enabled the use of the method of gauge independent atomic orbital (GIAO) to determine the ^{1}H-NMR chemical shifts. The impact of solvent in NMR analyses was taken into account in the polarizable continuum model developed by Tomasi and colleagues [23]. The programs Gaussian 09W [24] and Gauss-View molecular visualization were used to conduct every calculation [25].

DPPH free radical scavenging activity. The free radical scavenging activity of the compounds was determined with a small modification according to the Blois method (1958) using 1,1-diphenyl 2-picryl hydrazyl (DPPH) [26]. The principle of method is based on the reduction of 1,1-diphenyl 2-picryl hydrazyl radical (DPPH$^{\cdot}$) which is colored free radical of free radical pickers. DPPH$^{\cdot}$is a stable red free radical. When antioxidant compounds eliminate free radicals, the color turns from red to yellow. The decrease in the absorbance of the reaction mixture at 517 nm indicates the increased antioxidant activity in the free radical scavenging activity. Reagents used are: 0.1 mM DPPH$^{\cdot}$ (prepared in ethanol); α-tocopherol 1 mg/mL; Butylhydroxyanisole (BHA) 1 mg/mL; Butylhydroxytoluene (BHT) (1 mg/mL).

In the study, the synthesized compound was dissolved in ethyl alcohol as 1 mg / mL. The standard was dissolved in ethanol again as 1 mg/mL. The test compound and standards were put into test tubes at 50, 100, 250 µg/ml, respectively and completed with pure ethanol to give a total volume of 3 ml. Then 1 mL from the stock DPPH$^{\cdot}$solution was added to each sample tube. It was incubated in 30 minutes room temperature and darkness. After incubation, the absorbance's at 517 nm were measured against the ethanol-containing blot. As control, 3 mL of ethanol and 1 mL of DPPH$^{\cdot}$solution was used. Reduced absorbance gives the free radical scavenging activity of the remaining amount of DPPH$^{\cdot}$solution.

The calculations for DPPH radical scavenging activity in the reaction medium were calculated according to the following formula.

% Free Radical Clearing Activity = $(A_0 - A_1/A_0) \times 100$

A_0: Absorbance of the control reaction, A_1: Absorbance of the sample or standard

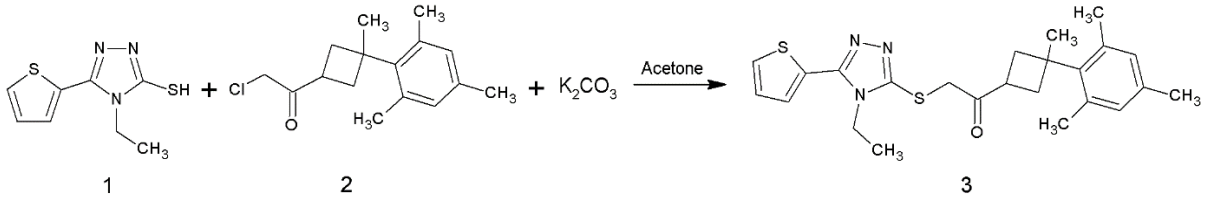


FIGURE 1
The reaction for the synthesis of title compound.

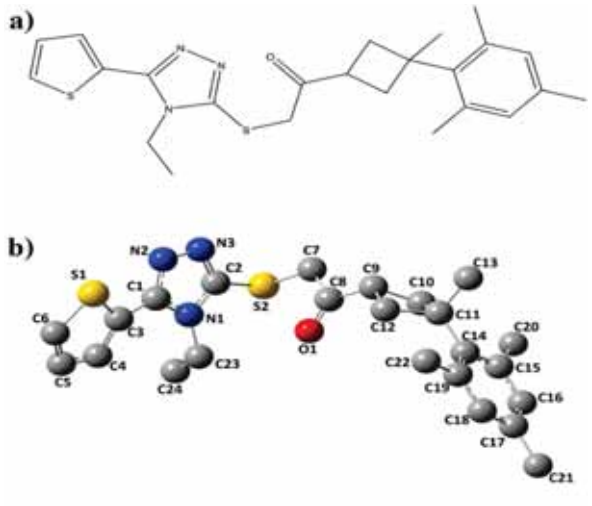


FIGURE 2
(a) Molecular structure of title compound. (b) The theoretical geometric structure of the title compound. (For the sake of clarity, H atoms not involved in the motifs shown have been omitted.

TABLE 1
Selected molecular structure parameters.

Parameters	Experimental [a]	B3LYP/cc-pVDZ
Bond lengths (Å)		
N(1)-C(2)	1.317 (3)	1.380
N(1)-C(1)	1.367 (3)	1.378
N(3)-C(2)	1.327(3)	1.319
O(1)-C(8)	1.205 (3)	1.215
S(2)-C(2)	1.744 (2)	1.770
S(2)-C(7)	1.790 (2)	1.833
RMSE[a]		0.019
Bond Angles (°)		
C(2)-N(1)-C(1)	102.26 (18)	103.75
C(1)-N(2)-N(3)	102.25 (19)	108.08
N(2)-C(1)-N(2)	114.7 (2)	109.96
N(1)-C(2)-N(3)	110.9 (2)	110.8
C(2)-S(2)-C(7)	98.93 (11)	99.02
O(1)-C(8)-C(7)	122.2 (2)	122.9
RMSE[a]		2.891
Dihedral angles (°)		
C(1)-N(1)-C(2)-S(2)	-178.84 (18)	-179.15
N(2)-N(3)-C(2)-S(2)	178.91 (16)	179.74
C(7)-C(8)-C(9)-C(12)	140.9 (2)	135.26
C(7)-S(1)-C(2)-N(3)	173.8 (2)	63.57
C(7)-S(1)-C(2)-N(1)	-7.5 (2)	-116.97
C(10)-C(11)-C(14)-C(1	-141.5 (2)	-142.53

[a] Experimental data taken from Ref. [29]

RESULTS AND DISCUSSION

Molecular geometry. The optimized parameters like bond angles, dihedral angles and bond lengths of **3** were taken by using the B3LYP/cc-pVDZ method. The theoretical geometric structure is given in Fig. 2. The geometric parameters which accounted with the experimental data from the study are listed in Table 1. It is clear that the theoretical calculations and the experimental results are for the solid phase and for the gas phase sequentially. The existence of a crystal field along with the intermolecular interactions connects the molecules together, which results with some differences in bond parameters between the experimental and calculated values in solid state.

Previously, we have reported the closely related 1,2,4-triaizole compound 4-ethyl-5-(2-hydroxyphenyl)-2H-1,2,4-triazole-3(4H)-thione (**4**) [27], which differs only in the 5-position (thiophen*versus*2-hydroxyphenyl). When the bond lengths and angles of the triazole rings in title compound and **4** are compared, it is seen that the values are very close to each other. However, the C1–C3 bond length of 1.45419 Å in **3** is significantly longer than the corresponding value in 4-ethyl-5-(2-hydroxyphenyl)-2H-1,2,4-triazole-3(4H)-thione, 1.473 Å.

Although close to being planar, the cyclobutane is puckered ring. The C10–C9–C12 plane forms a dihedral angle of 17.78º with the C12–C11–C10 plane. This value is small differences than those in the literatures; 22.99º [28] and 19.26º [29]. However, when the bond distances and angles of the cyclobutane ring in the title compound are compared with these, it is seen that there are no significant differences. The C=O bond distance is good agreement with literature values [30].

The most notable discrepancies are found in the orientation of the trizaole ring of the title compound, which is defined by torsion angels C7–S1–C2–N3 [173.8º] and C7–S1–C2–N1 [-7.5º]. The torsion angles have been calculated at 63.6º and -116.9º for B3LYP/cc-pVDZ level. The dihedral angles between the cycbutane ring (C9–C10–C11–C12) with the mesitylene ring (C14–C15–C16–C17–C18–C19) is –141.5º in the X-ray structure [30] and in the optimized structures the corresponding angle is –142.5º. In order to compare the experimental values with the theoretical results, root mean square error (RMSE) is used. Calculated RMSE for bond angles and bond lengths is 2.891° and 0.019Å for B3LYP/cc-pVDZ, respectively.

Nuclear Magnetic Resonance (NMR) spectra. Confidential producing of chemical shifts for average size molecules is provided by the processes for nuclear shielding calculation at the self-consistent field (SCF) level by means of GIAO's enable [31]. The computations for an isolated molecule are performed at its equilibrium geometry. The Gaussian 09W program package was used in the NMR structure computations presented here. The estimations observed were performed in dimethyl sulfoxide (DMSO) solution by means of polarizable continuum model (PCM) in addition to the gas phase in compliance with experimental chemical shifts attained in DMSO solution. The solvent influences must be taken into consideration since the existing spectral information is acquired in various solutions. The isotropic shielding values were employed for the computation of the isotropic chemical shifts δ concerning tetramethylsilane (TMS) $\delta_{iso}^{X} = \sigma_{iso}^{TMS} - \sigma_{iso}^{X}$. Where δ_{iso}– isotropic chemical shift and σ_{iso} – isotropic shielding constant value.

We have calculated ^{1}H chemical shift values (with respect to TMS) of 1.92–7.90 ppm at B3LYP/cc-pVDZ level, however the experimental results were observed to be 1.50–7.81 ppm. Aromatic protons resonate at 6.71-7.81 ppm experimentally, that have been calculated at 7.19-7.90 ppm. Additionally, the title compound gave distinctive peak at 4.15 ppm singlet experimentally, but calculated at 4.46 ppm. We have calculated ^{13}C chemical shift values (with respect to TMS) of 8.3–197.9 ppm with B3LYP/cc-pVDZ level, however the experimental results were observed to be 9.2–205.3 ppm. Chemical shift of hydrogens in mesitylene ring are appeared downfield, because of the effect of methyl groups in phenyl ring. The benzene ring carbon C14, C15, C16, C17, C18 and C19 chemical shift observe at 134.9, 127.2, 119.2, 126.3, 119.4 and 126.9 ppm. The results are consistent with the literature [27, 32]. As can be seen from Table 2, theoretical chemical shift outcomes of the title compound were compared with experimental data, showing generally closers both for ^{1}H and ^{13}C.

TABLE 2
Theoretical and experimental isotropic chemical shifts (with respect to tetramethylsilane all values in ppm) for the title compound.

Atom	Experimental (DMSO-d_6)	Calculated B3LYP/cc-pVDZ	Atom	Experimental (DMSO-d_6)	Calculated B3LYP/cc-pVDZ
C1	149.9	141.1	C21	12.8	12.1
C2	150.6	145.9	C22	15.2	13.9
C3	134.9	128.3	C23	35.2	33.6
C4	119.1	112.9	C24	9.2	8.3
C5	127.9	115.6	H4	7.57	7.75
C6	129.4	123.4	H5	7.26	7.59
C7	41.3	44.9	H6	7.81	7.90
C8	205.3	197.9	H7	4.15	4.46[a]
C9	40.3	32.3	H9	3.58	3.56
C10	41.34	36.8	H10	2.74	2.83[a]
C11	40.5	36.2	H12	2.51	2.28[a]
C12	32.3	29.2	H13	1.50	1.92[a]
C13	15.2	15.8	H16	6.71	7.19
C14	143.7	134.9	H18	6.71	7.22
C15	134.4	126.9	H20	2.52	2.50[a]
C16	129.4	119.4	H21	2.52	2.66[a]
C17	130.5	126.2	H22	2.52	2.58[a]
C18	128.8	119.3	H23	4.32	5.10[a]
C19	134.9	127.2	H24	1.63	1.97[a]
C20	15.1	13.7			

Note: The atom numbering according to Fig. 2 used in the assignment of chemical shifts.
[a] Average.

IR spectroscopy. Harmonic vibrational frequencies of **3** was calculated by utilizing DFT/B3LYP method coupled cc-pVDZ basis set and vibrational band assignment was achieved by Gauss-View molecular visualization software. At the same theory level, assessment of the harmonic vibrational frequencies of optimized structure was conducted and resulting frequencies were scaled by 0.9701 [33]. Facilitation of the assignment of the shown peaks achieved by analyses of the vibrational frequencies and resulting calculations for **3** were contrasted to experimental results shown in Table 3. Region at 4000–400 cm^{-1} was provided the FTIR spectra of **3** through the usage of KBr pellets on a Perkin–Elmer Spectrum one FT–IR spectrophotometer and presented in Fig.3. Overall, obtained calculations were shown adequate coherence with the experimental results.

C=C–C and C–H ring related vibrations normally used to readily determine the presence of aromatic rings in each structure. If compared to the aliphatic C-H stretch, stretching vibration of C-H manifests above 3000 cm^{-1} and regarded as a multiplicity of weak to mediocre bands [34]. In the present study, FTIR spectrum value of C-H stretching vibration was measured at 3000– 3030 cm^{-1} which was theoretically calculated in rage of 3064–3155 cm^{-1} via B3LYP method which was an indicator of adequate correlation between data.

Ordinarily six fundamentals which are CH_2 asym, asymmetrical stretch, CH_2 sym, symmetrical stretch, CH_2 rock, rocking and CH_2 scis, scissoring modes in name that are all belong to polarized in-plane vibrations, can be united to every CH_2 groups to assign CH_2 group frequencies. Furthermore, CH_2 twist, twisting and CH_2 wag, wagging modes of CH_2 group were supposed to be depolarized for out-of-plane bending vibrations. For methylene groups, C-H stretching vibration values would be lower in frequency as compared to values from aromatic C-H ring stretching. Stretching vibrations of the symmetrical and asymmetrical CH_2 manifest in regions of 2900-2800 cm^{-1} and 3000-2900 cm^{-1} ranges respectively [35, 36]. Resulting frequencies in range of 2920–2965 cm^{-1} through IR spectrum were ascribed to the CH_2 stretching mode of the titular molecule. Wavenumbers which were experimentally calculated via B3LYP/cc-pVDZ method were measured in range of 2959–3050 cm^{-1} were ascribed to CH_2 stretching vibrations as seen in Table 3.

The carbonyl characteristic frequency in a compound can widely be used and is an important band assigned in the region of 1650–1850 cm^{-1}.In the experimental IR spectrum, the C=O stretching vibration was given a band which positioned at 1712 cm^{-1} whereas the calculation was provided 27 cm^{-1} higher value which was at 1739 cm^{-1}. In our previous publication, C=O stretching vibration recorded 1705 cm^{-1} [32].

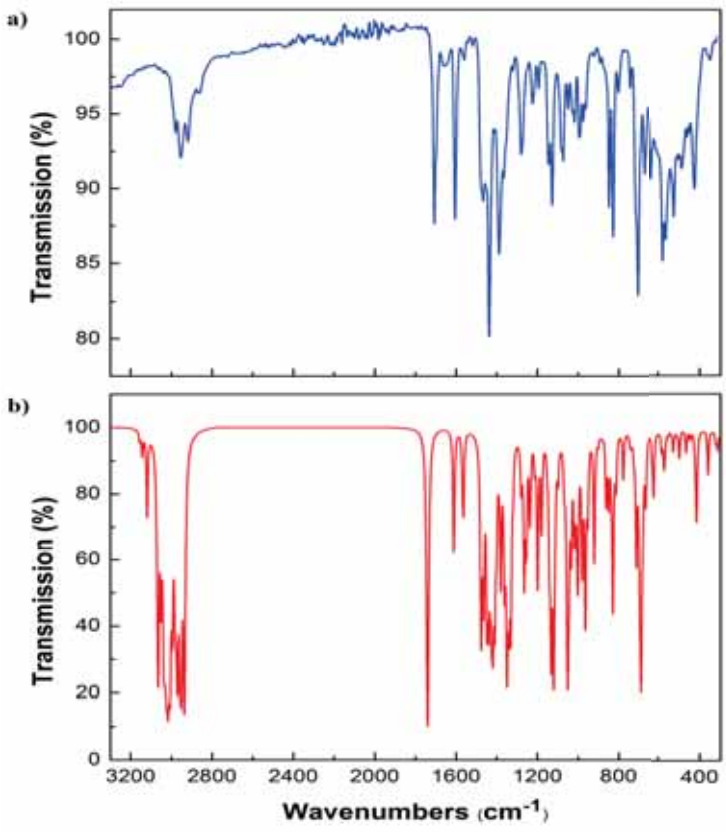


FIGURE 3
(a) Experimental FT-IR spectrum of the title compound. (b) Simulated IR spectra of title compound.

TABLE 3
Comparison of the experimental and calculated vibrational frequencies.

Assignments	Experimental IR with KBr	B3LYP/cc-pVDZ
υ_s (C–H) of R1	3030	3155
υ_{as} (C–H) of R1	-	3142
υ_{as} (C–H) of R1	3020	3118
υ_s (C–H) of R2	3000	3066
υ_{as} (C–H) of R2	-	3064
υ_{as} (C–H_2) of R3	2975	3050
υ_{as} (C–H_2) of R4	2960	3049
υ_s (C–H_3) of R4	2925	2996
υ_s (C=O)	1712	1739
υ (C=C) of R2	1635	1611
υ (C=C) of R1	1597	1562
υ (C=N) triazloe + υ(C=C) of R1	1480	1541
ω (C–H_3) of R2 + γ(C–H) of R2	1475	1464
α (C–H_2) of R4	1457	1448
α (C–H_2) of R3	1445	1434
α (C–H_3) of R2	1432	1427
ω (C–H_3) of R2	1394	1363
γ (C–H) of R1	1202	1198
υ (N–N)	1126	1097
υ (C–C) of R4	1075	1050
υ (C–S) of R1	1011	920
υ (C–S–C)	795	725

υ, stretching; α, scissoring; γ, rocking; ω, wagging; s, symmetric; as, asymmetric; β, bending; δ, of out plane bending R1; thiophene ring; R2; mezityl ring; R3; cyclobutane ring; R4; ethyl fragment.

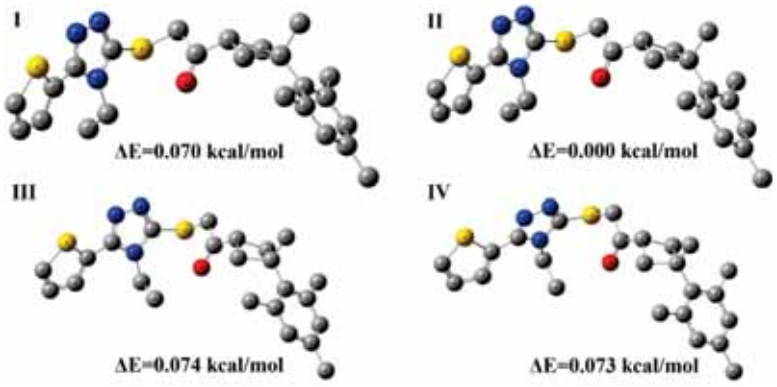


FIGURE 4
List of all the conformers with their optimized structure along with their energies.

The C=N stretching modes of the triazole derivatives are reported at 1541 cm^{-1} [27], 1592 cm^{-1} [37] and 1624 cm^{-1} [16] experimentally. For B3LYP method, stretching vibrations for triazole (C=N) bond were observed as be 1480 cm^{-1} experimentally whereas the calculation value was at 1541 cm^{-1}. In the 1-(3-Methyl-3-mesityl)-cyclobutyl-2-(5-thiophen-4-ethyl-2H-[1,2,4]triazol-3-ylsulfanyl)-ethanone system, the C=C and C-S-C stretching modes were observed to be 1597-1635, 795 cm^{-1} as experimentally and compares well with the value reported previously [1593-1601,590-665 cm^{-1}] [37].

When the all vibration bands of the triazole ring in the compound are compared with the previously reported triazole derivatives [16, 27, 37], it is seen that there are no significant differences. The other stretching, bending, twist, rocking, scissoring modes can be seen in Table 3. Despite the differences between observed and calculated values, the general agreement is good.

Conformational analysis. The conformational study using one dimensional potential energy surface (PES) scans was also performed to find out possible conformers and the most stable structure having minimum energy. PES scan was done by scanning the dihedral angles φ_1(C1–N1–C23–C24), φ_2(C10–C11–C14–C15) and φ_3(S1–C3–C1–N1),

using B3LYP/cc-pVDZ basis set. The variation of torsion angles was carried out at a step of 10º in the range of -180 – +180º rotation around the bond. The graphs obtained by varying the potential energy as a function of dihedral angles for all the bonds are given in Fig. 4.

Figure 5 shows the post-optimisation structure of each of the four conformers that were obtained as well as their relative energies. Meanwhile, Table 4 indicates the optimised energy and energy discrepancy of each conformer in relation to the conformer with the highest level of stability, which was conformer **II** (-1234880.390 a.u.), followed by conformer **I** (-1234880.320 a.u.). The two conformers show close similarities regarding the bond length of C–H, C-C, C=O, C–S, and C–N.

Values of φ1, φ2 and φ3 of the molecule are compared with experimental dihedral angles of similar molecules. Accordingly, These values were found as 110º [30] and -80º [38], for φ1, -136º [30] and -138º [39] for φ2, 175º [40] and 177º [41] for φ3. According to the results of the potential energy surface (PES) scans, the minimum values of energy are found as 100º and -80º for φ1, -140 for φ2 and 160º for φ3. As can be seen from these data, the calculated values are in great agreement with the experimental values. However, when the energy differences between HOMO and LUMO were calculated for the lowest energy four conformers, this difference was found to be the same (4.685 eV) for the four conformers. Accordingly, it can be said that these four conformers have the same desire to enter the reaction.

Nonlinear optical effects. Nonlinear optical (NLO) effects arise from the interactions of electromagnetic fields in various media to produce new fields altered in phase, frequency, amplitude or other propagation characteristics from the incident fields [42]. NLO is extensively studied at the moment because of its central role in technological innovations in various domains, including signal processing telecommunications and optical interconnections, where it mediates essential mechanisms such as frequency change, optical switching, optical logic, optical regulation, and optical memory [43, 44].

There has been ample discussion about the determination of total molecular dipole moment (μ), linear polarizability(α) and first-order hyperpolarizability (β) associated with the Gaussian output [45] and, in the context of analysis of organic NLO materials, there is clear preference for the DFT technique. The popular B3LYP technique is considered to possess highly effective prediction capacity, since it has shown consistency in the electric hyperpolarizability values it has yielded in different studies, as opposed to standard *ab initio* approaches [46, 47]. Moreover, the basis set cc-pVDZ was employed in the present study to determine hyperpolarizability, due to the fact that it is consistent and time-effective [48].

TABLE 4
Ground state optimized energy and energy difference of all the four conformers.

Conformers	Energy		Energy Difference*	
	Hartree	kcal/mol	Hartree	kcal/mol
I	-1967.92746199	-1234880.320	0.000111	0.070
II	-1967.92758035	-1234880.390	0.000000	0.000
III	-1967.92746193	-1234880.316	0.000117	0.074
IV	-1967.92746194	-1234880.313	0.000116	0.073

*Energies of the other four conformers relative to the most stable conformer II.

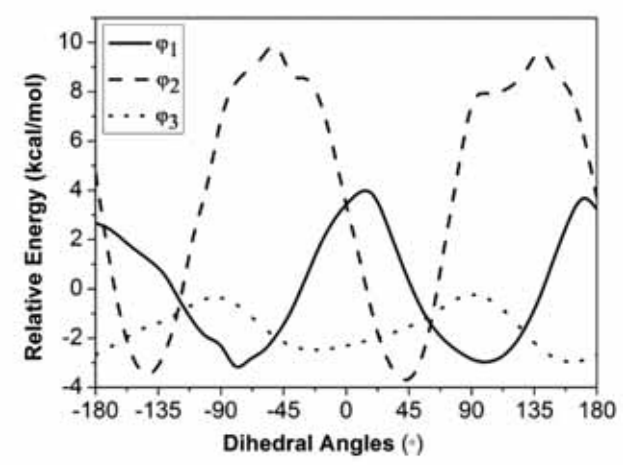


FIGURE 5
Potential energy surface scan with varying dihedral angle φ1, φ2 and φ3 of title compound.

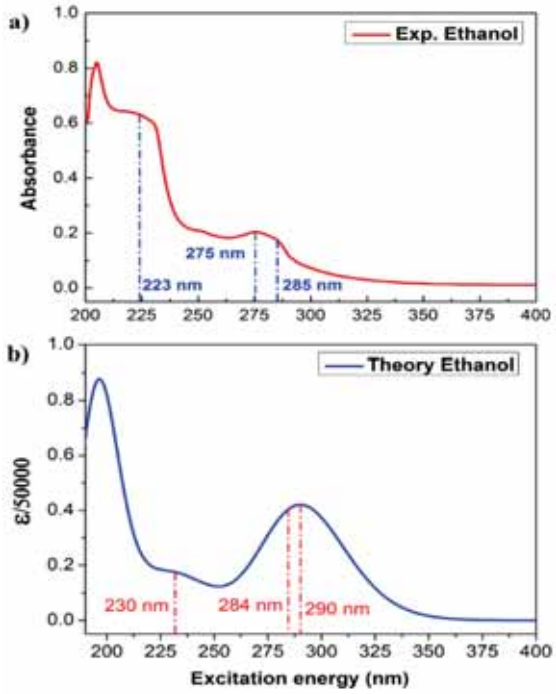


FIGURE 6
a) Experimental UV spectrum.
(b) TD-DFT//B3LYP/cc-pVDZ level UV spectrum of title compound.

The program Gaussian 09W permitted calculation of the electronic dipole moment μ_i (i = x, y, z), polarizability α_{ij} and the first hyperpolarizability β_{ijk} of **3** within the context of the combined approach of B3LYP and cc-pVDZ. A standard molecule usually employed to examine the NLO characteristics of molecular systems is urea, which in this case served as a threshold value to enable comparison. Thus, compared to urea's values α_{tot} = 3.831 Å^3 and β_{tot} = 0.37 × 10^{-30} cm^5/esu that were calculated via B3LYP/6-31G(d), 3 exhibited higher values, namely, α_{tot} = 47.739 Å^3 and β_{tot} = 4,56 × 10^{-30} cm^5/esu. Thus, it could be said that 3 is a contributor to NLO material formation based on the first hyperpolarizability magnitude.

Electronic absorption spectra. With the aim of studying electronic transitions, UV–vis spectroscopic analysis was performed for the title compound. It was recorded that the absorption spectral peaks to be at 223, 275 and 285 nm in ethanol as it is shown in Fig. 6. Using TD-DFT method and IEF-PCM (integral equation formalism-polarizable continuum model) [49, 50] model using B3LYP/cc-pVDZ basis set, the absorption band of **3** were calculated in the solvent (ethanol) phase.

Oscillator strengths (f), calculated absorption peaks (λ_{max}), positions of observed absorption peaks, and the assignments of the **3** molecule transitions were performed for the purpose of understanding the nature of electronic transitions. The main orbitals contributing to the chemical stability are the highest occupied molecular orbital (HOMO) and lowest unoccupied molecular orbital (LUMO) [51, 52]. HOMO (H) corresponds to the ability to donate electrons and thus indicates electron ionization. On the other hand, LUMO (L) being an indicator of electron affinity corresponds to the ability to accept electrons. Basically corresponding to the electron excitation from H to the L, electronic transition absorption is defined as the transition from the ground state to the first excited state. The first intense band at 285 nm corresponds to H/L transition calculated at 290 nm with oscillator strength 0.4774 nm. The transition originates from H/L+1 with oscillator strength 0.0362 nm corresponding to second absorption maxima at 275 nm. The third band at 223 nm corresponds to H–3/L+1 transition calculated at 230 nm.

One of the absorption bands at 275 nm is caused by the $\pi \rightarrow \pi^*$ transition and the other band at 285 nm is due to $\sigma \rightarrow \pi^*$ transition. It is expected that the transitions of $\pi \rightarrow \pi^*$ occur at a relatively lower wavelength as a consequence of the extended aromaticity of the mesitylene, triazole and thiophene rings. In this case, due to the presence of lone pair of electrons in the sulfur and nitrogen atoms in the molecular structure, the $\sigma \rightarrow \pi^*$ transition is more important. The atomic molecular orbital plots (HOMO-LOMO plot) for the frontier orbitals of solvent phase are plotted and presented in the Fig. 7.

Chemical reactivity. Knowledge about the chemical reactivity and site selectivity of a molecular system can be attained with the use of DFT. In the context of drug development and refinement of the physical and chemical properties of the drug molecule, a number of chemical reactivity descriptors play an important role [53]. In the following part, attention is directed to the parameters of chemical reactivity, namely, global and local reactivity descriptors, molar refractivity, and molecular electrostatic potential (MEP) map.

(1) Global reactivity descriptors. Several molecular parameters can be determined based on the energy values of HOMO and LUMO. The least amount of energy necessary to eliminate an electron from the atom or molecule in gaseous state is known as the ionization potential (I = - E_{HOMO}). The amount of energy discharged as a result of the addition of one electron to a gaseous molecule is called the electron affinity (A = - E_{LUMO}). An atom's predilection to attracting electrons is known as electronegativity χ = (IP + EA)/2. Weight transfer prevention in a molecule is denoted by chemical hardness η = (IP-EA)/2. Using these values other reactivity descriptors are calculated such as chemical potential $\mu = -\chi$, softness s = 1/2η and global electrophilicity index $\omega = \mu^2/2\eta$ [54–56]. Table 5 lists the parameter values of the electronic structure that were determined based on the B3LYP/cc-pVDZ technique.

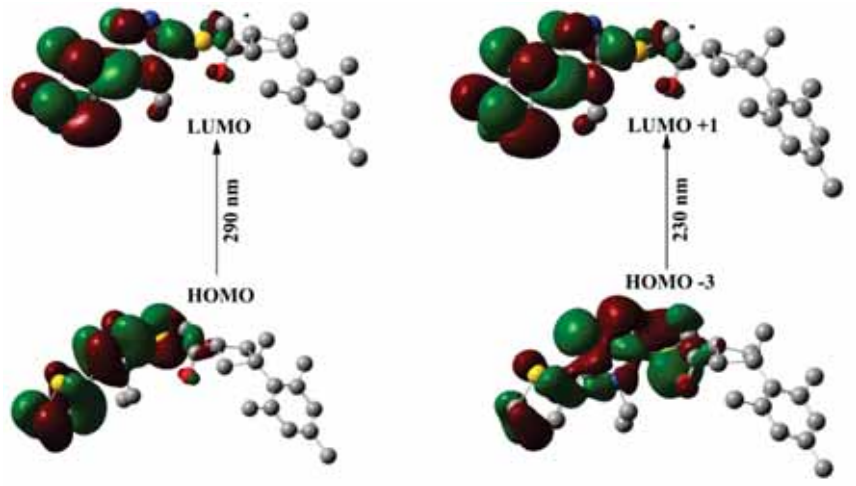


FIGURE 7
HOMO-LUMO plots for the selected transitions of title compound.

TABLE 5
Electronic structure parameters of the title compound.

Parameters	B3LYP cc-pVDZ
E_{HOMO} (eV)	-5.808
E_{LUMO} (eV)	-1.123
$\Delta E = E_{LUMO} - E_{HOMO}$ (eV)	4.685
I (eV)	5.808
A (eV)	1.123
χ (eV)	3.465
η (eV)	2.343
S (eV^{-1})	0.213
ω (eV)	2.563
Dipole moment (D)	
μ_{total}	4.3707
μ_x	3.3938
μ_y	1.4777
μ_z	2.3240

During system acquisition of an extra electronic charge from the environment, the measurement of energy stabilisation can be undertaken with the global electrophilicity index [57]. Electrophilicity is concerned with the acquisition of extra electronic charge by an electrophile as well as with the opposition put up by the system regarding electronic charge exchange with the environment. It is considered a suitable global chemical reactivity descriptor because it is informative not only about electron transfer (chemical potential), but also about stability (hardness).

The compound's chemical activity is usually indicated by the energy values of HOMO and LUMO and the difference of energy between them. A robust interaction and quick reaction are denoted by a small energy difference between HOMO and LUMO, while a weak interaction and slow reaction are denoted by a large energy difference between HOMO and LUMO [58]. The molecules with lower energy gap shows high reactivity and are more polarizable [59]. The value of the energy separation between the HOMO and LUMO is4.685eV for gas phase. In a similar work [30] conducted at the level of B3LYP/6-311G (d,p), this value was found to be 4.807eVfor the 1-(3-Methyl-3-mesityl)-cyclobutyl-2-(5-pyridin-4-yl-2H-[1,2,4]triazol-3-ylsulfanyl)-ethanone molecule.

(2) Local reactivity descriptors. A molecule's chemical reactivity and site selectivity are usually determined with the parameter of local reactivity called Fukui function f(r). In this case, the indicators of local reactivity have been determined by applying the principle of Hard and Soft Acid and Base (HSAB) alongside the DFT [60]. The expression of the f(r) takes the following form : [61]

$$f(r) = \left(\frac{\partial p(r)}{\partial N}\right)_{v(r)} = \left(\frac{\partial \mu(r)}{\partial V(r)}\right)$$

In the above, p(r) denotes the electron density in relation to the overall electron number N in the system at the fixed external potential V(r) that acts on an electron as a result of the totality of the system nuclei. The ideal areas where modification of the electronic density can be undertaken by a chemical species can be detected with this function.

Compared to the molecular areas with a small f(r), the areas with a large f(r) are softer from a chemical perspective. The description of the f(r) for reactivity assessment at atomic level based on the finite difference approximation is as follows:

$$f_k^+ = [q_k(N+1) - q_k(N)]$$
$$f_k^- = [q_k(N) - q_k(N-1)]$$
$$f_k^0 = [q_k(N+1) - q_k(N-1)]$$

The above three relationships are respectively associated with nucleophilic attack, electrophilic attack, and radical attack.

Assessed on the basis of natural population analysis, q_k represents the atomic charge at the *k*th atomic site in molecular species of neutral (N), anionic (N+1) or cationic (N-1) nature. The equations below facilitate the determination of the indices associated with Local Softness and electrophilicity:

$S_k^+ = Sf_k^+ , \ S_k^- = Sf_k^- , \ S_k^0 = Sf_k^0$

$\omega S_k^+ = \omega f_k^+ , \ \omega_k^- = \omega f_k^- , \ \omega_k^0 = \omega f_k^0$

In the above, the nucleophilic attack is denoted by +, the electrophilic attack is denoted by -, and the radical attack is denoted by O. Table 6 provides a series of f(r) values for the title compound. The key reactivity location in the title compound for the radical attack $(f_k^0, s_k^0, \omega_k^0)$ and the nucleophilic attack $(f_k^+, s_k^+, \omega_k^+)$ is S1, while for the electrophilic attack $(f_k^-, s_k^-, \omega_k^-)$ is S2.

(3) Molar refractivity. The dispersivity of valence electrons is influenced by the molecule's mass, charge and polarizability and is indicated by the molar refractivity (MR). The Lorentz-Lorentz equation defines the molecular property of MR: [62, 63]

$$\mathrm{MR} = \frac{n^2 - 1}{\mathrm{n}^2 + 2}\left(\frac{MW}{p}\right) = 1{,}333\pi\mathrm{N}\alpha$$

In the above equation, the refractive index and density are respectively denoted by n and r, the molecular weight and molar volume are MW and (MW/*p*), respectively, while Avogadro's number is denoted by N and the polarizability is represented by α. The density and wavelength of the light employed enable the calculation of the MR value. Linked to the determination of the molecule's real volume, MR is correlated with the forces controlling the interactions between the ligands and receptors. The approximation of the biological activity of the molecular system depends significantly on this property. MR has a 40-130 qualifying range and a mean value of 97 [64]. For the title compound, MR has a value of 120 e.s.u. MR should have a large value for a molecule of high polarizability. In this case, the polarizability and reactivity of a key pharmaceutical compound, 1-(3-Methyl-3-mesityl)-cyclobutyl-2-(5-thiophen-4-ethyl-2H-[1,2,4]triazol-3-ylsulfanyl)-ethanone, are dependent on these values.

(4) Molecular electrostatic potential (MEP). Molecular areas with different charges can be observed based on the molecular electrostatic potential surface (MEPS) [65]. The nature of the interactions between molecules can be deduced from the manner in which the charges are distributed. To facilitate observation and interpretation of the data related to electrostatic potential energy, the different intensities of the electrostatic potential energy values are represented through a colour spectrum with minimal and maximal values being indicated by red and blue, respectively. These values are commonly employed to qualitatively assess electrophilic and nucleophilic reactions. From lowest to highest, red, orange, yellow, green and blue chart the increase in electrostatic potential energy. A correlation is established by these potential surfaces between the overall charge distribution, dipole moment, partial charges, electronegativity, and chemical reactivity site of a molecule [66]. Figure 8 illustrates that the regions of the title compound with the highest electro-negativity and highest electro-positivity are the triazole group and the carbonyl group, respectively. The adherence of substrate and receptors depends to a significant extent on the electrostatic potential value.

TABLE 6
Calculated local reactivity properties of the selected atom using Hirshfeld [B3LYP/cc-pVDZ] derived charges.

Atom	f_k^0	s_k^0	ω_k^0	Atom	f_k^+	s_k^+	ω_k^+	Atom	f_k^-	s_k^-	ω_k^-
S1	0.1577	0.0336	0.4042	**S1**	0.0989	0.021	0.2535	**S2**	0.0824	0.0176	0.2111
S2	0.1378	0.0294	0.3532	**C6**	0.0642	0.0137	0.1645	**C6**	0.059	0.0126	0.1512
C6	0.1231	0.0262	0.3155	**C8**	0.0561	0.0120	0.1437	**S1**	0.0589	0.0125	0.1510
N2	0.0851	0.0181	0.2181	**S2**	0.0554	0.0118	0.1420	**N2**	0.0471	0.0100	0.1207
C8	0.0616	0.0131	0.1579	**O1**	0.0475	0.0101	0.1217	**N3**	0.0431	0.0092	0.1105

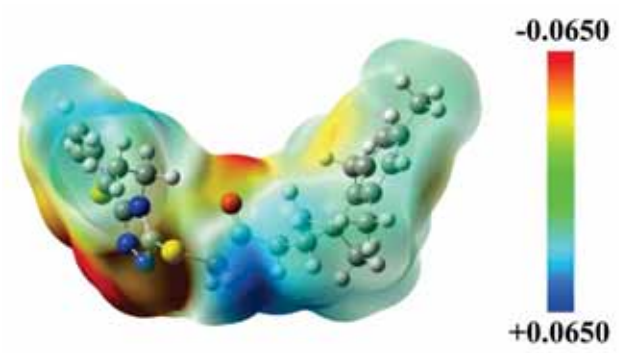


FIGURE 8
Molecular electrostatic potential map calculated at B3LYP/cc-pVDZ level.

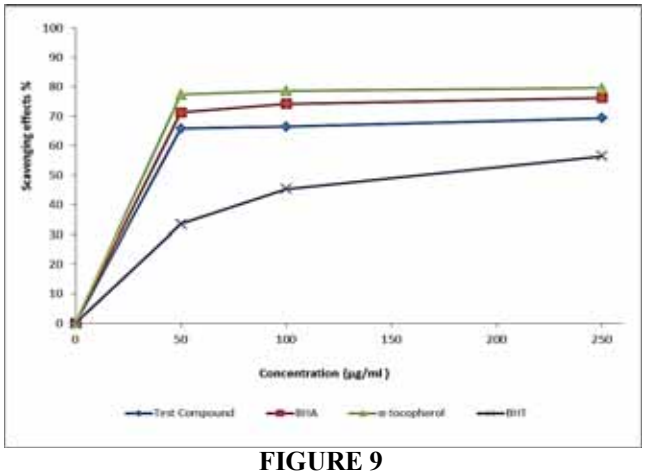


FIGURE 9
Scavenging effect of test compound, BHT, BHA and α-tocopherol at different concentrations (50-100-250 µg/mL)

Antioxidant activity. The antioxidant activity of the compound synthesized in the study was examined using the free radical scavenging activity method. The reduction ability of DPPH ratio ligands was determined by absorbance reduction at 517 nm induced by antioxidants and calculated percent inhibition values. The findings are given in Fig. 9.

The graph shows that the test compound showed better activity than the standards according to BHT. On the other hand it has been found that has a lower activity than the standard according to BHA and α-tocopherol. Accordingly, it can be said that the test compound has a good radical scavenging activity. This result can show that our test compound has good activity as a hydrogen donor because the antioxidants' effect on DPPH radical cleansing is thought to be due to their hydrogen donor capabilities [67]. DPPH is a stable free radical and accepts an electron or hydrogen radical to become a stable diamagnetic molecule [68]. DPPH-scavenging mechanism of our compounds could not clarified yet but our effort on this way is going on.

CONCLUSION

1-(3-Methyl-3-mesityl)-cyclobutyl-2-(5-thiophen-4-ethyl-2H-[1,2,4]triazol-3-ylsulfanyl)-ethanone are characterized and synthesized by UV–vis, FT–IR, ^{1}H–NMR, and ^{13}C–NMR spectral analysis methods. The DFT method was used in the examination of molecular geometries, electronic structures, NMR and vibrational, spectra of the title compound. TD-DFT calculations were used in the solution (EtOH) in order to predict the nature of the electronic transitions which are observed in the absorption spectra. The calculated chemical shift values and vibrational spectra match with the experimental data and the calculated geometry of the **3** is consistent with the X-ray crystallographic data. The NMR chemical shifts and calculated vibrational bands comply with the experimental results. Having been calculated using TD-DFT method, the electronic absorption and emission spectra were correlated to the experimental spectra. Three absorption peaks are recorded at 290, 284 and 230 nm in UV-vis spectrum which has transition from H→L (σ→π*), H→L+1 (π→π*), and H-3→L+1 (π→π*) respectively. The HOMO-LUMO energy gap is calculated4.685 eV for title compound. Chemical reactivity of 1-(3-Methyl-3-mesityl)-cyclobutyl-2-(5-thiophen-4-ethyl-2H-[1,2,4]triazol-3-ylsulfanyl)-ethanone was explained by means of global reactivity parameter. Fukui calculations show that S1 atom is susceptible for nucleophilic and radical attack whereas, S2 atom is prone for radical attack. Molecular electrostatic potential (MEP) reveals that the triazole group is the most electronegative and the C=O group is the most electropositive site of title compound. The antioxidative activity study revealed that the title compound tested showed good radical scavenging activity.

REFERENCES

[1] Koparir, M., Orek, C., Parlak, A.E., Soylemez, A., Koparir, P., Karatepe, M., Dastan, S.D. (2013) Synthesis and biological activities of some novel aminomethyl derivatives of 4-substituted-5-(2-thienyl)-2,4-dihydro-3H-1,2,4-triazole-3-thiones. Eur. J. Med. Chem. 63, 340–346.

[2] Shams el-Dine, S.A., Hazzaa, A.A. (1974) Synthesis of compounds with potential fungicidal activity. Part 2. Pharmazie. 29, 761–763.

[3] Sztanke, K., Tuzimski, T., Rzymowska, J., Pasternak, K., Kandefer-Szerszeń, M. (2008) Synthesis, determination of the lipophilicity, anticancer and antimicrobial properties of some fused 1,2,4-triazole derivatives. Eur. J. Med. Chem. 43, 404–419.

[4] Gadegoni, H., Manda, S. (2013) Synthesis and screening of some novel substituted indoles contained 1,3,4-oxadiazole and 1,2,4-triazole moiety. Chinese Chem. Lett. 24, 127–130.
[5] Ilango, K., Valentina, P. (2010) Synthesis and biological activities of novel 1, 2, 4-triazolo-[3, 4-b]-1, 3, 4-thiadiazole. Der Pharma Chem. 2, 16–22.
[6] Stillings, M.R., Welbourn, A.P., Walter, D.S. (1986) Substituted 1,3,4-thiadiazoles with anticonvulsant activity. 2. Aminoalkyl derivatives. J. Med. Chem. 29, 2280–2284.
[7] Jones, D.H., Slack, R., Squires, S., Wooldridge, K.R.H. (1965) Antiviral Chemotherapy. I. The Activity of Pyridine and Quinoline Derivatives against Neurovaccinia in Mice. J. Med. Chem. 8 676–680.
[8] Sugden, J.K., Yoloye, T.O. (1978) Medicinal applications of indole derivatives. Pharm. Acta Helv. 53, 65–92.
[9] Dembitsky, V.M. (2008) Bioactive cyclobutane-containing alkaloids. J. Nat. Med. 62, 1–33.
[10] Gutekunst, W.R., Baran, P.S. (2011) Total synthesis and structural revision of the piperarborenines via sequential cyclobutane C-H arylation. J. Am. Chem. Soc. 133, 19076–19079.
[11] Kole, G.K. Koh, L.L., Lee, S.Y., Lee, S.S., Vittal, J.J. (2010) A new ligand for metal-organic framework and co-crystal synthesis: mechanochemical route to rctt-1,2,3,4-tetrakis-(4'-carboxyphenyl)-cyclobutane. Chem. Commun. (Camb). 46, 3660–3662.
[12] Palafox, M.A., Rastogi, V.K., Tanwar, R.P., Mittal, L. (2003) Vibrational frequencies and structure of 2-thiouracil by Hartree-Fock, post-Hartree-Fock and density functional methods. Spectrochim. Acta - Part A Mol. Biomol. Spectrosc. 59, 2473–2486.
[13] Mohan, S., Sundaraganesan, N., Mink, J. (1991) FTIR and Raman studies on benzimidazole, Spectrochim. Acta Part A Mol. Spectrosc. 47, 1111–1115.
[14] Ten, G.N., Nechaev, V.V., Pankratov, A.N., Berezin, V.I., Baranov, V.I. (2010) Effect of hydrogen bonding on the structure and vibrational spectra of the complementary pairs of nucleic acid bases. II. adenine-thymine. J. Struct. Chem. 51, 854–861.
[15] Koparir, P., Sarac, K., Orek, C., Koparir, M. (2016) Molecular structure, spectroscopic properties and quantum chemical calculations of 8-t-buthyl-4-methyl-2H-chromen-2-one. J. Mol. Struct. 1123, 407–415.
[16] Cansiz, A., Orek, C., Koparir, M., Koparir, P., Cetin, A. (2012) 4-Allyl-5-pyridin-4-yl-2,4-dihydro-3H-1,2,4-triazole-3-thione: Synthesis, experimental and theoretical characterization. Spectrochim. Acta - Part A Mol. Biomol. Spectrosc. 91, 136–145.
[17] Becke, A.D. (1993) Density-functional thermochemistry. III. The role of exact exchange. J. Chem. Phys. 98, 5648.
[18] Lee, C., Yang, W., Parr, R. (1988) Development of the Colle- Salvetti correlation energy formula into a functional of the electron density. Phys Rev B. 37, 785–789.
[19] Woon, D.E., Dunning, T.H. (1993) Gaussian-Basis Sets for Use in Correlated Molecular Calculations .3. the Atoms Aluminum Through Argon. J. Chem. Phys. 98, 1358–1371.
[20] Helgaker, T., Jorgensen, P., Olsen, J. (2000) Molecular Electronic-Structure Theory. John Wiley & Sons Ltd.
[21] Runge, E., Gross, E.K.U. (1984) Density-functional theory for time-dependent systems. Phys. Rev. Lett. 52, 997–1000.
[22] Stratmann, R.E., Scuseria, G.E., Frisch, M.J. (1998) An Efficient Implementation of Time-Dependent Density-Functional Theory for the Calculation of Excitation Energies of Large Molecules. J. Chem. Phys. 109, 8218–8224.
[23] Barone, V., Cossi, M., Tomasi, J. (1997) A new definition of cavities for the computation of solvation free energies by the polarizable continuum model. J. Chem. Phys. 107, 3210.
[24] Frisch, M.J., Trucks, W., Schlegel, H.B., Scuseria, G.E., Robb, M.A., Cheeseman, J.R., Scalmani, G., Barone, V., Mennucci, B., Petersson, G.A., Nakatsuji, H., Caricato, M., Li, X., Hratchian, H.P., Izmaylov, A.F., Bloino, J., Zheng, G., Sonnenberg, J.L. (2010) Gaussian 09, Revision B.01. Gaussian Inc., Wallingford, CT.
[25] Dennington, R., Keith, T., Millam, J. (2009) GaussView, Version 5. Semichem Inc. Shawnee Mission. KS. Semichem Inc.
[26] Blois, M. (1958) Antioxidant determinations by the use of a stable free radical. Nature. 181, 1199–1200.
[27] Koparir, M., Orek, C., Koparir, P., Sarac, K. (2013) Synthesis, experimental, theoretical characterization and biological activities of 4-ethyl-5-(2-hydroxyphenyl)-2H-1,2,4-triazole-3(4H)-thione. Spectrochim. Acta - Part A Mol. Biomol. Spectrosc. 105, 522–531.
[28] Inkaya, E., Dinçer, M., Çukurovalı, A., Yılmaz, E. (2011) 2-Chloro-N-[4-(3-methyl-3-phenyl-cyclo-but-yl)-1,3-thia-zol-2-yl]-N′-(naphthalen-1-yl-methyl-idene)acetohydrazide. Acta Crystallogr. Sect. E Struct. Reports Online. 67, o310–o310.
[29] Dincer, M., Ozdemir, N., Yilmaz, I., Cukurovali, A., Buyukgungor, O. (2004) 1-Methyl-1-phenyl-3-[1-hydroxyimino-2-(succinimido)ethyl]cyclobutane. Acta Crystallogr. C. 60, o674-6.

[30] Inkaya, E., Dinçer, M., Ekici, O., Cukurovali, A. (2013) 1-(3-methyl-3-mesityl)-cyclobutyl-2-(5-pyridin-4-yl-2H-[1,2,4]triazol-3-ylsulfanyl)-ethanone: X-ray structure, spectroscopic characterization and DFT studies. Spectrochim. Acta. A. Mol. Biomol. Spectrosc. 101, 218–27.

[31] Jameson, C.J., de Dios, A.C. (1992) Abinitio calculations of the intermolecular chemical-shift in nuclear-magnetic-resonance in the gas-phase and for adsorbed species. J. Chem. Phys. 97, 417–434.

[32] Orek, C. Koparir, P., Koparir, M. (2012) N-cyclohexyl-2-[5-(4-pyridyl)-4-(p-tolyl)-4H-1,2,4-triazol-3-ylsulfanyl]-acetamide dihydrate: synthesis, experimental, theoretical characterization and biological activities. Spectrochim. Acta. A. Mol. Biomol. Spectrosc. 97, 923–34.

[33] Foresman, J.B., Frisch, Æ. (1996) Exploring Chemistry with electronic structure methods. (2nd ed.) Pittsburgh, PA Gaussian Inc. 266, 278–283.

[34] Coates, J. (2000) Interpretation of Infrared Spectra. A Practical Approach. In: Meyers, R.A. (Ed.) Encyclopedia of Analytical Chemistry. John Wiley & Sons Ltd. Chichester. 10815–10837.

[35] Sajan, D., Binoy, J., Pradeep, B., Venkata Krishna, K., Kartha, V.B., Joe, I.H., Jayakumar, V.S. (2004) NIR-FT Raman and infrared spectra and ab initio computations of glycinium oxalate. Spectrochim. Acta - Part A Mol. Biomol. Spectrosc. 60, 173–180.

[36] Furic, K., Mohacek, V., Bonifacic, M., Stefanic, I. (1992) Raman spectroscopic study of H2O and D2O water solutions of glycine. J. Mol. Struct. 267, 39–44.

[37] Cansız, A., Cetin, A., Orek, C., Karatepe, M., Sarac, K., Kus, A., Koparir, P. (2012) 6-Phenyl-3-(4-pyridyl)-1,2,4-triazolo-[3,4-b][1,3,4]thia-diazole: Synthesis, experimental, theoretical characterization and biological activities. Spectrochim. Acta Part A Mol. Biomol. Spectrosc. 97, 606–615.

[38] Demir, S., Dinçer, M., Çetin, A., Dayan, O., Cansiz, A. (2006) 5,5'-Pyridine-2,6-diylbis[4-ethyl-2,4-dihydro-1,2,4-triazole-3(2H)-thione]. Acta Crystallogr. Sect. E. 62, o2198--o2199.

[39] Şen, F., Dinçer, M., Çukurovalı, A., Yılmaz, I. (2011) (Z)-1-(3-Mesityl-3-methyl-cyclo-but-yl)-2-(morpholin-4-yl)ethanone oxime. Acta Crystallogr. Sect. E Struct. Reports Online. 67, o958–o959.

[40] Yildirim, S.Ö., Akkurt, M., Koparir, M., Cansiz, A., Sekerci, M., Heinemann, F.W. (2004) 3-(2-Furyl)-4-(4-methoxyphenyl)-1H-1,2,4-triazole-5(4H)-thione. Acta Crystallogr. Sect. E. 60, o2368--o2370.

[41] Dege, N., Andac, O., Cansiz, A., Çetin, A., Sekerci, M., Dinçer, M. (2004) 5-(Furan-2-yl)-4-(*p*-tolyl)-2,4-dihydro-1,2,4-triazole-3-thione. Acta Crystallogr. Sect. E. 60, o1405--o1407.

[42] Sun, Y.X., Hao, Q.L., Wei, W.X., Yu, Z.X., De Lu, L., Wang, X., Wang, Y.S. (2009) Experimental and density functional studies on 4-(3,4-dihydroxybenzylideneamino)antipyrine, and 4-(2,3,4-trihydroxybenzylideneamino)antipyrine. J. Mol. Struct. THEOCHEM. 904, 74–82.

[43] Andraud, C., Brotin, T., Garcia, C., Pelle, F., Goldner, P., Bigot, B., Collet, A. (1994) Theoretical and experimental investigations of the nonlinear optical properties of vanillin, polyenovanillin, and bisvanillin derivatives. J. Am. Chem. Soc. 116, 2094–2102.

[44] Geskin, V.M., Lambert, C., Bredas, J.L. (2003) Origin of High Second- and Third-Order Nonlinear Optical Response in Ammonio/Borato Diphenylpolyene Zwitterions: The Remarkable Role of Polarized Aromatic Groups. J. Am. Chem. Soc. 125, 15651–15658.

[45] Thanthiriwatte, K.S., Nalin de Silva, K.M. (2002) Non-linear optical properties of novel fluorenyl derivatives—ab initio quantum chemical calculations. J. Mol. Struct. THEOCHEM. 617, 169–175.

[46] Maroulis, G., Begué, D., Pouchan, C. (2003) Accurate dipole polarizabilities of small silicon clusters from *ab initio* and density functional theory calculations. J. Chem. Phys. 119, 794.

[47] Maroulis, G. (2008) How large is the static electric (hyper)polarizability anisotropy in HXeI? J. Chem. Phys. 129, 044314.

[48] Qin, C., Si, Y., Yang, G., Su, Z. (2011) Quantum chemical study of structures, electronic spectrum, and nonlinear optical properties of polynuclear lithium compounds. Comput. Theor. Chem. 966, 14–19.

[49] Miertuš, S., Scrocco, E., Tomasi, J. (1981) Electrostatic interaction of a solute with a continuum. A direct utilization of AB initio molecular potentials for the prevision of solvent effects. Chem. Phys. 55, 117–129.

[50] Miertuš, S., Tomasi, J. (1982) Approximate evaluations of the electrostatic free energy and internal energy changes in solution processes. Chem. Phys. 65, 239–245.

[51] Schmalz, T.G., Seitz, W.A., Klein, D.J., Hite, G.E. (1988) Elemental Carbon Cages. J. Am. Chem. Soc. 110, 1113–1127.

[52] Bethune, D.S., Meijer, G., Tang, W.C. Rosen, H.J. (1990) The vibrational Raman spectra of purified solid films of C60 and C70. Chem. Phys. Lett. 174, 219–222.

[53] Padmanabhan, J., Parthasarathi, R., Elango, M., Subramanian, V., Krishnamoorthy, B.S., Gutierrez-Oliva, S., Toro-Labbé, A., Roy, D.R., Chattaraj, P.K. (2007) Multiphilic descriptor for chemical reactivity and selectivity. J. Phys. Chem. A. 111, 9130–9138.
[54] Calais, J.-L. (1993) Density-functional theory of atoms and molecules. R.G. Parr and W. Yang, Oxford University Press, New York, Oxford, 1989. IX + 333 pp. Price £45.00. Int. J. Quantum Chem. 47, 101.
[55] Parr, R.G., Yang, W. (1989) Density-Functional Theory of Atoms and Molecules. Oxford University Press. New York, Oxford.
[56] Gázquez, J.L. (2008) Perspectives on the Density Functional Theory of Chemical Reactivity. J. Mex. Chem. Soc. 52, 3–10.
[57] Parr, R.G., Szentpály, L.V., Liu, S. (1999) Electrophilicity Index. J. Am. Chem. Soc. 121, 1922–1924.
[58] Fleming, I., Wiley, J. (1979) Frontier Orbitals and Organic Chemical Reactions. J. Mol. Struct. 56, 306.
[59] Srivastava, K., Shimpi, M.R., Srivastava, A., Tandon, P., Sinha, K., Velaga, S.P. (2016) Vibrational analysis and chemical activity of paracetamol–oxalic acid cocrystal based on monomer and dimer calculations: DFT and AIM approach. RSC Adv. 6, 10024–10037.
[60] Ayers, P.W., Levy, M. (2001) Perspective on Density functional approach to the frontier-electron theory of chemical reactivity. In: Cramer, C.J., Truhlar, D.G. (Eds.) Theoretical Chemistry Accounts: New Century Issue. Springer. Berlin Heidelberg, 353–360.
[61] Parr, R.G., Yang, W. (1984) Density functional approach to the frontier-electron theory of chemical reactivity. J. Am. Chem. Soc. 106, 4049–4050.
[62] Padron, J.A., Carrasco, R., Pellon, R.F. (2002) Molecular descriptor based on a molar refractivity partition using Randic-type graph-theoretical invariant. J. Pharm. Pharm. Sci. 5, 258–266.
[63] Verma, R.P., Hansch, C. (2005) A comparison between two polarizability parameters in chemical-biological interactions. Bioorganic Med. Chem. 13, 2355–2372.
[64] Ghose, A.K., Viswanadhan, V.N., Wendoloski, J.J. (1999) A Knowledge-Based Approach in Designing Combinatorial or Medicinal Chemistry Libraries for Drug Discovery. 1. A Qualitative and Quantitative Characterization of Known Drug Databases. J. Comb. Chem. 1, 55–68.
[65] Weiner, P.K., Langridge, R., Blaney, J.M., Schaefer, R., Kollman, P.A. (1982) Electrostatic Potential Molecular Surfaces. Proc. Natl. Acad. Sci. 79, 3754–3758.
[66] Kumru, M., Küçük, V., Kocademir, M., Alfanda, H.M., Altun, A., Sari, L. (2015) Experimental and theoretical studies on IR, Raman, and UV-Vis spectra of quinoline-7-carboxaldehyde, Spectrochim. Acta - Part A Mol. Biomol. Spectrosc. 134, 81–89.
[67] Baumann, J., Wurm, G., von Bruchhausen, F. (1980) Prostaglandin synthetase inhibition by flavonoids and phenolic compounds in relation to their O2--scavenging properties (author's transl). Arch. Pharm. (Weinheim). 313, 330–337.
[68] Soares, J.R., Dinis, T.C., Cunha, A.P., Almeida, L.M. (1997) Antioxidant activities of some extracts of Thymus zygis. Free Radic. Res. 26, 469–478.

Received: **13.11.2017**
Accepted: **10.02.2018**

CORRESPONDING AUTHOR

Semra Turkoglu
Firat University,
Faculty of Health Sciences,
23119, Elazig – Turkey

e-mail: smrturkoglu@hotmail.com

© by PSP Volume 27 – No. 5/2018 pages 3006-3012 Fresenius Environmental Bulletin

EVALUATION OF THE PHYSICOCHEMICAL CHARACTERISTICS AND CHLOROPHYLL-A CONTENT OF LAKE YENICAGA, BOLU

Savas Kilic[1,*], Z Arzu Becer[2]

[1]Mediterranean Fisheries Research Production and Training Institute, Antalya, Turkey
[2]Akdeniz University, Fisheries Faculty, 07059 Antalya, Turkey

ABSTRACT

The aim of this study was to assess some physical and chemical water characteristics, and chlorophyll-a content of the Lake Yeniçağa. In addition, the suitability of the obtained data was evaluated in terms of the fish life. The present study carried out between March 2009 and July 2010. According to the results of the analysis, it was determined that they did not pose a danger for fish survival although ammonium, nitrite, and phosphate values were high in some months.

KEYWORDS:
Fish life, Lake Yeniçağa, physical and chemical analysis of water, water quality.

INTRODUCTION

Lake Yeniçağa is an important aquatic system due to the commercial and sportive fishery, many migratory birds, its surrounding's being used as a recreational area, and being a peat bed. The lake is located on an important bird migration route between Europe and Africa. As a result of hosting a large number of migratory birds, the 1800 ha lake area was put under protection [1]. There are wide peat areas in the north and west of the lake, and private peat soil businesses are active in this area.

Studies have been conducted on the physical and chemical characteristics of Lake Yeniçağa, its phytoplankton and zooplankton fauna, benthic invertebrates [2-6], and the biology, populations, and fisheries of some fish species in the lake [7-9]. In fishery biology studies, it is necessary to know the physical and chemical characteristics of the water in order to determine the vital characteristics of the living thing. In this study, it is aimed to investigate the physical and chemical characteristics of Lake Yeniçağa water and also the suitability of the obtained data in terms of the fish life.

MATERIALS AND METHODS

Lake Yeniçağa is a freshwater lake in the Western Black Sea Region, Bolu province, Yeniçağa District (Figure 1). In the south of the lake as a settlement area is the district center of Yeniçağa, Hamzabey Village on the north-west, and Deliler Village on the north-east. The area around the lake is surrounded by reeds, and there are wide meadow areas in the north and west. The lake, which has an average area of 260 ha, feeds from the Deliler from the east and Kuzuviran creeks from the northwest. The lake waters drain to Aşağı Dere and Mengen Brook, which come out from the northeastern side of the lake and are taken with canals. The deepest point of the lake is 5.2 m [4]. There are wide peat areas in the north and west of the lake, and private peat soil businesses are active in this area.

In order to determine some physical and chemical water characteristics of Lake Yeniçağa, measurements and sampling were made from five different points once a month between August 2009 and July 2010. Onsekizler site, which is the west end of the lake, Hamzabey Brook entrance, where the water of the Kuzuviran Creek that passes through Hamzabey Village mixes with the lake, the Deliler Canal, where the Deliler Creek that passes through Deliler Village mixes with the lake, Mezbahane site, where the district sewer drains to the lake, and the Lake Center, which are all locations that can represent the water characteristics of the lake, were selected to be the sampling points.

Water samples were taken with two one-litregrey plastic bottles about 30 cm below the surface of the lake. The water samples were brought to the laboratory, where the analyses would be performed, as soon as possible in refrigerated containers with ice bags. The water samples were stored in the refrigerator at +4°C until the analyses were made. The temperature (T), dissolved oxygen (DO), and pH of the lake water were measured in situ by the Hach brand HQ40d Model portable measuring device, its conductivity (EC) with WTW Multi 340i/SET device approximately 30 cm below the surface of the lake. Alkalinity (± 5 mg/l), am-

monium (NH_4^+) (± 0.52 mg/l), nitrate (NO_3^-) (± 0.11 mg/l), nitrite (NO_2^-) (± 0.0028 mg/l), orthophosphate (PO_4^{3-}) (± 0.09 mg/l), calcium (Ca^{2+}) (± 1.6 mg/l), magnesium (Mg^{2+}) (± 0.57 mg/l), chloride (Cl^-) (± 0.052 mg/l), and sulphate (SO_4^{2-}) (± 2.6 mg/l) analyses were performed using a Spectroquant NOVA 60 model photometer using Merck brand spectroquant test kits. 200 ml of the water sample was filtered through GF/C Whatman filter paper 47 mm in diameter for the determination of chlorophyll-a content. The filtered filter papers were placed in a plastic tube tacitly and wrapped in aluminium foil and stored in a refrigerator at -18°C until the analysis. Chlorophyll-a was analyzed according to the methanol method by Marker [10].

RESULTS AND DISCUSSION

The annual mean physical and chemical characteristics of Lake Yeniçaga water are presented in Table 1, and the monthly change is presented in Figure 2.

The temperature of lake waters varies depending on the seasons, the geographical position of the lake, the surface area, the depth, the mineral salts dissolved in it, and the sun rays absorbed [11]. The water temperature is one of the most important factors limiting the life, growth, and reproduction of the fish. Considering that the fishes of the Cyprinidae family perform their normal activities such as the growth, nutrition, and reproduction at water temperatures of 4-28°C [12-13]. It can be said that the temperature values (1.8°C- 26°C) measured in Lake Yeniçağa are within the suitable limits for European chub and velvetfish.

In the upper parts where photosynthesis is intense, excess oxygen enters certain depths of water and that the oxygen level of the environment can exceed the saturation level [14]. It is thought that the oxygen production in July increases due to the photosynthesis by phytoplankton and the dissolved oxygen of the environment exceeds the saturation level, and also the high pressure generated by the open air on the day of measurement increases the dissolved oxygen content in the water, when the water temperature and chlorophyll-a content are the highest. It is thought that the dissolved oxygen is at the lowest level at Onsekizler site, where the concentration of phytoplankton is the highest in September, due to eutrophication. The dissolved oxygen content must be at least 5 mg/l in order for Cyprinidae to survive. Since the dissolved oxygen values (5.16 mg/l- 16.23 mg/l) measured in Lake Yeniçağa do not fall below this limit, there is no danger for the fish life.

The electrical conductivity is an indicator of the total dissolved solids in the water. The electrical conductivity values of waters suitable for fishery generally varybetween 150-750 µS/cm [15]. The pH value varies in proportion to the change in the CO_2 content in the water. The changes might be due to the decrease in the CO_2 content as a result of the seasonal photosynthesis by phytoplankton and the changes in the total alkalinity and precipitation [16]. Taking into consideration that the optimum pH value for freshwater fish is between 6 and 9, it can be concluded that the pH (7.56 - 8.86) and electrical conductivity values (488 µS/cm- 769 µS/cm) measured in Lake Yeniçağa are suitable for the fish life.

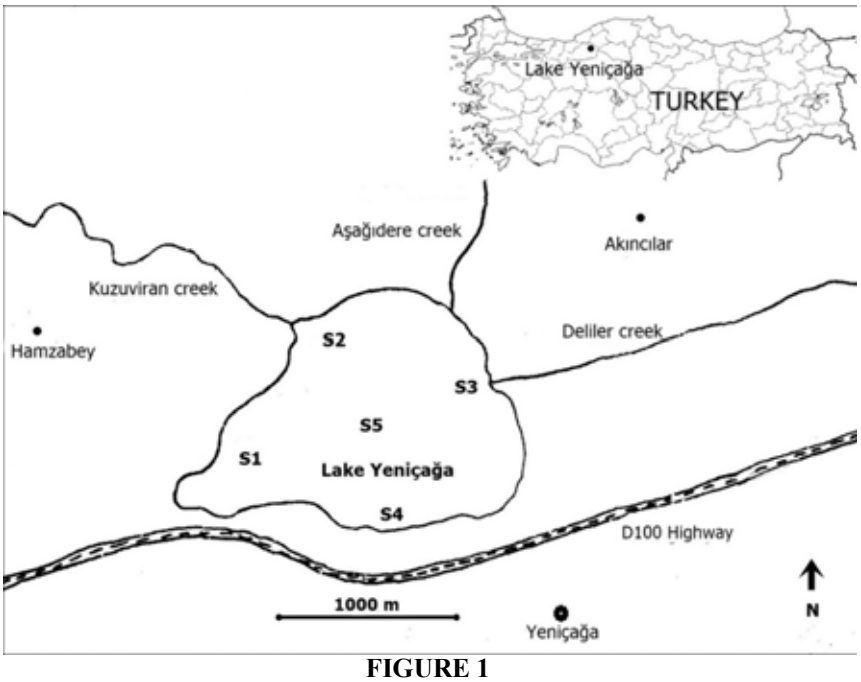
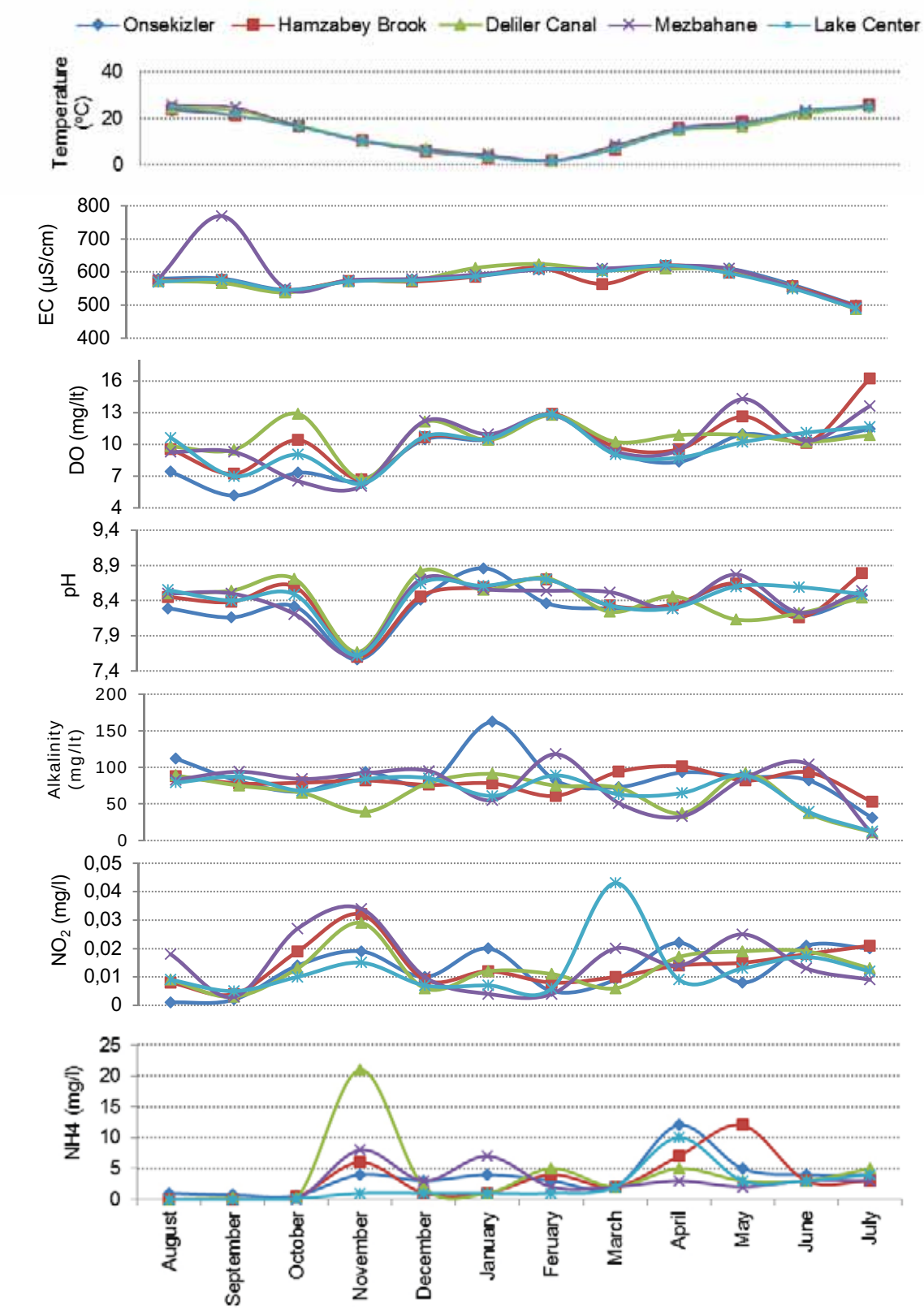


FIGURE 1
The location of Lake Yeniçağa in Turkey and water sampling points.


Onsekizler
Hamzabey Brook
Deliler Canal
Mezbahane
Lake Center
Temperature (°C)
40
20
0
EC (µS/cm)
800
700
600
500
400
DO (mg/lt)
16
13
10
7
4
pH
9,4
8,9
8,4
7,9
7,4
Alkalinity (mg/lt)
200
150
100
50
0
NO2 (mg/l)
0,05
0,04
0,03
0,02
0,01
0
NH4 (mg/l)
25
20
15
10
5
0
August
September
October
November
December
January
Feruary
March
April
May
June
July

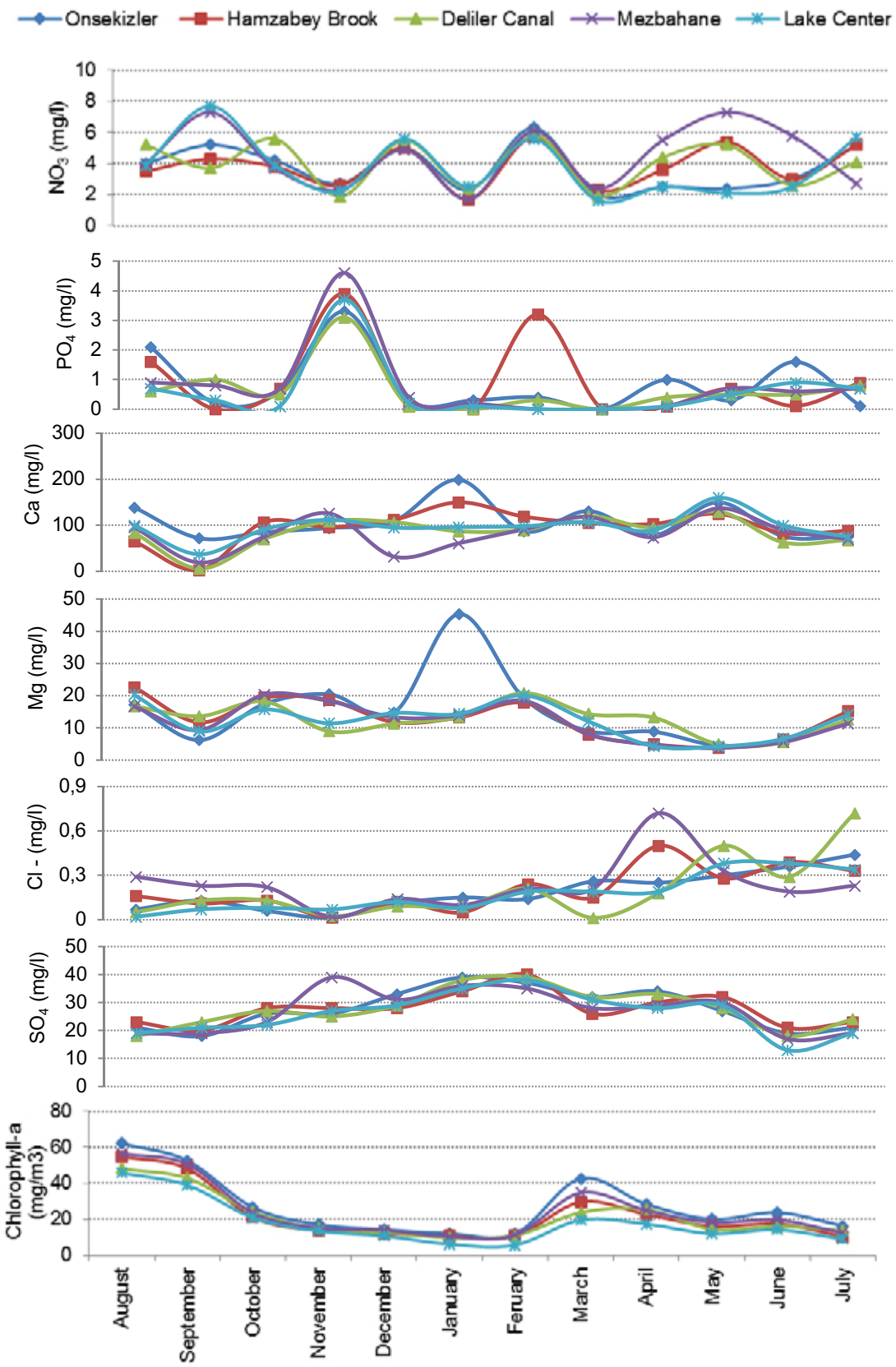


FIGURE 2
Monthly physical and chemical parameter values of the sampling points.

TABLE 1
Annual mean (lowest-highest) physical and chemical characteristics of Lake Yeniçağa water by the sampling points.

	Sampling points					
Parameters	Onsekizler	Hamzabey Brook	Deliler Canal	Mezbahane	Lake Center	Mean
T (°C)	14±2.3 (1.8- 24.9)	14.4±2.4 (1.8- 25.8)	14.6±2.4 (1.9- 25.2)	15.2±2.5 (2.1- 26.0)	14.4±2.4 (1.8- 25.1)	14.5±2.4 (1.9- 25.3)
EC (µS/cm)	579±9 (499- 614)	573±9 (497- 619)	577±11 (488- 624)	595±28 (493- 729)	575±10 (489- 621)	579±11 (493- 617)
DO (mg/l)	9.22±0.63 (5.16- 12.88)	10.52±0.77 (6.68-16.23)	10.62±0.47 (6.71-12.90)	10.35±0.72 (6.04-14.30)	9.82±0.55 (6.28-12.82)	10.02±0.54 (6.47-12.83)
pH	8.32±0.09 (7.56-8.86)	8.42±0.09 (7.60-8.79)	8.42±0.09 (7.67-8.81)	8.41±0.09 (7.61-8.77)	8.44±0.08 (7.62-8.70)	8.40±0.08 (7.61-8.63)
Alkalinity (mg/l)	87±9 (31-162)	80±4 (53-101)	64±8 (11-92)	75±9 (9-118)	68±7 (12-89)	75±5 (23-90)
NH_4^+ (mg/l)	3.6±0.9 (0.6-12.0)	3.3±1.0 (0-12.0)	4.0±1.6 (0-21.0)	2.8±0.7 (0-8.0)	2.2±0.8 (0-10.0)	3.2±0.7 (0.2-8.0)
NO_3^- (mg/l)	3.7±0.4 (2.0-6.3)	3.8±0.4 (1.7-5.7)	4.0±0.4 (1.9-5.9)	4.5±0.6 (1.7-7.3)	3.8±0.6 (1.6-7.7)	4.0±0.4 (2.0-5.9)
NO_2^- (mg/l)	0.013±0.002 (0.001-0.022)	0.014±0.002 (0.004-0.032)	0.021±0.002 (0.003-0.029)	0.015±0.003 (0.003-0.034)	0.013±0.003 (0.005-0.043)	0.015±0.002 (0.003-0.046)
PO_4^{3-} (mg/l)	0.9±0.3 (0-0.3)	0.9±0.4 (0-3.9)	0.7±0.2 (0-3.1)	0.8±0.4 (0-4.6)	0.6±0.3 (0-3.7)	0.8±0.3 (0-3.7)
Ca^{2+} (mg/l)	108±11 (72-199)	96±11 (3-150)	86±9 (6-130)	82±10 (19-137)	97±8 (37-160)	94±8 (27-140)
Mg^{2+} (mg/l)	15.3±3.2 (4.5-45.3)	12.8±1.8 (3.8-22.6)	12.8±1.4 (4.9-20.8)	12.0±1.7 (3.8-20.3)	12.2±1.6 (4.2-20.2)	13.0±1.6 (4.2-20.0)
Cl^- (mg/l)	0.190±0.038 (0.014-0.440)	0.206±0.042 (0.015-0.500)	0.202±0.061 (0.013-0.720)	0.241±0.050 (0.018-0.720)	0.176±0.037 (0.020-0.380)	0.203±0.037 (0.028-0.412)
SO_4^{2-} (mg/l)	28±2 (18-39)	28±2 (20-40)	28±2 (18-39)	27±2 (17-39)	26±2 (13-38)	27±2 (18-38)
Chlorophyll-a (mg/m^3)	27.2±4.8 (11.8-62.1)	22.2±4.3 (10.3-54.8)	21.3±3.6 (9.6-48)	24.2±4.4 (10.2-56.5)	17.7±3.6 (5.6-45.7)	22.5±4.1 (9.7-53.4)

The sulphate content exceeding 250 mg/l is an indication of contamination [17]. In general, it is estimated that the increases in sulphate values increase with precipitation, which is derived from fertilizers used in agricultural land, and industrial and domestic wastes. The sulphate values (13 mg/l- 40 mg/l) are not dangerous.

The alkalinity values of 30-500 mg/l $CaCO_3$ are accepted in natural waters [18]. The measured alkalinity values (9 mg/l- 162 mg/l) varied between the acceptable values.

The ammonia content exceeded 2.5 mg/l while the pH value was between 7.4 and 8.5 would lead to toxic effects on fish but the dissolved oxygen content would reduce the toxic effect of ammonia [15-19]. Similarly, higher oxygen values are thought to reduce the toxic effects of ammonia on fish although the average ammonia is calculated to be above 2.5 mg/l.

Contamination starts with the nitrite content in the water exceeding 1 mg/l [17]. It is thought that rainwaters carry agricultural, human, and animal wastes from agricultural land and settlement areas around the lake to the lake. According to the results, it is possible to mention the nitrite pollution in the lake. However, it has not reached a critical level in terms of the fish life. For fish and other aquatic organisms, the appropriate limits of nitrate are 5-10 mg/l, and if the nitrate nitrogen in the water exceeds 46 mg/l, the fish suffers respiratory distress and suffocate [20].

The high orthophosphate contents (0 mg/l- 4.6 mg/l) were observed in November. This can be explained by domestic and animal wastes originating from the district center around the lake, Hamzabey Village and Deliler Village settlements, and phosphate-containing fertilizers' used in agricultural land mixing with the lake water through rainwaters and creeks.

There should be at least 30-40 mg/l of calcium in the water suitable for fishing. It is thought that the periodic decrease in calcium values is due to the rain entering the lake through the creeks. The calcium values ranging from 82 mg/l to 108 mg/l on average are suitable values for life and development of the fish.

It is estimated that the seasonal change in magnesium values is derived from the creeks feeding the lake. The magnesium content of the water with the optimum fish fauna should be lower than 14 mg/l [19]. The average magnesium values of the sampling points by months in Lake Yeniçağa were measured to be above 14 mg/l in August, October, November, January, and February. However, it is shown that the points except for Onsekizler site (15.3 mg/l) are suitable environments for fish fauna

in terms of magnesium when the average magnesium values of the sampling points are examined.

As the oxygen content decreases, the toxic effect of chloride on the fish increases. The acceptable concentration value of chloride for fish is 4 mg/l [21]. There is no pollution caused by chloride in Lake Yeniçağa.

Chlorophyll-a is one of the important water quality parameters because it also shows the primary production and eutrophication levels [22]. Chlorophyll-a contents are the indicator of phytoplankton growth in the lake. The environmental factors affecting the phytoplankton also affect the chlorophyll-a content [23]. It is thought that the phytoplankton density increases with the increase in the nutrient level in the lake, and accordingly, it causes the increase in chlorophyll-a content.

CONCLUSION

In conclusion, ammonium, nitrite, and phosphate values were high levels in certain periods in the lake but they did not pose a danger for fish survival. It is estimated that the use of nitrogenous, phosphorous, and nitrate fertilizers on agricultural areas around the lake and the transportation of domestic and animal wastes in the surrounding villages to the lake with the Kuzuviran and Deliler Creeks increase the ammonium, nitrite and phosphate values of the lake. In order to improve the quality of water in Lake Yeniçağa, the domestic and industrial wastes from the villages around the lake and the district center should be treated with appropriate treatment systems and be released to the creeks and lake. Furthermore, the excessive and unnecessary use of fertilizers should be precluded.

ACKNOWLEDGEMENTS

This study was funded by the Akdeniz Universitiy Scientific Research Projects Coordination Unit under project number 2009.03.0121.003.

REFERENCES

[1] BirdLife International (2001) Important Bird Areas and Potential Ramsar Sites in Europe. BirdLife International. Wageningen, Netherlands, 126p.

[2] Akıncı, G. (2000) Some physical and chemical characteristics of Yeniçağa lake and determination and seassonal changes of zooplanktonic species (cladocera and copepoda). MSc Thesis. Hacettepe University, Institute of Graduate Studies in Science. Ankara.

[3] Saygı, B.Y. and Demirkalp, F.Y. (2004a) Trophic status of shallow Yeniçağa Lake (Bolu, Turkey) in relation to physical and chemical environment. Fresen. Environ. Bull. 13, 385-393.

[4] Saygı, B.Y. and Demirkalp, F.Y. (2004b) Primary production in shallow eutrophic Yeniçağa Lake (Bolu, Turkey). Fresen. Environ. Bull. 13, 98-104.

[5] Sümer, N. (2002) Flora of Yeniçağa. MSc. Thesis. University of Abant İzzet Baysal Department of Biology, Bolu.

[6] Özbek, M. and Sarı, M.H. (2007) Hirudinea (Annelida) fauna of some lakes located in western Black Sea Region. E.U. Journal of Fisheries and Aquatic Sciences. 24, 83-88.

[7] Kılıç, S. (2003) Population and fishing of carp (Cyprinus carpio L., 1758) in Yeniçağa Lake. MSc Thesis. Karadeniz Technical University Institute of Science. Trabzon.

[8] Kılıç, S. and Becer Özvarol, A.Z. (2008) Yeniçağa Gölü'nün (Bolu) av kompozisyonunun belirlenmesi üzerine bir çalışma. Su Ürünleri Mühendisleri Derneği Dergisi. 32, 18-21 (in Turkish).

[9] Kılıç, S., Becer Özvarol, A.Z., Yılmaz, S. and Özvarol, Y. (2010) Fishing, fish population and sustainable fishing management in the Lake Yenicaga (Bolu). Ecological Life Sciences. 5, 344-352.

[10] Marker, A.F.H. (1994) Chlorophyll a SCA Method Revision. Natural Environment Council, PR/395/3/A.

[11] Tanyolaç, J. (2000) Limnoloji. Hatiboğlu Yayınları No 67, Ankara (in Turkish).

[12] Baensch, H.A. and Riehl, R. (1991) Aquarien atlas. Bd. 3. Melle: Mergus. Verlag für Natur- und Heimtierkunde, Germany.

[13] Baensch H.A. and Riehl, R. (1995) Aquarien Atlas. Band 4. Mergus. Verlag GmbH, Verlag für Natur- und Heimtierkunde, Melle, Germany.

[14] Morkoç, E. (1991) Seasonal variations of primary production and limiting nutrients in the Izmit Bay using carbon-14 technique and their relationships with environmental factors. Phd Thesis. Istanbul University, Institute of Marine Sciences and Geopraphy. Istanbul (in Turkish).

[15] Bremond, R. and Vuichard, R. (1973) Parameters de la qualite des eaux. Ministere de la Protection de la Nature et de Environnement Documentation Française, Paris.

[16] Boyd, C.E. (1990) Water Quality in Ponds for Aquaculture. Agricultural Experiment Station Press, Auburn, Alabama.

[17] Nisbet, M. and Verneaux, J. (1970) Composantes chmiques des eaux courantes. Annales de Limnologie, 6, 161-190.

[18] Sarıhan, E. (1993) Balık Üretimi. Çukurova Üniversitesi Ziraat Fakültesi Basımevi. Adana, 41-55 (in Turkish).
[19] Ekmekçi, F.G. (1989) Sarıyar Baraj Gölü'ndeki ekonomik öneme sahip balık stoklarının incelenmesi. Doctorate Thesis. Hacettepe University Institute of Science, Department of Biology. Ankara, 225p (In Turkish).
[20] Yaramaz, Ö. (1992) Su Kalitesi. E.Ü. Su Ürünleri Fakültesi. İzmir (In Turkish).
[21] Alabaster, J.S. and Lloyd, R. (1982) Water Quality Criteria for Freshwater Fish. Butterworths, London.
[22] Kayaalp, G.T. and Polat, S. (2001) Estimation of chlorophyll-a for full completed and incompleted regression model. E.U. Journal of Fisheries and Aquatic Sciences. 18, 529-535.
[23] Türkoğlu, M., Yenici, E., İşmen, A. and Kaya, S. (2004) Variations of nutrient and chlorophyll-a in the Çanakkale Strait (Dardanelles). E.U. Journal of Fisheries and Aquatic Sciences. 21, 93-98.

Received: **15.11.2017**
Accepted: **05.02.2018**

CORRESPONDING AUTHOR

Savas Kilic
Mediterranean Fisheries Research Production and Training Institute,
Antalya – Turkey

e-mail: savasyay@gmail.com

© by PSP Volume 27 – No. 5/2018 pages 3013-3019 Fresenius Environmental Bulletin

STATISTICAL AND SPATIAL ANALYSES OF THE MANGANESE CONCENTRATIONS IN THE SHALLOW GROUNDWATER OF THE URBAN AREA OF SUZHOU, ANHUI PROVINCE AND ITS ENVIRONMENTAL IMPLICATIONS

Sun Linhua[1,2,*], Cheng Chen[1,2]

[1]School of Resources and Civil Engineering, Suzhou University, Anhui 234000, China
[2]National Engineering Research Center of Coal Mine Water Hazard Controlling, Anhui 234000, China

ABSTRACT

Groundwater is important for the development of the city of Suzhou, because most of the water used for domestic, industrial and agricultural purpose is obtained from the underground. In this study, a total of 62 shallow groundwater samples in the urban area of the city have been collected and their manganese (Mn) concentrations have been measured, then the data have been analyzed by statistical and spatial analyses. The results show that the Mn concentrations in the groundwater range from 19.0-728 μg/L (mean = 263 μg/L), and most of the samples (90.3%) were classified to be Class IV according to the groundwater quality standard of China, implying that the groundwater should be treated before drinking. The samples have medium coefficient of variation and low p-values of normal distribution test, suggesting that it may have been influenced by anthropogenic activities, which was further demonstrated by the consistent of the distribution of the samples with high Mn concentrations and the areas with high density of human, transportation and hardware manufacturing, as well as the high-high cluster of the spatial autocorrelation analysis. The environmental background values have been calculated to be 60.6-415 and 0-592 μg/L, based on the box plot and spatial autocorrelation analyses, respectively, which were related to their different basis (need normal distribution or not).

KEYWORDS:
Groundwater, manganese, spatial autocorrelation, statistical analysis

INTRODUCTION

Most of the water used for the industrial, agriculture and domestic purpose in north China is obtained from the underground. However, with the rapid development of the society and economy, the environmental condition of the groundwater was gradually becoming worse, because of the irrational exploration of the groundwater, and the anthropogenic pollution [1]. Therefore, the scientific issues related to the groundwater have attracted a large number of studies, such as the study related to the regional hydro-geology, hydrochemistry, groundwater pollution, restoration, modeling and management [2-4].

Trace elements, especially the toxic ones (e.g. Hg, Cd, Pb, Zn et al), have long been concerned by scientists because of their special characteristics and hazardous for the human health [5, 6]. Among these metals, iron (Fe) and manganese have attracted the most attention because of their high contents in the groundwater, and most of the other metals in the water can be affected by the Fe and Mn oxides and hydroxides. And therefore, a series of studies have been carried out for the removal of them from the water [7-9].

Suzhou is an important city with coal production in China, and it is also a city with long period of groundwater utilization. The water for industrial and domestic purpose is mainly obtained from the underground, especially the shallow and deep pore water. In recent years, with the continuous development of the urban economy and scale, the demand for industrial and domestic water is increasing, and the problems related to the development and utilization of groundwater resources are exposed more and more, which restricts the sustainable development of the city and the health of the people in the area [10-12]. The recent study about the drinking water in the city has reported a low standard-reaching rate of Mn (only 65%) [13].

Because of the importance of groundwater for the development of the city, a total of 62 groundwater samples from the shallow wells in the urban area have been collected and analyzed for their Mn concentrations, and the statistical and the spatial autocorrelation analyses have been applied to the data, for getting the information about: (1) the Mn con-

centration and their spatial distribution, (2) spatial autocorrelation and clustering identification and (3) the environment background value of Mn in the groundwater, which can provide scientific information for the protection and utilization of the shallow groundwater in the area.

MATERIALS AND METHODS

Study area. Suzhou is the north gate of the Anhui province, China. It is located at the south of the Huang-Huai plain, with adjacent to Xuzhou of Jiangsu and Heze of Shandong in the north, Yongcheng of Henan in the west, Suqian of Jiangsu in the east. The annual precipitation is 857 millimeters, with an average temperature of 14.4 degrees (centigrade). There are many rivers in the area, including the Kui, Sui, Tuo and Hui Rivers. However, the groundwater is the main water source for industrial production, agriculture activities and urban living in the city.

Sampling and analysis. A total of 62 shallow groundwater samples were collected from the shallow wells (<30m), and the sample's locations are shown in Figure 1. Before sampling, a 2.0 L polyethylene bottle that has been cleaned in the laboratory have been rinsed three times by the water, and then the samples were acidified to be pH<2 by HNO_3 to prevent the adsorption of the elements by the bottle, and finally labeled and sent to the laboratory for processing. The GPS location and site conditions (including the flow of people, life, industry and traffic related information) have been recorded. In the laboratory, all of the samples were filtered by 0.22 μm film before analysis for removing debris. The concentrations of Mn was analyzed by atomic absorption spectrometer, and the quality control was carried out by standard sample (the correlation coefficient between actual concentration and measured concentration was higher than 0.99). All of the analysis was conducted in the Engineering Research Center of Coal Mine Exploration, Anhui province, China.

Data treatment. Firstly, all of the data were processed for statistical analysis by the Mystat 12 software, for calculating the maximum, minimum and mean values, standard deviation, coefficient of variation and the p-value of the normal distribution test, and then the contour map of the Mn concentrations was constructed by the Surfer 11 software (with natural neighbor grid method), and finally the spatial autocorrelation analysis by the Geoda 1.8.3 software. Finally, the local spatial autocorrelation is processed to obtain the significant map and the spatial clustering map.

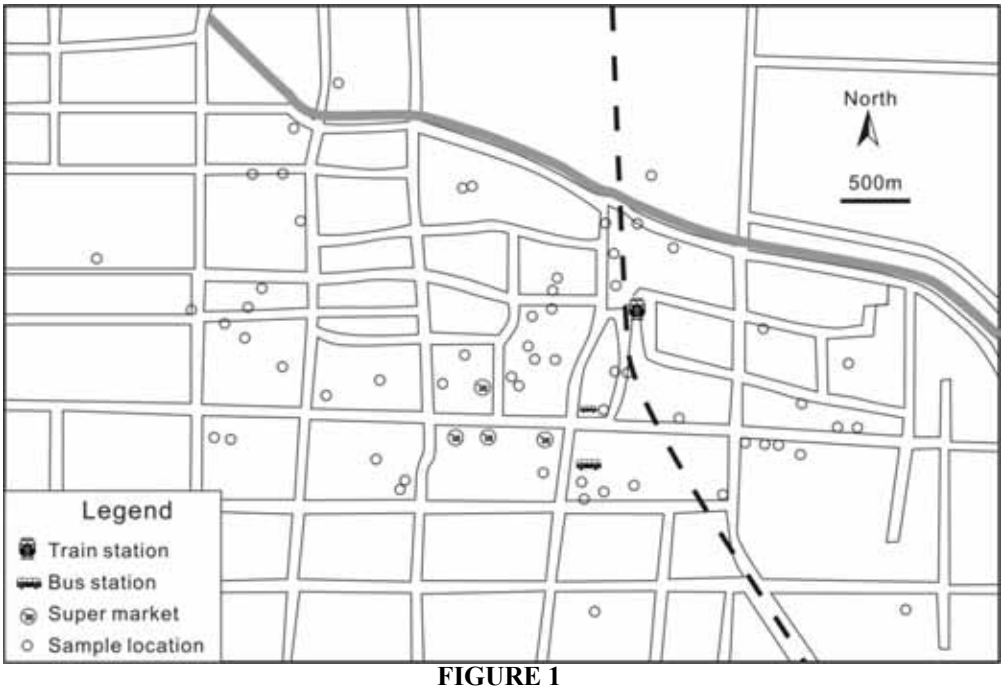


FIGURE 1
Locations of the groundwater samples in this study.

TABLE 1
Descriptive statistics of Mn concentrations in this study (μg/L).

	N	Min	Max	Mean	SD	CV	p-value
Mn	62	19.0	728	263	137	0.519	<0.01

Environmental background. The environmental background is the concentrations (mostly, the range of concentrations) of the elements in the relative clean area (with low or no contribution of anthropogenic activities), and is the basis for determine the pollution degree of the regional environment [14, 15]. For the management of the groundwater, environmental background is also important, because it is needed for identifying the pollution of the groundwater and, it is also the destination of the environmental protection [16].

At present, there are two kinds of methods for determine environmental background values, including the geochemical method and statistical method. Among these two, the statistical method is the most commonly used one, because it is hard to find a place without anthropogenic influence, which was needed for the geochemical method. There are some specific methods related to the statistical method: e.g. the relative cumulative frequency, the normal distribution, the regression analysis, the outlier test, the iterative standard deviation and so on [14, 15]. And all of these methods have a same basis that the background values of the sample obey the normal distribution (or lognormal distribution).

In this study, two kinds of methods have been applied for the determination of the environment background value:

(1) the box plot by the Mystat 12, which based on the assumption that the environmental background value in line with the normal distribution. After processing, the samples outside of the lower and upper hinge of the box plot were removed (repeated until no abnormal samples), and then calculate the mean and standard deviation of the rest of the samples. The environmental background value was then calculated to be mean± 2*standard deviation.

(2) based on the spatial autocorrelation analysis, the basis is that there is no significant change of the concentrations in the sample relative to its adjacent samples, or namely “no mutation ”. Therefore, the samples for calculating the environmental background values only consider the “non-significant” samples (not belong to the high-high, low-low, high-low and low-high clusters) after spatial autocorrelation analysis, and the environmental background value was also calculated by the mean±2*standard deviation.

RESULTS AND DISCUSSION

Concentrations. Based on the situation of the groundwater quality in China and the health of people, as well as the goal for environmental protection, the National Standard of China (GB/T 14848-93) have classified the groundwater quality into five degrees with Mn concentrations: Class I and II (≤0.05 mg/L), natural background; Class III (≤0.10 mg/L), suitable for drinking, industrial and agricultural use; Class IV (≤1.0 mg/L), suitable for industrial and agricultural use (can also be used for domestic purpose after treatment); Class V (>1.0 mg/L), not suitable for any purpose. In this study, the Mn concentrations of the groundwater are 19.0-728 μg/L (mean = 263 μg/L) (Table 1). In comparison with the National Standard of China, one sample is classified to be Class I and II, five samples are classified to be Class III, and 56 samples are classified to be Class IV, which suggest that the groundwater in the study area might have been polluted by Mn releasing processes (either natural or anthropogenic).

Coefficient of variation (CV = standard deviation / mean) has long been used for identifying the anthropogenic contribution for the pollution in the environmental studies [17, 18], previous studies revealed that when CV < 0.10, it means low anthropogenic contribution, whereas CV > 0.90 means high anthropogenic contribution. In this study, the CV of the Mn concentrations of the groundwater samples is 0.519, which indicates that the groundwater has probably been influenced by anthropogenic activities. Additionally, the p-value of the normal distribution test is <0.01, which means that the Mn concentrations in this study cannot pass the normal distribution test ($p > 0.05$), which also suggests the anthropogenic contribution [14, 15]. Even after log transformation, the CV is still > 0.10 and the p-value < 0.05, which also means anthropogenic influence.

Spatial distribution. The contour map of the Mn concentrations in this study is shown in Figure 2. As can be seen from the figure, two areas with high Mn concentrations can be found in the central and central-northeast of the study area. In comparison with the sample locations in the Figure 1, it can be found that the groundwater samples with high Mn concentrations are located in the area between the train station, bus stations and the business area. Our observation during sampling found that this area is characterized by high density of people, transportation, hardware manufacturing and business. And therefore, the high Mn in this area might be contributed by natural and anthropogenic sources simultaneously, because except for the weathering of Mn bearing rock, the manufacturing of hardware and the discharge of garbage can release Mn into the environment [17].

Spatial autocorrelation analysis. The local spatial autocorrelation (LISA) has been applied for the calculation of spatial clustering in this study, and according to the classification of the Moran'I index [19], all of the samples can be subdivided into two major categories after calculation: “not significant” and “significant”. Samples classified into the former are considered as “no mutation”

relative to its adjacent samples, and the samples classified into the latter can be divided into four sub categories: high-high, low-low, low-high and high-low, which represent the relationship between a sample and its surrounding ones. Moreover, the concentration of the high-high samples can be called as “hot spot”, and the concentration of the low-low samples is identified as “freezing spot”, whereas the low-high and high-low samples are abnormal ones, which may be related to the influence of other factors [20-23]. The results of spatial autocorrelation analysis are shown in Figure 3.

As can be seen from the figure, 35 samples are classified to be “not significant” samples, whereas the sample numbers classified to be high-high, low-low, low-high and high-low clusters are 10, 8, 6 and 3, respectively. It can also be noticed from the figure that the samples divided into the high-high cluster are mainly concentrated in the area between the railway station (north), bus station (south) and its western commercial district. Therefore, this area can be called as "hot spot". This area is also consistent with the distribution of the samples with high Mn concentrations (Figure 2), which implying that the releasing of Mn from the steel (railway, bus, hardware manufacturing) and living garbage is the main influence factor. In contrast, the low-low cluster samples are all located in the west of the study area, where is the newly constructed urban area with low density of human. Further, for the low-high and high-low abnormal samples, they reflect that the concentrations of Mn in these samples are "mutation" relative to the surrounding ones, and may be a reflection of natural (low-high) or anthropogenic disturbance (high-low) [20-23].

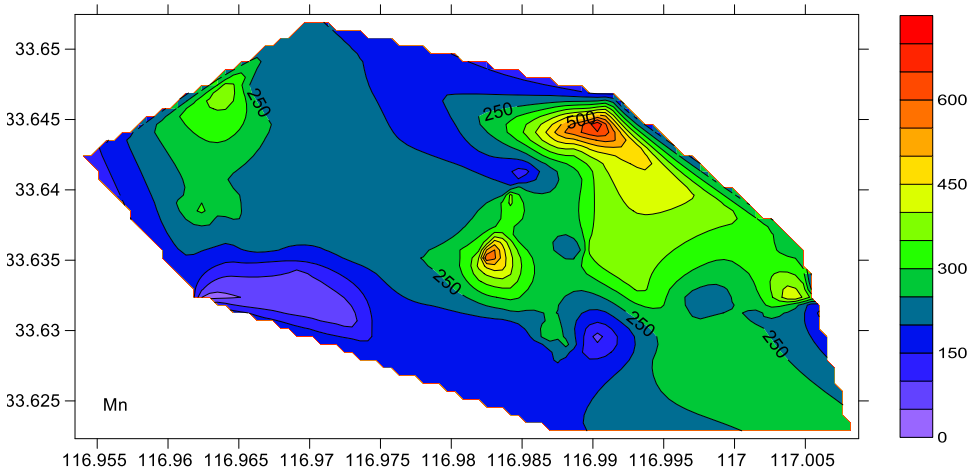


FIGURE 2
Contour map of Mn concentrations (μg/L).

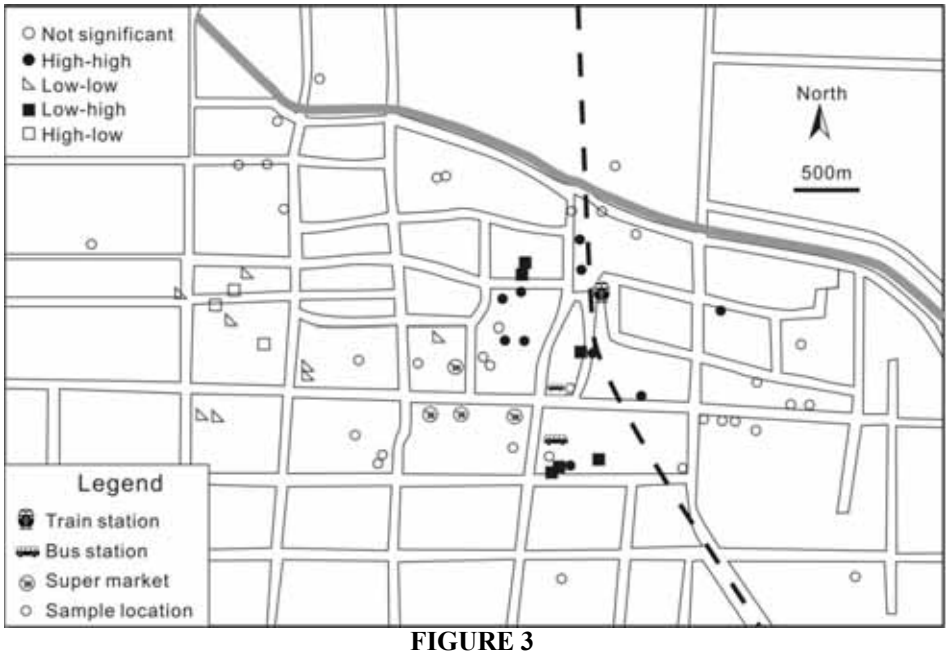


FIGURE 3
Results of spatial autocorrelation analysis.

TABLE 2
Descriptive statistics of Mn concentrations of the samples after outlier removal (μg/L).

	N	Min	Max	Mean	SD	CV	p-value
Mn[1]	56	54.0	426	238	88.7	0.373	>0.15
Mn[2]	35	54.0	728	280	156	0.558	<0.01

Note: 1 and 2 are the samples after outlier removal based on the box plot and spatial autocorrelation analysis, respectively.

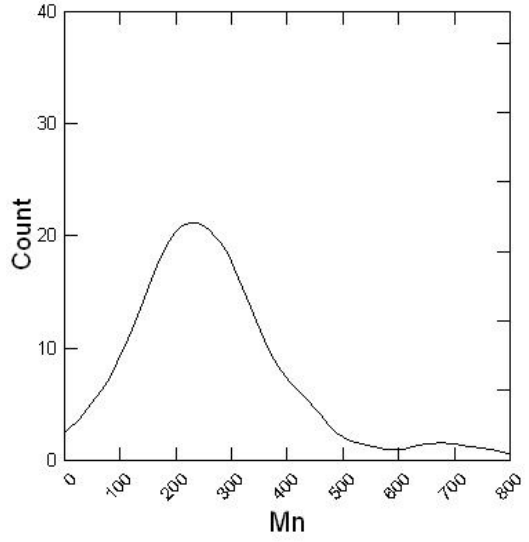


FIGURE 4
Density plot of the Mn concentrations (μg/L).

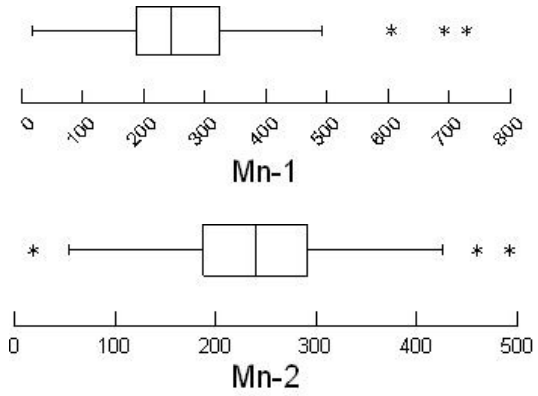


FIGURE 5
Box plot of the Mn concentrations (μg/L).

Implications for the environmental background. Figure 4 is the density plot of Mn concentrations. It can be seen from the figure that the concentrations of Mn have at least two peaks, which probably have two kinds of information: one is that the Mn in the groundwater might have been influenced by anthropogenic activities (the second peak), and another is that the Mn in the groundwater without anthropogenic influence might follow the normal distribution (the first peak in the Figure 4). Moreover, based on the box plot of the Mn concentrations, there are 3 samples with concentrations higher than 500 μg/L are identified to be outliers (Mn-1 in Figure 5), and another 3 samples can be identified as outliers with the second application of the box plot (Mn-2 in Figure 5). After the removal of the six ones, the remaining 56 samples were calculated and the average value was 238 μg/L with standard deviation to be 88.7 μg/L (Table 2). Therefore, the background value calculated by the statistics method was 60.6-415 μg/L.

As to the spatial autocorrelation analysis, the above mentioned 35 samples belong to the "not significant" category were calculated, and the mean value was 280 μg/L with the standard deviation was 156 μg/L (Table 2). Therefore, the background value calculated by the spatial autocorrelation analysis method was 0-592 μg/L (less than 0 and replaced by 0).

Further discussion. For comparison, the iterative standard deviation, distribution function method [24] and QQ plot [25] have also been applied for calculation the environmental background. The results show that the environmental background values of Mn in the groundwater are 88.7-399 μg/L (iterative standard deviation) and 48.9-441 μg/L (distribution function), respectively. As can be seen from the QQ diagram (Figure 6), it is hard to find an inflection point, and therefore, it is hard to determine the environmental background value through the method.

According to the results obtained by the above methods, it can be found that the calculated environmental background values are different with each other, and the main reason for this difference is their different basis: for the statistical methods (including box plot, QQ plot and iterative standard deviation, distribution function), the basis is that the background samples follow the normal distribution, they calculated the environmental background to be 48.9-441 μg/L, whereas the spatial analysis focused on the "no mutation" feature, the environmental background calculated by it is 0-592 μg/L.

Different methods should be chosen for the environmental background estimation according to different conditions: if the distribution of the element/pollutant can be determined or demonstrated (most commonly normal or lognormal), the statistics method (or the method with same principle, such as the iterative standard deviation and the probability distribution plot [24, 25]) can be considered. However, if the distribution of data is uncertain, the method of spatial analysis should be chosen. Considering about the Mn in this study, it is

hard to determine which distribution is follow, because it is hard to find a straight line in the QQ plot even before or after lognormal transformation (Table 1 and Figure 6). And therefore, the spatial autocorrelation method should be chosen.

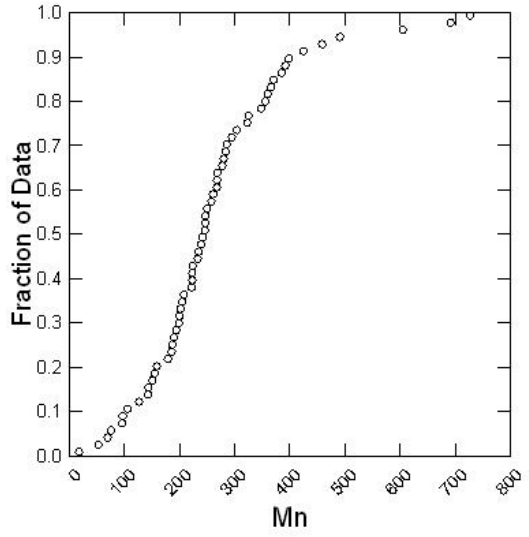


FIGURE 6
QQ plot of the Mn concentrations (μg/L).

CONCLUSIONS

Based on the statistical and spatial analyses of the Mn concentrations of the shallow groundwater in Suzhou, Anhui province, China, the following conclusions have been made:

(1) Most of the samples (90.3%) were classified to be Class IV according to the groundwater quality standard of China, which means that the groundwater should be treated before drinking. The samples have medium coefficient of variation and low p-values of normal distribution test, implying that it may have been influenced by anthropogenic activities.

(2) The spatial distribution of the Mn concentration suggests that the samples with high concentrations of Mn are located in the area consistent with the hot spot identified by spatial autocorrelation analysis, and indicating that the area has been influenced by anthropogenic activities.

(3) The environmental background values have been calculated to be 60.6-415 and 0-592 μg/L with box plot and spatial autocorrelation analyses, respectively.

ACKNOWLEDGEMENTS

This work was financially supported by the Scientific Research Program of the Students in Suzhou University (KYLXLKZD17-22) and the Key Research Program of Suzhou University (2016yzd08).

REFERENCES

[1] Liu, G.D., Wu, W.L., Zhang, J. (2005) Regional differentiation of non-point source pollution of agriculture-derived nitrate nitrogen in groundwater in northern China. Agriculture, Ecosystems & Environment. 107(2), 211-220.

[2] Zhang, W.L., Tian, Z.X., Zhang, N., Li, X.Q. (1996) Nitrate pollution of groundwater in northern China. Agriculture, Ecosystems & Environment. 59(3), 223-231.

[3] Rodríguez-Lado, L., Sun, G., Berg, M., Zhang, Q., Xue, H., Zheng, Q., Johnson, C.A. (2013) Groundwater arsenic contamination throughout China. Science. 341(6148), 866-868.

[4] Zhang, X., Pei, D., Hu, C. (2003) Conserving groundwater for irrigation in the North China Plain. Irrigation Science. 21(4), 159-166.

[5] Alinnor, I.J., Obiji, I.A. (2010) Assessment of trace metal composition in fish samples from Nworie River. Pakistan Journal of Nutrition. 9(1), 81–85.

[6] Begum, A., Ramaiah, M., Khan, I., Veena, K. (2009) Heavy metal pollution and chemical profile of Cauvery River Water. Journal of Chemistry. 6(1), 47–52.

[7] Mouchet P. (1992) From conventional to biological removal of iron and manganese in France. Journal-American Water Works Association. 84(4), 158-167.

[8] Ellis, D., Bouchard, C., Lantagne, G. (2000) Removal of iron and manganese from groundwater by oxidation and microfiltration. Desalination. 130(3), 255-264.

[9] Katsoyiannis, I.A., Zouboulis, A.I. (2006) Use of Iron- and Manganese-Oxidizing Bacteria for the Combined Removal of Iron, Manganese and Arsenic from Contaminated Groundwater. Water Quality Research Journal of Canada. 41(2), 117-129.

[10] Li, L., Qin, F.G., Chen, M.H. (2004) Elementary analysis on high iron content of groundwater. Ground Water. 26(4), 260-261.

[11] Liu, Q., Liang, H. (2014) The application of electrometric method and numerical simulation to evaluate groundwater resources in the Suzhou city, Anhui province. Chinese Journal of Engineering Geophysics. 11(5), 688-692.

[12] Lin, M.L., Peng, W.H. (2016) Concentrations and health risk assessment of heavy metals in groundwater in rural areas of Suzhou City. Water Resources Protection. 32(06), 114-120.

[13] Yu, B., Zhi, Y.H. (2017) Analysis on the outcomes of drinking water monitoring in urban areas in Suzhou of Anhui province from 2015 to 2016. Journal of Tropical Diseases and Parasitology. 15(2), 102-140.
[14] Reimann, C., Filzmoser, P., Garrett, R.G. (2005) Background and threshold: critical comparison of methods of determination. Science of the Total Environment. 346(1), 1-16.
[15] Reimann, C., Garrett, R.G. (2005) Geochemical background—concept and reality. Science of the total environment. 350(1), 12-27.
[16] Liu, W.B., Feng, C.E., Gao, C.R. (2014) Background value of groundwater environment in Hetao Plain. Earth Science Frontiers. 21(4), 147-157.
[17] Sarkar, D., Datta, R., Hannigan, R. (2011) Concepts and applications in environmental geochemistry. vol. 5. Elsevier.
[18] Sun, L.H., Cheng, B.X., Chen, S.H. (2017) Trace metal concentrations in the river water near the urban area: a case study in Suzhou, northern Anhui province, China. Fresen. Environ. Bull. 26, 4017-4022.
[19] Anselin, L. (1995) Local indicators of spatial association-LISA. Geographical Analysis. 27(2), 93-115.
[20] Moran, P.A.P. (1948) The interpretation of statistical maps. Journal of the Royal Statistical Society. Series B (Methodological). 10(2), 243-251.
[21] Ord, J.K., Getis, A. (1995) Local spatial autocorrelation statistics: distributional issues and an application. Geographical Analysis. 27(4), 286-306.
[22] Diniz-Filho, J.A.F., Bini, L.M., Hawkins, B.A. (2003) Spatial autocorrelation and red herrings in geographical ecology. Global Ecology and Biogeography. 12(1), 53-64.
[23] Zhao, X.F., Huang, X.J., Zhang, X.Y., Zhu, D.M., Lai, L., Zhong, T.Y. (2009) Application of spatial autocorrelation analysis to the COD, SO2 and TSP emission in Jiangsu Province. Environmental Science. 30(6), 1580-1587.
[24] Nakić, Z., Posavec, K., Bačani, A. (2007) A visual basic spreadsheet macro for geochemical background analysis. Ground Water. 45(5), 642-647.
[25] Panno, S.V., Kelly, W.R., Martinsek, A.T., Hackley, K.C. (2006) Estimating background and threshold nitrate concentrations using probability graphs. Ground Water. 44(5), 697-709.

Received: **16.11.2017**
Accepted: **05.02.2018**

CORRESPONDING AUTHOR

Sun Linhua
School of Resources and Civil Engineering,
Suzhou University,
Anhui 234000 – China

e-mail: sunlinh@126.com

© by PSP Volume 27 – No. 5/2018 pages 3020-3027 Fresenius Environmental Bulletin

EFFICIENT REGENERATION AND *AGROBACTERIUM TUMEFACIENS* MEDIATED GENETIC TRANSFORMATION OF POTATO (*SOLANUM TUBEROSUM* L.)

Hussein Abdullah Ahmed[1,2], Surendra Barpete[1,*], Guray Akdogan[1], Gulsum Aydin[3], Cengiz Sancak[1], Sebahattin Ozcan[1]

[1]Department of Field Crops, Faculty of Agriculture, University of Ankara, 06110, Diskapi, Altindag, Turkey
[2]Department of Field Crops, Faculty of Agriculture and Natural Sciences, Usak University, Eylul Kampusu, Usak, Turkey
[3]Department of Biotechnology, Faculty of Science, University of Selcuk, Alaeddin Keykubat Yerleskesi Selcuklu, Konya, Turkey

ABSTRACT

Potato (*Solanum tuberosum* L.) is highly demandable world food crop and has become a staple food in many parts of the world including Turkey, India and China. Potato under in vitro culture condition is recalcitrant and genotype dependent. Therefore, we tested several factors to enhance regeneration and genetic transformation efficiency of Turkish potato genotypes. The influence of physical factors and conditions in *Agrobacterium* mediated transformation of the potato leaves was tested. Using the best combination (10 mg L^{-1} ZR, 10 mg L^{-1} NAA) with Agrobacterium-mediated transformation, we regenerated independent putative transformants 61.6% of the total explants cultured. GUS and nptII positive plants were confirmed by molecular analysis (PCR) that showed transformation rate of 24.16%. The protocol described here is simple, efficient, and produces transgenic plant in 7-8 weeks after inoculation with *Agrobacterium bacterium*.

KEYWORDS:
Solanum tuberosum, Agrobacterium tumefaciens, Transformation, potato, Co-cultivation

INTRODUCTION

Potato (*Solanum tuberosum* L.) is an important crop that can help to alleviate growing hunger problem in the world by providing a balanced diet, as it is rich in many nutrient contents and carbohydrate [1]. The total world potato production is estimated at 3815 million tons [2] and is the third most important food crop in the world after rice and wheat in terms of human consumption.

Potato is prime candidate for improvement through biotechnology techniques and breeding strategy for nutritional quality and production. Many diseases, pests and weeds can cause significant losses in production of potato [3]. Therefore, it is very important to grow potatoes that are efficient with more resistant to herbicides, pests and diseases with nutritional content [1, 4]. *Agrobacterium tumefaciens* has been widely used for the introduction of a large number of foreign genes into plant cells to develop transgenic plants with enhanced resistance to biotic and abiotic stresses [4]. Gene transfer via *A. tumefaciens* is a complex process affected by a number of genetic factors associated with the bacteria, host plant cells and the interaction of these factors [5, 6, 7]. Leaves, stems, tubers, petiole, protoplasts and micro-tubers have been used as the explants to develop transgenic potato lines [1, 8]. However, the transformation efficiency is significantly dependent on genotype [9, 10, 11] and reliable regeneration protocol [12]. Thus, a genotype specific regeneration and transformation method needs to be developed [13, 14]. This study aimed to develop an efficient regeneration and genetic transformation procedure using *A. tumefaciens* for the local potato genotypes of Turkey.

MATERIALS AND METHODS

Plant material and culture condition. Four potato genotypes namely Innovator, Marabel, Tokat-10/1 and Tokat-6/24 were used for optimization of regeneration protocol. The tubers of genotypes were washed with running tap water to remove traces of soil then surface sterilized using 2.5% sodium hypochlorite for 20 min. This was followed by 3 × 5 min rinsing with sterile double distilled water. The tubers were sprouted at 24 °C under dark conditions for six weeks. The sprouts (2-3 cm) were excised from the tubers that again re-sterilized with 1.25% sodium hypochlorite for 20 min and rinsed with 3 × 5 min sterile distilled water. Thereafter, the apical buds explants were cultured on MS regeneration medium [15] supplemented with 3% sucrose and solidified with 0.3% Gelrite. The explants were sub-cultured to fresh media at three weeks interval. Plantlets height 8-10 cm with 6-8 leaves were obtained after four weeks of culture explants. Leaf discs (0.5 cm^2) and internode explants were prepared for culture. Leaf discs were

inoculated on axial side by submerging in the medium. Several plant growth regulators combinations were tested for plant regeneration (data not shown). Thereafter, two standardized plant regeneration protocol were selected and applied for four potato genotypes.

All culture media were autoclaved at 121 °C (1.5 kg cm^{-2} pressure) for 20 min and pH was adjusted to 5.6–5.8 with 1 N NaOH or 1 N HCl. All cultures were grown at 25 ± 2 °C with a 16/8h light/dark cycle photoperiod. The light was supplied at an intensity of 25 µmol photons m^{-2} s^{-1} using cool-white fluorescent lamps.

1st Regeneration Medium (RM1). Four-weeks old leaves were used for preparing leaf discs of 0.5 cm diameter. The leaf discs were cultured on MS medium supplemented with 4 mg L^{-1} gibberellic acid (GA_3), 1 mg L^{-1} 6-benzylaminopurine (BAP), 0.1 mg L^{-1} naphthalene acetic acid (NAA), 3% sucrose and 0.3% gelrite for callus induction and shoot regeneration. The shoots were rooted on MS medium devoid plant growth regulators.

2nd Regeneration Medium (RM2). Leaf discs were cultured on MS medium containing 10 mg L^{-1} trans-zeatin riboside (ZR), 10 mg L^{-1} NAA, 3% sucrose and 0.3% gelrite under dark conditions for three days. Thereafter, explants were transferred to callus induction MS medium supplemented with 2 mg L^{-1} ZR, 0.2 mg L^{-1} NAA, 0.02 mg L^{-1} GA_3. After 2 weeks of culture, the calli were transferred to shoot regeneration MS medium containing 2 mg L^{-1} ZR, 0.2 mg L^{-1} GA_3, 3% sucrose and 0.3% gelrite. The regenerated shoots were transferred to MS medium containing 0.2 mg L^{-1} indole-3-butyric acid (IBA) for rooting.

Agrobacterium Strain and Plant Transformation Vector. *A. tumefaciens* strain GV2260 [16] carrying binary plasmid p35S-GUS-INT [17] was used for plant transformation studies. The binary plasmid carried neomycin phosphotransferase II (*nptII*) marker gene under control of the nopaline synthase (NOS) promoter and β-glucuronidase (*GUS*) gene under control of the cauliflower mosaic virus (CaMV35S) promoter. *Agrobacterium* strain was inoculated in YEP medium (8 g L^{-1} nutrient broth, 1 g L^{-1} yeast extract, 0.24 g L^{-1} magnesium sulfate and 5 g L^{-1} sucrose) supplemented with 50 mg L^{-1} kanamycin.

Infection media (Inoculation & co-cultivation). Five different methods were tested for optimization of transformation via *A. tumefaciens*.

Gene transfer protocol (1st, 2nd & 3rd). The leaf discs of Takat-10/1 (4-5 mm^2) were inoculated for 30 min on liquid RM2 medium with *A. tumefaciens* culture diluted 1:20, 1:40 and 1:80 for 1st, 2nd and 3rd gene transfer protocol respectively. Thereafter, the infected leaf discs were co-cultivated with same medium solidified with gelrite for 48 h. After co-cultivation, explants were sub-cultured on same regeneration selection medium containing 75 mg L^{-1} kanamycin and 500 mg L^{-1} duocid.

Gene transfer protocol (4th). In the 4th gene transfer protocol, leaf dices inoculated with *A. tumefaciens* culture diluted 1:50 in liquid MS medium supplemented with 5 mg L^{-1} GA_3, 1 mg L^{-1} BAP, 1 mg L^{-1} IAA, 1 mg L^{-1} 2,4-D 100 µM acetosyringone and 5 mM betaine for 30 min. Thereafter, the infected leaf discs co-cultivated on MS solid regeneration medium containing 5 mg/L GA_3, 1 mg L^{-1} BAP, 1 mg L^{-1} IAA for 48 h. Then, leaf discs were transferred to RM2 containing 75 mg L^{-1} kanamycin and 500 mg L^{-1} duocid after co-cultivation.

Gene transfer protocol (5th). The leaf discs were mixed with *A. tumefacines* suspension that diluted 1:30 in MS liquid regeneration medium containing 0.37 M acetosyringone for 10 min. Thereafter, co-cultivated on solid medium supplemented with 2 mg L^{-1} ZR, 0.2 mg L^{-1} NAA, 0.02 mg L^{-1} GA_3 for 72 h. Thereafter, the explants were sub-cultured on regeneration medium (RM2) containing 75 mg L^{-1} kanamycin and 500 mg L^{-1} duocid.

Rooting and acclimatization of transgenic plantlets. The regenerated shoots (5-6 cm) on RM2 were rooted on MS medium containing 0.2 mg L^{-1} IBA, 500 mg L^{-1} Duocid and 75 mg L^{-1} kanamycin. The root initiations were started after one week of culture inoculation. Roots were thin but healthy in culture medium. Thereafter, the rooted plants were removed, washed and transferred to plastic pots containing mixture of peat, perlite and soil (1:1:1). Each pot was covered with a transparent polyethylene bag to create a high relative humidity; afterwards, the polythene bags were gradually opened. The acclimatized plants were maintained under ambient daylight conditions at 19–23 °C in a greenhouse. Transformation efficiency was calculated by dividing total number of polymerase chain reaction positive plants divided by the total number of explants used in the experiments, and this was expressed as a percentage.

GUS (β-glucuronidase) histochemical assay. All regenerated and survived plants were examined for GUS histochemical assay. Therefore, the samples were immersed in X-gluc {100 mM sodium phosphate (pH=7.0), 10 mM EDTA, 0.1% Triton X–100 and 1 mM 5-bromo-4-chloro-3-indolyl-β-D-glucuronic acid} solution and incubated at 37 °C overnight and fixed with 70% ethanol. A characteristics blue color spots shown the expression of GUS (*β-glucuronidase*) gene in the positive plant tissues.

The proper control plant for GUS histochemical assay was done that explants showing no blue color spot.

Molecular evaluation of putative transformants. The genomic DNA of putative transgenic plants used as template for Polymerase Chain Reaction (PCR) analyses using the *Phire Plant Direct PCR Kit (Thermo Scientific,* Cat. #F-130WH*)* used according to the manufacturer's recommendations. PCR was carried out using the gene-specific primer to amplify the internal fragment of *nptII* (459 bp) from putative transgenic plants. The amplification reaction proceeded with gene-specific primers *nptII* (forward: TTGCTCCTGCCGAGAAAG-3' and reverse 5'-R-GAAGGCGATAGAAGGCGA-3'). The PCR was performed at 98 °C for 5 min, 98 °C for 5 sec, 58 °C for 15 sec, and 72 °C for 3 min followed by 40 cycles. The plasmid DNA was used as positive control, whereas DNA from untransformed plants was used as negative control. The amplified DNA fragments were electrophoresed on 1.5% agarose gel and visualized by ethidium bromide staining under ultraviolet (UV) light.

Statistical analysis. The all experimental data were subjected to one-way analysis of variance (ANOVA, SPSS for Windows v. 11., SPSS, USA), and the post hoc tests were performed using least squares difference (LSD). Data given in percentages were subjected to arc sine ($\sqrt{X}$) transformation [18] before statistical analysis.

RESULTS AND DISCUSSION

The development of reliable regeneration protocol is crucial step for potato genetic transformation [19]. Because, genotype is important factor that affecting frequency of plant regeneration as well as genetic transformation in potato [19, 20, 21]. In a first set of experiment, contamination free leaf discs and internode explants were cultured on various PGRs combinations that exhibited explant swelled and callus production on leaf discs; whereas, internode explant show less callus induction from cut end (data not shown). The selection of healthy leaf explants (0.5 cm^2) from potato stock plant is critical for generating a high frequency of callus, shoot and root regeneration. The callus initiation was observed at the cut edges of leaf discs after 7-8 days of culture. After two weeks of culture inoculation, green compact calli were produced from leaf explants on all the combination of auxin, Cytokinin and Zeatin Riboside (ZR). The leaf discs explants were produced more calli, with NAA more effective than ZR for callus induction. Leaf discs explants did not produced callus at the lower level of ZR. Therefore, the two best PGRs-explant combinations that regenerated the highest number of shoots were: leaf explants on MS medium containing 4 mg L^{-1} GA_3, 1 mg L^{-1} BAP, 0.1 mg L^{-1} NAA (RM1) and 10 mg L^{-1} ZR, 10 mg L^{-1} NAA (RM2) were used for four potato genotypes.

In the second set of experiments, the leaf explants of four potato genotypes were cultured on RM1 and RM2 selected media from previous experiments. All the four potato genotypes were shown callus induction and shoot initiation after two and four weeks of culture respectively. Although, shoot regeneration frequency in RM1 did not show any statistically significant differences (ANOVA) between of genotypes, whereas; shoot regeneration frequency and number of shoots per explants were significant ($P<0.01$) in RM2. The cultured leaf explants in Magenta boxes containing 75 ml of medium resulted in vigorous growth of callus, shoot initiation as compared to the explants cultured in test tube, and glass bottles. These kinds of glassware's were used commonly and frequently in previous studies [22, 23]. The reason of improvement of culture growth in the Magenta boxes is probably due to the greater availability of sufficient quantity of nutrients and proper air space [23]. However, the result of present study indicated that incubation of culture explants in 16h light and 8 h dark photoperiod with a temperature of 25±2°C with a light intensity of 25 μmm^2 s^1 developed healthy and vigorous stock plants. The regenerated shoots behavior in both types of media is compared, shoot induction on RM2 was most favorable with maximum shoot regeneration frequency (90.00%) and number of shoots (10.83) noted on genotype Tokat-10/1 (Table 1).

The results are in agreement with Ewing et al. [24] and Khatun et al. [8]. They found that plant regeneration capability and behavior depends on the genotype and growth medium during the plant regeneration. However, it is also important to develop an efficient plant regeneration system prior to genetic transformation are in agreement with Pierik [25] and Uranbey et al. [26, 27].

The regeneration rate of each genotype differs depending on regeneration media. The shoot regeneration frequencies were ranged 41.03 – 51.90% and 30.98 - 90.00% on RM1 and RM2 respectively. Therefore, it is significant to determine local genotypes with high regeneration capabilities for efficient genetic transformation. Therefore, RM2 and potato genotype Tokat-10/1 with high regeneration capacity was used for *Agrobacterium-mediated* transformation studies. Moreover, vigorous and healthy stock plants of potato genotype Tokat-10/1 were maintained on MS basal medium supplemented with 3% sucrose. Shoot tips plus one axillary bud (approximately 2–3 cm in length) of genotype Tokat-10/1 was used as explant and subcultured that developed 8–10 leaves at 4-weeks culture peri-

od that used as explant source for transformation studies.

***Agrobacterium-mediated* gene transfer.** In the last leg of experiments, leaf discs of genotype Tokat-10/1 was infected with five different ratio of agrobacterium dilution (strain GV2260 carrying plasmid p35S-GUS-INT) for oncogenic efficiency and subsequently plant regeneration. The results of experiment shown that mixtures and dilution of bacterial cultures with ratios of 1:20, 1:40, 1:50 and 1:80 for 30 min incubation with bacteria did not shown significant genetic transformation efficiency on Tokat-10/1; whereas, 1:30 dilution for 10 min @ 72 h exhibited 24.16% transformation efficiency. Since the aim of these infections was to test whether transformation efficiency increased by mixed infections and could gave potato plants transformed with T-DNA from the disarmed Agrobacterium.

A simple and rapid transformation protocol for the potato genotype Tokat-10/1 has not been reported previously. Potato genotype Tokat-10/1 is sensitive to photoperiod and produces tubers under short-day conditions. Therefore, a rapid and efficient transformation protocol for this genotype would facilitate research in Turkish environment. Numbers of *Agrobacterium*-mediated gene transfer protocol for potato have already been developed [28, 29]. However, they mainly focus on commercial varieties such as "Bintje", "Desire" "Russet Burbank" and "Shepody" [30, 31, 32, 33]. The transformation frequency is significantly dependent on genotype reported by Vinterhalter et al. [34] and Cingel et al. [10]. However, efficiency of infection was highly influenced by strain of *Agrobacterium tumefaciens* that plays significant role for genetic transformation [6]. Apart from this, the Agrobacterium host strain LBA4404 has been commonly used for transformation of potato as well as cotton transformation [6, 14]. Earlier study emphasized that the Agrobacterium host strain GV2260 contributed to superior transformation efficiency compared to LBA4404 in potato. Therefore, we used the GV2260 host strain exclusively in these experiments. The current protocol reduced the time for tedious washing procedure and dark incubation of explants that commonly used in potato transformations. The addition of growth regulators to the infection medium was exhibited to the vigor growth of callus on leaf discs explants and had no significant effect on the efficiency of transformation and regeneration. These are agreement with Barpete et al. [6] and Anayol et al. [35]. They found that adding of PGRs in infection media increase the transformation and regeneration efficiency of cultured explant.

The cultured explants swelled and developed callus from the cut surface on selected medium containing 50 mg L^{-1} of kanamycin after 6–7 days of incubation on. The rest of explants showed no signs of growth or exhibited necrosis in the culture. The number of explants were induced callus that ranging from 07 to 89 explants out of 120 explants cultured. The protocol number 5th were best and showed green calli that initiated first shoot buds after three weeks of culture in the RM2 (Figure 1a).

The emerged shoots with a height of 5-6 cm were excised and rooted on MS medium containing 0.2 mg L^{-1} IBA, 500 mg L^{-1} Duocid and 75 mg L^{-1} kanamycin (Figure 1b). The regenerated plants were washed in running tap water to remove trace of medium then transferred to pots (Figure 1c). Regenerated plantlets were acclimatized in the greenhouse and allowed to set mini potato tubers. Thereafter, the histochemical GUS assay and PCR analysis were performed to confirm the presence of transgenes in putative transgenic plants. Histochemical GUS analysis was performed with leaf, shoot and tuber sample collected from putative transgenic plants. The dark or light blue regions were seen on different tissues incubated in histochemical reagent. *GUS* gene expressions were confirmed by blue spots that recorded 24.16% out of 46.66% tested putative plant (Figure 1d). Leaf explants were expressing higher GUS activity as compare to the shoot and tuber explant. PCR analysis of the GUS positive explants confirmed the presence of *nptII* gene by exhibiting a 459 bp fragment on the agarose gel, non-transgenic plants and control plants did not show any amplified fragment on the agarose gel (Figure 2).

TABLE 1
Effect of different regeneration medium on adventitious shoot regeneration in different potato cultivars and genotypes

Genotypes	1st *Regeneration Medium* (RM1)		2nd *Regeneration Medium* (RM2)	
	Shoot Regeneration Frequency (%)	Number of shoots/ explant	Shoot Regeneration Frequency (%)	Number of shoots/explant
Tokat 10/1	41.03b	3.00 b*	90.00 a*	10.83 a*
Tokat 6/24	42.73b	2.26 b	72.78 ab	9.16 a
Innovator	46.86b	1.93 b	63.93 b	2.66 b
Marabel	51.90a	4.60 a	30.98 c	2.30 b

* Means represented with different letters within each column are significantly different according to LSD test on 1 % significance level

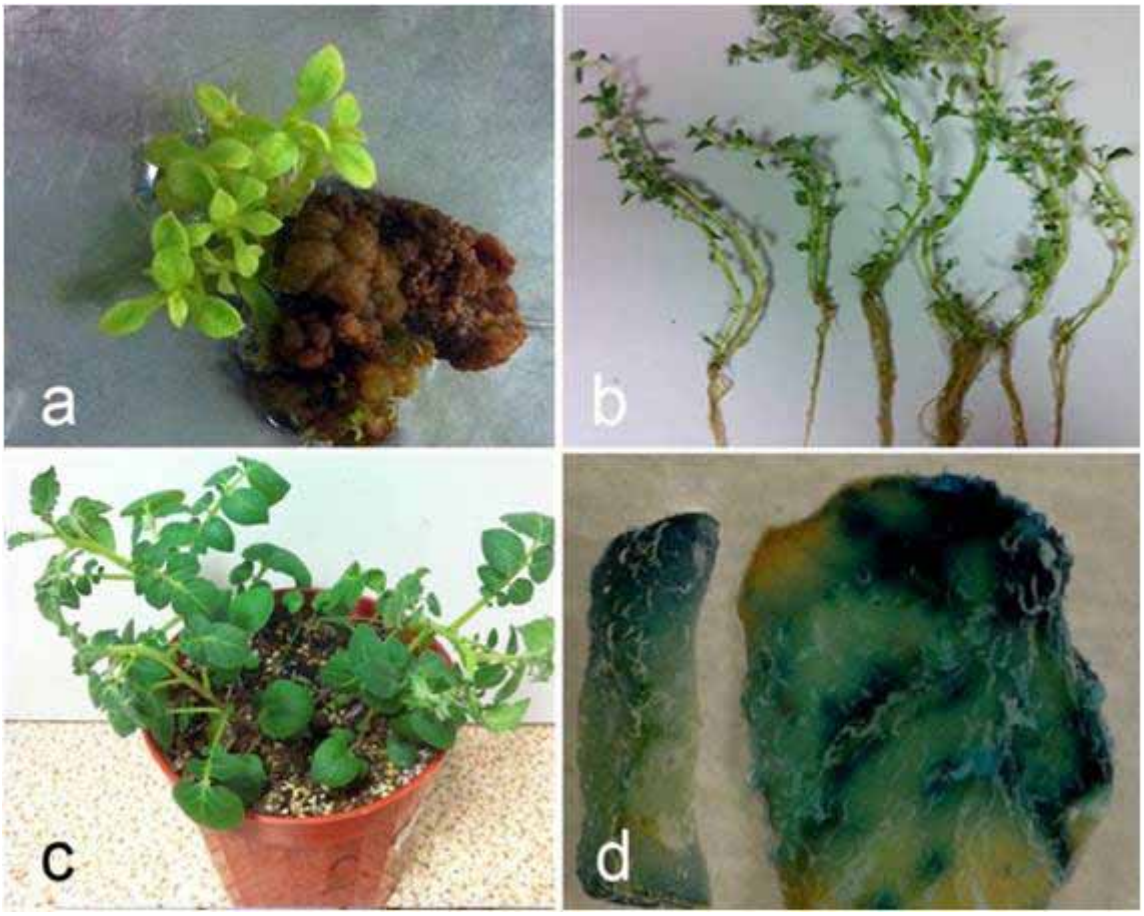


FIGURE 1
Agrobacterium-mediated genetic transformation of Tokat 6/24 potato genotype a) Kanamycin resistant shoot development on regeneration medium after 10-12 weeks of culture initiation, b) Rooting of kanamycin-resistant shoots on medium containing kanamycin, c) Acclimatization of rooted plantlets in growth chamber d) GUS gene expression on stem and on leaflets

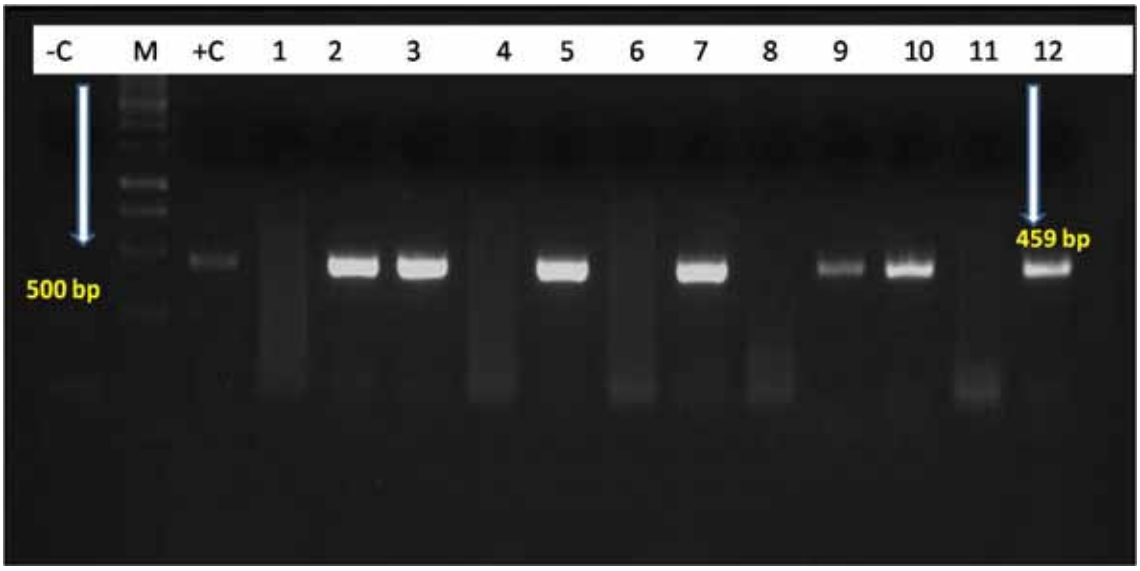


FIGURE 2
Confirmation of npt-II gene in plants growing in greenhouse by PCR. M: Marker; -C: negative control (untransformed plant); +C: Positive control (pBin19 Ti plasmid); Lane 1-12: putative trancgenic plant.

TABLE 2
The leaf discs explants of potato genotype Tokat-1/10 were cultured on RP2 medium after infection with *Agrobacteirum strain* GV2260- p35S - NPT II on three different transformation protocol their genetic transformation frequency (%)

Protocol	No. of explant	Agrobacterium culture diluted	Inoculation time	Cocultivation Period	Callus resistant to kanamyscin (Kn)	Shoots Resistant to Kn	Rooted shoots resistant to Kn	GUS +ve & NPT II +ve plants	Tranformation efficency (%)
1st	120	1:20	30 min	48 h	16	6	2	-	0.00
2nd	120	1:40	30 min	48 h	14	5	3	1	0.83
3rd	120	1:80	30 min	48 h	07	-	-	-	0.00
4th	120	1:50	30 min	48h	23	8	4	3	2.50
5th	120	1:30	10 min	72h	89	74 (61.6%)	56 (46.6%)	29	24.16

*kanamyscin denote as Kn

In nutshell, 120 explants were cultured but no transgenic plants were obtained with the 1st and 3rd protocols; whereas, only 1 and 3 positive plant were obtained from 2nd and 4th protocol respectively. In the 5th protocol 74 (61.6%) explants of the explants formed kanamycin resistant shoots, 56 (46.6%) of the explants were rooted and transgene expression was verified by histochemical GUS assay and PCR assay confirmed 29 (24.16%) explant were positive for all the parameter used (Table 2).

In the study, shoot regeneration and acclimatization are developed as early as 4 and 8 weeks respectively after Agrobacterium infection compared to 10-12 weeks in earlier reports of potato transformation [22, 36]. Thereafter, we continued to use this protocol for transformation and have regenerated over 350 independent transgenic lines after first year. This protocol may be useful in several genotypes for the introduction and regeneration of agronomically important traits without the problem of somaclonal variation. Therefore, it would be beneficial for a large-scale application to potato transformation.

ACKNOWLEDGEMENTS

The present work is partially supported by the Scientific and Technological Research Council of Turkey (TUBITAK). The authors would like to thank Prof. Dr. Gungor Yilmaz (University of Gaziosmanpasa, Department of Field Crops) and Dr. Huseyin Onaran (Niğde Potato Research Institute) for providing the plant material. The authors would like to thank Dr Jitendra Kumar (Department of Plant Pathology, University of Minnesota, USA) for valuable suggestion and improvement of the present manuscript.

The authors declare that they have no conflict of intrest for the manuscript entitled “Efficient regeneration and *Agrobacterium tumefaciens* mediated genetic transformation of potato (*Solanum tuberosum* L.)”.

All authors discussed, planned and carried out experiments collectively. All authors have made substantial contributions to conception and design, acquisition of data, analysis and interpretation of data. All authors have been involved in drafting the manuscript or revising it critically for important intellectual content. All authors read and approved the final manuscript to be published.

REFERENCES

[1] Veale, M.A., Slabbert, M.M. and Van, E.L. (2012) Agrobacterium-mediated transformation of potato cv. Mnandi for resistance to the potato tuber moth (Phthorimaea operculella). South Afr. J. Bot. 80, 67-74.

[2] FAOSTAT (2017) http://www.tarimpusulasi.com/images/files/PATATES%20DOSYASI.pdf.

[3] Nowicki, M., Foolad, M.R., Nowakowska, M. and Kozik, E.U., (2012) Potato and tomato late blight caused by Phytophthora infestans: An overview of pathology and resistance breeding. Plant Disease. 96, 4-17.

[4] Tavazza, R., Tavazza, M., Ordas, B.R.J., Ancora, G. and Benvenuto, E. (1988) Genetic transformation of Potato (Solanum tuberosum): An efficient method to obtain transgenic plants. Plant Sci. 59, 175-181.

[5] Ziemienowicz, A. (2014) Agrobacterium-mediated plant transformation: Factors, applications and recent advances. Biocatal. Agricult Biotechno. 3, 95-102.

[6] Barpete, S., Bakhsh, A., Anayol, E., Özcan, S. F., Oğuz, M.C., Karakoç, O.C. and Özcan, S. (2016a) Inducing osmotic stress leads to better genetic transformation efficiency in cotton (Gossypium hirsutum L.). Turk. J. Biol. 40, 826-836.

[7] Khabbazi, S.D., Barpete, S., Sancak, C. and Ozcan, S. (2017) Preconditioning effect of bap on in vitro multiplication of mature embryo of Lentil (Lens Culinaris Medik.) Fresen. Environ. Bull. 26, 191-125.
[8] Khatun, A., Hasan, M.M., Bachchu, M.A.A., Moniruzzaman, M. and Nasiruddin, K.M. (2012) Agrobacterium-mediated genetic transformation of potato (Solanum tuberosum L.) var Cardinal and Heera. The Agricult. Scientific J. Krishi Found. 10, 81-86.
[9] Heeres, P., Schippers, R.M., Jacobsen, E. and Visser R.G.F. (2002) Transformation of a large number of potato varieties: genotype-dependent variation in efficiency and somaclonal variability. Euphytica. 124, 13-22.
[10] Cingel, A., Vinterhalter, B., Vinterhalter, D., Dragosavac, D.A., Smigocki, A. and Ninkovi S (2010) Agrobacterium-mediated transformation of two Serbian potato cultivars (Solanum tuberosum L. cv. Draga_evka and cv. Jelica). Afr. J. Biotechno. 9, 4644-4650.
[11] Barpete, S., Oğuz, M.C., Özcan, S.F., Anayol, E. and Ahmed, H.A. (2015) Effect of temperature on germination, seed vigor index and seedling growth of five Turkish cotton (Gossypium hirsutum L.) cultivars. Fresen. Environ. Bull. 24, 2561-2566.
[12] Barpete, S., Özcan, S.F., Khawar, K.M. and Özcan, S. (2016b) Effect of plant growth regulators and physical factors on in vitro high frequency regeneration of Grass pea. J. Anim. Plant Sci. 26, 1087-1093.
[13] Haberlach, G.T., Cohen, B.A., Reichert, N.A., Baer, M.A., Towill, L.E. and Helgeson, J.P. (1985) Isolation, culture and regeneration of protoplasts from potato and several related Solanum species. Plant Sci. Lett. 39, 67-74.
[14] Butler, N.M., Baltes, N.J., Voytas, D.F. and Douches, D.S. (2016) Geminivirus-Mediated Genome Editing in Potato (Solanum tuberosum L.) Using Sequence-Specific Nucleases. Front Plant Sci., 7, 1045.
[15] Murashige, T. and Skoog, F. (1962) A revised medium for rapid growth and bioassay with tobacco tissue cultures. Physiol. Planta. 15, 473-497.
[16] Deblaere, R., Bytebier, B., De Greve, H., Deboeck, F., Schell, J., Vanmontagu, M. and Leemans, J. (1985) Efficient octopine Ti plasmid-derived vectors for Agrobacterium-mediated gene transfer to plants. Nucleic Acids Res. 13, 4777-4788.
[17] Vancanneyt, G., Schmidt, R., O'conner, S.A., Willmitzer, L. and Rosh, S.M. (1990) Construction of an intron-containing marker gene: Splicing of the intron in transgenic plants and its use monitoring early events in Agrobacterium-mediated plant transformation. Mol. Gen. 220, 245-250.
[18] Snedecor, S.W. and Cochran, W.G. (1967) Statistical methods. The Iowa State University Press, Iowa, USA, 327-329.
[19] Borna, R.S., Hoque, M.I. and Sarker, R.H. (2010) Agrobacterium mediated genetic transformation for local cultivars of potato (Solanum tuberosum L.) using marker genes. Plant Tiss Cult. Biotechno. 20, 145-155.
[20] Ahloowalia, B.S. (1982) Plant regeneration from callus culture in potato. Euphytica. 31, 755-759.
[21] Romano, A., Raemakers, K., Bernardi, J., Visser, R. and Mooibroek, H. (2003) Transgene organisation in potato after particle bombardment-mediated (co-) transformation using plasmids and gene cassettes. Transgen. Res. 12, 461–473.
[22] Wenzler, H., Mignery, G., May, G. and Park, W. (1989) A rapid and efficient transformation method for the production of large numbers of transgenic potato plants. Plant Sci. 63, 79–85.
[23] González, R.G., Sánchez, D.S., Guerra, Z.Z., Campos, J.M., Quesada, A.L., Valdivia, R.M., Arencibia, A.D., Bravo, K.Q. and Caligari, P.D.S. (2008) Efficient regeneration and Agrobacterium tumefaciens mediated transformation of recalcitrant sweet potato (Ipomoea batatas L.) cultivars. Asia Pac. J. Mol. Biol. Biotechno. 16, 25-33.
[24] Ewing, E., Higgins, A. and Simpson, J. (1985) Cutting as simplified models of the potato plant. In: Li, P.H. (Ed) Potato Physiology. Academic Press. San Diego, New York. 153-207.
[25] Pierik, R.L.M. (1987) In vitro culture of higher plants. Martinus Nijhoff Publishers. Boston. Horticult. 35, 28-33.
[26] Uranbey, S., Basalma, D., Sancak, C., Er, C. and Ozcan, S. (2005a) Agrobacterium-mediated transformation in potato using different explant and co-cultivation media and histochemical detection of pathogenesis related promoters. Biol. Bratis. 60, 685-690.
[27] Uranbey, S., Sevimay, C.S., Kaya, M.D., İpek, A., Sancak, C., Başalma, D., Er, C. and Özcan, S. (2005b) Influence of different co-cultivation temperatures, periods and media on Agrobacterium tumefaciens-mediated gene transfer. Biol. Planta. 49, 53-57.
[28] Onamu, R., Legaria, J.P., Sahagún, J.C., Rodríguez, J.L. and Pérez, J.N. (2012) In vitro regeneration and Agrobacterium-mediated transformation of Potato (Solanum tuberosum L.) Cultivars Grown in Mexico. Plant Tiss. Cult. Biotech. 22, 93-105.
[29] Forsyth, A., Weeks, T., Richael, C. and Duan, H. (2016) Transcription Activator-Like Effector Nucleases (TALEN)-Mediated Targeted DNA Insertion in Potato Plants. Front. Plant Sci. 7, 1572.

[30] Stiekema, W.J., Heidekamp, F., Louwerse, J.D., Verhoeven, H.A. and Dijkhuis, P. (1988) Introduction of foreign genes into potato cultivars Bintje and Desiree using an Agrobacterium tumefaciens binary vector. Plant Cell Rep. 7, 47-50.
[31] Ishida, B., Synder, G. and Belknap, M. (1989) Using in vitro micro tubers in transformation of potato. Plant Cell Rep. 8, 325-328.
[32] Beaujean, A., Sangwan, R.S., Lecardonnel, A. and Sangwan, N.B.S. (1998) Agrobacterium-mediated transformation of three economically important potato cultivars using sliced internodal explants: an efficient protocol of transformation. J. Exp. Bot. 49, 1589–1595.
[33] Gustafson, V.S., Mallubhota, J., Macdonnel, M., Sanyal, B.B., Chakravarty, G., Wang-Pruski, C., Rothwell, P., Audy, D., Dekoeyer, M., Siahbazi, B.F. and Gan, S.R. (2006) Transformation and plant regeneration from leaf explants of Solanum tuberosum L. cv. Shepody. Plant Cell Tiss. Org. Cult. 85, 361-366.
[34] Vinterhalter, D., Zdravkovi, K.S., Miti, N., Dragievi, I., Cingel, A., Raspor, M. and Ninkovi, S. (2008) Protocols for Agrobacterium-mediated transformation of potato. In: Texeira De Silva, J. (Ed.) Fruit, Veg. Cereal. Sci. Biotechno. 1-15.
[35] Anayol, E., Bakhsh, A., Karakoç, O.C., Onarıcı, S., Köm, D., Aasim, M., Özcan, S.F., Barpete, S., Khabbazi, S.D, Önol, B., Sancak, C., Khawar, K.M., Ünlü, L. and Özcan, S. (2016) Towards better insect management strategy: restriction of insecticidal gene expression to biting sites in transgenic cotton. Plant Biotechno. Rep. 10, 83–94.
[36] Banerjee, A.K., Prat, S. and Hannapel, D.J. (2006) Efficient production of transgenic potato (S. tuberosum L. ssp. andigena) plants via Agrobacterium tumefaciens-mediated transformation. Plant Sci. 170, 732-738.

Received: **17.11.2017**
Accepted: **09.02.2018**

CORRESPONDING AUTHOR

Surendra Barpete
Department of Field Crops,
Faculty of Agriculture,
University of Ankara,
06110 Diskapi, Altindag – Turkey

e-mail: surendrabarpete@gmail.com

© by PSP Volume 27 – No. 5/2018 pages 3028-3034 Fresenius Environmental Bulletin

SPATIOTEMPORAL ANALYSIS OF ANTARCTIC SNOWMELT CHANGES USING MICROWAVE RADIOMETER DATA (1978-2015)

Xingdong Wang[1,2,*], Cheng Wang[2], Bin Li[1]

[1]College of Information Science and Engineering, Henan University of Technology, Zhengzhou, Henan, 450001, China
[2]Institute of Remote Sensing and Digital Earth, Chinese Academy of Sciences, Beijing, 100094, China

ABSTRACT

Antarctic surface snowmelt variations are sensitive indicators of climate change due to the direct interface with the atmosphere and ocean. Here, we have utilized the sensitivity of microwave radiometer data to detect the presence of liquid water in the snow caused due to snowmelt conditions and analyze a variety of spatiotemporal characteristics of the Antarctic snowmelt cycle over a 36-year period from 1978 to 2015 by applying an improved wavelet transform using SMMR and SSM/I data. The spatial distribution of snowmelt areas shows that most are located on the edges of Antarctic ice shelves. Snowmelt areas are affected by land cover type, surface elevation, and geographic location. The temporal distribution of snowmelt areas shows that the Antarctic snowmelt changes systematically over time. There are the roughly 5-year periodic variations in the melt intensity, which shows that the Antarctic snowmelt will adjust to climate change. In addition, the Antarctic snowmelt varies with the seasons; it is particularly acute in summer, with peak melt in December and January and low melt in March. To a certain extent, the results reveal Antarctic snowmelt spatiotemporal change characteristics.

KEYWORDS:
Snowmelt detection, microwave radiometer, wavelet transform, Antarctica, climate change, spatiotemporal change characteristics

INTRODUCTION

Global climate and environmental change is an important issue in today's world. Antarctica is a key region in this regard with the Antarctic ice and snow changes being one of the most important factors affecting global climate and environmental change [1-2]. The polar regions play the role of an 'amplifier' for global climate and environmental change. Both historical and modern observations show that the magnitude of polar climate and environmental change is twice as large as changes in middle and low latitude regions, therefore, the polar climate is easier to monitor for subtle changes. Both observations and simulation results show that the inter-annual variations in the extent and surface characteristics (mainly reflectance) of Antarctic ice and snow significantly affect global water vapor circulation, global heat balance, and climate change, which can be seen in temperature and precipitation distributions [3-4]. The polar regions control the exchange of heat, moisture, and momentum between the atmosphere and the surface; this directly affects global atmospheric circulation and climate, which is the key factor for global climate and environmental change [5]. The interaction between the Antarctic ice sheet and adjacent geospheres has a huge impact on the global climate and environment. The Antarctic snowmelt will cause changes in the surface humidity and then cause ice shelf collapse and ice movement [6]. By means of long time series of microwave radiometer data, the Antarctic snowmelt spatiotemporal change characteristics are effectively analyzed, which could promote the study of global climate and environmental change.

The spaceborne microwave radiometers can be used macroscopically, rapidly, objectively and effectively to monitor and assess the Antarctic snowmelt changes, providing an important means of measuring snowmelt changes in Antarctic areas that are difficult for people to access and measure directly. In particular, microwave radiometers can be used to retrieve snowmelt information under all weather conditions because microwaves can penetrate clouds. The brightness temperature of the microwave radiometers is highly sensitive to the liquid water changes in the snow. Therefore, we can use the microwave radiometer data to monitor and measure the surface snowmelt over the ice sheet. For studying the snowmelt spatiotemporal changes in Greenland and other regions, many snowmelt detection methods have been developed and applied to microwave radiometer SMMR (Scanning Multichannel Microwave Radiometer) and SMM/I (Special Sensor Microwave/Imager) [5, 7-13]. Torinesi et al. [3] found that the interannual variability in local snowmelt showed good regularity based on microwave radiometer data from 1980 to 1999, but

the regularity was poor for all Antarctica. Liu et al. [14] used the microwave radiometer data (1978-2004) to study the Antarctic snowmelt and found that most of the snowmelt indicators showed a negative interannual trend. Picard and Fily [4] developed a model for daily snowmelt changes using the temporally different characteristics of four microwave radiometer datasets for Antarctica and applied this model to determine daily variability in the Antarctic snowmelt over 26 years. Tedesco [15] compared six Antarctic ice sheet snowmelt detection algorithms using microwave radiometer data from 1979 to 2008 and analyzed the Antarctic snowmelt spatiotemporal changes, the trend of the melting index and the different regional abnormal snowmelt phenomena.

In the present paper, we obtained the average snowmelt onset date, end date, and duration as well as the annual changes of the snowmelt areas and the seasonal changes of the snowmelt pixels, for the 36-year period from 1978 to 2015, based on the improved wavelet transform method [16-17]. Based on this, the Antarctic snowmelt spatiotemporal change characteristics are obtained. The Antarctic snowmelt spatiotemporal mechanism is analysed and combined with the Antarctic surface snowmelt observations.

MATERIALS AND METHODS

Datasets. Microwave radiometers passively receive the thermal radiation of ground objects [18], and the measured microwave radiometric brightness temperature is very sensitive to variations in the snow's liquid water content; the brightness temperature will show dramatic changes over the snowmelt onset and end dates. At present, there are several microwave radiometers in general use: SSM/I, Advanced Microwave Scanning Radiometer-EOS (AMSR-E), and SMMR. This paper mainly uses SMMR and SSM/I microwave radiometer data from 26 October 1978 to 30 June 2015 derived from the NSIDC (National Snow and Ice Data Center). The selected data channel is the 18 GHz horizontal polarization channel of the SMMR and the 19 GHz horizontal polarization channel of the SSM/I with F8, F11, F13, and F17 platforms; their ranks and data accuracy are the same and stored in the same format. Over the 36 year period, two different kinds of SSMR and SSM/I sensors were used, and the sensors were equipped with different platforms (F8, F11, F13, and F17). Therefore, it is necessary to study the different sensors' data and normalize each to the same platform.

The overlap dates for the five kinds of data are from 20 August to 9 July 1987, from 29 April to 3 December 1991, from 30 December to 3 May 1995, and from 30 September 2008 to 1 January 2009. Using these overlapping data sets, we can perform a regression treatment to calibrate the SMMR data to the F8 platform of the SSM/I, and calibrate the F11, F13, and F17 platforms to the F8 platform. We do this using Eqn (1),

$$T_1 = a * T_2 + b \quad (1)$$

where T_1 is the SSM/I brightness temperature data for the 19GHz band of the F8 platform, and T_2 is the brightness temperature data for the F11, F13 and F17 platforms, respectively; a (slope) and b (intercept) are regression parameters.

Liu et al. [2] calculated the conversion between the SMMR and SMM/I and between the F11 and F8 platforms of SSM/I; they also calculated the regression coefficients for the F13 and F8 platforms for the SSM/I. Different sensor and platform data conversion parameters are shown in Table 1. The regression coefficients are used to convert all data to the F8 platform.

After all the data are normalized, we use the improved wavelet-transform snowmelt detection algorithm to extract the 36-year snowmelt information from the microwave radiometer data (there is not data from 21 August 1987 to 12 January 1988, so there is no Antarctic snowmelt information for 1987). The Antarctic summer is from December to February, so for convenience, the year is defined from 1 July to 31 June of the following year, and the former year is adopted as the label (so 1991 goes from 1 July 1991 to 31 June 1992).

Methods. The basic principle of the snowmelt detection algorithm based on wavelet transform [2, 17] is that the edges of dramatic changes in the long time series brightness temperature data reflect the snow melt or freeze-up onset dates [19-20]. The snowmelt onset date for each year is the date of the first sharp rising edge on the curve of brightness

TABLE 1
Regression parameter from different sensors and platform data

Data transformation	Slope	Intercept	Correlation coefficient
Transform SMMR 18 GHz into SSM/I F8 19 GHz	1.06	-2.79	R>0.99
Transform SSM/I F11 and F13 19 GHz into SSM/I F8 19 GHz	1.008	-1.17	R>0.99
Transform SSM/I F17 19 GHz into SSM/I F8 19 GHz	1.0286	-3.0094	R>0.99

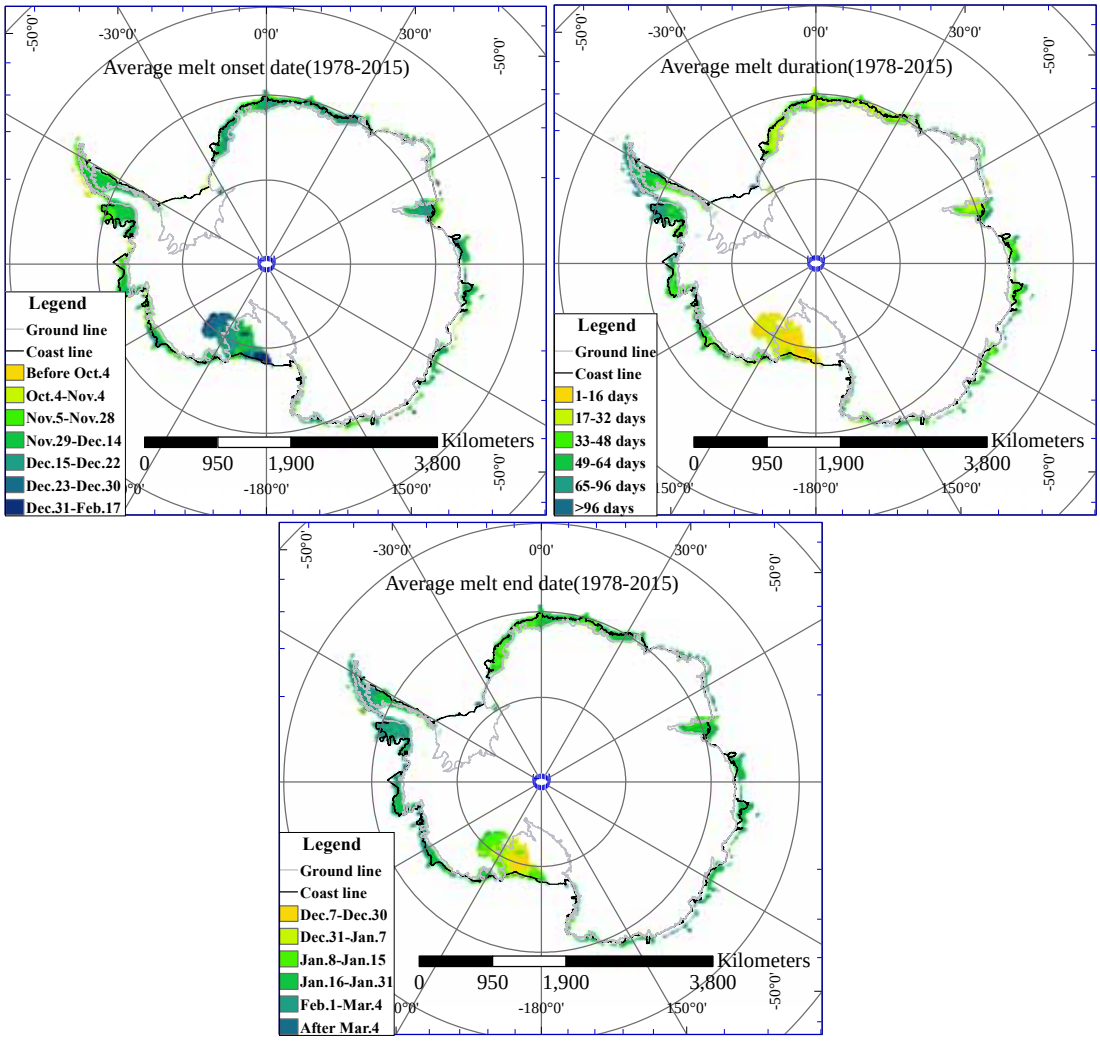


FIGURE 1
Antarctic ice-sheet average melt onset date, duration, and end date for 1978-2015

temperature vs. time, and the melt end date for each year is the date of the last sharp falling edge on this curve; the total melt duration of a pixel is the sum of each individual melt duration in a year for the pixel. This method can detect whether each pixel is experienced freezing or thawing as well as the freeze-thaw date.

The basic steps are as follows:

(1) The long time series of brightness temperature data are pre-processed.

(2) A multi-scale wavelet decomposition by wavelet transform is performed on the pre-processed data to decompose the edge information under different scales.

(3) Determine the optimal classification threshold for dry snow and wet snow based on a variance analysis model and the generalized Gauss model.

(4) Obtain the melt onset date, end date, and duration of each pixel based on step (3).

(5) The neighbourhood operation [2] detects and corrects potential errors, ultimately determining the final snowmelt onset date, duration, and end date.

RESULTS AND DISCUSSION

Antarctic snowmelt spatial analysis. Through the above process, the Antarctic average melt onset date, duration, and end date were obtained from 1978 to 2015 (Figure 1); the total melt areas were about 1,621,875 km^2, accounting for 11.67 percent of the total ice-sheet areas. We can see from Figure 1 that the melt areas were mainly distributed on the edge of the Antarctic ice shelves, including Ross Ice Shelf, Amery Ice Shelf, Ronne Ice Shelf, Larsen Ice Shelf, Getz Ice Shelf, Abbot Ice Shelf, Wilkins Ice Shelf, Brunt Ice Shelf, Riiser-Larsen Ice Shelf, Fimbut Ice Shelf, West Ice Shelf, and Shackleton Ice Shelf, etc. On the whole, earlier melt onset dates and later melt end dates are associated with longer melt durations.

The Antarctic ice-sheet melt shows obvious

regional variations. On the whole, the melt strength of the Antarctic Peninsula is the largest, showing average melt onset dates before mid-December for Wilkins Ice Shelf and Larsen Ice Shelf; it also has average melt durations of more than 60 days and has melt end dates after 1 February. For the two largest ice shelves, Long Ice Shelf and Ross Ice Shelf, the average melt duration is relatively short (generally less than 10 days). Most of the south Antarctic regions did not experience melt over the 36-year period.

Due to its low specific heat capacity, rock will have a more pronounced temperature change than ice and snow under the same solar radiation conditions; this makes ice that is in contact with rock melt more easily than other ice. This can be seen for the Larsen Ice Shelf and Wilkins Ice Shelf, which are located in a rocky area of the Antarctic Peninsula: these ice shelves are affected by the cover of low specific heat capacity rocks, so the snow is more easily melted compared to Ross Ice Shelf and Long Ice Shelf which have very few rocks. The average melt duration represents a complex change in the melt intensity, which is affected by latitude. For the Antarctic regions, the solar radiation intensity is generally relatively weaker in the high latitude regions, which causes lower surface temperatures than in the low latitude regions. The results of this work show that almost no melt processes occur in most of the high latitude areas in Antarctica, while the Antarctic Peninsula, located at lower latitudes, had sustained, high-intensity melt.

The Hengduan Mountains and the Antarctic Peninsula are the most widely distributed areas of the Antarctic continent. However, because the most of the Hengduan Mountains are located at high latitudes, this makes the melt intensity there very different from the Antarctic continent's melt intensity.

Figure 2 shows that higher altitudes are associated with shorter average melt durations; this is due to the influence of the atmosphere's vertical temperature gradient from 0-500 m above sea level. The average altitude is less than 20 m above sea level, and the average melt duration was over 50 days. The average duration was dominated by the fringe field of the ice shelves and the sea. In the regions with average altitudes from 20-200 m, the average melt duration was less than 50 days, especially at altitudes of 100 m, such as Fimbul Ice Shelf, Amery Ice Shelf, and Riise-Larsen Ice Shelf, which had average melt durations of about 30 days. For the regions with average altitudes from 200-500 m, such as Gates Ice Shelf and Abbott Ice Shelf, the average melt duration increased with increasing altitude, and the average melt duration was about 40 days; this is due to the influence of the atmosphere's vertical temperature gradient. At altitudes of approximately 400 m, the average melt duration decreased to about 25 days. The majority of melt regions are distributed in the Antarctic Peninsula at altitudes above 500 m, where the combination of low latitudes, resulting in more intense solar radiation, and the distribution of rocks with low heat capacity ratios allow these regions to have a high-strength melt.

In short, the comprehensive effects of the cover types, altitude, and geographical location (latitude) give the Antarctic snowmelt patterns a complex spatial distribution.

Antarctic snowmelt temporal analysis. From Figure 3 we can see that the inter-annual variation of the Antarctic snowmelt region is relatively large, and the largest melt areas were in 2012 (from 1 July 2012 to 31 June 2013) with a melt area of 1,611,250 km^2. The minimum melt area was 565,000 km^2 in 1999, a factor of three smaller than the 2012 melt area. From the melt trend in Figure 3, the following periodic melt law can be seen: after the emergence of a large melt intensity, the second year will show a substantial decline, and there will be a smaller melt one or two years later. Four or

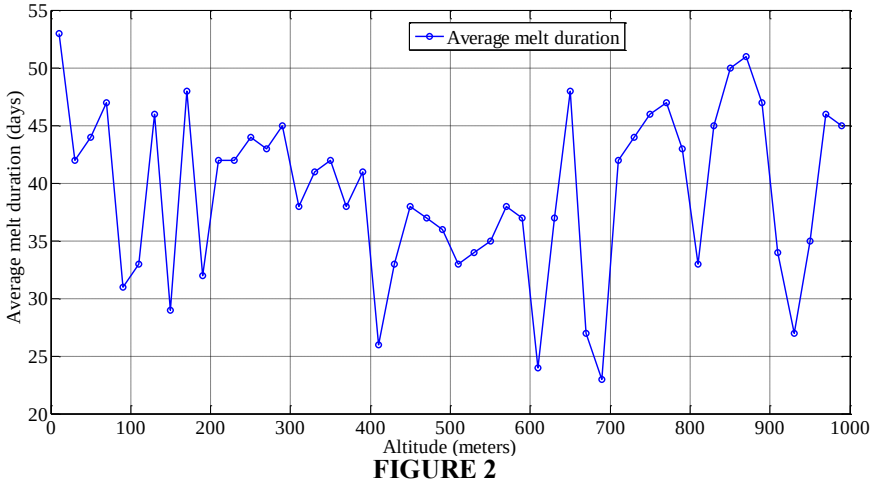


FIGURE 2
Relationship between average melt duration and altitude

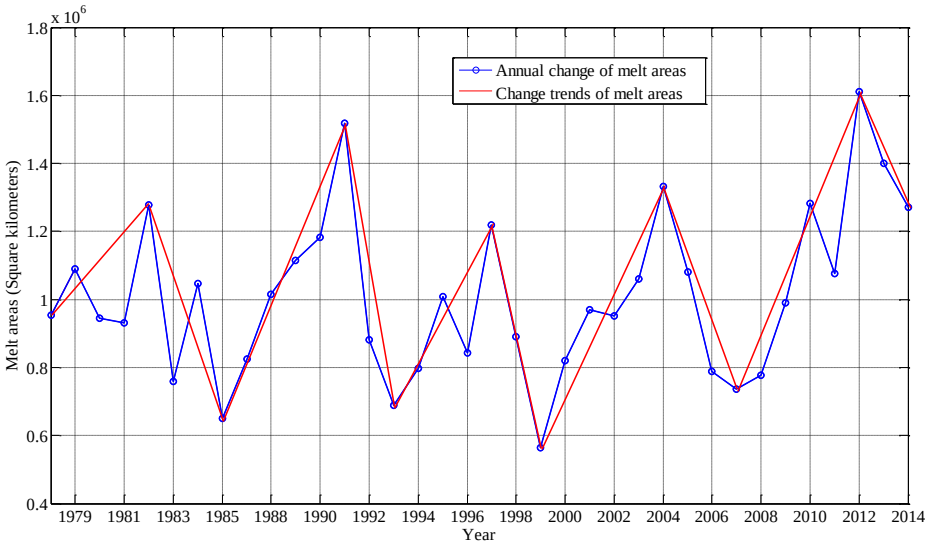


FIGURE 3
Antarctic melt-area annual change

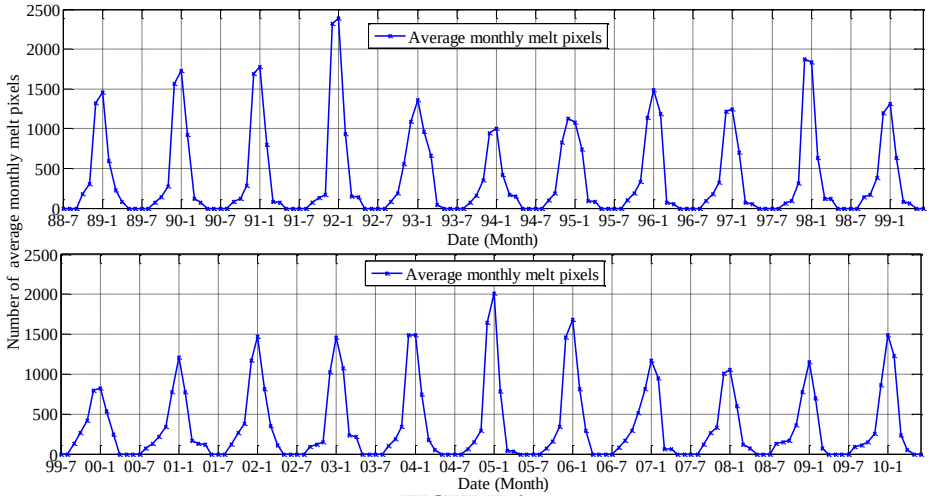


FIGURE 4
Monthly change in number of average melt pixels

five years after the smaller melt intensity, there will appear another large melt intensity; for example, 1985 had a small melt intensity, and there is a second maximum melt extent in 1991 (this pattern repeats roughly every 5 years for 36 years). From the periodic variation it can be seen that the Antarctic ice sheet has a certain adjustment to the climate change, and it is negative feedback on climate change. The periodic variations in the melt intensity show that the Antarctic ice sheet will adjust to climate change on a specific timescale, and it provides a negative feedback on climate change.

As shown by Figure 4, the melt of the Antarctic ice sheet has a very obvious seasonal rhythm, and summer (from December to February) has a sharp melt, with the melt reaching its peak in December and January. Starting in February, the melt areas begin to decrease, and the melt areas are very rare in March. This shows that the Antarctic ice-sheet melt (mainly on the surface of the ice shelves) will undergo a refreezing process after the summer melting of the ice sheet. With the refreezing of ice and snow, the melt areas are reduced sharply; the average melt areas in February were only about 50 percent compared to January, while the melt areas in March are further reduced. For 22 years, in March melt areas are basically stable at about 750,000 km^2. After May, Antarctica enters the winter season, and very few melt events occur until October when the Antarctic ice sheet enters the melt season.

CONCLUSIONS

Based on microwave radiometer data (1978-2015), we find (1) The Antarctic total snowmelt areas are closely related to the spatial variation of the ice sheet cover type, altitude, and latitude. (2)

The Antarctic snowmelt undergoes rapid fluctuations and periodic changes (5-year periodic changes) in the melt intensity. (3) The Antarctic snowmelt areas with large time variations are mainly distributed in Ross Ice Shelf and Ronne Ice Shelf, and the melt conditions of these regions determine the total variation of the Antarctic ice-sheet melt areas. In contrast, Larsen Ice Shelf and Wilkins Ice Shelf of the Antarctic Peninsula have maintained stable widespread melting of snow and ice, maintaining a consistently high intensity of melting of snow and ice in the summer.

ACKNOWLEDGEMENTS

This research was supported by the National Key Research and Development Program of China (No. 2016YFA0600302), National Natural Science Foundation of China (No. 41606209), Fundamental Research Funds for the Henan Provincial Colleges and Universities (No. 2015QNJH16), and Funded by Key Laboratory of Global Change and Marine-Atmospheric Chemistry (No. GCMAC1605). We thank the Chief Editor of the Journal and the anonymous reviewers for their time and effort, which will significantly improve the manuscript.

REFERENCES

[1] Oza, S.R. (2015) Spatial-temporal patterns of surface melting observed over Antarctic ice shelves using scatterometer data. Antarctic Science. 27(4), 403-410.

[2] Liu, H.X., Wang, L. and Jezek, K.C. (2005) Wavelet-transform based edge detection approach to derivation of snowmelt onset, end and duration from satellite passive microwave measurements. International Journal of Remote Sensing. 26(21), 4639-4660.

[3] Torinesi, O., Fily, M. and Genthon, C. (2003) Variability and trends of the summer melt period of Antarctic ice margins since 1980 from microwave sensors. Journal of Climate. 16(7), 1047-1060.

[4] Picard, G. and Fily, M. (2006) Surface melting observations in Antarctica by microwave radiometers: Correcting 26-year time series from changes in acquisition hours. Remote Sensing of Environment. 104(3), 325-336.

[5] Mernild, S.H., Mote, T.L. and Liston, G.E. (2011) Greenland ice sheet surface melt extent and trends: 1960-2010. Journal of Glaciology. 57(204), 621-628.

[6] Li, X.W., Wang, X.D., Wang, C., Zhang, L. (2017) Antarctic snow melt detection based on the synergy of SSM/I and QuikSCAT. Antarctic Science. 29(6), 561-568.

[7] Abdaati, W. and Steffen, K. (2001) Greenland ice sheet melt extent: 1979-1999. Journal of Geophysical Research. 106(D24), 33983-33988.

[8] Dupont, F., Royer, A., Langlois, A., Gressent, A., Picard, G., Fily, M., Cliche, P., Chum, M. (2012) Monitoring the melt season length of the Barnes Ice Cap over the 1979-2010 period using active and passive microwave remote sensing data. Hydrological Processes. 26(17), 2643-2652.

[9] Mote, T.L. (2007) Greenland surface melt trends 1973-2007: Evidence of a large increase in 2007. Geophysical Research Letters. 34(22), L22507.

[10] Tedesco, M., Brodzik, M., Armstrong, R., Savoie, M. and Ramage, J. (2009) Pan arctic terrestrial snowmelt trends (1979-2008) from spaceborne passive microwave data and correlation with the Arctic Oscillation. Geophysical Research Letters. 36(21), 272-277.

[11] Fettweis, X., Gallee, H., Lefebre, F. and van Ypersele, J.P. (2006) The 1988-2003 Greenland ice sheet melt extent using passive microwave satellite data and a regional climate model. Climate Dynamics. 27(5), 531-541.

[12] Fettweis, X., van Ypersele, J.P., Gallee, H., Lefebre, F., Lefebvre, W. (2007) The 1979-2005 Greenland ice sheet melt extent from passive microwave data using an improved version of the melt retrieval XPGR algorithm. Geophysical Research Letters. 34(5), 247-260.

[13] Smith, T., Bookhagen, B., Rheinwalt, A. (2017) Spatiotemporal patterns of High Mountain Asia's snowmelt season identified with an automated snowmelt detection algorithm, 1987-2016. Cryosphere. 11(5), 2329-2343.

[14] Liu, H.X., Wang, L. and Jezek, K.C. (2006) Spatiotemporal variations of snowmelt in Antarctica derived from satellite scanning multichannel microwave radiometer and Special Sensor Microwave Imager data (1978-2004). Journal of Geophysical Research-Earth Surface. 111(F1), F01003.

[15] Tedesco, M. (2009) Assessment and development of snowmelt retrieval algorithms over Antarctica from K-band spaceborne brightness temperature (1979-2008). Remote Sensing of Environment. 113, 979-997.

[16] Wang, X.D., Xiong, Z.Q., Li, X.W. and Liang, L. (2013) Antarctic snowmelt detection based on improved wavelet transform. Acta Electronica Sinica. 41(2), 402-406.

[17] Liang, L., Guo, H.D., Li, X.W. and Cheng, X. (2013) Automated ice-sheet snowmelt detection using microwave radiometer measurements. Polar Research. 32 (13), 89-99.

[18] Fretwell, P., Pritchard, H.D., Vaughan, D.G., Bamber, J.L., Barrand, N.E., Bell, R., Bianchi, C., Bingham, R.G., Blankenship, D.D., Casassa, G. (2013) Bedmap2: improved ice bed, surface and thickness datasets for Antarctica. Cryosphere. 7(1), 375-393.
[19] Joshi, M., Merry, C.J., Jezek, K.C. and Bolzan, J.F. (2001) An edge detection technique to estimate melt extent on the Greenland ice sheet using passive microwave data. Geophysical. Geophysical Research Letters. 28(18), 3497-3500.
[20] Steiner, N. and Tedesco, M. (2014) A wavelet melt detection algorithm applied to enhanced-resolution scatterometer data over Antarctica (2000-2009). Cryosphere. 8(1), 25-40.

Received: **17.11.2017**
Accepted: **19.02.2018**

CORRESPONDING AUTHOR

Xingdong Wang
College of Information Science and Engineering,
Henan University of Technology,
Zhengzhou, Henan, 450001 – China

e-mail: zkywxd@163.com

© by PSP Volume 27 – No. 5/2018 pages 3035-3042 Fresenius Environmental Bulletin

EFFECT OF LOCUST BEAN (*CERATONIA SILIQUA* L.) EXTRACT WASTE ON CLOGGING OF IN-LINE EMITTERS

Servet Tekin*

Kahramanmaras Sutçu Imam University, Faculty of Agriculture, Department of Biosystems Engineering, 46040 Kahramanmaras, Turkey

ABSTRACT

This study was conducted by means of the drip test bench set up in the workshop of Agricultural Faculty Biosystems Engineering Department of Kahramanmaras Sutçu Imam University, Turkey in 2017. In the experiment, the locust extract waste, which emerges as by product during the gum extraction from locust bean, was used for opening the emitters on an in-line drip lateral with %85 clogging ratio. Due to its high acid content, the locust extract was diluted by 1:4 ratio with water. Regular canal water irrigation was considered as a reference at the beginning of the treatment. Locust extract waste (LW) and canal water (CW) were applied to the clogged drip irrigation system under the pressure of 1 atm by 2 irrigation treatments with 2 repetitions. In the study, Distribution Uniformity (DU), Adjusted Christiansen Uniformity Coefficient (adjCU), Coefficient of variation (CV) and emitter flow rate variation (Qvar) values of each subject emitter were determined. As a result of the study, the values of DU, adjCU, CV and Qvar in the clogged emitter in which canal water applied were found to be 48.45%, 69.01%, 0.39 and 0.77, respectively, while in the locust extract applied emitter these values were calculated to be 77.52%, 97.01%, 0.04 and 0.17. According to the results, it was concluded that locust extract waste was highly effective in unclogging for emitters.

KEYWORDS:
Drip irrigation, locust bean extract waste, clogging, in-line emitter

INTRODUCTION

In Turkey, the Locust tree (*Ceratonia siliqua* L.) is native to the Mediterranean region and grows spontaneously in the area of about 1750 km^2 extending along the South Coasts of Turkey from Tarsus, Mersin to Marmaris district. Its varieties grown in Turkey are fleshy, sesame and wild types [1]. Turkey, especially its Mediterranean region, has vast lands to be used for locust bean cultivation and locust bean cultivation is gaining importance gradually in Turkey since it is in its native soil [2]. Although the fruit of locust tree is of little significance in terms of production and trade capacity both in the world and in Turkey, it has various areas of utilization. Therefore, specify of its utilization areas increases locust bean's importance and more attention is paid to its cultivation and production with growing demand for it. However, it is the seeds of locust bean that gives importance to the plant. The seeds are processed to obtain locust bean gum, which is an important food additive used in the food industry. 3 different processes are employed for locust bean gum production: 1) 95% sulfuric acid treatment, 2) 1% sodium hydroxide treatment and 3) Mechanical shelling [3]. The most preferred method employed in Turkey is treating seeds with 95% sulfuric acid. This method, the sulfuric acid treatment of seeds to remove shell and obtain the gum, generates a waste containing high amount of sulfuric acid which is harmful for the environment.

The limited availability of clean water resources around the world, rapid population growth, droughts caused by global warming and climate change, the gradual increase in urban and industrial water requirements put pressure on water resources used in agricultural irrigation [4,5,6]. Considering that 75% of water resources is used for agricultural purposes, the utilization of pressurized irrigation techniques that apply water more efficiently is inevitable [7]. Drip irrigation systems have started to be used increasingly in recent years [8, 9, 10, 11].

Drip irrigation systems, one of modern irrigation techniques, have some drawbacks and the most important of all is clogging of emitters over time and significant decrease in system performance. Clogging is the most common and serious problem in drip irrigation systems. It is difficult and costly to detect, clean or to replace the clogged emitters. Partially or completely clogging of emitters decreases water distribution uniformity and irrigation efficiency. Clogging is generally caused by neglecting water quality parameters at the planning stage or when the system is not operated properly and the necessary maintenance is not carried out. The clogging of emitters over time depends on the properties of the water used for irrigation [8, 9, 12, 13, 14, 15].

Physical clogging is one of the main clogging factors that caused by the suspended solids found in water (such as silt and fine sand). On the other hand, high concentration of dissoluble salts in irrigation

water constitute a significant level of clogging problem and high values of Ca, Mg, Fe, Mn and HCO_3 and high pH values and temperature lead to chemical clogging. If irrigation water has high pH values (pH>7.5) and includes high concentrations of Ca and Mg, Ca and Mg precipitate in the form of carbonates and cause partially or completely clogging in emitters. If the solubility of salts dissolved in water is low, these elements may lead to clogging. The solubility of the substances in water depends on the temperature, pH value, the redox potential of the water and the concentration of dissolved solids in water [14, 16, 17] researched chemical and biological clogging in drip irrigation systems and their effects on system performance and showed that chemical and biological clogging were more significant in lateral ends due to the low flow rate at the lateral ends.

Various chemicals have been used in order to prevent the dissolved salts to clog emitters. Chlorination is required to control the development of organic bacteria in the emitters and inside the tube and to prevent precipitation of salts. The control of chemical clogging, which can be defined as the precipitation of salts, is quite difficult. One of the approaches for preventing chemical clogging is decreasing pH value of water with acid injection to levels in which precipitation does not occur. When applied at low concentrations, acid injection (phosphoric acid, hydrochloric acid and sulfuric acid) prohibits $CaCO_3$ and $MgCO_3$ from precipitation and prevents emitter clogging. Acid injection lowers pH of water, decreases salt precipitation and increases the effect of chlorination. Data about acid injection doses to be used for drip irrigation was reported by [18]. The quantity and dose of acid for injection depend on the water quality and the amount of water to be applied. The acid dosage applied according to the recommendations enables the neutralization of 80% of the bases found in water and expected to lower the pH value of water to the range of 5.0-5.5 immediately after injection. The acid injection rates should be controlled precisely by using acid-resistant injection pumps [19, 20, 21, 22]. However, acid treatments may lead to corrosion in the system and are inevitably harmful to both operators and the environment.

The aim of this study is to utilize the acidic wastes of locust bean gum processing plants for preventing dissolved salts of irrigation water from clogging emitters and to determine the effects of acidic wastes on emitter performance (distribution Uniformity (DU), adjusted Christiansen uniformity (adjCU), coefficient of variation (CV) and emitter flow rate variation (Qvar). In addition, we are of the opinion that utilization of the locust extract waste to prevent clogging, which is one of the major problems of increasingly used drip irrigation systems in recent years will contribute to both economy and environmental protection.

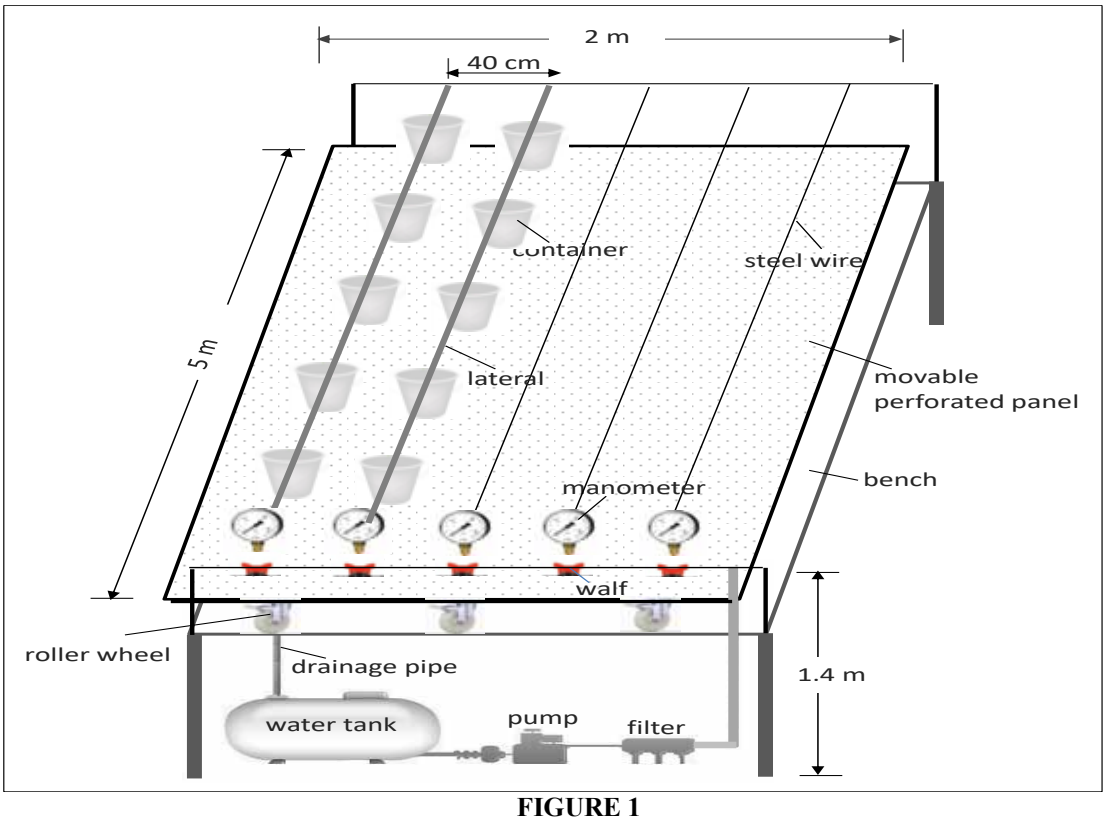


FIGURE 1
Drip irrigation test bench

MATERIALS AND METHODS

The locust extract waste used in this study was obtained from the wastes from gum production of INCOM locust bean processing plant in Mersin province, Turkey. The plant uses 95% sulfuric acid treatment method to produce locust bean gum and the process generates wastes with high sulfuric acid content. The locust bean waste used in the study was analyzed and the pH value and soluble SO_4 content were found 1.25 and 28%, respectively. In the experiment, an in-line emitter with an emitter range of 33 cm, diameter of Ø16 mm and flow velocity of 4 L h^{-1} was used. The in-line emitters used in the study were obtained from laterals which had been used for a long time in agricultural activities and then had been discarded due to emitter clogging. Two different water sources were used in the study and the canal water (CW) and locust waste (LW) were introduced to clogged emitter laterals with two repetitions.

The study was carried out in Kahramanmaraş Sütçü İmam University Agricultural Faculty Biosystems Engineering Department laboratories. In order to conduct the experiments, a drip irrigation test bench, which is 5 m long, 2 m wide, 1.20 m above the ground and consists of a hanger system, main pipeline and hangers for laterals, was set up. Laterals used for tests were located 40 cm above the test bench (Figure 1).

The canal water was introduced to clogged in-line laterals prior to locust extract waste treatment. Locust extract waste was then stored in 1 ton capacity plastic container and supplied to the system by a pump with s 0.5 HP power and 2.52 m^3 h^{-1} maximum flow rate. A filter was placed at the main pipeline entrance and two valves were placed following the filter to control the recirculation exit and main pipeline entrance. Although operating pressure could be kept at preferred levels by means of the valves, the pressure was adjusted by an added inventor to the system. The pressure of the incoming water was measured by a manometer at the beginning of each lateral. The trials were conducted under the pressure of 1 atm. To determine the viscosity variation, the water temperature was measured with a thermometer throughout the test. The water temperature change during the measurements did not exceed 23 ° C (± 0.5 °C).

In order to determine the pressure-flow rate interaction, 28 emitters were selected for each type of emitter and flow rate for each emitter was measured with 2 repetitions. The measurements for all laterals on the test bench were performed synchronously. Measurement of flow was carried out with water cans placed beneath the emitters after 10 min of water supply to obtain stabilized flow. The mobile panel, which was placed above test bench, was pulled horizontally after the treatment and the flow rate of emitters was measured volumetrically. The parameters of performance evaluation in the study were determined by equations below.

1) Coefficient of variation (CV) of emitters was calculated using the following equation [12, 23].

$$CV = \frac{\left(q_1^2+q_2^2+....+q_n^2-n{q_{ort}}^2\right)^{1/2}}{q_{avg}\left(n-1\right)^{1/2}} \quad (1)$$

Where CV: Coefficient of variation (CV) of emitters; q_1, q_2, ..., q_n: emitters' drip rate (L h^{-1}); q_{avg}: average drip rate (L h^{-1}); n: number of emitters.

2) Distribution Uniformity (DU) was calculated using the following equation [24].

$$DU = 100\left(\frac{q_{lq}}{q_{avg}}\right) \quad (2)$$

Where DU: Distribution Uniformity (%); q_{lq}: averages of ¼ with the smallest value (lower quarter) of the emitters (L h^{-1}); $q_{avg:}$ average drip rate (L h^{-1}).

3) Adjusted Christiansen Uniformity Coefficient (adjCU) was calculated using the following equation.

$$adjUC = 100(1-0.798\times c-CV) \quad (3)$$

Where CV is *Coefficient of variation.*

4) Emitter flow rate variation was calculated using the following equation.

$$q_{var} = \frac{(q_{max-}q_{min})}{q_{max}} \quad (4)$$

Where, q_{max}: maximum drip discharge (L h^{-1}), q_{min}: minimum drip discharge (L h^{-1}).

RESULTS

Variations in Average Flow Rates of Emitters. The variations in flow rates of emitters by treatments are given in Table 1 and Figure 2. Table 1 and Figure 2 reveal that non-uniform changes occur in the flow rates of emitters that were clogged at the beginning. After locust extract waste treatment for LW-1 and LW-2 treatments, however, it is determined that the flow variations have a uniform characteristic. It can be concluded that this change resulted from the high HSO_4 content of locust waste.

The results of CW treatment tests were summarized in Table 1. As it can be seen from the table, while the average flow rate (q_{avg}) in CW treatments was 0.86-0.87 L h^{-1}, the average flow rate for LW treatments was measured as 1.30 L h^{-1}. It was concluded that the acid in locust extract waste reduces the precipitation of salts by lowering the pH value of the water and increases the chlorination efficiency and consequently results in unclogging of the emitters.

Coefficient of variation (CV). The coefficient of variation of emitters was assessed according to [25, 26]. The CV values obtained in the study are given in Figure 3. As it can be seen in Figure 3, the initial CV value determined under the pressure of 1

atm for CW treatment was in the range of 38.12% and 39.14%. These values are higher than the limit values proposed by [26, 27]. The CV values determined for CW treatment are in an unacceptable class due to exceeding 5%. In the LW treatment, however, CV values were determined in the range of 3.30%-4.20% and these values are in the top class.

TABLE 1
Flow rate (L h^{-1}) variations of emitters along lateral for canal water (CW) and locust extract waste (LW) treatments

Emitter number	CW-1	CW-2	LW-1	LW-2
1	1.12	1.16	1.31	1.30
2	1.28	1.25	1.34	1.32
3	1.24	1.24	1.30	1.30
4	1.14	1.16	1.31	1.32
5	0.74	0.79	1.40	1.38
6	1.06	1.02	1.22	1.22
7	0.80	0.84	1.24	1.26
8	0.46	0.44	1.31	1.31
9	0.78	0.80	1.26	1.26
10	0.60	0.66	1.21	1.21
11	1.26	1.25	1.34	1.34
12	0.72	0.74	1.26	1.26
13	0.74	0.74	1.46	1.42
14	1.12	1.12	1.30	1.30
15	0.42	0.44	1.26	1.32
16	0.62	0.64	1.30	1.30
17	0.41	0.41	1.30	1.30
18	0.43	0.44	1.20	1.28
19	0.47	0.47	1.28	1.28
20	0.32	0.30	1.31	1.31
21	1.31	1.24	1.32	1.32
22	1.25	1.20	1.32	1.32
23	1.22	1.20	1.30	1.32
24	1.28	1.28	1.36	1.36
25	1.04	0.80	1.30	1.30
26	0.42	0.42	1.32	1.32
27	0.80	0.80	1.26	1.28
28	1.21	1.24	1.27	1.28
$q_{avg.}$	**0.87**	**0.86**	**1.30**	**1.30**

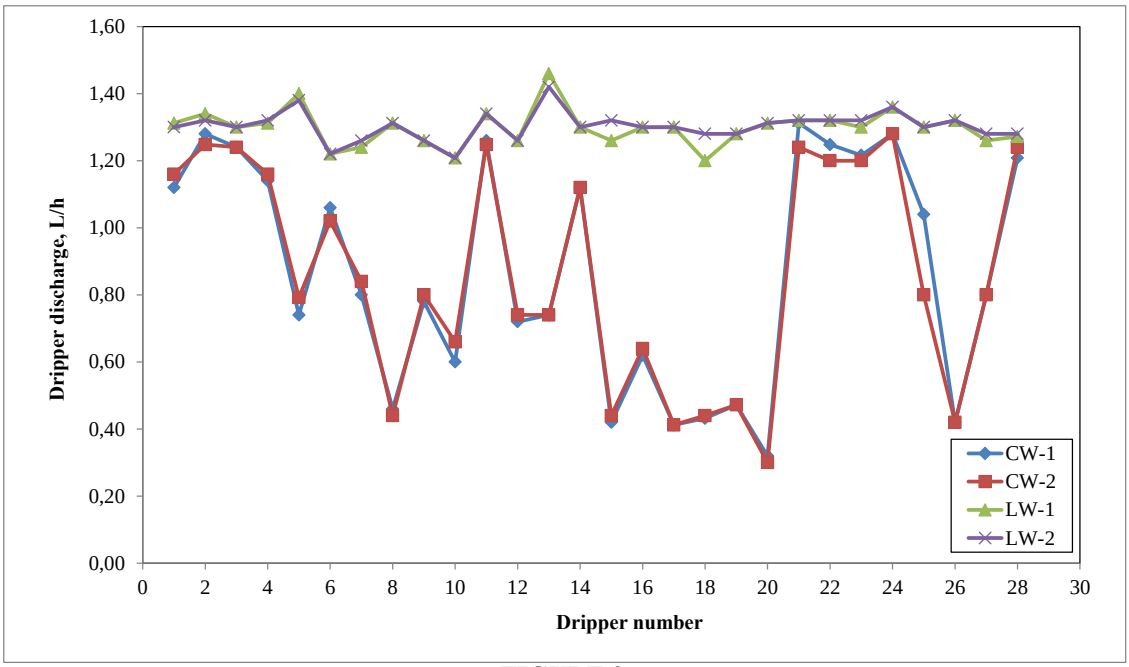


FIGURE 2
Flow rate variations of emitters along lateral for canal water (CW) and locust waste (LW) treatments

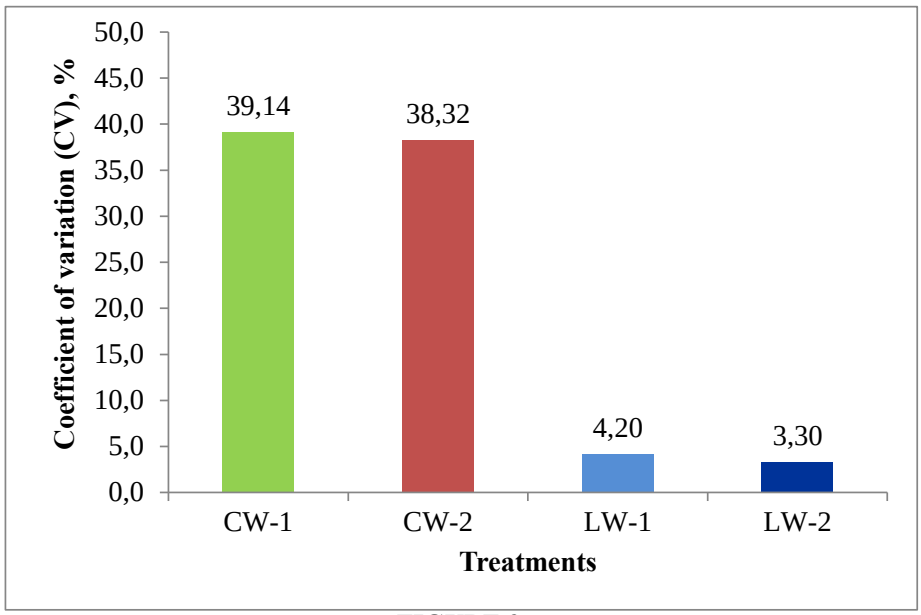


FIGURE 3
Coefficient of variation of emitters by treatments

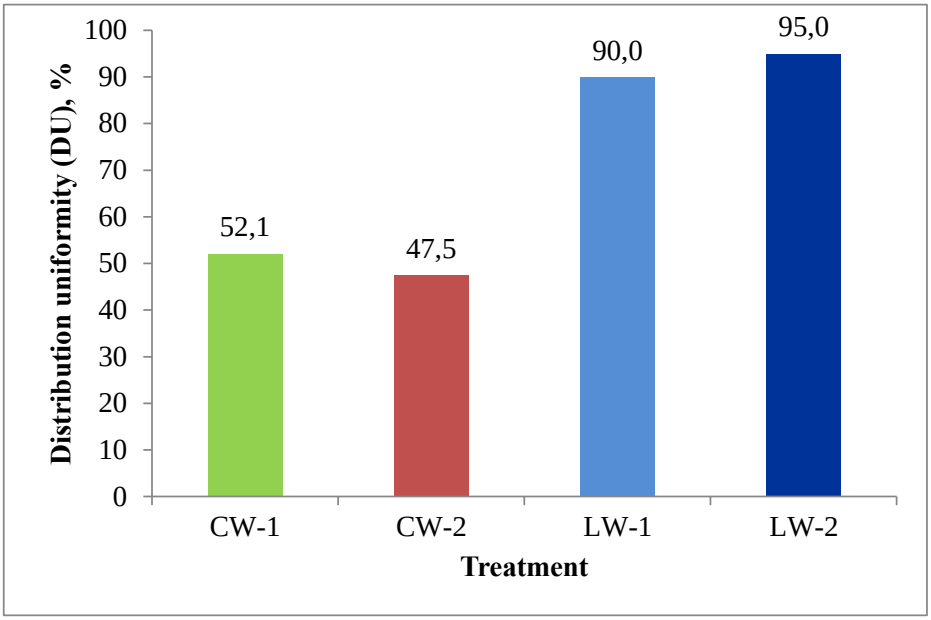


FIGURE 4
Distribution uniformity of emitters by treatment

Distribution uniformity (DU). Distribution Uniformity of emitters was assessed according to [26] and obtained DU values are given in Figure 4. As it is represented in Figure 4, the initial DU values of drip irrigation laterals were between the range of 47.5%-52.1%, and after the LW treatment these values increased to 90%-95%. In terms of classification, these values belong to top class and are desired for drip irrigation. It can be concluded that the acidic content of LW led to these higher values. The average DU values by different treatments indicate that water quality had a strong effect on DU values. Distribution Uniformity, as found in the studies conducted by [28, 29, 30], exceeded 94% and took place in the top class in general.

Adjusted Christiansen Uniformity (adjCU). The Adjusted Christiansen Uniformity (adjCU) values of average emitter flow rates of the treatments are given in Figure 5. The adjUC values for all treatments were found higher than 90%. While the highest average adjCU value was observed in CW treatment with 68.8%-69.4%, highest adjCU value was observed in LW treatment. It can be concluded that these high values resulted from unclogging of emitters and from laminar flow and that the acids found in LW showed a repellent effect in eliminating clogging as well.

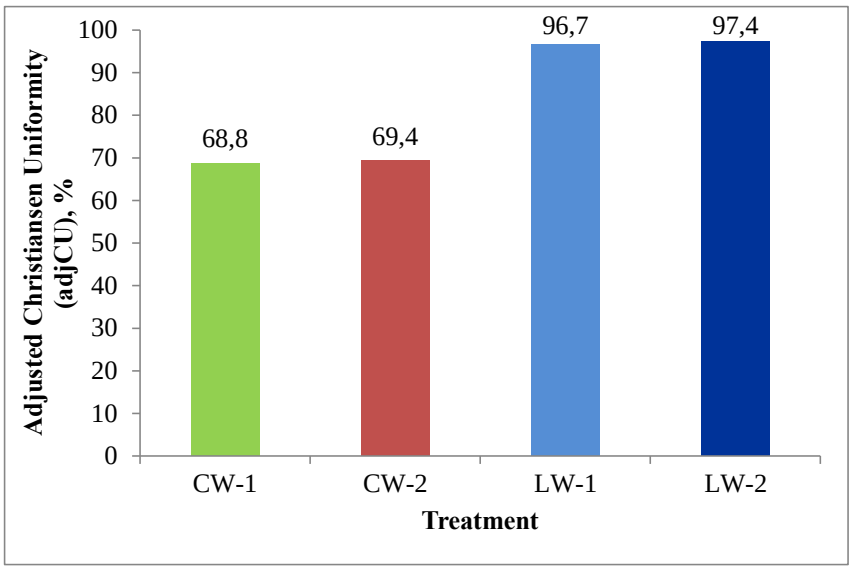


FIGURE 5
Adjusted Christiansen uniformity of emitters by treatments

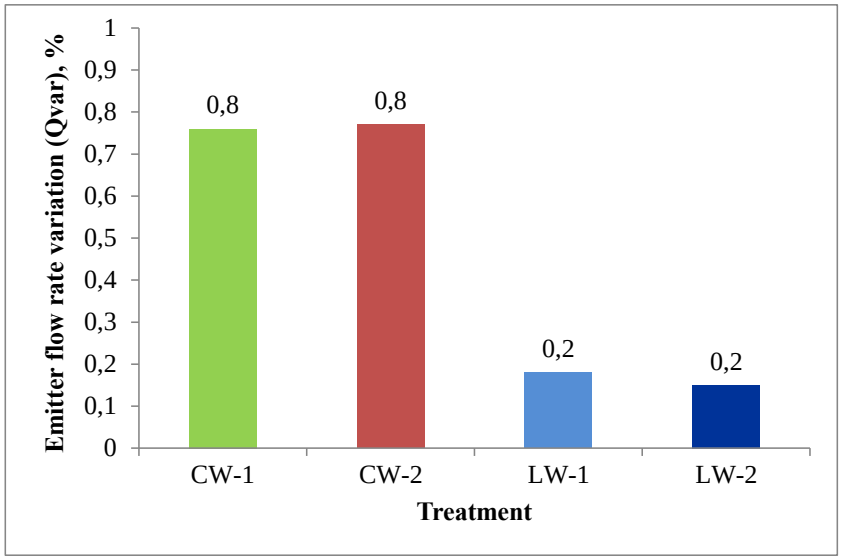


FIGURE 6
Emitter flow rate variation of emitters by treatments

Emitter flow rate variation (Qvar). The values of emitter flow rate variation (Qvar) by treatment are given in Figure 6. While the lowest flow rate variation of the first lateral in the CW treatment was 75%-76%, it was found 15%-18% for LW. The highest flow rate variation was observed in CW treatment, whereas the lowest variation was observed in LW treatment. It can be concluded that diminishing variation of flow rate results from the acids found in LW.

CONCLUSION

One of the most important constraints of drip irrigation systems is that the emitters become clogged in time, resulting in a significant decrease in system performance. Detecting, cleaning or replacement of clogged emitters is quite difficult and costly. Partial or complete clogging of the emitters decreases the water distribution uniformity and irrigation efficiency, which may lead to production and quality losses consequently.

In this study, the effect of locust bean waste on preventing chemical clogging in in-line emitter lateral pipelines, which is the main problem encountered in drip irrigation systems, was investigated.

As a result of this study, the DU, adjUC, CV and Qvar values of clogged emitters for CW treatment were found 48.45%, 69.01%, 0.39 and 0.77, respectively, and for LW treatment were found 77.52%, 97.01%, 0.04 and 0.17, respectively. Considering the average flow rates comparison, it is con-

cluded that locust bean extract waste is more efficient in preventing clogging.

It is important for users who are to apply locust bean waste to drip irrigation system to bear in mind that locust waste has a high acidic content and its usage needs to be paid attention. In addition, it is recommended that new studies should be carried out to investigate the adverse effects of sulfide, the amount of which is high in locust waste, on the environment.

In conclusion, it was determined that locust bean waste is effective in preventing emitters from clogging, however, it is also highly harmful to the system if used undiluted.

REFERENCES

[1] Ahraz, A. (2003) Locust bean gum (keçiboynuzu zamkı) E-410'un Türkiye'de üretimi. Gıda Teknolojisi. 7, 36-37 (in Turkish).

[2] Karkacier, M. and Artik, N. (1995) Keçiboynuzunun (*Ceratonia siliqua* L.) fiziksel özellikleri, kimyasal bileşimi ve ekstraksiyon koşulları. Gıda Tekonolojisi Derneği. 3, 131-136 (in Turkish).

[3] Yurdagel, Ü. and Teke, İ. (1985) Keçiboynuzu meyvesinin kavrulması ile oluşan renk değişimlerinin araştırılması. Gıda Tekonolojisi Derneği. 1, 39- 42 (in Turkish).

[4] Rolbiecki, S., Rolbiecki, R., Kuśmierek-Tomaszewska, R., Dudek, S., Żarski, J. and Rzekanowski, C. (2015) Requirements and effects of drip irrigation of mid-early potato on a very light soil in moderate climate. Fresen. Environ. Bull. 24, 3895-3902.

[5] Bayramoglu, E. and Demirel, O. (2016) Investigation of the irrigation possibility of *ilex aquifolium* L. plants by drip irrigation. Fresen. Environ. Bull. 25, 1779-1785.

[6] Kaman, H., Cetin, M. and Kırda, C. (2017) Monitoring and assessment of irrigation management in a large irrigation project area. Fresen. Environ. Bull. 26, 3986-3994.

[7] Demirel, K., Genc, L., Bahar, E., Inalpulat, M., Smith, S. and Kizil, U. (2014) Yield estimate using spectral indices in eggplant and bell pepper grown under deficit irrigation. Fresen. Environ. Bull. 23, 1237-1242.

[8] Granberry, D.M., Harrison, K.A. and Kelley, W.T. (2012) Drip chemigation: injecting fertilizer, acid and chlorine. Univ. of Georgia, Cooperative Extension, Athens, GA, 1130.

[9] Noori, J.S. and Thamiry, H.A. (2012) Hydraulic and statistical analyses of design emission uniformity of trickle irrigation systems. Journal of Irrigation and Drainage Engineering. 138, 791-798.

[10] Yazar, A., Tangolar, S., Sezen, S.M., Bozkurt-Çolak, Y., Gence,l B., Bilir Ekbiç, H. and Sabır, A. (2010) Bağlarda su yönetiminde yeni yaklaşımlar: yaprak su potansiyeli kullanılarak Çukurova koşullarında yüksek kaliteli verim için optimum sulama zamanının belirlenmesi. TÜBİTAK-TOVAG-106747 No'lu proje sonuç raporu (in Turkish).

[11] Qui, J., Qian, Y., Fenglin, Z. and Lvdan, Z. (2017) Impact of drip irrigation and buried straw layer on the soil cultivated environment: a case study under greenhouse. Fresen. Environ. Bull. 26, 5413-5419.

[12] Keller, J. and Bliesner, R.D. (1990) Sprinkle and trickle irrigation. An Avi Book. Van Nostrand Reinhold Pub. New York.

[13] Bozkurt, S. and Özekici, B. (2006) The effect of fertigation management in different types of in-line emitters on trickle irrigation system performance. Journal of Applied Sciences 6(5). 1165-1171.

[14] Nakayama, F.S. and Bucks, D.A. (1986) Trickle irrigation for crop production. Elsevier Science Publishers. Amsterdam, Netherlands.

[15] Kırnak, H., Doğan, E., Demür, S. and Yalçın, S. (2004) Determination of hydraulic performance of trickle irrigation emitters used in irrigation systems in the Harran Plain. Turkish Journal of Agriculture and Forestry. 28, 223-230.

[16] Capra, A. and Scicolone, B. (1998) Water quality and distribution uniformity in drip/ trickle irrigation systems. Journal of Agricultural Engineering Research. 70(4), 355–365.

[17] Tarchitzky, J., Rimon, A., Kenig, E., Dosoretz, C.G. and Chen, Y. (2013) Biological and chemical fouling in drip irrigation systems utilizing treated wastewater. Irrigation Science. 31, 1277-1288.

[18] Tyson, A.W. and Harrison. K.A. (1985) Chlorination of drip irrigation systems to prevent emitter clogging. Misc. Publ. 183. Cooperative Extension Service, University of Georgia.

[19] Nakayama, F.S. and Bucks, D.A. (1981) Emitter clogging effects on trickle irrigation uniformity. Transactions of the ASAE 24(1), 77-80.

[20] Pitts, D.J., Haman, D.Z. and Smajstrla, A.G. (1990) Causes and prevention of emitter plugging in microirrigation systems. Institute of Food and Agricultural Sciences Bulletin. 258.

[21] Benham, B. and Ross, B. (2002) Filtration, treatment and maintenance considerations for micro-irrigation Systems. Virginia State University- Publication. 442-757.

[22] Liu, H. and Huang, G. (2009) Laboratory experiment on drip emitter clogging with fresh water and treated sewage effluent. Agricultural Water Management. 96(5), 745–756.

[23] ASAE. (2003) Field evaluation of micro irrigation systems. EP458. American Society of Agricultural Engineers. 760−765.
[24] Keller, J. and Karmeli, D. (1974) Trickle irrigation design parameters. Transaction of the ASAE. 17(4), 678-684.
[25] Wu, I.P. and Gitlin, H.M. (1974) Drip irrigation design based on uniformity. Transactions of the ASAE. 17(3), 157-168.
[26] ASAE. (1994) Design and Installation of Microirrigation Systems. EP405 American Society of Agricultural Engineers. 724-727.
[27] Tüzel, H. (1993) Damla sulama sistemlerinde sulama yeknesaklığının değerlendirilmesi. Ege Üniversitesi Ziraat Fakültesi Dergisi. 30, l19-126 (in Turkish).
[28] Çamoğlu, G. and Yavuz, M.Y. (2004) Yerli ve yabancı yapım damlatıcıların sulama performansları yönünden karşılaştırılması. Uludağ Üniversitesi Ziraat Fakültesi Dergisi. 18(1), 181-191 (in Turkish).
[29] Hezarjaribi, A., Dehghani, A.A., Helghi, M.M. and Kiani, A. (2008) Hydraulic performances of various trickle irrigation emitters. Journal of Agronomy. 7(3), 265-271.
[30] Mangrio, A.G., Asif, M., Ahmed, E., Sabir, M.W., Khan, T. and Jahangir, I. (2013) Hydraulic performance evaluation of pressure compensating (PC) emitters and micro-tubing for drip irrigation system. Science, Technology and Development. 324, 290-298.

Received: **20.11.2017**
Accepted: **30.01.2018**

CORRESPONDING AUTHOR

Servet Tekin
Kahramanmaras Sutçu Imam University,
Faculty of Agriculture,
Department of Biosystems Engineering,
46040 Kahramanmaras – Turkey

e-mail: servettekin@ksu.edu.tr

© by PSP Volume 27 – No. 5/2018 pages 3043-3050 Fresenius Environmental Bulletin

MECHANISM OF ADSORBING URANIUM BY ORGANIC MATTER IN PADDY SOIL NEAR URANIUM MINE TAILING POND

Jingying Chen[1,2], Zumin Qiu[1,*], Bai Gao[3]

[1]School of Resources Environmental & Chemical Engineering, Nanchang University, Nanchang 330031, China
[2]State Key Laboratory Breeding Base of Nuclear Resources and Environment, East China University of Technology, Nanchang, 330013, Jiangxi, China
[3]School of Water Resources & Environmental Engineering, East China University of Technology, Nanchang 330013, China

ABSTRACT

Uranium mining would produce a great deal of acid wastewater and waste residue. Both of them contain numerous poisonous and pernicious substances, including heavy metals and radionuclide, which would cause serious soil pollution near the tailing pond. By taking the paddy soil near a uranium mine tailing pond in Southern China as the research object, this paper employed methods like infrared spectroscopy, scanning electron microscope, granule size and specific surface area to analyze elements of change of functional group, morphology, granule-size composition, specific surface area as well as aperture before and after adsorbing uranium through field sampling and lab analysis, so as to lucubrate the mechanism of adsorbing uranium by organic matters in paddy soil from a micro perspective.

The result showed that, if the soil structure remained unchanged, organic matter's major basic groups C-N, C-O, C-H, -OH and N-H and soil's basic groups like Si-O, C=O and C=C interacted and generated strong complex with UO_2^{2+}, so the soil was allocated with a stronger electrostatic uranium adsorption of the soil; organic matters affect the size of soil granules and then their adsorption capacity; paddy soil possessed II-type isothermal adsorption curve, C-type hysteresis loop as well as parallel-plate split-shaped open pore with narrow apertures of 2~50 mm in materials of mesopore (mesoporous) before and after removing organic matters; paddy soil's specific surface, pore volume, aperture and adsorption capacity were all decreased after removing organic matters, which indicated that organic matters would raise the soil's adsorption of uranium. The soil's adsorption capacity and volume of uranium is in direct proportion to its volume of organic matters under natural conditions.

KEYWORDS:
Soil Organic Matter, Uranium, Adsorption Mechanism

INTRODUCTION

Uranium is a vital raw material in nuclear energy. Uranium mining may produce a great deal of uranium-containing wastes, which may cause serious pollution and threaten the ecological security by migrating into the soil through ways of tailing mine leachate and sewage irrigation [1]. Hence, it is of great importance to explore the uranium's migration and transformation in the soil. Researches have shown that [2-4], uranium, in the form of UO_2^{2+}, is mainly absorbed by iron exchange with H^+ of humus acid during the migration period, whereas organic matters are a vital element in the migration and transformation period in the soil. At present, numerous researches on adsorption models of uranium in the soil have been made, but few on adsorption models of uranium in organic matter in the uranium tailing pond soil [5-11]. By taking the paddy soil downstream a uranium mine tailing pond as the research object, this paper employed paddy soil with organic matters contained as adsorbent and uranium solution with different gradient concentrations as adsorption object to study the contribution of organic matters to the soil's adsorption of uranium. The research result offers parameters for impact evaluation of tailing pond, certain application value for guiding to renovate characteristics of polluted soil in our country's tailing ponds, and food safety and ecological safety in mine ponds.

EXPERIMENTAL METHOD

Sample Pretreatment. Collected soil samples were mixed evenly, reduced to 100 g by quartering, naturally air dried, removed impurities, grinded and sifted through 100 meshes. The removal of organic matters in the soil was made by carrying out a full oxidation decomposition using H_2O_2[12], adding 30% of hydrogen dioxide solution in the soil, fully mixing the turbid liquid to decompose organic matters until there was no bubble inside, adding a small amount of H_2O_2 solution to stir until no bubble produced,

sifting through meshes after dried by air, and storing for use.

Adsorption Experience. Firstly, this paper selected few paddy soils polluted by uranium to remove organic matters: added about 0.5 g of soil samples (original soils and soils with organic matters removed) and 10 mL of uranium standard solution with certain concentration in a series of centrifuge tubes with volume of 50 mL, adjusted pH of turbid liquid and controlled adsorption conditions by dilute nitric acid and NaOH solution, and vibrated in constant temperature vibrator. Further, this experiment also included parallel samples for comparison. Secondly, this paper took out of and centrifuged soil samples at set time, measured the mass concentration of uranium in liquid supernatant, and calculated its adsorption efficiency and contribution ratio of organic matters. Thirdly, this paper lucubrated the mechanism of adsorbing uranium by paddy soil after removing organic matters using infrared spectroscopy, scanning electron microscope, granule size and specific surface area, plus discussed impacts of soil structure, grain size and specific surface area on the adsorption effect.

MECHANISM OF URANIUM ADSORPTION BY ORGANIC MATTERS IN THE SOIL

Analysis on Functional Group (Infrared Spectroscopy) in Soil Samples before and after Adsorption. This paper adopted Nicolet IS5 Fourier transform infrared spectrometer produced by Thermo Fisher Scientific Co., Ltd. The experience used KBr compacting test to scan within the scope of 4000cm^{-1}-400cm^{-1}.

Figure 1 is the infrared spectrogram of uranium adsorption by paddy soil before and after removing organic matters. From the comparison of infrared spectroscopy curves at 1# and 2#, we can know that there were quite few changes in original paddy soil and paddy soil with organic matters removed: no significant change at spectral peaks and no new band, but only certain displacements of spectral peaks appeared. It showed that the soil's structure remained unchanged after removing organic matters.

From the comparison of infrared spectroscopy curves at both 1# and 3# and 2# and 4# in Figure 1, we can know that spectral peaks were displaced and new bond appeared after adsorption. The stretching vibrations of -OH and N-H of original paddy soil moved from approximately 3620 cm^{-1} and 3437 cm^{-1} to higher until 3697~3445 cm^{-1} with elevated peak intensity and sharpened peak shape, while stretching vibrations of -OH and N-H of paddy soil with organic matters removed moved from about 3697 cm^{-1} and 3438 cm^{-1} to 3621 ~3446 cm^{-1} with raised peak intensity. The stretching vibrations of C-H of original paddy soil and paddy soil with organic matters removed moved from 2900 cm^{-1}, 2918 and to 2920, 2900 cm^{-1}, wherein the former's peak intensity and peak shape basically remained unchanged, while the latter had a significantly reduced peak intensity and flattened peak shape. The stretching vibrations of C=O and C=C at 1629 cm^{-1} and 1654 cm^{-1} of original paddy soil and paddy soil with organic matters removed moved to 1617, 1618 cm^{-1}, wherein the latter had a widened peak shape and increased peak intensity, while the latter had a narrowed peak shape and weaken peak intensity. The strong adsorption peaks respectively appeared near 1445 and 1447 cm^{-1} of the original paddy soil and paddy soil with organic matters removed after the adsorption, which may be free C-H bending vibration peak and C-OH stretching vibration peak. The stretching vibration peaks of Si-O, C-N, C-O off-plane coiling vibration peaks of original paddy soil moved from 1080 cm^{-1} to 1031 cm^{-1}, while paddy soil with organic matters removed moved from 1032 cm^{-1} to 1078 cm^{-1}, but both of them had small changes in peak shape and intensity. Generally speaking, characteristic adsorption peaks of uranium appeared in 800~1100 cm^{-1}. Due to the existence of massive basic groups like Si-O and C-O in the soil, U-O characteristic peak was sheltered from these characteristic adsorption peaks. The stretching vibration of -OH may be caused by functional groups of alcohol, phenol or carboxylic acid. The stretching vibration peaks of C=O and C=C may be caused by conjugated double bond of carbonyl in aldehyde, ester, ketone or carboxylic acid. Part displacement of adsorption peaks before and after the adsorption may be caused by the replacement of H^+ formed by hydroxyl, amidogen and other elements by UO_2^{2+}. C-H stretching vibration peak and C-H bending vibration peak and C-OH stretching vibration peak may be caused by the combination of H^+ and carbon-containing compounds.

From the spectrogram, we can know that the soil structure remained relatively complete after the adsorption. From changes in basic groups before and after removing organic matters, we can know that organic matters in paddy soil may contain many basic groups like C-N, C-O and C-H, which can allocate the soil surface with large negative charges and raise the soil's electrostatic adsorption of uranyl ions. Besides, active basic groups like -OH, N-H, Si-O, C-N, C=O and C=C plays an inevitable role in determining the uranium adsorption capacity of paddy soil.

Analysis on Sample Morphology (Scanning Electron Microscope) before and after Adsorption. This paper adopted Nova Nano SEM 450 high-resolution field emission scanning electron microscope produced by FEI Chech Co., Ltd. This paper dried, metal sprayed, observed in scanning electron microscope and draw up images of processed samples.

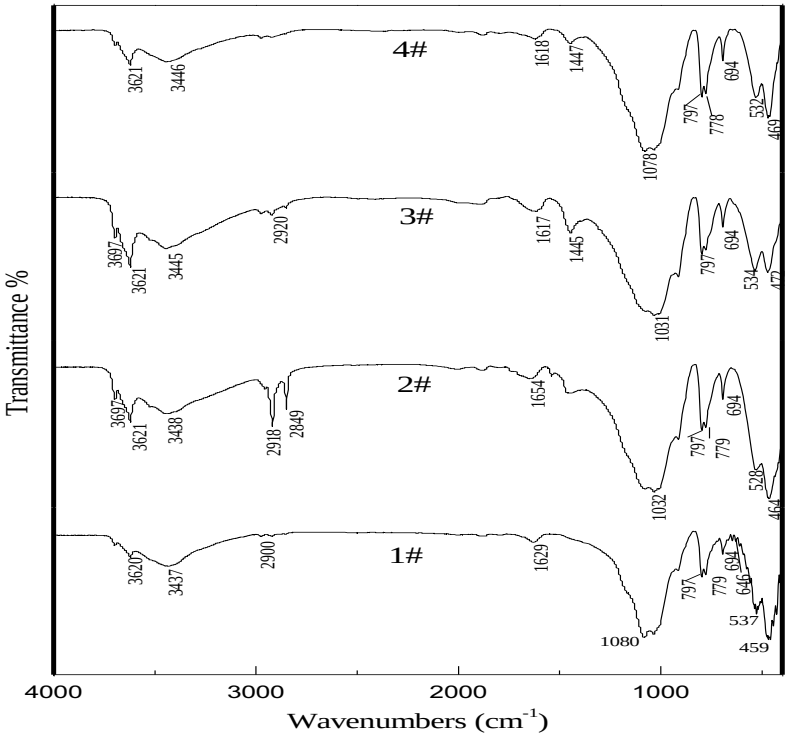


FIGURE 1
Infrared Spectrogram of Uranium Adsorption by Paddy Soil before and after Removing Organic Matters
1# Paddy Soil before Adsorption; 2# Paddy Soil with Organic Matters Removed before Adsorption; 3# Paddy Soil after Adsorption; 4# Paddy Soil with Organic Matters Removed after Adsorption;

Analysis on Scanning Electron Microscope of Uranium Adsorption by Paddy Soil before and after Removing Organic Matters. This paper observed surface topography of granules (100 meshes, 0.15 mm) for the uranium adsorption by paddy soil before and after removing organic matters by the scanning electron microscope, as shown in Figure 2.

It can be known from Figure 2 that, there were a series of twisty honeycomb aggregations or irregular porous structures with surface irregularity. On one hand, pole space increases soil's superficial area and exposes more adsorption loci; on the other hand, it also offers necessary channels and enough adsorption space for uranyl ion and metal ions in adsorption solution for internal diffusion. From the comparison of 1# and 2#, we can know that after adsorbing uranium, the original paddy soil had a narrowed pole space in that most adsorption loci were occupied by UO_2^{2+}; however, surface irregularity still remained significant, this was because functional groups on surfaces of organic matters in the soil took part in in uranium adsorption. After removal of organic matters, through surface irregularity still remained significant, we found that both porous structures and surface adsorption loci reduced, which was mainly due to the wide pore space, reduced soil porosity, many tiny irregular structures with many small pore spaces. It follows that after removal of organic matters, pole size would be reduced; after uranium adsorption, paddy soil with organic matters removed would possess an unchanged basic structure, filled part of small space, large irregular structures with large space, which may be caused by the accumulation of uranyl ions on these irregular structures.

The soil has massive obligate adsorption basic groups, and organic matters can act with UO_2^{2+} to produce clathrate or chelate, which can elevate the soil's uranium adsorption capacity and change the soil's surface morphology.

Analysis on Granule Size of Soil before and after Adsorption. This paper used Mastersizer 2000 laser granule analyzer produced by the Britain's Malvern Instruments Ltd to measure samples' granularity: fully dispersing samples of certain amount in distilled water media, conducting ultrasonic treatment after dilution and testing on laser granule analyzer.

Figure 3 is the distribution diagram of granule size of paddy soil before and after adsorption. Table 1 is the distribution table of granule size of paddy soil before and after adsorption, of which D10, D50 and D90 are diameters on X-axis of 10%, 50% and 90% on Y-axis and D50 is also known as median particle diameter or medium particle diameter, which is generally used to represent the particle size of that group.

It can be seen from Table 1 that medium particle diameters of the original paddy soil before and after adsorption are 9.164 and 9.099 um, while medium particle diameters of the paddy soil with organic matters removed before and after adsorption are 14.244 and 18.845 um. As per the soil's proportion in various particle sizes and international classification standard for soil texture, all above are silt, which is at the level of soil particle, whose name is silty loam. After removing organic matters, paddy soil's particle size was increased, but its texture type remained unchanged. It can be known from Fig. 3.1 that, particle sizes of the original paddy soil before adsorption are mainly distributed between 0.3 and 80um with peak near 10um, particle sizes of the original paddy soil after adsorption are mainly distributed between 0.4 and 60um with peak at 8~9um, showing a reduction in particle sizes; particle sizes of paddy soil with organic matters removed before adsorption are mainly distributed between 0.3 and 60um with peak at 10um: organic matters may affect particle sizes of paddy soil, or removal of organic matters may change sizes of paddy soil, particle sizes of paddy soil with organic matters removed after adsorption are mainly distributed between 0.3 and 90um with peak at 20~30um, whose distribution curve of particle sizes is relatively sharp and main product is coarse dust.

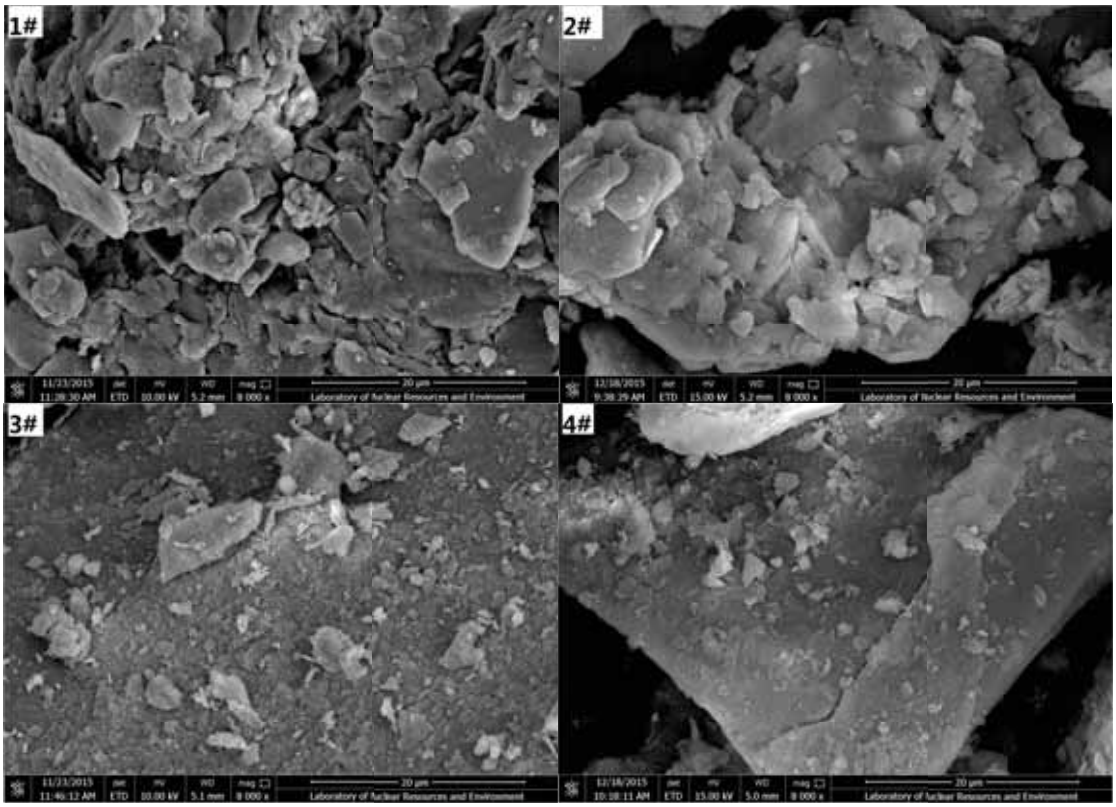


FIGURE 2
Scanning Electron Microscope Diagram of Paddy Soil before and after the Adsorption
1# Paddy Soil before Adsorption; 2# Paddy Soil with Organic Matters Removed before Adsorption; 3# Paddy Soil after Adsorption; 4# Paddy Soil with Organic Matters Removed after Adsorption;

TABLE 1
Particle Size Distribution of Paddy Soil before and after Adsorption

Particle size distribution (um)	Before Adsorption		After Adsorption	
	Paddy Soil	Paddy Soil with Organic Matters Removed	Paddy Soil	Paddy Soil with Organic Matters Removed
D10	1.800	2.895	2.371	3.410
D50	9.164	14.244	9.099	18.845
D90	31.348	34.238	29.216	52.640

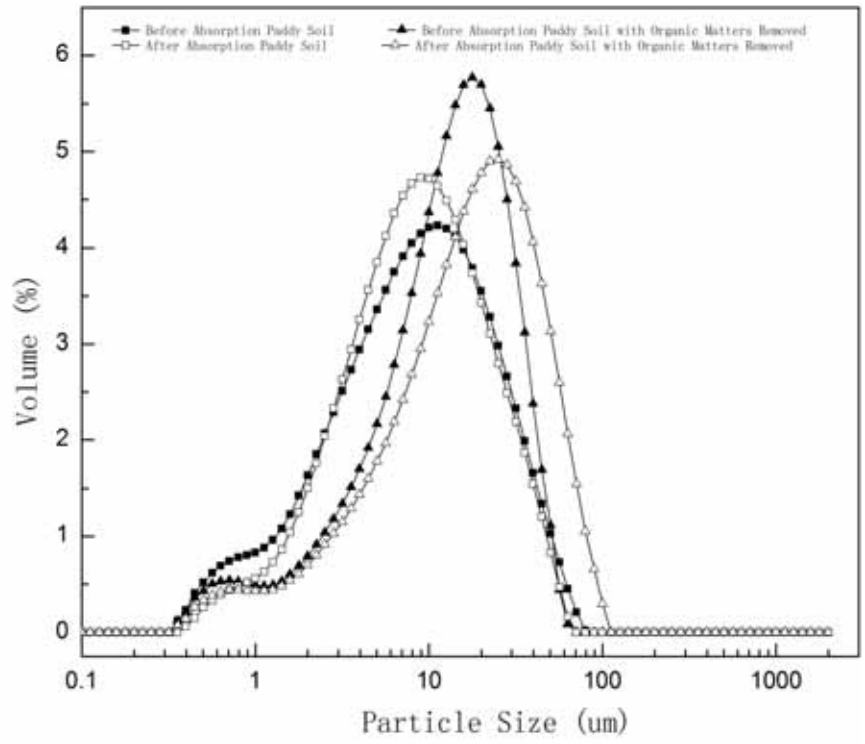


FIGURE 3
Particle Size Distribution of Paddy Soil before and after Adsorption

TABLE 2
Specific Surface Area, Pore Volume and Pore Diameter of Paddy Soil before and after Removal of Organic Matters

Soil Sample	Specific Surface Area (m^2/g)		Pore Volume (cm^3/g)	Pore Diameter (nm)
	BET	Langmuir		
Original Paddy Soil	21.68	48.41	0.044	19.79
Soil with Organic Matters Removed	16.61	34.91	0.039	19.61

Analysis on Specific Surface Area, Pore Volume and Pore Diameter of Soil Sample before and after Adsorption. This paper used Quantachrome Nova specific surface area and pore diameter distribution analyzer produced by Quantachrome to measure the specific surface area, pore volume and pore diameter of soil samples.

(1) Analysis on Adsorption & Desorption Curves and BET Pore Diameters of Soil Samples before and After Removal of Organic Matters. This paper employed inert gas (N_2 or Ar) to represent adsorption materials by physical way to obtain specific surface area, distribution of pore volume and diameter, surface properties and other information of adsorption materials.

It can be known from Table 2 that by BET method and Langmuir method, the original paddy soil's specific surface areas of $21.68m^2/g$ and $48.41m^2/g$, pore volume of $0.044cm^3/g$ and pore diameter of 19.79nm and the original red soil's specific surface areas of $18.69m^2/g$ and $40.55m^2/g$, pore volume of $0.039cm^3/g$ and pore diameter of 19.61nm; after removing out of organic matters, the paddy soil's specific surface areas of $1.61m^2/g$ (BET) and $4.91m^2/g$ (Langmuir), pore volume of $0.039cm^3/g$ and pore diameter of 19.61nm and the red soil's specific surface areas of $13.30m^2/g$ (BET) and $29.49m^2/g$ (Langmuir), pore volume of $0.036cm^3/g$ and pore diameter of 19.59nm, indicating a reduced trend when compared with the original paddy soil. It follows that its adsorption capacity was accordingly diminished, which agrees with the measured result in adsorption experiment and verifies the induction in the analyzed scanning electron microscope. From the size of specific surface area, we can conclude that soil samples in this experiment have not been provided with strong adsorption capacity. Internationally, pore sizes are usually divided into three types: micropore with pore diameter ≤2nm; mesopore with pore diameter of 2~50nm; macropore with pore diameter ≥50nm. Therefore, it can be judged that paddy soil with organic matters

removed is a kind of mesopore (mesoporous) material.

Figure 4 is adsorption-desorption curve and pore diameter distribution of paddy soil before and after removal of organic matters. It can be seen from the pore diameter distribution curve that, there are two most probable pore sizes of the original paddy soil: 6.60 nm and 15.2 nm; but one most probable pore size in soil with organic matters removed: 19.606 nm, indicating that the pore space scope of soil with organic matters removed is diminishing and does harm to the improvement of adsorption capacity, which agrees with the analyzed result of scanning electron microscope.

It can be seen from Figure 4 that both adsorption curve and desorption curve of soil samples are II-type adsorption isotherms. They slowly increase at the initial stage and rapidly increase in the latter stage and no adsorption saturation has obtained even the saturated vapor pressure is nearly reached, showing that there are macropores of certain amount and endless scope in the paddy soil with organic matters removed. There's no superposition or adsorption loop in the whole period, indicating that the whole adsorption process is accompanied by adsorption and desorption all the time. Adsorption loop is a kind of C-type curve, adsorption branch and desorption branch rise up or rise down suddenly at the saturated vapor pressure. The shape of adsorption loop could reflect the pore structure with the most typical pore is parallel-plate split-shaped open pore. According to the capillary condensation theory and Kelvin equation [13], in the adsorption process, capillary condensation occurred first in narrow pores and wide pores came second; desorption occurred first in wide pores under high relative pressures and in narrow pores under sufficiently low relative pressures.

Loop location is connected with pressure when capillary condensation occurs: low pressure refers to small pore size. The closing time for upper and lower ends of adsorption hysteresis loop counters to the width of pore size distribution of soil samples: farther distance of closing points on upper and lower ends refers to wider pore size distribution and vice versa. Figure 4 shows a large adsorption-desorption loop and there's basically no separation between them, so the pore structures of paddy soil before and after removal of organic matters are primarily mesopores or micropores with narrow pore sizes distributed.

(2) Analysis on Specific Surface Area and Pore Diameter of Soil Samples before and After Adsorption. Table 3 shows specific surface area, pore volume and pore diameter of soil samples before and after adsorption. Compared with data in Table 2, all data increased or decreased within a small range, apart from large increase in the specific surface area using Langmuir method. The reason may be the irons' direct adsorption of on surfaces of adsorbents or their entering into pores inside adsorbents.

From the pore size distribution in Figure 5, there are some changes in pore size distribution after adsorption. There is only one most probable pore size of the original paddy soil after adsorption: 19.69nm, whose distribution diminishes at macropores; two most probable pore sizes of paddy soil with organic matters removed: 18.642 and 24.982nm. The analysis from scanning electron microscope obtained the same result.

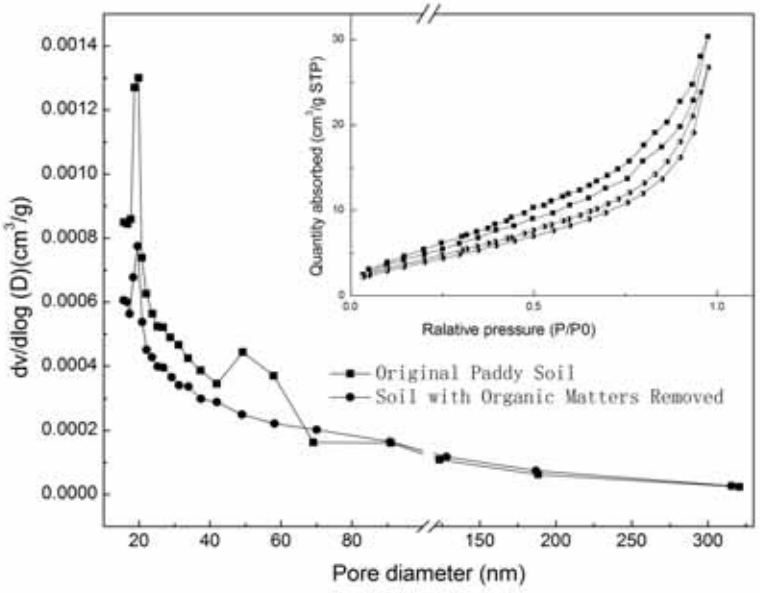


FIGURE 4
N2 Adsorption-Desorption Curve and Pore Diameter Distribution of Paddy Soil before and after Removal of Organic Matters

TABLE 3
Specific Surface Area, Pore Volume and Pore Diameter of Soil Samples before and after Adsorption

Soil Sample	Specific Surface Area (m^2/g)		Pore Volume (cm^3/g)	Pore Diameter (nm)
	BET	Langmuir		
Original Paddy Soil	25.89	85.99	0.046	14.85
Paddy Soil with Organic Matters Removed	15.81	46.52	0.038	15.63

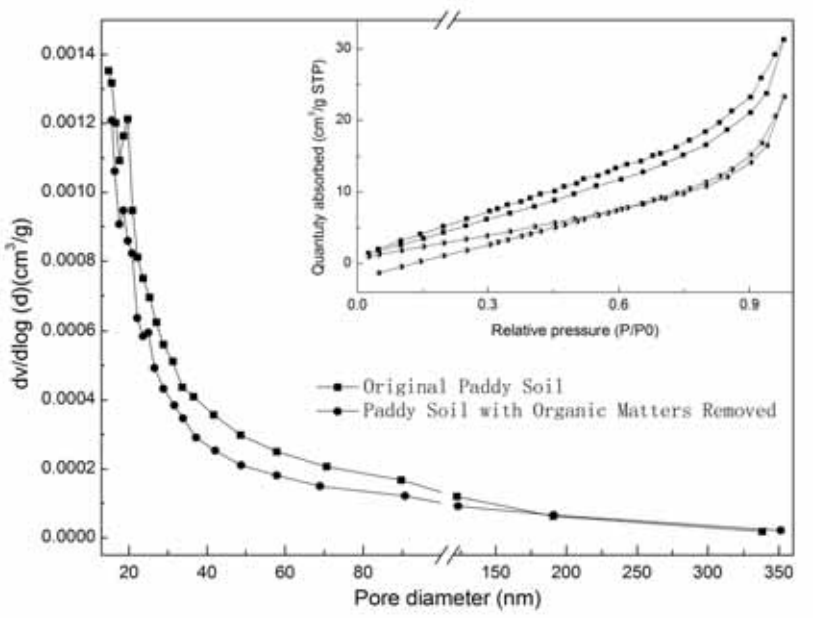


FIGURE 5
N2 Adsorption-Desorption Curve and Pore Diameter Distribution of Paddy Soil with Organic Matters Removed before and after Removal of Organic Matters

CONCLUSIONS

(1) The infrared spectrogram analysis demonstrated that the spectrogram of paddy soil had few changes with some displacements of peaks before and after removing organic matters; there were few new bands after adsorption, but the soil structure still remained complete. It can be seen from changes on spectrogram that organic matters in paddy soil may contain massive basic groups like C-N, C-O and C-H, which can allocate the soil surface with large negative charges and generated strong complex with, so the soil was allocated with a stronger electrostatic uranium adsorption of the soil. Besides, active basic groups like Si-O, C-N, C=O and C=C plays an inevitable role in determining the uranium adsorption capacity of paddy soil and red soil;

(2) The scanning electron microscope analysis showed that after removing organic matters, the paddy soil had a flattened surface and reduced adsorption loci; the soil structure had few changes before and after adsorption, which can generate the surface adsorption with, including adsorption on external surfaces and adsorption in the layers;

(3) The analysis from scanning electron microscope, specific surface area and pore diameter showed that after removing organic matters, pore space scope of paddy soil was reduced and then its adsorption capacity, indicating that organic matters can improve the soil's adsorption capacity and volume of uranium, which accords with the experimental result;

(4) The particle diameter analysis showed that paddy soil before and after removing organic matters is silt and particle diameter of paddy soil are raised after removal of organic matters, showing that organic matters have a significant impact on particle diameter of soil; after the adsorption, changes in particle diameters of original paddy soil are not obvious, while those of paddy soil with organic matters removed are relatively obvious;

(5) The analysis of specific surface area, pore volume and pore diameter showed that paddy soil possessed II-type isothermal adsorption curve, C-type hysteresis loop as well as parallel-plate split-shaped open pore with narrow apertures of 2~50 mm in materials of mesopore (mesoporous) before and after removing organic matters; paddy soil's specific

surface, pore volume, aperture and adsorption capacity were all decreased after removing organic matters, indicating that organic matters would elevate the soil's adsorption of uranium, which accords with the experimental result.

ACKNOWLEDGEMENTS

This work was supported by the National Natural Science Foundation of China (21407023, 41362011, 41662024), Jiangxi Province Natural Science Foundation of China(20171BAB203027), Open fund project of State Key Laboratory Breeding Base of Nuclear Resources and Environment (Z1507).

REFERENCES

[1] Akabzaa, T.M., Armah, T.E.K., Baneong-Yakubo, B.K. (2006) Prediction of acid mine drainage generation potential in selected mines in the Ashanti Metallogenic Belt using static geochemistry methods. Environmental Geology. 52(5), 957-964.

[2] Borovec, Z., Kribek, A., Olar, V. (1979) Sorption of Uranyl humic acids. Chem. Geol. 27, 39-46.

[3] Tao, Z.Y., Li, W.J., Zhang, F.M, Ding,Y.Q., Yu, Z. (2003) Am(III) adsorption on oxides of aluminium and silicon: effects of humic substances, pH, and ionic strength. J Colloid Interf. Sci. 265, 221-226.

[4] Zhu, H., Liao, J., Zhang, D., Kang, H., Liu, Q., Yang, Y., Liu, N. (2007) Extraction and Absorption of Soil Humic Acid on U (VI). Atomic Energy Science and Technology. 41(6), 683-688.

[5] Zhang, Y. (2012) Experimental Research on U (VI) Absorption of Humus and U (VI) Reduction of Humus/Shewanella Putrefaciens. University of South China & College of Environment and Safety, Hengyang.

[6] Mountney, A.W. (1992) Computer simulation of metalion-humic and fulvic acid interaction. J. Soil. Sci. 43, 679-688.

[7] Bednar, A.J., Medina, V.F., Ulmer-Scholle, D.S., Frey, B.A., Johnson, B.L., Brostoff, W.N., Larson, S.L. (2007) Effects of organic matter on the distribution of uranium in soil and plant matrices. Chemosphere. 70, 237-247.

[8] Li, J., Guo, Z., Liang, Y., Yang, H., Yu, S. (2011) Research on Impacts of Humic Acid and Acid Rain on Migration in the Soil. China Environmental Science. 31, 84-88.

[9] Montavon, G., Mansel, A., Seibert, A., Keller, H., Kratz, J.V., Trautmann, N. (2000) Complexation Studies of UO_2^{2+} with humic acid at low metalion concentrations by indirect speciation methods. Radiochim Acta. 88, 17-24.

[10] Jiang, H., Zhou, S., Zeng, G., Liu, Y., Li, H., Ouyang, S. (2015) U (VI) Absorption Dynamics and Thermodynamics of Insoluble Humic Acid. Journal of Safety and Environment. 15(1), 193-198.

[11] Anirudhan, T.S., Radhakrishnan, P.G. (2009) Kinetics, thermodynamics and surface heterogeneity assessment of uranium (VI) adsorption onto cation exchange resin derived from a lignocellulosic residue. Applied Surface Science. 255(9), 4983-4991.

[12] Bao, Y.Y., Zhou, Q.X, Wan, Y. Xie, X.J. (2009) Effect of soil organic; matter on adsorption and desorption of oxytetracycline in soils. China Environmental Science. 29(6), 651-655.

[13] Wang, Z., Zhang, M., Mei, H., Sun, L., Li, S., Wu, Q. (2002) Chemical and Physical Theory of Capillary Condensation and Absorption-Desorption Loop. Xinjiang Petroleum Geology. 23(3), 233-235.

Received: **21.11.2017**
Accepted: **23.02.2018**

CORRESPONDING AUTHOR

Zumin Qiu
School of Resources Environmental &
Chemical Engineering,
Nanchang University,
Nanchang 330031 – China

e-mail: qiuzm@ncu.edu.cn

© by PSP Volume 27 – No. 5/2018 pages 3051-3058 Fresenius Environmental Bulletin

INFLUENCE OF DISINFECTANT ADDED TO DRINKING WATER ON QUAIL GROWTH PERFORMANCE AND EGG QUALITY

Ali Karabayir[1,*], Mustafa Ogutcu[2], Nazan Arifoglu[3]

[1]Canakkale Onsekiz Mart University, Faculty of Agriculture, Department of Animal Science, 17020, Canakkale, Turkey
[2]Canakkale Onsekiz Mart University, Faculty of Engineering, Department of Food Engineering, 17020, Canakkale, Turkey
[3]Canakkale Onsekiz Mart University, Canakkale College of Applied Sciences, Department of Food Technology, 17020, Canakkale, Turkey

ABSTRACT

In the present study, the effect of disinfectant addition into drinking water on quail (*Coturnix coturnix japonica*) growth performance, egg quality, and water quality parameters was investigated. Drinking water quality was positively affected by addition of disinfectant (sodium N-chloro-p-toluenesulfonamide trihydrate). Microbial load of drinking water was reduced by disinfectant addition. Feed intake of the quails provided with disinfected drinking water was lower, while water intake and live weight gain was similar between the trial groups. Quail egg quality was affected by addition of disinfectant. The eggs of the quails provided disinfected drinking water had lower egg weight, shell strength and thickness, but the protein and mineral composition was not affected by disinfectant addition. The Haugh units of the eggs of the quails provided with disinfected water were higher, thus these types of eggs could be readily more suitable for the bakery industry. It can be concluded that addition of disinfectant into quail drinking water may improve the status and egg quality of quails.

KEYWORDS:
Egg quality, quail, *Coturnix coturnix japonica,* disinfectant, drinking water, growth performance

INTRODUCTION

Water is the most important ingredient of poultry farming, since it is used in management and as drinking water. Generally, in poultry farming city network, underground and surface waters are used. It is well known that water quality greatly affects health and vitality of poultry farming. The quality parameters of water are characterized as flavour, acidity, alkalinity, smell, colour, turbidity, salinity, conductivity, pH, biochemical oxygen demand, hardness, anions and cations concentrations, herbicides, pesticides and bacteria. Among these characteristics the most important criteria are toxicity and microbial contaminants that may cause many diseases as well as lethal effects on poultry farming [1-4]. On the other hand, water is not only contaminated from various sources, but also it may be contaminated by other environmental factors. Hence, water quality in poultry farms should be frequently controlled and if necessary some methods should be applied such as addition of cleaning and softening agents, filtration, magnetic precipitation or disinfections [1, 4-5].

In poultry farming, water intake depends on several factors such as type of animal, age, sex, activity, water quality, water and environmental temperature, and feed intake. Moreover, poultry carcasses consist of 55-77% water, while poultry eggs have 65% water. These data show that water quality directly affects quality of poultry products such as meat and eggs [6].

One of the important commercial poultry farming species is quail. Particularly, in Asian countries (Turkey, China, Japan, etc.) there is continuously increasing quail production and consumption. Quail eggs are preferred by consumers for their several beneficial properties such as protecting from stomach ulcers, strengthening the immune system, promoting memory health, increasing brain activity and stabilizing the nervous system [7]. In literature several studies related to quail growth performance and quality of eggs are presented. Studies on quail growth performance and egg quality; such as addition of acetyl salicylic acid [8], different dissolved oxygen concentrations in drinking water [9], lycopene [10], cinnamon and rosemary oils [11], and canola meal [12] were previously reported.

On the other hand, the health status of poultry has a direct effect on the quality of poultry products. Thus, in order to maintain good health status, water sanitation is gaining significance especially in intensive poultry farming [3, 13-15]. In order to improve the quality of drinking water, disinfectant addition is becoming a common application in poultry farming. Maharjan et al. [14] evaluated the impact of broiler farm water system sanitation practices and concluded that daily water sanitation helps in providing microbiologically safe water to broil-

ers. Taking into account the fact that disinfectant addition may improve the health status and product quality, in the present study sodium N-chloro-p-toluenesulfonamide trihydrate (Halamid) was used as a disinfectant in the drinking water of quails. Halamid is a disinfectant especially effective on gram-negative bacteria approved by Food and Drug Administration (FDA) for use in aquaculture [16]. The objective of the present study was to investigate the effects of Halamid added drinking water on quail growth performance and laying characteristics. The other main aim of the study was to determine the effects of adding disinfectant into drinking water on the quality characteristics of the quail eggs.

MATERIALS AND METHODS

Materials. A total of 40 quails (*Coturnix coturnix japonica*) at age of 3-7 days were purchased from a commercial farmer in Bayramic-Canakkale province of Turkey and were fed *ad libitum* a standard starter feed (25% crude protein and 3000 kcal of metabolizable energy (ME) per kg of diet) until the quails reached average weight of 51.7±1.5 g. The quails were divided into two groups and each group included two subgroups with a population of 10 birds per cage. All quails were fed standard diets in each cage. One of the cage was given drinking city network water, while the other cage was given drinking water containing 2% disinfectant (Halamid: sodium N-chloro-p-toluenesulfonamide trihydrate) solution. Halamid is a commercial biodegradable disinfectant purchased from Axcentive SARL (Chemin de Champouse, France). It is a white crystalline powder having a weak chlorine odour. Halamid is currently approved by FDA especially against gram-negative bacteria [16]. During the study, the quails were fed *ad libitum* a two-phase standard feed: grower feed (24% crude protein and 2900 kcal of metabolizable energy (ME) per kg of diet) from 0-21 days; a laying diet (20% crude protein and 2900 kcal of ME per kg of diet) from 22-49 days, purchased from feed market in Bayramic-Canakkale province of Turkey. All of the chemicals used in the chemical analyses were of analytical grade and purchased from Sigma-Aldrich and Merck.

Methods. Quail water analysis. The drinking water samples were collected once a week from each water tank. The pH, temperature, electrical conductivity (EC) and dissolved oxygen (DO) measurements were done immediately. The pH and temperature values of the water samples were measured by using a pH meter (Sartorius PP-50, Gottingen, Germany), while electrical conductivity (EC) and dissolved oxygen (DO) values were determined by using a Hanna HI98311 EC meter (Hanna Instrument Inc., USA) and Hanna HI9146 DO meter (Hanna Instrument Inc., USA), respectively.

The elemental composition of the water samples was analysed by using Perkin Elmer Optima 8000 ICP-OES. The elemental compositions of the samples were expressed in mg/L.

For the microbiological examination of the samples, water sampling first from the source and then from the bowls in the quail cages was accomplished and total coliforms, *Escherichia coli* and total bacteria determination was done according to Standard Methods for the Examination of Water and Wastewater [17]. The results were expressed as colony forming units (CFU) per 100 ml.

Quail performance features. The growth performance of the quails was monitored for 49 days. Feed and water intake was recorded daily and the results were calculated weekly as g/cage. For the live weight measurements, the quails were numbered and the individual live weights of the quails were determined weekly and the results were expressed as g/cage. The feed efficiency rate was calculated using feed consumption and live weight gain [9].

Quail egg quality analysis. The shell thickness, yolk width, height, albumen width, height and length were measured by using digital calliper. Yolk (1), Albumen (2) and Haugh (3) indices were calculated by using the following equations.

$$Yolk\ (\%) = [Yolk\ height\ (mm) / Yolk\ diameter\ (mm)]\ x100 \quad (1)$$

$$Albumen\ (\%) = \frac{[Albumen\ Height\ (mm)]}{[Albumen\ lenght + Albumen\ width\ (mm)/2]}\ x\ 100 \quad (2)$$

$$Haugh\ Unit = 100 \log[Albumen\ height(mm) + 7.57 - 1.7\ Egg\ weight\ (g)^{0.37}] \quad (3)$$

The protein contents of the quail egg albumen and yolk were separately determined according to AOAC Official Method (939.02) Protein Kjeldahl Standard Method [18].

A Texture Analyzer TA-XT2i (Stable Microsystems, Surrey, UK) was used to determine the egg shell hardness and the measurements were done according to Xie et al. [19]. The puncture test parameters were 2 mm cylinder probe, weight head 50 kg, probe inlet velocity 2 mm/s, outlet velocity 2 mm/s. The puncture test results were calculated by TA-XT2i Software and the results were given as hardness values (N).

Mineral analysis. First, 0.5 g egg albumen and yolk were separately weighed into a crucible, then 1 ml HCL and 8 ml HNO_3 were added. The mixture was gradually heated from 50 to 200 ºC in 55 min using Berghof Speed Wave microwave oven. After the liquid solutions were diluted to 25 ml, the samples were analysed using Perkin Elmer Optima 8000 ICP-OES. The elemental compositions of the samples were expressed in mg/kg.

Statistical analysis. The results were represented as mean ± standard deviation. The data were analysed by ANOVA and the multiple comparisons of the means accomplished by Tukey's test. Statistical analysis was performed with Minitab v.17.1.0 [20].

RESULTS AND DISCUSSION

Features of drinking water quality. Water is regarded as the source of life. Besides, poultry meat consists of 55-77% water, while 65% of poultry eggs are composed of water. The roles of water in poultry are transport of nutrients, digestion, absorption, regulation of body temperature and excretion of body wastes. Hence, particularly daily water intake is important for poultry farming. On the other hand, type of animal, water quality, water temperature, ambient temperature, feed consumption and diet also affect poultry water consumption. The daily water intake of poultry may vary depending on some quality criteria such as pH, temperature, flavour, turbidity and electrical conductivity [1, 5]. Therefore, the physical and sensorial quality of drinking water should be monitored and controlled. Generally, the pH values of both drinking water samples were in the neutral pH range (Fig. 1.). The pH values of the network water (NW) samples ranged from 6.95 to 7.41, while those values for Halamid added water (HAW) samples varied from 6.99 to 7.36. In literature, it was reported that the pH values of quail drinking water should be desirably in the range of 6.8-7.5 [4]. These literature findings are close to our findings. The concentration of dissolved oxygen affects taste, odour, colour and chemistry of water, while it is essential for aquatic life [21]. The dissolved oxygen (DO) values of the NW and HAW samples ranged between 3.21-5.76 and 2.72-5.47 mg/l, respectively. Sarin et al. [22] reported that DO values of typical network water ranged from 1 to 4 mg/L. These results are different from our findings. Fairchild and Ritz [4] reported that the normal ground water had little or no concentrations of dissolved oxygen. The fact that water DO values were greater than zero indicated that groundwater was in contact with surface water. On the other hand, the concentration of DO affects the solubility and stability of other elements such as Fe, Mn and S [21]. In terms of pH and DO values, there were no significant differences between the water samples. The EC values of the NW and HAW samples ranged between 304-342 and 1426-1731 µs/cm, respectively. There were statistically significant differences between the water samples. These results implied that NW sample had lower amounts of TDS than the HAW sample. In literature, it was reported that water samples with EC values less than 1670 µ/cm have a relatively low level of salinity and in general it is regarded that they present no serious threat to any livestock or poultry. Additionally, water samples with EC values ranging between 1670 and 5000 µ/cm were regarded as satisfactory for all classes of livestock [23]. As seen from Fig. 1, the temperature values of both water samples varied between 22 and 27 ºC. In literature, feed intake and death rate values decrease with increasing the conductivity of water. Moreover, positive correlations among live weight and DO and pH values of drinking water were recorded [24, 25].

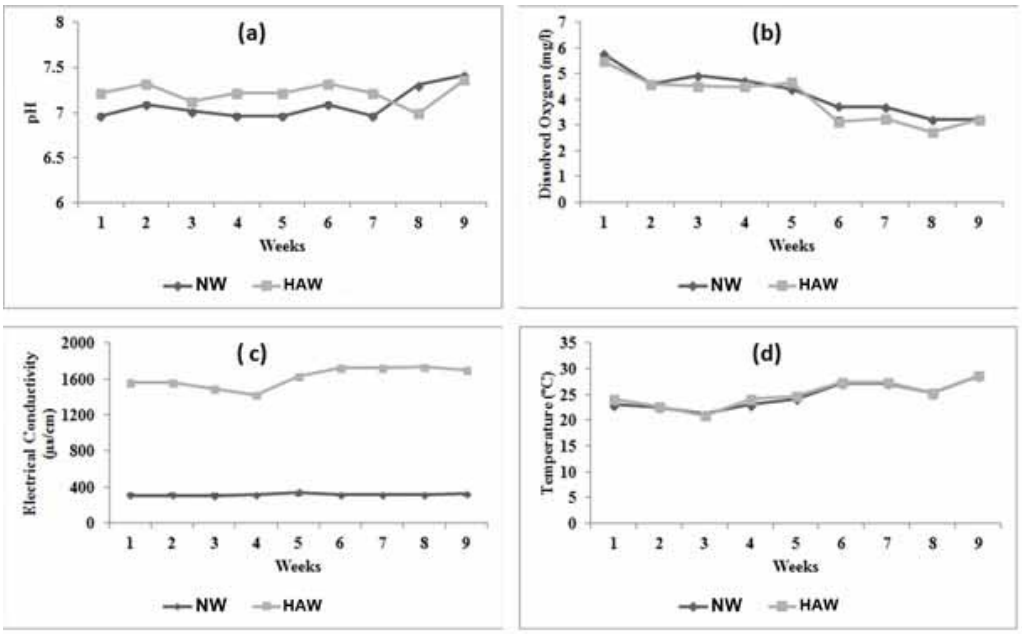


FIGURE 1
Some physico-chemical parameters of the drinking water samples (HAW: Halamid added water, NW: Network water).

The microbiological quality of drinking water is an important issue in poultry farming. Microbiological water quality was generally tested for total bacteria, coliform and faecal coliform bacteria counts. Especially, coliform bacteria are normally found in the digestive systems of human and poultry, so presence of coliforms is an indicator of faecal contamination [4]. As it is well known, the cause for many epidemic diseases in poultry farms was drinking water. As a result of these diseases, poultry may either die or be weakened. In Table 1, the microbiological results of NW and HAW water samples are given. The HAW sample had no *E. coli*, coliform and total bacteria, while for the NW sample 110 CFU/100ml E. coli, 210 CFU/100 ml coliform and 85 CFU/ml total bacteria were recorded. Additionally, considering the samples taken from water bowl, the NW samples had *E. coli* 4500 CFU/100 ml, coliform counts 4500 CFU/100 ml, total bacteria counts 310 CFU/ml, while the HAW sample had *E. coli* 87.50 CFU/100 ml, coliform counts 525 CFU/100 ml and total bacteria counts 70 CFU/ml. These findings demonstrated that the HAW sample was more effective in improving the microbiological quality of drinking water. Fairchild and Ritz [4] reported that when the number of microorganisms is found at high level in water, it indicates that water supply is contaminated. For poultry farming, the maximum acceptable level of coliform and total bacteria values should not exceed 0-50 CFU/ml and 0-100 CFU/ml, respectively [4, 6]. Based on the above results, potential bacterial diseases of poultry farming such as colibacillosis (*Escherichia coli*) and fowl typhoid (*Salmonella gallinarum*) might be prevented by adding disinfectant into drinking water [13]. During the trial period, no diseases were observed in the quails.

TABLE 1
Microbiological properties of the drinking waters samples.

Sample	*E. coli** (CFU/100ml)	Coliforms (CFU/100ml)	Total Microorganisms (CFU/ml)
HAW	0.00±0.00B**	0.00±0.00B	0.00±0.00C
HAW-Bowl	87.50±12.5B	525.00±75.00B	70.00±10.00B
NW	110.00±10.00B	210.00±10.00B	85.00±5.00B
NW-Bowl	4500.00±500.00A	4500.00±500A	310.00/10.00A

CFU: Colony forming unit, HAW: Halamid added water, NW: Network water.
*The results are presented as Mean±Standard Deviation (SD).
*Capital letters in the same column show significant differences ($p<0.05$)

TABLE 2
Mineral composition of the drinking water samples.

Minerals	HAW* (mg/l)	NW (mg/l)	Limits (mg/l)	Remarks [4]
Zinc (Zn)	0.02±0.00A**	0.02±0.00A	0-1.5	Higher levels are toxic. Growth retardation may be observed.
Barium (Ba)	0.009±0.00A	0.009±0.00A		-
Iron (Fe)	0.007±0.00A	0.00±0.00B	0.2-0.3	Higher level occur bad odor and taste
Boron (B)	0.007±0.00A	0.004±0.00B		-
Manganese (Mn)	0.002±0.00A	0.001±0.00B	0.01-0.05	-
Chromium (Cr)	0.0005±0.00A	0.0003±0.00A		-
Magnesium (Mg)	9.84±0.01A	9.25±0.15B	14-125	Higher levels have laxactive effect. Levels higher than 50 mg/l may affect performance depending on the higher levels of sulfate.
Copper (Cu)	0.002±0.00B	0.003±0.00A	0.002-0.6	Higher levels occur bitter taste. It causes lesions in the mouth and gizzard.
Aluminium (Al)	0.02±0.00A	0.01±0.00B	0.05-0.2	-
Potassium (K)	1.58±0.01A	1.27±0.01B		-
Calcium (Ca)	44.59±1.22B	52.43±5.44A	0-60	-
Sodium (Na)	472.6±3.18A	9.63±0.13B	50-150	Depending on the higher level of sulfate and chloride, higher than 50 mg/l levels may be affect performance.

HAW: Halamid added water, NW: Network water.
*The results are presented as Mean±Standard Deviation (SD).
**Capital letters in the same line show significant differences ($p<0.05$)

The elemental compositions of the NW and HAW samples are given in Table 2. In Table 2, calcium (Ca), potassium (K), magnesium (Mg), sodium (Na) and zinc (Zn) levels of the HAW samples were 44.59, 1.58, 9.84, 472.6 and 0.02 mg/l, respectively. On the other hand, calcium (Ca), potassium (K), magnesium (Mg), sodium (Na) and zinc (Zn) levels of network water were 52.43, 1.27, 9.25, 9.63 and 0.02 mg/l, respectively. Fe, B, Mn, Mg, Al, K, and Na levels in the HAW sample were found higher than those of the NW sample, while Ca and Cu levels were found lower (Table 2). The elemental composition and level of both water samples were found to be within the legal limits according to literature data (Table 2), except for the Na level in the HAW sample [4]. This finding might be explained with the fact that the disinfectant used within this study (Halamid) is in the form of Na-salt and thus disinfectant containing water had a higher Na level.

Growth performance. The growth performance of the quails was monitored by daily feed and water intake, live weight gain, feed efficiency rate and death rate for seven weeks. The growth performance data of the quails are given in Fig. 2. According to Fig. 2, the feed intake values of the HAW group were lower than that of the NW group. The feed intake levels of the HAW and NW quail groups ranged between 236.7-319.07 g/cage/week and 227.6-379.8 g/cage/week, respectively. In literature, feed intake levels of quails were reported as 35.98-37.07 g/bird/day [12], 22.67-30.01 g/bird/day [15], 31.18 g/bird/day [10]. Literature findings are close to our findings. Moreover, the water intake level of the HAW and NW groups ranged between 355-566 ml/cage/week and 415.7-475.7 ml/cage/week, respectively. Also, there were statistically significant differences between HAW and NW quail groups (p=0.018). However, there were no statistically significant differences between HAW and NW groups in terms of water intake values (p>0.05). These results imply that the addition of disinfectant to drinking water did not affect water intake level, while it affected feed intake level. The quail live weight was monitored for seven weeks and the results are shown in Fig. 2c. The live weight levels of the HAW quail group increased from 51.7 to 193.53 g, while the live weight level of the NW quail group increased from 51.7 to 219.28 g at the end the trial period. There were no statistically significant differences between the HAW and NW quail groups with respect to live weight levels (p>0.05). These results demonstrated that disinfectant addition to drinking water did not affect live weight levels of quails. Safari & Zahedi [26] reported that quail live weight ranged from 15.5 to 193.25 g. These findings are similar to our results. The weekly feed efficiency rates of HAW and NW quail groups changed between 1.23-4.71 and 1.04-6.43, respectively. As seen from Fig. 2d, the feed efficiency rate values decreased during the trial for both groups. The other important parameter in poultry farming was survival level. The survival levels of the HAW quail group were 97.78%, while the NW quail group were 100% (data not shown). Hassan et al. [8] reported that the live weights of quails (34-39 week age) provided with drinking water containing acetyl salicylic acid (0-1.5 g/L) to be in the range of 156.0-217.9 g. Moreover, in the same study, it was shown that adding 1.5 g/L acetyl salicylic acid to the drinking water of quails under heat stress improved body weight, fertility, hatchability, embryonic mortality, egg production, egg specific gravity, and sperm storage capacity [8]. Both literature and our findings demonstrated that drinking water characteristics are effective on quail performance and eggs.

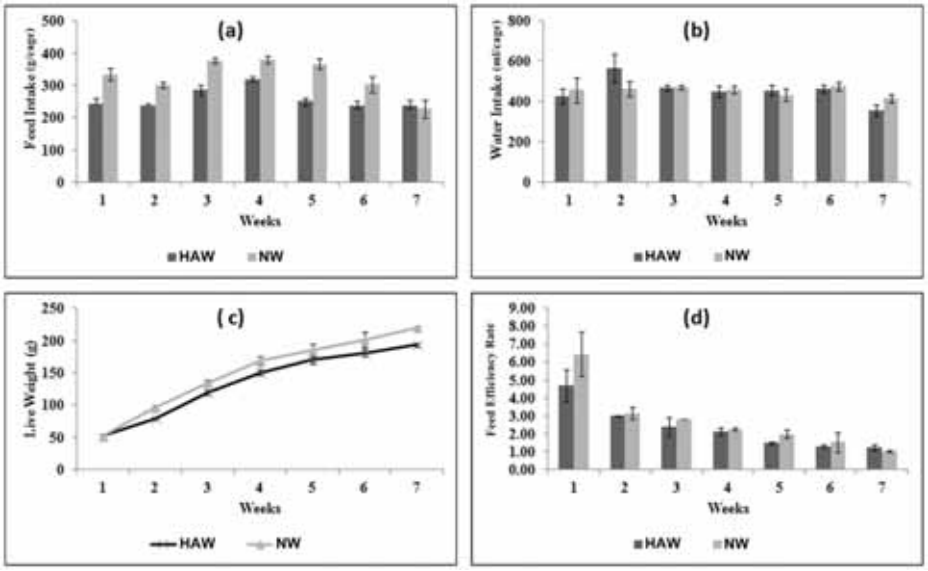


FIGURE 2
Growth-performance features of the quails (HAW: Halamid added water, NW: Network water).

TABLE 3
Quality parameters of the quail eggs.

Features	HAW*	NW
Egg Weight (g)	8.78±1.10b**	10.57±0.24a
Protein (%)	20.11±2.95a	20.33±2.24a
Shell Strength (N)	7.44±1.94b	10.02±2.62a
Shell Thickness (mm)	0.25±0.06b	0.30±0.05a
Yolk Width (mm)	24.23±3.33b	25.99±2.63a
Yolk Height (mm)	6.79±1.79a	6.99±1.95a
Yolk Index	28.83±9.56a	27.13±7.81a
Albumen Width (mm)	51.39±10.42b	61.62±8.62a
Albumen Length (mm)	67.51±14.34b	81.06±15.70a
Albumen Height (mm)	2.83±0.52a	3.11±0.56a
Albumen Index	5.07±1.92a	4.42±0.84a
Haugh Unit	97.83±2.14a	81.52±3.63b

HAW: Halamid added water, NW: Network water.
*The results are presented as Mean±Standard Deviation (SD).
**Small letters in the same line show significant differences ($p<0.05$)

Quality properties of quail eggs. Quail eggs contain significant nutritional contents of amino acids, fatty acids, vitamin E, sex hormone P and minerals such as zinc and iron. Hence, quail eggs are regarded as good sources of nutrients for human body [7]. The quail eggs quality characteristics of the HAW and NW groups are shown in Table 3. The egg weight of the HAW group was 8.78 g, while the NW group eggs were 10.78 g. In literature, quail eggs weights were reported as 11.79-12.17 g by Simsek et al. [11] 10.35-11.46 g by Saki et al. [12], 10.19 g by Korenekova et al. [27], and 11.52 g by Sahin et al. [10]. Our HAW group egg weights are lower than literature data, while NW group egg weights are similar to literature data. The shell strength and thickness values of the HAW group eggs were 7.44 N and 0.25 mm, respectively. On the other hand, the shell strength and thickness values of the NW group eggs were 10.02 N and 0.30 mm, respectively. In literature, shell strength and thickness values of quail eggs were reported as 12.09 N and 0.25 mm, respectively [27, 28]. These literature results are similar to our findings. In terms of egg weight, shell strength, shell thickness, yolk width, albumen weight, albumen length, and Haugh unit, there were statistically significant differences between the HAW and NW group quail eggs. As seen from Table 3, the NW group quail eggs had higher values of egg weight, shell strength and shell thickness. Haugh unit was defined as an indicator of the albumen quality for bakery industry [10]. The Haugh unit of the HAW and NW group eggs were 97.83 and 81.82, respectively. Moreover, the HAW group quail eggs had significantly higher Haugh unit values. In this case, HAW group eggs are more valuable than NW group eggs for the bakery industry. On the other hand, protein, yolk height and index, albumen height and index were fairly similar for both egg groups.

The elemental compositions of the albumen and yolk portions of the HAW and NW egg groups are given in Table 4. The egg yolk portions of both groups had lower level compared with yolk portions of both egg groups. Zinc (Zn), iron (Fe), calcium (Ca), and phosphorus (P) level of the HAW group yolk portion of eggs were 21.10, 38.07, 729 and 2315 mg/kg, respectively. On the other hand, Zinc (Zn), iron (Fe), calcium (Ca), and phosphorus (P) level of the NW group yolk portion of the eggs were 27.50, 38.58, 867.5 and 4242 mg/kg, respectively. These results demonstrated that the HAW group eggs had lower Zn, Ca and P values than that of the NW group eggs. Korenekova et al. [27] reported that the amount of zinc in albumen and yolk ranged between 71.08-73.49 and 63.84-67.1 mg/kg, respectively. These literature data are similar to our results. The Zn, Ca and P concentrations of egg yolks of quails provided with HAW were lower, thus it can be stated that addition of Halamid into drinking water of quail might decrease the mineral utilization of the birds. These results are correlated with the findings of egg weight and egg shell parameters (Table 3). However, egg protein content was not affected by Halamid supplementation, while Haugh unit, a significant egg quality parameter, increased with Halamid addition.

TABLE 4
Mineral composition of the quail eggs.

Mineral	Yolk-HAW* (mg/kg)	Albumen-HAW (mg/kg)	Yolk-NW (mg/kg)	Albumen-NW (mg/kg)
Zinc (Zn)	21.1±0.23B**	5.80±0.10D	27.50±0.40A	8.09±0.13C
Cobalt (Co)	0.09±0.02	0.04±0.01	0.15±0.11	0.12±0.04
Iron (Fe)	38.07±2.29A	-	38.58±0.34A	1.83±0.20B
Manganese (Mn)	1.10±0.01A	0.68±0.01D	1.05±0.01B	0.76±0.01C
Chromium (Cr)	0.29±0.22	0.13±0.04	0.32±0.03	0.20±0.10
Magnesium (Mg)	118.7±2.42C	117.1±1.94C	150.8±0.98B	196.8±1.19A
Calcium (Ca)	729±5.18B	245.9±1.61C	867.5±8.26A	227.1±2.62D
Copper (Cu)	1.04±0.04A	0.65±0.03B	0.96±0.21AB	0.70±0.16B
Sodium (Na)	351.4±1.03D	1584±28.07B	530.2±8.50C	1702±11.15A
Potassium (K)	785.6±4.87D	1114±2.02B	1057±8.21C	1183±11.87A
Aluminium (Al)	1.00±0.02C	0.89±0.11C	4.21±0.08B	16.06±0.08A
Phosphorus (P)	2315±33.77B	108.1±2.66C	4242±87.08A	122.9±1.21C

HAW: Halamid added water, NW: Network water
*The results are presented as Mean±Standard Deviation (SD).
**Capital letters in the same line show significant differences ($p<0.05$)

CONCLUSIONS

In conclusion, the findings of this study provide evidence about the effect of drinking water quality on quail growth performance and its egg quality. Disinfectant addition to water decreases the microbiological load of the drinking water of quails. But, the eggs of the quails provided disinfectant added water had lower egg weight, shell strength and thickness. One of the main results is that the high sodium level of the disinfectant may have decreased production values. However, the eggs of both groups were similar in protein and mineral composition. Besides, in this study it was found out that the quail eggs are good sources of protein and zinc, iron and phosphorus. The quail eggs have a higher Haugh unit and they might be valuable for use in bakery industry.

ACKNOWLEDGEMENTS

This study was approved by Çanakkale Onsekiz Mart University Animal Experiments Local Ethics Committee (approval No: 2017/05-02).

REFERENCES

[1] Carter, T.A., and Sneed R.E. (1996) Drinking water quality for poultry. Published by: North California Cooperative Extension Service. Available From: https://www.bae.ncsu.edu/ extension/ext-publications/water/drinking/pst42-wqg-poultry-sneed.pdf.

[2] Flachowsky, G. (2003) Contributions of agriculture to improve food security and food safety. Fresen. Environ. Bull. 12, 467-489.

[3] Antary, T., Alawi, M., Estityha, H. and Al-Oqlah, K. (2012) Comparison study of chlorinated pesticides in animal products within fourteen years in Jordan. Fresen. Environ. Bull. 21, 117-122.

[4] Fairchild, B.D. and Ritz, C.W. (2015) Poultry drinking water primer. UGA Extension Bulletin. 1301, 6p. Available from: http://extension.uga.edu/publications/files/pdf/B%201301_4.PDF.

[5] Karabayir, A., Ogutcu M. and Arifoglu, N. (2017) Water quality characterization of extensive laying hen farms. Fresen. Environ. Bull. 11, 6687-6692.

[6] Leeson, S., and Summers, J.D. (2009) Commercial poultry nutrition. 3rd ed. Ontario, Canada: Nottingham University Press.

[7] Tunsaringkarn, T., Tungjaroenchai, W. and Siriwong, W. (2013) Nutrient benefits of quail (*Coturnix coturnix japonica*) eggs. Int. J. Sci. Res. 3, 1-8.

[8] Hassan, S., Mady, M., Cartwright, A., Sabri, H. and Mobarak, M. (2003) Effect of acetyl salicylic acid in drinking water on reproductive performance of Japanese quail (*Coturnix coturnix japonica*). Poult. Sci. 82, 1174-1180.

[9] Dincer, E., Karabayir, A. and Mendes, M. (2007) Effects of drinking water differing in dissolved oxygen concentration on growth performance of broiler. Arch. Geflügelkd. 71, 169-174.

[10] Sahin, N., Akdemir, F., Orhan, C., Kucuk, O., Hayirli, A. and Sahin, K. (2008) Lycopene-enriched quail egg as functional food for humans. Food Res. Int. 41, 295-300.

[11] Simsek, U.G., Ciftci, M., Ozcelik, M., Azman, M.A., Tonbak, F. and Ozhan, N. (2015) Effects of cinnamon and rosemary oils on egg production, egg quality, hatchability traits and blood serum mineral contents in laying quails (*Coturnix coturnix japonica*). Vet. J. Ankara Univ. 62, 229-236.

[12] Saki, A., Goudarzi, A.S.M., Ranjbaran, M., Ahmadi, A., Khoramabadi V. (2017) Evaluation of biochemical parameters and productive performance of Japanese quail in response to the replacement of soybean meal with canola meal. Acta Sci. Anim. Sci. 39(1), 51-56.

[13] Amaral, L.A. (2004) Drinking water as a risk factor to poultry health. Rev. Bras. Ciênc. Avíc. 6, 191-199.

[14] Maharjan, P., Clark, T., Kuenzel, C., Foy, M. K. and Watkins S. (2016) On farm monitoring of the impact of water system sanitation on microbial levels in broiler house water supplies. J. Appl. Poultry Res. 25, 266-271.

[15] Kurnaz, E. and Filazi, A. (2011) Determination of metal levels in the muscle and livers of chickens. Fresen. Environ. Bull. 20, 2903-2908.

[16] Trushenski, J.S., and Bowker J.D. (2014) Q&A: Halamid Aqua (Chloramine-T) approved by FDA to treat fish diseases – what it means for fisheries. Fisheries. 39, 378-379.

[17] Rice, E.W., Baird, R.B., Eaton, A.D. and Clesceri L. (2012) Standard methods for the examination of water and wastewater. American Public Health Association, American Water Works Association, Water Environment Federation: Washington, DC.

[18] AOAC (1980) Official methods of analysis. 13th ed. Association of Official Analytical Chemists, Washington, DC.

[19] Xie, L., Hettiarachy, N.S., Ju, Z.Y., Meullenet, J., Wang, H., Slavık, M.F. and Janes, M.E. (2002) Edible film coating to minimize eggshell breakage and reduce post-wash bacterial contamination measured by dye penetration in eggs. J. Food Sci. 67, 280-284.

[20] Minitab. (2000) MINITAB statistical software, release 13 for windows. Minitab Inc. State College, USA.
[21] Scatena, F. (2000) Drinking water quality. In: Dissmeyer, G.E. (ed.) USDA Forest Service Southern Research Station Asheville, North Carolina, 7-25.
[22] Sarin, P., Snoeyink, V., Bebee, J., Jim, K., Beckett, B., Kriven, W. and Clement, J. (2004) Iron release from corroded iron pipes in drinking water distribution systems: effect of dissolved oxygen. Water Res. 38, 1259-1269.
[23] Bagley, C.V., Amacher, J.K. and Poe, K.E. (1997) Analysis of water quality for livestock. AH/Beef. 28, 1.
[24] Barton, T., Hileman, L. and Nelson, T. (1986) A survey of water quality on Arkansas broiler farms and its effect on performance. Proceedings of the 21st Meeting on Poultry Health and Condemnations. University of Arkansas. Fayetteville, AR, 1-33.
[25] Zimmermann, N. and Douglass, L. (1998) A survey of drinking water quality and it's effects on broiler growth performance on Delmarva. Poult. Sci. 77, 1-121.
[26] Safari, A. and Zahedi A. (2016) The effect of different levels supplementation of Glycyrrhiza glabra extract on growth performance in male quail. International Journal of Advanced Biological and Biomedical Research. 4, 214-219.
[27] Korenekova, B., Skalicka, M., Nad, P., Saly, J. and Korenek, M. (2007) Effects of cadmium and zinc on the quality of quail's eggs. Biol. Trace Elem. Res. 116, 103-109.
[28] Skalicka, M., Korenekova, B., Nad, P. and Saly, J. (2008) Influence of chromium and cadmium addition on quality of Japanese quail eggs. Acta Vet. Brno. 77, 503-508.

Received: **21.11.2017**
Accepted: **18.02.2018**

CORRESPONDING AUTHOR

Ali Karabayir
Canakkale Onsekiz Mart University,
Faculty of Agriculture,
Department of Animal Science,
17020, Canakkale – Turkey

e-mail: alikarabayir@comu.edu.tr

© by PSP Volume 27 – No. 5/2018 pages 3059-3067 Fresenius Environmental Bulletin

GROWTH RESPONSE OF URBAN WEEDS IN SINGLE AND MULTI-METAL CONTAMINATED SOIL, CHINA

Kan-kan Shang[1,*], Jie Wang[2], Gilles Vincent[1]

[1]Shanghai Chenshan Plant Science Research Centre, Chinese Academy of Sciences, Shanghai Chenshan Botanical Garden, Shanghai, 201602, China,
[2]Shanghai Key Lab for Urban Ecological Processes and Eco-Restoration, East China Normal University, Shanghai, 200241, China

ABSTRACT

To evaluate the impact of Cu, Zn and Pb on weed communities in urban environments, a field experiment was conducted in soils with high levels of single and multi-metal contamination in Shanghai, China. Soil properties, floristic composition, cover and biomass of the plant community and growth of different ecotypes was studied under contaminated soil as well as control conditions. Results showed that66 plant species belonging to 24 families were present in all plots, 31 species occurring only in spring and 8 in autumn, as well as 27 co-occurring in two seasons. Community composition was generally significantly different among treatments in spring and autumn. There was no significant difference in species richness or diversity between single-metal contamination and control. Presence of heavy metals dramatically impeded the growth of aboveground biomass as well as roots, and resulted in a significant decline in biomass of metal-sensitive species. Multi-contamination (Cu + Zn + Pb) had a strong influence on weeds, as evidenced by a significant decline in species richness, cover and biomass of the community and in growth of metal-sensitive species. A large number of species were eliminated, while metal-tolerant species, mainly grasses, appeared in higher relative dominance in multi-contaminated sites. These findings give new insight for using weeds as a good indicator of complex metal-related stresses.

KEYWORDS:
Field comparative experiment, indicator species, growth response, root morphology, urban pollution

INTRODUCTION

In China, heavy metal contamination in urban soil has become a serious issue, given the rapid pace of industrialization and urbanization over the last three decades. Urban soils are subject to continuous accumulation of organic and inorganic contaminants from either localized or diffuse sources [1-2]. Heavy metals are typical contaminants in urban environments and may originate from many different sources, such as vehicle emissions, energy and fuel production, fertilizer and pesticide application, municipal waste and industrial discharges [3-4]. The most common heavy metal contaminants are: Cr, Cu, Pb, Zn, Ni, Cd and Hg, with concentration higher than 1000mg/kg [4]. All of these persistent metals pose a significant risk to plant, animal and human health[5-6], and their ubiquity has become an urgent health issue in urban ecosystems [4, 7].

Metals are required by plants in a wide range of concentrations. But high concentrations of both essential (e.g. Fe, Mn, Zn, Cu) and nonessential (e.g. Co, Ni, Pb, Cd, Cr, Hg) metals in soil may inhibit growth, decrease biomass, lead to plant death [8-10] and influence plant assemblages [11]. Numerous studies have found that heavy metal-contaminated soil damages root systems directly, with symptoms ranging from disruption of the root cuticle and reduced root hair proliferation, to severe deformation of root structure and impediment of root growth using pot experiments [12-16]. Among the few field studies on the effects of metals on structure and composition of vegetation, many present a certain ambiguity due to mixed contamination as well as wide heterogeneity of soil properties, temperature, moisture and other environmental factors [17-18]. Brown [19] found that heavy metal-tolerant communities can form distinct zones clearly separated from surrounding heavy metal-sensitive vegetation, but that a number of unexamined soil factors exert significant impact on the species compositions of heavy metal-contaminated sites. Babalonaset al. [20] also found that soil conditions played a key role in the development of vegetation patchiness in studies of vegetation on soils with a naturally high content of heavy metals. On the other hand, many uncertainties can be identified when trying to extrapolate effects observed in laboratory experiments to real-world situations in the field, such as coexistence of many pollutants, pH, or thickness of organic layer [21-22]. Therefore, a rigorous, well-defined field study is essential in order to validate laboratory data in actual field situations while maintaining soil conditions relatively uniform except for the type and level of metal contamination [23].

TABLE 1
Mean values of pH, conductivity and metal concentration of the contaminated soil after equilibrium of spiking metal in 2015

Treatments	pH	EC (us/cm)	Cu_{HNO3} (g/kg)	Zn_{HNO3} (g/kg)	Pb_{HNO3} (g/kg)
Control	7.99	207.0	89.3	75.5	20.0
Cu-spiked	8.04	222.5	1128.3	93.3	18.1
Zn-spiked	8.23	191.9	23.7	2453.5	23.3
Pb-spiked	8.15	198.4	18.3	83.7	840.6
3M-spiked	8.03	195.2	521.1	1300.5	1468.4

Weeds play a role as spontaneous vegetation and are highly sensitive to any environmental changes affecting an urban area [24]. Ruderal vegetation will appear distributed in a spatial pattern corresponding to variation of the site's specific attributes, including water conditions, pH, soil structure and associated biotic and abiotic stresses [25]. Certain weed assemblages can also be associated with the presence of anthropogenic metal-contaminated soil [26]. After industrial or mining activities are shut down, brown fields on the sites are often left to revegetate spontaneously [7, 27]. On the other hand, weeds represent a potentially insightful choice for metal accumulation studies, since many are hardy, tolerant, adaptable to harsh conditions, and able to spread over large areas while yielding a considerable amount of biomass [5, 28]. Furthermore, comparative studies of perennial plants indicate that species in stressful environments exhibit traits that might confer stress tolerance (poor competitive ability, low growth rate and delayed reproduction), whereas comparisons of ecotypes within annual species show divergence in traits associated with stress avoidance (rapid development and early reproduction) [29]. The numerous qualities of spontaneously-growing weeds make them good candidates for a study of the effects of heavy metal contamination on community structure and plant growth.

To determine the effects of heavy metals on plant development in situ, an artificial gradient must be created to compare plant growth in different heavy metal-contaminated soils with an uncontaminated control [13]. The objectives of this investigation were to: (i) evaluate the effects of high levels of Cu, Zn and Pb in soil on weeds in an urban environment; (ii) document the growth response of different plant ecotypes under contaminated conditions; and (iii) explore the effects of the interaction of different metals on weed growth.

MATERIALS AND METHODS

Site and experimental design. The Chenshan Botanical Garden (31°04′39″N, 121°11′12″E) in Shanghai, China was selected as an appropriate site for the experimental trial. This site has a subtropical monsoon climate. Its annual average temperature is 17.8 °C and the annual rainfall is 1457.9 mm, with 60% of the rainfall concentrated in the rainy season (May to September). The split-plot experimental design comprised four large, uniform blocks divided into five 10 m × 10 m plots, in which various treatments were applied randomly. These treatments included spiking the soil with salts of different metals (Cu, Zn and Pb- spiked), a treatment containing a mix of the three metals (3M-spiked), and an uncontaminated control (Control). In order to simulate conditions as close as possible to the contamination currently characteristic of urban soil in China [3], appropriate amounts of $CuCl_2$, $ZnCl_2$ and $PbCl_2$, each in the form of a dry powder, were used to spike the soil for each treatment described above. The diverse metal salts were applied on the soil surface of each plot in the fall of 2014, mechanically incorporated into the first 25-30 cm, and left to equilibrate for four months, before initiating study of the weed communities. During the first year (2015) after experiment set-up, weed investigations and measurements were conducted. The concentrations of Cu, Zn and Pb were first measured in April 2015 (Table 1).

Soil sampling and analysis. Soil samples were taken from the 0-30 cm layer in June and September 2015, after equilibrium of metal salts and soil had been reached. In each plot, a composite sample drawn randomly from four sites was evaluated to determine the physicochemical properties. Soil samples were placed in polyethylene bags and brought to the laboratory, then air-dried at room temperature for two weeks. All air-dried soil samples were sieved through a 2-mm nylon sieve to remove coarse debris, and then ground with a mortar and pestle until all particles passed through a 0.149-mm nylon sieve.

Soil pH and electrical conductivity were determined in the supernatants of 1:5 soil and water mixtures using a Hach pH meter (Hach Company, USA) or electrical conductivity instrument (Leici Company, China). Total nitrogen and phosphorus were analyzed using an automatic intermittent analyzer (Smart-Chem) after digestion with H_2SO_4 inglass tubes. Soil organic matter was analyzed using a Vario TOC analyzer (Elementar Company, Germany). Soil bulk density cores were also collected using a 100 cm^3 cylinder from each soil profile,

oven-dried at 105ºC for 24h, and weighed to determine bulk density, soil water content and soil total porosity.

Community composition and biomass estimation. Based on the life history characteristics of vegetation on the site, ruderal species life forms were classified into perennial and annual species, further divided into winter annual and summer annual species [30]. Accordingly, weed investigations were conducted in spring (May to June) and autumn (September) of 2015. In each plot, species were recorded by botanical name in the field or identified subsequently in the Shanghai Chenshan Herbarium (CSH). The maximum height of each species and community was measured. The cover of each species for each plot was estimated on a five-degree Braun-Blanquet scale [31], and total cover of the community was estimated based on the cover of each species. This measurement was derived by comparing the data collected by two researchers during each season, to ensure that all species had been recorded.

Three 0.5 m ×0.5 m sub-plots along the diagonals were selected for collection of above-and belowground biomass in each plot. Fresh biomass was weighed in the field, and then oven-dried to a constant weight at 70ºC in the laboratory.

Common species growth and root morphology. To determine the effect of high levels of heavy metals on plant growth, one species per season (spring, autumn) was chosen for additional investigation: *Chenopodium serotinum* (Chenopodiaceae), with a taproot system, and *Eleusine indica* (Gramineae), with a fibrous root system. These particular species were selected because they were present in almost all twenty plots. Above- and belowground biomass of five individuals of each targeted species per season species was collected. The length as well as live and dry biomass of above- and belowground parts were measured in the laboratory. Aboveground tissues and cleaned roots were oven-dried at 70ºC to constant weight.

The roots of all samples were handled with extreme care during cleaning, oven drying and weighing for keeping the integrity. Root morphology, including total root length, projection area, surface area and diameter, tips and root volume were then measured using special scanner systems (Epson expression 1680 and WinRHIZON).

Data analyses. The relative dominance of each weed species, identity of dominant species and Shannon-Wiener index of diversity were determined according to the method followed by a previous study of the urban weed community in Shanghai [24]. In order to further test for significant differences in community assemblage among sampling sites, a permutational multivariate analysis of variance ('PERMANOVA') was performed. Analyses were based on Bray-Curtis dissimilarity on untransformed data of relative dominance, with 1000 permutations. All variables were analyzed using a one-way ANOVA and a Least Significant Different (LSD) test. For all tests, the classical level of 0.05 was used as p-value threshold. Analyses were performed using SPSS statistical software version 13.0 and Excel (Microsoft Inc.) software packages.

RESULTS

Soil physicochemical properties. Among treatments, bulk density (BD), soil water content (SWC) and soil total porosity (STP) were 1.4-1.5 Mg/m^3, 26.0-32.6 %, and 42.6-48.9%, respectively. Total nitrogen (TN), total phosphorus (TP) and soil organic matter (SOM) were 0.73-1.04g/kg, 0.010-0.022 g/kg and 15.6-17.5 g/kg, respectively. As expected, compared to control, there was no significant difference in physical properties (BD, SWC, STP) or nutrient content (TN, TP, SOM) after addition of heavy metals and mechanical mixing (Table 2).

Effect on community composition and biomass. A botanical inventory of the study site identified 66 species belonging to 24 families, 21 perennials and 45 annual species over the duration of the investigation (Table 3). Twenty-seven species co-occurred in spring and autumn, 31 were present only in spring and 8 in autumn. Community composition was generally significantly different among treatments in spring and autumn (PERMANOVA, $P < 0.05$). Many species common and abundant in the control plot were significantly reduced in abundance and even eliminated in multi-contaminated sites, such as *Acalypha australis*, *Lamium amplexicaule*, *Polypogon fugax*, *Polygonum lapathifolium*, and *Ranunculus japonicas*.

TABLE 2
Soil physicochemical properties under single and multi-contaminated conditions in 2015

Parameters	Control	Cu-spiked	Zn-spiked	Pb-spiked	3M-spiked
BD(Mg/m^3)	1.4±0.1a	1.4±0.1a	1.4±0.1a	1.4±0.2a	1.5±0.1a
SWC (%)	27.5±5.6a	28.0±7.7a	26.0±2.5a	32.6±4.5a	26.3±4.1a
STP (%)	45.3 ±3.9a	46.1±7.4a	43.5±2.1a	48.9±11.6a	42.6±2.7a
TN (g/kg)	0.86±0.49a	0.77±0.04a	0.79±0.71a	0.73±0.58a	1.04±0.83a
TP (g/kg)	0.010±0.005b	0.025±0.005a	0.022±0.010ab	0.022±0.010ab	0.017±0.007ab
SOM (g/kg)	16.5±3.2a	15.6±1.1a	17.1±5.1a	17.5±1.11a	17.3±6.1a

TABLE 3
Floristic composition, life form, and relative dominance of the weed communities under single and multi-contaminated conditions

Latin name	Family	Life form	Spring					Autumn				
			C	Cu	Zn	Pb	3M	C	Cu	Zn	Pb	3M
Setaria viridis	Gramineae	A	**20.8**	**13.4**	**20.6**	**44.8**	**6.0**	**49.8**	**32.9**	14.4	**50.4**	**21.7**
Solidago canadensis	Compositae	P	**8.9**	1.2	2.3	0.7	0.7	**10.4**	**4.7**	1.5	2.4	0.4
Humulus scandens	Moraceae	A	**6.9**	4.3	1.8	3.2	9.7	0.5	0.7	0.5	0.2	0.3
Digitaria sanguinalis	Gramineae	A	5.8	3.7	1.3	0.2	1.0	**13.7**	**6.1**	**22.3**	**12.5**	5.0
Euphorbia humifusa	Euphorbiaceae	A	2.7	0.8	0.4	0.3	1.2	0.2	2.2	0.5	0.2	1.2
Abutilon theophrasti	Malvaceae	A	0.9	1.7	0.4	1.1	2.1	0.1	0.4			
Alternanthera philoxeroides	Amaranthaceae	P	0.7	**37.8**	**35.0**	1.3	**39.3**	0.2	**13.9**	**20.6**	0.1	**24.0**
Cyperus rotundus	Cyperaceae	P	0.5	**5.4**	**7.5**	0.2	**14.4**	0.5	2.2	1.6	3.8	2.0
Cynodon dactylon	Gramineae	P	0.4	2.3	0.3	0.3	**7.2**	<0.1	8.9	6.6	2.5	**13.6**
Echinochloa crusgalli	Gramineae	A	0.4	3.4	**8.1**	0.3	1.6	**8.4**	3.7	2.5	**12.2**	3.5
Calystegia hederacea	Convolvulaceae	P	0.3	0.1	0.2	0.3	2.3	0.3	1.3	0.4	0.1	0.2
Eclipta prostrata	Compositae	A	0.3	0.6	0.7	0.4	1.6	0.7	3.5	4.1	2.2	1.5
Eleusine indica	Gramineae	A	0.2	0.2	1.2	<0.1	2.2	5.2	**6.0**	**16.9**	4.0	**17.4**
Agrimonia pilosa	Rosaceae	P	0.3	0.5	0.1	0.7	0.9	0.4	1.2	0.1	0.3	
Rorippa indica	Cruciferae	A	0.1	0.2	0.3	0.4	0.2			0.1		
Polygonum lapathifolium	Polygonaceae	A	**16.6**	1.5	0.7	8.7		1.2	2.1		0.7	
Acalypha australis	Euphorbiaceae	A	0.6	1.6	0.8	0.4		0.3	1.3	0.4	0.6	
Sonchus oleraceus	Compositae	A	0.3	0.6	0.2		0.3		0.1		0.1	0.4
Artemisia annua	Compositae	A	0.5	0.6		0.2					0.2	
Erigeron annuus	Compositae	A	0.7	1.1		0.2		0.5	1.2			
Polygonum aviculare	Polygonaceae	A	0.1	0.7							0.1	
Polygonum perfoliatum	Polygonaceae	P	0.8		0.5	0.5			0.3			
Phragmites australis	Gramineae	P	0.4		0.3		1.9	0.2		0.6	0.5	2.2
Cirsium setosum	Compositae	P	0.2		0.1	0.2		0.1		0.1	0.1	0.1
Solanum nigrum	Solanaceae	A	0.2		1.4	0.7		0.2		0.2	0.2	
Cayratia japonica	Vitaceae	P	0.1		0.2		0.9		0.7	0.1		2.6
Turczaninowia fastigiata	Compositae	P		1.0		0.2		0.7	1.7		1.0	0.6
Chenopodium serotinum	Chenopodiaceae	A	**11.7**	**10.5**	**9.0**	**32.8**	4.5					
Ranunculus japonicus	Ranunculaceae	A	**9.2**	0.6	0.4	0.2						
Rumex nepalensis	Ranunculaceae	P	0.9	3.6	1.7	0.6						
Aeschynomene indica	Leguminosae	A	0.8	0.4	0.7	0.2						
Lamium amplexicaule	Labiatae	A	1.6	0.8	0	0.4						
Polypogon fugax	Gramineae	A	1.6	0.2	0.4	0.1						
Chenopodium album	Chenopodiaceae	A	3.2		1.7							
Cerastium arvense	Caryophyllaceae	A	0.2		0.1	0.1						
Artemisia argyi	Compositae	P	<0.1		<0.1		<0.1					
Bothriospermum zeylanicum	Boraginaceae	A	0.1									
Galinsoga parviflora	Compositae	A	0.2									
Geranium wilfordii	Geraniaceae	A	0.1									
Elsholtzia ciliata	Labiatae	A	0.2									
Gnaphalium affine	Compositae	A	0.3									
Veronica anagallis-aquatica	Scrophulariaceae	P	0.2									
Kalimeris indica	Compositae	P	<0.1									
Achyranthes bidentata	Amaranthaceae	P	<0.1									
Portulaca oleracea	Portulacaceae	A		0.1	0.5		0.9					
Siegesbeckia orientalis	Compositae	A		0.5	0.2							
Medicago polymorpha	Leguminosae	P		0.2								
Phytolacca acinosa	Phytolaccaceae	P		0.1								
Rumex japonicus	Polygonaceae	P		0.1								
Cardamine hirsuta	Cruciferae	A			0.1							
Coronopus didymus	Cruciferae	A			0.1							
Euphorbia helioscopia	Euphorbiaceae	A			0.1							
Amaranthus tricolor	Amaranthaceae	A			0.6							
Mazus miquelii	Scrophulariaceae	A				<0.1						
Salvia plebeia	Labiatae	A				0.1						
Vicia sepium	Leguminosae	A				0.1						
Galium aparine var. *tenerum*	Rubiaceae	A					0.3					
Myosoton aquaticum	Caryophyllaceae	A					0.7					
Leptochloa chinensis	Gramineae	A						2.9	1.3	0.3	3.2	1.2
Echinochloa colonum	Gramineae	A						1.3	1.1	2.9	1.6	1.1
Sesbania cannabina	Leguminosae	A						0.5	1.2	0.9	0.2	
Setari aglauca	Gramineae	A						0.9	0.4	1.3		
Ixeris japonica	Compositae	P						0.2	0.6			
Echinochloa caudata	Gramineae	A						0.6		1.3	0.8	1
Carpesium abrotanoides	Compositae	P						<0.1				
Youngia japonica	Compositae	A							0.3			

Note: A: annual species, P: perennial species, C: control, Cu: Cu-spiked, Zn: Zn-spiked, Pb: Pb-spiked, 3M: 3M-spiked. Bold character mean the relative dominance value of dominant species in the plot.

This resulted in the decline of species richness, calculated as the number of species per sample plot in metal-contaminated sites, with a significant difference between sub-plots exposed to multi-contamination and other treatments (Table 4). The dominant species under conditions of both single and multi-contamination also varied dramatically in comparison with control. The relative dominance of *Alternanthera philoxeroides* in both seasons, *Cyperus rotundus* in spring and *E. indica* in autumn occurred in Cu, Zn and multi-contaminated sites and increased dramatically. Furthermore, *Setaria viridis* maintained relatively high dominance levels in comparison with control in both seasons, and *Echinochloa crusgalli*, *Leptochloa chinensis* and *Echinochloa colonum* achieved a similar status in autumn. Many species that appeared during the study period were observed only in contaminated sites, but at low frequencies (Table 3); these species included *Portulaca oleracea, Medicago polymorpha, Phytolacca acinosa,* and *Rumex japonicus*. Total plant cover was significantly influenced by contamination. Community cover under multi-contamination in both seasons and Cu contamination in autumn were reduced significantly ($p<0.05$). The one exception was the Pb contaminated site in spring, where community diversity (Shannon-Wiener) showed no significant differences among treatments (Table 4).

Aboveground, root and total plot biomass were significantly influenced by heavy metal contamination in spring and autumn (Figure 1). Biomass in multi-contaminated sites decreased dramatically compared to sites with single contamination. For example, in spring, the total community biomass in Cu, Zn and Pb contaminated sites produced 61.3%, 73.4% and 53.2% of the biomass of the control site, and only 19.5% of control in multi-contaminated sites. The same trends were found for the production of total biomass in autumn, when the community in Cu, Zn and Pb contaminated sites produced 46.8%, 89.9% and 55.4% of biomass found in control, and 42.7% of control in multi-contaminated sites.

Effect on growth of common species. The growth performance of *C. serotinum* and *E. indica* was significantly affected by single and multi-contamination (Figure 2). Compared to control, the length of aboveground biomass and roots of *C. serotinum* was reduced significantly in Cu, Zn single and multi-contaminated sites ($p<0.05$). Aboveground biomass produced in single-contaminated sites reached 65.2%-91.1% of control and only 54.7% of control in multi-contaminated sites. Root biomass produced in single-contaminated sites reached 52.6%-128.2% of control, and only 19.2% of control in multi-contaminated sites. As for *E. indica*, there was no significant difference in length of aboveground biomass or roots between contaminated sites and control. The biomass of aboveground biomass and roots in Cu and Pb contaminated sites decreased significantly in comparison with control ($p<0.05$).

TABLE 4
Effects of heavy metal contamination on species richness, coverage and Shannon-Wiener diversity index

Treatments	Spring			Autumn		
	Number of species	Coverage (%)	Shannon-Wiener index	Number of species	Coverage(%)	Shannon-Wiener index
Control	20.5±2.5a	50.8±5.1a	1.88±0.30a	17.8±2.5a	59.3±8.5a	1.61±0.25ab
Cu-spiked	18.8±2.9a	48.3±8.5a	1.83±0.15a	17.5±1.9a	35.3±4.1b	2.20±0.10a
Zn-spiked	18.5±2.4a	42.5±27.2ab	1.87±0.24a	14.5±3.3ab	42.3±15.4b	1.61±0.54ab
Pb-spiked	19.0±2.9a	40.0±16.3ab	1.19±0.44b	15.5±0.6a	45.5±9.9ab	1.56±0.58b
3M-spiked	11.3±2.9b	23.0±11.2b	1.56±0.65ab	11.8±1.7b	33.3±5.4b	1.60±0.40ab

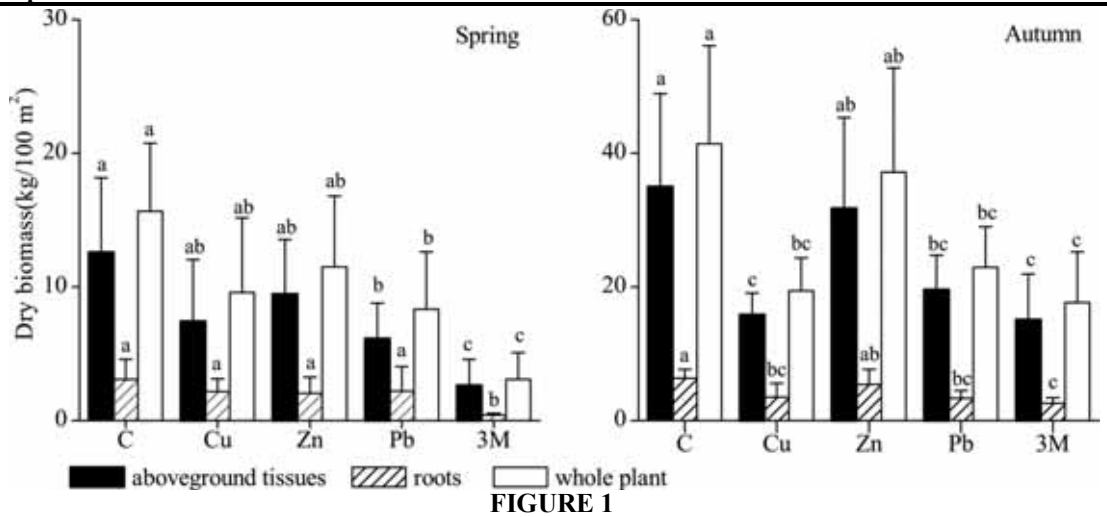


FIGURE 1
Effect of heavy metal contamination on aboveground, roots and total plant biomass of weed community plot. C: control, Cu: Cu-spiked, Zn: Zn-spiked, Pb: Pb-spiked, 3M:3M-spiked, the same as following.

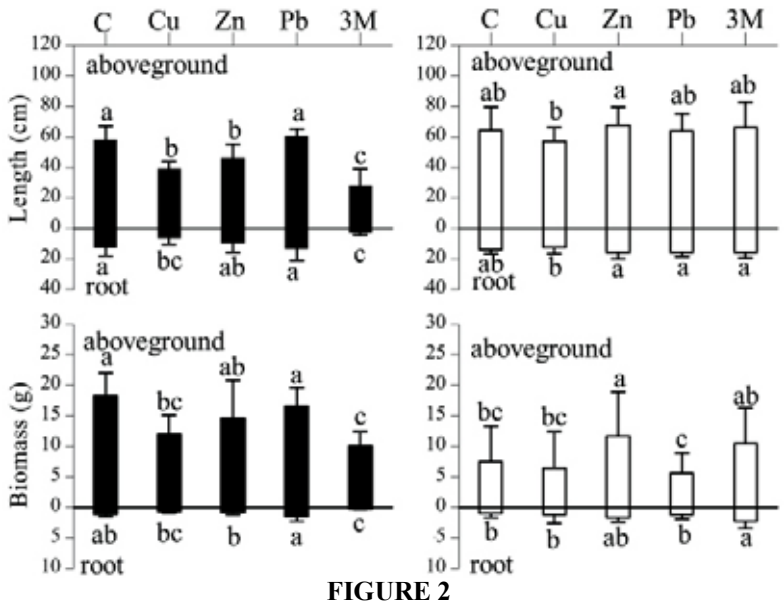


FIGURE 2
Effect of heavy metal contamination on length and biomass for aboveground and roots of *C. serotinum* and *E. indica.* Black: *C. serotinum*in spring, white: *E. indica* in autumn.

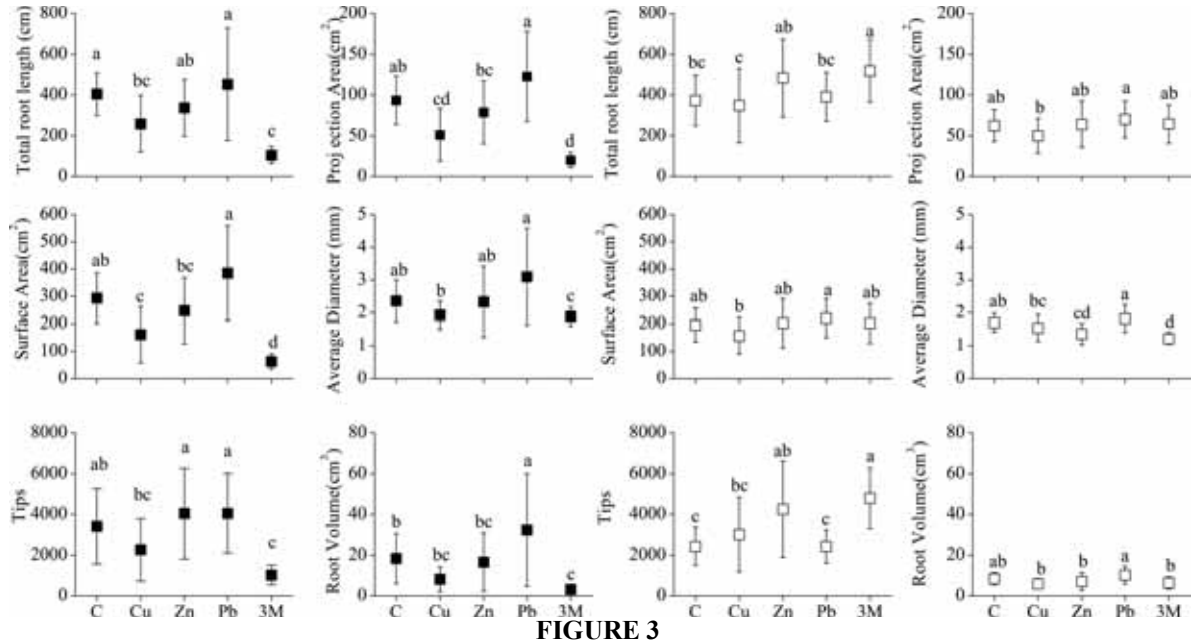


FIGURE 3
Effect of heavy metal contamination on root morphology of *C. serotinum* and *E. indica*. Black: *C. serotinum* in spring, white: *E. indica* in autumn.

Metal contamination had a more serious impact on the root morphology of *C. serotinum* than *E. indica* (Figure 3). Compared to control, total root length, projection area, surface area, average diameter, tips and root volume of *C. serotinum* were reduced significantly in Cu and multi-contaminated sites ($p<0.05$), while declining slightly in Zn and increasing in Pb. In *E. indica*, only average root diameter decreased significantly in multi-contaminated soil ($p<0.05$). Many parameters of root morphology in Zn, Pb and multi-contaminated plots were slightly higher than in control.

DISCUSSION AND CONCLUSION

The effects observed on weeds included alterations (mainly reductions) in floristic composition, cover, species richness, community biomass and growth of common species under contaminated conditions in comparison with uncontaminated plots, and were statistically significant in multi-contaminated plots. These results are consistent with general observations made previously that the presence of heavy metals in soil strongly determines the species composition of plant communities and their growth [12, 21, 23].

Community composition was generally significantly different among treatments in the two seasons. However, there were no significant differences in species richness or diversity between single contamination and control (Table 4). A previous field study on single contamination found that species richness and plant cover generally decreased with increasing contamination by Cu alone [23]. In that study, species richness or dominance of metal-sensitive species decreased, while metal-tolerant species increased under heavy metal contamination. Accordingly, *A. australis*, *L. plexicaule*, *P. fugax*, *P. lapathifolium* and *R. japonicas*, all metal-sensitive species, were eliminated in multi-contaminated sites. It should be noted that the occurrence and distribution of new species in metal-contaminated soils, even at low frequencies, may, in fact, be a function of conditions suitable for propagation, recruitment and stress avoidance, as well as tolerance to physiologically stressful conditions [32]. Moreover, metal-tolerant species, mainly grasses such as *C. rotundus*, *E. indica*, *D. sanguinalis*, *C. dactylon* and *E. crusgalli,* had higher relative dominance, as did the invasive species *A. philoxeroides*, in contaminated sites (Table 3). These species of Gramineae have been recognized as metal-tolerant, and often produce ecotypes that are able to colonize metal-contaminated substrates [13, 32]. Another species belonging to the genus *Alternanthera* had the potential to tolerate and accumulate Cd and Pb, especially at lower metal levels [10]. Members of the Cyperaceae have been known to be highly resistant to petroleum pollution [33]. Thus, the presence of some weeds, especially grasses, could be a good indicator of complex metal-related stresses.

Many authors have reported that heavy metals have an impact on plant growth, particularly root growth [2, 12, 16]. Reduced plant size seems to be characteristic of plants growing in heavy metal-contaminated soils, and may be due to limited root growth, and, consequently, limited water and mineral intake by plants [12, 34-35]. As a metal-sensitive species, the root morphology of *C. serotinum* was influenced significantly by metal contamination, especially in Cu and multi-contaminated sites (Figure 3). These results correlate with the significant decrease in the growth and biomass of *C. serotinum* in spring, and community biomass accumulation over the two seasons (Figure 1, 2). In contrast, *E. indica,* as a metal-tolerant species, was able to alter its root growth pattern and morphology and adapt to the evaluated metal stress (Figure 2, 3). Although total root length, projection area, surface area, average diameter, tips and root volume of *E.indica* increased slightly in comparison with control, none of these indices presented any significant changes in Zn, Pb and multi-contaminated plots (Figure 2). Previous results showed that root length, surface-area and volume of metal-tolerant species increased notably under 1224 μM zinc or 200uM lead +1224μM zinc treatments, whereas in a metal-sensitive species, these parameters decreased significantly [12]. In general, the growth response to contaminated conditions found in this study was obviously different according to plant ecotypes, such as metal-sensitive species *C. serotinum* and metal-tolerant species *E. indica*.

The distribution and growth of weeds and their communities also depends on numerous environmental factors, including metal stress, soil moisture and nutrient conditions, mechanical impediments, as well as temperature and nutrient availability [18, 21, 25]. In this experiment, in compared to control, single contamination had minimal effects on weed distribution and growth, but multi-contamination strongly influenced weeds, as evidenced by species richness, cover and biomass of the community and growth of sensitive species (Tables 3, 4 and Figures 1-3). This can be attributed to heavy metal stress, because there were no changes in soil characteristics among metal treatments (Table 2). Soil metal concentrations above which toxicity was likely were reported, namely 60-125 mg/kg for Cu, 70-400 mg/kg for Zn and 100-400 mg/kg for Pb [11]. The artificial metal content provided as a treatment here was clearly over this threshold (Table 1). Moreover, interactions among metals, including antagonistic, additive and synergistic effects, may have influenced plant growth. Wang et al. observed antagonistic behavior under low concentrations of the combined Cd and Zn treatment, and synergistic behavior under high concentrations of the combined Cd and Zn treatment [15]. Numerous studies conducted as pot experiments have also confirmed that phytotoxic metals in soil may inhibit growth, decrease biomass and even result in the death of plants [8-10]. Together, these effects translated into severe impacts on species richness and floristic composition of the community in this field study. In conclusion, the significant differences in plant response mechanisms between single and multi-contaminated sites in our experiment may be caused primarily by additive interaction of multi-metal phytotoxicity.

ACKNOWLEDGEMENTS

This study received financial support through a grant from the Shanghai Administration Bureau of Landscape and City Appearance (No. G152426) and National Natural Science Foundation of China (No. 31770468). We would like to thank Michel Labrecque and Kun Song for their critical review of the manuscript, Guowei Zhang and XiaoXu Li for their technical assistance, and Karen Grislis for her improvement of English grammar and expression.

REFERENCES

[1] Mahar, A., Wang, P., Ali, A., Awasthi M.K., Lahori, A.H., Wang, Q., Li, R.H., Zhang Z.Q. (2016) Challenges and opportunities in the phytoremediation of heavy metals contaminated soils: A review. Ecotoxicology and Environmental Safety. 126, 111-121.

[2] Nguyen, T.X.T., Amyot, M., Labrecque, M. (2017) Differential effects of plant root systems on nickel, copper and silver bioavailability in contaminated soil. Chemosphere. 168, 131-138.

[3] Wei, B.G., Yang, L.S. (2010) A review of heavy metal contaminations in urban soils, urban road dusts and agricultural soils from China. Microchemical Journal. 94, 99-107.

[4] Cai, M.F., McBride, M.B., Li, K.M. (2016) Bioaccessibility of Ba, Cu, Pb, and Zn in urban garden and orchard soils. Environmental Pollution. 208,145-152.

[5] Liu, Z.L., Chen, W., He, X.Y., Huang, Y.Q., Zhang, Y., Ding, W.H. (2017) Influence of cadmium on growth and antioxidative capacity of *Weigela folorida* 'Red Prince'. Fresen. Environ. Bull. 26, 7137-7141.

[6] Jadia, C.D., Fulekar, M.H. (2009) Phytoremediation of heavy metals: Recent techniques. African Journal of Biotechnology. 8, 921-928.

[7] Desjardins, D., Nissim, W.G., Pitre, F.E., Naud, A., Labrecque, M. (2014) Distribution patterns of spontaneous vegetation and pollution at a former decantation basin in southern Quebec, Canada. Ecological Engineering. 64, 385-390.

[8] Ryser, P., Sauder, W.R. (2006) Effect of heavy-metal-contaminated soil on growth, phenology and biomass turnover of *Hieraciumpiloselloides*. Environmental Pollution. 140, 52-61.

[9] Rai, P.K. (2016) Biodiversity of roadside plants and their response to air pollution in an Indo-Burma hotspot region: implications for urban ecosystem restoration. Journal of Asia-Pacific Biodiversity. 9, 47-55.

[10] Tauqeer, H.M., Ali, S., Rizwan, M., Ali, Q., Saeed, R., Lftikhar, U., Ahmad, R., Farid, M., Abbasi, G.H. (2016) Phytoremediation of heavy metals by *Alternanthera bettzickiana*: Growth and physiological response. Ecotoxicology and Environmental Safety. 126, 138-146.

[11] Séleck, M., Bizoux, J.P., Colinet, G., Faucon, M., Guillaume, A., Meerts, P., Piqueray, J., Mahy G. (2013) Chemical soil factors influencing plant assemblages along copper-cobalt gradients: implications for conservation and restoration. Plant Soil. 373, 455-469.

[12] Lejeune, K., Galbraith, H., Lipton, J., Kapustka, L.A. (1996) Effects of metals and arsenic on riparian communities in southern Montana. Ecotoxicology. 5, 297-312.

[13] Brun, L.A., Corff, J.L., Maillet J. (2003) Effects of elevated soil copper on phenology, growth and reproduction of five ruderal plant species. Environmental Pollution. 122, 161-368.

[14] Orcen, N. (2017) Stomatal parameters and growth responses of nicotiana and *Atriplex* to Cd, Pb and Cd-Pb-contaminated soil. Fresen. Environ. Bull. 26, 6340-6345.

[15] Wang, S.F., Zhao, Y., Guo, J.H., Zhou, L.Y. (2016) Effects of Cd, Cu and Zn on *Ricinus communis* L. Growth in single element or co-contaminated soils: Pot experiments. Ecological Engineering. 90, 347-351.

[16] Muradoglu, F., Encu, T., Gündogdu, M., Canal S.B. (2016) Influence of lead stress on growth, antioxidant enzyme activities and ion changes in root and leaf of strawberry. Fresen. Environ. Bull. 25, 1125-1133.

[17] Clark, R.K., Clark, S.C. (1981) Floristic diversity in relation to soil characteristics in a lead mining complex in the Pennines, England. New Phytology. 87, 799-815.

[18] Becker, T., Brändel, M. (2007) Vegetation-environment relationships in a heavy metal-dry grassland complex. Folia Geobotanica. 42, 11-28

[19] Brown, G. (1994) Soil factors affecting patchiness in community composition of heavy metal-contaminated areas of Western Europe. Vegetatio. 115, 77-90.

[20] Babalonas, D., Mamolos, A.P., Konstantinou, M. (1997) Spatial variation in a grassland on soil rich in heavy metals. Journal of Vegetation Science. 8, 601-604.

[21] Woch, M.W., Kapusta, P., Stefanowicz, A.M. (2016) Variation in dry grassland communities along a heavy metals gradient. Ecotoxicology. 25, 80-90.

[22] Strandberg, B., Axelsen, J.A., Pedersen, M.B., Jensen, J., Attrill M.J. (2006) Effect of a copper gradient on plant community structure. Environmental Toxicology and Chemistry. 25, 743-753.

[23] Gil-Díaz, M., Pinilla, P., Alonso, J., Lobo, M.C. (2017) Viability of a nanoremediation process in single or multi-metal(loid) contaminated soils. Journal of Hazardous Materials. 321, 812-819.

[24] Tian, Z.H., Song, K., Da, L.J. (2015) Distribution patterns and traits of weed communities along an urban-rural gradient under rapid urbanization in Shanghai, China. Weed Biology and Management. 15, 27-41.

[25] Osmond, C.B., Austin, M.P., Berry, J.A., Billings, W.D., Boyer, J.S., Dacey, J.W.H., Nobel, P.S., Smith, S.D., Winner, W.E. (1987) Stress physiology and the distribution of plants. Bioscience. 37, 38-48.

[26] Gallagher, F.J., Pechmann, I., Bogden, J.D., Grabosky, J., Weis, P. (2008) Soil metal concentrations and vegetative assemblage structure in an urban brownfield. Environmental Pollution. 153, 351-361.
[27] Marques, A.P.G.C., Rangel, A.O.S, Castro, S.P.M.L. (2009) Remediation of heavy metal contaminated soils: phytoremediation as a potentially promising clean-up technology. Critical Reviews in Environmental Science and Technology. 39, 622-654.
[28] Minkna, T.M., Mandzhieva, S.S., Chaplygin, V.A., Bauer, T.V., Burachevskaya, M.V., Nevidomskaya, D.G., Sushkova, S.N., Sherstnev, A.K., Zamulina S.I. (2017) Content and distribution of heavy metals in herbaceous plants under the effect of industrial aerosol emissions. Journal of Geochemical Exploration. 174, 113-120.
[29] Stanton, M.L., Roy, B.A., Thiede, D.A. (2000) Evolution in stressful environments. I Phenotypic variability, phenotypic selection, and response to selection in five distinct environmental stresses. Evolution. 54, 93-111.
[30] Chen, X.S., Wang, W.B., Liang, H., Da L.J. (2014) Dynamics of ruderal species diversity under the rapid urbanization over the past half century in Harbin, Northeast China. Urban Ecosystems. 17, 455-472.
[31] Braun-Blanquet, J. (1964) Pfazensoziologie, Grundzüge der vegetationskunde. 3rd edition. Springer-Verlag, Wien, New York.
[32] Ernst, W.H.O. (2006) Evolution of metal tolerance in higher plants. Forest, Snow and Landscape Research. 80, 251-274.
[33] Merkl, N., Schultze-Kraft, R., Infante, C. (2005) Assessment of tropical grasses and Legumes for phytoremediation of petroleum contaminated soils. Water Air and Soil Pollution. 165, 195-209.
[34] Austruy, A., Wanat, N., Moussard, C., Vernay, P., Joussein, E., Ledoigt, G., Hitmi, A. (2013) Physiological impacts of soil pollution and arsenic uptake in three plant species: *Agrostis capillaris*, *Solanum nigrum* and *Vicia faba*. Ecotoxicology and Environmental Safety. 90, 28-34.
[35] Canal, S.B., Bozkurt, M.A. (2017) Effects of iron application against cadmium toxicity on growth and anti-oxidative enzyme activity in lettuce. Fresen. Environ. Bull. 26, 2615-2621.

Received: **22.11.2017**
Accepted: **23.02.2018**

CORRESPONIDING AUTHOR

Kankan Shang
Shanghai Chenshan Plant Science Research Centre,
Chinese Academy of Sciences,
Shanghai Chenshan Botanical Garden,
Shanghai, 201602 – China

e-mail: shangkankan@163.com

© by PSP Volume 27 – No. 5/2018 pages 3068-3074 Fresenius Environmental Bulletin

THE EFFECTS OF DIFFERENT COMBINATION OF COMBINED FERTILIZER DOSES ON SOME AGRONOMIC CHARACTERISTICS OF TURF MIXTURE

Mustafa Yilmaz*

Pamukova Vocational School, Sakarya University, Sakarya, Turkey

ABSTRACT

This study was conducted to determine the effects of different combination of combined fertilizer doses applications on turfgrass characteristics of a turf mixture in Sakarya/Pamukova ecological conditions in Turkey, during 2013-2015 years. The research was conducted in randomized block design with four replications. As a material, a cool season turf mixture consisting of 40% *Lolium perenne* L., cv. Integra, 25% *Festuca rubra rubra* L., cv. Eugene, 20% *Festuca rubra commutata* Gaud., cv. Survivor and 15% *Poa pratensis* L., cv. Evora were used. Nine different combination of NPK fertilizer doses (0-0-0, 5-2.5-2.5, 10-5-5, 15-7.5-7.5, 20-10-10, 25-12.5-12.5, 30-15-15, 35-17.5-17.5 and 40-20-20 g m^{-2} respectively) were applied. At the end of study, shoot growth, creeping yield and dry matter content and yield, root yield and plant growth form (habitus) were determined. At the study, the most promising data were taken from 30-15-15 g m^{-2} fertilizer dose compare to control.

KEYWORDS:
Cool season, turf mixture, fertilizer doses, creeping yield, dry matter yield, root yield, shoot growth.

INTRODUCTION

Turf and turf grasses are the most important botanical elements for safeguarding the environment. Turf areas fill people with contentment through an appeal created by the harmony of green colors and also have lots of benefits such as controlling erosion in roadsides, grazing lands and problematic agricultural areas [1]. However, in order to accomplish all of these functions; the intended plant material's origin, properties, cultivation procedure and techniques of fighting diseases and pests must be identified and selection must be carried out accordingly. Selection of the wrong plant material can cause failure of the project as well as big economic losses [2, 3, 4].

Achievement of quality good enough to fulfill expectations and continuity for a long period of time are factors that are more important than the establishment of turfgrass. For durability of the established turfgrass, first, the correct plant species and mixtures need to be selected in accordance with both the ecological and application purpose. Because it is well known that mixtures perform better than pure sowing. In areas with unstable environmental conditions, using a mixture of various agreeable cultivars rather than just one is more advantageous [2, 3, 5]. After selection of the most suitable plant material for the turfgrass to be established, additional consideration needs to be given to maintenance and restoration activities such as fertilization, irrigation, cutting, weed control, and disease and pest management. The most important prominent in fertilization of turfgrasses is to provide the soil with sufficient nutrients during the period when plants require them the most. For this purpose, turfgrasses should be fertilized with consideration to the last frost date of spring and the first frost date of autumn, according to the ecological conditions in which they were established [2, 3].

Among the macro nutrients, turfgrasses need a) nitrogen; for shoot and root growth, enhancement of shoot frequency and color, and endurance against disease and pests, heat, cold and drought, b) phosphorus; for transfer of secondary nutrients, improvement of root development and regrowth, c) potassium; for boosting growth and development, regulating water intake and continuity, and enhancing endurance against heat and cold [2, 3, 6].

For nitrogen, phosphorus and potassium (NPK), the most essential macro nutrients used in turfgrasses, best results were reported in the doses 25-20-20 by Acikgoz [2], 25-15-15 by Avcioglu [3], 12/90-15-15 by Beard [5], 30-7-20 by Hope [7], 10-30 by Petrovic [8], and Turner and Hummel [9], 25-20-20 by Oral [10], 24-15-15 by Yilmaz [11], 60-90 by Bilgili and Acikgoz [12,13], 50-50-50 by Salman and Avcioglu [14] and 25-15-15 g m^{-2} by Yilmaz et al., [15]. Certain researchers studying turfgrasses and mixtures [16-27] reported different research results with the same doses.

Furthermore, among researchers who studied the topics of shoot height, herbage yield, dry matter content, dry matter yields and root yield; the best in-

dicators of whether plants adapted well to their cultivation area, Klapp [28] 1.200, Jung and Baker [29] 429-523, Fiala [30] 1.400-1.700, Genckan [31] 100-4.500 (mean: 800), Birant [32] 128, Yilmaz [33] 688, Yilmaz and Avcioglu [34] reported a root yield of 315-1.200 g m^{-2}. Tarman [35], on the other hand, stated that root dry matter amounts were approximately 80% of dry herbage yield.

This research was conducted to determine the performance of a quadruple mixture of newly introduced cultivars with different doses of combined fertilizer and to suggest the most suitable dose.

MATERIALS AND METHODS

The research was carried out in the Vocational Training School research areas of the Pamukova district in the Sakarya province, situated in the eastern Marmara region (N 40˚ 30' 20.462, E 30˚ 10' 9.263 and 80 m above sea level).

Climatic data of the research period between November 2013-November 2015 and long term average have been presented in Table 1.

In the first year, precipitation was 596.6 mm, average temperature was 14.7 ˚C and relative humidity was 77.4%, while in the second year these values were 845.5 mm, 14.7 ˚C and 78.0% respectively. In the same order, long term average was 685.9 mm, 14.7 ˚C and 76.9%. This shows that precipitation in the first year was below long term average, but considerably above it in the second year. Average temperatures were the same for both years and with long term average.

Soil samples taken from 0-20 cm depths of the research area were analyzed in the Vocational Training School's laboratory and research area soils were found; clayey-loamy, slightly alkaline (pH: 7.4), saltless (0.024%), medium limy (8.6%), deficient in available phosphorus (10.61 kg ha^{-1}), potassium (190 kg ha^{-1}) and organic substances (0.94%) [6].

Used in the study; a cool-season turf mixture consisting of 40% *Lolium perenne* L., cv. Integra and 20% *Festuca rubra commutata* Gaud, cv. Survivor, (developed by American Pennington Seed), along with 25% *Festuca rubra rubra* L., cv. Eugene and 15% *Poa pratensis* L., cv. Evora, cultivars (developed by Denmark DLF Trifolium Seed). The mixture was sown according to the widely proposed sowing norm for practical applications of 50 g m^{-2} [2, 3].

The research was established on November 1, 2013, observation and measurements were carried out between April 1, 2014 and November 31, 2015; in spring, summer, autumn and winter. Plot sizes were 2×1 m and 1- meter distance were left between plots.

Nine different NPK (Combined) fertilizer doses (0-0-0, 5-2.5-2.5, 10-5-5, 15-7.5-7.5, 20-10-10, 25-12.5-12.5, 30-15-15, 35-17.5-17.5 and 40-20-20 g m^{-2}) were applied in the research. 15-15-15 composed and 26% Ammonium Nitrate fertilizers, recommended for use in fertilization of turfgrasses by Acikgoz [2] and Avcioglu [3], were used. Upon consideration of suggestions by researchers who reported that application of fertilizers needed by turfgrass only once or twice a year was insufficient in meeting expectations [27] and that application intervals needed to be more frequent, [25, 36, 37] annual fertilizer doses were applied between the last frost date of spring (April 21) and the first frost date of autumn (November 5) in 5 equal amounts with 40 day intervals (April 20, June 1, July 10, August 20, September 1). Irrigation was realized via a rotary sprinkler system. Upon reaching heights of 6-10 cm, plants were mown at a height of 4 cm with a gas lawn mower, 18 times per year (spring 6, summer 6, autumn 6 and winter 0).

TABLE 1
The climate dates of Geyve district for 2013-2015 years and Long Term Average (l.t.a.)(*)

	Total precipitation (mm)			Average temperature (ºC)			Relative humidity (%)		
Months	2013-14	2014-15	l.t.a.	2013-14	2014-15	l.t.a.	2013-14	2014-15	l.t.a.
November	29.2	83.2	49.0	10.1	10.1	10.2	83.8	86.6	83.8
December	55.2	101.8	96.5	1.6	8.0	4.3	82.7	91.5	86.6
January	20.8	141.0	94.7	6.7	3.5	4.4	80.7	86.9	84.2
February	11.2	146.6	78.3	7.7	6.6	6.8	76.1	82.2	80.0
March	52.8	48.1	64.4	9.9	8.9	9.1	75.4	78.9	63.8
April	33.0	94.2	57.1	14.3	11.0	13.8	71.6	72.5	70.3
May	66.8	23.4	53.3	18.4	18.7	18.3	73.8	70.4	72.5
June	93.0	48.8	42.8	21.5	20.9	22.2	74.6	76.8	69.6
July	35.0	2.0	10.0	24.7	24.2	24.8	71.0	69.3	65.6
August	9.0	5.2	6.9	25.2	25.7	25.2	70.4	68.0	65.4
September	114.2	66.0	64.5	20.5	23.2	21.3	76.9	73.0	68.4
October	76.4	85.2	68.4	15.6	15.8	15.4	83.2	85.0	78.4
Tot. /Mean	**596.6**	**845.5**	**685.9**	**14.7**	**14.7**	**14.7**	**76.7**	**78.4**	**74.1**

(*): Sakarya Meteorology Directorate Bulletin

TABLE 2
Shoot growth (cm) and green herbage yield (g m^{-2})

N - P - K (g m^{-2})	Shoot growth			Green herbage yield		
	1st year	2nd year	Mean	1st year	2nd year	Mean
0 - 0 - 0	60.5	61.5	61.0	1705	1762	1733
5 - 2.5 - 2.5	84.6	87.3	86.0	2176	2247	2211
10 - 5 - 5	96.4	97.5	97.0	3005	3091	3048
15 - 7.5 - 7.5	108.7	111.5	110.1	3436	3567	3501
20 - 10 - 10	120.6	122.3	121.5	3936	3992	3964
25 - 12.5 - 12.5	132.4	135.4	133.9	4261	4289	4275
30 - 15 - 15	144.6	147.3	146.0	4413	4461	4437
35 - 17.5 - 17.5	146.4	149.7	148.1	4462	4499	4480
40 - 20 - 20	145.2	148.5	146.9	4336	4359	4347
Mean	115.5	117.9	-----	3525	3585	-----
LSD 5%	*F: 2.81*	*Y: 1.68*	*F×Y: 4.75*	*F: 28.11*	*Y: 12.82*	*F×Y: 48.61*

F: Fertilizer combination, Y: Year, F×Y: Interaction.

In this study, the sum of all the measurements taken before each cutting gave shoot development (plant height) values. During cuttings, plot yields were weighed to determine green herbage yield and samples taken from these were weighed again after having been dried at 70 ˚C for 48 hours, then proportioned in order to calculate both dry matter content and dry matter yields. In both years of the experiment, 20×20×20 cm soil samples taken after the last cutting were leached, filtered, then root masses within were dried, weighed and were proportioned to attain yield calculations. Furthermore, root samples were examined and their forms were categorized as fescue, rhizome and stolon.

The experiment was conducted with four replications in the design of randomized blocks, statistical analyses of data were performed using the TOTEMSTAT Statistical Program [38] and LSD values (5%) were stated underneath the Tables.

RESULTS AND DISCUSSION

In statistical analyses carried out with data from the study, statistical differences between years of research were found insignificant. That is why, in the tables, data was not presented yearly, instead the analysis results of mean data obtained from the eight-year research were given.

Shoot growth. Shoot growth values obtained in the study were listed in Table 2.

Second year data were relatively higher than first year. In terms of fertilizer doses, the 35-17.5 - 17.5 dose achieved highest mean value (148.1 cm). In the way of fertilizer × year interaction, highest plant height was obtained from the 35-17.5-17.5 dose in the second year while the lowest value was seen in the control plot in the first year.

Among the cultivars used, *Lolium* had fastest plant growth and longest plant height, while the *Poa* species had slowest plant growth and shortest height. However, it was not possible to determine how much each species in the mixture had grown with measurements carried out before each cutting. For this reason, the highest plant height - not plant species - was taken into consideration in measurements. It is a known fact that frequently cut plants tend constantly to grow in order to develop vegetative parts, while uncut plants tend immediately to produce seeds. Plant height data obtained in this study were higher than heights reached by plants which were purely sown and were never cut [2, 3, 5].

Green herbage yield (Creeping yield). Green herbage yield data obtained in the study were given in Table 2. When examined in terms of years, second year data were found higher than, but close to the values of the first year. This was because data collection did not start immediately after establishment of the experiment before winter; but in spring, when it had fairly improved. Assessment of fertilizer doses and year × fertilizer doses show that, once again, highest mean values were attained from the 35-17.5-17.5 and 30-15-15 doses.

As a whole, data revealed that the lowest number was taken from the control plot in the first year. Total green herbage yield from 18 cuttings was 1705 g m^{-2} and average per cutting was 94.7 g m^{-2}. The highest number was achieved in the 35-17.5-17.5 g m^{-2} dose in the second year with 4499 g m^{-2} and average per cutting was 249.9 g m^{-2}. High green herbage yield is a typical indicator of strong vegetation cover, its durability for a long period of time, and good adaptability to its ecology [2, 3, 5].

Dry matter content and yield. Dry matter content and yield obtained in the study were presented in Table 3.

TABLE 3
Dry matter content (%) and dry matter yield (g m^{-2})

N - P - K (g m^{-2})	Dry matter content			Dry matter yield		
	1st year	2nd year	Mean	1st year	2nd year	Mean
0 - 0 - 0	27.52	27.61	27.57	469	486	478
5 - 2.5 - 2.5	28.66	28.78	28.72	624	647	635
10 - 5 - 5	28.82	28.96	28.89	866	895	881
15 - 7.5 - 7.5	29.11	29.45	29.28	1000	1050	1025
20 - 10 - 10	29.75	29.88	29.82	1171	1193	1182
25 - 12.5 - 12.5	30.15	30.28	30.22	1285	1299	1292
30 - 15 - 15	30.63	31.00	30.82	1352	1383	1367
35 - 17.5 - 17.5	30.46	30.52	30.49	1359	1373	1366
40 - 20 - 20	30.62	30.72	30.67	1328	1339	1333
Mean	**29.52**	**29.69**	**-----**	1041	1064	-----
LSD 5%	*F: 0.11*	*Y: 0.08*	*F×Y: 0.17*	*F: 12.23*	*Y: 6.12*	*F×Y: 24.28*

TABLE 4
Root yield (g m^{-2}) and growth form (Habitus) of mixture

N - P - K (g m^{-2})	Root yield			Growth form (Habitus)	
	1st year	2ndyear	Mean	1st year	2nd year
0 - 0 - 0	356	370	363	Festuca	Fescue+VeryLittleRhizome
5 - 2.5 - 2.5	476	517	496	Fescue+VeryLittle Rhizom	Fescue+Little Rhizome
10 - 5 - 5	689	716	702	Fescue+Little Rhizome	Fescue+Little Rhizome
15 - 7.5 - 7.5	813	856	834	Fescue+Little Rhizome	Fescue+Rhizome
20 - 10 - 10	946	985	965	Fescue+Rhizome	Fescue+Rhizome
25 - 12.5 - 12.5	1043	1085	1064	Fescue+Rhizome	Fescue+ Plenty Rhizome
30 - 15 - 15	1124	1177	1150	Fescue+Plenty Rhizome	Fescue+ Plenty Rhizome
35 - 17.5 - 17.5	1145	1192	1169	Fescue+ Plenty Rhizome	Fescue+ Plenty Rhizome
40 - 20 - 20	1105	1149	1127	Fescue+ Plenty Rhizome	Fescue+ Plenty Rhizome
Mean	**855**	**894**	**-----**		
LSD 5%	*F: 21.1*	*Y: 14.7*	*F×Y:18.5*		

TABLE 5
The ratio of varieties in the mixture (%) and seed counts (Number)[*]

Cultivars	Growth form (Habitus)	The ratio in the mixture (%)	The amount in the mixture (g)	Number of seeds (Per 1 gram)	Total number of seeds in the mixture
L. perenne	Fescue	40	20.0	450-550 (500)	10000
F. r. rubra	Rhizome	25	12,5	1100-1200 (1150)	14375
F. r. commutata	Fescue	20	10.0	1100-1200 (1150)	11500
P. pratensis	Rhizome	15	7.5	4500-5000 (4750)	35625
Total		**100**	**50**	**-----**	**71500**

[*] (Acikgoz, [2]; Avcioglu, [3]; Beard, [5])

Both dry matter content and dry matter yield values were slightly higher in the second year. Assessment of the numbers in terms of fertilizer doses showed that the 30-15-15 dose scored highest in dry matter content (30.82%) and yield (1367 g m^{-2}), while the control plot gave lowest values (27.57% and 478 g m^{-2}). In terms of year × fertilizer dose interactions, highest dry matter content (31.00%) and yield (1383 g m^{-2}) was once again achieved by the 30-15-15 dose. Increase in fertilizer amounts generally enhances the dry matter yield of turf, but is not recommended as it also increases cutting frequency. Therefore, N feed in fertilizer application should be moderate [2, 3, 5, 18]. In the present study, increase in fertilizer doses likewise increased dry matter content.

High green herbage and dry herbage yields of plants are indicators of good adaptation to their ecology [2, 3, 5]. The data obtained revealed that plants in the mixture adapted strongly and quickly to their environment.

Root yield. Root yield values were given in Table 4. Second year was higher than the first in terms of root yield. Highest root yield (1169 g m^{-2}) in the fertilizer doses was obtained from the 35-17.5-17.5 dose, and lowest (363 g m^{-2}) yield was seen in the

control plot. In terms of year × fertilizer dose interaction, highest root yield was achieved from the 35-17.5-17.5 dose (1192 g m^{-2}) in the second year, while lowest yield (356 g m^{-2}) was observed in the control plot in the first year. High root yield showed that plants in the turf mixture adapted strongly to the area and were able to exhibit their true performance. Additionally, the mixture's life form consisting predominantly of rhizomes was a preferred property in terms of covering and holding the soil. Root yields of 356-1192 g m^{-2} obtained in this research were in agreement with 315-1200 g m^{-2} root yields reported by certain researchers [28, 29, 31, 33, 34]. The results were relatively lower than the 1400-1700 g m^{-2} reported by Fiala [30]. They were higher than the data of Birant [32], who studied cool season turfgrasses, which could not show their full performance in Izmir conditions and which achieved a yield of 128 g m^{-2}. Furthermore, data from this study validate Tarman [35], who reported that the root dry matter amounts were approximately 80% of dry herbage yield.

Growth form (Habitus). Habitus created by plants in the samples taken for measurement of root weights were examined at the end of the study and were presented in Table 4.

The mass, which was determined as fescue in the control plot in the first year of the experiment, developed a number of rhizomes the second year, and both with increases in fertilizer doses and with years, the number of rhizomes in the root mass remarkably increased. For a better understanding of this increase, particular characteristics of species' seeds used in the study were given in Table 5.

Among the plants used in the study; *Lolium perenne* and *Festuca rubra commutata* create fescue, while *Festuca rubra rubra* and *Poa pratensis* develop rhizomes [2, 3, 5].

The most important factor affecting mixture rates in mixed sowings is thousand seed weight, which is related to seed size, and hence the number of seeds in 1 gram. In order to equate the number of seeds broadcast to the area, the percentage of coarse-seeded cultivars is kept higher. In this study 50 g m² of seeds were broadcast. Of this amount, 20 grams were (40%) *Lolium perenne*, 12.5 grams were (25%) *Festuca rubra rubra*, 10 grams were (20%) *Festuca rubra commutata* and 7.5 grams were (15%) *Poa pratensis*. Table 5 shows that the two cultivars creating fescue, which constituted 60% of the area (*Lolium perenne* and *Festuca rubra commutata*) had 21.500 seeds in total; whereas the two cultivars which constituted 40% (*Festuca rubra rubra* and *Poa pratensis*) had 50000 seeds in total. Thus, rhizome-predominant turf texture is considered normal.

CONCLUSION

Consideration of the research findings as a whole show that most favorable results were obtained from the 30-15-15 and 35-17.5-17.5 g m^{-2} doses. These doses are in agreement with and support the findings of Petrovic [8], Turner and Hummel [9], Oral [10], Yilmaz et al., [15], Ledeboer and Skogley [16], Sills and Carrow [17], Goatley et al., [19], Garling and Boehm [22], Jiang and Huang [23], Russi et al., [24], Barton and Colmer [26], Walker et al., [27], Yilmaz [33], Yilmaz and Avcioglu [34] and Tarman [35] who carried out studies in regions with similar ecological conditions to the research area. However, the doses were significantly lower than the recommended dose of 60-90 g m^{-2} by Bilgili and Acikgoz [12,13], Engelsjord and Singh [20] and Zhang et al., [21] who conducted research in similar climatic conditions. Bursa is a hotter region and thus required more frequent irrigation, which in turn resulted in greater leaching of plant nutrients and required the use of greater fertilizer amounts. This may explain why their fertilizer doses were higher. Furthermore, application methods and times, as well as the usage of a different fertilizer source may be cited among other reasons. On the other hand, the doses identified as most suitable in this study were lower than the 50-50-50 g m^{-2} doses recommended by Salman and Avcioglu [14] and Birant [32] who conducted research in an ecologically hotter region and sandy-permeable soils. This is because in regions with hot temperatures irrigation is more frequent and due to the sandy nature of soil, irrigation water leaches nutrients away from plants. The need for more water and more plant nutrients increased the amount of fertilizer used.

The values obtained regarding properties studied in the research were within the limits set by Acikgoz [2], Avcioglu [3] and Beard [5] for desirable turfgrass, because plant genera and cultivars included in the mixture were compatible with each other and suitable to the research ecology and sowing-maintenance procedures were carried out according to technique.

Among the properties studied; factors like shoot height, green herbage and root yield do not seem to directly influence turfgrass quality; however, high data pertaining to these properties is important since they show that plants have adapted strongly to the area and were able to fulfill their true potential. The life form of the mixture is expected to consist predominantly of rhizomes and this is a property which is preferred in terms of covering and holding the soil.

The research area ecology was highly suitable for cultivation of cool-season turfgrass. According to long term average data, annual precipitation was 685.9 mm and was distributed evenly to the seasons and months (winter: 269.5, autumn: 181.9, spring: 174.8 and summer: 59.7 mm). The most important

point of consideration here is that the research area received rain in all the seasons and months of the year. Assessment of precipitation from a different perspective shows that the research area respectively received; 87.2-389.4 of rain in winter, 152.6-165.7 in spring, 137.0-56.0 in summer and 273.8-176.0 mm in autumn in the first and second year (Table 1). Additionally, according to long term average data, the research area experiences rain and cool temperatures 128.6 days of the year, and has an average temperature of 14.7 ˚C. It is possible to say that these conditions create a suitable ecological environment for cool-season turfgrass to demonstrate their true performance.

Taking into consideration all the numbers obtained in the study, most favorable data were numerically achieved by the 30-15-15 and 35-17.5-17.5 g m^{-2} doses. Scientifically, environmentally (to prevent soil and water pollution) and economically the 30-15-15 g m^{-2} NPK fertilizer is recommended.

REFERENCES

[1] Tallarino, R. and Argenti, G. (2001) Indagini sull'evoluzione della composizione floristica di pieste da sci inerbite in Val Badia (Studies on the evolution of floristic composition in revegetated ski runs in Val Badia) Italia Forestale Montana. 56, 143-155.

[2] Acikgoz, E. (1994) Turfgrass Establishment and Maintenance Technique. Cevre Ltd. Co. Press 4. 1, Ofset, January 1994, On-Mat Co., Bursa.

[3] Avcioglu, R. (1997) Turf Technique (Turf Establishment & Management). Ege University Press, Izmir, Turkey.

[4] Demiroglu, G., Avcioglu, R. Kır, B. and Salman, A. (2011) Investigations on texture weed invasion and density features of some cool season turf grass cultivars in Mediterranean Environment, Int. Journal of Agriculture & Biology. 13(4), 461-468. ISSN Online:1814-9596.

[5] Beard, J.B. (1973) Turf grass: Science and Culture. Prentice-Hall Inc., Englewood Cliffs, New Jersey.

[6] Brohi, A.R. and Aydeniz, A. (1991) Fertilizers and Fertilization. Cumhuriyet University, Agricultural Faculty Press: 10, Course Book: 3, Tokat, 880p.

[7] Hope, F. (1983) Rasen. Verlag Eugen Ulmer, Stuttgart, Germany.

[8] Petrovic, A.M. (1990) The fate of nitrogenous fertilizers applied to turfgrass. Journal of Environmental Quality. 19, 1-14.

[9] Turner, T.R. and Hummel, N.W. (1992) Nutritional requirements and fertilization, In: Waddington, D.V., Carrow, R.N., Shearman, R.C. (Eds.) Turfgrass, American Society of Agr., Crop Sci. Soc. of America, Soil Sci. Soc. of America, Madison, WI, 385-440.

[10] Oral, N. (1998) The Investigations on the Seed Mixtures, Seeding Rate, N-fertilization in the Turfs Established in Bursa Region. Ph.D. Thesis. Uludag U. Fac. of Agr., Bursa, Turkey.

[11] Yilmaz, M. (2003) Effects on Performances of Turfgrass of Fertilizer Application in Different Dozes in Tokat Ecological Conditions. Gaziosmanpasa University, Journal of the Agricultural Fac. ISSN: 1300-2910, 20(1), 117-122.

[12] Bilgili, U. and Acikgoz, E. (2007) Effect of Nitrogen Fertilization on Quality Characteristics of Four Turf Mixtures Under Different Wear Treatments. Journal of Plant Nutrition. 30, 1139-1152.

[13] Bilgili, U. and Acikgoz, E. (2011) Effects of slow-release fertilizers on turf quality in a turf mixture. Turkish Journal of Field Crops. 16(2), 130-136.

[14] Salman, A. and Avcioglu, R. (2010) Performances of some cool season turf grasses in different fertilizer doses. J. of Faculty of Agri. Ege Univ. Izmir, Turkey, 47(3), 309-319.

[15] Yilmaz, M., Demiroglu, G. Salman, A. and Avcioglu, R. (2011) Determination of some properties of different doses of fertilizers applied in a turfgrass. Turkey 9. Field Crops Congress, 12-15 September 2011, Bursa, 1696-1701.

[16] Ledeboer, F.B. and Skogley, C.R. (1973) Effect of various nitrogen sources, timing, and rates on quality and growth rate of cool-season turfgrasses. Agronomy J. 65, 243-246.

[17] Sills, M.J. and Carrow, R.N. (1983) Turfgrass growth, N use and water use under soil compaction and N fertilization. Agronomy Journal. 75, 488-492.

[18] Bowman, D.C. (2003) Daily vs. periodic nitrogen addition affects growth and tissue nitrogen in perennial ryegrass turf. Crop Science. 43, 631-638.

[19] Goatley, J.M., Maddox, V. Lang, D.V. and Crouse, K.K. (1994) "Tifgreen" Bermudagrass response to late-season application of nitrogen and potassium. Agronomy J. 86, 7-10.

[20] Engelsjord, M.E. and Singh, B.R. (1997) Effects of slow-release fertilizers on growth and on uptake and leaching of nutrients in Kentucky bluegrass turfs established on sand-based root zones. Can. J. Plant Science. 77, 433-444.

[21] Zhang, M., Nyborg, M. and Malhi, S.S. (1998) Comparison of controlled-release nitrogen fertilizers on turfgrass in a moderate temperature area. Hort. Sci. 33, 1203-1206.

[22] Garling, D.C. and Boehm, M.J. (2001) Temporal effects of compost and fertilizer applications on nitrogen fertility of golf course turfgrass. Agro. Jour. 93, 548-555.

[23] Jiang, Y. and Huang, B. (2001) Effects of calcium on physiological responses of tall fescue and Kentucky bluegrass to drought stress. Int. Turfgrass Soc. Res. J. 9, 297-302.
[24] Russi, L., Annicchiarico, P. Martiniello, P. Tomasoni, C. Piano, E. and Veronesi, F. (2004) Turf Quality and Reliability in Varieties of Four Turf grass Species in Contrasting Italian Environments. International Turfgrass Society Res. Jou. 9, 917-921.
[25] Mangiafico, S.S. and Guillard, K. (2006) Fall fertilization timing effects on nitrate leaching and turfgrass color and growth. J. Environ. Quality. 35, 163-171.
[26] Barton, L. and Colmer, T.D. (2006) Irrigation and fertiliser strategies for minimising nitrogen leaching from turfgrass. Agricultural Water Management. 80, 160-175.
[27] Walker, K.S., Bigelow, C.A. Smith, D.R. Van Scoyoc, G.E. and Reicher, Z.J. (2007) Above ground Responses of Cool-Season Lawn Species to Nitrogen Rates and Application Timings. Crop Science. 47, 1225-1236.
[28] Klapp, E. (1971) Wiesen und Weiden. Paul Parey, Berlin und Hamburg, 271p.
[29] Jung, G.A. and Baker, B.S. (1985) Orchardgras. In: Heath, M.E., Barnes, R.F. and Metcalfe, D.S. (Eds.) Forages. Chapter: 24, Iowa State Univ. Press, Ames, Iowa, USA, 224-232.
[30] Fiala, K. (1992) Changes in the Biomass of Living and Dead Roots of Grasslands Due to Anthropogenic Factors. Rostlinna Vyroba. 34(2), 159-168.
[31] Genckan, M.S. (1992) Rehabilitation of Meadow-Range Culture Management. Ege University, Faculty of Agriculture Pub. No: 483, 2nd Edition, Bornova-Izmir, 655p.
[32] Birant, M. (1996) Investigations on the effect of different nitrogen levels on the agronomic and vegetational characteristics of some turfgrasses under Bornova conditions. Ph. D. Thesis. Ege Univ. Fac. of Agr. Izmir, Turkey.
[33] Yilmaz, M. (2000) Investigation on seed yield and turf properties of some grasses grown for turf grass and erosion control purposes in Tokat. Ph.D. Thesis. Ege Univ. Fac. of Agr. Izmir, Turkey.
[34] Yilmaz, M. and Avcioglu, R. (2003) Investigations on Root Growth Performances of Some Cool Season Grasses Grown for Erosion Control and Turfgrass. Journal of the Agricultural Faculty of Gaziosmanpasa University. ISSN: 1300-2910, 20(1), 123-129.
[35] Tarman, O. (1972) Forage crops Meadow and Pasture Culture. Volume I: General Principles. Ankara Univ. Faculty of Agr. Publishing: 464, Course Book: 157, 222p.
[36] Wehner, D.J. and Martin, D.L. (1989) Melamine/urea and oxamide fertilization of Kentucky bluegrass. Communications in Soil Science and Plant Analysis. 20, 1659-1673.
[37] Lawson, D.M. (1996) Fertilizers for Turf: The Sports Turf Research Institute. Bingley, West Yorkshire, England.
[38] Acikgoz, N., Ilker, E. and Gokcol, A. (2004) Assessment of Biological Research on the Computer. Ege University, TOTEM, Izmir.

Received: **23.11.2017**
Accepted: **07.02.2018**

CORRESPONDING AUTHOR

Mustafa Yilmaz
Sakarya University,
Pamukova Vocational School,
Sakarya – Turkey

e-mail: mustafayilmaz@sakarya.edu.tr

© by PSP Volume 27 – No. 5/2018 pages 3075-3080 Fresenius Environmental Bulletin

TOXIC EFFECT OF ATRAZINE HERBICIDE ON THE HEMATOLOGICAL INDICES OF SNOW CARP (*SCHIZOTHORAX PLAGIOSTOMUS*): AN INDIGENOUS FISH SPECIES OF ECONOMIC IMPORTANCE

Farman Ali[1,*], Muhammad Qayash Khan[2], Muhammad Zubair Anjum[3], Irfan Khattak[4]

[1]Department of Agriculture, Abdul Wali Khan University, Mardan, Pakistan.
[2]Department of Zoology, Abdul Wali Khan University, Mardan, Pakistan.
[3]Department of Zoology PMAS-Arid Agriculture University Rawalpindi, Pakistan.
[4]College of Veterinary Science and Animal Husbandry, Abdul Wali Khan University, Mardan, Pakistan

ABSTRACT

The present study was carried out to investigate the toxic effect of atrazine (herbicide) on snow trout (*Schizothorax plagiostomus*), a species of economic importance in Pakistan. The 24, 48 and 72 h LC_{50} of atrazine, calculated by Probit analysis, were found as 110.041, 31.943 and 12.190 mg/l, respectively, using a static renewal bioassay system. Significant decrease was observed in hemoglobin (Hb), Red blood cells (RBCs), Mean corpuscular hemoglobin (MCH), Mean corpuscular hemoglobin concentration (MCHC) and total proteins, while significant elevation was noticed in the White blood cells (WBCs), neutrophil, lymphocytes and Mean corpuscular volume (MCV). The reduced level of hemoglobin and erythrocytes show the anemic condition, while increase in WBCs and other blood parameters indicates the pathological status of *S. plagiostomus*. These results provide the baseline information of atrazine toxicity to *S. plagiostomus* and special concern on its use by agriculture sector, particularly in Pakistan.

KEYWORDS:
Schizothorax plagiostomus, atrazine, toxic effect, hematological indices

INTRODUCTION

The use of herbicide for weed control is a common agricultural practice throughout the world. The extensive use of Atrazine (2-chloro-4-ethylamino-6-isopropylamino-*s*-triazine) herbicide to improve agricultural production has a devastating effect on the non-targeted aquatic flora and fauna. This herbicide is extensively used by farmers for weed control in corn, sorghum, sugarcane, and other agricultural crops of economic importance. Although less toxic to aquatic species, atrazine persists in the environment and is among the most detected pesticides, contaminating rivers, streams, ponds, ground water and reservoirs [1, 2].

Carp fishes have been widely studied for its exposure to toxicants and pollutants [3-5].

Schizothorax plagiostomus is snow carp commonly known as Swati in Khyber Pakhtunkhwa and Gulguli in Punjab, Pakistan. It is widely distributed in the mountain and sub-mountain tributaries of River Indus and has been reported from the northern areas, Khyber Pakhtunkhwa and northern Punjab [6]. The fresh water fish fauna of Pakistan is represented by a minimum of 193 fish species, in which 86-species (8-exotic and 78-indigenous) are of special importance. Among these, the *S. plagiostomus* inhabiting the Indus River and its tributaries is an indigenous fresh water fish species of economic importance, declared vulnerable by IUCN [7, 8].

Several studies on the toxic effect of atrazine on ichthyofauna have proved that the herbicide has variable toxicity; both in respect of fish type exposed and dose concentration. The lethal dose of atrazine in different fish species has been assigned in the range of 30 to 45 mg/L [9, 10]. Rainbow trout (*Onchorhynchus mykiss*) when exposed to different concentrations of atrazine herbicide, had a lethal dose of 1000 µg/L. Hematological parameters are important tool to diagnose the animal health status when exposed to different toxicants. These parameters are considered a reliable diagnostic tools to assess the toxic effect of different toxicants either singly [11] or in combination on fish health [12]. Atrazine herbicide has a significant toxic effect on the hematology of common carp, *Cyprinus carpio* [13]. The toxicity effect of atrazine on the fat oxidation and antioxidant enzyme activity in *Channa punctatus* has also been investigated [14]. A study on the toxic effect of atrazine on Zebra fish concludes that atrazine significantly affects its various stages during embryonic development [15]. On the contrary, atrazine has been reported to have no significant toxic effect on *Pimpephaleus promelas* and *Xenopus laveis* embryos when exposed to different concentrations of atrazine [16]. Atrazine causes histological changes in the fingerlings of *Labeo rohita* [17]. The

effect of different environmental chemicals on various fish species indicates that the bioaccumulations of these chemicals occur in their fatty tissues and are absorbed through fish skin and gills [18]. The median lethal concentration (LC_{50}) is worldwide accepted method for acute toxicity assessment. The LC_{50} of a test chemical kills 50% of the test organisms after definite length of time exposure.

The effect of atrazine herbicide on different fresh water fish species has been assessed, however, no such investigations have been done to assess the toxic effect of atrazine herbicide on the hematological indices of *S. plagiostomus* in Pakistan. Keeping in view the importance of atrazine toxicity to fish fauna and its environmental hazards, the present study was aimed to analyze the effects of various concentrations of the atrazine on some blood biochemical indices of snow trout (*S. plagiostomus*).

MATERIALS AND METHODS

A total of 60 snow trouts, with an average weight of 200.80 ± 10.60 g and a mean length of 18.20 ± 1.20 cm, were captured from Khan Khwar district Shangla by using cast net. The fish were divided into four groups and transferred to the trout race ways settled at Alpuri Trout Hatchery for acclimatization and experimentation. One group was kept as a control and the remaining three groups were exposed to 50, 100 and 150 mg/l of atrazine, respectively for 24, 48 and 72 hours. Herbicide atrazine (brand name Premixrtra) was used to prepare the stock solution according to Gram/volume approach. The amount of herbicide for a proposed exposure experiment was calculated and dissolved in a specific volume of river water to prepare a stock solution. Then according to planned herbicide concentration, specific volume of stock solution was poured into the race ways. Since *S. plagiostomus* is a phytophagous fish, which feeds on algae attached to pebbles and stones, therefore, riverine pebbles with attached algae were collected from the bed of Khan Khwar adjacent to the Trout Hatchery Complex for feeding to the fish. Blood sampling was done at 24, 48 and 72 hours interval by using 2mm heparinized syringe to puncture the caudal peduncle. Five fish were made to bleed at each sampling time and the blood was transferred to the laboratory in EDTA added vials.

Probit analysis for determination of the 24, 48 and 72 hours LC_{50} values, and Multiple Analysis of Variance (MANOVA) were carried out using the statistical package for social sciences (SPSS) version 20 [19].

RESULTS

Table 1 shows the physico-chemical characteristics of the test water. The water temperature ranged between 21.2–22.1 ^{0}C and the pH varied from 7.0–7.5. The conductivity was found in the range of 200–220 µm/cm, while the concentration of dissolved oxygen varied between 10.2–11.2 mg/l throughout the experiment. The total hardness of test water remained in the range of 207–211 mg/l during the entire experiment.

TABLE 1
Physico-chemical properties of test water with minimum and maximum range

Parameters	Unit	Mean	Range
Water temperature	^{0}C	21.48	21.2–22.1
pH	-	7.3	7–7.5
Dissolved oxygen	mg·L^{-1}	10.68	10.2–11.2
Conductivity	µMcm^{-1}	208.8	200–220
Total hardness	mg·L^{-1}	209	207–211

Fish behavior and toxicity symptoms. The imbalance and erratic behavior of fish subjected to different concentrations of atrazine herbicide was observed throughout the experiment. The early response of fish showed alertness and restlessness, and thereafter the fish stopped swimming and remained static in vertical position. After some time the static specimens again started fast swimming and restlessness with suffocation. The specimens exposed to the high concentration of atrazine herbicides, swam erratically and their fins became hard and stretched. The increased opercula movement, gulping for air at surface and choking of gills with copious amount of thick mucus were observed. The fish lost their balance with rolling movement and became lethargic. Finally, they ceased the movement and sank to the bottom with their bellies turned upward and died.

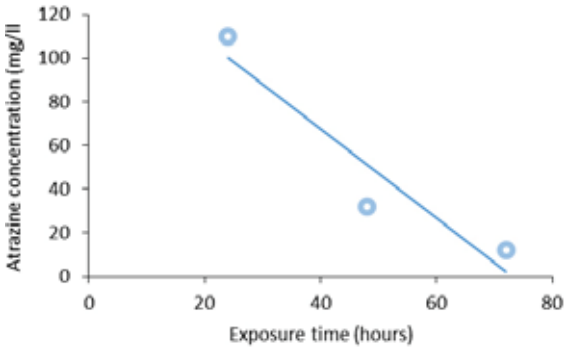
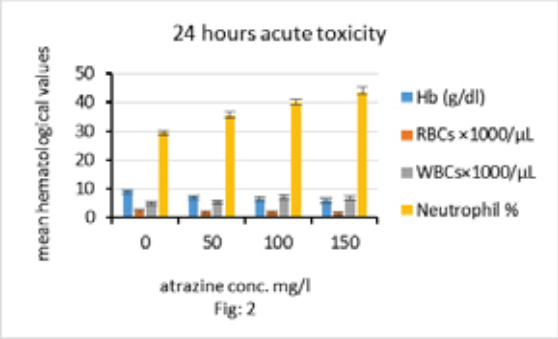
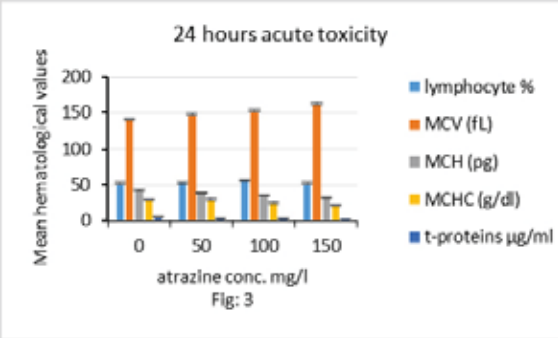


FIGURE 1
Increase in fish mortality is associated with the increases in exposure time and concentrations (r2 = 0.894).

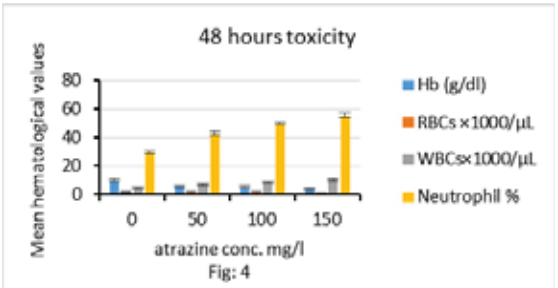
Estimation of LC_{50}. The LC_{50} values (with 95% confidence limits) of different concentrations of atrazine (Fig. 2) were found to be 110.041, 31.943 and 12.19 mg·L^{-1} for 24, 48 and 72 h respectively. Dose and time dependent increase was observed in

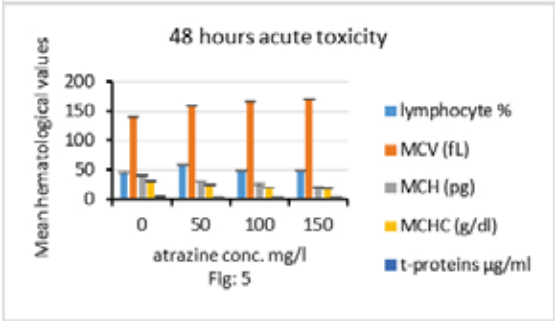
mortality rates. A direct proportional relationship between fish mortality and atrazine concentration was observed. The regression value calculated was 0.894. No mortality was found in the control group throughout the experiment.





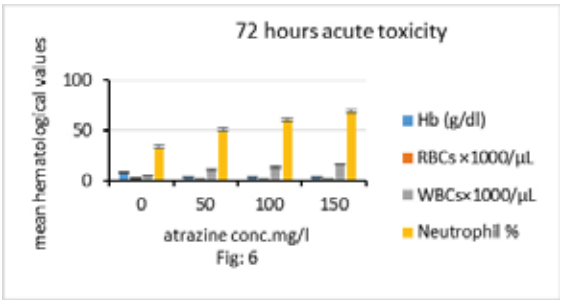
FIGURES 2 & 3
Changes observed in the hematological values of *S. plagiostomus* after 24-hours exposure to different concentrations of atrazine herbicide.

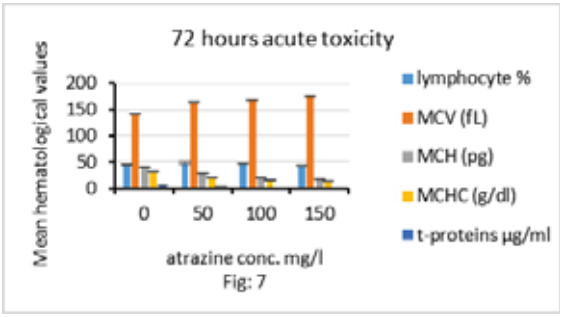




FIGURES 4 & 5
Changes observed in the hematological values of *S. plagiostomus* after 48-hours exposure to different concentrations of atrazine ±SE

The mean values of hematological parameters of control and test specimens exposed to 50, 100 and 150 mg/l of atrazine herbicide for 24, 48 and 72 hours respectively, are shown in table 2 and figures 2 to 6. Compared to control group, RBCs, HB, MCH, MCHC and total proteins were found to show significant decline, whereas neutrophil and MCV exhibited overall increase in all treatment groups. The lymphocyte count was found to exhibit minor fluctuations in all groups.





FIGURES 6 & 7
Changes observed in the hematological values of *S. plagiostomus* after 72-hours exposure to different concentrations of atrazine.

DISCUSSION

In the present study, the comparison of control group with that of treated ones clearly showed a marked decline in Hb, RBCs, MCH, MCHC and total proteins, while other blood parameters including MCV and WBCs were elevated significantly at the end of the experimental period in atrazine treated specimens of *S. plagiostomus* (Table 2).

Similar declining pattern in Hb, RBCs, MCH, MCHC and total proteins in different fish species was reported earlier by Ramesh *et al.* [13] and Hanke and Gluth [20] following subjection to different concentrations of atrazine herbicide. From the present findings, it is proposed that hematopoietic tissue get affected by atrazine causing low release of RBCs into blood circulation. Significant reduction in blood protein serum in the present study is supported by a previous study [21] where they reported that increased energy demand might increase protein consumption, a process where proteins are metabolized to provide energy, and therefore the protein serum

TABLE 2
Mean values of hematological parameters recorded for *Schizothorax plagiostomus* in response to different concentrations of atrazine for 24, 48 and 72 hours exposure.

Exposure hours	Parameters	Atrazine dose (mg/l±SE)			
		Control	50	100	150
24	Hb	9.4 ±0.2	7.4 ±0.3	6.6 ±0.4	6.3 ±0.3
	RBCs	2.7 ±0.1	2.3 ±0.2	2 ±0.2	1.7 ±0.1
	WBCs	5.2 ±0.4	5.6 ±0.3	7.5 ±0.5	7 ±0.6
	Neutrophil	29.5 ±0.6	35.8 ±0.9	40.2 ±0.9	43.5 ±1.9
	Lymphocytes	51.9 ±2.3	52.7 ±2	56.3 ±1.2	52.4 ±1.7
	MCV	140.6 ±2	147.7 ±1.5	153 ±1.6	162.5 ±1.8
	MCH	43.1 ±1.1	38.7 ±0.5	35.5 ±1	32 ±1.8
	MCHC	30 ±0.6	30 ±1.2	25.1 ±1.3	20.9 ±0.8
	Total proteins	5.4 ±0.2	4.7 ±0.3	4±0.2	3.3 ±0.1
48	Hb	10.2 ±0.6	5.9 ±0.3	5.4 ±0.6	4.5 ±0.4
	RBCs	2.5 ±0.2	2.0 ±0.3	1.8 ±0.2	1.6 ±0.3
	WBCs	5 ±0.4	7.3 ±0.7	8.8 ±0.4	10.5 ±0.2
	Neutrophil	29.7 ±1.3	42.5 ±2.1	50.0 ±1.3	55.3 ±2.3
	Lymphocytes	45.1 ±2.2	58.9 ±1.1	48.9 ±1.1	47.7 ±1.1
	MCV	139.8 ±1.5	158.0 ±1.3	165.7 ±1.1	170.8 ±1.0
	MCH	40.4 ±1	29.8 ±0.5	25.3 ±1.6	20.1 ±1.9
	MCHC	30.6 ±0.6	25.0 ±1.2	19.9 ±0.7	19.0 ±0.8
	Total proteins	5.1 ±0.2	3.5 ±0.2	3.0 ±0.1	2.8 ±0.1
72	Hb	8.0 ±0.2	3.8 ±0.3	3.4 ±0.4	3.5 ±0.5
	RBCs	2.8 ±0.2	1.3 ±0.2	1.1 ±0.1	1.4 ±0.2
	WBCs	5.1 ±0.4	11.0 ±0.5	13.2 ±0.7	16.0 ±0.8
	Neutrophil	33.1 ±2.2	50.4 ±2.8	60.1 ±2.0	68.6 ±2.4
	Lymphocytes	45.2 ±1.2	48.3 ±2.0	48.4 ±0.7	43.8 ±1.0
	MCV	140.5 ±0.9	162.9 ±1.6	167.5 ±1.3	174.7 ±1.2
	MCH	40.8 ±1.7	29.6 ±1.4	20.9 ±1.1	17.0 ±1.2
	MCHC	32.4 ±1.3	20.2 ±0.4	16.7 ±0.3	13.6 ±0.8
	Total proteins	5.6 ±0.2	2.7 ±0.2	1.6 ±0.2	0.8 ±0.1

reduces [21]. Hussein et al. [22] have assessed the atrazine effect on *Oreochromis niloticu* and *Chrysichthyes auratus* and concluded that total protein decline in the blood plasma of these fishes was due to globulin reduction which have indicated the suppression of fish immune system. The probable reason of total protein decline in the blood plasma of *S. plagiostomus* may be due to toxic effect of atrazine on the kidneys, spleen and liver [22].

Significant increase in MCV as clearly depicted in Table 2 in all treated groups during this study, is supported by previous study [23], which has shown that increase in MCV values is a clear reflection of reduction in TEC values because MCV and TEC have an inverse relationship with each other. Significant decline of Hb, MCH and MCHC in all treated groups in the present study contradict the finding of Jyoti Sharma and Seema Langer [23], where they found that increased level in MCH and MCHC inversely affect the hemoglobin level in *Gara gotyla gotyla* in response to Manganese metal toxicity [23].

It is understood that WBCs play a key role in animal defense mechanism. WBCs consist of granulocytes (basophils, neutrophils and eosinophils) and a-granulocytes (monocytes and lymphocytes). In the present study, lymphocytes exhibited minor fluctuations, while significant increase was found in neutrophil in all treatment groups in response to atrazine herbicide.

CONCLUSION

The findings of this study suggest that atrazine has strong effect on the blood biochemical indices of *S. plagiostomus*, which are dose and time dependent. Therefore, it is recommended that the use of the herbicide atrazine should be avoided or be used at a minimum level by the farmers, particularly in those areas where agricultural land has a close proximity with the natural water resources inhabiting the population of *S. plagiostomus*.

REFERENCES

[1] Battaglin, W.A., Thurman, E.M., Kalkhoff, S.J., Porter, S.D. (2003) Herbicides and transformation products in surface waters of the midwestern United States. Journal of the American Water Resources Association. 39, 743-756.

[2] Scribner, E.A., Thurman, E., Goolsby, D.A., Meyer, M.T., Battaglin, W.A., Kolpin, D.W. (2005) Summary of significant results from studies of triazine herbicides and their degradation products in surface water, ground water, and precipitation in the midwestern United States during the 1990s. U.S. Geological Survey.

[3] Mutlu, E. (2016) The effects of lead-induced toxicity on metabolic biomarkers in common carp (C*yprinus carpio* l.). Fresen. Environ. Bull. 25, 1420-1428.

[4] Du, J-L., Cao, L-P., Jia, R., Yin, G-J. (2016) The protection of glycyrrhiza polysaccharide on 2, 3, 7, 8-tetrachlorodibenzo-p-dioxin induced Jian carp (*Cyprinus carpio* var. jian) liver injury using precision-cut liver slices. Fresen. Environ. Bull. 25, 1997-2007.

[5] Mutlu, E., Demir, T., Kutlu, B. (2015) A comparative study on the effects of lead and zeolite on serum biochemistry of carp fish, *Cyprinus Carpio Linnaeus*, 1758 (Cyprinidae). Fresen. Environ. Bull. 24, 4390-4396.

[6] Mirza, M.R. (2006) A note on the fishes of Allai Khoar, NWFP, Pakistan. Punjab Univ J Zool. 21, 73-75.

[7] Rafiq, M. (2007) Biosystematics and distribution of the freshwater fishes of Pakistan with special reference to the subfamilies Noemacheilinae and Schizothoracinae: PhD thesis. PMAS-Arid Agriculture University. Rawalpindi.

[8] Rafique, M., Khan, N. (2012) Distribution and status of significant freshwater fishes of Pakistan. Records: Zool Surv Pakistan. 21, 90-95.

[9] Elia, A.C., Waller, W.T., Norton, S.J. (2002) Biochemical responses of bluegill sunfish (*Lepomis macrochirus*, Rafinesque) to atrazine induced oxidative stress. Bull. Env. Contam. Toxicol. 68, 809-816.

[10] Aaronson, M.J., Kirby, K.W., Tessari, J.D. (1980) Identification and confirmation of atrazine in pond water. Bull Env. Contam. Toxicol. 25, 492-497.

[11] Jezierska, B., Witeska, M. (2001) Metal toxicity to fish. Monografie University of Podlasie (Poland).

[12] Vosylienė, M.Z., Kazlauskienė, N., Svecevičius, G. (2003) Effect of a heavy metal model mixture on biological parameters of rainbow trout *oncorhynchus mykiss*. Env. Sci. Pollut. Res.10, 103-107.

[13] Ramesh, M., Srinivasan, R., Saravanan, M. (2009) Effect of atrazine (Herbicide) on blood parameters of common carp *Cyprinus carpio* (Actinopterygii: Cypriniformes). Afr. J. Env. Sci. Technol. 3, 453-458.

[14] Nwani, C.D., Lakra, W.S., Nagpure, N.S., Kumar, R., Kushwaha, B., Srivastava, S.K. (2010) Toxicity of the Herbicide Atrazine: Effects on Lipid Peroxidation and Activities of Antioxidant Enzymes in the Freshwater Fish *Channa punctatus* (Bloch). Int. J. Env. Res Public Health. 7, 3298-3312.

[15] Wiegand, C., Krause, E., Steinberg, C., Pflugmacher, S. (2001) Toxicokinetics of atrazine in embryos of the zebrafish (*Danio rerio).* Ecotoxicol Environ Saf. 49, 199-205.

[16] Scahill, J.L. (2008) Effects of atrazine on embryonic development of fathead minnows (*Pimephales promelas*) and *Xenopus laevis*. Bios. 79, 139-149.

[17] Jayachandran, K., Pugazhendy, K. (2009) Histopathological changes in the gill of *Labeo rohita* (Hamilton) fingerlings exposed to atrazine. American-Eurasian Journal of Scientific Research. 4, 219-221.

[18] Ortiz, J.B., de Canales García, M.L.G., Reiriz, M.C.S. (2003) Histopathological changes induced by lindane (g-hch) in various organs of fishes. Scientia Marina. 67, 53-61.

[19] SPSS, I. (2011) IBM SPSS statistics for Windows, version 20.0. New York: IBM Corp.

[20] Gluth, G., Hanke, W. (1985) A comparison of physiological changes in carp, *Cyprinus carpio*, induced by several pollutants at sublethal concentrations. I. The dependency on exposure time. Ecotoxicol. Environ. Saf. 9, 179-188.

[21] Das, P.C., Ayyappan, S., Jena, J., Das, B. (2004) Acute toxicity of ammonia and its sub-lethal effects on selected haematological and enzymatic parameters of mrigal, *Cirrhinus mrigala* (Hamilton). Aquaculture Research. 35, 134-143.

[22] Hussein, S., El-Nasser, M., Ahmed, S. (1996) Comparative studies on the effects of herbicide atrazine on freshwater fish *Oreochromis niloticus* and *Chrysichthyes auratus* at Assiut, Egypt. Bull. envir. contam. Toxicol. 57, 503-510.

[23] Sharma, J., Langer, S. (2014) Effect of manganese on haematological parameters of fish, *Garra gotyla gotyla*. J. Entomol. Zool. Stud. 2, 77-81.

Received: **24.11.2017**
Accepted: **23.02.2018**

CORRESPONDING AUTHOR

Farman Ali
Department of Agriculture,
Abdul Wali Khan University
Mardan, 23200 – Pakistan

e-mail: drfarman@gmail.com

© by PSP Volume 27 – No. 5/2018 pages 3081-3086 Fresenius Environmental Bulletin

INFLUENCE OF DIFFERENT PRIMING MATERIALS ON GERMINATION OF SORGHUM HYBRIDS (*SORGHUM BICOLOR* L. MOENCH. X *SORGHUM SUDANENSE* STAPH.) SEEDS

Negar Ebrahim Pour Mokhtari[1,*], Hasan Yavuz Emeklier[2]

[1]Gaziantep University, Islahiye Vocational School, Organic Farming Department, Gaziantep, Turkey
[2] Department of Field Crops, Ankara University, Ankara, Turkey

ABSTRACT

Maximum germination percentage achieves immediately after harvesting and gradually decreases with storage time. Seed aging is the main problem of seed storage. Seed priming enhances seed germination performance after aging and able to promote rapid and more uniform seed germination and plant growth. The purpose of this Communication is to compare the efficacy of different seed priming osmotica on the germination of aged and unaged hybrid silaj sorghum seed. Sugar Grazer II and Digestivo hybrid silage sorghum cultivars were used as the plant material. As the priming material, 5 different chemicals (8 mg/L putrescine, 2 mg/L jasmonic acid, 100 mg/L kinetin, 50 mg/L KNO_3 and 4.5 mg/L salicylic acid) were applied to aged and unaged seeds. Under laboratory conditions, the greatest first count germination (98.00%) was obtained from jasmonic acid treated aged Sugar Grazer II seeds and the greatest first count germination in Digestivo cultivar (98.00%) was obtained from KNO_3 treated unaged seeds. The greatest germination percentage (97.33%) was obtained from jasmonic acid-treated aged Sugar Grazer II.

KEYWORDS:
Accelerated Aging, Germination, Priming, Seed, Sorghum.

INTRODUCTION

Seed quality can have a profound influence on the establishment and the yield of a crop. Maximum germination percentage achieves after harvesting and gradually decreases with storage time. Seed aging is the main problem of seed storage [17]. The priming is a technical that reduces the effects of aging by reducing Malondialdehyde (MDA) and free radicals production and maintenance antioxidant activities [2]. In priming, seeds are soaked in different solutions with high osmotic potential. This prevents the seeds from absorbing in enough water for radicle protrusion, thus suspending the seeds in the lag phase [20]. Primed seeds pass phases imbibition and lag phase of germination and are ready for germination in the base of physiological and biochemical conditions Increasing in the rate of seed germination has been associated with the initiation of germination related processes [19], repair processes [18] restores the initial germinative ability, reduces the level of lipid peroxidation and increase in various free radical scavenging enzymes [1]. For example in seed treatment with salicylic acid, treatment was accompanied by a transient increase in the H_2O_2 level [23]. It seems possible that salicylic acid may exert its protective effect partially through the transiently increased level of H_2O_2. Polyamines including spermidine, putrescine and spermine are able to play act as regulators in various fundamental cellular processes such as cell division, proliferation, cell death, DNA and protein synthesis [9, 6]. Xu [25] revealed that tobacco (*Nicotiana tabacum* L.) seed priming with putrescine improved germination percentages, germination index, seedling length and dry weight in comparison with controls. Another plant growth regulator is Cytokinins. They can also be used as priming agent; Iqbal [10] showed that application of CK at 100 or 200 mg L^{-1} increased the germination rate and early seedling growth of wheat when compared with hydropriming treatment. Methyl jasmonate (MeJA) collectively referred to as jasmonates, are important cellular regulators involved in diverse developmental processes, such as seed germination, tuber formation, tendril coiling, root growth and fertility [24]. There are many reports showing that MeJA inhibits germination of seeds in angiosperms, such as sunflower [7], tobacco [16]. Seed priming treatments using salts such as potassium nitrate (KNO_3) have been effective in improving germination under improper conditions. Mohammadi [15] found that among the priming treatments, primed seeds with potassium nitrate showed the highest values for all traits and priming with KNO_3 than control, increased germination percentage, germination rate and seedling dry weight by 28.3, 129.4 and 58.1 percentage, respectively. Kattimani [11] indi-

cated that primed seeds with nitrate solutions produced vigorous seedlings, more dry matter accumulation and root length in compared with non-primed seeds.

Sorghum seeds generally lose their biological characteristics in a short time. Such a case then influence plant genetic characteristics and storage conditions. Sorghum seeds generally have 1000-seed weights of between 12-40 g and they need quite well-prepared seed beds for production. Therefore, when the sowing was not made in mellowed soils in a shallow fashion, germination and emergence rates will be quite low. On the other hand, since seed vigor is lost rapidly, sorghum seeds should be preserved under quite well conditions. Therefore, this study was conducted under laboratory conditions to investigate the effects of different priming chemicals on aged and unaged seeds of two hybrid sorghum cultivars (Sugar Grazer II and Digestivo).

MATERIALS AND METHODS

Experiments were conducted under laboratory conditions. Aged and unaged seeds of Sugar Grazer II and Digestivo hybrid silage sorghum (*Sorghum bicolor* L. Moench. x *Sorghum sudanense* Staph.) cultivars were used as the seed material of the experiments. Five different chemicals (8 mg/L putrescine, 2 mg/L jasmonic acid, 100 mg/L kinetin, 50 mg/L KNO_3 and 4.5 mg/L salicylic acid) were used for priming treatments. A control treatment without priming was also included into the experiments. For laboratory experiments, seeds were prepared for each treatment at the end of priming process. Germinated seeds were counted on forth and tenth day. Seedling root length and fresh weights were also measured at the end of tenth day. Fresh seedlings were dried in an oven at 70℃ for 48 hours. Dried samples were cooled in a desiccator and weighted in a precise balance to get seedling dry weights.

Accelerated aging test. For aging, seeds were placed in plastic boxes and supplemented with distilled water to provide high relative humidity. Seeds were placed in a single layer over the wire section of the box as not to touch each other. Aging boxes were placed in zip lock bags to prevent moisture loss and they were aged in an oven previously heated to 42°C at 100% relative humidity and dark for 24 hours. Following the aging procedure, aged seeds were placed in jars, closed with stretch film and kept in a fridge at 5°C for 24 hours to have the seed moisture balanced [26]. Experiments were conducted in 3 replications. Experimental results were subjected to variance analyses with Jump statistical software in accordance with Randomized Blocks Factorial Experimental Design. Significant differences were tested with F test and means were grouped with Duncan test.

TABLE 1
Effects of seed priming treatments on first count germination (%), Germination percentage (%), seedling root lengths, seedling fresh weight and seedling dry weight of aged and unaged seeds of sorghum cultivars*

	Seed aging	Priming	First count germination	Germination percentage (%)	Seedling root lengths	Seedling fresh weight	Seedling dry weight
		Putrescine	90.33 d	91.66 c	15.08 a	0.21 b	0.023 c
	Aged	Jasmonic acid	98.00 a	97.33 a	14.34 b	0.13 d	0.023 c
Sugar		Kinetin	96.00 b	92.33 b	10.33 d	0.09 e	0.018 d
Graze II		KNO_3	92.33 c	92.66 b	13.56 c	0.18 c	0.030 a
		Salicylic acid	87.66 e	91.66 c	15.09 a	0.25 a	0.027 b
		Control	84.00 f	87.66 d	9.87 e	0.08 f	0.014 e
		Putrescine	94.00 b	95.00 b	11.39 d	0.15 d	0.018 d
	Unaged	Jasmonic acid	95.00 a	95.66 a	14.05 a	0.22 a	0.023 a
		Kinetin	86.33 d	90.33 e	11.00 e	0.08 f	0.014 e
		KNO_3	93.66 b	94.33 c	12.26 c	0.18 c	0.022 b
		Salicylic acid	88.00 c	91.66 d	13.34 b	0.20 b	0.021 c
		Control	86.33 d	87.66 f	10.03 f	0.09 e	0.014 e
		Putrescine	93.66 a	93.33 b	14.87 c	0.33 b	0.034 a
	Aged	Jasmonic acid	90.33 d	90.00 d	16.19 a	0.31 c	0.034 a
Digestivo		Kinetin	90.00 d	91.33 c	10.86 e	0.14 e	0.023 c
		KNO_3	92.66 b	93.00 b	12.33 d	0.40 a	0.033 b
		Salicylic acid	91.66 c	95.00 a	15.77 b	0.27 d	0.034 a
		Control	89.00 e	89.00 e	9.71 f	0.10 f	0.017 d
		Putrescine	92.00 d	92.00 c	16.26 b	0.41 a	0.031 c
	Unaged	Jasmonic acid	93.33 c	93.00 b	16.62 a	0.34 b	0.027 d
		Kinetin	97.00 b	96.33 a	10.61 d	0.09 e	0.021 e
		KNO_3	98.00 a	92.33 c	16.08 b	0.19 d	0.032 b
		Salicylic acid	93.66 c	96.66 a	15.58 c	0.31 c	0.034 a
		Control	83.00 e	86.66 d	9.84 e	0.08 f	0.017 f

* Letters indicate different groups at 0.01 level.

First count germination. According to the Table 1, seed priming treatments had significant effects on first count germination of two different sorghum hybrids ($p<0.01$). First count germination (%) of unaged Sugar Grazer II seeds varied between 86.33-95.00% with the greatest value from jasmonic acid-primed seeds and the lowest value from the control seeds. Kinetin-primed seeds were also placed in the same statistical group with the control seeds. First count germination (%) of aged Sugar Grazer II seeds varied between 84.00 - 98.00% with the greatest value from jasmonic acid-primed seeds and the lowest value from the control seeds. First count germination (%) of unaged Digestivo seeds varied between 83.00 - 98.00% with the greatest value from KNO_3-primed seeds and the lowest value from the control seeds. First count germination (%) of aged Digestivo seeds varied between 89.00 - 93.66% with the greatest value from putrescine primed seeds and the lowest value from the control seeds. When the first count germination responses of aged and unaged seeds to different chemical under laboratory conditions were compared, it was observed that aged and unaged Sugar Grazer II seeds had the greatest first count germination (%) with jasmonic acid priming. Exogenous jasmonate treatments supported morphological and physiological changes and yielded the greatest first count germination Unaged Digestivo seeds had the greatest first count germination with KNO_3 priming and aged seeds with putrescine priming. Because of the changes observed in seed compounds with aging procedures, seeds had different responses to different chemicals, thus yielded different results. The different responses of different cultivars were because of physiological characteristics of the seeds and it was an expected case. Present findings about the effects of putrescine treatments on germination (%) comply with the findings of Tekin and Bozcuk [21] reported for sunflower and findings of Çavuşoğlu [5] reported for barley; present findings for KNO_3 treatments comply with the results of Madakadze [13] for switch grass, results of Büyükçıngıl [3] for grain sorghum; findings for jasmonic acid treatments comply with the findings of Tiryaki [22] reported for sorghum.

Germination percentage (%). As can be seen in Table 1, seed priming treatments had significant effects on germination percentage of two different sorghum hybrids ($p<0.01$). Germination percentage of unaged Sugar Grazer II seeds varied between 87.66 - 95.66% with the greatest value from jasmonic acid-primed seeds and the lowest value from the control seeds. Germination percentage of aged Sugar Grazer II seeds varied between 87.66 - 97.33% with the greatest value from jasmonic acid-primed seeds and the lowest value from the control seeds. Germination percentage of unaged Digestivo seeds varied between 86.66 - 96.66% with the greatest value from salicylic acid-primed seeds and the lowest value from the control seeds. With regard to the greatest germination power, salicylic acid and kinetin-primed seeds were placed into the same statistical group. Germination percentage of aged Digestivo seeds varied between 89.00 - 95.00% with the greatest value from salicylic acid-primed seeds and the lowest value from the control seeds. When the germination power responses of aged and unaged seeds to different chemicals under laboratory conditions were compared, it was observed that aged and unaged Sugar Grazer II seeds had the greatest germination percentage with jasmonic acid priming. Exogenous jasmonic acid treatments supported morphological and physiological changes and yielded the greatest germination powers. Unaged and aged Digestivo seeds had the greatest germination percentage with salicylic acid priming treatments. Present findings on germination power comply with the results of Büyükçıngıl [3] reporting positive effects of jasmonic acid and salicylic acid treatments on germination power of sorghum seeds and with the findings of Çanakçı [4] reporting positive effects of salicylic acid treatments on barley seeds.

Seedling root length. Table 1, reperesent, seed priming treatments had significant effects on seedling root lengths of two different sorghum hybrids ($p<0.01$). Seedling root lengths of unaged Sugar Grazer II seeds varied between 10.03 -14.05 cm with the greatest value from jasmonic acid-primed seeds and the lowest value from the control seeds. Seedling root lengths of aged Sugar Grazer II seeds varied between 9.87 - 15.09 cm with the greatest value from salicylic acid-primed seeds and the lowest value from the control seeds. However, with regard to the greatest root length, salicylic acid-primed seeds and putrescine-primed seeds were placed in the same statistical group. Seedling root lengths of unaged Digestivo seeds varied between 9.84 - 16.62 cm with the greatest value from jasmonic acid-primed seeds and the lowest value from the control seeds. Seedling root lengths of aged Digestivo seeds varied between 9.71 - 16.19 cm with the greatest value from again jasmonic acid-primed seeds and the lowest value from the control seeds. When the responds of aged and unaged seeds to different chemicals were compared with regard to seedling root lengths under laboratory conditions, it was observed that unaged seeds of Sugar Grazer II and both the aged and unaged seeds of Digestivo cultivar yielded the greatest seedling root lengths with jasmonic acid priming. Aged seeds of Sugar Grazer II yielded the greatest seedling root lengths with salicylic acid priming. Aged and unaged seeds of the same cultivars may have different responses against different chemicals. Present findings on seedling root lengths and posi-

tive effects of jasmonic acid treatments on seedling root lengths comply with the findings of Büyükcıngıl [3] for grain sorghum; positive impacts of salicylic acid treatments on seedling root lengths comply with the findings of Çanakçı [4] for barley.

Seedling fresh weight. Table 1 order, seed priming treatments had significant effects on seedling fresh weights of two different sorghum hybrids ($p<0.01$). Seedling fresh weights of unaged Sugar Grazer II seeds varied between 0.08 - 0.22 g with the greatest value from jasmonic acid-primed seeds and the lowest value from kinetin-primed seeds. Seedling fresh weight of aged Sugar Grazer II seeds varied between 0.08 - 0.25 g with the greatest value from salicylic acid-primed seeds and the lowest value from the control seeds. Seedling fresh weights of unaged Digestivo seeds varied between 0.08 - 0.41 g with the greatest value from putrescine-primed seeds and the lowest value from the control seeds. Seedling fresh weight of aged Digestivo seeds varied between 0.10 - 0.40 g with the greatest value from KNO_3-primed seeds and the lowest value from the control seeds. Considering the seedling fresh weights of both cultivars based on seed aging and priming treatments, it was observed that unaged Sugar Grazer II seeds had the greatest seedling fresh weights with jasmonic acid priming and aged seeds with salicylic acid priming. When the seedling fresh weights of Digestivo cultivar were compared with the values of Sugar Grazer II, it was observed that unaged Digestivo seeds had higher seedling fresh weights with putrescine priming and aged seeds with KNO_3 priming. Aging results in changes in seed compounds thus aged and unaged seeds had different values and this was an expected case. Present dings about the effects of putrescine treatments on seedling fresh weights comply with the findings of Tekin and Bozcuk [21] reported for sunflower seeds; findings on jasmonic acid treatments were similar with the results of Büyükçıngıl [3] reported for sorghum seeds. Positive impacts of salicylic acid treatments on seedling fresh weights of the present study also comply with the findings of Khodary [12] and Çanakçı [4]. Present findings about the positive effects of KNO_3 treatments on seedling fresh weights comply with the findings of Büyükçıngıl [3] reported for grain sorghum.

Seedling dry weight. As can be seen in Table 1, seed priming treatments had significant effects on seedling dry weights of two different sorghum hybrids ($p<0.05$). Seedling dry weights of unaged Sugar Grazer II seeds varied between 0.014 - 0.023 g with the greatest value from jasmonic acid-primed seeds and the lowest value from kinetin-primed seeds. However, control seeds and kinetin-primed seeds were placed in the same statistical group. Seedling dry weights of aged Sugar Grazer II seeds varied between 0.014 - 0.030 g with the greatest value from KNO_3-primed seeds and the lowest value from the control seeds. Seedling dry weights of unaged Digestivo seeds varied between 0.017 - 0.034 g with the greatest value from salicylic acid-primed seeds and the lowest value from the control seeds. Seedling fresh weight of aged Digestivo seeds varied between 0.017-0.034 g with the greatest values from putrescine, jasmonic acid and salicylic acid-primed primed seeds and the lowest value from the control seeds. With regard to the greatest seedling dry weights, KNO_3-pirmed seeds were placed in the same statistical group with putrescine, jasmonic acid and salicylic acid-primed seeds (Table 1). When the seedling fresh weight responses of aged and unaged seeds to different chemicals under laboratory conditions were compared, it was observed that unaged Sugar Grazer II seeds had the greatest seedling dry weights with jasmonic acid priming and aged seeds with KNO_3 priming. The greatest seedling dry weights of unaged Digestivo seeds were obtained from salicylic acid treatments and the greatest values of aged seeds was obtained from putrescine, jasmonic acid and salicylic acid treatments. Aging causes various changes in seed bioactive compounds and such changes then result in different responses. Thus aged and unaged seeds had different values as it was expected. Present findings about the positive effects of salicylic acid treatments on seedling dry weights comply with the findings of Mendoza [14] for peppers, findings of Khodary [12] for maize and findings of Çanakçı [4] for barley seeds. Current findings on KNO_3 treatments comply with the findings of Erdoğan [8] reported for Iskenderiye trefoil. Findings about the positive effects of jasmonic acid treatments on seedling dry weights comply with the findings of Büyükçıngıl [3] reported for sorghum seeds. Considering the laboratory experiments, it was observed that reactions on chemicals used as priming activator on aged and unaged seeds were different. Present findings revealed that jasmonic acid-priming yielded better outcomes. Priming processes may yield different outcomes in different cultivars. It is possible to mention that priming chemicals could be successful in stimulation activation of seed vigor.

REFERENCES

[1] Bailly, C., Benamar, A., Corbineau, F. and Côme, D. (1998) Free radical scavenging as affected by accelerated ageing and subsequent priming in sunflower seeds. Physiol Plant. 104, 646-652.

[2] Basra, S.M.A., Ahmad, N., Khan, M.M., Iqbal, N. and Cheema, M.A. (2003) Assessment of cotton seed deterioration during accelerate. Seed Sci Technol. 31,531-540.

[3] Büyükçıngıl, Y. (2007) Priming Uygulamasının Sorgum (*Sorghum bicolor* L. Moench) Tohumlarının Düşük Sıcaklıktaki Çimlenme Ve Çıkış Performansı Üzerine Etkileri. KSÜ, Fen Bilimleri Enistitüsü, Tarla Bitkileri Ana Bilim Dalı. Master Thesis. 56p.

[4] Çanakçı, S. (2010) Arpa (*Hordeum vulgare* L.) tohumlarının çimlenmesi, çeşitli büyüme parametreleri ve pigment miktarları üzerine salisilik asit ve ferulik asit'in etkileri. Fırat Üniversitesi Fen Bilimleri Enstitüsü Dergisi. 22 (1), 37-45.

[5] Çavuşoğlu, K., Kılıç, S. and Kabar, K. (2007) Arpa tohumlarının çimlenmesi sırasında gibberalik asit, kinetin ve etilen ile tuz stresinin hafifletilende bazı morfolojik ve anatomik gözlemler. SDÜ Fen Edebiyat Fak. Fen Dergisi (E-Dergi). 2(1), 27-40.

[6] Childs, A., Mehta, D., Gerner, E. (2003) Polyamine-dependent gene expression. Cell Mol. Life Sci. 60,1394-1406.

[7] Corbineau, F., Rudnicki, R.M. Come, D. (1988) The effects of methyl jasmonate on sunflower (*Helianthus annuus* L.) seed germination and seedling development. Plant Growth Regul. 7, 157-169.

[8] Erdoğan, G. (2008) Değişik kimyasal uygulamalarinin farkl iskenderiye üçgülü (*Trifolium alexandrinum* L.) çeşidi tohularının düşük sıcaklıkdaki çimlenme ve çıkış performansları üzerine etkileri. Master Thesis. Kahramanmaraş Sütçü İmam Üniversitesi, Kahramanmaraş, 60p.

[9] Igarashi, K, Kashiwagi, K. (2000) Polyamines: mysterious modulators of cellular functions. Biochem. Bioph. Res. Co. 271, 559-564.

[10] Iqbal, M., Ashraf, M. (2006) Wheat seed priming in relation to salt tolerance: growth, yield and levels of free salicylic acid and polyamines. Ann. Bot. Fenn. 43, 250-259.

[11] Kattimani, K.N., Reddy, Y.N. and Rajeswar Rao, B. (1999) Effect of pre-sowing seed treatment on germination, seedling emergence, seedling vigoure and root yield of Ashwagandha (Withania somnifera Daunal.). Seed Science Technology. 27, 483-488.

[12] Khodary, S.E.A. (2004) Effect of salicylic acid on the growth, photosynthesis and carbohydrate metabolism in salt-stressed maize plants. International Journal of Agriculture and Biology 6, 5-8.

[13] Madakadze, I.C., Prithiviraj, B., Madakadze, R.M., Stewart, K., Peterson, P., Coulman, B.E., and Smith, D.L. (2000) Effect of preplant seed conditioning treatment on the germination of switchgrass (*Panicum virgatum* L.). Seed Sci. & Technol. 28, 403-411.

[14] Mendoza, A.B., Rodriguez, H.R., Torres, V.R., Davila, J.H., Mezquitic, J.G.R., Tellez, E.B., Rangel A.S. and Garcia, M.A.B. (2002) Seed Treatment with Salicylates Modifies Stomatal Distrubution, Stomatal Density, and The Tolerance to Cold Stress in Pepper Seedlings. Proceedings of the 16th International Pepper Conference Tampico, Tamaulipas, Mexico, November 10-12.

[15] Mohammadi, G.R. (2009) The effect of seed priming on plant traits of late-spring seeded soybean (*Glycine max* L.). American-Eurasian Journal of Agriculture & Environmental Science. 5 (3), 322-326.

[16] Preston, C.A., Betts, H. and Baldwin, I.T. (2002) Methyl jasmonate as an allelopathic agent: sagebrush inhibits germination of a neighboring tobacco, *Nicotiana attenuata.* J. Chem. Ecol. 28, 2343 2369.

[17] Sveinsdottir, H., Yan, F., Zhu, Y., Peiter, T. and Schubert, S. (2009) Seed ageing-induced inhibition of germination and post-germination root growth is related to lower activity of plasma membrane H(+) ATPase in maize roots. J. Plant Physiol. 166(2), 128-135.

[18] Sivritepe, H.O. and Dourado, A.M. (1995) The effect of priming treatments on the viability and accumulation of chromosomal damage in aged pea seeds. Ann. Bot. 75,165-171.

[19] Soeda, Y., Konings, M.C.J.M., Vorst, O., van Houwelingen, A.M.M.L., Stoopen, G.M., Maliepaard, C.A., Kodde, J., Bino, R.J., Groot, S.P.C. and van der Geest, A.H.M (2005) Gene expression programs during *Brassica oleracea* seed maturation, osmopriming, and germination are indicators of progression of the germination process and the stress tolerance level. Plant Physiol. 137, 354368.

[20] Taylor, A.G., Allen, P.S., Bennett, M.A., Bradford, K.J., Burrisand, J.S. and Misra, M.K. (1998) Seed enhancements. Seed Sci. Res. 8, 245-256.

[21] Tekin, F. and Bozcuk, S. (1998) Effects of Salt and Exogenous Putrescine on Seed Germination and Early Seedling Growth of *Helianthus annuus* L. var. Santafe. Turkish Journal of Biology. 22(3), 331-340.

[22] Tiryaki, I., Korkmaz, A., Ozbay, N. and Nas, M.N. (2005) Effect of Priming Supplemented with Plant Growth Regulators on Sorghum (*Sorghum bicolor* L. Moench) Seed Germination and Seedling Emergence at Low Temperature. Türkiye VI. Tarla Bitkileri Kongresi, Antalya.

[23] Wahid, A., Perveen, M., Gelani, S., Basra, S.M.A (2007) Pretreatment of seed with H_2O_2 improves salt tolerance of wheat seedlings by alleviation of oxidative damage and expression of stress proteins. J Plant Physiol. 164, 283-294.

[24] Wasternack, C. (2007) An update on biosynthesis, signal transduction and action in plant stress response, growth and development. Annals of Botany. 100, 681– 697.
[25] Xu, S., Hu, J., Li, Y., Ma, W., Zheng, Y. and Zhu, S. (2011) Chilling tolerance in *Nicotiana tabacum* induced by seed priming with putrescine. Plant Growth Regul. 63, 279-290.
[26] Zamani, A., Sadat Nouri, S.A. Tavakol Afshar, R. Iran Nezhad, H. Akbari G.A. and Tavakoli, A. (2010) Lipid Peroxidation and Antioxidant Enzymes Activity under Natural and Accelerated Aging in Safflower (*Carthamus tinctorius* L.) Seed. Iranian Journal of Field Crop Science. 41(3), 545-554.

Received: **24.11.2017**
Accepted: **30.01.2018**

CORRESPONDING AUTHOR

Negar Ebrahim Pour Mokhtari
Gaziantep University,
Islahiye Vocational School,
Organic Farming Department,
Gaziantep – Turkey

e-mail: n_mokhtary@yahoo.com

© by PSP Volume 27 – No. 5/2018 pages 3087-3093 Fresenius Environmental Bulletin

DETERMINATION OF YIELD PERFORMANCE OF EARLY AND MAIN SEASON POTATO COMMERCIAL CANDIDATE VARIETIES

Ercan Ozkaynak*, Yasemin Orhan, Tugba Simsek

Yüksel Tohum, Kurşunlu Mah. Madenler Sok. No: 12/A, Antalya, Turkey

ABSTRACT

In this research, about 115.000 potato seeds from different genetic backgrounds obtained and evaluated 2008 to 2015 for developing new varieties. At the end of 9 years potato breeding program 7 advanced potato lines (The early season: 12-03-85, 12-55-07, 12-55-16, 12-69-39; main season: 12-68-05, 13-67-25 and 22-99-33) submitted for registration as commercial varieties. The aim at the research compared to performance of early and main season commercial candidate potato varieties with commercial varieties for agronomic, tuber and quality traits. 7 commercial candidate potato variety tested in 4 replicated trials in four potato regions of Turkey (For the early season, Adana and İzmir; for the main season, Antalya and Niğde). As a result, 4 of seven candidate commercial varieties determined as a suitable for French fries, chips and fresh potato market. In the first step, these 7 commercial candidate varieties will be using large-scale in Turkey, after that these varieties can use other countries such as Morocco, Pakistan, Azerbaijan and other Turkic Republics, South Korea, etc.

KEYWORDS:
Domestic, French fries, potato breeding, tuber yield

INTRODUCTION

Potato breeding is based on a phenotypic and genotyping selection scheme that cycle every 6 to 10 years (50 traits including quality and yield). Potato varieties are developed by crossing hundreds of genotypes in breeding programmes. After crossing, large populations of F1 seedlings are generally grown for visual selection. A single tuber is usually taken from each F1 plant selected for planting in the next season. During the next two to three seasons, clones are cultivated and screened for further evaluations and propagated to increase the number of seed tubers. After a number of years, superior clones are tested in replicated trials in different locations to estimate the genotype x environment interaction [1].

Although, last ten years important advances in molecular breeding provide opportunities for rapid genetic gain [2], yet the use of molecular approaches requires quantitative genetic analysis of the highly heterozygous breeding populations for development of the complex quality and yield traits with low heritability. Thus, phenotypic selection in potato still remains the common practice in breeding programmes.

Potato production in Turkey totally depends on foreign varieties, which are mainly from European countries such as Netherlands, France etc. It is thought that dependency of seed production system on imported seed as well as limited research and development efforts are main reasons for the situation. Currently, there are about 190 registered potato cultivars in the 'national variety' list and ten of them was bred via crossing in Turkey. These Turkish varieties has never had a change in commercial production because last 3-4 years old new varieties. However, only 25 to 30% demand for high quality and certified seed is supplied. The remaining demand is obtained either from stocked harvested small seeds by the growers, or from uncertified seed tubers sold at local markets [3, 4, 5]. There is a need to improve high yield, high quality and good adaptation ability new potato varieties for Turkey. In Turkey, generally tubers planted in beginning of January to middle of June planting season in Mediterranean and Aegean region (early season). Early season potato production was about 20% of total potato production. In main season, potato production was made long season 15th April to end of October. This study was conducted to determine to performance of agronomic, tuber, yield and quality traits of new superior potato candidate varieties for early season and main season growing conditions in Turkey.

MATERIALS AND METHODS

Plant material and experiment. Tetraploid cross populations including European varieties, exotic cultivars and local genotypes were used as parents for developing new varieties in the breeding programme. Approximately 115.000 seeds from dif-

ferent genetic backgrounds were obtained and evaluated between 2008 and 2015. The experiments were carried out during two periods (early season: January-June); medium and late season: May-October) in the experimental regions of Adana, İzmir, Antalya and Niğde in 2015. Early season field experiments were conducted at commercial fields of Adana and Izmir (Ödemiş) in the West-Mediterranean region of Turkey (January-June season). Medium-late season experiments were carried out in highlands of Antalya (Korkuteli) and Niğde. Five commercial potato varieties (Orkestra (mid early, ware potato), Marabel (early, retail fresh), Musica (mid early, retail fresh), Florice (mid early, retail fresh), Safrane (mid early, ware potato) and four candidate varieties (12-03-85 (early), 12-55-07 (early-mid early), (12-55-07 (mid early) and 12-69-39 (mid early) were used as a material in the present early season study. In main season experiment; Marabel (early, retail fresh), Agria (mid early-late, retail fresh -processing potato), Madeline (mid early, retail fresh), Melody (mid early, retail fresh), Granola (late, retail fresh) commercial varieties and three candidate varieties (12-68-05 (mid early), 13-67-25, mid early) and 22-99-33 (early-mid early) were used as material.

Cultural Practices, measured traits and statistical analysis. Potato commercial varieties and candidate varieties were planted, spaced 30 cm apart in ridges and 70 cm wide, in field conditions. Fertilizer was broadcast at 60/80 kg ha^{-1} N, 40/50 kg ha^{-1} P_2O_5 and 80/100 kg ha^{-1} K_2O in different experiment fields and locations. Weeds were controlled by hand after emergence. Disease control and irrigation was carried out according to practice. Except tuber yield other components were given as an average data of two locations. Main stem number were measured 5 randomised plant in replication at the end of flowering time. Marketable tuber yield (%) were determined the percentage of bigger 30mm in early season and 35 mm medium-late season. Tuber shape: 100 x (tuber long (mm) / tuber width (mm) in 20 tuber in each replication. 112-129: short oval tuber, 130-149: oval tuber, 150-169: long oval tuber, 170-199: long tuber and > 200 very long tuber. Flesh colour were measured 20 tuber in each replication. For cooking type baked and boiling potato performance were determined. For baked potato performance, 10 clear tuber in each replication were made 8 short holes with fork. After tubers baked in oven 175 C in two hours. After two hours tuber structure and colour were determined. Dry matter content (%) was measured by Zeal potato hydrometer and starch content (%) was determined with a polarimetric procedure [6]. The experiments were laid out in a Completely Randomized Block Design with four replication. 54 tubers of each cultivars were planted in two rows in each replication. Tuber yield were subjected to analysis of variance and differences were compared with LSD tests using MSTAT-C statistic program [7].

RESULTS

As a result of the early season trials during the research study, in commercial varieties generally were obtained 4-5 and 5-6 main stems, while candidate varieties were produced 5-6 main stems. In terms of the average tuber weight, the highest values were obtained, as the averages of Adana and İzmir, with the commercial varieties of Safrane and Florice. Among the candidate varieties, the highest value was obtained as 122g with 12-55-16 and a higher average tuber weight than the control variety Marabel was found. The marketable tuber ratio was varied between 90% and 96%. While the commercial variety Florice was given a marketable tuber ratio of 96%, the candidate varieties were produced a marketable tuber ratio of 94% and 95%. Tuber shape was determined as oval with the varieties Marabel and 12-69-39, long with Musica, and long oval with all other varieties. While the tuber flesh colour was yellow for the commercial varieties Marabel, Musica and the candidate variety 12-03-85, it was determined as light yellow for other control varieties and candidates.

In the analyses of cooking quality and nutrient contents, candidates, except for 12-55-16 and 12-55-07, variety candidates, and commercial control varieties were showed firm cooking tuber structure. The dry matter and starch ratio are the two most essential quality criteria for potatoes. In terms of dry matter, values of 18.0-23.9% were obtained based on commercial varieties and candidate varieties in the regions of Adana and İzmir. The highest dry matter ratio was obtained in the variety candidates 12-55-07 and 12-55-16. The distribution in terms of starch ratio varied between 10.5% and 17.7%. Of the candidate varieties, the variety 12-55-07 was given higher starch ratio than other candidates. In general, higher starch and dry matter ratios were determined in the Adana region.

Breeding studies are carried out for potato by taking into consideration some 50 different characteristics before the potential is established for commercial varieties. Table 1 gives some traits which are important for developing varieties for potato. Tuber yield is the most important character besides the plant, tuber, agronomic and quality characteristics of potato. Early season results for tuber yields were given in Table 2 collectively, on a regional basis. If Table 2 is examined, the highest yields were obtained for Florice and Safrane commercial varieties under Adana conditions, and variety 12-69-39, among the candidates, was statistically included in the same group as those varieties. The lowest yields were obtained with the commercial variety Marabel, and among the candidate varieties, 12-55-07 and 12-55-16 varieties were included in the same group as Orkestra and Musica varieties. The average tuber yield in the Adana area was found as 4381 kg decare^{-1}, which was obtained as 5573 kg decare^{-1}, under

İzmir conditions. Tuber yield was highest in Florice and Orkestra varieties under İzmir conditions, the control varieties being followed by 12-55-16 and 12-69-39 candidate varieties. All the four candidate varieties presented higher tuber yield than the control variety Marabel. The general average tuber yield was determined as 4977 kg decare^{-1} in the early season experiment. In view of the combined data as the average value of both areas, the highest yields were obtained in the Florice and Safrane commercial varieties, while, among the candidate varieties, the 12-69-39 and 12-55-16 varieties gave the highest yields. The lowest value of tuber yield was determined for the candidate variety 12-03-85.

Agronomic, plant, tuber and quality characteristics of 3 candidate varieties and 5 control commercial varieties under the main crop conditions were given in Table 3. In terms of the number of main stems, candidate varieties gave 5-6 pieces of stems as the average number of regions. As for the average tuber weight, 12-68-05 and 13-67-25 varieties of the candidate varieties surpassed commercial varieties by giving the highest values with 105g. The marketable tuber ratio ranged from 91% to 96% and the highest rate was obtained in the 13-67-25 candidate variety and the Granola commercial variety with 95%. The tuber shape was determined as short oval tuber for the candidate 12-68-05, oval tuber for Marabel, and long oval tuber for other varieties. In terms of flesh colour, among the candidates, 13-67-25 was determined as the variety having yellow flesh colour. Other candidates were determined as having light yellow tuberous colour. In terms of cooking quality, Marabel, Madeline, Granola, 13-67-25 showed a firm cooking tuber structure, while Agria and 22-99-33 varieties displayed medium fairly firm-floury tuber structure. In respect of dry matter ratio, 22-99-33, of the candidate varieties, were produced high values (20.4% and 21%) in both regions. The 12-68-05 variety gave a fairly high dry matter ratio, as was the case with the commercial variety Melody. As regards to the starch ratio, the highest value among candidate varieties was obtained for the variety 22-99-33 in the Niğde region.

TABLE 1
Early season experiment average values of plant, tuber and quality traits two locations (Adana and İzmir)

Varieties	MSN	ATW (g)	MTY (%)	TS	FC	Cooking type	Dry matter content (%)		Starch content (%)	
							Adana	İzmir	Adana	İzmir
Marabel	5-6	91	90	Oval	Yellow	Firm, AB	21.4	19.6	17.7	14.2
Orkestra	4-5	117	94	Long oval	Light yellow	Firm, A	19.5	19.0	15.3	15.0
Musica	5-6	109	92	Long	Yellow	Firm, A	20.8	20.6	15.0	14.7
Safrane	4-5	142	95	Long oval	Light yellow	Firm, A	21.3	20.3	15.7	14.7
Florice	4-5	147	96	Long oval	Light yellow	Firm, A	18.4	18.0	13.7	12.5
12-55-16	5-6	122	95	Long oval	Light yellow	Slightly mealy, B	22.4	21.0	14.0	10.5
12-55-07	5-6	103	94	Long oval	Light yellow	Slightly mealy, B	23.9	23.2	14.3	13.0
12-69-39	5-6	102	94	Oval	Light yellow	Firm, AB	21.4	21.3	12.4	12.0
12-03-85	5-6	93	91	Long oval	Yellow	Firm, AB	20.5	20.8	11.3	11.8

MSN: stem number per main, ATW: Average tuber weight, MTY: Marketable tuber yield, TS: Tuber shape, FC: Flesh colour.

TABLE 2
Early season tuber yield results of combined Adana and İzmir locations 2015*

Variety	Tuber Yield (kg/da)		
	Adana	İzmir	General Mean
Marabel	2246 d	4757 d	3502 d
Orkestra	4497 b	6171 a	5334 bc
Musica	4307 b	5939 ab	5123 bc
Safrane	5501 a	5768 b	5635 ab
Florice	5679 a	6260 a	5970 a
12-55-16	4457 b	5672 b	5065 bc
12-55-07	4518 b	5106 c	4937 c
12-69-39	5245 a	5356 bc	5301 bc
12-03-85	2977 c	5166 c	4072 d
General Mean	4381	5573	4977
Commercial Varieties Mean	4446	5779	5113
(%) CV	11.93	12.93	8.75
F Value	18.78**	10.03**	9.47**
LSD	689	475	593

*: Within columns, means followed by the same letter are not significantly different by ANOVA protected LSD test ($p<0.01$)

TABLE 3
Main season experiment average values of plant, tuber and quality traits two locations (Antalya and Niğde)

Varieties	MSN	ATW (g)	MTY (%)	TS	FC	Cooking type	Dry matter content (%)		Starch content (%)	
							Niğde	Antalya	Niğde	Antalya
Marabel	5-6	98	91	Oval	Yellow	Firm, AB	16.6	17.7	11.5	12.2
Agria	4-5	98	94	Long oval	Yellow	Slightly mealy, B	17.8	18.9	14.0	13.2
Granola	5-6	91	95	Long oval	Light yellow	Firm, A	17.9	17.5	10.2	11.4
Melody	4-5	100	94	Long oval	Yellow	Firm, AB	20.4	19.8	11.6	12.2
Madeline	6-7	99	93	Long oval	Yellow	Firm, A	16.8	17.6	10.8	11.3
22-99-33	5-6	100	94	Long oval	Light yellow	Slightly mealy, B	20.4	21.0	15.9	12.6
12-68-05	5-6	105	95	Short oval	Light yellow	Firm, AB	19.6	20.4	12.2	12.4
13-67-25	5-6	105	96	Long oval	Yellow	Firm, A	17.5	18.2	10.6	11.2

MSN: stem number per main, ATW: Average tuber weight, MTY: Marketable tuber yield, TS: Tuber shape, FC: Flesh colour.

TABLE 4
Main season tuber yield results at combined Antalya and Niğde locations 2015

Variety	Tuber yield (kg/da)		
	Antalya	Niğde	General Mean
Marabel	3107 d	3574 c	3341 d
Agria	3217 d	3894 bc	3556 cd
Granola	3580 bc	3921 bc	3751 c
Melody	4142 a	4068 abc	4105 b
Madeline	3364 cd	4061 abc	3713 c
22-99-33	3374 cd	3698 bc	3536 cd
12-68-05	4208 a	4551 a	4380 a
13-67-25	3911 ab	4207 ab	4059 b
General Mean	3613	3997	3805
Commercial Varieties Mean	3482	3904	3693
(%) CV	6.64	10.95	9.85
F Value	12.47**	10.92**	8.47**
LSD	339	352	320

*: Within columns, means followed by the same letter are not significantly different by ANOVA protected LSD test ($p<0.01$).

In the main crop experiment under Antalya conditions, the highest value was obtained with the 12-68-05 candidate variety in terms of the tuber yield, followed by the Melody variety (Table 4). Among the other candidate varieties, 13-67-25 and 22-99-33 varieties gave higher yields than the commercial varieties Marabel and Agria. The highest yield for the main crop was produced by 12-68-05 and 13-67-25 candidate varieties under Niğde conditions (Table 4). In commercial varieties, Melody and Madeline varieties showed good performance. Under the main crop conditions, tuber yields were found as 3613 kg decare^{-1} in the Antalya region and 3997 kg decare^{-1} in the Niğde region. The overall average was determined as 3805 kg decare $^{-1}$. When the combined tuber yield values are examined, 12-68-05 candidate variety ranked first, followed by 13-67-25 as the second and commercial type Melody as the third. As averages of two regions, 22-99-33 candidate variety produced higher tuber yield than Marabel variety.

DISCUSSION

The study involved 7 candidate varieties taken into the trial during the early and late seasons. In this study, the number of main stems was determined as 4-6. The number of main stems is a variety special trait and it is directly affected by the physiological ages of the seed tubers, their sizes and the number of eyes per tuber. Under the main crop conditions, 3 varieties of late season candidate varieties showed superior performance due to tuber yield and other characteristics. 13-67-25 and 12-68-05 candidate varieties took the center stage with high tuber yield as average of the two regions. The dry matter contents of both candidate varieties were found to be quite high.

Particularly the 13-67-25 candidate variety was considered as a variety with high quality, long oval tuber. According to the field observations of 13-67-25 and 12-68-05 candidate varieties, PVY virus resistance and mildew resistance are also high. 22-99-33 candidate variety is a special variety. 22-99-33, which is an early-mid early variety, was regarded as an industrial variety due to the dry matter rate. 22-99-33 candidate variety was also identified as a variety with a quite high starch ratio. 22-99-33 candidate variety has standard, long oval, high-quality tuber properties. In field observations, PVY virus resistance and mildew tolerance of 22-99-33 variety were found to be slightly lower than the other two candidates (12-68-05 and 13-67-25). As regards to the dormancy, the variety 22-99-33 displays the structure of a variety suitable for industrial production as one with a long dormancy.

During the early crop season, 4 candidate varieties were taken into experiment. In terms of earliness, 12-03-85 variety was observed to be the one which is earlier than Marabel, the most cultivated commercial variety of the early period in Turkey. The 12-03-85 variety also came to the forefront with a homogenous tuber structure and yellow tuber flesh colour. In field observations, the PVY virus tolerance of the 12-03-85 variety was observed to be weaker than the other varieties. 12-69-39 variety, even though being mid-early in terms of maturity, is the latest of the candidate varieties tested during early season. The 12-69-39 variety was identified as a candidate variety with a strong plant structure, standard and quality tuber characteristics. Although the 12-69-39 candidate variety exists in the mid-early group among the 7 varieties, it is a variety coming to the forefront in that it is the only kind suitable for breeding during both early and late seasons. Among the 4 varieties tested at early season, the 12-69-39 candidate variety was found to be the one with the highest tolerance to PVY virus and mildew based on field observations.

It is reported that PVY, which is the most common virus in the world and the primary one of the viruses affecting potato production the most, can cause 10-90% loss of crops in potato depending on the variety [8, 9]. This virus is mechanically transmitted by tuber and aphids. For a campaign, it is necessary to use clean tubers and to fight vectors. Fighting with vectors is mostly done chemically, but does not provide complete protection. Therefore, it seems that the best solution is to develop these virus-resistant varieties. Commercial candidate varieties 13-67-25, 12-68-05 and 12-69-39 were evaluated as high PVY tolerant varieties according to field observations.

12-55-07 and 12-55-16 candidate varieties are the sibling varieties from the same breeding pedigree. 12-55-07 variety is one with early- mid-early maturation property. It was determined as the variety with the highest dry matter ratio. 12-55-07 variety with homogenous, standard tubers is a fresh and industrial variety. Specifically its advantage of meeting the needs for chips and French Fries of industrial factories during the early period thanks to its early season structure, will bring 12-55-07 candidate variety to the forefront. 12-55-16 variety is also considered as a fresh and French Fries industrial candidate variety. The mildew tolerance in mid-early variety 12-55-16 is quite high under field conditions. For the early period, two commercial varieties Florice and Safrane came to the forefront with their high yield. Both are varieties with large, but low-quality tubers and do not have a chance to be grown in other potato regions.

12-55-07 and other candidate varieties appear to be the varieties rising to prominence both as they can be produced during early period and due to their yield and quality characteristics. The commercial varieties Orkestra and Madeline are the varieties having the potential of being produced, and, as such, which are produced, more extensively in different regions of Turkey, as compared to the Safrane and Florice varieties. The yield potentials of the candidate varieties are compatible with the Orchestra and Madeline varieties. In terms of disease resistance, Florice came into prominence as regards to mildew which is more important particularly during the early period, while the mildew tolerances of Safrane and Orkestra varieties were found to be lower. Among the candidates, 12-69-39 variety stands out with a high mildew tolerance. Since the early season growing in Turkey (January-June) coincides with the time of the temperate, rainy Mediterranean climate, potato mildew emerges as an important disease in this period. Varieties with high mildew tolerance during early season growing provide great advantage.

The dry matter rate is closely related with the efficiency of transmission of the assimilation products to the tuber [10, 11] and is largely controlled by the genetic structure. Dry matter rate is a character that can be affected by ecological conditions, duration of vegetation and, partly, soil and plant nutrition characteristics, besides genetic structure [12, 13, 14]. The results obtained from the candidate and commercial varieties share similarity with the results of [15, 16, 17] who reported that the dry matter ratio is affected by environmental factors as well as the genetic structure and that generally the varieties with industrial characteristics have a higher dry matter content.

The early-season potato growing period (Mediterranean and Aegean coastal zones like in the other Mediterranean countries) is shorter than the normal growing period and the temperature values are lower and photoperiod is shorter. Generally, high yield potential are obtained in Turkey for potato under normal conditions during the main crop season (May-October, Middle Anatolia Region) than in the early season (January-June) [3]. During the main crop sea-

son in 2015, plant development was adversely affected and the yield decreased due to high temperature values during the flowering and tuber formation period of the plant specially high temperatures of June, July, August and beginning of September. It was reported that the high temperature during the growth period of potato reduced the yield, and that especially the high temperature values during periods close to the harvest time, accelerated the physiological aging in the tubers [18, 19].

It is expected that the Turkish potato sector can show considerable developments in the next ten years if it combines suitable geographic position for international trade (Mediterranean coast, Middle East and Asia regions), the increasing seed potato demand in neighbouring countries (Iraq, Romania, Turkic Republics, Pakistan etc.) and the current growth of the Chips, French Fries and Starch industry. However, R&D investments and studies should be increased to realize the expected development in the potato sector. Similarly, it is necessary to subsidize investments in breeding activities and seed potato production in order to diminish the dependency on imported seed. In addition, it is important to ensure organization of the different actors like farmers, seed producers, processing industry representatives etc. in the sector Potato production is considered as a high cost in Turkey due to high input use and high input prices.

CONCLUSIONS

Although the potato production and culture has a shorter history in Turkey compared to other European and neighbour Mediterranean and Middle East countries, now Turkey is one of the important potato-producing countries in the world due to high-speed developments in the potato sector, especially during the last 20 years. Ten companies endeavoured the seed potato sector have R&D activities. However, the R&D activities in these potato companies are not at the intended level, and the vast majority of the research activities are limited to variety adaptation studies [3]. However, the Turkish potato sector has still not realized its full potential and must realize a mentality change as soon as possible. As a first step, new varieties must be breed and develop high adaptation ability, high disease tolerant, high yield and good quality for fresh and processing market. In second, new superior varieties must be produced and used first Turkey after than all over the world. Last step, the seed production system has to change from multiplication of imported seed to production of high-quality seed within country.

Many different characteristics, such as high yield, good quality, and resistance to diseases and pests, are desirable in potato varieties [20]. In the study, the 115.000 potato true potato seed lines were propagated and selected 2008 to 2015 with an acceptable tuber type and shape continued in the variety development process for subsequent years for the evaluation of agronomic, quality and disease resistance traits and/or used as parental lines in our recurrent selection programme. Superior advanced lines were selected from the breeding programme. These were grown in different potato fields of Turkey. Seven advanced superior lines were submitted for commercial variety registration.

As a conclusion, in this study seven advanced commercial candidate potato varieties was developed and tested in Turkey's potato growing regions. All commercial candidate potato varieties will be use large-scale next 10 years in Turkey and other countries like Morocco, Egypt, Tunisia, Russia, Pakistan, Azerbaijan and other Turkic Republics, South Korea, Bulgaria with high adaptation ability, high yield and good quality characteristics.

ACKNOWLEDGEMENTS

We gratefully acknowledge the financial support of the Scientific and Technological Research Council of Turkey and its TEYDEP foundation (Projects 3110172 and 1140133).

REFERENCES

[1] Carputo, D., and Frusciante, L. (2011) Classical Genetics and Traditional Breeding. In: Bradeen, J.M., Kole, C. (Eds.) Genetics, Genomics and Breeding of Potato. Published by Science Publishers. Enfield, NH 03748, USA, 20-40.

[2] Slater, A.T., Cogan, N.O.L. Hayes, B. Schultz, L., Dale, M.F.B. Bryan, G.J. and Forster, J.W. (2014) Improving breeding efficiency in potato using molecular and quantitative genetics. Theor. Appl. Genet. 127, 2279-2292.

[3] Çalışkan, M.E., Onaran, H. and Arıoğlu, H.H. (2010) The Overview to the Turkish Potato Sector: Challenges, Achievements and Expectations. Potato Agrophysiology. Proceedings of the International Symposium on Agronomy and Physiology of Potato, Proceeding Book. 20-24 September 2010, Nevşehir, Turkey, 1-11.

[4] Günel, E., Kuşman, N. Tuğrul, K.M. Yılmaz, A. Ağırnaslıgil, T. and Onaran, H. (2010) Starch and Sugar Plant Production. Turkey VII. Technical Congress of Agricultural Engineers. 11-15 January 2010, Ankara, Turkey, 77-396.

[5] Arslanoglu, F., Aytaç, S. and Karaca-Öner, E. (2011) Morphological characterization of the local potato (*Solanum tuberosum* L.) genotypes collected from the Eastern Black Sea Region of Turkey. African J. Biotechnology. 10(6), 922-932.

[6] Haase, N.U. (2003) Estimation of dry matter and starch concentration in potatoes by determination of under-water weight and near infrared spectroscopy. Potato Research. 46(4), 117-127.
[7] Freed, R., Einensmith, S.P. Guetz, S. Reicosky, D. Smail, V.W. and Wolberg, P. (1989) User's Guide to MSTAT-C Analysis of Agronomic Research Experiments. Michigan State Univ. USA.
[8] Ramakrishnan, A.B., Ritland, C.E. Sevillano, R.H.B. and Riseman, A. (2015) Review of potato molecular markers to enhance trait selection. American J. Pot. Res. 92, 455-472.
[9] Slater, A., Cogan, N.O.L. Rodoni, B. Daetwyler, H. Hayes, B. Caruana, B. Badenhorst, P. Spangenberg, G. and Forster, J. (2017) Breeding differently-The digital revolution: High throughput phenotyping and genotyping. 20th EAPR Conference. 9-14 July 2017, Paris France.
[10] Tekalign, T. and Hammes, P.S. (2005) Growth and productivity of potato as influenced by cultivar and reproductive growth: II. Growth analysis, tuber yield and quality. Scientia Horticulturae. 5, 29-44.
[11] Parlar, H., Gschwendtner, O. Anschütz, A. Leupold, G. and Görg, A. (2001) Influence of selected parameters on the 2 isoelectric adsorptive bubble separation (iabs) of potato proteins. Advances in Food Sciences. 23(1), 1-10.
[12] Yılmaz, H.A. and Güllüoğlu, L. (2002) Determination of agronomic and quality traits of some potato (*Solanum tuberosum* L.) varieties growing Harran plain. III. Nation Potato Congress, 23-27 September 2002, İzmir, Turkey, 179-192.
[13] Omran, A.A. and Hussien, H.A. (2015) Production and evaluation of gluten-free 184 cookies from broken rice flour and sweet potato. Advances in Food Sciences. 37(4), 184-192.
[14] Zhu, Z., Yuan, P. Rao, L. Chen, L. and Liu, X. (2017) Scenario simulation of ecosystem service value based on landscape transformation. Fresen. Environ. Bull. 26, 1812-1824.
[15] Pawelzik, E., Delgado, E. Poberezny, J. and Rogoziňska, I. (1999) Effect of different climatic conditions on quality of certain German and Polish potato varieties. Abstract 14th Trien. Conference EAPR, Sorrento. 635-636.
[16] Ekin, Z. (2009) Determination of yield and quality characters of some potato (*Solanum tuberosum* L.) varieties under Ahlat ecological conditions. J. Agric. Fac. HRU. 13(3), 1-10.
[17] Asmamaw, Y., Tekalign, T. and Workneh, T.S. (2010) Specific gravity, dry matter concentration, pH and crisp-making potential of Ethiopian potato (*Solanum tuberosum* L.) cultivars as influenced by growing environment and length of storage under ambient conditions. Potato Research. 53, 95-109.
[18] Kaya, C., Kara, T. Karakuş, A. and Sefaoğlu, F. (2016) Determination of performance of advanced potato breeding clones under growers conditions. Journal of Central Field Crops Research Institute. 25(2), 49-54.
[19] Jurišić, B. and Vidicki, B. (2014) Influence of some ecological factors and forest practice on the 2310 spatial pattern of species richness and distribution of lowland forests at landscape level (a case study: floodplain forest area of Ravni Srem, Serbia). Fresen. Environ. Bull. 23, 2310-2321.
[20] Asano, K., Kobayashi, A. Tsuda, S. Nishinaka, M. and Tamiya, S. (2012) DNA marker-assisted evaluation of potato genotypes for potential resistance to potato cyst nematode pathotypes not yet invading into Japan. Breeding Science. 62, 142-150.

Received: **04.12.2017**
Accepted: **21.02.2018**

CORRESPONDING AUTHOR

Ercan Ozkaynak
Yüksel Tohum,
Kurşunlu Mah. Madenler Sok. No: 12/A,
Antalya – Turkey

e-mail: eozkaynak@yukseltohum.com

© by PSP Volume 27 – No. 5/2018 pages 3094-3101 Fresenius Environmental Bulletin

SUPPLY RESPONSE OF MAIN LEGUMES IN TURKEY BY VECTOR ERROR CORRECTION APPROACH

R Figen Ceylan*

Department of Agricultural Economics, Faculty of Agriculture, Akdeniz University, 07070, Antalya, Turkey

ABSTRACT

Measuring the impact of price and non-price factors on annual agricultural products is an agricultural policy subject that continues to receive attention. In this study it was aimed to question the response of quantity supplied for main legumes as lentils, dried beans and chickpeas that are produced specifically in South-eastern regions of Turkey. Vector error correction methodology was incorporated to estimate the short-run dynamics of the quantity supplied as well as the static supply relationships between 1991 and 2013.Iimpacts of economical or ecological shocks were considered within the analysis for 1991 and 2013. Persistent declination of both the amount supplied and the producer price was recognised, even if the dependency of dried beans on its price was found relatively lower than the other staples. However, the declination in the amount and prices had shown that, well-built strategies to convince producers in order not to leave their lands and to support development of processing units are required specifically for South-eastern parts of Turkey.

KEYWORDS:
Legumes, Price, Supply Response, VEC

INTRODUCTION

One of the most important issues in agricultural economics is supply response of crops as the responsiveness of farmers to incentives determines agriculture's contribution to the overall economy. The situation is more important in Turkey, where the sector is the largest employer.

Agricultural supply response represents change in agricultural output due to a change in agricultural output price and other relevant factors. The concept of supply response is dynamic and different from supply function, which resides on a static concept. The supply function describes a price quantity relationship, where all other factors are held constant. On the other hand, the response relation is a more dynamic concept. It shows the change in quantity supplied with relevance to the changes in prices as well as changes in supply shifters such as prices of other products and costs of inputs like land and labour. Therefore, it approximates the amount supplied to the long run [1]. The production growth through incentives, while effective in the recent years, may be relatively difficult in the future. This may be induced by an economic or demand crisis or financial difficulties which result in reduced subsidies. Some agricultural policy experts are interested in observing the response of supply and demand to farm inputs accordingly [2].

The recent studies in the agricultural economics mostly focus on cointegration and error correction studies of time series data. The supply response of maize farmers to prices in Nigeria was analysed using cointegration and Auto Regressive Distributed Lag (ARDL) model between 1961 and 2008. The empirical findings showed that maize supply responds significantly and positively in the long run to its own price and negatively (positively) to the price of cassava (yam). Other results revealed that maize supply failed to respond price changes significantly in the short run. While short-run causality runs only from price of cassava to maize supply, long-run causality runs from joint price effect to maize supply [3].

Cointegration and error correction modelling approaches was used to estimate aggregate supply response for maize using data for Trans Nzoia District of Kenya for 1980 and 2003. Results indicated that high maize and low fertiliser costs positively influenced the aggregate maize supply. The elasticity of supply to fertiliser costs was -1.05 for the short-run and -1.26 for the long-run. The elasticity of supply to maize price was 0.53 for the short-run and 0.76 for the long-run. These findings indicated that the market liberalisation targeting for changing producer price incentives is reasonable and advisable [4]. Departing from this research, another Kenyan maize study confirmed inelastic response of maize production to its price, fertiliser costs, agro-investments and marketing board purchases between 1972 and 2008 [5].

Response of rubber farmers to price and non-price factors were analysed from 1970 to 2008 in Nigeria. Response of rubber supply to its own price was low with an estimated elasticity of 0.373 for the short-run and 0.204 for the long-run. Price sustainability and opportunity to increase supplies leaded to low responsiveness and promotion of sustainable marketing outlets and high quality exportable crop

production were suggested [6].

Legumes (pulse crops), which are the major vegetative protein sources for human nutrition, are important for the World and for Turkey. Chickpeas (45 %), lentils (38 %) and dried beans (17 %) are the most significant pulse crops of Turkey. Legumes are mainly produced in the South-eastern Anatolia, which is one of the least economically developed regions of Turkey. These crops are of considerable significance to the regional economy, which has relatively inefficient conditions and constraints compared to western regions regarding water supplies and reach to information. Although government policy actions intend to lessen the economic disparities among regions and prevent migration from rural to urban, the impact on legumes production has been a dramatic decline in the last fifteen years [7]. Departing from this inference, this study aimed to understand the effect of supply shifter factors on three major pulses of Turkey in the long and short run.

DATA CHARACTERISTICS AND MODELLING FRAMEWORK

Data. As it was aimed to understand the impacts of price and non-price factors on the amount of produced for chickpeas, dried beans and lentils, it is first necessary to understand the data characteristics. Yet, it is important to note that the secondary data analysed was withdrawn from the databases of Turkish Statistical Institute for the target products between 1991 and 2013. Accordingly, we first intended to look at the descriptive characteristics of the data for the above mentioned crops.

Quantity of Production. The production amount has varied specifically for lentil and chickpeas since the beginning of the analysis period as demonstrated in Figure 1. However, the amount of dried beans produced has remained relatively stable. The total production has remained around 200 thousand tons despite an almost 28 % decline in 2008 for chickpeas. Amount of lentils produced has declined steadily from

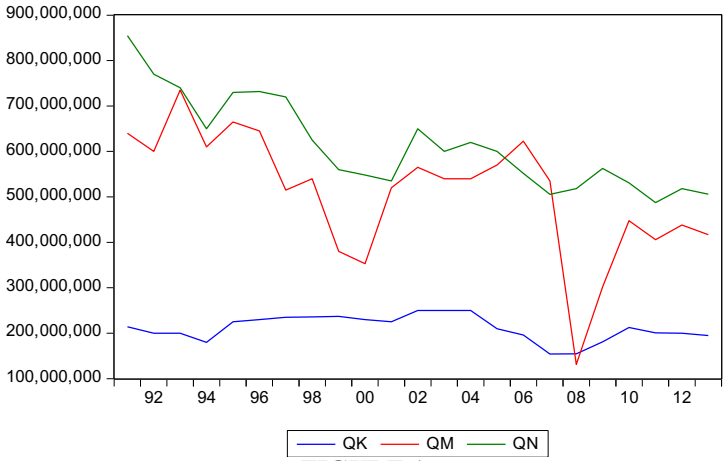


FIGURE 1
The amount of production for lentil (Q_m), chickpeas (Q_n) and dried beans (Q_k)

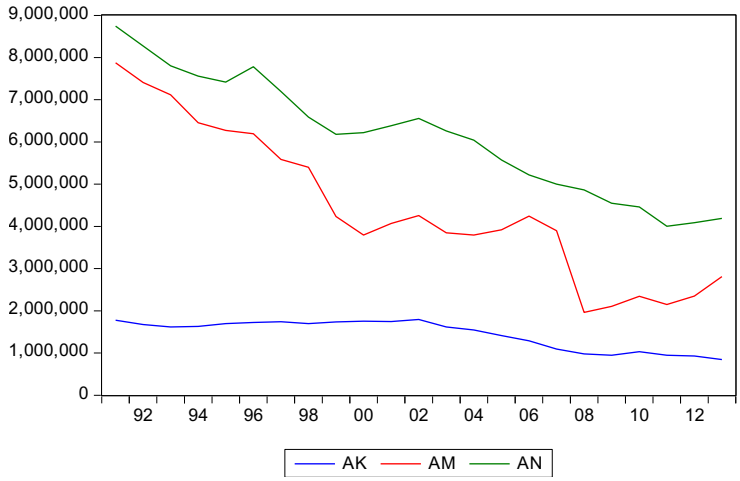


FIGURE 2
The production area for lentil (A_m), chickpeas (A_n) and dried beans (A_k)

around 855 thousand tons in 1991 to 506 thousand tons in 2013 with sharp reductions in 1994 and 2000 followed by induced production. The total declination accounted for 41 %. The change in lentil production was significant. From 640 thousand tons in 1991, the amount declined to 420 thousand tons in 2013 with 34 %. However, there are more sharp downsizing movements in 2000 (44 %) and 2008 (80 %) in comparison with the starting point, which are worth to diagnose. The variations of production amount are quite visible in Figure 1.

Area of Production. The field devoted for production of these three main staples had also declined with a higher variation for lentils. The lentil production fields had declined by 64 % to almost 3 million acres in 2013 while the declination was 52 % for chickpeas to 4 million and dried beans to below 1 million acres. The steady declination is also visible from Figure 2.

Producer Price. Outlet producer price per kg of these three crops had also evolved for as well as shown in Figure 3. While the real price had declined by 21 % for dried beans and by 40 % for lentils, the price for chickpeas had increased by almost 50 %. Besides, there had been seasonal shocks in 1995 and 2008 for all of the products in either direction followed by inverse movements. The reasoning behind the uprising in 1995 was the 1994 economic crisis induced by Mexican Peso crisis and the above expectations rise in price levels that became visible through more than 100 % rise in CPI levels [8]. Yet, the reason of the boom in 2008 however is the climatic conditions and attached declination experienced in the summer of 2007 [7].

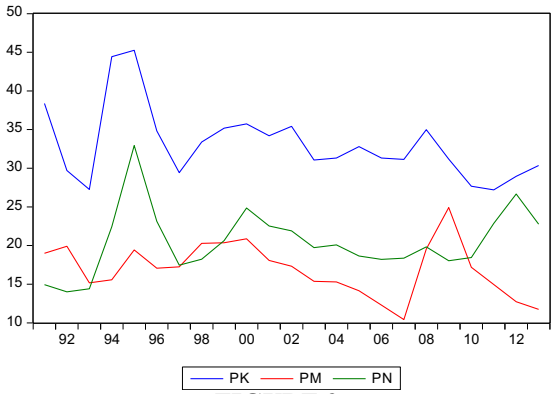


FIGURE 3
Real prices for lentil (P_m), chickpeas (P_n) and dried beans (P_k)

Methodology. Modelling Framework. Before proceeding, it is essential to note that the explanation of amount of agricultural products produced needs consideration with regards to the inter-period relationships. There are various methods applied for determination of the effects on quantity supplied. However, one of the most preferred methodologies is the Nerlovian approach that uses expected prices and non-price factors in explaining the production amount expectations [9].

Accordingly, the main function used to form the expectations framework is as following:

$$Q_t^* = a + bP_t^* + cZ_t \quad (1)$$

$Q_t^* = expected\ production\ amount\ for\ time\ t$
$P_t^* = expected\ price\ level\ for\ time\ t$
$Z_t = non - price\ vector\ for\ time\ t$

In order to integrate expectations, we need the previous year's data for annual agricultural crops. When detailed, it can be understood that the farmers decide what to produce, and how to exchange it with complementary and/or competitive products looking at the previous year's prices and factors as land and existing production capacity. Therefore, the expectation-oriented system is formed by integrating the differenced variables in the system. Besides, all data needs to be normalised by using logarithmic transformation.

$$Q_t - Q_{t-1} = \delta(Q_t^* - Q_{t-1}) \quad (2)$$

$$P_t^* = \theta P_{t-1} + (1-\theta) P_{t-1}^* \quad (3)$$

$$lnQ_t = C_0 + C_1 lnP_{t-1} + C_2 lnQ_{t-1} + C_3 lnZ_t \quad (4)$$

In this representation while C_1 refers to short-run price elasticity, $C_1/1\text{-}C_2$ refers to long-run price elasticity of the amount produced [1, 10].

Estimation of equations formed of non-stationary level variables generally tends to mislead the economic and statistical interpretations [11, 12]. Accordingly, the error correction system depending on co-integration of the auto-correlated variables of same order in a time series analysis was set forward in 1980s [12, 13, 14]. The objective behind was to reach a sound economic interpretation of the changes in the level of production. The co-integration methodology refers to estimation of the short run relationship between integrated variables. In this situation, the co-integration and joint estimation of the variables needs to be tested towards the static equations that refer to the long-run explanation of quantity supplied [15].

Static Equations. The static equations used to explain quantity supplied of these specific legumes are as following.

Lentil

$$lnQ_{mt} = \propto_1 + \alpha_2 lnQ_{mt-1} + \alpha_3 lnP_{mt-1} + \alpha_4 lnA_{mt-1} + \alpha_5 lnP_{kt-1} + \alpha_6 lnP_{nt-1} + \varepsilon_t \quad (5)$$

$Q_{mt} = lentil\ production\ amount\ in\ year\ t - kg$
$Q_{mt-1} = lentil\ production\ amount\ in\ year\ t_1 - kg$
$P_{mt-1} = real\ lentil\ price\ in\ year\ t_1 - per\ kg$
$A_{mt-1} = harvested\ field\ for\ lentils\ in\ year\ t_1 - decares$
$P_{kt-1} =$

$real\ dried\ beans\ price\ in\ year\ t_1 - per\ kg$

$P_{nt-1} = real\ chickpeas\ price\ in\ year\ t_1 - per\ kg$

Chickpeas

$$lnQ_{nt} = a_1 + a_2 lnQ_{nt-1} + \alpha_3 lnP_{nt-1} + \alpha_4 lnA_{nt-1} + \varepsilon_t \quad (6)$$

$Q_{nt} = chickpeas\ production\ amount\ in\ year\ t - kg$

$Q_{nt-1} = chickpeas\ production\ amount\ in\ year\ t_1 - kg$

$P_{nt-1} = real\ chickpeas\ price\ in\ year\ t_1 - per\ kg$

$A_{nt-1} = harvested\ field\ for\ chickpeas\ in\ year\ t_1 - decares$

Dried Beans

$$lnQ_{kt} = b_1 + b_2 lnQ_{kt-1} + b_3 lnP_{kt-1} + b_4 lnP_{mt-1} + \varepsilon_t \quad (7)$$

$Q_{kt} = dried\ beans\ production\ amount\ in\ year\ t - kg$

$Q_{kt-1} = dried\ beans\ production\ amount\ in\ year\ t_1 - kg$

$P_{kt-1} = real\ dried\ beans\ price\ in\ year\ t_1 - per\ kg$

$P_{mt-1} = real\ lentil\ price\ in\ year\ t_1 - per\ kg$

FINDINGS

The distribution of the data. Before proceeding, the data obtained on level needs to be tested for normality of distribution in order to meet the assumptions of estimation.

TABLE 1
Normality Test Results

	Jarque-Bera (p)		Jarque-Bera (p)		Jarque-Bera (p)
Q_k	1,05 (0,59)	A_k	3,18 (0,20)	P_k	6,29 (0,04)
Q_m	3,63 (0,57)	A_m	1,33 (0,51)	P_m	0,10 (0,94)
Q_n	2,25 (0,32)	A_n	1,13 (0,57)	P_n	6,17 (0,05)

Due to the normality test results indicated in Table 1, it can be noted that specifically the price indicators are not normally distributed and need be normalised for further analysis and logarithmic transformation is used accordingly.

Stationary Testing. Firstly, it is essential to check the correlograms of the logged data. Looking at the Q-statistics that were indicated in Table 2, it is understood that data on level were not stationary. Depending on the theory, it can be concluded that differencing the data can grant stationarity.

Subsequently, it is also essential to check existence of unit root of the data via ADF testing [13]. The results leaded the decision on whether the inter-period relationships could be overcome within the analysis.

Due to the findings demonstrated in Table 3, other than real price factors, all of the remaining variables have first order autocorrelation. The price variables on the other hand can be noted as not autocorrelated as they are also stationary on level. For implication of the concerned methodology, it is also essential to check the stationarity level of the lagged variables before explaining the equation system in details and considering the error correction process.

Apparently, the unit root process for the lagged variables revealed the same outcomes that they are mostly stationary in their first lags as can be seen in Table 4.

TABLE 2
Q-statistic Results

	Q-stat (p)		Q-stat (p)		Q-stat (p)
lnQ_k	13,50 (0,00)	lnA_k	19,64 (0,00)	lnP_k	3,03 (0,08)
$D(lnQ_k)$	0,31 (0,58)*	$D(lnA_k)$	2,38 (0,12)*	$D(lnP_k)$	< 0,01 (0,93)*
lnQ_m	4,26 (0,04)	lnA_m	18,69 (0,00)	lnP_m	5,64 (0,18)
$D(lnQ_m)$	1,34 (0,25)*	$D(lnA_m)$	< 0,01 (0,99)*	$D(lnP_m)$	0,04 (0,84)*
lnQ_n	13,52 (0,00)	lnA_n	19,57 (0,00)	lnP_n	6,69 (0,01)
$D(lnQ_n)$	0,27 (0,60)*	$D(lnA_n)$	0,47 (0,49)*	$D(lnP_n)$	0,90 (0,34)*

*, stationary at 1 % level of significance

TABLE 3
Unit Root Test Results (with constant)

	ADF (p)		ADF (p)		ADF (p)
lnQ_k	-2,08 (0,22)	lnA_k	0,90 (0,99)	lnP_k	-3,20 (0,03)**
$D(lnQ_k)$	-3,93 (< 0,01)*	$D(lnA_k)$	-3,04 (0,04)*	$D(lnP_k)$	-4,96 (< 0,01)*
lnQ_m	-2,93 (0,06)	lnA_m	-1,39 (0,56)	lnP_m	-3,11 (0,04)**
$D(lnQ_m)$	-5,52 (< 0,01)*	$D(lnA_m)$	-4,38 (< 0,01)*	$D(lnP_m)$	-4,59 (< 0,01)*
lnQ_n	-2,12 (0,24)	lnA_n	-0,65 (0,84)	lnP_n	-5,39 (< 0,01)*
$D(lnQ_n)$	-4,95 (< 0,01)*	$D(lnA_n)$	-2,59 (0,02)**	$D(lnP_n)$	-4,33 (< 0,01)*

*, stationary at 1 % level of significance; **, stationary at 5 % level of significance

TABLE 4
Unit Root Test Results for Lagged Variables (with constant)

	ADF (p)		ADF (p)		ADF (p)
lnQ_{k-1}	-2,06 (0,26)	lnA_{k-1}	0,54 (0,98)	lnP_{k-1}	-3,10 (0,04)**
$D(lnQ_{k-1})$	-3,94 (< 0,01)*	$D(lnA_{k-1})$	-3,00 (0,05)**	$D(lnP_{k-1})$	-4,72 (< 0,01)*
lnQ_{m-1}	-2,88 (0,07)	lnA_{m-1}	-1,04 (0,72)	lnP_{m-1}	-3,34 (0,03)**
$D(lnQ_{m-1})$	-5,36 (< 0,01)*	$D(lnA_{m-1})$	-4,45 (< 0,01)*	$D(lnP_{m-1})$	-4,53 (< 0,01)*
lnQ_{n-1}	-2,14 (0,23)	lnA_{n-1}	-0,15 (0,93)	lnP_{n-1}	-4,97(< 0,01)*
$D(lnQ_{n-1})$	-4,71 (< 0,01)*	$D(lnA_{n-1})$	-4,10 (< 0,01)*	$D(lnP_{n-1})$	-4,06 (< 0,01)*

*, stationary at 1 % level of significance; **, stationary at 5 % level of significance

TABLE 5
Co-integration test results

LENTILS		CHICKPEAS		DRIED BEANS	
Dep. Var.	**D(et)**	**Dep. Var.**	**D(et)**	**Dep. Var.**	**D(et)**
e(-1)	-1,04	e(-1)	-1,03	e(-1)	-1,20
t(p(t))	0,00*	t(p(t))	0,00*	t(p(t))	0,00*

*, stationary at 1 % level of significance

TABLE 6
Results for lentil production between 1991 and 2013

LONG-TERM				SHORT TERM			
Variable	**Est.**	**t-stat**	**(p)**	**Variable**	**Est.**	**t-stat**	**(p)**
Q_{m-1}	0,58	1,52	0,15	**$D(Q_{m-1})$**	0,75	7,17	0,00
P_{m-1}	0,97	2,30	0,04	**$D(P_{m-1})$**	0,03	0,08	0,93
A_{m-1}	0,03	0,07	0,95	**$D(A_{m-1})$**	-1,50	-2,35	0,03
P_{k-1}	-0,15	-0,17	0,87	**$D(P_{k-1})$**	0,26	0,78	0,45
P_{n-1}	0,19	0,35	0,73	**$D(P_{n-1})$**	-0,07	-0,28	0,78
α_1	5,12	0,99	0,33	**ECM2(-1)**	-0,23	-0,91	0,38
				α_1	-0,07	-1,45	0,17
R^2	0,42	**F-stat**	2,28 (0,09)	**R^2**	0,90	**F-stat**	21,33 (0,00)
D-W	2,07	**M.D.V.**	19,98	**D-W**	1,99	**M.D.V.**	-0,01

Co-integration. The data being recognised as non-stationary with detected unit roots, the co-movement of the data needed to be verified. Therefore, the residuals of the static equations formed for three crops (equations 7, 8, 9) were tested for their unit roots in order to make inferences about the short run co-integration. The reasoning behind was to understand whether a linear combination of the non-stationary series are stationary and could produce significant inferences through linear estimation [16]. The results are provided in the Table 5.

Accordingly, it was understood that quantity supplied of lentils, chickpeas and dried beans can be estimated by co-integrating the non-stationary series with I(1). The non-stationary series can be used to estimate the short-run relationships with co-integration methodology. Accordingly, the short-run static estimators were reformed to incorporate the co-integration correction.

$$D(lnQ_{mt}) = \propto_1 + \alpha_2 D(lnQ_{mt-1}) + \alpha_3 D(lnP_{mt-1}) + \alpha_4 D(lnA_{mt-1}) + \alpha_5 D(lnP_{kt-1}) + \alpha_6 D(lnP_{nt-1}) + \varepsilon_t \quad (8)$$

$$D(lnQ_{nt}) = a_1 + a_2 D(lnQ_{nt-1}) + \alpha_3 D(lnP_{nt-1}) + \alpha_4 D(lnA_{nt-1}) + \varepsilon_t \quad (9)$$

$$D(lnQ_{kt}) = b_1 + b_2 D(lnQ_{kt-1}) + b_3 D(lnP_{kt-1}) + b_4 D(lnP_{mt-1}) + \varepsilon_t \quad (10)$$

RESULTS AND DISCUSSION

Lentils. For the concerned crops, the factors that affect amount of production were determined and their effects were estimated for the long and short term after co-integration. The results are demonstrated in Table 6.

For lentil supplies, more than 50 % of the previous year's production was reflected in the contemporary level of production. This means that experiences and preferences of the farmer are considerably important in the decision making process. Besides, the production amount is highly responsive to the price. The long term price elasticity (0,97) indicates that a unit rise in log of real price leaded to a unit rise in the log of production amount. Considering the declination in the amount and real price between 1991 and 2013, it can be said that the supply mechanism followed its own path. However, the short term response is even more significant. The elasticity of 2,31 (0,97/(1-0,58)) can be read that lentil producers prefer to shift to competitive or complementary products easily due to a price reduction in the short term. This also can explain the steady reduction in prices and lentil supplies and the low responsiveness to the harvested area with 0,03 elasticity.

In addition, the real price of the chickpeas

(0,19) affect the production of lentils positively in the long run, while dried beans (-0,15) affect it in the adverse direction. Yet the impacts are said to be not too significant. It is indecisive apparently to conclude that whether consumers choose between dried beans and lentils or consume chickpeas and lentils together. To understand whether they are alternatives to each other, it is important to check the remaining relationships.

Considering the spill-over of short term cyclical movements in the production to long term, the co-integrated relationship provided some inferences. The estimate of the error correction coefficient revealed that the shocks of the previous period were purified by 23 % in the current period. This meant that inter-period effects were important but the out-of equilibrium conditions were also in control of the sector. And the short-term production amount is most significantly determined by the previous terms production amount, almost by 75 %. Besides, the production shock of 2008 was attributed to the climatic shock appeared in 2007 [7, 17]. The impacts of the drought had been visible in production figures in 2008 as seen in Figure 1.

Chickpeas. The production of chickpeas could have been explained by its previous supplies, price and area harvested. The findings are demonstrated in Table 7. Looking at the long term results, the long term price elasticity was 0,35. Meaning the 35 % of the rise in the real price is reflected as rise in the amount of production. One-third of the production was followed by the previous year. Yet, the short term price elasticity was 55 % (0,35/(1-0,37)). And the effect of rise in fields harvested was 13 %. Therefore, it can be concluded that, chickpeas are more dependent on the production area and producer loyalty is more important than lentils. Besides, looking at the short-run, it was notable that 91 % of the temporary shocks were offset in the following period.

Apparently, there was a steady decline in chickpeas production for the analysis period. Therefore, even if the price and land of production is said to impact chickpeas production, there appeared a continuous decline in both the harvested area and the price. This was mainly attributed to the more water dependent characteristic of chickpeas production and the drought summer periods that have been experienced.

Dried Beans. Dried bean production was also explained by its previous price, previous supplies and previous price of lentil. The findings are indicated in Table 8. Besides, both its own price and price of the lentil have positive impacts on the amount of production. Yet, the price elasticity of dried beans and lentils were 22 % and 24 % in a consecutive order. Besides, the price of the dried beans was more effective in the long-run with around 60 % (0,22/(1-0,63)) of elasticity. Considering the short term shocks and how the equilibrium was reached back, the dynamics are rather significant. Any sharp change in the current period is offset with a high speed of adjustment.

TABLE 7
Results for chickpeas production between 1991 and 2013

LONG-TERM				SHORT TERM			
Variable	**Est.**	**t-stat**	**(p)**	**Variable**	**Est.**	**t-stat**	**(p)**
Q_{n-1}	0,37	1,82	0,08	$D(Q_{n-1})$	0,22	0,73	0,48
A_{n-1}	0,13	1,75	0,09	$D(A_{n-1})$	0,16	2,08	0,05
P_{n-1}	0,35	2,61	0,02	$D(P_{n-1})$	0,64	1,46	0,16
α_1	6,90	2,74	0,01	**ECM2(-1)**	-0,91	-2,46	0,02
				α_1	0,01	0,20	0,84
R^2	0,83	**F-stat**	28,67 (0,00)	R^2	0,50	**F-stat**	4,04 (0,02)
D-W	2,04	**M.D.V.**	20,21	**D-W**	2,16	**M.D.V.**	-0,01

TABLE 8
Results for dried beans production between 1991 and 2013

LONG-TERM				SHORT TERM			
Variable	**Est.**	**t-stat**	**(p)**	**Variable**	**Est.**	**t-stat**	**(p)**
Q_{k-1}	0,63	4,83	<0,01	$D(Q_{k-1})$	0,73	2,66	0,02
P_{k-1}	0,22	1,65	0,12	$D(P_{k-1})$	0,33	2,54	0,02
P_{m-1}	0,24	2,50	0,02	$D(P_{m-1})$	0,21	2,31	0,03
α_1	5,67	2,29	0,03	**ECM2(-1)**	-1,14	-3056	<0,01
				α_1	0,01	0,39	0,70
R^2	0,72	**F-stat**	15,39 (0,00)	R^2	0,57	**F-stat**	5,23 (<0,01)
D-W	1,92	**M.D.V.**	19,16	**D-W**	2,01	**M.D.V.**	-0,001

While there appeared a seasonal decline in 2007-2008, the cyclical movement around the average production has continued and the reduction is again attached to the summer conditions of 2007. 63 % of the existing production affecting the future production meant that the dried bean production had producer loyalty on a considerable extent.

POLICY IMPLICATIONS

The impacts of price and non-price factors on the production amount of main legumes were analysed within the study between 1991 and 2013 in order to undermine how important is the price. Therefore, it can be shortly noted that price and price related incentive and deterrents are important factors for estimating the production amount of these staples. To exemplify, all lentils, chickpeas and dried beans production schedules are open for the price motivations, lentils being the most affected with 97 % elasticity in the long run. The corresponding rates were 35 % for chickpeas and 22 % for dried beans. Besides, all these staples follow the previous period's production experiences. This finding both refers to the professionalization of the producer and persistent demand from the consumers. Yet, even if the rates do change, consideration of price related factors as supply motivators is still valid for these staples as it is a strict case for wheat production [10].

However, when the continuous decline in production of these staples is considered together with the findings, it is visible that real prices have been declining. Even after the seasonal shocks of 1995 and 2008, of which the reasoning were explained above as economic and climatic disruptions, the prices declined back to their normal downsizing way. Accordingly, declining prices leaded declinations in supplies of these staples and this finding is in conformity with the reached elasticity levels. In this manner, there needs policy solutions to reverse the impact of the declining prices. These solutions cannot be named as price subsidies or quantity-attached support systems. What is needed is more related with keeping the land in production and developing food processing industry in close proximity to the production fields, therefore in the South-eastern Anatolia in Turkey. When the producers are given incentives through reduced packaging or transportation expenses, or they are supported to establish their own processing facilities, it would be easier to keep the supply adequate for rising population and increasing export requirements from the Southern neighbours.

REFERENCES

[1] Tripathi, A. (2008) Estimation of Agricultural Supply Response by Cointegration Approach. Indira Gandhi Institute of Development Research, Visiting Research Scholar Programme, Mumbai, India.

[2] Ayinde, O.E, Bessler, D.A., Oni, F.E. (2014) Analysis of Supply Response and Price Risk on Rice Production in Nigeria. Selected Paper Prepared for Presentation at the Agricultural & Applied Economics Association's 2014 AAEA Annual Meeting, Minneapolis, MN. July 27-29.

[3] Ogundari, K., Nanseki, T. (2013) Maize Supply Response to Prices in Nigeria: application of ARDL a Co-Integration Analyses. 23rd New Zealand Econometric Study Group Meeting. 21 February 2013, New Zealand.

[4] Mose, L.O., Burger, K., Kuvyenhoven, A. (2007) Aggregate Supply Response to Price Incentives: The Case of Smallholder Maize Production in Kenya. African Crop Science Society. 8, 1271-1275.

[5] Onono, P.A., Wawire, N.W.H., Ombuki, C. (2013) The Response of Maize Production in Kenya to Economic Incentives. International Journal of Development and Sustainability. ISSN: 2168-8662. 2(2), 530-543.

[6] Mesike, C.S., Okoh, R.N. and Inoni, O.E. (2010) Supply Response of Rubber Farmers in Nigeria: An Application of Vector Error Correction Model. Agricultural Journal. 5(3), 146-150.

[7] Anonymous (2013) GAP International Agricultural Research Centre, Legumes Report. http://arastirma.tarim.gov.tr/gaputaem/Belgeler/tar%C4%B1msal%20veiler/gaputaem%20gncel/Baklagil%20Raporu.pdf.

[8] Sarıgedik, I. (2008) 1994 – 2001 Krizlerine Genel Bakış ve Kriz Yönetimi (General Overview of 1994 – 2001 Crisis and Crisis Management). MA Thesis. Ankara University Social Sciences Institute. Ankara.

[9] Nerlove, M. (1958) The Dynamic of Supply: Estimation of Farmers' Response to Prices. The Johns Hopkins University Press, London.

[10] Ozkan, B., Ceylan, R.F., Kızılay, H. (2011) Supply Response for Wheat in Turkey: A Vector Error Correction Approach. Mediterranean Journal of Economics, Agriculture and Environment. 3(2011), 34-38.

[11] Johansen, S. (1988) Statistical Analysis of Cointegrating Vectors. Journal of Economic Dynamics and Control. 12, 231-254.

[12] Granger, C.W.J. (1981) Some Properties of Time Series Data and Their Use in Econometric Model Specification. Journal of Econometrics. 16(1), 121-130.

[13] Dickey, D.A., Fuller, W.A. (1981) Likelihood Ratio Statistics for Autoregressive Time Series with a Unit Root. Econometrica. 49, 1057-1072.
[14] Engle, R.F., Granger, C.W.J. (1987) Cointegration and Error Correction: Representation, Estimation and Testing. Econometrica. 55, 251-276.
[15] Griffiths, W.E., Carter Hill, R., Lim, G.C., (2008) Using EViews for Principles of Econometrics. Wiley, 384p.
[16] Anwarul Huq, A.S.M., Arshad, F.M. (2010) Supply Response of Potato in Bangladesh: A Vector Error Correction Approach. Journal of Applied Sciences. 10(11), 809 – 902.
[17] Ozdem, M.A., TEPGE (2012) Dünya ve Türkiye'de Kurubaklagiller. (Legumes in the World and in Turkey) TEPGE – Institute of Agricultural Economics and Policy Development, ISSN: 1303–8346 / 7, 1-9.

Received: **12.12.2017**
Accepted: **18.02.2018**

CORRESPONDING AUTHOR

R Figen Ceylan
Department of Agricultural Economics,
Faculty of Agriculture,
Akdeniz University,
07070, Antalya – Turkey

e-mail: ceylan.figen@gmail.com

© by PSP Volume 27 – No. 5/2018 pages 3102-3106 Fresenius Environmental Bulletin

UPTAKE OF URANIUM BY PLANTS GROWING AROUND AN OLD URANIUM MILL TAILING IN NORTHEAST CHINA

Dong Yan[1], Kuke Ding[1], Yingxue He[1], Li Fan[1], Rui Zuo[2], Xiaoyan Jiang[1,*]

[1]Department of Radiology, National Institute for Radiological Protection, Chinese Center for Disease Control and Prevention, Beijing 100088, China
[2]College of Water Sciences, Beijing Normal University, Beijing 100875, China

ABSTRACT

In the uranium mining areas, uranium was usually discharged to the environment when the mining process occurred. A study was undertaken to investigate uranium concentrations in soil and plants around an old uranium mill tailing in northeast China. As a result, eight plant species samples were collected, including five families. Concentrations of uranium (dry weight, DW) in plants showed wide range of variations from 42.7 μg/g (roots of *Cichorium intybus*) to 0.180 μg/g (stems of *Erigeron annuus*). The contents of uranium in Compositae were higher than that of other plants species in the investigated samples, and which in plant tissues were roots > leaves > stems. *Oenothera biennis* displayed a high roots concentration ratio (CR) of 4.90 (mean value), followed by *Cichorium intybus* (2.98) and *Artemisia mongolica* (2.85). The species *Lepidium apetalum* leaves exhibited the maximum transportation factor (TF) of 0.626 (mean value) in this study. In summary, *Artemisia mongolica* and *Oenothera biennis* showed relatively high ability to remove uranium from their ambient soil, and could be used greatly towards phytoremediation in the study area.

KEYWORDS:
Uptake, Uranium, Plants, Uranium mill tailing

INTRODUCTION

Uranium (U) is a naturally occurring radionuclide existing almost entirely as ^{238}U (99.27%) in hexavalent state (U^{6+}), as ^{235}U in minor quantities (0.72%), and as ^{234}U in trace quantities (0.0055%) [1]. Uranium, at even natural levels, can provoke a radiation dose and chemical toxicity concern [2]. However, excessive amounts of uranium have been released into the environment through the activities associated with the nuclear industry and many other anthropogenic sources, such as mining and milling operations, disposal and discharge of industrial waste and effluent, disposal of medical wastes, military applications, and the use of phosphate fertilizer in agricultural land [1]. Therefore, understanding the behavior of natural radionuclides in soil-plant environmental system is essential for improving the radiological assessment and building the scientific knowledge of the migration of natural radioactive sources into plants around uranium mine [3]. Furthermore, plants have also been explored as an economical approach to remediation of soils contaminated with heavy metals and radionuclides. When contamination is a result, effective methodologies for environmental remediation are required.

The potential of some plants to accumulate uranium has been observed in several studies performed in field or laboratory conditions, supporting their possible use in uranium biomonitoring or phytoremediation of uranium contaminated soil or water [2, 4, 5]. For example, Shahandeh and Hossner [6] screened thirty four plant species for uranium accumulation from uranium contaminated soil, the results showed that sunflower (*Helianthus annuus*) and Indian mustard (*Brassica juncea*) accumulated more uranium than other plant species. However, domestic plant species in each area is different, and each plant species has different environmental adaptability. Little information is available on the accumulation of uranium in the plants around the uranium mill tailing in northeast China so far, and more extensive exploration is needed.

Specifically, the objective of this study was to collect and identify the plants that would serve as accumulators growing in the local natural environment of the uranium mining area. The identified plants could potentially be utilized for phytoremediation of uranium contaminated soil.

MATERIALS AND METHODS

Study area. The abandoned uranium mine is located in the northeast of China. The mine has a temperate continental monsoon climate with an annual average temperature of 8.2℃, an annual average rainfall of 800 mm. Ore minerals are mainly nasturan, uraninite, and uranium carbide stone. Uranium exists mainly in the form of dispersed adsorption and isomorphism. The uranium mine covers an area of approximately 0.25 km^2, and exploits approximately 3×10^4 t of uranium ore every year from 2006.

Sample collection and pre-treatment. The study was intended to identify plant species that growing near by the uranium mill tailing the potential to accumulate uranium. Soil and plants were collected from two points beside the uranium tailings accumulation site, one was about 10 m away, and the other was about 100 m away in autumn 2016. The sampling site was defined by a 5 m × 5 m square, the soil sample was taken at each corner and the intersection of its diagonals. Five partial soil samples weighing 0.5 kg each were collected from an average depth of 10 cm and mixed to obtain one composite sample with an amount of approximately 2.5 kg. In this square range, eight whole dominate plant species were collected, gently removed the soil particles adhering and packed in clean plastic bags. Then, the soil and plant samples were transported to the laboratory.

In the laboratory, the plant samples were washed thoroughly, first in running water followed by deionized water. Then each plant species was separate into two fractions, one stayed whole plant and the other divided into the following sections: root; stem; leaf; and blossoms if possible. *Erigeron annuus*, *Trifolium repens* and *Lepidium apetalum* had blossoms tissue, and *Cichorium intybus* showed basal leaves. All the sample parts were dried in an oven at 65 °C for 48 h. All the data in this paper were on this dry weight basis. The dried plants tissues were ground into a homogeneous powder for further analysis. The soil samples were initially air dried at room temperature for 2 weeks and subsequently oven-dried at 50 °C to a constant weight. Then soil were milled and sieved through a 0.149 mm mesh sieve.

Analysis procedure. Dried soil samples (0.1000 g) were digested with a mixture of HNO_3-HF-$HClO_4$ (3 mL of HNO_3, 1 mL of HF, 1 mL of $HClO_4$) in a Teflon pressure digest vessel at 165 °C for 4 h. The sample was then heated at 90 °C in an electric hot plate to expel residual HF and $HClO_4$; 1 mL of HNO_3 was added to the dry digestion mixture and diluted with ultrapure water (prepared with Milli-Q ultrapure water purification system) to obtain a final volume of 10 mL. Precisely weighed quantities of plant sample (0.2000 g) was digested with a mixture of HNO_3-H_2O_2 (2 mL of HNO_3, 1 mL of H_2O_2) using a high-pressure closed Teflon vessel at 165 °C for 4 h. The extracted solution, which was clear and free of organic substances, was left to cool, and their volumes was adjusted to 10 mL with ultrapure water. A digestion blank was prepared in every digestion cycle. All reagents used in the analysis were guaranteed reagents.

The total uranium analyses of extracting solutions (soil and plant samples) were performed on an inductivity coupled plasma mass spectrometer (ICP-MS, NexION 300D, Perkin Elmer, American). Values of uranium were expressed in μg/g DW. These chemical analyses were performed at the Analytical Laboratory of Beijing Research Institute of Uranium Geology, China.

Determination of transportation factor (TF) and concentration ratio (CR). This study anticipated the identification of plant species that were capable of accumulating uranium at high level. The accumulation ability was determined through calculation of transportation factor (TF) and concentration ratio (CR) [7]. TF was defined as the ratio of the elemental concentrations in aboveground plant tissues to those in roots, which was used determine the effectiveness of plants in migrating elements from the roots to the aerial parts [8]. CR referred to the ratio of the elemental concentrations in plant tissues to those in cultivated soil, which was expressed as the elemental accumulation and uptake in plants from the ambient soil [9].

RESULTS AND DISCUSSION

Uranium in soil and plants. The soil uranium concentrations of the two sampling sites, 10 and 100 m away from the mill tailing, were 15.2 and 10.7 μg/g, respectively. Compared with the soil background value of 3.03 μg/g in this region, the uranium content in the uranium mining area was higher. However, the average uranium content in the soil was considerably lower than that found in the literature for normal concentration range of 6.03 to 46.5 μg/g in the vicinity of a uranium mill tailing in south China [10]. According to the study of Shepherd et al. [11], considering the chemical toxicity of uranium to non-human biota, the soil uranium was suggested to 250 μg/g in dry soil. And based on this criterion, the uranium concentrations in the mine soils were lower.

Although uranium was not essential or beneficial to plants, many species would absorb uranium and incorporate it into their biomass along with other metals. The concentration of uranium in a plant had been shown to be dependent upon the degree of uranium contamination in the soil [2]. In this study, eight plant species were collected, and significant variation was found in absorption and accumulation pattern of uranium between different plant species and also between different tissues of the same species as shown in table 1. The mean concentration value of uranium (dry weight, DW) ranged from 42.7 μg/g (roots of *C. intybus*) to 0.180 μg/g (stems of *E. annuus*). Within the whole plants the highest uranium accumulation were found in the *A. mongolica* (21.0 μg/g DW), followed by those of *O. biennis* (16.6 μg/g DW), *A. scoparia* (13.0 μg/g DW) and *C. intybus* (10.5 μg/g DW). Therefore, the contents of uranium in Compositae were higher than that of other plants species in the investigated samples. This result was similar to early studies on the surrounding plants of an old uranium mine [1]. Among the plant tissues, the highest content of uranium was the roots,

followed by leaves and stems. This distribution characteristic of uranium in plants was similar to that of many other studies, including aquatic plants and trees [3, 12-14]. Obviously, the plants blossoms contain a lot of uranium, which could not be neglected. Reason why concentrations of uranium in roots was much higher than other tissues may include uranium adsorbed to roots cell walls [15]. The observed variation might be due to cumulative factors such as of plant species and organ concerned, and absorption, adsorption and other physicochemical, physiological and morphological mechanisms of metal retention in the tissues [1].

Uranium CR and TF in plants. It has been truly observed that uranium concentration in plants vary between species [1, 12]. Using CR values, some plant species could be considered high uranium accumulators as concentrations from plant tissues were higher than those found in soil [2]. As shown in table 2, the plant species *A. mongolica*, *C. intybus*, *O. biennis*, *C. album* and *T. repens* presented the CR values greater than 1. This characteristic could support the consideration of the species as uranium accumulators [16]. In these five plant species, the whole plants CR of *A. mongolica* and *O. biennis* were higher than 1, and roots CR of all were higher than 1, which also revealing a great phytoextraction ability. In the aerial parts of plants, *C. intybus* showed high CR of leaves and *T. repens* showed high CR of stems. Compared with the data in IAEA Technical Reports Series No.472 [17], which mentioned the results of stems and leaves CR in the plants were range from 0.0086 to 0.41 with an average of 0.036.

The TF indicated uranium translocation ability from roots to aerial parts. In this study, the mean values of TF were in the range from 0.626 (leaves TF of *L. apetalum*) to 0.0156 (stems TF of *O. biennis*), which were lower than 1. In the view of both CR and TF were usually >1 in accumulators, the species in this study were relatively not competent. However, the high values of TF might be due to the soil characteristics such as pH, and phosphate, carbonate, and organic matter content, which affects the chemical form of uranium along with the plant's physiological characteristics like nutrient uptake strategies and organic acid exudation [18]. Moreover, the rate of uranium translocation from roots to upper parts was probably species-dependant [12]. On the other hand, the uranium concentrations in roots of the sampling plants were many fold higher than the aerial parts of the same plant species, and then the TF values of the aerial parts were much lower than 1. This characteristic of most plants had also been reported in other studies. For example, Shahandeh and Hossner [6] reported that uranium concentration in roots of different plants collected from the same site was 30-50 times higher than uranium concentration in shoots. Therefore, if the screening of uranium accumulation plants from local plant species around mill tailing, the high CR of whole plants could be considered, for example *A. mongolica* and *O. biennis* would be a good choice.

TABLE 1
Uranium concentrations in plant species (μg/g, value on dry weight basis, DW; mean±SD)

Family	Plant species	Stems	Leaves	Roots	Blossoms	Whole plants
	Erigeron annuus	0.180±0.0690	2.31±1.85	12.8±3.69	0.656±0.404	5.82±1.87
Asteraceae	*Artemisia scoparia*	0.354±0.203	3.17±2.33	7.47±1.04	--	13.0±11.1
(or Compositae)	*Artemisia mongolica*	1.07±0.902	7.77±6.14	36.9±5.95	--	21.0±14.1
	Cichorium intybus	--	9.18±6.62	42.7±30.1	--	10.5±5.88
Onagraceae	*Oenothera biennis*	0.773±0.657	5.17±4.67	73.3±7.75	--	16.6±9.03
Chenopodiaceae	*Chenopodium album*	1.50±0.740	5.95±3.23	14.9±6.91	--	5.01±2.11
Leguminosae	*Trifolium repens*	1.94±1.11	4.02±2.78	14.7±1.95	0.835±0.475	7.37±3.74
Brassicaceae	*Lepidium apetalum*	0.553±0.303	3.14±2.01	4.66±0.640	0.914±0.576	3.31±1.83

"--" means no data.

TABLE 2
Uranium CR of plants (mean±SD)

Plant species	Stems	Leaves	Roots	Blossoms	Whole plants
Erigeron annuus	0.0134±0.00300	0.158±0.115	0.969±0.117	0.0466±0.0231	0.438±0.0684
Artemisia scoparia	0.0254±0.0113	0.220±0.142	0.580±0.0209	--	0.880±0.705
Artemisia mongolica	0.0726±0.0570	0.533±0.381	2.85±0.0360	--	1.48±0.832
Cichorium intybus	--	0.639±0.400	2.98±1.81	--	0.756±0.323
Oenothera biennis	0.0525±0.0416	0.347±0.301	4.90±4.38	--	1.19±0.490
Chenopodium album	0.109±0.0381	0.429±0.175	1.09±0.344	--	0.370±0.0987
Trifolium repens	0.139±0.0618	0.282±0.166	1.19±0.358	0.0599±0.0263	0.535±0.196
Lepidium apetalum	0.0398±0.0164	0.222±0.117	0.362±0.0135	0.0648±0.0332	0.238±0.100

"--" means no data.

TABLE 3
Uranium TF of plants (mean±SD)

Plant species	Stems	Leaves	Blossoms
Erigeron annuus	0.0136±0.00146	0.151±0.101	0.0459±0.0183
Artemisia scoparia	0.0445±0.0210	0.389±0.258	--
Artemisia mongolica	0.0257±0.0203	0.189±0.136	--
Cichorium intybus	--	0.210±0.00693	--
Oenothera biennis	0.0156±0.00547	0.0795±0.00974	--
Chenopodium album	0.0990±0.00375	0.381±0.0403	--
Trifolium repens	0.145±0.0952	0.305±0.230	0.0624±0.0407
Lepidium apetalum	0.112±0.0496	0.626±0.345	0.183±0.0985

"--" means no data.

CONCLUSION

The average uranium content in soil was 13.0 μg/g, which was 3-5 times of the background value in the study region. It was found that the uranium concentration detected in the studied root samples showed several times or tens of times higher than that observed in their above ground parts, and uranium concentrations observed in Compositae were relatively high.

In this study, CR values of five plant species sampled were higher than 1, but all the TF values were lower than 1. Considering the CR and TF of the eight sampling plant species, *A. mongolica* and *O. biennis* would be promising candidates for phytoremediation. With economical and technical benefit, the study would be of great help to clean up uranium contaminated regions using the studied plant species in future environmental projects.

ACKNOWLEDGEMENTS

This study was financially supported by Beijing Municipal Natural Science Foundation (7172146) and National Natural Science Foundation of China (41672228). We are grateful to the Analytical Laboratory of Beijing Research Institute of Uranium Geology in China for their testing works.

REFERENCES

[1] Favas, P.J.C., Pratas, J.O., Mitra, S., Sarkar, S. K. and Venkatachalam, P. (2016) Biogeochemistry of uranium in the soil-plant and water-plant systems in an old uranium mine. Science of the Total Environment. 568, 350-368.

[2] Caldwell, E.F., Duff, M.C., Ferguson, C.E., Coughlin, D.P., Hicks, R.A. and Dixon, E. (2012) Bio-monitoring for uranium using stream-side terrestrial plants and macrophytes. Journal of Environmental Monitoring. 14, 968-976.

[3] Al-Hamarneh, I.F., Alkhomashi, N. and Almasoud, F.I. (2016) Study on the radioactivity and soil-to-plant transfer factor of ^{226}Ra, ^{234}U and ^{238}U radionuclides in irrigated farms from the northwestern Saudi Arabia. Journal of Environmental Radioactivity. 160, 1-7.

[4] Sreedhar, Y., Nagaraju, A., Thejaswi, A. and Bhargava, Y. (2017) Reclamation of abandoned mine land: a case study from Tummalapalle uranium mining area, Cuddapah district, Andhra Pradesh, south India. Fresen. Environ. Bull. 26, 1373-1382.

[5] Jha, V.N., Tripathi, R.M., Sethy, N.K. and Sahoo, S.K. (2016) Uptake of uraniumby aquatic plants growing in fresh water ecosystem around uranium mill tailings pond at Jaduguda. Science of the Total Environment. 539, 175-184.

[6] Shahandeh, H. and Hossner, L.R. (2002) Role of soil properties in phytoaccumulation of uranium. Water, Air, and Soil Pollution. 141, 165-180.

[7] Yan, D., Zhao, Y., Wang, S., Xu, D. and Zhou, L. (2014) Characteristics of cesium and strontium transport in a soil-soybean system. Fresen. Environ. Bull. 23, 175-183.

[8] Wang, X., Chen, C. and Wang, J. (2017) Phytoremediation of strontium contaminated soil by *Sorghum bicolor* (L.) Moench and soil microbial community-level physiological profiles (CLPPs). Environmental Science and Pollution Research. 24, 7668-7678.

[9] Trok, M., Smodi, B. and Eler, K. (2011) Natural radionuclides in trees grown on a uranium mill tailings waste pile. Environmental Science and Pollution Research. 18, 819-826.

[10] Li, G., Hu, N., Ding, D., Zheng, J., Liu, Y., Wang, Y. and Nie, X. (2011) Screening of plant species for phytoremediation of uranium, thorium, barium, nickel, strontium and lead contaminated soils from a uranium mill tailings repository in south China. Bulletin of Environmental Contamination and Toxicology. 86, 646-652.

[11] Sheppard, S. C., Sheppard, M.I., Gallerand, M. and Sanipelli, B. (2005) Derivation of ecotoxicity thresholds for uranium. Journal of Environmental Radioactivity. 79, 55-83.

[12] Shtangeeva, I. (2010) Uptake of uranium and thorium by native and cultivated plants. Journal of Environmental Radioactivity. 101, 458-463.
[13] Erne, M., Smodi, B. and Trok, M. (2011) Uptake of radionuclides by a common reed (*Phragmites australis* (Cav.) Trin. ex Steud.) grown in the vicinity of the former uranium mine at Zirovski vrh. Nuclear Engineering and Design. 241, 1282-1286.
[14] Favas, P. J.C., Pratas, J. O., Varun, M., D'Souza, R. and Paul, M.S. (2014) Accumulation of uranium by aquatic plants in field conditions: Prospects for phytoremediation. Science of the Total Environment. 470, 993-1002.
[15] Ebbs, S.D., Brady, D.J. and Kochian, L.V. (1998) Role of uranium speciation in the uptake and translocation of uranium by plants. Journal of Experimental Botany. 49, 1183-1190.
[16] Trotta, A., Falaschi, P., Cornara, L., Minganti, V., Fusconi, A., Drava, G. and Berta, G. (2006) Arbuscular mycorrhizae increase the arsenic translocation factor in the As hyperaccumulating fern *Pteris vittata* L. Chemosphere. 65, 74-81.
[17] IAEA (2010) Handbook of parameter values for the prediction of radionuclide transfer in terrestrial and freshwater environments. Vienna, IAEA Technical Reports Series No.472.
[18] Duquene, L., Vandenhove, H., Tack, F., Van der Avoort, E., Van Hees, M. and Wannijin, J. (2006) Plant-induced changes in soil chemistry do not explain differences in uranium transfer. Journal of Environmental Radioactivity. 90, 1-14.

Received: **18.12.2017**
Accepted: **06.02.2018**

CORRESPONDING AUTHOR

Xiaoyan Jiang
Department of Radiology,
National Institute for Radiological Protection,
Chinese Center for Disease Control and Prevention,
Beijing 100088 – China

e-mail: fangsheshengtai@126.com

© by PSP Volume 27 – No. 5/2018 pages 3107-3116 Fresenius Environmental Bulletin

PREDICTING SITE INDEX FOR ORIENTAL SPRUCE (*PICEA ORIENTALIS* L. (LINK)) USING ECOLOGICAL FACTORS IN THE EASTERN BLACK SEA, TURKEY

Ismet Yener[1,*], Lokman Altun[2]

[1]Artvin Coruh University, Faculty of Forestry, 08100, Artvin, Turkey
[2]Karadeniz Technical University, Faculty of Forestry, 61080, Trabzon, Turkey

ABSTRACT

Oriental spruce is a very important commercial timber species in Turkey. Its distribution area is recognized as one of the 25 biodiversity hotspots in the world. The present study aims to model site index (SI) of oriental spruce stands using some topographic, climatic and edaphic variables in a mountainous ecoregion of the Eastern Black Sea, Turkey. Within this scope, 60 sample plots were visited in the study area, and the height, diameter at breast height and age of sample trees were measured. A soil pit was also dug in each sample plot for analyzing soil properties. Then, some physical (sand, silt, clay, plant available water capacity) and chemical properties (pH, electrical conductivity, organic matter content and exchangeable cations) were examined on each soil sample. Finally, regression tree and multiple linear regression methods were used to model SI. Their adjusted coefficient of determination (R^2_{adj}) values were found to be as 0.70 and 0.53, respectively. According to the outperformed model, longitude, soil K^+ content and landform were the most important factors affecting the SI. The results show that the regression tree model which is proposed in the present study may be used by forest planners and silviculture experts as a decision support tool for scheduling proper forestry activities.

KEYWORDS:
Site index, oriental spruce, regression tree, multiple linear regression.

INTRODUCTION

Forest site quality is defined as the sum of factors, including climatic, edaphic, topographic and biotic, affecting the capacity to produce forests or other vegetation [1]. The most-used and most-preferred indicator to measure forest productivity for pure and even-aged stands is site index (SI) described as top height at standard age calculated from average height of 100 dominant trees per hectare [2, 3]. The SI method can be used for only forested areas but not unforested areas because of fire, insects, disease and poor stocking [4, 5]. Therefore, there is a need for an indirect estimation using ecological variables. One of the approaches being analytical is modeling the SI as a function of miscellaneous climatic, topographic and edaphic variables [6-8].

Due to complicated interactions between forest growth and ecological factors, nonparametric techniques such as regression tree (RT), fuzzy logic, neural network and general additive model have been increasingly used recently by some researchers [9-16] to estimate SI from environmental variables in addition to parametric statistical techniques such as multiple linear regression (MLR). However, the nonparametric RT technique is better than the parametric techniques as it allows for interactions and nonlinear relations among many predictors [17].

Oriental spruce is one of the most important timber species and spreads from Georgian border to Ordu-Melet River in Turkey [18-20]. Its area coverage is 334472 ha according to the Turkey's national forest inventory [21]. Although many studies have been carried out to evaluate site productivity using environmental factors for many species so far, studies focused on oriental spruce (*Picea orientalis* L. (Link)) are very few. Therefore, there is an urgent need for predicting site index of that species practically.

The aim of this study was; i) to develop site index models from ecological factors using MLR and RT, and ii) to compare these models in terms of predictive performance. Hence, forest owners could make wise decision about their land management and land-use planning.

MATERIALS AND METHODS

Site description. The study area is located between 40°34'-40°57' N latitudes and 37°52'-39°25' E longitudes. It covers Colchis part of Black Sea Region including Ordu, Giresun, and Trabzon provinces (Figure 1). The elevation of oriental spruce sites changes between 800 and 2000 m above sea level [22]. This region is characterized by mountain-

ous topography with steep slopes. Soil parent material varies widely from sedimentary marl, conglomerate and sandstone to igneous granite, basalt, andesite, dacite, rhyodacite and diabase [23]. The soil texture ranges from clay loam, silty clay loam to sandy loam, loam and loamy clay. Humus form includes both moder and mulls [24]. The soil in the region is generally acidic due to high precipitation causing leaching of nutrients [25].

The study area, accommodating many endemic species, located in the one of the 200 ecological regions having top priority in the world. It is also included in the 25 biodiversity hotspots requiring conservation and protection according to IUCN [26]. The study area shows Eastern Black Sea climate under Black Sea macroclimate type, temperate in winter, warmer in summer and quite rainy in all seasons. The annual mean temperature and the annual mean precipitation ranges between 5 - 10 °C and 800 - 2100 mm, respectively [27, 28]. The growing season in the region is about six months (from May to October).

The studied spruce stands were even-aged, naturally regenerated and uniformly stocked having no evidence of fire, storm or bug damages. Along with oriental spruce, beech (*Fagus orientalis*), fir (*Abies nordmanniana)*, Scotch pine (*Pinus sylvestris)* and alder (*Alnus glutinosa)* species existed in these stands. However, they were dominated by one species; oriental spruce. Regarding understory vegetation, *Sorbus aucuparia, Prunus officinalis, Ilex colchica, Sambucus nigra, Vaccinium myrtillus, Lonicera caucasica, L. xylosteum, Ribes biebersteinii, R. Orientale, Rhododendron ponticum, and R. Luteum* species were widely spread on the forest floor [29].

Data collection and analyses. The sampling and field measurements were performed during the summer season of 2010 and 2011. For this, 60 circular sample plots with 11.28 m radius (0.04 ha) were determined using stratified random sampling method. Some topographic, climatic and edaphic variables were used to model SI which means top height at 100 years old [30]. Average age of the stands was calculated for four dominant trees in a sample plot by counting annual rings at diameter breast height (1.3 m) and then 10 years were added for seedling age. Top height of the stands was calculated by averaging the height of these four dominant trees in each sample plot [31]. Then, SI was calculated from SI curves developed by Akalp [32] based on anamorphic guide curve method.

In each sample plot; aspect (ASP) [33], slope position (LFRM), elevation (ELEV) and slope (SLP) were determined [34]. For regression analysis, the aspect values (azimuth) were transformed using the equation developed by Beers et al. [35]. Slope positions were determined as distance to the ridge (from the ridge=0 to the bottom=100) [36]. Coordinates (LAT and LONG) at each sample plots were recorded by handheld GPS with 5 m accuracy.

In each sample plot a soil pit was dug up to bedrock, described according to Çepel [37], and a disturbed soil sample was taken at 0-15 cm soil depth. Soil samples were air-dried and sieved through 2-mm mesh before analysis. All measurements and observations about soil profile, including soil depth, litter layer thickness, humus type, stoniness, root intensity, soil structure were recorded in a soil inventory sheet.

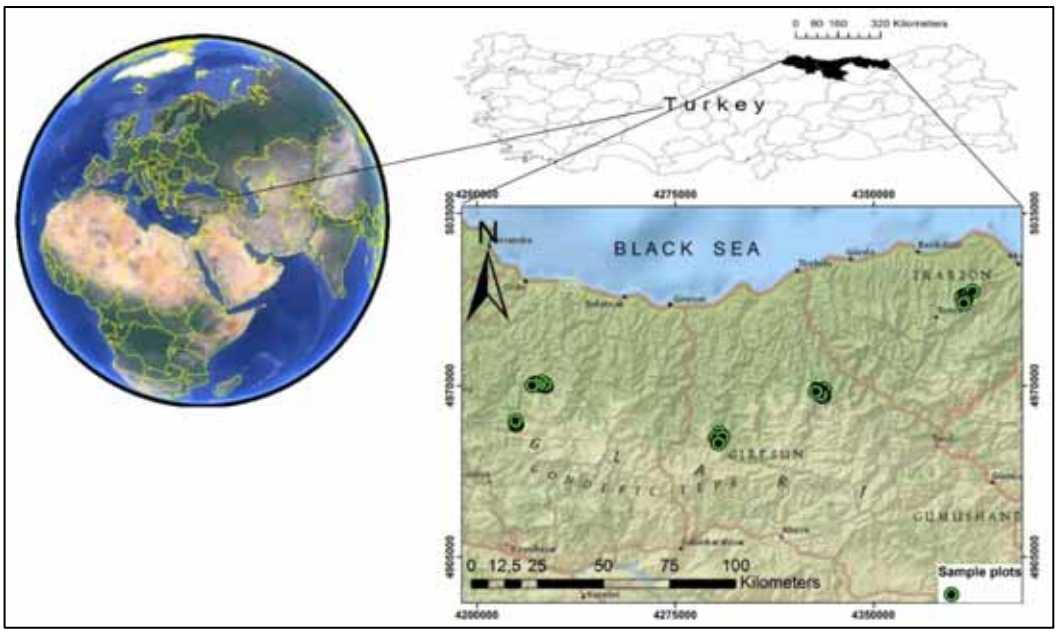


FIGURE 1
Sampling sites in the study area (Canik-Giresun Mountainous Ecoregion)

Some physical and chemical analyses were also conducted on soil samples. Soil texture analysis was performed according to Bouyoucos hydrometer method [38]. Soil acidity (pH) was determined by glass electrode (1/2.5 soil-water) in distilled water, and organic matter (OM) was determined by Walkley-Black wet digestion method [39]. Available water capacity [40] was calculated as the difference between field capacity and permanent wilting point by pressure desorption method [41]. Soil exchangeable cations were extracted using 1 N ammonium acetate and measured by flame-photometer (for Na^+ and K^+) and atomic absorption spectrophotometer (for Mg^{++} and Ca^{++}) [42].

Annual mean temperature (TEMP), annual mean precipitation (PREC) and annual mean minimum-maximum temperature were obtained from meteorological stations closest to the sampling plots. Using these, temperature and precipitation in growing season (TEMPV and PRECV) were computed. Then, climatic data were extrapolated using 5 °C km^{-1} temperature lapse rate and 450 mm km^{-1} increase in precipitation according to Erinç [43] and Akman [44]. Actual evapotranspiration (AET) was also computed according to Thornthwaite [45] method.

The relationship between SI of oriental spruce and 24 ecological variables was examined tabularly. First, simple correlation analysis was used to investigate the individual effects of ecological variables on SI of oriental spruce. Finally, multiple linear regression and regression tree techniques were used to model SI from ecological variables. SPSS 20.0 [46] and DTREG v19 [47] were used for the statistical analyses.

RESULTS AND DISCUSSION

Descriptive statistics for the topographic, edaphic and climatic variables were given in Table 1. According to the table, SI for oriental spruce ranged from 14.4 to 30.3 m. Average SI was determined as 20.3 m. Site productivity classes of total 60 sample plots were determined as low (38-plot), medium (16-plot) and high (6-plot).

Relations between SI and ecological variables. Correlation analysis results showed that SI of oriental spruce was positively correlated with longitude, land slope, distance to the ridge, annual mean temperature, mean temperature during growing season, mean total precipitation in growing season, AET, sand, pH and soil depth (Table 2). On the other hand, the elevation, aspect, silt, organic matter, plant available water capacity and K^+ were negatively correlated with SI. No correlations were found between SI and latitude, annual mean total precipitation, soil stoniness, Na^+, Ca^{++} and Mg^{++}.

TABLE 1
Descriptive statistics for variables

Variables and their abbr.	Units	Minimum	Maximum	Mean	SD*
Site Index	m	14.4	30.3	20.3	3.8
Longitude	m	403557	534736	469006.3	45860.8
Latitude	m	4490327	4533588	4507569.3	13460.4
Elevation	m	1333	1939	1660.9	146.2
Slope	%	1	75	35.1	19.7
Distance to Ridge	m	0.0	100.0	47.1	31.2
Aspect	°	0	351	203.0	102.2
Temperature	°C	4.9	7.6	6.1	0.7
Precipitation	mm	1639	2115	1932.0	128.7
Temp in Growing Season	°C	10.1	12.9	11.4	0.7
Precipitation in Growing Season	mm	772	1030	932.4	72.6
Actual Evapotranspiration	mm	470	549	503.3	21.4
Thornthwaite Moisture Index		200	350	284.5	36.9
Sand	%	45	86	68.5	9.3
Clay	%	3	31	16.8	5.9
Silt	%	7	27	15.1	4.9
Organic Matter	%	2.9	22.0	8.1	4.1
pH		4.0	5.4	4.8	0.4
Available Water Capacity	%	5	19	12.1	3.7
Soil Depth	m	15	130	95.3	26.5
Stoniness	%	5.0	52.5	25.7	17.5
Na^+	ppm	49	86	63.5	9.1
K^+	ppm	22	218	68.7	41.0
Ca^{++}	ppm	2	2117	441.5	505.3
Mg^{++}	ppm	5	453	124.9	110.0

*Standard deviation

TABLE 2
Pearson correlation between ecological variables and SI

Variable		(1)	(2)	(3)	(4)	(5)	(6)	(7)	(8)	(9)	(10)	(11)	(12)	(13)
(1)	SI	1	**.36***	-.07	**-.30***	**.30***	**.49***	**-.29***	**.42***	.22	**.40***	**.26***	**.41***	-.01
(2)	LONG		1	**.61***	**.30***	-.07	-.01	-.02	.25	**.82***	-.25	**.84***	-.24	**.69***
(3)	LAT			1	.14	**-.53***	-.23	-.11	-.31	.22	-.25	.22	**-.30***	**.29***
(4)	ELEV				1	**-.28***	**-.58***	**.36***	**-.96***	**.69***	**-.98***	**.64***	**-.97***	**.87***
(5)	SLP					1	**.45***	-.02	**.43***	.02	**.37***	.05	**.42***	-.16
(6)	LFRM						1	**-.26***	**.65***	-.20	**.63***	-.16	**.64***	**-.41***
(7)	ASP							1	**-.32***	.20	**-.35***	.18	**-.33***	.28
(8)	TEMP								1	**-.55***	**.99***	**-.50***	**.99***	**-.79***
(9)	PREC									1	**-.59***	**.99***	**-.56***	**.94***
(10)	TEMPV										1	**-.54***	**.99***	**-.82***
(11)	PRECV											1	**-.50***	**.92***
(12)	AET												1	**-.79***
(13)	MITH													1
(14)	SAND													
(15)	CLAY													
(16)	SILT													
(17)	OM													
(18)	pH													
(19)	AWC													
(20)	MDEP													
(21)	STON													
(22)	Na^{+}													
(23)	K^{+}													
(24)	Ca^{++}													
(25)	Mg^{++}													

Variable		(14)	(15)	(16)	(17)	(18)	(19)	(20)	(21)	(22)	(23)	(24)	(25)
(1)	SI	**.31***	-.22	**-.30***	**-.39***	**.30***	**-.26***	**.31***	-.20	-.18	**-.31***	.01	-.09
(2)	LONG	.08	-.09	-.06	-.08	-.03	-.04	.16	-.13	-.18	-.14	-.20	**-.28***
(3)	LAT	-.18	-.03	**.31***	**.46***	**-.62***	**.36***	-.12	-.02	.15	-.09	**-.36***	**-.33***
(4)	ELEV	**-.32***	.20	**.27***	.08	.02	.20	-.05	.00	-.12	.07	-.15	-.09
(5)	SLP	**.29***	-.09	**-.34***	**-.51***	**.50***	**-.43***	.16	.01	-.24	-.07	.17	.08
(6)	LFRM	**.29***	**-.28***	-.20	-.14	.24	-.18	.17	.02	-.12	-.07	.16	.03
(7)	ASP	-.10	.10	.05	-.05	.04	.16	-.09	.13	-.15	.08	-.08	-.01
(8)	TEMP	**.38***	-.19	**-.36***	**-.26***	.19	**-.30***	.13	-.02	.01	-.07	.22	.13
(9)	PREC	.01	.01	-.07	-.22	.22	-.11	.17	-.15	**-.29***	-.08	-.13	-.19
(10)	TEMPV	**.36***	-.19	**-.34***	-.20	.12	**-.27***	.11	-.03	.06	-.08	.19	.11
(11)	PRECV	.04	.00	-.10	-.25	.24	-.14	.18	-.15	**-.30***	-.09	-.12	-.19
(12)	AET	**.38***	-.18	**-.37***	-.25	.17	**-.29***	.13	-.02	.03	-.07	.22	.13
(13)	MITH	-.15	.09	.09	-.05	.08	.06	.05	-.07	-.18	-.02	-.16	-.18
(14)	SAND	1	**-.80***	**-.83***	.05	.15	**-.57***	.22	**-.35***	-.17	-.22	-.17	**-.28***
(15)	CLAY		1	**.42***	**-.29***	.01	**.39***	-.21	**.26***	.15	**.25***	.22	**.33***
(16)	SILT			1	.18	-.25	**.53***	-.20	**.30***	.09	.14	.10	.14
(17)	OM				1	**-.47***	**.29***	**-.36***	.20	**.37***	.16	-.18	-.05
(18)	pH					1	**-.41***	**.29***	.08	-.04	.14	**.49***	**.42***
(19)	AWC						1	-.22	**.26***	.16	.10	-.14	-.08
(20)	MDEP							1	**-.34***	-.11	**-.36***	-.04	-.10
(21)	STON								1	.15	**.37***	**.26***	**.35***
(22)	Na^{+}									1	.02	**.32***	**.29***
(23)	K^{+}										1	**.31***	**.41***
(24)	Ca^{++}											1	**.78***
(25)	Mg^{++}												1

* correlation is significant at the 0.05 or 0.01 level.

Regarding the topographic factors; landform, longitude, elevation, land slope and slope aspect were correlated with SI. The positive effect of the landform (distance to ridge) on SI (r=0.49) can be attributed to decrease in soil skeleton and increase in soil depth [1]. Similar results were found by some other researchers [48, 49]. The positive correlation between longitude and SI (r=0.36) can be attributed to decrease both in land slope and elevation. The negative correlation between elevation and SI (r=-0.30) may be related to negative climatic conditions affecting growing period, soil formation and micro-organism activities [1]. A surprising correlation between aspect and SI (r=-0.29) was found. Although oriental spruce is among the shade tolerant tree species, SI increased from north to south aspects. Similar results were found by some other researchers [5, 50]. While Vanderschaaf and Prisley [50] explained that issue with increasing growing period and photosynthesis rate, the others [51, 52] associated it with improving ecological conditions resulted from warming in south aspects especially in daytimes in case of appropriate humidity in mountainous areas.

Among the climatic factors; temperature, temperature in growing season, precipitation in growing season and actual evapotranspiration were positively correlated with SI. AET is the sum of transpiration and evaporation under natural condition depending on amount of soil water [53].

The positive effect of AET on SI (r=0.41) was an expected finding like mentioned in some studies [54-56]. This effect can be attributed to high temperature besides effective rainfall positively affecting the growing period, photosynthesis, litter decomposition, formation of soil organic matter, carbon balance, some physiological and enzymatic activities [57]. The temperature is also known one of the most important stress factors that the plants are mostly vulnerable [58].

While silt (r=-0.30), organic matter (r=-0.39), available water capacity (r=-0.26) and potassium content (r=-0.31) were negatively correlated with SI, pH (r=0.30) and soil mechanical depth (r=0.31) were positively correlated with it. The positive effect of pH and mechanical soil depth on SI was also documented by other studies [8, 59, 60]. The negative effect of increasing organic matter content on SI may be related to decreasing pH affecting nutrient take up by plants.

Modeling SI. Topographic, climatic, edaphic and integrated models (Eq. (1), Eq. (2), Eq. (3), Eq. (4)) were developed by MLR stepwise method. Adjusted R^2 (R^2_{adj}) for these models were found as to be 0.43, 0.45, 0.25 and 0.53, respectively (Table 3).

Topographic;

$$SI=629.99+0.00007*LONG+0.0001*LAT -0.012*ELEV \quad (1)$$

Climatic;

$$SI=-41.54+4.006*TEMP+0.019*PREC \quad (2)$$

Edaphic;

$$SI= 28.015-0.458*OM-0.238*CLAY \quad (3)$$

Integrated;

$$SI=-236.3+0.00003*LONG+13.357*TEMPV +0.056*ELEV-.020*K^+ \quad (4)$$

In this study, 43.3% of the variation was explained by topographic factors including longitude, latitude and elevation. Many studies have used topographic variables to model SI. Klinka et al. [61], for example, computed SI variance for Engelmann spruce as 64% using elevation and latitude. This value was computed by Ercanli et al. [59] for oriental spruce as 65.6% with slope, elevation and aspect variables. However, SI variance modeled by topographic factors could be lower as much as 24.5%, as well [62].

The climatic factor, also an important variable affecting site index, has been used in a number of studies. Our climatic model explains the 45.4% of the variation within the SI. The positive effects of temperature and precipitation on plant metabolism and photosynthesis rates are well-known phenomena [1]. In addition to these, models may include other climatic variables such as actual evapotranspiration, moisture index, water surplus and water deficit [54-56].

TABLE 3
Parameters of MLR and RT models

MLR Models	R^2_{adj}	RMSE	Unstandardized Coefficient		F	RT Models	R^2_{adj}	RMSE
			B	SE				
Topographic	0.433	2.87			16.01	**Topographic**	0.549	2.53
Constant			629.999	154.934		LONG		
LONG			0.00007	0.0		LFRM		
LAT			0.0001	0.0		ASP		
ELEV			-0.012	0.003				
Climatic	0.454	2.82			25.48	**Climatic**	0.519	2.62
Constant			-41.541	9.136		PRECV		
TEMP			4.006	0.592		MITH		
PREC			0.019	0.003		AET		
Edaphic	0.248	3.31			10.72	**Edaphic**	0.414	2.89
Constant			28.015	1.813		OM		
OM			-0.458	0.109		K^+		
CLAY			-0.238	0.077				
Integrated	0.535	2.60			20.39	**Integrated**	0.700	2.07
Constant			-236.3	50.3		LONG		
LONG			0.00003	0.0		K^+		
TEMPV			13.357	2.6		LFRM		
ELEV			0.056	0.013				
K^+			-0.020	0.008				

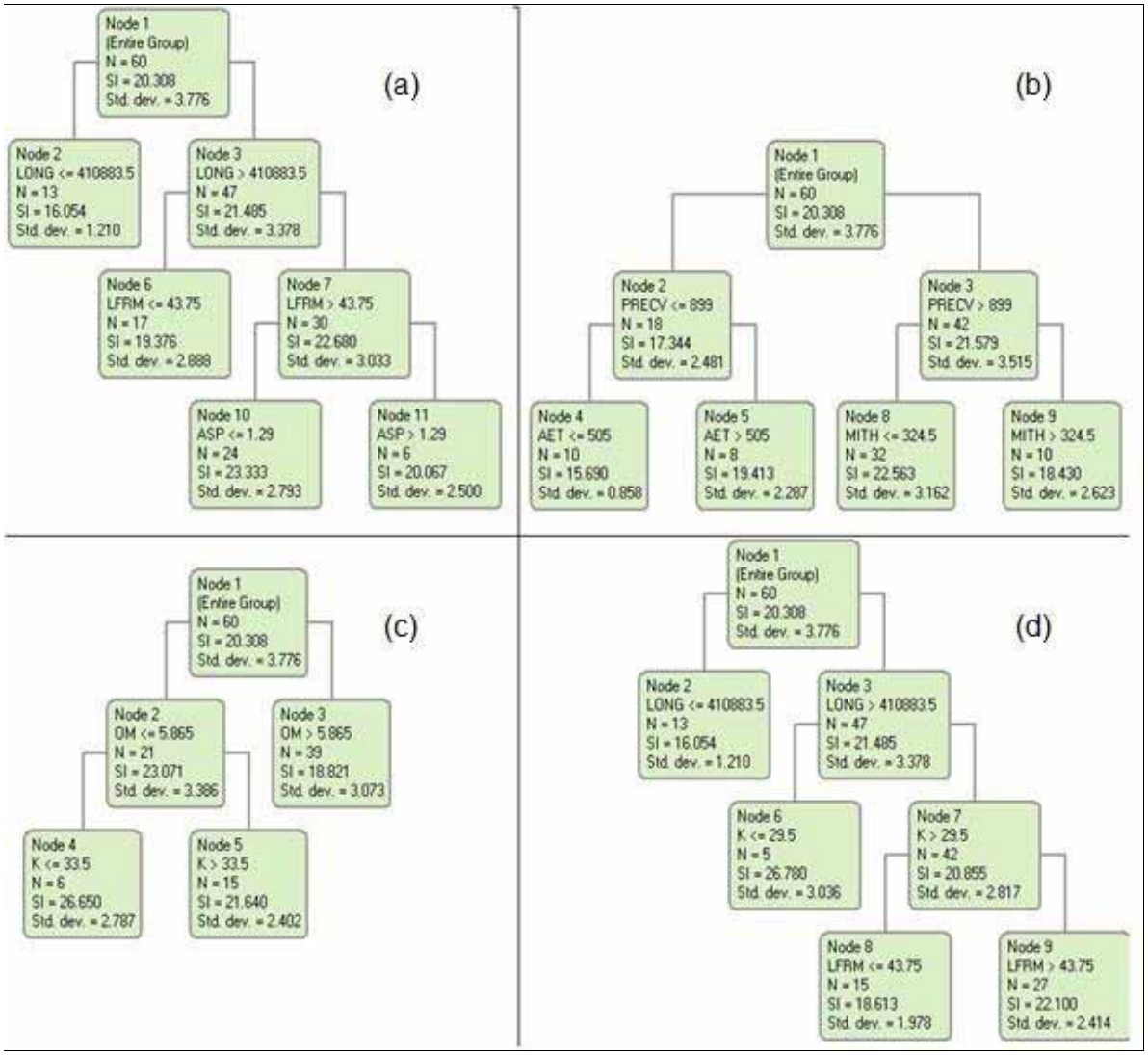


FIGURE 2
Regression tree models (a; topographic, b; climatic, c; edaphic, d; integrated)

Edaphic variables had the lowest effect on the SI compared to the other ecological variables in the present study. The edaphic model only explained 24.8% of the variation in SI of oriental spruce. Many models developed by the others included only the forms of edaphic variables with variable variation rate. Sanchez-Rodriguez et al. [60], for example, showed that soil depth, pH, total N and foliar P concentration accounted for 60% of SI variation for Monterey pine. In the same study, 42.5% of the variation in SI was explained by fine textured soil, silt content in B_s horizon and organic carbon content in A_{el} for Scotch pine. Another model developed by Chen et al. [7] which included soil moisture regime and soil nutrient regime along with topographic variables, accounted for 61% of the total variation in SI.

RT analysis was also performed to model SI using ecological variables. The integrated, topographic, climatic and edaphic models accounted for 55%, 52%, 41% and 70% respectively. RT models can be seen in Table 3 and Figure 2. Integrated RT model including LONG, K^+, LFRM accounted for 70% of the variation in SI of oriental spruce. The integrated RT model having the highest coefficient of determination included at least one variable from each group except for climatic group.

The primary split for the integrated SI model (Fig. 2d) was based on longitude, with the highest SI (21.49 m) on the sample plots whose longitude was bigger than 410833.5 m. After this point, it was based on soil K^+ content, with the highest SI (26.78 m) on the plots whose K^+ content was lower than 29.5 ppm. The last split was based on LFRM (distance to ridge). The highest SI was 22.10 m on the plots whose distance to ridge was longer than 43.75 m. In this model, the most important factor affecting SI was longitude. Plots, whose longitude was bigger than 410883.5 m, had slight slopes and long distance to ridge. Moreover, it positively affected the soil AWC, OM and stoniness. Aertsen et al. [9], also reported similar results like that. In their study, the longitude explained the largest proportion of the total variance.

In the present study, all RT models were superior to MLR models in terms of R^2_{adj} and RMSE values (Table 3). Similar results were found by other researchers [62, 63]. They reported that determining the effect of any ecological variable on SI was difficult using traditional statistical techniques even with a comprehensive listing of interaction terms [64].

Topographic RT model (Figure 2a) accounted for 54.9% of the variation in site index with a RMSE value of 2.53 m. It included longitude, landform and aspect variables. The increase in SI with longitude may be related to the amount of precipitation in the growing season (r=0.84). Landform and aspect also affect weathering, soil formation, soil texture and growing period [1].

Edaphic RT model (Figure 2c), consisting of OM and K^+, explained 41.4% of the variance. OM was also included in edaphic MLR model. The negative effect of OM on SI may be related to relatively low pH (r=-0.47). It affects exchangeable bases uptake, thus giving rise to phytotoxic effect [65]. Mg content was determined as the most important factor affecting growth of the chestnut stands in Spain using RT model explaining 42% of the SI variance [10].

Along with the edaphic and topographic models, a climatic model (Figure 2b), accounting for 51.9% of the variance, was also developed. It consisted of PRECV, MITH and AET. Although a slightly increase in precipitation in growing season positively affected SI, an increase in moisture index negatively affected it. AET was directly related to annual mean temperature which had important effects on photosynthesis, growing season period, soil formation and microbial activity. The RT model developed by Mckenny and Pedlar [64] for jack pine also included precipitation and temperature in growing season along with the total depth of mineral soil.

CONCLUSION

Compared with parametric and nonparametric statistical techniques, RT was found to be superior to MLR for predicting SI in all model groups. Among the model groups, integrated models outperformed to the other groups but they were not practical on-the-ground. Thus, it is better to use topographic or climatic models as they have both easily accessible and cost-effective variables. In this study, we developed eight MLR and RT models consisting topographic, climatic, edaphic and integrated variables. All of them are site-specific, thus they are only valid for the areas similar to ours. Specifically, afforestation sites and unstocked forestlands are suitable for running our models. However, these models should be improved and widen to other regions by additional studies in the future.

ACKNOWLEDGEMENTS

This research was supported by Karadeniz Technical University Scientific Research Project Unit, Turkey (Ref. No. 2009.113.001.05). We thank Dr. Teoman Guner and his staff for allowing us to work in the laboratory and their valuable help; Dr. Kursad Ozkan and Dr. Aydın Kahriman for their contribution in statistical analyses. We would also like to thank Can Vatandaslar for his valuable proofreading, and Cambasi, Ekindere, Akilbaba, Harsit and Vakfikebir Forest Enterprises for granting access permission to the forests and providing us accommodation.

REFERENCES

[1] Spurr, S.H. and Barnes, B.V. (1991) Forest ecology. Wiley, New York.

[2] Chen, H.Y.H., Klinka, K. and Kabzems, R.D. (1998) Site index, site quality, and foliar nutrients of trembling aspen: relationships and predictions. Canadian Journal of Forest Research-Revue Canadienne De Recherche Forestiere. 28(12), 1743-1755.

[3] Monserud, R.A., Moody, U. and Breuer, D.W. (1990) A soil-site study for inland Douglas-fir. Canadian Journal of Forest Research. 20(6), 686-695.

[4] Kayahara, G.J., Klinka, K. and Marshall, P.L. (1998) Testing site index site-factor relationships for predicting Pinus contorta and Picea engelmannii x P-glauca productivity in central British Columbia, Canada. Forest Ecology and Management. 110(1-3), 141-150.

[5] Kimsey Jr., M.J., Moore, J. and McDaniel, P. (2008) A geographically weighted regression analysis of Douglas-fir site index in north central Idaho. Forest Science. 54(3), 356-366.

[6] Bravo-Oviedo, A. and Montero, G. (2005) Site index in relation to edaphic variables in stone pine (Pinus pinea L.) stands in south west Spain. Annals of Forest Science. 62(1), 61-72.

[7] Chen, H., Krestov, P.V. and Klinka, K. (2002) Trembling aspen site index in relation to environmental measures of site quality at two spatial scales. Canadian Journal of Forest Research. 32(1), 112-119.

[8] Szwaluk, K.S. and Strong, W.L. (2003) Near-surface soil characteristics and understory plants as predictors of Pinus contorta site index in southwestern Alberta, Canada. Forest Ecology and Management. 176(1-3), 13-24.

[9] Aertsen, W., Kint, V., van Orshoven, J., Ozkan, K. and Muys, B. (2010) Comparison and ranking of different modelling techniques for prediction of site index in Mediterranean mountain forests. Ecological Modelling. 221(8), 1119-1130.

[10] Afif-Khouri, E., Alvarez-Alvarez, P., Fernandez-Lopez, M.J., Oliveira-Prendes, J.A. and Camara-Obregon, A. (2011) Influence of climate, edaphic factors and tree nutrition on site index of chestnut coppice stands in north-west Spain. Forestry. 84(4), 385-396.
[11] Crookston, N.L. and Rehfeldt, G.E. (2005) Using Forest Inventory and Analysis Data to Model Plant-Climate Relationships. Washington DC. USDA. 243-250.
[12] Harrington, C.A. and Gould, P.J. (2010) Growth of Western Redcedar and Yellow-Cedar. USDA Forest Service - General Technical Report PNW-GTR. 97-102.
[13] McKenney, D.W. and Pedlar, J.H. (2003) Spatial models of site index based on climate and soil properties for two boreal tree species in Ontario, Canada. Forest Ecology and Management. 175(1-3), 497-507.
[14] Moisen, G.G. and Frescino, T.S. (2002) Comparing five modelling techniques for predicting forest characteristics. Ecological Modelling. 157, 209-225.
[15] Perry, M.D. (2014) Use of Climatic Water Balance Metrics as Site Productivity Predictors. The University of Montana. Thesis Dissertations. Professional Papers. Paper 4244.
[16] Sabatia, C.O. and Burkhart, H.E. (2014) Forest Ecology and Management Predicting site index of plantation loblolly pine from biophysical variables. Forest Ecology and Management. 326, 142-156.
[17] Prasad, A.M., Iverson, L.R. and Liaw, A. (2006) Newer Classification and Regression Tree Techniques: Bagging and Random Forests for Ecological Prediction. Ecosystems. 9(2), 181-199.
[18] Anşin, R. and Özkan, Z.C. (1997) Tohumlu Bitkiler. Trabzon: Karadeniz Teknik Üniversitesi.
[19] Atalay, İ. (1984) Doğu Ladini (Picea orientalis L.) Tohum Transfer Rejiyonlaması. Ankara: Orman Genel Müdürlüğü.
[20] Kayacik, H. (1955) The Distribution of Picea orientalis (L.) Carr. Kew Bulletin. 10(3), 481-490.
[21] Anonymous (2014) Türkiye Orman Varlığı. Ankara: Orman Ve Su İşleri Bakanliği Orman Genel Müdürlüğü Orman İdaresi ve Planlama Dairesi Başk.
[22] Akgül, E. (1989) Doğu Ladininin Ekolojisi. In: Erkuloğlu, Ö.S. (ed.) Doğu Ladini. Ankara: Ormancılık Araştırma Enstitüsü. 27-57.
[23] Anonymous (2002) Maden Tetkik ve Araştırma Genel Müdürlüğü, 1/500.000 Ölçekli Trabzon ve Samsun Paftaları. Ankara: Maden Tetkik ve Araştırma Enstitüsü.
[24] Akgül, E. (1975) Türkiye'de Doğu Ladininin Yayılış Sahası Topraklarında Tespit Edilen Başlıca Özelliklerle Bunlar Arasındaki İlişkiler. Ankara: Ormancılık Araştırma Enstitüsü.
[25] Guner, S., Tufekcioglu, A. and Celik, N. (2017) Effects of Thinning, Liming, and Nitrogen Application on The Growth of A Young Oriental Beech (Fagus Orientalis Lipsky) Forest Stand. Fresen. Environ. Bull. 26, 6727-6733.
[26] Eminagaoglu, O., Kutbay, H., Bilgin, A. and Yalcin, E. (2006) Contribution to The Phytosociology and Conservation of Tertiary Relict Species in Northeastern Anatolia (Turkey). Belg J Bot. 139(1), 124-130.
[27] Atalay, İ. (2002) Türkiye'nin Ekolojik Bölgeleri. İzmir: Orman Bakanlığı.
[28] Atalay, İ. (2010) Uygulamalı Klimatoloji. İzmir: Çevre ve Orman Bakanlığı Ağaçlandırma ve Erozyon Kontrolu Genel Müdürlüğü.
[29] Anşin, R. (1980) Doğu Karadeniz Bölgesi Florası ve Asal Vejetasyon Tiplerinin Floristik İçerikleri. Associate Professorship Thesis. Trabzon: Karadeniz Teknik Üniversitesi.
[30] Skovsgaard, J.P. and Vanclay, J.K. (2008) Forest site productivity: a review of the evolution of dendrometric concepts for even-aged stands. Forestry. 81(1), 13.
[31] van Laar, A. and Akça, A. (2007) Forest Mensuration. Springer, Netherlands.
[32] Akalp, T. (1978) Türkiye'deki Doğu Ladini (Picea orientalis Link. Carr) Ormanlarında Hasılat Araştırmaları. Ankara: Ormancılık Araştırma Enstitüsü.
[33] Raspe, O. and Kohn, J.R. (2002) S-allele diversity in Sorbus aucuparia and Crataegus monogyna (Rosaceae: Maloideae). Heredity. 88, 458-465.
[34] Schoeneberger, P.J. (2002) Field book for describing and sampling soils. National Soil Survey Center, Natural Resources Conservation Service, U.S. Dept. of Agriculture.
[35] Beers, T.W., Dress, P.E. and Wensel, L.C. (1966) Notes and Observations: Aspect Transformation in Site Productivity Research. Journal of Forestry. 64(10), 691-692.
[36] Zech, W Çepel, N. (1972) Güney Anadolu'daki Bazı Pinus Brutia Meşcerelerinin Gelişimi İle Toprak ve Relief Özellikleri Arasındaki İlişkiler. İstanbul Üniversitesi Yayın No: 1753, Orman Fakültesi Yayın No: 191, İstanbul, 107p.
[37] Çepel, N. (1978) Orman Ekolojisi. İstanbul: Istanbul Universitesi, Orman Fakultesi.
[38] Bouyoucos, G.J. (1962) Hydrometer Method Improved for Making Particle Size Analyses of Soils. Agron J. 54(5), 464-465.
[39] Walkley, A. (1947) A critical examination of a rapid method for determining organic carbon in soils-Effect of variations in digestion conditions and of inorganic soil constituents. Soil Science. 63(4), 251-264.

[40] Krawczyk, U., Petri, G. and Kery, A. (1991) Hplc Analysis of Procyanidins in Crataegus Extract. Arch Pharm. 324(2), 97-99.
[41] Burt, R. (2004) Soil Survey Laboratory Methods Manual: Soil Survey Investigations. United States Department of Agriculture Natural Resources Conservation Service. Report No. 42, Version 4.0 Report No. 42, Version 4.0.
[42] Pansu, M. and Gautheyrou, J. (2007) Handbook of Soil Analysis: Mineralogical, Organic and Inorganic Methods. Springer. Berlin Heidelberg.
[43] Erinç, S. (1984) Klimatoloji ve Metotları. İstanbul: İstanbul Üniversitesi Coğrafya Enstitüsü.
[44] Akman, Y. (2010) İklim ve Biyoiklim. Ankara: Palme Yayıncılık.
[45] Thornthwaite, C.W. (1948) An Approach toward a Rational Classification of Climate. Geographical Review. 38(1), 55-94.
[46] IBM Corp. (2011) IBM SPSS Statistics for Windows, Version 20.0. Armonk, NY: IBM Corp.
[47] Sherrod, P.H. (2003) DTREG predictive modeling software. Software available at http:// www dtreg com.
[48] Dasdemir, I. (1992) Türkiye' deki doğu ladini (picea orientalis l. carr.) ormanlarında yetişme ortamı faktörleri-verimlilik ilişkisi. Ankara: Ormancilik Arastirma Enstitusu.
[49] Kalay, H.Z. (1989) Trabzon Orman Bölge Müdürlüğü Saf Doğu Ladini (Dorukağaç) (Picea orientalis (L.) Link) Büklerinin Gelişimi ile Bazı Toprak Özelliklerinin ve Fizyografik Etmenlerin Arasındaki İlişkilerin Denel Olarak Araştırılması. Trabzon: Karadeniz Teknik Universitesi.
[50] Vanderschaaf, C.L. and Prisley, S.P. (2006) Factors Affecting Site Productivity of Loblolly Pine Plantations Across the Southeastern United States. Proceedings of the Fifth Forestry and Natural Resources GIS Conference. Athens, GA: Warnell School of Forestry and Natural Resources, University of Georgia. 175-187.
[51] Roise, J.P. and Betters, D.R. (1981) An Aspect Transformation with Regard to Elevation for Site Productivity Models. Forest Science. 27(3), 483-486.
[52] Stage, A.R. and Salas, C. (2007) Interactions of elevation, aspect, and slope in models of forest species composition and productivity. Forest Science. 53(4), 486-492.
[53] Ozyuvaci, N. (1999) Meteoroloji ve Klimatoloji. Istanbul: Istanbul Universitesi, Orman Fakultesi.
[54] Corona, P., Scotti, R. and Tarchiani, N. (1998) Relationship between environmental factors and site index in Douglas-fir plantations in central Italy. Forest Ecology and Management. 110(1-3), 195-207.
[55] Klinka, K. and Carter, R.E. (1990) Relationships Between Site Index and Synoptic Environmental-Factors in Immature Coastal Douglas-Fir Stands. Forest Science. 36(3), 815-830.
[56] Wickramasinghe, A. (1988) Modeling Tree Growth Potential Based on Effective Evapotranspiration. Forest Science. 34(4), 864-881.
[57] Enez, K., Sariyildiz, T., Aricak, B. and Savaci, G. (2016) Initial Litter Quality Variables and Disturbed Site Characteristics by Forest Harvesting Practices Influence Litter Decomposition Rates of Scots Pine, Trojan Fir and Sweet Chestnut in Northwest of Turkey. Fresen. Environ. Bull. 25, 4732-4741.
[58] Sevik, H. and Karaca, U. (2016) Determining the Resistances of Some Plant Species to Frost Stress Through Ion Leakage Method. Fresen. Environ. Bull. 25, 2745-2750.
[59] Ercanli, I., Gunlu, A., Altun, L. and Baskent, E.Z. (2008) Relationship between site index of oriental spruce Picea orientalis (L.) Link and ecological variables in Macka, Turkey. Scandinavian Journal of Forest Research. 23(4), 319-329.
[60] Sanchez-Rodriguez, F., Rodriguez-Soalleiro, R., Espanol, E., Lopez, C.A. and Merino, A. (2002) Influence of edaphic factors and tree nutritive status on the productivity of Pinus radiata D. Don plantations in northwestern Spain. Forest Ecology and Management. 171(1-2), 181-189.
[61] Klinka, K., Wang, Q., Carter, R.E. and Chen, H.Y.H. (1996) Height growth-elevation relationships in subalpine forests of interior British Columbia. Forestry Chronicle. 72(2), 193-198.
[62] Güner, Ş.T., Comez, A., Ozkan, K., Karatas, R. and Celik, N. (2016) Modelling the productivity of Anatolian black pine plantations in Turkey. Istanbul University Faculty of Forestry. 66(1), 159-172.
[63] Gulsoy, S., Suel, H., Celik, H., Ozdemir, S. and Ozkan, K. (2014) Modeling Site Productivity of Anatolian Black Pine Stands in Response to Site Factors in Buldan District, Turkey. Pakistan Journal of Botany. 46(1), 213-220.
[64] Mckenny, D.W. and Pedlar, J.H. (2003) Spatial Models of Site Index Based on Tree Species in Ontario, Canada. Forest Ecology and Management. 175, 497-507.
[65] Bakker, M.R. (1999) The effect of lime and gypsum applications on a sessile oak (Quercus petraea (M.) Liebl.) stand at La Croix-Scaille (French Ardennes) II. Fine root dynamics. Plant and Soil. 206(1), 109-121.

Received: **19.12.2017**
Accepted: **18.02.2018**

CORRESPONDING AUTHOR

Ismet Yener
Artvin Coruh University,
Faculty of Forestry,
08100, Artvin – Turkey

e-mail: yener@artvin.edu.tr

© by PSP Volume 27 – No. 5/2018 pages 3117-3123 Fresenius Environmental Bulletin

THE EFFECTS OF ACARICIDE DIPPING METHODS ON BULB MITE [*RHIZOGLYPHUS ECHINOPUS* (FUMOUZE & ROBIN) (ACARI: ASTIGMATA)] THAT HARMFULL ON GARLIC

Cihan Cilbircioglu[1,*], Sultan Cobanoglu[2]

[1]Kastamonu University, Taskopru Vocational School, Organic Agricultural Department, Kastamonu, Turkey
[2]Ankara University Agriculture, Plant Protection Department, Ankara, Turkey

ABSTRACT

Rhizoglyphus echinopus (Fumouze & Robin) (Acari: Astigmata) is the most important harmful mite species in garlic (Alliaceae: *Allium sativum* L.) areas in Kastamonu. This mite causes darkening and decaying especially in the underground part of the garlic, causing significant damage. In this study, the effects of acaricide Azadirachtin indica, Abamectin and Hexythiazox were investigated. on the *R. echinopus* damage of garlic heads during the garlic cultivation period. For this purpose, garlic seeds were dipped in acaricide solutions and later planted. Whether or not the effects of the acaricides on the harmful mite concentration in the soil were tried to be revealed by the exit rates of the plants. Trials were carried out in two different locations from garlic farming areas in Kastamonu province during the 2015-2016 vegetation period. Each extract was tested in 16 plots by four repetitive and four parcels were identified as controls and no application was made to these parcels. As a result were identified that Azadirachtin indica, Abamectin and Hexythiazox were not significantly different from control, no effect on *R. echinopus* in the head of the garlic and has been determined that natural equilibrium has been established in the control plots.

KEYWORDS:
Garlic Acari, *Rhizoglyphus echinopus*, Acaricide, Population density, Kastamonu

INTRODUCTION

Garlic (*Allium sativum* L.) (Asparagales: Amaryllidaceae) is one of the most commonly produced vegetable crops in the world. Garlic is used as a spice mash, a canned product, a dried powder, a garlic oil, and as garlic pellets. Garlic has a wide range of uses and positive effects on human health such as asthma, hypertension, bronchitis, cancer, circulatory weaknesses, colds, colitis, and coughing [1].

Although garlic is now grown in almost every region of the world, it preffer under temperate climates on sandy, loamy, and argilliferous soils, especially rich in germanium and selenium [2]. The best quality garlic in the world is grow in Taşköprü Plain where 85% of the soil has a permeable, loamy-argillifereous structure. In addition, Taşköprü has an optimum climate for garlic cultivation with warm, humid spring [3]. Adequate rainfall is received in February and March when garlic germinates, and the crop can be grown without additional irrigation in Kastamonu [2].

According to United Nations Food and Agricultural Organization, 24.3 million metric tons of garlic were grown worldwide in 2013. Nearly 80% of this global production was belong to China, India, South Korea, Egypt, and Russia [4].

Garlic is an important crop in Turkey, where over 87.000 tons are produced annually; which accounted for 0.36% of the total world production in 2013 [5]. The greatest production area in Turkey is in Taşköprü Province, especially near the city of Kastamonu (25.2% of total production in Turkey). Taşköprü garlic is recognized as one of the best garlic varieties in Turkey and the rest of the world. In 2012, there were 18.500 ha of Taşköprü garlic with 16.650 tons of production and yields of 900 kg/ha [3]. In Taşköprü, 3.500 families (about 40.000 people) are employed in garlic production.

Diseases and pests can cut garlic yields by 10-50%, and mites are one of the most important problems on onions, garlic, and bulbous ornamental plants [6, 7, 8, 9, 10, 11, 12, 13, 14].

The two most common mite species, *Rhizoglyphus echinopus* and *Rhizoglyphus robini*, are probably cosmopolitan and damage a variety of crops including onions (*Allium cepa*), garlic (*Allium sativum*), other *Allium* species, *Lilium, Hyacinthus* and many other vegetables, cereals, and ornamentals in storage, in the greenhouse and in the field. Management of these soil pests is complicated by the lack of appropriate sampling methods for assessing field populations and predicting outbreaks, a lack of integrated management alternatives, and a limited

knowledge of their field biology and ecology. Management of bulb mites is complicated by their short generation time, high reproductive potential, broad food niche, interactions with other pests and pathogens, and unique adaptations for dispersal. Historically, control of these acarine pests has relied on the use of synthetic miticides and insecticides, but this option is now limited due to documented resistance and with drawal of registration of some products. Alternative control strategies, including cultural and biological control, have shown limited success, but need to be further developed and implemented [8, 9].

Use of chemicals has been limited in recent years, and biological or cultural methods have been advocated [15]. Natural plant extracts with bological activities against diseases and insects are being investigated, and herbal intesticides have been found to be effective against several pests [16].

Neem products affect feeding, growth, and development of insects and mites [17, 18, 19, 20].

Avermectin is a macrocyclic lactone derivative that is generated as a fermentation product from a actinomycete bacteria (Actinobacteria), Streptomyces avermitilis (ex Burg) Kim & Goodfellow (Actinomycetales: Streptomycetaceae), that is found naturally in the soil. It is accepted by United States Environment Proteciton Agency (EPA) as second class toxic pesticide [21].

Hexythiazox is a mixture of four stereoisomers chemical compounds from the group of thiazolidines and carboxamides and acaricide effective on mite eggs and nymphs, but not adults.

Sorаurer [22] concluded that the method of nicotine sulfate and carbon disulphide fumigation for two hours or dipping method the head parts in tobacco extract were successful against *R. echinopus*. In addition to this, the researcher reported that the application of the fir tree oil had a killing effect of 60% to 90% on mites and the application of hot water to the garlic heads at 55 °C is 100%. effective.

Ertürk [23] researched that the damage of *Rhizoglyphus echinopus* (Fumouze & Robin) (Acarina: Acaridae) on bulbous plants, fumigated with methyl bromide on Hyacinthus bulbs against the eggs of *R. echinopus* and reported that fumigant is 100% effective on the egg of mite.

Garman [24] reported that the plant bulbs were dipped in hot water and then the cold steam application was successful on *R. echinopus* in Lilium and Hyacinthus bulbs in storage.

From the scientific studies above, in this study the possibilities of fighting with *R. echinopus* for two years between 2014 and 2016 were investigated in the garlic cultivation area of two different localities in Taşköprü district of Kastamonu province. For this purpose, it is aimed to determine how the harmful mite populations of the underground parts of the garlic, that is to say the head, are affected by the application of acaricides by spraying the seed garlic teeth.

MATERIALS AND METHODS

This study was performed in 2015-2016 on a 0.2 hectare fields located in Yukarıemerce and Alisaray Village in Taşköprü/ Turkey (Figure 1). A local variety, Taşköprü garlic, was planted at 1250 kg per hectare on March into 3 x 10 meter plots. To prevent cross contamination for comparison acariside effects, each plot was separated by a three meters of empty space. The experiment was set up as a randomized complete block design with four treatments (three acaracides and an untreated control) replicatied four times (Figure 2). Thus, there was a total of 16 plots covering about one hectare. Plots were randomly assigned. Before planting, garlic cloves were treated by dipping them in Abamectin (Avirmec EC®) at 30 ml/100 L water, azadirachtin (NeemAzal-T/S®) at 30 ml/100 L water and Hexathiazox (Yoksorrun 5EC®) at 50 ml/100 L. water. Garlic cloves were immersed in one of the three acaricide-water treatments for 15 minutes before planting. Each application is planned in 4 replications, did not spray on green parts of garlic.

Since the flow of garlic is dense in the head part, the dipping method of the head parts has been specially selected. The method of applying acaricides to pre-planting methods by dipping method was tested against *R. echinopus* mites and it was tested whether it is a high success rate application.

After the spraying, counting is done on 7th, 14th, 21st and 28th days until the green parts are developed; five garlic plants were taken from each plot after extracting in Berlese funnel, the mites collected in ethyl alcohol were thoroughly mixed and homogenized. Then have taken 1 ml of alcohol and counted the amount of mite in it and afet this process is repeated three times, were averaged number of mites so were determined the number of mites in 1 ml alcohol. Because of taking 5 pieces of garlic head sample the number of mites found was divided by 5 and the number of mites per garlic was calculated. Climate data (temperature and humidity values) for the study areas were obtained from the meteorological station.

RESULTS

Within the scope of the study, data obtained from studies of compound trials in the garlic field of Alisaray and Yukarıemerce Village of Taşköprü District during 2015 and 2016 vegetation period Tukey (P=0.05) in the direction of the obtained data, all census days, all different applications and at (α=0.05) level there was no significant difference in statistical significance between the drug trial parcels and the control parcels ($P \geq 0.05$). When were determined Table 1, Table 2, Table 3 and Table 4; Abamectin, Neemazal and Hexathiazox that were applied in all different localities and census periods

the result were not effective against the population density of *R. echinopus* at head of garlic. This situation shows that Abamectin, Neemazal and Hexathiazox are not fully effective in suppressing the density of *R. echinopus* on the garlic head (Figure 3, Figure 4).

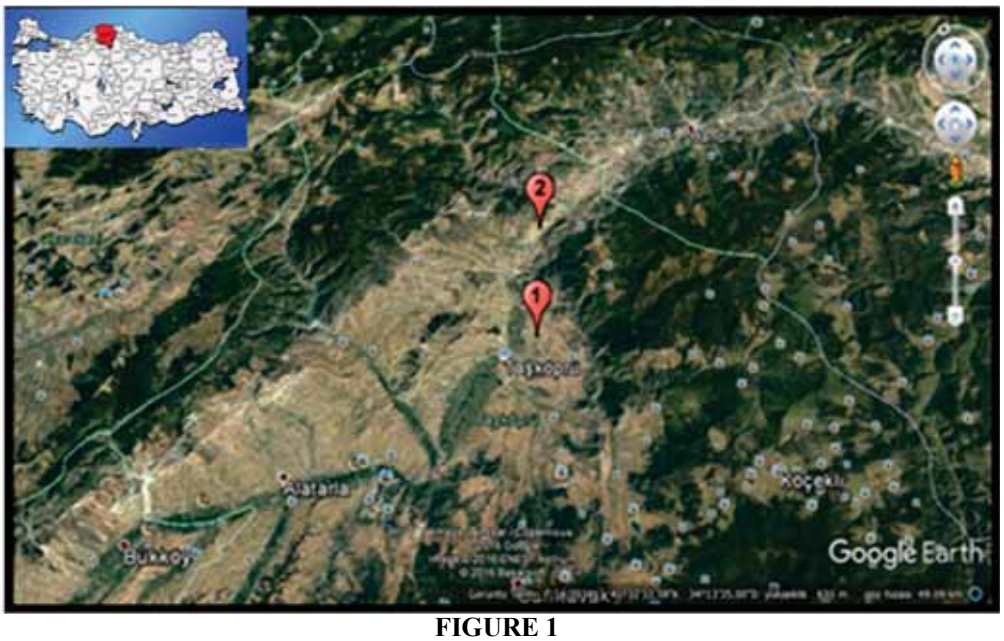


FIGURE 1
Locations where experiments are conducted (1= Alisaray field, 2=Yukarıemerce field).

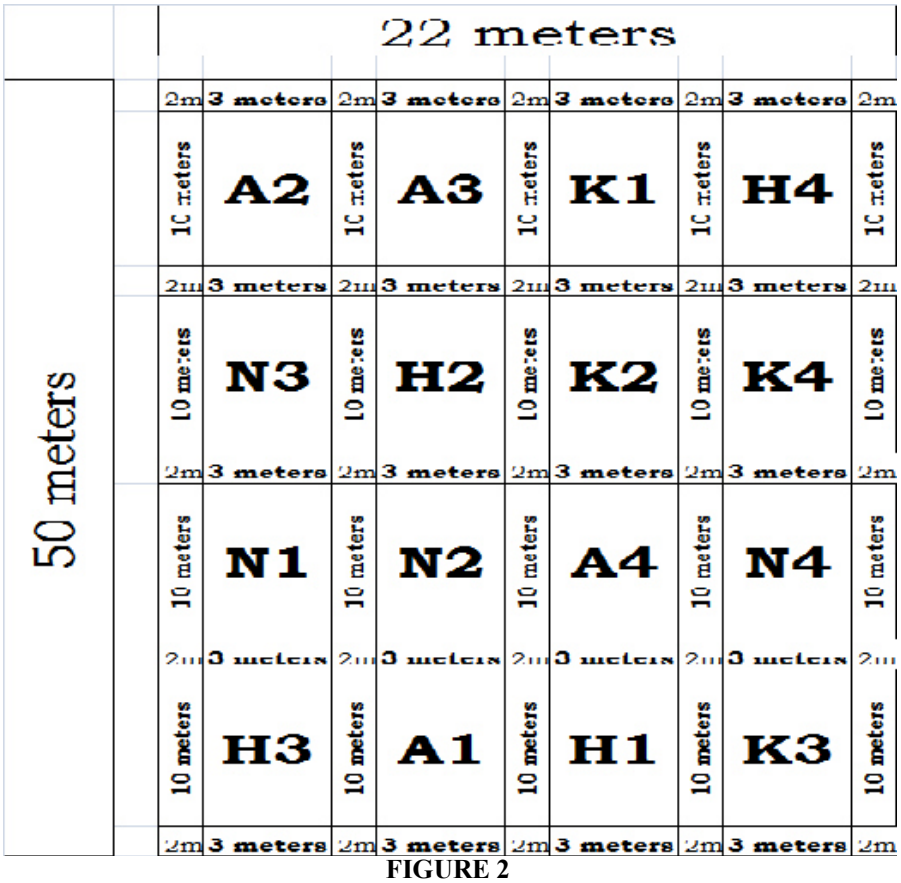


FIGURE 2
Acaricides trial parcels and their distribution
(A means: Avirmectin, H means: Hexythiazox, N means: Neemazal)

TABLE 1
Percentage of avarage mite density on garlic heads in acaricide trial parcels in Yukarıemerce Village Parcels in 2015 (Mean+ standard deviation)*

YUKARIEMERCE VILLAGE PARCELS (2015)					
Applied Materials	**After 3 days**	**After 7 days**	**After 14 days**	**After 21days**	**After 28 days**
Abamectin	34.25± 18.25	6.25± 1.11	8.25± 4.05	2.25± 1.31	32.25± 10.44
Neemazal (Azadirachtin indica)	15.50± 5.61	8.25± 2.75	6.00± 2.16	2.00± 1.00	12.75± 7.12
Hexathiazox	8.50± 2.90	4.00± 1.16	4.25± 1.93	0.25± 0.25	15.75± 13.12
Control	9.25± 2.36	10.25± 3.42	15.5± 8.47	4.75± 2.39	38.25± 12.00
Statistical Values	P= 0.289, df:12, F: 1.523	P: 0.282 df:12, F: 1.315	P: 0.405 df:12, F: 1.013	P: 0.184 df:12, F: 1.611	P: 0.388 df:12, F: 1.299

* Assessed by Tukey method (P ≥0.05).

TABLE 2
Percentage of avarage mite density on garlic heads in acaricide trial parcels in Yukarıemerce Village Parcels in 2016 (Mean+ standard deviation)*

YUKARIEMERCE VILLAGE PARCELS (2016)					
Applied Materials	**After 3 days**	**After 7 days**	**After 14 days**	**After 21days**	**After 28 days**
Abamectin	33.50± 1.55	21.25± 3.57	8.25± 4.05	22.00± 6.14	2.50± 0.29
Neemazal (Azadirachtin indica)	36.25± 4.52	23.50± 3.12	4.00± 2.16	24.75± 4.31	7.25± 2.95
Hexathiazox	36.00± 6.00	24.00± 2.52	4.25± 1.93	28.00± 4.38	6.75± 2.14
Control	38.25± 3.38	35.00± 7.27	15.9± 8.47	32.25± 6.68	5.25± 1.80
Statistical Values	P= 0.852, df:12, F: 0.216	P: 0.192 df:12, F: 1.858	P: 0.403 df:12, F: 1.013	P: 0.566 df:12, F: 0.649	P: 0.390 df:12, F: 1.098

* Assessed by Tukey method (P ≥0.05).

TABLE 3
Percentage of avarage mite density on garlic heads in acaricide trial parcels in Alisaray Village Parcels in 2015 (Mean+ standard deviation)*

ALISARAY VILLAGE PARCELS (2015)					
Applied Materials	**After 3 days**	**After 7 days**	**After 14 days**	**After 21days**	**After 28 days**
Abamectin	0.50± 0.50	12.75± 4.29	7.50± 1.76	5.25± 1.65	4.75± 1.70
Neemazal (Azadirachtin indica)	1.25± 0.95	15.50± 4.91	6.25± 2.01	6.50± 2.25	6.50± 1.55
Hexathiazox	1.25± 1.25	11.25± 3.38	5.75± 2.46	5.25± 2.98	3.50± 1.04
Control	1.00± 0.58	24.25± 5.54	11.75± 5.92	12.75± 4.09	18.50± 3.77
Statistical Values	P= 0.928, df:12, F: 0.216	P: 0.242 df:12, F: 1.598	P: 0.626 df:12, F: 0.616	P: 0.305 df:12, F: 1.542	P: 0.788 df:12, F: 9.230

* Assessed by Tukey method (P ≥0.05).

TABLE 4
Percentage of avarage mite density on garlic heads in acaricide trial parcels in Alisaray Village Parcels in 2016 (Mean+ standard deviation)*

ALISARAY VILLAGE PARCELS (2016)					
Applied Materials	**After 3 days**	**After 7 days**	**After 14 days**	**After 21days**	**After 28 days**
Abamectin	7.00± 3.11	6.75± 2.69	5.75± 2.06	5.25± 2.66	5.50± 2.72
Neemazal (Azadirachtin indica)	9.50± 3.77	7.25± 2.50	8.00± 3.49	6.25± 1.65	6.75± 2.29
Hexathiazox	2.50± 1.04	8.50± 2.18	8.25± 2.21	7.00± 3.24	6.75± 3.12
Control	6.00± 1.08	2.50± 0.87	2.25± 0.69	6.50± 1.85	6.50± 1.50
Statistical Values	P= 0.265, df:12, F: 1.287	P: 0.260 df:12, F: 1.433	P: 0.310 df:12, F: 1.425	P: 0.956 df:12, F: 0.091	P: 0.984 df:12, F: 0.058

*Assessed by Tukey method (P ≥0.05).

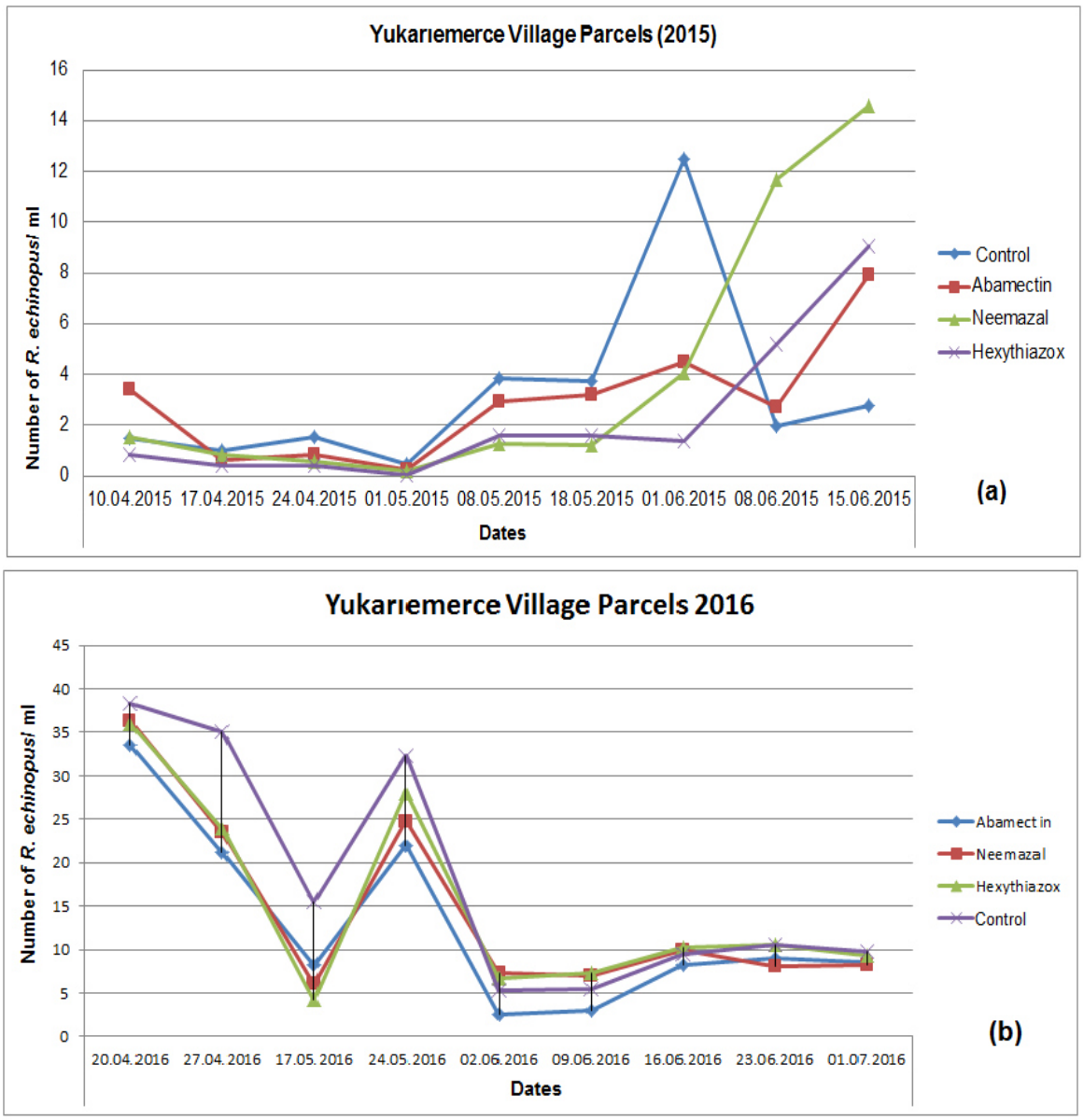


FIGURE 3
Mite density in garlic parcels where planted in different acaricide solutions in Yukarıemerce Village in 2015 and 2016 vegetation period (average number of mites/ ml)

CONCLUSIONS

In the study the possibility of fighting with garlic mites were investigated in garlic growing areas in Kastamonu. In the scope of the study, in order to find a solution to the struggle of harmful mite species in the garlic, it was investigated how the seeds were sprayed and the harmful population was affected with the least acaricide application. Thus, it was tried to shed light on the mite problem which is a major problem of the breeders in the region.

As a result; the application of three acaricides (Abamectin, Azadirachtin indica and Heathiazox) with dipping method did not show a different effect on the mite density, especially in the head of garlic. The temperature and humidity values in the region are very different from their normal values influenced this situation. It is evaluated that the location, humidity and temperature values of mite population densities are effective. All three acaricides were not different from each other and from control plots according to their effects. Care should be taken not to distort this natural balance that is formed in the region. According to the fact that the effects on the mite density of all three acaricides are not different when the harmful mite intensity increased it was evaluated that it would be appropriate to prefer Azadirachtin indica, which is not harmful to the environment and harmful to the natural balance.

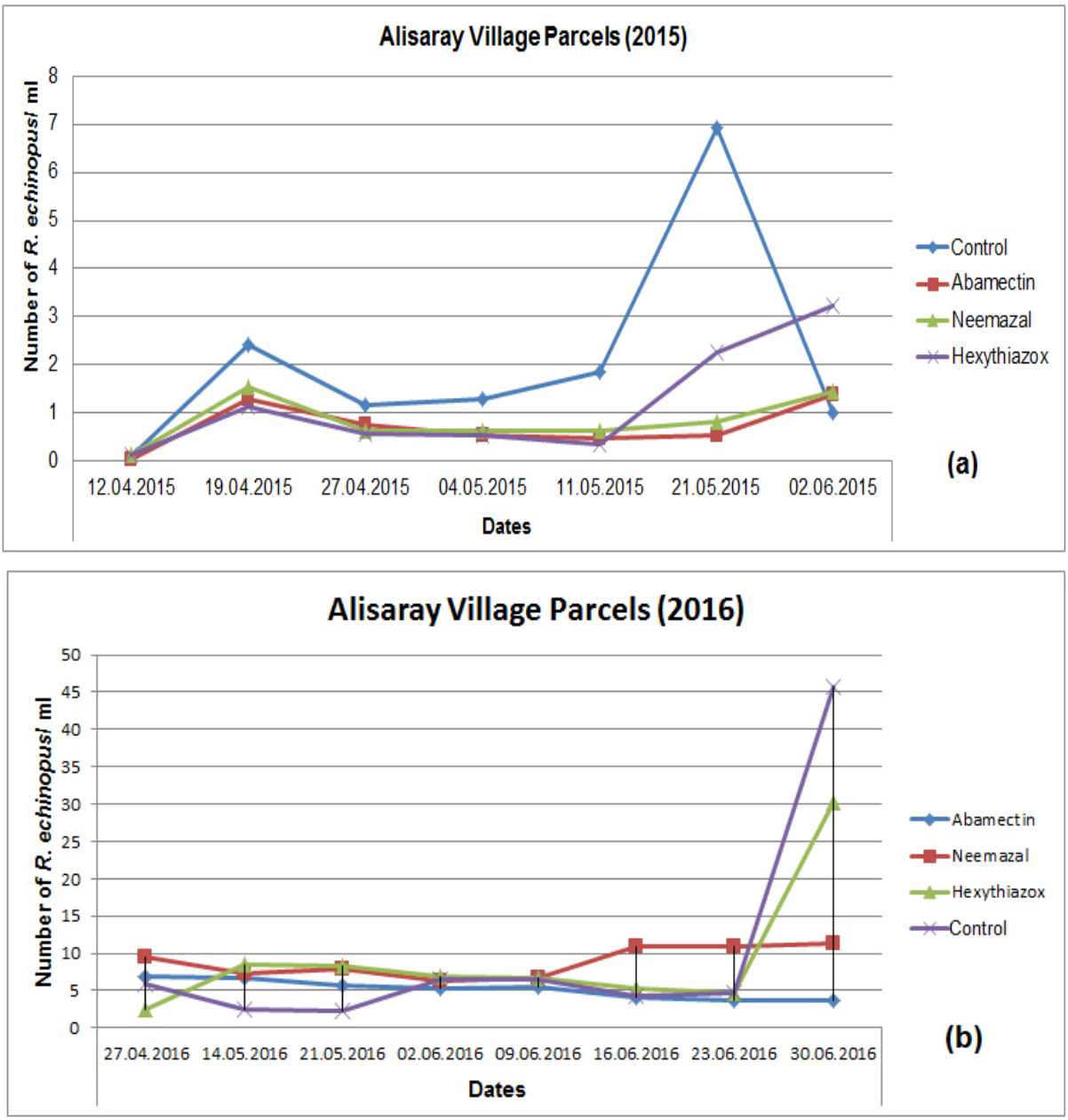


FIGURE 4
Mite density in garlic parcels where planted in different acaricide solutions in Alisaray Village in 2015 and 2016 vegetation period (average number mites/ ml)

ACKNOWLEDGEMENTS

We would like to express our appreciation to the TUBİTAK TOVAG, which supported this study (Project No: 114O416).

REFERENCES

[1] Kaul, M.K. (1997) Medicinal Plants of Kashmir and Ladakh: Temperate and Cold Arid Himalaya. Indus Publishing Co., New Delhi, India, 173p.

[2] Taban, S., Çıkili, Y., Kebeci, F., Taban, N., Sezer, S.M. (2004) Fertility status and potential nutritional problems of Taşköprü garlic soils. Ankara Univ. Faculty Agric. Sci. J. 10, 297-304.

[3] Anonymous (2012) Taşköprü garlic panel information note. North Anatolian Development Agency, Kastamonu, Turkey, 132p.

[4] FAO. (2015) FAOSTAT. Statistics Division, Food and Agriculture Organization (FAO). United Nations.

[5] Cılbırcıoğlu, C. (2017) Determination of Mite (Acari) Species of Garlic, Their Distribution and Population Development of Important Species in Kastamonu. Ph. D. Thesis. Ankara University, Graduate School of Science and Technology. Ankara.
[6] Chen, J.S., Lo, K.C. (1989) Susceptibility of two bulb mites, *Rhizoglyphus robini* and *Rhizoglyphus setosus* (Acarina: Acaridae), to some acaricides and insecticides. Exp. Appl. Acarol. 6, 55–66.
[7] Madanlar, N., Önder, F. (1996) Mites associated with cultivated mushrooms in Turkey. Poster No. 15-138, XX. Internat. Congr. Entomol. 25-31 Aug. 1996. Firenze, Italy.
[8] Díaz, A., Okabe, K., Eckenrode, C.J., Villani, M.G., Oconnor, B.M. (2000) Biology, ecology, and management of the bulb mites of the genus *Rhizoglyphus* (Acari: Acaridae). Exp. Appl. Acarol. 24, 85-113.
[9] Straub, R.W. (2004) Onion arthropod pest management. Available at: http://ipmworld.umn.edu /chapters/straub.htm.
[10] Bayram, Ş., Çobanoğlu, S. (2007) Mite fauna (Acari: Prostigmata, Mesostigmata, Astigmata) of coniferous plants in Turkey. 12th Internat. Congr Acarol., Amsterdam, The Netherlands. Türk. Entomol. Derg. 31, 279-290.
[11] Göven, M.A., Çobanoğlu, S., Güven, B. (2009) Predator mite fauna of the Aegean Coast vineyards. Plant Protect. Bull. 49, 1-10.
[12] Kılıç, T. (2010) Fresh onions in İzmir: Determination of insects and mites found and pest monitoring of population changes. Ph.D. Thesis. Ege University, Graduate School of Science and Technology. İzmir, 130p.
[13] Denizhan, E. (2012) A new record for Turkey eriophyoid fauna: *Aceria tulipae* (Keifer, 1938) (Acari: Eriophyoidea). Plant Protect. Bull. 52, 119-122.
[14] Kılıç, T., Çobanoğlu, S., Yoldaş, Z., Madanlar, N. (2012) Mite (Acari) species determined in fresh onion fields in Izmir province. Türk. Entomol. Derg. 36, 401-411.
[15] Önoğur, E., Çetinkaya, N. (1999) General Principles of Plant Protection in Ecological Agriculture. Ecological Agriculture Education Course Notes, İzmir Provincial Directorate of the Ministry of Agriculture and Rural Affairs, E. Ü. Faculty of Agriculture, ETO Association Publications, İzmir, Turkey.
[16] Tepe S. (2010) Bitki korumada doğal pestisitlerin kullanımı. Derim Dergisi. 18(3), 113-121.
[17] Schmutterer, H. (1990) Properties and potential of natural pesticides from the neem tree *Azadirachta indica*. Annu. Rev. Entomol. 35, 271-297.
[18] Koul, O. (2004) Neem – a global perspective. In: Koul, O., Wahab, S. (Eds.) Neem, Today and in the New Millennium. Kluwer Academic Publishers, The Netherlands, 1-19.
[19] Isman, M.B. (2006) Botanical insecticides, deterrents and repellents in modern agriculture and an increasingly regulated world. Annu. Rev. Entomol. 51, 45-66.
[20] Copping, L.G., Duke, S.O. (2007) Natural products that have been used commercially as crop protection agents. Pest Manage. Sci. 63, 542-554.
[21] Hoy, M., Conley, J. (1987) Toxicity of pesticides to western predatory mite. Calif. Agric. 41, 12-14.
[22] Sorauer, P. (1913) Handbuch der Pjlanzetlkrankheiten. Vol. 1-6. Berlin, Parey.
[23] Ertürk, H. (1953) *Rhizoglyphus echinopus* Akarlarına karşı *Hyacinthus* (sümbül) Soğanlarının Methyl bromide ile Fümigasyomu. İzmir-Bornova Ziraat Mücadele Enstitüsü. 5, 31-37.
[24] Garman, P. (1949) Mite species from apple trees in Connecticut. Conn. Agr. Expt. Sta. Bull. 520, 1-27.

Received: **22.12.2017**
Accepted: **19.02.2018**

CORRESPONDING AUTHOR

Cihan Cilbircioglu
Kastamonu University,
Taşköprü Vocational School,
Organic Agriculture Programme,
Kastamonu – Turkey

e-mail: cihancilbirci@hotmail.com

© by PSP Volume 27 – No. 5/2018 pages 3124-3132 Fresenius Environmental Bulletin

EFFECTS OF DIFFERENT KIND OF SOURCES IN NOISE EXPOSURE: ANTALYA AS A CASE STUDY

Nesimi Ozkurt[1], Deniz Sari[1], Samet Feyyaz Hamamci[1], Melike Nese Tezel[1,*], Muhammet Erdol[1], Mustafa Ece[2], Nazli Yalcindag[2], Nese Yugruk-Akdag[3]

[1]TUBITAK Marmara Research Center, Environment and Cleaner Production Institute, Kocaeli, Turkey
[2]Antalya Metropolitan Municipality, Antalya, Turkey
[3]Yildiz Technical University, Architectural Faculty, Building Physics Department, Besiktas, Istanbul, Turkey

ABSTRACT

The results of the analyses carried out according to the European Noise Directive for determining the efficacy of different noise sources in areas being exposed to high levels of noise are presented. The study area was selected to cover of all noise sources exposure areas which are critical according to limit values. Comparison of 55 dB(A) and higher noise level impact indicates that road, Antalya airport, and entertainment places are the three noisiest sources of all followed by railway and industrial zones during 24 hrs. time period in Antalya city. 65 dB(A) and higher noise levels for road, Antalya airport, and entertainment places exceeded and their exposed population were 73,300, 9,500, and 2,900 respectively. The violations observed for 75 dB(A) and higher noise levels for road and entertainment places for which exposed population were 17,400, and 700 respectively. The average noise levels sourced from airport, railway, and industrial zones essentially conform to the 75 dB(A) limit for daily time interval. Nearly %10 of population exposed from road noise, %1 both from Antalya airport and entertainment places for 55 dB(A) and higher noise levels during the night time period. However, for railway and industrial zones average noise levels for night time period conformed to the regulatory standards. For 65 dB(A) and higher noise levels, only %3 of population exposed from road noise.

KEYWORDS:
Modeling, Noise source, Exposure, Noise map

INTRODUCTION

Noise, which is considered an important component of environmental pollution today, causes many negative consequences from the disturbing effects on daily activities to physiological or psychological complaints. Gradually intensifying in parallel with technological developments and population growth, noise disturbs people in both closed and open spaces based on the actual conditions, and such disturbances are known to create serious problems on occasions. Occupational Safety & Health Administration (OSHA) classifies the effects of noise in the following three groups based on the level of significance:

- Primary Effects, which include noise-induced temporary threshold shift, noise-induced permanent threshold shift, acoustic trauma and tinnitus.
- Effects on Communication and Performance, which may include isolation, annoyance, difficulty in concentrating, absenteeism and accidents.
- Other Effects, which may include stress, muscle tension, ulcers, increased blood pressure and hypertension [1].

As an important research on effects of noise, the study conducted by Saeki et al., clearly revealed the annoying, performance decreasing and fatiguing effects of noise during mental memory task [2]. In another study, effects of different noise combinations on sleep were researched [3]. In that study, road traffic noise used as a single noise source and construction or movie noise combined with road traffic noise were used as combined noise sources. The results showed that the combined noise source including construction noise decreased the number of participants who fell asleep within an hour and increased the number that were awakened prematurely when compared to the effects of road traffic noise combined with movie noise. Klæboe et al. conducted a survey study in Norway, in 18 study areas from two cities and with a total of nearly 4,000 respondents and revealed the relationship between road noise exposure and noise annoyance [4]. Another research carried out by Kluizenaar and Miedema investigated the effects of traffic noise on cardiovascular health and analyzed the negative effects of noise on hypertension, cardiovascular disease and cardiovascular mortality by use of questionnaires, measurements and hospital admission databases [5]. Similarly, Pierra et al. made a study of the effects of nocturnal road traffic noise on sleep and human health [6]. Another study conducted by Jakovljeic et al. showed a strong correlation between noise levels, personal characteristics and some housing conditions [7]. The

literature includes many papers about the negative effects of noise on sleep [3, 8-12].

Researches on the effects of noise reveal that noise start to cause annoyance over 55 dBA. Level of annoyance clearly increases at noise levels exceeding 65 dBA and serious problems develop over time. According to the World Health Organization (WHO), noise levels that must not be exceeded in residential areas are 55 dBA for the daytime and 45 dBA for the nighttime. The Organization also clearly states that noise levels higher than 40 dBA should cause sleep disturbances [13]. When it is taken into account that an important part of the world's population is exposed to noise levels exceeding 65 dBA during the daytime, scale of the problem can be easily understood. Certain targets were set within the scope of the "Fifth Environmental Action Program" started by the European Commission in 1996, which included keeping average exposure to noise under 65 $L_{Aeq,}$ never allowing the level of exposure to exceed 85 L_{Aeq} and keeping it at 55 L_{Aeq} for quiet areas [14]. In line with these targets, member countries of the European Union were required to prepare noise maps and action plans for the purposes of revealing the actual scale of noise exposure and developing action plans for controlling noise [15]. In response, European Union member countries speeded up ongoing studies towards noise control and legislated common directives for the development of noise maps for all settlements and presentation of actual conditions of noise exposure [16-22]. In December 2012, information concerning people who are exposed to different noise levels and to different noise sources for the noise indicators L_{den} and L_{night} in European settlements with more than 100,000 inhabitants, as well as all main transport networks should have been reported by member countries. This information is now being integrated into the existing database containing noise data for the whole Europe: Noise Observation and Information Service for Europe [23].

In strategic noise maps, combined effects of different noise sources in a certain area are evaluated. On the other hand, there are also studies which try to find out the effects separately for each of various noise sources including roads, railroads, airports, entertainment places and industrial zones. In their study, Brito and Coelho prepared noise maps which aimed to show affected areas of different noise sources in Fortaleze, a Brazilian city with a population of 2.8 million [24]. Similarly, Dimitrios et al. worked on the noise exposure caused by the port and the nearby road in the Greek city of Piraeus in order to find which source was dominant at various locations of the city [25]. Panagopoulos et al. prepared noise maps of the roads of Thessaloniki city to "classify" the city area into zones according to different noise levels. Results indicate that 6.5% of the population was exposed to noise levels above 65 dBA during nighttime [26]. In another research carried out by Baltrėnas et al., noise measurements were taken near the main streets in the southern part of Panevežys, Lithuania. The performed measurements show, the noise level limit in the daytime was exceeded by 65%, in the evening by 88%, and at night by 71% of all the total measurements made [27]. Vogiatzis was studied Larnaka International Airport in Cyprus and mentioned that aircraft noise is an important parameter of degradation of the soundscape environment in the immediate area of airports [28]. In Turkey, there are also recent studies about noise impact of sources on surrounding communities. Ozkurt et al. studied airport noise and their impacts on communities around the İstanbul Ataturk Airport and İzmir Adnan Menderes Airport [29, 30]. Noise exposure levels were calculated on the surrounding communities both for current flight operations in 2012 and also for future capacities of Ankara Esenboga Airport [31]. Hamamci et al. was characterized the lands affected by airport noise in terms of land cover/use characteristics around Ankara Esenboga, Antalya and Izmir Adnan Menderes Airports [32].

Antalya, a southern city of Turkey on the Mediterranean coast, has been a focus of interest for both local and international tourists thanks to its very long holiday season and various facilities offered for visitors. While more than 600 entertainment venues located along the coast of the city make an important contribution to the attractiveness of Antalya in terms of tourist activities, they also cause many environmental problems, noise pollution being in the lead. Sari et al. assessed the noise exposure levels sourced by entertainment facilities such as discos, bars and pubs etc. in the city center of Antalya. The level of entertainment noise exposure in the city was calculated according to the European Noise Directive [33]. In addition, roads are also known to be effective noise sources for many areas of the city.

In this study, results of the analyses carried out for determining the efficacy of different noise sources in areas being exposed to high levels of noise are presented.

DATA AND METHODOLOGY

Study area and data. Antalya is a city in the Mediterranean coast of southwestern Turkey and is surrounded by mountains situated on coastal cliffs. The city of Antalya is located between the longitudes 29° 14' E and 32° 27' E, and latitudes 36° 06' N and 37° 27' N, covering a total area of 138,000 hectares. The population of agglomeration in the city is more than 1 million [33].

TABLE 1
Model input data in study area

Model area (km^2)	Households	Population	Schools	Hospitals	City area (km^2)
704	231,600	900,700	4,160	72	2,027



FIGURE 1
Location of noise sources in study area

The geographical data for the study area had been collected from the archives belonging to Antalya Metropolitan Municipality. The geographical data used for the model consists of the location and height information of the buildings, number of floors, land use, topography and all other obstacles located in Antalya City. The data was utilized for establishing the elevation, building (residential), auxiliary building (industrial, commercial), hospital and school layers in the software.

Road-traffic data and railway data were acquired from Antalya Metropolitan Municipality. They include road segments, traffic volume, vehicle speed, and composition of vehicle types. In the year 2012, traffic data for Antalya Airport were collected by the General Directorate of State Airports Authority. The flight statistics and types of aircraft are according to the German document "Instructions on the Calculation of Noise Protection Areas" [34]. The representative sound pressure levels for entertainment places were obtained from emission library of SoundPLAN. The SoundPLAN is a graphics oriented noise prediction program which is used for noise planning, noise assessment and the development of noise mitigation measures. According to SoundPLAN emission library, sound power levels were used as 66 dBA for cafe bistro-beer garden (up to about 300 persons), 71 dBA for cafe bistro-beer garden (more than 300 persons), 80 dBA for restaurants with music, 90 dBA for pub-bar-discotheque and 105 dBA for entertainment venue with live music [35]. The model input data in study area was given in Table 1. The location of noise sources was shown in Fig.1.

Noise modeling. The models are numerical representations of the reality and are able to produce an accurate estimate of the noise exposure experienced in the cities. Noise modeling is used to evaluate current or future noise levels in agglomerations and to produce different noise maps. These maps, which show contours of equal noise, are a powerful tool for illustrating the impact of noise from a source or combination of sources to surrounding communities [36]. Noise mapping is acknowledged as one of the best ways for understanding the issues related to

environmental noise. Developing a noise map requires detailed information about the noise sources, physical environment and population structure of the area and the relevant environmental and acoustical conditions. Modern noise mapping methods rely heavily on computer noise modeling. In this study, the SoundPLAN 7.3 software package was used to develop a model of noise levels. The results of these simulations were exported to maps and day-time and night-time noise layers were created at a 10-m spatial resolution in the raster data format by use of a bilinear interpolation algorithm. Fig.2 and Fig.3 shows 55 dB(A) and higher exposure areas of noise sources at daytime and nighttime, respectively.

Estimating population exposure. Noise disturbance significantly impacts many areas with high population density and affects the inhabitants in their daily life, sleep, work and study. The literature suggests that the risk of hypertension and myocardial infarction increases with prolonged exposure to the noise generated by airports and roads [37-40].

The number of people exposed to noise is determined by means of façade level calculations on households. Two different methods are available to assess the number of people exposed to noise:

Proportional exposure. proportional attribution of the number of inhabitants of a given building to each façade level point.

Highest level exposure. in compliance with END all inhabitants of a building are assigned to the level of the most exposed façade.

In this study, "highest level exposure" method was used to calculate size of the exposed population.

EU noise indicators L_{den} and L_n are to be determined by means of the assessment method described hereafter. The definition of the L_{den} level (day–evening–night) is defined by the following formula:

$$L_{den} = 10log_{10}\frac{1}{24}\left[\left(12 * 10^{\frac{L_d}{10}}\right) + \left(4 * 10^{\frac{L_e+5}{10}}\right) + \left(8 * 10^{\frac{L_n+10}{10}}\right)\right]$$

where:

(a) Lday (L_d) is the A-weighted long-term average sound level as defined in standard "Acoustics - Description, measurement and assessment of environmental noise - Part 1: Basic quantities and assessment procedures" [41], determined over all the day periods of a year,

(b) Levening (L_e) is the A-weighted long-term average sound level as defined in ISO 1996-1:2003, determined over all the evening periods of a year,

(c) Lnight (L_n) is the A-weighted long-term average sound level as defined in ISO 1996-1:2003, determined over all the night periods of a year.



FIGURE 2
55 dB(A) and higher exposure areas of noise sources at daytime, L_{den}

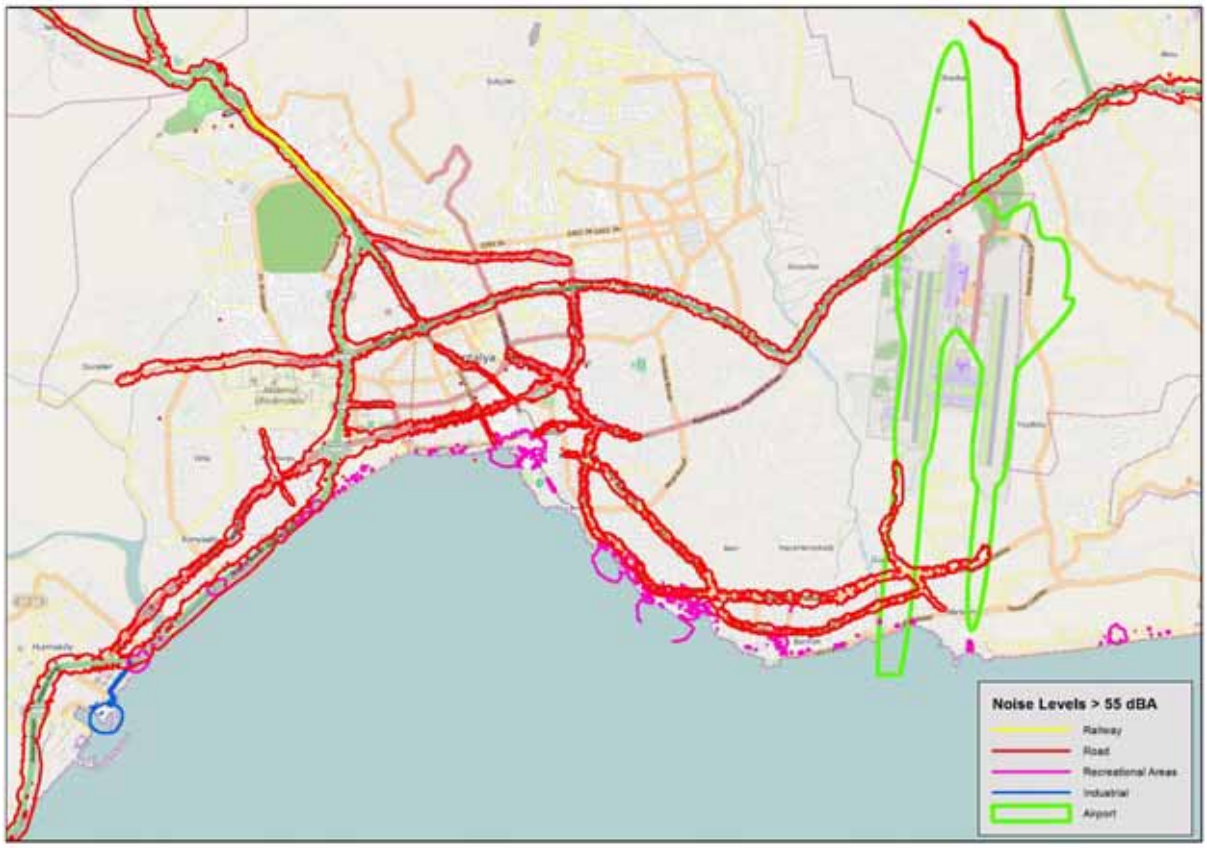


FIGURE 3
55 dB(A) and higher exposure areas of noise sources at nighttime, L_n



FIGURE 4
Spatial pattern of population affected by noise at daytime, L_{den}



FIGURE 5
Spatial pattern of population affected by noise at nighttime, L_n

In SoundPLAN software, each building can carry a series of attributes such as residential, school and hospital. The "residential" attribute identifies buildings for which both the number of people and the number of dwellings exposed to certain noise levels are calculated. The attributes "school" and "hospital" identifies sensitive buildings. The number of buildings per noise level band is counted for these attributes.

The exceedance maps for threshold values of 55, 65 and 75 dB(A) were prepared at an elevation of 4 m above the ground in the study area for all noise indicators. The number of households, sensitive buildings, and population situated in the areas that are exposed to these noise levels were also calculated for two time zones. In Fig.4 and Fig.5, spatial pattern of population affected by noise were given at daytime and nighttime, respectively.

RESULTS AND DISCUSSION

Comparison of 55 dB(A) and higher noise level impact indicates that road, Antalya airport, and entertainment places are the three noisiest sources of all followed by railway and industrial zones during 24 hrs. time period in Antalya city. 65 dB(A) and higher noise levels for road, Antalya airport, and entertainment places exceeded and their exposed population were 73,300, 9,500, and 2,900 respectively. The violations observed for 75 dB(A) and higher noise levels for road and entertainment places for which exposed population were 17,400, and 700 respectively. The average noise levels sourced from airport, railway, and industrial zones essentially conform to the 75 dB(A) limit for daily time interval.

In addition, nearly %10 of population exposed from road noise, %1 both from Antalya airport and entertainment places for 55 dB(A) and higher noise levels during the night time period. However, for railway and industrial zones average noise levels for night time period conformed to the regulatory standards. For 65 dB(A) and higher noise levels, only %3 of population exposed from road noise. There are negligible amount exposure from 75 dB(A) and higher noise levels were determined for the same time period. Comparison of noise impacts of sources on population at daytime and nighttime were shown in Fig.6 and Fig.7, respectively.

CONCLUSIONS

As it can be observed, high exposure values are estimated from road and airport noise, lower values are determined from railway and industrial zones' noise for both 24 hrs. and night time periods. This is mainly due to the higher number of vehicles on roads and more flight numbers in Antalya airport and the dense population in residences live near these noise sources.

From this comparison, it is evident that population affected by railway, entertainment places, and industrial zones noise decrease their rating and road and aircraft noise raise, that is coherent with the annoyance assumptions, considering a greater annoyance for road and aircraft noise and smaller for other noise sources in the study area.

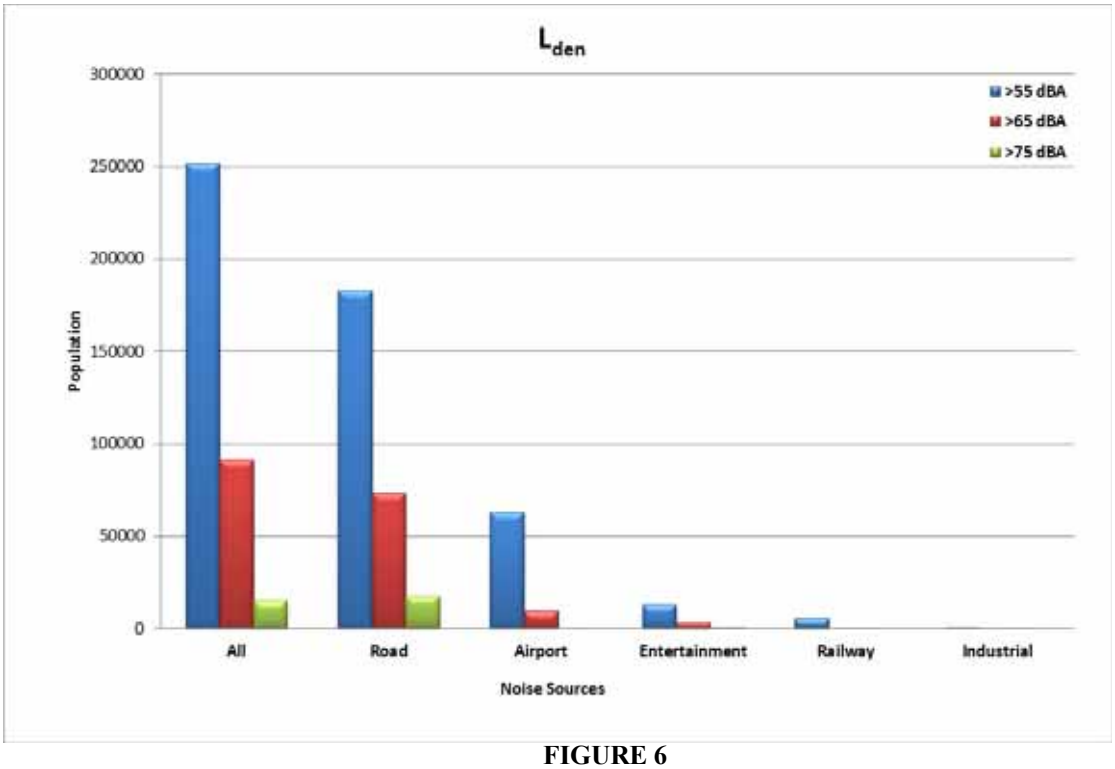


FIGURE 6
Comparison of noise impacts of sources on population at daytime, L_{den}

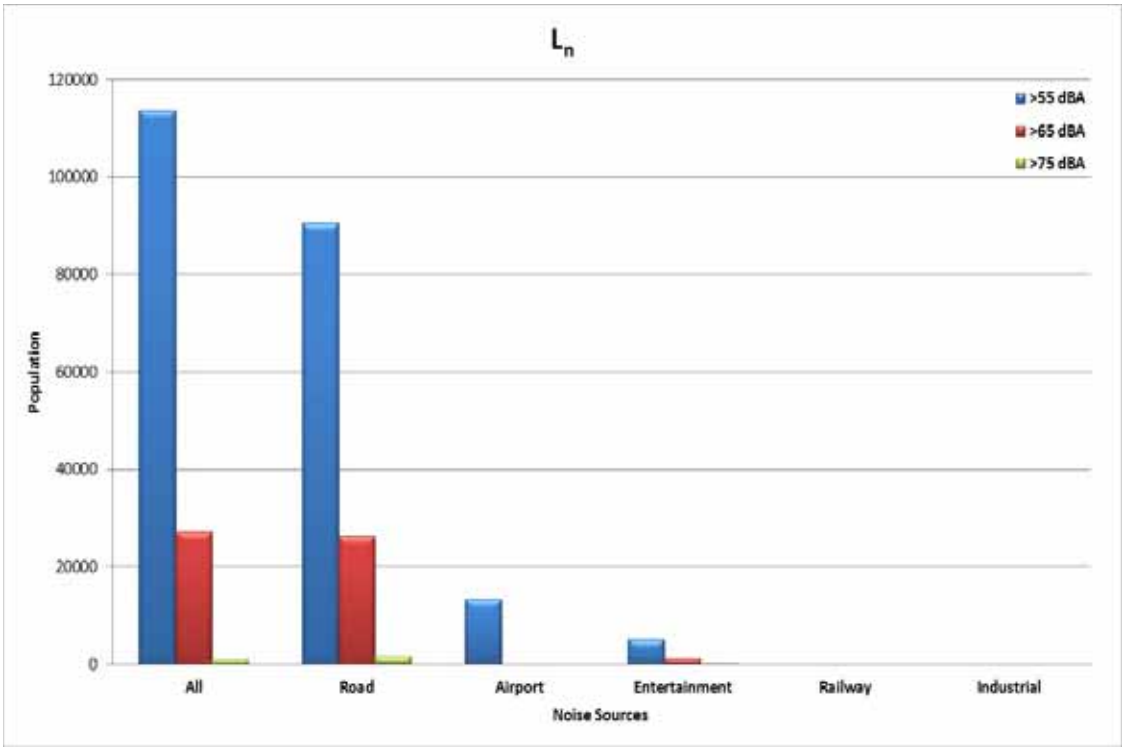


FIGURE 7
Comparison of noise impacts of sources on population at nighttime, L_n

ACKNOWLEDGEMENTS

The authors appreciate the support of TUBITAK Marmara Research Center, Environment and Cleaner Production Institute. The authors also would like to thank Antalya Metropolitan Municipality and General Directorate of State Airports Authority for permission to use the project data.

The authors have declared no conflict of interest.

REFERENCES

[1] OSHA (2013) Occupational Safety and Health Administration (OSHA) Technical Manuel - Section III: Chapter 5. In: 01.12.2017, United States Department of Labor. Available from: https://www.osha.gov/dts/osta/otm/new_noise/.

[2] Saeki, T., Fujii, T., Yamaguchi, S. and Harima, S. (2004) Effects of acoustical noise on annoyance, performance and fatigue during mental memory task. Applied Acoustics. 65(9), 913-921.

[3] Lee, P.J., Shim, M.H. and Jeon, J.Y. (2010) Effects of different noise combinations on sleep, as assessed by a general questionnaire. Applied Acoustics. 71(9), 870-875.

[4] Klaeboe, R., Amundsen, A.H., Fyhri, A. and Solberg, S. (2004) Road traffic noise - the relationship between noise exposure and noise annoyance in Norway. Applied Acoustics. 65(9), 893-912.

[5] Kluizenaar, Y. and Miedema, H. (2009) Road traffic and cardiovascular health effects-Road traffic noise and air pollution. In: INTER-NOISE 2009. Ottawa, Ontario, Canada.

[6] Pirrera, S., De Valck, E. and Cluydts, R. (2010) Nocturnal road traffic noise: A review on its assessment and consequences on sleep and health. Environment International. 36(5), 492-498.

[7] Jakovjevic, B., Paunovic, K. and Belojevic, G. (2009) Road-traffic noise and factors influencing noise annoyance in an urban population. Environment International. 35(3), 552-556.

[8] Basner, M., Mullner, U. and Griefahn, B. (2010) Practical guidance for risk assessment of traffic noise effects on sleep. Applied Acoustics. 71(6), 518-522.

[9] Eberhardt, J.L. (1988) The influence of road traffic noise on sleep. Journal of Sound and Vibration. 127(3), 449-455.

[10] Eberhardt, J.L. and Akselsson, K.R. (1987) The disturbance by road traffic noise of the sleep of young male adults as recorded in the home. Journal of Sound and Vibration. 114(3), 417-434.

[11] Ohrstrom, E., Rylander, R. and Bjorkman, M. (1988) Effects of night time road traffic noise-an overview of laboratory and field studies on noise dose and subjective noise sensitivity. Journal of Sound and Vibration. 127(3), 441-448.

[12] Van Kamp, I., Gidlöf-Gunnarsson, A. and Persson Waye, K. (2013) The effects of noise disturbed sleep on children's health and cognitive development. In: ICA 2013. 133, Montreal, Canada, 3506.

[13] WHO (2011) WHO night noise guidelines for Europe, In: 06.06.2016, World Health Organization. Available from: http://www.euro.who.int/en/health-topics/environment-and-health/noise/policy/who-night-noise-guidelines-for-europe.

[14] EC (1996) Future Noise Policy, European Commission Green paper. In: Com (96), Commission of the European Communities, Brussels, Belgium.

[15] End, Directive (2002) 2002/49/EC - Relating to the assessment and management of environmental noise in 189/12. The European Parliament and of the Council: Official Journal of the European Communities.

[16] Eriksson, C., Nilsson, M.E., Stenkvist, D., Bellander, T. and Pershagen, G. (2013) Residential traffic noise exposure assessment: application and evaluation of European Environmental Noise Directive maps. Journal of Exposure Science and Environmental Epidemiology. 23(5), 531-538.

[17] Ibbeken, S. and Krüger, M. (2013) Noise Mapping for Major Roads for the State of Baden-Wuerttemberg according to the Environmental Noise Directive. In: INTER-NOISE 2013. Inssbruck, Austria, 208.

[18] King, E.A., Murphy, E. and Rice, H.J. (2011) Implementation of the EU environmental noise directive: Lessons from the first phase of strategic noise mapping and action planning in Ireland. Journal of Environmental Management. 92(3), 756-764.

[19] King, E.A. and Rice, H.J. (2009) The development of a practical framework for strategic noise mapping. Applied Acoustics. 70(8), 1116-1127.

[20] Murphy, E. and King, E.A. (2010) Strategic environmental noise mapping: Methodological issues concerning the implementation of the EU Environmental Noise Directive and their policy implications. Environment International. 36(3), 290-298.

[21] Niemeyer, L., Cortês, M. and Ribas, L. (2013) Sustainable urban planning for Brazilian cities: noise management in the context of urban sprawl. In: INTER-NOISE 2013. Inssbruck, Austria, 212.

[22] Vaisis, V. and Janusevicius, T. (2009) Modelling of noise level in the northern part of Klaipeda city. Journal of Environmental Engineering and Landscape Management. 17(3), 181-188.
[23] Guardia, N. and Nugent, C. (2013) Overview of the Current State of the Environmental Noise Directive Implementation in Europe and Exploitation of Results. In: INTER-NOISE 2013. Inssbruck, Austria, 204.
[24] Brito, A. and Coelho, J. (2013) The Creation of the noise map of the city of Fortaleza. In: INTER-NOISE 2013. Inssbruck, Austria, 211.
[25] Dimitrios, A., Konstantinos, B. and George, C. (2013) Residential exposure to port noise and noise mapping: A case study of Piraeus, Greece. In: INTER-NOISE 2013. Inssbruck, Austria, 206.
[26] Panagopoulos, J., Bizakis, A., Zisopoulou, D., Karayannis, A., Kolletis, N., Tzekakis, E. and Kassomenos, P. (2016) Environmental noise mapping in Thessaloniki Greece. In: Vogiatzis, K., Kouroussis, G., Crocker, M. and Pawelczyk, M. (Eds.) Proceedings of the 23rd International Congress on Sound and Vibration: From Ancient to Modern Acoustics, Int Inst Acoustics & Vibration: Auburn.
[27] Baltrenas, P., Petraitis, E. and Janusevicius, T. (2010) Noise level study and assessment in the southern part of Panevežys. Journal of Environmental Engineering and Landscape Management. 18(4), 271-280.
[28] Vogiatzis, K. (2012) Airport environmental noise mapping and land use management as an environmental protection action policy tool. The case of the Larnaka International Airport (Cyprus). Science of The Total Environment. 424(Supplement C), 162-173.
[29] Ozkurt, N., Hamamci, S.F. and Sari, D. (2015) Estimation of airport noise impacts on public health. A case study of İzmir Adnan Menderes Airport. Transportation Research Part D: Transport and Environment. 36, 152-159.
[30] Ozkurt, N., Sari, D., Akdag, A., Kutukoglu, M. and Gurarslan, A. (2014) Modeling of noise pollution and estimated human exposure around Istanbul Ataturk Airport in Turkey. Science of the Total Environment. 482, 486-492.
[31] Ozkurt, N. (2014) Current assessment and future projections of noise pollution at Ankara Esenboga Airport, Turkey. Transportation Research Part D-Transport and Environment. 32, 120-128.
[32] Hamamci, S.F., Dogru, A.O., Sari, D., Ozkurt, N. and Seker, D.Z. (2017) Determining Characteristics of Lands Affected by Noise Pollution of Airports. Fresen. Environ. Bull. 26, 69-74.
[33] Sari, D., Ozkurt, N., Hamamci, S.F., Ece, M., Yalcindag, N., Akdag, A. and Akdag, N. (2014) Assessment of noise pollution sourced from entertainment places in Antalya, Turkey. In: INTER-NOISE 2014. Melbourne, Austria.
[34] AzB, (1999) Neue zivile Flugzeugklassen fo9r die Anleitung zur Berechnung von Larmschutzbereichen (Entwurf). Berlin: Umweltbundesamt.
[35] SoundPLAN, (2014) SoundPLAN User's Manuel, Braunstein + Berndt GmbH SoundPLAN International LLC.
[36] Sari, D., Ozkurt, N., Akdag, A., Kutukoglu, M. and Gurarslan, A. (2014) Measuring the levels of noise at the Istanbul Ataturk Airport and comparisons with model simulations. Science of The Total Environment. 482-483, 472-9.
[37] Babisch, W.F., Beule, B., Schust, M., Kersten, N. and Ising, H. (2005) Traffic noise and risk of myocardial infarction. Epidemiology. 16(1), 33-40.
[38] Bluhm, G.L., Berglind, N., Nordling, E. and Rosenlund, M. (2007) Road traffic noise and hypertension. Occupational and Environmental Medicine. 64(2), 122-126.
[39] Jarup, L., Babisch, W., Houthuijs, D., Pershagen, G., Katsouyanni, K., Cadum, E., Dudley, M. L., Savigny, P., Seiffert, I., Swart, W., Breugelmans, O., Bluhm, G., Selander, J., Haralabidis, A., Dimakopoujou, K., Sourtzi, P., Velonakis, M., Vigna-Taglianti, F., Hyena Study Team (2008) Hypertension and exposure to noise near airports: the HYENA study. Environmental Health Perspectives. 116(3), 329-333.
[40] Rosenlund, M., Berglind, N., Pershagen, G., Hallqvist, J., Jonson, T. and Bellander, T. (2006) Long-term exposure to urban air pollution and myocardial infarction. Epidemiology, 17(4), p. 383-390.
[41] ISO_1996-1 (2003) Acoustics - Description, measurement and assessment of environmental noise, In: Part 1: Basic quantities and assessment procedures.

Received: **22.12.2017**
Accepted: **24.01.2018**

CORRESPONDING AUTHOR

Melike Nese Tezel
TUBITAK Marmara Research Center,
Environment and Cleaner Production Institute
P.O. Box 21,
41470 Gebze, Kocaeli – Turkey

e-mail: nese.tezel@tubitak.gov.tr

© by PSP Volume 27 – No. 5/2018 pages 3133-3139 Fresenius Environmental Bulletin

PROBLEMS MEASURED AND EVALUATED OF IRRIGATED AGRICULTURAL AND NON-IRRIGATED AGRICULTURAL SOILS

Ahu Alev Abaci-Bayan*

Ahi Evran University, Faculty of Agriculture, Soil Science and Plant Nutrition of Department, Kirsehir

ABSTRACT

Healthy and balanced nutrition of a country's population as well as its future generations is possible by ensuring sustainable economic development through protecting the environment and biological diversity. In this study, the areas where two different agricultural systems applied were determined and soil samples were taken from 0-30 cm depth and soil analyses were carried out for ecological and agricultural evaluation.It was found that the saturation percentage of the soils varied between 41.80-84.70%, its pH varied between 7.27-8.19, the total amount of $CaCO_3$ varied between 2.55-21.24%, total salinity ratio 0.003-0.040%, organic matter content varied between 1.25-3.86%, the amount of beneficial P_2O_5 varied between 1.92-9.00 kg da^{-1} and the amount of available K_2O was found so high. In the study, it was concluded that the application of phosphorus and potassium fertilizer should be taken into account since the P_2O_5 level is high in irrigated soils and the soils are clay loam and the amount of K_2O is at an adequate level in both cultivated soils.

KEYWORDS:
Kirsehir, soil charactesitic, irrigated agricultural, non-irrigated agricultural

INTRODUCTION

It has been stated that 3200 million hectares of land in the world are potentially suitable for agriculture; however, only 1450 million hectares of them are still cultivated and that the majority of the remaining land of 1750 million hectares is less suitable for agriculture and environmentally sensitive soils. In the world, non-irrigated farminghas been carried out in 1200 million hectares, whereas irrigated agriculture has been carried out in 250 million hectares (17%). It is estimated that the total area, in which drainage is conducted, 150-200 million hectares (10-14%), and 100-150 million hectares of theseare located in rainy areas while 25-50 million hectares are located in irrigated areas [1].

It has been determined that the ecological conditions determine which of the agricultural systems, including irrigated, non-irrigated and moist agriculture will be put into practice in a region where the most effective factor in the field agricultural system is water. Irrigated agriculture is an agricultural system which has been applied in places where water cannot be met by natural rainfall but can be provided through irrigation, which is necessary for the normal development and crop production of plants. The quantity and quality of the products decreases and salinity-desertification problems soon begin if proper quality water is not used in irrigation no matter how efficient the soil is, how well modern irrigation methods are used. The quality of irrigation water is determined by the amount of dissolved salts in the waterand irrigation water mostly contains sodium, magnesium and calcium salts. Soil-plant-water relationships in irrigated farming lands and their effects on human and environment have not been considered thoroughly. Because of this, the producers tend to use excessive water because they could not be trained adequately, consequently they encounter many problems such as drainage, high groundwater, salinity and sodium. Among other agricultural systems, non-irrigated farmingis non-irrigated field farming, which is carried out in soilsan having annual rainfall of up to 500 mm or irregular rain distribution according to seasons. Non-irrigated farming is a mandatory method where rainfall is a limiting factor for plants. 60-65% of the total area in the world, while 81.7% of a total of 27.7 million hectares of cultivated land in Turkey, annual precipitation is less than 500 mm and non-irrigated farming has been applied. Fallow non-irrigated farming has been carried out in 74% of the non-irrigated farming areas, namely 16.8 million hectares. Because the water is limited in non-irrigated farming areas, the main purpose of non-irrigated farming is to maintain the water obtained from the precipitation as long as possible in the soil for a long time and to use the water most effectively [2].

The agricultural productivity of the soil and the content of plant nutrients are important for increasing agricultural production. The positive or negative physical and chemical properties of soils

and the lack or excess of plant nutrients is among the factors that affect the yield and quality of agricultural crops. If there are not enough plant nutrients to grow the plants in the soil, the appropriate type and amount of fertilizer is given to the soil to cover the deficit. A good fertilization is achieved by determining the amount and type of the fertilizer that the plant needs, and giving this fertilizer to the soil in accordance with its technique at the right time. The type and amount of fertilizer required for soil in the laboratory are determined by obtaining various soil samples from a specific area. Thanks to soil analysis, the nutrients which are found in the soil structure and needed for soil can be determined accurately. Hence, which fertilizer, how and in what quantities will be applied are determined through soil analysis.

In this study, physical and chemical analyzes were performed on the samples taken in order to determine the soil structure of some non-irrigated and irrigated farming carried out in Kırşehir province. Additionally, soil analysis results have been examined in terms of productivity and some suggestions have been made.

MATERIALS AND METHODS

Soil samples taken from 0-30 cm depth of irrigated and non-irrigated agricultural land are dried under laboratory conditions and prepared for an analysis by being crushed with a wooden hammer and sieved with a 2 mm sieve. According to the basis reported by Demiralay (1993) [3], percentage of saturation with water, 100 g of soil samples sieved with a 2 mm sieve were taken and soil colloid surface areas were saturated with water. Soil reaction (pH) was measured potentiometrically in saturation sludge by using a pH meter [4]. Total salinity in the saturation sludge was measured by the electrical pH conductivity probe [4]. Total lime was determined on a volume basis using Scheibler calcimetre with 10% hydrochloric acid [5]. The organic material was determined titrimetrically by oxidizing the organic carbon with 1.0 N $K_2Cr_2O_7$ ve H_2SO_4 and 0.5 N $FeSO_4.7H_2O$ by the 'Walkley-Black' method of wet decomposition [6]. Exchangeable potassium was extracted as reported by Helmke and Sparks (1996) according to the Ammonium acetate method (NH_4OAc, 1.0 N, pH:7) and the amount of potassium passing through the solution was determined in a flame photometer [7]. Beneficial phosphorus was determined by using 0.5 M sodium bicarbonate ($NaHCO_3$) using a UV-VIS spectrophotometer at a wavelength of 880 nm coulometrically according to the method developed by Olsen et al. (1954) [8]. Statistical evaluation was done by calculating standard deviation, variance, skewness, kurtosis, coefficient of variation and correlation.

RESULTS AND DISCUSSION

The average water saturation percentage of the study area soil at 0-30 cm depth was found to be 54.55% for irrigated areas, while it was found to be 54.08% for non-irrigated areas andsome soil analysis results are given in Table 1 and Table 2. The coefficient of variation for watery saturation percentages of irrigated soils was determined to be 27.99 %, while 20.08 % for non-irrigated soils and these values were found to be moderately variable. Because, the coefficient of variation is considered to be slightly variable if it is <15 and to be intermediate-level variable and to be highly variable if it between 16-35 if it is >36 [9].

The saturating condition which is used to determine the soil structures is given in Table 3. When the soils of the study area are evaluated according to Table 3, it is stated that both areas generally have a clay loam structure. The soil structure is one of the important physical properties that determines the level of soil fertility and is of great importance in terms of fertilization [10]. In addition, the analysis results of the soils based on the agricultural system used in the study areas are given in Figure 1.

It was observed that the average soil pH was 7.87 in irrigated areas from the study area, while it decreased to 7.64 in non-irrigated areas. When the soil is classified according to pH values, soils with a pH of 7.4-7.8 are usually mildly alkaline and those with a pH of 7.9-8.4 are considered to be moderately alkaline [12]. The percentage of variation coefficient of soil pH was found less than <15 for irrigated and non-irrigated farming, which indicates that the pH value of these areas is slightly variable. Accordingly, as a result of the evaluation of the study area soil according to Table 4, the pH of non-irrigated soils were found slightly alkaline and the pH of irrigated soils exhibited a moderately alkaline reaction. Soil reaction is a soil feature that significantly influences plant growth and availability of plant nutrients. If the annual amount of rainfall is low, it causes the soil pH to be high. The variable H^+ ion is less common in arid regions. Due to the influence of the prevailing climate condition, the bases in the soil are prevented from being washed away and turned into acid-reactive state [10].

TABLE 1
Soil analysis of results in irrigated agriculture areas

Soil No	Product	Texturing class	Saturation percentage	pH	Total salt	Total lime ($CaCO_3$)	Organic matter	Available Phosphorus (P_2O_5)	Exchangeable Potassium (K_2O)
			%		%	%	%	kg da^{-1}	kg da^{-1}
1	Walnut	Clay loam	60.53	7.53	0.011	15.83	3.72	13.61	287.38
2	Walnut	Loam	35.50	7.87	0.003	6.73	1.55	14.77	121.00
3	Walnut	Clay loam	54.45	7.95	0.010	21.24	1.51	8.55	114.95
4	Walnut	Clay loam	53.79	8.19	0.009	20.18	1.26	8.02	96.80
5	Walnut	Clay loam	61.60	7.95	0.011	14.18	1.38	7.88	104.36
6	Sunflower seeds	Loam	44.00	7.81	0.018	4.34	2.01	16.96	1614.59
7	Sunflower seeds	Clay	84.70	7.83	0.033	7.64	3.22	3.16	427.28
8	Sunflower seeds	Loam	41.80	7.81	0.003	3.22	2.46	1.92	170.01
	Minimum	-	35.50	7.53	0.003	3.22	1.26	1.92	96.80
	Maximum	-	84.70	8.19	0.033	21.24	3.72	16.96	1614.59
	Average	-	54.55	7.87	0.012	11.67	2.14	9.36	367.05
	Variance		233.12	0.03	0.00	50.48	0.84	29.08	267327.41
	Standard deviation		15.27	0.18	0.01	7.11	0.92	5.39	517.04
	Skewness		0.95	-0.13	1.58	0.21	0.91	0.02	2.57
	Kurtosis		1.41	2.10	3.02	-1.83	-0.61	-1.22	6.81
	Coefficient of variation (%)		27.99	2.35	80.50	60.88	42.82	57.61	140.86

TABLE 2
Soil analysis of results in non-irrigated agriculture areas

Soil No	Product	Texturing class	Saturation percentage	pH	Total salt	Total lime ($CaCO_3$)	Organic matter	Available phosphorus (P_2O_5)	Exchangeable potassium (K_2O)
			%		%	%	%	kg da^{-1}	kg da^{-1}
9	Barley	Loam	46.75	7.56	0.020	2.55	1.25	2.16	143.54
10	Barley	Clay loam	63.80	7.49	0.018	7.56	1.95	2.85	540.72
11	Barley	Clay loam	53.90	7.60	0.011	6.81	1.66	2.70	510.47
12	Barley	Loam	46.20	7.78	0.011	6.37	1.37	2.78	186.04
13	Barley	Loam	47.30	7.83	0.013	8.24	1.28	5.41	453.75
14	Barley	Loam	44.00	7.81	0.011	6.66	2.08	1.92	160.33
15	Barley	Clay	75.68	7.77	0.040	13.40	3.86	2.54	546.39
16	Barley	Clay loam	55.00	7.27	0.011	3.31	1.85	9.00	70.18
	Minimum	-	44.00	7.27	0.011	2.55	1.25	1.92	70.18
	Maximum	-	75.68	7.83	0.040	13.40	3.86	9.00	546.39
	Average	-	54.08	7.64	0.017	6.86	1.91	3.67	326.43
	Variance		117.90	0.04	0.00	10.95	0.72	5.78	41542.16
	Standard deviation		10.86	0.20	0.01	3.31	0.85	2.40	203.82
	Skewness		1.31	-0.93	2.20	0.83	2.09	1.98	-0.03
	Kurtosis		1.16	0.19	5.11	1.78	4.97	3.66	-2.43
	Coefficient of variation (%)		20.08	2.57	58.76	48.23	44.35	65.51	62.44

TABLE 3
Percentage of saturation condition [11]

Percentage of saturation	Meaning class
<%30	Sandy
%31-50	Loam
%51-70	Clay loam
%71-110	Clay
>%111	Heavy clay

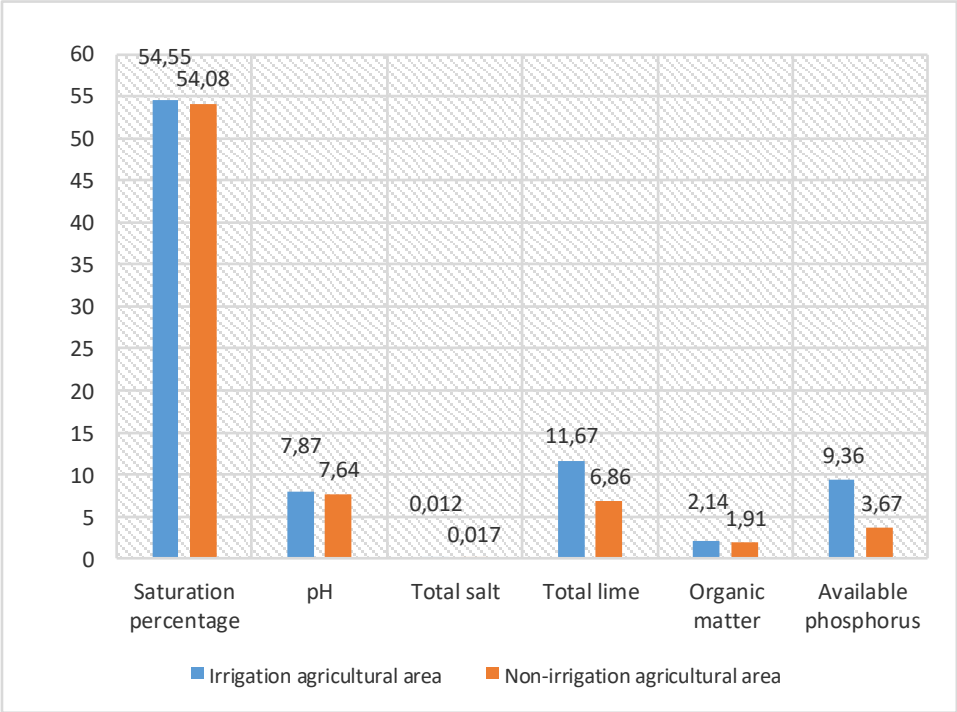


FIGURE 1
Analysis results of irrigation and non-irrigation agricultural soils

TABLE 4
According to the classification of soil pH [12]

pH values	Reaction
<4.5	Excess acid
4.5-5.0	Very strong acid
5.1-5.5	Strong acid
5.6-6.0	Medium acid
6.1-6.5	Light acid
6.6-7.3	Neutral
7.4-7.8	Light alkaline
7.9-8.4	Medium alkaline
8.5-9.0	Strong alkaline
>9.1	Very strong alkaline

TABLE 5
Total soil content of soils (%) [11]

Total soil (%)	Meaning class
<%0.15	Without salt
%0.15-0.35	Lightly salt
%0.35-0.65	Medium salty
>%0.65	Very salty

It was found that the average % salt content of the irrigated study soilwas 0.012%, while it was 0.017% for the non-irrigated soil. When the study area was classified according to total salt content percentage, it was determined that all of the soil contained less than 0.15%, which is the limit value for salinity and, it was determined that the soil was in the unsalted class when assessed according to Table 5. It was concluded that there is no problem in terms of salinity in the study area soils. The coefficient of variation of both study area soils is found >36, which means that the total salt content is highly variable.

The total lime content of the study area soil was found to be 11.67% for irrigated farming, while it was found to be 6.86% for non-irrigated farming soils. In order to determine the lime status of the soil in Table 6, % total lime contents are given and

classified accordingly as medium lime when the average values of the field soils are taken into account. However, in some irrigated areas, the total lime content was found to be too high. The excessive amount of lime in the soil prevents plant nutrients such as phosphorus, iron and zinc from being taken up by the plant. The coefficient of variation of both study area soils is found >36, which means that the total lime content is highly variable.

Soil organic matter is the most important structural component of soil and consists of plant and animal wastes. When the research area is compared with respect to the content of organic matter, the average area of organic matter in irrigated areas was 2.14% and the amount of organic matter in dry areas was 1.91%. The classification of soils by organic matter content is given in Table 7. Accordingly, it was determined that the organic matter content of the study area soil is included in the moderate and low classes, respectively. In these areas, it was foundthat application of the barn, vermicompost barnyard manure application, green fertilization and application of organic matter content should be done. The coefficient of variation of both soil samples is >36, which indicates that the total organic matter content is highly variable.

Phosphorus is among the plant nutrients that are most needed by the plant. It was determined that the average amount of phosphorus (P_2O_5) content in the soil of the irrigated farming areawas 9.36 kgda^{-1}, while it was 3.67 kg da^{-1} in the soil of non-irrigated farming area. The classification of soils according to their phosphorus content is given in Table 8. Accordingly, the study area was determined to be a soil with high and low levels of phosphorus in terms of the available phosphorus content of the soil. It was found that the amount of phosphorus available is particularly high in irrigated areas, while it is low in non-irrigated areas. Considering the analysis results of the soil, phosphorous fertilizers can be applied if needed. The coefficient of variation of both study area soils was >36, which indicated that the beneficial phosphorus contents were highly variable. Figure 2 shows the exchangeable potassium contents of agricultural areas.

TABLE 6
Total lime contentof soils (%) [11]

Total lime (%)	Meaning class
<%1	Less lime
%1-5	Lime
%5-15	Medium lime
%15-25	Excess lime
>%25	Too much lime

TABLE 7
Total organic matter content of soils (%) [11]

Organic matter (%)	Meaning class
<%1	Very little
%1-2	Little
%2-3	Medium
%3-4	Good
>%4	High

TABLE 8
Available phosphorus content of the soil (kg da^{-1}) [11]

kg P_2O_5 da^{-1}	Meaning class
<3	Very little
3-6	Little
6-9	Medium
9-12	High
>12	Very high

Potassium element is among the plant nutrients that are widely found in the soil. Thin soils contain more potassium than coarse soils [10]. It was shown in Figure 2 that the average available potassium (K_2O) content of the irrigated area in the study was found to be 367.05 kg da^{-1}, while it was found to be 326.43 kg da^{-1} in non-irrigated farming soils. The classification of soils according to their

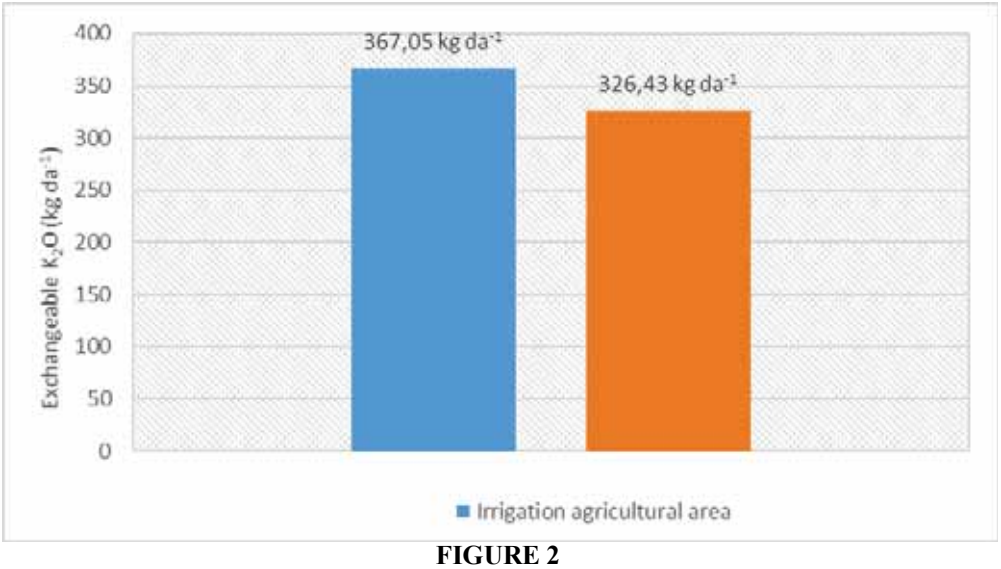


FIGURE 2
Exchangeable potassium status of irrigated and non-irrigation agricultural soils

available potassium content is given in Table 9, and according to this classification, the study area was determined to be sufficient in terms of available potassium content of the soils. Potassium fertilization is not needed since there is no difference in plant growth and yield as a result of potassium fertilization due to the sufficient amount of potassium in the soil of the region. The coefficient of variation of both study area soils was >36, which indicated that the beneficial phosphorus contents were highly variable.

TABLE 9
Exchangeable potassium content of the soil (kg da^{-1}) [11]

K_2O kg da^{-1}	Meaning class
<20	Very little
20-30	Little
>30	Adequate

As a result of the statistical analysis on the soil structure of the study area, it was found that there is a positive correlation between the water saturation percentages of irrigated agriculture soil and total salinity value at $p < 0.05$ significance level. It has been determined by [13] that the total salinity value is higher in the horizons where the saturation value is high in the Gavur Lake soil. It was observed that there was a negative correlation between pH value of field soils and organic matter content at $p < 0.05$ significance level. Similar findings were found in [13] and [14] have also been reported, and as the soil pH increases, the content of organic matter decreases.

Dry agricultural areas of research lands made correlation analysis total salinity values and percent saturation with water as a result of $p < 0.05$ significance level is positive, in percent saturation with water to the organic matter content $p < 0.01$ was found positive relationship cardinality. The organic matter content of soils causes the increase of the specific surface area of the soils and the soil becomes sature with higher moisture contents [13]. It has been observed by [15] that the percentage of saturation of the soil with water increases due to the dose rate increase of the hazelnut compost, which can be applied to the soil, [16] examined the physical and chemical relationships of 24 soil samples and found a positive relationship between organic matter and saturation value. Organic matter with a total salinity $p<0.01$ level of significance was found a positive correlation. The Golbasi Lakes horizon where the low total salinity of soil the soil is found to be low in organic matter content [13]. Total lime with between potassium $p<0.05$ level of significance was found a positive correlation. [17] by the application of lime soil pH of the soil, available phosphorus, potassium and can also in many research studies to increase the amount of calcium was determined [18-19-20-21-22].

CONCLUSION

It was found that hot and dry climatic conditions and high clay coverage lead soil to be rich in potassium plant nutrients and soil potassium excess has been observed in many study area soils rather than potassium deficiency. When the average values of the analysis results of the study area soils are taken into account, it was determined that the soil is clay loam, and the soil is unsalted and medium calcareous, and also available potassium element is sufficient. In irrigated areas, it was found that the amount of available phosphorus amount is high, the amount of organic matter is moderate, and the area soil exhibited a moderate alkaline reaction. In non-irrigated farming areas, it was concluded that the amount of available phosphorus and organic matter is low, and the soil is characterized by mild alkalinity. It was determined that the practices which increase of organic matter content, such as barnyard manure, vermicompost application, green fertilization, should be carried out in the study area soil. In conclusion, it was determined thatthe phosphorous fertilizer application should be reduced in the soil where the content of phosphorus is high, and fertilizer application should be done based on the plant nutrient needs by carrying out soil analyses regularly.

REFERENCES

[1] FAO. (1994) Forest Resources Assessment 1990-non-tropical developing countries Mediterranean region. FO: MISC/94/3. Rome. www.fao.org/docrep/007/t3910e/t3910e00.htm
[2] Kendirli, B., Cakmak, B. (2005) Problems and Solutions in Irrigated Farmland in Turkey. Ministry of Agriculture and Rural Affairs. July-August 2005. Number:164. Ankara, 28-32.
[3] Demiralay, I. (1993) Physical Analysis of Soil. Atatürk University, Agricultural Faculty Publications No: 143, Erzurum.
[4] Thomas, G.W. (1996) Soil pH and Acidity. In: Sparks, D.L. (ed.) Method of Soil Analysis: Chemical Methods. Part 3. SSSA. Madison, WI. 475-491.
[5] Gulcur, F. (1974) Physical and Chemical Analysis Methods of Soil. Istanbul University, Faculty of Forestry Publications No: 1970, Faculty of Forestry Publications No: 201, İstanbul.
[6] Nelson, D.W., Sommers, L.E. (1996) Total Carbon, Organic Carbon, and Organic Matter. In: Sparks, D.L. (ed.) Method of Soil Analysis: Chemical Methods. Part 3. SSSA, Madison, WI. 961-1011.

[7] Helmke, P.A., Sparks, D.L. (1996) Lithium, Sodium, Potassium, Rubidium, and Calcium, in Sparks, D.L., (Ed) Methods of Soil Analysis, Part 3, Chemical Methods, SSSA Book Series Number 5, SSSA., Madison, WI. 551-574.
[8] Olsen, S.R., Cole, V., Watanabe, F.S., Dean, L.A. (1954) Estimation of Available Phosphorus in Soils by Extraction with Sodium Bicarbonate. U.S.D.A. Circular Number 939, U.S. Government Printing Office, Washington.
[9] Wilding, L.P., Bouma, J., Goss, D.W. (1994) Impact of Spatial Variability on Interpretative Modelling. In: Bryant, R.B. and Arnold, R.W. (Eds.) Quantitative Modellling of soil Forming Processes. SSSA Special publication no:39, SSSA Inc. Madison, WI. 65-75.
[10] Eyupoglu, F. (1999) Soil Fertility Status of Turkey. General Directorate of Rural Services, soil and Fertilizer Research Institute Publications, General publications No:220, Technical publications No:67. Ankara.
[11] Ulgen, N., Yurtseven, N. (1995) Turkey Fertilizer and Manure Guide. Soil and Fertilizer Research Institute publications. General Publication No:209, Technical Publication No: 66. Ankara.
[12] Ergene, A. (1993) Principles of Soil Science. Atatürk University, Publications No: 586, Agricultural Faculty Publications No: 267, Textbook Series No: 42, Erzurum.
[13] Abacı Bayan, A.A. (2016) Soil Characteristics, Efficiency Levels and Problems of Wetlands In the Eastern Mediterranean Region. University of Kahramanmaras Sutcu Imam, Graduate School of Natural and Applied Sciences Department of Soil Science and Plant Nutrition, Phd Thesis.
[14] Jeanneau, L., Jaffrezic, A., Pierson-Wickmann, A.C., Gruau, G., Lambert, T., Petitjean, P. (2014) Constraints on the Sources and Production Mechanisms of Dissolved Organic Matter in Soils from Molecular Biomarkers. Vadose zone Journal. 13(7).
[15] Birol, Y., Bender Ozenc, D. (2011) The Effect of Hazelnut Zuruf Compost on the Physical Properties of Compressed Clayey Soil. National Soil and Water Symposium 25-27 May 2011 Ankara.
[16] Aygun, C., Kara, I., Sever, A.L., Erdogdu, I., Atalay, A.K., Avag, A., Mermer, A., Özaydınlı, A., Yıldız, H., Urla, Ö., Aydoğdu, M., Ünal, E., Aydoğmuş, O., Dedeoğlu, F., Tuğaç, M.G., Torunlar, H., Cebel, H., Başkan, O., Keçeci, M., Depel, G. (2013) Determination of Some Physical and Chemical Properties of the Bilecik Provincial Territory. III. National Soil and Water Resources Congress 22-24 October 2013-Tokat.
[17] Ozyazici, G. (2014) Effect of Lime and Sugar Industry Waste First Carbonification Sludge on the Yield and the Some Soil Properties in Hazelnut (*Corylus avellana* L.) Grown in Acid Soil. Turkey Agricultural Research Journal. 1, 176-185.
[18] Aydın, A., Sezen, Y. (1990) The effect of lime on the availability of some macro and micro nutrients with some properties of acid soil of the Eastern Black Sea Region. Atatürk University Faculty of Agriculture Journal. 21(1), 94-105.
[19] Murata, M.R., Hammes, P.S., Zharare, G.E. (2002) Soil amelioration effects on nutrient availabiliy and productivity of ground nut on acid sandy soils of Zimbabwe. Experimental Agriculture. 38, 317-331.
[20] Kovacevic, V., Rastija, M. (2010) Impacts of liming by dolomite on the maize and barley grain yields. Poljoprivreda. 16(2), 3-8.
[21] Karalic, K., Loncaric, Z., Popovic, B., Ivezic, V. (2013) Phosphorus and potassium availability change by liming of acid soils. IV. International Symposium, Agrosym 2013, 119-124.
[22] Osundwa, M.A., Okalebo, J.R., Ngetich, W.K., Ochuodho, J.O., Othieno, C.O., Langat, B., Omenyo, V.S. (2013) Influence of agricultural lime on soil properties and wheat (*Triticum aestivum L.*) yield and acidic soils of Uasin Gishu County, Kenya. American Journal of Experimentel Agriculture. 3(4), 806-823.

Received: **25.12.2017**
Accepted: **23.02.2018**

CORRESPONDING AUTHOR

Ahu Alev Abaci-Bayan
Ahi Evran University,
Faculty of Agriculture,
Soil Science and Plant Nutrition of Department, Kirsehir

e-mail: ahuabaci@gmail.com

© by PSP Volume 27 – No. 5/2018 pages 3140-3147 Fresenius Environmental Bulletin

ARBUSCULAR MYCORRHIZAL FUNGI IN *CYNODON DACTYLON* (L.) PERS. (BERMUDA GRASS) FROM TEMPERATE BLACK SEA COASTAL REGIONS

Sahin Palta*

Bartin University, Faculty of Forestry, Department of Forest Engineering, Division of Watershed Management, Subdivision of Range Management, Bartin, Turkey.

ABSTRACT

Arbuscular mycorrhizal fungi (AMF) exist in herbaceous plants' rhizospheres from the Black Sea temperate zone. The AMF is significant for herbaceous plants during their life processes and stages; it has vital importance under the marginal climate conditions and protects plants against soil-borne diseases. The aim of this research is to investigate the symbiotic status of AMF species with *Cynodon dactylon* (L.) PERS., within the temperate coastal regions of the Black Sea. In order to achieve this aim, 20 samples of Bermuda grass were collected from the study area. AMF spore abundance and diversity were determined in the study area during the 2016 dry season. Also, physical and chemical properties of the rhizosphere soils were analyzed, including the pH, $CaCO_3$ content, organic carbon, available P, available K, soil texture, and total N. Furthermore, 12 arbuscular mycorrhyzal fungi species were diagnosed. Identified spores belonged to *Ambispora*, *Dentiscutata*, *Funneliformis*, *Cetraspora*, *Claroideoglomus*, *Acaulospora*, *Scutellospora*, *Rhizoglomus*, and *Gigaspora* genus. The diagnosed dominant AMF genus was *Gigaspora.* The soil of rhizosphere had low organic carbon, low available P, low available K, low total N, high $CaCO_3$ content, almost neutral pH, and sandy soil. The symbiotic status of *Cynodon dactylon* with arbuscular mycorrhizal fungi species demonstrated that the indigenous *Cynodon dactylon* carried substantial potential as a host plant for AMF species in sandy soils from Black Sea temperate coastal regions.

KEYWORDS:
Arbuscular mycorrhizal fungi (AMF), *Cynodon dactylon,* soil properties, symbiosis.

INTRODUCTION

The Black Sea region in Turkey possesses distinctive ecological conditions that nestles and homes many herbaceous plants, some of which are endemic and include rare species such as *Pancratium maritimum* L. from the Amaryllidaceae family in sandy soil.

Droughts and salinities have become an unavoidable reality in terms of global warming. Natural resources are the most important wealth and genetic resources [1]. There is an important relationship among AMF root colonization, soil characteristics, and host plants [2]. The symbiotic relationships of plants with arbuscular mycorrhizal fungi is sigificant in terms of life processes of plants. The plants that have symbiotic mutualistic relationships with AMF are relatively more advantageous compared with the non-AMF plants. The AMF supplies water and mineral nutrients to the plants and protects them against soil-borne diseases, salt, and drought stress and contributes to moving toxic materials contamineted to the host plants [3, 4, 5, 6, 7]. The symbiosis between AMF and host plants is mutualistic; the AMF utilizes some of the carbon budget of the plants, which they produce during photosynthesis and supply soil water and nutrients, mainly nitrogen and phosphorus, to the host plants [8, 9, 10, 11].

The limiting soil characteristics such as low nutrient availability and water deficiency are stress-causing situations that reduce crop yields around the whole world [12]. The symbiosis between host plant and AMF is crucial from the point of enhancing water supply and plant nutrition [13, 14, 15, 16].

Plant diversity and community may be affected by the AMF community in that it establishes symbiotic mutualistic relationships with plants [17, 18]. Besides, AMF diversity and community may be influenced by host plant species [19, 20, 21, 22, 23]. Also, it was reported that AM fungi may have an impact on ecosystem processes, such as carbon cycle, productivity, and nutrient mobilization [24].

Bermuda grass [*Cynodon dactylon* (L.) PERS. (Gramineae)] is a perennial native herbaceous plant in the temperate coastal region of the Black Sea. Bermuda grass is especially indigenius to the tropical and temperate regions around the world. *C. dactylon* contains carbohydrates, proteins, minerals, carotenoids, flavonoids, and glycosides. Bermuda grass has been utilized for traditional medicine because it features antiviral, antimicrobial, antibacterial, and injury-healing properties [25].

C. dactylon is a significant grass species commonly utilized within playgrounds and greenbelt areas. It has been noted that the total plant dry weight of some Bermuda grass was not substantially influenced by low N supplement [26]. It was also noted that *C. dactylon* exhibited natural tolerance against submergence because it improved photosynthesis after re-aeration and developed aerenchyma [27]. Besides, it was stated that the AMF inoculation improved the reproduction of the *C. dactylon* after cutting [28]. Furthermore, it was noted that AMF inoculation enhanced the photosynthetic rate of host plants [29,30]. It was declared that plants with mycorrhiza had higher chlorophyll content in order to encourage photosynthesis [28].

Several studies were carried out to analyze the relationships between native arbuscular mycorrhizal fungi and native plants in Turkey's Black Sea region. The aim of this research is to determine the symbiotic status between AMF species and *Cynodon dactylon* (L.) PERS. in sandy soils in temperate coastal regions of the Black Sea. Thus, this research would contribute to investigations into the distribution of AMF biodiversity and the ecological properties of native arbuscular mycorrhizal fungi in those temperate coastal regions.

MATERIALS AND METHODS

Study area. The study area is located in a temperate coastal region in the Bartın province within the northwestern Black Sea, Turkey (Fig. 1). The geographical coordinates of the research area are within 32° 22′ eastern longitude and 41° 37′ northern latitude. The altitude of the study area is almost zero m asl. The meteorological data utilized in this study belong to the meteorological station of the Bartın province. According to the meteorological data (of 30 years between 1982 and 2011), the annual average temperature is 12.6°C, while the annual average precipitation is 1044 mm [31,32]. The study area is dominated by the humid mesothermal climate type [33]. The mean temperature of the coldest month (January) and the hottest month (July) are 4.1°C and 22.2°C, respectively. The average precipitation of the driest month (May) and the wettest month (October) are 49 mm and 123 mm, respectively [32].

Soil Sampling. Soil samples were collected during the vegetation period of 2016 (dry season). In the study area, 20 different composite root zone samples that involve soil and root fragments were randomly taken from the near hairy root line and deeper (0–30 cm deep) from *Cynodon dactylon*. The rhizosphere soil samples were sieved using a 2 mm sieve from the study area, placed in polyethylene bags, and stored at 4°C until analysis. Thus, 20 soil samples were transferred from the study area and analyzed. Besides, during the dry season, the samples were collected because the fungal sporulation was estimated to be higher during that period within arid and semi-arid ecosystems [34]. The soil samples of rhizosphere collected from the study area were separated into portions in order to analyze some of the chemical and physical properties of soil and AMF diversity and abundance.



FIGURE 1
Bartın Watershed [2].

Isolation and identification of arbuscular mycorrhizal fungi. Spores of AMF were isolated by the wet sieving method, which then was followed by the sucrose centrifugation [35,36]. Initially, isolated spores were analyzed under water through a dissecting microscope. They were classified dependent upon their morphological characteristics. The species definition relied on the diagnosis based on [37] and on scientific literatures about the new genera and families (i.e., [38]) and through considering and referring to the international AMF database [39]. For this study, it was decided that the suggestion by [40] was a relatively more appropriate classification, involving relatively recent diagnosed new taxa (i.e., [41]).

Chemical and physical properties of the soils. The standard methods were applied for the analysis of the soil chemical and physical characteristics. These standard methods included the hydrometer method for the identification of the particle size distribution of the soil [42]. A pH meter was used to identify pH in 1:2.5 soil/water suspension [43]. The EC meter was preferred for the determination of electrical conductivity in 1:5 soil/water suspension [44]. The Kjeldahl method and Walkley–Black wet oxidation method were applied for the analysis of soil total nitrogen and organic carbon, respectively [45, 46]. The available phosphorus was determined based on the methodology of [47]. The Scheibler calcimeter method was practiced for identifying the $CaCO_3$ content [48].

RESULTS AND DISCUSSION

Soil properties. Chemical and physical properties of the soil were analyzed such as pH, $CaCO_3$ content, organic carbon, available P, available K, soil texture, and total N. Furthermore, the rhizosphere soil had low organic carbon, low available P, low available N, high $CaCO_3$ content, almost neutral pH, and sandy soil (Table 1).

The results of these sandy soil properties indicated that the soil was relatively unfavorable for plant growth. It was reported that the sandy soils had high permeability because they have large porosity, and they quickly warm up. The sandy soils were dry in the dry seasons or areas when and where drought is predominant. Plant nutrients are low due to the lack of clay in sandy soils [49,50].

TABLE 1
Properties of rhizosphere soil of *Cynodon dactylon.*

Soil Properties	Sand (%)	Clay (%)	Silt (%)	pH (H_2O)	Electrical Conductivity (dS m^{-1})	$CaCO_3$ (%)	Organic Carbon (%)	Total Nitrogen (%)	Available Phosphorus (ppm)	Available Potassium (ppm)
Minimum	90.50	5.30	2.40	7.04	0.01	17.85	0.72	0.04	4.20	77.98
Maximum	93.20	7.50	4.10	7.20	0.01	18.97	0.75	0.06	4.70	81.25
Average	91.40	6.00	2.60	7.12	0.01	18.16	0.74	0.05	4.46	79.52

TABLE 2
Identified AMF spores in rhizosphere soil of *Cynodon dactylon.*

Order	Family	Species
Diversisporales	Acaulosporaceae	*Acaulospora laevis* Gerd. & Trappe
	Gigasporaceae	*Dentiscutata reticulata* (Koske, D.D. Mill. & C. Walker) Sieverd., F.A. Souza & Oehl
		Cetraspora pellucida (T.H. Nicolson & N.C. Schenck) Oehl, F.A. Souza & Sieverd
		Gigaspora albida N.C. Schenck & G.S. Sm.
		Gigaspora decipiens I.R. Hall & L.K. Abbott
		Gigaspora margarita W.N. Becker & I.R. Hall
		Scutellospora calospora (T.H. Nicolson & Gerd.) C. Walker & F.E. Sanders
Glomerales	Claroideoglomeraceae	*Claroideoglomus claroideum* (N.C. Schenck & G.S. Sm.) C. Walker & A. Schüßler
		Claroideoglomus etunicatum (W.N. Becker & Gerd.) C. Walker & A. Schüßler
	Glomeraceae	*Funneliformis geosporum* (T.H. Nicolson & Gerd.) C. Walker & A. Schüßler
		Rhizoglomus fasciculatum (Thaxt.) Sieverd., G.A. Silva & Oehl
		Ambispora gerdemannii (S.L. Rose, B.A. Daniels & Trappe) C. Walker, Vestberg & A. Schüßler

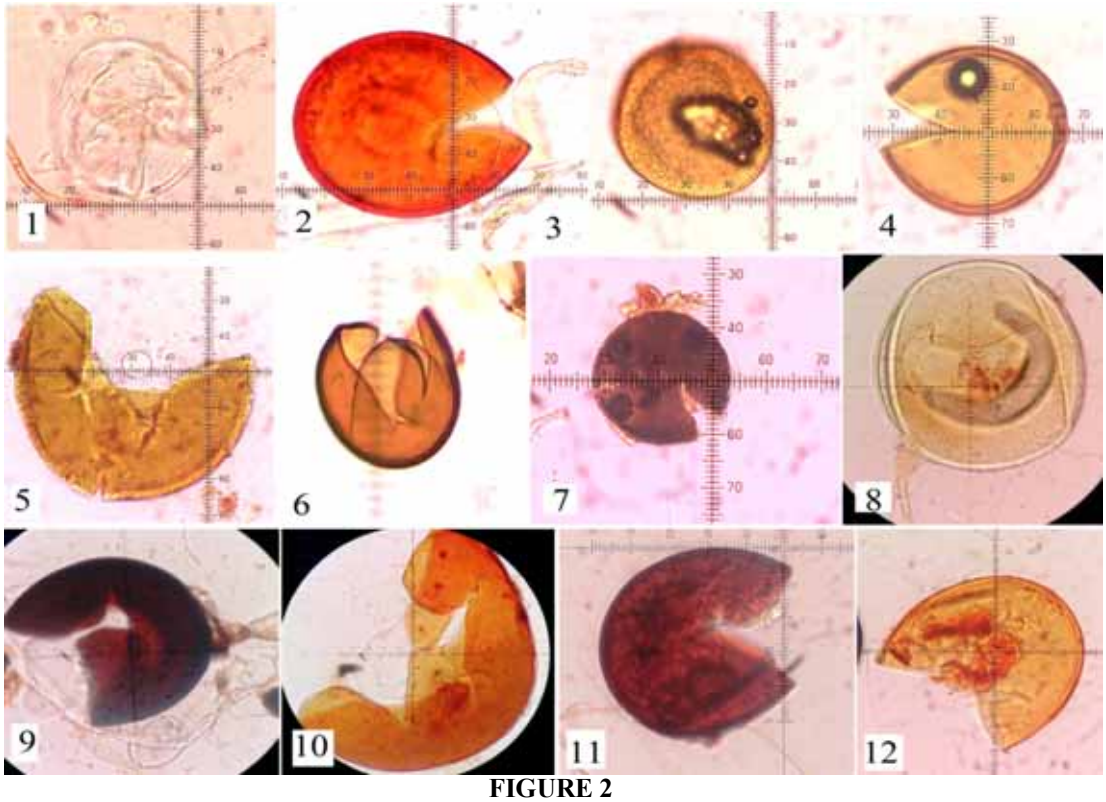


FIGURE 2

Isolated AMF spores from rhizosphere soil of Bermuda grass. 1) *Ambispora gerdemannii* (71x83µ), 2) *Acaulospora laevis* (132µ), 3) *Cetraspora pellucida* (103µ), 4) *Claroideoglomus claroideum* (105µ), 5) *Claroideoglomus etunicatum* (82x152µ), 6) *Dentiscutata reticulata* (105x135µ), 7) *Funneliformis geosporum* (63µ), 8) *Gigaspora albida* (315µ), 9) *Gigaspora decipiens* (252x345µ), 10) *Gigaspora margarita* (225x435µ), 11) *Rhizoglomus fasciculatum* (151µ), 12) *Scutellospora calospora* (138x175µ).

Arbuscular mycorrhizal fungi. AMF spore abundance and diversity were determined in this study during the 2016 dry season. The spore density of AMF was 18.75 spores 25 g^{-1} soil in the study field (Table 2). The 12 different AMF species were diagnosed belonging to nine different genera: *Ambispora* (1); *Acaulospora* (1); *Cetraspora* (1); *Claroideoglomus* (2); *Dentiscutata* (1); *Funneliformis* (1); *Gigaspora* (3); *Rhizoglomus* (1); *Scutellospora* (1) (Table 2, Figure 2).

Glomus mosseae and *Glomus intraradices* were diagnosed from *Gramineae* family plants from Turkey [51]. Besides, it was stated that the species of *Glomus* genus were the common (mainly *G. Occultum*, *G. intraradices*, and *G. mosseae*) AMF around the world [52,53]. Yet, it was found that the dominant order was *Diversisporales*, and the dominant genus was *Gigaspora* in this study. It was declared that distribution of AMF biodiversity related to the salinity, soil pH, deterioration of soil structure (fertilization, tillage etc.), amount of phosphorus [54], vegetation status [55], and hydrological status of the soil [56, 57].

The results of the study demonstrated that the AMF carried low spore counts in rhizosphere soil in *Cynodon dactylon*. This status does not mean that the symbiotic relationship between AMF and *Cynodon dactylon* is poor; as stated, the growth of the AMF is generally in balance with the growth of the host plant [58]. Considering the physical and chemical properties of the soil of the study area, it was shown that these soils included insufficient nutrients such as low organic carbon, available K, available P, total nitrogen, and high lime content. All of these soil properties would have restricted the growth and development of *Cynodon dactylon*. Therefore, the spore density of the AMF in the rhizosphere of *Cynodon dactylon* may also have been low. It was impressed that the growth of the AMF was slowed and decreased when the carbon source decreased due to the host plant [59, 60]. Besides, the soil texture of the study area was sandy, which has low water-holding capacity because it has high drainage capacity. However, it was also reported that the soil water availability was significant for a AMF-host plant relationship, particularly in terms of the functioning and biodiversity [34].

It was stated that soil characteristics were considerable parameters affecting the AMF composition in the rhizosphere soil of the host plant [61]. Futhermore, soil properties such as available phosphorous, pH, etc. were able to alter the AMF composition, raising the frequency of mutualists from genera *Scutellospora*, *Gigaspora*, *Funneliformis*, and *Acaulospora* [40, 62]. Similarly for this study, it was found that the spore densities

were 1 g^{-1}1 soil and AMF species were 16, belonging to nine genera in the sand dunes in the rhizosphere soil of *Asteriscus maritimus* (L.) Less [63]. In this study, *Gigaspora* was found to be the dominant species, but no spores were obtained from *Gigaspora* in sand dunes [63]. Besides, it was reported that the dominant family was *Glomeraceae* [63], but it was *Gigasporaceae* in this study.

It is believed that the AMF had important contributions to *Cynodon dactylon* to provide resistant against drought and water deficiency, particularly in the soils that carry limiting properties. It was reported that the inoculation of AMF triggered the improvement of *Cynodon dactylon* in red mud compared with that of the controls [64]. Also, it was stated that the inoculation of AMF enhanced the vitality and improvement of *Cynodon dactylon* by promoting the nutrient uptake, decrasing metal translocation to the aerial portion of grass and tolerance to metal stress conditions, alkaline, sodic, and saline [64]. Furthermore, it was reported that the AMF decreased the harmful impacts of soil such as nutrient deficiency, insufficient organic matter, high pH, or high salinity [65,66].

CONCLUSIONS

The symbiotic status of *Cynodon dactylon* with the arbuscular mycorrhizal fungi species demonstrated that the indigenous Bermuda grass offered substantial potential as the host plant for AMF species, even though the habitat was influenced by the high lime content and low nutrient availability in sandy soils from Black Sea temperate coastal regions. The dominant order was *Gigasporales*, which offered the largest variety of species in the study. It is supposed that, based upon these marginal soil properties, AMF spor density was found low in this study. It is thought that AMF contributes to *Cynodon dactylon* to supply resistance against unfavorable soil conditions. Therefore, as in this research, arbuscular mycorrhizal fungi are substantial in that they sustain their vital activities, thus establishing a simbiotic mutualistic relationship with *Cynodon dactylon* under limiting soil properties. These arbuscular mycorrhizal fungi should be isolated and used in planting studies in similar ecological areas. Thus, it is expected that the succession of the planting and afforestation studies would increase with these AMF in sandy soils. Accordingly, this region may have special ecosystem conditions in terms of distribution of AMF biodiversity and composition. Therefore, the region and similar regions should be conserved against environmental degradation and pollution.

ACKNOWLEDGEMENTS

I would like to acknowledge Tancredo Augusto Feitosa de Souza from the Federal University of Paraíba, for his assistance during the diagnosis of the AMF spores in this study.

REFERENCES

[1] Palta, Ş., Genç Lermi, A. (2017) Determination of Some Properties of Herbaceous Plants in Understory of Urban Forestry in Bartın Province. COMU J. Agric. Fac. 5(2), 1-8.

[2] Palta, Ş., Genç Lermi, A., Beki, R. (2016) The Effect of Different Land Uses on Arbuscular Mycorrhizal Fungi İn The Northwestern Black Sea Region. Environmental monitoring and assessment. 188(6), 350.

[3] Gianinazzi-Peason, V., Gianinazzi S. (1983) The physiology of vesicular-arbuscular mycorrhizal roots. Plant Soil. 71, 197-209.

[4] Heald, C.M., Bruton, B.D., Davis. R.M. (1989) Influence of *Glomus intraradices* and soil phosphorus on *Meloidgyne incognita* infecting. The Journal of Nematology. 21(1), 69-73.

[5] Rosendahl, C.N., Rosendahl, S. (1991) Influence of vesicular-arbusclar mycorrhizal fungi (*Glomus* spp.) on the response of cucumber (*Cucumis sativus* L.) to salt stress. Environ. Exp. Bot. 31(3), 313-318.

[6] Davies, F.T.J., Potter J.R., Linderman, R.G. (1992) Mycorrhiza and repeated drought exposure affect drought resistance and extraradical hyphae development of pepper plants independent of plant size and nutrient content. Plant Physiology. 139, 289-294.

[7] Małachowska-Jutsz, A., Kalka, J. (2010) Influence of mycorrhizal fungi on remediation of soil contaminated by petroleum hydro-carbons. Fresen. Environ. Bull. 19, 3217-3223.

[8] Demir, S. (1998) Bazı kültür bitkilerinde Vesiküler-Arbusküler Mikorrhiza (VAM) Oluşumu Ve Bunun Bitki Gelişimi Ve Dayanıklılıktaki Rolü Üzerinde Araştırmalar. PhD Thesis. Ege Üni, FBE, Bitki koruma ABD. İzmir. 114p.

[9] Rhodes, L.H. (1980) The use of mycorrhizae in crop production systems. Outlook on Agriculture. 10(6), 275-281.

[10] Bolan, N.S., Robson, A.D., Barrow, N.J. (1987) Effects of Vesicular-Arbuscular Mycorhizae the availability of iron phosphates to plants. Plant and Soil. 99, 401 - 410.

[11] Li, X.L., Marschner, H., George, E. (1991) Extension of the phosphorus depletion zone in VA mycorrhizal white clover in a calcareous soil. Plant and Soil. 135, 41-48.

[12] Szaboles, I. (1991) Desertification and salinization. In: Choukr-Allah, R. (Ed.) Plant Salinity Research: New Challenges. I.A.V. Hassan II. Agadir, Morocco. 3–18.
[13] Smith, S.E., Read, D.J. (2008) Mycorrhizal Symbiosis. 3rd ed. Academic Press Inc. London, UK, 815p.
[14] Kyriazopoulos, A.P., Orfanoudakis. M., Abraham, E.M., Parissi, Z.M., Katergari, A. (2017) Growth Characteristics of *Medicago Sativa* L. Under Limited Irrigation as Affected by Arbuscular Mycorrhiza Fungi Inoculation. Fresen. Environ. Bull. 26, 955-961.
[15] Erdogan, O., Bagdatli, C. (2017) The Effects of Arbuscular Mycorrhizal Fungi (Amf) and Deficit Irrigation Levels on Yield and Growth Parameters of The Silage Maıze (*Zea mays* L.). Fresen. Environ. Bull. 26, 2948-2955.
[16] Cakmakci, Ö., Cakmakci, T., Demirer Durak, E., Demir, S., Sensoy, S. (2017) Effects of Arbuscular Mycorrhizal Fungi in Melon (*Cucumis melo* L.) Seedling Under Deficit Irrigation. Fresen. Environ. Bull. 26, 7513-7520.
[17] van der Heijden, M.G.A., Klironomos, J.N., Ursic, M., Moutoglis, P., Streitwolf-Engel, R., Boller, T., Wiemken, A., Sanders, I.R., (1998) Mycorrhizal fungal diversity determines plant biodiversity, ecosystem variability and productivity. Nature. 396, 69-72.
[18] van der Heijden, M.G.A., Streitwolf-Engel, R., Riedl, R., Siegrist, S., Neudecker, A., Ineichen, K., Boller, T., Wiemken, A., Sanders, I.R. (2006) The mycorrhizal contribution to plant productivity, plant nutrition and soil structure in experimental grassland. New Phytologist. 172, 739-752.
[19] Sanders, I.R., Fitter, A.H., (1992) Evidence for differential responses between host-fungus combinations of vesicular-arbuscular mycorrhizas from a grassland. Mycological Research. 96, 415-419.
[20] Bever, J.D., Morton, J.B., Antonovics, J., Schultz, P.A., (1996) Host dependent sporu-lation and species diversity of arbuscular mycorrhizal fungi in a mown grassland. Journal of Ecology. 84, 71-82.
[21] Vandenkoornhuyse, P., Husband, R., Daniell, T.J., Watson, I.J., Duck, J.M., Fitter, A.H., Young, J.P.W. (2002) Arbuscular mycorrhizal community composition associated with two plant species in a grassland ecosystem. Molecular Ecology. 11, 1555-1564.
[22] Vandenkoornhuyse, P., Ridgway, K.P., Watson, I.J., Fitter, A.H., Young, J.P.W. (2003) Co-existing grass species have distinctive arbus-cular mycorrhizal communities. Molecular Ecology. 12, 3085-3095.
[23] Goomaral, A., Undarmaa, J., Matsumoto, T., Yamato, M. (2013) Effect of plant species on communities of arbuscular mycorrhizal fungi in the Mongolian steppe. Mycoscience. 54, 362 - 367.
[24] Rillig, M.C. (2004) Arbuscular mycorrhizae and terrestrial ecosystem processes. Ecology Letters. 7, 740-754.
[25] Ashokkumar, K., Kumarakurubaran, S., Muthukrishnan, S.D. (2013) *Cynodon dactylon* (L.) Pers.: An updated review of its phytochemistry and pharmacology. Journal of Medicinal Plants Research. 7(48), 3477-3483.
[26] Li, D., Chen, J., Zong, J., Wang, Y., Guo, H., Zhang, B., Liu, J. (2017) Variation in Growth Response and Nitrogen Accumulation and Partitioning of Bermudagrass Under Low Nitrogen Levels. Fresen. Environ. Bull. 26, 654-660.
[27] Tan, S., Zhu, Z., Zhang, K., Xu, H., Zhang, Q. (2013) Effects of Submergence on Morpho-Physiological Characteristics and Recovery of Bermudagrass (*Cynodon dactylon*). Fresen. Environ. Bull. 22, 2535-2543.
[28] Wu, J., Sun, B., Wang, Y., Xin, G., Ye, S., Peng, S. (2011) Arbuscular Mycorrhizal Fungal colonization improves regrowth of bermuda-grass (*Cynodon Dactylon* L.) After Cutting. Pak. J. Bot. 43(1), 85-93.
[29] Fan, Y.Q., Luan, Y.S., An, L.J., Kun, Y. (2008) Arbuscular mycorrhizae formed by Penicillium inophilum improve the growth, nutrient uptake and photosynthesis of strawberry with two inoculum-types. Biotechnology Letters. 30, 1489-1494.
[30] Sheng, M., Tang, M., Chen, H., Yang, B.W., Zhang, F.F., Huang, Y.H. (2008) Influence of arbuscular mycorrhizae on photosynthesis and water status of maize plants under salt stress. Mycorrhiza. 18, 287-296.
[31] TSMS (2013) Turkish State Meteorological Service. Daily meteorological data. Ankara, Turkey.
[32] Öztürk, M., Bolat, İ., Ergün, A. (2015) Influence of air–soil temperature on leaf expansion and LAI of Carpinus betulus trees in a temperate urban forest patch. Agricultural and Forest Meteorology. 200(2015), 185–191.
[33] Atalay, I. (2011) Climate Atlas of Turkey (in Turkish). Istanbul, Turkey: Inkılâp Bookstore Press.
[34] da Silva, I.R., de Mello, C.M.A., Neto R.A.F., da Silva D.K.A., de Melo, A.L., Oehl, F., Maia, L. C. (2014) Diversity of arbuscular mycorr-hizal fungi along an environmental gradient in the Brazilian semiarid. Appl. Soil Ecol. 84,166–175.

[35] Gerdemann, J.W., Nicolson, T.H. (1963) Spores of mycorrhizal Endogonespecies extracted from soil by wet sieving and decanting. Trans Br Mycol Soc. 1, 43–66.
[36] Jenkins, W.R. (1964) A rapid centrifugal flotation technique forseparating nematodes from soil. Plant Dis Rep. 48, 692.
[37] Schenck, N.C., Perez, Y. (1990) Manual for the Identification of VA Mycorrhizal Fungi. 3rd ed. Gainesville: Synergistic Publications.
[38] Oehl, F., Souza, F.A., Sieverding, E. (2008) Revision of Scutellospora anddescription of five new genera and three new families in the ar-buscular mycorrhiza-forming Glomeromycetes. Mycotaxon. 106, 311–360.
[39] INVAM (2017) International Culture Collection of Arbuscular and Vesicular–Arbuscular Mycorrhizal Fungi. http://www.-invam.caf.wvu. edu.
[40] Oehl, F., Sieverding, E., Palenzuela, J., Ineichen, K., Silva, G.A. (2011) Advances in Glomeromycota taxonomy and classification. IMA Fungus. 2, 191–199.
[41] Sieverding, E., Silva, G.A., Berndt, R., Oehl, F. (2014) *Rhizoglomus*, a new genus of the Glomeraceae. Mycotaxon. 129, 373-386.
[42] Bouyoucos, G.J. (1962) Hydrometer method improved for making particle size analyses of soils. Agron. J. 54, 464-465.
[43] Rowell, D.L. (1994) Soil science: methods and applications. Longman Scientific and Technical. Singapore.
[44] Rhoades, J.D. (1982) Soluble Salts. In: Page, A.L. (Ed.) Methods of soil analysis. Part 2 Chemical and Microbiological Properties. SSSA Book series No: 9, Madison, 149-157.
[45] Walkley, A., Black, A.I. (1934) An examination of the Degtjareff method for determining soil organic matter, and proposed modification of the chromic acid titration method. Soil Sci. 37, 29–38.
[46] Bremner, J.M., Mulvaney, C.S. (1982) Nitrogen-total. In: Page, A.L. (Ed.) Methods of soil analysis. Part 2 Chemical and Microbiological Properties. SSSA Book series No: 9, Madison, 595-622.
[47] Olsen, S.R., Cole, C.V., Watanabe, F.S., Dean, L.A. (1954) Estimation of Available Phosphorus in Soils by Extraction with Sodium Bicarbonate. U.S. Department of Agriculture Circular No. 939.
[48] Allison, L.E, Moodie, C.D. (1965) Carbonate. In: C.A. Black (Ed.) Methods of soil analysis. American Society of Agronomy. Wisconsin, 1379-1396.
[49] Kantarcı, M.D. (2000) Toprak İlmi. İstanbul Üniversitesi Toprak İlmi ve Ekoloji Anabilim Dalı, İ.Ü. Yayın No. 4261, Orman Fakültesi Yayın No. 462, İstanbul, 420p.
[50] Bruand, A., Hartmann, C., Lesturgez, G. (2005). Physical properties of tropical sandy soils: A large range of behaviours. Management of Tropical Sandy Soils for Sustainable Agriculture. A holistic approach for sustainable development of problem soils in the tropics. Khon Kaen, Thailand.
[51] Demir, S., Sipahioğlu, H.M., Kaya, İ., Akköprü, A., Usta, M. and Aysan, E. (2007) Van ve çevresinde Gramineae familyasına ait bitkilerde Arbüs-küler Mikorhizal Fungusların (AMF) tür çeşitliliğinin Nested-PCR yöntemiyle belirlenmesi. TÜBİTAK-TOGTAG 3367 No'lu Proje Kesin Raporu, 38p.
[52] Schenck, N.C., Smith, G.S. (1982) Additional new and unreported species of mycorrhizal fungi (Endogonaceae) from Florida. Mycologia. 74(1), 77-93.
[53] Morton, J.B. and Bentivenga, S.P. (1994) Levels of diversity in endomycorrhizal fungi (Glomales, Zygomycetes) and their role in defining taxonomic and non - taxonomic groups. Plant and Soil. 159, 47-59.
[54] Abbott, L.K., Robson, A.D. (1991) Factors influencing the occurrence of vesicular-arbuscular mycorrhizas. Agriculture, Ecosystems & Environment. 35, 121–150.
[55] Johnson, N.C., Tilman, D. and Wedin, D. (1992) Plant and soil controls on mycorrhizal fungal communities. Ecology. 73, 2034–2042.
[56] Ingham, E., Wilson, M. (1999) The Mycorrhizal colonization of six wetland species at sites differing in land use history. Mycorrhiza. 9, 233–235.
[57] Miller, S., Bever, J. (1999) Distribution of Arbuscular Mycorrhizal Fungi in stands of the wetland grass Panicum Hemitomon along a wide hydrologic gradient. Oecologia. 119, 586–592.
[58] Saito, M. (2000) Symbiotic exchange of nutrients in Arbuscular Mycorrhizas: Transport and transfer of phosphorus. In: Kapulnik, Y., Douds D.D. (eds.) Arbuscular Mycorrhizas: Physiology and Function. Kluwer Academic Publishers. 85-106.
[59] Johnson, P.N. (1976) Effects of soil phosphate level and shade on plant growth and mycorrhizas. New Zeland Journal of Botany. 14, 333-340.
[60] Ferguson, J.J., Menge, J.A. (1982) The influence of light intensity and artificially extended photoperiod upon infection and sporulation of Glomus fasciculatus on Sudan grass and on root exudationof Sudan grass. New Phytologist. 92, 183-192.

[61] de Souza T.A.F., Rodriguez-Echeverría, S., Andradea, L.A., Freitas, H. (2016) Arbuscular mycorrhizal fungi in *Mimosa tenuiflora* (Willd.) Poir from Brazilian semi-arid. Brazilian Journal of Microbiology. Environmental Microbiology. 47, 359–366.

[62] Carneiro, R.F.V., Cardozo Júnior, F.M., Pereira, L.F., Araújo, A.S.F., Silva, G.A. (2012) Fungos micorrízicos arbusculares como indicadores darecuperacão de áreas degradadas no Nordeste do Brasil. RevCienc Agron. 43, 648–657.

[63] Estrada, B., Beltrán-Hermoso, M., Palenzuela, J., Iwase, K., Ruiz-Lozano, J.M., Barea, J.M., Oehl, F. (2013) Diversity of arbuscular mycorrhizal fungi in the rhizosphere of *Asteriscus maritimus* (L.) Less., a representative plant species in arid and saline Mediterranean ecosystems. Journal of Arid Environments. 97, 170-175.

[64] Babu, G., Reddy, S. (2011) Influence of arbuscular mycorrhizal fungi on the growth and nutrient status of bermudagrass grown in alkaline bauxite processing residue. Environmental Pollution. 159, 25-29

[65] Entry, J.A., Rygiewicz, P.T., Watrud, L.S., Donnelly, P.K. (2002) Influence of adverse soil conditions on the formation and function of arbuscular mycorrhizas. Advanced Environ-mental Research. 7, 123e138.

[66] Oliveira, R.S., Boyer, L.R., Carvalho, M.F., Jeffries, P., Vosátka, M., Castro, P.M.L., Dodd, J.C. (2010) Genetic, phenotypic and functional variation within a *Glomus geosporum* isolate cultivated with or without the stress of a highly alkaline anthropogenic sediment. Applied Soil Ecology. 45, 39-48.

Received: **25.12.2017**
Accepted: **24.02.2018**

CORRESPONDING AUTHOR

Sahin Palta
Bartın University,
Faculty of Forestry,
Department of Forest Engineering, Division of Watershed Management,
Subdivision of Range Management,
Bartın - Turkey

e-mail: spalta@bartin.edu.tr

© by PSP Volume 27 – No. 5/2018 pages 3148-3155 Fresenius Environmental Bulletin

PROTECTIVE EFFECT OF ELLAGIC ACID AGAINST CARBON TETRACHLORIDE (CCl_4) – INDUCED OXIDATIVE BRAIN INJURY IN RATS

H Turan Akkoyun[1,*], Aydin Sukru Bengu[2], Aykut Ulucan[2], Mahire Bayramoglu-Akkoyun[3], Okan Arihan[4]

[1]Faculty of Veterinary Science, Department of Physiology, Siirt University, Siirt, Turkey
[2]Vocational School of Health Services, Department of Medical Services and Technics Bingol University, Bingol, Turkey
[3] Faculty of Veterinary Science, Department of Biochemistry, Siirt University, Siirt, Turkey
[4]Faculty of Medicine, Department of Physiology, Van Yuzuncu Yil University, Van, Turkey

ABSTRACT

In this study, it was aimed to investigate protective effects of Ellagic acid in rats which have brain damage formed with carbon tetrachloride (CCl_4). 28 male Wistar albino rats were separated into 4 groups as Control, CCl_4., Ellagic acid and CCl_4+ Ellagic acid. From the brain tissue homogenate malondialdehyde (MDA), glutathione (GSH), superoxide dismutase (SOD), gluthation peroxidase (GSH-Px), catalase (CAT) levels were measured and routine histopathological investigation was performed. An increase in MDA level ($p<0.01$) whereas a decrease in CAT, GSH-Px, SOD ($p<0.01$) and GSH ($p<0.05$) levels in CCl_4 administered group compared to control was observed. In our study, in the control and Ellagic acid administered groups, no microscopic findings were observed in the brain, while severe lesions were seen in the CCl_4 administered group and only mild congestion lesions were seen in the CCl_4 + Ellagic acid group. Results of this study suggest a protection by ellagic acid against CCl_4 induced brain damage. This protection is possibly via induction of antioxidant protective mechanism which is shown both by biochemical and histopathological methods.

KEYWORDS:
Brain damage, Carbon tetrachloride, Ellagic Acid, Rat

INTRODUCTION

Reactive oxygen species are among the etiology of degenerative diseases. Exposure to radiation, heavy metals and xenobiotics cause increase in free radicals and oxidative stress [1,2]. Carbon tetrachloride (CCl_4) poisoning resembles oxidative stress as an experimental model [3]. CCl_4 exerts toxic effects in various organs such as kidney, testis, heart, lung, brain and mainly on liver [4]. CCl_4 toxicity probably is due to formation of trichloromethyl radical. In the presence of oxygen, CCl_4 reacts with oxygen to form trichloromethyl peroxide radical [5, 6]. Following CCl_4 toxication, augmented oxidative stress due to increased free radical formation is thought to be the reason behind tissue damage [7]. Ellagic acid is a polyphenolic compound found in pomegranate, mulberry, walnut, green tea, strawberry and eucalyptus leaf [8,9]. Ellagic acid have different mechanisms of action in bioactivity studies but most proven ones are antioxidant, anti-fibrotic, anti-carcinogenic, anti-plasmodial activity and chemoprotective property [10, 11]. Such properties of ellagic acid are thought to be beneficial against organ damage. Therefore this study was aimed to investigate protective effect of ellagic acid against CCl_4 induced acute brain damage in rats.

MATERIALS AND METHODS

Animals. This study was conducted in Bingol University with the approval of Bingol University Animal Experiments Local Ethical Commission (04.04.2017 -2017/04,04-01). 28 male Wistar-Albino rats weighing 250-300 gr were used. Rats were kept in a room with 20-22ºC constant temperature within twelve (12h) hours of light-dark cycle (lights on 07:00-19:00; lights off 19:00-07:00). Rats were given water and standard pellet food *ad libitum* and acclimatized to their cages for adaptation. Only feeding was ceased 12 hours prior to experiments.

Experimental Design. Rats were divided into four groups containing 7 animals each; Group I (Control, n=7): Animals in this group was injected with distilled water, 250-300 grams of body weight daily for 7 days [12]. Group II (CCI4, n=7): Administered 0.5 ml/kg CCI4 (i.p.) daily for 7 days [12]. Group III (Ellagic acid, n=7): Administered ellagic acid (5 mg/kg/day) (oral gauge) daily for 7 days [13]. Group IV (CCl4+ Ellagic acid, n=7): Administered 0.5 ml/kg CCl_4 (i.p.) daily for 7 days + ellagic acid 5 mg/kg/day with oral gauge. Brain tissue samples were obtained from all groups at the

end of 7th day under i.p. 60 mg/kg ketamine hydrochloride and 10 mg/kg Xylasine anesthesia. Brain tissue was obtained, washed with saline, dried and stored in deep freeze (-80^{0}C) biochemical (MDA, GSH, SOD, GSH-Px, CAT) analysis were conducted.

BIOCHEMICAL ASSAYS

Measurement of MDA Level. MDA levels in tissues were determined spectrophotometrically with method of Ohkawa et al. 532 nm concentration was given as nmol/mg protein [14].

Measurement of GSH Level. Tissue GSH levels were determined with the method defined by Tietze (1969) and Fairbans et al. (1999). 405 nm concentration was given as µmol/mg protein [15, 16].

Measurement of SOD Level. SOD (EC 1.15.1.1) activity in the tissue was determined by at 505 nm wavelength according to using method of Sun et al. (1988). This method relies on Xanthine oxidase induced production of O_2^-radical and avoidance of nitroblue tetrazolium (NBT) reduction with the help of SOD enzyme. [17]. The results were expressed as IU/mg protein in terms of specific activity.

Measurement of GSH-Px Level. Activity of GSH-Px (E.C.1.11.1.9) was determined by using Paglia et al. (1967). Decrease of absorbance via oxidation of NADPH to NADP during such reactions was read with Microplate Reader at 340 nm GSH-Px activity was measured [18]. The results were expressed as IU/mg protein in terms of specific activity.

Measurement of CAT Level. CAT (EC 1.11.1.6) activity was measured according to the method described by Aebi 1974. H_2O_2 gives maximum absorbance in 240 nm wavelength. It relies on disintegration of H_2O_2 by catalase into water and oxygen and it is observed as the decrease in absorbance in UV spectrometer. Decrease in absorbance is related with catalase enzyme activity. Decrease of absorbance with sample addition was read in every 15 second for 5 min. For calculation values of every minute linear absorbance decrease is evaluated [19]. The results were expressed as IU/mg protein in terms of specific activity.

Histopathological analysis of the brain. After treatment, eight rats in each group were anaesthetized with diethyl ether, euthanized by decapitation under deep anesthesia and necropsied. After that the cerebrum were excised and isolated immediately. Also, brain tissue samples were fixed in 10% neutral-buffered formalin for 48 h. The tissue samples were processed as routine protocol of dehydration with alcohol series (50%, 70%, 96% and 100%), clearance in xylene and then embed in paraffin before being sectioning at 5 µm thickness with rotary microtome (Leica, RM2125) [20]. The slides were stained with hematoxylin and eosin for histological examination [21]. Finally the slides were examined and photographed using light microscopy (Leica, DM2500).

Statistical analysis. Results were evaluated with SPSS 20(Statistical Program- Software System) program. Data were expressed as X ± SEM. One way ANOVA was conducted and intragroup comparisons were done with post-hoc Tukey' test.

RESULTS

MDA levels were found higher in CCl_4 administered group (CCl_4) compared to control group (Cont) ($p<0.01$). In addition, increase in CCl_4+ Ellagic Acid administered group was significant ($p<0.05$) and also decrease in CCl_4 + Ellagic Acid compared to lone CCl_4 administered group was found significant ($p<0.01$) (Figure 1) GSH was found significantly lower in CCl_4 and in CCl_4 + Ellagic Acid group compared to control ($p<0.05$) (Figure 2), Decrease in SOD values in CCl_4 and CCl_4 + Ellagic acid groups compared to control group was found statistically significant ($p<0.01$). In addition increase in SOD level in CCl_4 + Ellagic acid group compared to CCl_4 group was found significant ($p<0.05$). (Figure 3), Increase in GSH-Px level in Ellagic acid and CCl_4 + Ellagic Acid compared to CCl_4 group were found significantly higher ($p<0.05$) (Figure 4), CAT enzyme activity levels were found significantly lower in CCl_4 + Ellagic acid group compared to control ($p<0.01$). In addition, this level was found significantly higher in Ellagic acid compared to CCl_4 group ($p<0.05$). Also increase in CCl_4 + Ellagic acid was significantly higher compared to CCl_4 group ($p<0.01$) (Figure 5). In control group (Group-1) no significant histopathological differences were noted and the brain tissues were in normal histological architecture (Figure 6- A). In the CCl_4 administered group (Group-2) in brain, perineural vacuolation, neuronophagia, mild congestion of blood vessels and glial cell proliferation around damaged neuronal cell bodies to give rise to so-called satellitosis were found most frequently in cerebral cortex. Common lesion in the cerebral cortex are as follows; necrosis of most of pyramidal neurons with pyknotic nuclei, neuronal shrinkage and mild microgliosis (Figure 6-B). In addition, no significant histopathological evidences were observed after administration of Ellagic acid group (Group-3) in the section of rat brain, which is similar to control group (Figure 6-C). Only mild congestion lesion of blood vessels in cortex has been observed in CCl_4 + Ellagic acid group (Group-4) (Figure 6 -D).

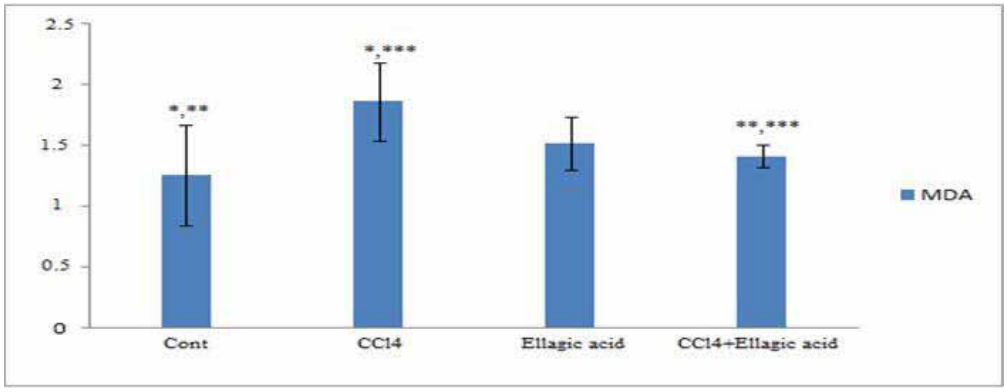


FIGURE 1
MDA levels (nmol/mg protein) of brain tissues of different groups b(*), b1(***)=p<0.01, c(**)=p<0.05

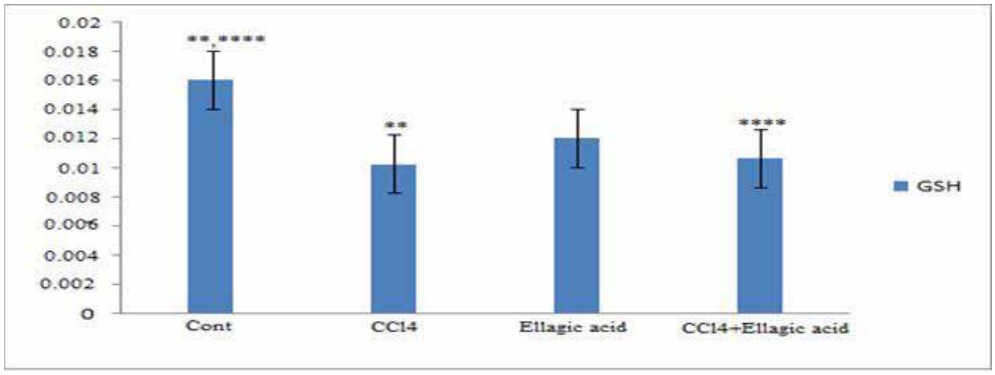


FIGURE 2
GSH levels (µmol/mg protein) of brain tissues in different groups b (*), b1(***)=p<0.01, c(**), c1(****)=p<0.05

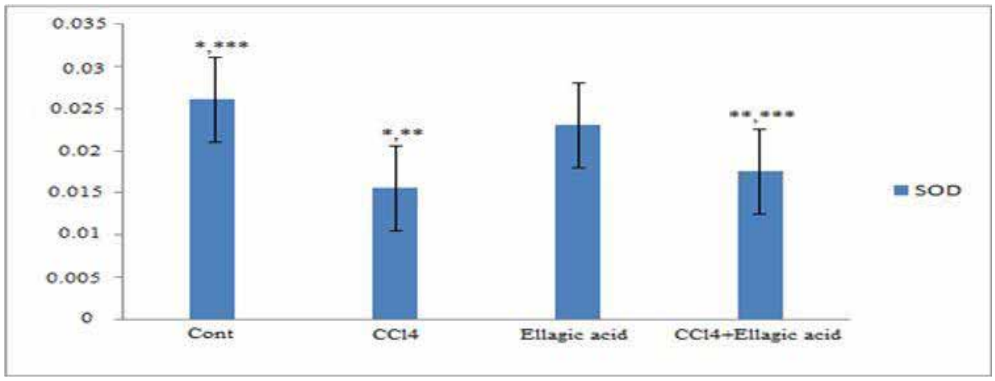


FIGURE 3
SOD levels (IU/mg protein) of brain tissues of groups b(*), b1(***)=p<0.01, c(**)=p<0.05

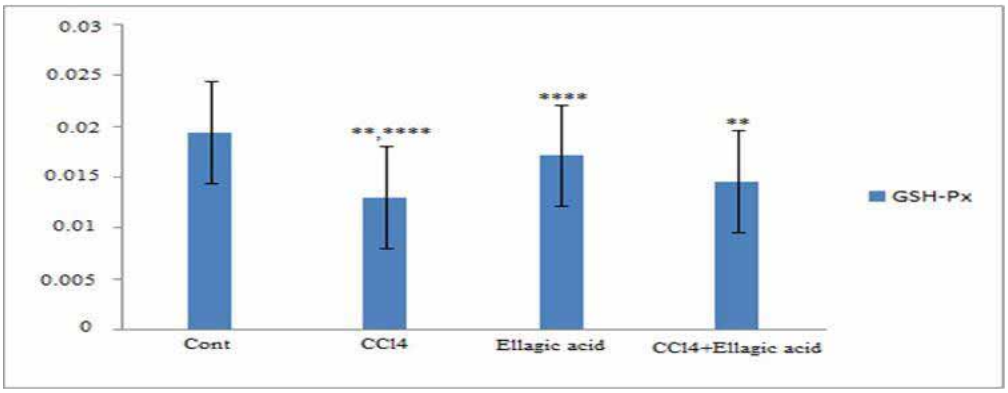


FIGURE 4
GSH-Px levels (IU/mg protein) in brain tissues of groups c(**),c1(****)=p<0.05

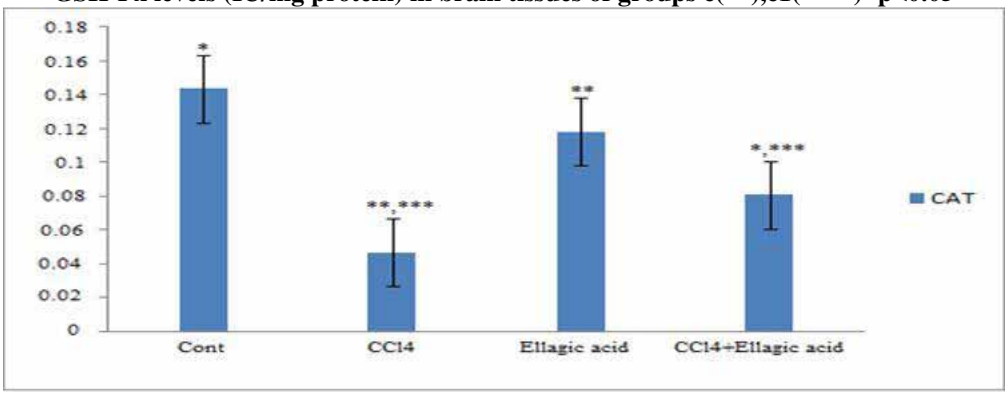


FIGURE 5
CAT levels (IU/mg protein) in brain tissues of groups b (*), b1(***)=p<0.01, c(**),c1(****)=p<0.05

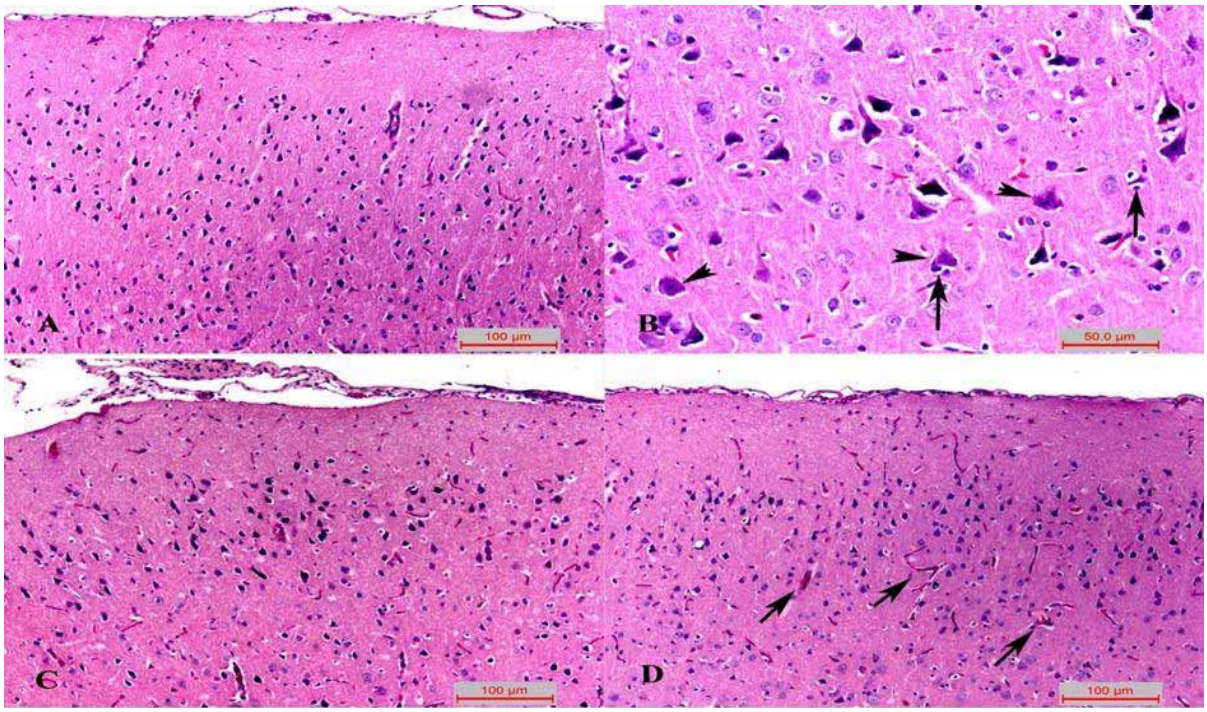


FIGURE 6
Histopathology of brain tissues. (A): Control group (Group-1), normal histological architecture x10. (B): CCl_4 administered group (Group-2), perineural vacuolation, neuronophagia and satellitosis (arrows); necrosis of pyramidal neurons with pyknotic nuclei and neuronal shrinkage (arrow heads) x20. (C): Ellagic acid group (Group-3), normal histological structure x10. (D): CCl_4 + Ellagic acid group (Group-4), mild congestion of blood vessels in cortex (arrows) x10. H&E staining.

DISCUSSION

CCI_4 is a toxic agent which causes free radical formation due to its toxic effect [22]. CCI_4 is transformed by cytochrome P450 enzyme into trichloromethyl (CCI_3) and trichloromethylperoxile (CCI_30_2) free radicals which are more toxic. Following their production lipid peroxidation occurs which causes tissue oxidative damage [23-26]. Oxidative stress is the disruption of the balance between free radicals and antioxidant defense system which may be caused by a pathological event. Organisms are protected against oxidative stress via enzymatic and non-enzymatic systems [27]. In many of the previous studies with CCl_4, it was shown that antioxidant defense systems are involved in protection of the animals against this toxication [28, 29]. MDA is among substances formed by lipid peroxidation and a commonly used parameter as an indicator for oxidative stress [30]. In our study CCI_4 injected group had a significant rise in brain MDA levels compared to control group. Increase of MDA proves augmentation of lipid peroxidation in brain and oxidative stress as an outcome in brain due to CCI_4. Similarly it is reported that MDA levels in the brains of CCI_4 administered animals rise [2]. CCl_4 + Ellagic acid administered group showed a decrease in MDA level due to Ellagic acid ($p<0.05$) (Figure 1). This decrease may be due to amelioration of the oxidative damage in the brain caused by free radicals by ellagic acid. Literature reports support our data in this aspect. Ellagic acid was also tested on STZ induced diabetes in rats in literature and ellagic acid protected brain and sciatic nerve against lipid peroxidation [31]. In a study focusing on cisplatin induced oxidative stress on heart and liver showed protective effect of Ellagic acid [32]. GSH involves in certain steps in defense processes against oxidative damage caused by free radicals, peroxides and other toxic substances and protects cells [33]. Therefore decrease of GSH makes cells more prone to such hazards. Attenuation of GSH in living organisms leads to tissue malformations and injuries [34]. In our study CCI_4 injected group showed significant decrease in GSH level compared to control however ellagic acid alleviated this decrease to some extent ($p<0.05$). (Figure 2). This protection might be related with antioxidant nature of ellagic acid. Recent studies provided evidence for protective effect of ellagic acid against oxidative stress. Literature studies present decrease of GSH in 6th hour due to CCl_4 [35] or in heart and liver of rats due to cisplatin [32]. Mentioned decreases in GSH levels might be due to overuse of GSH for decreasing toxic effects of CCI_4. SOD is an important enzyme which scavenges peroxide anion radicals and inhibits lipid peroxidation due to free radicals [36]. Brain tissue SOD activity was significantly lower in CCI_4 and CCl_4 + Ellagic acid injected group compared to control ($p<0.01$) (Figure 3). Similar studies present an important decrease in brain tissue SOD activity in CCI_4 administered groups [2, 4, 37]. Reason for this decrease was explained as induction of hydrogen peroxide and peroxynitrite formation in brain tissue by CCI_4 and decrease of such enzymes during removal of such reactive substances from tissue. Literature studies are in accordance with our findings. SOD levels significantly increased in CCI_4+Ellagic acid administered group compared to lone CCI_4 injected group ($p<0.05$) (Figure 3). In a study focusing on hepatoprotective effect of ellagic acid in rats, SOD activity was found lower in CCI_4 injected group compared to CCI_4 + Ellagic acid administered group [38]. Literature findings support our results in this parameter. GSH-Px plays an important role in cell defense against reactive oxygen species. GSH-Px levels in our study significantly increased in CCl_4 + Ellagic acid administered group compared to lone CCI_4 administered group ($p<0.05$) (Figure 4). Other researchers found an increase in GSH-Px activity in CCl_4 + Ellagic acid administered group compared to lone CCl_4 injected group in rats in a study focusing on hepatoprotective activity of ellagic acid in rats [38]. CAT is among important enzymes which avoids free radical accumulation and lipid peroxidation [39]. In our study although CAT was decreased in CCI_4 + Ellagic acid group compared to control ($p<0.01$), increase in ellagic acid compared to CCI_4 group was also found significant ($p<0.05$). In addition increase in CCI_4 + Ellagic acid group compared to CCI_4 group was also found significant ($p<0.01$) (Figure 5). In literature CCI_4 administered group showed a significant decrease in brain tissue CAT activity [2, 4, 37]. Similarly decrease in kidney tissue CAT activity was reported in CCI_4 administered rats [40]. Literature reports also support our findings. In our study, difference between the groups was observed in histopathological findings in the brains as a result of microscopic examination. In the control and Ellagic acid administered groups, no microscopic findings were observed in the brain, while severe lesions were seen in the CCl_4 administered group and only mild congestion lesions were seen in the CCl_4 + Ellagic acid group. Although administration of CCl_4 was reported to cause severe necrosis and hemorrhage at the meninges in the rat brain, it has not been observed in our study. Histopathological findings which are observed in rat brain tissues due to CCl_4 toxicities, CCl_4 administered group (Group-2) such as perineural vacuolation, neuronophagia, mild congestion of blood vessels and satellitosis, necrosis of most of pyramidal neurons with pyknotic nuclei, neuronal shrinkage and mild microgliosis found most frequently in cerebral cortex, are similar to some CCl_4 toxicity studies [2, 41]. Ellagic acid administration was reported for its neuroprotective activity by decreasing neuronal damage and necrosis in streptozotocin-induced diabetic rat

brains [31]. In our study, it might be proposed that Ellagic acid has neuroprotective effect against CCl_4 induced oxidative rat brain damage in CCl_4 + Ellagic acid group (Group-4) similar to their control group and our findings (Figure 6).

CONCLUSION

Results of this study suggest a protection by ellagic acid against CCl_4 induced brain damage. This protection is possibly via induction of antioxidant protective mechanism which is shown both by biochemical and histopathological methods.

ACKNOWLEDGEMENTS

Authors declare no conflict of interest.

REFERENCES

[1] Kim, H.J., Odend'Hal, S., Bruckner, J.V. (1990) Effect of oral dosing vehicles on the acute hepatotoxicity of carbon tetrachloride in rats. Toxicology and applied pharmacology. 102, 34-49.

[2] Jayakumara, T., Sakthivel, M., Thomas, P.A., Geraldine, P. (2008) Pleurotus ostreatus, an oyster mushroom, decreases the oxidative stress induced by carbon tetrachloride in rat kidneys, heart and brain. Chemico-Biological Interactions. 176, 108-120.

[3] McGregor, D., Lang, M. (1996) Carbon tetrachloride: genetic effects and other modes of action. Mutation Research/Reviews in Genetic Toxicology. 366, 181-195.

[4] Tirkey, N., Pilkhwal, S., Kuhad, A., Chopra, K. (2005) Hesperidin, a citrus bioflavonoid, decreases the oxidative stress produced by carbon tetrachloride in rat liver and kidney. BMC pharmacology. 5, 1-8.

[5] Hartley, D.P., Kolaja, K.L., Reichard, J., Petersen, D.R. (1999) 4-Hydroxynonenal and malondialdehyde hepatic protein adducts in rats treated with carbon tetrachloride: immunochemical detection and lobular localization. Toxicology and applied pharmacology. 161, 23-33.

[6] Melin, A.M., Perromat, A., Deleris, G. (2000) Pharmacologic application of Fourier transform IR spectroscopy: in vivo toxicity of carbon tetrachloride on rat liver. Biopolymers. 57, 160-168.

[7] Recknagel, R.O., Glende, E.A., Dolak, J.A., Waller, R.L. (1989) Mechanisms of carbon tetrachloride toxicity. Pharmacology & therapeutics. 43, 139-154.

[8] Han, H.D., Lee, M.J., Kim, J.H. (2006) Antioxidant and Apoptosis-inducing Activities of Ellagic Acid. Anticancer Research. 26, 3601-3606.

[9] Seeram, N.P., Adams, L.S, Henning, S.M., Niu, Y., Zhang, Y., Nair, M.G., Heber, D. (2005) In vitro antiproliferative, apoptotic and antioxidant activities of punicalagin, ellagic acid and a total pomegranate tannin extract are enhanced in combination with other polyphenols as found in pomegranate juice. The Journal of nutritional biochemistry. 16, 360-367.

[10] Baek, B., Lee, S.H., Kim, K., Lim, H.W., Lim, C.J. (2016) Ellagic acid plays a protective role against UV-B-induced oxidative stress by up-regulating antioxidant components in human dermal fibroblasts. The Korean Journal of Physiology & Pharmacology. 20, 269-277.

[11] Festa, F., Aglitti, T., Duranti, G., Ricordy, R., Perticone, P., Cozzi, R. (2001) Strong antioxidant activity of ellagic acid in mammalian cells in vitro revealed by the comet assay. Anticancer Research. 21, 3903-3908.

[12] Manjrekar, A.P., Jisha, V., Bag, P.P., Adhikary, B., Pai, M.M., Hegde, A., Nandini, M. (2008) Effect of Phyllanthus niruri Linn. treatment on liver, kidney and testes in CCl 4 induced hepatotoxic rats. Indian journal of Experimental Biology. 46, 514-20.

[13] Bharathi, E., Jagadeesan, G. (2014) Antioxidant potential of hesperidin and ellagic acid on renal toxicity induced by mercuric chloride in rats. Biomedicine & Preventive Nutrition. 4, 131-136.

[14] Ohkawa, H., Ohishi, N., Yagi, K. (1979) Assay for lipid peroxides in animal tissues by thiobarbituric acid reaction. Analytical biochemistry. 95, 351-358.

[15] Tietz, F. (1969) Enzymatic method for quantitative determination of nanogram amounts of total and oxidized glutathione: Applications to mammalian blood and other tissues. Analytical Biochemistry. 27, 502-522.

[16] Fairbans, V.F, Klee, G.G. (1999) Biochemical aspects of hematology. Tietz Textbook of Clinical Chemistry. 3rd ed. Philadelphia, Pennsylvania: WB Saunders Company. 1698-1704.

[17] Sun, Y., Oberley, L.W., Li, Y. (1988) A simple method for clinical assay of superoxide dismutase. Clinical chemistry. 34, 497-500.

[18] Paglia, D.E., Valentina, W.N. (1967) Studies on the quantitative and qualitative characterization of erythrocyte glutathione peroxidase. The Journal of laboratory and clinical medicine. 70, 158-169.

[19] Aebi, H. (1974) Catalase. In: Bergmeyer, H.V. (ed.) Methods in enzymatic analysis. Academic press. New York, 2, 674-84.

[20] Bancroft, J.D., Gamble, M.(2002) Tissue processing and microtomy, Theory and Practice of

Histological Techniques. 5th edition. Harcourt Publishers Limited, Churchill Livingstone London, 85–107.
[21] Lilli, R.D. (2008) The Hematoxylin and Eosin, In: Gamble, M. Histopathologic Technique and Practical Biochemistry. 8th edition. Elsevier Limited. London: Churchill Livingstone.
[22] Sanzgiri, U.Y., Srivatsan, V., Muralidhara, S., Dallas, C.E., Bruckner, J.V. (1997) Uptake, distribution, and elimination of carbon tetrachloride in rat tissues following inhalation and ingestion exposures. Toxicology and applied pharmacology. 143, 120-129.
[23] Weber, L.W., Boll, M., Stampfl, A. (2003) Hepatotoxicity and mechanism of action of haloalkanes: carbon tetrachloride as a toxicological model. Crit Rev Toxical. 33, 105-36.
[24] Thrall, K.D, Vucelick, M.E., Gies, R.A., Benson, J.M. (2000) Comparative metabolism of carbon tetrachloride in rats, mice, and hamsters using gas uptake and PBPK modeling. Journal of Toxicology and Environmental Health. Part A. 60, 531-548.
[25] Ohta, Y., Kongo, M., Sasaki, E., Nishida, K., Ishiguro, I. (2000) Therapeutic effect of melatonin on carbon tetrachloride-induced acute liver injury in rats. Journal of pineal research. 28, 119-26.
[26] Rao, P.S., Mangipudy, R.S., Mehendale, H.M. (1997) Tissue injury and repair as parallel and opposing responses to CCI4 hepatotoxicity: a novel dose-response. Toxicology. 118, 181-93.
[27] Gülcen, B., Karaca, Ö., Kuş, M.A., Çolakoğlu, S., Ögetürk, M., Kuş, İ. (2012) Deneysel Karbon Tetraklorür Zehirlenmesinde Akciğer Doku Hasarı ve Melatonin Hormonunun Koruyucu Rolü: Işık mikroskobik ve biyokimyasal bir çalışma. Düzce Tıp Dergisi. 14, 37-42
[28] Ozturk, F., Gul, M., Ateş, B., Ozturk, I.C., Cetin, A., Vardi, N. (2009) Protective effect of apricot (Prunusarmeniaca L.) on hepatic steatosis and damage induced by carbon tetrachloride in wistar rats. British Journal of Nutrition. 102, 1767-75.
[29] Ozturk, I.C., Ozturk, F., Gul, M., Ateş, B., Cetin, A. (2009) Protective effects of ascorbic acid on hepatotoxicity and oxidative stress caused by carbon tetrachloride in the liver of Wistar rats. Cell biochemistry and function. 27, 309-15.
[30] Kamal, A.A.M., Gomaa, A., El Khafif, M., Hammad, A.S. (1989) Plasma lipid peroxides among workers exposed to silica or asbestos dusts. Environmental Research. 49, 173-180.
[31] Uzar, E., Alp, H., Cevik, M.U., Fırat, U., Evliyaoglu, O., Tufek, A., Altun, Y. (2012) Ellagic acid attenuates oxidative stress on brain and sciatic nerve and improves histopathology of brain in streptozotocin-induced diabetic rats. Neurological Sciences. 33, 567-574.
[32] Yüce, A., Ateşşahin, A., Çeribaşı, A.O., Aksakal, M. (2007) Ellagic Acid Prevents Cisplatin-Induced Oxidative Stress in Liver and Heart Tissue of Rats. Basic Clinical Pharmacology Toxicology. 101, 345-349.
[33] Sies, H. (1999) Glutathione and its role in cellular functions. Free Radical Biology and Medicine. 27, 916-921.
[34] Limon-Pacheco, J.H., Hernandez, N.A., Fanjul-Moles, M.L., Gonsebatt, M.E. (2007) Glutathione depletion activates mitogen-activated protein kinase (MAPK) pathways that display organ-specific responses and brain protection in mice. Free Radical Biology and Medicine. 43, 1335-1347.
[35] Yalçın, A., Erlaçin, S., Yüce, G., Onat, T. (1997) CCl4 uygulanan sıçanlarda karaciğer GSH, GST ve selenyum düzeyleri. Ege Tıp Dergisi. 36, 13-15.
[36] Escobar, J.A., Rubio, M.A., Lissi, E.A. (1996) SOD and catalase inactivation by singlet oxygen and peroxyl radicals. Free Radical Biology and Medicine. 20, 285-290.
[37] Lesiuk, S.S., Czechowska, G., Stryjecka-Zimmer, M., Slomka, M., Madro, A., Celinski, K., Wielosz, M. (2003) Catalase, superoxide dismutase, and glutathione peroxidase activities in various rat tissues after carbon tetrachloride intoxication. Journal of Hepato-Biliary-Pancreatic Sciences. 10, 309-315.
[38] Singh, K., Khanna, A.K., Chander, R. (1999) Hepatoprotective activity of ellagic acid against carbon tetrachloride induced hepatotoxicity in rats. Indian Journal of Experimental Biology. 37, 1025-1026.
[39] Halliwell, B., Gutteridge, J.M. (1985) Free radicals in biology and medicine. Clarendon Press. Oxford, 331-332.
[40] Srinivasan, M., Rukkumani, R., Ram Sudheer, A., Menon, V.P. (2005) Ferulic acid, a natural protector against carbon tetrachloride-induced toxicity. Fundamental clinical pharmacology. 19, 491-496.
[41] Ojo, O.A., Ojo, A.B., Ajiboye, B., Akintayo, C., Oyinloye, B.E., Ojo, A.A. (2016) Carbon Tetrachloride-induced oxidative stress in Wistar rat brain: Neurocurative potential of Ficus asperifolia (Miq). 9, 1334-1338.

Received: **29.12.2017**
Accepted: **13.02.2018**

CORRESPONDING AUTHOR

H Turan Akkoyun
Siirt University,
Faculty of Veterinary Science
Department of Physiology
TR-56100 Siirt – Turkey

e-mail: turanakkoyun@hotmail.com

© by PSP Volume 27 – No. 5/2018 pages 3156-3161 Fresenius Environmental Bulletin

STUDY ON THE CHARACTERISTICS AND UTILIZATION OF A TRICLOPYR BUTOXYETHYL ESTER DEGRADING BACTERIUM, *LACTOBACILLUS BUCHNERI* TBE-6

Jiang-wei Zhu[1,*], Yan Zhao[2], Xiao-lou Li[3], Wei-hong Chen[4], Rong Huang[4]

[1]Collaborative Innovation Center of Sustainable Forestry in Southern China of Jiangsu Province, Nanjing Forestry University, Nanjing 210037, China
[2]Shanghai Institute of Quality Inspection and Technical Research, Shanghai 200233, China
[3]Architecture and Environmental Engineering Department, Sichuan Vocational and Technological College, Suining 629000, China
[4]Pudong Agrotechnology Extension Center, Shanghai 201201, China

ABSTRACT

A strain TBE-6 capable of degrading triclopyr butoxyethyl ester (TBEE) was isolated from farmland soil. TBE-6 was identified as *Lactobacillus buchneri* based on 16S rRNA and analysis of morphology, physiological and biochemical characters. The optimal pH value and temperature were 6.5 and 37□ respectively. The strain TBE-6 had the ability to degrade TBEE, triclopyr and TCP. The degradation rate of TBEE (100mg/L) by the strain TBE-6 could reach 94.4% in 5d. The combined applications of the strain TBE-6 and the strain TR-13 was considered an effective means for rapidly degrading TBEE. The degradation rate of TBEE (100mg/L) by the strain TBE-6 and the strain TR-13 could reach about 98.6% in 5d. In addition, the strain TBE-6 showed a high tolerance to TBEE. It was considered that the strain TBE-6 could be applied for bioremediation of TBEE, triclopyr or TCP pollution.

KEYWORDS:
Triclopyr butoxyethyl ester, biodegradation, *Lactobacillus buchneri*

INTRODUCTION

Triclopyr butoxyethyl ester {2-butoxyethyl 2-(3,5,6-trichloropyridin-2-yl) oxyacetate, it also could be called as TBEE} was a registered herbicide used extensively in the control of broadleaf weeds and woody plants on forests, rangeland and plantation crops, such as oil palm [1-3]. In such applications the TBEE could potentially reach surface water and soils, which raises concerns about potential hazards to ecosystem, particularly aquatic life and soil organisms [4, 5]. Therefore, the degradation and environmental fate of TBEE in ecosystem were paid more attention. Potential environmental routes of removal of TBEE were hydrolysis, biodegradation, photolysis and sorption to sediment, especially microbial degradation [3, 6-8].

The major intermediate metabolites of TBEE degradation were triclopyr and 3,5,6-trichloro-2-pyridinol (TCP) [9, 10]. Particularly, TCP was a charged molecule at neutral pH and more leachable into the water system than TBEE and triclopyr [11, 12]. It was moderately mobile due to its greater water solubility, which could cause the widespread contamination in soil and aquatic environment [13]. It was considered that TCP was more hazardous pollutants than the parent compound. Therefore, in the degradation process of organic pollutants, not only need to focus on the parent pollutants, but also must pay attention to their intermediate products.

In this study, *Lactobacillus buchneri* TBE-6, a strain that could degrade TBEE was isolated, its degradation characteristics was studied. The strain TBE-6 has the ability to degrade TBEE and its major metabolites triclopyr and TCP. It was considered that the strain TBE-6 could be applied for bioremediation of TBEE, triclopyr or TCP pollution.

MATERIALS AND METHODS

Chemicals and Media. Chemicals: triclopyr butoxyethyl ester (TBEE, 97.0%) was supplied by the Dow Chemical Company. All other chemicals used were of analytical grade and commercially available.

Culture media. ①Inorganic salt medium: $MgSO_4 \cdot 7H_2O$ 0.2 g, K_2HPO_4 0.1g, $(NH_4)_2SO_4$ 0.1 g, $CaSO_4$ 0.05 g, $FeSO_4 \cdot 7H_2O$ 0.01 g, water 1.0 L, pH 7.0. ②Isolation medium: inorganic salt medium containing TBEE (100mg/L) was used to isolate TBEE degrading bacteria. ③Enrichment medium: beef extract powder 3.0 g, yeast extract powder 5.0 g, peptone10.0 g, sodium chloride 5.0 g, water 1.0 L, pH7.0.

Isolation and identification of TBEE degrading bacteria. The soil sample was collected from the woodland in Nanjing City, China, in which triclopyr butoxyethyl ester has been used for more than seven

years. 6.0 g of soil samples were placed in 100ml inorganic salt medium containing 100 mg/L TBEE for shaking culture at 37°C, and the concentration of the residual TBEE in medium was determined every 24h [14, 15]. The culture solution with 3d degradation rate ≥75% was switched to enrichment medium containing same concentration TBEE, and continuously switched for more than 5 times. After the degradation ability was verified again, the above enrichment medium was coated on inorganic salt culture plate containing TBEE for culture at 37°C. The eugonic bacterial colonies were selected and repeatedly streaked on the culture plate to obtain the pure culture. The new isolates were identified by using 16SrRNA sequence analysis.

Tolerance of the strain TBE-6 on TBEE. TBEE was added to the inorganic salt medium, and the concentration of TBEE were 50mg/L, 100mg/L, 200mg/L, 400 mg/L and 800 mg/L, respectively. The strain TBE-6 was inoculated respectively for shaking cultivation at 37°C. OD_{600} was determined regularly, so as to evaluate the tolerance of strain TBE-6 on TBEE.

Degradation of TBEE by strain TBE-6. 5% strain TBE-6 inoculum was inoculated in inorganic salt medium containing 100mg/L TBEE, and then placed in a shaker to culture (37°C). The concentration of TBEE and triclopyr were determined every 24h [16].

Degradation of triclopyr and TCP by strain TBE-6. The inorganic salt medium containing 100mg/L triclopyr (or TCP) was inoculated with 5% strain TBE-6 inoculum, and then put it into the shaker (37°C). The concentration of triclopyr (or TCP) was determined regularly [17, 18].

Degradation of triclopyr butoxyethyl ester by combining strain TBE-6 and strain TR-13. The strain TR-13 was a triclopyr degrading bacterium deposited in our laboratory. It was identified as *Bacillus cereus* according to 16S analytical method (GenBank accession number KY649624). The strain TR-13 could effectively degrade triclopyr to 3,5,6-trichloro-2-pyridinol(TCP) at a faster rate, but it could not degrade TCP alone. Because the strain TBE-6 degrades triclopyr only at a slower rate, the combined applications of the strain TBE-6 and the strain TR-13 was considered an effective way to rapidly degrade triclopyr butoxyethyl ester.

5% strain TBE-6 inoculum and 4% strain TR-13 inoculum were inoculated simultaneously in inorganic salt culture medium containing 100mg/L triclopyr butoxyethyl ester, and then incubate in incubator. The concentration of triclopyr butoxyethyl ester and triclopyr were determined every 24h.

RESULTS AND DISCUSSION

Identification and characterization of TBEE degrading bacteria. A strain capable of using TBEE as the sole carbon sources and energy source was isolated from soil, named TBE-6. It was a gram-positive, non-spore forming, facultative anaerobic, rod prokaryote(0.4-0.8×2.0-2.5 um in size). It forms rough, opalescent and opaque colonies on the nutrient agar plate. The optimal pH and temperature were 6.5 and 37°C respectively. It was positive in tests for catalase, amylolysis, glucose fermentation, but the indole test was negative [19, 20]. The strain TBE-6 was identified as *Lactobacillus buchneri* according to 16S sequence analysis (16S sequence: GenBank accession number MF491867).

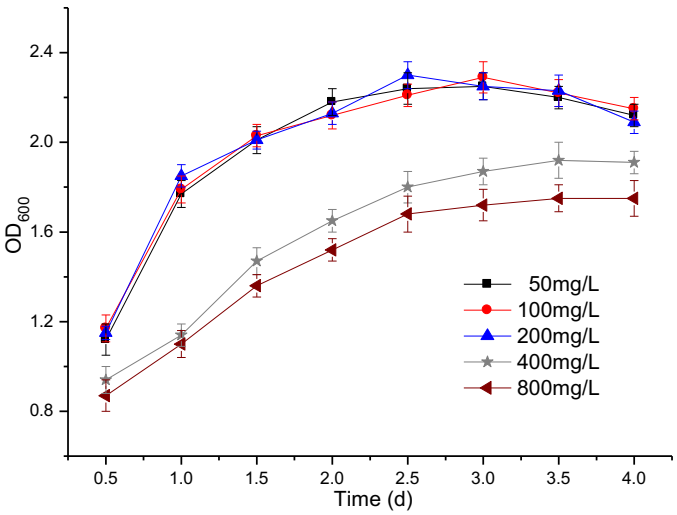


FIGURE 1
Effect of concentration of TBEE on the growth of strain TBE-6

Tolerance of the strain TBE-6 on TBEE. The concentration of TBEE increased from 50mg/L to 200mg/L, and the growth on the strain TBE-6 did not change significantly($P>0.05$). However, if the concentration was further increased to 400mg/L or 800mg/L, the growth of strain TBE-6 would decrease gradually (Fig.1). The results showed that the growth on the strain TBE-6 had been inhibited by 400mg/L or 800mg/L TBEE, but it was still growing. Therefore, it was preliminarily considered that the strain TBE-6 could tolerate at least 800mg/L TBEE under the experimental conditions. According to the experimental results, it was inferred that the strain TBE-6 had excellent tolerance and degradation ability on TBEE, which could be used in a wider range of TBEE concentrations. In addition, it was possible that the strain TBE-6 was used in the bioremediation of TBEE pollution. The degradation ability of the strain TBE-6 might be closely related with the long-term use of TBEE in the sampling area. Generally, soil microorganism that continuously encounter the artificially synthesized compound might induce the ability to degrade the compound [21, 22].

Degradation of TBEE by the strain TBE-6. The results in Fig. 2 showed that TBEE could be degraded by the strain TBE-6, and triclopyr was an important intermediate metabolite. To inoculate the strain TBE-6 in inorganic salt medium contained TBEE could substantially improve the degradation rate of TBEE. The degradation rate of TBEE (100mg/L) by the strain TBE-6 could reach 94.4% in 5d. At the same time, it was found that the concentration of triclopyr was dynamically changing in the degradation process of TBEE. In addition, in the process of degradation of TBEE to triclopyr, part of triclopyr would be further degraded, the other part

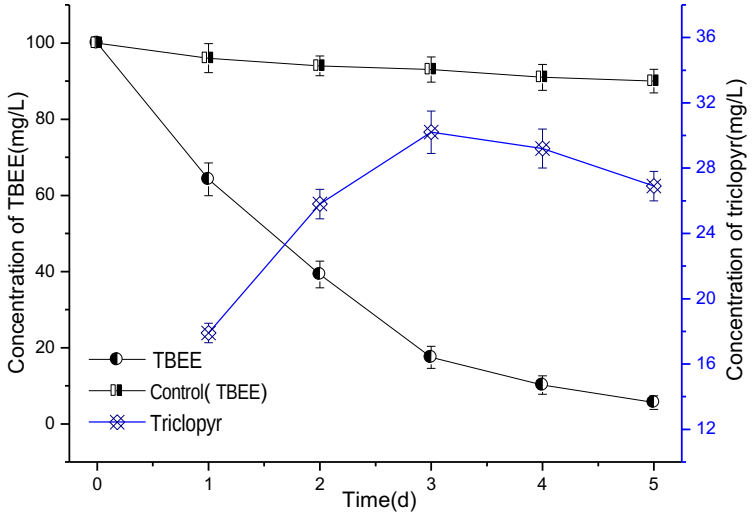


FIGURE 2
Degradation curve of TBEE by the strain TBE-6 and the concentration of triclopyr

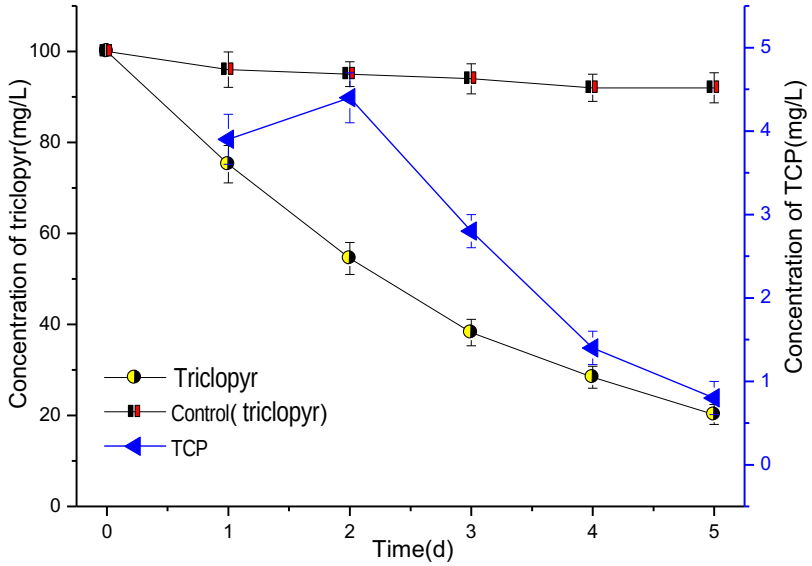


FIGURE 3
The curve on triclopyr degradation by the strain TBE-6 and the concentration of TCP

was temporarily accumulated. For example, on the fifth day, the concentration of TBEE was 5.6 mg/L (94.4 mg/L TBEE had been degraded), the theoretical concentration of triclopyr should be 67.9 mg/L, but the measured concentration was 26.9 mg/L. It indicated that some of triclopyr had been degraded, or there were other degradation pathways of TBEE in which the triclopyr was not its intermediate product.

Degradation of triclopyr and TCP by the strain TBE-6. The above experimental results had shown that triclopyr was an important intermediate product for TBEE degradation. Whether the strain TBE-6 could degrade triclopyr, and its degradation rate were the important part of this study. The results in Fig. 3 showed that the strain TBE-6 could degrade triclopyr and its degradation rate could reach about 80% in 5d. In addition, TCP had been identified as an important intermediate product for triclopyr degradation. During the process of triclopyr degradation, the concentration of TCP first increase, and then gradually reduced, indicating that the TCP produced in this process could be degraded by strain TBE-6. The results shown in Fig. 4 also confirmed that the strain TBE-6 could effectively degrade TCP, and the degradation rate was 99.4% in 4d, 5d degradation rate could reach 100%.

Degradation of TBEE by the strain TBE-6 and TR-13. It was considered that the biodegradation pathway of TBEE was as follows: TBEE → Triclopyr → TCP →…→ CO_2+H_2O [23]. During the degradation of TBEE, the degradation rate of intermediate metabolites and the accumulation of intermediates will affect the entire degradation process. Because the degradation rate of triclopyr (100mg/L) by the strain TR-13 could reach about 92% in 5d [24], the strain TBE-6 degrades triclopyr less rapidly than the strain TR-13, and there was a certain degree of triclopyr accumulation during the degradation of TBEE by the strain TBE-6, the combined applications of the strain TBE-6 and the strain TR-13 was considered an effective means for

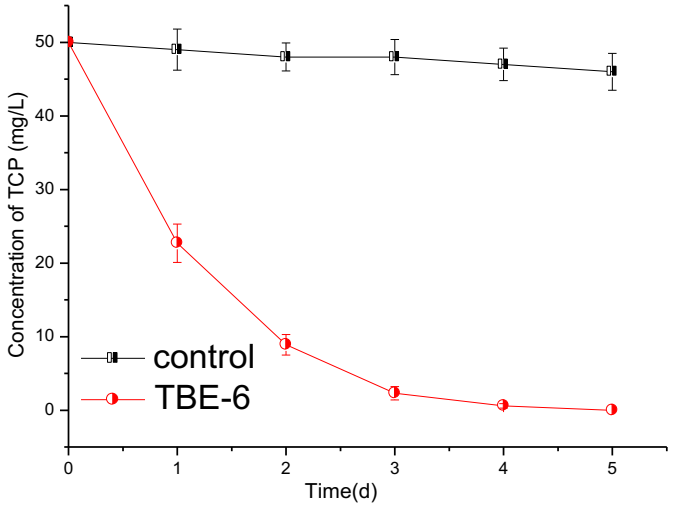


FIGURE 4
The curve on TCP degradation by the strain TBE-6

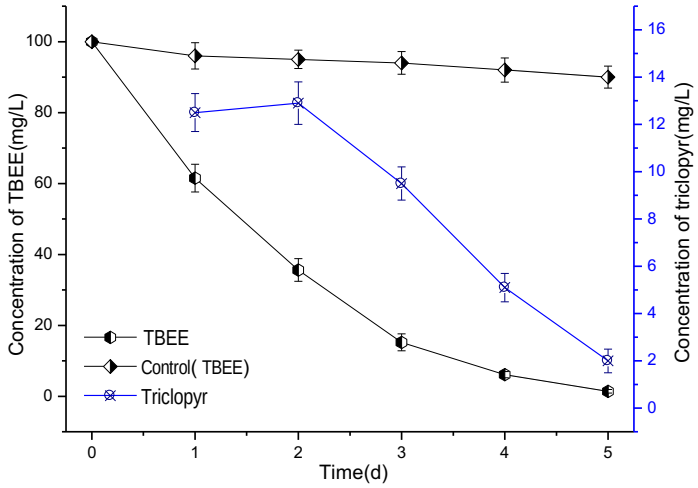


FIGURE 5
The curve on TBEE degradation by the strain TBE-6 and the strain TR-13

rapidly degrading TBEE. The results in Fig. 5 showed that TBEE could be rapidly degraded by the strain TBE-6 and the strain TR-13. The degradation rate of TBEE (100mg/L) by the strain TBE-6 and the strain TR-13 could reach about 98.6% in 5d. The fitted equation was $C=100e^{-0.5185t}$, $R^2=0.9914$, half life=1.38 d. These data indicated that the degradation rate of TBEE when the two strains were combined was higher than when the strain TBE-6 alone was used. In addition, the concentration of triclopyr shown in Fig. 5 was significantly lower than that in Fig. 2. It indicates that the combined application of the strain TBE-6 and the strain TR-13 in the degradation of TBEE will help to reduce the accumulation of intermediate (triclopyr) , and effectively increase the biodegradation rate of TBEE.

CONCLUSION

In this study, *Lactobacillus buchneri* TBE-6 was isolated from soil, which could degrade TBEE into triclopyr and TCP. The strain TBE-6 had the ability to degrade TBEE, triclopyr and TCP, respectively. The degradation rate of TBEE (100mg/L) by the strain TBE-6 could reach 94.4% in 5d. The combined applications of the strain TBE-6 and the strain TR-13 was considered an effective means for rapidly degrading TBEE. The degradation rate of TBEE (100mg/L) by the strain TBE-6 and the strain TR-13 could reach about 98.6% in 5d. In addition, the strain TBE-6 could tolerate at least 800mg/L TBEE and showed a high tolerance to TBEE. It was considered that the strain TBE-6 could be applied for bioremediation of TBEE, triclopyr or TCP pollution.

ACKNOWLEDGEMENTS

This study was funded by the Natural Science Fundation of Jiangsu Provincial Universities (No.17KJB610004) and China Postdoctoral Science Foundation (No.2017M611827), and partially by the Priority Academic Program Development of Jiangsu Higher Education Institutions.

REFERENCES

[1] Netherland, M.D., Jones K.D. (2015) A three-year evaluation of triclopyr for selective whole-bay management of Eurasian watermilfoil on Lake Minnetonka, Minnesota. Lake & Reservoir Management. 31(4), 306-323.

[2] Thompson, D.G., Kreutzweiser, D.P., Capell, S.S., Thomas, D.R., Staznik, B., Viinikka, T. (1995) Fate and effects of triclopyr ester in a first-order forest stream. Environmental Toxicology & Chemistry. 14(8), 1307-1317.

[3] Mccall P.J., Gavit P.D. (1986) Aqueous photolysis of triclopyr and its butoxyethyl ester and calculated environmental photodecomposition rates. Environmental Toxicology & Chemistry. 5(10), 879-885.

[4] Thompson, D.G., Staznik, B., Fontaine, D.D., Mackay T., Oliver, G.R., Troth J. (1991) Fate of triclopyr ester (release®) in a boreal forest stream. Environmental Toxicology & Chemistry. 10(5), 619-632.

[5] Guilherme, S., Santos, M.A., Gaivão, I., Pacheco, M. (2015) Genotoxicity evaluation of the herbicide garlon(®) and its active ingredient (triclopyr) in fish (anguilla anguilla l.) using the comet assay. Environmental Toxicology. 30(9), 1073-1081.

[6] Massiha, A., Issazadeh, K. (2011) Microbial degradation of pesticides in surface soil using native strain in Iran. International Conference on Biotechnology and Environment Management. IACSIT Press, Singapoore. IPCBEE vol.18, 76-81.

[7] Kreutzweiser, D.P., Holmes, S.B., Eichenberg, D.C. (1994) Influence of exposure duration on the toxicity of triclopyr ester to fish and aquatic insects. Archives of Environmental Contamination & Toxicology. 26(1), 124-129.

[8] Vassios, J.D., Nissen, S.J., Koschnick, T.J., Heilman, M.A. (2014) Triclopyr absorption and translocation by Eurasian watermilfoil (myriophyllum spicatum) following liquid and granular applications. Weed Science. 62(1), 22-28.

[9] Guo, M., Wu, W., Song, N., Shan, Z., Kong, D. (2013) Degradation characteristics and mechanism of triclopyr-2-butoxyethyl ester in the environment. Acta Scientiae Circumstantiae. 33(5), 1278-1285.

[10] Fox, A.M., Haller, W.T., Getsinger, K.D., Petty, D.G. (2002) Dissipation of triclopyr herbicide applied in Lake Minnetonka, MN concurrently with Rhodamine WT dye. Pest Management Science. 58(7), 677-686.

[11] Abraham, J., Silambarasan, S. (2013) Biodegradation of chlorpyrifos and its hydrolyzing metabolite 3,5,6-trichloro-2-pyridinol by *Sphingobacterium sp*. JAS3. Process Biochemistry. 48(10), 1559-1564.

[12] Petty, D.G., Getsinger, K.D., Woodburn, K.B. (2003) A review of the aquatic environmental fate of triclopyr and its major metabolites. Journal of Aquatic Plant Management. 41(2), 69-75.

[13] Yang, L., Zhao, Y.H., Zhang, B.X., Yang, C.H., Zhang, X. (2005) Isolation and characterization of a chlorpyrifos and 3,5,6-trichloro-2-pyridinol degrading bacterium. Fems Microbiology Letters. 251(1), 67-73.

[14] Mccall, P.J., Laskowski, D.A., Bidlack, H.D. (1988) Simulation of the aquatic fate of triclopyr butoxyethyl ester and its predicted effects on coho salmon. Environmental Toxicology & Chemistry. 7(7), 517-527.
[15] Carney, E.W., Billington, R., Barlow, S.M. (2007) Developmental toxicity evaluation of triclopyr butoxyethyl ester and triclopyr triethylamine salt in the cd rat. Reproductive Toxicology. 23(2), 165-174.
[16] Ebadi, A.G. (2008) Determination of residues of triclopyr in fishes of Caspian Sea (Iran). Asian Journal of Chemistry. 20(5), 3497-3501.
[17] Koch, H.M., Angerer, J. (2001) Analysis of 3,5,6-trichloro-2-pyridinol in urine samples from the general population using gas chromatography-mass spectrometry after steam distillation and solid-phase extraction. Journal of Chromatography B Biomedical Sciences & Applications. 759(1), 43-49.
[18] Anwar, S., Liaquat, F., Khan, Q.M., Khalid, Z.M., Iqbal, S. (2009) Biodegradation of chlorpyrifos and its hydrolysis product 3,5,6-trichloro-2-pyridinol by bacillus pumilus strain C2A1. Journal of Hazardous Materials. 168(1), 400-405.
[19] Mazzucotelli, C.A., Ponce, A.G., Kotlar, C.E., Moreira, M.D.R. (2013) Isolation and characterization of bacterial strains with a hydrolytic profile with potential use in bioconversion of agroindustial by-products and waste. Ciencia E Tecnologia De Alimentos. 33(2), 295-303.
[20] Sun, P., Cui, J., Jia, X., Wang, W. (2017) Isolation and characterization of bacillus amyloliquefaciens L-1 for biocontrol of pear ring rot. Horticultural Plant Journal. 3(5), 183-189.
[21] Petric, I., Karpouzas, D.G., Bru, D., Udikovic-Kolic, N., Kandeler, E., Djuric, S. (2015) Nicosulfuron application in agricultural soils drives the selection towards NS-tolerant microorganisms harboring various levels of sensitivity to nicosulfuron. Environmental Science & Pollution Research. 23(5), 1-14.
[22] Felsot, A., Maddox, J.V., Bruce, W. (1981) Enhanced microbial degradation of carbofuran in soils with histories of furadan use. Bulletin of Environmental Contamination & Toxicology. 26(1), 781-788.
[23] Zhu, J., Dai, L., Yang, N., Li, X., Zhao, Y. (2017) Study on biodegradation mechanism of triclopyr butoxyethyl ester and utilization of a triclopyr butoxyethyl ester degrading bacterium, *Bacillus coagulans* TBE-9. Fresen. Environ. Bull. 26, 7561-7567.
[24] Zhu, J., Xie, K., Zhao, Y. (2017) Isolation and utilization of a triclopyr degrading bacterium, *Bacillus cereus* TR-13. Fresen. Environ. Bull. 26, 8119-8124.

Received: **29.12.2017**
Accepted: **12.02.2018**

CORRESPONDING AUTHOR

Jiang-wei Zhu
Collaborative Innovation Center of Sustainable Forestry in Southern China of Jiangsu Province,
Nanjing Forestry University,
Nanjing 210037 – China

e-mail: jw_zhu2016@qq.com

© by PSP Volume 27 – No. 5/2018 pages 3162-3165 Fresenius Environmental Bulletin

FERTILITY VARIATION AND GENE DIVERSITY BASED ON CONE AND SEED PRODUCTION IN A CLONAL SEED ORCHARD OF *PINUS NIGRA* ARNOLD

Zafer Kaya, Halil Baris Ozel*

Bartin University, Faculty of Forestry, 74100, Bartin, Turkey

ABSTRACT

Black pine or also called Anatolian black pine [*Pinus nigra* Arn. subsp. *pallasiana.* (Lamb.) Holmboe.] is one of the most important forest tree species used in multiple purposes such as conversion of unproductive forest to productive by plantation generally for extreme region (i.e., arid and frost area) in Turkish forestry. Improved seeds produced from seed orchards have an important factor in success of the conversion. Estimation of fertility variation among genotypes is one of the important tools used to produce improved seeds. Female, male, total, and cone fertility variations, and also gene diversity based on cone and seed production were estimated in a clonal seed orchard of the species for three consecutive years.

Male fertility (2.63, 2.07 and 1.12) was higher than that of female (1.24, 1.24 and 1.06) for the years, while it was opposite (1.07 and 1.14) for combined years. Fertility variation of cone was higher than total fertility variation for strobili production for the years. The relative status numbers estimated based on the total fertility ranged from 77.5% to 91.9% for the reproductive characters and years. Estimated gene diversity in seed crop were higher than 0.98.

KEYWORDS:
Black pine, flowering, reproductive, sibling coefficient, status number.

INTRODUCTION

Black pine or also called Anatolian black pine [*Pinus nigra* Arn. subsp. *pallasiana.* (Lamb.) Holmboe.] is one of the most important forest tree species for Turkish forestry and the "National Tree Breeding and Seed Production Programme" [1]. The species covers about 21% of total forest area by 4.7 million ha, of which about 2.1 million ha are considered to be unproductive forests [2]. The present unproductive forest area of the species and Turkey is getting larger potential of the species for plantation because of resistance to disadvantages areas (i.e., arid area). For the purpose, 165 seed orchards were established at 1135 ha in the species [3]. Seed orchards produced improved seeds are an important seed source for forestry and successful of the plantations. Estimation of fertility variation defined as an individual ability to give progeny is one of the important tools used different purposes such as gene conservation, seed production programs, managing forest genetic resources, evolutional and genetic management of populations for plant breeding [4-8] to produce higher quality and quantity improved seeds. To monitor and determine the genetic diversity of seed crops, some genetic parameters such as genetic relatedness, inbreeding, and gene diversity should be also calculated based on fertility variation [9]. Knowledge of fertility variation estimated based on reproductive characters is getting importance because of its easy, cheap and light survey. Many studies have been carried out on fertility variation in different plant species because these advantages [e.g., 7, 10-16].

The purposes of this study are to evaluate fertility variation among orchard parents and its effect on gene diversity of seed (i.e., status number), and to contribute to breeding and seed production programme of the species.

MATERIALS AND METHODS

Seed orchard and data collection. The studied seed orchard of Black pine, was established in Eflani-Karabuk in 8 ha at northern part of Turkey in 2002. Grafts were planted at spacing 8 m x 8 m, and the seed orchard is composed of 40 clones (total of 1620 ramets) [17]. The data of female and male strobilus were collected from six ramets chosen randomly from each clone at the beginning of May and September of 2013, 2014 and 2015.

Number of female ($N_{♀}$) and male ($N_{♂}$) strobilus, and cone number (N_{cone}) data were collected on fifteen grafts, chosen at random, from each of fourty clones, chosen at random, at the beginning of May for strobili and at the beginning of September for cone of the years.

Fertility variation, status number and gene diversity. The female fertility (ψ_f) and male fertility (ψ_m) variation was estimated as [18]:

$$\psi_f = N\sum_{i=1}^{N} f_i^2 = CV_f^2 + 1,$$

$$\psi_m = N\sum_{i=1}^{N} m_i^2 = CV_m^2 + 1 \quad \text{(1a and b)}$$

where N is the census number, f_i is the female fertility (i.e., relative female flower production) of the i^{th} individual, m_i is the male fertility (i.e., relative male flower production) of the i^{th} individual and CV_f and CV_m are the coefficients of variation in female and male flower production among individuals, respectively.

Total fertility variation (Ψ) was calculated by strobili production [8] and also based on number of cone (Ψ_{cone}) as [19]:

$$\Psi = \left(\frac{CV_f^2 + CV_m^2}{4}\right) + 0.5\left(N\sum_{n=1}^{N}\frac{f_n m_n}{\sum f \sum m} + 1\right),$$

$$\Psi_{cone} = N\sum_{i=1}^{N} cone_i^2 \quad \text{(2a and b)}$$

where N is the census number, CV_f is the coefficient of variation in female fertility, and CV_m is the coefficient of variation in male fertility, f_n and m_n are the number of female and male strobilus of the n^{th} individual; f and m are used as index for the female and male strobilus, respectively. Where $cone_i$ is the fertility for cone production of the individual i.

If the clones are unrelated and non-inbred, the status numbers of female ($N_{s(f)}$) and male parents ($N_{s(m)}$) are calculated as [20]:

$$N_{s_{(f)}} = \frac{1}{\sum_{i=1}^{N} f_i^2}, \quad N_{s_{(m)}} = \frac{1}{\sum_{i=1}^{N} m_i^2} \quad \text{(3 a and b)}$$

where $p_{i(f)}$ is the female fertility of the clone i, $p_{i(m)}$ is the male fertility of the clone i and N is the census number in the seed orchard. Here, fertility is estimated based on the strobilus assessment.

Status number (N_s) on total fertility (i.e., clone fertility) was calculated as following [21]:

$$N_s = \frac{4N}{[\Psi_f + \Psi_m + 2 + 2r\sqrt{(\Psi_f - 1)(\Psi_m - 1)}]},$$

$$N_{s_{(cone)}} = \frac{1}{\sum_{i=1}^{N} cone_i^2} \quad \text{(4 a and b)}$$

where ψ_f and ψ_m are the fertility variations of female and male parents, which are equivalent to CV_f^2 +1 and CV_m^2 +1, respectively (Kang 2001). Here, CV_f and CV_m are the coefficients of variation in female and male strobilus production among individuals, and r is the correlation coefficient between female and male strobilus production. Relative status number (N_r) was calculated as $N_r = N_s / N$ [20].

Gene diversity (GD) in seed crop was estimated based on status number (N_s) on total fertility as [11]: GD=1-0.5/ N_s

RESULTS AND DISCUSSION

Fertility variation of male strobili ($\Psi_{(♀)}$) was higher than that of female ($\Psi_{(♂)}$), while it was opposite for polled years (1.14 & 1.07) (Table 1). The status number (N_s) and relative status number (N_r) of female and male parents were acceptable level (N_r >80%), except male parents in 2013 and 2014 (Table 1).

Averages of female and male strobilius were 145 and 706 for combined years in the orchard, while large difference was reported among clone and within clone for the years [22]. Averages of female and male strobilus were found 78 and 187 in a clonal seed orchard of the species based on one year data [9]. Large differences among clones showed importance of individual selection and seed harvesting year. The variation was in good accordance with other Black pine and Scots pine studies [9, 23]. It was also reported in clonal seed orchards of *Tectona grandis* [13]. The studied seed orchard was rather young in age to peak strobilus production. It was reported that fertility variation is higher when seed orchard was young [6, 18]. Beside, there could be many genetic and environmental effects such as year and management of orchard [24-26]. For instance, it was Ata (1995) reported that good seed year was once in two or three years in natural stands of the species [27].

TABLE 1
Fertility variation ($\Psi_{(♀)}$ & $\Psi_{(♂)}$), status number ($N_{s(♀)}$ & $N_{s(♂)}$) and relative status number ($N_{r(♀)}$) & $N_{r(♂)}$) in gametic gene pool for female (♀) and male (♂) parents

	2013		2014		2015		General	
($\Psi_{(♀)}$ & $\Psi_{(♂)}$)	1.24	2.63	1.24	2.07	1.06	1.12	1.14	1.07
$N_{s(♀)}$ & $N_{s(♂)}$	24.2	11.4	28.2	16.9	29.2	27.6	24.5	26.3
$N_{r(♀)}$ & $N_{r(♂)}$	0.81	0.38	0.80	0.48	0.94	0.89	0.88	0.94

TABLE 2
Fertility variation (Ψ), status number (N_s), relative status number (N_r) and relative gene diversity (*GD*) in total gametic gene pool in the studied seed orchards

	$\Psi_{(♀+♂)}$ & Ψ_{cone}		$N_{s(♀+♂)}$ & $N_{s(cone)}$		$N_{r(♀+♂)}$ & $N_{r(cone)}$		$GD_{(♀+♂)}$ & $GD_{(cone)}$	
2013	1.10	1.15	36.5	34.7	91.1	86.7	0.986	0.986
2014	1.17	1.27	34.2	31.4	85.5	78.6	0.985	0.984
2015	1.09	1.29	36.8	30.9	91.9	77.5	0.986	0.984
General	1.05	1.23	37.9	32.6	94.9	81.4	0.987	0.985

Status number (N_s) for the total fertility ($\Psi_{(♀+♂)}$) and cone fertility (Ψ_{cone}) was moderately high for the years (Table 2), indicating that orchard was functioning efficiently for seed harvesting area. It was also supported by higher relative gene diversity (*GD>0.98*), and fertility variations estimated by strobili and cone productions (Table 2).

Fertility variation of female ($\Psi_{(♀)}$) strobili was higher than that of male strobili ($\Psi_{(♂)}$) for polled years (Table 1). They were estimated 1.06 and 1.12 in a clonal seed orchard of the species [9]. Fertility variation estimated based on cone production was found 1.81 in total of three plantation populations of Ehrami black pine [28]. It was suggested that the sibling coefficient of seed orchards as a heuristic rule of thumb could be set to two [21].

Status number (N_s) for the total fertility ($\Psi_{(♀+♂)}$) and cone fertility (Ψ_{cone}) was moderately high for the years (Table 2). However, fertility variation and related parameters such as status number could be balanced by forest tending or other forestry practices (i.e., harvesting equal seed crop from each clone).

ACKNOWLEDGEMENTS

Authors acknowledge administrative support from The Research Directorate of Forest Tree Seeds and Tree Breeding of Turkey. Authors thank to Prof. Dr. Nebi Bilir from Suleyman Demirel University for his valuable comments in the paper.

REFERENCES

[1] Koski, V., Antola, J. (1993) National tree breeding and seed production programme for Turkey 1994-2003. The Research Directorate of Forest Tree Seeds and Tree Breeding. Ankara, Turkey.

[2] General Directorate of Forestry (2016) Forest Inventory of Turkey. General Directorate of Forestry Press. Ankara, Turkey.

[3] General Directorate of Forestry (2015) Website of the Research Directorate of Forest Tree Seeds and Tree Breeding of Turkey. Ankara, Turkey.

[4] Griffin, A.R. (1982) Clonal variation in Radiata pine seed orchard. Some flowering, cone and seed production traits. Australian Forest Research. 12, 295-302.

[5] El-Kassaby, Y.A. (1995) Evaluation of tree-improvement delivery system: factors affecting genetical potential. Tree Physiology. 15, 545-550.

[6] Bila, AD. (2000) Fertility variation and its effects on gene diversity in forest tree populations. Ph.D Thesis. Swedish University of Agricultural Science. Umeå, Sweden. Acta Universitatis Agriculturae Sueciae, Silvestria, 166p.

[7] Kang, K.S., Bila, A.D., Harju, A.M., Lindgren, D. (2003) Fertility variation in forest tree populations. Forestry. 76, 329-344.

[8] Bilir, N., Kang, K.S., Lindgren, D. (2005) Fertility variation in six populations of Brutian pine (*Pinus brutia* Ten.) over altitudinal ranges. Euphtyica. 141, 163-168.

[9] Bilir, N., Kang, K.S., Ozturk, H. (2002) Fertility variation and gene diversity in clonal seed orchards of *Pinus brutia*, *Pinus nigra* and *Pinus sylvestris* in Turkey. Silvae Genetica. 51, 112-115.

[10] Bila, A.D., Lindgren, D., Mullin, T.J. (1999) Fertility variation and its effect on diversity over generations in a Teak plantation (*Tectonia grandis* L.f.). Silvae Genetica. 48, 109-114.

[11] Kang, K.S., Lindgren, D. (1998) Fertility variation and its effect on the relatedness of seeds in *Pinus densiflora*, *Pinus thunbergii* and *Pinus koraiensis* clonal seed orchards. Silvae Genetica. 47, 196-201.

[12] Bilir, N., Prescher, F., Ayan, S., Lindgren, D. (2006) Growth characters and number of strobili in clonal seed orchards of *Pinus sylvestris.* Euphytica. 152, 293-301.

[13] Varghese, M., Nicodemus, A., Nagarajan, B., Lindgren, D. (2006) Impact of fertility variation on gene diversity and drift in two clonal seed orchards of teak (*Tectona grandis* Linn. f.). New Forests. 31, 497-512.

[14] Bilir, N., Kang, K.S. (2014) Estimation of fertility variation by strobili and cone productions in Taurus cedar (*Cedrus libani* A. Rich.) populations. IUFRO Forest Tree Breeding Conference, Prague.

[15] Ozel, H.B., Bilir, N. (2015) Fertility variation and status number in a clonal seed orchard of Scotch Pine (*Pinus sylvestris* L.). Fresen. Environ. Bull. 214, 2035-2038.
[16] Yazici, N., Bilir, N. (2017) Aspectual Fertility Variation and Its Effect on Gene Diversity of Seeds in Natural Stands of Taurus Cedar (Cedrus libani A. Rich.). I. J. Genomics. 2017, 5p.
[17] General Directorate of Forestry (2001) Working report of 2000 and working plan of 2001. The Research Directorate of Forest. Tree Seeds and Tree Breeding Press. Ankara, Turkey.
[18] Kang, K.S., Lindgren, D. (1999) Fertility variation among clones of Korean pine (*Pinus koraiensis* S. et Z.) and its implications on seed orchard management. For. Genetica. 6, 191-200.
[19] Bilir, N. (2011) Fertility variation in Wild rose (*Rosa canina* L.) over habitat classes. International Journal of Agriculture and Biology. 13, 110-114.
[20] Lindgren, D., Gea, L., Jefferson, P. (1996) Loss of genetic diversity monitored by status number. Silvae Genetica. 45, 52-59.
[21] Kang, K.S. (2001) Genetic gain and gene diversity of seed orchard crops. Ph.D Thesis. Swedish University of Agricultural Science, Umeå, Sweden. Acta Universitatis Agriculturae Sueciae, Silvestria. 187p.
[22] Bilir, N., Özel, H.B. (2017) Variation in strobili and cone production among clones in a Pinus nigra seed orchard. The International Conference on Agriculture, Forest, Food Sciences and Technologies (ICAFOF). Cappadocia, May 15-17, 798p.
[23] Bilir, N., Prescher, F., Lindgren, D., Kroon, J. (2008) Variation in Seed Related Characteristics in Clonal Seed Orchards of *Pinus sylvestris*. New Forests. 36, 187-199.
[24] Eriksson, G., Jonsson, A., Lindgren, D. (1973) Flowering in a clonal trial of *Picea abies* (Karst.). Stud. For. Suec. 110, 4-45.
[25] Hedegart, T. (1976) Breeding systems, variation and genetic improvement of teak (*Tectona grandis* L.f.). In: Burley, J., Styles, B.T. (eds.) Tropical Trees: Variation, Breeding and Conservation. Linnean Society Symposium Series 2. Academic Press, New York.
[26] Zobel, B., Talbert, J. (1984) Applied forest tree improvement. John Wiley & Sons, New York.
[27] Ata, C. (1995) Technique of Silviculture. Karaelmas University, Bartin Forestry Faculty publishers, Bartin, Zonguldak
[28] Bilir, N., Catal, Y., Tekocak, S., Cercioglu, M. (2017) Fertility variation in endemic populations of Ehrami black pine (*Pinus nigra* Arnold. subsp. *pallasiana* var. *pyramidata*). Journal of Forestry Research. 28, 683-686.

Received: **04.01.2018**
Accepted: **06.02.2018**

CORRESPONDING AUTHOR

Halil Baris Ozel
Bartın University
Faculty of Forestry,
Department of Forest Engineering
74100, Bartın – Turkey

e-mail: halilbarisozel@gmail.com

© by PSP Volume 27 – No. 5/2018 pages 3166-3173 Fresenius Environmental Bulletin

THE EFFECT OF MIXING *SOLIDAGO CANADENSIS* L. SOIL WITH THAT OF NEIGHBOURING *IMPERATA CYLINDRICAL* (L.) P. BEAUV. ON NITROGEN TRANSFORMATIONS

Liya Zheng, Bangliang Deng, Qian Liu, Xiang Zheng, XiaoFeng Xu, ShuLi Wang, LiJun Huang, Xiaomin Guo, Dekui Niu*

Jiangxi Provincial Key Laboratory of Silviculture, Co-Innovation Center of Jiangxi Typical Trees Cultivation and Utilization, College of Forestry, Jiangxi Agricultural University, Nanchang 330045, China

ABSTRACT

Plant invasions can alter soil nitrogen cycling as a result of differences in physiological traits. *Solidago canadensis* L. has a rapidly expanding range and displaces diverse grass species throughout eastern China. In new invasion sites where distribution is patchy, *S. canadensis* and neighbouring species all contribute soil inputs; however, whether there is a mixing effect remains unknown. The aim of this study is to investigate the influence of plant invasions on soil nitrogen transformation. We examined the effects of an invasive plant, *S. canadensis*, on soil properties and the nitrogen mineralization (including ammonification and nitrification) process 0–30 cm below the surface using lab incubations. We considered different habitats within the invaded sites. Invasive soils (i.e., soils dominated by species considered invasive) had higher soil organic carbon, total nitrogen, and total biomass than native soils, but dissolved organic carbon, ammonium nitrogen, and nitrate nitrogen were not significantly different. Soil nitrogen mineralization rates were intermediate in mixed soils compared to invasive and native soils, thus indicating additive effects associated with *S. canadensis* invasions.

KEYWORDS:
Solidago canadensis, nitrogen mineralization, mixed soil, additive effect, plant invasion

INTRODUCTION

Invasive plants have not only seriously threatened the native biodiversity and stability of many ecosystems [1], they have also caused considerable economic loss worldwide [2]. Plant invaders can induce the alteration of abiotic and biotic properties of their neighbouring soils [3]. The complexity of soil ecosystems has only begun to be understood over the last decade; studies have uncovered critical effects of microbes on nutrient cycling, plant growth, and community dynamics [4]. Therefore, soil nitrogen (N) cycling in areas dominated by invasive species might be different compared to native soils. N transformations have a vital effect on inorganic N supply, and inorganic and organic N contribute differentially to the growth advantage of invaders because of different uptake mechanisms of inorganic and organic N [5]. N mineralization is not only a foundational step in soil organic N transformation, but it is also one of the most important processes in soil N cycling. During the N mineralization process, soil organic N is mineralised into inorganic N primarily in the forms of ammonium N (NH_4^+–N) and nitrate N (NO_3^-–N), or it is transformed into an intermediate transitional fraction, such as soluble organic N (SON), which can then be mineralised into inorganic N. Historically, most studies on invasive soil N mineralization have focused on soluble inorganic N, but mixed soils have received little attention. Therefore, an accurate simulation of the N mineralization process in invasive, native, and mixed soils is important to guide strategies for the control of invasive alien plants.

Solidago canadensis L. (henceforth "*Solidago"*) is one of the most hazardous invasive plants in China [6]. The invasive perennial forb is native to North America, and it was introduced to China as an ornamental plant in the mid-1930s [7]. It has reportedly spread to many provinces in southeastern China, disturbed industrial and agricultural areas, and it is becoming a serious invasive plant that can compete aggressively with many native species, such as the native perennial forb *Imperata cylindrica* (L.) P. Beauv. (henceforth "*Imperata"*). This forb is broadly distributed in humid and loose, light-weight soil, and it has a long, cylindrical, stout rhizome.

The success of *Solidago* invasion is partially related to the release of allelopathic compounds, among other benefits, from AM fungi; this dynamic potentially differentiates *Solidago* soils from co-occurring native soils [8]. *Solidago* invasion may form dense monocultures and lead to the displacement of native species, which greatly reduces the biodiversity of the invaded area [1]. As invasions progresses, *Solidago* distribution might be patchy and coexist with native species, forming mixed soils in the transition zones (i.e., nearby soils with *Solidago* and surrounding *Imperata* may be influenced by both native

and invasive soils). A study has shown that the soil physicochemical properties and microbial composition of termite nest soils differed from control soils, and they produced altered C and N cycling rates in soil mixtures [9]. Differences in physiological traits, roots, and the litter input between moso bamboo (*Phyllostachys edulis* (Carrière) J. Houzeau, synonym *Phyllostachys heterocycla* Carrière) and native trees can cause non-additive effects on soil C and N properties [10]. During the stages of invasion, invasive plants are still expanding into areas dominated by native plants, and the abiotic and biotic impacts in these mixed forests may differ relative to invader monocultures [11].

We collected soils to conduct an incubation experiment to examine the effects of invasion on soil N transformations. We address the following questions: 1) How do soil N mineralization characteristics vary among non-invaded soils, mixed soils, and *Solidago* soils? 2) Could differences in physiological traits and nutrient use between *Solidago* and *Imperata* cause non-additive effects on soil N mineralization when mixed together?

MATERIALS AND METHODS

Sample collection and analysis. The study was conducted in Nanchang, Jiangxi Province, China (longitude 115°47′ 22″–115°49′35″ E and latitude 28°43′49″–28°45′35″N). The region has a subtropical humid monsoon climate with a long-term mean annual temperature of 17.4 °C. The mean annual precipitation is 1,744 mm, and rainfall occurs more during the spring and autumn with rainy seasons in May and June. The annual frost-free period is about 270 days with an annual sunshine of 1,723 h. The soils are classified as red soils at the site (humic planosols following the FAO system).

In September 2016, we surveyed the study site to identify four blocks (5 m × 5 m). The area was dominated by both *Imperata* and *Solidago*; both species were mainly distributed along the highway and in abandoned lands. Within each block we established two quadrats (1 m × 1 m) that were approximately 3 m away from each other. Aboveground vegetation inside the eight fixed quadrats was completely removed by hand. Eight samples of the top 30-cm soil layers in the interior of each quadrat were collected, and all roots were removed from the soil sample of each plot. The aboveground vegetation and the roots were naturally air-dried to a constant weight. We collected *Solidago* soils and *Imperata* soils and produced a mixed soil by mixing equal masses of the native and invaded soils. The stones, plant and animal residues were removed from the fresh soil, then soils were passed through a 2 mm sieve for analysis. Fresh samples were used to measure soil dissolved organic carbon (DOC; Vario TOC, Elementar, Germany), and soil available nitrogen (AN, which includes extractable ammonium and nitrate) [8, 12]. Soil pH values were measured using a glass electrode (soil/water ratio of 1:2.5). Air-dried samples ground with a 0.15-mm sieve were used to estimate soil total organic carbon (TOC) and total nitrogen (TN) [8, 12].

Soil incubation experiment. Lab incubation was used to determine differences in N transformation rates (ammonification, nitrification, and nitrogen mineralization) among *Solidago* soils, mixed soils, and *Imperata* soils. We incubated soil samples (~25 g dry weight equivalent determined by a subsample) of the three soil types in 150 mL conical flasks in the dark at 25 °C and with 60% water filled pore space (WFPS). We used fresh soils to determine initial and final AN concentration after incubation to calculate N transformation rates (mg N kg^{-1}soil day^{-1}). Soil samples were measured at five-day intervals to determine N transformation rates over the 25 days of incubation (a total of 60 incubated soil samples= 3 soil types × 4 blocks × 5 times). We calculated the soil net N ammonification rate, nitrification rate, and mineralization rate based on the following the equations:

Net N ammonification rate = $(ammonium_a - ammonium_0) / T_{days}$

Net nitrification rate = $(nitrate_n - nitrate_0) / T_{days}$

Net N mineralization rate = $[(nitrate_n + ammonium_a) - (nitrate_0 + ammonium_0)] / T_{days}$

where $ammonium_0$ and $ammonium_a$ are initial and final ammonium concentrations (mg NH_4^+–N kg^{-1}soil), respectively; $nitrate_0$ and $nitrate_n$ represent initial and final nitrate concentrations (mg NO_3^-–N kg^{-1}soil), respectively; and T_{days} is the incubation time in days.

Statistical analyses. We used Student's t-tests to examine the differences in pH, DOC, NH_4^+–N, NO_3^-–N, AN, TN, C/N ratio, and TOC between native and invaded soils. We used repeated-measures ANOVA to examine dependence of three net N transformation rates on soil types, incubation time, and their interactions. We used post-hoc tests to examine differences among means at each time point. We calculated expected value of N transformation rates based on values obtained when each soil was incubated alone. We also used t-tests to examine the differences between observed and expected value of soil N transformations.

RESULTS

Test soil parameters. Relative to native soils, *Solidago* soils had slightly, but not significantly, higher DOC concentrations, AN concentration, and C/N ratios, but pH values were not significantly higher (Table 1). The TOC and TN concentrations were significantly ($p<0.05$) higher in *Solidago* soil

compared to *Imperata* soil (Table 1). NH_4^+–N and NO_3^-–N concentrations were positively correlated with TOC and TN concentrations, but negatively correlated with pH values (Table 2).

Soil nitrogen mineralization. The pattern of change of NH_4^+–N accumulative concentrations in the invasive species was a bimodal curve (Fig. 1A). The accumulation of NH_4^+–N reached its maximum on the fifth day and its lowest on the fifteenth day (14.25 ± 4.24 N mg kg^{-1} d^{-1} and 1.43 ± 0.36 N mg kg^{-1} d^{-1}, respectively). Mixing *Solidago* and *Imperata* soils displayed a similar pattern in accumulation of NH_4^+–N with the invasive species. NO_3^-–N concentrations varied over time with generally higher values over 25 days of incubation (Fig. 1B), and NO_3^-–N concentrations were significantly different among the three soil types ($P<0.05$). The inorganic N content varied over time and it was significantly different among soils (Fig. 1C). There was no significant interactive effect of species and time over 25 days of the nitrogen mineralization process.

The net ammonification rate was positive during the early incubation period, but it was negative by the fifteenth day (Fig. 2A), suggesting that the N immobilization had a greater effect than N mineralization on the N transformation process. The net nitrification rate increased proportionally contrary to the net N ammonification rate (Fig. 2B), which implied that ammonium availability might control nitrification in these soils.

The soil N mineralization rates were intermediate in mixed soils compared to *Solidago* and *Imperata* soils. *Solidago* soils mineralized more rapidly than *Imperata* soils (Fig. 2C). For mixed soils, there were no significant differences between the observation value and the expected value (Fig. 3).

Plant biomass. *Solidago* had a larger aboveground biomass than *Imperata* ($P<0.05$), but the belowground biomass of *Solidago* (362 ± 35.68 g) and *Imperata* (351 ± 31.30 g) were quite similar, thus suggesting balanced resource acquisition between the invasive species and the native species. *Solidago* produced a higher total biomass than *Imperata* (Fig. 4); however, its shoot-root ratio was lower relative to *Imperata* ($P<0.05$).

DISCUSSION

Invasion effects on soil characteristics. The invasive *Solidago* benefited more from arbuscular mycorrhizal (AM) fungi than native plants [8, 13], which potentially improved the ability of the plant to uptake nutrients, hence increasing the quantity and quality of TOC and TN inputs (Table 1). A previous study demonstrated that invasive *Solidago* and native plant species were not affected by soil history, rather the soil biota community of *Solidago* promoted the growth of native species [14]. We found that there were no significant differences in NH_4^+–N, NO_3^-–N, and DOC between invasive and native species (Table 1), perhaps because AM fungi act to share resources among neighbouring plants, thus *Imperata* benefits from the presence of *Solidago.* This was consistent with another study that observed no difference in the effect strength of plant-soil feedback between invasive and native plants [15]. Therefore, native and invasive species mediated by alterations in the soil biota community caused a balanced acquisition of resource. Indeed, soil DOC had also been used as a measure of available resources for microbes [16]. However, our results suggest that these soil properties are not altered in the early stages of invasion.

TABLE 1

Dependence of soil C and N characteristics (means ± standard error) on species (*Solidago, Imperata*) in one-way ANOVAs. Means with the same lowercase letters in the same row are not significantly different in LSD tests at α = 0.05

Treatments	pH	TOC g kg^{-1}	TN g kg^{-1}	C/N	DOC mg kg^{-1}	NH_4^+-N mg kg^{-1}	NO_3^--N mg kg^{-1}
Solidago	6.82±0.52a	15.00±1.88a	1.56±0.13a	9.62±0.74a	537.12±20.35a	6.43±2.30a	5.8±0.58a
Imperata	7.51±0.73a	10.42±1.38b	1.13±0.08b	9.22±0.55a	525.65±26.92a	1.67±0.54a	3.5±0.53a

Note: TOC, total organic carbon; TN, total nitrogen; DOC, dissolved organic carbon; NH_4^+-N, ammonium N; NO_3^--N, nitrate N.

TABLE 2

Pairwise correlation coefficients among soil C and N characteristics

Parameters	TOC	TN	C/N ratio	NH_4^+-N	NO_3^--N	AN	pH
TN	0.954**						
C/N ratio	0.783*	0.568					
NH_4^+–N	0.693	0.809*	0.188				
NO_3^-–N	0.779*	0.832*	0.445	0.712*			
AN	0.764*	0.869**	0.278	0.977**	0.845**		
pH	0.102	-0.154	0.665	-0.572	-0.137	-0.477	
DOC	0.004	0.055	-0.058	0.272	0.508	0.361	-0.096

*P<0.05; **P<0.01

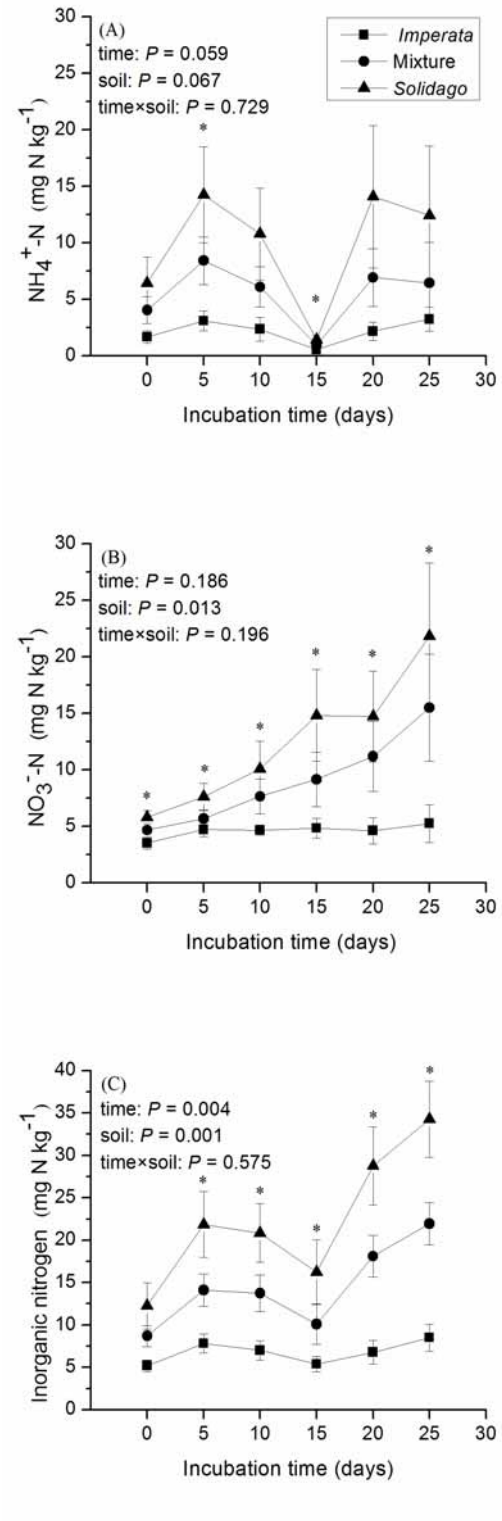


FIGURE 1
The dependence of accumulative concentrations of NH_4^+-N (A), NO_3^--N (B), and inorganic N (C) on soil types (*Solidago* soils, mixed soils, or *Imperata* soils) throughout the incubation period (means ± standard error). *P<0.05

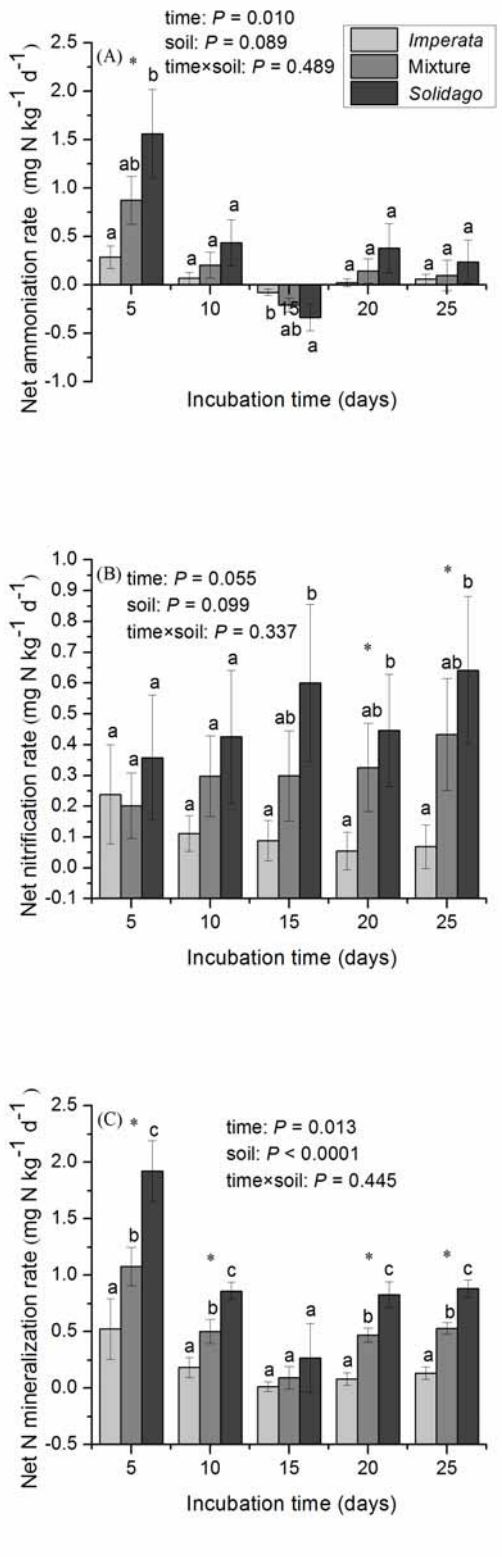


FIGURE 2
The difference of soil net N ammonification (A), nitrification (B), and mineralization rate (C) on soil types (*Solidago* soils, mixed soils, or *Imperata* soils) throughout the incubation period (means ± standard error). Means with the same letters were not significantly different in post hoc tests at P = 0.05. *P< 0.05

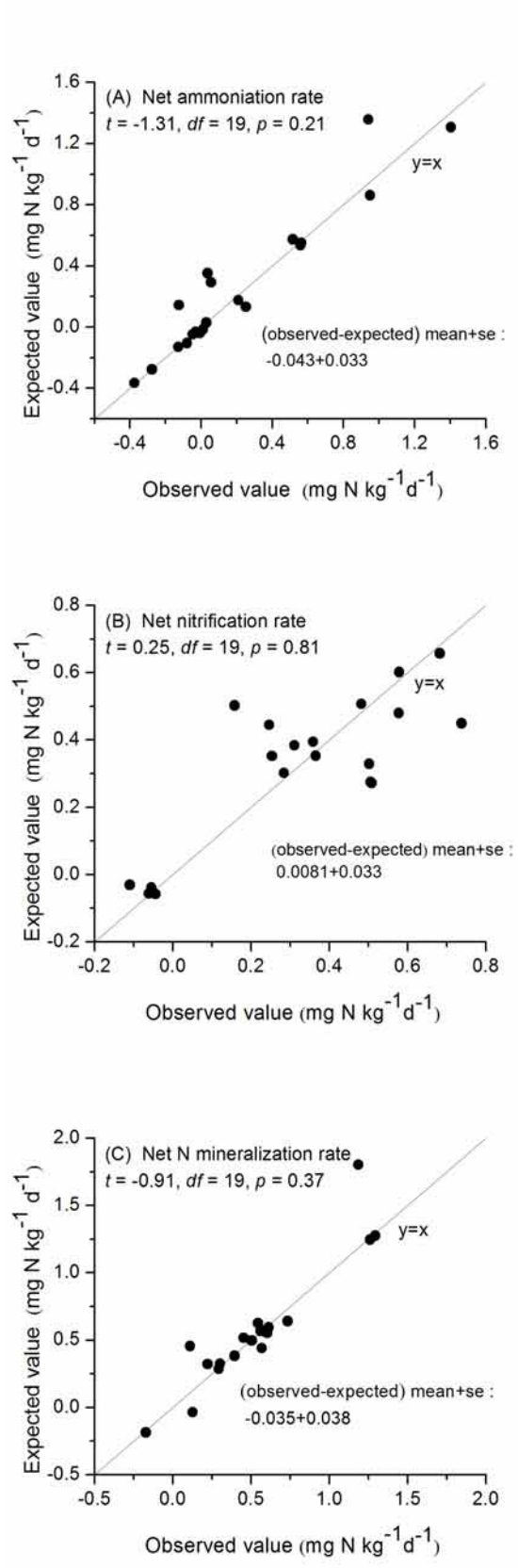


FIGURE 3
The dependence of comparison between expected and observed values of N ammonification (A), nitrification (B), and mineralization rate (C) in mixed soils

We observed lower pH values from *Solidago* soils (Table 1), indicating that *Solidago* have a preference for acidic and low-saline soils. The available N concentrations were negatively correlated with pH values (Table 2), which is similar to what was found by Aciego Pietri and Brookes [17], who observed that soil NH_4^+–N and NO_3^-–N concentrations were maximal at the lowest pH (pH 3.7).

Soil N mineralization. Soil N mineralization can be greatly influenced by temperature and moisture [18]. However, in this study, the temperature and moisture were strictly controlled during the incubation process. The temperature (25 °C) was chosen because the average outdoor temperature was 25 °C when the soil was collected. Therefore, the observed differences in N mineralization rates were likely correlated with microbial communities and available soil carbon (C) and N [19]. Invasive species promote the N mineralization rate, unlike the native species; this might have been induced by the higher TOC and TN concentrations related to the higher microbial biomass and activity in the soil N transformations [20, 21]. Soil N mineralization is correlated positively with total soil C and N concentrations [22], which indicates that soil microbial activities and N substrate availabilities have an important effect on regulating N mineralization.

The accumulation of NH_4^+–N and the net ammonification rate decreased in the early stages of incubation, but it increased after the fifteenth day, which might be a result of the changes in soil microbial community structure and activity [3]. The soluble and available small molecular nutrients were likely more abundant during the early incubation period, which promoted higher microbial activity of ammonification bacteria. Over time, the small molecular nutrients gradually decomposed and primarily larger molecular nutrients remained. As a result, the soil microbial community structure and activity were altered, the net ammonification rate gradually decreased, and the N immobilization was higher than ammonification by the fifteenth day (Fig. 1A). Because microbial community structure tended to be dominated by polymer microorganisms that could better utilize the large molecular nutrients, the net ammonification rate and accumulation of NH_4^+–N increased later in the incubation period. The available NH_4^+–N was the substrate resource of nitrification, leading to the proportional increase of the net nitrification rate in contrast to the net N ammonification rate (Fig. 2B). Soil N mineralization had a similar pattern to ammonification in the early stages of incubation, which is consistent with the finding that invasive species cultured alone could exhibit limited contributions to its success in *Solidago*-soil interaction during the early stages of invasion [23].

The mixed soils could be considered as a transition invasion zone where invasive *Solidago* co-oc-

curs with the native *Imperata*. In our study, the mixing of *Solidago* and *Imperata* soils resulted in additive effects on N mineralization compared to mineralization rates in isolated soils of each species. Mixing soil samples from multiple experimental units ignores uncertainty and generates incorrect estimates of soil biota effects on plants [24]. Many previous studies on mixed soils were conducted outdoors, it is just in a relative mixed area as for the mixed soils sampling [9, 10]. Therefore, the non-addictive effects were observed in these experiments because the mixing of soil samples is biased. Our experiment is a strictly controlled blend of soils, so there is no mixing effect on N mineralization. Our results are consistent with the finding [24] that mixed soil samples (MSS) can produce faulty results, and different research questions require precise techniques to be sufficiently addressed.

Plant biomass. Other experimental studies have observed a loss of more than 50% of the total biomass of native species when competing with *Solidago* [25]. In our experiment, *Solidago* produced a higher total biomass than *Imperata* (Fig. 4), which is likely attributable to the competitive advantage provided by its tall stature compared to the shorter species. *Solidago* has strong competitive effects on native species due to its large size and its ability to grow at least as tall as neighbouring species [26, 27]. The strong competitive interactions make plant size a mediator of competitive ability and a very important factor when invading habitats occupied by smaller native species [28]. These results are consistent with the finding that *Solidago* allocated more biomass to the aboveground parts when growing with *Euthamia graminifolia* (L.) Nutt compared to *Solidago* growing in monocultures [29].

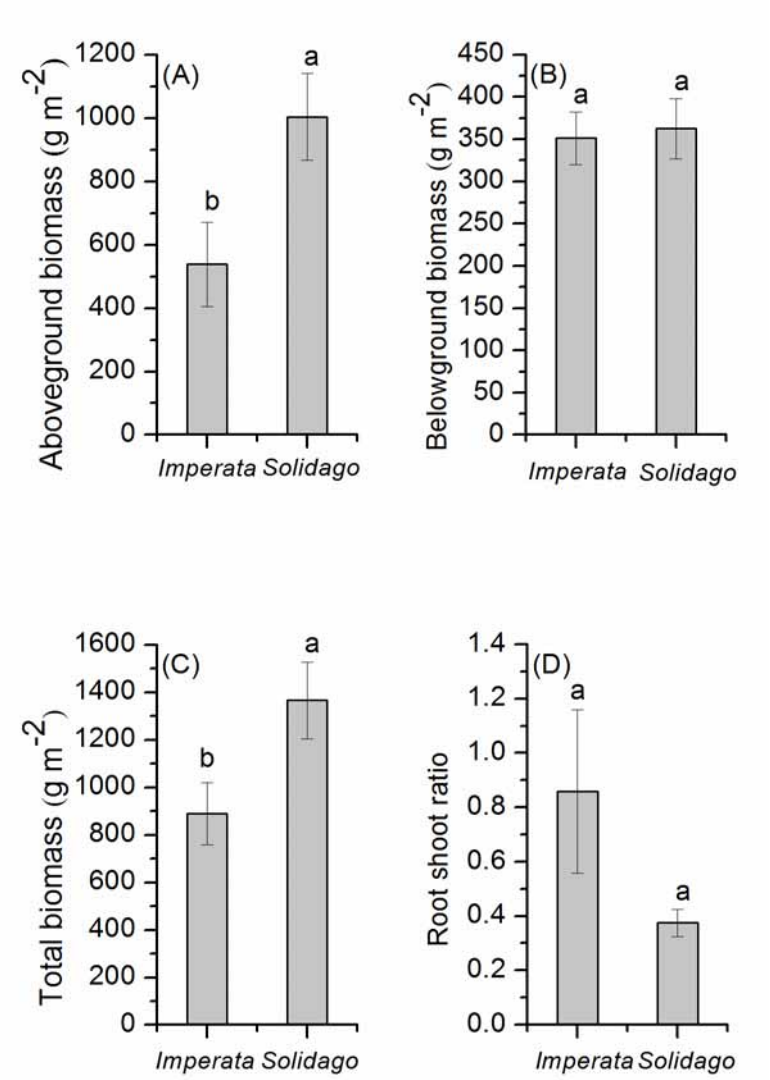


FIGURE 4
The dependence of aboveground biomass (A), belowground biomass (B), total biomass (C), and root/shoot ratio (D) between *Solidago* and *Imperata* (means ± standard error). Means with the same letters were not significantly different in post hoc tests at P = 0.05

ACKNOWLEDGEMENTS

The authors thank WenWu Meng and his friend for their assistance and patience in the field work and three reviewers for their contributions to the improvement of the earlier manuscript. This study was supported by the National Natural Science Foundation of China (No.31360177, No.41501317).

REFERENCES

[1] Ehrenfeld, J.G. (2010) Ecosystem consequences of biological invasions. Annual Review of Ecology Evolution and Systematics. 41, 59-80.

[2] Mack, R.N., Simberloff, D., Lonsdale, W.M., Evans, H., Clout, M., Bazzaz, F.A. (2000) Biotic invasions: causes, epidemiology, global consequences, and control. Ecological Applications. 10(3), 689-710.

[3] Chang, E.H., Chiu, C.Y. (2015) Changes in soil microbial community structure and activity in a cedar plantation invaded by moso bamboo. Applied Soil Ecology. 91, 1-7.

[4] Hodge, A., Fitter, A.H. (2013) Microbial mediation of plant competition and community structure. Functional Ecology. 27(4), 865–875.

[5] Yu, H.W., Yang, J.X., Gao, Y., He, W.M. (2016) Soil organic nitrogen endows invasive Solidago canadensis with greater advantages in low-phosphorus conditions. Ecosphere. 7(3), e01254.

[6] Dong, M., Lu, J., Zhang, W., Chen, J., Li, B. (2006) Canada goldenrod (*Solidago canadensis*): An invasive alien weed rapidly spreading in China. Acta Phytotaxonomica Sinica. 44(1), 72-85.

[7] Jin, L., Gu, Y.J., Xiao, M., Chen, J.K., Li, B. (2004) The history of *Solidago canadensis* invasion and the development of its mycorrhizal associations in newly-reclaimed land. Functional Plant Biology. 31(10), 979-986.

[8] Zhang, L., Zhang, Y., Zou, J., Siemann, E. (2014) Decomposition of Phragmites australis litter retarded by invasive *Solidago canadensis* in mixtures: an antagonistic non-additive effect. Scientific Reports. 4, 5488.

[9] Hu, Y., Zhang, L., Deng, B., Liu, Y., Liu, Q., Zheng, X., Zheng, L., Kong, F., Guo, X., Siemann, E. (2017) The non-additive effects of temperature and nitrogen deposition on CO_2 emissions, nitrification, and nitrogen mineralization in soils mixed with termite nests. Catena. 154, 12-20.

[10] Li, Z., Zhang, L., Deng, B., Liu, Y., Kong, F., Huang, G., Zou, Q., Liu, Q., Guo, X., Fu, Y. (2017) Effects of moso bamboo (*Phyllostachys edulis*) invasions on soil nitrogen cycles depend on invasion stage and warming. Environmental Science Pollution Research. 24, 24989–24999.

[11] Cremer, M., Kern, N.V., Prietzel, J. (2016) Soil organic carbon and nitrogen stocks under pure and mixed stands of European beech, Douglas fir and Norway spruce. Forest Ecology and Management. 367, 30-40.

[12] Sparks, D.L., Page, A.L., Helmke, P.A., Loeppert, R.H., Soltanpour, P.N., Tabatabai, M.A., Johnston, C.T., Sumner, M.E. (1996) Methods of soil analysis. Part 3 - chemical methods. Soil Science Society of America Inc, Madison.

[13] Sun, Z.K., He, W.M. (2010) Evidence for Enhanced Mutualism Hypothesis: *Solidago canadensis* Plants from Regular Soils Perform Better. PLoS ONE. 5(11), e15418.

[14] Schittko, C., Wurst, S. (2014) Above- and belowground effects of plant-soil feedback from exotic *Solidago canadensis* on native Tanacetum vulgare. Biological Invasions. 16(7), 1465-1479.

[15] Dostál, P., Palečková, M. (2011) Does relatedness of natives used for soil conditioning influence plant-soil feedback of exotics? Biological Invasions. 13(2), 331-340.

[16] Huang, Y., Zou, J., Zheng, X., Wang, Y., Xu, X. (2004) Nitrous oxide emissions as influenced by amendment of plant residues with different C:N ratios. Soil Biology and Biochemistry. 36(6), 973-981.

[17] Aciego Pietri, J.C., Brookes, P.C. (2008) Nitrogen mineralisation along a pH gradient of a silty loam UK soil. Soil Biology and Biochemistry. 40(3), 797-802.

[18] Zaman, M., Chang, S.X. (2004) Substrate type, temperature, and moisture content affect gross and net N mineralization and nitrification rates in agroforestry systems. Biology and Fertility of Soils. 39(4), 269-279.

[19] Liang, Y., He, X., Chen, C., Feng, S., Liu, L., Chen, X., Zhao, Z., Su, Y. (2015) Influence of plant communities and soil properties during natural vegetation restoration on arbuscular mycorrhizal fungal communities in a karst region. Ecological Engineering. 82, 57-65.

[20] Berendse, F. (1990) Organic Matter Accumulation and Nitrogen Mineralization During Secondary Succession in Heathland Ecosystems. Journal of Ecology. 78(2), 413-427.

[21] Kitayama, K. (1996) Soil nitrogen dynamics along a gradient of long-term soil development in a Hawaiian wet montane rainforest. Plant and Soil. 183(2), 253-262.

[22] Yan, E.R., Wang, X.H., Huang, J.J., Li, G.Y., Zhou, W. (2008) Decline of soil nitrogen mineralization and nitrification during forest conversion of evergreen broad-leaved forest to plantations in the subtropical area of Eastern China. Biogeochemistry. 89, 239-251.

[23] Dong, L.J., Sun, Z.K., Yan, G., He, W.M. (2015) Two-year interactions between invasive *Solidago canadensis* and soil decrease its subsequent growth and competitive ability. Journal of Plant Ecology. 8(6), 617-622.
[24] Cahill, J.F., Cale, J.A., Karst, J., Bao, T., Pec, G.J., Erbilgin, N. (2017) No silver bullet: different soil handling techniques are useful for different research questions, exhibit differential type I and II error rates, and are sensitive to sampling intensity. New Phytologist. 216(1), 11.
[25] Fenesi, A., Geréd, J., Meiners, S.J., Tóthmérész, B., Török, P., Ruprecht, E. (2015) Does disturbance enhance the competitive effect of the invasive *Solidago canadensis* on the performance of two native grasses? Biological Invasions. 17(11), 3303-3315.
[26] Goldberg, D.E., Werner, P.A. (1983) The effects of size of opening in vegetation and litter cover on seedling establishment of goldenrods (*Solidago spp.*). Oecologia. 60(2), 149-155.
[27] Walck, J.L., Baskin, J.M., Baskin, C.C. (1999) Relative Competitive Abilities and Growth Characteristics of a Narrowly Endemic and a Geographically Widespread *Solidago* Species (Asteraceae). American Journal of Botany. 86(6), 820-828.
[28] Yuan, Y.G., Bing, W., Zhang, S.S., Tang, J.J., Tu, C., Hu, S.J., Yong, J.W.H., Xin, C. (2013) Enhanced allelopathy and competitive ability of invasive plant *Solidago canadensis* in its introduced range. Journal of Plant Ecology. 6(3), 231–235.
[29] Szymura, M., Szymura, T.H. (2016) Interactions between alien goldenrods (*Solidago* and *Euthamia* species) and comparison with native species in Central Europe. Flora. 218, 51-61.

Received: **08.01.2018**
Accepted: **10.02.2018**

CORRESPONDING AUTHOR

Dekui Niu
Jiangxi Provincial Key Laboratory of Silviculture,
Co-Innovation Center of Jiangxi Typical
Trees Cultivation and Utilization,
College of Forestry,
Jiangxi Agricultural University,
Nanchang 330045 – China

e-mail: ndk2157@163.com

© by PSP Volume 27 – No. 5/2018 pages 3174-3179 Fresenius Environmental Bulletin

THE EFFECTS OF ORGANIC AMENDMENTS ON CADMIUM UPTAKE OF SPINACH (*SPINACIA OLERACEA L.*) AND PLANT GROWTH UNDER CADMIUM TOXICITY

Sibel Boysan-Canal[1,*], Mehmet Ali Bozkurt[1], Selma Kipcak[2]

[1]Department of Soil Science and Plant Breeding, Faculty of Agriculture, Yuzuncu Yil University, Van, Turkey
[2]Department of Baskale Vocational High School, Yuzuncu Yil University, Van, Turkey

ABSTRACT

It has been well-documented that organic amendments reduce heavy metal uptake by plants thereby diminishing their movement in soil. The aim of the present pot experiment is to investigate the potential effects of organic amendments sewage sludge (SS), sheep manure (SM), cattle manure (CM), peat, and humic acid (HA)) on plant growth, cadmium uptake and antioxidative enzyme activity in spinach (*Spinacia oleracea L.*). The pot experiment was 100 mg kg^{-1} cadmium applied to soils with the sequence of: 0%, 10% and 20% levels of SS, SM, CM, Peat and HA with two different levels of 500 and 1000 mg kg^{-1} applied. Organic amendment applications, including 10% and 20% Cd + SS and 20% Cd +CM and 20% Cd+ SM significantly decreased cadmium uptake, respectively, 80.19%, 77.70%, 78.76%, and 73.12% compared to cadmium application alone. Cadmium application alone caused higher activity in ascorbate peroxidase (APX) activity and malondialdehyde (MDA) content than control. Organic amendments resulted in decreased APX activity and MDA content. All organic amendment applications significantly decreased cadmium uptake in spinach. However, SS was more effective than others applications, due to the low amount of heavy metal in SS. Additionally, another account for its effectiveness may be that the other organic matter level of the SS is higher than the other organic amendments.

KEYWORDS:
Spinach (*Spinacia oleracea L.*), Cadmium, Organic amendments, Antioxidative *enzyme*

INTRODUCTION

Cadmium(Cd) is one of the most toxic heavy metals. Accumulation and diffusion of Cd in agricultural soils occur through phosphor fertilizer, sewage sludge (SS), industrial production, motor vehicles, agricultural medicine of fungicides. Excessive amount of Cd in soil is associated with decrease in plant growth, photosynthesis, chlorophyll synthesis, as well as impairment in physiological and morphological features of plant [1]. Excessive Cd is involved in oxidative stress, which results from the production of hydrogen peroxide (H_2O_2) and superoxide radical ($.O2^-$) and hidroxyl radical (.OH). Plant cells have antioxidative protection systems set in motion to deal with harmful effects of reactive oxygen species [2]. Formation of metallo-organic compounds through giving organic matter to soil may increase heavy metal availability in plants; on the other hand, interaction between metal and solid phase of humic acid may cause decrease availability heavy metal. Thus, potential harmful effects on environment may be mitigated [3]. Cd uptake by high plants is dependent on Cd concentration and availability in soil. The bioavailability of Cd in soil interacts with soil organic matter. Because ligands included in organic materials bond with Cd ions that result in decreased Cd uptake [4]. Most studies have documented that organic fertilizers have substantial potential to diminish mobility of heavy metals in soil. The field experiment of cattle, swine, and poultry waste compost incorporated into soil, Sato et al. [5] reported that Cd concentration was 34-38% lower in spinach harvested from animal waste compost treated fields than chemical fertilizer-treated fields. In another study, Han et al. [6] demonstrated that the application of slurry composting and bio filtration liquid fertilizer significantly affected mobilization and bioavailability of heavy metal in soil, as well as Cd uptake, which in turn affected the phyto extraction of plant. Heavy metal uptake and toxicity may be differ as a function of type and chemical compound structure of the organic fertilizers [7]. In a pot experiment to explore the growth and metal accumulation in water spinach established on heavy metal contaminated soil, with chicken manure and coconut tree sawdust at application rates of 0%, 1% and 3% (w/w) were incorporated within the soil. Both organic amendments significantly decreased soil extractable metals and plant metal uptake [8]. In another study, the effects of organic amendments, including farm yard manure, poultry manure, press mud and activated carbon on heavy metal uptake into and growth of berseem under nickel contaminated

conditions. Applications of organic amendments decreased heavy metal uptake by plants at high levels of nickel [9].

As a leaf vegetable, spinach is important in the human diet. Spinach has nutritional value and wealth anti-oxidant content. Moreover, spinach is a source of vitamin A, vitamin C, vitamin E, vitamin K, vitamin B2, vitamin B6, magnesium, iron, selenium, calcium, folic acid, zinc, copper, folate, betaine, potassium, and omega-3 fatty acids [10]. The aim of this study is to investigate the influence of various organic amendments on cadmium uptake, plant growth and anti-oxidative enzyme activity in spinach *(Spinacia oleracea L.)* under Cd toxicity condition.

MATERIALS AND METHODS

Characterization of soil and organic amendments. Soil samples were taken from a large brown soil group in the entisols order in the town of Edremit in Van province, Turkey. Physical and chemical properties of soil and organic fertilizers used in the experiment are given in Table 1. The experiment of soil in the was characterized by alkaline pH, unsalted, medium calcareous, low organic matter and low nitrogen. These soil characteristics were alike the soil properties of the study by Alpaslan et al. [11]. SS was taken from the Van Municipality Wastewater Treatment Plantation. Cd, Cu and Zn contents in SS were under the threshold values recommended in the soil pollution control guideline [12]. Cattle and sheep manure was taken from the nearby farm. Peat was supplied as commercial product. As soil conditioner humic acid was supplied as commercial product Humas-15.

Pot Experiment. Soil was collected from top 20 cm, air dried for pot experiment in climate room condition. In pots in the experiment, 100 mg kg^{-1} Cadmium (Cd), applied to soils with the sequence of: 0%, 10% and 20% levels of SS, SM, CM, peat, and HA with two different levels of 500 and 1000 mg kg^{-1} applied. In the present study, 12 applications were made according with a randomized plot design. Pot experiment was conducted in a total of 48 pots, with 4 repetitions in each application. 2 kg pots included 3 plants in each. 12 applications consisted of combinations of Cd, SS, SM, CM, peat, and HA. The applications are as follows:

1. Control
2. Cd: Cadmium100 mg kg^{-1}
3- Cd+%10 S.M.
4- Cd+%20 S.M.
5-Cd+%10 S.S.
6-Cd+%20 S.S.
7- Cd+%10 C.M.
8- Cd+%20 C.M.
9-Cd+%10 Peat
10-Cd+%20 Peat
11-Cd+HA1:500mg kg^{-1}
12-Cd+HA2:1000mg kg^{-1}

Chemical analyses Soil and Organic Amendments. The soil samples and organic manures were air dried in a shadowy place and passed through a 2 mm sieve. In line with the guidelines, using 1:2.5 soil-water mixture and organic manure-water mixture, soil and organic manures pH were measured [13]. The electrical conductivity(EC) of soil and organic manures were measured in soil and water suspension and organic manure and water suspension at ratio of (1:5 (w/v) using EC meter (Termo Scientific,USA). Lime content was calculated using Scheibler calcimeter [14]. Soil organic matter was determined using by Walkley Black method [15]. Total N was measured using Kjeldahl method in soil and organic manures by [16]. Available Fe, Cu, Zn, Mn, and Cd were extracted with DTPA and then measured using AAS technique [17].

TABLE 1
Characteristics of Soil and Organic Amendments Used in the Experiment

	Soil	Sewage Sludge	Humic Acid	Sheep Manure	Cattle Manure	Peat
pH(1/2.5)	8,02	8,07	8,00	8,81	8,35	8,11
Salt, dSm^{-1}	0,673	8,43	-	5,97	11,12	2,01
Lime, %	14,08	3,15	-	3,33	2,78	2,96
Organic Material,%	1,16	39	10	29	33	28
Total N,%	0,07	1,85	0,50	1,42	1,57	1,40
	Extractable with DTPA			**Total elements**		
Cd,$mgkg^{-1}$	0,040	1,03	-	0,69	0,91	0,79
Cu, $mgkg^{-1}$	0,89	117	40	21,84	26,43	10,6
Zn, $mgkg^{-1}$	0,25	677,	100	55,12	86,13	29,13
Mn, $mgkg^{-1}$	6,99	239	100	283	258	171
Fe, $mgkg^{-1}$	3,59	7900	-	595,7	584,7	586,6

TABLE 2
Effects of organic amendments applications on yield parameters of spinach under cadmium contamination condition

Applications	Plant length (cm)	Leaf number	Fresh plant weight (g pot^{-1})	Dry plant weight (g pot$^{-1)}$	Root length (cm)	Fresh root weight (g pot^{-1})	Dry root weight (g pot$^{-1)}$
Control	14,13 **bc***	7,92 **bc**	6,12 **def**	0,48 **ef**	11,88 **ab**	0,19**cd**	0,04 **cde**
Cd (100mg kg^{-1})	11,67 **cdef**	6,75 **c**	4,15 **fg**	0,40 **f**	10,13 **abcd**	0,10**de**	0,02 **efg**
Cd + %10SM	14,83 **ab**	8,50 **b**	10,56 **bc**	1,09 **bc**	12,42 **a**	0,40**a**	0,06 **a**
Cd + %20SM	15,09 **ab**	11,17 **a**	10,27 **bc**	1,08 **bc**	10,58 **abc**	0,33**ab**	0,05 **ab**
Cd + %10SS	16,68 **a**	8,42 **b**	11,59 **b**	1,23 **ab**	10,50 **abc**	0,28**b**	0,05 **ab**
Cd + %20SS	17,36 **a**	8,42 **b**	14,09 **a**	1,44 **a**	10,96 **abc**	0,31**ab**	0,05 **ab**
Cd + %10CM	12,49 **bcde**	8,83 **b**	8,15 **cd**	0,87 **cd**	10,75 **abc**	0,32**ab**	0,05 **ab**
Cd + %20CM	13,02 **bcd**	8,25 **bc**	7,23 **de**	0,77 **de**	9,67 **abcd**	0,24**b**	0,04 **bcd**
Cd + %10 Peat	10,81 **defg**	7,83 **bc**	4,00 **fg**	0,50 **ef**	10,71 **abc**	0,13**de**	0,03 **def**
Cd + %20Peat	10,40 **efg**	8,25 **bc**	5,37 **ef**	0,55 **ef**	9,00 **abcd**	0,14**de**	0,03 **def**
Cd + HA1	8,40 **g**	7,75 **bc**	2,13 **g**	0,28 **f**	8,22 **cd**	0,05**e**	0,02 **fg**
Cd + HA2	9,87 **fg**	8,33 **bc**	2,37 **g**	0,30 **f**	7,19 **d**	0,05**e**	0,01 **g**

Note*: Statistically significant mean differences are indicated with different letters in the same column ($p<0.05$).

The amount of organic matter in SS, SM, CM and peat was determined using combustion method suggested by Kacar [16]. Air dried plant and organic manure samples (SS, SM, CM, Peat) were burned with a mixture of HNO_3-H_2O_2 acids in microwave system to measure the concentration of Cd, Fe, Zn, Cu and Mn by using atomic absorption spectrophotometer [18]. SPSS 13.0 software package was used for statistical analyses [19].

Enzyme Analysis and Lipid Peroxidation. Ascorbate peroxidase (APX) activity was determined following the decrease of ascorbate by measuring the change in absorbance at 290 nm for 1 min in 2 ml of a reaction mixture containing 50 mM KH_2PO_4 (pH 7.0), 1 mM EDTA-Na2, 0.5 mM ascorbic acid, 0.1 mM H_2O_2 and 50 ml of crude enzyme extract [20].

The levels of lipid peroxidation were measured in terms of malondialdehyde (MDA) content, a product of lipid peroxidation. Leaf sample (0.5 g) was homogenised in 10 mL of 0.1% trichloro acetic acid (TCA). The homogenate was centrifuged at 15,000g for 5 minutes. To 1.0 ml aliquot of the supernatant 4.0 ml of 0.5% thiobarbituric acid (TBA) in 20% TCA was added. After centrifugation at 10,000g for 10 min, the absorbance of supernatant was recorded at 532 nm. The value for non-specific absorption at 600 nm was subtracted. The MDA equivalent was calculated [21].

RESULTS AND DISCUSSION

Effects of Organic Amendments on Spinach Growth. Plant length, number of leaves, number of fresh leaves, fresh and dry leaf weight, length of root, fresh and dry root weight of Spinach in various organic amendments under 100 mg kg^{-1}Cd condition are presented in Table 2. Plant length, leaf number, fresh and dry plant weight, root length, fresh and dry root weight decreased with Cd application alone which was statistically unsubstantial. The highest mean values of fresh and dry leaf weight, and plant length were observed in Cd + 20% SS application: 14.09 g pot^{-1}, 1.44 g pot^{-1}, and 17.36 cm, respectively. The highest mean values of root length, fresh and dry root weight were observed in Cd + 10% SM application: 12.42 cm, 0.40 g pot^{-1}, and 0.06 g pot^{-1}, respectively.

These results showed that SS and SM applications increased yield criteria in spinach. These findings were because of high organic matter and nutrient content higher level SM and SS than other organic amendments. Kamari et al. [8] reported that chicken manure was more effective on fresh and dry plant weight of spinach due to organic material content above compared to coconut tree sawdust in heavy metal contaminated soils. SS which includes high salt and heavy metal content has unfavorable results in physiological and metabolic activity in spinach plant [22]. However, Han et al. [23] reported that SS application resulted in better growth in leaf, root and shoot of birch seedlings under cadmium contamination conditions.

Effects of Organic Amendments on Cadmium Uptake and Micro Element Bioavailability. The highest cadmium content in plant was observed in 100 mg kg^{-1} Cd application. On the other hand, lowest cadmium bioaccumulation was occurred in Cd + 10% SS application. In comparison to Cd application alone other amendment applications were resulted in significantly decrease in heavy metal bioavailability as follows: Cd + 10% SS (80.19%), Cd + 20% CM (78.76%), Cd + 20% SS (77.70%), Cd + 20% SM (73.12%), Cd +10% CM (69.55%), Cd + 10 SM (68.58%), Cd + 10% peat (45.13%), Cd + HA1 (500mg kg^{-1}) (25.36%), Cd + HA2 (1000mg kg^{-1}) (20.54%) and Cd + 20% Peat (17.83%) (See, Table 3, Figure 1).

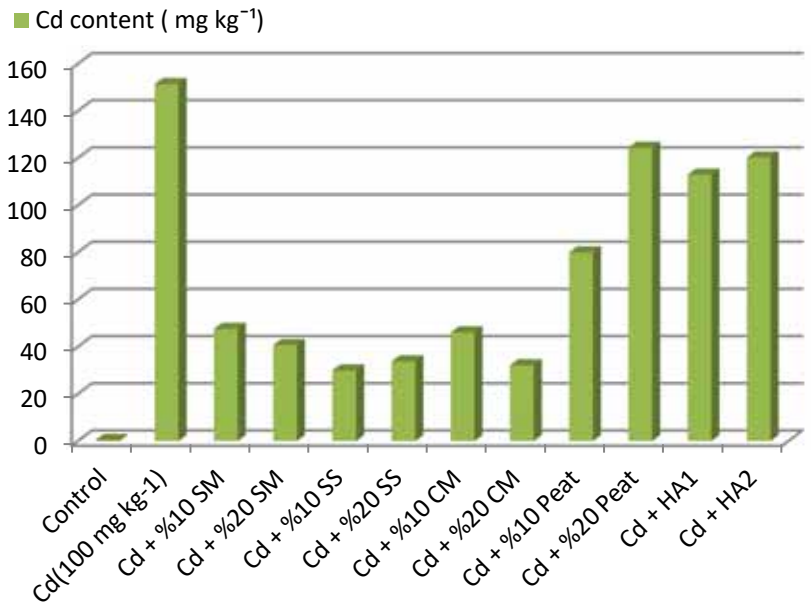


FIGURE 1
Effects organic amendments applications cadmium uptake of spinach under cadmium contamination condition.

All organic amendment applications significantly caused decrease in cadmium uptake into the plant under cadmium contaminated condition. Bioaccumulation of heavy metals in plant tissue and their absorption are dependent on organic material, pH, temperature, and availability of nutrient elements. Organic materials play role in prevention to an extent to which they produce chelated compounds with heavy metals. Organic materials in soil diminishes bioavailability of heavy metals thereby altering them to less soluble forms. Heavy metals are adsorbed through organic acids (e.g., humic acid, fulvic acid) involved within organic materials [24]. Nevertheless, SS was predictor of a significant reduction in cadmium uptake into plant relative to other organic fertilizers. Higher organic material content in SS than other organic fertilizers may account for the discrepancy between organic amendments in soil. SS applications with sufficient amounts seems to be ameliorative in chemical and physical characteristics of soil that leads to increase in crop yield**.** In a similar study, Han et al. [23]. asserted that preventive effects of SS on heavy metal toxicity can be explain through relative reduction in heavy metal bioaccumulation rates. This may be due to that plant growth is associated with the increased synthesis of heavy metal-binding proteins in sewage sludge.

100mg kg^{-1} Cd application significantly increased Cu, Mn and Fe bioavailability in spinach compared to control. This finding was in consonant with the previous data that subsequent applications of 50 mg kg^{-1} Cd was associated with Fe, Zn, Cu and Mn uptake in spinach in the commencement; whereas Fe and Mn uptake into plant significantly increased after eight weeks of application [25]. As can be seen in Table 3, Zn and Cu accumulation in plant was increased in Cd + 10%SS and Cd + 20% SS applications relative to Cd application alone due to high Zn and Cu content in SS. In a field experiment conducted by Canal and Bozkurt [26] accelerated Cd and Zn bioavailability in lettuce plant in SS application under cadmium contaminated soil was documented. On the other hand, accumulation of Fe and Mn content in spinach plant was greater than other applications in Cd + HA1 (Table 3). HA play a regulatory and restorative role for physical and chemical conditions in soils [27]. HA was associated with plant growth, as well as Fe and Zn uptake into plants in certain conditions [28].

Effects of Organic Amendments on APX enzyme activity and MDA level. In comparison to control, APX enzyme activity in spinach was significantly greater in 100 mg kg^{-1} Cd application. whereas, all organic amendments applications were associated with decrease in APX enzyme activity in spinach when compared to cadmium application alone. The lowest level of APX activity was observed in control (Table 4).

MDA, an indicator of lipit peroxidation, was the highest in Cd alone application. A significant reduction in MDA content was associated with all organic amendment applications (Table 4). In a similar study, Cr increased catalase (CAT), superoxide dismutase (SOD), and peroxidase (POD) activity in Zea mays. whereas Farm yard manure(FMY)+Cr and vermicompost+Cr applications in plant decreased Cr accumulation in shoots and roots and CAT, SOD, and POD activity [29].

TABLE 3
Effects of organic amendments applications on micro element content and cadmium uptake of spinach under cadmium contamination condition (mg kg^{-1}).

Applications	Cd	Fe	Zn	Cu	Mn
Control	0,43**g***	593,5 **d**	16,11 **g**	5,33 **ef**	57,66 **d**
Cd(100 mg kg^{-1})	151,4 **a**	879,3 **b**	21,48 **g**	7,24 **b**	76,49 **c**
Cd + %10 SM	47,57 **d**	621,9 **d**	18,28 **g**	6,10 **cd**	74,76 **c**
Cd + %20 SM	40,70 **d**	460,5 **e**	28,51 **f**	6,02 **cd**	77,85 **c**
Cd + %10 SS	29,98**f**	247,8 **f**	191,6 **b**	6,43 **c**	51,22 **d**
Cd + %20 SS	33,77 **ef**	217,9 **f**	259,4 **a**	7,96 **a**	53,96 **d**
Cd + %10 CM	46,10 **de**	435,8 **e**	21,83 **g**	5,94 **cd**	75,35 **c**
Cd + %20 CM	32,15 **f**	254,0 **f**	28,23 **f**	5,80 **de**	75,74 **c**
Cd + %10 Peat	80,05 **c**	569,0 **d**	28,63 **f**	5,20 **f**	104,1 **b**
Cd + %20 Peat	124,4 **b**	802,6 **bc**	35,76 **e**	6,07 **cd**	78,51 **c**
Cd + HA1	113,0 **b**	1096,6 **a**	78,87 **d**	6,20 **cd**	135,4**a**
Cd + HA2	120,3 **b**	759,4 **c**	121,8**c**	6,00 **cd**	127,8 **a**

Note*: Statistically significant mean differences are indicated with different letters in the same column ($p<0.05$).

TABLE 4
Effects of organic amendments applications on APX enzyme activity and MDA content of spinach under cadmium contamination condition.

Applications	APX mmol g^{-1} F.W.Min^{-1}	MDA nmol g -1 F.W.
Control	0,54**d***	3,71 **f**
Cd(100 mg kg^{-1})	1,75 **a**	9,89 **a**
Cd + %10 SM	0,97 **cd**	4,84 **cde**
Cd + %20 SM	0,76 **cd**	3,89 **f**
Cd + %10 SS	1,13**b**	5,36 **cd**
Cd + %20 SS	1,18 **b**	5,23 **cd**
Cd + %10 CM	1,03 **bc**	5,59 **c**
Cd + %20 CM	0,91 **bc**	4,53 **def**
Cd + %10 Peat	1,00 **bc**	8,33 **b**
Cd + %20 Peat	1,17 **b**	5,43 **cd**
Cd + HA1	0,71 **cd**	5,07 **cd**
Cd + HA2	0,87 **bcd**	4,01 **ef**

Note*: Statistically significant mean differences are indicated with different letters in the same column ($p<0.05$).

CONCLUSION

Organic material amendments were associated with decreased cadmium uptake into spinach plant. SS had more positive effects relative to organic fertilizers. A possible account for this finding may be that urban SS utilized in the study seems to higher levels of organic matters compared to other organic fertilizers.

REFERENCES

[1] Jhanji, S., Setia R.C., Kaur N., Kaur, P. and Setia, N. (2012) Role of nitric oxide in cadmium-induced stress on growth, photosynthetic components and yield of Brassica napus L. Journal Environ. Biol. 33, 1027-1032.

[2] Zhang, Y., Sun, G., Yang, M., Wu, H., Zhang, J., Song, S., Ma, E., Guo, Y. (2011) Chronic accumulation of cadmium and its effects on antioxidant enzymes and malondialdehyde in Oxya chinensis (Orthoptera: Acridoidea). Ecotoxicology and Environmental Safety. 74, 1355-1362.

[3] Gondar, D. and Bernal, M.P. (2009) Copper binding by olive mill solid waste and its organic matter fractions. Geoderma. 149, 272–279.

[4] He, Q.B. and Singh, B.R. (1993) Effect of organic matter on the distribution, extractability and uptake of cadmium in soils. J. Soil Science. 44(4), 641-650.

[5] Sato, A., Takeda, H., Oyanagi, W., Nishihara, E. and Murakami, M. (2010) Reduction of cadmium uptake in spinach (Spinacia oleracea L.) by soil amendment with animal waste compost. Journal of Hazardous Materials. 181, 298-304.

[6] Han, S.H., Kim, D.H., Ultra, V.U., Kim N.S. and Aggangan, N.S. (2012) Physiological response of Cd- and Pb-treated Populus alba x glandulosa seedling amended with SCB liquid fertilizer. Asia Life Sciences. 21(2), 481-498.

[7] Tejada, M. Gómez, I and Del Tora, M. (2011) Use of organic amendments as a bioremediation strategy to reduce the bioavailability of chlorpyrifos insecticide in soils. Effects on soil biology. Ecotoxicology and Environmental Safety. 74, 2075-2081.

[8] Kamari, A., Yusoff, S.N.M., Putra, W.P, Ishak, C.F., Hashim, N., Mohamed, A., Phillip, E., (2014) Metal uptake in water spinach grown on contaminated soil amended with chicken manure and coconut tree sawdust. Environmental Engineering and Management Journal. 9(13), 2219-2228.

[9] Shahid, M., Sabir, M., Ali, M.A. and Ghafoor, A. (2014) Effect of organic amendments on phytoavailability of nickel and growth of berseem (Trifolium alexandrinum) under nickel contaminated soil conditions. Chemical Speciation and Bioavailability. 26(1), 37-42.
[10] Şensoy, S., Turkmen, Ö. and Gorgun, Y. (2011) Determination of Suitable Sowing Dates for Spinach Production in Van Ecological Condition. YYÜ. Tarım Bilimleri. Dergisi. 21(2), 140-145.
[11] Alpaslan, M., Güneş, A. and İnal A. (1998) Deneme Tekniği Ankara Üniversitesi Ziraat Fakültesi Yayınları: 1501, Ders Kitabı:423, Ankara.
[12] Anonymous (2005) T.C. Resmi Gazete. Toprak Kirliliği Kontrolü Yönetmeliği Yayın No: 25755, Ankara.
[13] Jackson, M.L. (1958) Soil Chemical Analysis. Prentice Hall Inc. New Jersey, USA.
[14] Hızalan, E. and Ünal, E. (1966) Topraklarda Önemli Analizler. Ankara Üniversitesi Ziraat Fakültesi Yayınları: 273, Ders Kitabı: 466, Ankara.
[15] Walkley A (1947) A critical examination of a rapid method for determining organic carbon in soils: Effect of variation in digestion conditions and inorganic soil constituent. Soil Science.63, 251-263.
[16] Kacar B (1994) Bitki ve toprağın kimyasal analizleri: III Toprak Analizleri. A.Ü.Z. Eğitim Araştırma ve Geliştirme Vakfı Yayınları: 3, Ders Kitabı: 705, Ankara.
[17] Lindsay, W.L. and Norvell, W.A. (1978) Development of a DTPA soil test for zinc, iron, manganese and copper. Soil. Science. Society American Journal.42, 421-428.
[18] Kacar B, İnal A, (2008) Bitki Analizleri. Nobel Yayın Dağıtım. ISBN:978-605-395-036-3. Ankara, 892p.
[19] Düzgüneş, O., Kesici, T., Kavuncu, O. and Gürbüz, F. (1987) Araştırma ve Deneme Metodları (İstatistik Metodları-II). Ankara Üniversitesi Ziraat Fakültesi Yayınları: 1021, Ankara. 381p.
[20] Nakano, Y. and Asada, K. (1981) Hydrogen peroxide in spinach chloroplasts. Plant Cell Physiolog. 22, 860-867.
[21] Hodges, D.M., DeLong, J.M., Forney, C.F. and Prange, R.K. (1999) Improving the thiobarbituric acid-reactive-substances assay for estimating lipid peroxidation in plant tissues containing anthocyanin and other interfering compounds. Planta. 207, 604-611.
[22] Singh, R.P. and Agrawal, M. (2008) Potential benefits and risks of land application of sewage sludge. Waste Management. 28, 347-35.
[23] Han, S.H, Lee, J.C, Oh, C.Y. and Kim, P.G. (2006) Alleviation of Cd toxicity by composted sewage sludge in Cd-treated Schmidt birch (Betula schmidtii) seedling. Chemosphere. 65, 541-546.
[24] Kwiatkowska-Maline, J. (2017) Functions of organic matter in polluted soils: The effect of organic amendments on phytoavailability of heavy metals. Applied Soil Ecology (In Press).
[25] Salaskar, D., Shrivastava, M. and Kale, S.P. (2011) Bioremediation potential of spinach (Spinacia oleracea L.) for decontamination of cadmium in soil. Current Science. 101(10), 1359-1363.
[26] Canal-Boysan, S. and Bozkurt, M.A. (2017) Effects of iron application against cadmium toxicity on growth and anti-oxidative enzyme activity in lettuce. Fresen. Environ. Bull. 26, 2615-2621.
[27] Tamer, N., Başalma, D., Türkmen, C. and Namlı, A. (2016) Organik toprak düzenleyicilerin toprak parametreleri ve ayçiçeği (Helianthus annuus L.) bitkisinin verim ve verim öğeleri üzerine etkileri. Toprak Bilimi ve Bitki Besleme Dergisi. 4(1), 11-21.
[28] Sergiev, I., Todorova, D., Moskova, I., Georgieva, N., Nikolova, A., Simova, S., Polizoev, D. and Alexieva, V. (2013) Protective effect of humic acids against heavy metal stress in triticale. Compt. rend. Acad. bulg. Sci. 66(1), 53-60.
[29] Dheeba, B., Sampathkumar, P. and Kannan, K. (2014) Chromium accumulation potential of Zea mays grown under four different fertilizers. Indian Journal of Experimental Biology. 52, 1206-1210.

Received: **13.01.2018**
Accepted: **18.02.2018**

CORRESPONDING AUTHOR

Sibel Boysan-Canal
Department of Soil Science and Plant Breeding,
Faculty of Agriculture,
Yuzuncu Yil University,
Van – Turkey

e-mail: sibelboysan@hotmail.com

© by PSP Volume 27 – No. 5/2018 pages 3180-3184 Fresenius Environmental Bulletin

PLASMA IRISIN AND HEAT SHOCK PROTEIN 70 LEVELS IN PRIMARY RAYNAUD'S PHENOMENON AND SYSTEMIC SCLEROSIS

Nevzat Gozel[1,*], Ahmet Karatas[2], Meltem Yardim[3], Mesude Seda Kinaci[1], Ramazan Ulu[4], Fatih Demircan[5], Faruk Kilinc[6] , Fethi Ahmet Ozdemir[7], Suleyman Aydin[3], Suleyman Serdar Koca[2]

[1]Department of Internal Medicine, School of Medicine, Firat University, Elazig, Turkey.
[2]Department of Rheumatology, School of Medicine, Firat University, Elazig, Turkey.
[3]Department of Biochemistry, School of Medicine, Firat University, Elazig, Turkey.
[4]Department of Nephrology, School of Medicine, Firat University, Elazig, Turkey.
[5]Department of Internal Medicine, Private Etik Life Hospital, Istanbul, Turkey
[6]Department of Endocrinology, School of Medicine, Firat University, Elazig, Turkey.
[7]Department of Molecular Biology and Genetics, Faculty of Science and Art, Bingol University, Bingol, Turkey.

ABSTRACT

The pathogenesis of Raynaud's phenomenon (RP) is not fully elucidated, yet. The aim of the present study was to evaluate plasma irisin and heat shock protein (HSP) 70 levels in both primary RP and secondary RP associated with systemic sclerosis (SSc). 15 patients with primary RP, 30 patients with RP secondary to SSc, and 30 healthy controls (HC) were included in the study. Raynaud Condition Score (RCS) were performed in the primary RP and SSc groups. Modified Rodnan skin severity score (MRSS) was determined for the SSc patients. Plasma irisin and HSP 70 levels were analyzed by ELISA method. When compared to the HC group, plasma irisin and HSP 70 levels were lower in the secondary RP group, but not in the primary RP group. Plasma irisin and HSP 70 levels were not directly related with RCS in the both primary and secondary RP groups. Moreover, they were not correlated with MRSS in the secondary RP group. The results of present study can suggest that irisin and HSP 70 levels are not associated with primary RP. Its level was lower in the secondary RP (SSc) patients. Therefore, it can be concluded that decreased irisin and HSP 70 levels are related with SSc instead of RP.

KEYWORDS:
Raynaud's phenomenon, systemic sclerosis, irisin, heat shock protein 70

INTRODUCTION

Raynaud's phenomenon (RP) is a vasospastic disorder characterized by episodic attacks of triphasic discolorations, and pain on fingers [1]. At its onset, skin paleness is dependent on digital arterial vasospasm. Deoxygenation of static venous blood induces cyanosis; then reactive hyperemia develops secondary to ischemia [2, 3]. It can occur primarily or can be secondary to an underlying cause [4]. Secondary RP can be seen in association with systemic lupus erythematosus, systemic sclerosis (SSc), mixed connective tissue disease, Sjögren syndrome and polymyositis/dermatomyositis, and also various etiologic factors as medications, traumatic damage, hyperviscosity syndromes, and endocrine disorders.

Systemic sclerosis is a chronic inflammatory disease with unknown etiology characterized by autoimmunity, vasculopathy, and fibrosis which may also involve skin, and organs [5]. In most of the patients RP is seen in association with skin stiffness. The pathogenesis of the disease is not known completely, while genetic predisposition, and immune activation triggered by external stimuli, and vasculopathy play an important role in its pathogenesis [6, 7]. In the most of SSc patients, RP is seen as a first finding. Years after onset of RP, skin stiffness and visceral involvements can develop [8].

Irisin is a protein hormone produced by skeletal muscles. Peroxisome proliferator-activated receptor (PPAR) γ coactivator 1α (PGC-1α) is a molecule which assumes a task in the regulation of genes that play an important role in the glucose, lipid, and energy metabolism. The stimulated PGC-1α increases the production of protein called fibronectin type III domain containing 5 (FNDC5). FNDC5 degrades, and induces the formation of irisin. Irisin levels have been demonstrated to decrease in low-grade inflammatory diseases as chronic renal failure, type 2 diabetes mellitus, and obesity [9].

Heat shock proteins (HSPs) belong to a group of proteins which increase with exposure to pathologic conditions as environmental stress, heat, toxic substance, oxidative stress, ischemia, infection, and inflammation [10]. According to their molecular weights numerous HSPs have been defined. HSP 70 is the most frequently studied molecule in this

group, and it aids in folding of newly synthetized polypeptides. Besides, it separates erroneously folded and precipitated proteins, and ensure their proper folding. HSP 70 inactivates apoptosis. As a matter of fact, it plays important roles in oncogenesis, neurodegenerative and autoimmune diseases via conduction of signals, cellular differentiation, and regulation of cell cycle [11, 12]. Besides, increased HSP 70 levels were found in patients with SSc [13].

The aim of the study was to investigate the levels of irisin, and HSP 70 in patients with primary RP and RP secondary to SSc.

MATERIALS AND METHODS

Participants. A total of 15 primary RP, 30 patients with RP secondary to SSc, and 30 healthy volunteers were included in the study. The participants those were admitted to the outpatient clinics of Departments of Internal Medicine, and Rheumatology in University Hospital were enrolled. Healthy control (HC) group consisted of the participants who consulted to the outpatient clinics of Internal Medicine without any detected inflammatory, and vascular disease. Patients younger than 18, and older than 65 years of age, those with known heart disease, hypertension, difficulties in socio-cultural cooperation, pregnant women, and those unwilling to participate in the study were not included in the study.

Samples. Five milliliters of blood samples were retrieved from left antecubital veins of the participants in the sitting erect position. Blood samples were placed in tubes containing aprotinin. Tubes were slightly agitated, and transferred without delay to the laboratory of biochemistry in ice batteries. Therein, blood samples were centrifuged at 3500 rpm under 4 ^{o}C ambient temperature for 10 minutes to obtain plasma. Then samples were transferred into aprotinin containing tubes, and stored at -20 ^{o}C till the day of analysis. Plasma irisin (Hangzhou Eastbiopharm Co., LTD, China,: CV(%) = SD/mean ×100; Intra-Assay: CV< 10%; Inter-Assay: CV< 12%; Sensitivity: 0.023 µg/ml) and HSP 70 (Shanghai Yehua Biological Technology Co., Shanghai, China: CV(%) = SD/mean ×100; Intra-Assay: CV< 10%; Inter-Assay: CV< 12%; Sensitivity: 1.02 ng/mL) concentrations were measured with ELISA method using appropriate commercial kits.

Clinical scoring. In patients with primary and secondary RP, daily frequency, duration, and severity of attacks were determined using Raynaud's Condition Scores (RCS). Besides, the severity of cutaneous involvement in SSc patients in the secondary RP group was also determined using Modified Rodnan Skin Scoring (MRS) system.

Statistical analysis. For statistical analysis of data SPSS program was used. Data obtained in the study were expressed as mean ± standard deviation. In statistical analyses *Kruskall-Wallis*, and *post-hoc Mann-Whitney U* were used. Categorical data were analyzed using *chi-square* test. Pearson correlation analysis was used to determine the correlations. P< 0.05 was considered as the level of significance.

RESULTS

Demographic and clinical variable of the data were presented in the Table 1. The mean age was higher in the secondary RP group when compared with the HC group ($p<0.05$). There was no difference in terms of mean age between primary and secondary RP groups ($p>0.05$).

Plasma irisin and HSP 70 levels were similar in the primary RP and HC groups ($p>0.05$). However, their levels were lower in the secondary RP group compared to the primary RP and HC group ($p<0.05$ for both) (Table 1).

TABLE 1
The demographics and laboratory data in the study groups

	HC (n=30)	Primary RP (n=15)	Secondary RP (n=30)
Mean age (years)	27.6±10	30.2±7.9	49.4±13[a]
SBP (mmHg)	105±20.3	111.1±12.6	119±17.6[a]
DBP (mmHg)	67± 7.2	76.0±9.2	76±10.2[b]
Creatinine (mg/dL)	0.6± 0.2	0.6± 0.1	0.6±0.1
ESR (mm/h)	9.9±8.2	7.1±7.5	18.3±11.1[a,e]
CRP (mg/L)	3.9±1.9	4.1±1.8	4.5±3.0[c]
Glucose (mg/dL)	86±6.8	85.5± 8.6	105±19.9[b,d]
Total cholesterol (mg/dL)	168.9±32.5	158.9±30.8	200.6±44.1[b,c]
LDL cholesterol (mg/dL)	93.5±20.1	93.5±24.5	124.1±41.0[b,c]
HDL cholesterol (mg/dL)	54.3±17.0	54.3±16.5	52.4±16.6
Triglyceride (mg/dL)	115.7±9.9	101.4± 54.5	146.2±108.7
Irisin (µg/mL)	4.79±6.6	4.21±3.2	2.65±4.1[a,c]
HSP 70 (ng/mL)	262.6±215.6	235.5±174.2	132.1±80.5[a,c]

Data were expressed as mean±SD.
SBP, systolic blood pressure; DBP, diastolic blood pressure; ESR, erythrocyte sedimentation rate; CRP, C-reactive protein; LDL, low density lipoprotein; HDL, high density lipoprotein; HSP, heat-shock protein.
When compared to the HC group: [a]p<0.05, [b]p<0.01
When compared to the primary RP group: [c]p<0.05, [d]p<0.01, [e]p<0.001.

In the HC group, irisin and HSP 70 levels were negatively correlated with diastolic blood pressure (r=-0.429; p=0.018, and r=-0.409, p=0.025, respectively). However, in the primary RP and the secondary RP groups, they were not significantly correlated with blood pressures. A positive correlation existed between HSP 70 and irisin levels in the primary RP, and the HC groups (r=0.645; p=0.009 and r=0.676; p=0.0001, respectively).

In all three groups, total cholesterol, LDL, HDL and triglyceride levels were within normal limits. Levels of total cholesterol, and LDL were higher in the secondary RP group than in the HC group ($p<0.05$ for both). However, there was no significantly difference in terms of HDL, and triglyceride levels between the secondary RP and HC group ($p>0.05$). In the primary RP group, irisin level was negatively correlated with total cholesterol and HDL levels (r=-0.693, p=0.018, and r=-0.616, p=0.044, respectively). Moreover, there was a negatively correlation between HSP 70 and total cholesterol levels in the primary RP group (r=-0.754, p=0.007).

Raynaud's Condition Scores were detected as 4.70±2.38 in the primary RP, and 6.33±1.54 in the secondary RP group. As for RCS, a statistically significant difference was detected between two groups ($p<0.05$). On the other hand, in both groups plasma irisin and HSP 70 levels were not correlated with RCS ($p>0.05$). In the secondary RP group mean MRDS was determined as 13.07±9.16. Irisin and HSP 70 levels were not correlated with MRS ($p>0.05$).

DISCUSSION

In our study, plasma irisin and HSP 70 levels were similar in the primary RP group and healthy volunteers. On the other hand, their levels were lower in the SSc group compared to the healthy subjects and the primary RP group. Irisin and HSP 70 levels were not related with primary RP. However, their levels were lower in the secondary RP group. These results suggest that the lower levels of irisin and HSP 70 can be associated with SSc, instead of RP.

Raynaud's phenomenon is a disorder characterized by the onset of paroxysmal vasospasm manifesting on terminal ends of extremities [14]. It generally appears as the first symptom in patient with SSc. SSc is the most frequent cause of secondary RP [15]. RP is actually a vascular dysfunction. The cause of vascular dysfunction is still unknown in the RP, but abnormalities in the endothelium may contribute to the development of RP. The irisin secreted by the endothelium may be related to RP. According to the best of our knowledge, the present study evaluating irisin levels in RP and SSc is the first.

Irisin is a recently identified myokine. Those are peptides released by the skeletal muscle. It has been shown that irisin hormone induces the relaxation of mesentery arteries [16]. The effects of irisin hormone on the proliferation of vascular endothelial cells and on apoptosis have also been demonstrated. Besides, irisin increases the expression of matrix metalloproteinase (MMP) in endothelial cells. Irisin plays an important role in the maintenance of endothelial homeostasis by stimulating angiogenesis of endothelial cells [17]. At a certain concentration irisin accelerates cell metabolism. It inhibits cellular proliferation, and stimulates cellular differentiation [18]. In an experimental study, it has been determined that intravenous irisin induced vascular dilation related to ATP-sensitive potassium channel with resultant decrease in blood pressure [19]. However, in our study, the level of irisin was not altered in the primary RP group.

Irisin plays a role in energy metabolism. The decrease in PPARs those are involved in the formation of the irisin has been shown to enhance fibrosis in an animal model of SSc. It has also been demonstrated that PPAR agonists exert anti-fibrotic effects by inhibiting differentiation of myofibroblasts [20]. In a study, serum irisin level has been reported to decrease in diabetic patients who developed macrovascular complications [21]. Besides, protective effects of irisin on atherosclerotic vascular diseases have been shown in an experimental study [22]. However, in a study performed on patients with Behçet's disease, a negative correlation between serum irisin levels and endothelial wall thickness has been detected [23].

As in irisin, HSP 70 level was not directly related with RP; however, HSP 70 level was lower in the SSc (secondary RP) group, in our study. Its level was not related with RCS in both primary and secondary RP groups. These results suggest that it level decreases due to SSc, but not RP. Conversely, in SSc, higher HSP 70 level and its positive correlation with MRSS have been shown, previously [13]. HSP 70 gene expression has been reported to be 8 times higher in fibroblasts of SSc patients relative to normal fibroblasts [24]. On the other hand, HSPs mediate immunoregulation. HSP 70 has protective effects against diverse stress conditions and anti-inflammatory activity. The protective effects of HSP 70 against inflammatory response and pulmonary fibrosis have been demonstrated [25]. The decrease of HSP 70 level in SSc can be more conceivable. Its decreased level can support the widespread fibrosis in SSc.

However, HSP 70 level was not correlated with MRSS, in our study. This result might be related to the immunosuppressive treatment received by the patients [26]. The patients in the secondary RP group received immunosuppressive treatment such as prednisolone and azathioprine, already.

Our study has some limitations. Firstly, the number of study participants was small. Before the study, power analysis was not performed to determine the number of participants. On the other hand, our study had a cross-sectional design. Prospective follow-up, and serial analyses of the patient could provide more valuable outcomes.

CONCLUSIONS

In conclusion irisin and HSP 70 levels decrease in the secondary RP group, although their levels do not alter in the primary RP. Moreover, RCS is not related with plasma irisin and HSP 70 levels. These results suggest that irisin and HSP 70 are not directly related with RP. Their decreased level in the secondary RP can be caused by SSc. Therefore, new predictive and prognostic studies are required to perform about irisin and HSP 70 in RP and SSc.

REFERENCES

[1] Belch, J.J. (1990) The phenomenon, syndrome and disease of Maurice Raynaud. British journal of rheumatology. Brit J Rheumatol. 29, 162-5.

[2] O'Connor, C.M. (2001) Raynaud's phenomenon. J Vasc Nurs. 19, 87-92.

[3] Bakst, R., Merola, J.F., Franks, A.G. and Sanchez, M. (2008), Raynaud's phenomenon: pathogenesis and management. J. Am. Acad. Dermatol. 59, 633-53.

[4] Wigley, F.M. (1993) Raynaud's phenomenon. Curr Opin Rheumatol. 5, 773-84.

[5] Varga, J. and Abraham, D. (2007) Systemic sclerosis: a prototypic multisystem fibrotic disorder. J Clin Invest. 117, 557-67.

[6] Denton, C.P. and Black, C.M. (2004) Scleroderma--clinical and pathological advances. Best Pract Res Clin Rheumatol. 18, 271-90.

[7] Rosenbloom, J., Castro, S.V. and Jimenez, S.A. (2010) Cellular and molecular mechanisms and novel therapies. Ann Intern Med. 152, 159-66.

[8] Van den Hoogen, F., Khanna, D., Fransen, J. (2013) Classification criteria for systemic sclerosis: an American College of Rheumatology/European League against Rheumatism collaborative initiative. Arthritis Rheum. 65, 2737-47.

[9] Liu, J.J., Wong, M.D., Toy, W.C. (2013) Lower circulating irisin is associated with type 2 diabetes mellitus. J Diabetes Complications. 27, 365-9.

[10] Lindquist, S. and Craig, E.A. (1988) The heat-shock proteins. Annu Rev Genomics. 22, 631-77.

[11] Pockley, A.G. (2003) Heat shock proteins as regulators of the immune response. Lancet. 362, 469-76.

[12] Otaka, M., Odashima, M. and Watanabe, S. (2006) Role of heat shock proteins (molecular chaperones) in intestinal mucosal protection. Biochem Biophys Res Commun. 348, 1-5.

[13] Ogawa, F., Shimizu, K., Hara, T. (2008) Serum levels of heat shock protein 70, a biomarker of cellular stress, are elevated in patients with systemic sclerosis: association with fibrosis and vascular damage. Clin Exp Rheumatol. 26, 659-62.

[14] Kuryliszyn-Moskal, A., Kita, J. and Hryniewicz, A. (2015) Raynaud's phenomenon: new aspects of pathogenesis and the role of nailfold videocapillaroscopy. Reumatologia. 53, 87-93.

[15] Barsotti, S., Stagnaro, C., d'Ascanio, A. and Della Rossa, A. (2016) One year in review 2016: Systemic sclerosis. Clin Exp Rheumatol. 34 Suppl. 100(5), 3-13.

[16] Jiang, M., Wan, F., Wang, F. and Wu, Q. (2015) Irisin relaxes mouse mesenteric arteries through endothelium-dependent and endothelium-independent mechanisms. Biochem Biophys Res Commun. 468, 832-6.

[17] Wu, F., Song, H., Zhang, Y. (2015) Irisin Induces Angiogenesis in Human Umbilical Vein Endothelial Cells In Vitro and in Zebrafish Embryos In Vivo via Activation of the ERK Signaling Pathway. PLoS One. 10, 1-17.

[18] Xie, C., Zhang, Y., Tran, T.D. (2015) Irisin controls growth, intracellular Ca^{2+} signals, and mitochondrial thermogenesis in cardiomyoblasts. PLoS One. 10, 13-21.

[19] Zhang, W., Chang, L., Zhang, C. (2015) Central and peripheral irisin differentially regulate blood pressure. Cardiovascular drugs and therapy / sponsored by the International Society of Cardiovasc Ther. 29, 121-128.

[20] Sertznig, P. and Reichrath, J. (2011) Peroxisome proliferator-activated receptors (PPARs) in dermatology: Challenge and promise. Dermatoendocrinol. 3, 130-5.

[21] Zhang, M., Chen, P., Chen, S. (2014) The association of new inflammatory markers with type 2 diabetes mellitus and macrovascular complications: a preliminary study. Eur Rev Med Pharmacol Sci. 18, 1567-72.

[22] Lu, J., Xiang, G., Liu, M. (2015) Irisin protects against endothelial injury and ameliorates atherosclerosis in apolipoprotein E-Null diabetic mice. Atherosclerosis. 243, 438-48.

[23] Icli, A., Cure, E., Cumhur Cure, M. (2016) Novel myokine: irisin may be an independent predictor for subclinic atherosclerosis in Behcet's disease. J Investig Med. 64, 875-81.

[24] Deguchi, Y., Shibata, N. and Kishimoto, S. (1990) Elevated transcription of heat shock protein gene in scleroderma fibroblasts. J Clin Exp Immunol. 81, 97-100.
[25] Tanaka, K., Tanaka, Y., Namba, T. (2010) Heat shock protein 70 protects against bleomycin-induced pulmonary fibrosis in mice. Biochem Pharmacol. 80, 920-31.
[26] Udelsman, R., Blake, M.J., Stagg, C.A. and Holbrook, N.J. (1994) Endocrine control of stress-induced heat shock protein 70 expression in vivo. Surgery. 115, 611-6.

Received: **15.01.2018**
Accepted: **03.03.2018**

CORRESPONDING AUTHOR

Nevzat Gozel
Firat University, Faculty of Medicine,
Department of Internal Medicine,
23119 Elazig – Turkey

e-mail: drngozel@hotmail.com

© by PSP Volume 27 – No. 5/2018 pages 3185-3190 Fresenius Environmental Bulletin

EFFICACY OF HOT WATER AND CHEMICAL SEED TREATMENTS ON BACTERIAL SPECK OF TOMATO IN TURKEY

Sumer Horuz[1,*], Aysegul Ocal[2], Yesim Aysan[2]

[1]Erciyes University, Faculty of Agriculture, Department of Plant Protection, 38039, Kayseri, Turkey
[2]Cukurova University, Faculty of Agriculture, Department of Plant Protection, 01330, Adana, Turkey

ABSTRACT

Bacterial speck, caused by *Pseudomonas syringae* pv. *tomato* (Pst), is an economically important disease of tomato, that causes yield loss of marketable fruit. Management of bacterial speck is a challenge in commercial nurseries, fields or greenhouses. This is due to the limited efficacy of current disease management strategies, since the pathogen acquires resistance to antibiotics and copper-based compounds in Turkey. The pathogen is seed- borne and no disease resistant tomato cultivars are commercially available. Therefore, it is essential to develop alternative disease control strategies. In this study, physical and chemical seed treatments that provide disease suppression were assayed individually or combined under climatic conditions and the colonization ability of *Pseudomonas syringae* pv. *tomato* on/in inoculated seeds was compared with untreated seeds. All seed treatments significantly reduced the *Pseudomonas syringae* pv. *tomato* population on seeds and significantly decreased disease incidence and disease severity. Mean bacterial populations on the plate dilutions was diminished up to 100% in hot water treated tomato seeds. The efficacies of treatments on disease incidence and severity provide evidence of significance and greater than 57%. Treatments did not significantly affect seed germination and seed germination ranged from 76% to 91%. Based on our results, we recommend that hot water seed treatment be used to combat bacterial speck as a first step of disease management in nurseries.

KEYWORDS:
Control, copper, physical, *Pseudomonas syringae* pv. *tomato*

INTRODUCTION

The cultivated tomato (*Solanum lycopersicum* L., formerly *Lycopersicon esculentum* Miller) is an important food crop that has achieved popularity with almost 165 million tonnes production worldwide [1]. Plant disease become the limiting factor in tomato production in many parts of the world when resistant cultivars are not planted. There are nearly 200 known tomato diseases causing significant economic losses in nurseries, greenhouses and fields [2]. Bacterial speck, caused by *Pseudomonas syringae* pv. *tomato*, is one of the most economically important bacterial diseases in many tomato-growing regions of the world [3, 4]. Lesions occur on leaflets and may spread to stems and flowers. Yield reductions can result from defoliation, flower abortion and fruit damage [5]. Reduction of crop yield and fruit quality is especially seen when the tomato plants are grown under plastic covers or in greenhouses under cool and humid conditions [6]. The plant foliage should keep dry in greenhouses to avoid from favor enviromental conditions for pathogen development.

The first step of bacterial speck management is the use of pathogen-free seeds. However, disease management in the field mainly depends on the use of copper-based bactericides [7]. both in non-organic and organic agriculture production systems, unfortunately, chemical applications do not always effectively reduce bacterial speck severity [8]. For decades, heavy use of copper compounds have lead to copper resistance development of bacterial populations. Loss of copper sensitivity of *P. syringae* pv. *tomato* populations was reported [9, 10, 11]. Bacterial speck management in the presence of copper-resistant *P. syringae* pv. *tomato* populations is extremely difficult. Thus, a range of disease management strategies must be integrated [12, 13]. Acibenzolar-S-methyl, a plant defense activator, has been recommended for field management of bacterial speck as an alternative to copper-based bactericides, particularly where copper-resistant populations predominate [14, 15]. Biocontrol agents including *Azospirillum brasilense, Bacillus pumilus, B. amyloliquefaciens, Pseudomonas fluorescens* and bacteriophages offer eco-friendly approaches for the management of bacterial speck [6, 16, 17, 18, 19, 20].

The pathogen, *Pseudomonas syringae* pv. *tomato* survives from season to season in/on tomato seeds and during seed germination the bacterial population increases [11]. Hence, seed treatments have gained importance for reducing bacterial speck outbreaks in tomato. Seed treatments are employed to eradicate or reduce pathogen inoculum on/in seeds.

For decades, chemical and physical seed treatments have been developed to control *Pseudomonas syringae* pv. *tomato* on/in tomatoes [16, 21]. In this study, we aimed to (1) evaluate the colonization ability of *Pseudomonas syringae* pv. *tomato* on/in inoculated seeds treated with twelve chemical and physical seed treatments, and (2) determine the efficacy of these treatments (individually or in combination) on bacterial speck development and seed germination.

MATERIALS AND METHODS

Pathogen, growth conditions and inoculum preparation. *Pseudomonas syringae* pv. *tomato* strain CG-1-1r from the culture collection of Professor Dr. Yesim Aysan (Cukurova University, Faculty of Agriculture, Department of Plant Protection, 01330, Adana, Turkey) used in this study for seed inoculations [22]. *Pseudomonas syringae* pv. *tomato* strain CG-1-1r was grown on King's Medium B and incubated at 25 °C for 48 h. To prepare *Pseudomonas syringae* pv. *tomato* inoculum, a suspension was generated in saline buffer (NaCI 0.85%) and the concentration was adjusted to A_{600}:0.2 OD with a spectrophotometer (Shimadzu UV-120-01, North America). The bacterial suspension was ten-fold serially diluted with saline buffer and 100 µl aliquots were spread plated onto KB. The concentration of the bacterial inoculum was estimated to be $1.5x10^8$ CFU ml^{-1} and this concentration was used in further studies.

Inoculation of tomato seeds. Tomato seeds of the susceptible cultivar H-2274 were immersed into 250 mL of a *Pseudomonas syringae* pv. *tomato* strain CG-1-1r suspension for 30 min and filtered through double-layered cheesecloth. Seeds were air dried at room temperature (25±2°C) for 24 h in a laminar flow and divided into three lots (100 seeds/lot) before seed treatments.

Physical and chemical seed treatments. The physical and chemical treatments applied to seeds and the exposure times were as follows (per 0.1 liter sterilized water): 50 ºC hot water for 30 min; streptomycin sulphate, 0.02 g for 5 min; cupric acetate, 0.1% and 0.2% for 1 or 3 min; sodium hypochlorite, 2% and 3% for 1, 3 or 5 min. Combinations of chemical treatments were also included according to average results of first experiment. The solutions were freshly prepared before immersion of tomato seeds. Each sample (n=300 seeds) was rinsed as previously described and treated seeds transferred to dry in a laminar flow hood for 24 h at room temperature.

Effect of treatments on the survival of *Pst* on tomato seeds. The colonization ability of *Pst* was compared on treated and untreated seeds. Initially, *Pseudomonas syringae* pv. *tomato* strain CG-1-1r was gradually maintained resistant to rifampicin (100 mg/l). Fourteen g of tomato seeds (cultivar H-2274) were inoculated with pathogen suspension as previously described. Two days after inoculation, each sample (n=1 g) of pathogen-inoculated seeds was treated as described above. All treated tomato seeds were shaken on a shaker at 150 rpm for 30 min and air-dried in a laminar flow cabinet for 24 h. Each seed sample was put into glass tubes containing 9 ml sterilized nutrient broth and shaken at 250 rpm for 3 h. Each treatment was ten-fold serially diluted with nutrient broth including 1/10, 1/100, 1/1000 and 1/10 000 serial dilutions. Aliquots of 100 µl were spread onto KB medium supplemented with rifampicin, 100 mg/l, and incubated at 25°C for 72 h. Bacterial colonies were counted and the results were compared with positive control. Mean bacterial populations were calculated using the plate-count technique (number of colonies*dilution of sample*10).

Efficacy of seed treatments at chamber room conditions. Artificially inoculated and treated tomato seeds (n=150 seeds per treatment) were sown in small plastic pots 20x12x3 cm (lengthxwidhtxheight) containing sterilized soil and incubated under climatic room with the following conditions: 22-25°C, 75% humidity and 16 h of light alternating with 8 h of darkness. Fifteen days after planting, each cotyledon was examined for speck symptoms. Bacterial speck seedling transmission (number of seedlings displaying typical bacterial speck symptoms divided by the number of seedlings that germinated*100) was recorded. Disease severity was evaluated visually and scored using a modified range of 0 to 3 (0 shows a healthy-looking plant; 1 signifies 1 speck on cotyledon; 2 signifies 2-3 specks; and 3 signifies more than 4 specks), as previously described [23]. Efficacy of seed treatments on seed germination percentage (number of germinated seedlings divided by the number of seeds that sown*100) were also determined.

Experimental design and statistical analysis. The seeds subjected to various seed treatments were randomly placed in a growth chamber. Each treatment was replicated three times and each plastic pot containing fifty seeds was used per replicate. Data from each pot was combined and the entire experiment was analyzed by analysis of variance (ANOVA) at $P \leq 0.05$. The efficacy of treatments was evaluated using the Abbott formula (the number of cotyledons with speck symptoms in control - the number of cotyledons with speck symptoms in seed treatments/ the number of cotyledons with speck symptoms in control*100). All experiments were repeated twice in controlled conditions. Initially, first and second treatments were statistically analyzed separately, but, both treatments yielded similar results. Hence, data from all experiments were com-

bined and the average of two experiments was statistically evaluated. The same evaluations were done in the experiment of combined chemical seed treatments.

RESULTS

Effect of treatments on the survival of *Pst* on tomato seeds. Three days after inoculations, the forming colonies on plates were recorded. 100 bacterial colonies were counted on four ten-fold diluted positive control plates. Treatments conducted with sodium hypochlorite (2-3%), copper acetate (0.1-0.2%), hot water (50 °C) and streptomycine sulphate (0.2 g$^-$) reduced bacterial colonization on seed compared to control plates (Table 1). No bacterial growth was observed on the plate dilutions of hot water treated tomato seeds.

Efficacy of seed treatments under growth chamber conditions. All single physical and chemical seed treatments significantly reduced lesion development on tomato seedlings (Table 2). 50°C water was the only treatment that suppressed bacterial speck in first two experiments. Foliar disease incidence in treated seeds ranged from 0.00% to 26.45% and severity ranged from 0.00% to 11.05%, respectively. The efficacies of treatments on disease incidence and severity were greater than 57%. All treated seeds displayed 76% to 91% germination and treatments did not significantly reduce seed germination (Table 2). These results correlated with earlier study on bacterial colonization on seeds. According to both studies, hot water seed treatment was the most suppressive treatment reaching to 100% both in bacterial colonization (one g of tomato seeds) and seed treatment (150 seeds per treatment).

According to first experiments conducted with individual physical and chemical seed treatments, combinations of copper acetate (0.2%) and sodium hypochloride (2%) were studied as a second trial to enhance efficacy on pathogen inoculum. Combinations of copper acetate and sodium hypochlorite reduced lesion appearance on seedlings (Table 3). The combined treatments were also significant statistically differed from control seedlings (Table 3). Efficacies on disease incidence and severity were higher than 90%. Most sown seeds germinated and germination percentages ranged from 80% to 97%.

TABLE 1
Colonization of bacterial speck on each one g of tomato seeds

Seed Treatments	Mean bacterial populations (CFU/g)
Control	$1,0*10^7$
Streptomycin sulphate	$1,9*10^6$
Cupric acetate, 0.1% 1 min	$1,6*10^6$
Cupric acetate, 0.1% 3 min	$2,9*10^6$
Cupric acetate, 0.2% 1 min	$2,3*10^6$
Cupric acetate, 0.2% 3 min	$4,3*10^4$
Sodium hypochloride 2% 1 min	$3,4*10^6$
Sodium hypochloride 2% 3 min	$3,2*10^6$
Sodium hypochloride 2% 5 min	$2,3*10^6$
Sodium hypochloride 3% 1 min	$3,0*10^3$
Sodium hypochloride 3% 3 min	$1,5*10^3$
Sodium hypochloride 3% 5 min	$4,0*10^1$
Hot water, 50°C, 30 min	0,00

TABLE 2
Efficacy of seed treatments evaluated by disease incidence (DI) and disease severity (DS) (Means of two experiments with three replicates of each a hundred seedlings)

Seed Treatments	Disease incidence (%)	Efficacy%	Disease severity (%)	Efficacy%	Germination %
Control	$66,30^{a*}$		$28,13^a$		$83,00^a$
Cupric acetate, 0.1% 1 min	$26,45^b$	59,50	$11,05^b$	57,45	$88,85^a$
Cupric acetate, 0.1% 3 min	$15,30^c$	76,45	$7,90^b$	71,25	$81,60^a$
Sodium hypochloride, 2% 1 min	$7,15^d$	89,85	$3,00^c$	89,65	$82,45^a$
Sodium hypochloride, 3% 3 min	$6,75^d$	89,90	$2,45^c$	91,25	$82,40^a$
Streptomycin sulphate, 0,02 g$^-$	$6,15^d$	91,10	$2,55^c$	90,80	$81,20^a$
Sodium hypochloride, 3% 1 min	$4,05^d$	93,80	$1,45^c$	94,20	$90,10^a$
Sodium hypochloride, 3% 5 min	$3,10^d$	95,10	$1,50^c$	94,05	$76,35^a$
Cupric acetate, 0.2% 3 min	$2,58^d$	96,20	$0,85^c$	97,35	$79,40^a$
Cupric acetate, 0.2% 1 min	$1,66^d$	97,40	$0,55^c$	97,85	$85,60^a$
Sodium hypochloride, 2% 3 min	$1,42^d$	97,90	$0,45^c$	98,30	$91,40^a$
Sodium hypochloride, 2% 5 min	$1,00^d$	98,70	$0,35^c$	98,90	$88,70^a$
Hot water, 50°C, 30 min	$0,00^d$	100,00	$0,00^c$	100,00	$80,90^a$

* Means followed by the same letters within each column are not significantly different (P≤0.05) according to Duncan's Multiple Range Test

TABLE 3
Efficacy of combined seed treatments evaluated by disease incidence (DI) and disease severity (DS) (Means of two experiments with three replicates of each a hundred seedlings)

Seed Treatments	Disease incidence (%)	Efficacy %	Disease severity (%)	Efficacy %	Germination %
Control	72,35[a*]		43,62[a*]		91,33[a]
Cupric acetate, 0.2% 1 min+ Sodium hypochloride, 2% 3 min	5,21[b]	92,80	1,94[b]	95,54	93,33[a]
Cupric acetate, 0.2% 3 min+ Sodium hypochloride, 2% 3 min	1,10[c]	98,48	0,56[bc]	98,72	97,33[a]
Cupric acetate, 0.2% 1 min+ Sodium hypochloride, 2% 5 min	0,00[c]	100,00	0,00[c]	100,00	94,67[a]
Cupric acetate, 0.2% 3 min+ Sodium hypochloride, 2% 5 min	0,00[c]	100,00	0,00[c]	100,00	80,00[a]

* Means followed by the same letters within each column are not significantly different (P≤0.05) according to Duncan's Multiple Range Test

DISCUSSION

Seed borne diseases can seriously affect crop yield and quality. Thus, the most crucial control strategy is exclusion or reducing the pathogen inoculum during production. Unfortunately, seed infection can not be easy to avoid and thus, various seed treatments are used to reduce/eliminate seedborne inoculum. *Pst* can be destructive in commercial greenhouses during wet conditions in Turkey. Hence, it is important to eliminate the pathogen from seeds before seedling growth. The goal of this study was to find the best seed treatment/s for disease control in nurseries. Results of the seed treatments showed that physical and chemical treatments effectively reduced bacteria associated with seeds.

Today, tomato crops are threatened by many seed-borne bacterial pathogens including bacterial speck [5]. Seeds are the primary inoculum sources for bacterial pathogen infestation. No effective spray application in the field or greenhouses has been proven yet. The only way to solve the problem is by providing pathogen-free seeds. Because growers prefer to product tomato in the same greenhouses or fields every growth season, the population of the inoculum greatly rise in the area [24]. Thus, the damages may increasingly advanced owing to the pathogen dissemination and disease control may get difficult. The thermal seed treatment described here is one possible solution to the problem.

Currently, pysical seed treatments like hot water, electron beam treatments and hot air treatments are commercially in use for seed disinfection [25]. The risks in using physical seed treatments are 1) they may reduce the inoculum but may not fully eliminate seed inoculum and 2) may affect seed vitality. Thus, it's vital to find the most reliable heat and immersing period in hot water. The high efficacy of hot water treatments were well studied [26, 27]. Our study has also confirmed that soaking tomato seeds in hot water (50 °C, 30 min) eliminated the CFU of seed-associated bacteria by hundred percent. Also this treatment did not effect seed germination and no visual disease symptoms appeared on seedlings. Since [26] reported that it may be difficult to maintain 56 °C under commercial conditions to eliminate *Clavibacter michiganensis* subsp. *michiganensis* from tomato seeds, our study suggests that commercial nurseries may use this temperature (50 °C) for bacterial pathogens by providing thermostat controlled bath circulator.

Chemical control predominantly relies on copper based compounds, but the reduction in sensitivity to copper in *Pst* populations were reported [28, 29, 30]. Our findings indicate the increase in copper resistance in copper treated seeds even in used bacterial strain. Since antibiotic usage is restricted in large-scale of tomato production [16], our results demonstrated the less sensitivity to streptomycin with a high growth in petri dishes and symptom appearance in seedlings compared to control.

The combination of effective seed treatments may enhance disease control. Thus, seed treatments may help reduce losses caused by plant associated bacteria during tomato growth. When the combined treatment was applied to infested seeds, the control achieved was significant [16]. In this study, combined treatments efficiently controlled lesion development on seedlings.

Unfortunately, we do not recommend to store treated seeds for years, since we have no report whether the treatment affects the seed germination. In summary, we suggest that some tomato seed lots should be treated with water at 50 °C for 30 min or combined treatments be applied before getting seedlings in commercial nurseries. Then, this sample should be tested to ensure if seed germination is not adversely affected. This study suggests these applications to be employed in commercial nurseries in Turkey before seedling growth.

ACKNOWLEDGEMENTS

Acknowledgements are extended to Assoc Prof Dr Zeki Gokalp (Certified English Translator and an expert in Biosystems Engineering) for his critical reading and thorough syntactic corrections of the manuscript. This study was partially founded by Erciyes University Scientific Research Projects Unit (Grant no: FBA-2016-6457).

REFERENCES

[1] Food and Agricultural Organization (2016) Tomato production worldwide. http://faostat.fao.org/beta/en/#data/QC

[2] Jones, J.B., Zitter, T.A., Momol, T.M. and Miller, S.A. (2014) Compendium of tomato diseases and pests. 2nd edition. APS Press, St Paul, Minnesota, USA, 168p.

[3] Aysan, Y. Mirik, M., Cetinkaya-Yildiz, R. and Sahin, F. (2007) Outbreak of bacterial speck disease in a nursery in the Eastern Mediterranean region of Turkey. Acta Horticulturae. 729, 441.

[4] Basim, H., Basim, E., Yilmaz, S., Dickstein, E.R. and Jones, J.B. (2004) An outbreak of bacterial speck caused by Pseudomonas syringae pv. tomato on tomato transplants grown in commercial seedling companies located in the Western Mediterranean region of Turkey. Plant Disease. 88, 1050.

[5] Miller, S.A. and Jones, J.B. (2014) Bacterial speck. In: Jones, J.B, Zitter, T.A., Momol, T.M. and Miller, S. (Eds.) Compendium of tomato diseases and pests. 2nd edition. APS Press. St. Paul, Minnesota, 55121, USA, 54-55.

[6] Bashan, Y. and Bashan, L.E. (2002a) Protection of tomato seedlings against ınfection by Pseudomonas syringae pv. tomato by using the Plant Growth-Promoting Bacterium Azospirillum brasilense. Applied and Environmental Microbiology. 68, 2637–2643.

[7] Conlin, K.C. and McCarter, S.M. (1983) Effectiveness of selected chemicals in inhibiting Pseudomonas tomato in vitro and in controlling bacterial speck. Plant Dis. 67, 639-644.

[8] Trueman, C.L. (2015) Copper alternatives for management of bacterial spot (Xanthomonas gardneri) and bacterial speck in processing tomatoes. Acta Horti. 1069, 243-249.

[9] Alexander, S.A. (1999) First report of copper-tolerant Pseudomonas syringae pv. tomato in Virginia. Plant Dis. 83, 964.

[10] Benlioglu, K. and Benlioglu, S. (1998) Pseudomonas syringae pv. tomato'ya karşı bakır dayanıklılığı üzerinde çalışmalar. 8th Turkish Phytopathol. Congress. 21-25 September, Ankara, 52-56.

[11] Cuppels, D.A. and Elmhirst, J. (1999) Disease development and changes in natural Pst populations on field tomato plants. Plant Dis. 83, 759-764.

[12] Cemen, A., Aysan, Y., Horuz, S. and Saygılı, H. (2017) Biological control of tomato bacterial speck disease using bacteriophages. Integrated control in protected crops, temperature climate. IOBC, WPRS Bulletin. 124, 146.

[13] Karabuyuk, F. and Aysan, Y. (2016) Aqueous plant extracts as seed treatments on tomato bacterial speck disease. 3rd International Symposium Biological Control of Plant Bacterial Diseases (Biocontrol 2016). 11-14 April 2016. Belgrad, Serbia. Abstracts Book. 39p.

[14] Graves, A.S and Alexander, S.A. (2002) Managing bacterial speck and spot of tomato with Acibenzolar-S-methyl in Virginia. Plant health (Online).

[15] Louws, F.J., Wilson, M., Campbell, H.L., Cuppels, D.A., Jones, J.B., Shoemaker, P.B., Sahin, F. and Miller, S.A. (2001) Field control of bacterial spot and bacterial speck of tomato using a plant activator. Plant Dis. 85, 481–488.

[16] Bashan, Y. and Bashan, L.E. (2002b) Reduction of bacterial speck (Pseudomonas syringae pv. tomato) of tomato by combined treatments of plant growth-promoting bacterium, Azospirillum brasilense, streptomycin sulfate, and chemo-thermal seed treatment. European Journal of Plant Pathology. 108, 821–829.

[17] Ji, P., Campbell, H.L., Kloepper, J.W., Jones, J.B., Suslow T.V., Wilson M. (2006) Integrated biological control of bacterial speck of tomato under field conditions using biological control agents and plant growth-promoting rhizobacteria. Biol. Cont. 36, 358–367.

[18] Jones, J.B., Jackson, L.E., Balogh, B., Obradovic, A., Iriarte, F.B., Momol, M.T. (2007) Bacteriophages for Plant Disease Control. Annual Review of Phytopathol. 45, 245-262.

[19] Lanna Filho, R., de Souza, R.M., Ferreira, A., Quecine, M.C., Alves E., de Azevedo, J.L. (2013) Biocontrol activity of Bacillus against a GFP-marked Pseudomonas syringae pv. tomato on tomato phylloplane. Australasian Plant Pathology. 42, 643–651.

[20] Silva, J.R.C., de Souza, R.M., Zacarone, A.B., da Silva, L.H.C.P., dos Santos Castro, A.M. (2008) Control with endophytic bacteria and in vitro inhibition of Pseudomonas syringae pv. tomato, agent of bacterial speck of tomato. Ciênc. agrotec. 32, 1062-1072.

[21] Kritzman, G. (1993) A chemi-termal treatment for control of seedborne bacterial pathogens of tomato. Phytoparasitica. 21(2) 101-109.

[22] Karabuyuk, F., Kirli, M.M., Horuz, S. and Aysan, Y. (2014) Seedborne tomato bacterial diseases observed in commercial nurseries and fields in Adana. Turkey 5th seed congress with international participation. 19-23 October 2014. Diyarbakir. Abstracts Book Page 682.

[23] Yunis, H., Bashan, Y., Okon, Y. and Henis, Y. (1980) Two sources of resistance to bacterial speck of tomato caused by Pseudomonas tomato. Plant Disease. 64, 851–852.

[24] Gunes, M. and Aysan, Y. (2016) Tomato bacterial disease in plastic greenhouses and fields in Mersin, Turkey. 5th International Symposium on Tomato Diseases. Malaga, Spain. June 13-16, 2016. Abstracts book Page 128.
[25] Van Der Wolf, J.M., Birnbaum, Y., Van Der Zouwen, P.S. and Groot, S.P.C. (2008) Disinfection of vegetable seed by treatment with essential oils, organic acids and plant extracts. Seed Sci. & Technol. 36, 76-88.
[26] Fatmi, M., Schaad, N.W. and Bolkan, H.A. (1991) Seed treatments for eradicating Clavibacter michiganensis subsp. michiganensis from naturally infected tomato seeds. Plant Dis. 75, 383-385.
[27] Ivey, M.L.L. and Miller, S.A. (2005) Evaluation of hot water seed treatment for the control of bacterial leaf spot and bacterial canker on fresh market and processing tomatoes. Acta Horticulturae. 695, 197-204.
[28] Bender, C.L. and Cooksey, D.A. (1986) Indigenous plasmids in Pseudomonas syringae pv. tomato: Conjugative transfer and role in copper resistance. American Soc. for Microbiol. 165, 534-541.
[29] Cooksey, D.A., Azad, H.R., Cha, J.S. and Lim, C.R. (1990) Copper resistance gene homologs in pathogen and saprophytic bacterial species from tomato. App. and Envir. Microbiol. 56, 431-435.
[30] Pernezny, K., Vaclav, K., Blanka, K. and Iveth, H. (1995) Bacterial diseases of tomato in the Czech and Slovak Republics and lack of streptomycin resistance among copper-tolerant bacterial strains. Crop Prolection. 14(4), 267-270.

Received: **18.1.2018**
Accepted: **18.02.2018**

CORRESPONDING AUTHOR

Sumer Horuz
Erciyes University,
Faculty of Agriculture,
Department of Plant Protection,
38039, Kayseri – Turkey

e-mail: sumer_536@yahoo.com

© by PSP Volume 27 – No. 5/2018 pages 3191-3198 Fresenius Environmental Bulletin

EFFECTIVENESS OF VARIOUS ATTRACTANTS FOR MEDITERRANEAN FRUIT FLY, CERATITIS CAPITATA (WIEDEMANN) (DIPTERA: TEPHRITIDAE) ON POMEGRANATE FRUITS IN TURKEY

Nihat Demirel*, Ahmet Emin Yildirim, Gamze Kilic

Mustafa Kemal University, Faculty of Agriculture, Department of Plant Protection, 31034 Hatay, Turkey

ABSTRACT

The Mediterranean fruit fly, *Ceratitis capitata* (Wiedemann) (Diptera: Tephritidae), is a serious pest on pomegranate fruits in Turkey. The objective of this study was to determine effectiveness of various attractants to Mediterranean fruit fly, *Ceratitis capitata* (Wiedemann) (Diptera: Tephritidae) on pomegranate fruits in Hatay province of Turkey. The Decis traps baited with various attractants impregnated in paper handkerchief dispensers were used. After two years of the study, effectiveness of various attractants to *C. capitata* varied in each of the pomegranate variety and sampling year. In the first year, the highest mean of catches on 'Hicaz' pomegranate were observed on the combination of ammonium acetate + ammonium bicarbonate attractant traps. In addition, the highest mean of catches on 'Katırbaşı' pomegranate were observed on the combination of ammonium acetate + ammonium bicarbonate + putrescine attractant traps. However, the lowest mean of catches on 'Hicaz' and 'Katırbaşı' pomegranate were observed on the combination of ammonium bicarbonate + trimethylamine + putrescine attractant traps in both studies. In the second year, the highest mean of catches on 'Hicaz' I, II pomegranate were observed on the combination of ammonium acetate + ammonium carbonate attractant traps in both studies. On the other hand, the lowest mean of catches on 'Hicaz' I, II pomegranate were observed on the combination of ammonium acetate + trimethylamine + putrescine and a single ammonium acetate attractant traps. The highest mean of catches on Katırbaşı pomegranate were observed on the combination of ammonium acetate + trimethylamine + cadaverine attractant traps, whereas the lowest mean of catches were observed on the combination of ammonium acetate + trimethylamine + putrescine and a single ammonium acetate attractant traps. The highest percentages of damage ratios were observed on 'Hicaz' (18%) in 2015 and (14%) in 2016.

KEYWORDS:
Mediterranean fruit fly, attractant, traps, pomegranate, Turkey

INTRODUCTION

Pomegranate, *Punica granatum* L. (Punicaceae: Myrtiflorae), is an important tropical and subtropical tree [1], widespread in Turkey where it comprises approximately 30.530 ha with a total produce of 465.200 tons of fruit per annum, and Hatay province's share is 1.288 ha and 20.430 tons [2]. The Mediterranean fruit fly (Medfly), *Ceratitis capitata* (Wiedemann) (Diptera: Tephritidae), is one of the most important fruit pests throughout the world [3, 4]. The Medfly is a highly adaptive polyphagous tropical fruit fly which attacks more than three hundred and fifty botanical species [5, 6]. The females puncture the fruits and lay eggs below the skin of the host fruits, which are destroyed by larval feeding [7]. The Medfly caused significant damages on pomegranate fruits in Turkey [8]. Insecticidal protection from *C. capitata* is possible by using a cover spray or a bait spray [9]. Protein bait sprays mixed with organophosphates or low toxicity insecticides are successfully used as area-wide integrated pest management techniques to control *C. capitata* populations [10, 11]. Traps baited with trimedlure and attractants are important tools for detection, monitoring and controlling of the *C. capitata* [12, 13]. The trimedlure contained in Jackson traps, and McPhail traps baited with hydrolyzed protein were the primary detection tools used in medfly detection programmes [14, 15]. Traps baited with lures are also continuously used to monitor and control population size and spread [12, 16]. The purpose of the current study was to determine efffectiveness of various attractants to Medfly, *Ceratitis capitata* (Wiedemann) (Diptera: Tephritidae) on pomegranate fruits in Hatay province of Turkey.

TABLE 1
Various lures (attractants) used at pomegranate orchards in Antakya district of Hatay province.

Treatments (Lures)[a]	2015 Lures (gr)/trap[z]	2016 Lures (gr)/trap[z]
Ammonium acetate	0.08	0.42
Ammonium carbonate	0.08	0.42
Ammonium bicarbonate	0.08	---
Diammonium phosphate	0.08	----
Ammonium acetate+Ammonium carbonate	0.08+0.08	0.42+0.42
Ammonium acetate +Ammonium bicarbonate	0.08+0.08	---
Ammonium acetate + Trimethylamine + Putrescine	0.08+0.08+0.01	0.42+0.13+0.01
Ammonium acetate + Ammonium carbonate +Putrescine	0.08+0.08+0.01	----
Ammonium acetate+Ammonium bicarbonate + Putrescine	0.08+0.08+0.01	---
Ammonium carbonate+Trimethylamine + Putrescine	0.08+0.08+0.01	---
Ammonium bicarbonate+Trimethylamine+ Putrescine	0.08+0.08+0.01	----
Ammonium acetate+ Trimethylamine +Cadaverine	-----	0.42+0.13+0.01
Ammonium bicarbonate + Diammonium phosphate	0.08+0.08	----

[a]Lures abbreviations: Ammonium acetate (AA), Ammonium carbonate (AC), Ammonium bicarbonate (AB), Diammonium phosphate (DAP), Ammonium acetate + Ammonium carbonate (AA+AC), Ammonium acetate + Ammonium bicarbonate (AA+AB), Ammonium acetate + Trimethylamine + Putrescine (AA+TMA+P), Ammonium acetate + Ammonium carbonate + Putrescine (AA+AC+P), Ammonium acetate + Ammonium bicarbonate + Putrescine (AA+AB+P), Ammonium carbonate + Trimethylamine + Putrescine (AC+TMA+P), Ammonium bicarbonate + Trimethylamine + Putrescine (AB+TMA+P), Ammonium acetate + Trimethylamine + Cadaverine (AA+TMA+C), Ammonium bicarbonate + Diammonium phosphate (AB+DAP).
[z]Putrescine and Cadaverine used as (mg) and rest of the treatments (lures) used as (gr).

MATERIALS AND METHODS

The study was conducted in 2015-2016 to determine effectiveness of various attractants for Medfly, *Ceratitis capitata* (wiedemann) (Diptera: Tephritidae) on pomegranate fruits in Hatay province of Turkey.

Traps Baited with Attractant in 2015. Two studies were conducted at two different pomegranate orchards in Antakya district of Hatay province. The first study was carried out at the 'Hicaz' pomegranate orchards. The second one was conducted at the 'Katırbaşı' pomegranate orchards. The Decis type traps and baited with ammonium acetate (AA), ammonium carbonate (AC), trimethylamine (TMA), ammonium bicarbonate (AB), Diammonium phosphate (DAP) and 1,4-diaminobutane (putrescine) (P) were used as synthetic food-based lures in both studies. A single and combinations of two and three lures were used in the study (Table 1). Attractant or mixed attractants impregnated into paper handkerchiefs pages were used in this study. Each of the paper handkerchief package (10x7.5 cm) had a 3-mm diameter hole and contained 25 g attractant or mixed of attractants, 2 ml of 10% propylene glycol to decrease water evaporation and 2 ml of 2% dichlorvos (DDVP). Both studies were conducted as randomized complete block design with 12 treatments and 5 replications. The traps were placed at 1.5-2m high on southeastern side of the pomegranate trees (1 trap per three trees) on 10th August 2015. Attractant and propylene glycol and dichlorvos (DDVP) in the traps were replaced with the new ones in every 45 days. Traps were removed on 15th December and brought to the laboratory and captured adults of *C. capitata* were counted.

Traps Baited with Attractant in 2016. Three studies were conducted at two different pomegranate orchards in Antakya district of Hatay province. The first study was carried out at the 'Hicaz' pomegranate orchards. The second study was conducted at the 'Katırbaşı' pomegranate orchards. The last study was carried out at the 'Hicaz' pomegranate orchards. The Decis type traps and baited with ammonium acetate (AA), ammonium carbonate (AC), trimethylamine (TMA), diaminoalkane (cadaverine) (C) and 1,4-diaminobutane (putrescine) (P) were used as synthetic food-based lures with all studies. Single and combinations of two and three lures were used in the study (Table 1). Attractant or mixed attractants impregnated into paper handkerchiefs pages were used in the study. Each of the paper handkerchief package (10x7.5 cm) had a 3-mm diameter hole and contained 25 g attractant or mixed of attractants, 2 ml of 10% propylene glycol to decrease water evaporation and 2 ml of 2% dichlorvos (DDVP). The first and second study were conducted as randomized complete block design with 5 treatments and 10 replications. The last study was conducted as randomized complete block design with 5 treatments and 15 replications. All traps were placed at 1.5-2m high on southeastern side of the pomegranate trees (1 trap in every three

trees) on 28nd August 2016. Attractant and propylene glycol and dichlorvos (DDVP) in the traps were replaced with the new ones in every 45 days. All traps were removed on 10th December and brought to the laboratory and captured adults of *C. capitata* were counted.

All data were analyzed by analysis of variance (ANOVA) with using the SAS software and means were separated by using the Least Significant Difference (LSD) Multiple Comparison Tests ($P < 0.05$) [17].

Damages Rates in 2015-2016. The fruit damage assessment was measured by the percentage of medfly punctures during the harvest in both year. For this purpose, during the harvest time, except from the trap baited with attractant lure hanging tree, three-hundred fruits were chosen randomly from thirty trees in each of the orchards and checked for medfly punctures and infested fruits were counted. The percentage of fruit damage was calculated by dividing the number of infested fruits by the total number of sampled fruits in each orchards to evaluate the percentage of the damaged fruits in each of the orchard.

RESULTS AND DISCUSSION

Traps Baited with Attractant in 2015. Effectiveness of various attractants to *C. capitata* on pomegranate fruits varied in each of the sampling year. In the first study, a total of 6444 medfly adults were caught by attractant traps at the 'Hicaz' pomegranate and the highest mean of catches were caught by the combination of ammonium acetate + ammonium bicarbonate attractant traps ($F=5.69$; $P= 0.0001$) (Figure 1). The lowest mean of catches were caught by the combination of ammonium bicarbonate + trimethylamine + putrescine, ammonium carbonate + trimethylamine + putrescine and ammonium acetate+ammonium bicarbonate + putrescine, single of ammonium carbonate, ammonium bicarbonate and diammonium phosphate attractant traps.

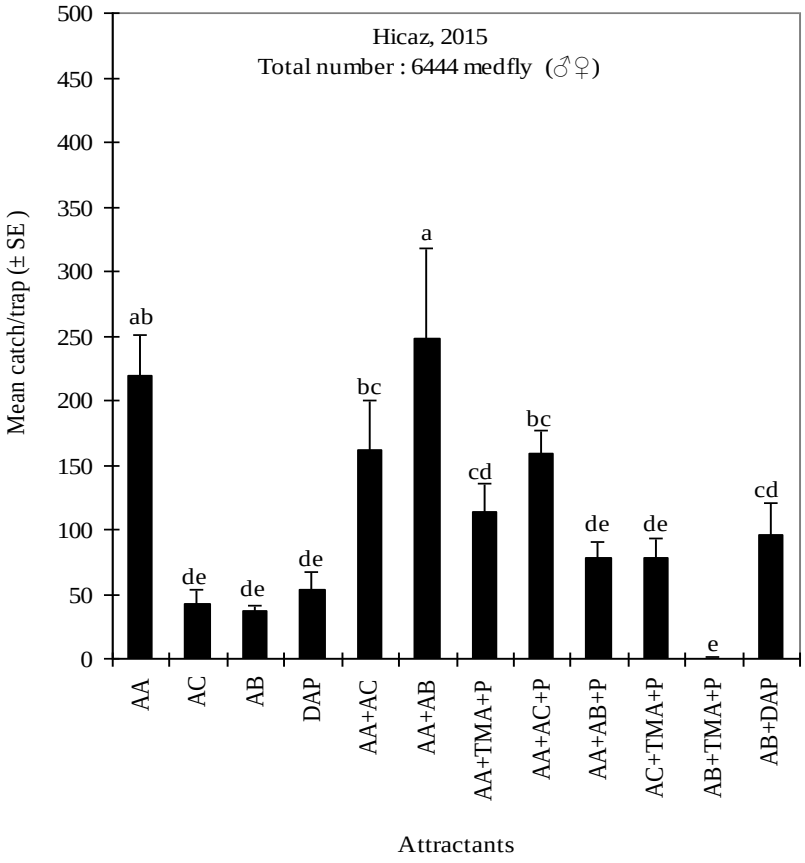


FIGURE 1
Mean and standard error of the number of captured adults per traps baited with attractants (10 August–15 December, 2015) at the Hicaz pomegranate orchard in Antakya district. Different letters above bars indicate significant differences according to Least Significant Difference (LSD) Multiple Comparison Tests ($P < 0.05$).

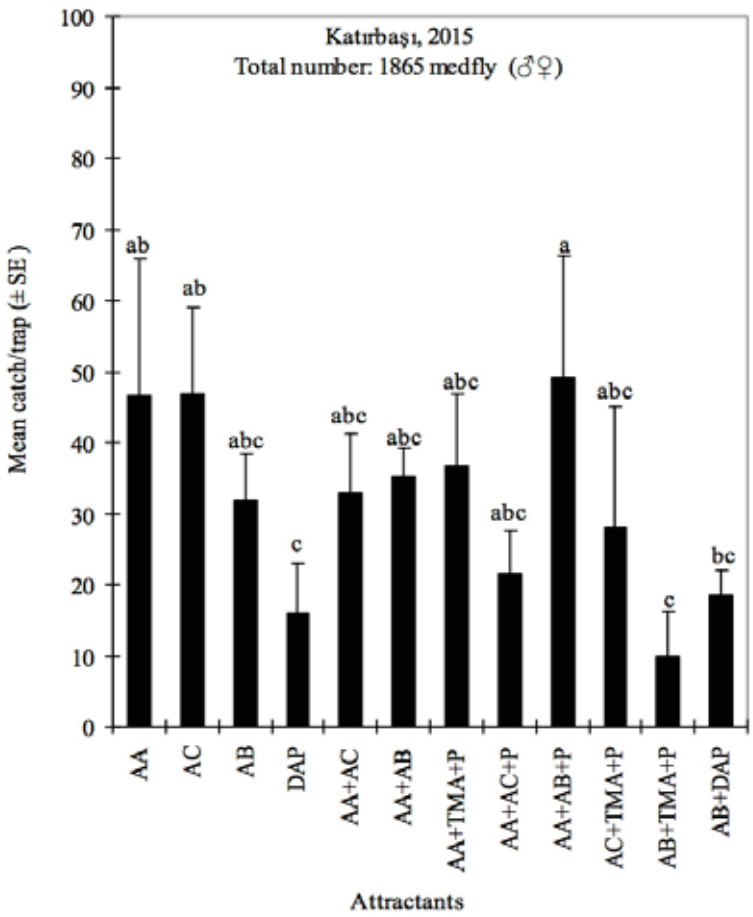


FIGURE 2
Mean and standard error of the number of captured adults per traps baited with attractants (10 August–15 December, 2015) at the Katırbaşı pomegranate orchard in Antakya district. Different letters above bars indicate significant differences according to Least Significant Difference (LSD) Multiple Comparison Tests (P < 0.05).

In the second study, a total of 1865 medfly adults were caught by attractant traps at the 'Katırbaşı' pomegranate and the highest mean of catches were caught by the combination of ammonium acetate + ammonium bicarbonate + putrescine attractant traps (F=2.22; P= 0.0203) (Figure 2). The traps baited with ammonium acetate and ammonium carbonate caught significantly high number of medfly during the study. The lowest mean of catches were caught by the combination of ammonium bicarbonate + trimethylamine + putrescine and single treatment of diammonium phosphate attractant traps.

Traps Baited with Attractant in 2016. In the first study, a total of 2485 medfly adults were caught by attractant traps at the 'Hicaz' pomegranate and the highest mean of catches were caught by the combination of ammonium acetate + ammonium carbonate attractant traps (F=2.27; P= 0.0261) (Figure 3). The lowest mean of catches were caught by the combination of ammonium acetate + trimethylamine + putrescine attractant traps.

In the second study, a total of 5482 medfly adults were caught by attractant traps at the 'Katırbaşı' pomegranate and the highest mean of catches were caught by the combination of ammonium acetate + trimethylamine + diaminoalkane (cadaverine) attractant traps (F= 5.10; P= 0.0001) (Figure 4). The lowest mean of catches were caught by the combination of ammonium acetate + trimethylamine + putrescine attractant traps.

In the last study, a total of 1495 medfly adults were caught by attractant traps at the 'Hicaz' pomegranate and the highest mean of catches were caught by the combination of ammonium acetate + ammonium carbonate attractant traps (F= 1.93; P= 0.0316) (Figure 5). The lowest mean of catches were caught by the single treatment of ammonium acetate and ammonium carbonate and the combination of ammonium acetate + trimethylamine + putrescine and ammonium acetate + trimethylamine + diaminoalkane (cadaverine) attractant traps.

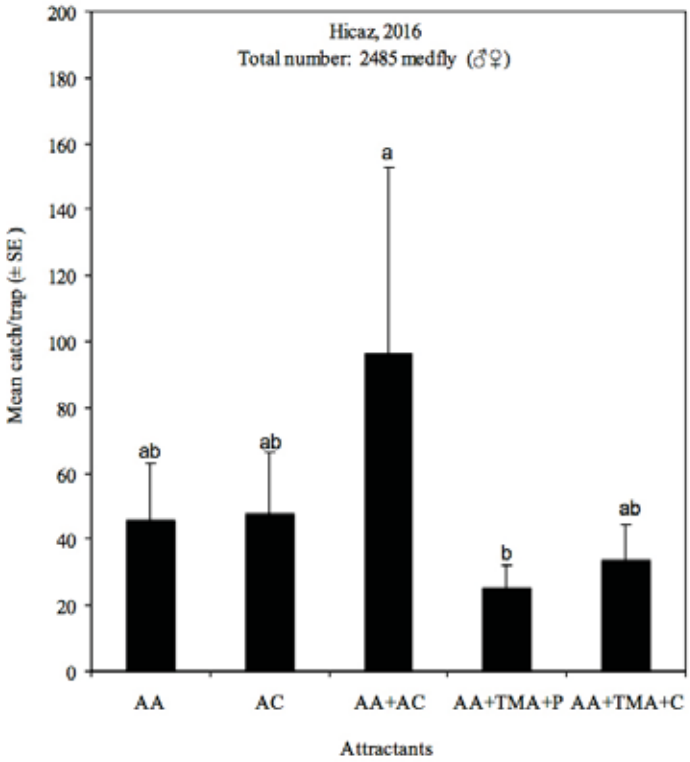


FIGURE 3

Mean and standard error of the number of captured adults per traps baited with attractants (28 August–10 December, 2016) at the Hicaz I pomegranate orchard in Antakya district. Different letters above bars indicate significant differences according to Least Significant Difference (LSD) Multiple Comparison Tests (P < 0.05).

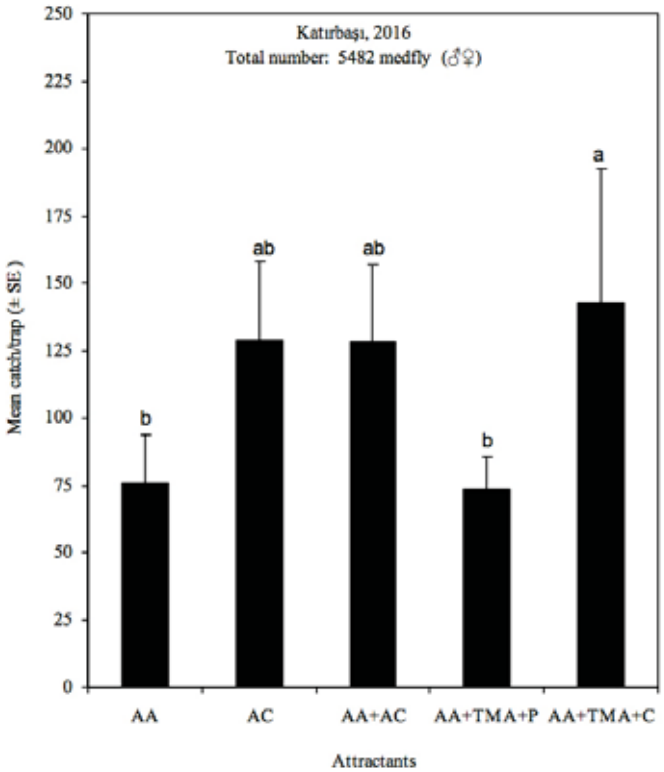


FIGURE 4

Mean and standard error of the number of captured adults per traps baited with attractants (28 August–10 December, 2016) at the Katırbaşı pomegranate orchard in Antakya district. Different letters above bars indicate significant differences according to Least Significant Difference (LSD) Multiple Comparison Tests (P < 0.05).

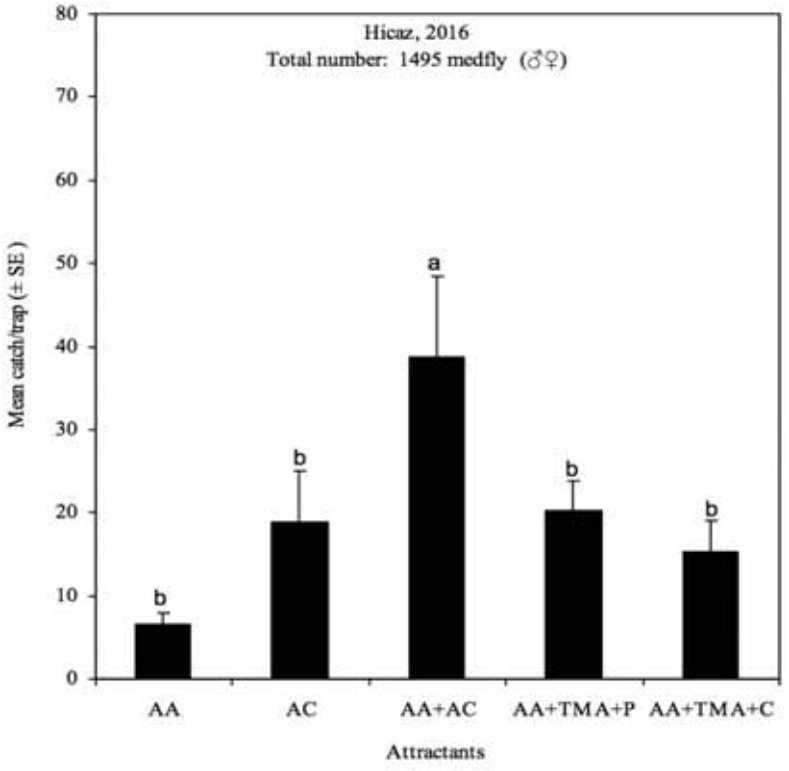


FIGURE 5
Mean and standard error of the number of captured adults per traps baited with attractants (28 August–10 December, 2016) at the Hicaz II pomegranate orchard in Antakya district. Different letters above bars indicate significant differences according to Least Significant Difference (LSD) Multiple Comparison Tests (P < 0.05).

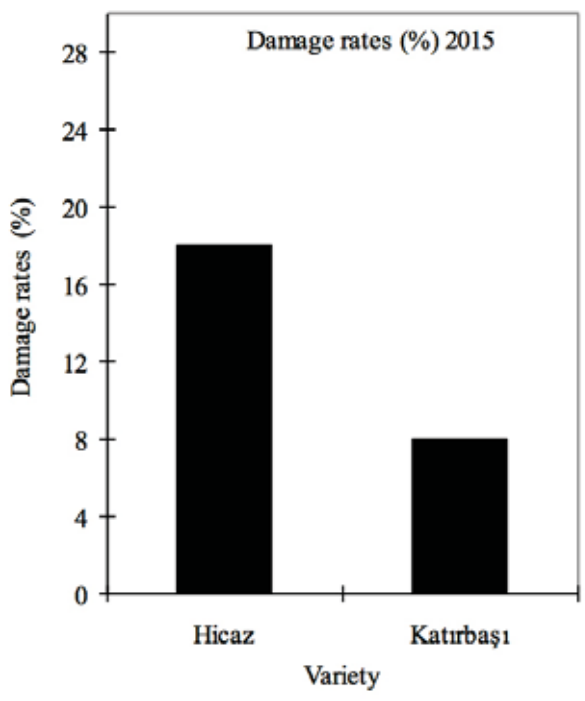


FIGURE 6
Percentage of the damaged fruits by medfly in pomegranate orchards in Antakya district in 2015.

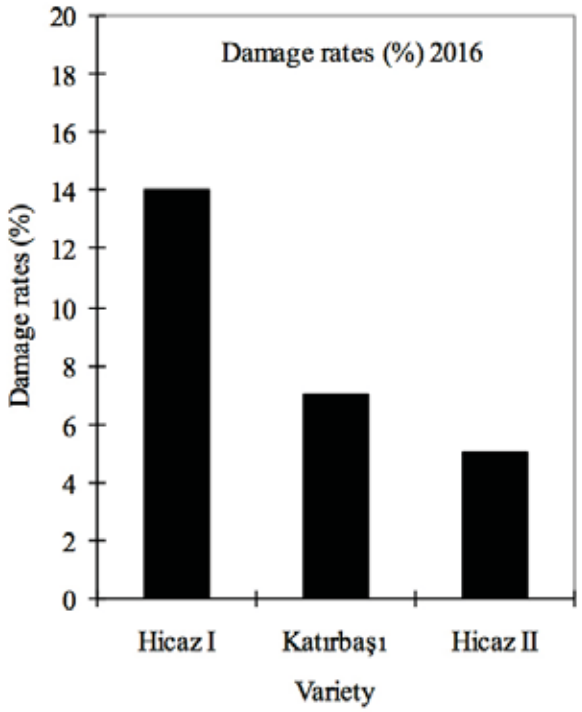


FIGURE 7
Percentage of the damaged fruits by medfly in pomegranate orchards in Antakya district in 2016.

Damages rates in 2015-2016. The damage ratio of medfly varied each of the sampling variety and year. In the first year, the highest percent of damage rate was observed with 18 percent on 'Hicaz' pomegranate fruit (Figure 6). The damage rate was 8 percent on 'Katırbaşı' pomegranate fruit. In the second year, the highest percent of damage rate was observed with 14 percent 'Hicaz I' pomegranate fruit (Figure 7). The damage rates were 7 percent on 'Katırbaşı' and 5 percent on 'Hicaz II' pomegranate fruits.

The trimedlure, ceralure, protein-based baits and lures are critical components to detect, monitor and control of *C. capitata* on various fruits in the world [15]. Traps baited with protein-based baits and lures are also used for capture of male and female *C. capitata* [13]. The food-based lures capture both females and males [15, 16], whereas food-based baits has been the high capture of nontarget insects [18]. Gothilf and Levin [19] reported that an ammonium carbonate has long been known to attract females. Several studies have demonstrated and confirmed the high selectiveness and effectiveness of the combinations of several synthetic food attractants based on ammonium acetate, putrescine and trimethylamine for *C. capitata* females capture [16, 20, 21]. A two year study were conducted by Demirel [8] to evaluate population density and damage rates of medfly on various pomegranate orchards in Turkey. The result of the study point out that the medfly caused 14% damage ratio on Hicaz pomegranate and 25 % on Katırbaşı pomegranate fruits.

CONCLUSIONS

The present study was conducted by traps baited with various attractants determine efffectiveness of various attractants to Medfly, *Ceratitis capitata* (Wiedemann) (Diptera: Tephritidae) on pomegranate fruits in Hatay province of Turkey. As a result of two years of investigations, effectiveness of various attractants varied in each of the sampling year. In the first year, the highest mean of catches on 'Hicaz' pomegranate were observed on the combination of ammonium acetate + ammonium bicarbonate attractant traps. In addition, the highest mean of catches on 'Katırbaşı' pomegranate were observed on the combination of ammonium acetate + ammonium bicarbonate + putrescine attractant traps. In the second year, the highest mean of catches on 'Hicaz' I, II pomegranate were observed on the combination of ammonium acetate + ammonium carbonate attractant traps. In addition, the highest mean of catches on 'Katırbaşı' pomegranate were observed on the combination of ammonium acetate + trimethylamine + cadaverine attractant traps. The highest damage ratios of medfly were observed on 'Hicaz' pomegranate fruit in both years.

ACKNOWLEDGEMENTS

This project was supported by University of Mustafa Kemal of Scientific Research Projects (BAP) (project number: 13601).

REFERENCES

[1] Morton, J. (1987) Pomegranate In: Morton, J.F. (ed.) Fruits of warm climates. Julia F. Morton, Miami, Florida, USA, P. 352–355.
[2] Anonymous (2016) Türkiye istatistik kurumu. https://biruni.tuik.gov.tr/bitkiselapp/bitkisel.zul .20.01.2018.
[3] Christenson, L.D., Foote, R.H. (1960) Biology of fruit flies. Annual Review of Entomology. 5, 171-192.
[4] Demirel, N. (2007) Behavior paradigms in the Mediterranean fruit fly, Ceratitis capitata (Weidemann). Journal of Entomology. 4(2), 129-135.
[5] Papadopoulos, N.T., Carey, J.R., Katsoyannos, B.I. and Kouloussis N.A. (1996) Overwintering of the Mediterranean fruit fly (Diptera: Tephritidae) in northern Greece. Annals of the Entomological Society of America. 89, 526-534.
[6] Liquido, N.J, Shinoda, L.A. and Cunningham, R.T. (1991) Host Plants of the Mediterranean Fruit Fly (Diptera Tephritidae): An Annotated World Review. Entomological Society of America. Miscellaneous Publications. No. 77.
[7] Thomas, M.C., Heppner, J.B., Woodruff, R.E., Weems, H.V., Steck, G.J. and Fasulo, T.R. (2010) Mediterranean Fruit Fly, *Ceratitis capitata* (Wiedemann) (Insecta: Diptera: Tephritidae). University of Florida, IFAS Extension. EENY-214.
[8] Demirel, N. (2016) Population density and damage ratios of Mediterranean fruit fly, *Ceratitis capitata* (Wiedemann) (Diptera: Tephritidae) on pomegranate orchards in Turkey. Entomology and Applied Science Letters. 3(5), 1-7.
[9] Roessler, Y. and Chen, C. (1994) The Mediterranean fruit fly, *Ceratitis capitata*, a major pest of citrus in Israel, its regulation and control. Bulletin OEPP/EPPO Bulletin. 24, 813-816.
[10] Burns, R.E., Harris, D.L., Moreno, D.S. and Eger, J.E. (2001) Efficacy of spinosad bait sprays to control Mediterranean and Caribbean fruit flies (Diptera: Tephritidae) in commercial citrus in Florida. Florida Entomologist. 84. 672-678.

[11] Urbaneja, A., Chueca, P., Monton, H., Pascual-Ruiz, S., Dembilio, O., Vanaclocha, P., Abad-Moyano, R., Pina, T. and Castanera, P. (2009) Chemical alternatives to malathion for controlling Ceratitis capitata (Diptera: Tephritidae), and their side effects on natural enemies in Spanish citrus orchards. J. Econ. Entomol. 102, 144-151.

[12] Gazit, Y., Rössler, Y., Epsky, N.D. and Heath, R.R. (1998) Trapping females of the Mediterranean fruit fly (Diptera: Tephritidae) in Israel: comparison of lures and trap type. Journal of Economic Entomology. 91(6), 1355-1359.

[13] Navarro, V., Alfaro, F., Dominguez, J., Sanchis, J. and Primo, J. (2008) Evaluation of traps and lures for mass trapping of Mediterranean fruit fly in citrus groves. J. Econ. Entomol. 101, 126–131.

[14] Gilbert, J., Bingham, R.R. (1999) Insect Trapping Guide. California Department of Food and Agriculture. MF, 1–9.

[15] IAEA (2003) Trapping guidelines for area-wide fruit fly programmes. Insect Pest Control Section, International Atomic Energy Agency. Vienna, Austria.

[16] Epsky, N.D., Hendrichs, J., Katsoyannos, B.I., Vasquez, L.A., Ros, J.P., Zumreoglu, A., Pereira, R., Bakri, A., Seewooruthun, S.I. and Heath, R.R. (1999) Field evaluation of female-targeted trapping systems for Ceratitis capitata (Diptera: Tephritidae) in seven countries. J. Econ. Entomol. 92(1), 156–164.

[17] SAS Institute, (1998) User's Guide, version 6. SAS Institute, Cary, NC, USA.

[18] Boulahia-Kheder, S., Loussaïef, F., Ben Hmidène, A., Trabelsi, I., Jrad, F., Akkari, Y. and Fezzani, M. (2012) Evaluation of two IPM programs based on mass-trapping against the Mediterranean fruit fly *Ceratitis capitata* on citrus orchards. Tunisian Journal of Plant Protection. 7, 53-66.

[19] Gothilf, S. and Levin, G. (1989) Attraction of the Mediterranean fruit fly to ammonium and protein bait. In: Cavalloro, R. (ed). Fruit flies of economic importance. A.A. Balkema, Rotterdam, 387-391.

[20] Miranda, M.A., Alonso, R. and Alemany, A. (2001) Field evaluation of Medfly (Dipt., Tephritidae) female attractants in a Mediterranean agrosystem (Balearic Islands, Spain). Journal of Applied Entomology. 125, 333- 339.

[21] Alemany, A., Alonso, D. and Miranda, M.A. (2004) Evaluation of improved Mediterranean fruit fly attractants and retention systems in the Balearic Islands (Spain). In: Barnes, B.N. (ed.) Proceedings of the 6th International Symposium on Fruit Flies of Economic Importance. Isteg Scientific Publications, Centurion. 355–359.

Received: **23.1.2018**
Accepted: **18.02.2018**

CORRESPONDING AUTHOR

Nihat Demirel
Mustafa Kemal University,
Faculty of Agriculture,
Department of Plant Protection,
31034, Hatay – Turkey

e-mail: ndemirel@mku.edu.tr

© by PSP Volume 27 – No. 5/2018 pages 3199-3205 Fresenius Environmental Bulletin

DETERMINATION OF THE EFFECT OF SOME ORGANIC AND ORGANO-MINERAL FERTILIZERS ON TOTAL PHENOLIC, FLAVONOID AND ANTHOCYANIN CONTENT OF BOGAZKERE (VITIS VINIFERA L.) GRAPES

Gultekin Ozdemir*

Dicle University, Faculty of Agriculture, Department of Horticulture, 21280 Diyarbakir, Turkey

ABSTRACT

This study was conducted to determine the impacts of organic and organo-mineral fertilizers on total phenolic, flavonoid and anthocyanin activities of Bogazkere (*Vitis vinifera* L. cv.) grapes. Study treatments included organic fertilizers (green fertilizer (vetch), green fertilizer (barley), green fertilizer (vetch + barley), farmyard manure, bactoguard, lifebac NP, humanica) and organo-mineral fertilizers (bactolife quality organo, bactolife high organo, bactolife high organo, bactolife super organo power). The organic, and organo-mineral fertilizer applications positively influenced the total phenolic, flavonoid and anthocyanin productions. The maximum total phenolic production was significantly higher under bactolife buper brgano bower (550.47 µg GAE/mg in pulp) application. The total flavonoid production in berry pulp (45.07 µg QUE/mg), seed (26.76 µg QUE/mg) and skin (20.27 µg QUE/mg) were the highest under the bactolife super organo power. Total anthocyanin content of berry skin and pulp of Bogazkere grape cultivar was the highest under the organic humanica.

KEYWORDS:
Grape, Bogazkere, Berry, Phenolic, Flavonoid, Anthocyanin

INTRODUCTION

Turkey has about 7% of the world's area of vineyards, and produces 6.4% of the world's grape production. In addition, productivity in Turkey has improved by about 40% in the last 15 years, from 6654 kg ha^{-1} in 1998 to 9249 kg ha-1 in 2012 [1].

Boğazkere are red grape cultivars of *Vitis vinifera* L. grown in southeastern Turkey, especially Diyarbakir province. It is an important red grape variety for Turkey, which produces wellbalanced and characteristics wines, with fruity notes such as strawberry, cherry, and blackberry-like odours [2, 3].

Grape is one of the most important protective food [4-7] not only due to its special nutritive value but also owing to its wide spread production. Some authors have studied the protective effect, total phenolic and flavonoid contents of different grape cultivars and ecological regions in Turkey [8- 20].

The types and concentration of the phenolic compounds depend on the grape variety, ripening, climatic conditions, wine making practices (the use of enzymes, maceration conditions, and fermentation temperature), and ageing [37].

Among the types of grapes, especially red grapes and grape juice, the major phenolic compounds found in red wine are called as flavonoids, anthocyanins and flavonols [3].

Grape yields and quality were mainly affected by soil fertility and fertilization [21, 22]. Fertilizer management one of the main factors responsible for grapes phytochemical profiles. Very little work has been reported on the effect of organic and organo-mineral fertilizers on grapes in Turkey [23-25].

There are various types of fertilizers available for use in vineyards. Currently, the use of organic and organo-mineral fertilizers has attracted the interest of producers focus on improving the productive performance cultivated grape cultivars [26-28].

The objective of the present study was to determine the effects of organic and organo-mineral fertilizers on total phenolic, flavonoid and anthocyanin content of berry skin, pulp and seed of Bogazkere (*Vitis vinifera* L.) grapes.

MATERIALS AND METHODS

The study was performed under Bogazkere (*Vitis vinifera* L) local grape variety. Boğazkere are red grape cultivars of *Vitis vinifera* L. grown in Diyarbakir province.

Vineyard area. The experiments were carried out in a 8 years old private vineyard in Dicle town, which is located in Diyarbakir province of Turkey, in the years of 2016. The study site was initiated on a Vertisol soil with parent materials mostly consisting of marn and lacustrine transported material. The

experiment was conducted under a semi-arid climate with a mean maximum air temperature of 28-38°C and minimum air temperature 10-12°C during growing season, respectively.

The reduced tillage was conducted at 2-3 cm depth of soil in October and November in the years of 2016. Some physical and chemical properties are tabulated (Tab. 1).

Fertilizer applications. The present study included twelve fertilizer applications; (1) Control, (2) Green Fertilizer (Vetch; 90 kg ha^{-1}), (3) Green Fertilizer (Barley; 30 kg ha^{-1}), (4) Green Fertilizer (Mixture of Vetch (75%) and Barley (25%); 9 kg da^{-1} vetch and 3 kg da^{-1} barley), (5) Farm Manure (3 tons da^{-1}), (6) Bactoguard (35% organic matter, 24% organic carbon, and 2.5% organic N), (7) Lifebac-NP (containing natural *Bacillus subtilis and Bacillus megatherium* isolate $1x10^9$ cfu/ml), (8) Humanica (50% organic matter, %55 humic + fulvic acid), (9) Bactolife Quality Organo (4-0-8+0.2% Fe, Mn, Zn and Cu), (10) Bactolife High Organo (5-5-0+0.2% Fe, Mn, Zn and Cu), (11) Bactolife High Organo 5-5-5 +0.2% Fe, Mn, Zn and Cu), and (12) Bactolife Super organo-Power (10-0-0+0.2% Fe, Mn, Zn and Cu).

The control plots did not receive any applications from any fertilizers. The crop was grinded and mixed in the soil when vetch bloomed was 50 % whereas farmyard manure was incorporated within 0-20 cm soil depth during the spring plowing under consideration of the worked had been done by same researchers [21]. Each treatment had replicated three times in the randomized block design for two years. Bactoguard, Lifeback-NP and Humanica fertilizers were used as commercial organic treatments [29]. Bactoguard (20 L with 1 tons of water ha^{-1}) and organo-mineral fertilizers (30 L with 1 tons of water ha^{-1}) were applied 3 times in soil starting with leaf formation with 25-day intervals until harvesting (before and after flowering and when grape reaches the size of a nut). Bactoguard derived from plants which liquid organic fertilizer, provides effective protection against cold, hail, water, and salt stresses due to containing organic acids, amino acids, antioxidant enzymes and hormones in natural form. Bactoguard had 35% organic matter; 2.5% nitrogen (N); 24% organic carbon. Lifeback-NP was sprayed 100 mL per vine with sap water to holes opening to coral trace of vines and going down to hair roots. Lifeback-NP is a microbial fertilizer containing natural *Bacillus subtilis and Bacillus megaterium* isolates and proliferates rapidly by covering plant roots/leaves and generates nutrient-intake promoting secretions without feeding from plants. In addition, Lifeback-NP enables plants to fix free nitrogen in the atmosphere through their leaves and roots. Humanica was applied 3 kg per vine to crown trace of vines mixed with soil between February and March. Humanica contained organic matter (40%), total acid (Humic + Fulvic; 50%), and maximum humidity (35%) and soil conditioning fertilizer based on Leonardite which has a dark color and soft texture. Soils properties require reconditioning if their structures suffer disruption along with efficiency and productivity losses. Organo-mineral applications contained Bactolife Super Organo Power, Bactolife Quality Organo, Bactolife High Organo (Nitrogen (5%), P_2O_5 (5%)), and Bactolife High Organo (Nitrogen (5%), P_2O_5 (5%), and K_2O (5%)) organic matter content (20%) [29].

Total phenolic, flavonoid and anthocyanin analysis. The content of total phenolic in the grape berry skin, pulp and seed were determined according to the Folin–Ciocalteau method [30]. Gallic acid was employed as the calibration standard and the results were expressed as gallic acid equivalents (GAE) (µg GAE/mg of berry sample). The absorbance was measured using a UV-vis spectrophotometer at a wavelength of 765 nm [3, 20]. Fresh sample (1 gram) was homogenized with ultraturraks, incubated at 4°C for 12 hours, and centrifuged at 1200 rpm for 50 min whereas supernatants were filtered through 0.22 m. Measurement of the flavonoid concentration of the grape berry skin, pulp and seed were based on the method described by Park et al., with a slight modification [31]. A 1 ml aliquot of the sample was added to a test tube containing 0.1 ml of 10% aluminum nitrate, 0.1 ml of 1 M potassium acetate and 3.8 ml

TABLE 1
Chemical properties of the experimental field soils before the experiment (mean ± standard deviation, n = 20)

Soil Properties	Means	Soil Properties	Means
pH (1:2 soil:water) (%)	7.82±0.30	Electric conductivity (dS/m)	0.95±0.04
Clay (%)	39.12±1.2	Organic matter (%)	2.36±0.23
Silt (%)	28.23±1.1	$CaCO_3$ (%)	7.80±0.11
Sand (%)	32.65±2.3	Available P (mg/kg)	3.15±1.20
CEC† (%)	20.44±1.4	Available Fe (mg/kg)	3.40±0.60
Exchangeable Mg ($cmol_c$/kg)	2.10±0.40	Available Mn (mg/kg)	7.10±1.10
Exchangeable Ca $cmol_c$/kg	14.35±1.40	Available Zn (mg/kg)	2.20±0.88
Exchangeable K $cmol_c$/kg	3.20±0.73	Available Cu (mg/kg)	5.40±1.10
Exchangeable Na $cmol_c$/kg	0.40±0.07	Available B (mg/kg)	0.20±0.06

†CEC: Cation Exchange Capacity

of methanol. The mixture was then incubated for 40 min at room temperature and the absorbance was determined at 415 nm. Spectrophotometric analysis was performed using a five-point calibration curve generated with pure quercetin (Sigma) as the standard. The flavonoid content in the Okuzgozu berry samples were expressed in micrograms of quercetin equivalents (QUE) per ml of a sample [3, 20]. The total anthocyanin of grape berry pulp and seed extracts were measured [32] pH differential method.

Statistical analysis. The experiments were performed in a complete randomized block design with three replicates. Each replicate consisted of five vines. The results are expressed in mean ± SD. One-way ANOVA (PROC-GLM procedure) was used to analyze the effects of organic and organo-mineral fertilizers on total phenolic, flavonoid and anthocyanin content of Bogazkere (*Vitis vinifera* L. cv.) grapes. When statistically significant effects ($P<0.05$) were detected, the least significant difference (LSD) tests were used to separate means after one-way ANOVA. Data were analyzed using SPSS 15.0 for Windows.

RESULTS AND DISCUSSION

In this study, results showed that different treatment of organic and organo-mineral fertilizers had significant effect on Bogazkere grape berry total phenolic (berry skin, pulp, seed), total flavonoid (berry skin, pulp, seed) and total anthocyanin (berry skin, pulp) profiles (Table 2-4).

Total phenolic. The treatments of Bactolife Super Organo Power (OM4) and Bactolife High Organo 5-5-5 (OM3) were found more effective in producing total phenolic content of grape berry skin, pulp and seed content than other treatments and control. The maximum total phenolic content at 126.69 µg GAE/mg of grape berry skin, at 550.47 µg GAE/mg of berry pulp, at 346.22 µg GAE/mg of berry seed were recorded on organo-mineral fertilizer Bactolife Super Organo Power treatment (Table 2). The average percentage of total phenolic skin, pulp, and seed increase was 8.75%, 3.44%, and 3.39 % when compared to control, respectively. These findings are supported by the findings of [33, 34].

Total flavonoid. The data presented in Table 3 indicated the maximum total flavonoid (µg QUE/mg) content of berry skin (20.27 µg QUE/mg), pulp (45.07 µg QUE/mg) and seed (26.76 µg QUE/mg) of Bogazkere grape cultivar were recorded on organo-mineral fertilizer Bactolife Super Organo Power (OM4) application. The next best treatment in this regard was Bactolife High Organo 5-5-5 (OM3). The average percentage of total flavonoid skin, pulp, and seed increase was 377.40%, 41.45%, and 121.40 % when compared to control, respectively. The lowest total flavonoid content was observed in control vine berries. The results obtained in the present investigations are in conformity with those obtained by [33, 34, 35] in grapes.

TABLE 2
Total phenolic (µg GAE/mg) content of berry skin, pulp and seed of Bogazkere grape cultivar

Treatments*	Total phenolic (µg GAE/mg)	Total phenolic (µg GAE/mg)	Total phenolic (µg GAE/mg)
	Skin	Pulp	Seed
C	106.51 ± 0.17^{a}	517.00 ± 0.25^{a}	323.59 ± 0.10^{a}
V	108.83 ± 0.04^{b}	519.47 ± 0.16^{ab}	325.67 ± 0.13^{b}
B	110.57 ± 0.18^{c}	521.58 ± 0.05^{bc}	327.90 ± 0.02^{c}
B+V	111.85 ± 0.28^{d}	523.99 ± 0.47^{c}	329.31 ± 0.07^{d}
FM	112.94 ± 0.42^{e}	529.28 ± 0.45^{d}	331.61 ± 0.15^{e}
O1	114.31 ± 0.21^{f}	537.38 ± 0.44^{e}	332.86 ± 0.18^{f}
O2	115.92 ± 0.07^{g}	539.51 ± 0.25^{ef}	335.27 ± 0.33^{g}
O3	117.73 ± 0.18^{h}	541.84 ± 0.06^{efg}	337.58 ± 0.20^{h}
OM1	119.25 ± 0.19^{ı}	543.86 ± 0.04^{fgh}	339.35 ± 0.21^{ı}
OM2	121.57 ± 0.20^{i}	545.65 ± 0.14^{gh}	341.56 ± 0.18^{i}
OM3	123.62 ± 0.03^{j}	547.73 ± 0.13^{hı}	343.76 ± 0.05^{j}
OM4	126.69 ± 0.06^{k}	550.47 ± 0.21^{i}	346.22 ± 0.22^{k}
Average	115.82 ± 0.99	534.81 ± 1.94	334.56 ± 1.18
p-value**	<0.001	<0.001	<0.001

* C: Control, Untreated, V: Green Fertilize (Vetch), B: Green Fertilizer (Barley), FM: Farm Manure, O1: Bactoguard, O2: Lifebac NP, O3: Humanica, OM1: Bactolife Quality Organo, OM2: Bactolife High Organo 5-5-0, OM3: Bactolife High Organo 5-5-5, OM4: Bactolife Super organo Power.

** p-value from one-way ANOVA. Means in columns followed by different letters are significantly different by LSD protected by ANOVA (Analysis of Variance) at $p < 0.05$ ($n = 6$).

TABLE 3
Total flavonoid (µg QUE/mg) content of berry skin, pulp and seed of Bogazkere grape cultivar

Treatments*	Total flavonoid (µg QUE/mg)	Total flavonoid (µg QUE/mg)	Total flavonoid (µg QUE/mg)
	Skin	Pulp	Seed
C	2.08 ± 0.01[a]	24.27 ± 0.15[a]	7.71 ± 0.31[a]
V	4.14 ± 0.25[b]	28.98 ± 0.47[c]	12.03 ± 0.38[b]
B	2.53 ±0.30[a]	26.49 ± 0.18[b]	9.82 ± 0.39[c]
B+V	5.82 ± 0.04[c]	30.36 ± 0.21[c]	13.65 ± 0.09[d]
FM	6.95 ± 0.11[d]	31.71 ± 0.26[de]	14.84 ± 0.07[e]
O1	8.05 ± 0.02[d]	32.76 ± 0.11[e]	16.18 ± 0.10[f]
O2	10.31 ± 0.10[e]	34.43 ± 0.15[f]	17.32 ± 0.07[g]
O3	12.10 ± 0.41[f]	36.24 ± 0.46[g]	18.91 ± 0.08[h]
OM1	17.52 ± 0.05[ı]	42.52 ± 0.12[i]	24.54 ± 0.14[ı]
OM2	15.69 ± 0.26[h]	40.49 ± 0.14[ı]	22.59 ± 0.22[i]
OM3	13.67 ± 0.32[g]	38.65 ± 0.08[h]	20.49 ± 0.16[j]
OM4	20.27 ± 0.20[i]	45.07 ± 0.44[j]	26.76 ± 0.06[k]
Average	9.93 ± 0.97	34.33 ± 1.04	17.07 ± 0.95
p-value**	<0.001	<0.001	<0.001

* C: Control, Untreated, V: Green Fertilize (Vetch), B: Green Fertilizer (Barley), FM: Farm Manure, O1: Bactoguard, O2: Lifebac NP, O3: Humanica, OM1: Bactolife Quality Organo, OM2: Bactolife High Organo 5-5-0, OM3: Bactolife High Organo 5-5-5, OM4: Bactolife Super organo Power.
** p-value from one-way ANOVA. Means in columns followed by different letters are significantly different by LSD protected by ANOVA

TABLE 4
Total antosiyanin (Malvidin- 3-o-glikozit (mg/kg)) content of berry skin, pulp and seed of Bogazkere grape cultivar

Treatments*	Total antosiyanin (Malvidin- 3-o-glikozit (mg/kg))	Total antosiyanin (Malvidin- 3-o-glikozit (mg/kg))
	Skin	Pulp
C	16.006,0 ± 0.30[a]	624.67 ± 0.07[a]
V	16.008,4 ± 0.44[ab]	627.28 ± 0.31[b]
B	16.010,9 ± 0.36[bc]	629.49 ± 0.21[c]
B+V	16.013,0 ± 0.14[c]	632.10 ± 0.71[d]
FM	17.017,0 ± 0.18[d]	633.53 ± 0.13[d]
O1	17.018,6 ± 0.77[d]	635.89 ± 0.30[e]
O2	17.029,6 ± 0.25[g]	643.48 ± 0.24[h]
O3	17.036,1 ± 0.53[ı]	650.30 ± 0.20[i]
OM1	17.027,5 ± 0.16[fg]	641.26 ± 0.44[g]
OM2	17.022,5 ± 0.50[e]	637.76 ± 0.19[f]
OM3	17.032,5 ± 0.21[h]	646.67 ± 0.70[ı]
OM4	17.025,5 ± 0.23[f]	639.46 ± 0.03[fg]
	16.687,3 ± 1.08	636.82 ± 1.27
p-value**	<0.001	<0.001

* C: Control, Untreated, V: Green Fertilize (Vetch), B: Green Fertilizer (Barley), FM: Farm Manure, O1: Bactoguard, O2: Lifebac NP, O3: Humanica, OM1: Bactolife Quality Organo, OM2: Bactolife High Organo 5-5-0, OM3: Bactolife High Organo 5-5-5, OM4: Bactolife Super organo Power.
** p-value from one-way ANOVA. Means in columns followed by different letters are significantly different by LSD protected by ANOVA (Analysis of Variance) at $p < 0.05$ ($n = 6$).

Total anthocyanin. The data in Table 4 reveal that total anthocyanin (Malvidin- 3-o-glucoside (mg/kg)) content of berry skin (17.036,1 mg/kg) and pulp (950,30 mg/kg) of Bogazkere grape cultivar was the highest in organic treatment Humanica. The lowest total anthocyanin content was observed in control treatment (berry skin (16.000,0 mg/kg) and pulp (624,67 mg/kg). The average percentage of total anthocyanin skin and pulp increase was 4.13% and 1.94% when compared to control, respectively. The results are supported by the findings reported by [36].

CONCLUSION

Results conducted that total phenolic (µg GAE/mg), flavonoid (µg QUE/mg) and anthocyanin (Malvidin- 3-o-glucoside (mg/kg)) content in Boğazkere grape skin, pulp and seed of berries showed important differences according to the organic and organo-mineral fertilizer applications.

In this study, results showed that optimum plant nutrition especially organo-mineral application increased the phytochemical potential due to fertilizer use efficiency, enzymatic potential of fertilizer and plant ion balance. Overall, the results of this study suggest that microbial and organo-mineral fertilizer application have the potential to increase the quality of the vine plants. Therefore, integrated use of organic and organo-mineral fertilizer showed promising potential for improving total phenolic, flavonoid and anthocyanin content of Bogazkere (*Vitis vinifera* L.) gapes.

Fertilizer management one of the main factors responsible for grapes quality and especially their phytochemical profiles. In conclusion, to get the best quality of grapes growers can use this results to prepare fertilization programs in their vineyards.

REFERENCES

[1] Soylemezoglu, G., Atak, A., Boz, Y., Unal, A., Saglam, M. (2016) Viticulture in Turkey. Chronica Horticulturae. 56, 27-31.

[2] Cabaroglu, T., Canbas, A., Lepoutre, J.P., Gunata, Z. (2002) Free and bound volatile composition of red wines Vitis vinifere L. cv. Öküzgözü and Boğazkere grown in Turkey. America Journal of Enology and Viticulture. 53, 64-68.

[3] Ozdemir, G., Pirincciogluı, M., Kizil, G., Kizil M. (2017) Determination of total phenolic and flavonoid content of berry skin, pupl and seed fractions of Öküzgözü and Boğazkere grape cultivars. Scientific Papers. Series B. Horticulture. 61, 219-224.

[4] Wang, X.L., Wang, C.X., Fan, J.C., Shi, P.H., Wu, J.F. (2017) Natural grape polyphenols for preparing spherical CO_3O_4 nanoaggregates as heterogeneous catalysts for catalytıc oxidation of orange II with sulfate radicals. Fresen. Environ. Bull. 26, 1637-1645.

[5] Pirincciogluı, M., Kizil, G., Kizil, M., Ozdemir, G., Kanay, Z., Ketani, M.A. (2012) Protective effect of Okuzgozu (Vitis vinifera L. cv.) grape juice against carbon tetrachloride induced oxidative stress in rats. Food & Function. 3, 668-673.

[6] Miao, L., Shu-Hua, Y., Jian-Xin, H., Peng, L., Yi, Z., Shuang, D., Xin-Liang, C., Jia-Yi, G., Jun, W., Jian-Bin, H. (2016) The protective effect of grape-seed proanthocyanidin extract on oxidative damage induced by zearalenone in Kunming mice liver. Int J Mol Sci. 17, 808.

[7] Pirincciogluı, M., Kizil G., Ceken Toptanci, B., Ozdemir, G., Kizil, M. (2017) Protective effect of okuzgozu (vitis vinifera l. cv.) seed extract against hydroxyl radical induced DNA damage. Scientific Papers-Series B-Horticulture. 61, 205–208.

[8] Deryaoglu, A., Canbas, A. (2003) Physical and Chemical Changes Occured During Maturation of Okuzgozu Grape Variety Grown in Elazig Region. The Journal of Food. 28, 131-140.

[9] Aras, O. (2006) Determination of the Total Carbohydrate, Protein, Mineral Substances and Phenolic Compounds of Grape and Grape Products. M.Sc. Thesis. Suleyman Demirel University, Graduate School of Natural and Applied Sciences, 59p.

[10] Orak, H.H. (2007) Total Antioxidant Activities, Phenolics, Anthocyanins, Polyphenoloxidase Activities of Selected Red Grape Cultivars and Their Correlations. Scientia Hort. 111, 235-241.

[11] Babalik, Z., Cetin, S., Hallac Turk, F., Gokturk Baydar, N. (2009) Determination of Phenolic Compounds of Cavus Grape Cultivars under Different Training Systems. 7th Symposium on Viticulture and Technologies. 5-9 October, Turkey, 228-293.

[12] Baydar, G.N., Ozkan, G., Yasar, S. (2007) Evaluation of the Antiradical and Antioxidant Potential of Grape Extracts. Food Control. 18, 1131-1136.

[13] Uluocak, E. (2010) The physical and chemical changes during ripening period of some wine grape varieties grown in Kazova (Tokat) Ecology. M.Sc. Thesis. Gaziosmanpasa University, Graduate School of Natural and Applied Sciences, 89p.

[14] Kelebek, H. (2009) Researches on the Phenolic Compounds Profile of Okuzgozu, Bogazkere and Kalecik Karasi Cultivars Grown in Different Regions and Their Wines. PhD Thesis. Cukurova University, Graduate School of Natural and Applied Sciences, 251p.

[15] Bayir, A. (2011) Investigation of Phenoloic Content and Antiradical Activity of Grape, Mulberry and Myrtle. PhD Thesis. Akdeniz University, Graduate School of Natural and Applied Sciences, 147p.

[16] Cangi, R., Saracoglu, O., Uluocak, E., Kilic, D., Sen A. (2011) The Chemical Changes of Some Wine Grape Varieties During Ripening Period in Kazova (Tokat) Ecology. Igdir Univ. J. Inst. Sci. & Tech. 1, 9-14.

[17] Toprak, F.E. (2011) Phytochemical Characteristics in Kalecik Karasi Grape Cultivar (Vitis vinifera L.) Grown in Ankara and Nevsehir. M.Sc. Thesis. Ankara University, Graduate School of Natural and Applied Sciences, 64p.

[18] Kaplama, P. (2012) Antioxidant Activities Anthocyanin Profiles and some Physical and Chemical Properties of Grape Cultivars Grown in Erzincan. M.Sc. Thesis. Ataturk University, Graduate School of Natural and Applied Sciences, 87p.

[19] Pehlivan, E.C., Uzun, H.I. (2015) Effects of Cluster Thinning on Yield and Quality Characteristics in Shiraz Grape Cultivar. Yuzuncu Yil University Journal of Agricultural Sciences. 25, 119-126.

[20] Ozdemir, G., Beren Sogut, A., Pirinccioglu, M., Kizil G., Kizil, M. (2016) Changes in the phytochemical components in wine grape varieties during the ripening period. Scientific Papers. Series B. Horticulture. 60, 85-93.

[21] Ozdemir, G., Tangolar, S., Gursoz, S., Cakir, A., Tangolar, S.G., Ozturkmen, A.R. (2008) Effect of different organic manure applications on grapevine nutrient values. Asian Journal of Chemistry. 20, 1841-1847.

[22] Oner, N., Tok, H.H., Saglam, M.T. (2015) Effects on the yield and quality of grape juice in merlot grape varieties foliar fertilizer application. Journal of Tekirdag Agricultural Faculty. 12, 82-99.

[23] Altindisli, A. (2005) Effects of some organic fertilizers on yield and quality of Round seedless (Round sultana) grape variety. Researching sustainable systems. Proceedings of the First Scientific Conference of the International Society of Organic Agriculture Research (ISOFAR), held in Cooperation with the International Federation of Organic Agriculture Movements (IFOAM) and the National Association for Sustainable Agriculture, Australia (NASAA), Adelaide Convention Centre. Adelaide, South Australia. 21-23 September, 498-501.

[24] Tangolar, S., Ozdemir, G., Gursoz, S., Cakir, A., Tangolar, S.G. (2007) The effects of some organic fertilizer applications on phenological growth with cluster berry and must characteristics of grapevine (Vitis vinifera L. Cilores). Mediterranean Agricultural Sciences. 20, 319-325.

[25] Yagmur, B., Ozlu, E., Ates, F., Simsek, H. (2017) The response of soil health to different tillage practices in organic viticulture farming. J Soil Sci Plant Health. 1, 1-11.

[26] Colapietro, M. (2011) The organo-mineral fertilizers may enhance the production of table grapes. Informatore Agrario. 67, 55-59.

[27] Mehofer, M., Schmuckenschlager, B., Hanak, K., Vitovec, N., Schober, V. (2013) Investigations into the influence of organic fertilizer on the nitrogen content in the soil and the musts of grapes from the varieties 'Blauburger', 'Pinot noir', 'Blaufränkisch' and 'Riesling'. Mitteilungen Klosterneuburg, Rebe und Wein, Obstbau und Früchteverwertung. 63, 117-131.

[28] Kizgin, B., Karakus, H., Ozdemir, G. (2017) Effect of organic and organo-mineral fertilizers on grapevine leaf chlorophyll content. Proceedings X Conference of Agronomy Students. Cacak, Serbia. 23-25 August, 10, 221-225.

[29] Turan, M., Kitir, N., Alkaya, U., Gunes, A., Tufenkci, S., Yildirim, E., Nikerel, E. (2016) Making soil more accessible to plants: the case of plant growth promoting rhizobacteria. In: Rigobelo, E.C. (ed.) Plant growth. InTech, Rijeka.

[30] Singleton, V.L., Rossi Jr, J.A. (1965) Colorimetry of total phenolics with phosphomolybdic-phosphotungstic acid reagents. Amer. J. Enol. Vitic. 16, 144–158.

[31] Park, S.J., Lee, S.G., Shin, S.C., Lee, B.Y., Ahn, Y.J. (1997) Larvicidal and antifeeding activities of oriental medicinal plant extracts against four species of forest insect pests. Appl. Entomol. Zool. 32, 601–608.

[32] Giusti, M., Wrolstad, R. (2001) Characterization and measurement of anthocyanins by UV-visible spectroscopy. In: Giusti, M.M. and Wrolstad, R.E. (Eds.) Current Protocols in Food Analytical Chemistry. John Wiley and Sons, Inc. Hoboken, F1.2.1.-F1.2.13.

[33] Gul, H., Acun, S., Sen, H., Nayir, N., Turk, S. (2013) Antioxidant activity, total phenolics and some chemical properties of Okuzgozu and Narince grape pomace and grape seed flours. Journal of Food, Agriculture & Environment. 11, 28-34.

[34] Zhang, M.X., Liu, C.H., Nan, H.J., Li, Z. (2014) Phenolic compound pro les in skins of white wine and table grape cultivars grown in the national grape germplasm resource nursery of China. South African Journal of Enology and Viticulture. 36, 154-164.

[35] Malusà, E., Laurenti, E., Ghibaudi, E., Rolle, L. (2004) Influence of organic and conventional management on yield and composition of grape cv. 'Grignolino'. Acta Hort. (ISHS). 640, 135-141.

[36] Nedelkovski, D., Cvetković, J., Beleski, K., Poposka, H. (2017) Phenolic composition of Vranec grapevine cultivar (Vitis vinifera L.) grafted on different rootstock. Bulg. J. Agric. Sci. 23, 389-395.

[37] Kelebek, H.K., Canbas, A., Cabaroglu, T., Selli S. (2007) Improvement of antocyanin content in the cv Öküzgözü wines by using pectolytic enzymes. Food Chemistry. 105, 334-339.

Received: **28.01.2018**
Accepted: **23.02.2018**

CORRESPONDING AUTHOR

Gultekin Ozdemir
Department of Horticulture,
Faculty of Agriculture
University of Dicle,
Diyarbakir – Turkey

e-mail: gozdemir@dicle.edu.tr

© by PSP Volume 27 – No. 5/2018 pages 3206-3211 Fresenius Environmental Bulletin

THE VARIABLE OF LEAF MICROMORPHOGICAL CHARACTERS ON GROWN IN DISTINCT CLIMATE CONDITIONS IN SOME LANDSCAPE PLANTS

Mehmet Cetin[1], Hakan Sevik[2], Nurcan Yigit[3], Halil Baris Ozel[4,*], Burak Aricak[3], Tugrul Varol[4]

[1]Kastamonu University, Faculty of Engineering and Architecture, Department of Landscape Architecture, Kuzeykent, 37150, Kastamonu, Turkey
[2]Kastamonu University, Faculty of Engineering and Architecture, Department of Environmental Engineering, Kuzeykent, 37150, Kastamonu, Turkey
[3]Kastamonu University, Faculty of Forestry, Department of Forest Engineering, Kuzeykent, 37150, Kastamonu, Turkey
[4]Bartin University, Faculty of Forestry, Department of Forest Engineering, Agdaci Campus74100, Bartin, Turkey

ABSTRACT

Unlike other designs, the working of Landscape Architecture is the use of plants to put the design of this work on the foreground. When landscaping is finished applying in the open space area is valued at the rate, it may be out of old one that is the usual use. Under the circumstances, the selection of landscaping plants is crucial affected and the conclusion of the use of species is not incorporate in the area's natural vegetation. Nevertheless, Turkey is under the influence of three different climate types. These types of climatic features are entirely different from each other. However, some types of plants, all places are using these climates types. In this research, the changes in the leaves of micromorphological characters were evaluated which the some of tree leaves are grown under different climate conditions. This research showed that it is to identify the influence of the type of place growing conditions by using electron microscope (SEM = Scanning Electron Microscope) in the laboratory at Kastamonu University, University Central Research Laboratory, Research and Application Center. As a result, it found out micromorphological characters at the leaf specimens belonging to species such as; stoma density (1 mm^2 in area), stoma length (µm), stoma width (µm), pore aperture (µm) and pore length (µm).

KEYWORDS:
Micromorphogical character, stoma, leaf, SEM, Climate.

INTRODUCTION

With the rapid development process experienced in the world, structural changes in economic, social, cultural, and political areas have accelerated the process of urbanization and have caused the destruction of green spaces. The fact that rapid urbanization and industrialization has moved human being away from the nature has made him, being a part of the nature, move a part of the nature to his living space. As a result, especially landscape works have become a part of modern life [1, 2, 3, 4].

Plants are the source of life for living beings, and they carry out many functions at the places where they exist. In the place they grow, plants reduce a lot of pollutants such as nitrogen and sulphur oxides, carbon dioxide (CO_2) carbon monoxide (CO), volatile organic compounds (VOCs), particles, ozone, NO_2, formaldehydes and heavy metals [2, 5, 6, 7, 8, 9, 10]. Also plants reduce noise [11, 12, 13]; increase aesthetic value [14, 15, 16]; wood and non-woods forest products [17, 18] have a positive psychological effect, provide energy conservation [19, 20, 21]; prevent erosion, reduce wind speed and hold the soil with their roots, thus preventing washing away of the soil with rainfalls and streams, and protect wildlife and hunting resources [22, 23]. Open-green areas with plantation are important activity areas for both adults and children [1, 24, 25]. Besides, plants increase the productivity of people working in the environment they grow in [26] as well as relieving physiological stress and reducing negative emotions [27].

Plants, which are the most important part of landscape works, play aesthetically and functionally important roles in the design of landscape spaces. This is because plant materials are vibrant, dynamic, malleable, decorative, aesthetical, economic, and functional, which makes them rich, diverse, and living ornamental materials for creating buildings and spaces [18]. In landscape works, practitioners can change micro-environmental conditions to a certain degree. This causes species to be cultivated in places that are not their natural areas of spread. Although these species continue, their healthy growth in the environments they are in, some structural changes may take place at micro level. This may manifest itself especially in those species that are grown in large areas where different climatic types prevail.

Turkey is under the influence of three main climatic types that have quite different characteristics from each other. Within the scope of landscape works, many plants are grown in areas where these three climatic types prevail. These plants generally do not morphologically differ from each other significantly. However, there is not enough information about how they differ at the micromorphological level. In this study, it is aimed to determine how some micromorphological characters change in three plant species grown in certain areas of Turkey where different climatic types prevail.

MATERIALS AND METHODS

The study was conducted on the plants collected from the areas dominated by three climatic types prevailing in Turkey, which are described below.

a) Black Sea Climate: It is rainy every season. In the Eastern Black Sea Region, maximum precipitation is in autumn, and minimum precipitation is in spring. Annual precipitation is 2000-2500 mm. In the Western Black Sea Region, maximum precipitation is in autumn, and minimum precipitation is in spring. Annual precipitation is 1000-1500 mm. In the Central Black Sea Region, maximum precipitation is in winter, and minimum precipitation is in summer. Annual precipitation is 700-1000 mm. The average number of days with snowy weather is 18 in the areas where the Black Sea climate prevails. Average annual temperature is 13-15°C. Average temperature in January is 6-7°C, while average temperature in July is 21-23°C. Annual temperature difference is 13-15°C [28].

b) Mediterranean Climate: Summers are hot and dry, while winters are warm and rainy. Maximum precipitation is in winter, and minimum precipitation is in summer. The precipitation difference is quite big between summer and winter. Average annual precipitation is 600-1000 mm. Average annual temperature is 18-20°C. Average temperature in January is 8-10°C. Average temperature in July is 28-30°C. Annual temperature difference is 15-18°C [29].

c) Continental Climate: Summers are hot and dry, and winters are cold and snowy. In the Central Anatolia Region, maximum precipitation is in spring, and minimum precipitation is in summer. In the Central Anatolia Region, average precipitation is 300-400 mm; average temperature in winter is 1-2°C; average temperature in summer is 22-23°C; average annual temperature is 10-12°C; and annual precipitation is 500-600 mm. Figure 1 presents the map of climate types prevailing in Turkey [29].

The study was conducted on *Cotoneaster franchetti*, *Cercis siliquastrum*, and *Acer negundo* species cultivated in areas where the above-mentioned three climate types prevail. The leaf samples collected from the said species within the

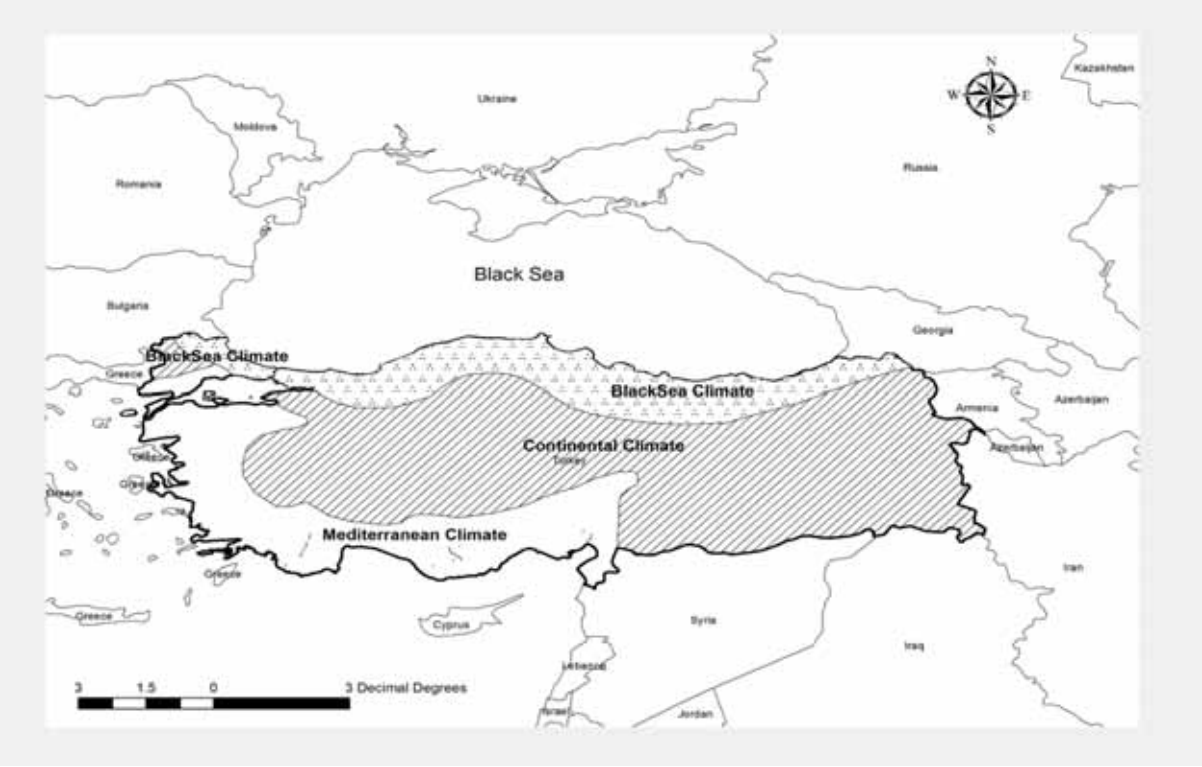


FIGURE 1
The map of climate types in Turkey [29].

TABLE 1
The change of the micromorphological characters by species

Species	STDEN	STL	STW	PORL	PORW
Cotoneaster franchetti	186,18	20,71 c	13,45 c	14,38 c	4,76 c
Cercis siliquastrum	159,87	18,24 b	10,03 a	12,06 b	2,92 b
Acer negundo	186,51	13,40 a	11,12 b	6,68 a	2,01 a
F Value	2,509ns	65,559***	55,300***	125,776***	77,117***

TABLE 2
The change of the micromorphological characters by climate type

Climate Type	STDEN	STL	STW	PORL	PORW
Continental	110,36 a	18,24 c	11,33	10,36	3,33
Mediterranean	206,21 b	18,16 b	11,53	11,09	3,11
Black Sea	216,00 b	15,94 a	11,74	11,67	3,26
F Value	90,928***	4,026*	0,389 ns	1,109 ns	0,194ns

TABLE 3
The change of the micromorphological characters in each species by climate type

Species	Climate	STDEN	STL	STW	PORL	PORW
Cotoneaster franchetti	Continental	92,15 a	17,11 a	12,44 a	11,44 a	4,65 a
	Mediterranean	257,62 c	24,09 c	14,46 c	16,08 b	5,64 b
	Black Sea	208,77 b	20,92 b	13,46 b	15,63 b	3,98 a
	F	2036,199***	135,354***	123,316***	75,670***	7,451**
Cercis siliquastrum	Continental	119,46 a	20,54 c	11,01 b	13,85 c	3,00 b
	Mediterranean	200,31 c	17,58 b	9,61 a	11,53 b	2,09 a
	Black Sea	159,85 b	16,60 a	9,47 a	10,79 a	3,68 c
	F	651,554***	29,426***	3,608*	14,010***	12,681***
Acer negundo	Continental	119,46 a	17,07 c	10,54 a	7,98 c	2,33 b
	Mediterranean	160,69 b	12,83 b	10,52 a	7,41 b	1,61 a
	Black Sea	279,38 c	10,32 a	12,29 b	4,66 a	2,10 b
	F	1951,713***	56,699***	6,388**	13,762***	8,664**

scope of the study at the end of August were pressed and dried. Then they were taken to the laboratory for examination under an electron microscope. Scale images were obtained from the underside of the leaf blade and from the areas close to the middle point via a scanning electron microscope (SEM). .jpeg files were created from the obtained images. Following the completion of these processes, ImageJ, which is a computer measuring program, was used for the following micromorphological measures:

STDEN: Stomatal density (on an area of 1 mm^2)
STL: Stoma length
STW: Stoma width
PORL: Pore length
PORW: Pore width

The obtained data were evaluated via SPSS and subjected to analysis of variance and Duncan's test.

RESULTS AND DISCUSSIONS

Table 1 presents the results of Duncan's test and analysis of variance carried out for determining whether or not there are differences between the species in terms of the micromorphological characters examined.

According to the table, STDEN does not vary among the species at a statistically significant level, but all the other characters vary among the species at a statistically significant level, at a confidence level of 99.9%. Table 2 presents the results of Duncan's test and analysis of variance carried out for determining whether or not the micromorphological characters examined vary by climate type.

According to Table 2, the micromorphological characters examined in the study do not significantly vary by climate type, and only STDEN and STL are affected by climate at a statistically significant level. Table 3 presents the results of Duncan's test and analysis of variance carried out for determining how the micromorphological characters examined vary in each species by climate type.

According to Table 3, all the micromorphological characters examined in the study vary by climate type at a statistically significant level. *Cotoneaster franchetti* was found to have the lowest values for all the characters in continental climate and the highest values in the Mediterranean climate. *Cercis siliquastrum* and *Acer negundo* were determined to have the lowest values for SDEN in continental climate. *Cercis siliquastrum* was seen to have the highest values in the Mediterranean climate, while *Acer negundo* was detected to have the highest values in the Black Sea climate. *Cercis siliquastrum* was found to have the lowest values

for all the characters except for PORW in the Black Sea climate and the lowest values for PORW in the Mediterranean climate. *Cercis siliquastrum* was determined to have the highest values for all the characters except for PORW in continental climate and the highest values for PORW in the Black Sea climate. *Acer negundo* was seen to have the lowest values for STL and PORL in the Black Sea climate and the highest values in continental climate. This species was detected to have the lowest values for STW and PORW in the Mediterranean climate and the highest values in the Black Sea climate.

CONCLUSIONS

The results of the study show that the micromorphological characters vary from one climate type to another at a statistically significant level for all the species. It is noteworthy that the lowest values for STDEN, which is known as one of the most important indicators of the reaction of plants to environmental conditions, were obtained in continental climate. In general, this result is consistent with the results of previous studies. Xu and Zhou [30] state that stomas control CO_2 and water vapor entry into leaves and are affected by environmental conditions. There are also studies reporting that stomatal density or dimensions vary by factors such as water stress ([31, 32, 33], light [18], plant density, length, and leaf surface [34, 35, 36, 37], salt stress [4].

It is notable that stomatal density is reported to be associated with water stress in particular. In the present study, the lowest values for STDEN were obtained in continental climate. In Turkey, average annual precipitation is 500-600 mm in the areas covered by continental climate, 600-1000 mm in the areas dominated by the Mediterranean climate, and over 700 mm in the areas where the Black Sea climate prevails. This means that the number of stomas is associated with precipitation and thus water stress.

The other characters were determined to vary from plant to plant. This may be due to the differences between the anatomical structures of plants. As a matter of fact, previous research reports that plants cultivated under equal conditions give different reactions to different stress factors. For example, among the saplings exposed to a water stress of -8 bars, germination percentage falls to 65% in *Pinus brutia* and to 0% in *Sophora japonica* and *Cupressus arizonica* under the same conditions. Germination percentage goes down to 0% even in the saplings of *Ailanthus altissima* exposed to a water stress of -6 bars [24]. Similar results were obtained in different origins of the same species as well [1, 25, 38]. This implies that species may give different reactions to the same climatic conditions.

The study results show that there are significant differences between plants in terms of micromorphological characters. However, it is interesting that especially each plant reacts differently to the climate conditions in which it is grown. According to these results, it can be said that the genetic structure of the species is one of the most effective factors on micromorphological characters. Morphological and anatomical characters generally occur as a result of the interaction between genetics and the environment and they are shaped by the effect of genetic factors [39] in addition to many environmental factors [18, 24]. This also explains that species can give different reactions to the same climate conditions. The fact that micromorphological characters also vary significantly by species has been shown in the studies carried out [40, 41].

RECOMMENDATIONS

The results of the study indicate that micromorphological characters significantly vary among the individuals cultivated in different climate types. Although there is a significant level of variation from species to species, continental climate has an obvious effect in terms of STDEN. Thus, it can be said that STDEN has a considerable potential for the determination of the stress levels of plants. Contrary to other methods, STDEN is easy to determine and produces a result in a short time. Therefore, there is a need for detailed research aimed at clearly revealing the relationship of this character with plant stress level. Research on this subject should be diversified and maintained.

ACKNOWLEDGEMENTS

This study was supported by Kastamonu University Scientific Research Projects Coordinator within the scope of KÜ-BAP01 / 2016-12 project. We thank Kastamonu University Scientific Research Projects Coordinator for their support (Project Number: KU-BAP01/2016-12).

REFERENCES

[1] Sevik, H., Cetin, M. (2016a) Evaluation of Topiary Applications and Problems: A Case Study of Kastamonu. International Journal of Multidisciplinary Thought. 05(05), 45–50.

[2] Sevik, H., Ahmaida, E.A., Cetin, M. (2017a) Change of the Air Quality in the Urban Open and Green Spaces: Kastamonu Sample. In: Ecology, Planning and Design. Chapter 31. St. Kliment Ohridski University Press. Sofia. ISBN: 978-954-07-4270-0, 409-422.

[3] Cetin, M., Adiguzel, F., Kaya, O., Sahap, A. (2018) Mapping of bioclimatic comfort for potential planning using GIS in Aydin. Environment, Development and Sustainability. 20(1), 361-375.
[4] Zhao, R.X., Zhang, Q.B., Wu, X.Y., Wang Y. (2001) The effects of drought on epidermal cells and stomatal density of wheat leaves. Inner Mongolia Agricultural Science and Technology. 6, 6–7.
[5] Ceburnis, D., Steinnes, E. (2000) Conifer needles as biomonitors of atmospheric heavy metal deposition: comparison with mosses and precipitation role of the canopy. Atmospheric Environment. 34, 4265-4271.
[6] Papinchak, H., Holcomb, E.J., Orendovici, B.T. and Decoteau, D.R. (2009) Effectiveness of houseplants in reducing the indoor air pollutant ozone. HortTechnol. 19(2), 286-290.
[7] Ozel, H.B., Ozel, H.U., Varol, T. (2015) Using Leaves of Oriental Plane (*Platanus orientalis* L.) to Determine the Effects of Heavy Metal Pollution Caused by Vehicles. Polish Journal of Environmental Studies. 24(6), 2569-2575.
[8] Yang, D.S., Pennisi, S.V., Son, K-C., Kays, S.J. (2009) Screening indoor plants for volatile organic pollutant removal efficiency. HortScience. 44(5), 1377-1381.
[9] Yigit, N. (2016) Micromorphological Studies on Plants and Their Importance. St. Kliment Ohridski University Press. Sofia. ISBN 978-954-07-4137-6.
[10] Sevik, H., Cetin, M., Kapucu, O., Aricak, B., Canturk, U. (2017b) Effects of light on morphologic and stomatal characteristics of Turkish Fir needles (*Abies nordmanniana subsp. bornmulleriana Mattf.*). Fresen. Environ. Bull. 26, 6579-6578
[11] Yigit, N., Sevik H., Cetin, M., Gul, L. (2016a) Clonal variation in chemical wood characteristics in Hanönü (Kastamonu) Günlüburun black pine (*Pinus nigra* Arnold. subsp. *pallasiana* (Lamb.) Holmboe) seed orchard. Journal of Sustainable Forestry. 35(7), 515-526.
[12] Yigit, N., Sevik, H., Cetin, M., Kaya, N. (2016b) Determination of the Effect of Drought Stress on the Seed Germination in Some Plant Species. Water Stress in Plants. ISBN:978-953-51-2621-8, chapter 3: InTech, 43-62.
[13] Aricak, B., Enez, K., Özer Genc, C., Sevik, H. (2016) A Method Study to Determine Buffering Effect of The Forest Cover on Particulate Matter and Noise Isolation. 1st International Symposium of Forest Engineering and Technologies (FETEC 2016), 177-185.
[14] Cetin, M. (2016a) Changes in the amount of chlorophyll in some plants of landscape studies. Kastamonu University Journal of Forestry Faculty. 16(1), 239-245.
[15] Cetin, M. (2016b) A Change in the Amount of CO_2 at the Center of the Examination Halls: Case Study of Turkey. Studies on Ethno-Medicine. 10(2), 146–155.
[16] Guney, K., Cetin M., Sevik, H., Guney, K.B. (2016) Influence of germination percentage and morphological properties of some hormones practice on *Lilium martagon* L. seeds. Oxidation Communications. 39(1), 466-474.
[17] Altunel, T. (2011) Odun Dışı Orman Ürünlerinin Değerlendirilmesinde Dünya'dan Örnekler. 2. Uluslararası Odun Dışı Orman Ürünleri Sempozyumu. 8-10 Eylül 2011. Isparta.
[18] Sevik H., Cetin M., Kapucu O. (2016) Effect of light on needle morphologic and stomatal characteristics of Turkish Fir (*Abies nordmanniana subsp. bornmulleriana* Mattf.). International Conference on Forestry and Environment: Challenges and Prospects. 65.
[19] Cetin, M., Topay, M., Kaya L.G., Yilmaz, B. (2010) Efficiency of bioclimatic comfort in landscape planning process: case of Kütahya. Turkish Journal of Forestry. 1(1), 83-95, 2010.
[20] Ozel, H.B., Ertekin, M. (2011) Growth models in investigating oriental beech (*Fagus orientalis* Lipsky.) juvenilities growth performance in the Western Black Sea in Turkey (Devrek-Akçasu Case Study). Romanian Biotechnological Letters. 16(1), 5850-5857.
[21] Ozel, H.B., Ertekin, M. (2012) The change of stand structure in Uludağ fir (*Abies nordmanniana subsp. bornmuelleriana* Mattf.) forests along an altitudinal gradient. Kastamonu University Journal of Forestry Faculty. 12(3), 96-104.
[22] Kırdar, E., Özel, H.B., Ertekin, M. (2010) Effects of pruning on height and diameter growth at stone pine (*Pinus pinea* L.) afforestations. Bartın Orman Fakültesi Dergisi. 12(18), 1-10.
[23] Ozel, H.B., Bilir, N. (2016) Effects of light and moisture on growth and morphological characteristics of horse chestnut (*Aesculus hippocastanum* L.) seedlings in the western black sea region in Turkey. Agriculture & Forestry/Poljoprivreda i Sumarstvo. 62(1), 65-69.
[24] Sevik H., Cetin M. (2015) Effects of water stress on seed germination for select landscape plants. Polish Journal of Environmental Studies 24(2), 689-693.
[25] Sevik H., Cetin M. (2016b) Effects of some hormone applications on germination and morphological characters of endangered plant species *Lilium artvinense* L. Onion scales. Bulgarian Chemical Communications. 48(2), 256-260.

[26] Djukanovic, R., Wargocki, P., Fanger, P.O. (2002) Cost-benefit analysis of improved air quality in an office building. Proceedings of Indoor Air. 2002(1), 808-813.
[27] Chang, C., Chen, P. (2005) Human Response to Window Views and Indoor Plants in the Workplace. HortScience. 2005(40) 1354-1359.
[28] Ertuğrul, M., Varol, T., Özel, H.B. (2014) Climate changes in prospect for the West Black Sea Forests. International Journal of Bartin Faculty of Forestry. 16(23-24), 35-43.
[29] Varol, T., Ertuğrul, M. (2015) Climate change and Forest Fire Trend in the Aegean and Mediterranean Regions of Turkey. Fresen. Environ. Bull. 24, 3436-3444.
[30] Xu, Z., Zhou, G. (2008) Responses of leaf stomatal density to water status and its relationship with photosynthesis in a grass. Journal of experimental botany. 59(12), 3317-3325.
[31] Yang, H.M., Wang, G.X. (2001) Leaf stomatal densities and distribution in *Triticum aestivum* under drought and CO_2 enrichment. Acta Phytoecologica Sinica. 25, 312–316.
[32] Zhang, Y.P., Wang, Z.M., Wu Y.C., Zhang, X. (2006) Stomatal characteristics of different green organs in wheat under different irrigation regimes. Acta Agronomica Sinica. 32, 70–75.
[33] Liu, S., Liu, J., Cao, J., Bai, C., Shi, R. (2006) Stomatal distribution and character analysis of leaf epidermis of jujube under drought stress. Journal of Anhui Agricultural Science. 34, 1315–1318.
[34] Wang, R.Z., Gao, Q. (2003) Climate-driven changes in shoot density and shoot biomass in *Leymus chinensis* (Poaceae) on the Northeast China Transect (NECT). Global Ecology and Biogeography. 12, 249–259.
[35] Zhang, X.Y., Wang, H.M., Hou, Z.D., Wang, G.X. (2003) Stomatal density and distributions of spring wheat leaves under different planting densities and soil moisture levels. Acta Phytoecologica Sinica. 27, 133–136.
[36] Yang, L., Han, M, Zhou, G., Li J. (2007) The changes of water-use efficiency and stoma density of *Leymus chinensis* along Northeast China Transect. Acta Ecologica Sinica. 27, 16–24.
[37] Gazanchian, A., Hajheidari, M., Sima, N.K., Salekdeh, G.H. (2007) Proteome response of *Elymus elongatum* to severe water stress and recovery. Journal of Experimental Botany. 58, 291–300.
[38] Yucedag, C., Kaya, L.G., Cetin, M. (2018) Identifying and assessing environmental awareness of hotel and restaurant employees' attitudes in the Amasra District of Bartin. Environmental Monitoring and Assessment. 190(2), 60.
[39] Sevik, H. (2012) Variation in seedling morphology of Turkish fir (*Abies nordmanniana subsp. bornmulleriana* Mattf). African Journal of Biotechnology. 11(23), 6389-6395.
[40] Galmés, J., Flexas, J., Savé, R., Medrano, H. (2007) Water relations and stomatal characteristics of Mediterranean plants with different growth forms and leaf habits: responses to water stress and recovery. Plant and Soil. 290(1), 139-155.
[41] Maiti, R., Rodríguez, H.G., Balboa, P.R., Moncivais, J.M., Tijerina, H.D., Díaz, J. G., Kumari, A. (2016) Leaf surface anatomy in some woody plants from northeastern Mexico. Pak. J. Bot. 48(5), 1825-1831.

Received: **13.2.2018**
Accepted: **18.02.2018**

CORRESPONDING AUTHOR

Halil Baris Ozel
Bartın University,
Faculty of Forestry,
Agdaci Campus,
74100 Bartın – Turkey

e-mail: halilbarisozel@gmail.com

© by PSP Volume 27 – No. 5/2018 pages 3212-3217 Fresenius Environmental Bulletin

NOTICE

TOWARD AN INTEGRATED SAFE AND SUSTAINABLE FOOD SYSTEM

Sule Turhan[1,*], Erkan Rehber[2], Burcu Erdal[1], Hasan Vural[1]

[1]Uludag University, Faculty of Agriculture, Department of Agricultural Economics, Bursa, Turkey
[2]Economist and Author, Bursa, Turkey

ABSTRACT

There are considerable development to establish quality standards and schemes to have safe foods and sustainable agriculture alternatives to protect natural resources and environment. From one hand, there are strict quality and safety measures used in conventional agriculture and some considerable development to have same controlled and certified sustainable systems such as organic farming on the other hand. In fact, alternatives agriculture systems have not guaranteed food safety, even if they intent do. Recently, there are movements in both consolidation of the wide range measures used in conventional agriculture and used them in the alternative productions systems. In short a worldwide strong tendency have shown to have a sound and consolidated strict quality and safety measures, as well as having a unified food system from seed to fork. This paper aims to review these developments shortly. Indeed these are big challenges. All stakeholders have to realize these rapid changes and need to be in common efforts to meet new food policy requirements.

KEYWORDS:
Food safety, sustainable agriculture alternatives, food regulations and standards

INTRODUCTION

Most industrial countries achieved farming practices, which are more intensive with high level of inputs leading to tremendous yield increases sustained food surpluses by the second half of the 20th century. Especially WW II war caused the appearance of some technologies that have been used in agriculture. Modern plant breeding, improved agronomy and the development of inorganic fertilizers and modern pesticides fueled this movement. These advances were much slower in reaching developing countries. Nevertheless, some foundations led in establishing an international agricultural research system to help transfer and adapt scientific advances to developing countries. The breeding of improved varieties, combined with the expanded use of fertilizers, other chemical inputs, and irrigation led to dramatic yield increases in Asia and Latin America, beginning in the late 1960s. In 1968, William S. Gaud coined the term “Green revolution” to describe this phenomenal growth in agriculture [1].

Despite its success at increasing aggregate food supply, the green revolution has also created some problems mainly as adverse impacts on the environment. The increasing use of agrochemical based pest and weed control in some crops has affected the surrounding environment as well as human health. Increase in the area under irrigation has led to a rise in the salinity of the land. Although high yielding varieties had provided a considerable production increase, it has led to significant genetic erosion. The other main problem is about the quality of food that is output of the above-mentioned agricultural activities and contemporary processing-distribution systems.

The centralized food distribution system and the changes in the demographic and cultural practices of consumers are contributing factors to the apparent increase in the number of outbreaks of foodborne illness in the world. Recently genetically modified organism and nanotechnology used in food industry have been evaluated as new sources of foodborn health problems while proponents of these issues argue otherwise [2]. Fortunately, there are efficient actions to improve measures to overcome those problems mentioned above [3]. From one hand, strict quality and safety measures used in conventional agriculture have been developed and some considerable progress to have some controlled and certified sustainable systems such as organic farming have been achieved on the other hand. In fact, alternatives agriculture systems have not guaranteed food safety, even if they intent do. Recently there are movements in both consolidation of the wide range measures used in conventional agriculture and used them in the alternative productions systems [4]. In short a worldwide strong tendency have shown to have a strong and strict consolidated quality and safety measures, as well as having a unified food system from seed to

fork. This paper aims to summarize these developments.

DEVELOPMENTS IN FOOD SAFETY

World Health Organization (WHO) of United Nations (UN) has been involved in food safety since its establishment. Some charges related to food safety were included in the 1948 WHO Constitution. Many WHO activities about food safety are carried out in close collaboration with FAO. The Sixteenth World Health Assembly approved the establishment of the Joint FAO/WHO Food Standards Program, with the Codex Alimentarius Commission as its principal organ in May 1963. A group of experts convened jointly by the FAO and the World Health Organization (WHO) in 1983 concluded that illness due to contaminated food is perhaps the most widespread health problem in the contemporary world [4]. In 1992, the FAO/WHO-sponsored International Conference on Nutrition declared that access to nutritionally adequate and safe food is a right of each individual [6, 7]. The increasing public concern about food safety resulted in a high-level international forum "Enhancing Food Safety in a Global Community" held in Beijing in 2007 and Beijing Declaration of Food Safety was adopted. Declaration demonstrated a high-level commitment to resolving food safety problems to development comprehensive programs [8]. The concept of traceability can be used to explain a general foundation of such control systems in food sector. The new EU Traceability Regulation No.178/2002 which came into force in January 2005, defines 'traceability' as "the ability to trace and follow a food, feed, food-producing animal or substance intended to be, or expected to be incorporated into a food or feed, through all stages of production, processing and distribution" [9]. FAO and WHO created the Codex Alimentarius Commission in 1963. There is a wide range of different standards and regulations in the food sector like hygienic standards, sanitary and phytosanitary standards, or maximum levels related to the content of aflatoxin or pesticides [10]. Many companies take a standard (for example, the EUREPGAP1 standards) as the baseline for doing business in the food sector [10]. Certification, accreditation, inspection, testing, metrology and are the important activities to establish and implement of standards. During the last 20 years, however, the multilateral rules have become much more stringent on the development and use of standards [11]. Although differences in standards and regulations may lead to conflicts and disputes, they may also be a source of fruitful dialogue between countries, causing some countries to alter and improve their food safety systems. A summary about these standards and basic quality control schemes will be presented below.

Quality Standards. The International Organization for Standardization (ISO) is an international collaboration of national standards setting organization. The ISO story began in 1946 when delegates from 25 countries met at the Institute of Civil Engineers in London and decided to create a new international organization to facilitate the international coordination and unification of industrial standards. ISO officially began operation in February 1947 as a new organization. Today ISO has members from 163 countries and 3368 technical bodies to take care of standard development. Since 1947, ISO has developed and published commercial standards, many of which have become laws and/or national standards in contributing countries. ISO 9000 was first published in 1987. It was based on the BS 5750 series of standards from British Standard Institute (BSI) that were proposed to ISO in 1979. The original ISO 9000 series consisted of five standards: ISO 9000, 9001, 9002, 9003 and 9004, plus ISO 8402 which was published in 1986 and it focused on terminology. As a general quality control standard; ISO 9001, the world's most popular standard for quality management, is now under review, with an updated version was available since the end of 2015 [12].

Good Agricultural Practice (GAP). Quality assurance systems along the food production chain may include Good Agricultural Practices (GAP), Good Manufacturing Practices (GMPs), Good Hygienic Practices (GHPs). GAPs and GMPs (Good Manufacturing Practices) are a set of principles, regulations and technical recommendations applicable to production, processing and food transport, addressing human health care, environment protection and improvement of worker conditions and their families. The term "GAP" is a recognized terminology used in the international regulatory framework as well as in reference to private, voluntary and non-regulatory applications that are developed and applied by governments, civil society organizations and the private sector [13]. Due to a rise in food borne illness, the US Department of Agriculture (USDA) developed Good Agricultural Practices (GAPs) in 1998, partly as a guideline by which farmers could reduce the chance of microbial contamination of crops. Programs that aim to standardize GAPs globally and across industries include GLOBALGAP and the United Fresh Produce GAPs Harmonization Initiative [14]. In the EU, to assure food safety and to control relevant environmental and social issues, the European group of representatives from all stages of the food chain in the fruit and vegetables sector, with the support of producer organizations outside the EU, initiated a system named as the "EUREPGAP (Euro Retailer produce working group-Good Agriculture Practices)".

Hazard Analysis Critical Control Points (HACCP). The traditional approaches to food safety assurance (GAP, GMP etc.) are still essential parts of any foods control program, but they have certain limitations and shortcomings. HACCP, originally developed as a safety assurance tool by the private sector, is now introduced in the food safety legislation of many countries [15]. The Codex Alimentarius Commission for food safety recommends HACC that is used by most countries around the world since the 1960s. Its application in the control of food quality has been extended during 1990s in the developed world. HACCP could be used with interaction and interdependency as an international regulatory standard and as a private standard in industry assurance programs [16].

There is a great effort in the United States to establish the HACCP system as the prevailing approach to food safety. All food companies were required to apply HACCP principles in the EU since 1995. Within Europe, systems based on HACCP principles (as defined by Codex) have been incorporated into the EC Food Hygiene Regulations and animal feed legislation. In addition, the requirements made on suppliers in the food industry by their customers include a HACCP plan as a fundamental component Systems based on Codex guidance are a specific requirement for some of these private industry standards. Guidance is available that will assist businesses to comply with these requirements [17]. In Canada, government agencies have undertaken various programs involving HACCP systems to improve the safety of foods. Agriculture Canada has reorganized to meet consumer concerns and has formed a new Agri-Foods Safety Division to work with other federal food inspection agencies, the provinces and the agri-food industry. The Codex Alimentarius Commission promotes the practical implementation of HACCP systems in the food industry. The adoption of such assurance systems is a benefit to the international trade in food; this has attained further recognition with the development of International Standard ISO 22000. This standard combines the quality assurance requirements found in ISO 9000 and the food safety focused components found in a HACCP plan. The ISO 22000 standard emphasizes the role of ensuring that good practice is followed in food businesses, by what is referred to as the prerequisites program (PRP).

ALTERNATIVE AGRICULTURAL SYSTEMS: ORGANIC AGRICULTURE

Rio Declaration on Environment and Development, Chapter 14 of Agenda 21, adopted by the UN General Assembly in 1992, and Rome Declaration on World Food Security in 1996 were the corner stone of such activities [18, 19]. Under this concept many different descriptions of sustainable agriculture appeared such as organic, integrated, eco-agriculture, permaculture, vermiculture and biodynamic, etc. There are other approaches which represent alternatives to conventional production systems, and which are environmentally friendly but not organic. An example is low external input sustainable agriculture (LEISA).

Despite having historical roots, which go back to the first part of the 20th century, organic farming has began to develop as an economic sector in the last three decades. There are many definitions of organic farming (or agriculture) made by several scientists, legislations and public and private certification organizations. In fact, the concept of organic farming is a production system from field to consumer table. It consists of production, processing and distribution of organic food and fibers. The concept of organic farming has been evolving since first coined by Lord Northbourn (1940) in his book "Look to the Land" and Albert Howard who adopted Northbourne terminology, and published a book “A study of Organic Agriculture” in 1947 which was the first book having the term “organic agriculture” in the title. The organic movement has also originally been a farmer experienced activity in different parts of world simultaneously. Indigenous practices and knowledge have contributed to this movement and they will remain an important part of it in the future [20]. However, sometimes there are also different organic food concepts, which can be confused by consumers. However, there are some terms, such as free-range, hormone-free, and natural, can still appear on food labels, which are being confused with "organic". The true organic must be the only food labeled "organic" has been certified as meeting organic standards. On the other hand, it is also confusing that an organic label does not refer to residue free healthy food. It is a production system that is also aiming at supplying healthy and safe food [21]. But the organic label refers to an agricultural growing method i.e. it is not intended to be a health claim. When the concept and principles of organic farming are concerned, indigenous products, which are called “organics by defaults” and products which are collected in the wild named as “wild collected products” as well as the intentionally organically grown products have to be considered. The production methods called organic by default have been practiced in many less developed countries in Africa and Asia. Those who have been using natural farming methods are also termed as “de-facto organic farmers”. But they cannot be considered “organic farmers” because their way of farming is sometimes soil depleting and unproductive. With the availability of direct contact between farmer and consumer, trust can be maintained without any verification system. Its simplest way is represented by farm gate or farmers’ market. One typical example of such as system is “community supported agriculture” (CSA) has been

observed mostly in the USA. The concept of CSA was brought to the USA from Switzerland in 1984 which its root goes back 1960s in Europe. Over time two different types have emerged as farmer and consumer driven [22]. The other examples are WWOOF and Teikei. WWOOF is a worldwide network that allows volunteers to live and learn on organic practices. WWOOF brings together hosts and volunteers (WWOOFers) helping each other to make a healthier world. WWOOF also promotes cultural understanding of the many diverse peoples and cultures around the world through the intercultural exchange that takes place while sharing in the daily life of others. The Japanese "Teikei" is a unique form of a producer-consumer partnership developed in Japan in early 1970s [17].

INTEGRATION AND CONVERGENCE OF FOOD SAFETY MEASURES AND PRACTICES

When discussing organic farming as a feasible alternative to the contemporary agriculture, it is necessary to consider other ecological approaches as well as conventional agriculture itself as explained above. It is well known that, in general, Sanitary and Physosanitary (SPS) measures have been included even in production and trade of conventional agriculture. And also, some strict rules have been implemented in mainstream agricultural food chains from seed to consumer table that can be generally referred to as "traceability and quality monitoring systems" (1). These systems sometimes have stringent and more demanding standards such as "EUREPGAP". It is a fact that those ecologic agricultural practices and conventional farming are competitors of organic farming both from economic and food quality points of view.

It must be suggested the necessity of integration and consolidation of the efforts and regulated for food safety considering their complementary specifications. Food Safety and Sustainable Agriculture Forum organized in 2014, Beijing shows that it is a global awareness more than being an individual view. It is a necessary movement when considering theirs complementary functions. Such a revision has given a tighter vision of food safety and would enable better oversight in each of these categories [23]. ISO and food safety management (HACCP) came under the umbrella of ISO 22000 after September 2004. In designing this plan, it is important to keep in mind that both HACCP and ISO need to be generic, so that establishments have the opportunity to demonstrate how they are managing their process [23]. Global Food Safety Initiative (GFSI) is an international effort in this field. The benefits of global convergence, between GFSI recognized schemes and mutual recognition of food safety certification to retailers and food service operators acting on an international scale are clear. This is also leading to the efficient assurance of regulatory compliance for certification schemes in markets as diverse as the European Union, the Americas, Asia Pacific and the Middle East and Africa.

In fact, the implementations of alternatives agriculture including organic agriculture do not guarantee food safety, even if they intent to care about human and animal health and natural resources (land and water). There are considerable efforts to integrate quality assurance schemes like GAP and HACCP in the alternative agricultural practices mainly within the organic certified farming. For example, recently the safety and quality of organic foods have been questioned in the USA while the demand for organic food has increased rapidly over the past two decades. If consumer confidence is to remain high, the safety, quality and health benefits of organic foods must be assured [24]. Buyers of the organic products (including CSA members and farmers' market shoppers) have started to demand GAP certifications from their farmers, to verify the farmer's good practices. As a result, GAP and other Food Safety Audits have been on the rise, and may be demanded by most consumers (and legislation) in the near future. The principles of organic processing plans and HACCP plans are quite similar in terms of documentation and how analyzes could be done within each step of the process. For example, a HACCP plan can be utilized to establish procedures to assure that organic materials are not from non-organic materials and that they do not in contact with non-approved substances. In fact, a HACCP plan can incorporate an Organic Production and Handling System Plan to ensure organic integrity. There are some practical problems. For example, in the USA, one concern identified by operators of certified organic farms regarding GAP certification is that once approved, a farm's organic certification applies to all produce, grain and oilseed crops produced on that farm, whereas a GAP audit only certifies specific crops. One of the subsets of The Quality Low Input Food (QLIF) integrated project, which was designed directly to support the implementation of HACCP systems in the organic food sector [25]. The structure of the organic food supply chain was examined to identify those aspects that are common throughout the food industry and those that require special attention in organic systems. These differences arise during the production and processing stage and in the distribution chain, and are prescribed by organic legislation and standards. HACCP protocols and manuals for six commodities (wheat, field vegetables, apples, milk, eggs, and pork meat) have been developed within the QLIF Project that focuses on primary production. Consideration is also given to the use of HACCP to manage food quality and organic integrity in the supply chain in addition to the management of food safety hazards. These have been

used to disseminate HACCP knowledge to businesses in the organic food supply chain. The second phase of the project enabled the information in the training manuals to be disseminated to the organic sector by offering training workshops [17]. All food business operations in Europe and all businesses supplying food to a European retailer are required to implement HACCP since 2007. It is important to emphasize that this is not a legal requirement in primary production.

CONCLUSIONS

There are considerable development to establish quality standards and schemes to have safe foods. Recently, there is also a remarkable development to integrate and combine these efforts with the convergence using them both in conventional and alternative agricultural systems mainly in organic farming. These developments will serve to establish better measures for having safe food and sustainable agriculture through having rather a holistic production system from seed to fork.

Indeed, there are big gaps related developments and implementations these food safety rules among countries based on their development levels. Developed countries have their own standard and certification organizations and they have more power to be effective in establishing some rules and principles. However, most of the developing countries do not have their own organizations and professional institutions established to assist farmers and other actors of the food chain throughout production, handling, processing and marketing. Therefore, all stakeholders in developing countries need some financial and technical support to use production techniques to meet required standards and getting desired results such comprehensive food safety schemes and regulated systems. In this respect, the role of governments can be considered two fold. First of all, the enforcement of the legislation and regulation supervision of the inspection system can be considered a permanent responsibility of the government. On the other hand, research, education and provision of information are important instruments of the governments' policies. Especially at the beginning stage, governments have to support the whole system to have a sound and well functioning production chain, which will be able to operate without government support. Having an integrated system that is health promoting, economically viable, equitable, and ecologically sound creates some burdens both physical and financial. Many businesses can face challenges, but in particular, small-scale producers and traders in developing countries need support in planning and implementing food safety programs beside sustainable practices such as organic farming. Such a system, in fact needs additional paperwork and record keeping beside comprehensive knowledge. The farmers need to have theoretical and practical knowledge along with financial subsidies to implement such a comprehensive system.

The convergence of traditional and certified agricultural production and processing systems from the food safety points have been evolving toward a unified food system. All stakeholders have to realize these rapid changes and need to be in common efforts to meet new food policy requirements.

REFERENCES

[1] Rehber, E. (2011) Economics of Organic Farming (Extended and updated). Lambert Academic Publishing England. ISBN:978-3-8465-3300-0. 280p.

[2] Davies, J.G. (2006) Managing the Effects of Nanotechnology. Woodrow Wilson International Center for Scholars, Project on Emerging Nanotechnologies, Washington DC.

[3] Dagistan, E., Gül, M., Akpınar, G., Gülcan, S. (2017) The Future Prospects of Factors Affecting Consumer Attitudes on The Fruit Juice Market in Turkey. Fresen. Environ. Bull. 26, 6765-6772.

[4] Turhan, Ş., Vural, H., Ak, İ., Erdal, B. (2017) Consumer Trends for Organic Products: The Case of The Marmara Region in Turkey. Fresen. Environ. Bull. 26, 8160-8159.

[5] WHO (1984) The Role of Food Safety in Health and Development. Report of a Joint FAO/WHO Expert [meeting held in Geneva from 30 May to 6 June 1983], 79p.

[6] Kaferstein, F.K. (2003) Food Safety in Food Security and Food Trade. Food Safety as a Public Health Issue for Developing Countries Focus. 10, Brief 2 of 17.

[7] Rehber, E. (2012) Food for thought: "four Ss with one F": Security, safety, sovereignty, and shareability of food. British Food Journal. 114(3), 353 – 371.

[8] ITC (2008) An Introduction to ISO 22000, Food Safety Management Systems, Food Safety: An Overview. International Trade Center. 85(2008), 39p.

[9] EU (2006) Regulation (EC) No 178/2002 of the European Parliament and of the Council of 28, January 2002. In: Official Journal of the European Communities, F.K.

[10] Frohberg, K., Grote, U. and Winter, E. (2006) EU Food Safety Standards, Traceability and Other Regulations: A growing Trade Barrier to Developing Countries' Exports? Invited paper prepared for presentation at the International Association of Agricultural Economists Conference, Gold Coast, Australia. August 12-18 2006.

[11] Josling, T. (2006) The Institutional Framework for Food Regulation and Trade. Paper prepared for the IATRC Summer Symposium. Bonn, May 28-30.
[12] www.cyclopaedia.org.
[13] FAO (2007) Report of the FAO Internal Workshop on Good Agricultural Practices. Gap working paper-series. 4, 51p.
[14] Schneider, R.G., Schneider, K.R. and Archer, D.L. (2011) Food Safety on the Farm: An Overview of Good Agricultural Practices. Food Science and Human Nutrition Department. http://edis.ifas.ufl.edu/fs135.
[15] Rehber, E. and Ulusoy, Ş. (1998) HACCP System and Its Feasibility in Developing Countries: A CostBenefit Analysis Approach. 61th EAAE Seminar. Warsaw Agricultural University Press. Poland, October 22-24, 198-211.
[16] Yıldırım, E.M., Karaman, A.D., Yerlikaya, H. (2017) Overview of Pest Management Practices in Turkish Food Processing Facilities. Fresen. Environ. Bull. 26, 4637-4644.
[17] Stanley, R., Knight, C., Bodnar, F. (2011) Experiences and challenges in the development of an organic HACCP system NJAS - Wageningen Journal of Life Sciences. 58, 117– 121.
[18] Flachowsky, G. (2003) Contributions of Agriculture to Improve Food Security and Food Safety. Fresen. Environ. Bull. 12, 467-489.
[19] Subedi, S.P. (2003) The World Trade Organization, the European Union and the Liberalization of Trade in Agriculture. Managerial Law. 45(5-6), 27-47.
[20] Sligh, M. and Cierpka, T. (2007) The Organic Values In: Lockeretz, W. (ed.) Organic Farming, An International History. CAB International, Massachusetts, USA. 30.
[21] Rawson, J.M. (2006) Organic Agriculture in the United States: Program and Policy Issues. CRS Report for Congress, The Library of Congress.
[22] Adam, K.L. (2006) Community Supported Agriculture, ATTRA - National Sustainable Agriculture Information Service, Availability: ATTRA, 16p.
[23] Guillot, L. (2006) HACCP and ISO: Is it the Right Combination? Rearranging Task Codes in a Manner to Better Accommodate the Combination of HACCP and ISO. Food Quality & Safety magazine. April/May, 11-13.
[24] Cooper, J., Niggli, U. and Leifert, C. (2007) Handbook of organic food safety and quality. CRC Press, Woodhead Publishing. Cambridge, England, 521p.
[25] Niggli, U., and Leifert, C. (2007) Improving Quality and Safety of organic and Low-input Foods and Maximizing the Benefit of Consumer and Producers. In: Niggli, U., Leifert, C., Alföldi, T., Lück, L. and Willer, H. (eds.) Proceedings of the 3rd International Congress of the European Integrated Project Quality Low Input Food (QLIF), 15-22.

Received: **07.12.2017**
Accepted: **18.02.2018**

CORRESPONDING AUTHOR

Sule Turhan
Uludag University,
Faculty of Agriculture,
Department of Agricultural Economics,
TR 16059 Bursa – Turkey

e-mail: sbudak@uludag.edu.tr

AUTHOR INDEX

A

Abaci-Bayan, A. A. 3133
Abdel-Wahab, M. A. 2943
Abdul-Wahab, S. A. 2612
Acar, R. 2873
Ahmed, H. A. 3020
Akachat, A. 2968
Akdogan, G. 3020
Akkoyun, H. T. 3148
Alarifi, S. 2883
Al-dahmash, B. 2883
Alessia, M. S. 2883
Ali, D. 2883
Ali, F. 3075
AlKahtane, A. A. 2883
Alkahtani, S. 2883
Alnahdi, A. 2612
Alomar, S. Y. 2883
Al-Qahtani, A. A. 2883
Altun, L. 3107
Altun, M. 2635
Al-Yahya, H. 2883
Anjum, M. Z. 3075
Aricak, B. 3206
Arifoglu, N. 3051
Arihan, O. 3148
Aslan, H. 2853
Aydin, G. 3020
Aydın, H. 2800
Aydin, S. 3180
Aydin-Uncumusaoglu, A. 2900
Aysan, Y. 3185

B

Barpete, S. 3020
Bayat, A. 2963
Bayramoglu-Akkoyun, M. 3148
Baysoy, O. 2878
Baytut, O. 2853
Becer, Z. A. 3006
Bengu, A. S. 3148
Bolat, A. 2963
Boysan-Canal, S. 3174
Bozkurt, M. A. 3174
Budama-Kilinc, Y. 2642

C

Cakir, C. 2629
Cakir-Koc, R. 2642
Canturk, U. 2629
Can-Yilmaz, E. 2853
Cerit, I. 2963
Cetin, M. 2629, 3206
Ceyhan-Guvensen, N. 2761
Ceylan, R. F. 3094
Chen, B. 2844
Chen, C. 2671, 3013
Chen, J. 3043
Chen, W.-H. 3156
Cilbircioglu, C. 3117
Cobanoglu, S. 3117
Cui, X. 2844
Cymes, I. 2777, 2791

D

Daglioglu, Y. 2951
Demircan, F. 3180
Demirel, N. 3191
Deng, B. 3166
Ding, K. 3102
Ding, L. 2891

E

Ece, M. 3124
Ekberli, I. 2834
Elipek, B. 2853
Elkamel, A. 2612
El-Samawaty, A. E.-R. M. A. 2943
Emeklier, H. Y. 3081
Erdal, B. 3212
Erdol, M. 3124

F

Fan, L. 3102
Fan, S. 2662

G

Gao, B. 3043
Gerami, S. 2743
Gonulal, O. 2853
Gozel, N. 3180
Gumus, S. 2933
Guo, K. 2978
Guo, R. 2724
Guo, X. 2671, 3166
Guo, Y. 2703

H
Hacisalihoglu, S. 2933
Hamamci, S. F. 3124
He, Y. 3102
Horuz, S. 3185
Hu, S. 2913
Huang, L. 3166
Huang, R. 3156

I
Ikhile, E. 2612

J
Jia, X. 2818
Jiang, H. 2662
Jiang, X. 3102

K
Karaagac, H. A. 2963
Karabacak, E. 2853
Karabayir, A. 3051
Karatas, A. 3180
Kaya, Z. 2642, 3162
Keskin, D. 2761
Kezik, U. 2933
Khan, M. Q. 3075
Khattak, I. 3075
Kilic, G. 3191
Kilic, S. 3006
Kilinc, F. 3180
Kinaci, M. S. 3180
Kipcak, S. 3174
Koc, N. 2873
Koca, S. S. 3180
Kopacki, M. 2751
Koparir, M. 2992
Koparir, P. 2992
Krivokapic, S. 2690
Kucuk, C. 2878
Kurt, Y. 2853

L
Li, B. 3028
Li, F. 2724, 2735
Li, X.-L. 3156
Li, Y. 2703, 2724
Ling, L. 2809
Linhua, S. 3013
Liu, J. 2654
Liu, Q. 3166
Liu, X. 2844
Liu, Y. 2891
Liu, Z. 2654
Louhab, K. 2968
Lu, D. 2818
Lu, F. 2922

M
Ma, T. 2662
Ma, Y. 2662
Mahanpoor, K. 2682
Masoudi, M. 2743
Mei, Z. 2809
Metin-Kir, S. 2697
Mokhtari, N. E. P.
Mutlu, E. 2900

N
Nemlioglu, S. 2635
Nie, J. 2662
Niu, D. 3166
Niu, G. 2768

O
Ocal, A. 3185
Ogutcu, M. 3051
Okut, N. 2785
Orcen, B. B. 2642
Orek, C. 2992
Orhan, Y. 3087
Ozcan, S. 3020
Ozdemir, F. A. 3180
Ozdemir, G. 3199
Ozdemir, N. 2834
Ozel, H. B. 3162, 3206
Ozgen, I. 2829
Ozkaynak, E. 3087
Ozkurt, N. 3124
Ozturk, E. 2834

P
Palta, S. 3140
Pan, Z. 2703
Parafiniuk, S. 2751
Parlak, A. E. 2992
Petrovic, D. 2690
Petryk, A. 2867

Q
Qin, M. 2818
Qiu, Z. 3043

R
Rebbah, H. 2968
Rehber, E. 3212

S
Sancak, C. 3020
Sankur, F. 2761
Sanli, E. R. 2985
Sarac, K. 2992
Sari, D. 3124
Selcuk, N. 2785
Sevik, H. 2629, 3206
Sevilmis, U. 2963
Sezgin, N. 2635
Shang, K.-K. 3059
Shi, H. 2818
Shi, R. 2662
Siddiqui, W. A. 2809
Simşek, T. 3087
Skwarylo-Bednarz, B. 2751
Sui, B. 2818

T
Tang, D. 2768
Tang, J. 2671
Tang, Z. 2922
Tekin, S. 3035
Temelli, U. E. 2635, 2717
Tetik, O. 2963
Tezel, M. N. 3124
Tosunoglu, M. 2853
Turhan, S. 3212
Turkoglu, S. 2992

U
Ucarkus, E. 2642
Ulu, R. 3180
Ulucan, A. 3148
Unal, M. 2697
Uzar, S. 2800

V
Vardar, F. 2697
Varol, T. 3206
Vincent, G. 3059
Vural, H. 3212

W
Wang, C. 3028
Wang, G. 2724, 2735
Wang, J. 3059
Wang, M. 2818
Wang, Q. 2654, 2662
Wang, S. 3166
Wang, X. 3028
Wang, Y. 2735
Wen, J. 2844
Wu, B. 2844
Wu, C. 2978
Wu, S. 2724
Wu, Y. 2913

X
Xiang, B. 2978
Xiong, M. 2724
Xu, J. 2724
Xu, X. 3166
Xu, Y. 2818

Y
Yagmur, M. 2785
Yakupoglu, T. 2834
Yalcindag, N. 3124
Yan, D. 3102
Yan, X. 2844
Yan, Y. 2654
Yang, Q. 2735
Yang, Y. 2768
Yardim, M. 3180
Yassin, M. A. 2943
Yavas, I. 2649
Yavuz, M. 2985
Yener, I. 3107
Yesil, E. A. 2635
Yi1, N. 2913
Yigit, N. 3206
Yildirim, A. E. 3191
Yildirim, B. 2785
Yilmaz, M. 3068
Yilmaz-Ozturk, B. 2951
Yin, G. 2662
Yugruk-Akdag, N. 3124
Yurur, E. E. 2800

Z

Zarzycki, J.	2867	Zhao, Y.	3156
Zeng, H.	2703	Zheng, L.	3166
Zeynolabedin, R.	2682	Zheng, X.	3166
Zhang, M.	2844	Zhou, L.	2724
Zhang, Q.	2654	Zhu, J.-W.	3156
Zhang, S.	2654	Zhu, M.	2768
Zhang, W.	2703	Zuo, R.	3102
Zhao, S.	2978		

SUBJECT INDEX

A

ABAG 2933
Acaricide 3117
Accelereted Aging 3081
Acetamiprid 2735
Acne Vulgaris 2642
Acoustic index analysis 2922
acute toxicity 2951
additive effect 3166
additives 2985
Adsorbents 2649
Adsorption Mechanism 3043
aerosols 2968
Agrobacterium tumefaciens 3020
Air pollution 2743
algal cells 2951
Alnus glutinosa 2933
Ambient air quality 2612
Anamorphic fungi 2943
Antarctica 3028
Anthocyanin 3199
antibiotic sensitivity 2761
Antioxidant activity 2992
Antioxidative enzyme 3174
Apoptosis 2883
Arbuscular mycorrhizal fungi (AMF) 3140
architectural acoustic environment design 2922
Atmospheric pollutants 2612
atrazine 3075
attractant 3191

B

Berry 3199
bibliometrics 2654
bioaccumulation 2951
bioaccumulation factor 2867
biodegradation 2735, 3156
biodiversity 2800
Black pine 3162
Bogazkere 3199
Bostrichus capucinus 2829
Brain damage 3148
Brassica juncea 2913
Brine outfall 2635

C

Cadmium 3174
Camellia sinensis 2933
Carbon tetrachloride 3148
cat 2985
catalase 2878
Cd 2878
Cd contamination 2913
cellulose materials 2654
Cement 2717
Chitosan 2642, 2913
Chromosomal abnormalities 2697
Chrysanthemum 2751
CIP 10 2968
Climate 3206
climate change 3028
clinical specimens 2761
clogging 3035
cluester analysis 2785
Coconut Oil 2642
Co-cultivation 3020
$CoFe_2O_4$/Copper Slag 2682
computer-aided acoustic prediction 2922
Concrete 2717
contamination 2690
Control 3185
Cool season 3068
copper 3185
Coturnix coturnix japonica 3051
creeping yield 3068
Crested Wheatgrass [Agropyron cristatum (L.) Gaernt] 2873
Cynodon dactylon 3140

D

dam reservoirs 2791
degradation 2654
Dendrosotinus ferrugineus 2829
Dessert Wheatgrass [A. desertorum (Fisch. ex Link) Schult] 2873
DFT 2992
dinoflagellate 2800
disinfectant 3051
diversity 2853
DNA damage 2883
dog 2985
Domestic 3087
drinking water 3051
Drip irrigation 3035
dry matter yield 3068
Dust pollution 2968
Dye tracer 2635

E

Ecology 2800
economic growth 2818
Efficiency of irrigation 2809
Egg quality 3051
ejector nozzles 2751
Ellagic Acid 3148
energy resource 2654
Environmental Kuznets curve 2818
environmental quality 2818
Erosivity 2834
Escherichia coli 2761
Eskisehir 2717
Essential oil constituent 2785
exploratory spatial data analysis technology 2768
Exposure 3124

F

fallow land 2867
Farmland Soil 2662
fertilizer doses 3068
Ficus caria 2829
Field comparative experiment 3059
Fish life 3006
Flavonoid 3199
flowering 3162
food regulations and standards 3212
Food safety 3212
French fries 3087
Fresh water 2900
FT-IR 2992
Fukui descriptors 2992
functional analysis 2724
Fungicide 2697
fuzzy compre-hensive assessment method 2891

G

Garlic Acari 3117
GC-MS analysis 2785
geo-accumulation index 2844
Germination 3081
germination percentage 2649
GIS 2629
Gökçeada 2853
Grape 3199
greenhouse 2809
Groundwater 2809, 2791, 3013
growth performance 3051
growth response 3059
Guangxi 2818
Guidelines 2612

H

HaCaT cells 2883
Heap bioleaching 2844
heat shock protein 70 3180
heated and unheated conditions 2809
heavy metal 2662, 2900
heavy metals 2867
heavy metals pollution 2844
hematological indices 3075
Herbal detox 2985
Herbicide 2697,
hierarchical cluster analysis (HCA). 2900
hydroxyapatite 2703

I

Imbros 2853
index system 2891
indicator 2800
indicator species 3059
in-line emitter 3035
intensive care unit 2761
irisin 3180
irrigated agricultural 3133

J

J. oxycedrus 2499
Jarahi River 2468
Jordan 2418, 2427

K

Kastamonu 3117
kinetic energy 2834
Kirsehir 3133
Klebsiella pneumoniae 2761
Kutahya 2629

L

Lactobacillus buchneri 3156
Lagrangian–Eulerian finite 2671
Lake Yeniçağa 3006
Landslide 2933
leaf 3206
Legumes 3094
locust bean extract waste 3035

M

magnetosome biosynthesis 2724
Magnetospirillum 2724
Maize 2963
major facilitator superfamily 2724
manganese 3013
MCP 2883
Mediterranean fruit fly 3191
metal pollution index 2690
Meteorological Parameters 2743
Microbiology of outdoor air 2943
Micromorphogical character 3206
microorganism number 2878
microwave radiometer 3028
Middle East 2943
Mitotic index 2697
mixed soil 3166
Modeling 3124
Molds 2943
MTT assay 2883
multiple linear regression 3107
multivariate statistical analysis 2900

N

nanocomposite 2951
Nanoparticle 2642
Neonicotinoid Insecticide 2735
new host 2829
new record parasitoid 2829
nitrogen mineralization 3166
NO_2 2743
Noise map 3124
Noise source 3124
non-irrigated agricultural 3133
Numerical simulation 2671

O

Olive mill wastewater 2649
Organic amendments 3174
oriental spruce 3107
oxidative stress 2951

P

pathogen identification 2978
Pb 2878
pepper yield 2809
Permeable reactive barrier (PRB) 2703
Phenolic 3199
Photodegradation 2682
physical 3185
physical and chemical analysis of water 3006
phytoplankton 2800
plant invasion 3166
Plants 3102
polyurethane industry 2968
pomegranate 3191
Population density 3117
potato 3020
potato breeding 3087
Price 3094
Priming 3081
principal components analysis (PCA) 2900
protein expression 2724
Pseudomonas syringae pv. tomato 3185
Public Health 2717

Q

quail 3051
Quanzhou Bay artificial island 2671

R

rainfall intensity 2834
rainfall simulator 2834
Rapid detection 2978
Rat 3148
Raynaud's phenomenon 3180
Recreational potential 2629
Regional environmental regulation 2768
Regression model 2743
regression tree 3107
Remediation 2913
reproductive 3162
research trends 2654
resting cyst 2800
reverberation time control 2922
Rhizoglyphus echinopus 3117
Rhodamine B 2635
risk assessment 2844
Roadside soil 2878
root and stem rot diseases 2751
Root growth 2697
root morphology 3059
root yield 3068
r- toluidine 2682

S
Salinity 2873
Salt Lake 2853
Schizothorax plagiostomus 3075
sediment 2800
Seed 3081
seedling growth 2649
SEM 3206
shoot growth 3068
sibling coefficient 3162
Site index 3107
Snowmelt detection 3028
Soil 2690, 2735
soil charactesitic 3133
Soil Loss 2933
Soil Organic Matter 3043
soil properties 3140
Solanum tuberosum 3020
Solidago canadensis 3166
Sorghum 3081
sound absorption measurement 2922
Sources of Pollution 2662
spatial autocorrelation 2768, 3013
spatiotemporal change characteristics 3028
Specific Radioactivity 2717
Spinach (Spinacia oleracea L.) 3174
spraying 2963
Standards 2612
statistical analysis 3013
status number 3162
stoma 3206
Supply Response 3094
sustainable 2629
sustainable agriculture alternatives 3212
symbiosis 3140
systemic sclerosis 3180

T
Taguchi 2682
Tall Wheatgrass [A. elongatum (Host) P. Beauv.] 2873
Tongling 2662
toxic effect 3075
Trace metal 2690
Transformation 3020
traps 3191
Triangular mesh 2671
triclopyr butoxyethyl ester 3156
Tropical fungi 2943
tuber yield 3087
turf mixture 3068
Turkey 2829, 3191

U
Uptake 3102
Uranium 2703, 3043, 3102
Uranium mill tailing 3102
Urban forest 2629
urban pollution 3059
urease 2878
UV-visible spectrometry 2635

V
Valsa mali 2978
VEC 3094
vegetables 2690
vegetation 2867

W
water quality 2777, 2791, 3006
water reservoirs 2777
water resources 2777
water-saving irrigation developing level 2891
wavelet transform 3028
Weed control 2963
weight set 2891
wetlands 2853
wheat 2649
Wood canker 2978
WQI 2777, 2791

X
Xinjiang 2978

Z
Zeolite 2913
Ziziphora clinopodioides 2785
$(ZnO\text{-}TiO_2)_{NCM}$ 2951

1,2….,9
1,2,4-Triazole 2992
4,4-MDI 2968

FEB – GUIDE FOR AUTHORS

General

FEB accepts original papers, review articles, short communications, research abstracts from the entire sphere of environmental-chemistry,-biology,-microbiology,- technology, -biotechnology and-management, furthermore, about residue analysis/ and ecotoxicology of contaminants.

Acceptance or no acceptance of a contribution will be decided, as in the case of other scientific journals, by a board of reviewers. Papers are processed with the understanding that they have not been published before (except in form of an abstract or as a part of a published lecture, review or thesis);that they are not under consideration for publication elsewhere; that their publication has been approved by all co-authors, if any, as well as-tacitly or explicitly- by the responsible authorities at the institute where the work has been carried out and that, if accepted, it will not be published elsewhere in the same form, in either the same or another language, without the consent of the copyright holders.

Language

Papers must be written in English. Spelling may either follow American (Webster) or British (Oxford) usage but must be consistent. Authors who are less familiar with the English language should seek assistance from proficient colleagues in order to produce manuscripts that are grammatically and linguistically correct.

Size of manuscript

Review articles should not exceed 30 typewritten pages. In addition up to 5 figures may be included.

Original papers must not exceed 14 typewritten pages. In addition up to 5 figures may be included.

Short-Communications should be limited to 4 typewritten pages plus not more than 1 illustration.

Short descriptions of the authors, presentation of their groups and their research activities (with photo) should together not exceed I typewritten page. Short research abstracts should report in a few brief sentences (one-fourth to one page) particularly significant findings. Short articles by relative newcomers to the chemical innovation arena highlight the key elements of their Master and PhD-works in about I page.

Book Reviews are normally written in-house, but suggestions for books to review are welcome.

Preparation of manuscript

Dear authors,

FEB is available both as printed journal and as online journal on the web. You can now e-mail your manuscripts with an attached file. Save both time and money. To avoid any problems handling your text please follow the instructions given below:

When preparing your manuscripts have the formula K/SS (Keep It Simple and Stupid) in mind. Most word processing programs such as MS-Word offer a lot of features. Some of them can do serious harm to our layout. So please do not insert hyperlinks and/or automatic cross-references, tables of contents, references, footnotes, etc.

1. Please use the standard format features of your word processor (such as standard.dot for MS Word).
2. Please do not insert automatisms or secret link-ups between your text and your figures or tables. These features will drive our graphic department sometimes mad.
3. Please only use two fonts for text or tables "Times New Roman" and for graphical presentations "Arial".
4. Stylesheets, text, tables and graphics in shade of grey
5. Turn on the automatic language detection in English (American or British)
6. Please - check your files for viruses before you send them to us!!

Manuscripts should send to:parlar@wzw.tum.de
or:parlar@prt-parlar.de

Thank you very much!

STRUCTURE OF THE MANUSCRIPT

Title page: The first page of the manuscript should contain the following items in the sequence given: A concise title of the paper (no abbreviations). The names of all authors with at least one first name spelled out for every author. The names of Universities with Faculty, City and Country of all authors.

Abstracts: The second page of the manuscript should start with an abstract that summarizes briefly the contents of the paper (except short communications). Its length should not exceed 150-200 words. The abstract should be as informative as possible. An extended repetition of the paper's title is not considered to be an abstract.

Keywords: Below the Summary up to 6 key words have to be provided which will assist indexers in cross-indexing your article.

Introduction: This should define the problem and, if possible, the frame of existing knowledge. Please ensure that people not working in that particular field will be able to understand the intention. The word length of the introduction should be 150 to 300 words.

Materials and methods:
Please be as precise as possible to enable other scientists to repeat the work.

Results: Only material pertinent to the subject must be included. Data must not be repeated in figures and tables.

Acknowledgements: Acknowledgements of financial support, advice or other kind of assistance should be given at the end of the text under the heading "Acknowledgements". The names of funding organisations should be written in full.

References: Responsibility for the accuracy of references rests with the authors. References are to be limited in number to those absolutely necessary. References should appear in numerical order in brackets and in order of their citation in the text. They should be grouped at the end of the paper in numerical order of appearance. Abbreviated titles of periodicals are to be used according to Chemical or Biological Abstracts, but names of lesser known journals should be typed in full. References should be styled and punctuated according to the following examples:

ORIGINALPAPERS:
l. Author, N.N. and Author, N.N. (Year) Full title of the article. Journal and Volume, first and last page.
BOOK OR PROCEEDING:
2. Author, N.N. and Author, N.N. (Year) Title of the contribution. In: Title of the book or proceeding. Volume (Edition of klitor-s, ed-s) Publisher, City, first and last page

DOCTORAL THESIS:
3. Author, N.N. (Year) Title of the thesis, University and Faculty, City

UNPUBLISHED WORK:
Papers that are unpublished but have been submitted to a journal may be cited with the journal's name followed by "in press". However, this practice is acceptable only if the author has at least received galley proofs of his paper. In all other cases reference must be made to “unpublished work" or "personal communication".

Discussion and Conclusion: This part should interpret the results in reference to the problem outlined in the introduction and of related observations by the author/s or others. Implications for further studies or application may be discussed. A conclusion should be added if results and discussion are combined.

Corresponding author: The name of the corresponding author with complete postal address

Precondition for publishing:
A minimum number of 25 reprints must be ordered and prepaid.
1 - 4 pp.: 200,- EURO + postage/handling
5 - 8 pp.: 250,- EURO + postage/ handling
More than 8pp: 1.50 EURO/page x number of reprints +postage/ handling.
The prices are based upon the number of pages in our journal layout (not on the page numbers of the submitted manuscript).
Postage/ Handling: The current freight rate is Germany 10 €, Europe 18,00 €, International 30 €.
VAT: In certain circumstances (if no VAT registration number exists) we may be obliged to charge 7% VAT on sales to other EU member countries.MESAEP and SECOTOX members get a further discountof 20% (postage/ handling full).